THE UNIVERSITY *of* EDINBURGH

Characterising the Optical Properties of Galaxy Clusters with GMPhoRCC

Ross John Hood

Doctor of Philosophy
The University of Edinburgh
2014

Lay Summary

Galaxy clusters, the largest observable structures in the universe, are excellent tools to test our understanding of cosmology, galaxy formation and evolution. However in order to be useful for such analysis it is necessary to determine many of their properties such as mass, number of cluster members and redshift, a cosmological distance measure, which are often expensive and time consuming to determine directly. Presented in this thesis is GMPhoRCC, an algorithm which aims to characterise these properties quickly and reliably from readily available optical data and provides many advantages over existing methods. Of particular note is the quality control system, which can identify cases where the GMPhoRCC result catastrophically fails to match the properties of the cluster.

The development of GMPhoRCC is explored through comparisons with existing methods using clusters with previously determined properties. GMPhoRCC is found to provide more accurate and reliable measures of cluster properties, particularly redshift, compared with the XCS and maxBCG algorithms.

By creating artificial galaxy clusters with known attributes, the performance of GMPhoRCC is evaluated more thoroughly than can be achieved with existing clusters with estimated properties. Particular focus is given to assess the quality control system and confirms that it is able to identify the cases where the results are likely to be erroneous. In addition, the performance of GMPhoRCC is evaluated for a range of different cluster sizes and distances and is found to provide more reliable estimates separately for smaller and more distant clusters than is achieved with existing algorithms.

This thesis concludes with the application of GMPhoRCC to estimate the properties of ~ 7000 clusters, found through their emission of X-rays by the XCS team. In addition to providing these characterisations, future research with these X-ray clusters is explored. Of particular interest is how the optical properties

vary with X-ray, which helps to calibrate and improve the accuracy of the mass estimate, the most important and difficult property to determine.

Abstract

The properties of galaxy clusters, such as abundance and mass to light ratios, have long been used to investigate and constrain cosmology. With vast numbers of newly detected clusters, such as from the Planck mission (Planck Collaboration et al., 2013), full determination of cluster properties, particularly mass, can be hugely expensive and time consuming. Optical characterisation offers a cheap solution, using optical data alone to estimate cluster properties such as redshift. With the abundance of current optical data, such as from the Sloan Digital Sky Survey (SDSS), (Ahn et al., 2012) and upcoming all sky surveys, such as the Panoramic Survey Telescope and Rapid Response System (Pan-STARRS) 3π survey (Magnier et al., 2013), optical characterisation will play a key role in the investigation of the latest clusters. Presented in this thesis is the **G**aussian **M**ixture full **Pho**tometric **R**ed sequence **C**luster **C**haracteriser (GMPhoRCC), which aims to provide such an analysis, offering substantial advantages over existing algorithms.

GMPhoRCC identifies and models the red sequence, early-type galaxies which dominate the cluster, and uses the properties of this to estimate cluster redshift and richness, an optical mass proxy based on the number of cluster members. The main features include, full treatment of multi-modal distributions by modelling properties with error-corrected Gaussian Mixtures, model independence by using empirical photometric redshifts rather than assumed colour-redshift relations and quality control used to identify probable catastrophic failures in order to clean the characterisations. Using a sample of 5500 clusters taken from the GMBCG (Hao et al., 2010), NORAS (Böhringer et al., 2000), REFLEX (Böhringer et al., 2004) and XCS (Mehrtens et al., 2012) catalogues, GMPhoRCC redshift estimates are compared to spectra showing low scatter ($\sigma_{\Delta z} \sim 0.042$) around the actual value. In addition applying the quality control to produce a clean subset removes most outliers ($|z_{GMPhoRCC} - z_{spec}| > 0.03$) gives a much tighter agreement, $\sigma_{\Delta z} \sim 0.018$

showing significant improvement over maxBCG, $\sigma_{\Delta z} \sim 0.025$, and XCS, $\sigma_{\Delta z} \sim 0.050$.

In addition to comparisons with real clusters, an extensive evaluation of the GMPhoRCC selection function is presented using mock clusters. These mocks are produced by stacking red sequence galaxies from existing clusters, analysed using the SDSS DR9, in redshift-richness bins from which new sequences are resampled. This extends the similar approach of maxBCG and GMBCG where only rich clusters are used as seeds to generate mocks with a range of properties. Comparisons with mocks agree well with real clusters attaining low redshift scatters ($\sigma_{\Delta z} \sim 0.01$) with the clean subset removing the majority of outliers. In addition, with a definitive mock value, richness comparisons are possible and although show a larger fractional scatter ($\sigma_{\Delta n_{200}} \sim 0.12$) are centred on the mock value. Richness estimates are shown to be more sensitive to discrepancies in redshift, background fluctuations and poor modelling of the red sequence than redshift.

Completeness is estimated by considering the fraction of clusters found with characterisations within given bounds. First incomplete photometry, simulated by an i-band < 21 cut, is shown to remove members for clusters with $z > 0.45$. Redshift completeness, the fraction of clusters within 0.03 of the mock value, is not immediately hindered by the photometry, attaining 93% for $0.05 < z < 0.62$ for clusters with a richness greater than 20, showing improvement over maxBCG (with 90% for $0.1 < z < 0.3$) and a larger range than GMBCG (with 96% for $0.1 < z < 0.46$). Similar to results from GMBCG, richness attains lower completeness rates due to discrepancies introduced by projection effects, background fluctuations, and redshift errors. The fraction of clusters within 25% of the mock value, defining completeness, is measured as 91% for $0.07 < z < 0.45$ for clusters with richness greater than 20, 78% for those with richness between 10 and 20, and 64% for those with richnesses less than 10.

The application of GMPhoRCC follows, where characterisations are found for new XCS X-ray extended sources (Lloyd-Davies et al., 2011). Applying GMPhoRCC to these preliminary DR2 candidates ($\sim$ 10 times larger than the current catalogue) using the VLT Survey Telescope (VST) ATLAS catalogue (Shanks & Metcalfe, 2012) and the much deeper Canada-France-Hawaii Telescope Lensing Survey (CFHTLenS) (Heymans et al., 2012) provides characterisations beyond the SDSS footprint. Of the $13,956$ candidates, 6124 have optical coverage, 5580 in the SDSS, 523 in ATLAS and 819 in CFHTLenS with some overlap. Overall

characterisations are found for 4365 candidates, 1893 of which have an associated spectroscopic redshift. The clean subset comprises 1203 candidates, 904 with spectra. Considering XCS DR1, Mehrtens et al. (2012) presented 503 optically confirmed X-ray clusters of which 258 have spectroscopic redshifts and 108 have SDSS characterisations. GMPhoRCC provides characterisations for 360, 232 of which have spectroscopic redshifts. Overall GMPhoRCC provides 260 (149 of which are clean) new SDSS characterisations and 91 (61 of which are clean) new spectroscopic redshifts.

Finally this thesis concludes with a discussion of future research, focusing mainly on a preliminary analysis of a clean spectroscopic subset of XCS DR1 in order to illustrate the potential to constrain X-ray scaling relations with the upcoming XCS DR2. Additionally, potential research into the effect of environment on the red sequence is illustrated using the dependence of the CMR slope on X-ray temperature. While a slight dependence is found, the cluster sample is insufficient to contradict the independence on environment found by Hogg et al. (2004) and Hao et al. (2009).

Declaration

I declare that this thesis was composed by myself, that the work contained herein is my own except where explicitly stated otherwise in the text, and that this work has not been submitted for any other degree or professional qualification except as specified.

(*Ross John Hood, 2014*)

Acknowledgements

First and foremost, thanks are due to my supervisor, Bob Mann[1], whose support, guidance and patience have made this thesis possible.

This thesis makes extensive use of optical data from the Sloan Digital Sky Survey, SDSS-III. Funding for SDSS-III has been provided by the Alfred P. Sloan Foundation, the Participating Institutions, the National Science Foundation, and the U.S. Department of Energy Office of Science. The SDSS-III web site is `http://www.sdss3.org/`.

SDSS-III is managed by the Astrophysical Research Consortium for the Participating Institutions of the SDSS-III Collaboration including the University of Arizona, the Brazilian Participation Group, Brookhaven National Laboratory, Carnegie Mellon University, University of Florida, the French Participation Group, the German Participation Group, Harvard University, the Instituto de Astrofisica de Canarias, the Michigan State/Notre Dame/JINA Participation Group, Johns Hopkins University, Lawrence Berkeley National Laboratory, Max Planck Institute for Astrophysics, Max Planck Institute for Extraterrestrial Physics, New Mexico State University, New York University, Ohio State University, Pennsylvania State University, University of Portsmouth, Princeton University, the Spanish Participation Group, University of Tokyo, University of Utah, Vanderbilt University, University of Virginia, University of Washington, and Yale University.

Chapter 5 makes of use of additional optical data provided by the VLT Survey Telescope (VST) ATLAS catalogue (Shanks & Metcalfe, 2012 and Shanks et al in prep.) and from the Canada-France-Hawaii Telescope Lensing Survey (CFHTLenS), (Heymans et al., 2012 and Erben et al., 2013).

[1]Scottish Universities Physics Alliance, Institute for Astronomy, University of Edinburgh, Royal Observatory, Blackford Hill, Edinburgh, EH9 3HJ, UK

This work is based on observations obtained with MegaPrime/MegaCam, a joint project of CFHT and CEA/IRFU, at the Canada-France-Hawaii Telescope (CFHT) which is operated by the National Research Council (NRC) of Canada, the Institut National des Sciences de l'Univers of the Centre National de la Recherche Scientifique (CNRS) of France, and the University of Hawaii. This research used the facilities of the Canadian Astronomy Data Centre operated by the National Research Council of Canada with the support of the Canadian Space Agency. CFHTLenS data processing was made possible thanks to significant computing support from the NSERC Research Tools and Instruments grant program.

This work is based on VST ATLAS data products from observations made with ESO Telescopes at the La Silla Paranal Observatory under programme ID 177.A-3011(A,B,C) (see Shanks et al in prep.).

Additionally the author would like to thank Owen Turner[2] for his extensive work calibrating and testing a complete set of empirical photometric redshifts for the ATLAS catalogue using the method of Carliles et al. (2010) with an SDSS spectroscopic training set.

Finally to my Gran, who never stopped believing in me.
Gone but never forgotten.

[2]Scottish Universities Physics Alliance, Institute for Astronomy, University of Edinburgh, Royal Observatory, Blackford Hill, Edinburgh, EH9 3HJ, UK

Contents

List of Figures

4 Mock Galaxy Clusters

6 Discussion

List of Tables

3 GMPhoRCC: A New Characterisation Pipeline

4 Mock Galaxy Clusters

5 Characterising XCS Sources

Chapter 1

Introduction

Galaxy clusters are widely regarded as excellent probes of cosmology. As the largest observable objects these are great indicators of the large scale structure and evolution of mass distribution in the universe. As this is highly sensitive to the form of the expansion of the universe, their study gives valuable constraints on cosmological models (see Peebles, 1980, Sheth et al., 2001, Jenkins et al., 2001, Rozo et al., 2010 and Tinker et al., 2012 etc.). In addition clusters provide an excellent opportunity for studying galaxies themselves particularly formation, evolution and the impact of the environment (see Gladders et al., 1998 and Voit, 2005 etc.). Whether used to study galaxy evolution, large scale structure or containing cosmological models, galaxy clusters have proven to be a fruitful and active area of research.

In order to proceed with such cosmological analysis it is often necessary to detect and determine the properties of the clusters, which, particularly for mass and redshift, can be difficult and expensive. Without resorting to spectroscopy or weak lensing, which can be time consuming, expensive and cover only limited areas of the sky, optical characterisation methods have been developed to determine these properties from cheap photometry alone. With an abundant source of galaxy clusters from Planck (Planck Collaboration et al., 2013), XCS (Lloyd-Davies et al., 2011), GMBCG (Hao et al., 2010) etc. and with substantial optical data from the Sloan Digital Sky Survey (SDSS) (Ahn et al., 2012), Canada-France-Hawaii Telescope Lensing Survey (CFHTLenS) (Heymans et al., 2012) and the Panoramic Survey Telescope and Rapid Response System (Pan-STARRS) 3π survey (Magnier et al., 2013) the value of such research is clear and

is indeed the focus of this thesis.

While many methods of characterisation exist, such as, GMBCG (Hao et al., 2010), maxBCG (Koester et al., 2007b), XCS (Mehrtens et al., 2012) and redMaPPer (Rykoff et al., 2013) to name a few, these have several drawbacks and may even be linked to the much more difficult task of cluster finding preventing stand-alone use. With clusters dominated by a red sequence of early-type galaxies with similar ages, metallicities and colours, these methods are able to isolate and model cluster members to infer bulk properties such as redshift. Particularly with regards to maxBCG, and XCS, these assume a redshift-colour model to infer redshift from the red sequence colour. In addition it is noted that GMBCG and High et al. (2010) struggle in the cases with multi-modal distributions, where multiple peaks in the colour or redshift distributions lead to ambiguous characterisations and potential catastrophic failures.

The main aim of this research is the development of a new characterisation method to address these issues which can be used with multiple sources of optical data and potential galaxy clusters, leading ultimately to the analysis of new candidates. Presented in this thesis is the **G**aussian **M**ixture full **Ph**otometric **R**ed sequence **C**luster **C**haracteriser (GMPhoRCC), which is designed specifically to attain model-independent estimates of redshift, optical richness and the red sequence colour magnitude relation (CMR). GMPhoRCC offers many advantages over existing algorithms including proper treatment of multi-modal distributions and an extensive quality control system to remove potential catastrophic failures.

In addition to the development of GMPhoRCC this thesis includes an extensive evaluation of accuracy and the optical selection function with the use of empirical mock galaxy clusters. Using comparisons of the GMPhoRCC estimates to those from mocks which mimic SDSS photometry, accuracy with regards to the SDSS is assessed. Similarly by considering the fraction of the total mock catalogue which GMPhoRCC was able to attain suitable characterisations, completeness and an estimate of the optical selection function is evaluated.

With the ultimate goal to analyse new cluster candidates with GMPhoRCC the remaining focus of this research is the characterisation of new preliminary XCS DR2 sources. In addition to characterisations this includes preliminary calibrations and assessments necessary for using CFHTLenS and VLT Survey Telescope (VST) ATLAS data (Shanks & Metcalfe, 2012 and Shanks et al in prep.).

This thesis is structured as follows. Chapter 2 reviews the background theory of galaxy clusters covering cosmology, cluster properties, detection and existing characterisation methods. Chapter 3 details the development and calibration of GMPhoRCC with the SDSS and explores comparisons with existing methods. An extensive evaluation of GMPhoRCC accuracy and selection function using SDSS empirical mock galaxy clusters follows in Chapter 4. The application of GMPhoRCC to characterise new extended X-ray sources from XCS and the foundation for the use of optical data from VST ATLAS and CFHTLenS is presented in Chapter 5. This thesis concludes with a summary and discussion of future research in Chapter 6.

Throughout this thesis a flat ΛCDM cosmology is assumed with $\Omega_m = 0.27$, $\Omega_\lambda = 0.73$ and $h = 0.71$.

Chapter 2

Galaxy Clusters: The Background Theory

Galaxy clusters are widely regarded as excellent probes of cosmology. Whether used to study galaxy evolution, large scale structure or constraining cosmological models, galaxy clusters have proven to be a fruitful and active area of research. With an abundant source of galaxy clusters from Planck (Planck Collaboration et al., 2013), XCS (Lloyd-Davies et al., 2011), GMBCG (Hao et al., 2010) etc. and with substantial optical data from the Sloan Digital Sky Survey (SDSS) (Ahn et al., 2012), Canada-France-Hawaii Telescope Lensing Survey (CFHTLenS) (Heymans et al., 2012) and the Panoramic Survey Telescope and Rapid Response System (Pan-STARRS) 3π survey (Magnier et al., 2013) the value of such research is clear and is indeed the focus of this thesis. This preliminary Chapter, aims to provide the relevant background material concerning galaxy clusters which gives the foundation of the work presented in this thesis.

This Chapter is structured as follows. Section 2.1 gives an account of modern cosmology, focusing specifically on what can be learned from the study of galaxy clusters. Section 2.2 covers the properties of galaxy clusters discussing detection and characterisations. A review of existing characterisation methods is given in Section 2.3 covering their strengths and weaknesses. Finally this Chapter concludes in Section 2.4 with a review of the key points used throughout this thesis.

2.1 Cosmology with Galaxy Clusters

Throughout history study has shown time and time again that there is more to the universe than meets the eye. From the failings of early heliocentric models to the Great Debate the complexity of the universe has unfolded. Although not complete, modern cosmology has made tremendous progress in understanding and describing the universe as a whole. The first step towards this is to construct a framework from which our models and theories can be built. A full rigorous treatment of the formalism of cosmology can be found in Peacock (1999) and is outlined in the upcoming sections.

2.1.1 The Robertson-Walker Metric

On cosmological scales a rigorous treatment of matter, energy and space can only be achieved by considering Einstein's field equations.

$$R^{\mu\nu} - \frac{1}{2}g^{\mu\nu}R = -\frac{8\pi G}{c^4}T^{\mu\nu} - \Lambda g^{\mu\nu} \tag{2.1}$$

where $R^{\mu\nu}$ is the Ricci curvature tensor, R the Ricci curvature scalar, $g^{\mu\nu}$ the metric tensor, Λ the cosmological constant, G Newton's gravitational constant, c the speed of light, and $T^{\mu\nu}$ the stress-energy tensor.

By using the cosmological principle, the assumption that the universe is isotropic and hence homogeneous on large scales, these equations have been solved to give the Robertson-Walker metric (for details see Peacock, 1999).

$$\mathrm{d}s^2 = c^2\mathrm{d}\tau^2 = c^2\mathrm{d}t^2 - R^2(t)[\mathrm{d}r^2 + S_k^2(r)\mathrm{d}\psi^2] \tag{2.2}$$

where $\mathrm{d}s^2$ is the space time interval between two events, $R(t)$ is the scale factor which is a measure of the size of the universe, and r is the radial comoving co-ordinate. Comoving co-ordinates define a system such that comoving observers are at rest with respect to the local matter distribution and hence observe an isotropic universe. As predicted by General Relativity energy and matter curve space-time and $S_k(r)$ holds this information in the metric.

$$S_k(r) = \begin{cases} \sin(r) & (k=1) \\ \sinh(r) & (k=-1) \\ r & (k=0) \end{cases} \tag{2.3}$$

Here k is the curvature parameter with $k = 1$ denoting positive curvature (sphere-like) describing a closed universe. $k = 0$ describes zero curvature or a flat universe and $k = -1$ denotes negative curvature (saddle-like) describing an open universe.

2.1.2 The Friedmann Equation

One of the most important results of cosmology is that of an expanding universe. In order to describe the dynamics of this expansion we must first introduce some new parameters. First the dimensionless scale factor $a(t)$ defined to have a value of 1 at the present day, and also the Hubble parameter H

$$a(t) = \frac{R(t)}{R_0} \qquad H = \frac{\dot{a}}{a} \tag{2.4}$$

The value of the Hubble parameter today H_0 is directly observed from Hubble's law relating a galaxies recession speed, v and the distance from the observer r (more on distance in Section 2.1.4)

$$H = \frac{v}{r} \tag{2.5}$$

For simplicity it is also useful to define a dimensionless Hubble parameter, h.

$$h = \frac{H_0}{100 \text{ kms}^{-1} \text{ Mpc}^{-1}} \tag{2.6}$$

Using these parameters the dynamics of the scale factor, and hence the universe, can be expressed through the Friedmann equation.

$$H^2 = \frac{8\pi G}{3}\rho - \frac{kc^2}{R^2} \tag{2.7}$$

It is clear from the equation that a flat universe, $k = 0$, occurs for a specific 'critical' density ρ_c which can be used to define a dimensionless density parameter.

$$\Omega \equiv \frac{\rho}{\rho_{\mathrm{c}}} = \frac{8\pi G\rho}{3H^2} \tag{2.8}$$

Using this parameter and $\frac{1}{R^2} = \frac{a^2}{R_0^2}$ the Friedmann equation for present day values can be expressed as:

$$\frac{kc^2}{R^2} = H_0^2 a^{-2}[\Omega_0 - 1] \tag{2.9}$$

In order to use these equations it is important to relate the parameters to present day observables. A useful approximation to facilitate this is to separate the different components of density into pressure-less matter ρ_{m}, vacuum energy ρ_{v} and radiation ρ_{r}. Now to relate these to current day values note that $\rho_{\mathrm{m}} \propto a^{-3}$ i.e. the number density of the particles is reduced due to the expansion, $\rho_{\mathrm{r}} \propto a^{-4}$ from the dilution of the number density and also the redshift of the photon energy (see Section 2.1.3) and finally $\rho_{\mathrm{v}} =$ constant, which follows directly from the cosmological constant in the field equations. By using these the density of the universe can be re-written in terms of present day density parameters.

$$\frac{8\pi G\rho}{3} = H_0^2(\Omega_{\mathrm{v}} + \Omega_{\mathrm{m}} a^{-3} + \Omega_{\mathrm{r}} a^{-4}) \tag{2.10}$$

Combining these results gives an extremely useful form of the Friedmann equation depending only on present day observables.

$$H^2(a) = H_0^2[\Omega_{\mathrm{v}} + \Omega_{\mathrm{m}} a^{-3} + \Omega_{\mathrm{r}} a^{-4} - (\Omega - 1)a^{-2}] \tag{2.11}$$

This equation is crucial in determining the relation between redshift and comoving distance.

2.1.3 Redshift

As photons travel through the universe the space they are traversing expands resulting in an increased wavelength. This is effect is known as cosmological redshift and is a key signature of an expanding universe. The redshift, z is defined by the following where ν_{emit} is the frequency of the photon when emitted and ν_{obs} is the observed frequency.

$$1 + z = \frac{\nu_{\rm emit}}{\nu_{\rm obs}} \tag{2.12}$$

Now consider the comoving distance of such a photon. Since photons travel on null geodesics $\mathrm{d}\tau^2 = 0$ it is clear that that metric gives:

$$r = \int_{t_{\rm emit}}^{t_{\rm obs}} \frac{c\,\mathrm{d}t}{R(t)} \tag{2.13}$$

Since r is a comoving co-ordinate the integral must be the same for two photons emitted at different times, i.e. photons emitted later are observed later. Keeping r constant hence requires $\frac{\mathrm{d}t_{\rm emit}}{\mathrm{d}t_{\rm obs}} = \frac{R(t_{\rm obs})}{R(t_{\rm emit})}$ which implies that distant events are time dilated. This must also apply to frequency giving:

$$\frac{\nu_{\rm emit}}{\nu_{\rm obs}} = \frac{R(t_{\rm obs})}{R(t_{\rm emit})} = (1 + z) \tag{2.14}$$

Finally lead to the important relation between scale factor and redshift.

$$a(z) = (1 + z)^{-1} \tag{2.15}$$

Photometric Determination

Redshifts of objects can be determined by spectroscopy by studying absorption or emission lines in their spectra. Although this generally produces accurate results the limitations imposed by long integration times make this impractical to employ across a large survey. However redshifts can be determined photometrically from multi-band photometry as first pioneered by Baum (1962). This is essentially a type of very low resolution spectroscopy which can distinguish only strong features in the spectral energy distribution (SED) such as the 4000Å break. Today this method is implemented in two main forms, template matching methods and empirical training sets.

Template matching involves matching template galaxy SEDs to each object based on the multi-band photometry. These templates have various spectral types and redshifts associated with them. The various templates can come from various sources including, population synthesis models (Bruzual A. & Charlot, 1993) and

spectra of real objects (Coleman et al., 1980). A χ^2 best fit can be performed to determine the most suitable template and thus the photometric redshift. Many codes have been developed in ordered to determine photometric redshifts in this way such as `BPZ` (Benítez, 2000) and `hyperz` (Bolzonella et al., 2000). These methods have several drawbacks, most notably requiring knowledge of, or assumptions about, the galaxies spectral type and this can be an ambiguous property to determine. To avoid this problem empirical training sets can be used.

Empirical training sets employ a set of galaxies with known spectroscopic redshifts and broad-band photometry. These sets can then be used to derive a relationship between photometry and redshift. Many different methods have been developed using this such as, artificial neural nets (ANNs) (Li et al., 2006 and Yèche et al., 2010), support vector machines (SVM) (Wadadekar, 2005), kernel regression (Wang et al., 2007), k-d tree nearest neighbours (Csabai et al., 2007) and random forests (Carliles et al., 2010). ANNs were conceptually modeled after the brain where many neurons perform parallel calculations to derive empirical relations such as `annz` from Li et al. (2006). While the quality of the redshifts are subject to the training set low scatters have been achieved (Li et al., 2006) with $\sigma \sim 0.03$. SVM use a similar method of machine learning to determine redshifts giving a similar scatter about spectra as shown by Wadadekar (2005). Kernel regression uses a weighted average of nearest neighbours in the training set to attain photometric redshifts with the same levels of scatter about spectra. As with kernel regression, the k-d tree approach is a nearest neighbours method where neighbours in colour space are quickly identified by structuring the training set as a k-d tree. Photometric redshift is then calculated by fitting a local hyperplane to the spectroscopic redshifts and colours of the training set neighbours. Random forests are of particular interest providing redshifts with well understood Gaussian errors for the SDSS and VLT Survey Telescope (VST) ATLAS catalogue (Shanks & Metcalfe, 2012 and Shanks et al in prep.).[1] Here the photometric properties of a training set, such as colour, are split into a binary tree structure such that the scatter in the spectroscopic redshifts in each branch is minimised. Branching occurs until a minimum number of galaxies is attained. Each branch is assigned a photometric redshift as the average of the branch-consistent subset of training galaxies. By using a random subset of the input parameters and repeating, a random forest of many independent trees can be constructed. For each tree an input galaxy is assigned a branch and redshift based on photometry and by averaging across the full forest, and owing to the central limit theorem, a

[1] see Sections 3.2.2 and 5.1.1

photometric redshift can be found subject to a Gaussian error.

2.1.4 Distance Measures

Having determined the redshifts of objects it is possible to define various distance measures based on Hogg (1999), and the framework laid out in the previous sections.

First consider the comoving distance defined by:

$$D_{\mathrm{C}} = \int_{t_{\mathrm{emit}}}^{t_0} \frac{c\,\mathrm{d}t}{a(t)} \tag{2.16}$$

Now using $\frac{\mathrm{d}z}{\mathrm{d}a} = -a(t)^{-2}$ and combining Eq. 2.11 and 2.15 this can be solved using only redshift and the density parameters.

$$\begin{aligned} D_{\mathrm{C}} &= \int_0^z \frac{c}{H(z)}\mathrm{d}z \\ &= \int_0^z \frac{c}{H_0}[\Omega_{\mathrm{v}} + \Omega_{\mathrm{m}}(1+z)^3 + \Omega_{\mathrm{r}}(1+z)^4 - (\Omega - 1)(1+z)^2]^{-1/2}\mathrm{d}z \end{aligned} \tag{2.17}$$

Although this is the fundamental measure of cosmological distance this integral cannot in general be solved analytically and is solved in practice numerically.

Another important distance is the angular diameter distance D_{A} which is defined as the ratio between an objects actual transverse size and the angle it subtends on the sky. This is particularly important in converting angular separations in a survey to actual distances. From the metric this is given by:

$$D_{\mathrm{A}} = (1+z)^{-1} R_0 S_k(r) \tag{2.18}$$

which for a flat universe has the particularly simple form

$$D_{\mathrm{A}} = (1+z)^{-1} D_{\mathrm{C}} \tag{2.19}$$

Using the observed bolometric flux, S, and luminosity, L, of an object, another

useful measure is defined, luminosity distance, D_{L}.

$$D_{\mathrm{L}} = \sqrt{\frac{L}{4\pi S}} \tag{2.20}$$

It is trivial to show that this is related to the other distance measures defined in this section through the simple relation shown below.

$$D_{\mathrm{L}} = (1+z)D_{\mathrm{C}} \tag{2.21}$$

This distance is particularly important with regards to the K+e-corrections of Section 4.1.2 and is used to define the distance modulus, $DM(z)$, of Equation 4.1.

$$DM(z) \equiv 5\log\left(\frac{D_{\mathrm{L}}}{10\mathrm{pc}}\right) \tag{2.22}$$

With the formalism laid out cosmology can now begin to model the universe as a whole and arguably the greatest achievement has been the development of the ΛCDM model. The key components of this model attempts to explain the most puzzling and fundamental observations in the universe and are discussed in the upcoming sections.

2.1.5 The Big-bang and Inflation

Around 1920, using observations of galaxies, Hubble discovered that the recession velocities of these objects are directly proportional to their distance, a relation known as the Hubble law. This has remarkable consequences as this implies the universe is expanding. Combined with the discovery of the cosmic microwave background (CMB) this lead to the theory of the big bang. This suggests that at some finite time in the past the universe was extremely hot and dense which then expanded (and continues to do so) to give the conditions we observe today.

The CMB is an almost uniform microwave signal covering the whole sky and is a relic of the hot dense conditions of the early universe and is explained as follows. During this phase a plasma of particles and radiation filled the space with such a density that the universe was essentially opaque. As the universe

cooled and expanded a phase change occurred as neutral atoms formed from the plasma an era known as recombination. At this stage photons began to permeate the universe, as neutral atoms are less efficient at scattering radiation. These photons have undergone extreme redshift and are observed today as the CBM with a peak blackbody temperature around 2.73 K.

Examining the CMB in more detail shows that it is extremely uniform down to 1 part in 10^5. Combining this with the cosmological principle, that the universe is isotropic and homogeneous on large scales, leads to the horizon problem. While this suggests that the whole CMB was in causal contact to reach equilibrium, constraints by relativity prevent this, where causal patches are of the order $\sim 2^o$. An inflationary period of exponential expansion was introduced to explain the anomaly. Since this inflation is superluminal it suggests the whole universe existed in causal contact in the past allowing the equilibrium and observed uniformity of the CMB.

2.1.6 Dark Energy

With expansion of the universe already established questions arise about the future of this growth. With the birth of General Relativity and the apparent dominance of matter the fate of the expansion appeared to lie in the hands of gravity ultimately leading the universe to collapse. Until recently this was considered a reasonable consequence of gravity until observations of type Ia supernovae by Riess et al. (1998) contradicted this conclusion. Type Ia supernovae are well understood to have a universal luminosity and hence can be used as standard candles to probe distance. Riess et al. (1998) found several supernovae which were redshifted more for their luminosity distance than could be explained using a slowing expansion. The only explanation for the higher redshift (and hence faster recession) is an accelerating expansion.

Now a simple question arises, what kind of energy is driving this acceleration? Currently the exact form of this eludes observation hence the token name, dark energy. Leading theories suggest that this could be the result of zero-point or vacuum energy, the lowest energy state of the universe. This can be described using Einstein's famous cosmological constant Λ which from the field equations can be considered as a source of negative pressure to drive the expansion. Many more recent observations support these conclusions, e.g. from CMB, (Komatsu et al., 2011), (More on this in Section 2.1.8) and hence Λ's incorporation into the

model.

2.1.7 Dark Matter

Another perplexing observation was shown in Zwicky (1933) whilst studying the Coma galaxy cluster. Using the virial theorem[2] it was found that visible mass was not sufficient to bind the cluster given the velocities of the galaxies. The conclusion was that the cluster must be dominated by undetectable mass hence the name dark matter. This was not widely accepted until a similar effect was observed in the motion of stars around spiral galaxies. In this case the galaxies had insufficient mass to bind the outer stars and given their velocities they should have all been ejected.

Other evidence comes from a direct consequence of General Relativity, that matter curves space and can deflect light. Hence mass can act as a lens deflecting the images of background sources. In weak cases the lensing signal can be detected by a correlation on the alignment of objects in an image. The strength of the lensing signal is directly proportional to mass and independent of its form. Using this analysis on observations of clusters show that the visible matter is insufficient to explain the lensing signal, again pointing to dark matter.

Since dark matter has still not been detected directly this is a very active area of research. Various forms have been suggested such as cold dark matter (CDM) - slow moving particles unaffected by the electromagnetic force - and hot dark matter (HDM) - a similar concept with faster moving particles. The particular form has grand implications for structure formation in the universe. With a CDM model structure forms hierarchically where smaller particles collapses and merge together continuously forming more massive structures. Conversely HDM implies fragmentation where the largest structures form first with smaller components eventually breaking away. The favourite amongst cosmologists is a CDM explanation which is supported by current observations and hence is adopted by the model (see Section 2.1.8).

[2]The virial theorem equates a relaxed system's potential energy to twice the kinetic energy i.e. $2E_k + E_p = 0$

2.1.8 Constraining the Model

Describing the exact nature of the universe with ΛCDM is done using a variety of parameters. These include the density parameters for baryons, $\Omega_{\rm b}$, dark mater, $\Omega_{\rm c}$), vacuum energy, $\Omega_{\rm v}$, and also the Hubble parameter, H_0. They have an integral role in defining the formalism of cosmology and their values have great consequences for the universe. For example with sufficiently large vacuum energy the universe would expand indefinitely. As shown previously these parameters also impact the geometry of the universe dictating curvature. Hence constraining these parameters is vital in improving our understanding of the universe.

Using single observations often gives rise to degenerate constraints on these parameters as noted by Eisenstein et al. (1998) and Susperregi (2001). Hence in practice, combining observations from many sources such as the CMB and supernovae yields more fruitful constraints by breaking the degeneracy. For example, Komatsu et al. (2011) uses measurements of the CMB and the Baryon Acoustic Oscillations in the distribution of galaxies to constrain the simplest 6-parameter ΛCDM model.

Another important parameter is the amplitude of mass fluctuations on the $8h^{-1}$ Mpc scale, σ_8 which describes the structure and clustering in the universe. Accurately determining this parameter provides vital understanding of the structure in the universe. The growth of structure in the universe is exponentially influenced by σ_8^2 hence small variation have grand implications for the evolution of matter in the universe. This also affects how matter traces light which is important in understanding observations (see Bahcall et al., 2003).

By using the mass function of galaxy clusters many authors have investigated and constrained σ_8^2 and Ω_m, (Bahcall et al., 2003, Wen et al., 2010, White et al., 1993 and Rozo et al., 2010 to name a few.) The recent work by Rozo et al. (2010) uses the maxBCG cluster catalogue detailed by Koester et al. (2007a) derived using data from the Sloan Digital Sky Survey (SDSS) which is drawn from a 7398deg^2 patch of the sky covering the redshift range $0.1 < z < 0.3$.

2.2 The Properties of Galaxy Clusters

Galaxy clusters are among the largest directly observable structures in the universe which comprise a dark matter halo, intracluster medium (ICM) of hot gas and member galaxies. While direct observation of the dark matter halo is only possible with gravitational lensing, the ICM and galaxies provide several observational signatures which are used to detect and characterise clusters.

2.2.1 The Intracluster Medium

With the significant gravitational potential and release of energy in the formation of the galaxy cluster, the ICM is heated to extremely high temperatures ($\sim 10^7$ K) which results in distinct observational features, most notably the direct emission of X-rays and the interaction of the hot gas with the CMB resulting in the Sunyaev-Zel'dovich (SZ) Effect.

X-ray Emission

With the extremely high temperatures, the gas comprising the ICM becomes completely ionized resulting in X-ray emission through Bremsstrahlung radiation. Studies of the Abell clusters (Abell, 1958) by Kellogg et al. (1973) indeed confirmed extended X-ray emissions associated with the ICM. Using extended X-ray emission as a signature of the ICM (and hence galaxy clusters themselves) many surveys have been employed to detect clusters such as the Northern ROSAT All-Sky Galaxy Cluster Survey (NORAS) (Böhringer et al., 2000), ROSAT-ESO Flux Limited X-ray Galaxy Cluster Survey (REFLEX) (Böhringer et al., 2004), the XMM Large Scale Structure (XMM-LSS) Survey (Pierre et al., 2007) and the XMM Cluster Survey (XCS) (Romer et al., 2001 and Lloyd-Davies et al., 2011). These detections are particularly valuable as they X-ray emission is strongly correlated with the gravitational potential hence projection effects, common with optical detection[3], are negligible.

In addition to detection, X-ray observations, such as temperature and luminosity, offer the advantage of providing well understood tightly correlated mass proxies as shown by Zhang et al. (2011), Zhang et al. (2008) and Ettori (2013) etc.

[3] see Section 2.3

The Sunyaev-Zel'dovich Effect

In addition to direct observation, the ICM (and hence the cluster) can also be detected by the Sunyaev-Zel'dovich effect (SZ effect), introduced by Sunyaev & Zeldovich (1970). The SZ effect is the result of inverse Compton scattering of high energy electrons and CMB photons, in which some energy of the electrons is passed to the low energy CMB photons. This effect will shift the spectra of the CMB photons to higher frequencies, enhancing lower wavelengths and leaving a reduced intensity at the expected waveband. This can be detected in the CMB as temperature fluctuations, which can be calculated by considering the line integral of electron number density through the universe. It therefore can be seen that the most prominent SZ effect occurs in hot dense regions such as ICMs.

$$\frac{\Delta T_{SZ}}{T_{CMB}} = 4 \int \frac{kT}{m_e c^2} n_e \sigma_T \mathrm{d}l \tag{2.23}$$

where n_e is the electron number density, σ_T is the Thomson cross section and T is the temperature of the electron gas causing inverse Compton scattering.

The SZ effect is redshift independent since the signals are redshifted with the CMB, thus only depends on electron number density and temperature of the gas. Hence the SZ effect is an excellent technique for detecting clusters over a wide range of redshifts. Also the SZ observable the integrated Compton y-parameter, Y, scales with cluster mass as shown by comparing the cluster mass derived by gravitational lensing (Marrone et al., 2009 and Motl et al., 2005) and is thus an extremely useful technique to detect clusters.

Many surveys have taken advantage of this in order to detect clusters, such as those presented in Staniszewski et al. (2009) and Vanderlinde et al. (2010), however the most notable are those recently discovered by the Planck mission (Planck Collaboration et al., 2013), which comprise 861 clusters detected using the SZ effect across the whole CMB.

2.2.2 The Red Sequence

Observations of galaxy clusters, particularly noting those of the Coma and Virgo clusters from Bower et al. (1992a), have shown the members to be dominated by early-type galaxies with a low scatter colour magnitude relation (CMR). As

predominantly red galaxies, these members are known as the 'red sequence' and are characterised by the low scatter sloped CMR, with an example from cluster GMBCG J197.87292-01.34109 (GMBCG-1) shown in Figure 2.1. The slope of the CMR is the result of the mass metallicity relation, where more massive, brighter galaxies are able to more readily retain metal-rich material, either from supernovae ejection or mergers, resulting in redder colours. By studying these slopes, Gladders et al. (1998) found that metal-rich galaxies become redder faster with increasing age suggesting an evolution of the CMR slope. In addition, the similar colours (and hence metallicities), low scatter and CMR slopes suggested that the red sequence formed with a single starburst at high redshift, $z \sim 3$, are coeval and are passively evolving (Baum, 1959, Bower et al., 1992a, Gladders & Yee, 2000 and Eisenstein et al., 2001).

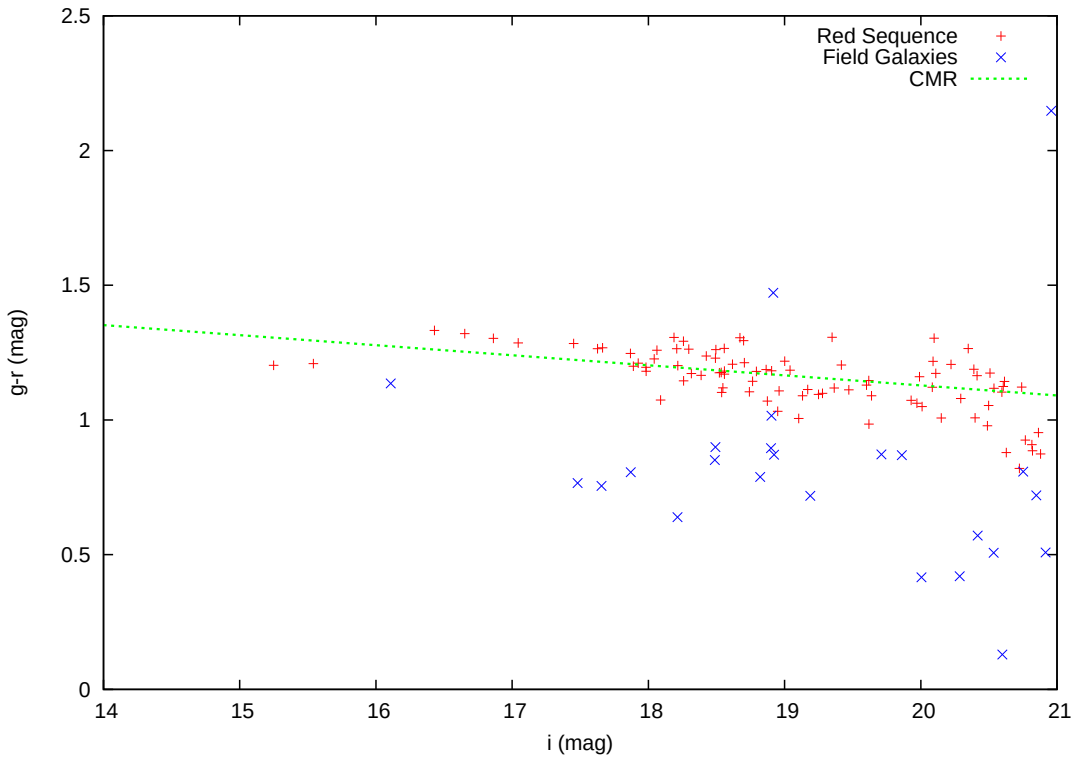

Figure 2.1 *The red sequence of GMBCG-1 showing the low scatter, sloped CMR.*

In addition to an enhanced surface density, the low scatter CMR and similar metallicities implies that galaxy clusters are also highly clustered in colour space. Many methods, such as, GMBCG (Hao et al., 2010), maxBCG (Koester et al., 2007b), ORCA (Murphy et al., 2012) and C4 (Miller et al., 2005), have been developed to exploit this in order to detect galaxy clusters by searching for spatial[4] and colour overdensities.

[4]particularly of the form of an NFW profile from Section2.2.3

2.2.3 Radial Profile

Direct measurement of the mass overdensity of clusters using gravitational lensing (Johnston et al., 2007) has shown that out to a few Mpc the density profiles are dominated by the dark matter halos. High resolution N-body simulations have shown that the equilibrium density profiles of dark matter halos follow NFW profiles (Navarro et al., 1997).

$$\frac{\rho(r)}{\rho_{crit}} = \frac{\delta_c}{(r/r_s)(1+r/r_s)^2} \tag{2.24}$$

where r_s is a scale radius, δ_c is a characteristic dimensionless density and $\rho_{\rm crit}$ is the critical density. It has been shown by Bartelmann (1996) that this can be rewritten in the form of a surface density shown below.

$$\Sigma(x) = \frac{2\rho_s r_s}{x^2-1} f(x) \tag{2.25}$$

where $x = r/r_s$ and defined as

$$f(x) = \begin{cases} 1 - \frac{2}{\sqrt{x^2-1}} \tan^{-1}\sqrt{\frac{x-1}{x+1}} & 1 < x \leq 20 \\ 1 - \frac{2}{\sqrt{1-x^2}} \tanh^{-1}\sqrt{\frac{1-x}{x+1}} & x < 1 \\ 0 & x = 1 \\ 0 & x > 20 \end{cases} \tag{2.26}$$

This is particularly important for optical cluster finders, such as maxBCG and GMBCG, as these often use galaxy overdensities in the form of an NFW surface profile to indicate the presence of a cluster.

2.2.4 Luminosity Function

Galaxy clusters have luminosity functions (LFs) well described by Schechter functions (Schechter, 1976 and Hansen et al., 2005) giving the number of galaxies with luminosity between L and $L + \mathrm{d}L$ as shown below:

$$\phi(L)\mathrm{d}L = \phi_*(\frac{L}{L_*})^\alpha e^{-\frac{L}{L_*}}\mathrm{d}L \tag{2.27}$$

where ϕ_* is a normalization point, α describes the faint end slope and L_* is a characteristic luminosity. The three parameters ϕ_*, L_* and α are used to fit this profile to the galaxy cluster. Using the following relationship the Schechter function can be rewritten in terms of magnitudes m with an example for GMBCG-1 shown in figure 2.2. The Schechter function with values, $\phi_* = 0.58$ galaxies/arcmin^2, $m_* = 17.7$ and $\alpha = -1$, is shown to be a good description of the cluster luminosity function.

$$\frac{L}{L_*} = 10^{-0.4(m-m_*)} \tag{2.28}$$

$$\begin{aligned} \phi(m)\mathrm{d}m = 0.4(\ln(10))\phi_* 10^{-0.4(m-m_*)(\alpha+1)} \\ \times \exp[-10^{-0.4(m-m_*)}]\mathrm{d}m \end{aligned} \tag{2.29}$$

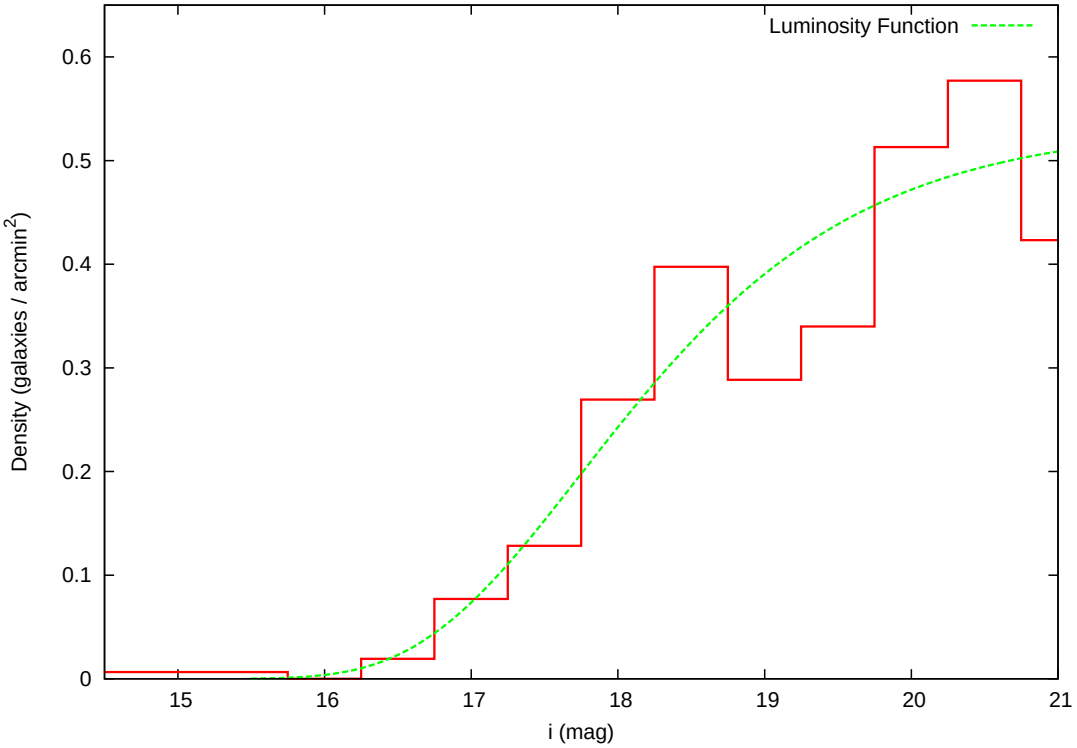

Figure 2.2 *The Schechter function with values, $\phi_* = 0.58$ galaxies/arcmin^2, $m_* = 17.7$ and $\alpha = -1$, is shown to be a good description of the luminosity function of GMBCG-1.*

2.2.5 Characterisations

There are a variety of different ways to characterise a galaxy cluster e.g. size, mass. One particular model predicts that clusters are virialised within regions where the average density is greater than the critical density by a factor of 200 (Peacock, 1999). The radius at which this is reached can be used to define a characteristic radius for a cluster r_{200}. Similarly a characteristic mass m_{200} can be defined as the mass contained within this radius. With dark matter as the dominant component of galaxy clusters, direct measurements of these are difficult and only available with gravitational lensing. Hence it is useful to define an easy to obtain, optical characterisation, to give a measure of the size of the cluster and ultimately serve as a mass proxy. Richness, a measure of the number of galaxies on the red sequence, is one such characterisation which has deep roots in the literature (Abell, 1958) and has been the focus of more recent research (Hao et al., 2010, Sheldon et al., 2009b, Hansen et al., 2009 and Rykoff et al., 2012).

Typically richness is a measure of the number of cluster members with colours consistent with the red sequence. While there are several ways to measure this consistently, a 2σ approach is common, where galaxies are considered if their colours are within 2σ, defined below:

$$\sigma^2 = (\sigma_{\rm col})^2 + (\sigma_{\rm cmr})^2 \tag{2.30}$$

of the expected red sequence colour as used by Koester et al. (2007b), Hao et al. (2010), High et al. (2010) and Mehrtens et al. (2012) to name a few. Here $\sigma_{\rm col}$ is the photometric colour error and $\sigma_{\rm cmr}$ is the intrinsic scatter of the red sequence brought about by the slight age variations of the galaxies. To maintain consistency across a range of redshifts additional cuts are placed on the brightness of the red sequence galaxies, where only those fainter than the BCG and brighter than a faint end cut off are considered. The faint end cut off is typically taken as $0.4L_*$ or equivalently $m_* + 1$ and in the cases of Koester et al. (2007b), Hao et al. (2010) and Rykoff et al. (2013), is derived from Blanton et al. (2003) using the luminosity function of field galaxies.

2.3 Existing Characterisation Methods

Many cluster detection/classification algorithms have been developed in recent years, maxBCG (Koester et al., 2007b), GMBCG (Hao et al., 2010) and C4 (Miller et al., 2005) to name a few, many of which take advantage of the red sequence, the dominant cluster members. It has been observed that across a wide range of redshifts, $z < 1$, clusters are dominated by early type elliptical galaxies. These galaxies are formed together with similar metallicities, with the majority of star formation occurring at high redshift $z > 2$ which then passively evolve. As a result these galaxies show as a low scatter colour-magnitude relation (CMR) known as the red sequence (see Section 2.2.2).

Many of the algorithms have been developed from or designed as optical cluster finders, which are not only tasked with classifying clusters but must also find them from large optical surveys. Without prior knowledge of the red sequence this is a difficult task essentially searching for surface overdensities which is highly susceptible to projection effects. Adding in extra information that clusters are dominated by the low scatter CMR helps to address this issue. By also searching for overdensities in colour space this drastically reduces the probability of contamination by field galaxies. Searching for clusters as spatial and colour overdensities is the basis of many of the algorithms discussed in this section. There are two main aspects of these classification algorithms, detection of the red sequence with cluster redshift and determination of richness.

2.3.1 C4

C4, detailed in Miller et al. (2005), is an optical cluster finder aimed at the spectroscopic release of SDSS DR2 Abazajian et al. (2004) which makes no such assumption about the form of the red sequence. C4 searches for overdensities in $7 - d$, position, redshift and colour space (not necessarily from a red sequence) outlined in the following steps.

1. Each galaxy is assigned a spatial aperture with a projected radius of $1h^{-1}$Mpc and a redshift aperture corresponding to a fixed comoving box $\pm 50h^{-1}$ in size. In this aperture the probability that each galaxy has the same colour as the target is computed and summed, assuming Gaussian errors and an intrinsic colour width.

2. Step 1 is repeated for 100 random galaxies using the target aperture. The median number count gives an estimate of the expected field contribution.

3. The probability that the target is a field galaxy is found using this median with a Gaussian approximation

4. Clusters are isolated as regions of low probability.

From here cluster redshifts simply come from the spectroscopic redshifts of cluster members. By only assuming clustering spatially and in colour galaxy clusters can be found and characterised without prior knowledge of the form of the red sequence. The C4 algorithm was designed to find clusters with the spectroscopic sample of SDSS DR2 which although giving very accurate redshifts is very limited is scope. In general an algorithm using galaxy redshifts need not be limited in this way as cheap photometric redshifts, although more inaccurate, are available across a far greater region. If the photometric redshifts are unbiased then they could be used in such an algorithm.

2.3.2 maxBCG

maxBCG, detailed in Koester et al. (2007b) is a matched filter optical finder, targeted at the larger SDSS DR5. Each galaxy in the target survey is assigned a likelihood that it is in fact a brightest cluster galaxy (BCG) lying at the centre of a cluster. This is done by considering not only spatial and colour clustering but also how well the galaxy conforms to the expected properties of a BCG. First considering the colour clustering, the red sequence is assumed to have a Gaussian intrinsic width about a redshift dependent expectation value. The probability that a galaxy with $g-r$ colour c_{g-r}, lies on the $g-r$ red sequence at redshift z given by:

$$P_{g-r}(z, c_{g-r}) = \frac{1}{\sqrt{s\pi}\sigma} \exp \frac{[c_{g-r} - \hat{c}(z)]^2}{2\sigma^2} \tag{2.31}$$

where σ is a combination of the galaxy colour errors σ_{g-r} and the intrinsic width of the red sequence σ^{RS}_{g-r}.

$$\sigma = \sqrt{\sigma^2_{g-r} + (\sigma^{RS}_{g-r})^2} \tag{2.32}$$

Observations of luminous red galaxies (LRGs) from Eisenstein et al. (2001) provides the basis of the colour-redshift model for red sequence galaxies. BCGs however are treated separately as these often have different optical properties than standard ellipticals. For BCGs the colour-redshift model is driven by observations of the brightest LRGs with $M_r < -21$. Although reducing the reliance on models this 'flat' form of the red sequence is not magnitude-dependent and hence does not fully describe the expected mass-metallicity relation encoded in a sloped CMR (see section 2.2.2 for more details).

The spatial clustering is described by an NFW profile, however it is noted as with Postman et al. (1996), maxBCG is insensitive to the parameters of the profile.

The redshift dependent likelihood can now be constructed as the product of the probability the galaxy is a BCG and the probability that the neighbouring galaxies are spatial distributed as an NFW and colour clustered as a red sequence. The likelihood a galaxy is a BCG is based on the galaxy colour and brightness given by:

$$\mathscr{L}_{BCG} \sim P_{g-r}^{BCG}(z) P_{r-i}^{BCG}(z) \exp -[(m_i - m)/\sigma_c]^2 \tag{2.33}$$

The extra exponential ensures a smooth cut off to ensure galaxies are bright enough to be considered BCGs. The width, σ_c, is taken as 0.3 magnitudes and cut off, m, is taken from magnitude-redshift relation derived from BCG observations.

After applying spatial and colour cuts around the target galaxy, the probability that an NFW red sequence exists centred on the galaxy is found by summing the probability of all the N_g neighbours.

$$\mathscr{L}_{RS} \sim \sum_{k=1}^{N_g} \Sigma(r_k) P_{g-r}(z, c_k) P_{r-i}(z, c_k) \tag{2.34}$$

combining these gives the total likelihood.

$$\mathscr{L} \sim \mathscr{L}_{BCG} \mathscr{L}_{RS} \tag{2.35}$$

The potential cluster redshift and final likelihood is found by maximising this function.

2.3.3 South Pole Telescope Cluster Analysis

The analysis of the South Pole Telescope (SPT) SZ clusters, presented in High et al. (2010), uses a background-subtracted red sequence to characterise the cluster. First a model red sequence is constructed which gives the expected colour of a galaxy with a given redshift and i-band magnitude. These are based on the stellar population models of Bruzual & Charlot (2003a) using passively evolving galaxies with a single starburst at $z \sim 3$. Using random metallicity-luminosity relations at various redshifts and fitting cubic splines, a full redshift dependent CMR is determined for the red sequence. While this considers a more complete treatment of the mass-metallicity relation in the CMR, these red sequences are still based on models adding extra dependence on further analysis.

Cluster redshift is found by considering an inner $2'$ cone used to sample the inner cluster, dominated by the red sequence. At various redshift slices the red sequence of this cone is isolated, based on the 2σ method of Section 2.2.2 using redshift appropriate colour based on the model. The density of the red sequence is calculated and background subtracted. The slice with the highest overdensity is assigned as the cluster redshift. This method is indeed able to recover reasonable cluster redshifts as demonstrated in Figure 2.3 where the previously considered cluster, GMBCG J197.87292-01.34109 (GMBCG-1), can clearly be seen as the peak at $z \sim 0.18$ which is in good agreement with the literature value of $z = 0.179$. Unfortunately however, this method breaks down in the case of a multi-modal distribution. Using the cluster GMBCG J239.47725+21.55627 (GMBCG-2) as an example, Figure 2.4 shows multiple redshift peaks where it is unclear which represents the cluster. In this case both peaks represent clusters which overlap on the 2-d sky surface. While this may seem like a rare event, consideration of the GMBCG catalogue in Section 2.3.4 shows this may be a common problem. Hence any new characterisation method will need to be designed to deal with these situations properly.

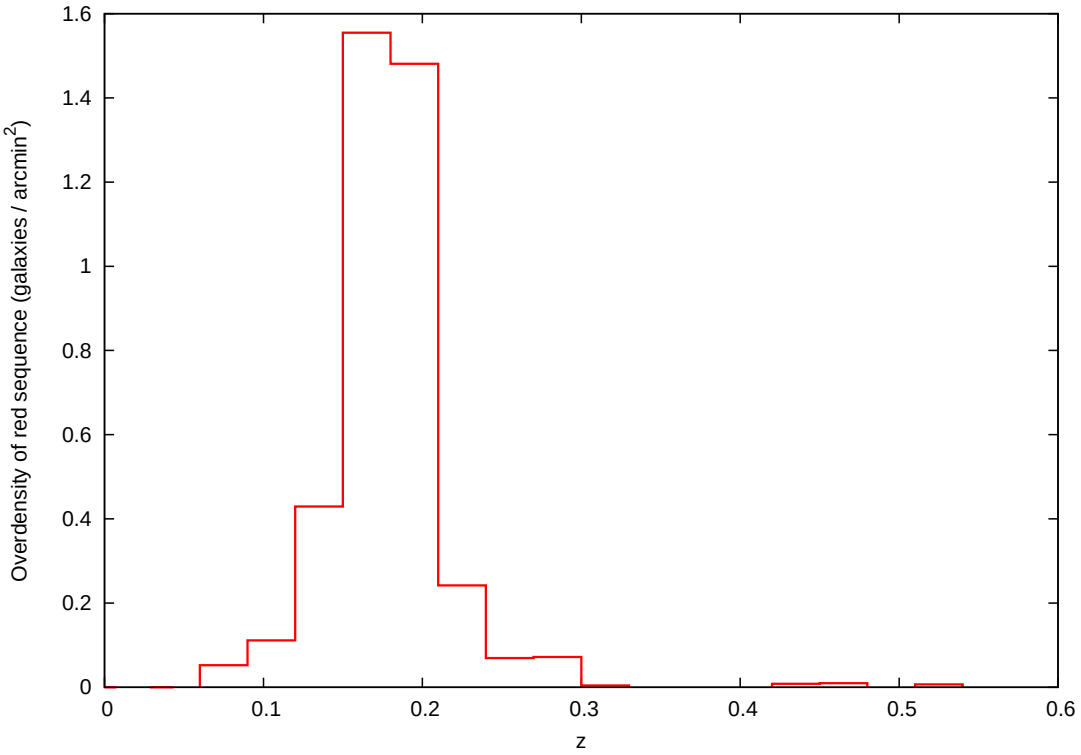

Figure 2.3 *A histogram of the red sequence overdensity as a function of redshift showing a clear peak around $z \sim 0.18$ representing the cluster GMBCG-1. In each bin the density of the red sequence is calculated and background subtracted using the 2σ method of Section 2.2.2 with a model of the expected colour for the given redshift.*

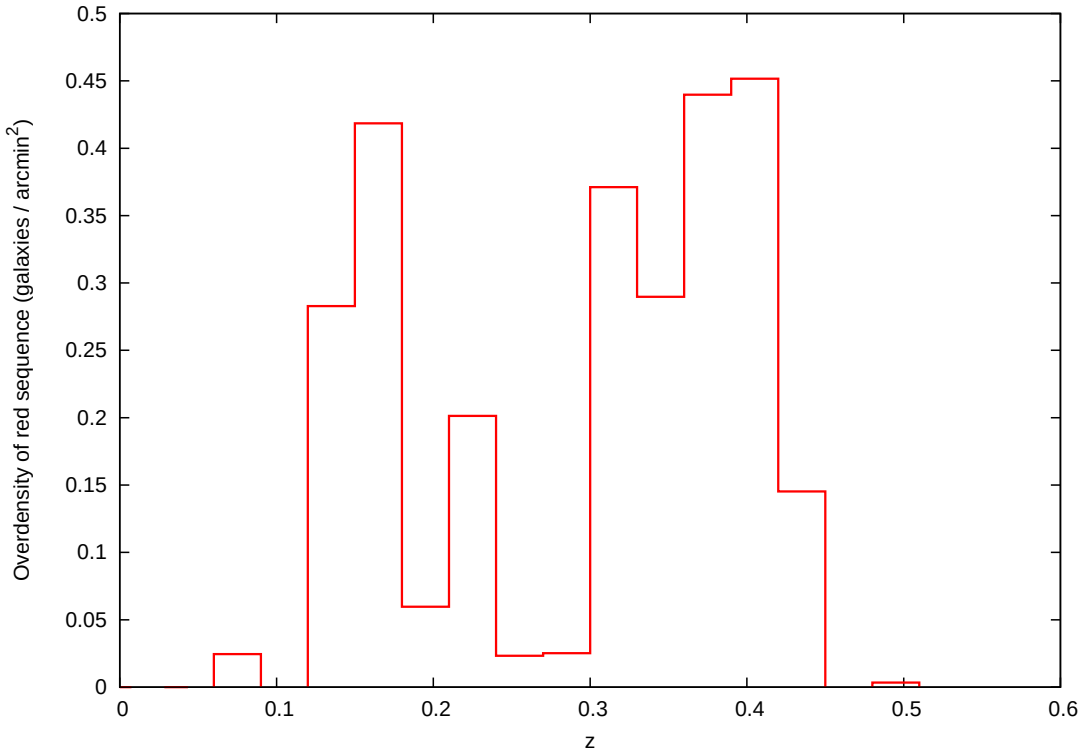

Figure 2.4 *A histogram of the red sequence overdensity as a function of redshift showing a multi-modal distribution. In each bin the density of the red sequence is calculated and background subtracted using the 2σ method of Section 2.2.2 with a model of the expected colour for the given redshift. The multiple peaks correspond to spatially overlapping clusters at different redshifts and without any additional information it is difficult to determine which represents the target cluster.*

2.3.4 GMBCG

The Gaussian Mixture Brightest Cluster Galaxy (GMBCG) algorithm from Hao et al. (2010) is an optical red sequence detector aimed the SDSS DR7. As a cluster finder this employs a similar percolation method as maxBCG, describing clusters as a BCG centroid with a surrounding red sequence. Each galaxy in the input is considered a potential BCG and the centre of a cluster. The surface and colour density of the surrounding red sequence are modelled and used to assigned a clustering strength as a measure of the probability that the candidate is a BCG in a cluster. Galaxies are removed from consideration if a more suitable BCG candidate is nearby belonging to the same red sequence. This repeats until the final BCG and red sequence list remains.

The cluster redshift is simply given as the photometric redshift of the BCG available from the SDSS DR7. In general these galaxies are bright, well understood galaxies and often have spectra and hence offer good estimates of the cluster redshift. From the characterisation stand point using the BCG only requires significant confidence in the ability to choose the correct galaxy, where an interloper would result in a catastrophic failure. Also any further characterisation is based on the existing knowledge of the cluster redshift from the finder part of the algorithm and hence is not suitable for stand-alone characterisations.

With regards to the red sequence, modelling proceeds using an error-corrected expectation maximisation technique to fit a Gaussian Mixture to the colours (see Section 3.1.1 for details on the fitting procedure). The Gaussian mixture allows the modelling of various structures in the colour distribution. Figure 2.5 shows an example Gaussian Mixture fit to the cluster GMBCG-1 where two colour components are clearly seen. This method simultaneously models the background and the red sequence as separate components. With the low scatter CMR and similar colours of the red sequence, the narrowest component is chosen to represent the cluster. In the case of GMBCG-1 the red sequence is given by the peak around $g - r \sim 1.2$. This again uses a single colour to describe the red sequence with the 2σ filtering of Section 2.2.2 which fails to consider the full CMR brought about by the mass-metallicity relation.

Considering the multi-modal GMBCG-2 shown in Figure 2.6, without the prior knowledge that both peaks represent clusters (as is provided by the finder part of the algorithm) it is again ambiguous which represents the cluster. In addition

considering the nearest neighbours on the 2-d sky surface of the whole GMBCG catalogue as shown in Figure 2.7, it is clear a significant fraction have another cluster with $5'$ showing that this may be a common occurrence. Again it is clear any new characterisation method will need to be designed to deal with multi-modal distributions properly.

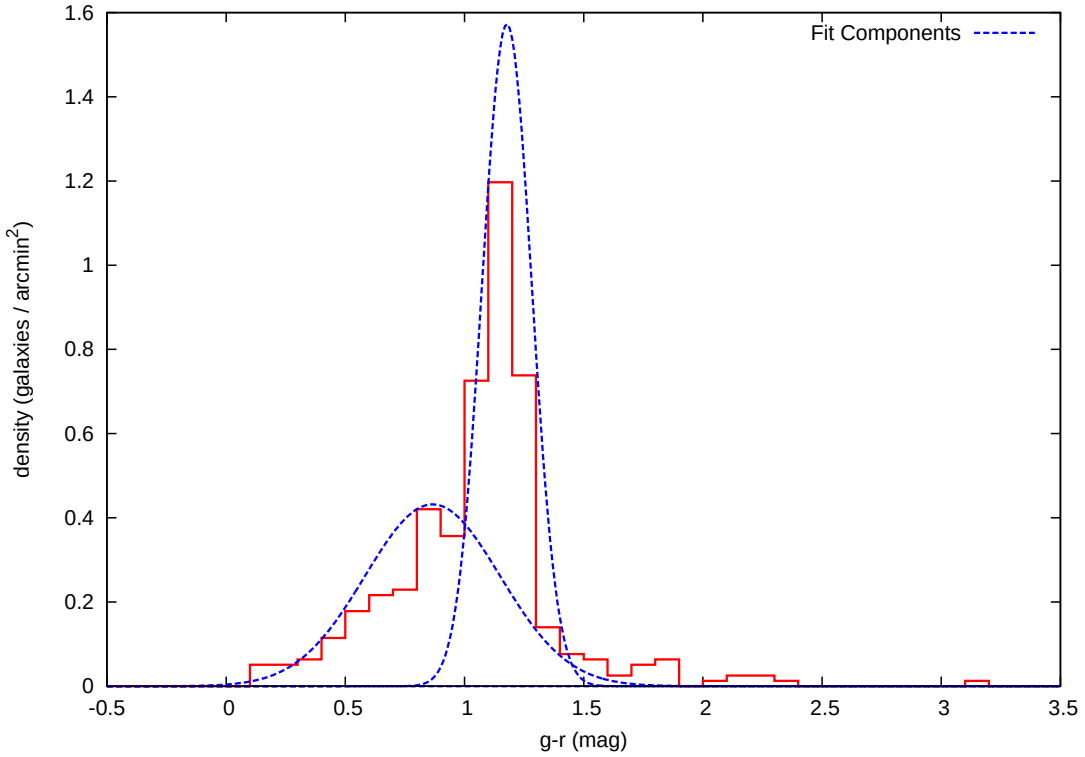

Figure 2.5 *A histogram of the $g-r$ colour density showing the components of the best fit Gaussian mixture for the cluster GMBCG-1. As the largest and narrowest component, it is clear the red sequence is modelled by the component peaked around $g-r \sim 1.2$.*

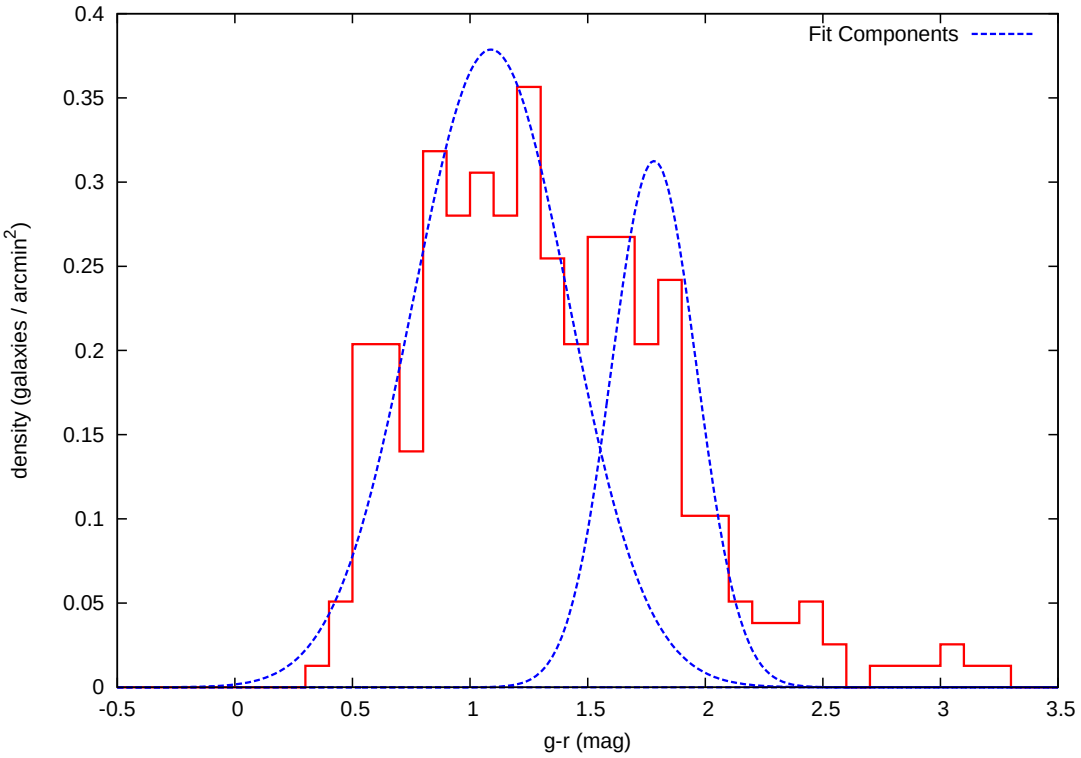

Figure 2.6 *A histogram of the $g-r$ colour density showing the components of the best fit Gaussian mixture for the cluster GMBCG-2. Again, as the result of spatially overlapping clusters, since both components are similar in width and amplitude it is difficult to determine which represents the target cluster red sequence.*

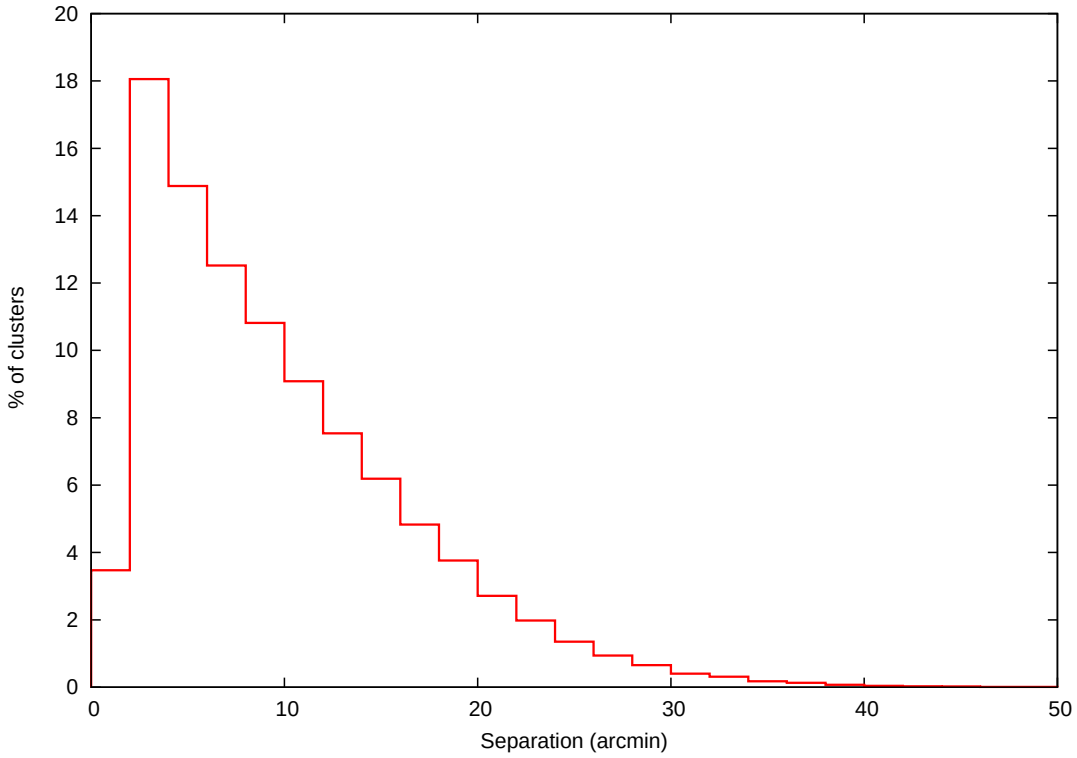

Figure 2.7 *A histogram of the angular separation between clusters in GMBCG and their nearest neighbour. Around* 20% *have an additional cluster within* 5 *arcmin which may produce ambiguities when characterising the target. With the frequency of these overlaps and potential background fluctuations it is clear that multi-modal distributions are an issue which must be addressed.*

2.4 Summary

Galaxy clusters are widely regarded as excellent probes of cosmology. As the largest observable objects these are great indicators of the large scale structure and evolution of mass distribution in the universe. As this is highly sensitive to the form of the expansion of the universe, their study gives valuable constraints on cosmological models (see Peebles, 1980, Sheth et al., 2001, Jenkins et al., 2001, Rozo et al., 2010 and Tinker et al., 2012 etc.). In addition clusters provide an excellent opportunity for studying galaxies themselves particularly formation, evolution and the impact of the environment (see Gladders et al., 1998 and Voit, 2005 etc.). Whether used to study galaxy evolution, large scale structure or constraining cosmological models, galaxy clusters have proven to be a fruitful and active area of research.

In order to proceed with such cosmological analysis it is often necessary to detect and determine the properties of the clusters, which, particularly for mass and redshift, can be difficult and expensive. Without resorting to spectroscopy or weak lensing, which can be time consuming, expensive and cover only limited areas of the sky, optical characterisation methods have been developed to determine these properties from cheap photometry alone.

Many characterisation methods exist such as maxBCG (Koester et al., 2007b), GMBCG (Hao et al., 2010) and the South Pole Telescope (SPT) cluster analysis (High et al., 2010) which rely on the detection of the red sequence to infer the bulk properties of the cluster. There are several drawbacks to these methods, particularly with regards to maxBCG and the SPT cluster analysis, which assume a redshift-colour model to infer redshift from the red sequence colour. This adds further model dependence to the analysis of such clusters. In addition many of these methods describe the red sequence as a simple colour neglecting the sloped CMR brought about by the mass-metallicity relation in clusters.

Further issues are encountered with multi-modal cluster distributions, where multiple peaks in the colour or redshift distributions lead to ambiguous characterisations and potential catastrophic failures. Particularly noting the large fraction of the GMBCG catalogue with clusters within $3'$ of another, multi-modal distributions can be common.

Any new characterisation method would ideally address these issues and include

features such as treatment of multi-modal distributions, model independence and full modelling of the red sequence CMR.

Chapter 3

GMPhoRCC: A New Characterisation Pipeline

Galaxy clusters are widely recognised as excellent probes of cosmology, whose properties, such as abundance and mass to light ratios, provide many constraints on cosmological models. In order to be used for such analyses, it is necessary to determine many cluster properties such as redshift and mass which unfortunately can be difficult to ascertain. The total cluster mass is particularly challenging to determine as clusters are dominated by dark matter where direct observation is only achievable through gravitational lensing. Presented in this chapter is GMPhoRCC, a new characterisation pipeline which aims to provide a modular, model-independent procedure to determine the optical properties of galaxy clusters using cheap photometric data alone. Specifically GMPhoRCC will estimate a red sequence colour magnitude relation (CMR), photometric redshift and richness, a measure of the number of cluster members which can be used a cheap optical mass proxy.

This chapter is structured as follows. Section 3.1 details the procedures and motivations behind the GMPhoRCC characterisation method. Section 3.2 explores the various calibrations and uses with the Sloan Digital Sky Survey DR9. To conclude Section 3.4 shows comparisons with existing cluster catalogues.

3.1 Development of GMPhoRCC

Presented in this section is the **G**aussian **M**ixture full **Pho**tometric **R**ed sequence **C**luster **C**haracteriser (GMPhoRCC) which is intended to provide model-independent, optical characterisation of potential clusters previously detected by other observations such as X-ray emission. The following lists several initial features drawn from several of the existing algorithms explored in Section 2.3 which have driven the development of GMPhoRCC.

1. Red sequence detection: GMPhoRCC will isolate the red sequence and use these galaxies to infer the optical properties of the cluster.
2. Photometric redshifts: In order to maintain model independence no colour-redshift relation can be assumed to find cluster redshift, instead it will be necessary to use empirical photometric redshifts of the red sequence.
3. Full red sequence CMR: Rather than using a single colour, the red sequence will be described by a full CMR determined by the GMPhoRCC.
4. Multiple red sequence bands: To maximise the efficiency of the GMPhoRCC and to cover a large range of cluster redshifts, multiple redshift dependent colour bands will be necessary as demonstrated in Hao et al. (2010).
5. Multi-modal distributions: Without resorting to a full finder approach where overlapping clusters can be separately identified and analysed, GMPhoRCC must deal with multi-modal distributions as several potential clusters.
6. Quality Control: Extending beyond simple error analysis it is necessary to assess the probability of catastrophic failure. By introducing quality control, several subsets can be produced where problem clusters and possible outliers can be identified and removed from the cleanest sample.

The main feature of GMPhoRCC is to identify the red sequence and use the properties of these galaxies to analyse the cluster. A basic outline of the procedure used to isolate the red sequence and ultimately determine redshift and richness is shown in Figure 3.1. While each of these steps are explored in detail in subsequent sections it is first noted that many of these require the modelling of cluster distributions such as colour and photometric redshifts which, as shown by GMBCG in Hao et al. (2010), can be approximated by a Gaussian mixture.

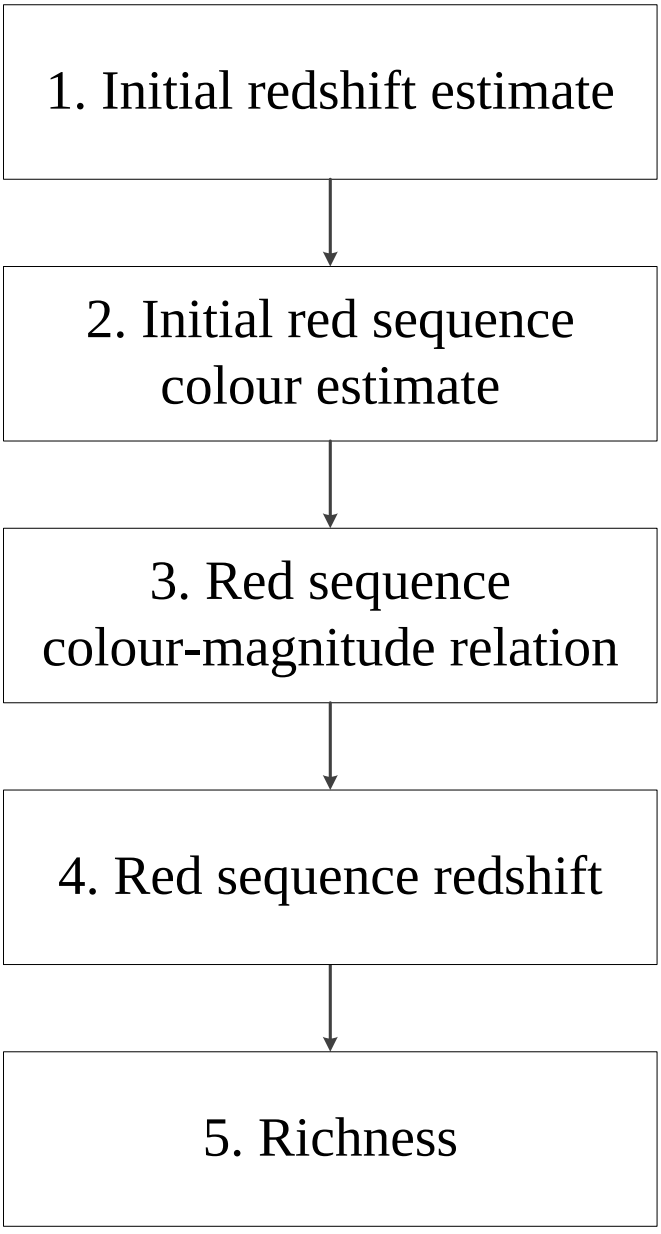

Figure 3.1 *A flowchart summarising the basic steps of GMPhoRCC to determine the red sequence CMR, cluster redshift and richness.*

3.1.1 Modelling cluster distributions

Cluster distributions, whether colour or redshift, are well modelled by Gaussian mixtures which use a sum of several Gaussian components to describe any features as shown by Hao et al. (2010). Figure 3.2 shows an example of a Gaussian mixture highlighting the constituent Gaussian components.

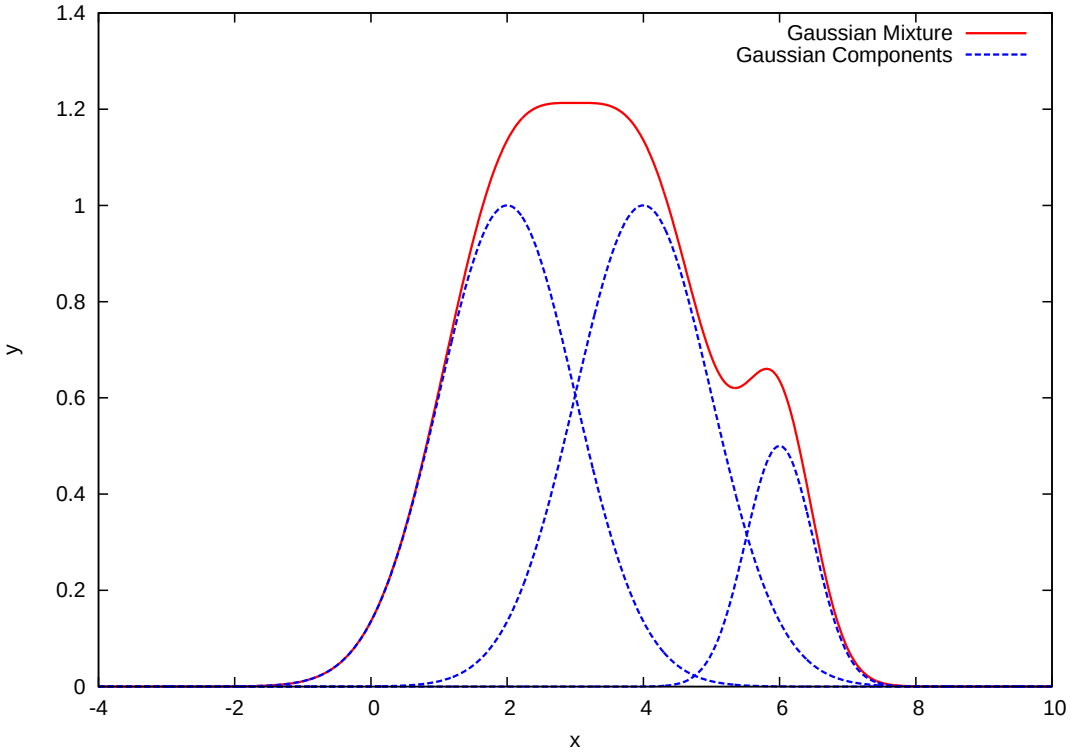

Figure 3.2 *An example of a Gaussian mixture highlighting the constituent components.*

Clusters are identified as overdensities hence any cluster distribution such as colour or redshift must be modelled with background subtraction.

$$\Sigma_{cluster} = \Sigma_{field} - \Sigma_{background} \tag{3.1}$$

where Σ represents a density. Whether in colour or redshift space these distributions are well modelled by error-corrected Gaussian mixtures (ECGM) which are determined by an expectation maximization procedure. Modelling clusters in this manner with background subtraction helps removes the ambiguity in component selection seen in GMBCG[1]. Rather than modelling the field only

[1] see Section 2.3.4

and identifying the separate mixture components which represent the cluster and background, the peak in the background-subtracted distribution represents the cluster. Values of interest, such as an approximate red sequence colour from the colour distribution, are determined with an associated uncertainty from the width of the distributions around the peaks.

Error-corrected Gaussian Mixtures: Expectation Maximisation

Fitting Gaussian mixtures to data is easily optimised using the expectation maximisation (EM) procedure as outlined in Press et al. (2002, §16.1). Extending this analysis to account for measurement errors as shown in Hao et al. (2009) is essential for modelling astrophysical data. The following derivation of the EM procedure is shown in detail in Hao et al. (2009), but for consistency with the rest of the analysis maintains the notation of Press et al. (2002, §16.1).

Applying a Gaussian mixture to the colour distribution of galaxies, the probability of galaxy n having colour $\tilde{c}_n$ given the parameters θ is defined below:

$$p(\tilde{c}_n \mid \theta) = \sum_k N(\tilde{c}_n \mid \mu_k, \sigma_k) P(k) \tag{3.2}$$

$$N(\tilde{c}_n \mid \mu_k, \sigma_k) = \frac{1}{\sqrt{2\pi\sigma_k^2}} \exp - \frac{(\tilde{c}_n - \mu_k)^2}{2\sigma_k^2} \tag{3.3}$$

where $\tilde{c}_n$ is the true colour of the galaxy and θ represents the collective parameters of the model namely μ_k, σ_k, $P(k)$, the component means, standard deviations and weights respectively. The colour of each galaxy has an associated measurement error which must be taken into consideration when fitting the Gaussian mixture.

$$p(\tilde{c}_n \mid c_n) = \frac{1}{\sqrt{2\pi\delta_n^2}} \exp - \frac{(\tilde{c} - c_n)^2}{2\delta_n^2} \tag{3.4}$$

where c_n is the measured galaxy colour with error δ_n. Combining these gives the likelihood function of the model given the single galaxy.

$$p(\theta \mid c_n) = \int p(\tilde{c}_n \mid \theta) p(\tilde{c}_n \mid c_n) \mathrm{d}\tilde{c}_n \tag{3.5}$$

Integrating this over $\tilde{c}_n$ and combining all galaxies gives the likelihood function of the model given the data with measurement errors.

$$p(\theta \mid \mathbf{c}) = \prod_{n=1}^{N} \left(\sum_{k=1}^{K} \frac{P(k)}{\sqrt{2\pi(\sigma_k^2 + \delta_n^2)}} \exp\left[-\frac{(c_n - \mu_k)^2}{2(\sigma_k^2 + \delta_n^2)} \right] \right) \tag{3.6}$$

where $\mathbf{c}$ is the complete set of galaxy colours, K is the total number of components and N is the number of galaxies. Finding the optimum parameters is simply a matter of finding those which maximise Equation 3.6. This problem is simplified greatly by introducing a hidden parameter z_n which labels the component from which c_n is sampled. This leads to the following pdf:

$$p(\mathbf{c} \mid z_n = k, \theta) = \prod_{n=1}^{N} p(c_n \mid z_n = k, \theta) = \prod_{n=1}^{N} \frac{1}{\sqrt{2\pi(\sigma_k^2 + \delta_n^2)}} \exp\left[-\frac{(c_n - \mu_k)^2}{2(\sigma_k^2 + \delta_n^2)} \right] \tag{3.7}$$

Finding the hidden variable can be done by expanding this pdf using Bayes' Theorem.

$$Pnk = p(z_n = k, \mid c_n, \theta) = \frac{p(c_n \mid z_n = k, \theta) p(z_n = k \mid \theta)}{\sum_{k=1}^{K} p(c_n \mid z_n = k, \theta) p(z_n = k \mid \theta)} \tag{3.8}$$

$$Pnk = \frac{p(c_n \mid z_n = k, \theta) P(k)}{\sum_{k=1}^{K} p(c_n \mid z_n = k, \theta) P(k)} \tag{3.9}$$

where it is noted that $p(z_n = k \mid \theta)$ is simply the weight of the component, $P(k)$. Using Equation 3.9 the likelihood function, Equation 3.6, can be rewritten in exponential family form

$$p(\theta \mid \mathbf{c}) = \exp\left[\sum_{n=1}^{N} \sum_{k=1}^{K} Pnk \left(-\frac{1}{2} \ln 2\pi - \frac{1}{2} \ln(\sigma_k^2 + \delta_n^2) - \frac{(c_n - \mu_k)^2}{2(\sigma_k^2 + \delta_n^2)} + \ln(P(k)) \right) \right] \tag{3.10}$$

With this form of the likelihood function it is now possible to optimise the parameters using the expectation maximization procedure. This involves iteratively updating θ by maximising the log-likelihood whilst constraining

$\sum_{k=1}^{K} P(k) = 1$ to maintain normality.

$$\mathscr{L}(\theta) = \sum_{n=1}^{N}\sum_{k=1}^{K} Pnk\left(-\frac{1}{2}\ln 2\pi - \frac{1}{2}\ln\left(\sigma_k^2 + \delta_n^2\right) - \frac{(c_n - \mu_k)^2}{2(\sigma_k^2 + \delta_n^2)} + \ln(P(k))\right) \tag{3.11}$$

This is done by using Lagrange Multipliers to maximise

$$\tilde{\mathscr{L}}(\theta) = \mathscr{L}(\theta) - \lambda\left[\sum_{k=1}^{K} P(k) - 1\right] \tag{3.12}$$

Maximising with respect to μ_k, σ_k and $P(k)$ gives the updated parameters $\hat{\mu_k}$, $\hat{\sigma_k}$ and $\hat{P(k)}$ respectively. Starting with $\hat{\mu}$:

$$\frac{\partial\tilde{\mathscr{L}}(\theta)}{\partial\mu_k} = \sum_{k=1}^{N}\left[Pnk\left(\frac{c_n - \hat{\mu_k}}{\sigma_k^2 + \delta_n^2}\right)\right] = 0 \tag{3.13}$$

rearranging this gives a recursion relation for μ_k

$$\hat{\mu_k} = \frac{\sum_{n=1}^{N} c_n Pnk}{\sum_{n=1}^{N} Pnk} \tag{3.14}$$

Similarly for $\hat{\sigma}_k$

$$\frac{\partial\tilde{\mathscr{L}}(\theta)}{\partial\hat{\sigma}_k} = \sum_{k=1}^{N} Pnk\left[\frac{\hat{\sigma}_k^2(1 + \delta_n^2/\hat{\sigma}_k^2) - (c_n - \mu_k)^2}{\hat{\sigma}_k^4(1 + \delta_n^2/\hat{\sigma}_k^2)^2}\right] = 0 \tag{3.15}$$

Unfortunately there is no analytical solution for $\hat{\sigma}_k$, however by replacing $\delta_n^2/\hat{\sigma}_k^2$ with δ_n^2/σ_k^2 an approximate value can be found. This step was shown by Hao et al. (2009) to be a reasonable approximation since $(c_n - \mu_k)$ is the dominant contributor. Using this approximation Equation 3.15

$$\frac{\partial\tilde{\mathscr{L}}(\theta)}{\partial\hat{\sigma}_k} = \sum_{k=1}^{N} Pnk\left[\frac{\hat{\sigma}_k^2(1 + \delta_n^2/\sigma_k^2) - (c_n - \mu_k)^2}{\hat{\sigma}_k^4(1 + \delta_n^2/\sigma_k^2)^2}\right] = 0 \tag{3.16}$$

which rearranges to yield

$$\hat{\sigma}_k = \left[\frac{\sum_{n=1}^{N} Pnk(c_n - \hat{\mu}_k)^2/(1 + \delta_n^2/\sigma_k^2)}{\sum_{n=1}^{N} Pnk/(1 + \delta_n^2/\sigma_k^2)} \right]^{1/2} \tag{3.17}$$

Finally for $P(k)$

$$\frac{\partial \tilde{\mathscr{L}}(\theta)}{\partial \hat{P}(k)} = \sum_{k=1}^{N} Pnk/\hat{P}(k) - \lambda = 0 \tag{3.18}$$

leading to

$$\hat{P}(k) = \frac{1}{\lambda} \sum_{k=1}^{N} Pnk \tag{3.19}$$

Now since $\sum_{k=1}^{K} P(k) = 1$ this leads to $\lambda = N$ and

$$\hat{P}(k) = \frac{1}{N} \sum_{k=1}^{N} Pnk \tag{3.20}$$

These recursive relations form the basis of the EM algorithm. First the expectation step or e-step is carried out, where the log-likelihood, $\mathscr{L}(\theta)$ and Pnks are calculated using initial estimates for the parameters. Next the maximisation step or m-step updates the parameters using the recursion relations which are fed straight back into an e-step. The process of e-step, m-step, e-step is repeated until the change in likelihood falls below some threshold value. A flow chart summarising the EM procedure is shown in Figure 3.3 with an illustration of convergence to the best fit shown in Figure 3.4.

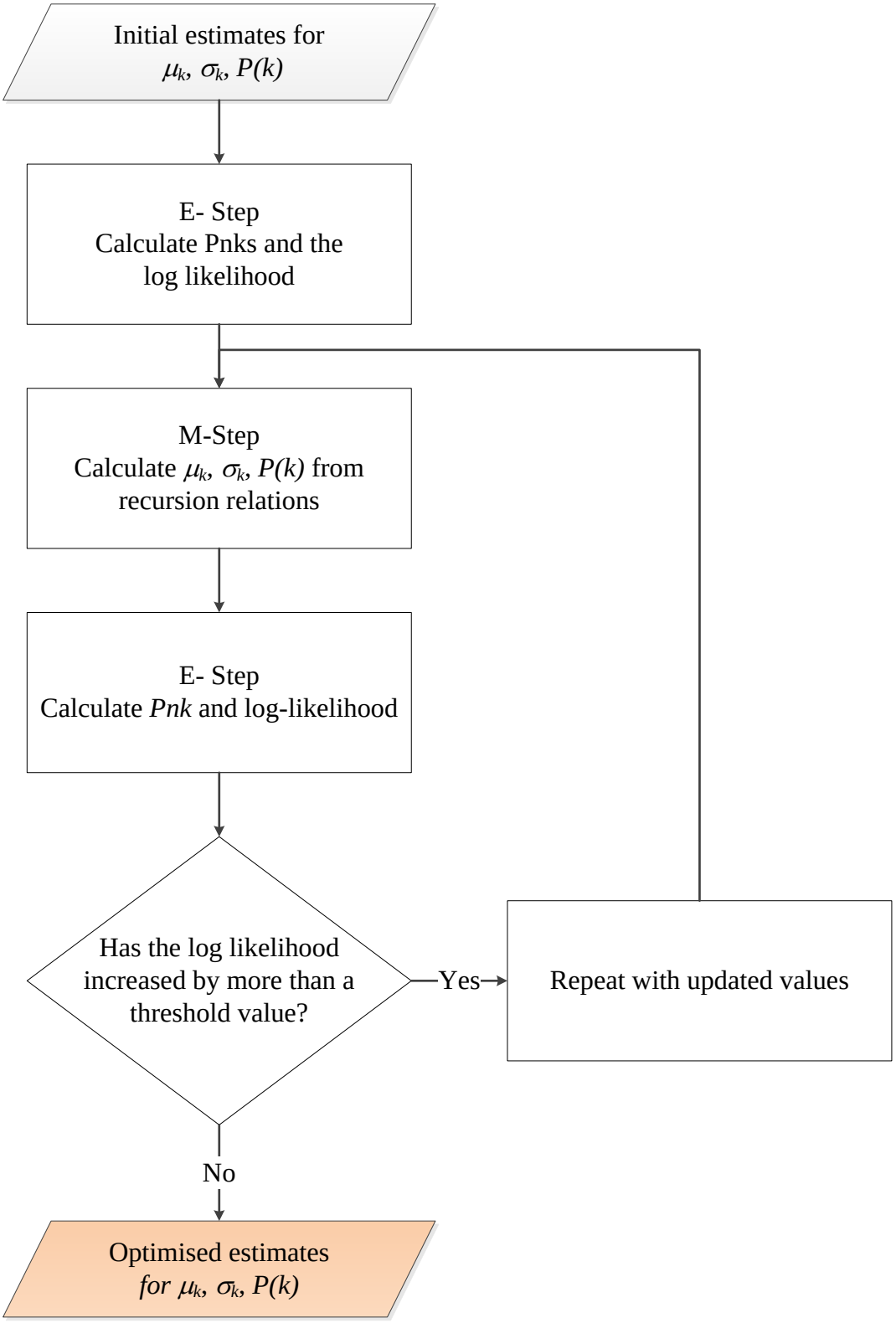

Figure 3.3 *A flowchart summarising the various steps in the EM algorithm.*

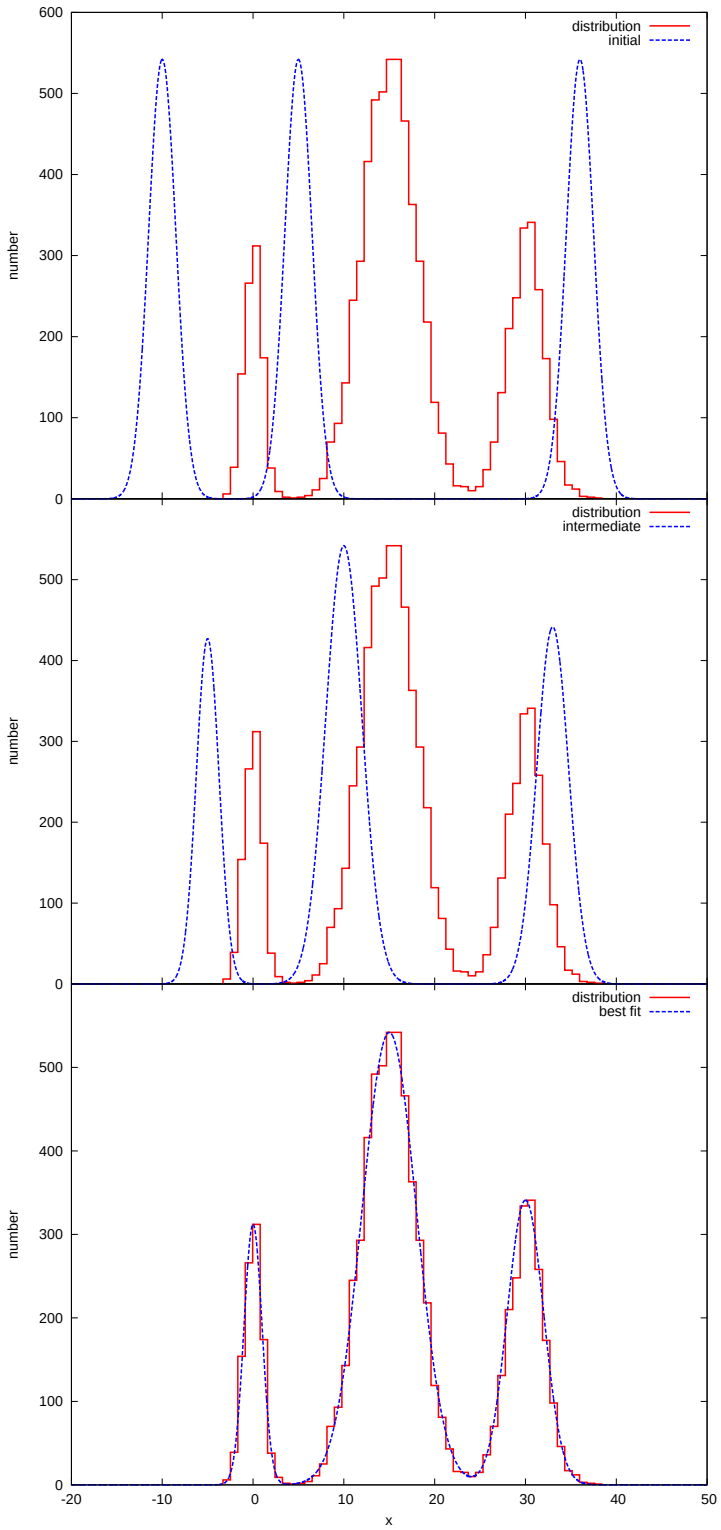

Figure 3.4 *An illustration of the expectation maximisation convergence to the best fit of an error-corrected Gaussian mixture to a distribution. From top to bottom the plots show the initial, an intermediate and best fit Gaussian mixture.*

Example: GMBCG-1

The following example shows the Gaussian mixture fits in practice using the cluster GMBCG J197.87292-01.34109 (GMBCG-1). In order to compare distributions from different areas it is necessary to normalise the Gaussian mixtures such that integrating over all parameter space returns the average density of the region. Figures 3.5 and 3.6 show the colour and redshift distributions for GMBCG-1. The widths are marked by the positions where the distribution is half the value of the peak giving an estimate of the asymmetric lower and upper error bars.

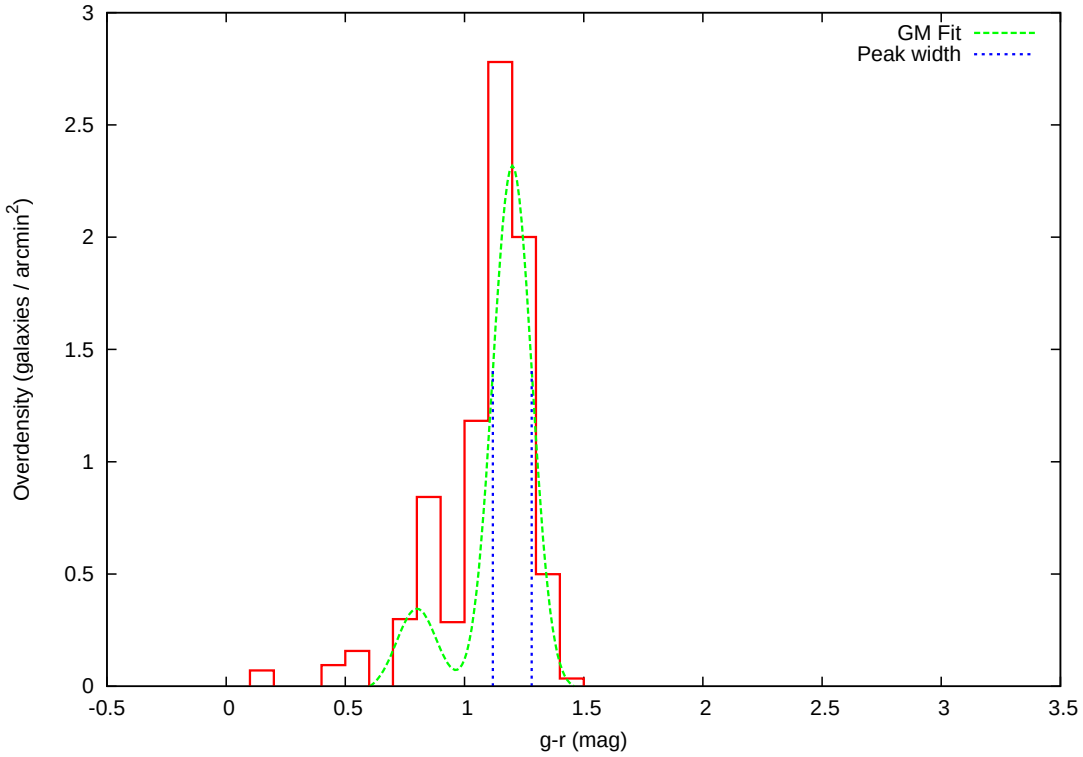

Figure 3.5 *A histogram of the $g-r$ colour overdensity of GMBCG-1 showing the best fit Gaussian mixture highlighting the associated width used as an error bar around the peak.*

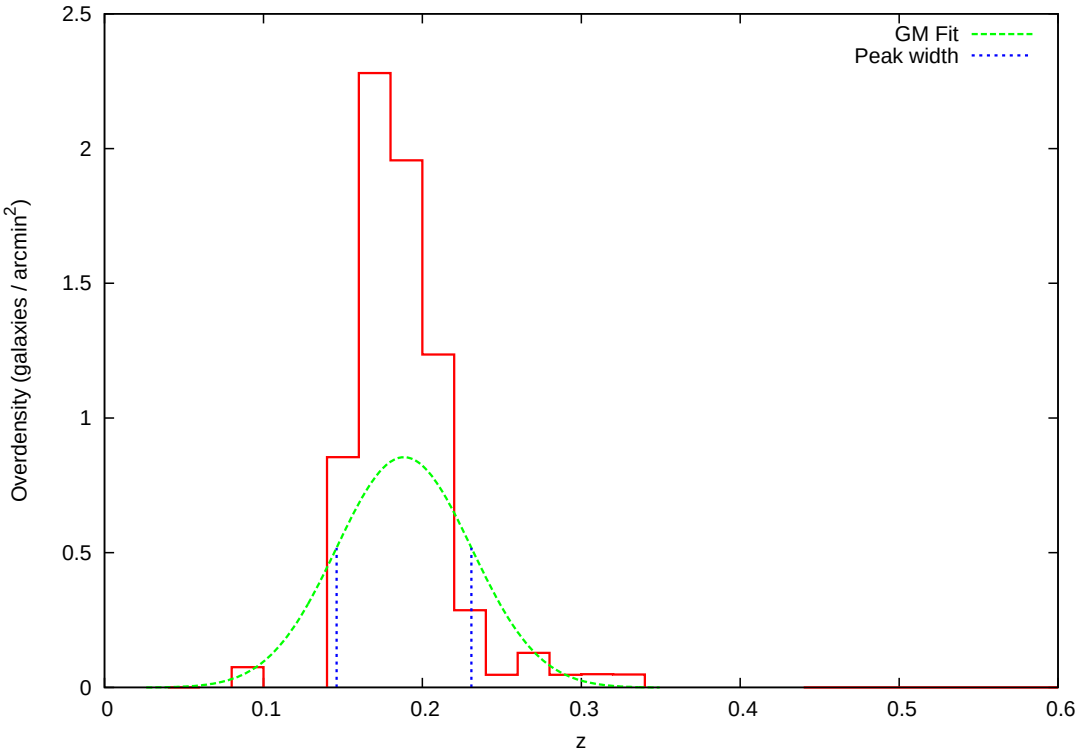

Figure 3.6 *A histogram of the redshift overdensity of GMBCG-1 showing the best fit Gaussian mixture highlighting the associated width used as an error bar around the peak.*

3.1.2 Preparing the optical data

As described in the Section 3.1.1 in order to model cluster distributions it is necessary to sample not only the cluster but also an appropriate background. A sample of the local background is taken in an annulus around the cluster region. The initial field is taken as an inner 0.5^o cone as the cluster region with an outer RA, Dec rectangle encompassing a larger cone of radius 1^o as the background annulus. This ensures coverage of the largest clusters while still giving sufficient area for the background. Section 3.2.3 details the analysis justifying these values. Care is needed to recover the area of each of these regions as there may be sections of the fields with no observations. This may simply signify unobserved areas of the sky or regions masked out due to poor photometry. By splitting the total field into 5′x5′ rectangular apertures a custom mask is constructed. This aperture is large enough that the probability of finding no galaxies is low hence empty apertures can be consider unobserved and assigned zero area. Summing the area across all the apertures recovers an accurate measure of the whole field. Figures 3.7 and 3.8 show an example field from SDSS DR9 around a cluster with and without a custom mask respectively.

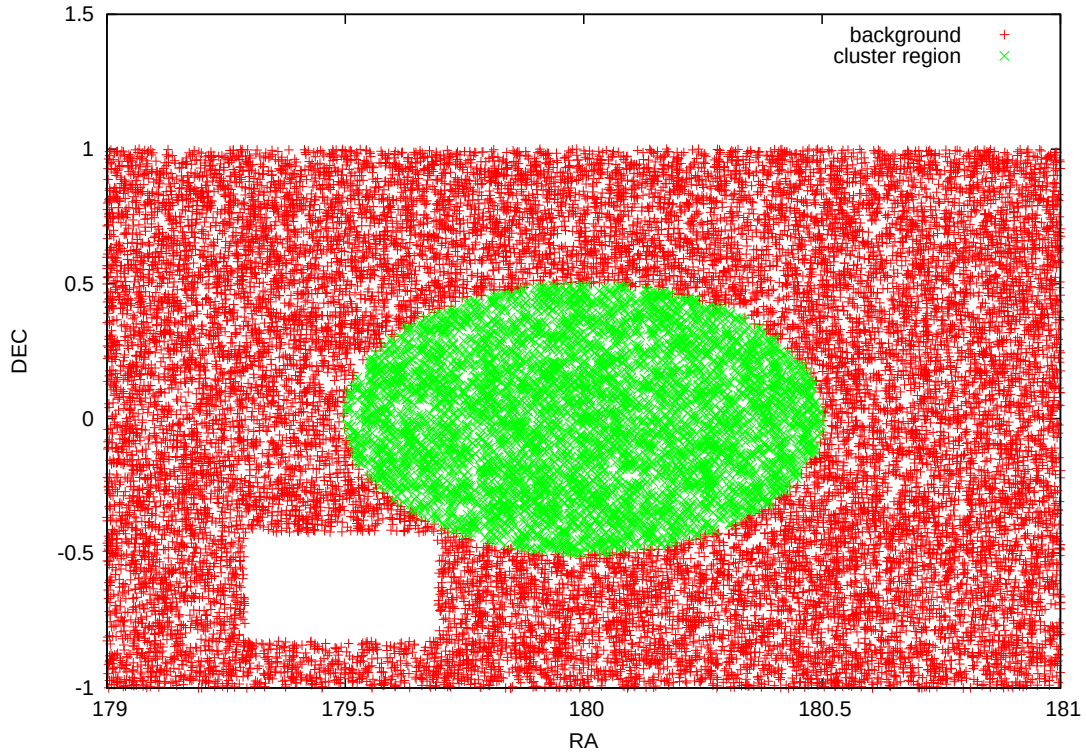

Figure 3.7 *A sample field in SDSS DR9 around a cluster showing an unobserved region.*

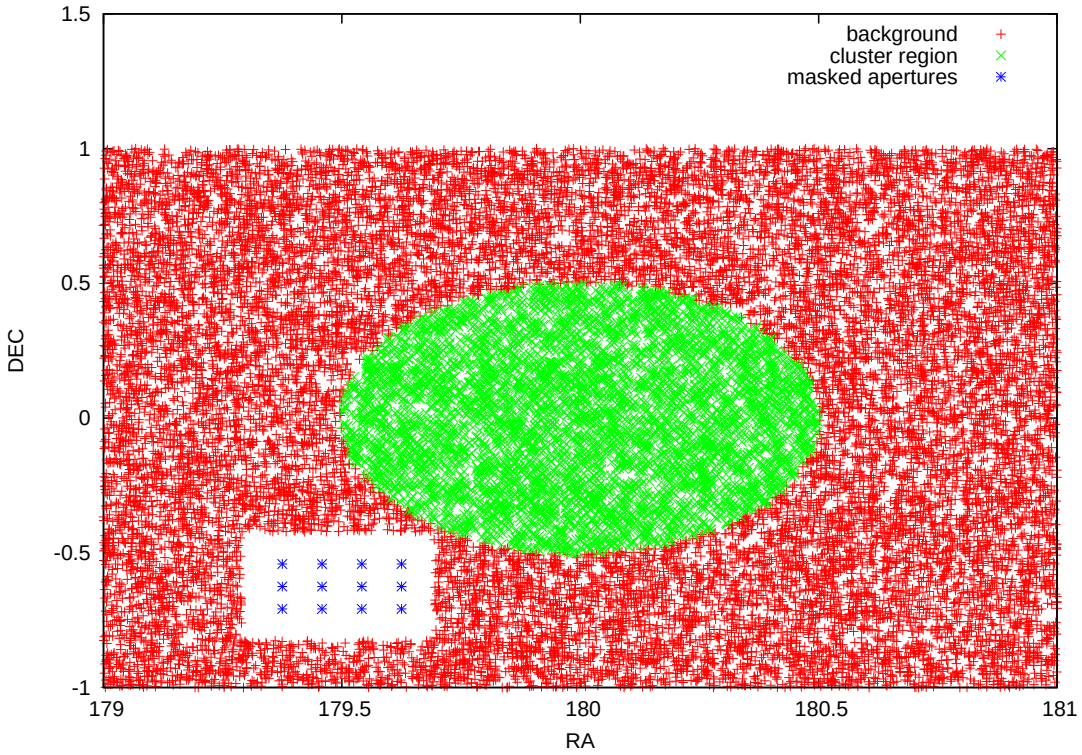

Figure 3.8 *The same sample field in SDSS DR9 from Figure 3.7 with a custom mask overlaid.*

3.1.3 Red sequence and redshift

With the framework in place to model the various cluster distributions from optical data the first step in GMPhoRCC is to identify the red sequence. The ultimate goal here is to determine a full CMR with intrinsic scatter, however there are several complications beyond simply fitting a linear function in the cluster region.

1. Selecting an appropriate cluster radius to investigate for the red sequence is not trivial and varies from cluster to cluster. Ideally a radius would be found which selects an inner region dominated by cluster members.

2. It was noted that GMPhoRCC should use a red sequence colour band most suited to the cluster redshift. Some colour bands show stronger clustering, higher cluster-background contrast and a stronger response in the colour-redshift relation as noted in Hao et al. (2010) and Rykoff et al. (2013). Although GMPhoRCC was not designed to use a colour-redshift relation having the multiple colour bands allows the possibility of adding this easily as an addition module to suit the user.

3. Fitting a full CMR blindly once the colour band and radius has been selected is still not ideal as there may be high contamination by field galaxies.

Finding an appropriate radius to use when examining the cluster distributions can be done by fitting in a range of radii and using the one which gives the largest overdensity. Radii of $1'$, $2'$, $3'$ and $4'$ are used to match different cluster sizes across a range of redshifts, again justified from the analysis in Section 3.2.3.

Next it may seem that fitting the joint redshift-colour distribution across a range of colour bands might be the most appropriate way to address the issue of band selection however this is not the case. The multi-dimensional expectation maximisation algorithm for fitting Gaussian mixtures cannot easily be extended to account for measurement errors present in astrophysical observations as noted by Hao et al. (2009). In this case the recurrence relations used to iteratively determine the parameters must themselves be solved numerically requiring significant computer resources. Even without this extension it was found in practice these functions struggle to recover the structure of the joint colour-redshift distribution and are highly sensitive to the initial estimate of the

parameters. While many cluster regions exhibit multi-modal distributions, the EM fitting often converges to wide single component mixture where much of the structure is lost resulting in poorer characterisations.

To get around this limitation the first step in GMPhoRCC, as shown in figure 3.1, is to find an initial estimate of cluster redshift by examining the peaks in the photometric redshift distribution from which appropriate colour bands can be determined. The primary peak, the one with largest overdensity, represents the primary potential cluster. A secondary cluster is considered if there is another peak with an amplitude of at least 20% of the primary. Table 3.1 shows the red sequence colour bands and the redshift ranges for which they are used. These values are in line with Hao et al. (2010) and the subsequent analysis in Section 4.2.1. These values ensure that the main spectral feature of the galaxies, the 4000Å break, remains in the band at a given redshift. This is important as this ensures the strongest colour clustering and contrast against the background. Additionally the redshift values overlap to account for possible failures of the initial estimate and help clusters where the 4000Å break sits between bands. Hence each potential cluster may require separate analysis in multiple bands from which a primary cluster can be selected.

Figure 3.9 expands on procedure 1 shown in Figure 3.1, illustrating the steps necessary to obtain an initial estimate of cluster redshift.

Red sequence band	redshift range
$g-r$	$0.0 \leq z < 0.5$
$r-i$	$0.3 \leq z < 0.8$
$i-z$	$0.6 \leq z$

Table 3.1 *The most suitable red sequence colour bands for the initial redshift estimate. These values overlap to account for uncertainty in the initial redshift and those close to a transition.*

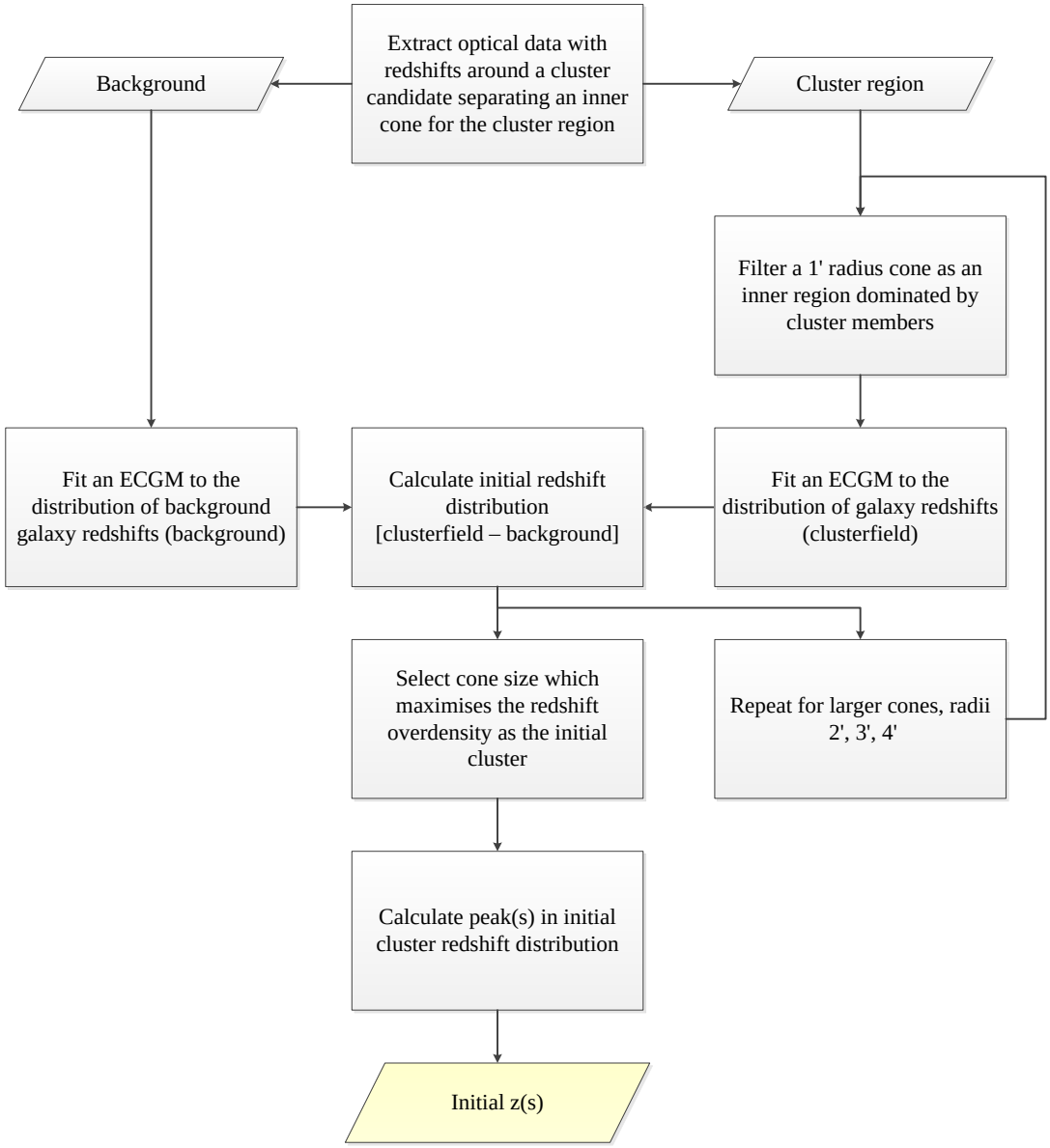

Figure 3.9 *A detailed flowchart showing the procedures of GMPhoRCC to determine an initial cluster redshift estimate highlighted as procedure 1 in Figure 3.1.*

Before fitting a CMR to the red sequence it is first necessary to remove potential contamination from field galaxies and this is done using the initial redshift and by considering the cluster colour distribution, highlighted as procedure 2 in Figure 3.1. First, galaxies are removed which do not conform with the initial redshift; specifically those where the galaxy redshift is more than 0.25 from the initial estimate and those fainter than would be considered in such a cluster. The faint end cut is taken as $m_*(z) + 2$ where the redshift dependent m_* is derived from the luminosity function of field galaxies and is explored in more detail in Section 3.1.4.

Next, peaks in the colour distribution of cluster, again across multiple radii, give an initial estimate of the red sequence colour and by filtering around this, unwanted contamination can be removed. This step is very similar to the initial redshift estimator and shown in detail in Figure 3.10.

Figure 3.10 *A detailed flowchart showing the procedures of GMPhoRCC to determine an initial red sequence colour estimate, highlighted as procedure 2 in Figure 3.1.*

Next, filtering occurs in a manner similar to that used to identify red sequence galaxies; all galaxies within 2σ of the initial colour estimate are kept for further analysis, where

$$\sigma^2 = \sigma^2_{colour} + \sigma^2_{RS} \tag{3.21}$$

Rather than using the common $\sigma_{RS} = 0.05$ to model the intrinsic scatter of a red sequence as selected by Hao et al. (2010), Koester et al. (2007b) and Mei et al. (2009), a broader cut, $\sigma_{RS} = 0.1$ is used to ensure that only field contamination is removed. The red sequence should now dominate these remaining galaxies and the CMR fitting procedure can now proceed.

Fitting a CMR may seem straightforward and there are indeed many regression methods to do this, such as ordinary least squares (OLS) or orthogonal linear regression (OLR), however without full treatment of the measurement errors the parameters found using these methods can be heavily biased as noted in Akritas & Bershady (1996). In order to appropriately fit a CMR it is necessary to account for not only measurement errors in both the colour and magnitude components but also the intrinsic scatter resulting from the age variations in the galaxies. Additionally, rather than assuming the size of the intrinsic width it is more useful to determine this from the fit, as the $\sigma_{RS} = 0.05$ may not be appropriate for all clusters. While Section 4.2.1 demonstrates that the standard $\sigma_{RS} = 0.05$ is sufficient across a range of redshifts for mock clusters, it is found in practice using a variable width red sequence increases the number of reliable GMPhoRCC characterisations of clusters from the maxBCG (Koester et al., 2007b), GMBCG (Hao et al., 2010) and XCS (Mehrtens et al., 2012) catalogues by 10%.

One particularly useful approach for fitting the CMR with full treatment of errors is the bivariate correlated errors and intrinsic scatter (BCES) method (Akritas & Bershady, 1996). This extends the standard OLS method to account for intrinsic scatter and potentially correlated errors in both the dependent and independent variables. The following derivation of the BCES method mirrors that shown in Akritas & Bershady (1996), however uses notation consistent with the rest of the analysis presented in this chapter applying specifically to fitting a CMR.

The first step defines the statistical model and the regression. The observed data are given by

$$(c_i, m_i, \mathbf{\Delta}_i),\ i = 1, ..., n \tag{3.22}$$

where c_i and m_i are the observed colours and magnitudes of the ith galaxy where the errors have a joint bivariate distribution with zero mean and covariance matrix $\mathbf{\Delta}_i$. The real colours and magnitudes, $\tilde{c}_i$ and $\tilde{m}_i$ respectively, are related to the observed data

$$\tilde{m_i} = m_i + \epsilon_{m,i} \tag{3.23}$$

$$\tilde{c_i} = c_i + \epsilon_{c,i} \tag{3.24}$$

where ϵ_i is drawn from the bivariate error distribution. The simple regression model is defined by

$$\tilde{c_i} = \alpha + \beta\tilde{m}_i + e_i \tag{3.25}$$

where e_i is drawn from a zero mean finite variance distribution representing the intrinsic scatter. In the case of the red sequence CMR this distribution is found in practice to be well approximated by a Gaussian (Hao et al. (2010) and Mei et al. (2009)). The parameters of the regression which minimise the squared residuals are given by the standard

$$\beta = \frac{C(\tilde{m}, \tilde{c})}{V(\tilde{m})} \tag{3.26}$$

$$\alpha = E(\tilde{c}) - \beta E(\tilde{m}) \tag{3.27}$$

where $C(\tilde{m}, \tilde{c})$ is the covariance of $\tilde{m}$ and $\tilde{c}$, $V(\tilde{m})$ is the variance of m_i and E denotes the expectation value. The BCES parameters are found by replacing the moments found from the true values with those from the observed data. First consider the expectation value, $E(\tilde{c})$, as ϵ_c is drawn from a zero mean distribution it follows from Equation 3.24 that

$$E(\tilde{c}) = E(c) \tag{3.28}$$

and similarly for $\tilde{m}$. Now consider variance, $V(\tilde{c})$, it is first noted that

$$\begin{aligned} E(c^2) &= E[E(c^2 \mid \Delta_{cc})] \\ &= E[E((c-\tilde{c})^2 + \tilde{c}^2 + 2\tilde{c}(c-\tilde{c}) \mid \Delta_{cc})] \\ &= E[E(\epsilon_c^2 + \tilde{c^2} + 2\tilde{c}\epsilon_c \mid \Delta_{cc})] \end{aligned} \tag{3.29}$$

where Equation 3.24 has been used to remove c with Δ_{cc} denoting the diagonal element of $\mathbf{\Delta}_c$ representing the error of c. As ϵ_c is drawn from the error distribution with zero mean this simplifies to

$$E(c^2) = E(\Delta_{cc}) + E(\tilde{c}^2) \tag{3.30}$$

Using Equation 3.28 and noting that the variance of a random variable, X, is given by $V(X) = E(X^2) - [E(X)]^2$, Equation 3.30 leads to

$$V(\tilde{c}) = V(c) - E(\Delta_{cc}) \tag{3.31}$$

and similarly for $\tilde{m}$. Considering covariance, $C(\tilde{m}, \tilde{c})$, first note

$$\begin{aligned} E(mc) &= E[E(mc \mid \mathbf{\Delta})] \\ &= E[E(\epsilon_m\epsilon_c + \tilde{m}\tilde{c} + \tilde{m}\epsilon_c + \tilde{z}\epsilon_c \mid \mathbf{\Delta})] \end{aligned} \tag{3.32}$$

where Equations 3.23 and 3.24 have been used to remove m and c. Again using the fact the ϵ has been drawn from a zero mean distribution, this simplifies to

$$E(mc) = E(\Delta_{cm}) + E(\tilde{m}\tilde{c}) \tag{3.33}$$

where Δ_{cm} is the off-diagonal component of $\mathbf{\Delta}$. Using Equation 3.28 and noting that the covariance of two random variables, X and Y, is given by $C(X,Y) =$

$E(XY) - E(X)E(Y)$, Equation 3.33 leads to

$$C(\tilde{m}, \tilde{c}) = C(m, c) - E(\Delta_{m,c}) \tag{3.34}$$

Using Equations 3.28, 3.31, 3.34, the regression parameters can be expressed using the observed data as shown below:

$$\beta = \frac{C(m, c) - E(\Delta_{mc})}{Vm - E(\Delta_{mm})} \tag{3.35}$$

$$\alpha = E(c) - \beta E(m) \tag{3.36}$$

Finally, replacing the population moments with sample moments, the BCES estimators are defined by

$$\hat{\beta} = \frac{\sum_{i=1}^{n} (m_i - \bar{m})(c_i - \bar{c}) - \sum_{i=1}^{n} \Delta_{cm,i}}{\sum_{i=1}^{n} (m_i - \bar{m}) - \sum_{i=1}^{n} \Delta_{mm_i}} \tag{3.37}$$

$$\hat{\alpha} = \bar{c} - \hat{\beta}\bar{m} \tag{3.38}$$

where $\bar{m}$ and $\bar{c}$ are the average magnitudes and colours respectively. While in general the magnitude and colour errors can be correlated, for example in the case of $r - i$ colours and i-band magnitudes, the CMR can be constructed in such a way as to provide uncorrelated errors with $\Delta_{mc} = 0$. In the case of $r - i$ vs i, fitting a regression model using r and i as the dependent and independent variables respectively, removes the correlation where the original CMR gradient, β_{r-i}, is calculated from the fitted gradient, β_r using $\beta_{r-i} = \beta_r - 1$. Figure 3.11 shows an illustration of the BCES convergence to the best fit linear function to a fictitious colour magnitude relation.

In practice the distribution of galaxies around the CMR found using the BCES estimators takes the form of a Gaussian whose width is a direct measure of the intrinsic scatter of the red sequence. The colour distribution around the CMR takes the form of a Gaussian. By correcting for the slope and using a single component, the width of the error-corrected Gaussian mixture gives a good estimate of the intrinsic scatter of the red sequence. In cases where galaxies

have large photometric errors these can account for the observed scatter entirely, dwarfing any intrinsic scatter and hence return artificially small values for the width, $\sim 10^{-10}$. To avoid these problems a minimum value for the width is assumed with $\sigma_{RS} = 0.05$. These steps, highlighted as procedure 3 in Figure 3.1, are shown in detail in Figure 3.12.

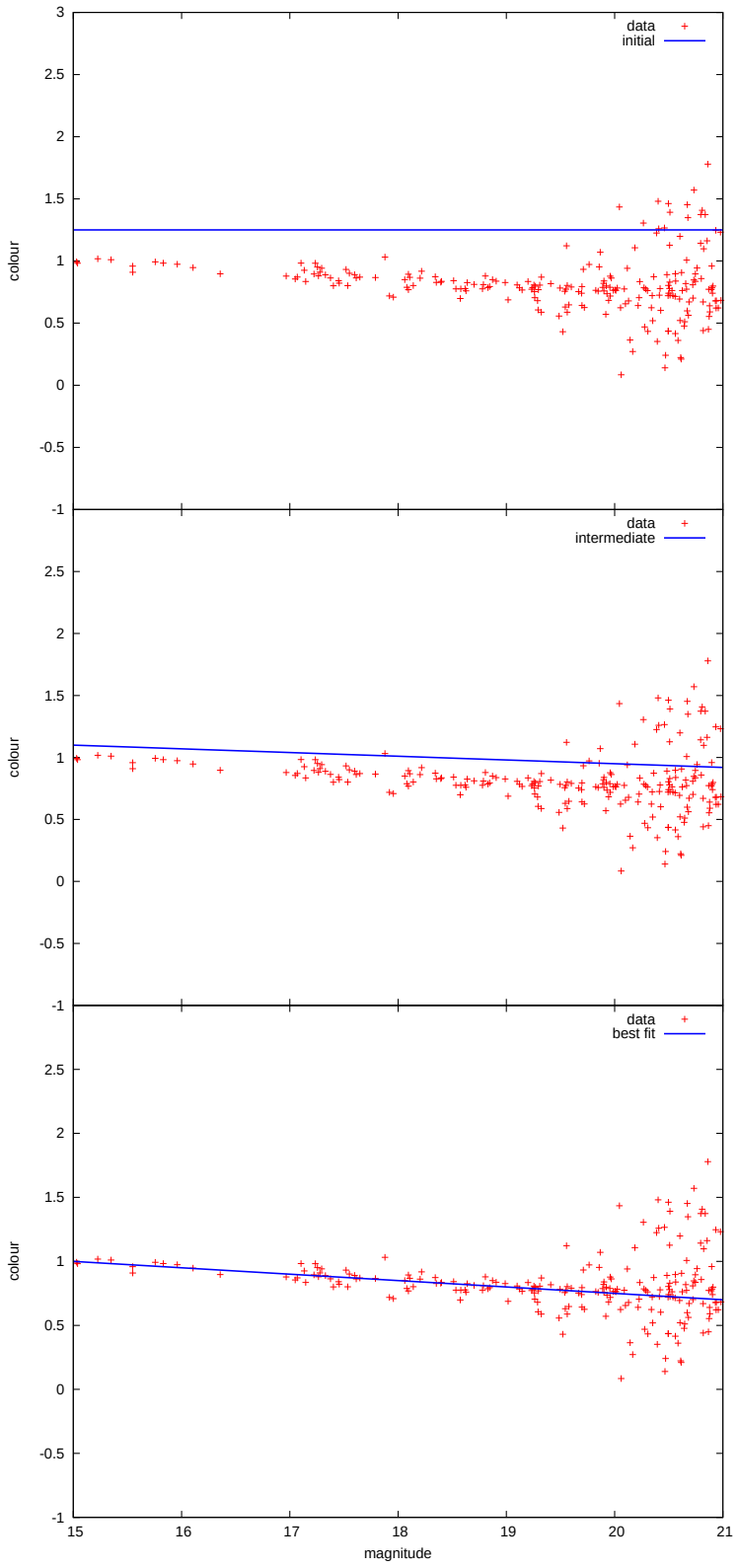

Figure 3.11 *An illustration of the BCES convergence to the best fit of a linear function to a fictitious colour magnitude relation. From top to bottom the plots show the initial, an intermediate and best fit CMRs.*

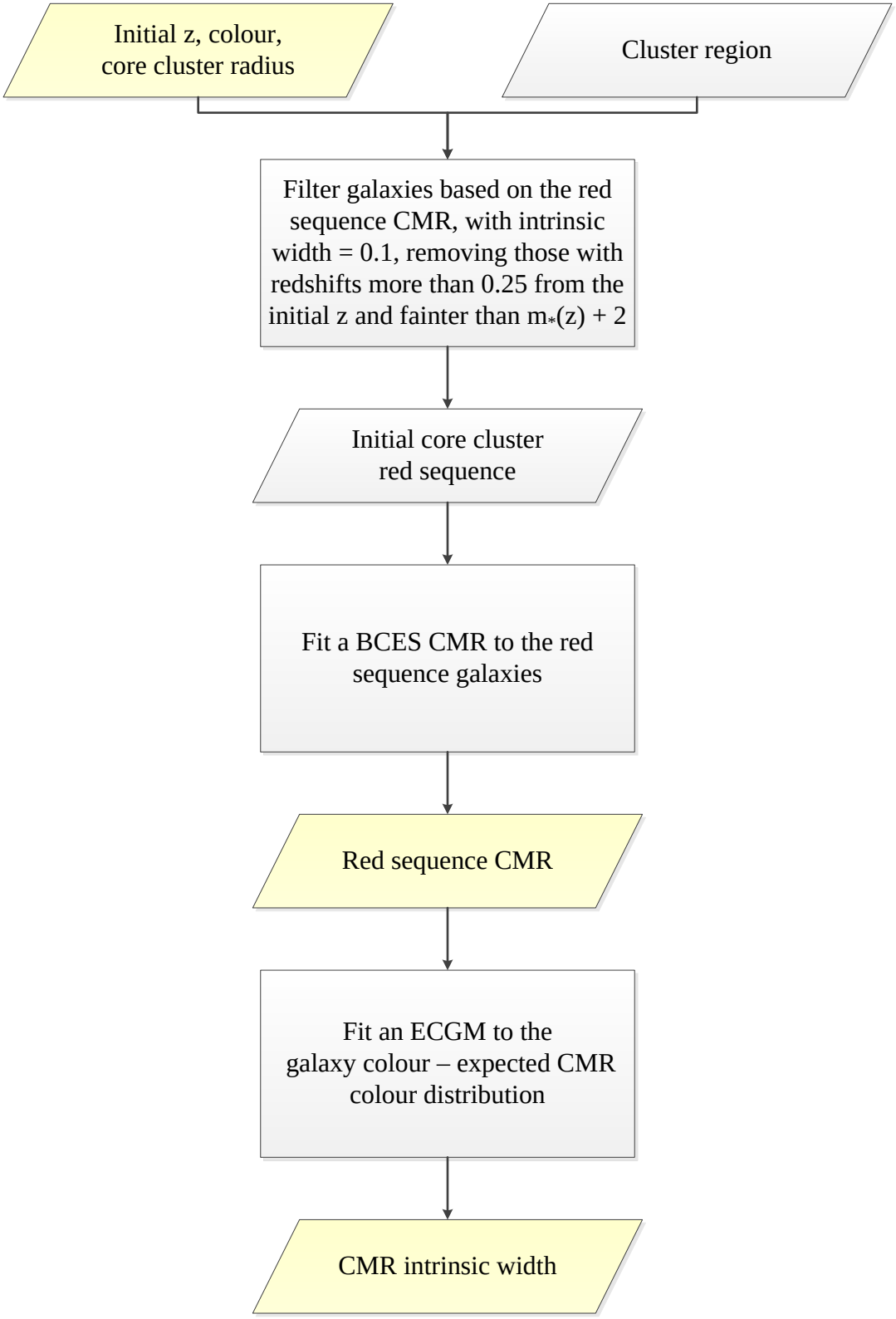

Figure 3.12 *A detailed flowchart showing the procedures of GMPhoRCC to filter remaining contamination and model the red sequence CMR, highlighted as procedure 3 in Figure 3.1.*

With the red sequence isolated using the 2σ approach, the peaks in the red sequence photometric redshift distribution provide the potential cluster redshift. Additional estimates such as spectroscopic or colour model redshifts can be added at this point if desired by the user. If spectroscopic redshifts are available, averaging these for the red sequence galaxies can provide a more reliable redshift estimator. Finally the BCG is identified as the brightest galaxy on the red sequence.

With all the potential clusters analysed, the final step is to select which represents the cluster. With multiple candidates it is not always easy to identify which represents the cluster and hence the selection process will return a primary as the most likely cluster and a secondary as another possibility. To help this process the potential clusters are first filtered to ensure the initial redshift, red sequence redshift and BCG redshift are all appropriate for the colour band used. Reducing the redshift overlap in Table 3.1 helps to remove the same candidates analysed in multiple bands. If this removes all the potential clusters the filter is not applied and the selection process continues.

Red sequence band	redshift range
$g-r$	$0.00 \leq z < 0.45$
$r-i$	$0.35 \leq z < 0.75$
$i-z$	$0.65 \leq z$

Table 3.2 *A tighter redshift-band relation for the red sequence than presented in Table 3.1. The reduced overlap helps to remove the same candidates analysed in multiple bands.*

The remaining candidates are then ranked, based first on the consistency of the three main redshift estimators, initial, red sequence and BCG. Four cleanness bands are introduced shown in Table 3.3 where the most desirable candidates have the lowest band value.

cleanness band	description
4	One or more of the main redshift estimators has not been found.
3	The red sequence and BCG redshift disagree by more than 0.1
2	All three estimators are not consistent with the colour band
1	All remaining candidates.

Table 3.3 *A list of the cleanness bands used to rank potential clusters.*

These consistency checks help to remove candidates which may not represent clusters but rather, random enhancements in the background or foreground.

Finally, to further rank clusters and break degeneracy, those where the red sequence redshift best matches the initial estimate provides the best selection, reducing the chance that the best candidates are spurious. The primary clusters are simply the cleanest candidates which best match the primary initial redshift estimate. A secondary cluster is assigned as the cleanest candidate associated with the earliest secondary peak (i.e. initial secondary redshifts considered first then colour then red sequence redshifts) which best matched the initial estimate. This selection procedure is shown in detail in Figure 3.13.

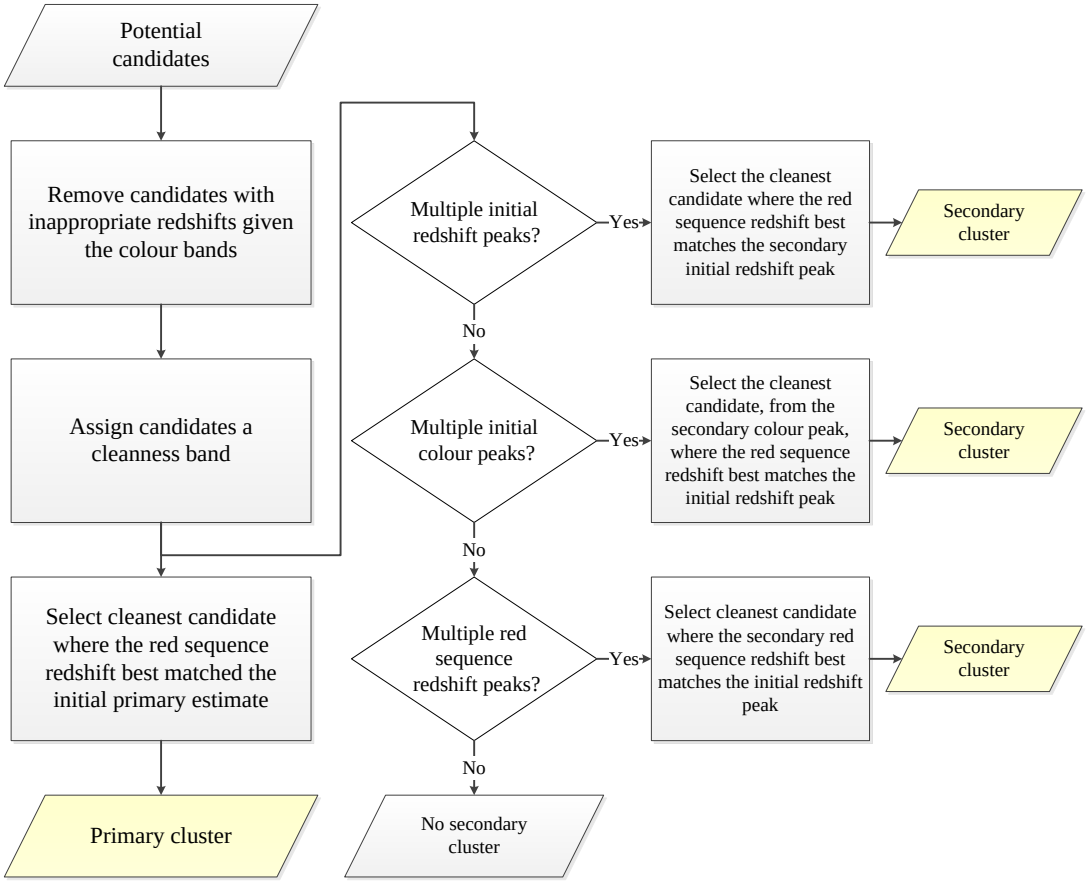

Figure 3.13 *A detailed flowchart showing the procedures of GMPhoRCC to select a primary and secondary cluster from a list of potential candidates.*

While comparing the GMPhoRCC estimates to previously characterised spectroscopic clusters, as explored in Section 3.4, it is found that on average 35% of targets characterised have an associated secondary cluster and of these only 13% (5% of the total) better matches spectra than the primary. In addition to the final selection process described here, other criteria were also considered. With a strong correlation observed between the BCG position and the cluster centre, candidates could be selected to prefer those where the BCG is closest to

the centroid. This however has not proven to be the best selection as candidate clusters can share the same BCG. Using this selection the fraction of clusters where the secondary is the best characterisation jumps from 5% to 22%. Again it has not only been shown that dealing with multi-modal distributions is necessary but also that the selection process of GMPhoRCC is able to reliably select the most appropriate characterisation from the potential candidates for the cluster.

Finally putting this together, Figure 3.14 expands procedure 4 from Figure 3.1 to show the steps taken by GMPhoRCC to estimate the red sequence redshift.

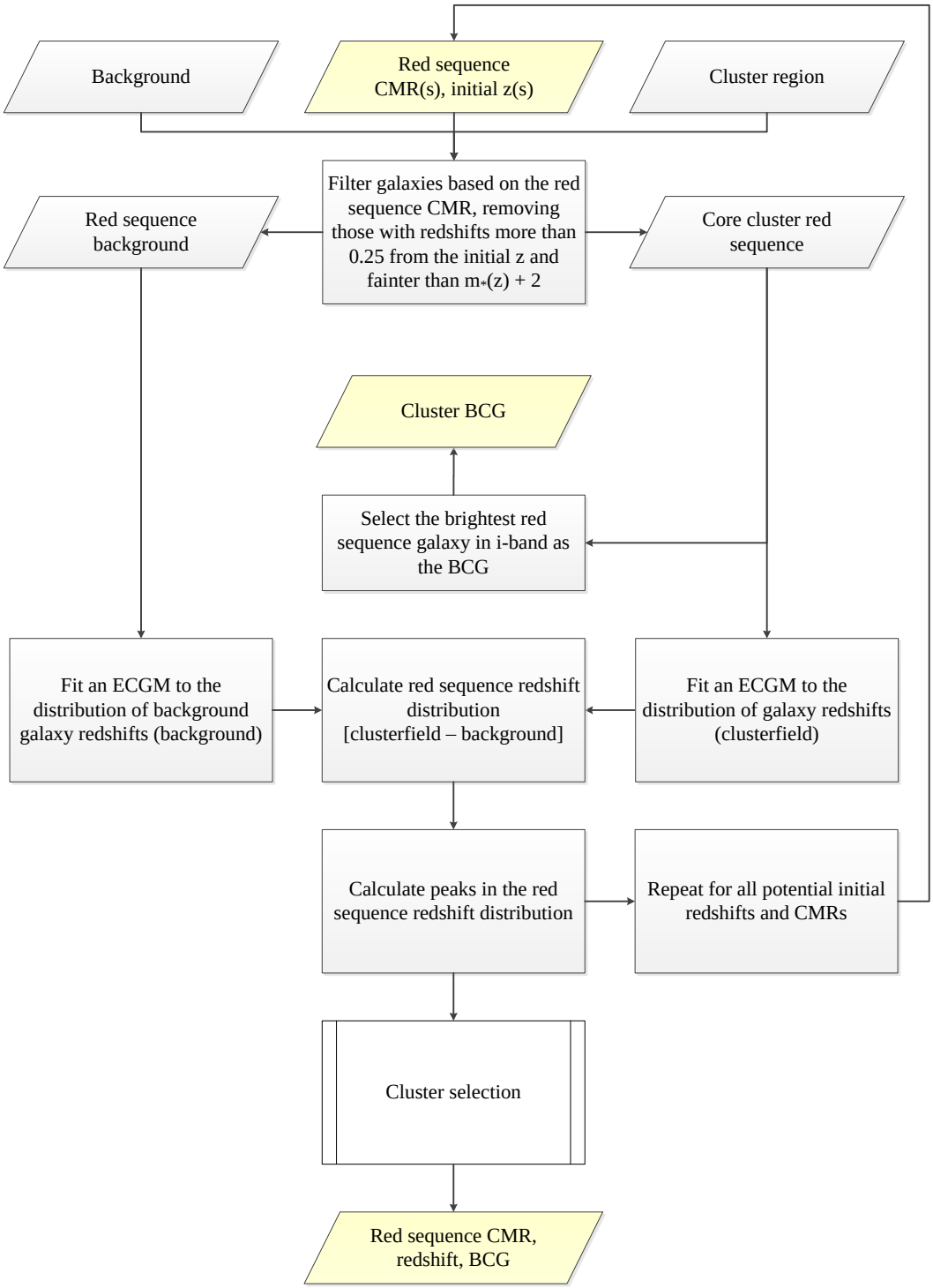

Figure 3.14 *A detailed flowchart showing the procedures of GMPhoRCC to estimate the cluster redshift from the red sequence CMR, highlighted as procedure 4 in Figure 3.1. The cluster selection process selects a primary and secondary cluster as outlined in Figure 3.13.*

3.1.4 Richness

Richness, a measure of the number of red sequence galaxies in the cluster, serves as a cheap optical mass proxy. With a range of radii, redshifts and red sequence colour bands it is essential to provide a consistent estimate of richness for all clusters.

GMPhoRCC measures richness as the number of red sequence galaxies fainter than the BCG and brighter than some redshift dependent cut-off, $m_*(z) + 1$. This takes the form of the maxBCG (Koester et al., 2007b) and GMBCG (Hao et al., 2010) richness which ensures the red sequence i-band magnitude range is consistent as a function of redshift. In agreement with maxBCG and GMBCG m_* is taken from the luminosity function of field galaxies determined by Blanton et al. (2003) and is shown in Figure 3.15.

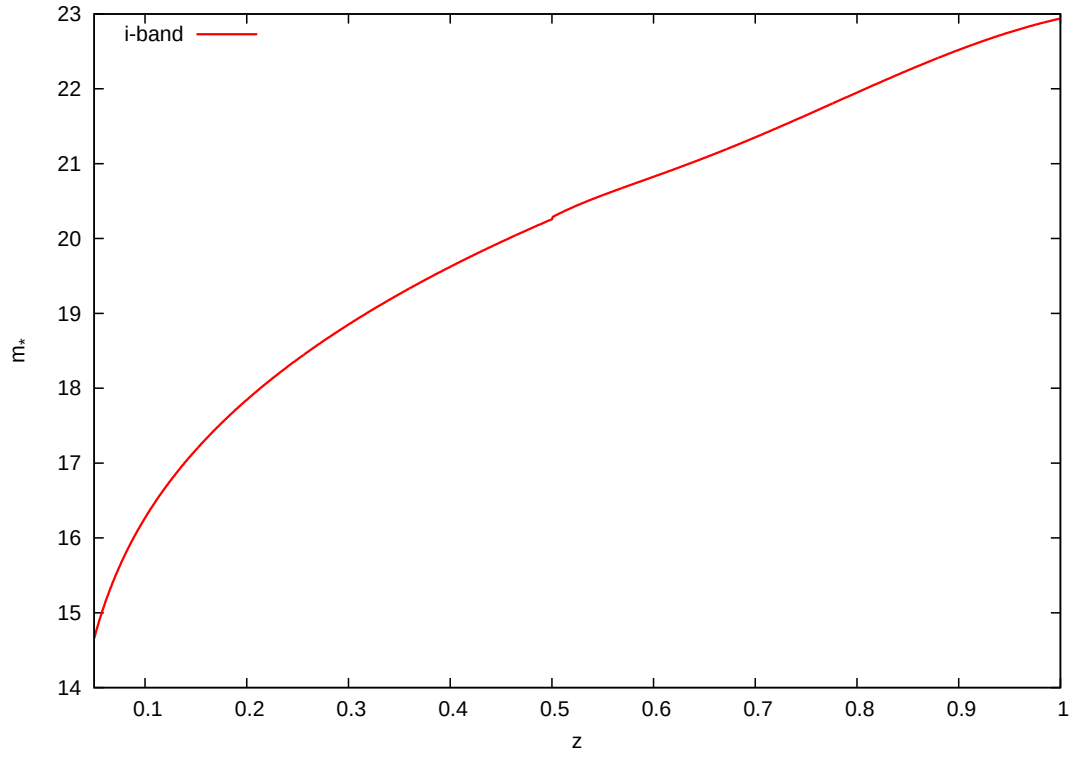

Figure 3.15 *The form of the m_* used to define the faint end cut-off to maintain a consistent magnitude range as a function of redshift.*

Since cluster radius varies with mass, to maintain a consistent mass proxy it is necessary to consider the richness inside a characteristic radius. One such radius is r_{200}, as discussed in Section 2.2.3; this is the radius inside which the average density is 200 times greater than the critical density. Since the cluster

mass is dominated by dark matter, measuring r_{200} directly is only possible using gravitational lensing and as such is not immediately available for GMPhoRCC. Many authors however use a fixed aperture such as $0.5\mathrm{h}^{-1}$Mpc to determine an intermediate richness, n_{gals}, in order to find r_{200}. By stacking the gravitational lensing signal of clusters in richness bins as demonstrated by Hansen et al. (2009), density profiles can be investigated as a function of richness. As expected, richness is indeed correlated with characteristic radius where scaling relations have been derived to determine r_{200} from n_{gals}. GMPhoRCC uses an intermediate richness defined inside a radius of $0.5\mathrm{h}^{-1}$Mpc in order to use the scaling relation (Equation 3.39) from Hansen et al. (2009) to find r_{200};

$$r_{200} = 0.133(n_{gals})^{0.539} \tag{3.39}$$

The final cluster richness, n_{200}, can then be determined inside this radius.

In addition to counting galaxies, richness is also estimated using the luminosity function method of High et al. (2010) explored in Section 2.3.3. This involves fitting a luminosity function within a magnitude range where the photometry is believed to be complete. Finding this range is simply done by inspecting a magnitude histogram where a limit can be assigned after which the density drops with increasing magnitude. Rather than using the binning approach to fit a Schechter function a new probabilistic approach has been developed which gives more reliable fits across a range of cluster richnesses. With appropriate normalisation the luminosity function, Equation 3.40, gives the number of galaxies within the magnitude range $m \rightarrow m+dm$ and hence the probability that a galaxy has a particular magnitude given the parameters of the Schechter function can be approximated by Equation 3.41.

$$\begin{aligned}\phi(m, \phi_*, m_*, \alpha)\mathrm{d}m = 0.4[\ln(10)]\phi_* 10^{-0.4(m-m_*)(\alpha+1)} \\ \times \exp[-10^{-0.4(m-m_*)}]\mathrm{d}m\end{aligned} \tag{3.40}$$

$$P(m|\phi_*, m_*, \alpha) = \frac{\phi(m, \phi_*, m_*, \alpha)\mathrm{d}m}{\text{Total Number of Galaxies}} \tag{3.41}$$

Using Bayes theorem, the likelihood of the parameters, $\mathscr{L}$, is given by combining

the probabilities from all galaxies.

$$\mathscr{L} = \prod_{k=1} P(\phi_*, m_*, \alpha | m_k) = \prod_{k=1} \frac{P(m_k|\phi_*, m_*, \alpha) P(\phi_*, m_*, \alpha)}{P(m_k)} \tag{3.42}$$

The cluster luminosity function is then defined by the parameters which maximise this likelihood. By assuming flat priors this is equivalent to minimising the log-likelihood shown in Equation 3.43.

$$\ln(\mathscr{L}) \propto \sum_{k=1} \ln \phi(m_k, \phi_*, m_*, \alpha) \tag{3.43}$$

In addition to using the High et al. (2010) fixed faint end ($\alpha = -1$), constraining the parameters to satisfy Equation 3.44 greatly increases the reliability of the fit.

$$\int \phi(m, \phi_*, m_*, \alpha) \mathrm{d}m = \text{Total Number of Galaxies} \tag{3.44}$$

This ensures a reasonable luminosity function is recovered which, when integrated across the previously determined magnitude range, returns the total number of galaxies observed.

Minimising Equation 3.43 subject to the constraint shown in Equation 3.44 proceeds using the standard sequential least squares method described by Kraft (1988).

Figure 3.16 compares this method with the binning approach of High et al. (2010) using galaxies randomly generated from a Schechter function. As expected, using the probabilistic framework provides the closest estimate of the generator and greatly improves performance where lower numbers of galaxies are available.

Although an improvement this method still produces unreliable results for very low numbers of galaxies hence, when fitting 5 or fewer data points, m_* is fixed based on the cluster redshift and the luminosity function of field galaxies determined by Blanton et al. (2003) and shown in Figure 3.15.

To serve as a suitable mass proxy it remains to prove that the GMPhoRCC richness is consistent across a range of redshifts and red sequence colour bands. While this is indeed true, a full analysis can only be done using mock clusters where the various properties can be controlled and hence is deferred to Section

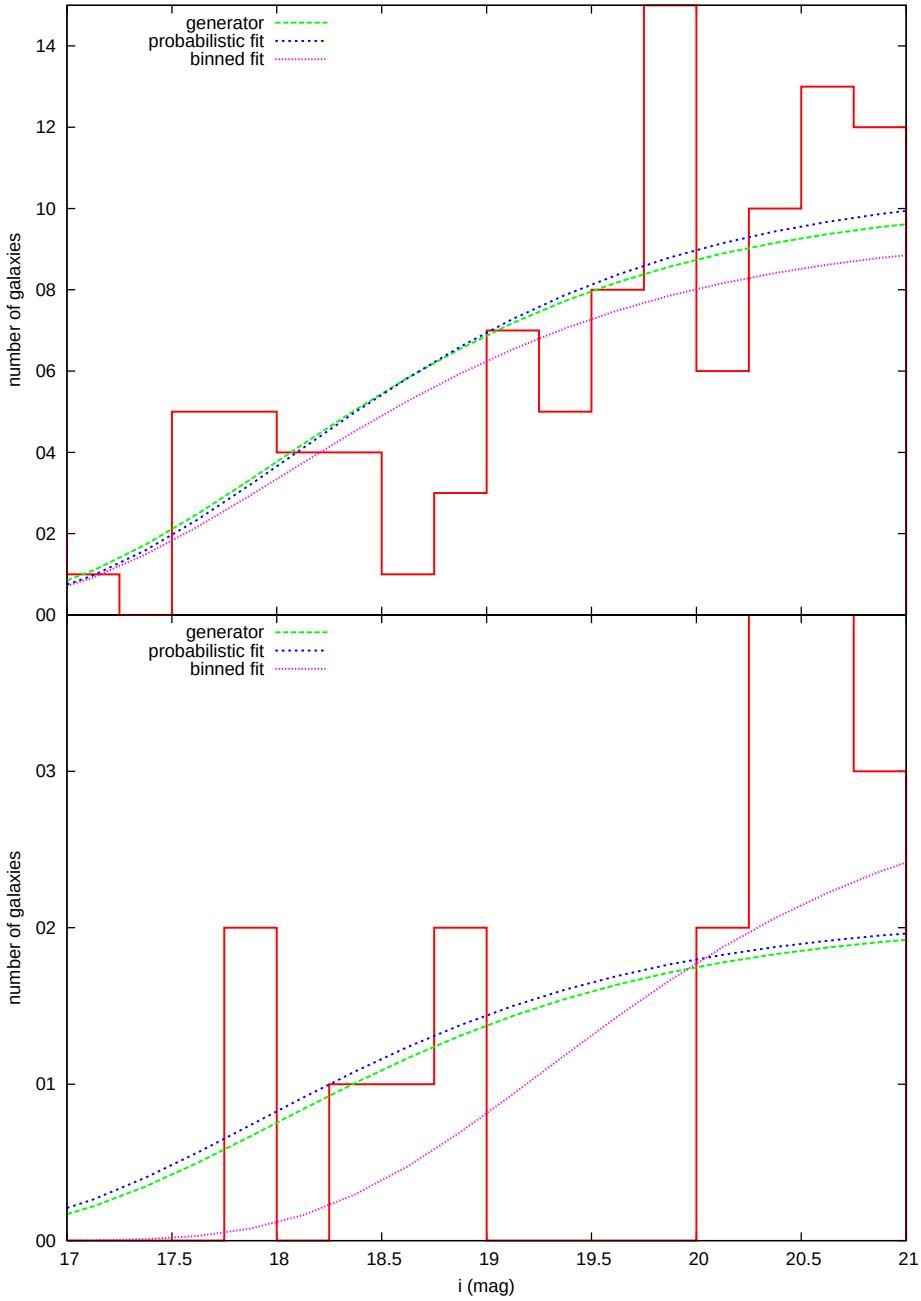

Figure 3.16 *The luminosity functions recovered using the binning and probabilistic methods with the top panel and bottom panels using* 100 *and* 20 *random galaxies respectively, drawn from a generator function. Although using a large number of galaxies the probabilistic method still provides the closest estimate of the generator. Considering the bottom panel, the advantage of the probabilistic method is clear providing a reasonable estimate of the generate despite the low number of galaxies.*

4.2.1.

Combining these methods, Figure 3.17 expands procedure 5 from Figure 3.1 in

more detail showing the steps taken to estimate cluster richness. By using an input radius of $0.5\mathrm{h}^{-1}$Mpc the intermediate richness, n_{gals} is determined, with n_{200} found by using r_{200}.

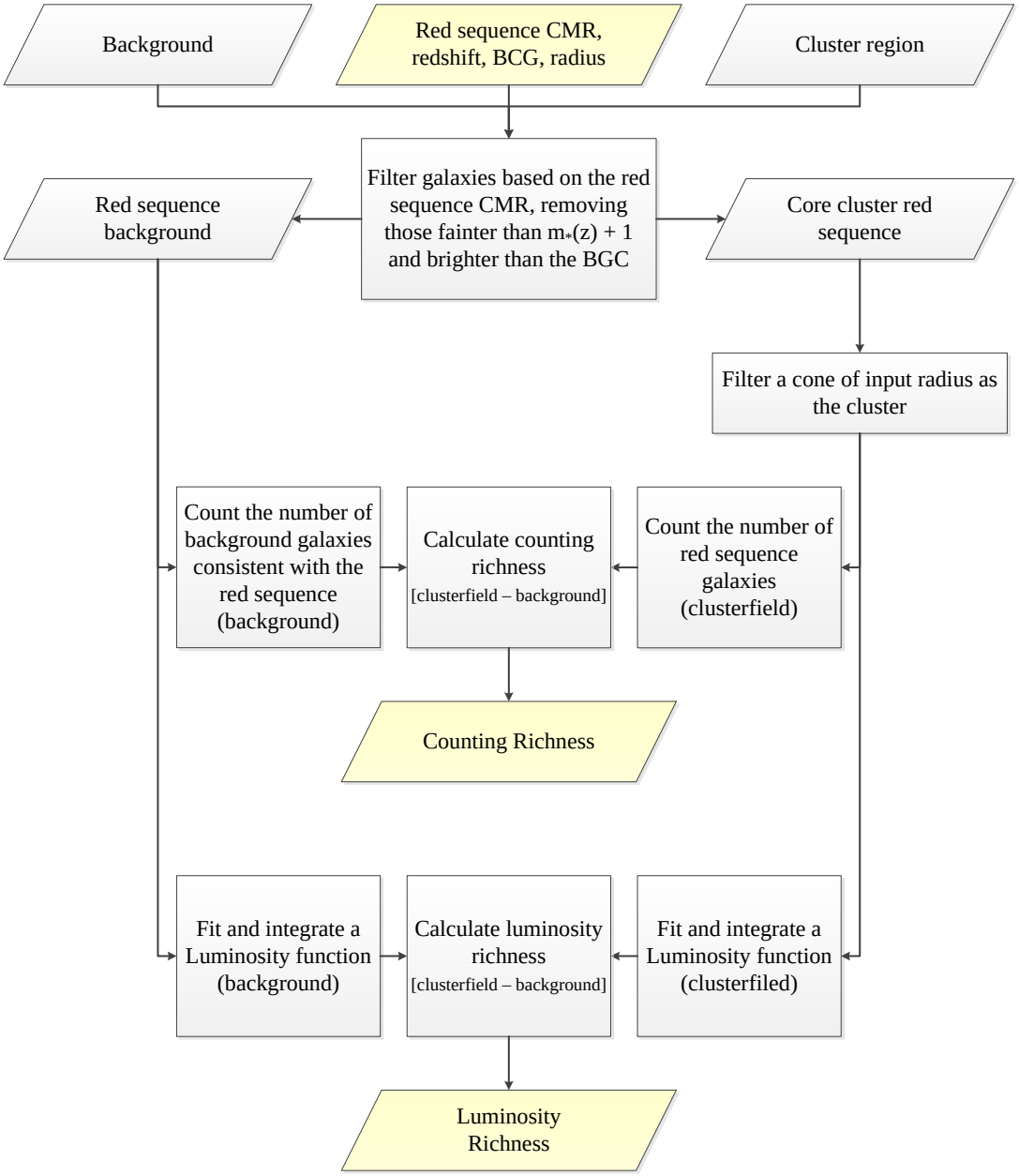

Figure 3.17 *A detailed flowchart showing the procedures of GMPhoRCC to estimate the cluster richness, highlighted as procedure 5 in Figure 3.1. An input radius of $0.5h^{-1}Mpc$ leads to the intermediate richness, n_{gals} with n_{200} given by r_{200}.*

3.2 Calibration with the Sloan Digital Sky Survey

Originally GMPhoRCC was intended to use the Pan-STARRS 3π survey as the source of optical data, providing the coverage and depth necessary to analyse the latest cluster catalogues, such as those from the Planck mission (Planck Collaboration et al., 2013). However delays with the optical data have shifted the focus to the Sloan Digital Sky Survey. The ninth data release presented in Ahn et al. (2012), provides coverage of $14,555$ square degrees in the northern hemisphere giving 95% completeness down to 21.3 magnitudes in i-band giving ~ 90 million suitable galaxies, ~ 1.5 million with spectra.

3.2.1 Photometry in DR9

The input optical data were selected from the Galaxy view of the PhotoObjAll table using the query summarised below to ensure cleanness and completeness in photometry.

```
SELECT * from GALAXY
WHERE

        (dered_i) < 21.0 AND

        (modelMagErr_g / dered_g) < 0.1 AND
        (modelMagErr_r / dered_r) < 0.1 AND
        (modelMagErr_i / dered_i) < 0.1 AND

        (insidemask)=0 AND
        (clean)=1 AND
        (extinction_i) < 0.5

        (dered_g - dered_r) BETWEEN -1.5 and 5 AND
        (dered_r - dered_i) BETWEEN -1.5 and 4 AND
        (dered_i - dered_z) BETWEEN -1.5 and 4 AND
```

Constraining the i-band magnitude ensures a consistent depth across the sky and provides a reasonable completion limit. Galaxies with extreme colours are

removed as these can adversely bias any Gaussian mixture fit. Also removing galaxies with photometric errors larger than 10% or flagged as sitting inside a mask helps maintain clean photometry reducing issues with possible nearby stars or poor seeing. Finally galaxies are removed which have been identified with either `BRIGHT`, `SATURATED`, `SATUR_CENTRE` or `AMOMENT` photometric flags.

3.2.2 Photometric redshifts

One of the fundamental properties of GMPhoRCC is the use of photometric redshifts[2] and with several available in DR9 it is necessary to select the most suitable. There are three main sources of redshifts available:

1. Template fitting. This involves fitting template galaxy spectral energy distributions (SEDs) to each object at various redshifts based on the multi-band photometry. The best fit provides a photometric redshift estimate.
2. Empirical. Here redshifts are found using an empirically trained relation between the galaxy photometric properties and redshift using a training set of galaxies with spectra.
3. Spectroscopic. These are determined by studying the full galaxy spectra and provide the most accurate and reliable measurement of redshift.

There are three main redshifts available in DR9. However to highlight the need for reliable estimates this section will also consider empirical redshifts from DR7 (consistent with GMBCG) and DR5 (consistent with maxBCG) as outlined below:

- $z_{spec-DR9}$. Around 1.5 million galaxy spectra are available in DR9 and as the most reliable estimate these redshifts are used where possible.
- z_{RF-DR9}. These DR9 redshifts are found empirically using a random forest machine learning technique developed by Carliles et al. (2010). Here the photometric properties of a training set, such as colour, are split into a binary tree structure such that the scatter in the spectroscopic redshifts in each branch is minimised. Branching occurs until a minimum number of galaxies is attained. Each branch is assigned a photometric redshift as

[2] see Section 2.1.3

the average of the branch-consistent subset of training galaxies. By using a random subset of the input parameters and repeating, a random forest of many independent trees can be constructed. For each tree an input galaxy is assigned a branch and redshift based on photometry and by averaging across the full forest, and owing to the central limit theorem, a photometric redshift can be found subject to a Gaussian error.

- z_{KF-DR9}. These DR9 redshifts are found empirically using a nearest neighbour fitting approach. Nearest neighbours in colour space are quickly identified by structuring the training set as a k-d tree. Photometric redshift is then calculated by fitting a local hyperplane to the spectroscopic redshifts and colours of the training set neighbours.

- z_{KF-DR7}. Following the same procedure as their DR9 counterparts these redshifts are trained from the smaller spectroscopic sample available from DR7.

- z_{NN-DR5}. These redshifts are obtained by training a neural net on the DR5 spectroscopic sample.

Using a photometric and spectroscopic subset of $\sim$ 30 million and $\sim$ 1 million galaxies respectively, Figure 3.18 confirms that each method can reasonably approximate the training set redshift distribution. However, larger differences are observed when extrapolating to other galaxies. These differences can have a huge impact on the red sequence redshift estimated by GMPhoRCC as shown in Figure 3.19. Here a spectroscopic subset of the GMBCG (Hao et al., 2010), NORAS (Böhringer et al., 2000), REFLEX (Böhringer et al., 2004) and XCS (Mehrtens et al., 2012) cluster catalogues are characterised with red sequence redshifts compared to spectra. There is a clear bias introduced by the poor z_{NN-DR5} photometric redshifts. With improved galaxy redshifts this issue has been resolved, with z_{RF-DR9} providing the best cluster estimates. While these results highlight the different methods it is noted that redshifts from later data releases are attained using larger spectroscopic training sets. Figure 3.20 shows how the GMPhoRCC estimate compares to spectra using the KF method to attain galaxy redshift from the DR9 and DR7 training sets. Although the DR9 training set is $\sim$ 50% larger than DR7, both KF redshifts give reasonable cluster estimates. Comparing the results attained using the various galaxy redshifts, Figure 3.21 shows that the RF and KF methods, particularly using the DR9 training set, provide the best GMPhoRCC estimates. In addition to attaining

the most accurate GMPhoRCC estimates, z_{RF-DR9} has well understood Gaussian errors, providing ideal redshifts for use with the error-corrected Gaussian mixture framework set out in Section 3.1.1, hence are used as the main source of photometric redshifts for GMPhoRCC.

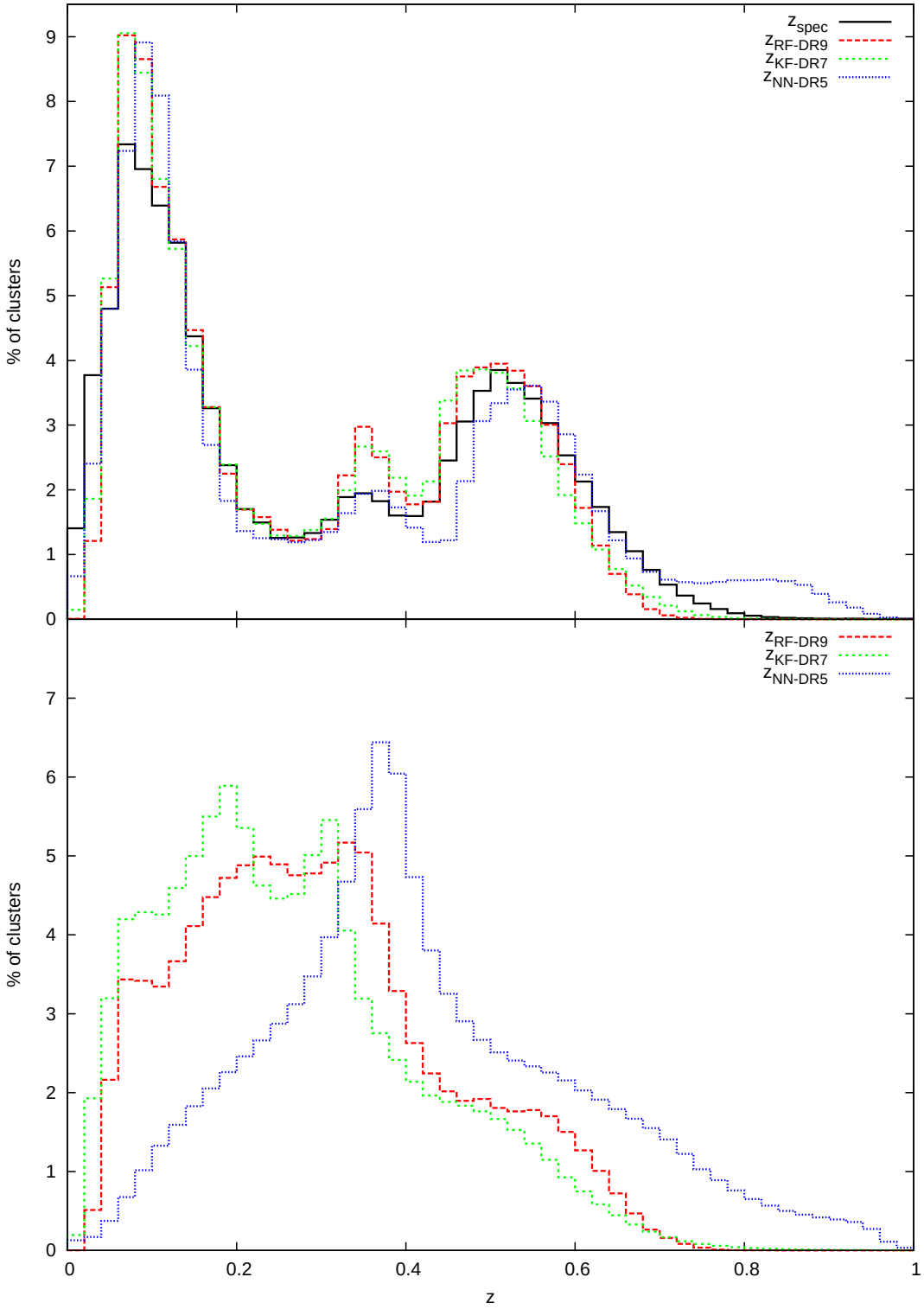

Figure 3.18 *A comparison of the different redshift distributions for the same 30 million galaxies. As expected the different methods are able to reasonably approximate the training set distributions.*

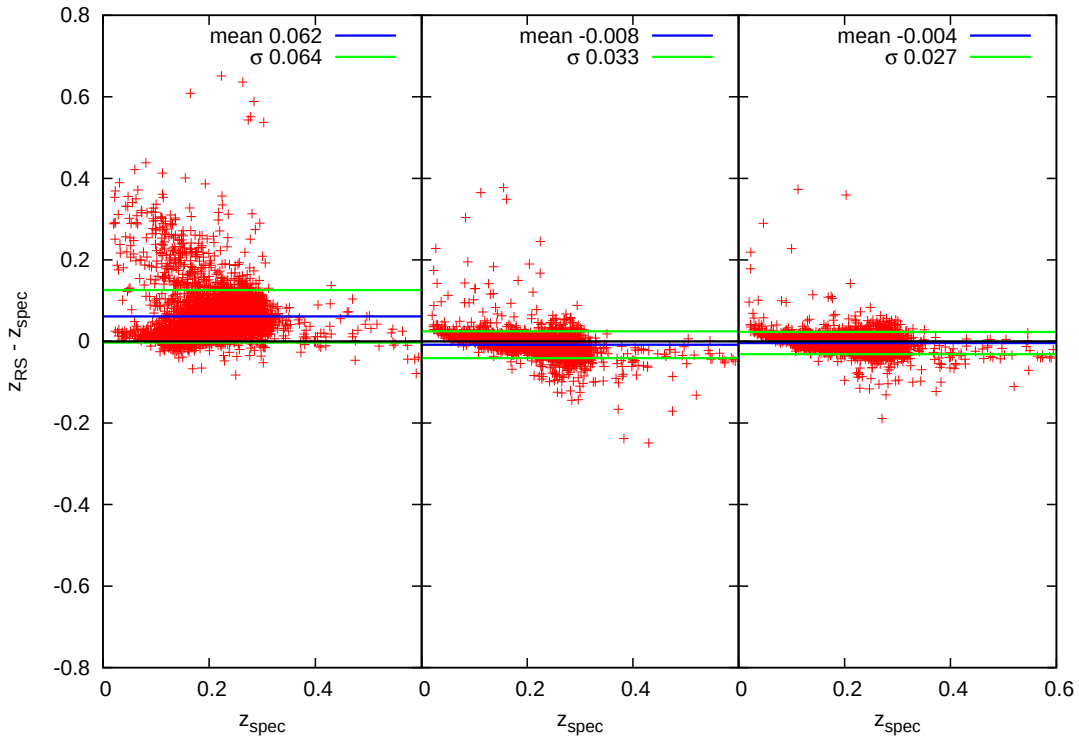

Figure 3.19 *A comparison of the GMPhoRCC red sequence redshift to spectra for a subset of the GMBCG, NORAS, REFLEX and XCS catalogues showing from left to right results using z_{NN-DR5}, z_{KF-DR7} and z_{RF-DR9} galaxy redshifts. There is a clear bias introduced by the poor z_{NN-DR5} photometric redshifts. With improved galaxy redshifts this issue has been resolved, with z_{RF-DR9} providing the best cluster estimates. With the larger training set (50% larger than DR7) and well understood Gaussian errors, z_{RF-DR9} provides the most appropriate photometric redshifts for use with GMPhoRCC.*

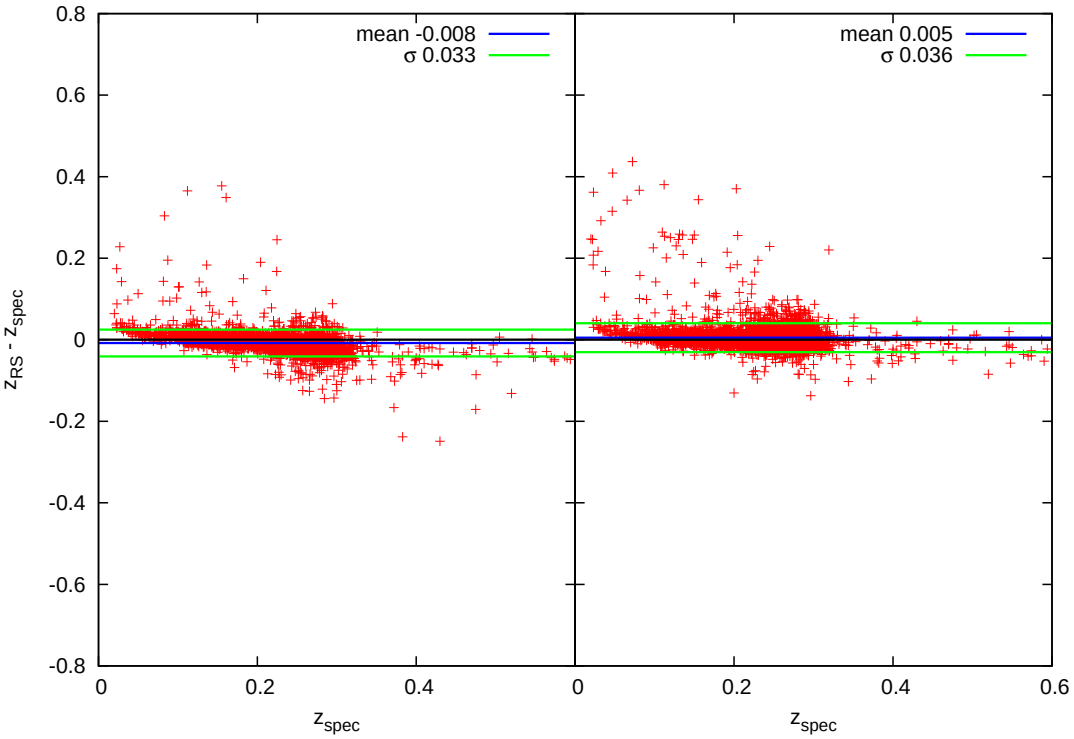

Figure 3.20 *A comparison of the GMPhoRCC red sequence redshift to spectra for a subset of the GMBCG, NORAS, REFLEX and XCS catalogues showing in the left and right panels, results using z_{KF-DR7} and z_{KF-DR9} respectively. Although the DR9 training set is $\sim 50\%$ larger than DR7, both KF redshifts give reasonable cluster estimates.*

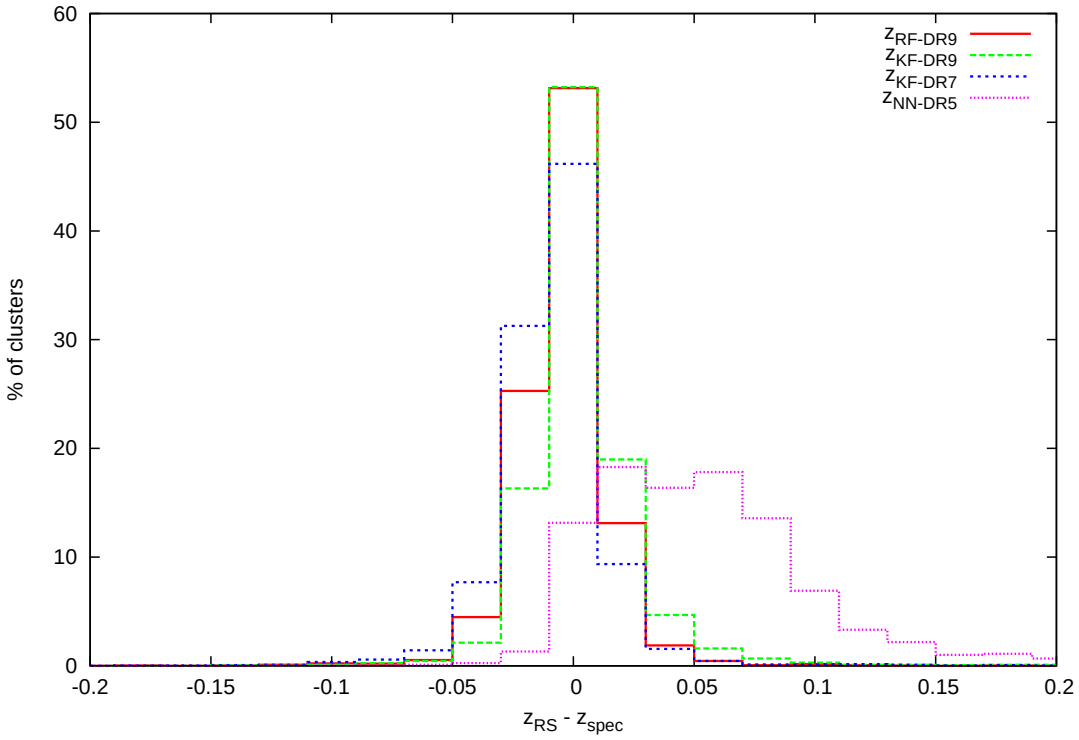

Figure 3.21 *A histogram comparison of the GMPhoRCC red sequence redshift to spectra for a subset of the GMBCG, NORAS, REFLEX and XCS catalogues using z_{RF-DR9}, z_{KF-DR7} and z_{NN-DR5} galaxy redshifts. This highlights the previously discussed bias introduced by the poor z_{NN-DR5} photometric redshifts. Again with improved galaxy redshifts this issue has been resolved with z_{RF-DR9} providing the best cluster estimates.*

3.2.3 Aperture Calibration

As described in Section 3.2.1, it is essential to select optical data to sample not only the cluster but also a local background. Without any prior information relating to the cluster size it is necessary to split the field to ensure a large enough region to encapsulate the largest candidates, and a background annulus with no significant cluster contribution. Figure 3.22 shows the angular size of the initial fixed aperture used to define n_{gals} as a function of redshift. For all but the very lowest redshift clusters a $30'$ radius cone will capture the fixed aperture. Extending this to r_{200} as shown in Figure 3.23 confirms the $30'$ cone covers even the richest clusters. Using GMBCG-1 as an example of a rich clusters, Figure 3.24 again shows a $30'$ radius cone to be a suitable cluster region.

In order to provide a background measure it is necessary to balance the area to provide adequate sampling without giving unnecessarily large numbers of galaxies which will degrade the computational performance of the fitting procedures. An RA-Dec rectangle is chosen to encompass a 1^o cone, this provides a background annulus similar in area to the initial cluster region. Using this rectangle rather than a cone is simply done for convenience as this is often the most efficient way to sample an optical database with indexing.

In order to model the red sequence as part of GMPhoRCC it is necessary to extract a core region of the cluster dominated by early type galaxies as shown in Section 3.1.3. This procedure is similar to that used in High et al. (2010), where a $2'$ cone is used to represent the cluster core however from Figures 3.22 and 3.23 this may not be suitable for all clusters. In order to sample the core across a range of redshifts and richnesses, cones with radii $1'$, $2'$, $3'$ and $4'$ are used. This provides small sampling suitable for low richness / high redshift clusters and large enough for high richness / low redshift. The core cluster radius is selected as the one which maximises the overdensity as shown in Section 3.1.3.

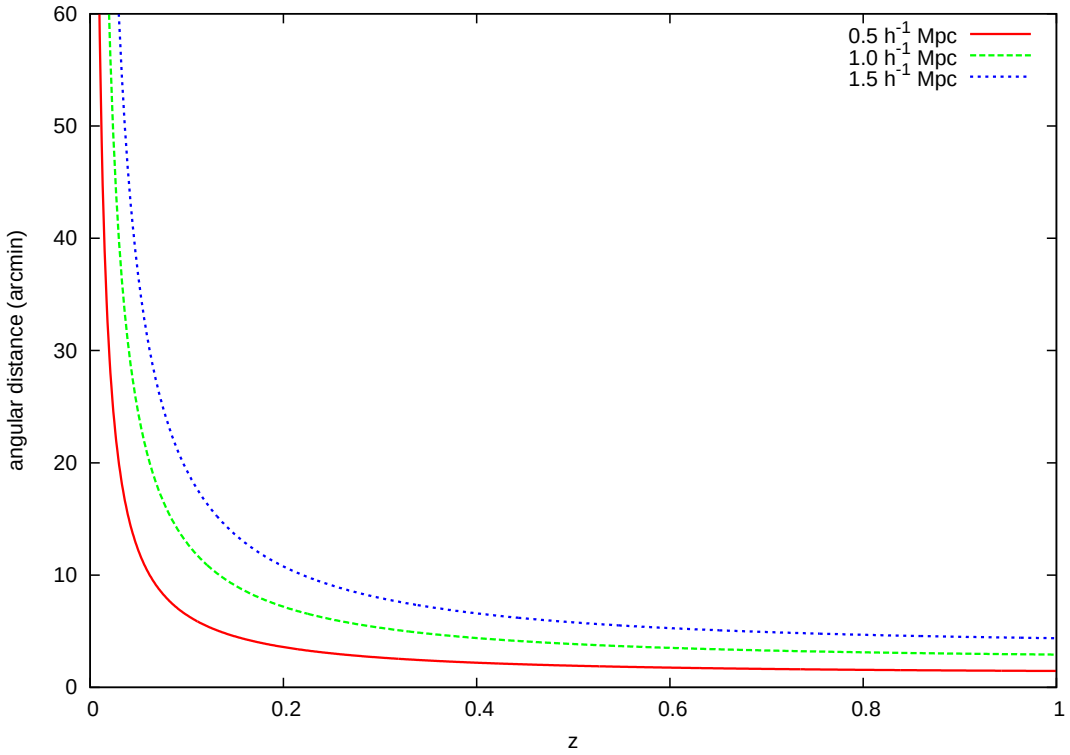

Figure 3.22 *The angular separation of a fixed comoving distance as a function of redshift. Setting the initial cluster regions as a* $30'$ *cone will encapsulate the* n_{gals} *fixed aperture for all but the very lowest redshift clusters.*

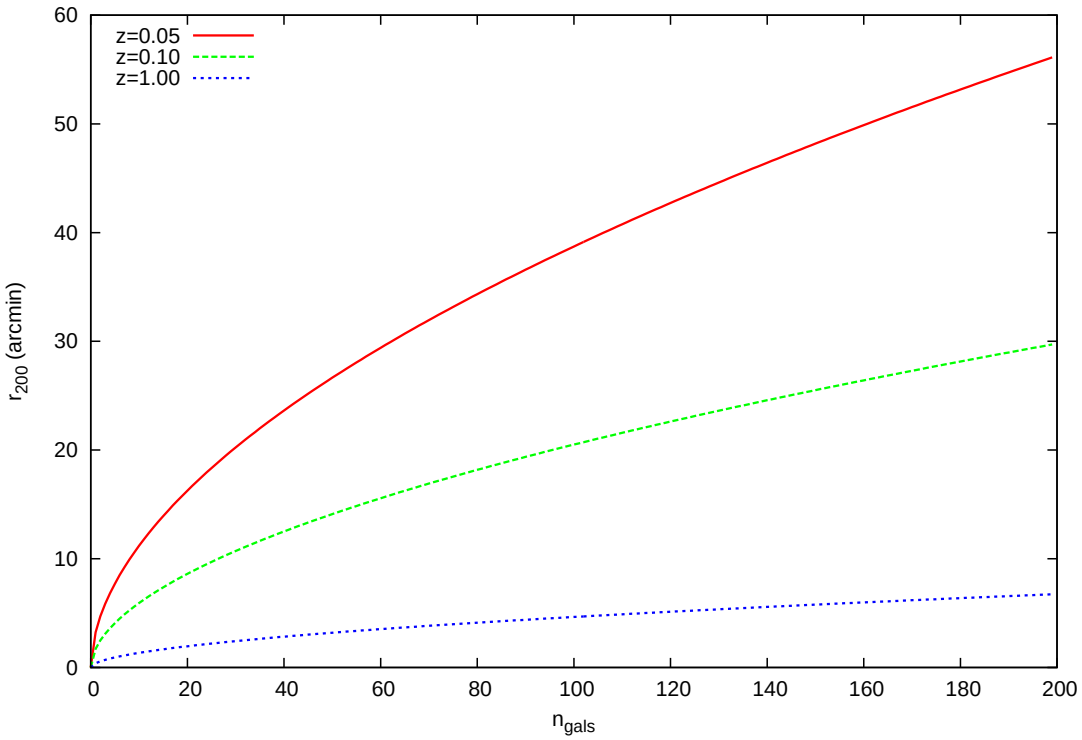

Figure 3.23 *The angular radius of r_{200} as a function of n_{gals}. Again a $30'$ radius cone has proven to be an appropriate size for the cluster region.*

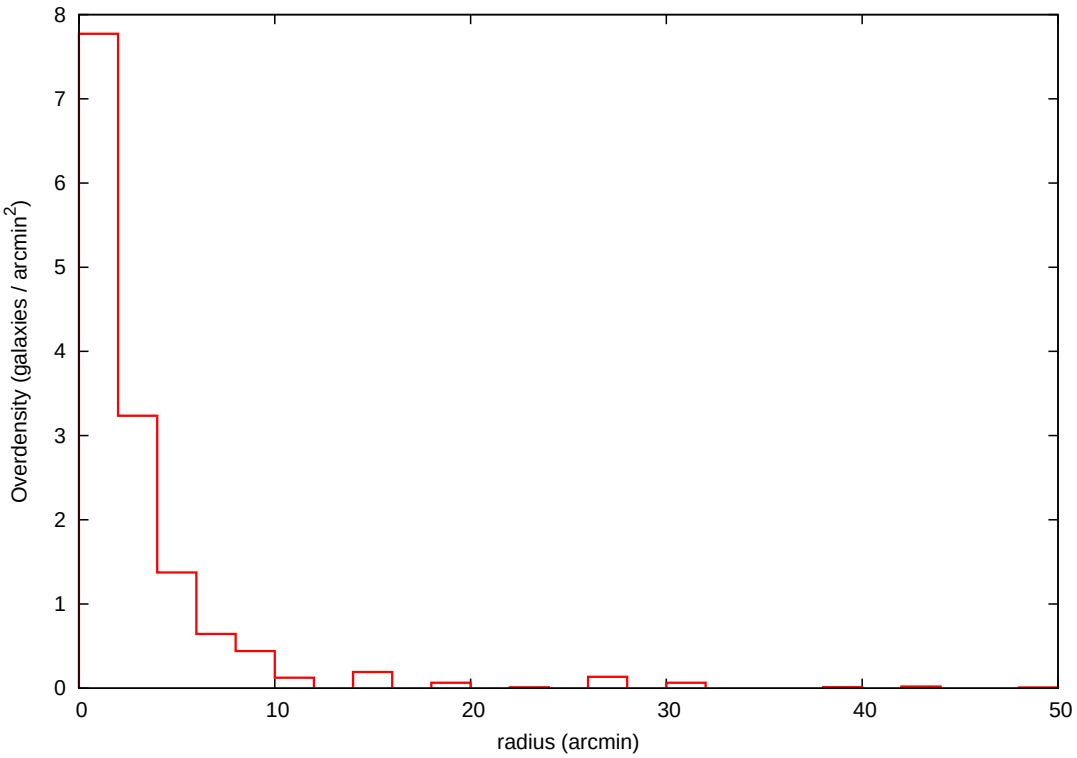

Figure 3.24 *The radial distribution of the rich cluster GMBCG-1. The cluster is completely encapsulated by a $30'$ cone.*

3.2.4 Quality Control

One of the main goals of GMPhoRCC is to provide a means of quality control to help identify possible catastrophic failures. As part of this many flags have been introduced to trace how the specific cluster has propagated through the algorithm. As shown in Section 2.3.4 a large source of ambiguity in cluster analysis is the presence of multi-modal distributions, where assigning values to redshift or red sequence colour is not straightforward. The first set of flags, detailed in Table 3.4, indicates issues with the various cluster distributions relating to multiple peaks with increasing severity. Unfortunately in practice many clusters (around 70%) show signs of multiple peaks and as such these flags alone are insufficient to identify problems.

Inconsistent redshifts or low richnesses may also indicate problems with the analysis and as such are the focus of the next set of flags shown in Table 3.5. Checking for consistencies in the red sequence and the BCG redshifts can be particularly useful if the underlying photometric redshifts are unreliable, as a bright galaxy, the BCG redshift should be more reliably estimated than the rest of the red sequence and in the case of DR9 may even have a spectroscopic measurement. If these inconsistencies dominate the target clusters it may be more useful to use the BCG redshift as a measure of the cluster as demonstrated in the GMBCG catalogue. Using DR7 redshifts these consistency checks are important and indeed suggest the BCG redshift is the more reliable estimate, however these problems are no longer an issue with the improved DR9 redshifts. Although there are few issues with redshift consistencies in DR9 these flags remain to help calibration with other optical sources such as Pan-STARRS.

The most significant indicator of catastrophic failure is the detection of very low richness. Firstly this indicates that the distribution modelling may be unreliable, fitting many parameters to only a few data points. However more importantly this could indicate an issue with the red sequence, either the candidate cannot be optically confirmed as a cluster or the red sequence has been missed altogether. In either case this is the strongest indication of catastrophic failure.

The final set of flags relates to non-detection and highlights exactly where in the algorithm the cluster is not found. This mainly indicates poor photometry where galaxies may be missing due to masking, high errors, poor seeing or the presence of unobserved regions.

Name	Value	Description
MULTI_BANDS	0x000000000001	Multiple bands considered
POOR_CMR_FIT	0x000000000002	Poor CMR fit, $\chi^2 > 5$
INAPPROPRIATE_Z	0x000000000004	One or more of the redshift estimates not appropriate for RS band
MULTI_INITIAL	0x000000000010	Multiple peaks in initial z distribution - relative heights < 5
MULTI_INITIAL_AMBIGUOUS	0x000000000020	Multiple peaks in initial z distribution - relative heights < 2
MULTI_INITIAL_CLOSE	0x000000000040	Primary and secondary peak within 0.1 of each other
MULTI_COLOUR	0x000000000100	Multiple peaks in the colour distribution - relative heights < 5
MULTI_COLOUR_AMBIGUOUS	0x000000000200	Multiple peaks in the colour distribution - relative heights < 2
MULTI_COLOUR_CLOSE	0x000000000400	Primary and secondary peak within 0.2 mag of each other
MULTI_ZFLAT	0x000000001000	Multiple peaks in the flat RS z fit - relative heights < 5
MULTI_ZFLAT_AMBIGUOUS	0x000000002000	Multiple peaks in the flat RS z fit - relative heights < 2
MULTI_ZFLAT_CLOSE	0x000000004000	Primary and secondary peak within 0.1 of each other
MULTI_ZRS	0x000000010000	Multiple peaks in the RS z fit - relative heights < 5
MULTI_ZRS_AMBIGUOUS	0x000000020000	Multiple peaks in the RS z fit - relative heights < 2
MULTI_ZRS_CLOSE	0x000000040000	Primary and secondary peak within 0.1 of each other

Table 3.4 *A list of the GMPhoRCC flags relating to the detection of multi-modal distributions. Unfortunately as $\sim 70\%$ of cluster have exhibit multi-modal distributions these are insufficient to identify catastrophic failures.*

By combining these flags, quality markers are assigned to clusters as an indicator of the reliability of the optical characterisation and are shown in Table 3.7. Finally the analysed clusters can be separated into various quality subsets, as shown in Table 3.8; 'clean' with quality < 2 representing the cleanest set with most problem clusters removed; 'mid' with quality < 3, a middle subset with only the worst clusters removed; and 'detection' with quality < 4, the full list of clusters considered to have been detected. While these subsets are largely independent of the optical input it is noted that the BCG and red sequence redshift consistency check is specific to the SDSS DR9 and should be calibrated based on the quality of the available redshifts.

Name	Value	Description
INCONSISTENT_Z_0_025	0x000000100000	Cluster z_{RS} and z_{BCG} are not consistent with each other, $\|z_{RS} - z_{BCG}\| > 0.025$
LOW_RICHNESS_N200_3	0x000000200000	Low counting richness recovered, $n_{200-count} < 3$
INCONSISTENT_Z_0_050	0x000001000000	Cluster z_{RS} and z_{BCG} are not consistent with each other, $\|z_{RS} - z_{BCG}\| > 0.050$
LOW_RICHNESS_N200_1	0x000002000000	Low counting richness recovered, $n_{200-count} < 1$
INCONSISTENT_Z_0_100	0x000004000000	Cluster z_{RS} and z_{BCG} are not consistent with each other, $\|z_{RS} - z_{BCG}\| > 0.100$
SPARCE_INITIAL	0x000010000000	< 5 Galaxies found in the cluster region for the initial z fit
SPARCE_COLOUR	0x000020000000	< 5 Galaxies found in the cluster region for the colour fit
SPARCE_ZFLAT	0x000040000000	< 5 Galaxies found in the cluster region for the flat RS z fit
SPARCE_ZRS	0x000080000000	< 5 Galaxies found in the cluster region for the RS z fit

Table 3.5 *A list of GMPhoRCC flags indicating issues with the redshift or richness estimates. These give the strongest indication an estimate may be erroneous.*

Using a spectroscopic sample of the GMBCG catalogue, the effect of the quality subsets can been seen. Figures 3.25 and 3.26 show how the GMPhoRCC redshift compares with spectra for the different quality subsets. It is clear that the quality subsets are able to progressively identify and remove the worst outliers with the clean set attaining the best estimates with lowest scatter. Rather promisingly the majority of clusters agree within $|z_{RS} - z_{spec}| < 0.01$ with the clean set attaining the highest fraction of clusters inside this bound. In addition to this, Figure 3.27 shows how the comparison compares for the various richness and redshift consistency checks used to calculate the quality marker. Clusters with inconsistencies between the BCG and red sequence redshift and separately those with low richness are those with the worst estimates, highlighting these as valuable indicators of probable catastrophic failures.

Meaningful comparisons with richness can be difficult to achieve as this requires the input catalogues and the specific richness measures to match (see Section 3.4.2).

Name	Value	Description
NO_OVERDENSITY_INITIAL	0x000100000000	No overdensity found in the cluster region for the initial z fit
NO_OVERDENSITY_COLOUR	0x000200000000	No overdensity found in the cluster region for the colour fit
NO_OVERDENSITY_ZFLAT	0x000400000000	No overdensity found in the cluster region for the flay RS z fit
NO_OVERDENSITY_ZRS	0x000800000000	No overdensity found in the cluster region for the RS z fit
NO_CLUSTER_INITIAL	0x001000000000	0 Galaxies found in the cluster region for the initial z fit
NO_CLUSTER_COLOUR	0x002000000000	0 Galaxies found in the cluster region for the colour fit
NO_CLUSTER_ZFLAT	0x004000000000	0 Galaxies found in the cluster region for the flat RS z fit
NO_CLUSTER_ZRS	0x008000000000	0 Galaxies found in the cluster region for the RS z fit
CLUSTER_INSIDE_MASK_0_5_MPC	0x010000000000	Empty apertures found inside $r < 0.5\mathrm{h}^{-1}$ Mpc of cluster centre
CLUSTER_INSIDE_MASK_R200	0x020000000000	Empty apertures found inside $r < r_{200}$ of cluster centre
CLUSTER_INSIDE_MASK_5_AM	0x040000000000	Empty apertures found inside $r < 5'$ of cluster centre
NO_DETECTION_REDSHIFT	0x100000000000	No detection in redshift module
NO_DETECTION_RICHNESS_NGALS	0x200000000000	No detection in richness, $n_{gals} < 0$ for both counting and luminosity method
NO_DETECTION_RICHNESS_N200	0x400000000000	No detection in richness, $n_{200} < 0$ for both counting and luminosity method
NO_COVERAGE	0x800000000000	No optical coverage

Table 3.6 *A list of GMPhoRCC flags relating to the non-detection of a cluster overdensity.*

Quality	Flags Value (decimal)	Indicator Flags
5	$140737488355328 \leq$ flags	NO_COVERAGE
4	$17592186044416 \leq$ flags < 140737488355328	NO_DETECTION_REDSHIFT NO_DETECTION_RICHNESS_NGALS NO_DETECTION_RICHNESS_N200
3	$16777216 \leq$ flags < 17592186044416	INCONSISTENT_Z_0_050 LOW_RICHNESS_1 INCONSISTENT_Z_0_100 SPARCE_INITIAL SPARCE_COLOUR SPARCE_ZFLAT SPARCE_ZRS NO_OVERDENSITY_INITIAL NO_OVERDENSITY_COLOUR NO_OVERDENSITY_ZRS NO_OVERDENSITY_ZRS NO_CLUSTER_INITIAL NO_CLUSTER_COLOUR NO_CLUSTER_ZFLAT NO_CLUSTER_ZRS CLUSTER_INSIDE_MASK_0_5_MPC CLUSTER_INSIDE_MASK_R200 CLUSTER_INSIDE_MASK_5_AM
2	$1048576 \leq$ flags < 16777216	INCONSISTENT_Z_0_025 LOW_RICHNESS_3
1	flags < 1048576	-

Table 3.7 *A list of the quality markers assigned to clusters based on the GMPhoRCC flags.*

Subset	Quality	Description
Detection	< 4	All clusters considered to have been detected i.e. estimates were found for both redshift and richness
Mid	< 3	An intermediate subset removing the worst outliers i.e. removing clusters with very low richness or large discrepancies between redshift estimates
Clean	< 2	The cleanest subset removing the majority of outliers i.e. removing cluster with low richness and discrepancies between redshift estimates

Table 3.8 *A list cluster subsets based on the GMPhoRCC quality markers used remove potentially erroneous characterisations.*

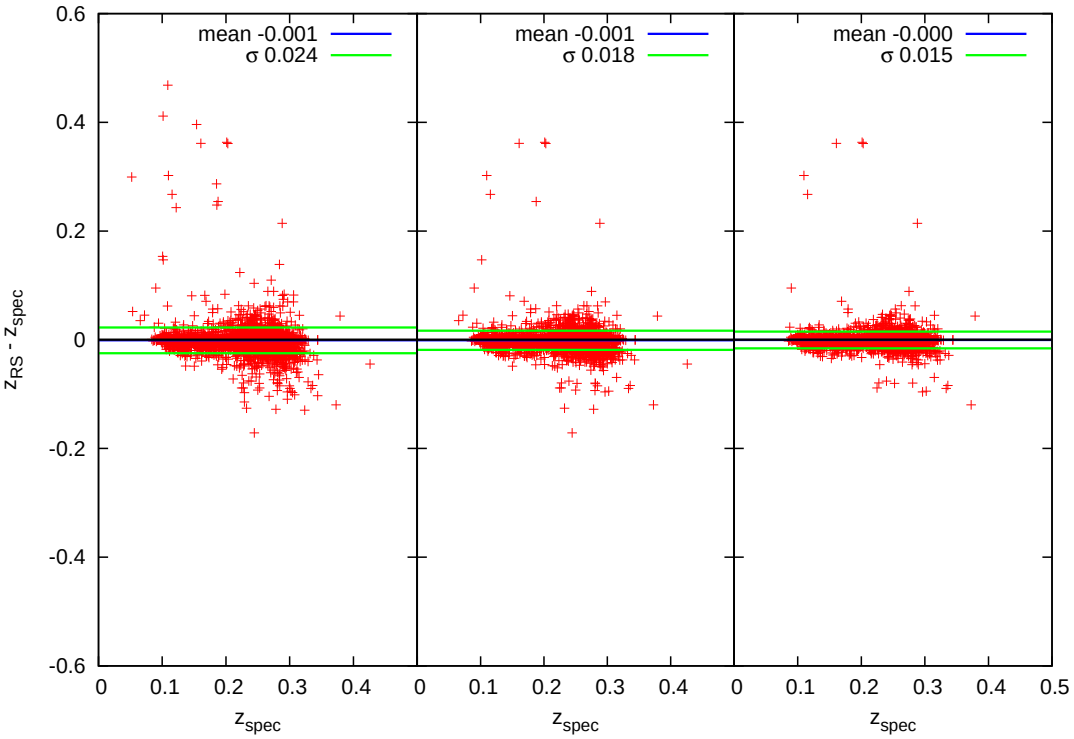

Figure 3.25 *A comparison of the GMPhoRCC red sequence redshifts to spectra using* 3776 *spectroscopic clusters from the GMBCG catalogue showing from left to right the detection, mid and clean subsets. The clean subset attains the fewest outliers and lowest scatter around the spectroscopic redshift highlighting the ability of the quality markers to identify problem clusters.*

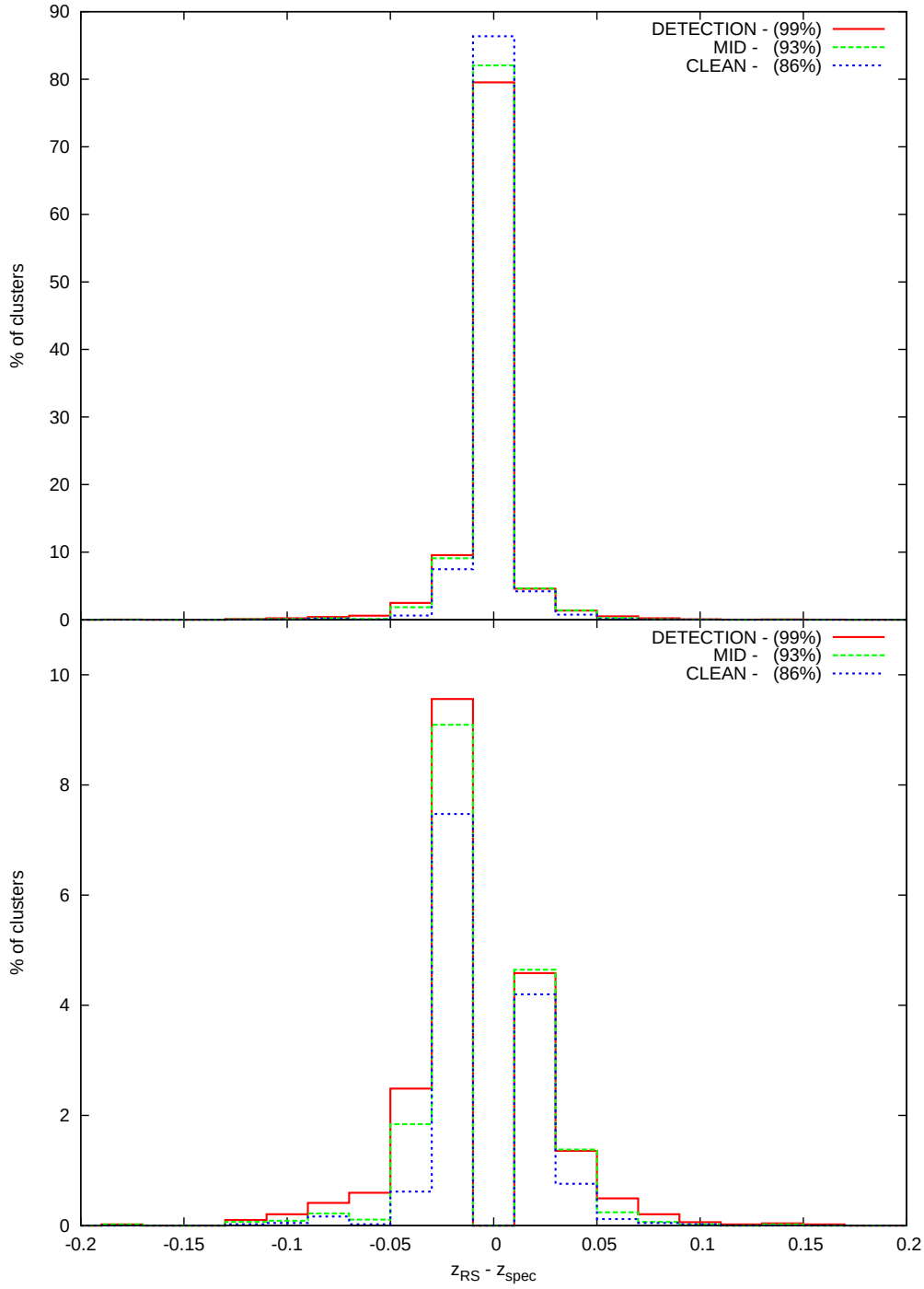

Figure 3.26 *A normalised histogram comparison of the GMPhoRCC red sequence redshift compared to spectra using* 3776 *spectroscopic clusters from the GMBCG catalogue. The comparison has been normalised and split into the separate quality bands where the legend shows the fraction of the total clusters in the subset. The bottom panel omits the middle bin to highlight the outliers where the clean subset can be seen to have removed the worst estimates with a greater fraction within* $|z_{RS} - z_{spec}| < 0.01$

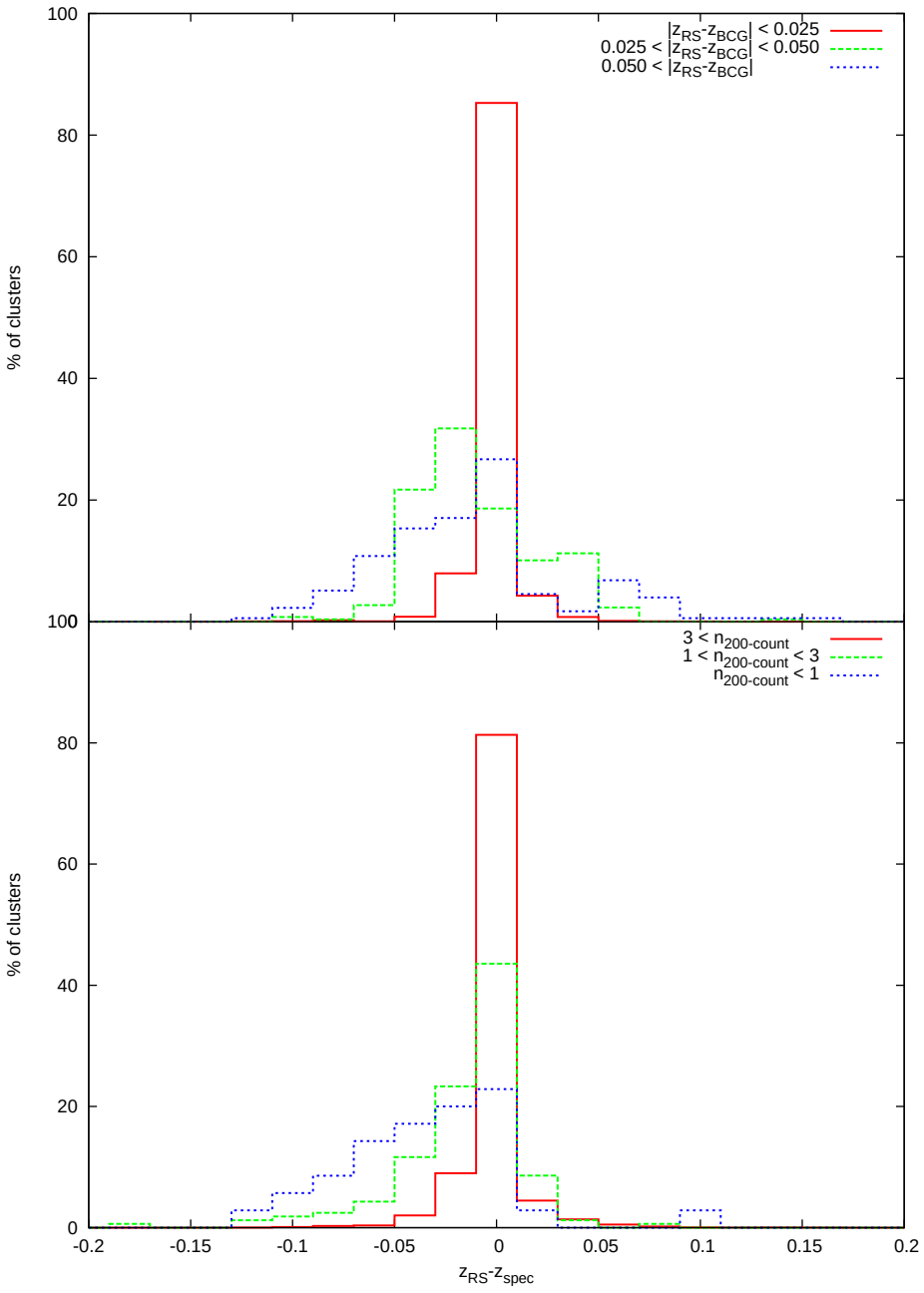

Figure 3.27 *A normalised histogram comparison of the GMPhoRCC red sequence redshift compared to spectra using* 3776 *spectroscopic clusters from the GMBCG catalogue. The top panel splits clusters based on the redshift consistency check used to calculate the quality marker, where it is clear those with larger discrepancies have the worst estimates. The bottom panel considers the low richness consistency checks, where those with the lowest richnesses attain the worst estimates. It is clear both the redshift and richness consistency checks as valuable tools to help identify potential catastrophic failures.*

3.3 The Complete GMPhoRCC

Consolidating the framework developed in this chapter the complete GMPhoRCC can now be defined. At the basic level this algorithm identifies a red sequence around a cluster candidate to provide model-independent estimates of redshift and richness. The main features include:

1. Red sequence detection: GMPhoRCC classifies candidates by isolating the red sequence and using these galaxies to infer the properties of the cluster.
2. Model Independence: Empirical photometric redshifts are used to remove the dependence on colour-redshift models used in many other algorithms.
3. Full red sequence CMR: The red sequence is modelled as a CMR recovering slope, intercept and intrinsic width.
4. Multiple red sequence bands: In order to characterise across a large range of redshift, maximise colour overdensity and improve contrast against the background, several redshift-dependent colour bands are used.
5. Multi-modal distributions: By analysing each peak in the various cluster distributions as potential candidates, a primary and secondary cluster is determined in ambiguous cases.
6. Extrapolation: With incomplete photometry richness can be extrapolated by fitting and integrating a luminosity function provided an adequate sample of bright galaxies remain.
7. Quality Control: Each cluster candidate is assigned a quality marker relating to how well the cluster has been characterised by GMPhoRCC. Several subsets are produced where problem clusters and potential outliers are identified and removed from the cleanest sample.

The basic form of the GMPhoRCC is outlined in Figure 3.28 with Figures 3.29 - 3.35 expanding on each of the procedures in detail. The first step, procedure 1 shown in Figure 3.29, estimates an initial redshift for the cluster by modelling the photometric redshift distribution from which appropriate red sequence colour bands can be selected. Procedure 2 shown in Figure 3.29, first filters around this initial estimate removing galaxies with inconsistent redshifts or too faint,

with the cut-off shown in Figure 3.31. Next, procedure 3 estimates an initial colour estimate by modelling the remaining galaxy colour distribution as shown in figure 3.30. Further filtering around this colour, Procedure 4 fits a CMR to the remaining galaxies to model the red sequence, as shown in Figure 3.32. By filtering the red sequence and modelling the redshift distribution a final estimate is found as shown in Procedure 5 and Figure 3.33. In the case of multi-modal distributions a primary and secondary characterisation is found using the selection process defined in Figure 3.34 using Tables 3.9 and 3.10. The final procedure estimates richness by two methods, counting galaxies and fitting and integrating a luminosity function as shown in Figure 3.35.

The various parameters produced by GMPhoRCC are shown in Table 3.11. In the case where GMPhoRCC was unable to determine a property a default value of -1 is used. Although these are independent of the optical input it is noted that the determination of the quality marker, as defined by Table 3.7, is calibrated specifically for use with the SDSS DR9. Constraints on the consistency of the BCG and red sequence redshift must be adjusted to match the specific input photometry and redshifts. Once appropriately calibrated these quality markers are used to define subsets of clusters as shown in Table 3.12 which remove those with potentially erroneous estimates.

Red sequence band	redshift range
$g-r$	$0.00 \leq z < 0.45$
$r-i$	$0.35 \leq z < 0.75$
$i-z$	$0.65 \leq z$

Table 3.9 *A tight redshift-band relation for the red sequence used to remove candidates with inappropriate redshift/band combinations.*

cleanness band	description
4	One or more of the main redshift estimators has not been found.
3	The red sequence and BCG redshift disagree by more than 0.1
2	All three estimators are not consistent with the colour band
1	All remaining candidates.

Table 3.10 *A list of the cleanness bands used to rank potential clusters where smaller numbers represent the most desirable candidates.*

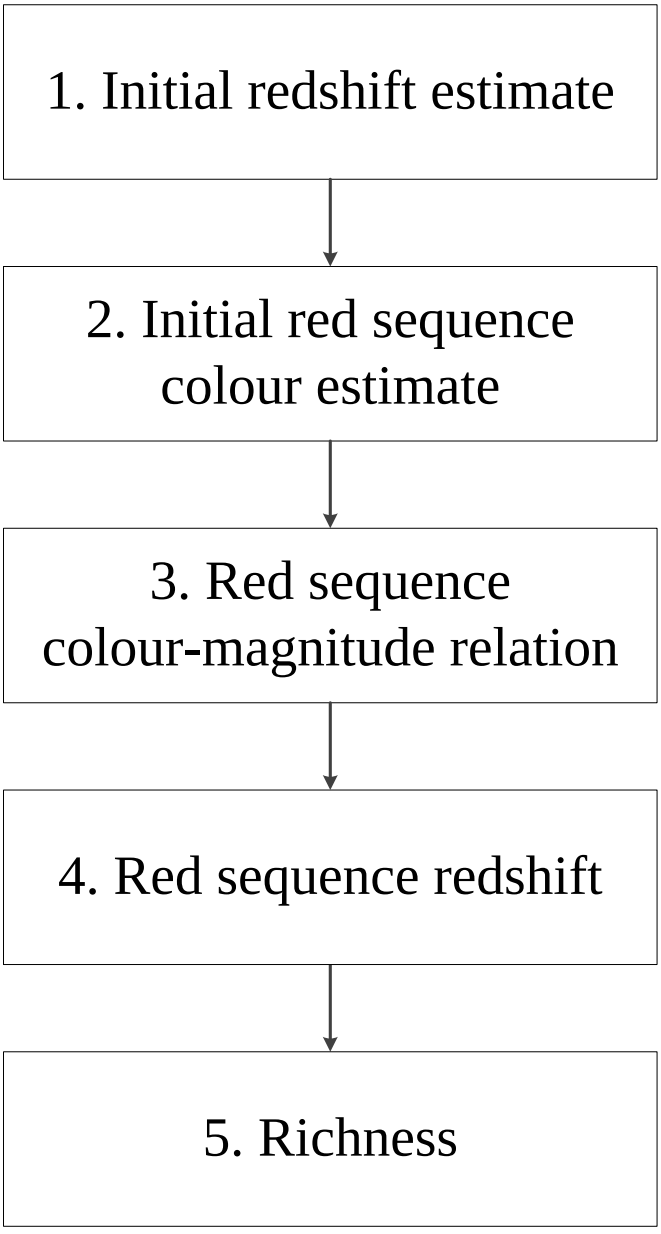

Figure 3.28 *A flowchart summarising the basic steps of GMPhoRCC to determine the red sequence CMR, cluster redshift and richness.*

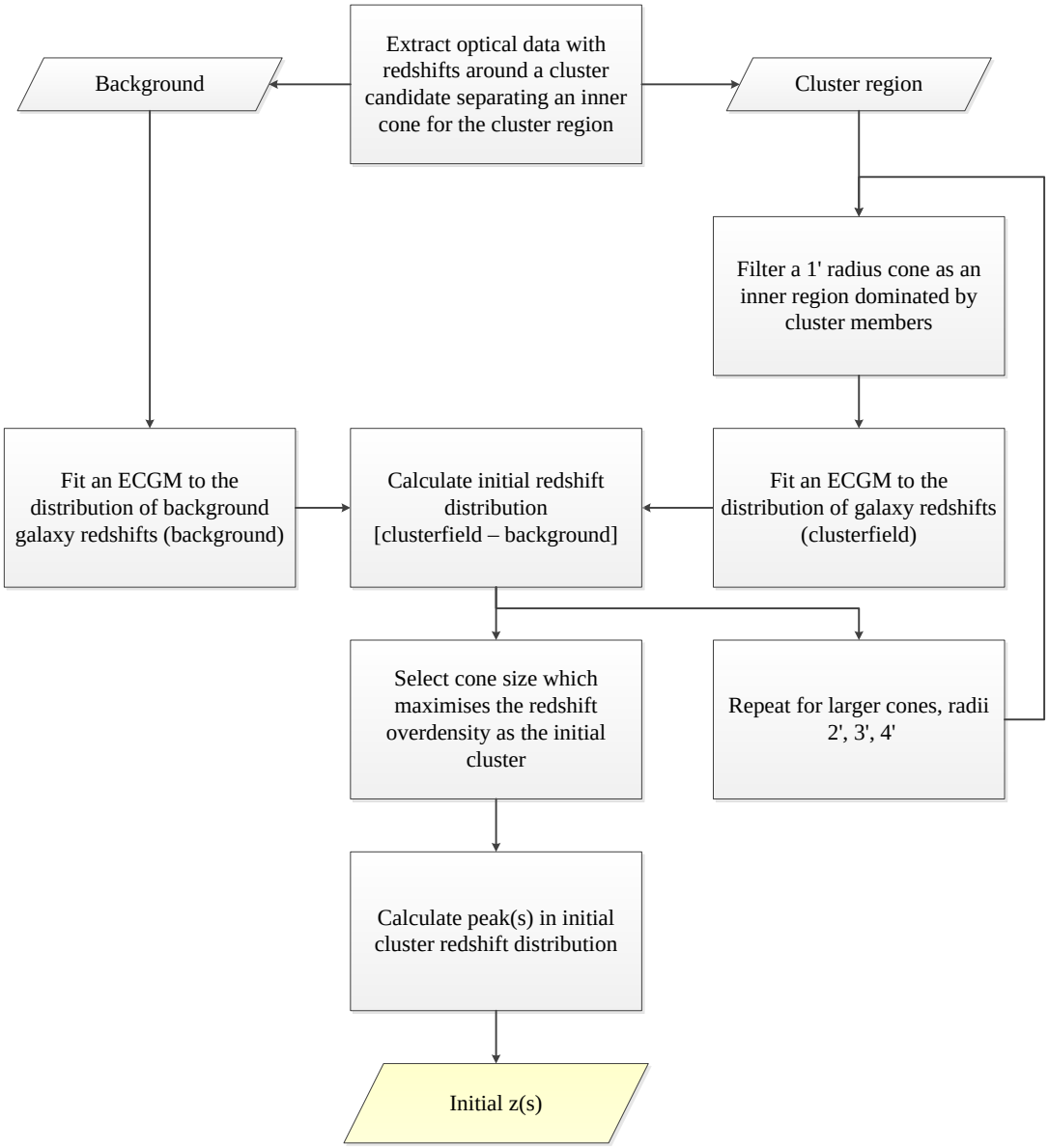

Figure 3.29 *A detailed flowchart showing the procedures of GMPhoRCC to determine an initial cluster redshift estimate highlighted as procedure 1 in Figure 3.28.*

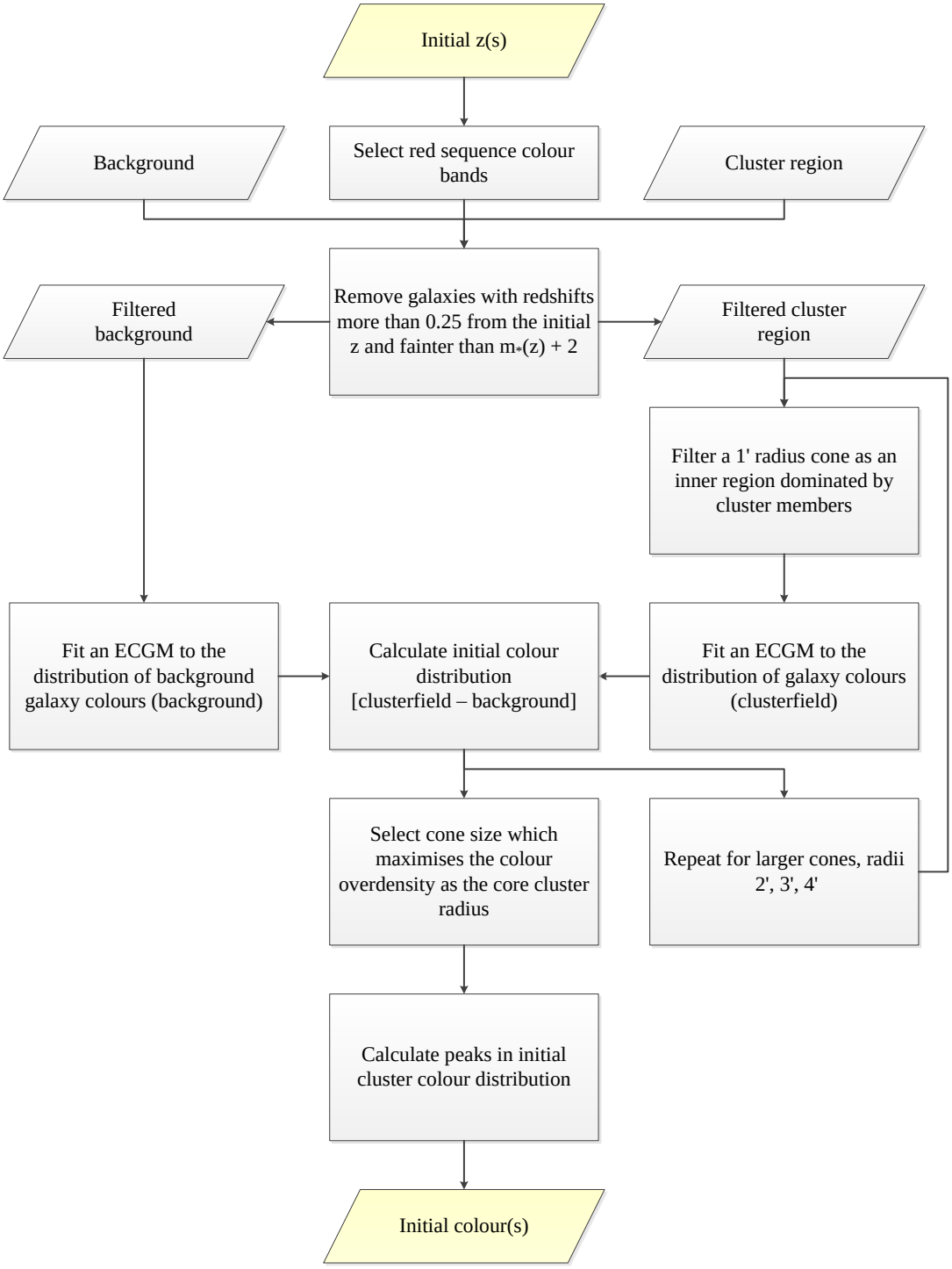

Figure 3.30 *A detailed flowchart showing the procedures of GMPhoRCC to determine an initial red sequence colour estimate, highlighted as procedure 2 in Figure 3.28. The form of m_*, used to define the faint end cut-off is shown in Figure 3.31*

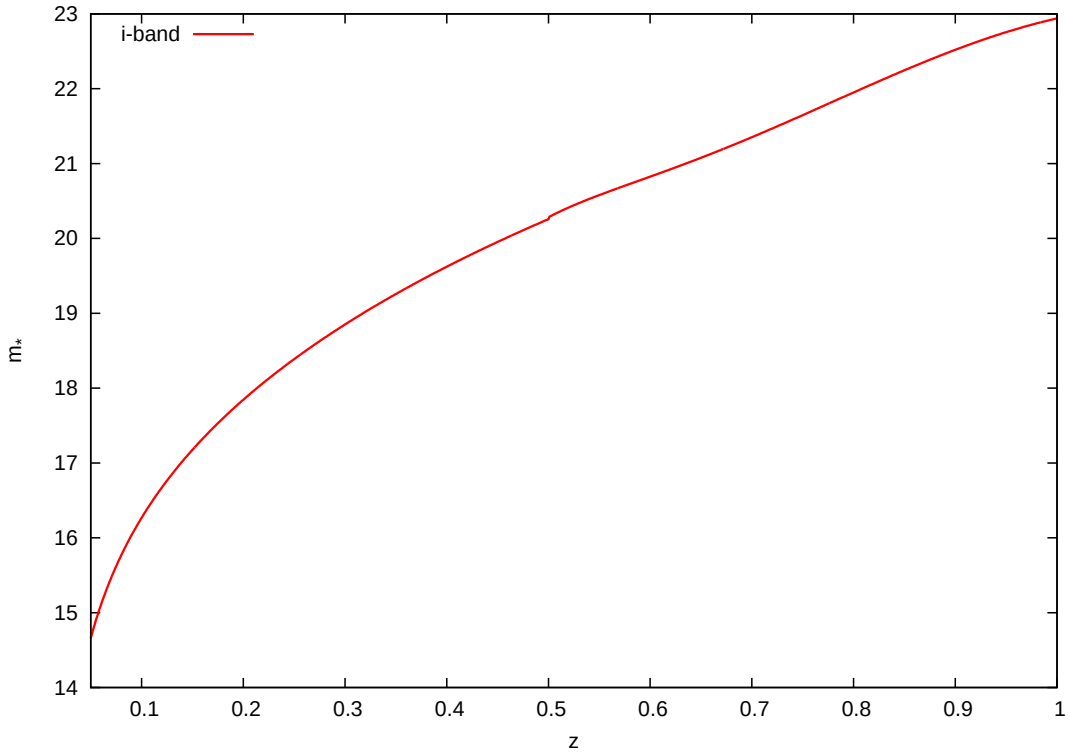

Figure 3.31 *The form of the m_* used to define the faint end cut-off to maintain a consistent magnitude range as a function of redshift.*

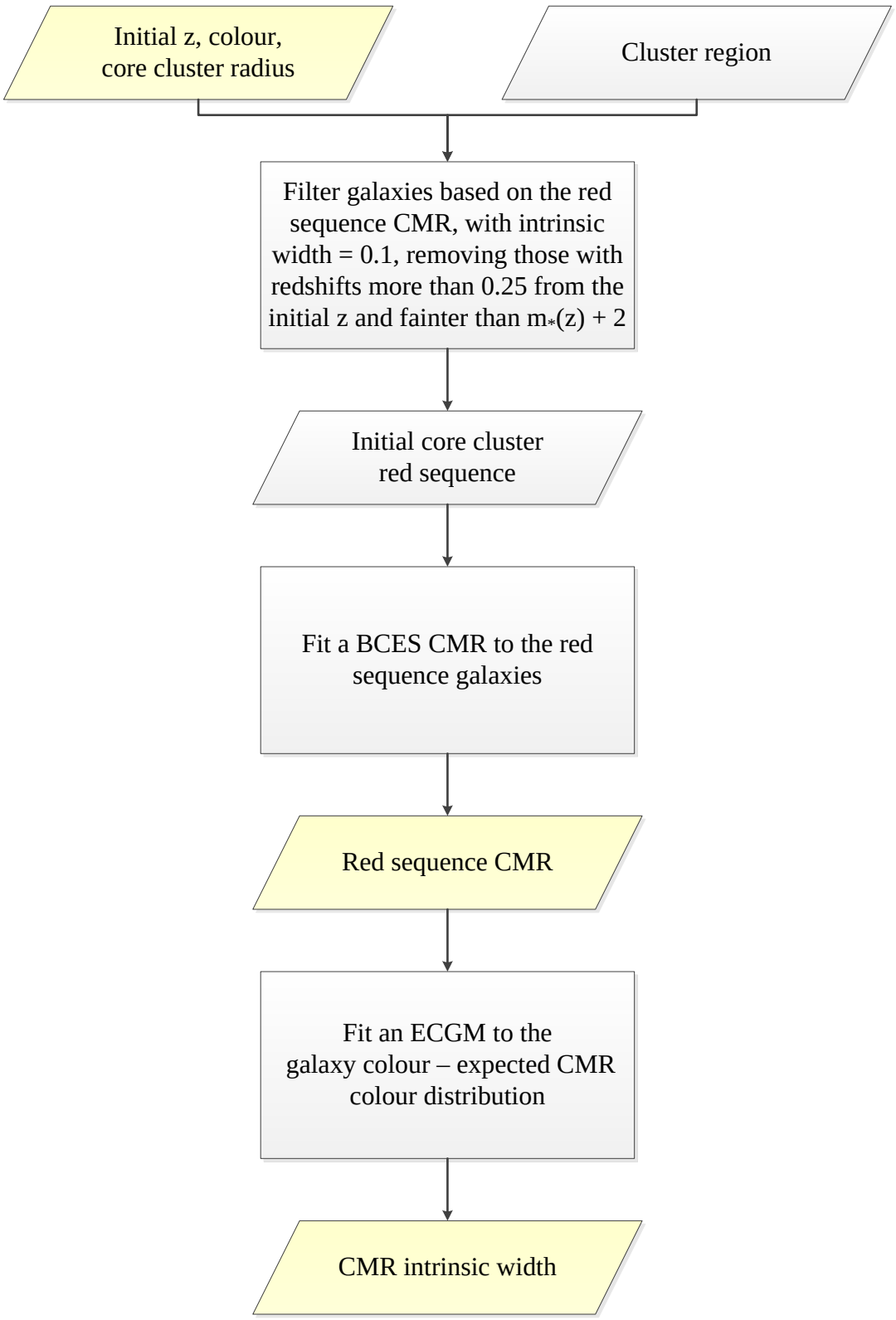

Figure 3.32 *A detailed flowchart showing the procedures of GMPhoRCC to filter remaining contamination and model the red sequence CMR, highlighted as procedure 3 in Figure 3.28.*

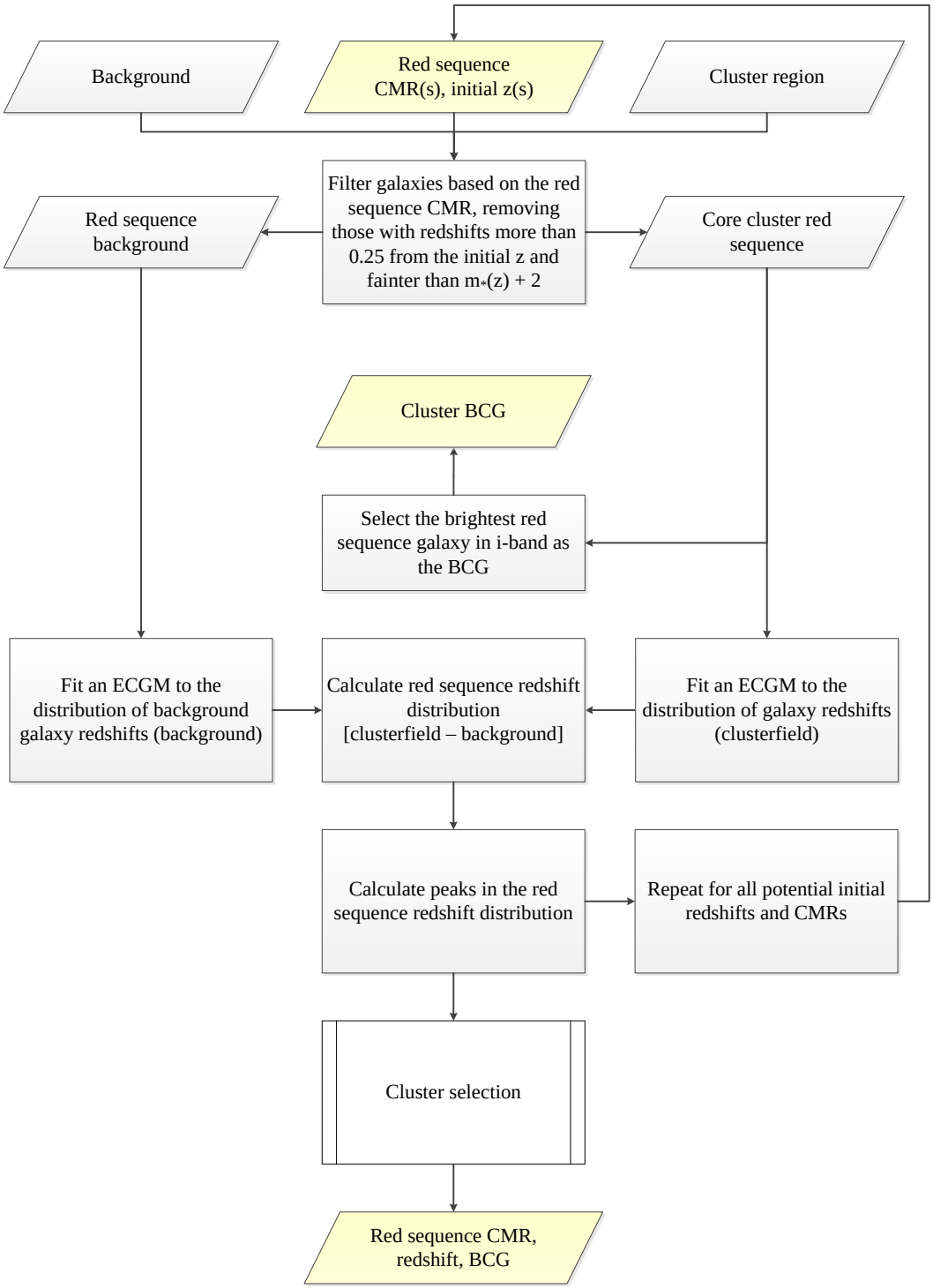

Figure 3.33 *A detailed flowchart showing the procedures of GMPhoRCC to estimate the cluster redshift from the red sequence CMR, highlighted as procedure 4 in Figure 3.28. The cluster selection process selects a primary and secondary cluster as outlined in Figure 3.34.*

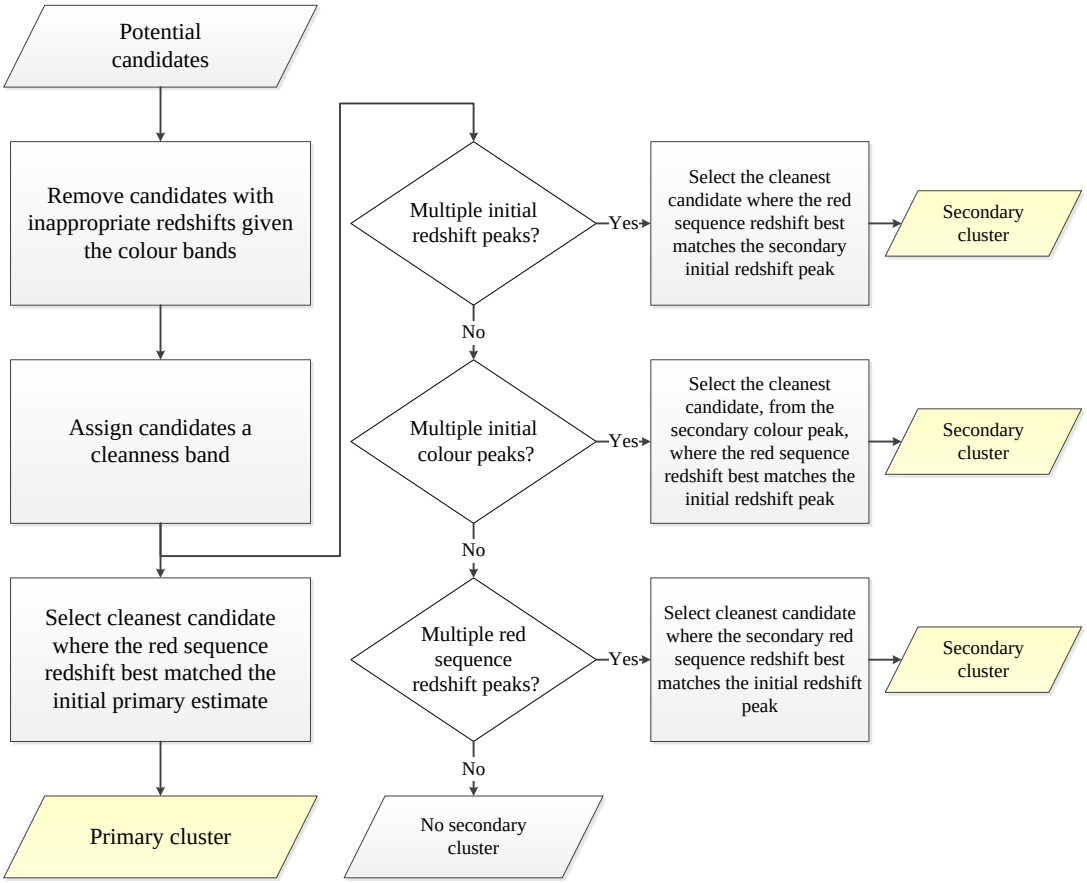

Figure 3.34 *A detailed flowchart showing the procedures of GMPhoRCC to select a primary and secondary cluster from a list of potential candidates.*

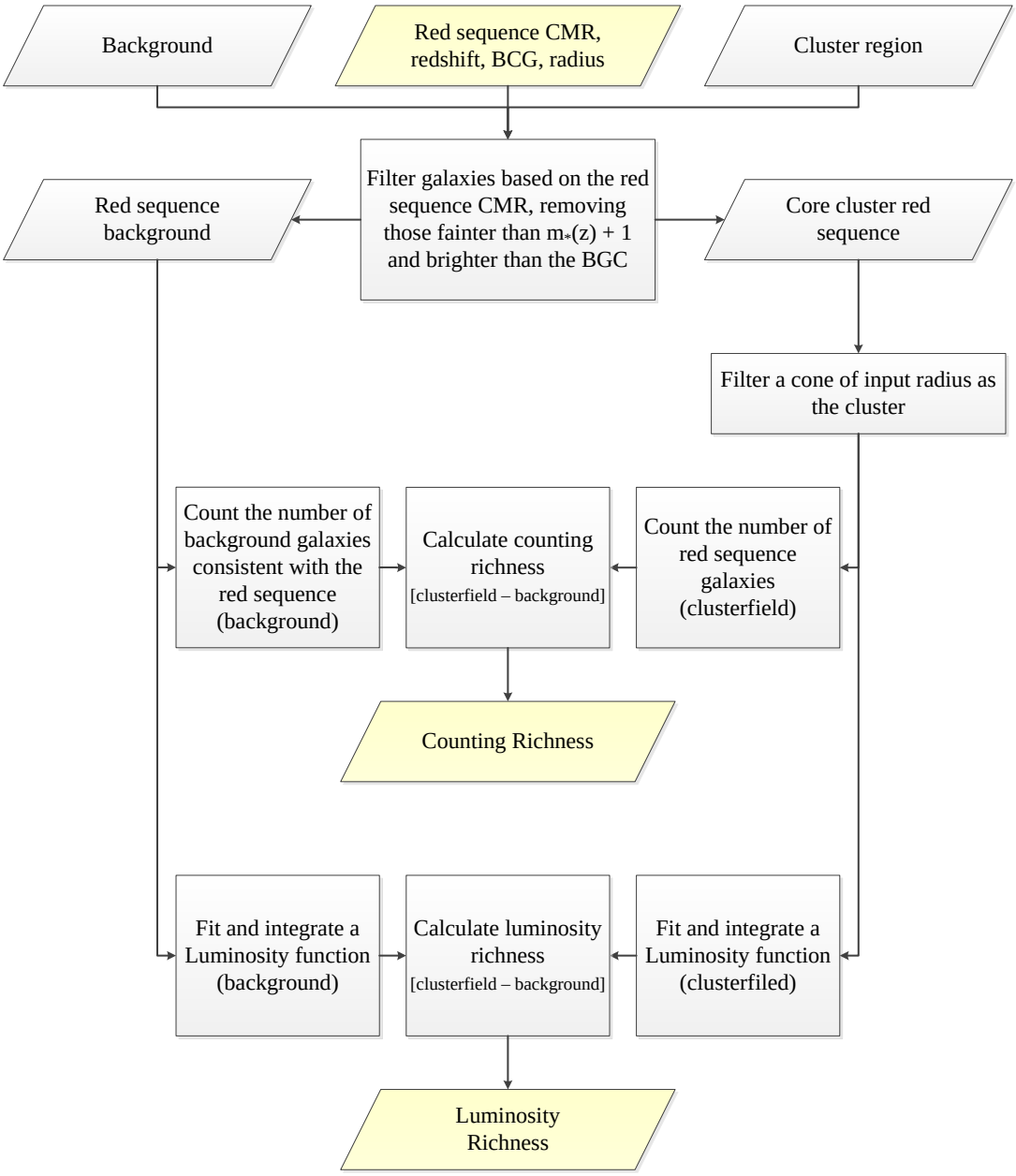

Figure 3.35 *A detailed flowchart showing the procedures of GMPhoRCC to estimate the cluster richness, highlighted as procedure 5 in Figure 3.1. An input radius of* $0.5h^{-1}Mpc$ *leads to the intermediate richness,* n_{gals} *with* n_{200} *given by* r_{200}.

Name	Description
band	The red sequence colour used to detect the cluster. 0 = $g-r$, 1 = $r-i$, 2 = $i-z$.
size	The angular radius in arcmin of the initial aperture used to model the red sequence.
z_initial	The position of the peak of the initial redshift distribution.
z_initial_peak	The size of the peak of the initial redshift distribution (galaxies / arcmin^2).
z_initial_errorm(p)	1-sigma error on the peak in the 'minus' ('positive') direction.
z_initial_info	A flag based on how the error was determined. 0 = No issues, 1 = Extrapolation needed due to multiple peaks.
rs_colour_(peak,error,info)	The position, amplitude and error of the peak in the initial red sequence colour distribution.
z_rs_(peak,error,info)	The position, amplitude and error of the peak in the red sequence photometric redshift distribution.
BCG_objID	The objID of the BCG.
BCG_dis	The angular distance in arcmin of the BCG from the cluster centre.
z_BCG_best_(err)	The best redshift with error of the BCG, spectra if available, photometric otherwise.
z_BCG_phot_(err)	The photometric redshift of the BCG, z_{RF-DR9}
z_BCG_spec_(err)	The spectroscopic redshift of the BCG.
z_gals_spec_(err)	A spectroscopic cluster redshift based on the spectra of the 5 brightest galaxies on the red sequence.
z_gals_spec_no	The number of galaxies available with spectra.
cmr_grad_(err)	The gradient of the red sequence CMR.
cmr_intercept_(err)	The intercept of the red sequence CMR.
cmr_width	The intrinsic width the red sequence CMR.
ngals_count_(err)	$n_{gals-count}$, the background-subtracted number of galaxies inside $0.5\mathrm{h}^{-1}$ Mpc on the red sequence with poissonian error.
ngals_lum_(err)	$n_{gals-lum}$, the background-subtracted richness inside $0.5\mathrm{h}^{-1}$ Mpc from integrating a LF with poissonian error.
r200_mpch-1	r_{200} in h^{-1} Mpc.
n200_count_(err)	$n_{200-count}$, the background-subtracted number of galaxies inside r_{200} on the red sequence with error.
n200_lum_(err)	$n_{200-lum}$, the background-subtracted richness inside r_{200} from integrating a LF with error.
flags	A hexadecimal combination of the GMPhoRCC flags.
quality	The quality marker based on the GMPhoRCC flags.

Table 3.11 *A list of outputs generated by GMPhoRCC using SDSS DR9 photometry. These properties are given for the primary and secondary cluster with the latter denoted by a '_sec' suffix. In the case where GMPhoRCC was unable to determine a property a default value of −1 is used. While the redshift labels are specific to SDSS DR9 these can be adjusted to match any optical input.*

Subset	Quality	Description
Detection	< 4	All clusters considered to have been detected i.e. estimates were found for both redshift and richness
Mid	< 3	An intermediate subset removing the worst outliers i.e. removing clusters with very low richness or large discrepancies between redshift estimates
Clean	< 2	The cleanest subset removing the majority of outliers i.e. removing cluster with low richness and discrepancies between redshift estimates

Table 3.12 *A list cluster subsets based on the GMPhoRCC quality markers used remove potentially erroneous characterisations.*

3.3.1 Computational Performance

GMPhoRCC is aimed primarily for use with standard desktop computers and as such does not require substantial computational resources. Development has proceeded using `python` 2.7.3 with the `scipy`[3] module providing many of the mathematics routines, particularly the sequential least squares method used to fit luminosity functions. GMPhoRCC experiences two main bottlenecks, first from the retrieval of the optical data either from a database or local files and secondly from fitting Gaussian mixtures. While little can be done with the data retrieval, the Gaussian mixture fitting is developed using `Fortran` 90 which provides a factor of 10 speed improvement over native `python` and is twice as fast as the `c++` version employed by Hao et al. (2010). The final performance improvement comes from the utilization of multiple threads available in even the most basic computers. While GMPhoRCC does not implement full parallelisation at the `Fortran` level, the `Parallel Python`[4] module allows for several cluster candidates to be analysed simultaneously. Although more were available little improvement was found beyond six threads due to the retrieval of the optical data.

As an example of typical performance, 6 threads from an Intel 3770k 4.2GHz processor with 16GB of PC3-19200 RAM, accessing the optical data locally from a hard disk has a characterisation time of 42 seconds per cluster per thread allowing the full characterisation of the XCS catalogue, 503 clusters, within 59 minutes.

[3] `http://www.scipy.org/`
[4] `http://www.parallelpython.com/`

3.3.2 Example Clusters

To demonstrate the characterisation procedure two clusters are considered, GMBCG-1, a previous example of an 'easy' well understood cluster and GMBCG J239.47725+21.55627 (GMBCG-2) an example showing ambiguous multi-modal distributions.

GMBCG-1

Figure 3.36 shows the well defined single peaked initial redshift and colour distributions of GMBCG-1 with clear indications of a cluster around $z \sim 0.18$ and $g-r \sim 1.2$. Filtering around these peaks and modelling the red sequence, Figure 3.37, shows a distinct CMR and peak in the final redshift distribution. The red sequence redshift, $z_{RS} = 0.18$ is in good agreement with the spectroscopic redshift $z_{spec} = 0.174$. Without a readily comparable richness the final plot, 3.38, shows the fitted luminosity function in good agreement with the distribution. With a well described luminosity function the two different richness methods are in very good agreement with $n_{gals-count} = 64$ and $n_{gals-lum} = 66$. With a well defined, single peaked, rich cluster GMPhoRCC, as expected shows little problems in the characterisation giving estimates in good agreement with spectra.

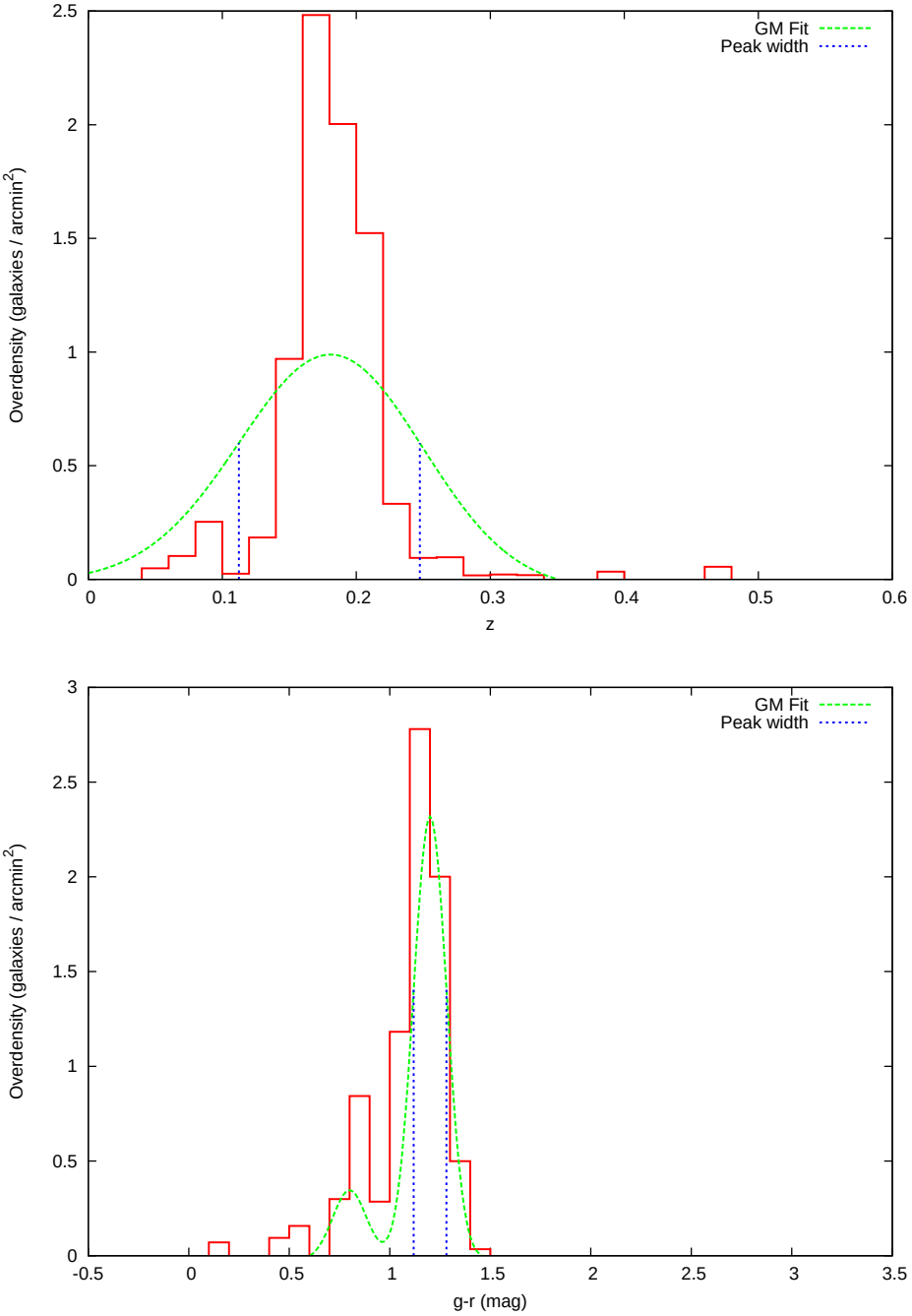

Figure 3.36 *Models of the initial redshift and colour distributions of GMBCG-1 shown in the top and bottom panels respectively. The initial redshift peak around $z \sim 0.18$ shows clear indication of a cluster. Similarly, after filtering, the initial colour peak around $g - r \sim 1.2$ clearly represents the cluster.*

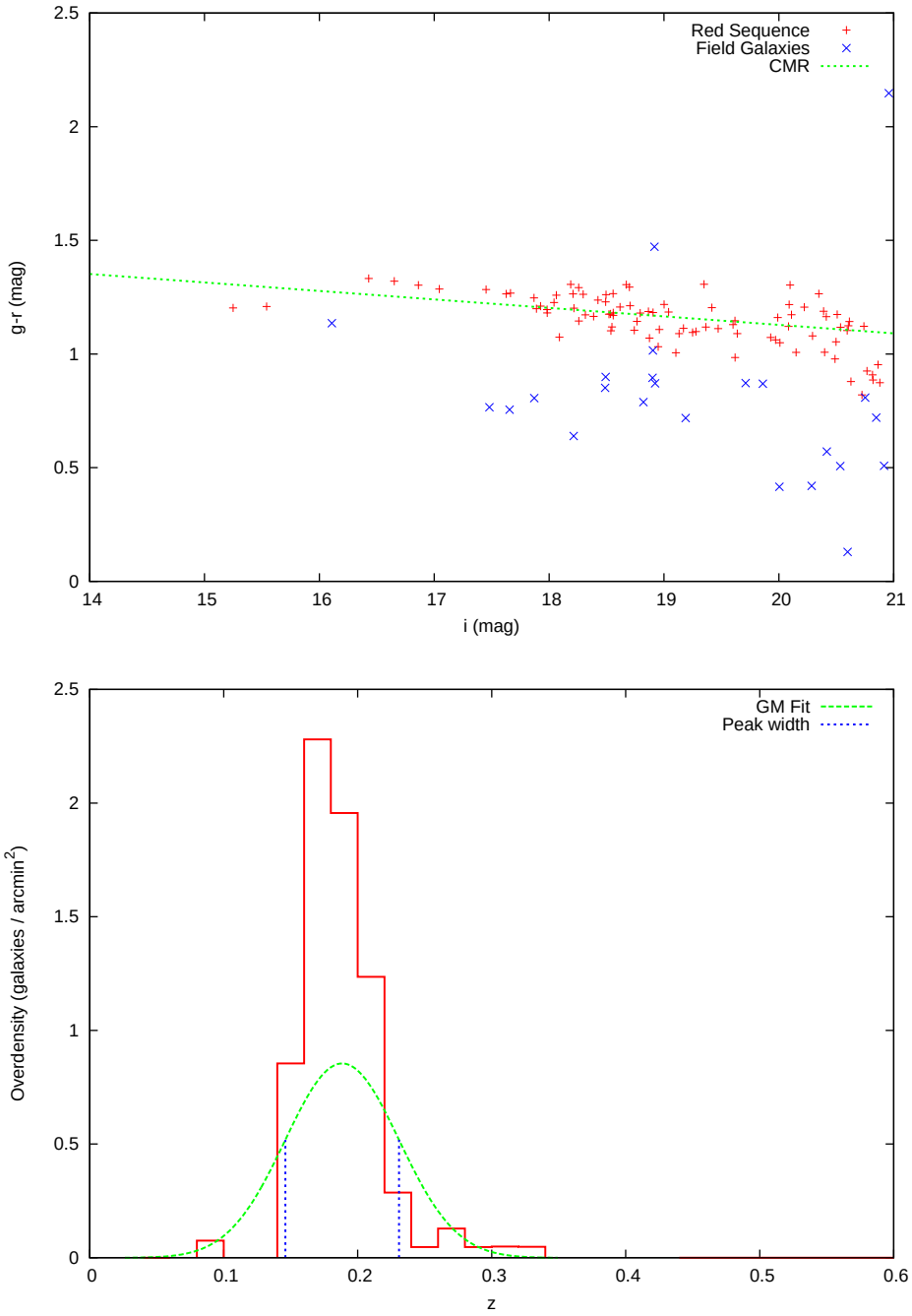

Figure 3.37 *The red sequence of GMBCG-1 showing the CMR and redshift distribution in the top and bottom panel respectively. The red sequence redshift, taken as the peak in the distribution with* $z_{RS} = 0.18$*, is in good agreement with the spectroscopic redshift* $z_{spec} = 0.174$

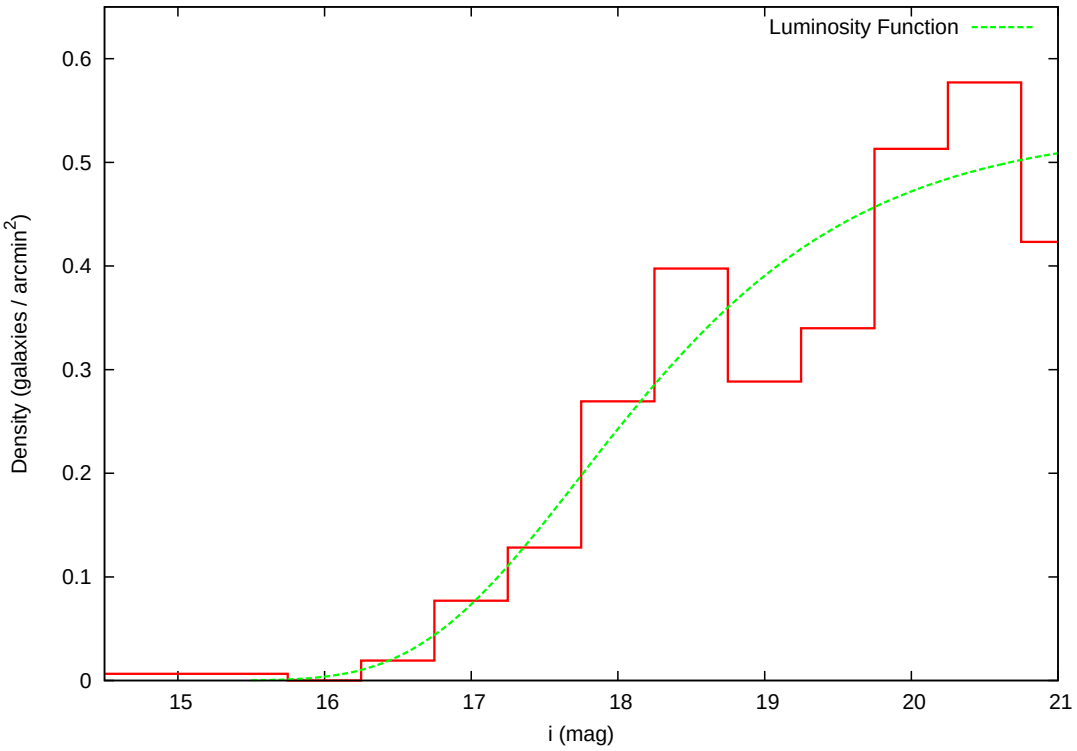

Figure 3.38 *The luminosity function of GMBCG-1 showing good agreement between the fit and the distribution.*

GMBCG-2

Figure 3.39 shows the bi-modal initial redshift distributions of GMBCG-2 where, in addition to the target around $z = 0.179$, another cluster around $z = 0.39$ is observed resulting in potential ambiguity for subsequent characterisation. Filtering around the low redshift peak a single broad colour peak is found around $g - r \sim 1.2$. Although multiple candidates are now considered, this initial step of filtering immediately helps the colour characterisation of the potential clusters contrary to the unconstrained distributions shown in Figure 2.6. Continuing filtering around this peak, Figure 3.40, shows a CMR and peak in the final redshift distribution. The red sequence redshift, $z_{RS} = 0.172$ is selected as the primary cluster and is in good agreement with the spectroscopic redshift, $z_{spec} = 0.179$, of the target. Although only partially covering the field, the secondary candidate is able to recover the higher redshift cluster with $z_{RS} = 0.375$. Again without a readily comparable richness the final plot, 3.41, shows the fitted luminosity function. With only a few galaxies the distribution does not appear to be well modelled by a Schechter function however the counting and luminosity richnesses are in good agreement with $n_{gals-count} = 13$ and $n_{gals-lum} = 14$. Even in ambiguous cases GMPhoRCC is able to appropriately select a candidate providing suitable characterisations.

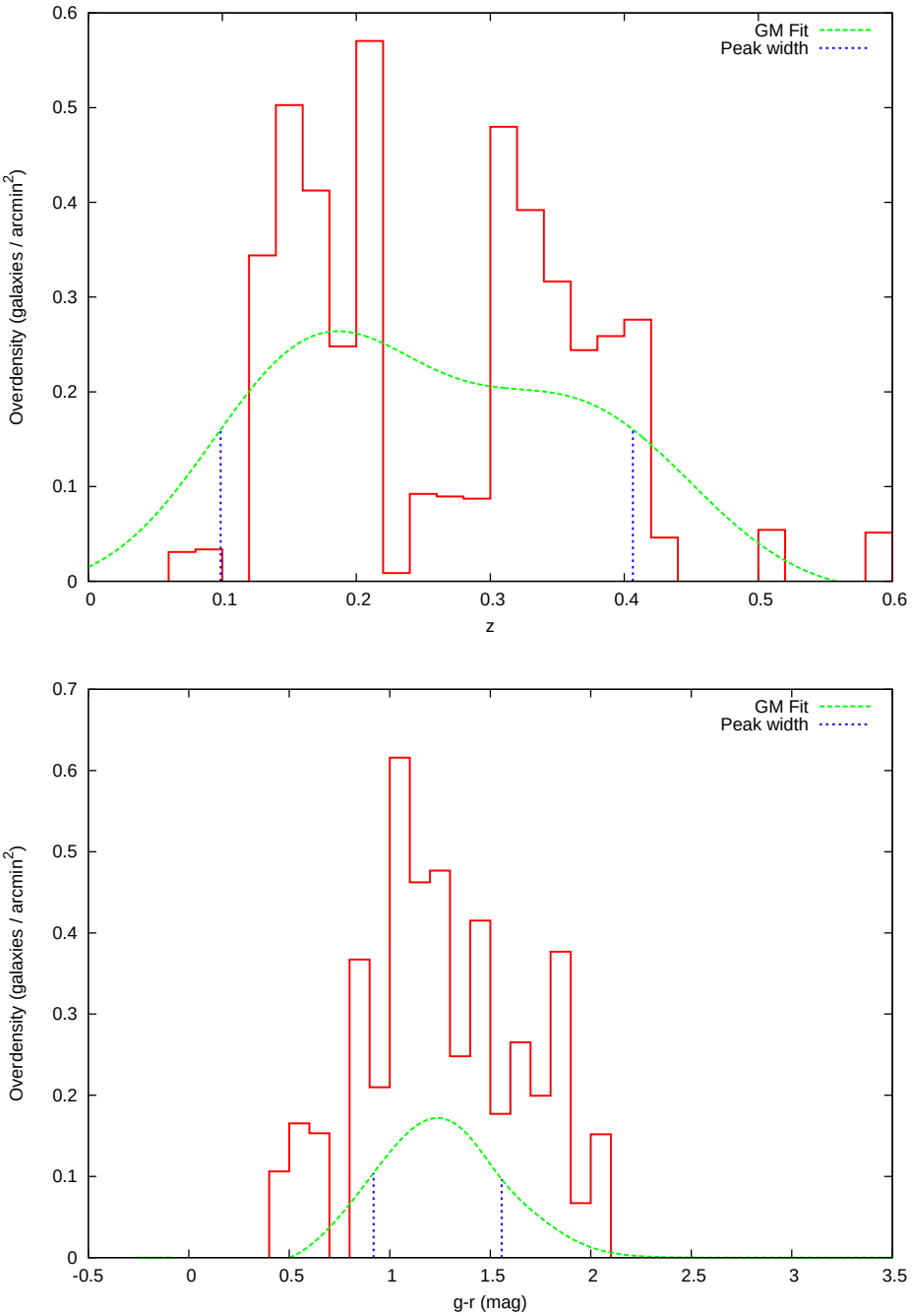

Figure 3.39 *Models of the initial redshift and colour distributions of GMBCG-2 shown in the top and bottom panels respectively. The initial redshift distribution shows two peaks corresponding to the target around* $z = 0.179$ *and another high redshift cluster at* $z = 0.39$*. After filtering around the low redshift primary candidate, the initial colour peak around* $g - r \sim 1.2$ *represents this cluster.*

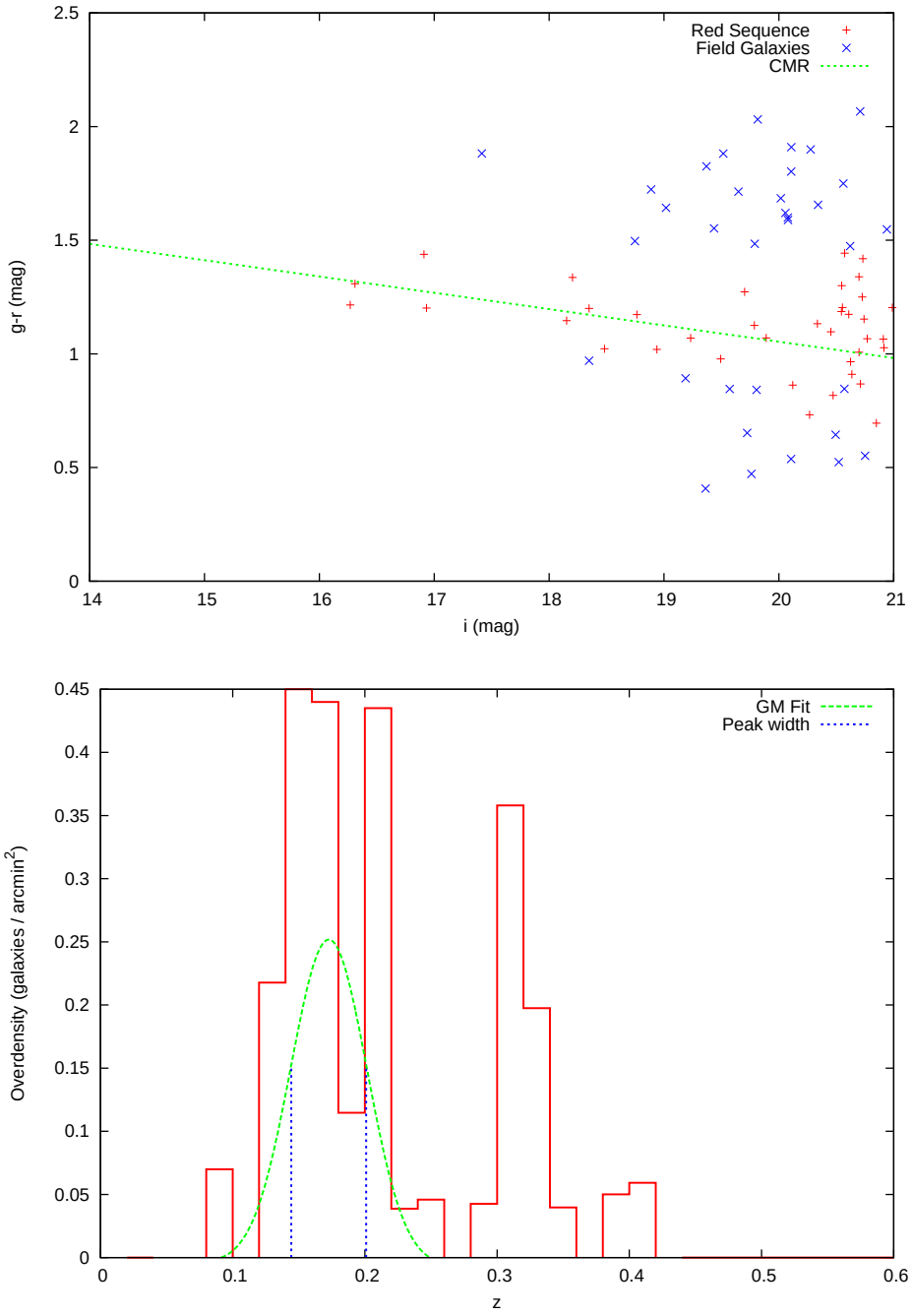

Figure 3.40 *The red sequence of GMBCG-2 showing the CMR and redshift distribution in the top and bottom panel respectively. Selected as the primary, the low redshift candidate from Figure 3.39 gives a CMR and redshift ($z_{RS} = 0.172$) consistent with the target at $z_{spec} = 0.179$. Even in ambiguous cases, GMPhoRCC is able to provide suitable characterisations by analysing several candidates and selecting the most appropriate.*

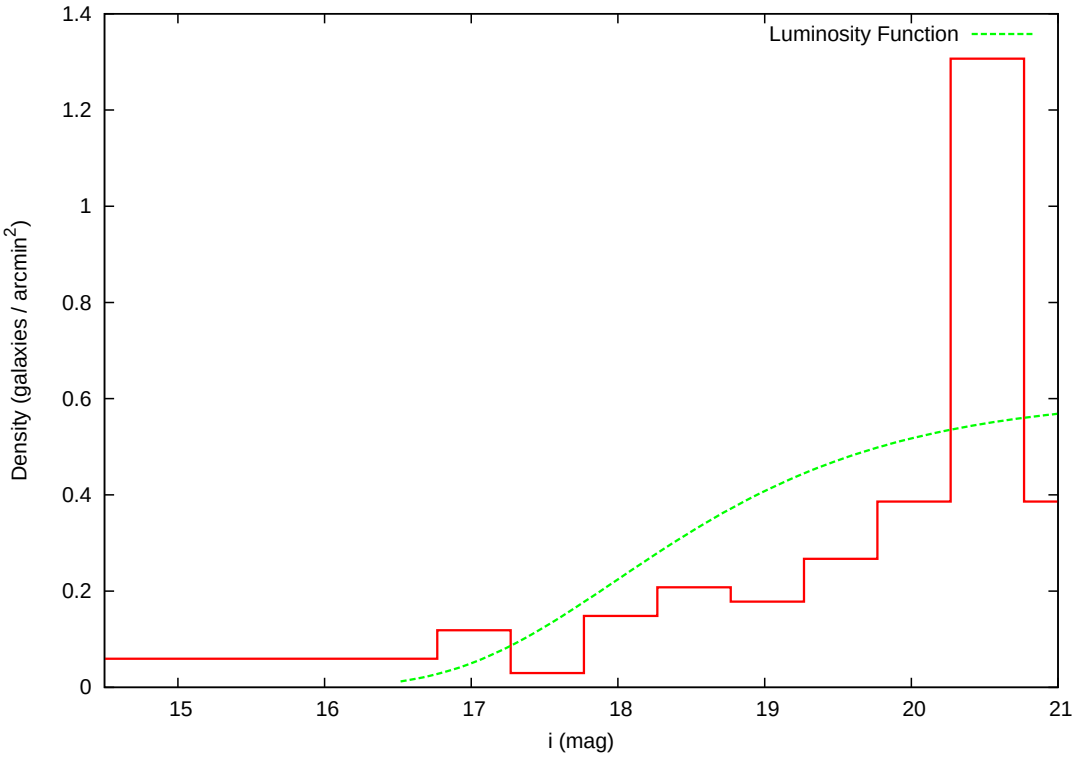

Figure 3.41 *The luminosity function of GMBCG-2. With only a few galaxies the distribution does not appear to be well modelled by a Schechter function however the counting and luminosity richnesses are in good agreement with* $n_{gals-count} = 13$ *and* $n_{gals-lum} = 14$.

3.4 Comparisons with existing catalogues

Throughout this chapter it has been seen that the development of GMPhoRCC has been driven by the desire to integrate the initial feature list and by comparisons with existing cluster catalogues. This gives valuable feedback on the performance of GMPhoRCC. This section explores comparisons using GMPhoRCC with the GMBCG, NORAS, REFLEX and XCS cluster catalogues. NORAS (Böhringer et al., 2000) and REFLEX (Böhringer et al., 2004) are both X-ray detected catalogues derived using observations from the ROSAT telescope providing 350 and 74 clusters respectively with coverage in the SDSS DR9. The XMM cluster Survey (XCS) provides 503 clusters detected from the XMM-Newton archive with X-ray and optical analysis detailed in Lloyd-Davies et al. (2011) and Mehrtens et al. (2012) respectively. Of these clusters 181 have coverage in DR9 with spectra. Finally a spectroscopic subset of the GMBCG catalogue (Hao et al., 2010) is used which has been cross matched with the maxBCG catalogue (Koester et al., 2007b). This provides a sample of 4895 of clusters with spectra and photometric estimates which, in addition to assessing the overall accuracy of GMPhoRCC, allows a comparison to the maxBCG estimates. Combining these catalogues gives 5500 clusters with optical coverage in the SDSS DR9.

3.4.1 Redshift Comparison

Of the 5500 clusters, redshift estimates were found for 99.7% and compared to spectra where Figure 3.42 highlights the results for each of the quality subsets. Although several discrepancies are present the cleaner subsets are able to identify and remove the worst outliers. Additionally, while the majority of all estimates are within $|z_{RS} - z_{spec}| < 0.01$, the clean subset has a larger fraction within this bound and less contamination with outliers as shown more clearly in Figure 3.43. As shown in Figure 3.44, it is noted that at low redshifts, $z < 0.1$, many cluster estimates are erroneous where limitations in field area and poor contrast against the background result in cases where field galaxies dominate the cluster distributions making it difficult to isolate the red sequence. Incompleteness and increasing measurement errors in the photometry at high redshift again cause issues with the red sequence detection. In addition to these redshift limitations it expected that low richness clusters produce the most outliers, where it is more

difficult to isolate and model the red sequence with a sparse number of galaxies. Without a definitive richness estimate (such as spectra for redshift) this analysis is deferred to Section 4.3.1 where mocks provide clusters with known properties.

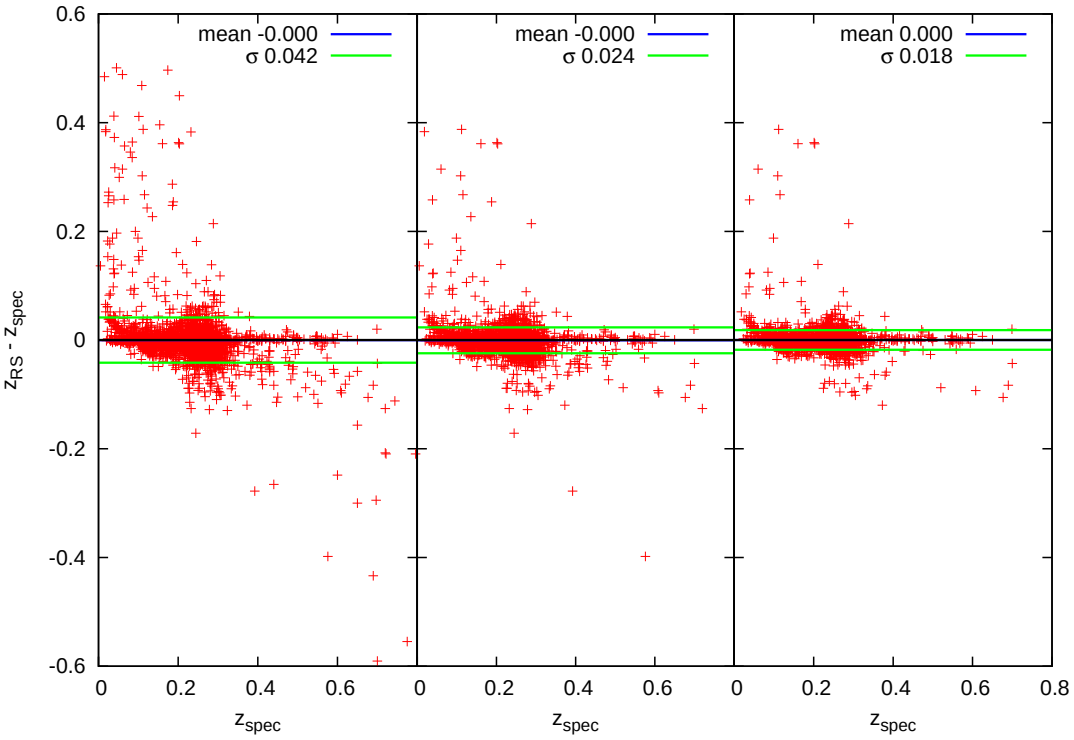

Figure 3.42 *A comparison of GMPhoRCC photometric red sequence redshifts to spectra using* 5500 *clusters with DR9 coverage from GMBCG, NORAS, REFLEX and XCS, showing from left to right, the detection, mid and clean subsets. While some discrepancies remain the majority of outliers have been removed in the clean subset. Although they have been correctly identified as problems, very low redshift clusters* ($z < 0.05$) *are not characterised well by GMPhoRCC due to poor contrast against the background and limitations in the field area.*

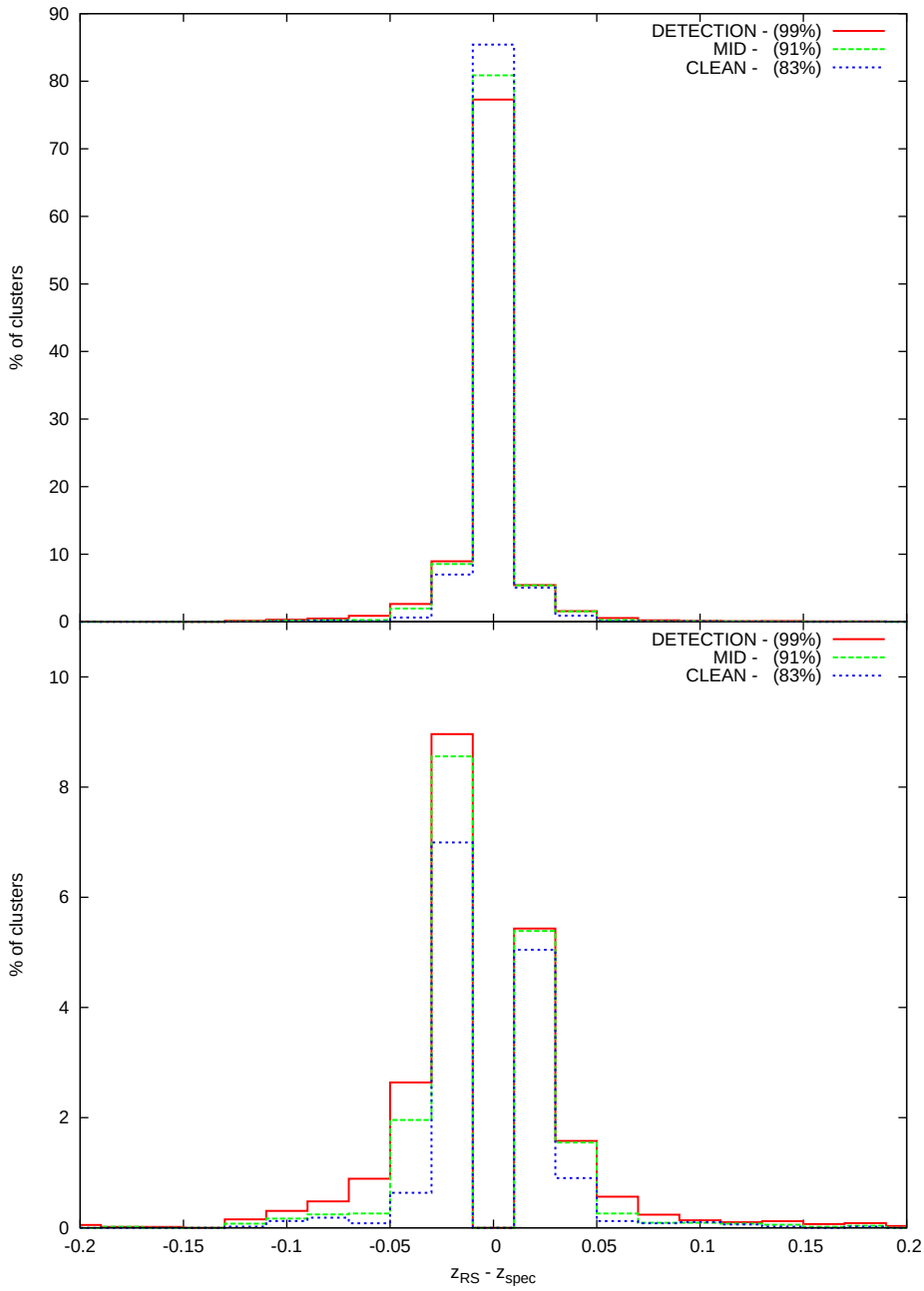

Figure 3.43 *A normalised histogram comparison of the GMPhoRCC photometric red sequence redshifts to spectra using* 5500 *clusters with DR9 coverage from GMBCG, NORAS, REFLEX and XCS. The comparison has been normalised and split into the separate quality subsets where the legend shows the fraction of the total clusters in each set. The bottom panel omits the middle bin to highlight the outliers where the clean subset can be seen to have removed the worst estimates with a greater fraction within* $|z_{RS} - z_{spec}| < 0.01$

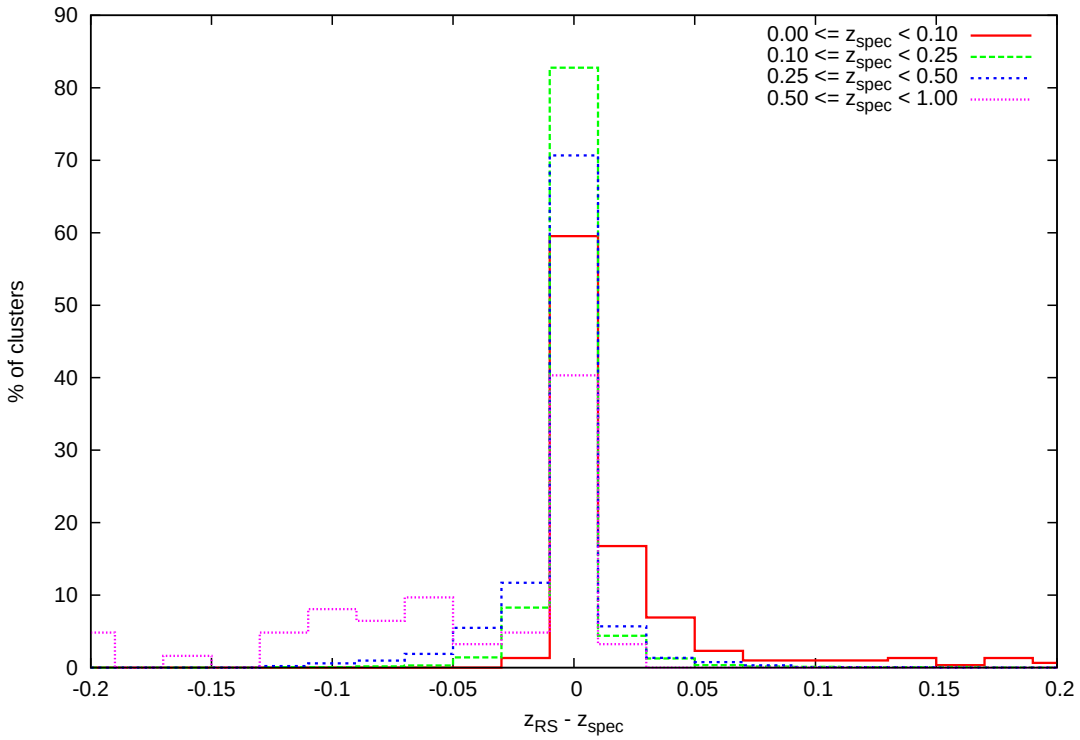

Figure 3.44 *A normalised histogram comparison of the GMPhoRCC photometric red sequence redshifts to spectra using* 5500 *clusters with DR9 coverage from GMBCG, NORAS, REFLEX and XCS. The comparison has been normalised and split into redshift bands to highlight any bias. At low redshifts limitations in field area and poor contrast against the background make it difficult to isolate the red sequence resulting in the larger fraction of outliers. Similarly incompleteness and increasing measurement errors in the photometry at high redshift cause issues with red sequence detection, resulting in the increased number of outliers.*

A subset of 133 XCS clusters have both spectroscopic and photometric redshifts available which provide an excellent resource to compare the performance of GMPhoRCC to the XCS analysis. Figures 3.45 and 3.46 shows that with the exception of a few outliers in the detection subset, GMPhoRCC provides a more accurate estimate with a lower scatter around the spectroscopic redshift than XCS. In addition to providing a more accurate redshift the estimate is independent of any colour-redshift model as employed by XCS.

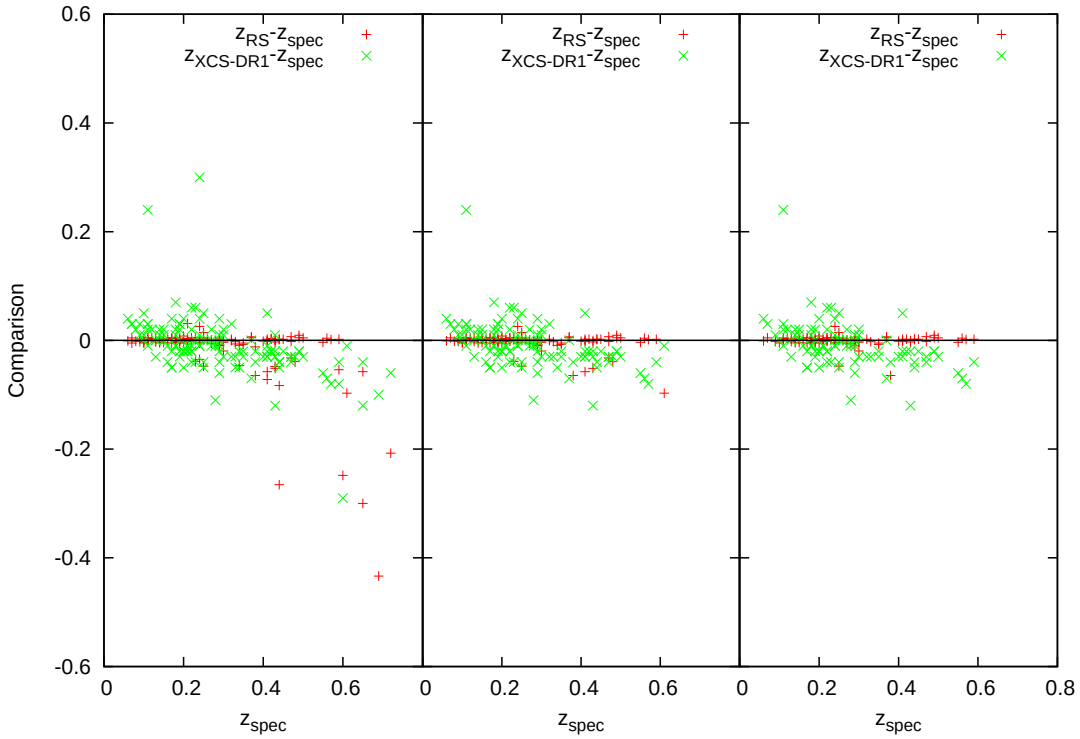

Figure 3.45 *Redshift comparisons for the GMPhoRCC and XCS photometric redshifts to spectra for a subset of* 133 *XCS clusters. With the exception of a few outliers in the detection subset. The GMPhoRCC red sequence redshift, z_{RS}, provides a more accurate estimate with lower scatter around the spectroscopic redshift than the XCS photometric estimate, $z_{XCS-DR1}$.*

In a similar approach as the previous XCS analysis, a subset of 4895 GMBCG clusters cross matched with the maxBCG catalogue have both spectroscopic and photometric redshifts available which can be used to compare the performance of GMPhoRCC to maxBCG. Figure 3.47 shows that while both estimates are in good agreement with spectra, GMPhoRCC attains fewer outliers with a larger fraction within 0.01 of the spectroscopic redshift. Again these improved redshifts are independent of any colour-redshift model as employed by maxBCG.

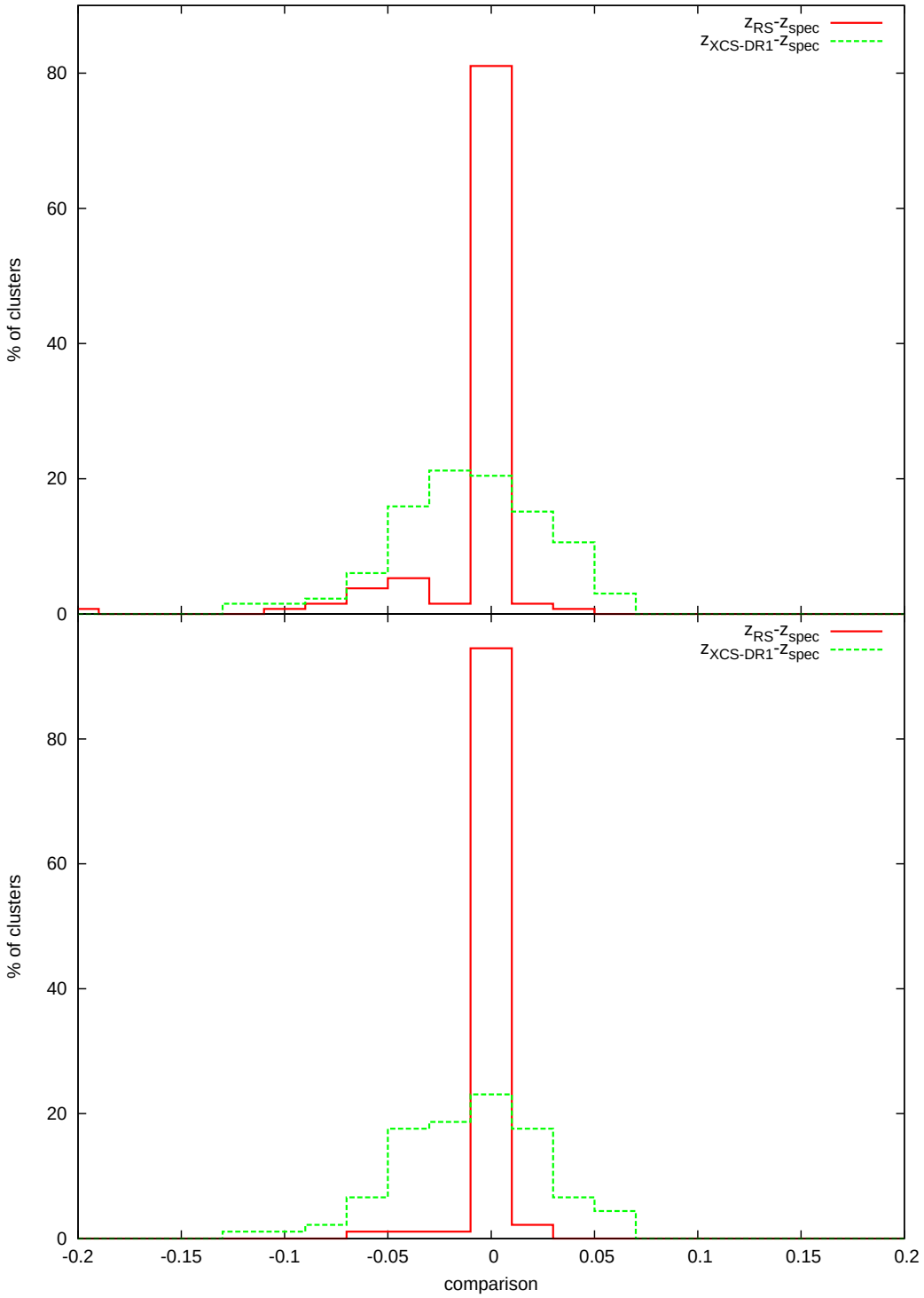

Figure 3.46 *A normalised histogram comparison of the GMPhoRCC and XCS photometric redshifts to spectra for a subset of* 133 *XCS clusters where the top and bottom panels show the detection and clean subsets respectively. Although the detection subset has a few more extreme outliers a much greater fraction than from XCS agree within* $|z_{phot} - z_{spec}| < 0.01$*, with the clean subset attaining the highest fraction in this band.*

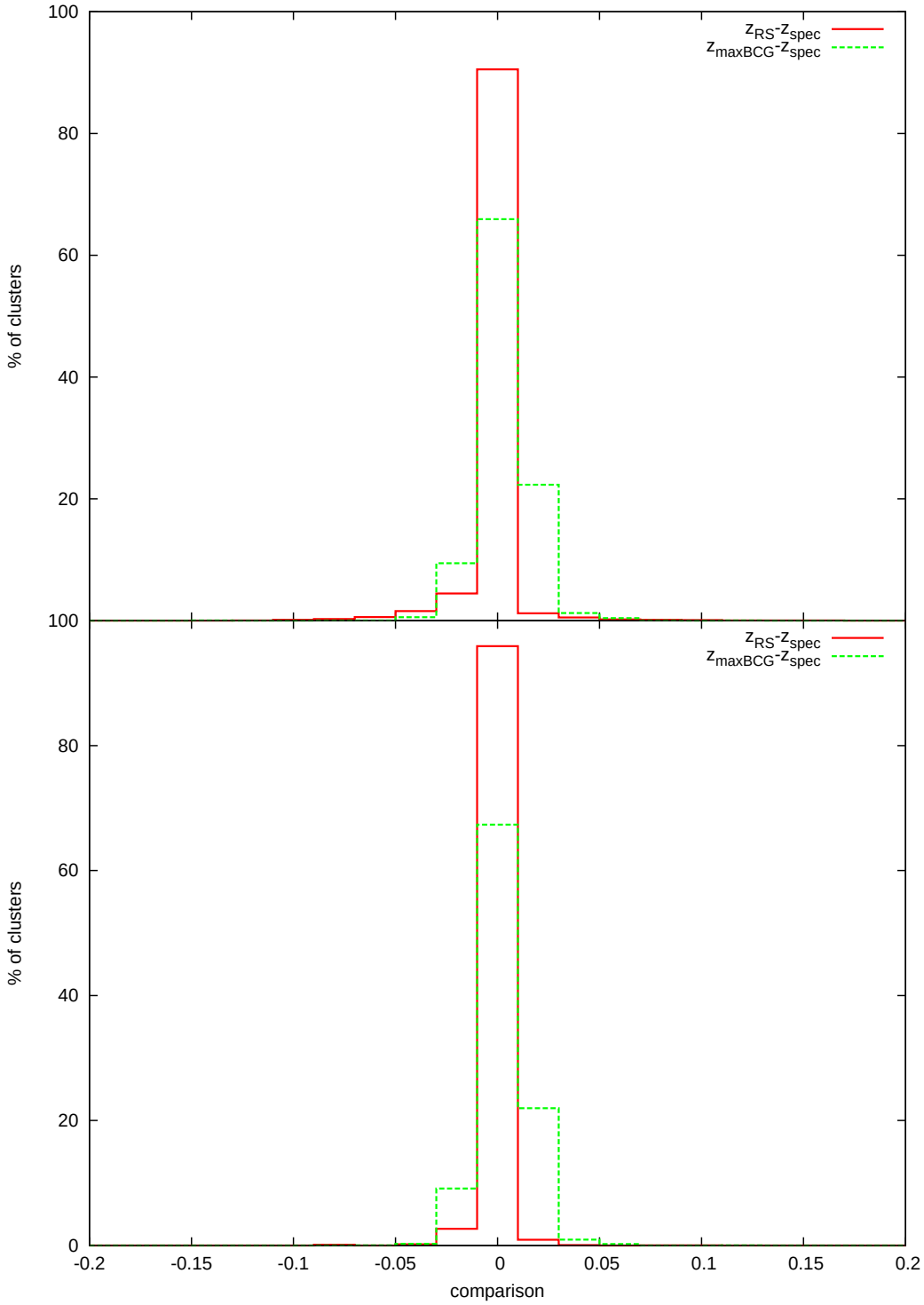

Figure 3.47 *A normalised histogram comparison of the GMPhoRCC and maxBCG photometric redshifts to spectra for a subset of* 4895 *maxBCG clusters where the top and bottom panels show the detection and clean subsets respectively. Again the detection subset has a few more extreme outliers however a much greater fraction than from maxBCG agree within* $|z_{phot} - z_{spec}| < 0.01$*, with the clean subset attaining the highest fraction in this band.*

3.4.2 Richness Comparison

Comparisons with richness are particularly difficult to achieve as these require close agreement with the input optical data and the precise definition of richness with that from the cluster catalogue. Considering GMBCG-1, also noted as the richest cluster in the maxBCG catalogue, Figures 3.48 and 3.49 show a field around the cluster with photometry cuts consistent with Section 3.2.1 and maxBCG respectively. While trying to best match the maxBCG photometry some ambiguity has lead to the complete masking of the cluster and hence these cuts are not used with GMPhoRCC. In addition to this, differences in the faint end cut-off, cluster redshift and BCG selection can result in very different richnesses for the same red sequence hence care must be taken when comparing richness estimates from different sources.

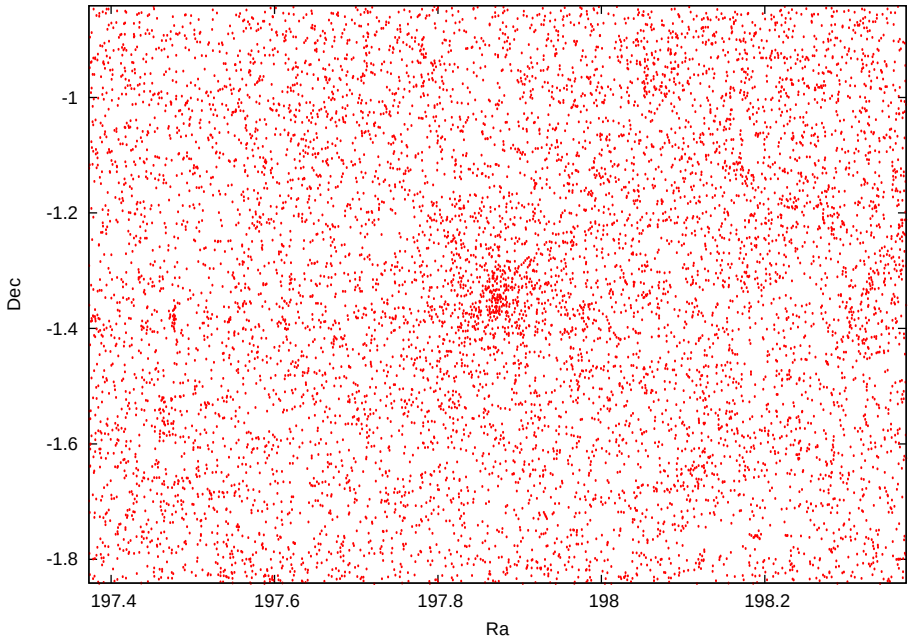

Figure 3.48 *A field centred on GMBCG-1 with photometry cuts consistent with Section 3.2.1.*

The DR9 optical input and GMPhoRCC richness, from Sections 3.2.1 and 3.1.4 respectively, best match the GMBCG catalogue. In order for a meaningful comparison to the GMBCG richness it is however still necessary to restrict the input data to DR7 primary galaxies and to remove the background subtraction from the GMPhoRCC richness. Figure 3.50 shows how the GMPhoRCC counting richness compares with GMBCG using 4895 spectroscopic clusters although a large spread is observed, the GMPhoRCC estimate is centred around the

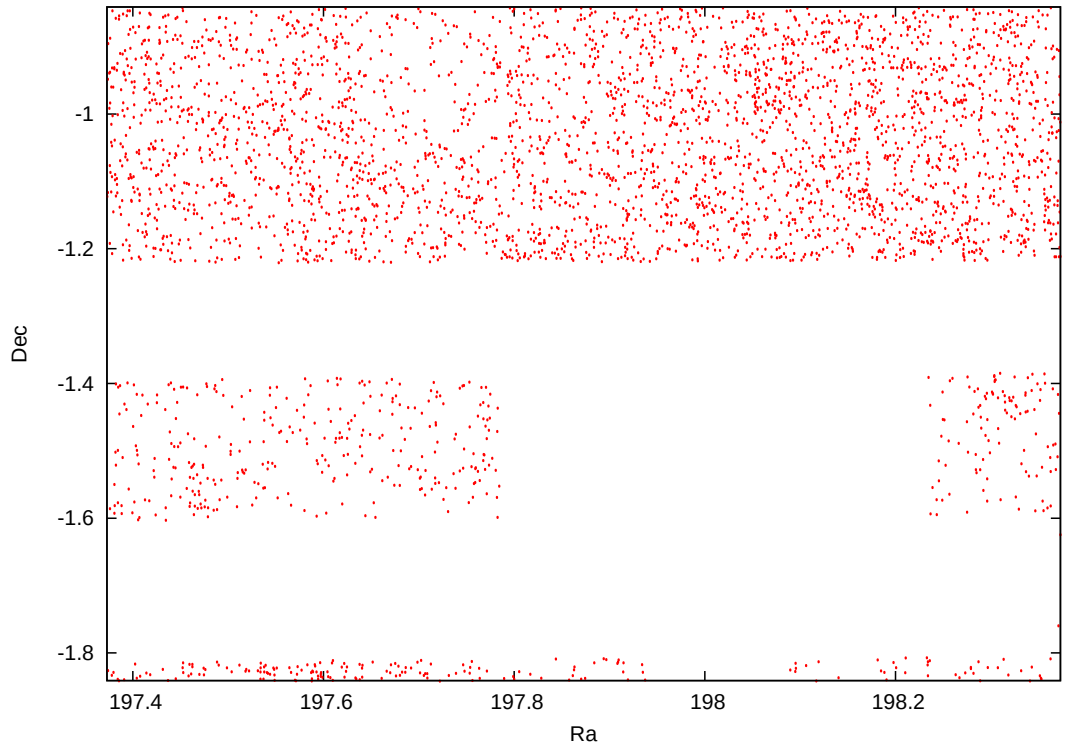

Figure 3.49 *A field centred on GMBCG-1 with masking and seeing photometry cuts used by maxBCG from Scranton et al. (2002). The cluster visible in Figure 3.48 has been completely removed.*

cluster value. It is noted that estimating richness is far more challenging than redshift, where precise red sequence modelling is required to recover all the cluster members. In addition, background fluctuations, issues with redshift, BCG selection and the intermediate richness propagate and are amplified in the n_{200} estimate. In addition to these issues, the luminosity method produces a slightly larger spread with more extreme outliers due to the extra uncertainty introduced by fitting a luminosity function, as shown in Figures 3.51 and 3.52.

By considering the quality subsets, Figure 3.53 shows the distributions more clearly with both estimates centred around the GMBCG value. While the clean subset attains the fewest outliers it is clear the quality sets have a much greater impact on the redshift estimates. This highlights the difficulty in identifying richness outliers, where only slight discrepancies in redshift, BCG and CMR result in the loss cluster members giving significant fractional differences particularly with low richness clusters.

In addition to this, these comparisons rely on the GMBCG richness which is subject to the various strengths, weaknesses and selection function associated

with this method and may not be an accurate representation of the 'true' cluster. Without a definite richness estimate comparisons with real clusters have limited value hence a full analysis of the GMPhoRCC richness is performed using mock galaxy clusters which have known properties. This allows a more comprehensive evaluation of the full GMPhoRCC characterisation and is explored in detail in Chapter 4.

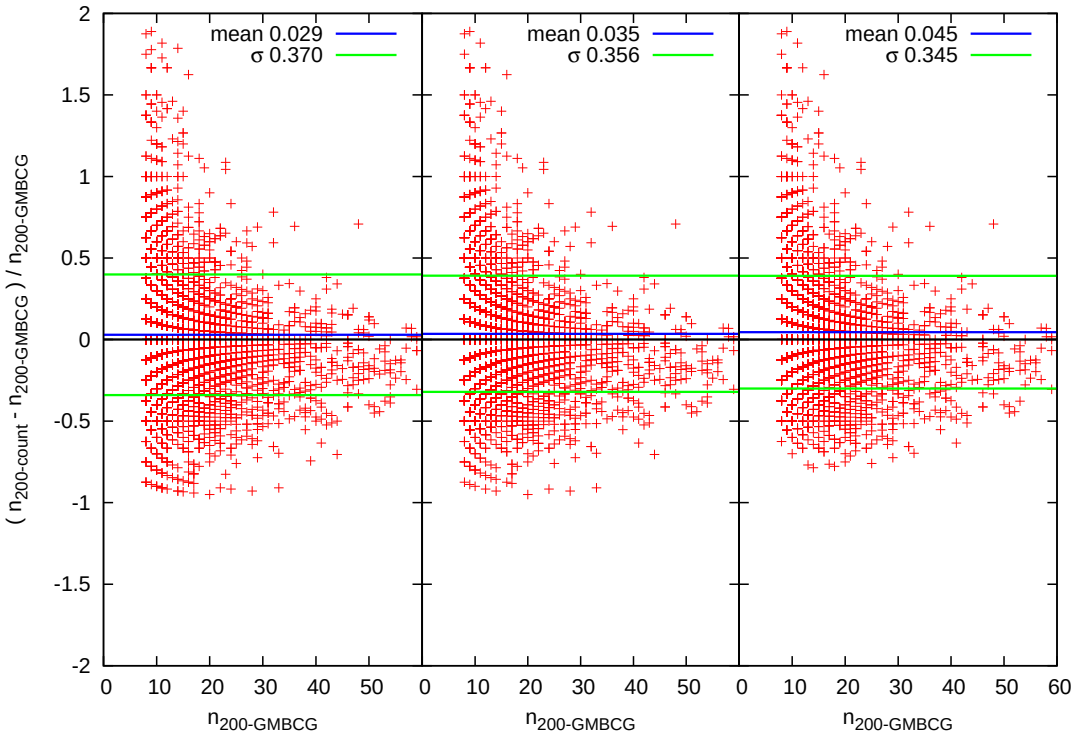

Figure 3.50 *A comparison of the GMPhoRCC $n_{200-count}$ to the GMBCG n_{200} value for a subset of* 4895 *spectroscopic clusters showing from left to right the detection, mid and clean subsets. Although a large spread is observed the estimates are centred around the GMBCG value where some outliers observed in detection have been removed in the clean subset resulting in the reduced scatter. It is noted that estimating richness is far more challenging than redshift where precise red sequence modelling is required to recover all the cluster members. In addition background fluctuations, issues with redshift, BCG selection and the intermediate richness propagate and are amplified in the n_{200} estimate. Combining these effect results in the observed large scatter and difficultly in removing outliers.*

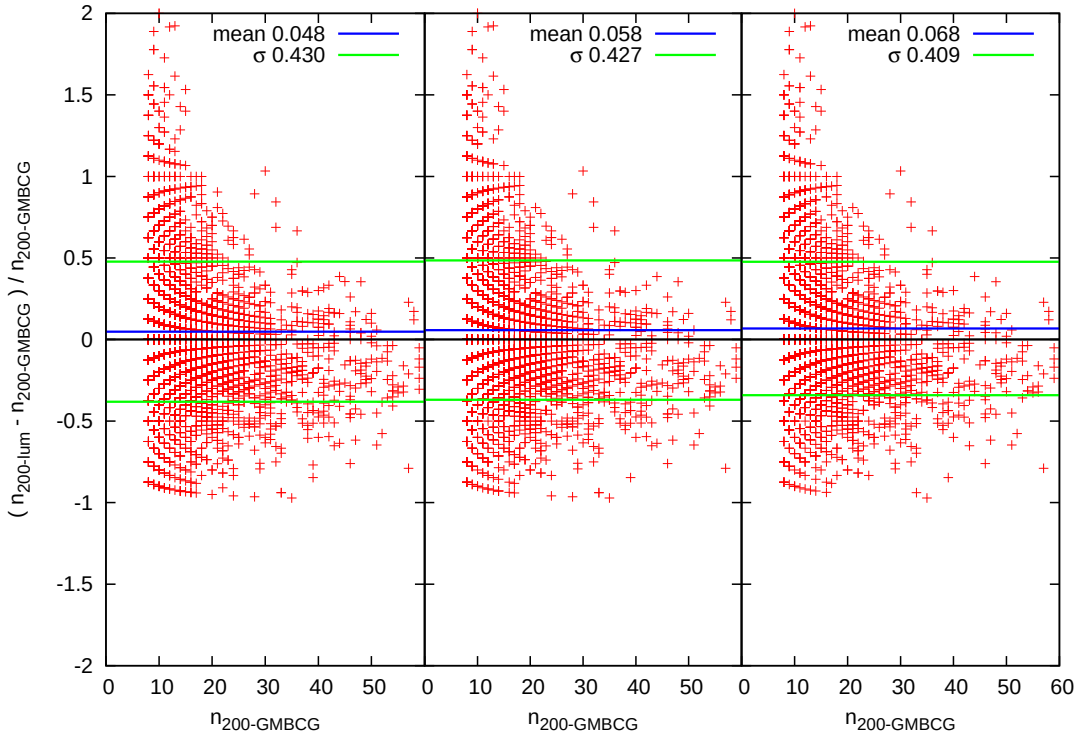

Figure 3.51 *A comparison of the GMPhoRCC $n_{200-lum}$ to the GMBCG n_{200} value for a subset of* 4895 *spectroscopic clusters showing from left to right the detection, mid and clean subsets. Although a large spread is observed the estimates are centred around the GMBCG value where some outliers observed in detection have been removed in the clean subset resulting in the reduced scatter. In addition to the issues regarding the counting luminosity, the extra uncertainty introduced by fitting and integrating a luminosity function results in a larger scatter and more outliers than observed in Figure 3.50.*

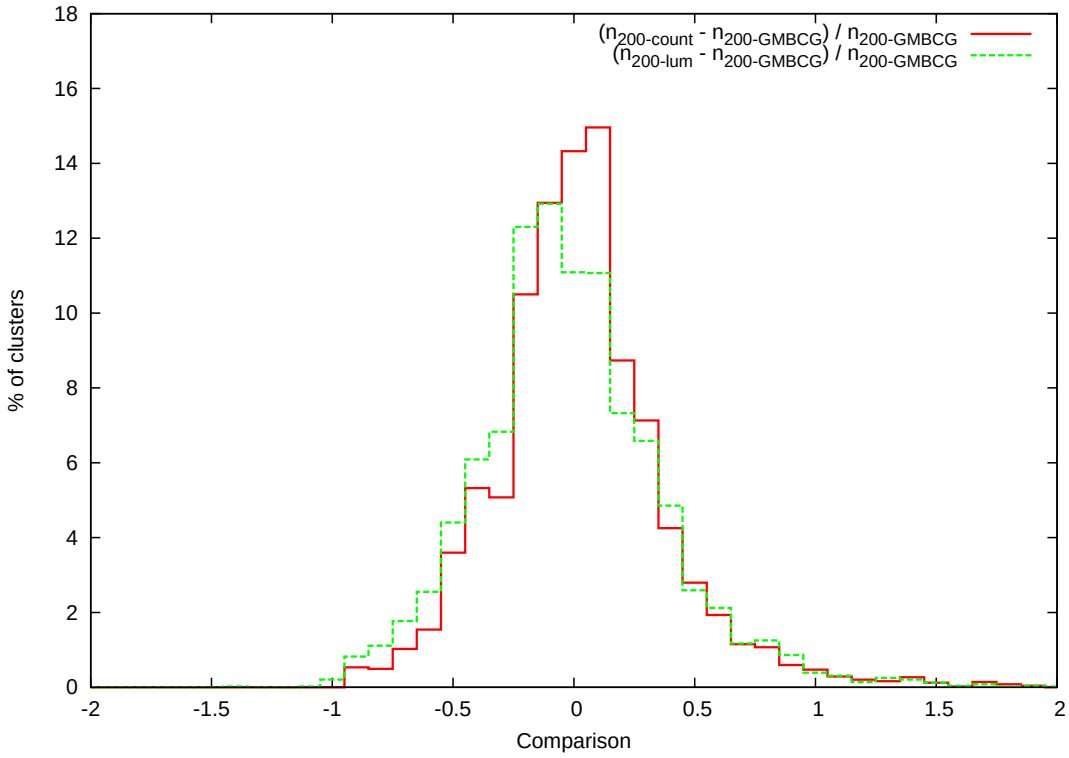

Figure 3.52 *A histogram comparison of both the GMPhoRCC n_{200} estimates for the detection subset using 4895 spectroscopic clusters from GMBCG. This highlights the slightly larger spread and more extreme outliers produced by the luminosity method compared to the counting richness.*

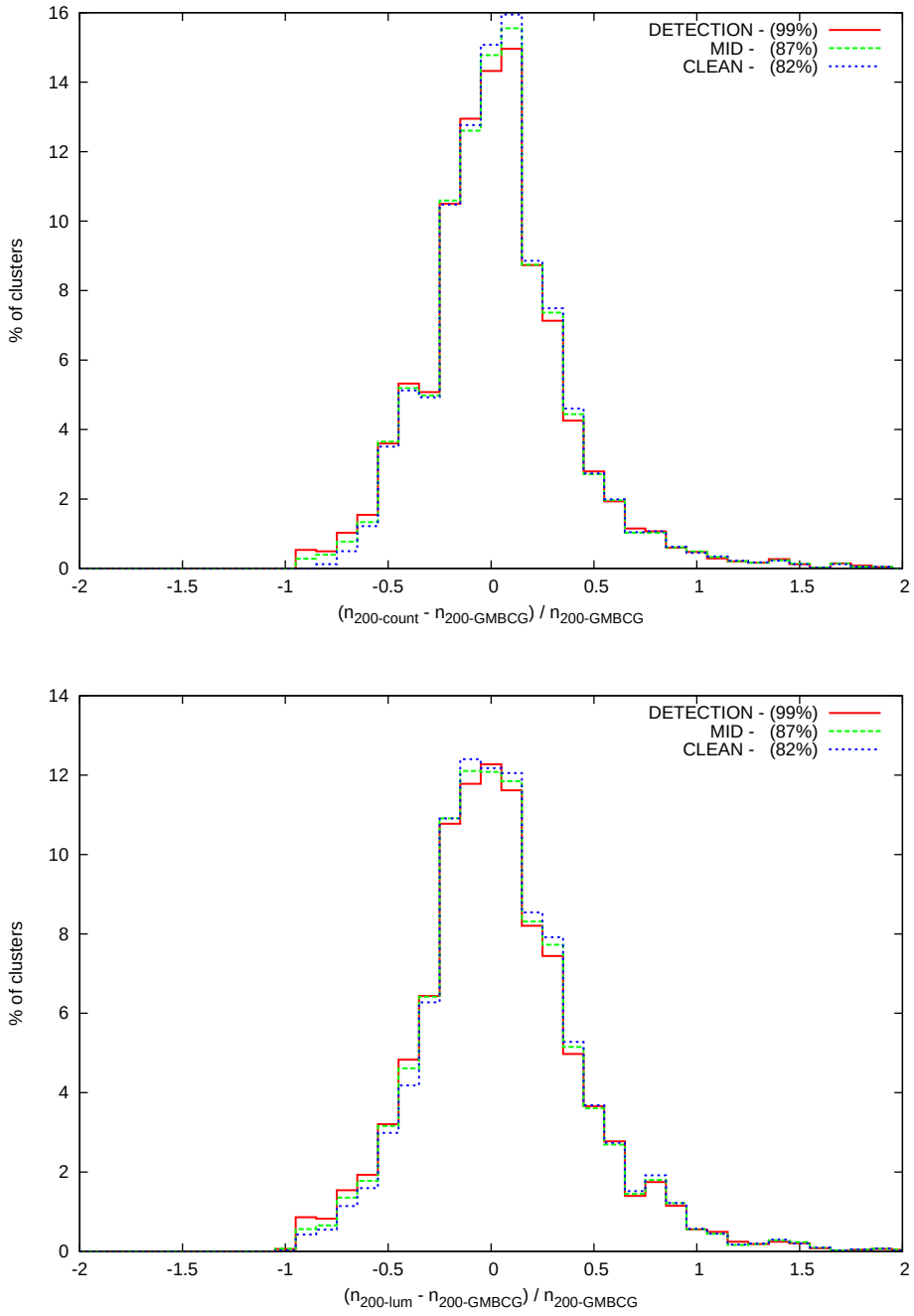

Figure 3.53 *A normalised histogram comparison of the GMPhoRCC n_{200} estimates to the GMBCG value using 4895 spectroscopic clusters with the top and bottom panels showing the counting and luminosity richnesses respectively. The comparison has been normalised and split into the separate quality bands where the legend shows the fraction of the total clusters in the subset. The counting subsets have estimates centred around the actual value with the clean attaining the fewest outliers. A slightly larger spread with more numerous and extreme outliers are observed in the luminosity estimates relative to counting due to the extra reliance and uncertainty introduced by fitting a luminosity function.*

3.5 Summary

Presented in this chapter is the **G**aussian **M**ixture full **Ph**otometric **R**ed sequence **C**luster **C**haracteriser (GMPhoRCC), which is designed to take potential cluster candidates, previously detected, and provide an optical confirmation and characterisation based on the red sequence. GMPhoRCC has been designed specifically to attain estimates of redshift, richness and the red sequence CMR and offers many advantages over existing algorithms including:

1. Treatment of multi-modal distributions.
2. Variable width red sequence.
3. Model independence.
4. Richness extrapolation.
5. Quality Control.

One of the most important features developed is the flag and quality control procedure. By flagging issues, particularly low richness and inconsistent red sequence and BCG redshifts, potential catastrophic failures can be identified and removed from cleaner subsets. By comparing GMPhoRCC estimates to those from existing catalogues the quality control has been calibrated. As richness is highly dependent on the input data and the particular definition and algorithm this was driven mainly using comparisons between GMPhoRCC and spectroscopic redshifts. While the majority of the flags and quality subsets are independent of the optical data it is noted that the consistency checks between the BCG and red sequence redshift are specific to the SDSS DR9 and must be calibrated to suit the available data.

With the quality controls calibrated, comparisons with real clusters from GMBCG, NORAS, REFLEX and XCS have shown that in addition to the high percentage ($\sim 75\%$) of all redshift estimates agreeing within $|z_{RS} - z_{spec}| < 0.01$, that the quality subsets are able to remove the majority of outliers.

Richness comparisons have proven to be more challenging relying on values highly sensitive to the exact definition, optical data and particular algorithm. In addition slight discrepancies in the redshift, BCG, and CMR result in the loss

of cluster members which, particularly with low richness clusters, can result in large fractional errors. This is reflected in the large scatter of estimates around the cluster value with only the most extreme outliers removed from the cleanest subsets.

Without a definite characterisation, comparisons with real clusters do not provide a complete assessment of GMPhoRCC, relying on an assumption that the analysis provided by other algorithms exactly describes the 'true' cluster. To get around this limitation, mock galaxy clusters can be constructed with known characterisations across a broad range of properties which can be used to provide comparisons. This allows a more comprehensive evaluation of the full GMPhoRCC characterisation and is explored in detail in Chapter 4.

Chapter 4

Mock Galaxy Clusters

While comparisons with existing catalogues are a useful tool to evaluate a characterisation method these can only take us so far. Existing methods are subject to their own strengths, weaknesses and selection functions hence a comparison with a controlled "truth" is required for absolute evaluation of a new method and this is often done using mock galaxy clusters. Mock clusters can be constructed with known redshifts, richnesses and colour magnitude relations (CMRs) which, when compared to GMPhoRCC estimates, gives insight into the overall performance as a function of cluster properties. One of the most important properties to investigate is completeness; this gives an estimate of how well GMPhoRCC can recover estimates as functions of redshift and richness. In contrast with cluster finders, this analysis relates only to the follow up characterisation from previously detected candidates which simplifies the analysis. Purity, although aimed more towards cluster finders, is another important trait estimating how many redshift and richness estimates are found by GMPhoRCC for fields with no clusters. In addition to these, redshift and richness comparisons can be done, similar to those shown in Section 3.4, to assess the accuracy of the GMPhoRCC estimates.

This chapter is structured as follows. Section 4.1 reviews some of the existing methods used to create mock clusters and their use to evaluate cluster finders, exploring many of the advantages and drawbacks of each. Section 4.2 details the empirical mocks used to assess GMPhoRCC, exploring the motivation behind this specific method and the properties of the resulting clusters. Section 4.3 explores the accuracy of GMPhoRCC, comparing estimates to the mock values.

To conclude Sections 4.4 and 4.5 investigate the purity and completeness of GMPhoRCC respectively to help estimate the selection function.

4.1 Review of Existing Mock Clusters

Mock clusters can be generated using two main methods, empirically using data from existing clusters or from simulations, constructing and populating dark matter halos from an underlying cosmological model.

4.1.1 Mocks from Simulations

Although using simulations to construct mocks gives a stronger tie to the underlying cosmology many of these mocks struggle to reproduce the observed optical properties of the cluster particularly the red sequence colour. Using these mocks naively risks optimising a code to fit the simulated data rather than real clusters. The following Sections gives an account of these mocks and their use to evaluate existing classification pipelines. Particular focus is given to how the more recent mocks recover the optical properties required.

maxBCG

maxBCG, (Koester et al., 2007b), is an optical red sequence cluster finder, using a probabilistic approach to identify spatial and colour clustering. In addition to an empirical Monte Carlo technique described in Section 4.1.2, maxBCG also uses mock clusters from N-body simulations to assess the algorithm. The exact construction of the mock clusters is not explicitly described but they generally consist of a dark matter halo and associated galaxies. A halo is considered detected if the red sequence galaxies of a maxBCG cluster exceed a fraction, 0.3, of the total, based on the ratio of areas of the average halo and r_{200} cluster. Completeness can be investigated as a function of halo mass, richness and redshift.

To apply this method to a red sequence finder/characterisation algorithm it is vital that the mocks accurately reflect the colours of the cluster members and their interaction with the halo. In general this is quite challenging for several reasons including limited resolution, complications in colour evolutions and unknown

behaviour at very high z, as noted by Song et al. (2012).

ORCA

ORCA, The Overdense red-sequence Cluster Algorithm (Murphy et al., 2012), is a red-sequence detector identifying surface and colour overdensities. Evaluation of this method comes from comparisons with maxBCG and a mock catalogue based on the Pan-STARRS medium deep survey (MDS). This mock was constructed by Cai et al. (2009) using a light cone from the Millennium Simulation, (Springel et al., 2005), which simulates a single tile of the MDS. The Millennium Simulation gives the cosmological framework to populate galaxies using the semi-analytic GALFORM model from Bower et al. (2006). This model assumes that galaxies are stripped of hot gas immediately following accretion onto the halo and join the red-sequence once the cold gas is depleted by star formation. This reproduces the bimodal colour distribution observed in clusters, however the rate of depletion results in galaxies redder than observed.

SZ Clusters from the South Pole Telescope

High et al. (2010) use an optical red sequence based algorithm to characterize SZ detected clusters from the South Pole Telescope. By identifying the colour from a colour-redshift model which maximizes the overdensity of galaxies, a red sequence is determined. Completeness and purity are evaluated in a similar manner as described in the previous Sections using the mock catalogues from Song et al. (2012). These mocks are based on high resolution N-body simulations with red and blue galaxies configured to match observations of real clusters. Completeness remains above 90% for $z < 1$; this not only reflects on the cluster finder but also highlights that the mocks represent red sequence clusters reasonably well.

4.1.2 Empirical Mocks

Empirical mocks rely on constructing a field with a random background and artificial cluster from existing optical data. As described in the subsequent review, artificial clusters are produced by taking observations of well known existing clusters and randomly sampling the red sequence to give a mock with a desired richness. In order to extrapolate the mock to a specific redshift the photometry

must be adjusted and this is done using K+e-corrections. This combines the change in the galaxy SED brought about by evolution (see 2.2.2), and the change due to observation at a different cosmological distance. K+e-corrections are fundamental components required to produce mocks across a range of redshifts and are explored in more detail in Section 4.1.2. Although many empirical mocks share these basic principles the exact input clusters and sampling vary across the different methods and are discussed in detail in the remaining sections.

K+e-correction

One fundamental component needed in order to construct empirical mocks across a range of redshifts is the ability to extrapolate photometry and this is done using K+e-corrections. K-corrections, outlined in Blanton et al. (2003), Blanton & Roweis (2007) and Hogg et al. (2002), account for the fact that while sources are observed at a redshift of z in a particular band, say R, the absolute magnitude has a rest-frame observation in another band, say Q, and are defined below:

$$m_R = M_Q + DM(z) + K_{QR}(z) \tag{4.1}$$

where m_R is the apparent magnitude in band R, M_Q is the absolute magnitude in band Q, $DM(z)$ is the distance modulus and $K_{QR}(z)$ is the K-correction. With M_Q independent of observed redshift, finding K-corrections allows the extrapolation of m_R to an apparent magnitude observed at another redshift. Specifically considering the method described in Blanton & Roweis (2007) and implemented in the code `KCORRECT` v4.2, K-corrections are found by fitting a spectral energy distribution (SED) as a linear combination of template spectra to the galaxy multi-band fluxes. From this SED the differences in fluxes observed in different bandpasses can be found.

K-Corrections alone are insufficient to extrapolate photometry to different redshifts as these assume the galaxy SED is constant which in general may not be the case. As galaxies evolve many factors can alter the SED, such as star formation bursts or the passive increase in metallicity caused by nuclear fusion in stars, and these effects must be accounted for while extrapolating photometry. By considering fictitious galaxies with specific populations and using stellar evolution models, the metallicity, mass and ultimately SED of the galaxy can be computed as a function of redshift. As a typical example, colour evolutions of LRGs are

explored in Tojeiro et al. (2011) by using several stellar population and evolution models to trace the full metallicity history of galaxies as a function of observed redshift and absolute magnitude.

Combining both K and evolution, K+e-corrections allow for the full extrapolation of photometry across a range of redshifts necessary to construct empirical mocks.

maxBCG

In addition to the simulation mocks, maxBCG uses a Monte-Carlo style sampling to produce empirical mocks to test the algorithm. The Monte-Carlo approach first creates a background using the maxBCG input by reassigning galaxy colours and randomizing positions to within $5'$. By running maxBCG over this background, purity is investigated. It was found that for $N_{200} = 10$ there is a 7% false-positive rate falling to $< 1\%$ for $N_{200} > 20$.

To investigate completeness, artificial clusters are added using data from Abell clusters stacked at various redshifts as a model (up to $z = 0.26$). At each redshift, radial distributions and colour distributions are modelled by power laws and 4th order polynomials respectively. Artificial clusters are then given a random redshift-richness value from the maxBCG catalogue (Koester et al., 2007a) and appropriate radial and colour models for the redshift. The colour distribution is K+e-corrected to match the specific cluster redshift using `KCORRECT` v4.1.4 (Blanton et al., 2003) with evolution correction derived from a Pegase-2 stellar population / galaxy formation model from Eisenstein et al. (2001). As an example of maxBCG-style K+e correction, the faint end cut-off used in Chapter 3 shown in Figure 4.1, shows how the apparent i-band magnitude of an LRG with an absolute magnitude of $M_i = -21.24$ changes with observed redshift.

Finally, an artificial cluster is considered detected if maxBCG finds a cluster within ± 0.025 in redshift with $N_{200} > N_{200-mock}$.

Construction in this way produces mocks which match the optical data precisely, allowing the evaluation of performance specific to the maxBCG input. By using observation of real galaxies the mocks recover the expected optical properties, such as colour, for the optical input. Matching the input is extremely important as performance is strongly correlated to the optical data. If several different optical sources are used however, separate mock analysis will be needed for each.

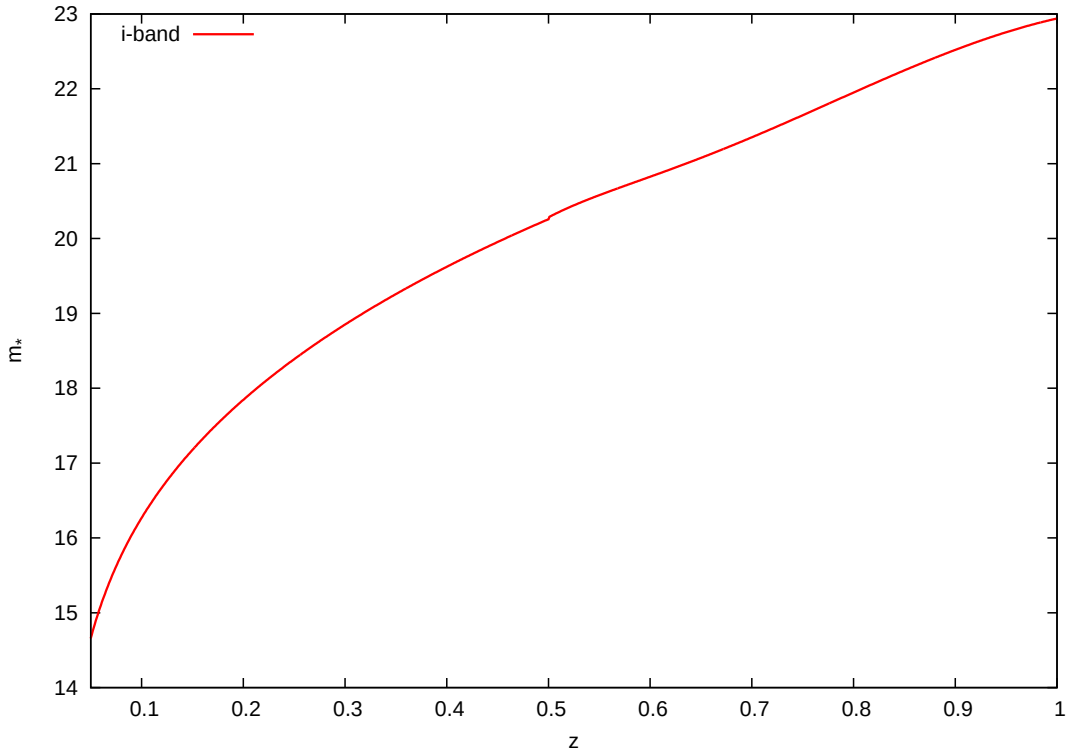

Figure 4.1 *The apparent i-band magnitude of an LRG with absolute magnitude, $M_i = -21.24$ as a function of redshift derived using maxBCG-style K+e-corrections.*

GMBCG

GMBCG (Hao et al., 2010), follows a similar Monte-Carlo technique as maxBCG to create simple mocks for evaluation. Their construction is as follows:

1. Background: Several large areas of the input are used with the rich ($N_{200} > 20$) clusters removed. The positions of these galaxies are randomized but they retain colours and redshifts.

2. Model Clusters: 49 rich clusters are selected in the range $0.01 < z < 0.55$ with $30 < N_{200} < 100$

3. Model Resampling: Randomly select a model BCG and a fixed number of cluster members randomly drawn from [10, 15, 20, 25, 30, 35, 40, 45, 50]

4. Adding Artificial Clusters: Randomly select a galaxy in the background to replace with the model BCG and add the cluster members maintaining relative positions.

Mock clusters are considered detected provided a redshift is found within ± 0.05 of the mock value. By cross matching the GMBCG clusters found using this input to the mock catalogue, completeness and purity can be estimated. Completeness is simply the fraction of the whole mock catalogue found and cross matched. Purity is the fraction of GMBCG clusters which is cross matched to the mock catalogue.

Again these mocks have the advantage of matching the optical data allowing a specific analysis relevant for the input. One possible concern is the reliance on the sampling of rich clusters to produce all the mocks across a range of richnesses. While it is necessary to have well understood clusters for resampling, generating all mocks from rich clusters relies on the independence of real cluster properties with richness, which may not be the case. To get around this, using seed clusters across a range of richnesses would be most desirable. Implementing this however is not straightforward and requires a sample of well observed low richness clusters which are difficult to produce.

4.2 Constructing SDSS Empirical Mocks

One of the simplest methods of generating mock clusters is to use empirical methods based on existing cluster detections. On the basic level this involves adding artificial clusters to field galaxies, derived from existing cluster detections and the targeted optical data. This has the advantage of producing mock clusters tailored to match the input, allowing the evaluation of GMPhoRCC characterisations produced using the specific optical data. This Section details the ingredients and recipes for constructing suitable empirical mocks to evaluate GMPhoRCC.

Firstly considering the artificial clusters, comprising a BCG and a red sequence, there are five main aspects listed below which must be reproduced to provide mocks suitable for use with GMPhoRCC.

- A suitable BCG
- Radial profile
- Redshift distribution
- Luminosity function

- CMRs / Colour distributions

All these properties can be reproduced from the properties of well observed seed clusters similar to those from maxBCG and GMBCG. However since these all depend on the cluster properties it is necessary to extend this technique across a large redshift and richness. With the introduction of quality bands, GMPhoRCC has the ability to identify very clean clusters which can be used to generate the mocks. Around $\sim 10,000$ of these clusters are found from the C4, GMBCG, REFLEX, NORAS and XCS catalogues using the clean sample with very good agreement between spectroscopic and GMPhoRCC redshifts, $|z_{spec} - z_{GMPhoRCC}| < 0.005$. By separately stacking the BCG and red sequence galaxies of these clusters in redshift/richness bins, a larger source is produced to sample cluster properties than from considering these individually. Stacking in this way ensures that each bin is dominated by cluster members where the bulk properties are representative of a cluster with the bin redshift and richness.

At this stage there are two methods which can be used for generating clusters with bin-appropriate properties, using generator functions or random sampling with replacement. By fitting CMRs, radial, luminosity and redshift distributions to the full list of red sequence galaxies these can be used as stacked generator functions, from which random galaxies can be drawn. Alternatively by sampling red sequence galaxies with replacement, similar to a bootstrapping method, the sampled galaxies are representative of the underlying distributions. Resampling provides the easiest solution, natively providing statistical noise and bin-appropriate measurement errors without any further effort. Figure 4.2 summarises the various steps used to generate the mock clusters used throughout this chapter using this sampling method.

Generation of the artificial clusters begins by randomly selecting a redshift and richness. Next a generator bin is selected randomly from the three closest to the desired mock. A random BCG is selected with red sequence galaxies repeatedly sampled until the desired n_{200} is met. At each stage galaxies are added, a red sequence CMR, n_{gals}, r_{200} and current n_{200} are found. This produces a cluster with a redshift corresponding to the bin. By adding $\Delta z = z_{cluster} - z_{bin}$ to each galaxy redshift with a K+e-correction to the photometry, an artificial cluster with desired redshift and richness is produced.

K-corrections are done using `KCORRECT` v4.2 from Blanton & Roweis (2007). To ensure the analysis of the mocks is insensitive to the evolutionary model, several

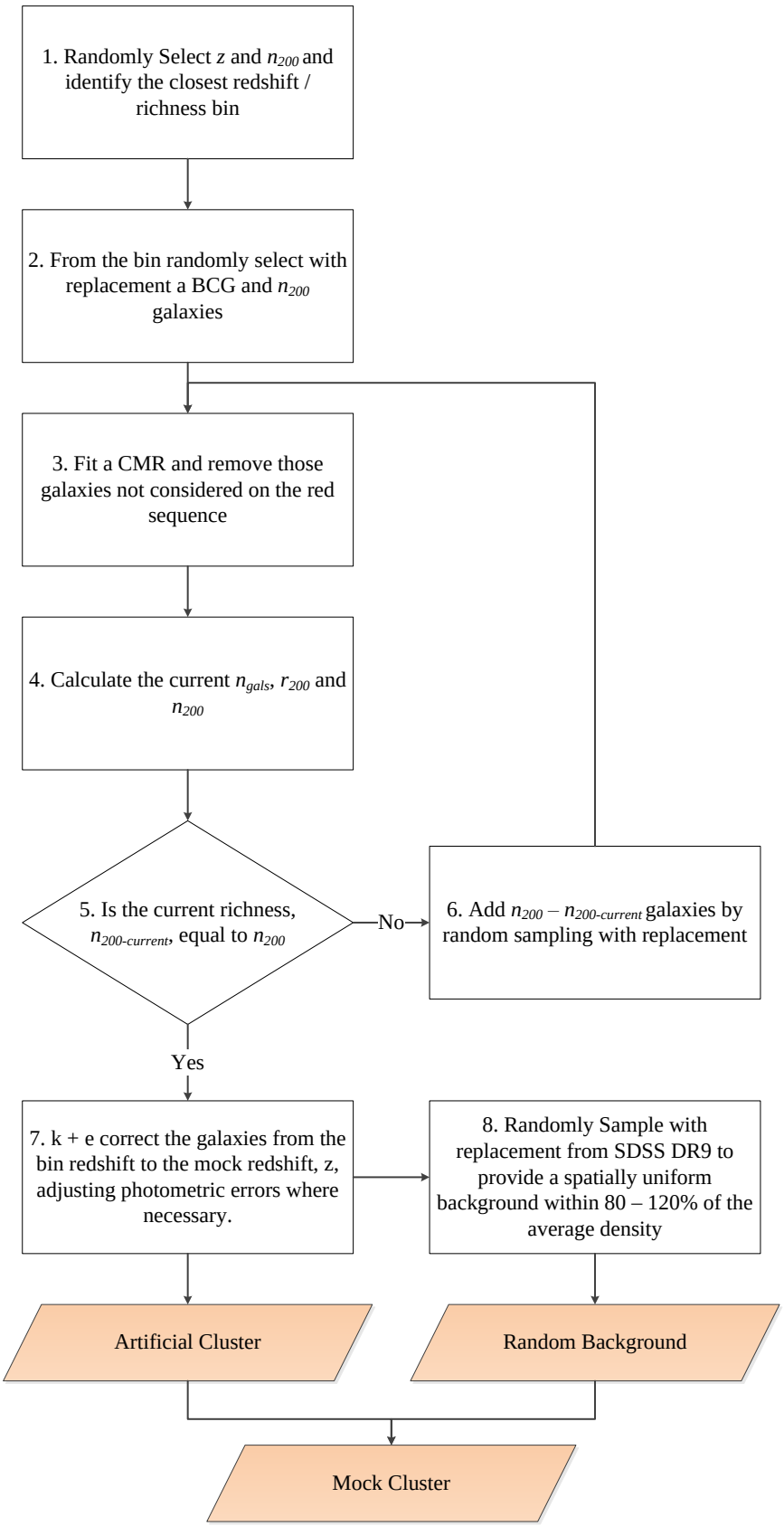

Figure 4.2 *A flowchart summarising the various steps in the construction of empirical SDSS DR9 mock galaxy clusters.*

are used to produce different sets of mock clusters. In addition to the maxBCG evolution outlined in Section 4.1.2, models from Tojeiro et al. (2011) are also used.

The evolution models of Tojeiro et al. (2011) are found by stacking the SDSS DR7 LRG sample (Abazajian et al., 2009) in redshift-colour-luminosity space to produce high signal-to-noise stacked spectra as a function of the photometric data. The stacked results of each cell are analysed using VESPA which models the galaxy spectra as a superposition of those from simple stellar populations (SSPs) of different metallicities and ages. From the superposition of SSPs the full star formation and metallicity history is computed. Finally from these the full evolution of colours is computed. The three SSP models considered by Tojeiro et al. (2011), BC03 (Bruzual & Charlot, 2003a), M10 (Maraston et al., 2009) and FSPS (Conroy & Gunn, 2010), result in different corrections which are used in this chapter to show the insensitivity of GMPhoRCC to the particular evolution used to construct the empirical mocks.

Next it is important to ensure the photometric errors are appropriate for a cluster at the desired redshift. This mainly affects high redshift artificial clusters which should possess higher errors than the low redshift seed due to the fainter photometry. To reproduce appropriate errors in each band, a sample of $\sim 500,000$ red sequence galaxies is used to model the error as a function of magnitude. By binning the galaxies the average error and standard deviation is found as a function of magnitude. A galaxy is assigned a new error by first interpolating a mean and spread based on the galaxy brightness and then by randomly sampling a Gaussian with those properties. This ensures random error generation which matches the bulk properties of the bin. To reflect this change it is necessary to reassign the galaxy magnitudes randomly using the larger Gaussian errors. Although photometric errors depend on a number of things including seeing, this method reproduces sensible errors providing good agreement with existing high redshift clusters as shown in fig 4.3.

With the artificial cluster generated the final step is to add a random background/foreground field. By sampling with replacement from DR9, a random background is generated which is representative of real field galaxies. These galaxies are added with a uniform spatial distribution matching within 80 - 120% of the average background density.

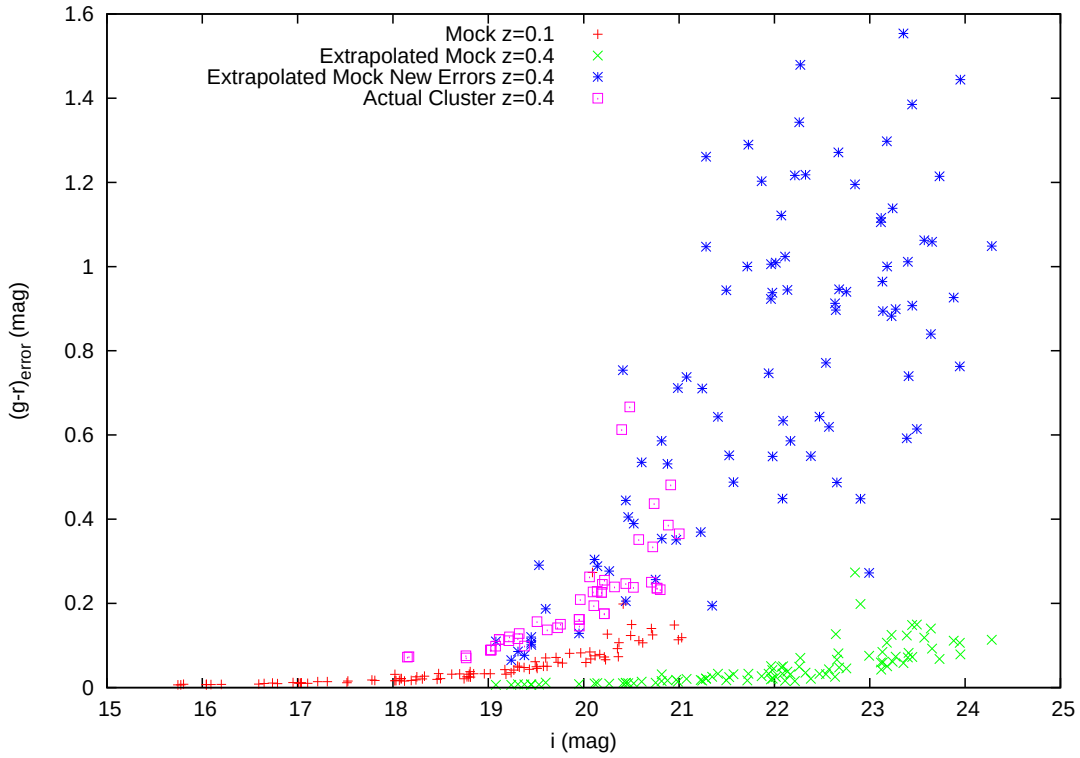

Figure 4.3 *A plot showing how the $g-r$ error compares between the $z = 0.1$ seed cluster, the extrapolated cluster at $z = 0.4$ with and without the new errors and a real $z = 0.4$ cluster. Without the new photometric errors it is clear that the extrapolated cluster underestimates the $g-r$ error. The new errors are seen to be in good agreement with an observed cluster at the same high redshift.*

4.2.1 The Properties of the Mock Clusters

Before any subsequent analysis can be done it is necessary to ensure the mocks are reasonable representations of real clusters. By comparing the bulk properties of the redshift/richness bins to that of a sample mock and a seed cluster it is shown indeed that the bins and mocks are good representations of clusters with the given properties.

Consider first the redshift/richness bin representing $8 \leq n_{200} < 11$ and $0.1 \leq z < 0.105$. Figures 4.4 and 4.5 show the redshift and $g-r$ colour distributions respectively for the bin, a sample mock and seed cluster showing them to be in good agreement.

Similarly, considering the higher redshift and richness bin, $40 \leq n_{200} < 45$, $0.425 \leq z < 0.455$, Figures 4.6 and 4.7 show the redshift and $r-i$ colour distributions respectively for the bin, a sample mock and seed cluster showing

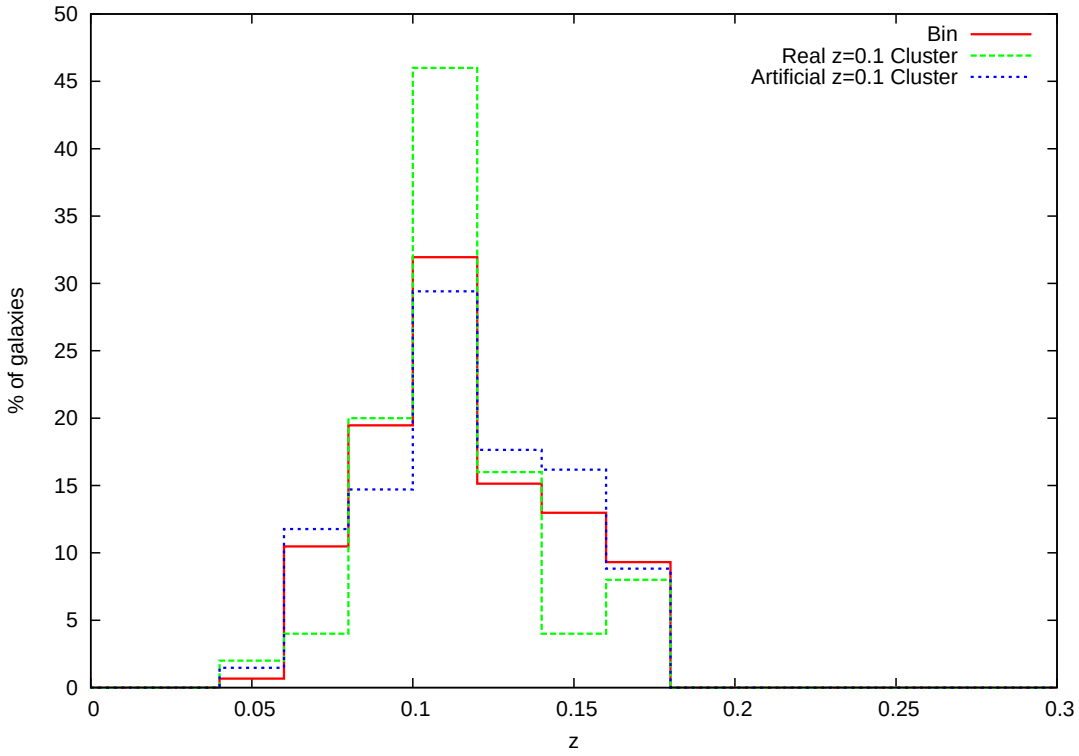

Figure 4.4 *A histogram showing the redshift distribution of a redshift/richness bin representing* $8 \leq n_{200} < 11$ *and* $0.1 \leq z < 0.105$ *compared with that from a sample mock and seed cluster from the same bin. The distributions show good agreement confirming the mock and bin to be good representations of real clusters with those properties.*

them to be in good agreement.

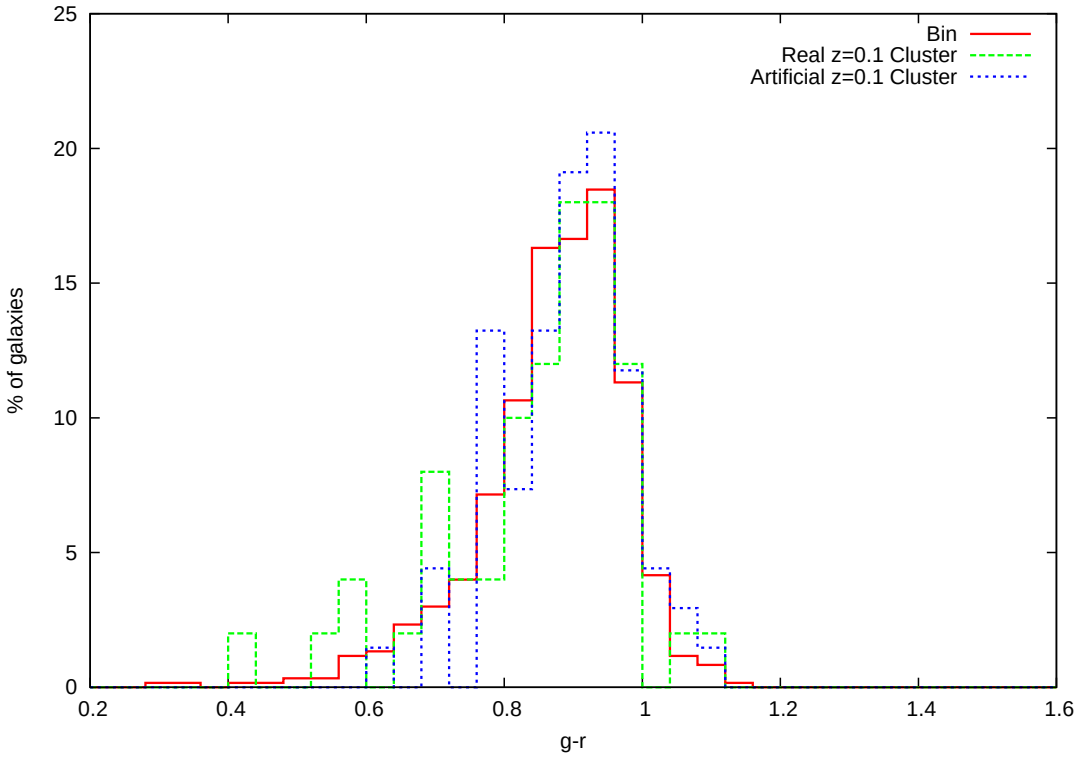

Figure 4.5 *A histogram showing the $g-r$ distribution of a redshift/richness bin representing $8 \leq n_{200} < 11$ and $0.1 \leq z < 0.105$ compared with that from a sample mock and seed cluster from the same bin. The distributions show good agreement again confirming the mock and bin to be good representations of real clusters with those properties*

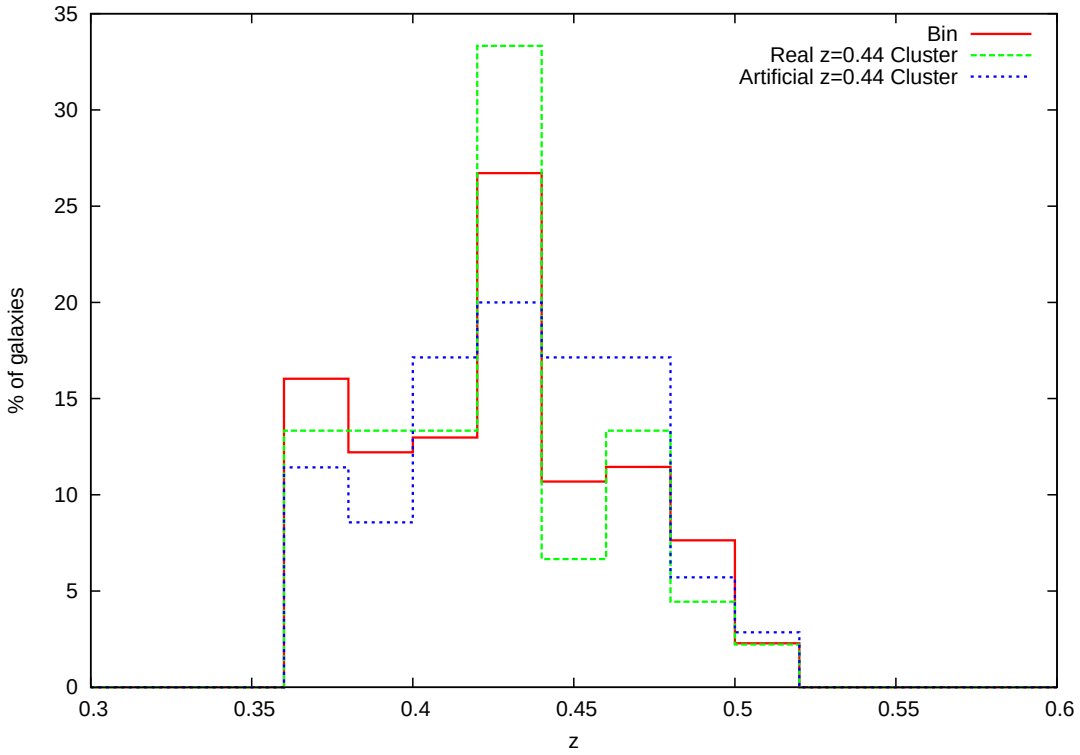

Figure 4.6 *A histogram showing the redshift distribution of a redshift/richness bin representing* $40 \leq n_{200} < 45$ *and* $0.425 \leq z < 0.455$ *compared with that from a sample mock and seed cluster from the same bin. The distributions show good agreement confirming the mock and bin to be good representations of real clusters with those properties*

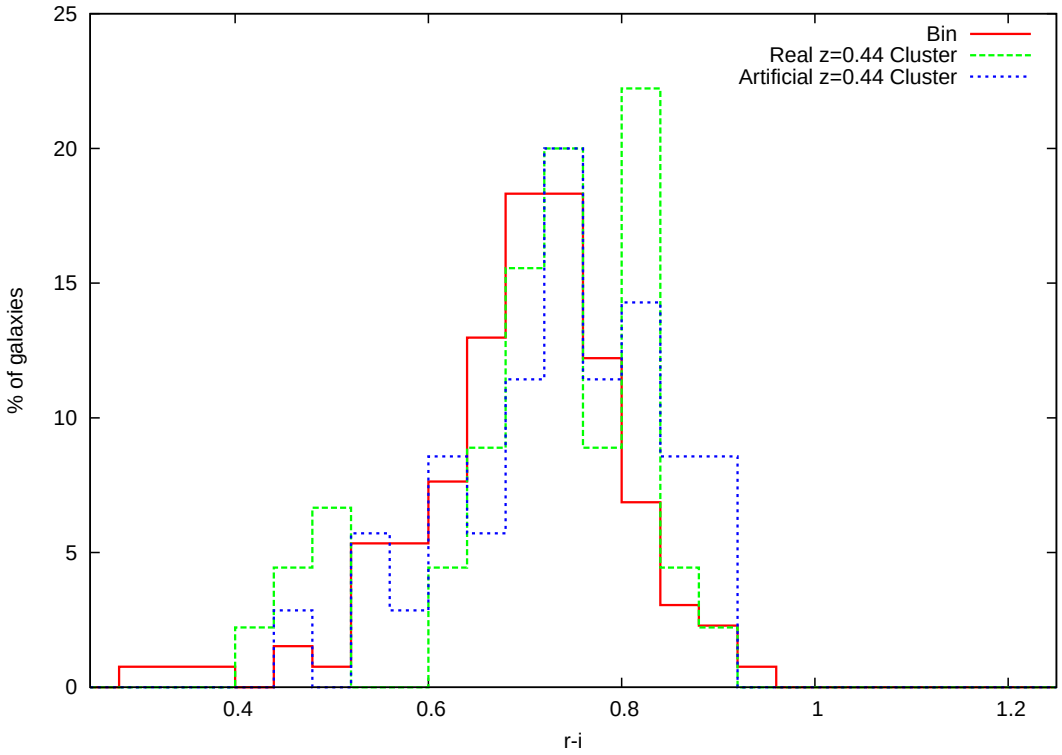

Figure 4.7 *A histogram showing the $r-i$ distribution of a redshift/richness bin representing $40 \leq n_{200} < 45$ and $0.425 \leq z < 0.455$ compared with that from a sample mock and seed cluster from the same bin. The distributions show good agreement again confirming the mock and bin to be good representations of real clusters with those properties*

Red Sequence Width

The following analysis using mocks explores how the intrinsic width of the red sequence varies with redshift, confirming that the fixed red sequence width of 0.05 used by GMBCG (Hao et al., 2010), maxBCG (Koester et al., 2007b) etc., is sufficient to describe the full scatter of the CMR. Although this is an adequate description of the scatter it is found in practice fitting a variable width increases the number of reliable GMPhoRCC characterisations of clusters from the maxBCG (Koester et al., 2007b), GMBCG (Hao et al., 2010) and XCS (Mehrtens et al., 2012) catalogues by 10%.

The mock catalogue for this analysis was produced by initially generating 80 clusters at $z = 0.1$ followed by K+e-corrections to give representations of these across a range of redshifts, $0.05 \leq z < 1.1$, resulting in a total of 4320 mocks. For each mock a red sequence CMR is fitted using all the colour bands i.e. $g-r$, $r-i$ and $i-z$ with the intrinsic width found by using the error-corrected expectation maximisation procedure to fit a Gaussian around the CMR as shown in Section 3.1.3. Figure 4.8 shows the widths of the red sequences across the redshift range generated using the maxBCG evolution outlined in Section 4.1.2, where 'mix' highlights where GMPhoRCC changes band to suit the redshift. In addition to showing that the fixed 0.05 scatter is sufficient to describe the cluster, the increase in width with redshift, in agreement with Rykoff et al. (2013), highlights the value of changing colour band as a function of cluster redshift as low scatter CMRs are easier to isolate and model. Figure 4.8 also shows that the larger realistic photometric errors[1] dominate the scatter of the CMR resulting in artificially small values for the intrinsic width agreeing with those observed from real clusters as discussed in Section 3.1.3. Again this highlights the need for a minimum value for the width, $\sigma = 0.05$.

Using the GMPhoRCC redshift-dependent colour band, Figure 4.9 compares the widths found using mocks generated using the different evolution models described in Section 4.1.2. The sudden large increases in widths observed using M10 and BC03 result from the introduction of bi-modal colour distributions. With the selection of evolution from Tojeiro et al. (2011) dependant on galaxy redshift, colour and absolute magnitude, the cluster galaxies follow several adjacent colour evolution tracks. While in general the evolution corrections from

[1]See Figure 4.3 where $z > 0.3$ red sequences are dominated with $i > 20$ galaxies with large (> 0.2) colour errors

the various tracks are similar, around $z \sim 0.2$ and $z \sim 0.4$ for M10 and BC03, significant differences lead to the introduction of bi-modal colour distributions and wider red sequences. While the different models give rise to different widths, GMPhoRCC is insensitive to the particular form of the evolution or red sequence since an optimal width is found for each cluster. This is demonstrated in more detail in subsequent sections, comparing results from mocks generated from different evolution models.

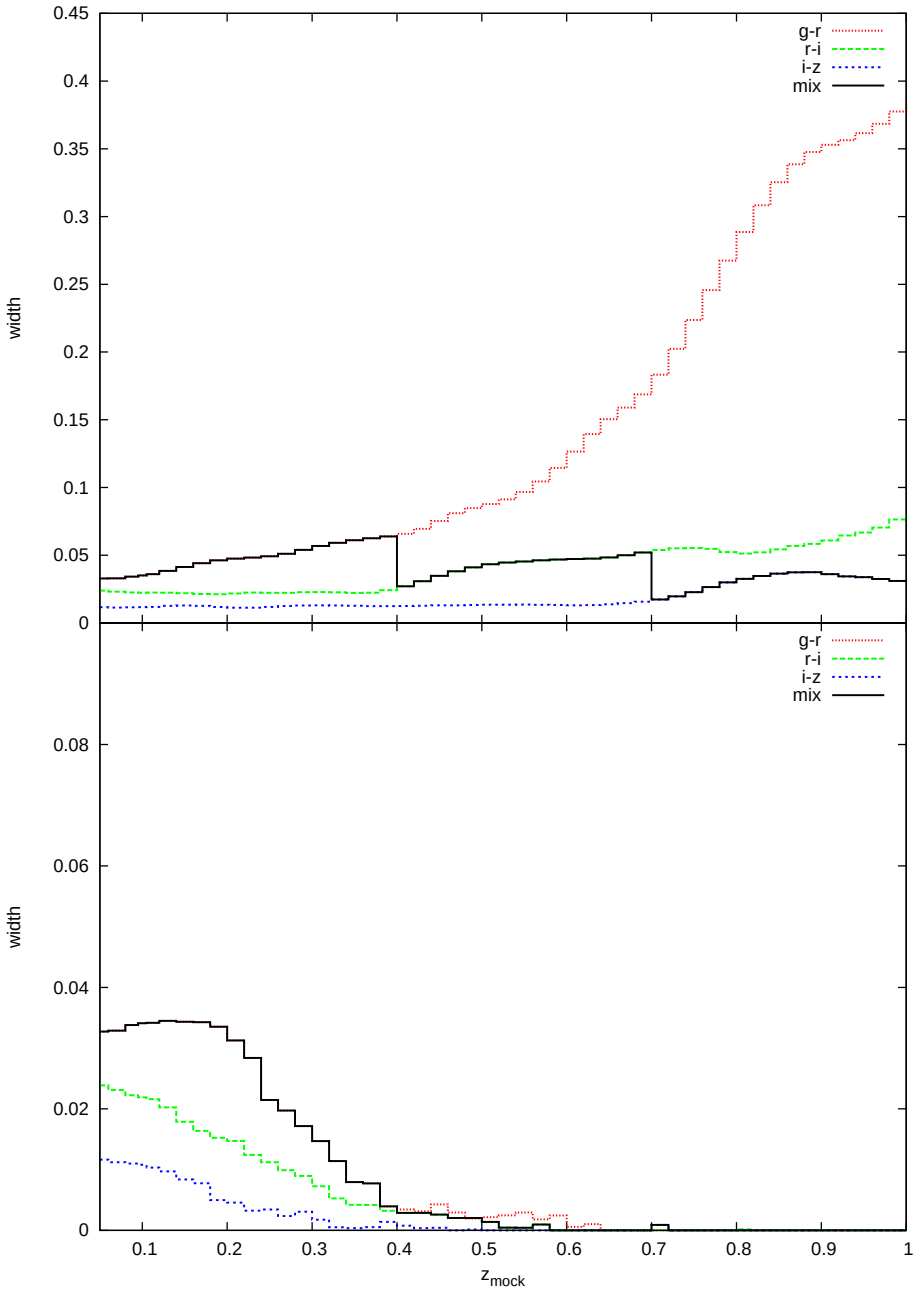

Figure 4.8 *The intrinsic width of the red sequence as a function of redshift for* 4320 *mocks generated with K+e-corrections using maxBCG-style evolution where the bottom and top panels show respectively results with and without realistic error extrapolation. In both cases a fixed width,* $\sigma = 0.05$*, is sufficient to describe the red sequence, however in practice fitting a variable width increases the reliability of the GMPhoRCC characterisation. The larger photometric errors used in the bottom panel (Typically* > 0.2 *for* $z > 0.3$ *red sequences, dominated by* $i > 20$ *galaxies as can be seen in Figure 4.3), dominate the scatter of the CMR resulting in artificially small values for the intrinsic width. Again this highlights the need for a minimum value for the width,* $\sigma = 0.05$*.*

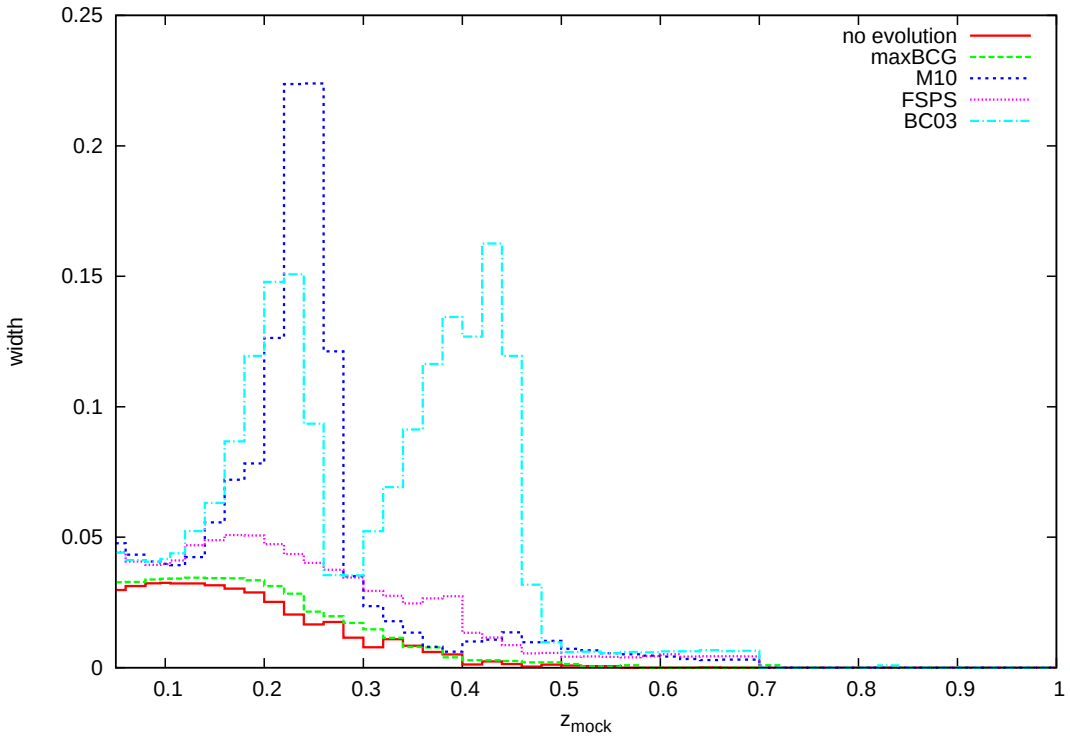

Figure 4.9 *The intrinsic width of the red sequence as a function of redshift for* 4320 *mocks generated with various K+e-corrections. Large sudden increases in widths observed with M10 and BC03 result from the introduction of bi-modal colour distributions. At these redshifts adjacent colour evolution tracks have significant differences in the correction resulting in bi-modal colour distributions and wide red sequences. While each evolution gives rise to a different form for the red sequence width, GMPhoRCC will be shown to be insensitive to the evolution model in subsequent sections.*

Richness

As discussed in Section 3.1.4 it is essential to show that the GMPhoRCC richness is consistent across a range of redshifts and colour bands. This can be done by considering the richnesses of the previous mock catalogue. The catalogue consists of 80 artificial clusters generated at $z = 0.1$ then K+e-corrected to produce representations across $0.05 \leq z < 1.1$. This allows the comparison of richness from the same mock observed at different redshifts.

While these results hold for n_{gals}, this Section focuses on n_{200} as this represents the best optical mass proxy. Figure 4.10 shows the median comparison between the mock and the original $z = 0.1$ richness as a function of redshift for the different evolution models outlined in Section 4.1.2. This highlights the importance of adding an evolution correction; many of the galaxies' i-band brightness becomes incorrectly fainter than the $m_* + 1$ cut off shown in Figure 3.15 resulting in the underestimated richness. Most importantly in the cases with evolution, the richness estimates are consistent across the various red sequence colour bands and up to $z_{mock} \sim 0.7$. Above this redshift the form of m_*, used to define the faint end richness limit, is no longer consistent with the SDSS as noted by Rykoff et al. (2013). In addition to this there are no significant differences between the evolution models, showing again the insensitivity to form of the red sequence and specific evolution.

While it is important to assess richness across a whole range of redshifts, in reality many of the high redshift clusters are too faint to be detected in the SDSS. By removing faint galaxies with $i \geq 21$ magnitudes, the mock catalogue can better match real clusters found in the SDSS. From Figure 3.15 it is expected that for $z > 0.45$ cluster galaxies will be lost due to the incomplete photometry resulting in reduced richness estimates which is exactly shown in Figure 4.11. In the region of complete photometry, $z < 0.45$, both estimates are shown to be consistent and insensitive to the evolution model. In addition the problem with m_* above $z > 0.7$ is dwarfed by the loss of cluster members due to incomplete photometry.

The main purpose of using the luminosity method is the hope that this can accurately extrapolate richness for clusters subject to incomplete photometry and Figure 4.12 shows that this is indeed the case. While the counting richness starts to fall off for $z > 0.45$ the luminosity richness remains consistent for $z < 0.55$. For $z > 0.55$ there are insufficient galaxies detected to adequately fit a luminosity function and both richness estimates become unreliable.

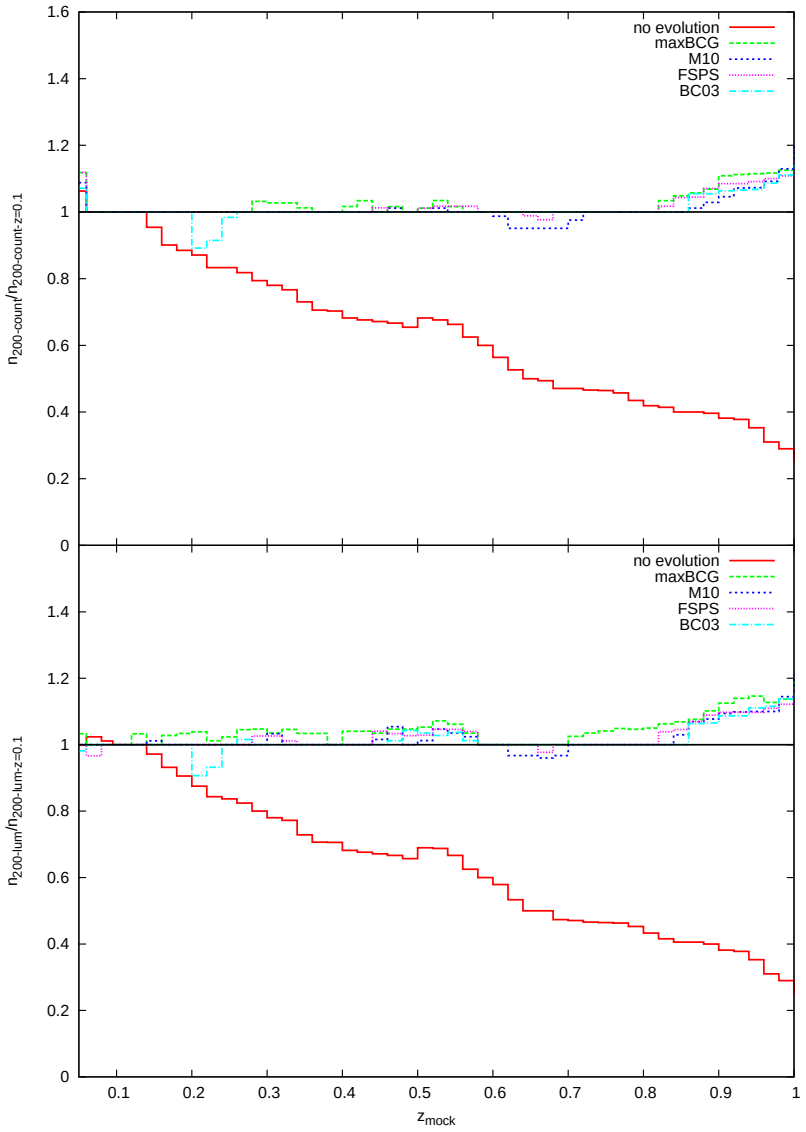

Figure 4.10 *A comparison of n_{200} as a function of redshift for 4320 mocks generated with various K+e-corrections where the top and bottom panels present the counting and luminosity richness respectively. The GMPhoRCC richness is shown to be consistent across the various red sequence colour bands and up to $z_{mock} \sim 0.7$. Above this redshift the form of m_*, used to define the faint end richness limit, is no longer consistent with the SDSS as noted by Rykoff et al. (2013). In addition to the richness consistence, it is clear that with no significant differences between the models GMPhoRCC is insensitive to the exact form of the evolution.*

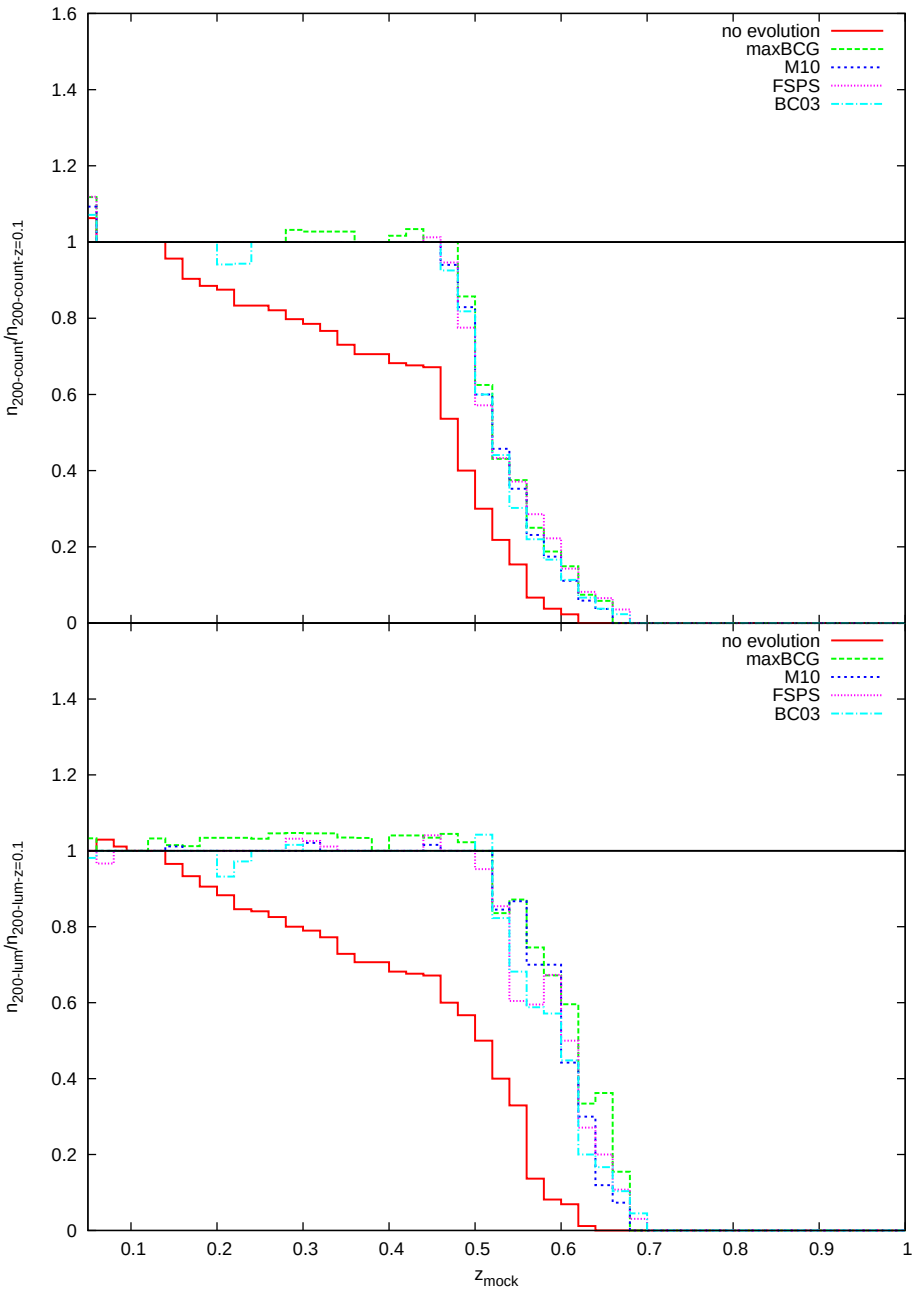

Figure 4.11 *A comparison of n_{200} as a function of redshift where the top and bottom panels present the counting and luminosity estimates respectively for* 4320 *mocks generated with various K+e-corrections using the SDSS complete photometry cut, $i < 21$ magnitudes. GMPhoRCC richness is shown to be consistent where photometry is complete, i.e. $z < 0.45$. Above this redshift cluster galaxies become too faint for reliable detection resulting in the reduction in richness.*

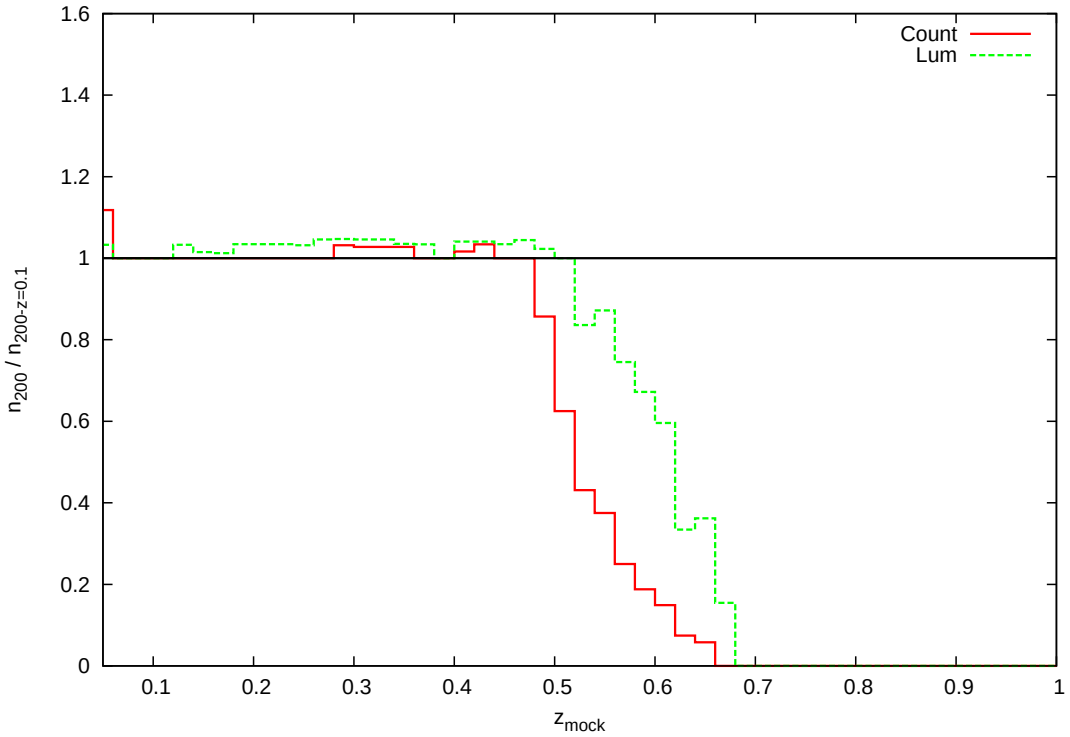

Figure 4.12 *A comparison of luminosity and counting n_{200} as a function of redshift for 4320 mocks generated with maxBCG-style K+e-correction using the SDSS complete photometry cut, $i < 21$ magnitudes. Luminosity richness is shown to be able to reliably extrapolate beyond the $z = 0.45$ completeness level, highlighted by the counting method, up to $z = 0.55$.*

4.3 GMPhoRCC Comparisons

In order to assess the accuracy of GMPhoRCC estimates, comparisons to actual mock cluster redshifts and richnesses are explored in this section. Mock catalogues were generated using K+e-corrections for each of the evolution models outlined in Section 4.1.2 with $0.05 < z < 1.1$ and $5 \leq n_{200} \leq 75$. This analysis focuses on accuracy and in order to highlight any possible bias as a function of cluster properties, the i-band< 21 cut to simulate incomplete photometry in the SDSS, as used in the previous section, is not used. Exploring the effect of incomplete photometry and the ability of GMPhoRCC to reliably estimate cluster properties across a range of redshift and richnesses is deferred to Section 4.5.

4.3.1 Redshift

The following analysis focuses on the red sequence photometric redshift estimate obtained by GMPhoRCC for mocks generated using maxBCG-style evolution.

Of the 7050 clusters, redshift estimates were found for 99.8% and compared to the mock value where Figure 4.13 highlights the results for each of the quality subsets. Although some discrepancies are present the cleaner subsets are able to identify and remove the worst outliers. Additionally, while the majority of all estimates are within $|z_{RS} - z_{mock}| < 0.01$, the clean subset has a larger fraction within this bound and less contamination with outliers as shown more clearly in Figure 4.14.

For the higher redshift clusters, $z > 0.6$, the large photometric errors make it difficult to isolate the red sequence resulting in the discrepancies. At the low redshift end, $z < 0.1$ poorer contrast against the background and limitations in the field area result in similar issues with fitting the red sequence. This agrees with the comparisons from existing catalogues shown in Section 3.4 and will help to define a reliable operational redshift range.

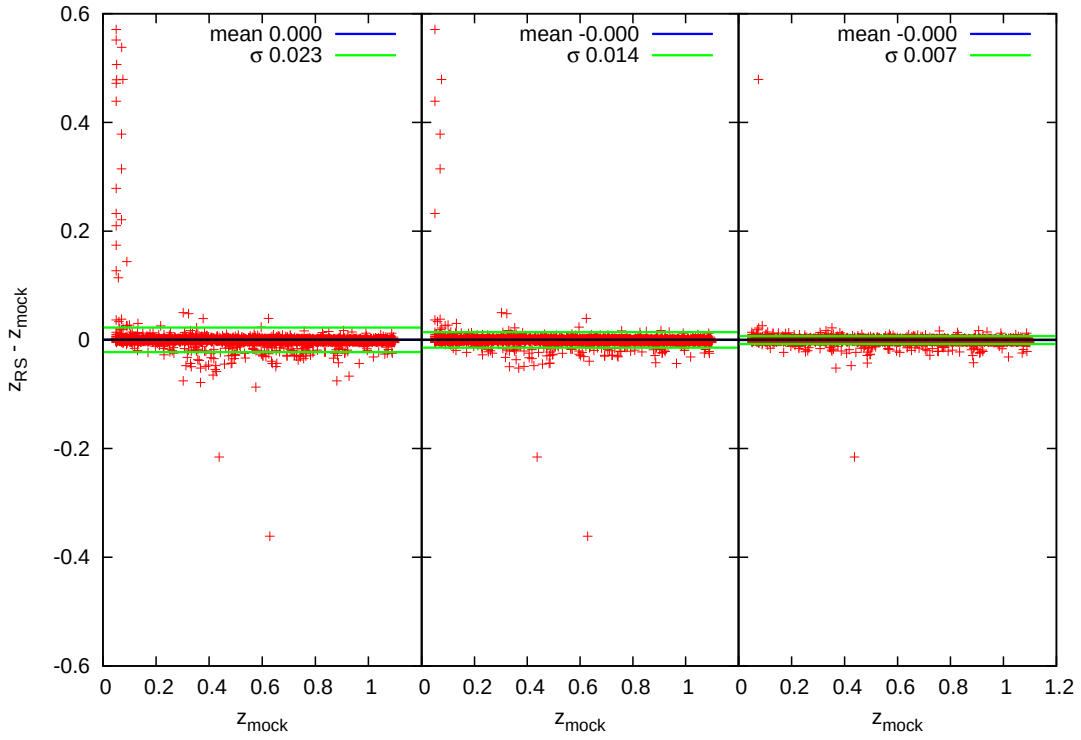

Figure 4.13 *A comparison of GMPhoRCC photometric red sequence redshift to the actual cluster value for* 7050 *mocks generated using maxBCG evolution showing from left to right the detection, mid and clean subsets. With the exception of two outliers, all catastrophic failures have been removed in the cleanest subset.*

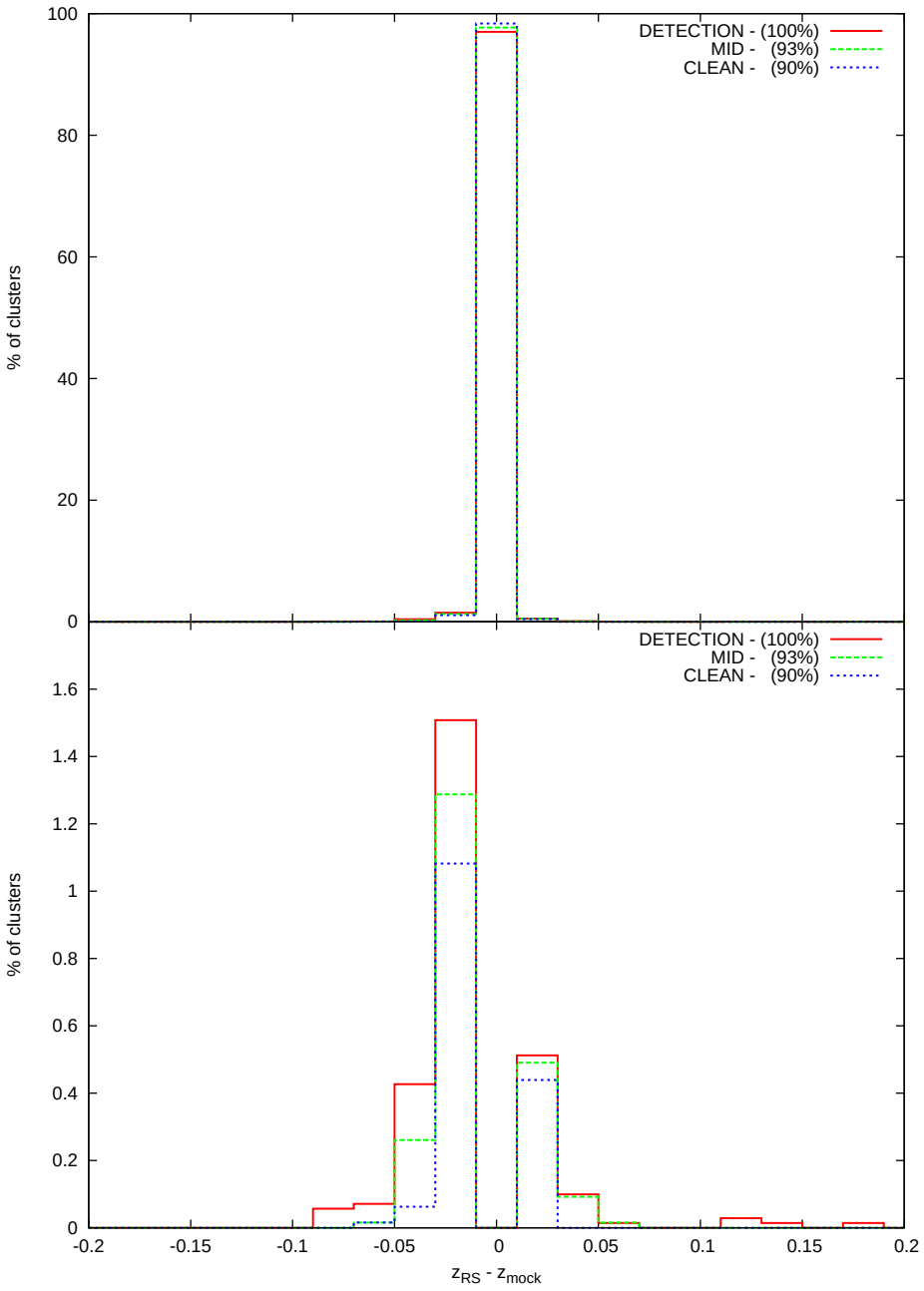

Figure 4.14 *A histogram comparison of GMPhoRCC photometric red sequence redshift to the actual cluster value for* 7050 *mocks generated using maxBCG evolution. The comparison has been normalised and split into the separate quality bands where the legend shows the fraction of the total clusters in the subset. The bottom panel omits the middle bin to highlight the outliers where the clean subset can be seen to have removed the worst estimates with a greater fraction within* $|z_{RS} - z_{mock}| < 0.01$

Expanding this comparison to mocks generated using different evolution models shown in Figures 4.15 shows no significant differences in the estimates for the detection subset. These similarities hold for each of the quality bands with the mid and clean sets comprising $\sim 92\%$ and $\sim 89\%$ of all the mocks respectively. GMPhoRCC is again shown to be insensitive to the exact form of the evolution model.

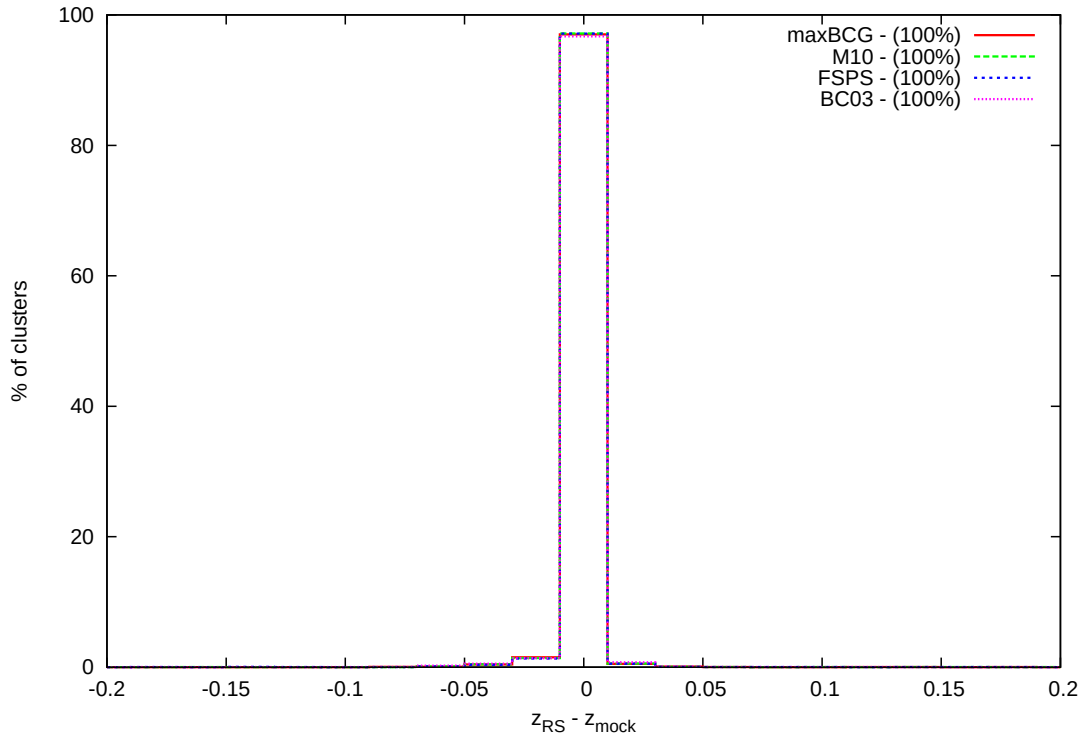

Figure 4.15 *A histogram comparison of GMPhoRCC photometric red sequence redshift to the actual cluster value for the detection subset for* 7050 *mocks generated using various evolution models. With no significant differences and the legend showing similar fractions of clusters in the detection subset it is clear GMPhoRCC is insensitive to the form of the evolution.*

Before exploring potential bias as a function of cluster properties it is useful to note that while modelling the red sequence accurately and identifying all the cluster members is the ultimate goal, the redshift estimate is not as sensitive to this as richness. Provided a suitable number of red sequence galaxies can be identified, these provide enough information to estimate the photometric distribution and give a reasonable redshift. Figure 4.16 shows this clearly by splitting the redshift comparison based on the three possible sources of the identified BCG. First identifying the BCG correctly gives strong indication the CMR suitably describes the cluster, which is the case for the majority (87%) of

the mocks. As expected, with good modelling the red sequence is easily identified and the redshift estimates are mostly within 0.01 of the actual value. In the case where another cluster member is incorrectly identified as the BCG, although a poorer CMR description of the red sequence is found, there are still enough cluster members to find a reasonable redshift. Finally a minor fraction, 9%, incorrectly identifies a field galaxy as the BCG, highlighting potentially the worst modelling of the red sequence. A small fraction of these cases indicate the failure to identify the red sequence completely and with very few cluster members, this results in outliers. Although containing outliers, the majority of the field galaxy BCG cases result from the presence of an interloper in an otherwise well described CMR. With the cluster members dominating reasonable redshift estimates can still be found.

Exploring these comparisons as a function of cluster redshift and richness, shown in Figures 4.17 and 4.18 respectively, reveals that while the estimates are in good agreement with the mock value, separately the low redshift and low richness clusters are the source of the most extreme outliers. This highlights the low redshift issues shown in the scatter plots, particularly Figure 4.13. Again for clusters with $z < 0.1$ poorer contrast against the background and limitations in the field area result in similar issues with fitting the red sequence. Similarly with only a few galaxies it is more difficult to isolate and model the red sequence where background fluctuations can dominate resulting in poorer estimates for low richness clusters.

Outside this low redshift or low richness regime (i.e. with $z > 0.1$ or $n_{200} > 10$) the redshift estimates appear in good agreement with the mock and show no bias. Constraints at higher redshift, $z > 0.5$, are not possible with this analysis as the effect of incomplete photometry has been ignored. Section 4.5 explores this in detail to assess the redshift and richness ranges of clusters which can be reliably analysed by GMPhoRCC.

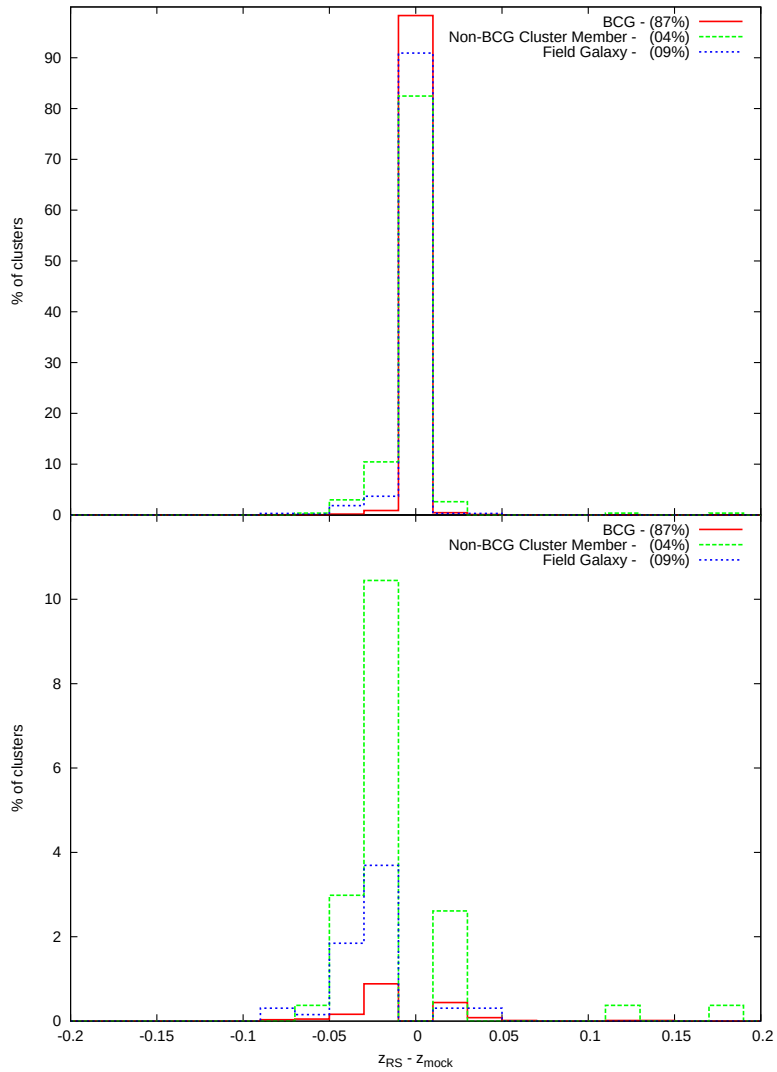

Figure 4.16 *A histogram comparison of GMPhoRCC photometric red sequence redshift to the actual cluster value for the detection subset for* 7050 *mocks generated using maxBCG evolution. The comparison has been split based on the source of the GMPhoRCC BCG and normalised where the legend shows the size of each subset relative to the total number of mocks. The bottom panel omits the middle bin to highlight the outliers. Matching the BCG correctly indicates suitable red sequence modelling and cluster member identification and hence provides the most accurate redshift estimates. Matching to another cluster member highlights a poorer CMR but is still sufficient to identify enough members to obtain a reasonable redshift. The cases of matching to a field galaxy results from an interloper contaminating a well modelled CMR where cluster members dominate resulting in a reasonable redshift. Alternatively a small fraction of the field galaxy cases indicate the complete failure to identify the red sequence and with very few members results in outliers.*

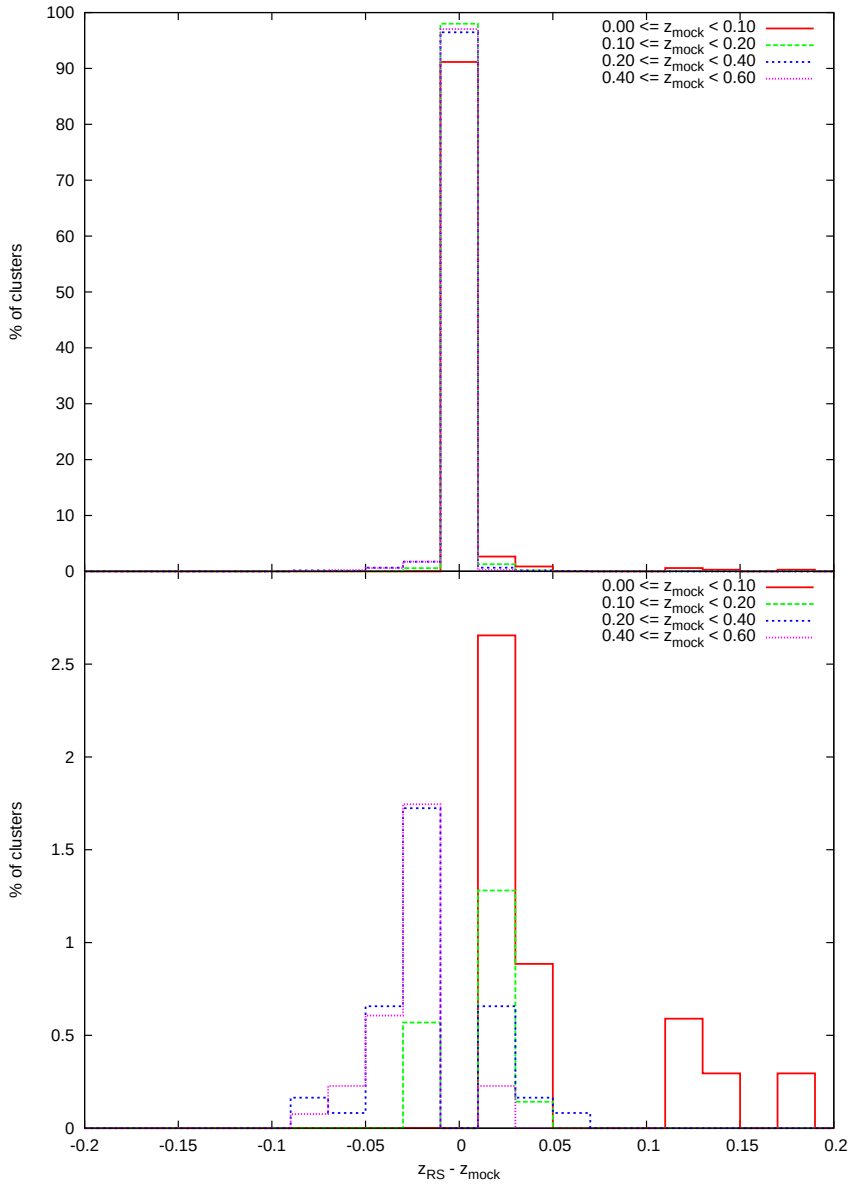

Figure 4.17 *A comparison of GMPhoRCC photometric red sequence redshift to the actual cluster value for the detection subset for* 7050 *mocks generated using maxBCG evolution. The comparison has been normalised and split into redshift bands where the bottom panel omits the middle bin to highlight the outliers and any bias. The source of the most extreme outliers is attributed to low redshift clusters where poor contrast against the background and limitations in the field area make it difficult to isolate and model the red sequence.*

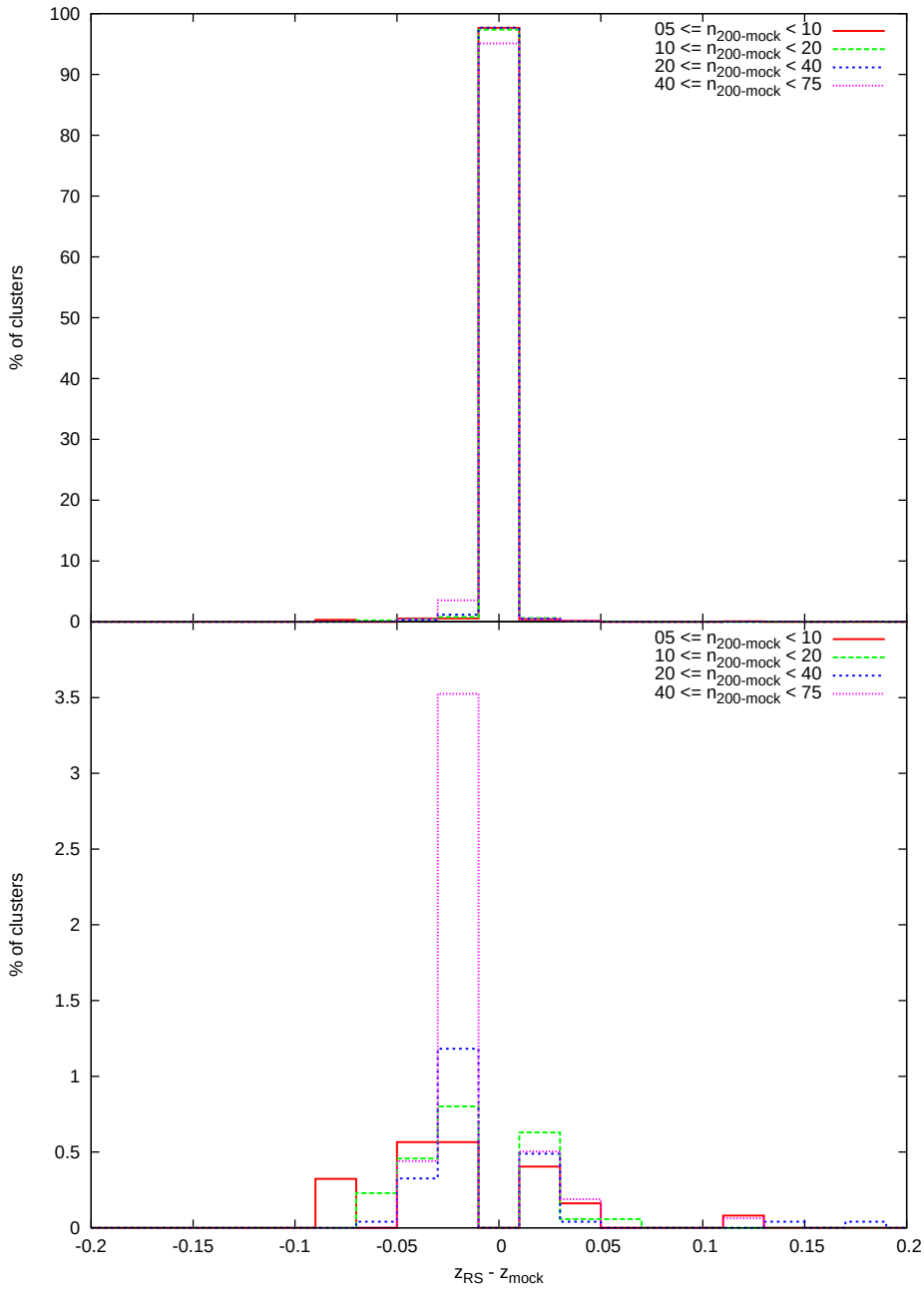

Figure 4.18 *A histogram comparison of GMPhoRCC photometric red sequence redshift to the actual cluster value for the detection subset for* 7050 *mocks generated using maxBCG evolution. The comparison has been normalised and split into richness bands where the bottom panel omits the middle bin to highlight the outliers and any bias. Low richness clusters are the source of the most extreme outliers where the low number of galaxies and larger contribution from the background makes it difficult to identify and model the red sequence.*

4.3.2 Richness

Mocks are particularly useful to assess the richness estimates as the 'true' value for real clusters is often difficult to measure and is sensitive to the input optical data and particular characterisation code.

First it is useful to consider the intermediate richness, n_{gals}, as any issues with this will propagate through GMPhoRCC resulting in poor estimates for r_{200} and ultimately n_{200}. Of the 7050 clusters, richness estimates were found using the counting method for 99.8% and compared to the mock value where Figure 4.19 highlights the results for each of the quality subsets. Similarly Figure 4.20 shows the luminosity richness comparison. These scatter plots are useful to highlight the outliers, however it is difficult to assess the distribution from these due to the integer values of n_{gals}. Figure 4.21 shows the distribution of the quality subsets more clearly.

First, considering the counting richness, although a large spread is observed, the GMPhoRCC estimate is centred around the cluster value. This large spread can be attributed to many factors including discrepancies in redshift, mismatched BCGs and background fluctuations. While redshift and BCG will be investigated in more detail later in this Section it is worth noting now that the typical number of interlopers added to richness varies from $\sim 0-5$ whereas the calculated correction is only $\sim 0-2$. In some cases this discreteness issue can lead to very large contributions from field galaxies or over-subtraction of the background contributing to the large spread.

The luminosity estimate is seen to produce more numerous and extreme outliers compared to the counting method. Fitting and integrating a Schechter function introduces additional sources of uncertainty over the counting method and provides an estimate which is sensitive to the quality of the fit. As a result of this, a larger spread is observed in the luminosity richness estimate as shown more clearly in Figure 4.22. Despite this, the luminosity method will be shown in Section 4.5 to be an important tool in order to extrapolate richness where photometry is incomplete.

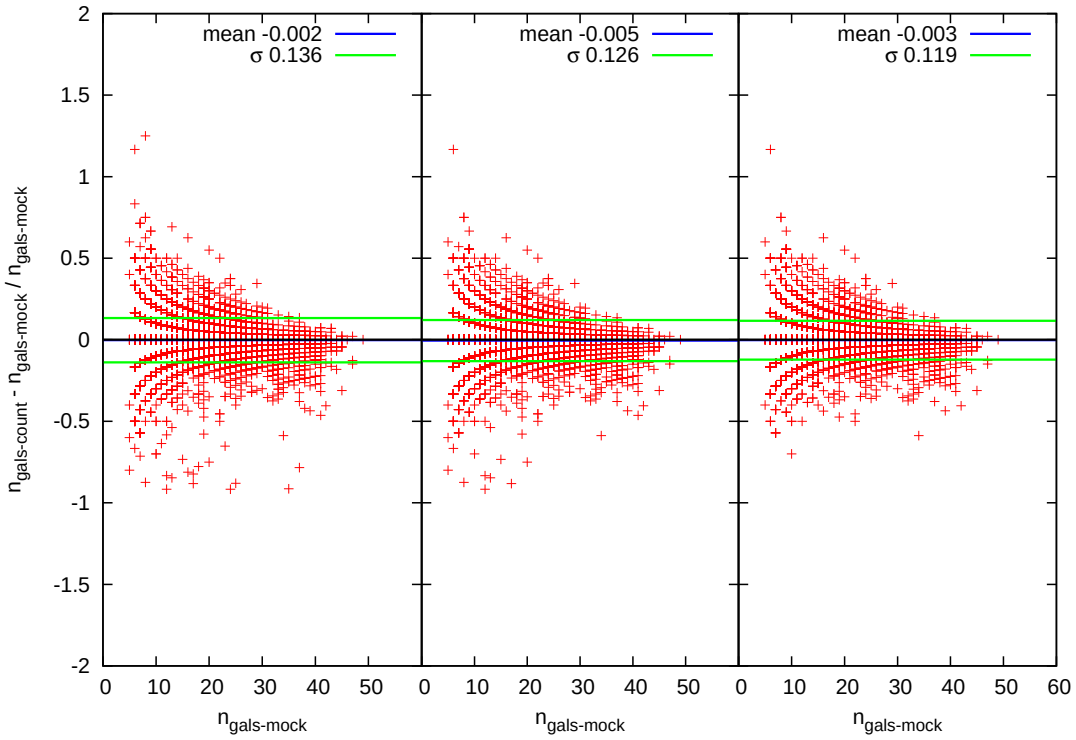

Figure 4.19 *A comparison of GMPhoRCC $n_{gals-count}$ estimate to the actual cluster value for* 7050 *mocks generated using maxBCG evolution showing from left to right the detection, mid and clean subsets. Although a large spread is observed the estimates are centred around the actual mock value where several of the worst outliers observed in detection have been removed in the clean subset.*

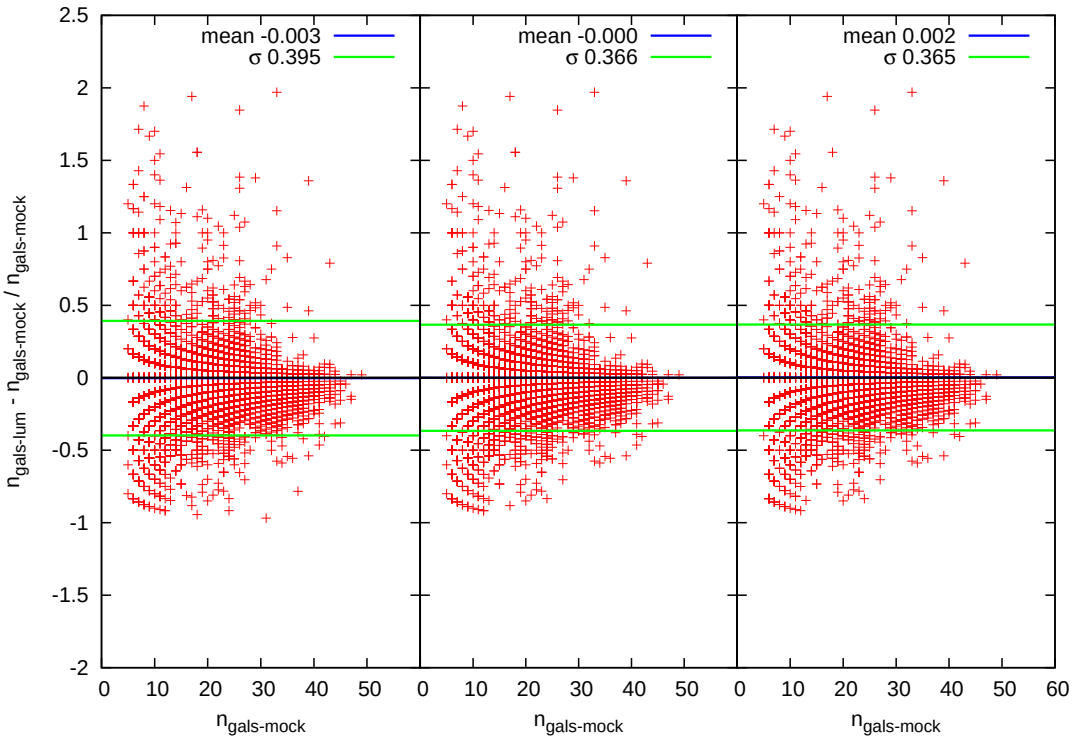

Figure 4.20 *A comparison of GMPhoRCC $n_{gals-lum}$ estimate to the actual cluster value for 7050 mocks generated using maxBCG evolution showing from left to right the detection, mid and clean subsets. A larger spread with more numerous and extreme outliers are observed relative to the counting estimate presented in Figure 4.19 due to the extra reliance and uncertainty introduced by fitting a luminosity function. While the effect of the quality subsets is more prominent with regards to redshift comparisons, several of the worst richness outliers observed in detection have been removed in the clean subset.*

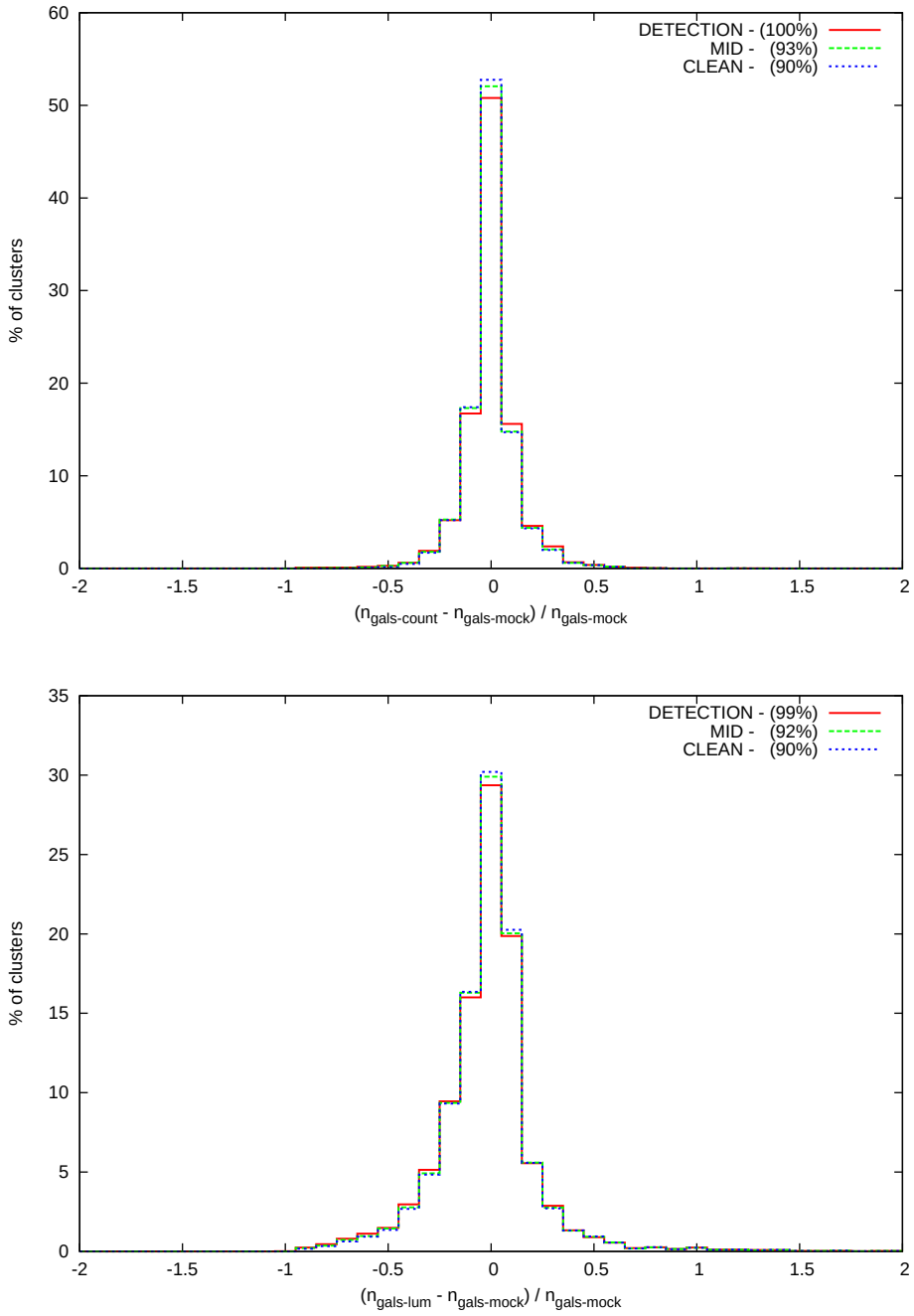

Figure 4.21 *A histogram comparison of the n_{gals} GMPhoRCC estimate to the actual cluster value with the top and bottom panels showing the counting and luminosity richnesses respectively for* 7050 *mocks generated using maxBCG evolution. The comparison has been normalised and split into the separate quality bands where the legend shows the fraction of the total clusters in the subset. Both estimates have richnesses centred around the actual value with the clean attaining the fewest outliers. A larger spread with more numerous and extreme outliers are observed with the luminosity richness relative to the counting estimate due to the extra reliance and uncertainty introduced by fitting a Schechter function.*

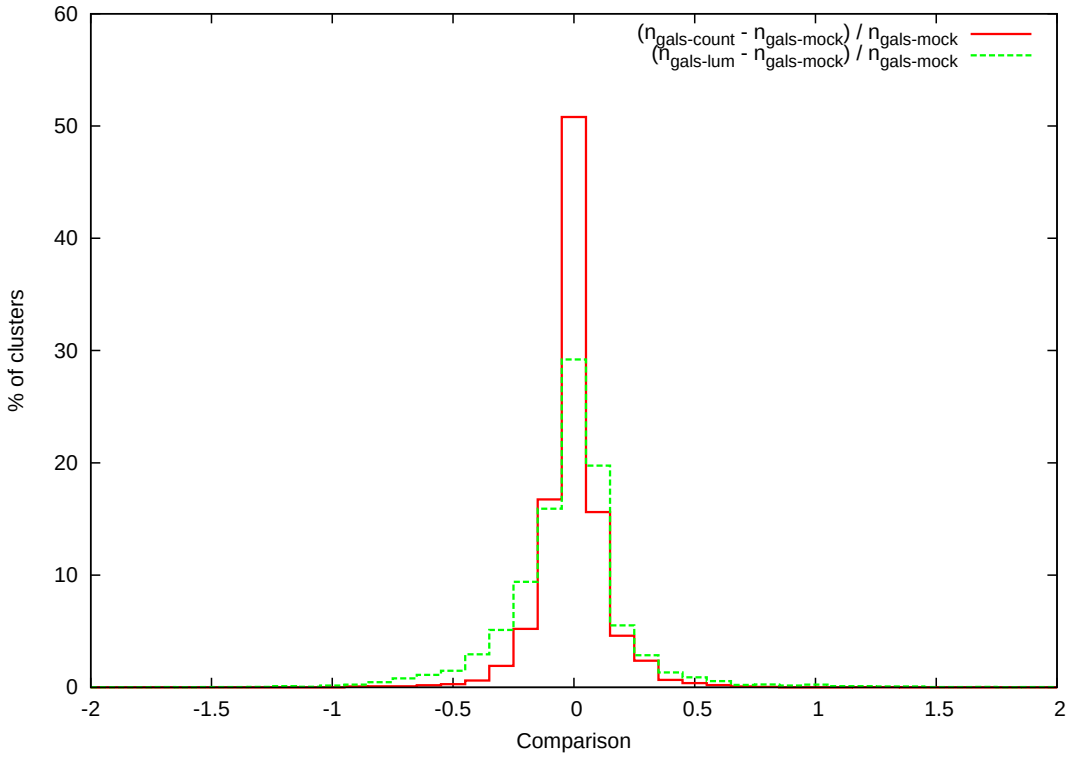

Figure 4.22 *A normalised histogram comparison of both the GMPhoRCC n_{gals} estimates for the detection subset for* 7050 *mocks generated using maxBCG evolution. This highlights the larger spread of the luminosity method compared to the counting richness.*

Again to ensure the GMPhoRCC estimates are accurate and reliable it is necessary to check there are no biases or dependencies introduced as a function of cluster properties. First considering the evolution used to generate the mocks, Figure 4.23 shows that there are no significant differences between the evolution models for the counting or luminosity richness from the detection set. These similarities hold for n_{200} and the other quality subsets where the mid and clean set comprise $\sim 92\%$ and $\sim 89\%$ of all the mocks respectively again showing the insensitivity of GMPhoRCC to the exact form of the evolution.

By considering the source of the identified BCG, Figure 4.24 demonstrates the importance of good red sequence modelling to attain an accurate richness estimate. The case of good modelling where the BCG has been correctly identified shows the greatest fraction of clusters where the estimate is in good agreement with the mock value. Alternatively poorer modelling, highlighted by identifying a fainter cluster member as the BCG, results in a slight underestimate as the magnitude range and hence number of galaxies considered is smaller. Identifying a field galaxy as the BCG may indicate the presence of an interloper in an otherwise well modelled red sequence which results in a slight overestimation due to the larger magnitude range and number of galaxies. Alternatively this may also indicate unsuitable red sequence modelling which gives rise to the worst outliers where many cluster members are not considered. The combination of both these effects leads to a wider scatter in the field galaxy case.

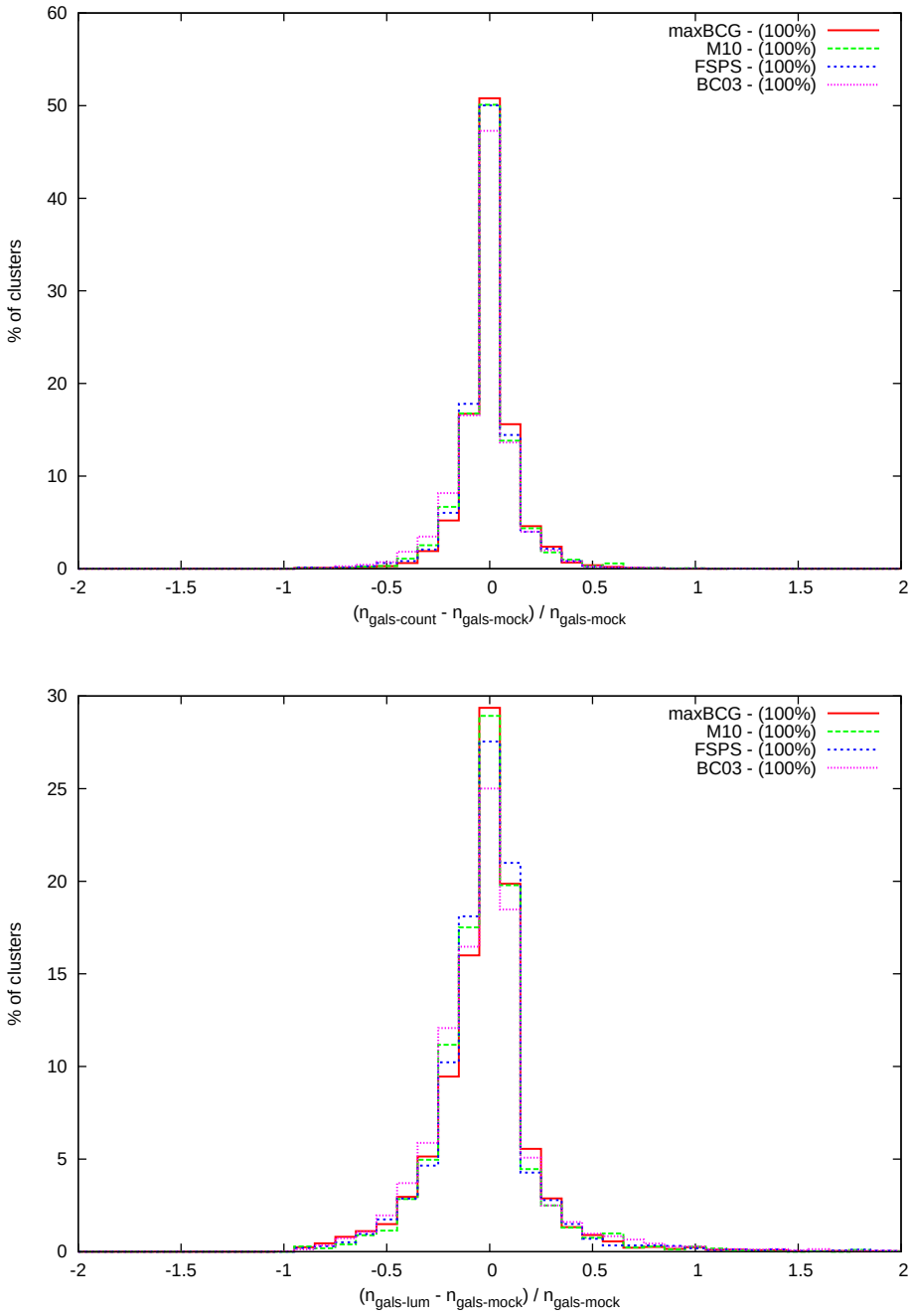

Figure 4.23 *A normalised histogram comparison of the GMPhoRCC n_{gals} estimates to the actual cluster value for the detection subset with the top and bottom panels showing the counting and luminosity richnesses respectively for* 7050 *mocks generated using various evolution models. In addition to the legend showing the similar fractions of clusters in the detection subset it is clear that the comparison does not vary significantly between evolution models.*

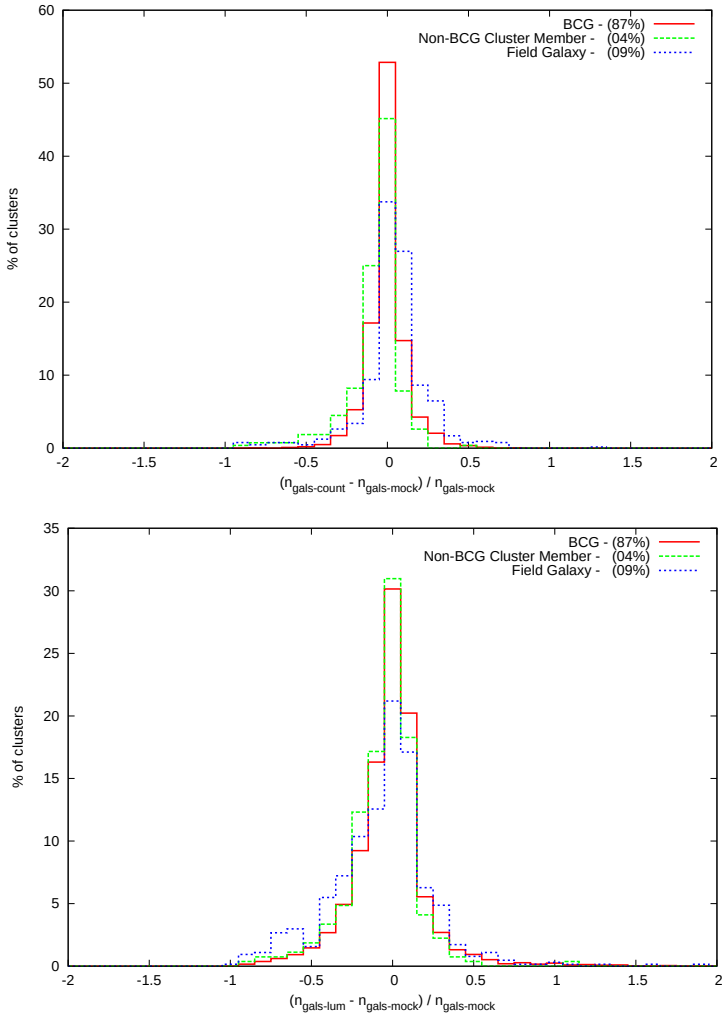

Figure 4.24 *A histogram comparison of GMPhoRCC n_{gals} estimate to the actual cluster value for the detection subset with the top and bottom panels showing the counting and luminosity richnesses respectively for* 7050 *mocks generated using maxBCG evolution. The comparison has been split based on the source of the GMPhoRCC BCG and normalised where the legend shows the size of each subset relative to the total number of mocks. Matching the BCG correctly indicates suitable red sequence modelling and cluster member identification and hence provides the larger fraction of estimates in good agreement with the mock value. Poorer red sequence modelling and matching to fainter cluster members gives rise to a narrower magnitude range and the possibility of missing red sequence galaxies resulting in a slight underestimation. Matching to field galaxy resulting from interlopers in an otherwise well modelled red sequence leads to slight overestimation due to the larger magnitude range and number of galaxies. Alternatively the field galaxy can indicate the complete failure to identify the red sequence and with very few members results in the worse outliers. The combination of both these effects leads to a wider scatter in the field galaxy case.*

While no bias is observed in either estimate with cluster redshift as demonstrated in Figure 4.25 it is noted that again the low redshift regime contains a larger fraction of the worst outliers.

Again, with cluster richness, no bias is observed with either estimate, however Figure 4.26 shows that a larger fraction of low richness clusters have poorer estimates. As with the redshift comparisons of Section 4.3.1 modelling the red sequence is difficult for sparsely populated clusters where the background forms a significant component of the field resulting in the poorer estimates.

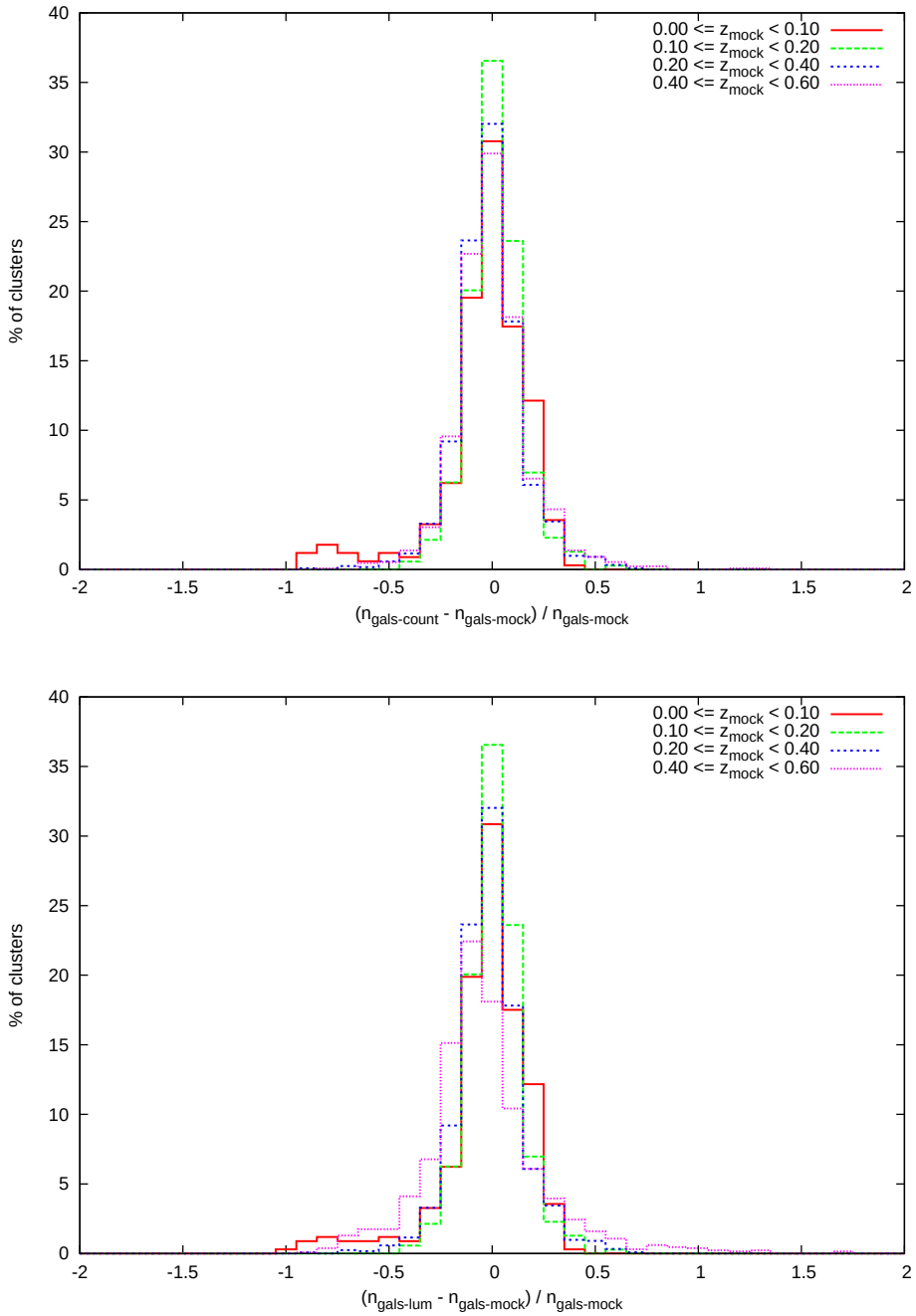

Figure 4.25 *A comparison of GMPhoRCC n_{gals} estimates to the actual cluster values for the detection subset with the top and bottom panels showing the counting and luminosity richnesses respectively for* 7050 *mocks generated using maxBCG evolution. The comparison has been normalised and split into redshift bands to highlight any bias. Both estimates show no dependence on redshift with the low redshift regime, $z < 0.1$, containing the worst outliers where modelling the red sequence is difficult due to poor contrast against the background and limitations in the field area.*

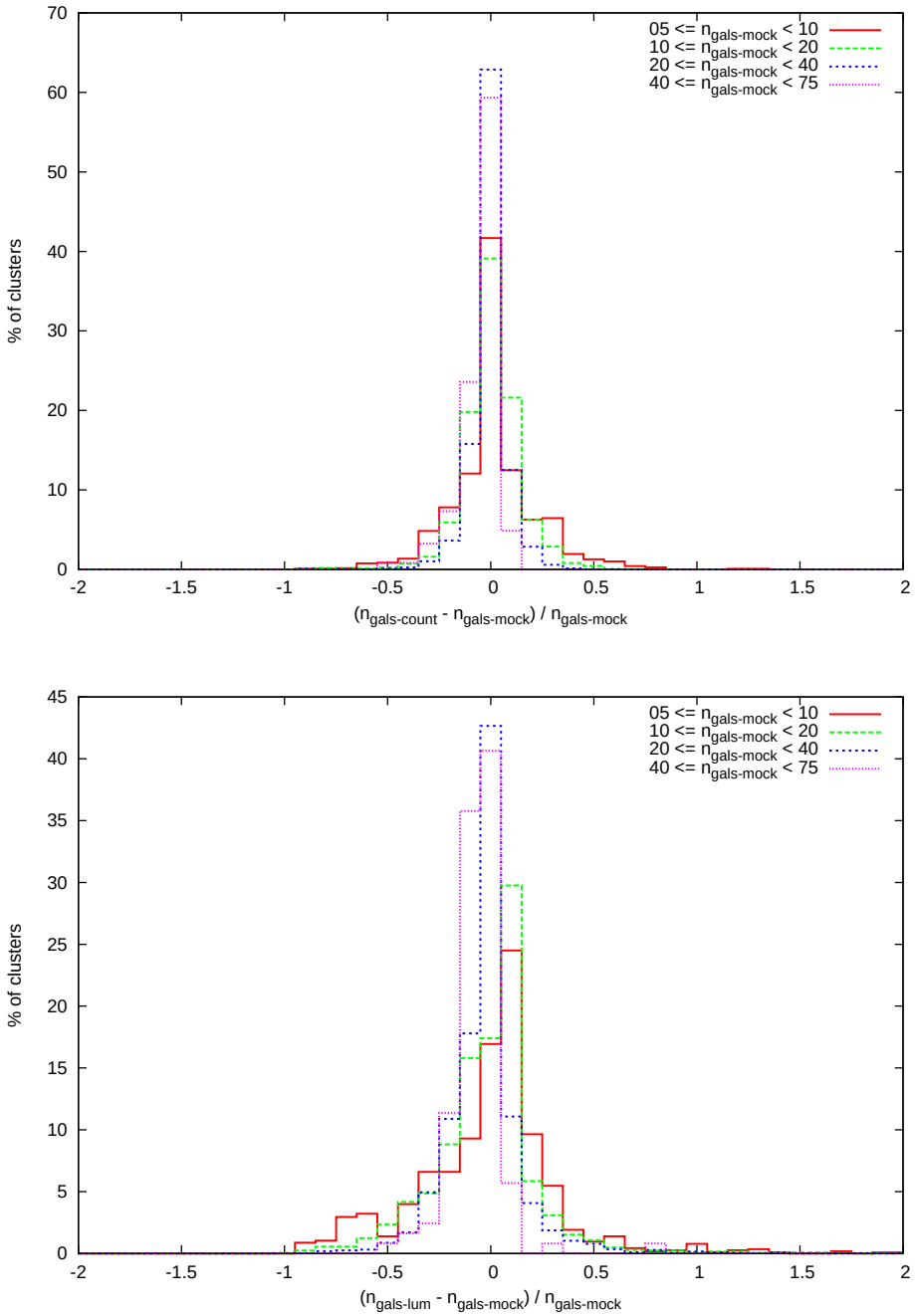

Figure 4.26 *A comparison of GMPhoRCC n_{gals} estimates to the actual cluster values for the detection subset with the top and bottom panels showing the counting and luminosity richnesses respectively for* 7050 *mocks generated using maxBCG evolution. The comparison has been normalised and split into richness bands to highlight any bias. The main source of outliers is attributed to low richness clusters where the low number of galaxies and larger contribution from the background makes it difficult to identify and model the red sequence.*

While no bias is present, it is noted that the GMPhoRCC richness estimate is sensitive to the redshift estimate. With an underestimated redshift the faint end limit of the red sequence is brighter resulting in a narrower magnitude range and underestimated richness. Overestimated redshifts result in a smaller angular radius and potential loss of members however this effect is negligible compared to those gained from the larger magnitude range and hence results in an overestimated richness. In addition to this any large discrepancies in redshift (under or overestimated) can indicate issues with modelling the red sequence which results in underestimated richnesses as shown in Figure 4.27. These issues are particularly important for the final richness estimate where discrepancies in redshift and BCG propagate affecting n_{gals}, r_{200} and ultimately n_{200}. As a result of this the n_{200} estimates are subject to a larger spread with more numerous and extreme outliers compared to n_{gals} as demonstrated in Figure 4.28. In addition any other issues with n_{gals} are similarly amplified in n_{200} as shown in Figure 4.29.

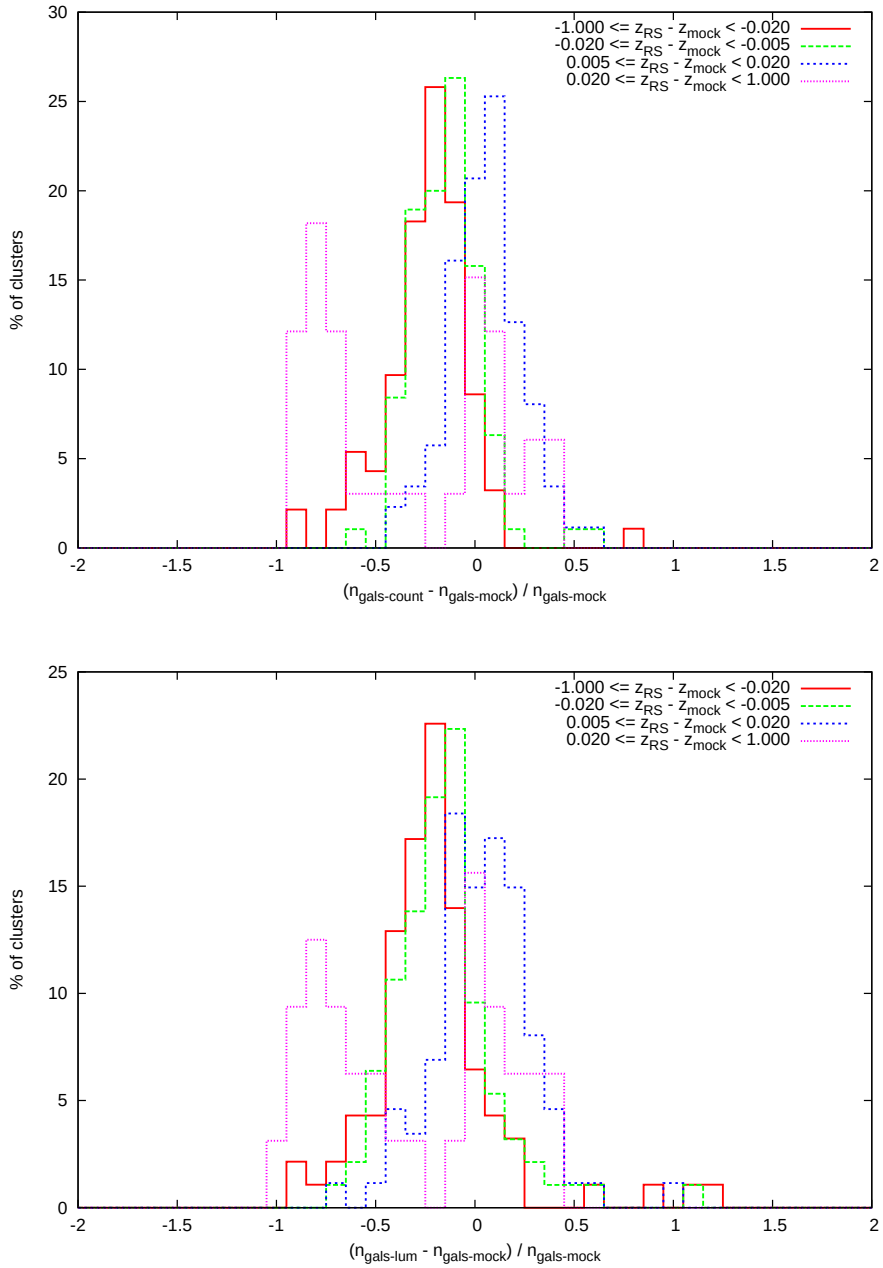

Figure 4.27 *A comparison of GMPhoRCC n_{gals} estimates to the actual cluster values for the detection subset with the top and bottom panels showing the counting and luminosity richnesses respectively for* 7050 *mocks generated using maxBCG evolution. The comparison has been normalised and split to highlight any bias as a function of how accurately redshift has been estimated. Clusters with catastrophic failures in the redshift estimate indicate issues with red sequence modelling resulting in the loss of many cluster members giving the underestimated richness. Slight underestimation of redshift results in a narrower magnitude range considered giving an underestimated richness. Similarly slight overestimation of redshift results in a larger magnitude range and hence a slightly overestimated richness.*

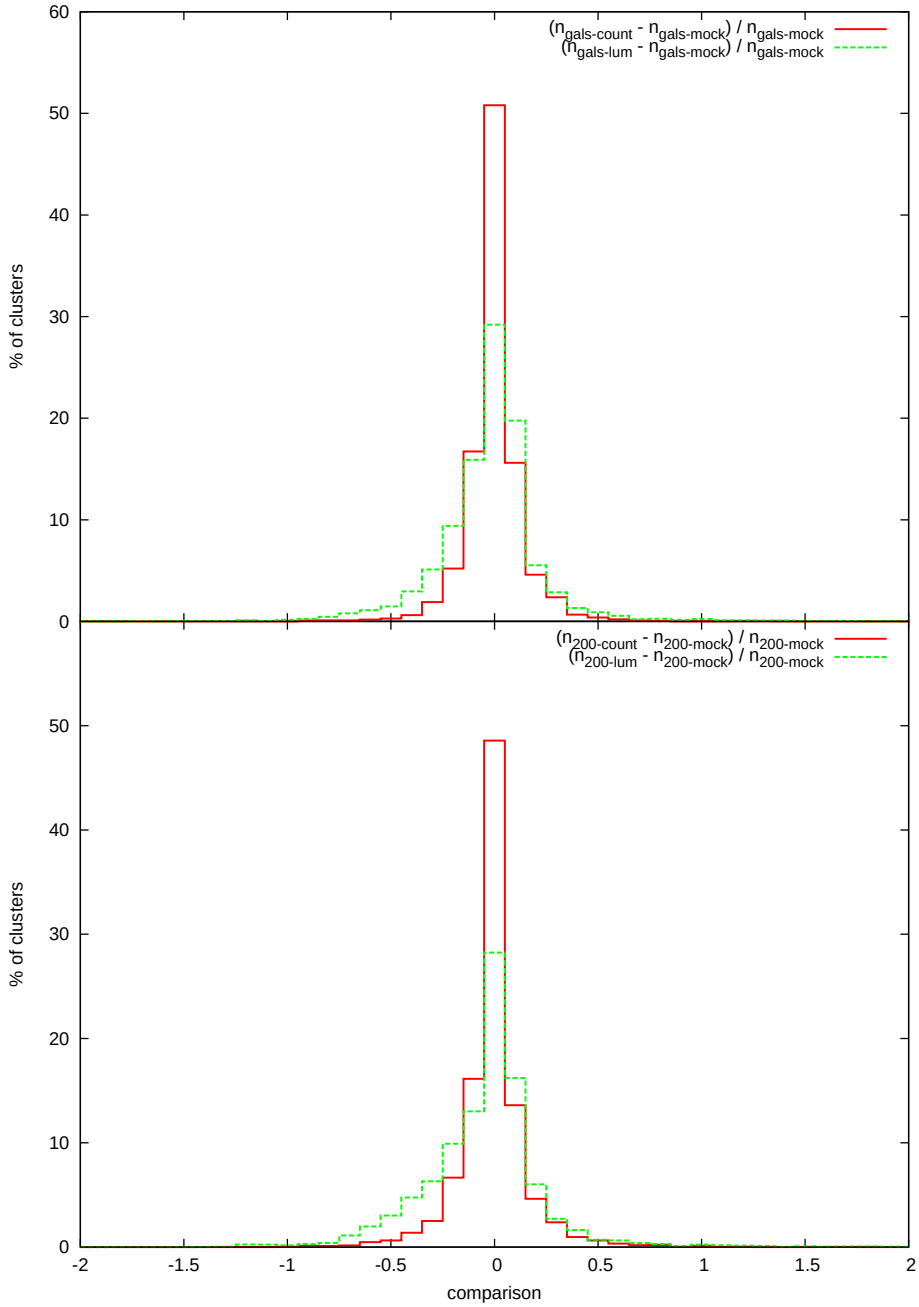

Figure 4.28 *A normalised histogram comparison of the GMPhoRCC richness estimates for the detection subset where the top and bottom panel show the n_{gals} and n_{200} estimates respectively for 7050 mocks generated using maxBCG evolution. The n_{200} estimate is subject to a larger spread with more numerous and extreme outliers due to the prorogation of errors in redshift, n_{gals} and r_{200}.*

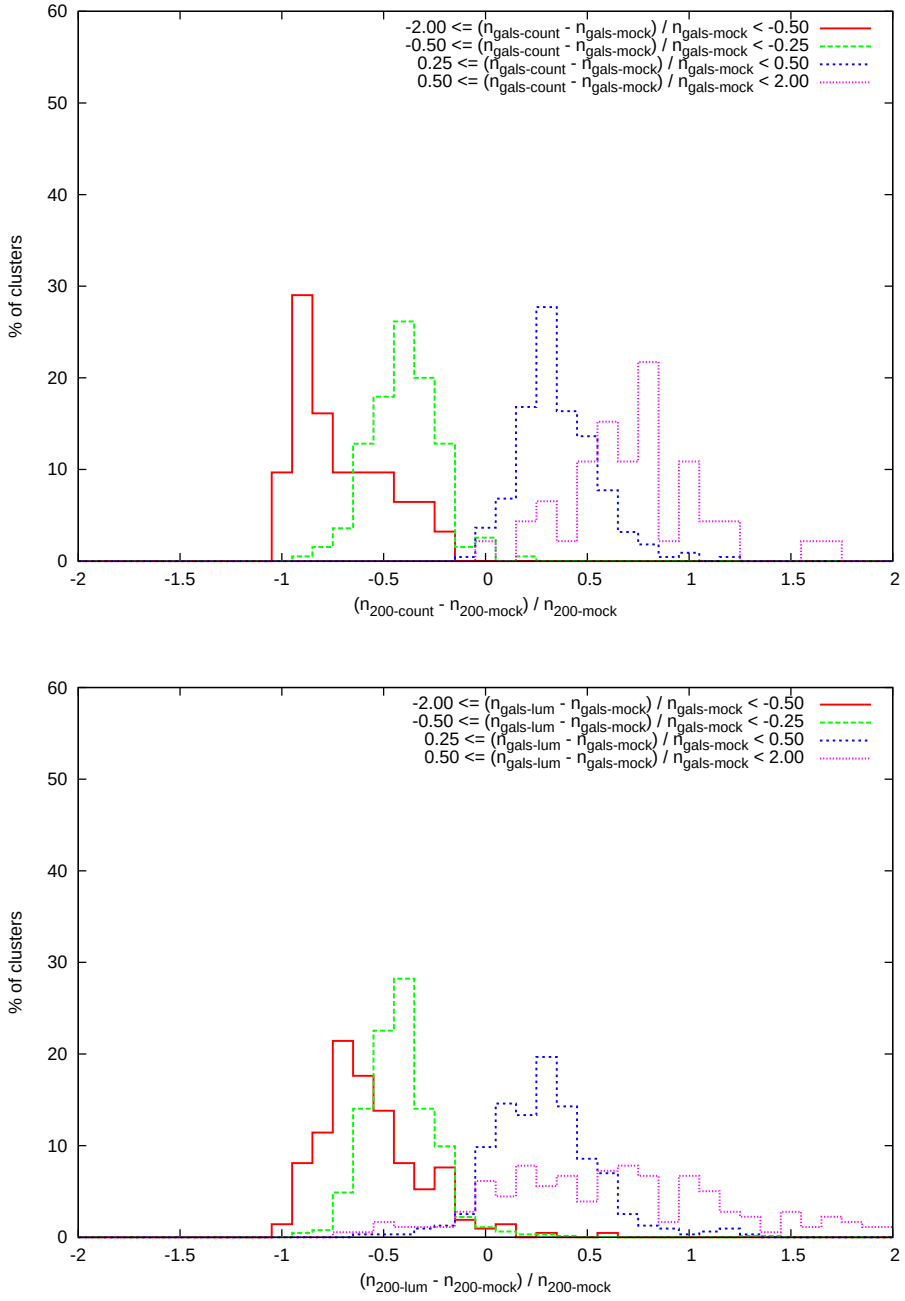

Figure 4.29 *A comparison of GMPhoRCC n_{200} estimates to the actual cluster values for the detection subset with the top and bottom panels showing the counting and luminosity richnesses respectively for* 7050 *mocks generated using maxBCG evolution. The comparison has been normalised and split to highlight any bias as a function of how accurately n_{gals} has been estimated. Any discrepancy in n_{gals} indicates an issue with the red sequence modelling and as a result mocks with the most discrepant n_{gals} estimate are the worst outliers here. In addition any issues with n_{gals} also adversely affects r_{200}, where an underestimated richness results in a smaller radius further reducing the estimate. Similarly overestimated n_{gals} further increases n_{200}.*

4.4 Purity

Although the target clusters for GMPhoRCC have already been detected in other wavebands (e.g. X-ray), it is important to understand purity when using the code to optically confirm a candidate or in cases where the candidate list is unclean and may be contaminated. By using the random backgrounds only of the mock catalogue used in the previous section, purity can be estimated as the fraction of fields where no cluster was detected i.e. detections in this case are impurities. Table 4.1 presents these purity results which represent the probability that given a candidate has a particular quality marker and richness that is in fact a cluster. Very few spurious characterisations are found with cleaner quality markers or high richness, i.e. these have the highest probability of representing real clusters. In particular candidates belonging to the clean subset, $q = 1$, have a negligible probability of resulting from a false detection. It is noted that GMPhoRCC attains extremely high levels of purity compared with maxBCG which attains $\sim 93\%$ for clusters with $n_{200} = 10$ and $\sim 99\%$ for $n_{200} = 15$. Similarly compared with GMBCG which attains purity levels of $\sim 75\%$ for $n_{200} > 10$ and $\sim 97\%$ for $n_{200} > 25$.

q	$n_{200} > 0$	$0 < n_{200} < 5$	$5 \leq n_{200} < 10$	$n_{200} \geq 10$
< 4	79.7%	80.7%	99.1%	100.0%
3	88.6%	89.2%	99.4%	100.0%
2	92.0%	92.1%	99.9%	100.0%
1	99.2%	99.4%	99.8%	100.0%

Table 4.1 *A list of the GMPhoRCC purity results based on counting richness and quality marker. Very few spurious characterisations are found with clean quality markers or high richness, i.e. candidates with clean quality markers or high richness have the highest probability of representing real clusters.*

4.5 Completeness

One of the most important properties to evaluate is completeness; this gives a measure of how well clusters are characterised across a range of redshifts and richnesses. Completeness is measured as the fraction of mock clusters where the estimated properties agree with the actual value within a given bound. The mock catalogues used in this analysis are those from Section 4.3, generated using

K+e-corrections for each of the evolution models outlined in Section 4.1.2 with $0.05 < z < 1.1$ and $5 \leq n_{200} \leq 75$. In order to simulate the effect of incomplete photometry in the SDSS, faint galaxies with i-band< 21 are removed. The following Sections investigate completeness with respect to redshift, richness and BCG matching. While model insensitivity will be shown, the following analysis focuses on mocks generated using maxBCG-style evolution.

4.5.1 Redshift Estimation

Using the maxBCG-style evolution mocks it can been seen in Figure 4.30 that for $z_{mock} < 0.6$, the majority of the GMPhoRCC estimates are in very good agreement with the mock value. At higher redshifts large fractions of the cluster galaxies can go undetected as they are too faint and as such, the red sequence becomes more difficult to isolate, resulting in the poorer redshift estimates. In addition to this, limitations in field area and poor contrast against the background for low redshift clusters, $z < 0.1$, makes the red sequence more difficult to isolate and model, resulting in the lower fraction of clusters with good redshift estimates.

Next considering the quality subsets, Figure 4.31 shows little difference between the bands in the region of complete photometry, $z < 0.45$. This shows that as the estimates are cleaned only a small number are removed which are in good agreement with the actual value. Above this redshift completeness reduces with cleaner subsets as many clusters with good redshift estimates are identified with low richness due to the incomplete photometry and are removed.

While it is expected that incomplete photometry results in a reduction in completeness the effect is not the same for all cluster richnesses. Considering low richness clusters, even with complete photometry, isolating the red sequence and estimating redshifts is challenging due to the low number of galaxies. Also as photometry becomes incomplete, estimating redshift for these is far more difficult than rich clusters as the number of galaxies drops even lower. Hence the redshift where the GMPhoRCC estimates become unreliable should be lower for groups than for high richness clusters and this is exactly what is seen in Figure 4.32 and summarised in Table 4.2. This effect is confirmed in all quality subsets and it is also noted obtaining 'clean' estimates is more difficult for lower richness clusters. Again due to the difficulty in modelling cluster distributions with only a few galaxies, a lower fraction of low richness clusters is observed in the clean subset.

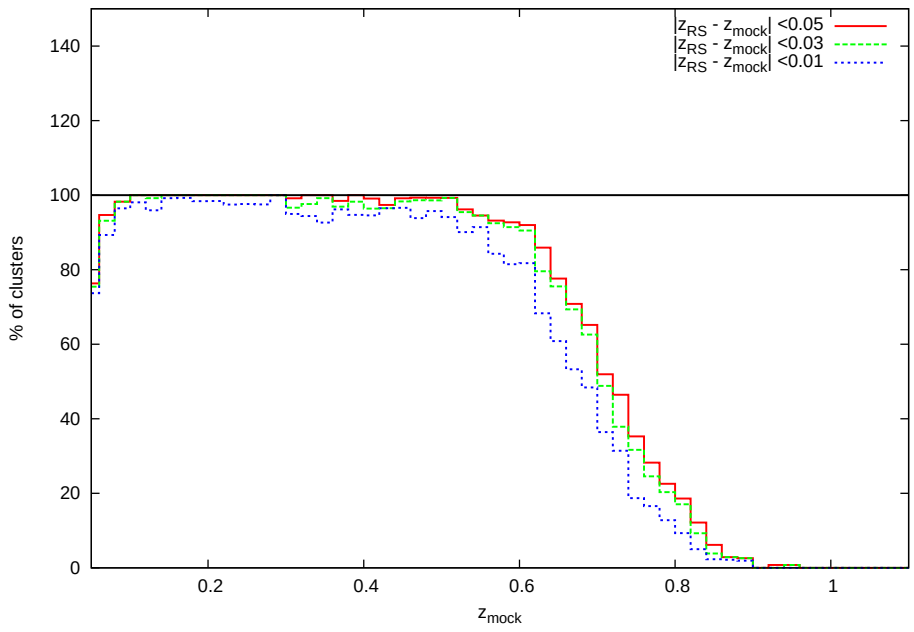

Figure 4.30 *The fraction of maxBCG evolution mock clusters where the redshift estimate is within various bounds of the actual value. For $z < 0.6$ most of the clusters are in very good agreement with the actual value. At higher redshifts many cluster galaxies are not detected due to incomplete photometry making it harder to isolate the red sequence and estimate redshift.*

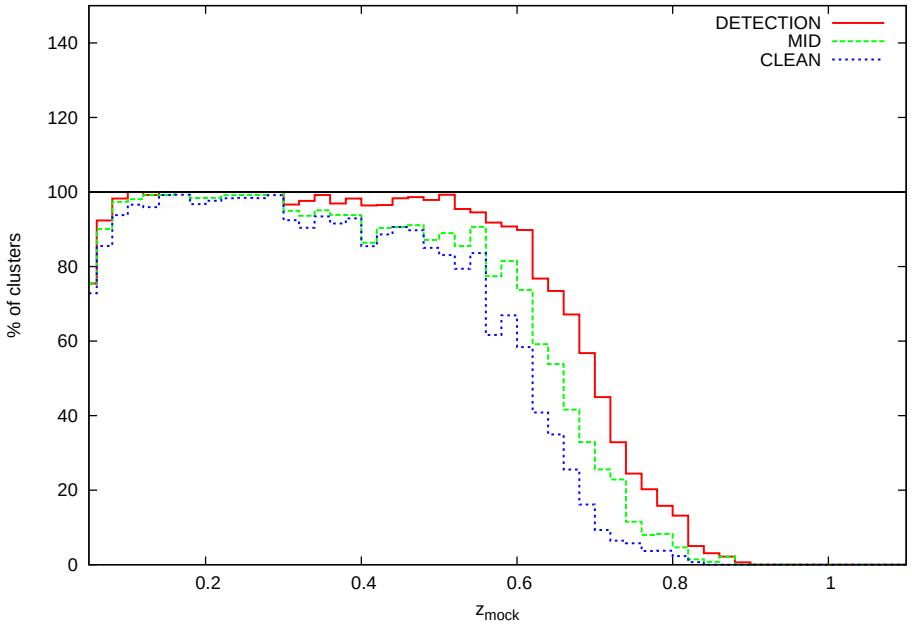

Figure 4.31 *The fraction of maxBCG evolution mock clusters for the various quality subsets where the redshift estimate is within* $|z_{RS} - z_{mock}| < 0.03$. *With little difference between the bands in the region of complete photometry,* $z < 0.45$ *it is clear that very few clusters with good redshift estimates are removed. Above this redshift completeness reduces with cleaner subsets as many clusters with good redshift estimates are identified with low richness due to the incomplete photometry and are removed.*

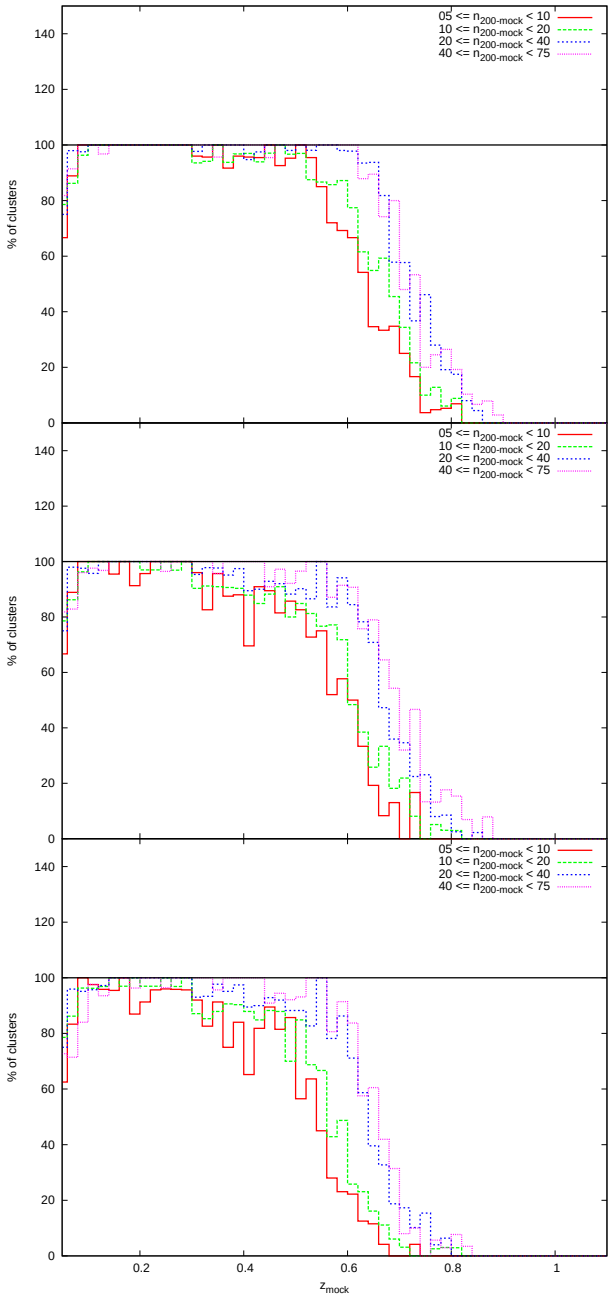

Figure 4.32 *The fraction of maxBCG evolution mock clusters for different richness bands where from top to bottom the panels show the detection, mid and clean subsets where the redshift estimate is within* $|z_{RS} - z_{mock}| < 0.03$. *Low richness clusters are more sensitive to incomplete photometry due to the already low number of galaxies. Isolating the red sequence and estimating redshift is more challenging for low richness clusters than their high richness counterparts at the same redshift. Hence the ability to reliably estimate cluster redshift drops more quickly with redshift for groups than rich clusters. Due to this difficulty the clean set is also subject to an earlier reduction in completeness and a lower fraction of low richness clusters across all redshifts.*

Subset	Richness	Redshift	Completeness
Detection	All	$0.05 < z < 0.65$	95.8%
	$5 \leq n_{200} < 10$	$0.07 < z < 0.55$	97.7%
	$10 \leq n_{200} < 20$	$0.07 < z < 0.55$	97.2%
	$20 \leq n_{200} < 40$	$0.05 < z < 0.65$	98.3%
	$40 \leq n_{200} < 75$	$0.05 < z < 0.65$	98.1%
Mid	All	$0.05 < z < 0.60$	92.6%
	$5 \leq n_{200} < 10$	$0.07 < z < 0.55$	91.7%
	$10 \leq n_{200} < 20$	$0.07 < z < 0.55$	93.0%
	$20 \leq n_{200} < 40$	$0.05 < z < 0.65$	93.8%
	$40 \leq n_{200} < 75$	$0.05 < z < 0.65$	94.8%
Clean	All	$0.05 < z < 0.60$	89.3%
	$5 \leq n_{200} < 10$	$0.07 < z < 0.50$	89.4%
	$10 \leq n_{200} < 20$	$0.07 < z < 0.50$	92.2%
	$20 \leq n_{200} < 40$	$0.05 < z < 0.62$	92.6%
	$40 \leq n_{200} < 75$	$0.05 < z < 0.62$	93.6%

Table 4.2 *A summary of the redshift completeness results.*

Although not directly comparable to a cluster finder completeness, it is noted that these GMPhoRCC completenesses improves on both maxBCG and GMBCG. Completeness, with regards to maxBCG, refers to the fraction of mock clusters detected within a redshift of 0.025 of the actual value which are at least as rich as the mock. GMPhoRCC exceeds the completeness rates over a larger redshift range than maxBCG which attains $\sim 95\%$ for $0.1 < z < 0.3$ and $n_{200} > 20$. Similarly, GMBCG attains high completeness rates, defined as the fraction of clusters detected within a redshift of 0.05 of the mock value, with $\sim 98\%$ for $0.1 < z < 0.46$ and $n_{200} > 25$ and $\sim 96\%$ for $0.1 < z < 0.46$ and $n_{200} > 10$. While the completeness rates are comparable, GMPhoRCC is able to extend the redshift range from $0.1 < z < 0.46$ to $0.05 < z < 0.62$.

While these results have been derived from maxBCG-style mocks, these hold for other forms of evolution as shown in Figure 4.33. All versions of the mocks show a reduction in completeness above $z > 0.55$ resulting from the loss of galaxies from incomplete photometry. With no significant differences observed, GMPhoRCC is again confirmed to be insensitive to the form of evolution.

Rather than considering completeness relative to the whole catalogue but instead relative to a subset with a given quality marker, q, and z_{RS} range, the accuracy of the GMPhoRCC redshift can be estimated. The fraction of clusters in a subset which achieve the $|z_{RS} - z_{mock}| < 0.03$ bound represents the probability that a cluster with a given quality marker and z_{RS} consistent with the subset, has a

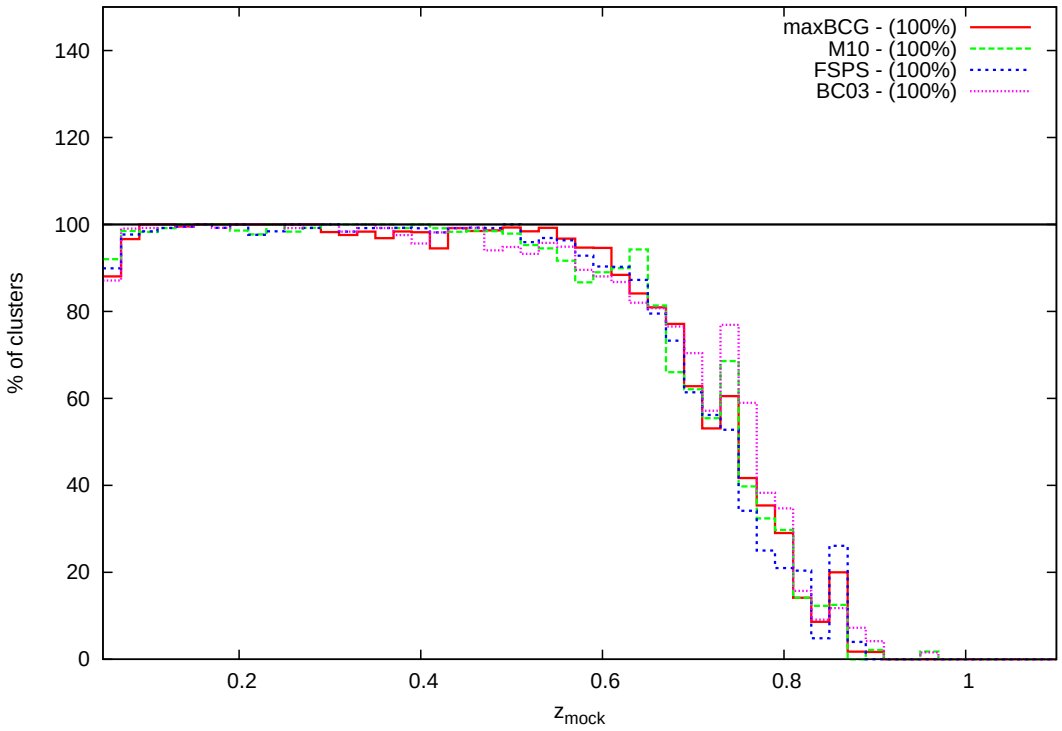

Figure 4.33 *The fraction of mock clusters generated using different forms of evolution from the detection subset where the redshift estimate is within* $|z_{RS} - z_{mock}| < 0.03$. *With no significant differences between the models GMPhoRCC is again shown to be insensitive to the form of the evolution used to generate the mocks.*

redshift estimate within 0.03 of the mock value. Figure 4.34 shows these fractions for the various quality markers and the $|z_{RS} - z_{mock}| > 0.03$ bound. In addition to the clean subset, $q = 1$, achieving a very high probability ($> 97\%$) that the redshift estimate is within 0.03 of the mock value, those with larger, less clean quality markers for $z < 0.45$ have low probabilities ($< 25\%$), again showing the ability of the quality subsets to identify and remove potential outliers. The sparse number of galaxies above $z > 0.45$ in the SDSS DR9 and the mock background results in a low chance of spurious high redshift estimates hence given $z_{RS} > 0.45$ there is a larger probability the redshift is associated with the cluster. In addition, those with good high redshift estimates are more likely to be flagged as low richness due to the incomplete photometry. This leads to larger, less clean quality markers and hence higher probabilities the estimate is associated with the cluster than expected for $q > 1$. While adjustments could be made to the quality subsets to take advantage of this increased probability it is noted that for $z > 0.45$ the larger, less clean quality markers mainly result from low numbers of galaxies due to incompleteness and hence the current quality subsets are necessary to maintain

cleanliness for both redshift and richness estimates. A full set of probabilities for each quality marker and several bounds are presented in Table 4.3.

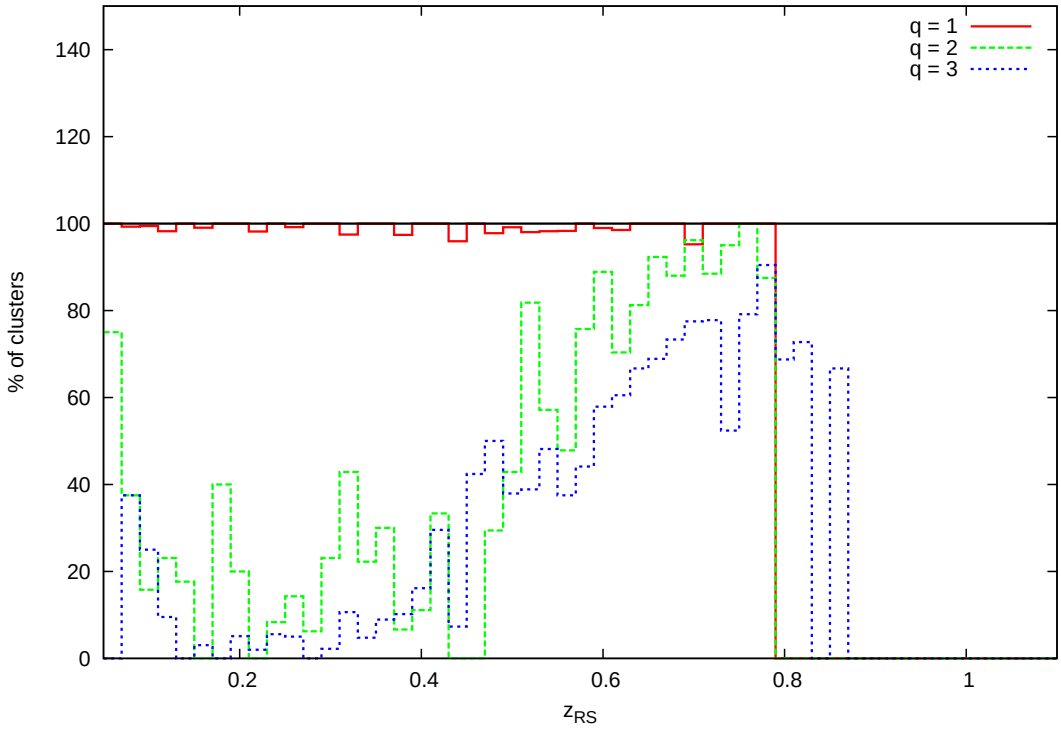

Figure 4.34 *The fraction of mock clusters with a given quality marker which achieve the* $|z_{RS} - z_{mock}| < 0.03$ *bound. In addition to the clean subset,* $q = 1$*, achieving a very high probability (*$> 97\%$*) that the redshift estimate is within* 0.03 *of the mock value, those with larger, less clean quality markers for* $z < 0.45$ *have low probabilities (*$< 25\%$*), again showing the ability of the quality subsets to identify and remove potential outliers. The sparse number of galaxies above* $z > 0.45$ *in the SDSS DR9 and the mock background results in a low chance of spurious high redshift estimates hence given* $z_{RS} > 0.45$ *there is a larger probability the redshift is associated with the cluster. In addition, those with good high redshift estimates are more likely to be flagged as low richness due to the incomplete photometry. This leads to larger, less clean quality markers and hence higher probabilities the estimate is associated with the cluster than expected for* $q > 1$*.*

q	Redshift Range	p($\Delta z < 0.01$)	p($\Delta z < 0.03$)	p($\Delta z < 0.05$)
3	$0.05 < z_{RS} < 0.50$	0.11	0.11	0.12
2	$0.05 < z_{RS} < 0.50$	0.16	0.19	0.25
1	$0.05 < z_{RS} < 0.80$	0.96	0.99	0.99

(a) *Low Redshift*

q	Redshift Range	p($\Delta z < 0.01$)	p($\Delta z < 0.03$)	p($\Delta z < 0.05$)
3	$0.50 < z_{RS} < 0.80$	0.45	0.61	0.66
2	$0.50 < z_{RS} < 0.80$	0.68	0.81	0.86

(b) *High Redshift*

Table 4.3 *A list of the probabilities that a redshift estimate is within various bounds of the actual value given the z_{RS} estimate and the quality marker of the cluster, where $\Delta z = |z_{RS} - z_{mock}|$. The bottom table shows the increase in probability for higher redshift and quality marker clusters. The sparse number of galaxies above $z > 0.45$ in the SDSS DR9 and the mock background results in a low chance of spurious high redshift estimates hence given $z_{RS} > 0.45$ there is a larger probability the redshift is associated with the cluster. In addition, those with good high redshift estimates are more likely to be flagged as low richness due to the incomplete photometry. This leads to larger, less clean quality markers and hence higher probabilities the estimate is associated with the cluster than expected for $q > 1$.*

4.5.2 BCG Identification

Identifying the correct BCG is not only hugely important for subsequent cosmology but also for calculating cluster richness. This analysis considers two scenarios, one where the BCG is correctly identified and one where another cluster member is selected as the BCG. While correctly matching the BCG shows the strongest evidence GMPhoRCC has suitably modelled the red sequence, even matching to a cluster member suggests the CMR is a reasonable representation of the cluster.

Mismatching the BCG results from two main issues, background interlopers and poor red sequence modelling. While mismatching to a background galaxy is easier to find with the quality bands due to inconsistencies in redshift, matching to another cluster member can be more challenging to identify. Figure 4.35 shows the fraction of maxBCG-style mocks where the BCG has been correctly matched or matched to a cluster member. As photometry becomes incomplete issues with fitting the red sequence due to the lower number of galaxies gives rise to the lower fraction matched above $z > 0.6$. In addition to this the difficulty in modelling the red sequence at low redshift, $z < 0.1$, due to poor contrast against the background and limitations in the field area, result in a smaller fraction of these mocks with correctly matched BCG.

By considering quality, Figure 4.36 shows very little difference between the subsets for $z < 0.55$. This highlights that very few clusters with suitably modelled red sequences are removed by the increasing cleanliness of the quality bands. This again shows the strength of the quality bands where possible catastrophic failures can be unidentified and removed while keeping clusters with good estimates. Above $z > 0.55$ completeness reduces with cleaner subsets as many clusters with correctly identified BCGs are considered to have low richness due to the incomplete photometry and are removed.

Again it is expected that a smaller fraction of low richness clusters have suitable CMRs due to the difficulty in modelling a sparse number of galaxies and this is reflected in the lower BCG match rates shown in Figure 4.37. Table 4.4 summarises and extends these results to correct BCG matching and cluster member BCG matching respectively for each of the quality subsets.

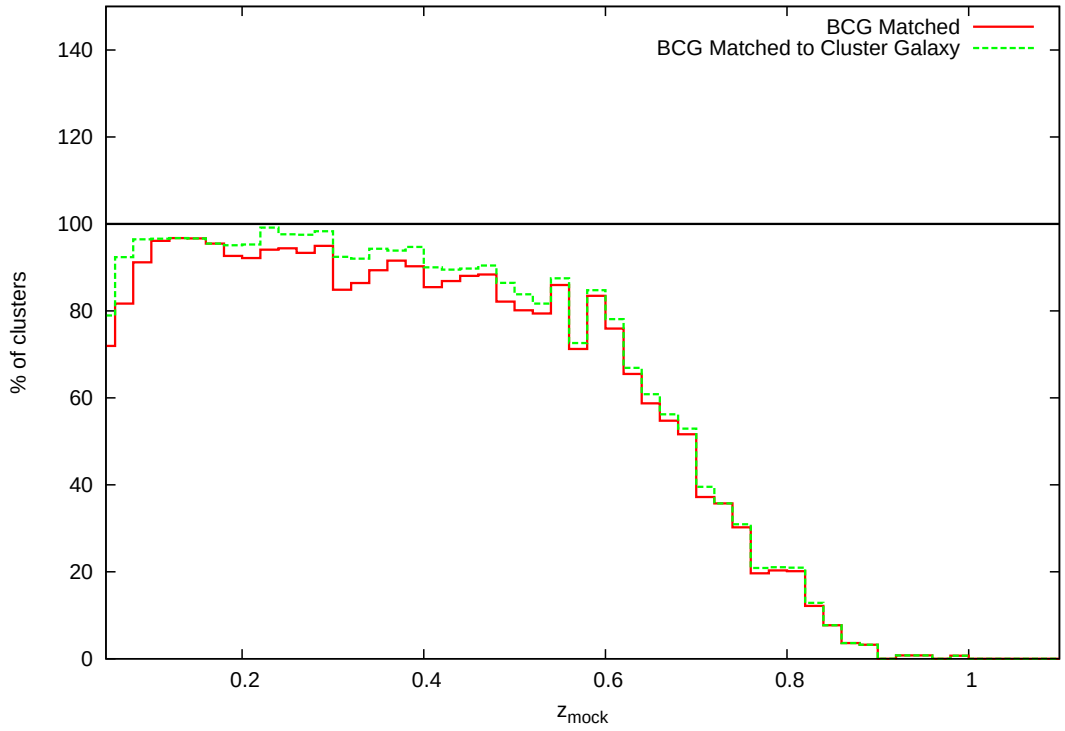

Figure 4.35 *The fraction of maxBCG evolution mock clusters with different BCG matching. For low redshift, $z < 0.6$ most of the clusters are in very good agreement with the actual value. At higher redshifts many cluster galaxies are not detected due to incomplete photometry making it harder to isolate the red sequence and identify the BCG. Difficulties in modelling the red sequence for $z < 0.1$ due to limitations in field area and poor background contrast, result in a lower fraction of these mocks with correctly matched BCG.*

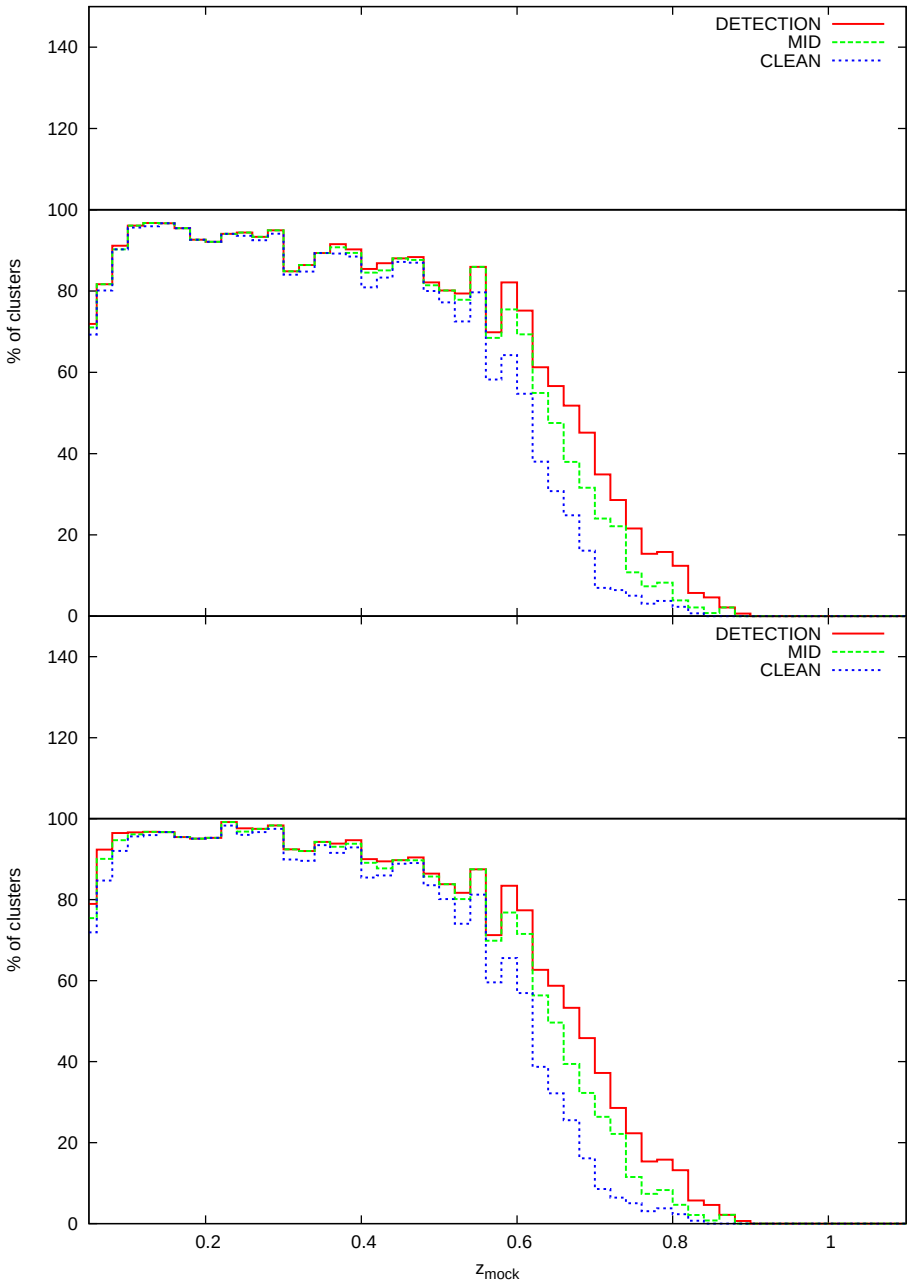

Figure 4.36 *The fraction of maxBCG evolution mock clusters where the BCG has been correctly matched in the top panel and matched to any cluster member in the bottom panel for the various quality subsets. With very little difference between the quality subsets for* $z < 0.55$*, it is clear very few clusters with suitably modelled red sequences are removed with increasing cleanness. Above* $z > 0.55$ *completeness reduces with cleaner subsets as many clusters with suitable CMRs are considered to have low richness due to the incomplete photometry and are removed.*

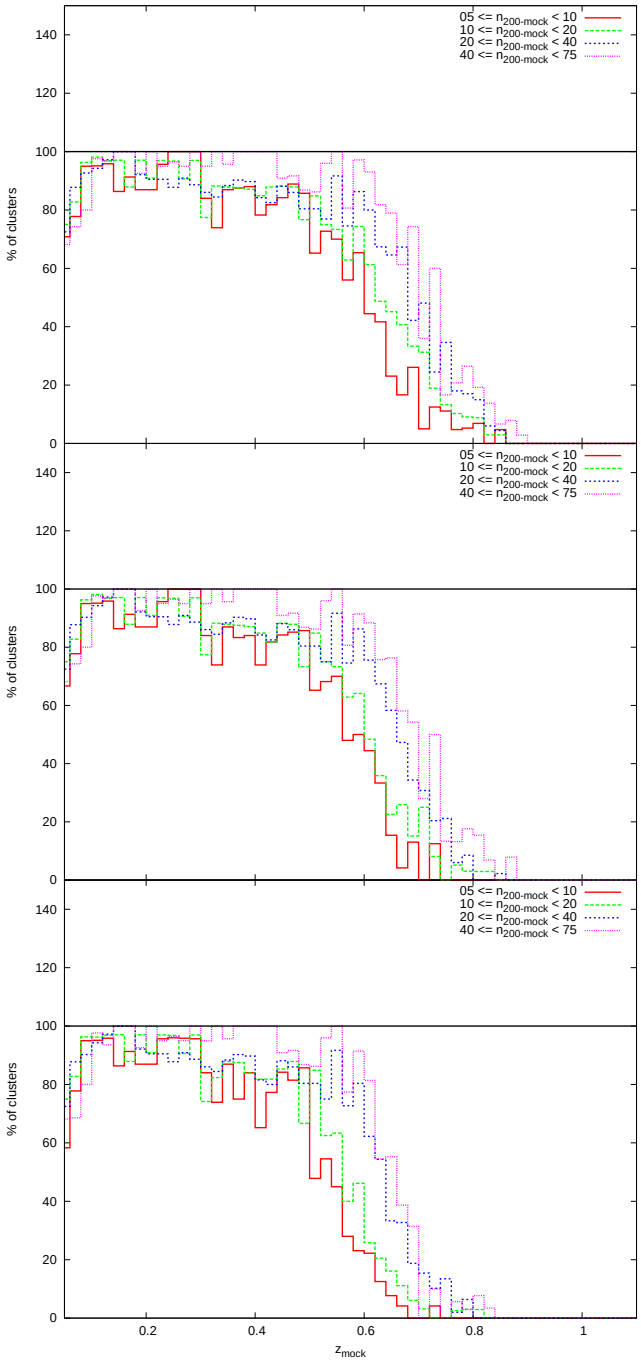

Figure 4.37 *From top to bottom, the fraction of maxBCG evolution mock clusters for different richness bands where the BCG has been correctly identified for the detection, mid and clean subsets.*

While BCG matching is an important property to assess, very little investigation has been done for existing algorithms regarding this and as such, comparisons are not possible.

While these results hold for other evolution models it is noted that the BC03

Subset	Richness	Redshift	Completeness
Detection	All	$0.05 < z < 0.60$	87.9%
	$5 \leq n_{200} < 10$	$0.05 < z < 0.55$	86.6%
	$10 \leq n_{200} < 20$	$0.05 < z < 0.55$	89.1%
	$20 \leq n_{200} < 40$	$0.05 < z < 0.62$	87.2%
	$40 \leq n_{200} < 75$	$0.05 < z < 0.62$	93.1%
Mid	All	$0.05 < z < 0.58$	87.8%
	$5 \leq n_{200} < 10$	$0.05 < z < 0.50$	87.3%
	$10 \leq n_{200} < 20$	$0.05 < z < 0.55$	88.7%
	$20 \leq n_{200} < 40$	$0.05 < z < 0.62$	86.9%
	$40 \leq n_{200} < 75$	$0.05 < z < 0.62$	92.6%
Clean	All	$0.05 < z < 0.58$	86.1%
	$5 \leq n_{200} < 10$	$0.07 < z < 0.50$	86.6%
	$10 \leq n_{200} < 20$	$0.05 < z < 0.55$	87.1%
	$20 \leq n_{200} < 40$	$0.05 < z < 0.62$	85.9%
	$40 \leq n_{200} < 75$	$0.05 < z < 0.62$	91.7%

(a) *Correctly identified BCG*

Subset	Richness	Redshift	Completeness
Detection	All	$0.05 < z < 0.60$	91.2%
	$5 \leq n_{200} < 10$	$0.05 < z < 0.55$	88.0%
	$10 \leq n_{200} < 20$	$0.05 < z < 0.55$	90.7%
	$20 \leq n_{200} < 40$	$0.05 < z < 0.62$	92.6%
	$40 \leq n_{200} < 75$	$0.05 < z < 0.62$	96.7%
Mid	All	$0.05 < z < 0.58$	90.9%
	$5 \leq n_{200} < 10$	$0.05 < z < 0.50$	88.8%
	$10 \leq n_{200} < 20$	$0.05 < z < 0.55$	90.2%
	$20 \leq n_{200} < 40$	$0.05 < z < 0.62$	92.2%
	$40 \leq n_{200} < 75$	$0.05 < z < 0.62$	95.4%
Clean	All	$0.05 < z < 0.58$	88.7%
	$5 \leq n_{200} < 10$	$0.05 < z < 0.50$	87.5%
	$10 \leq n_{200} < 20$	$0.05 < z < 0.55$	88.3%
	$20 \leq n_{200} < 40$	$0.07 < z < 0.62$	91.1%
	$40 \leq n_{200} < 75$	$0.05 < z < 0.62$	93.1%

(b) *BCG matched to any cluster member*

Table 4.4 *A summary of the completeness results where the top Table presents completeness where the BCG has been correctly identified and the bottom where the BCG has been matched to any cluster member. A smaller fraction of low richness clusters have suitable CMRs due to the difficulty in modelling a sparse number of galaxies resulting in lower completeness rates in both cases.*

evolution mocks suffer from lower matching rates as shown in Figure 4.38. As noted in Section 4.2.1, these mocks generally have much wider red sequences than

those from the other evolution models, due to the presence of bi-modal colour distributions, and as such have poorer contrast against the background making it far more difficult to suitably model a CMR.

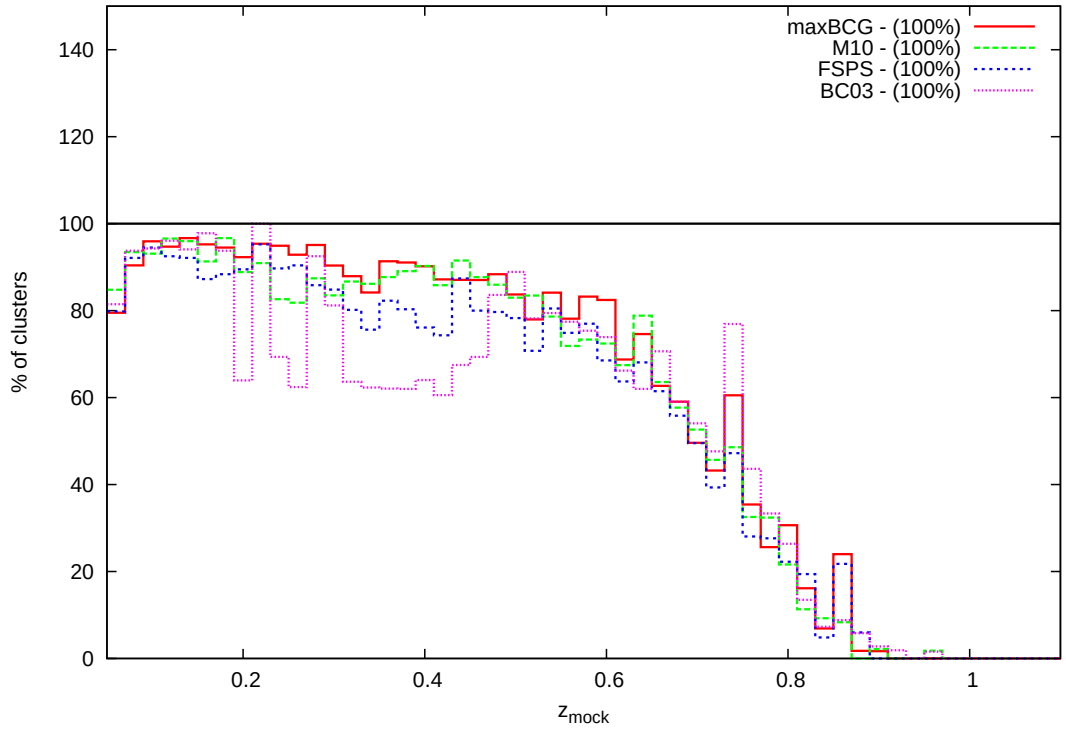

Figure 4.38 *The fraction of mock clusters generated using different forms of evolution where the BCG was correctly identified.*

Considering the BCG matching fractions with respect to subsets with a given quality marker, q and z_{RS} range rather than the whole mock catalogue, gives an estimate of the probability that the BCG has been matched to a particular source given the cluster is consistent with the subset. Figure 4.39 shows these fractions for clusters where the BCG has been correctly identified. In addition to the clean subset, $q = 1$, achieving a very high probability ($> 90\%$) that the BCG has been correctly identified, those with larger,less clean quality markers for $z < 0.45$ have low probabilities ($< 10\%$), again showing the ability of the quality subsets to identify and remove cases where the red sequence has not been well modelled. The sparse number of galaxies above $z > 0.45$ in the SDSS DR9 and the mock background results in a low chance of spurious high redshift estimates hence given $z_{RS} > 0.45$ there is a larger probability the CMR and BCG are associated with the cluster. In addition, those with suitable CMRs at high redshifts are more likely to be flagged as low richness due to the incomplete photometry. This leads to larger, less clean quality markers and hence higher probabilities the CMR and

BCG is associated with the cluster than expected for $q > 1$. Again no adjustments are made to the quality subsets since incomplete photometry becomes an issue for $z_{RS} > 0.45$ with the current subsets necessary to maintain cleanliness for both redshift and richness estimates. A full set of probabilities for each quality marker and the different BCG sources are presented in Table 4.5.

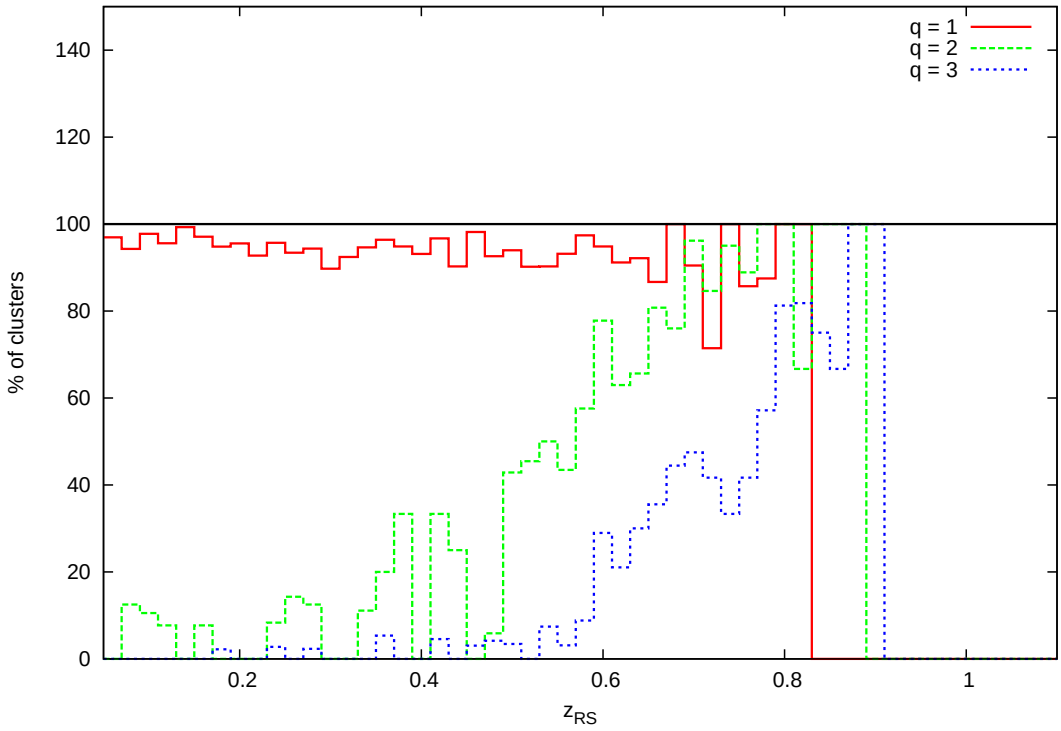

Figure 4.39 *The fraction of mock clusters with a given quality marker where the BCG has been correctly identified. In addition to the clean subset, $q = 1$, achieving a very high probability ($> 90\%$) that the BCG has been correctly identified, those with larger, less clean quality markers for $z < 0.45$ have low probabilities ($< 10\%$), again showing the ability of the quality subsets to identify and remove cases where the red sequence has not been well modelled. The sparse number of galaxies above $z > 0.45$ in the SDSS DR9 and the mock background results in a low chance of spurious high redshift estimates hence given $z_{RS} > 0.45$ there is a larger probability the CMR and BCG are associated with the cluster. In addition, those with suitable CMRs at high redshifts are more likely to be flagged as low richness due to the incomplete photometry. This leads to larger, less clean quality markers and hence higher probabilities the CMR and BCG is associated with the cluster than expected for $q > 1$.*

q	Redshift Range	p(BCG)	p(CM)
3	$0.05 < z_{RS} < 0.60$	0.03	0.03
2	$0.05 < z_{RS} < 0.50$	0.10	0.16
1	$0.05 < z_{RS} < 0.80$	0.94	0.97

(a) *Low Redshift*

q	Redshift Range	p(BCG)	p(CM)
3	$0.60 < z_{RS} < 0.80$	0.39	0.39
2	$0.50 < z_{RS} < 0.80$	0.72	0.75

(b) *High Redshift*

Table 4.5 *A list of the probabilities that the BCG has been matched to various sources given the cluster has a specific quality marker and redshift estimate, where p(BCG) and p(CM) represent the cases of correct BCG identification and cluster member BCG respectively. In both scenarios the clean set demonstrates the highest probability that the red sequence has been suitably modelled.*

4.5.3 Richness Recovery

While two richnesses are investigated by GMPhoRCC, n_{200} best represents an optical mass proxy, considering galaxies within a characteristic radius, rather than the fixed aperture of n_{gals}, and hence is the subject of this section. Section 4.3.2 has explored the accuracy of the GMPhoRCC estimates previously using mocks without the presence of incomplete photometry and found that although no bias is present there is typically a large scatter, $\sim 25\%$ around the mock value. In addition to any uncertainties in redshift, n_{gals} and r_{200} propagating through GMPhoRCC, large background fluctuations result in the large scatter and this is reflected in a lower fraction of clusters, compared with redshift completeness, attaining even the most relaxed richness bound as shown in Figure 4.40. Completeness, as the fraction of clusters attaining the richness bound, in both the counting and luminosity estimate tails off above $z > 0.45$ due to incomplete photometry where cluster galaxies become too faint for reliable detection. It is noted that the luminosity method is able to extrapolate richness resulting in a slower reduction with redshift and higher completeness than the counting method for $z > 0.45$. For the remainder of this Section richness completeness is considered as the fraction of clusters where the richness is within 25% of the mock value.

Considering quality, Figure 4.41 shows only a few clusters which attain the richness bound are removed as the subsets become cleaner. This again shows that cleaning the results using the quality subsets does not remove an excess of clusters with good estimates.

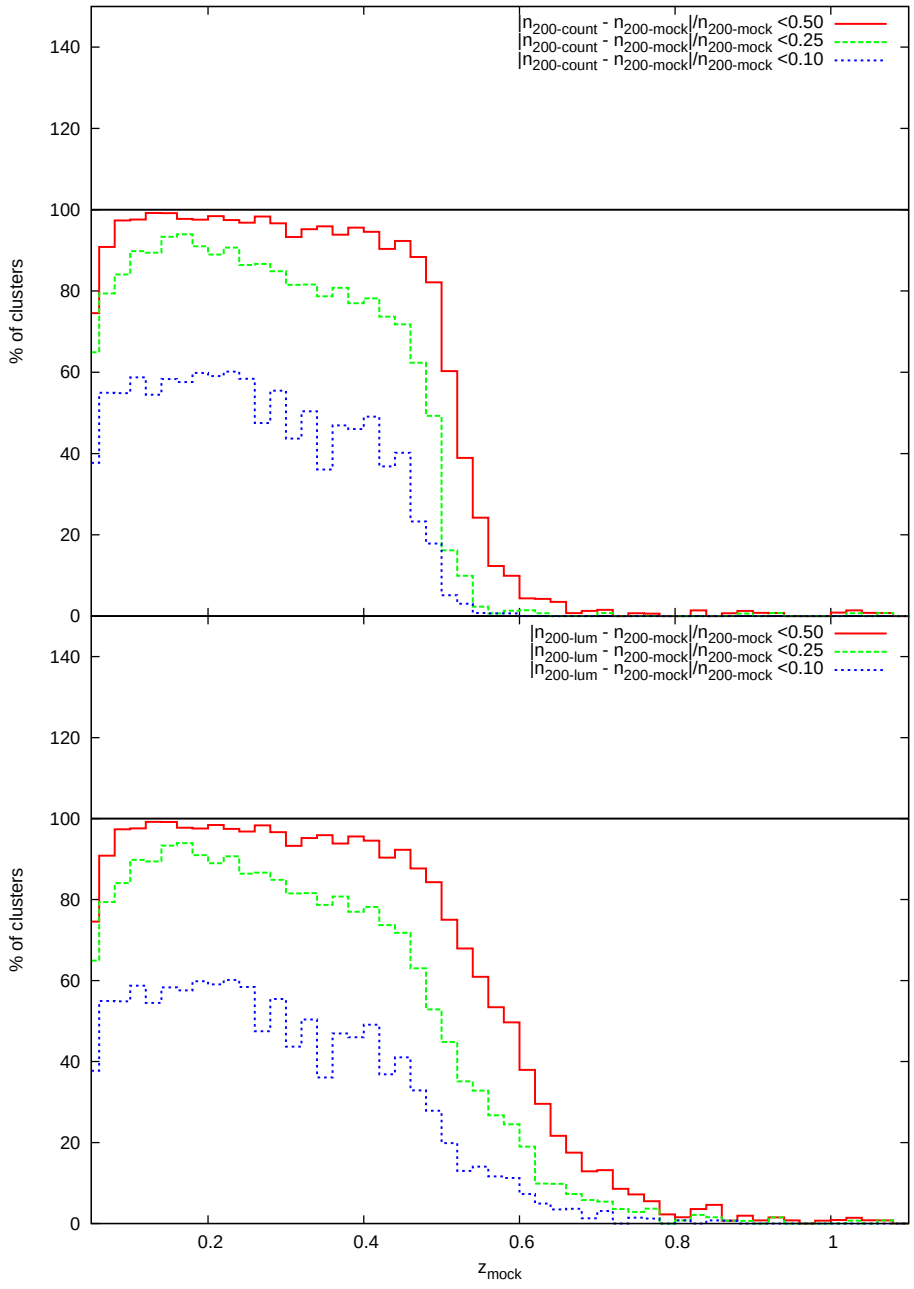

Figure 4.40 *The fraction of maxBCG evolution mock clusters where the n_{200} estimate is within various bounds of the actual value where the top and bottom panels show the counting and luminosity richness respectively. For higher redshifts, $z > 0.45$, cluster members become too faint for detection resulting in underestimated richnesses and a sharp decline in $n_{200-count}$ completeness. Similarly $n_{200-lum}$ is subject to a reduction in completeness above $z > 0.45$ however the luminosity method can extrapolate richness into regions of incomplete photometry attaining larger completeness rates that $n_{200-count}$ for $z > 0.5$.*

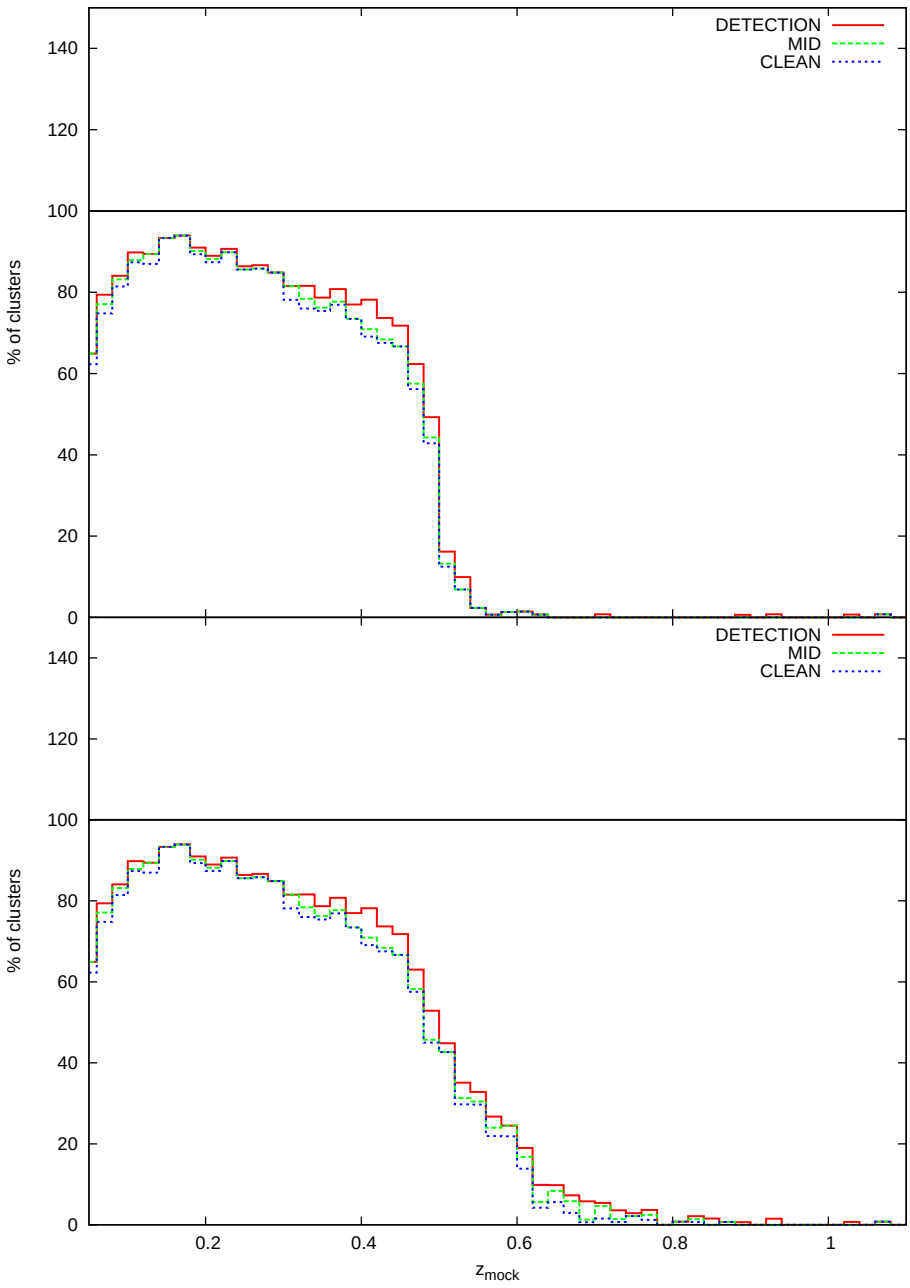

Figure 4.41 *The fraction of maxBCG evolution mock clusters where the n_{200} estimate is within 25% of the actual value for the different quality subsets where the top and bottom panels show the counting and luminosity richness respectively. With very little differences between the subsets it is clear that only a few clusters which attain the richness bound are removed as the quality becomes cleaner.*

As stated in the previous sections, low richness clusters are difficult to model and analyse due to difficulties in fitting distributions to a small number of galaxies, and this is reflected in the completeness rates shown in Figure 4.42. In addition to this, the lower completeness in the clean set, particularly for low richness clusters, reflects the difficulty in attaining 'clean' estimates. Low richness clusters suffer from reduced completeness rates not only as a result of these difficulties but from background fluctuations which, in this case can cause as much as an 80% discrepancy due to discreteness. Table 4.6 summarises and extends these results to the luminosity richness, $n_{200-lum}$.

While these richness completeness results may seem unsatisfactorily low, it is noted that other algorithms, particularly GMBCG, suffer from poor richness recovery. While this recovery is not quantified, it is noted in Hao et al. (2010) that GMBCG fails to match even intermediate richnesses due to the similar issues of projection and background fluctuations.

While these results hold in general for the other forms of evolution as shown in Figure 4.43, M10 and BC03 mocks suffers from a slight reduction in completeness around $0.2 < z_{mock} < 0.4$ due to the bi-modal colour distributions and wider red sequences compared to the other models as discussed in Sections 4.2.1 and 4.5.2.

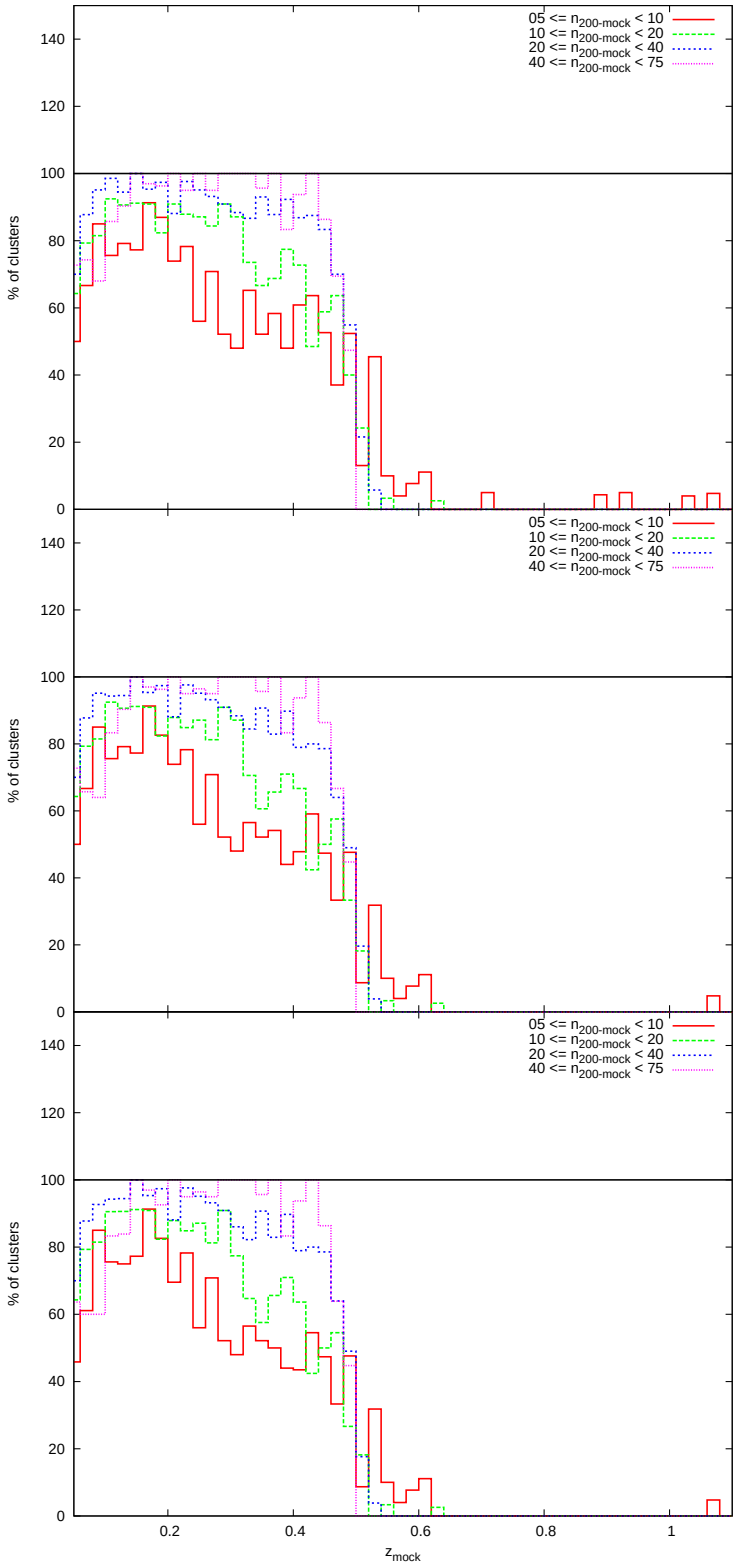

Figure 4.42 *The fraction of maxBCG evolution mock clusters for different richness bands where the $n_{200-count}$ estimate was within 25% of the actual value where the top, middle and bottom panels represent the detection, mid and clean subsets respectively.*

Subset	Richness	Redshift	Completeness
Detection	All	$0.07 < z < 0.45$	85.0%
	$5 \leq n_{200} < 10$	$0.07 < z < 0.45$	67.5%
	$10 \leq n_{200} < 20$	$0.07 < z < 0.45$	81.2%
	$20 \leq n_{200} < 40$	$0.07 < z < 0.45$	92.8%
	$40 \leq n_{200} < 75$	$0.07 < z < 0.45$	93.2%
Mid	All	$0.07 < z < 0.45$	83.3%
	$5 \leq n_{200} < 10$	$0.07 < z < 0.45$	65.6%
	$10 \leq n_{200} < 20$	$0.07 < z < 0.45$	79.2%
	$20 \leq n_{200} < 40$	$0.07 < z < 0.45$	91.0%
	$40 \leq n_{200} < 75$	$0.07 < z < 0.45$	92.3%
Clean	All	$0.07 < z < 0.45$	82.4%
	$5 \leq n_{200} < 10$	$0.07 < z < 0.45$	64.3%
	$10 \leq n_{200} < 20$	$0.07 < z < 0.45$	77.9%
	$20 \leq n_{200} < 40$	$0.07 < z < 0.45$	90.7%
	$40 \leq n_{200} < 75$	$0.07 < z < 0.45$	91.3%

(a) *The counting richness* $n_{200-count}$

Subset	Richness	Redshift	Completeness
Detection	All	$0.07 < z < 0.50$	81.8%
	$5 \leq n_{200} < 10$	$0.07 < z < 0.45$	67.5%
	$10 \leq n_{200} < 20$	$0.07 < z < 0.45$	81.2%
	$20 \leq n_{200} < 40$	$0.07 < z < 0.52$	87.5%
	$40 \leq n_{200} < 75$	$0.07 < z < 0.52$	88.0%
Mid	All	$0.07 < z < 0.50$	79.5%
	$5 \leq n_{200} < 10$	$0.07 < z < 0.45$	65.6%
	$10 \leq n_{200} < 20$	$0.07 < z < 0.45$	79.2%
	$20 \leq n_{200} < 40$	$0.07 < z < 0.52$	85.1%
	$40 \leq n_{200} < 75$	$0.07 < z < 0.52$	86.9%
Clean	All	$0.07 < z < 0.50$	78.6%
	$5 \leq n_{200} < 10$	$0.07 < z < 0.45$	64.3%
	$10 \leq n_{200} < 20$	$0.07 < z < 0.45$	77.9%
	$20 \leq n_{200} < 40$	$0.07 < z < 0.52$	84.8%
	$40 \leq n_{200} < 75$	$0.07 < z < 0.52$	86.0%

(b) *The luminosity richness* $n_{200-lum}$

Table 4.6 *A summary of results where the top and bottom Tables present completeness where the* $n_{200-count}$ *and* $n_{200-lum}$ *estimates respectively are within* 25% *of the mock value.*

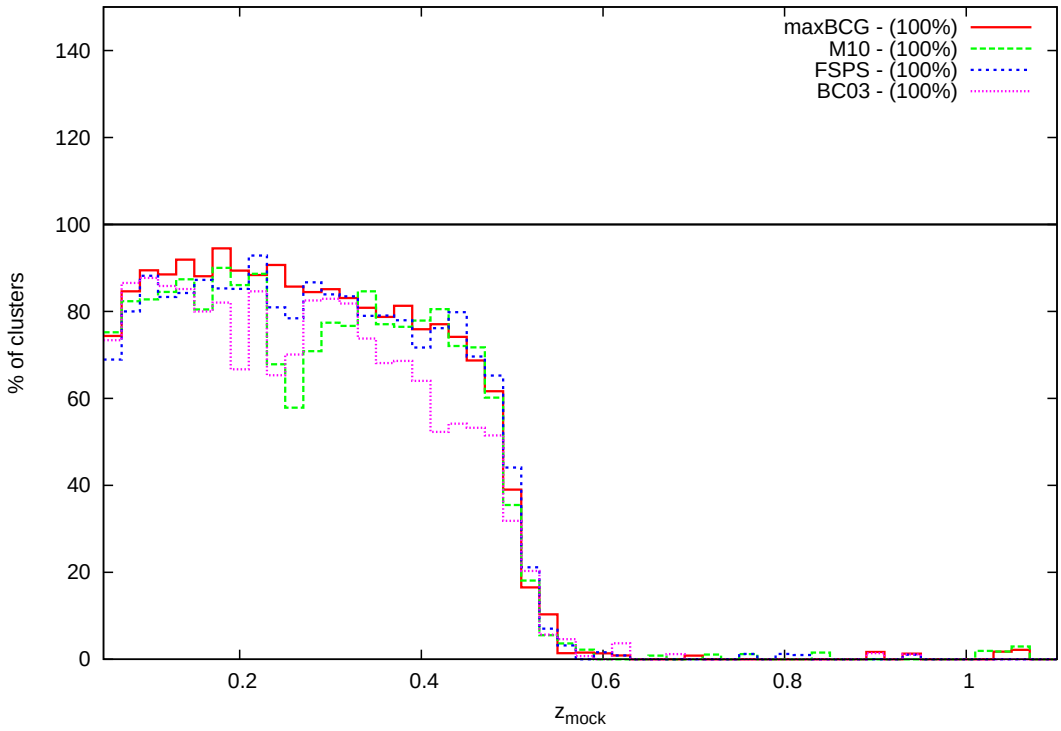

Figure 4.43 *The fraction of mock clusters generated using different forms of evolution where the $n_{200-count}$ estimate was within 25% of the original value. With little difference between the models GMPhoRCC is again shown to be insensitive to the form of the evolution used to generate the mocks.*

Considering completeness relative to a subset of mocks with a given quality marker, q, and z_{RS} range, rather than the whole catalogue, gives insight into the accuracy of the GMPhoRCC richness estimate. The fraction of clusters in a given subset where the $|n_{200-count} - n_{200-mock}|/n_{200-mock} < 0.25$ bound is achieved represents the probability that a richness estimate is within 25% of the mock value, given a cluster has a quality marker and z_{RS} consistent with the subset. Figure 4.44 shows these fractions for the various quality markers and the 25% bound. In addition to the clean subset, $q = 1$, achieving a very high probability ($> 85\%$) that the richness estimate is within 25% of the mock value, those with larger, less clean quality markers have low probabilities ($< 15\%$), again showing the ability of the quality subsets to identify and remove potential outliers. A full set of probabilities for each quality marker and several bounds are presented in Table 4.7. It is clear that for a high redshift estimate the luminosity method is able to extrapolate richness, attaining much higher probabilities of attaining the 25% bound ($\sim 30\%$ compared to $\sim 5\%$).

In general the probabilities are lower than the redshift and BCG counterparts shown in Tables 4.3 and 4.5 due to the large scatter in the richness estimates. Again this is due to the propagation of uncertainty in redshift, n_{gals} and r_{200} and the presence of potentially large background fluctuations.

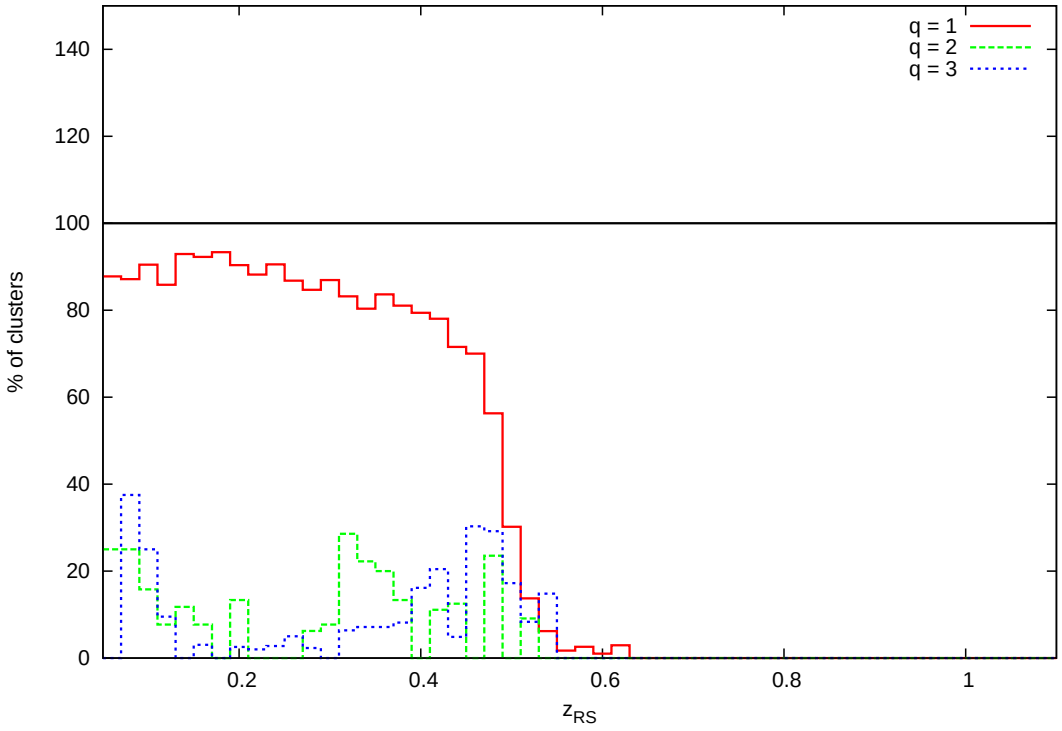

Figure 4.44 *The fraction of mock clusters with a given quality marker where the n_{200} estimate was within 25% of the original value. In addition to the clean subset, $q = 1$, achieving a high probability ($> 75\%$) that the richness estimate is within 25% of the mock value, those with larger, less clean quality markers have very low probabilities ($< 10\%$), again showing the ability of the quality subsets to identify and remove potential outliers.*

q	Redshift Range	p($\Delta n_c < 0.1$)	p($\Delta n_c < 0.25$)	p($\Delta n_c < 0.5$)
3	$0.05 < z_{RS} < 0.45$	0.03	0.06	0.08
2	$0.05 < z_{RS} < 0.45$	0.05	0.11	0.20
1	$0.05 < z_{RS} < 0.45$	0.53	0.86	0.97

(a) *The counting richness* $n_{200-count}$

q	Redshift Range	p($\Delta n_l < 0.1$)	p($\Delta n_l < 0.25$)	p($\Delta n_l < 0.5$)
3	$0.05 < z_{RS} < 0.50$	0.04	0.09	0.12
2	$0.05 < z_{RS} < 0.50$	0.05	0.11	0.20
1	$0.05 < z_{RS} < 0.50$	0.51	0.83	0.96

(b) *The luminosity richness* $n_{200-lum}$

q	Redshift Range	p($\Delta n_l < 0.1$)	p($\Delta n_l < 0.25$)	p($\Delta n_l < 0.5$)
3	$0.50 < z_{RS} < 0.80$	0.04	0.09	0.22
2	$0.50 < z_{RS} < 0.80$	0.04	0.11	0.24
1	$0.50 < z_{RS} < 0.80$	0.13	0.30	0.58

(c) *The luminosity richness* $n_{200-lum}$*, high redshift*

Table 4.7 *A list of the probabilities that the* n_{200} *estimate is within various bounds of the actual value given the* z_{RS} *estimate and the quality marker of the cluster. The top and bottom Tables present results for the counting and luminosity richnesses respectively, where* $\Delta n_c = |n_{200-count} - n_{200-mock}|/n_{200-mock}$ *and* $\Delta n_l = |n_{200-lum} - n_{200-mock}|/n_{200-mock}$*. In addition to the clean subset,* $q = 1$*, achieving the highest probabilities that the richness estimate is within given bounds of the mock value, those with larger, less clean quality markers have very low probabilities (*$< 17\%$*), again showing the ability of the quality subsets to identify and remove potential outliers.*

4.6 Summary

Presented in this chapter is the assessment of GMPhoRCC using mock galaxy clusters. Mocks are uniquely suited for this task, providing clusters with known properties rather than those characterised using other algorithms which are subject to their own weaknesses, strengths and selection functions. The mocks used were generated empirically from SDSS data which has the advantage over simulated mocks of providing clusters which best match the optical properties of those found in the target optical data. Very clean clusters from C4, GMBCG, REFLEX, NORAS and XCS catalogues analysed by GMPhoRCC were stacked in redshift/richness bins to provide a source dominated by red sequence galaxies with bin-appropriate properties. Resampling these galaxies with replacement until a given richness is met produces a cluster with suitable colour, redshift, radial and luminosity distributions at the bin redshift. Finally, K+e-corrections are able to extrapolate the photometry to match a cluster at any redshift. Section 4.2 shows the mocks generated this way and the bins themselves share bulk properties with typical real clusters.

Analysis of these mocks proceeded using those generated with the maxBCG-style evolution discussed in Section 4.1.2, however the results were shown to be insensitive to the form of the evolution. First considering redshift, this is relatively easier to estimate than richness, proving to be reasonably accurate even with poorer modelled red sequences where only a fraction of the members are recovered. Even with a smaller fraction, modelling the redshift distribution gives an excellent estimate for the cluster. It is noted that low richness clusters suffer from poorer estimates due to the difficulty in modelling with a low number of galaxies. In addition, poor contrast against the background and limitations in the field area give rise to a similar result at low redshift. The introduction of the quality subsets is seen to greatly improve the set of estimates, removing most of the outliers.

In contrast to redshift, richness is more difficult to measure accurately and the estimates exhibit typical scatters of $\sim 30\%$ around the mock value. Modelling the red sequence accurately is vital, since losing even a few galaxies can result in a large fractional deficits. Similarly, large background fluctuations can cause significant discrepancies particularly with low richness clusters. In addition, errors with redshift, BCG matching, the intermediate richness n_{gals} and r_{200} propagate through GMPhoRCC and are amplified in the final richness, n_{200}.

Again, it is noted that low richness clusters suffer from the poorest estimates as modelling the red sequence is difficult with only a few galaxies. Similarly low redshift clusters suffer from the worst outliers again due to poor contrast against the background and limitations in the field area.

These findings are confirmed in the investigation of completeness. By adding an $i-$band < 21 photometry cut, the effect of incomplete photometry in the SDSS DR10 can be simulated allowing the mocks to be used to explore completeness. Completeness gives a measure of the fraction of clusters which can be characterised by GMPhoRCC as a function of cluster properties and can gives an estimate of the optical selection function of GMPhoRCC. Incompleteness begins to affect clusters with a redshift $z > 0.45$, where galaxies become too faint for reliable detection and this is reflected in the various completeness measures.

First considering redshift, completeness was considered as the fraction of clusters where the redshift estimate was within $|z_{RS} - z_{mock}| < 0.03$. The redshift estimate was again shown to be very reliable with a high fraction of clusters attaining this bound in regions of complete photometry. Separately the low richness and low redshift clusters exhibit reduced completeness rates due to the difficulties in modelling the red sequence. In addition to this, GMPhoRCC is found to exceed the completeness of GMBCG and maxBCG particularly by extending the redshift range considered.

Richness is again observed to be more difficult to estimate as shown by the reduced completeness rates relative to redshift. Although these rates seem unsatisfactorily low, other algorithms such as GMBCG, have issues recovering richness due to projection effects and background fluctuations. It is noted that the luminosity method shows greater completeness above $z > 0.5$ clearly showing the ability to extrapolate richness in regions of incomplete photometry. For these high redshift clusters the luminosity estimate should be used as the optical mass proxy. In addition the higher completeness indicates that the counting method should be used for lower redshift clusters.

Combining these completeness results gives in insight into the redshift and richness ranges of clusters which GMPhoRCC can reliably characterise and this is summarised in Table 4.8. With the high completeness it is expected that these clusters have a high probability of attaining a redshift estimate within $|z_{RS} - z_{cluster}| < 0.03$. Similarly inside these ranges, a reasonably high probability is expected that the richness is within 50% with a lower probability the estimate

is within 25%

While the completeness analysis gives insight into the optical selection function it is equally important to assess the accuracy of the estimates once a cluster has been characterised. By considering completeness with respect to the various subsets with a given quality marker, q, and z_{RS} range rather than the whole mock catalogue, the probability that a clusters estimate is within a given bound can be assessed and this is summarised in Table 4.9. The quality markers are not only able to identify those where the estimate has a high probability of matching the mock value but also those with poorer estimates.

Throughout this chapter GMPhoRCC has been shown not only to produce estimates in good agreement with the mock value but is also able to identify those which are potentially erroneous.

Subset	Richness	Redshift	Completeness
Detection	$5 \leq n_{200} < 10$	$0.07 < z < 0.55$	97.7%
	$10 \leq n_{200} < 20$	$0.07 < z < 0.55$	97.2%
	$n_{200} \geq 20$	$0.05 < z < 0.65$	98.2%
Mid	$5 \leq n_{200} < 10$	$0.07 < z < 0.55$	91.7%
	$10 \leq n_{200} < 20$	$0.07 < z < 0.55$	93.0%
	$n_{200} \geq 20$	$0.05 < z < 0.65$	94.2%
Clean	$5 \leq n_{200} < 10$	$0.07 < z < 0.50$	89.4%
	$10 \leq n_{200} < 20$	$0.07 < z < 0.50$	92.2%
	$n_{200} \geq 20$	$0.05 < z < 0.62$	90.2%

(a) *Redshift Completeness*

Subset	Richness	Redshift	Completeness
Detection	$5 \leq n_{200} < 10$	$0.05 < z < 0.55$	86.6%
	$10 \leq n_{200} < 20$	$0.05 < z < 0.55$	89.1%
	$n_{200} \geq 20$	$0.05 < z < 0.62$	89.4%
Mid	$5 \leq n_{200} < 10$	$0.05 < z < 0.50$	87.3%
	$10 \leq n_{200} < 20$	$0.05 < z < 0.55$	88.7%
	$n_{200} \geq 20$	$0.05 < z < 0.62$	89.0%
Clean	$5 \leq n_{200} < 10$	$0.07 < z < 0.50$	86.6%
	$10 \leq n_{200} < 20$	$0.05 < z < 0.55$	87.1%
	$n_{200} \geq 20$	$0.05 < z < 0.62$	88.1%

(b) *Correct BCG Completeness*

Subset	Richness	Redshift	Completeness
Detection	$5 \leq n_{200} < 10$	$0.07 < z < 0.45$	67.5%
	$10 \leq n_{200} < 20$	$0.07 < z < 0.45$	81.2%
	$n_{200} \geq 20$	$0.07 < z < 0.45$	92.9%
Mid	$5 \leq n_{200} < 10$	$0.07 < z < 0.45$	65.6%
	$10 \leq n_{200} < 20$	$0.07 < z < 0.45$	79.2%
	$n_{200} \geq 20$	$0.07 < z < 0.45$	91.5%
Clean	$5 \leq n_{200} < 10$	$0.07 < z < 0.45$	64.3%
	$10 \leq n_{200} < 20$	$0.07 < z < 0.45$	77.9%
	$n_{200} \geq 20$	$0.07 < z < 0.45$	90.9%

(c) *Counting Richness Completeness*

Subset	Richness	Redshift	Completeness
Detection	$5 \leq n_{200} < 10$	$0.07 < z < 0.55$	67.5%
	$10 \leq n_{200} < 20$	$0.07 < z < 0.45$	81.1%
	$n_{200} \geq 20$	$0.07 < z < 0.50$	87.7%
Mid	$5 \leq n_{200} < 10$	$0.07 < z < 0.55$	65.6%
	$10 \leq n_{200} < 20$	$0.07 < z < 0.45$	79.1%
	$n_{200} \geq 20$	$0.07 < z < 0.50$	85.7%
Clean	$5 \leq n_{200} < 10$	$0.07 < z < 0.55$	64.3%
	$10 \leq n_{200} < 20$	$0.07 < z < 0.45$	77.9%
	$n_{200} \geq 20$	$0.07 < z < 0.50$	85.2%

(d) *Luminosity Richness Completeness*

Table 4.8 *A summary of the completeness results showing redshift and richness ranges of clusters which can be reliably characterised by GMPhoRCC*

q	Redshift Range	p($\Delta z < 0.01$)	p($\Delta z < 0.03$)	p($\Delta z < 0.05$)
3	$0.05 < z_{RS} < 0.45$	0.04	0.05	0.05
2	$0.05 < z_{RS} < 0.45$	0.16	0.19	0.22
1	$0.05 < z_{RS} < 0.80$	0.97	0.99	0.99

(a) *Redshift Estimates*

q	Redshift Range	p(BCG)	p(CM)
3	$0.05 < z_{RS} < 0.60$	0.03	0.03
2	$0.05 < z_{RS} < 0.50$	0.10	0.16
1	$0.05 < z_{RS} < 0.80$	0.94	0.97

(b) *BCG Identification*

q	Redshift Range	p($\Delta n_c < 0.1$)	p($\Delta n_c < 0.25$)	p($\Delta n_c < 0.5$)
3	$0.05 < z_{RS} < 0.45$	0.03	0.06	0.08
2	$0.05 < z_{RS} < 0.45$	0.05	0.11	0.20
1	$0.05 < z_{RS} < 0.45$	0.53	0.86	0.97

(c) *Counting Richness Estimates*

q	Redshift Range	p($\Delta n_l < 0.1$)	p($\Delta n_l < 0.25$)	p($\Delta n_l < 0.5$)
3	$0.05 < z_{RS} < 0.50$	0.04	0.09	0.12
2	$0.05 < z_{RS} < 0.50$	0.05	0.11	0.20
1	$0.05 < z_{RS} < 0.50$	0.51	0.83	0.96

(d) *Luminosity Richness Estimates*

q	Redshift Range	p($\Delta n_l < 0.1$)	p($\Delta n_l < 0.25$)	p($\Delta n_l < 0.5$)
3	$0.50 < z_{RS} < 0.80$	0.04	0.09	0.22
2	$0.50 < z_{RS} < 0.80$	0.04	0.11	0.24
1	$0.50 < z_{RS} < 0.80$	0.13	0.30	0.58

(e) *Luminosity Richness Estimates, high redshift*

Table 4.9 *A summary showing the probability an estimate is within a bound given the cluster quality marker and redshift estimate where* $\Delta z = |z_{RS} - z_{mock}|$, $\Delta n_c = |n_{200-count} - n_{200-mock}|/n_{200-mock}$, $\Delta n_{lum} = |n_{200-lum} - n_{200-mock}|/n_{200-mock}$ *and p(BCG) and p(CM) represent the probability that the BCG was respectively identified correctly and identified as any cluster member. With high and low probabilities achieved for the* $q = 1$ *and* $q > 1$ *sets respectively, the quality markers and subsets have proven to be able to identify cases where the estimates are likely to be erroneous.*

Chapter 5

Characterising XCS Sources

GMPhoRCC has proven to be a valuable tool for characterising galaxy clusters and now with significant understanding of performance and selection function, is ideal for use with new potential cluster candidates. The XMM cluster survey (XCS) (Romer et al., 2001, Lloyd-Davies et al., 2011 and Mehrtens et al., 2012) provides analysis of X-ray observations from the XMM-Newton telescope giving an extensive list of extended X-ray sources as potential cluster candidates[1]. Considering XCS DR1, GMPhoRCC has already proven in Section 3.4.1 to provide more accurate redshift estimates and with the increased coverage provided by the Sloan Digital Sky Survey (SDSS) DR10 over DR7 used in Mehrtens et al. (2012), is ideal to extend the current cluster list. In addition to the 503 optically confirmed clusters of XCS DR1, many other candidates were considered by Lloyd-Davies et al. (2011) and with newer sources available, XCS has proven to be a valuable source of X-ray detected clusters for characterisation. While the ultimate goal of this research was to provide characterisations for an upcoming XCS data release, the submission schedule of this thesis prevented such analysis as these extended sources are still in preparation. This chapter however, is a significant step toward this goal, providing characterisations for a preliminary XCS DR2 list which, combines the complete catalogue from Lloyd-Davies et al. (2011) with new extended sources in the Red Sequence Cluster Survey (RCS) (Gladders & Yee, 2005) region. Many of these extended X-ray sources however lie outside of the SDSS footprint hence the focus of this chapter is to not only provide characterisations using the SDSS but also lay the ground work for using additional optical data. Of particular interest is optical data provided by the VLT Survey

[1] see Section 2.2

Telescope (VST) ATLAS catalogue (Shanks & Metcalfe, 2012 and Shanks et al in prep.), providing coverage in the southern hemisphere and from the Canada-France-Hawaii Telescope Lensing Survey (CFHTLenS), (Heymans et al., 2012 and Erben et al., 2013) providing much deeper photometry than the SDSS. As the focus of weak lensing studies, CFHTLenS provides the unique opportunity of future research of cluster characterisations as a function of lensing observables.

This chapter is structured as follows. Section 5.1 explores the extra optical data provided by VST ATLAS and CFHTLenS with additional calibrations and comparisons presented in Section 5.2. This chapter concludes with the characterisations given in Section 5.3 with a discussion in Section 5.4.

5.1 Optical Data

In addition to those discussed in Lloyd-Davies et al. (2011), XCS provides new extended X-ray sources found specifically in the CFHTLenS / RCS region giving an extensive list of potential clusters for characterisation. While the original intent of this research was to provide characterisations for an upcoming XCS data release, the submission schedule of this thesis prevented such analysis as these extended sources are still in preparation. Hence these sources define a preliminary list of potential candidates for the second XCS data release. The distribution of these $13,956$ extended sources are shown in Figure 5.1 with those in the SDSS DR10 footprint highlighted. While the development, analysis and comparisons of Chapters 3 and 4 have all focused on SDSS DR9 as the source of optical data, this Chapter makes use of the more recent DR10. While no additional photometry is provided, a significant gain ($\sim 30\%$) in spectroscopic redshifts is achieved with the sample increasing from ~ 1.7 million to ~ 2.2 million as described in Ahn et al. (2013). It is clear from Figure 5.1 that while the SDSS provides a large coverage, additional sources of optical data are needed to characterise the full catalogue of sources.

Access to VST ATLAS (Shanks & Metcalfe, 2012 and Shanks et al in prep.) data provides additional SDSS-like photometry in the southern hemisphere with deeper photometry provided from CFHTLenS. Figure 5.2 shows the total combined optical coverage highlighting the areas of each survey. While some sources still have no optical coverage, the use of ATLAS allows for characterisations outside the SDSS footprint and with the deeper CFHTLenS data, characterisations of

clusters at higher redshifts than is possible using the SDSS. In addition to these current optical data, the Panoramic Survey Telescope and Rapid Response System (Pan-STARRS) 3π survey (Magnier et al., 2013) offers a future extension to the SDSS, providing deep, multi-band photometry with significant coverage across 3π steradians of the sky.

Of the $13,956$ candidates, 6124 have optical coverage, 5580 in the SDSS, 523 in ATLAS and 819 in CFHTLenS with some overlap.

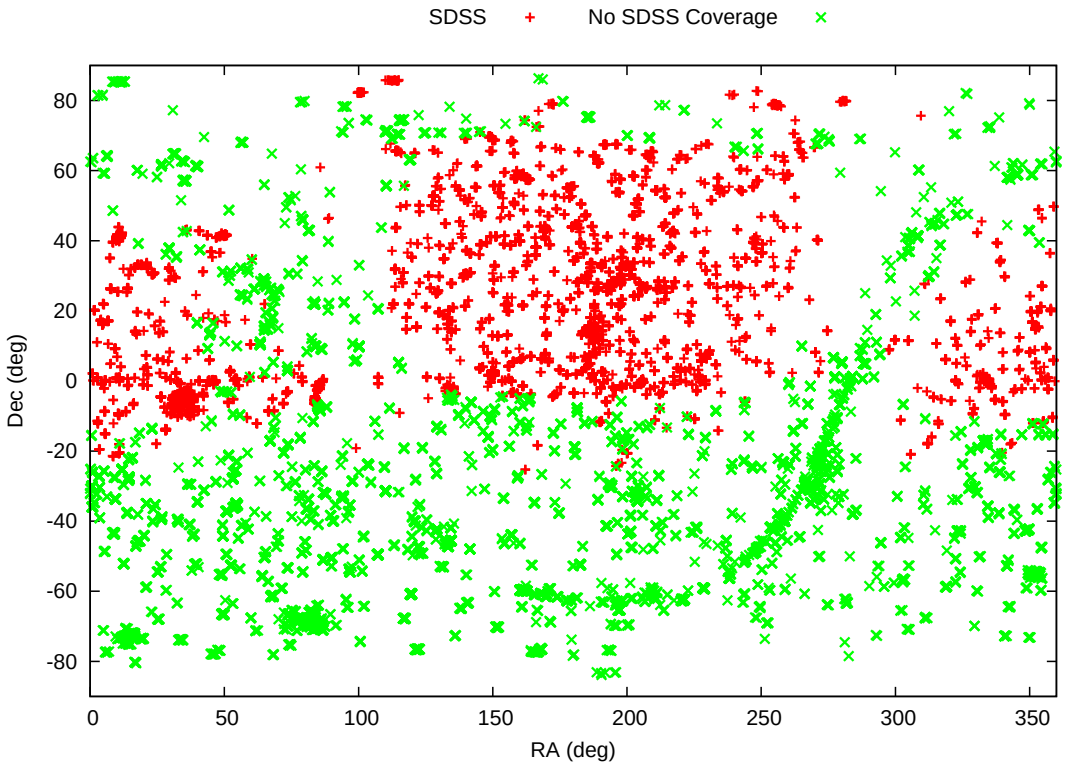

Figure 5.1 *The distribution of the preliminary XCS DR2 extended X-ray sources highlighting SDSS DR9 coverage. While the SDSS provides large coverage many sources lie outside this footprint, highlighting the need for additional sources of optical data.*

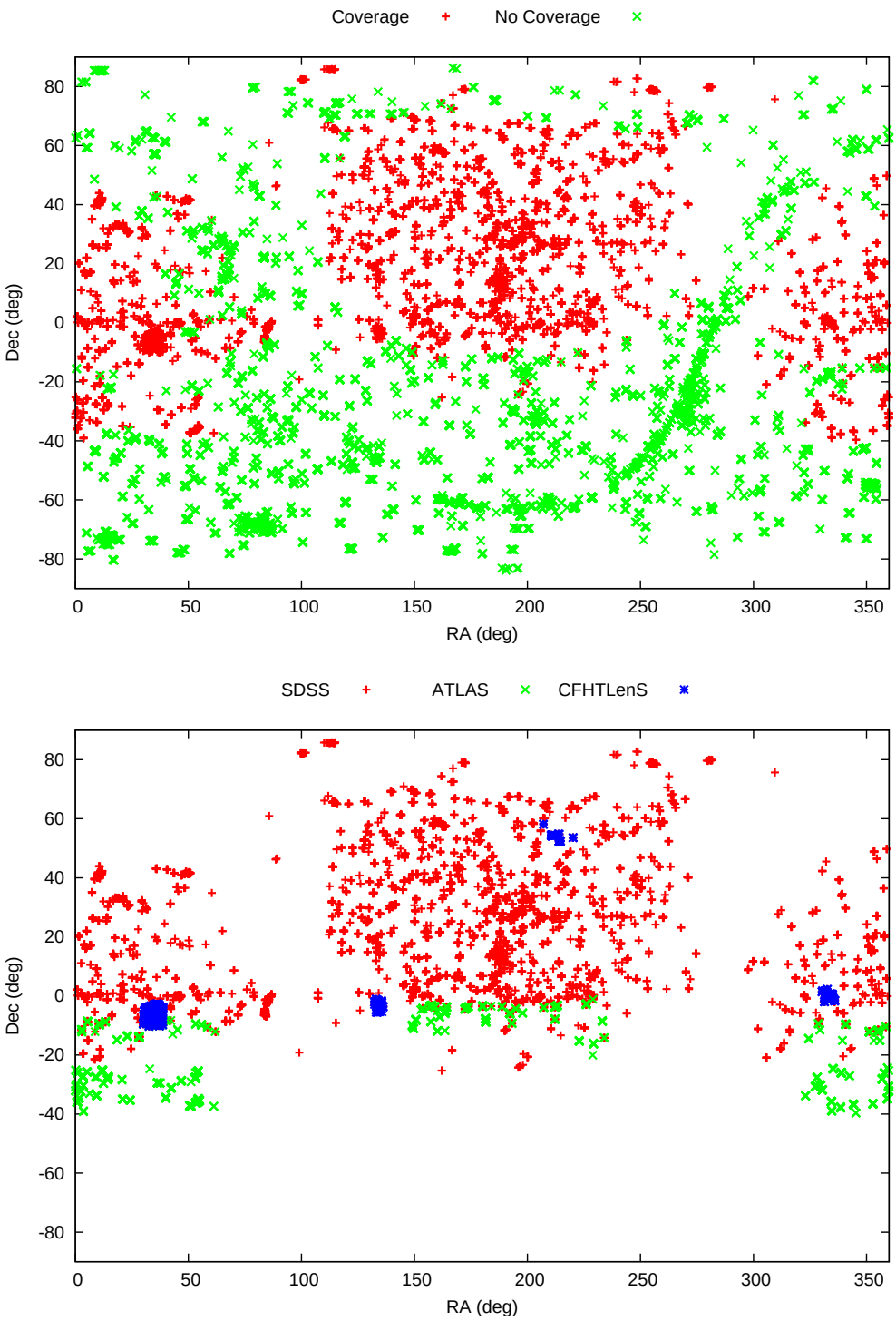

Figure 5.2 *The total optical coverage available for the preliminary XCS DR2 extended X-ray sources. The top panel shows the total coverage while the bottom highlights the coverage from the various optical sources. While some sources still have no optical coverage, the use of ATLAS and CFHTLenS allows for the characterisation outside the SDSS footprint.*

5.1.1 VST ATLAS

The ATLAS data provides SDSS u,g,r,i and z bands at a similar depth as the SDSS. Figure 5.3 shows the Petrosian i-band distribution of the ATLAS data compared to the SDSS showing the effect of incompleteness above $i > 20$. It is noted that while a full investigation of performance and completeness with regards to ATLAS requires extensive analyses similar to those shown in Chapter 4, that incomplete photometry above this level may result in the non-detection of faint members for clusters with $z > 0.32$ as expected from Figure 3.15. Compared to the SDSS these issues occur at a much lower redshift, where the sharp cut imposed at $i > 21$ in model magnitudes results in SDSS incompleteness for clusters with $z > 0.45$. The main purpose of the photometry cut in the SDSS is to remove a sparse number of galaxies with very poor photometric errors. A similar cut is not imposed on ATLAS at $i > 20$ as incompleteness has a more gradual effect where a large fraction of galaxies with good photometry would be removed.

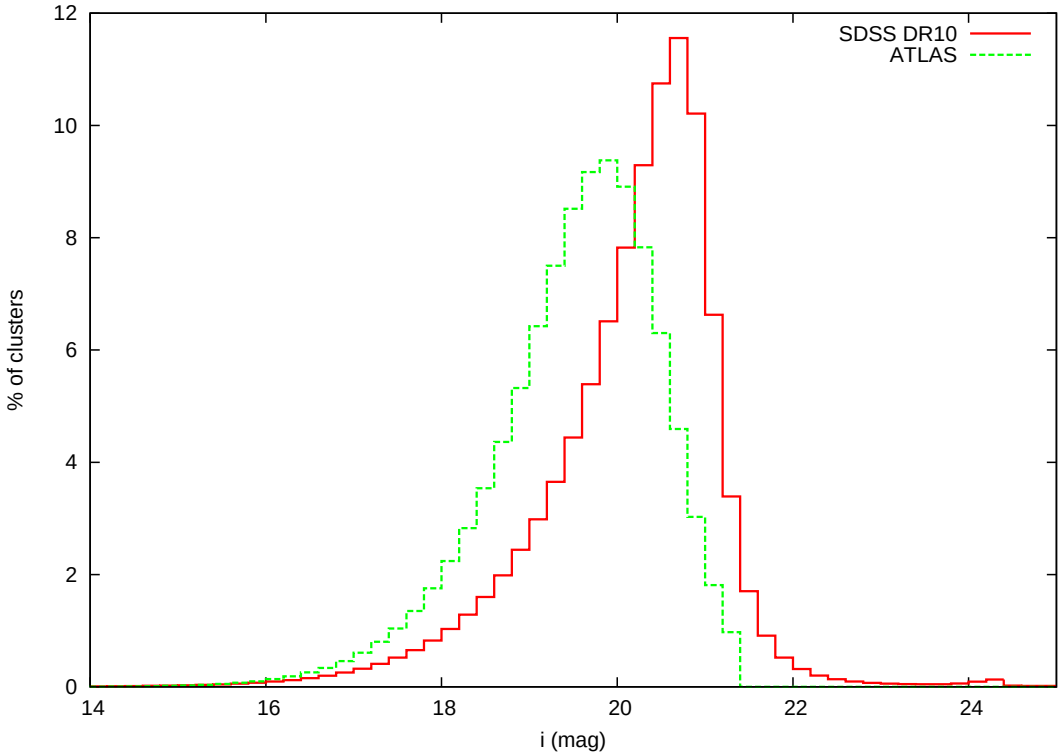

Figure 5.3 *The i-band distribution of the galaxies in ATLAS and the SDSS. Incomplete photometry can be seen to occur at a brighter level, $i > 20$, than the SDSS which may result in the non-detection of faint members for clusters with $z > 0.32$ as expected from Figure 3.15. Contrary to the sharp cut in the SDSS, galaxies in this region remain as they form a significant fraction of the ATLAS data.*

In addition to the multi-band photometry, GMPhoRCC requires photometric redshifts in order to characterise clusters and while the complete data release of ATLAS is intended to include these from SED template fitting, these are not ready for this analysis. Instead empirical photometric redshifts are provided courtesy of Owen Turner[2] using the random forest method of Carliles et al. (2010). The training set was produced in the cross-matched overlap region of the SDSS and ATLAS providing galaxies with SDSS spectroscopic redshifts and ATLAS photometry. Figure 5.4 shows the distribution of photometric redshifts for the ATLAS survey attained using this method. Although similar to the SDSS photometric distribution, it is noted that there are fewer very low redshift ($z < 0.05$) and high redshift ($z > 0.55$). While the low redshift end remains outside the GMPhoRCC selection function, the reduced high end is likely to restrict the range of cluster redshifts which can be characterised. Again for understanding of performance extensive analysis is required with ATLAS-specific mocks.

5.1.2 CFHTLenS

The CFHTLenS data provides SDSS u,g,r,i and z bands to a much deeper level than the SDSS. Figure 5.5 shows the i-band distribution of the CFHTLenS data with a hard faint end cut above $i > 24.2$. While the range of complete photometry extends beyond this, this cut ensures completeness for clusters up to $z = 1$. Above this redshift the optical red sequence technique suffers from reduced performance as the 4000Å break transitions into infrared bands as noted by High et al. (2010). In addition to reducing the computational burden, removing these galaxies prevents the faint end from dominating the field aiding the isolation of the red sequence.

CFHTLenS photometric redshifts are produced with advanced SED template fitting using the `BPZ` code of Benítez (2000) and Coe et al. (2006) with details shown in Hildebrandt et al. (2012). This method utilises a Bayesian approach to calculate the full redshift probability distribution of an object. It is noted that these redshifts suffer from non-negligible bias across the full magnitude range where, for example, brighter galaxies ($i < 20$) have overestimated photometric redshifts of the order ~ 0.03. An extensive investigation into this bias and possible

[2]Scottish Universities Physics Alliance, Institute for Astronomy, University of Edinburgh, Royal Observatory, Blackford Hill, Edinburgh, EH9 3HJ, UK

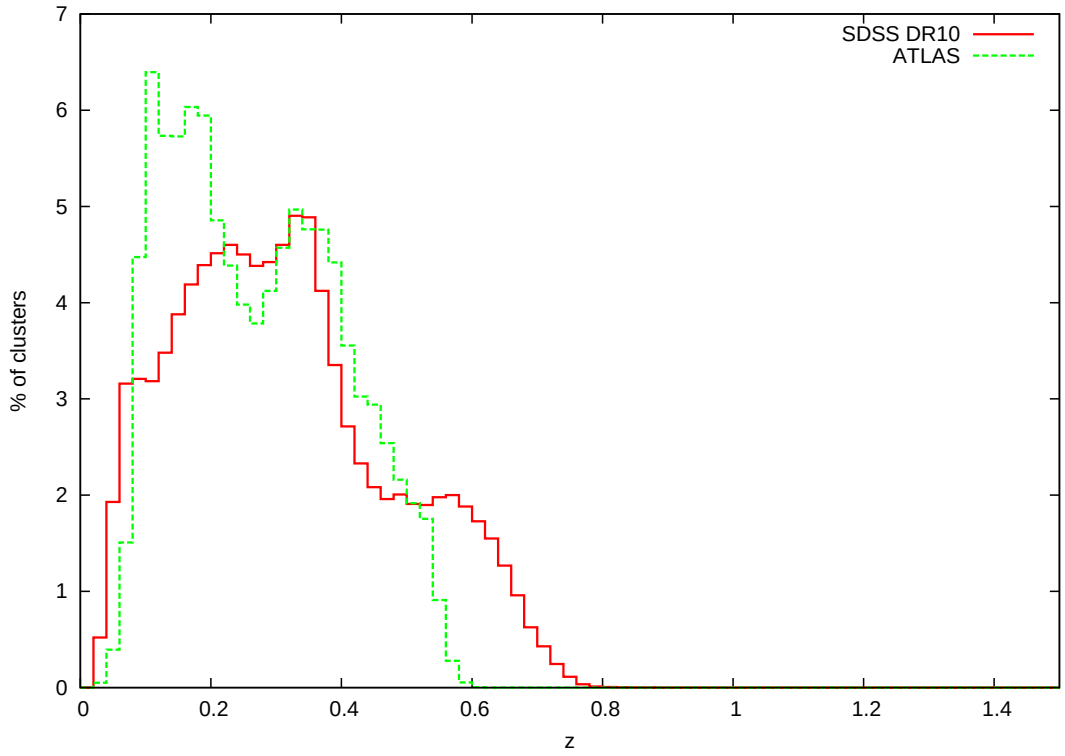

Figure 5.4 *The redshift distribution of the galaxies in the ATLAS survey attained using the random forest method of Carliles et al. (2010) with an SDSS spectroscopic training set. Although similar to the SDSS photometric distribution, it is noted that there are fewer very low redshift ($z < 0.05$) and high redshift ($z > 0.55$)*

corrections is detailed in Hildebrandt et al. (2012) and Velander et al. (2014) and is explored in more detail in Section 5.2.2. Figure 5.6 shows the distribution of photometric redshifts for the CFHTLenS data highlighting again the extra depth compared with the SDSS. Although many redshifts are available above $z > 1.5$, a hard cut is imposed to remove unnecessary galaxies and aid the isolation of the red sequence.

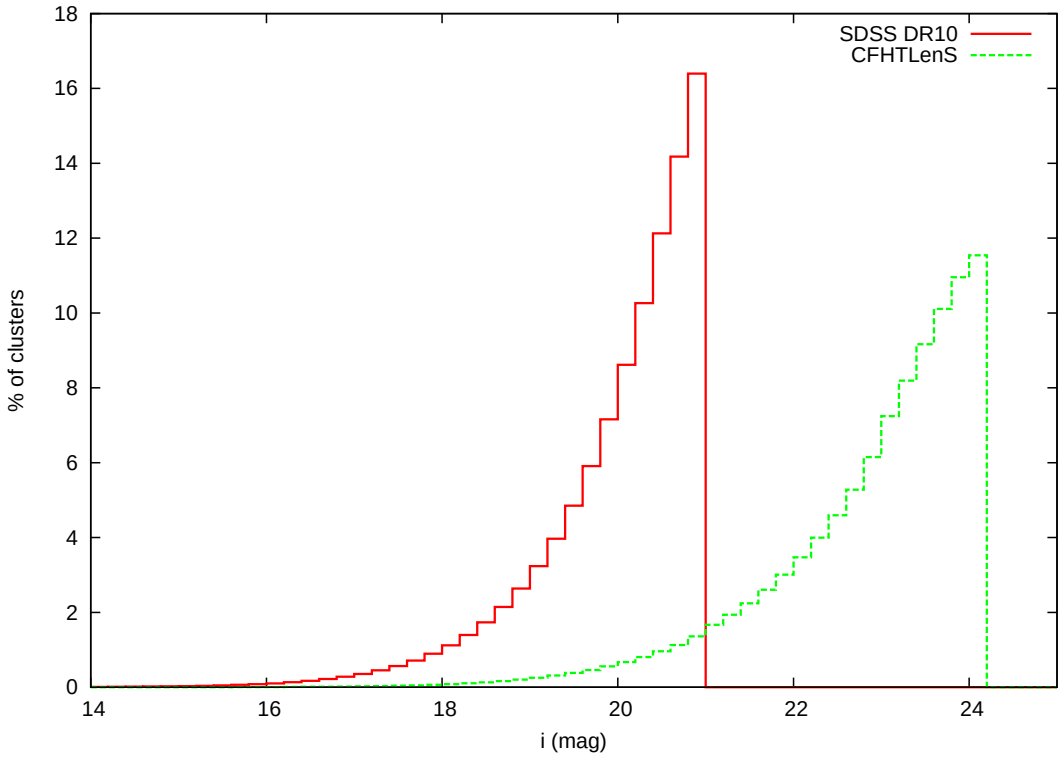

Figure 5.5 *The i-band distribution of the galaxies in CFHTLenS and the SDSS. CFHTLenS provides far deeper photometry than the SDSS where the sharp faint end cut is introduced to remove unnecessary galaxies to aid in the isolation of the red sequence whilst maintaining complete photometry for clusters up to $z = 1$, the limit of the optical red sequence method.*

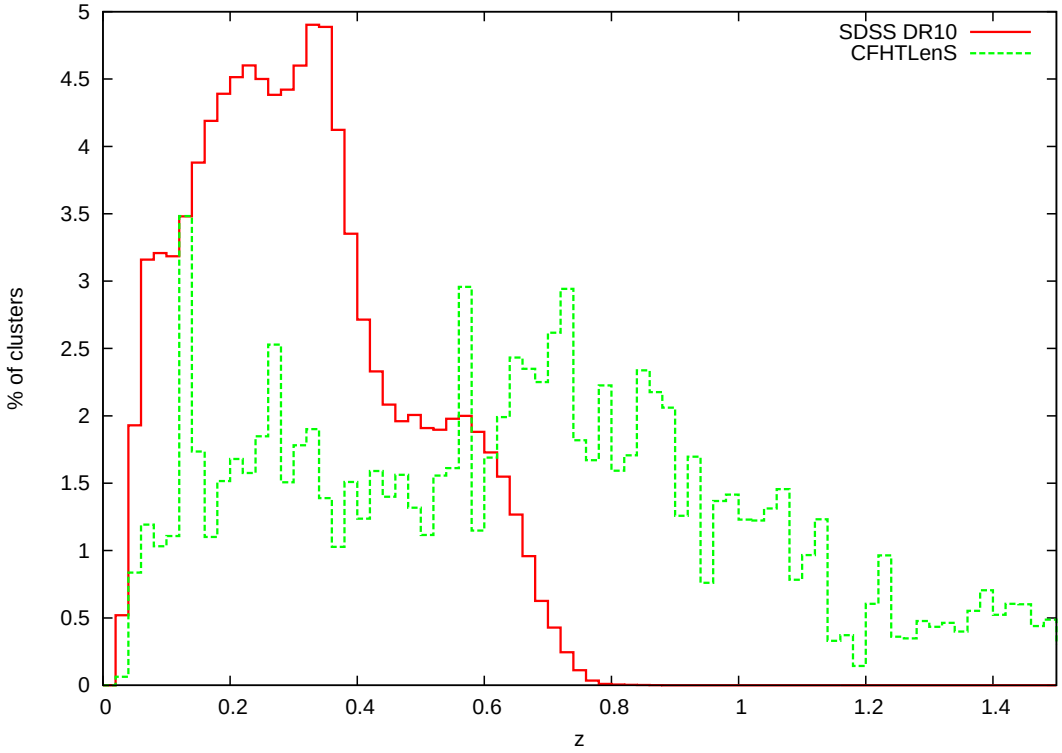

Figure 5.6 *The redshift distribution of the galaxies in CFHTLenS and the SDSS. The extra depth of CFHTLenS compared to the SDSS is highlighted and although redshifts are available above $z > 1.5$, a hard cut is imposed to remove unnecessary galaxies, aiding the isolation of the red sequence.*

5.2 Optical Calibrations

While the calibration of the GMPhoRCC quality markers and subsets of Section 3.2.4 is largely independent of the optical data, the redshift consistency checks however are specific to the SDSS and as such must be recalibrated for ATLAS and CFHTLenS. For such a calibration a small spectroscopic sample of GMBCG (Hao et al., 2010), NORAS (Böhringer et al., 2000), REFLEX (Böhringer et al., 2004) and XCS (Mehrtens et al., 2012) clusters with optical coverage are characterised and compared. While the quality markers are designed to remove failures in both redshift and richness estimates, there are no suitable comparisons for the latter hence the calibrations of this section are driven by redshift recovery. In addition to aiding the calibration these comparisons give an estimate of GMPhoRCC accuracy where a full evaluation requires the use of mock clusters or larger spectroscopic samples.

5.2.1 ATLAS

First considering ATLAS, 42 clusters with optical coverage are characterised by GMPhoRCC with comparison to spectra shown in Figure 5.7. In addition to the larger scatter, the ATLAS photometric redshifts appear to have a slight bias compared with the SDSS. Considering the larger errors however, the cluster redshifts are found to be consistent with the spectroscopic value. The source of the large scatter and errors is mainly attributed to the preliminary ATLAS photometry where, calibrations and work to ensure homogenisation across the survey, are ongoing. In addition to this it is noted that the galaxy photometric redshifts are preliminary with ongoing work aimed at further improvement.

The tight redshift consistency check used for the SDSS to remove outliers makes use of the fact that as a bright galaxy, the BCG generally has a more reliable photometric redshift, hence discrepancies between this and the overall distribution indicates a problem. In the case of ATLAS however, with the preliminary photometric calibrations and larger redshifts errors, the same consistency checks are not as strong an indicator of potential outliers, instead a broader check must be used. Figure 5.8 demonstrates the effect of the wider consistency checks used for ATLAS data. Although the consistency checks do not improve the slight bias, applying quality cuts based on these will

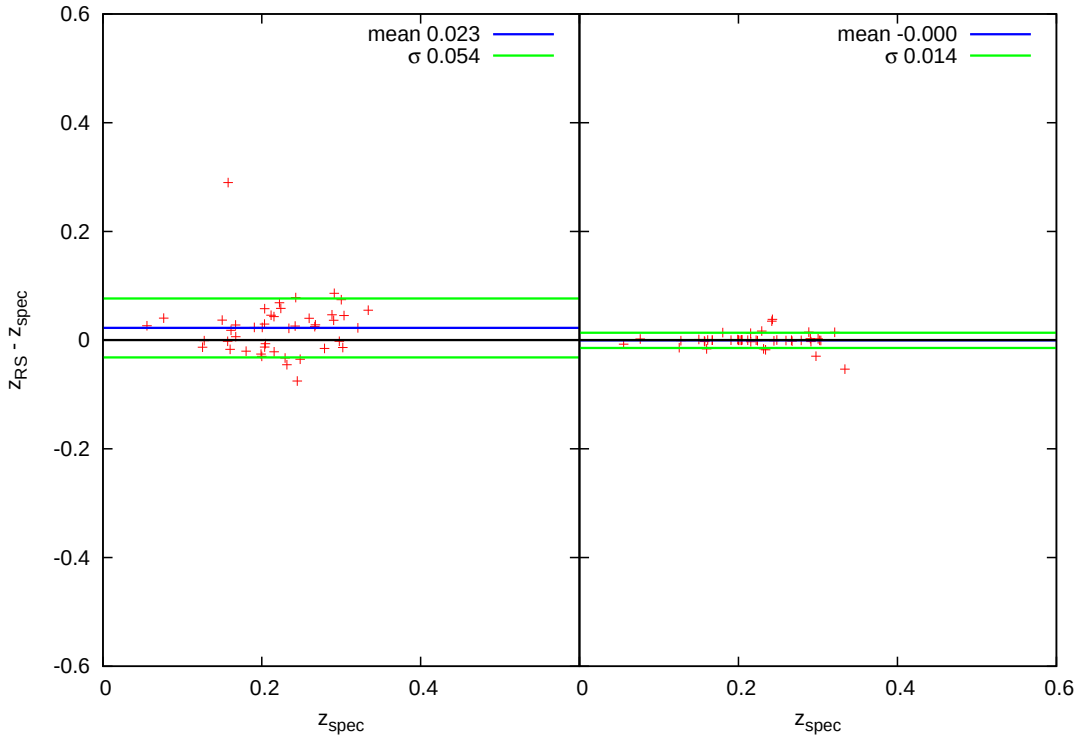

Figure 5.7 *A comparison of GMPhoRCC photometric red sequence redshifts to spectra using 42 clusters from GMBCG, NORAS, REFLEX and XCS where the left and right panel shows results using ATLAS and SDSS data respectively. In addition to the larger scatter, the ATLAS redshifts appear to have a slight bias compared with the SDSS, however, considering the larger errors, the estimates are consistent with the spectroscopic value.*

reduce the scatter of the estimates by removing the worst outliers. The SDSS consistency checks $0.025 \leq |z_{RS} - z_{BCG}| < 0.05$ and $|z_{RS} - z_{BCG}| \geq 0.05$ used to indicate quality markers 2 and 3 respectively are replaced by the broader $0.05 \leq |z_{RS} - z_{BCG}| < 0.1$ and $|z_{RS} - z_{BCG}| \geq 0.1$, with a full description of the ATLAS-specific quality marker given in Table 5.1. With the small cluster sample these new markers are preliminary, with a larger cluster sample these can be further calibrated.

Using Table 3.8 with the new marker, a set of ATLAS-specific quality subsets can be defined and are shown in Figures 5.9 and 5.10 for the previous cluster set. Although a slight bias and large scatter remains compared to the SDSS, the clean subset removes the most outliers attaining the smallest scatter of the ATLAS estimates.

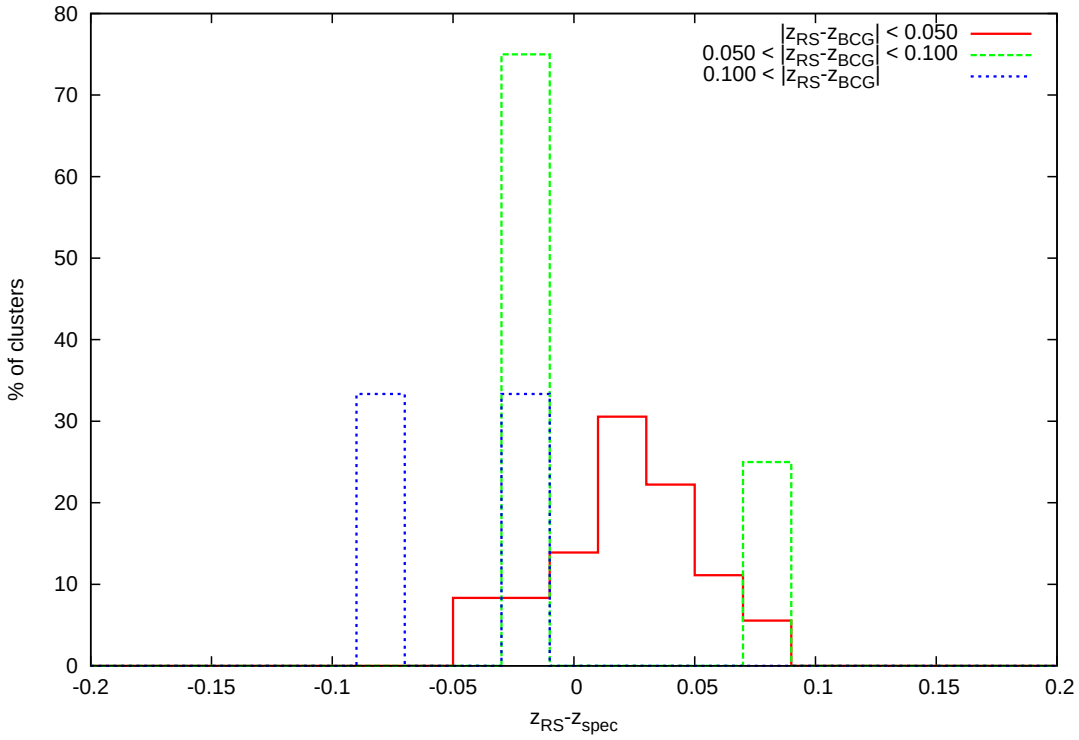

Figure 5.8 *A normalised histogram comparison of the GMPhoRCC red sequence redshifts compared to spectra, highlighting the broader redshift consistency checks, using* 42 *spectroscopic clusters with ATLAS coverage from the GMBCG, NORAS, REFLEX and XCS. Although the consistency checks do not improve the slight bias, applying quality cuts based on these reduces the scatter of the estimates by removing the worst outliers.*

Quality	Flags Value (decimal)	Indicator Flags
5	$140737488355328 \leq$ flags	NO_COVERAGE
4	$17592186044416 \leq$ flags < 140737488355328	NO_DETECTION_REDSHIFT NO_DETECTION_RICHNESS_NGALS NO_DETECTION_RICHNESS_N200
3	$33554432 \leq$ flags < 17592186044416	LOW_RICHNESS_1 INCONSISTENT_Z_0_100 SPARCE_INITIAL SPARCE_COLOUR SPARCE_ZFLAT SPARCE_ZRS NO_OVERDENSITY_INITIAL NO_OVERDENSITY_COLOUR NO_OVERDENSITY_ZRS NO_OVERDENSITY_ZRS NO_CLUSTER_INITIAL NO_CLUSTER_COLOUR NO_CLUSTER_ZFLAT NO_CLUSTER_ZRS CLUSTER_INSIDE_MASK_0_5_MPC CLUSTER_INSIDE_MASK_R200 CLUSTER_INSIDE_MASK_5_AM
2	$2097152 \leq$ flags < 33554432	LOW_RICHNESS_3 INCONSISTENT_Z_0_050
1	flags < 2097152	-

Table 5.1 *A list of the quality markers assigned to clusters based on the GMPhoRCC flags incorporating a broader redshift consistency check for ATLAS data.*

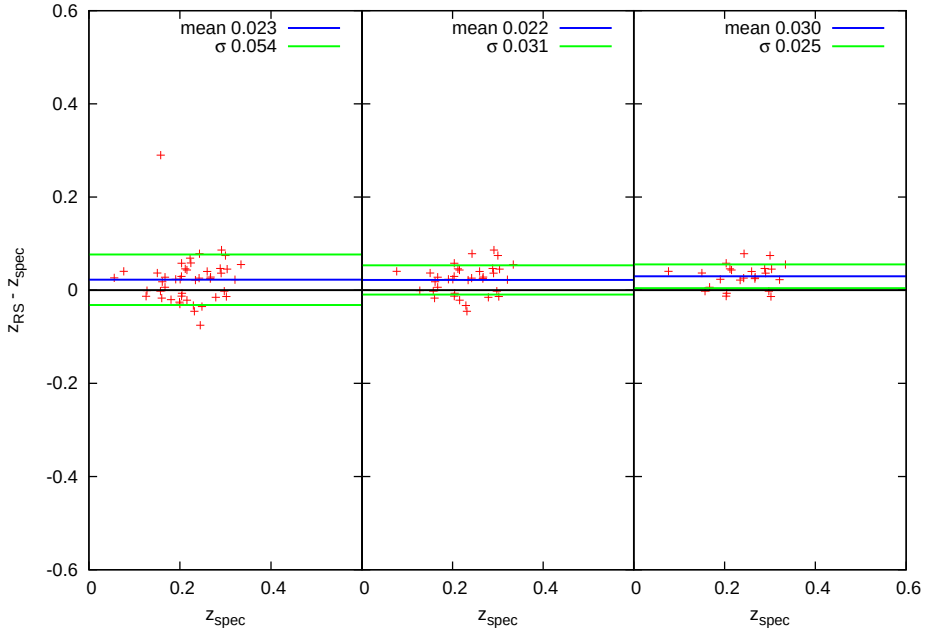

(a) *ATLAS*

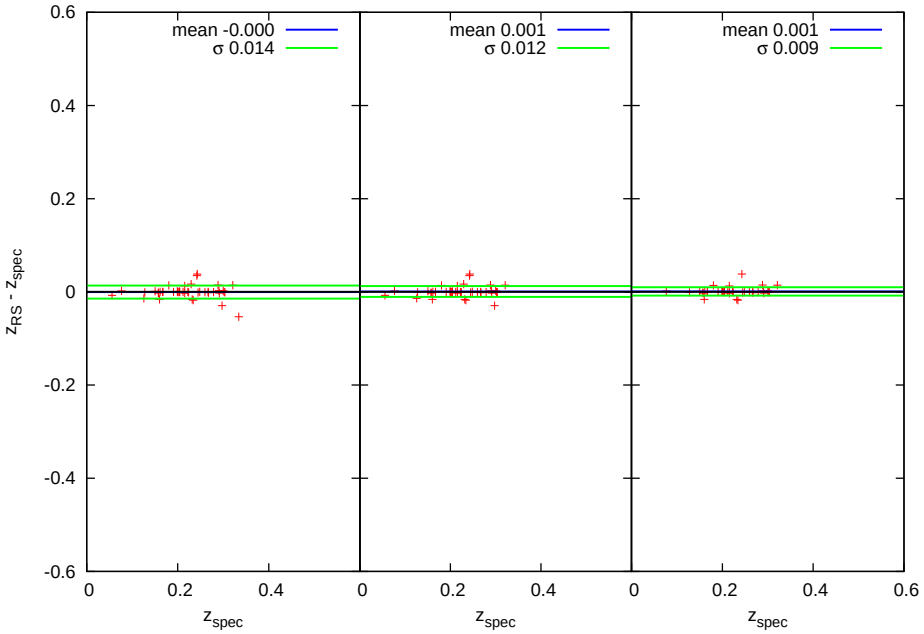

(b) *SDSS DR10*

Figure 5.9 *A comparison of GMPhoRCC photometric red sequence redshifts to spectra using* 42 *clusters with ATLAS and SDSS DR10 coverage from GMBCG, NORAS, REFLEX and XCS, showing from left to right, the detection, mid and clean subsets. Although a slight bias and large scatter remain compared to the SDSS, the clean subset removes the most outliers attaining the smallest scatter of the ATLAS estimates.*

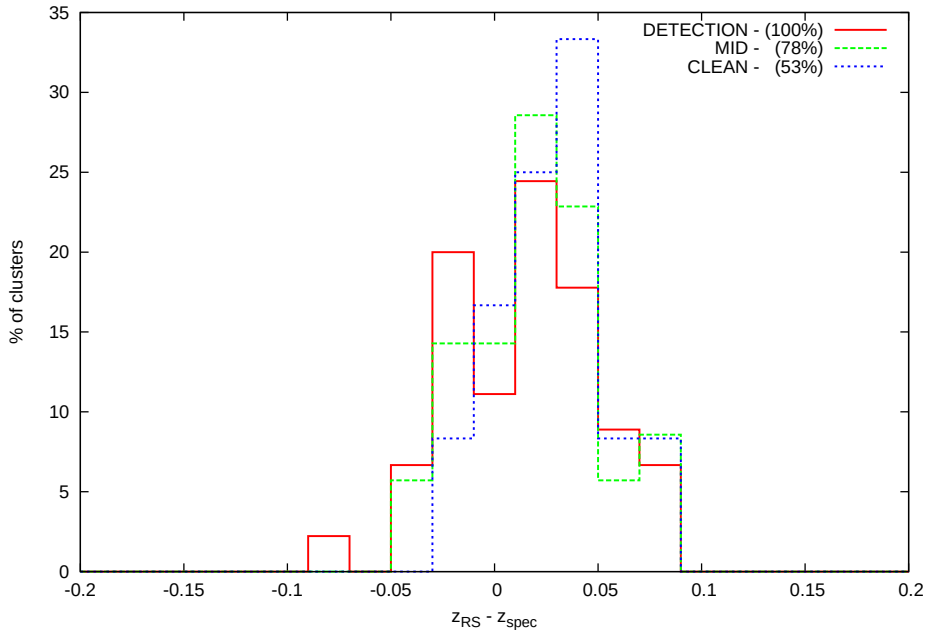

(a) *ATLAS*

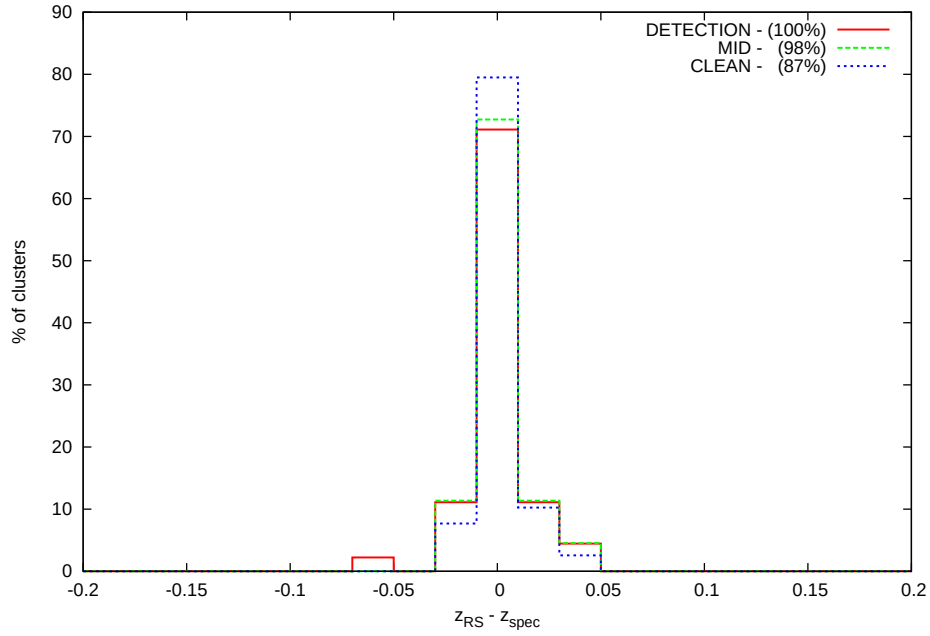

(b) *SDSS DR10*

Figure 5.10 *A normalised histogram comparison of the GMPhoRCC photometric red sequence redshifts to spectra using 42 clusters with ATLAS and SDSS coverage from GMBCG, NORAS, REFLEX and XCS. The comparison has been normalised and split into the separate quality subsets where the legend shows the fraction of the total clusters in each set. The slight bias and larger scatter compared with the SDSS is highlighted, with the clean set attaining the fewest outliers.*

5.2.2 CFHTLenS

Considering CFHTLenS, 60 clusters with optical coverage are characterised by GMPhoRCC with comparison to spectra shown in Figure 5.11. As with ATLAS, the CFHTLenS redshifts results in bias with a larger scatter compared with the SDSS. With significant effort to quantify and model the photometric redshift bias in Hildebrandt et al. (2012) and Velander et al. (2014) it is possible to add a correction to improve the estimates. By stacking the training set separately in magnitude and redshift space, Hildebrandt et al. (2012) has quantified the bias as function of the photometric properties of the target galaxies. Particularly using Figure 4. of Hildebrandt et al. (2012), a correction is applied to the photometric redshifts as a function of i-band magnitude with characterisation results shown in Figure 5.12. Typically these corrections are of the order ~ 0.03 for the dominant red sequence galaxies, those with $i < 19$ and although there is still a slight bias, this significantly improves the cluster estimates giving a lower scatter. In addition to these, correction from Velander et al. (2014) are also considered. Here the bias is modelled as a linear function of redshift in magnitude bins by using spectra from the VIMOS VLT Deep Survey (Garilli et al., 2008), DEEP2 (Newman et al., 2013) and the SDSS (Eisenstein et al., 2001). Here the corrections are of the order ~ 0.01 for the dominant bright galaxies and result in poorer cluster estimates with, larger scatter and more extreme outliers. With the best estimates, the Heymans et al. (2012) corrections are used for the remaining CFHTLenS analysis however it is noted that the small cluster sample rules out the possibility of a definitive set of corrections with further research required.

As with ATLAS, it is necessary to calibrate the redshifts consistency checks to calculate a CFHTLenS-specific quality marker. It is found that the BCG redshift is no more reliable than any other galaxy despite the brightness and with larger errors than those from the SDSS is not a strong indicator of the 'true' cluster redshift. Similarly with ATLAS, it is therefore necessary to use broader redshift consistency checks, the effect of which are shown in Figure 5.13. Although the consistency checks do not improve the slight bias, applying quality cuts based on these will reduce the scatter of the estimates by removing the worst outliers. The SDSS consistency checks $0.025 \leq |z_{RS} - z_{BCG}| < 0.05$ and $|z_{RS} - z_{BCG}| \geq 0.05$ used to indicate quality markers 2 and 3 respectively are replaced by the broader $0.05 \leq |z_{RS} - z_{BCG}| < 0.1$ and $|z_{RS} - z_{BCG}| \geq 0.1$, with a full description of the CFHTLenS-specific quality marker given in Table 5.2. Again with the small cluster sample these new markers are preliminary, with a larger cluster sample

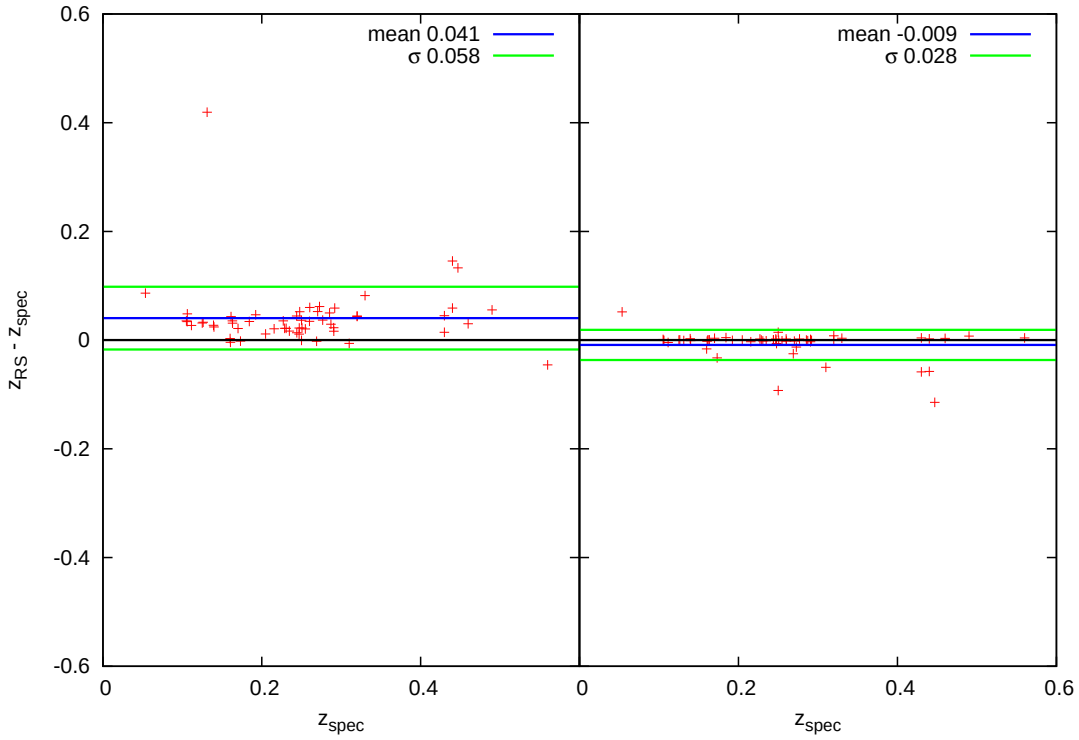

Figure 5.11 *A comparison of GMPhoRCC photometric red sequence redshifts to spectra using* 60 *clusters from GMBCG, NORAS, REFLEX and XCS where the left and right panel shows results using CFHTLenS and SDSS data respectively. In addition to the larger scatter the CFHTLenS redshifts appear to have a slight bias compared with the SDSS.*

these can be further calibrated.

Using Table 3.8 with the new marker, a set of CFHTLenS-specific quality subsets can be defined and are shown in Figures 5.14 and 5.15 for the previous cluster set. Although a slight bias and large scatter remains compared to the SDSS, the clean subset removes the most outliers attaining the smallest scatter of the CFHTLenS estimates.

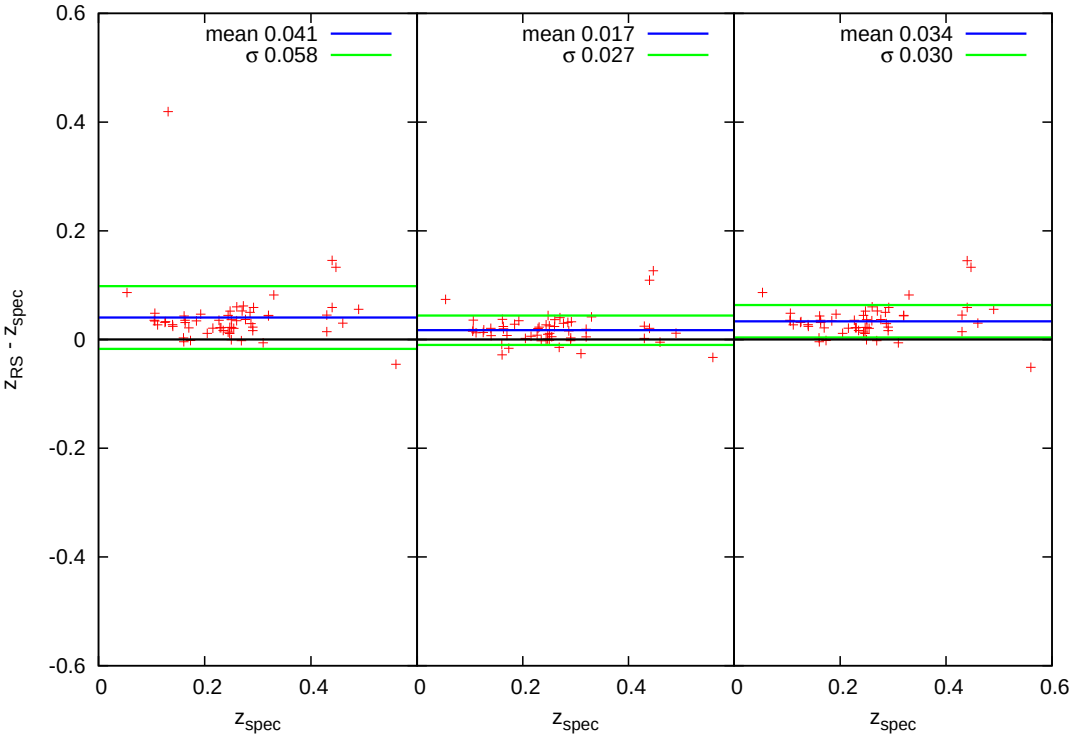

Figure 5.12 *A comparison of GMPhoRCC photometric red sequence redshifts to spectra with various bias corrections using* 60 *clusters with CFHTLenS coverage from GMBCG, NORAS, REFLEX and XCS. From left to right the panels show results using no corrections, Hildebrandt et al. (2012) based corrections and Velander et al. (2014) based corrections, respectively. While a slight bias remains it is clear the Hildebrandt et al. (2012) corrections produce the best estimates with the lowest scatter and given the typical errors these redshifts are consistent with spectra.*

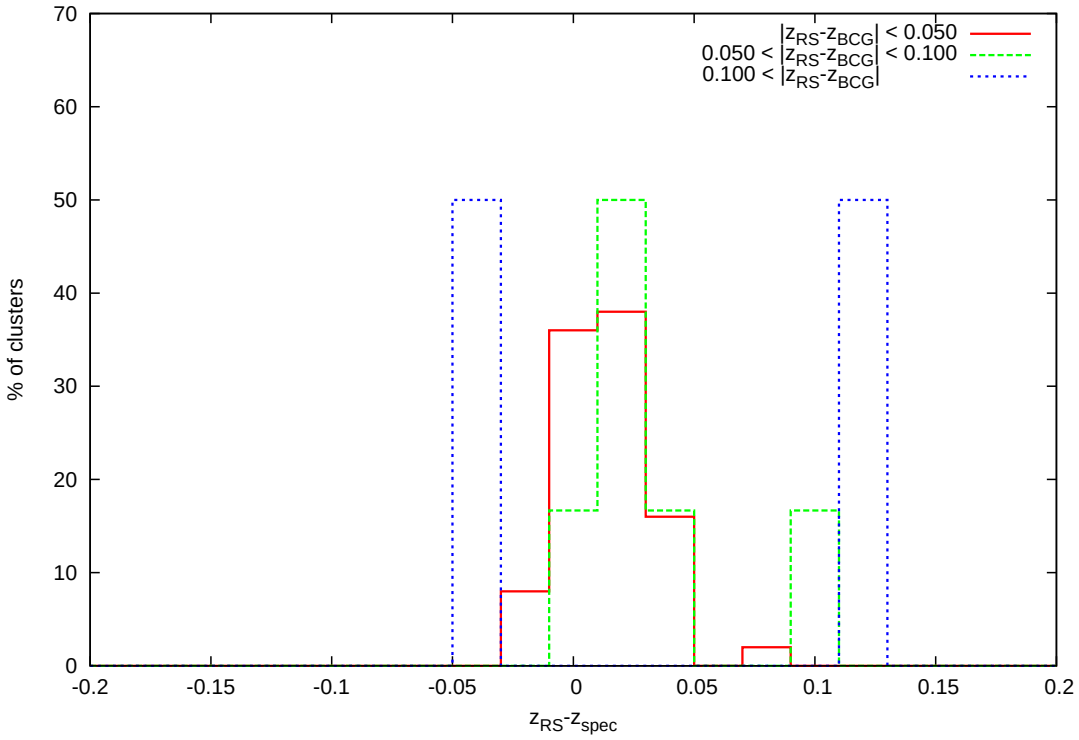

Figure 5.13 *A normalised histogram comparison of the GMPhoRCC red sequence redshifts compared to spectra, highlighting the broader redshift consistency checks, using* 60 *spectroscopic clusters from the GMBCG, NORAS, REFLEX and XCS with CFHTLenS optical data. Although the consistency checks do not improve the slight bias, applying quality cuts based on these reduces the scatter of the estimates by removing the worst outliers.*

Quality	Flags Value (decimal)	Indicator Flags
5	$140737488355328 \leq$ flags	NO_COVERAGE
4	$17592186044416 \leq$ flags < 140737488355328	NO_DETECTION_REDSHIFT NO_DETECTION_RICHNESS_NGALS NO_DETECTION_RICHNESS_N200
3	$33554432 \leq$ flags < 17592186044416	LOW_RICHNESS_1 INCONSISTENT_Z_0_100 SPARCE_INITIAL SPARCE_COLOUR SPARCE_ZFLAT SPARCE_ZRS NO_OVERDENSITY_INITIAL NO_OVERDENSITY_COLOUR NO_OVERDENSITY_ZRS NO_OVERDENSITY_ZRS NO_CLUSTER_INITIAL NO_CLUSTER_COLOUR NO_CLUSTER_ZFLAT NO_CLUSTER_ZRS CLUSTER_INSIDE_MASK_0_5_MPC CLUSTER_INSIDE_MASK_R200 CLUSTER_INSIDE_MASK_5_AM
2	$2097152 \leq$ flags < 33554432	LOW_RICHNESS_3 INCONSISTENT_Z_0_050
1	flags < 2097152	-

Table 5.2 *A list of the quality markers assigned to clusters based on the GMPhoRCC flags incorporating a broader redshift consistency check for CFHTLenS data.*

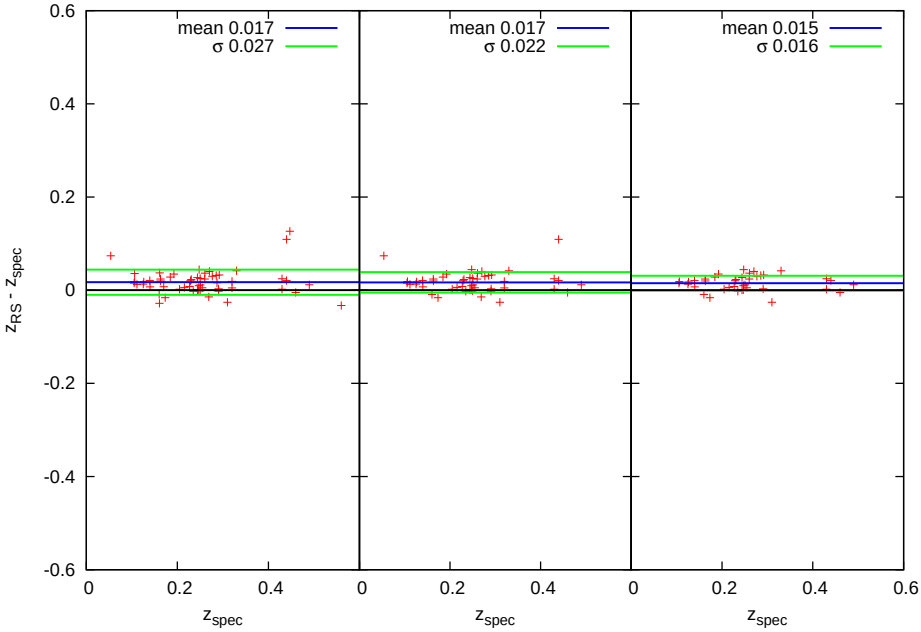

(a) *CFHTLenS*

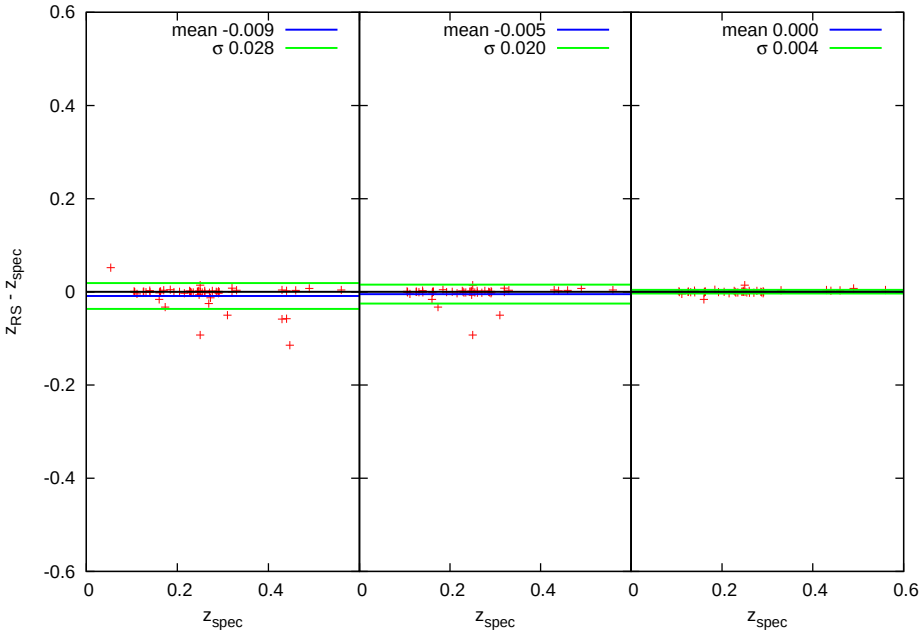

(b) *SDSS DR10*

Figure 5.14 *A comparison of GMPhoRCC photometric red sequence redshifts to spectra using* 60 *clusters with CFHTLenS coverage from GMBCG, NORAS, REFLEX and XCS, showing from left to right, the detection, mid and clean subsets. While the slight bias remains, the quality subsets can be seen to reduce the scatter in the estimates by removing the worst outliers*

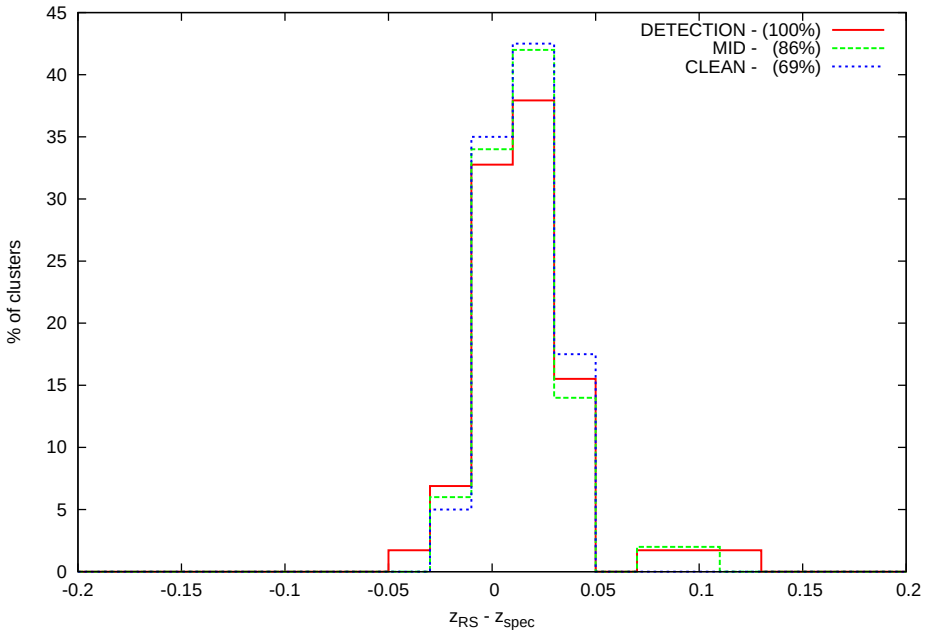

(a) *CFHTLenS*

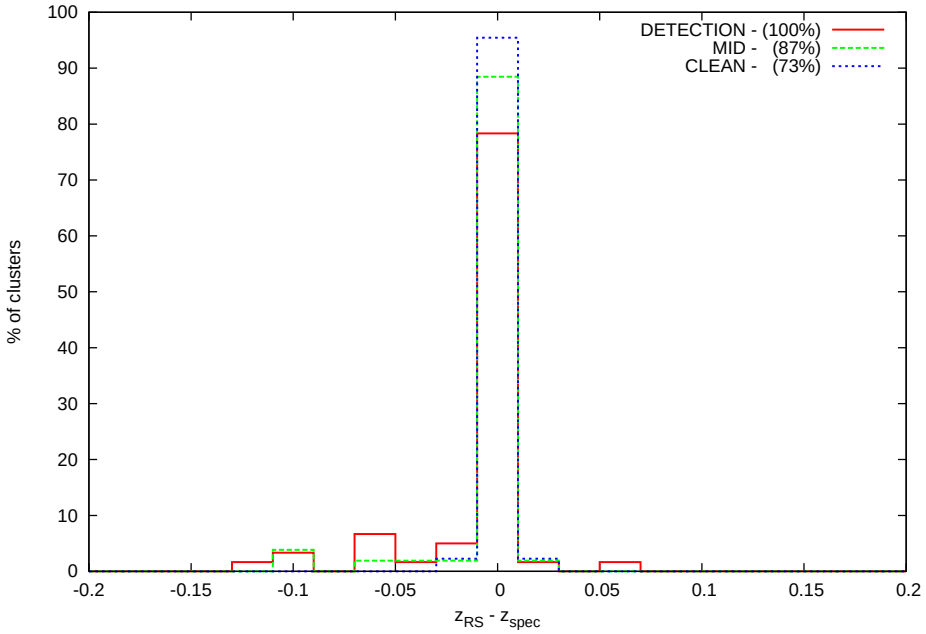

(b) *SDSS DR10*

Figure 5.15 *A normalised histogram comparison of the GMPhoRCC photometric red sequence redshifts to spectra using* 60 *clusters with CFHTLenS coverage from GMBCG, NORAS, REFLEX and XCS. The comparison has been normalised and split into the separate quality subsets where the legend shows the fraction of the total clusters in each set. Although the slight bias remains the clean set has the lowest scatter and fewest extreme outliers.*

5.3 Results

First considering XCS DR1, Mehrtens et al. (2012) presented 503 optically confirmed X-ray clusters of which 258 have spectroscopic redshifts and 108 have SDSS characterisations. GMPhoRCC provides characterisations for 360, 232 of which have spectroscopic redshifts. Overall GMPhoRCC provides 260 (149 of which are clean) new SDSS characterisations and 91 (61 of which are clean) new spectroscopic redshifts. Table 5.3 shows a sample of 20 clusters highlighting the important characterisations with a full list presented in Appendix A.

Of the 13,956 preliminary XCS DR2 candidates described in Section 5.1, 6124 have optical coverage, 5580 in the SDSS, 523 in ATLAS and 819 in CFHTLenS with some overlap. Overall characterisations are found for 4365 candidates, 1893 of which have an associated spectroscopic redshift. The clean subset comprises 1203 candidates, 904 with spectra.

Using the SDSS DR10 optical data, characterisations were found for 3882 candidates with spectroscopic redshifts found for 1893. The clean subset comprises 1203 extended X-ray sources, 904 with spectra. Table 5.4 shows a sample of 20 clusters highlighting the important characterisations with a full list presented in Appendix A. The performance of these characterisations is well understood where the GMPhoRCC selection function and accuracy follows from Chapter 4.

Of the 523 sources with ATLAS coverage, GMPhoRCC was able to produce characterisations for 274 with 64 in the clean subset. Table 5.5 shows a sample of 20 sources highlighting the important characterisations with a full list presented in Appendix A. These characterisations are preliminary and are subject to change with further improvements in the photometric redshifts. In addition full understanding of the accuracy and selection function of ATLAS requires a more extensive analysis similar those presented in Chapter 4 with the SDSS DR9.

Using CFHTLenS optical data, GMPhoRCC was able to produce characterisations for 702 of the 819 extended X-ray sources with coverage attaining 237 in the clean subset. Table 5.6 shows a sample of 20 sources highlighting the important characterisations with a full list presented in Appendix A. While care was taken to correct any redshift bias, the preliminary analysis of Section 5.2.2 suggest a slight bias might remain with $z_{phot} - z_{sec} \sim 0.015$ particularly for $z_{spec} < 0.4$.

name	z_{RS}	z_{BCG}	z_{spec-g}	cmr_{grad}	cmr_{inter}	cmr_{wid}	n_{gals-c}	n_{gals-l}	n_{200-c}	n_{200-l}	qual
XMMXCS J001116.1+005211.3	$0.364^{+0.061}_{-0.061}$	0.379 ± 0.057	$0.365 \pm 1.2e-04$	-0.128 ± 0.056	4.304 ± 1.070	0.001	9 ± 3	9 ± 4	5 ± 3	5 ± 3	1
XMMXCS J001737.4-005235.4	$0.212^{+0.047}_{-0.048}$	0.229 ± 0.038	$0.211 \pm 3.8e-05$	-0.049 ± 0.016	2.233 ± 0.287	0.054	21 ± 5	19 ± 5	28 ± 6	22 ± 5	1
XMMXCS J002314.1+001201.5	$0.260^{+0.052}_{-0.052}$	0.250 ± 0.039	$0.258 \pm 2.8e-05$	-0.032 ± 0.013	2.022 ± 0.239	0.001	12 ± 4	14 ± 4	12 ± 4	15 ± 4	1
XMMXCS J002650.0+171931.3	$0.474^{+0.115}_{-0.113}$	0.474 ± 0.146	-	-0.058 ± 0.036	1.943 ± 0.724	0.090	6 ± 4	-	5 ± 3	-	1
XMMXCS J002953.9+350507.5	$0.491^{+0.131}_{-0.130}$	0.471 ± 0.086	-	-0.031 ± 0.064	1.467 ± 1.253	0.058	21 ± 5	30 ± 6	20 ± 5	32 ± 7	1
XMMXCS J004119.5+252618.9	$0.137^{+0.031}_{-0.031}$	0.144 ± 0.025	-	-0.011 ± 0.015	1.250 ± 0.266	0.057	20 ± 5	23 ± 5	22 ± 5	26 ± 5	1
XMMXCS J004231.6+005119.9	$0.151^{+0.023}_{-0.024}$	0.159 ± 0.026	$0.151 \pm 2.2e-05$	-0.028 ± 0.009	1.597 ± 0.149	0.006	8 ± 3	8 ± 3	7 ± 3	8 ± 3	1
XMMXCS J004252.6+004303.1	$0.271^{+0.040}_{-0.040}$	0.275 ± 0.042	$0.270 \pm 4.0e-05$	-0.048 ± 0.050	2.321 ± 0.963	0.114	12 ± 4	38 ± 7	12 ± 4	11 ± 5	1
XMMXCS J004333.7+010109.6	$0.195^{+0.030}_{-0.029}$	0.203 ± 0.030	$0.196 \pm 2.1e-05$	-0.073 ± 0.021	2.557 ± 0.372	0.061	8 ± 3	10 ± 4	7 ± 3	8 ± 3	1
XMMXCS J004359.3+000706.8	$0.218^{+0.044}_{-0.045}$	0.226 ± 0.036	$0.218 \pm 2.0e-05$	-0.087 ± 0.030	2.944 ± 0.569	0.031	15 ± 4	17 ± 4	16 ± 4	20 ± 5	1
XMMXCS J005545.8+003840.8	$0.068^{+0.001}_{-0.001}$	0.089 ± 0.023	$0.067 \pm 6.4e-06$	-0.066 ± 0.020	1.913 ± 0.325	0.068	11 ± 3	14 ± 4	11 ± 3	13 ± 4	1
XMMXCS J010608.4+005031.4	$0.258^{+0.050}_{-0.050}$	0.277 ± 0.044	$0.259 \pm 2.8e-05$	-0.049 ± 0.018	2.351 ± 0.340	0.041	22 ± 5	27 ± 6	23 ± 5	37 ± 7	1
XMMXCS J010720.2+141604.2	$0.074^{+0.007}_{-0.008}$	0.073 ± 0.015	$0.074 \pm 1.2e-05$	0.007 ± 0.012	0.782 ± 0.188	0.027	9 ± 3	7 ± 3	7 ± 3	6 ± 3	1
XMMXCS J010858.7+132557.7	$0.146^{+0.025}_{-0.025}$	0.154 ± 0.023	$0.146 \pm 2.1e-05$	-0.037 ± 0.020	1.649 ± 0.342	0.105	6 ± 3	8 ± 3	6 ± 3	9 ± 3	1
XMMXCS J011624.2+325717.0	$0.471^{+0.104}_{-0.102}$	0.475 ± 0.076	-	-0.089 ± 0.061	2.610 ± 1.216	0.094	12 ± 4	19 ± 5	12 ± 4	-	1
XMMXCS J011922.6-011011.7	$0.186^{+0.029}_{-0.029}$	0.190 ± 0.029	$0.186 \pm 2.2e-05$	-0.016 ± 0.020	1.451 ± 0.368	0.071	5 ± 2	9 ± 3	3 ± 2	6 ± 3	1
XMMXCS J014430.3+021237.0	$0.166^{+0.041}_{-0.041}$	0.187 ± 0.031	$0.165 \pm 1.4e-05$	-0.063 ± 0.013	2.271 ± 0.221	0.023	10 ± 3	10 ± 3	10 ± 3	11 ± 3	1
XMMXCS J015315.0+010214.2	$0.059^{+0.001}_{-0.001}$	0.064 ± 0.016	$0.059 \pm 6.7e-06$	-0.011 ± 0.004	1.022 ± 0.054	0.006	6 ± 3	2 ± 2	4 ± 2	3 ± 2	1
XMMXCS J015558.0+053200.8	$0.454^{+0.109}_{-0.108}$	0.499 ± 0.086	$0.450 \pm 1.0e-04$	-0.041 ± 0.024	1.560 ± 0.480	0.001	4 ± 3	13 ± 4	5 ± 3	12 ± 4	1
XMMXCS J020341.6-074705.7	$0.443^{+0.075}_{-0.073}$	0.430 ± 0.066	$0.440 \pm 8.9e-05$	0.107 ± 0.052	-0.071 ± 1.033	0.201	12 ± 4	11 ± 4	13 ± 4	12 ± 4	1

Table 5.3 *A sample table of GMPhoRCC characterisations for XCS DR1 using SDSS DR10 optical data where* 260 *(*149 *of which are clean) new SDSS characterisations and* 91 *(*61 *of which are clean) new spectroscopic redshifts are found.*

name	z_{RS}	z_{BCG}	z_{spec-g}	cmr_{grad}	cmr_{inter}	cmr_{wid}	n_{gals-c}	n_{gals-l}	n_{200-c}	n_{200-l}	qual
XMMXCS J000349.3+020403.5	$0.116^{+0.030}_{-0.030}$	0.132 ± 0.039	$0.098 \pm 1.4e-05$	-0.023 ± 0.013	1.360 ± 0.217	0.043	15 ± 4	15 ± 4	17 ± 4	23 ± 5	1
XMMXCS J000521.4+201503.1	$0.390^{+0.085}_{-0.085}$	0.408 ± 0.062	-	-0.029 ± 0.098	2.207 ± 1.879	0.021	10 ± 4	10 ± 4	10 ± 4	10 ± 4	1
XMMXCS J001116.1+005211.3	$0.364^{+0.061}_{-0.061}$	0.379 ± 0.057	$0.365 \pm 1.2e-04$	-0.128 ± 0.056	4.304 ± 1.070	0.001	9 ± 3	9 ± 4	5 ± 3	5 ± 3	1
XMMXCS J001737.4-005235.4	$0.212^{+0.047}_{-0.048}$	0.229 ± 0.038	$0.211 \pm 3.8e-05$	-0.049 ± 0.016	2.233 ± 0.287	0.054	21 ± 5	19 ± 5	28 ± 6	22 ± 5	1
XMMXCS J001738.0-004856.5	$0.210^{+0.040}_{-0.041}$	0.223 ± 0.037	$0.200 \pm 3.7e-05$	-0.005 ± 0.021	1.362 ± 0.386	0.089	15 ± 4	15 ± 4	20 ± 5	18 ± 5	1
XMMXCS J001817.2+161744.2	$0.555^{+0.128}_{-0.129}$	0.562 ± 0.092	-	0.082 ± 0.045	-0.489 ± 0.858	0.091	7 ± 3	12 ± 4	6 ± 3	12 ± 4	1
XMMXCS J001847.99+160215.5	$0.541^{+0.100}_{-0.099}$	0.571 ± 0.096	$0.541 \pm 1.9e-04$	-0.039 ± 0.021	1.796 ± 0.391	0.001	14 ± 4	28 ± 6	14 ± 4	49 ± 8	1
XMMXCS J001848.2+160201.7	$0.542^{+0.112}_{-0.111}$	0.571 ± 0.096	$0.541 \pm 1.9e-04$	-0.053 ± 0.018	2.076 ± 0.362	0.001	16 ± 4	32 ± 6	16 ± 5	42 ± 8	1
XMMXCS J001919.91+162445.9	$0.333^{+0.085}_{-0.085}$	0.345 ± 0.051	-	0.052 ± 0.112	0.687 ± 2.156	0.042	11 ± 4	10 ± 4	11 ± 4	11 ± 4	1
XMMXCS J001919.9+162445.9	$0.333^{+0.085}_{-0.085}$	0.345 ± 0.051	-	0.052 ± 0.112	0.687 ± 2.156	0.042	11 ± 4	10 ± 4	11 ± 4	11 ± 4	1
XMMXCS J002113.4-082751.3	$0.093^{+0.062}_{-0.064}$	0.102 ± 0.032	-	0.046 ± 0.001	-0.216 ± 0.013	0.500	3 ± 2	3 ± 2	3 ± 2	3 ± 2	1
XMMXCS J002213.8-150543.3	$0.463^{+0.171}_{-0.171}$	0.485 ± 0.171	-	0.044 ± 0.104	0.006 ± 2.080	0.097	16 ± 5	19 ± 5	19 ± 5	28 ± 6	1
XMMXCS J002314.1+001201.5	$0.260^{+0.052}_{-0.052}$	0.250 ± 0.039	$0.258 \pm 2.8e-05$	-0.032 ± 0.013	2.022 ± 0.239	0.001	12 ± 4	14 ± 4	12 ± 4	15 ± 4	1
XMMXCS J002650.0+171931.3	$0.474^{+0.115}_{-0.113}$	0.474 ± 0.146	-	-0.058 ± 0.036	1.943 ± 0.724	0.090	6 ± 4	-	5 ± 3	-	1
XMMXCS J002742.9+171016.6	$0.141^{+0.029}_{-0.029}$	0.165 ± 0.030	-	-0.035 ± 0.025	1.683 ± 0.436	0.047	6 ± 3	4 ± 2	5 ± 2	4 ± 2	1
XMMXCS J002944.7+045222.1	$0.206^{+0.052}_{-0.053}$	0.210 ± 0.034	$0.206 \pm 3.2e-05$	-0.046 ± 0.029	2.136 ± 0.543	0.061	4 ± 2	5 ± 3	4 ± 2	5 ± 3	1
XMMXCS J002953.9+350507.5	$0.491^{+0.131}_{-0.130}$	0.471 ± 0.086	-	-0.031 ± 0.064	1.467 ± 1.253	0.058	21 ± 5	30 ± 6	21 ± 6	32 ± 7	1
XMMXCS J003054.0+262306.1	$0.508^{+0.152}_{-0.152}$	0.509 ± 0.078	-	-0.062 ± 0.050	2.066 ± 0.995	0.001	5 ± 3	13 ± 4	5 ± 3	12 ± 4	1
XMMXCS J003614.6+091408.9	$0.436^{+0.072}_{-0.072}$	0.439 ± 0.094	$0.436 \pm 1.1e-04$	0.087 ± 0.140	0.248 ± 2.703	0.067	21 ± 5	23 ± 5	30 ± 6	48 ± 8	1
XMMXCS J003647.5+090242.2	$0.389^{+0.093}_{-0.090}$	0.363 ± 0.057	$0.389 \pm 6.0e-05$	0.023 ± 0.042	0.239 ± 0.816	0.001	7 ± 3	6 ± 4	6 ± 3	4 ± 3	1

Table 5.4 *A sample table of GMPhoRCC characterisations for the preliminary XCS DR2 sources using SDSS DR10 optical data. Of the* 7227 *with coverage, characterisations were found for* 3882 *with spectroscopic redshifts found for* 1893*. The clean subset comprises* 1203 *extended X-ray sources,* 904 *with spectra.*

name	z_{RS}	z_{BCG}	cmr_{grad}	cmr_{inter}	cmr_{wid}	n_{gals-c}	n_{gals-l}	n_{200-c}	n_{200-l}	qual
XMMXCS J001328.5-272319.0	$0.436^{+0.058}_{-0.056}$	0.392 ± 0.047	0.090 ± 0.147	0.115 ± 2.902	0.026	8 ± 3	8 ± 3	6 ± 3	7 ± 3	1
XMMXCS J001415.6-302251.3	$0.267^{+0.134}_{-0.133}$	0.243 ± 0.078	-0.063 ± 0.058	2.548 ± 1.149	0.001	18 ± 4	18 ± 5	34 ± 6	9 ± 4	1
XMMXCS J001436.6-390012.8	$0.374^{+0.075}_{-0.075}$	0.361 ± 0.065	0.113 ± 0.055	-0.211 ± 1.032	0.001	5 ± 2	25 ± 5	4 ± 2	24 ± 5	1
XMMXCS J001956.5-253517.1	$0.113^{+0.054}_{-0.054}$	0.107 ± 0.029	0.020 ± 0.067	0.358 ± 1.146	0.108	3 ± 2	2 ± 2	3 ± 2	0 ± 1	1
XMMXCS J002041.4-254252.3	$0.147^{+0.088}_{-0.088}$	0.153 ± 0.042	-0.062 ± 0.019	2.093 ± 0.349	0.038	16 ± 4	19 ± 5	22 ± 5	24 ± 5	1
XMMXCS J002531.7-330246.4	$0.103^{+0.037}_{-0.038}$	0.095 ± 0.035	0.038 ± 0.019	0.276 ± 0.300	0.060	6 ± 3	6 ± 3	4 ± 2	5 ± 2	1
XMMXCS J003652.4-333905.3	$0.263^{+0.102}_{-0.101}$	0.308 ± 0.081	-0.042 ± 0.031	2.098 ± 0.595	0.036	7 ± 3	8 ± 3	5 ± 2	7 ± 3	1
XMMXCS J004134.0-092212.4	$0.087^{+0.051}_{-0.050}$	0.067 ± 0.033	-0.028 ± 0.018	1.208 ± 0.302	0.079	8 ± 3	12 ± 4	8 ± 3	14 ± 4	1
XMMXCS J004137.0-091932.1	$0.095^{+0.055}_{-0.055}$	0.068 ± 0.015	-0.024 ± 0.018	1.161 ± 0.320	0.061	16 ± 4	20 ± 5	16 ± 4	21 ± 5	1
XMMXCS J004144.6-092113.6	$0.087^{+0.045}_{-0.045}$	0.067 ± 0.033	-0.040 ± 0.015	1.436 ± 0.255	0.068	9 ± 3	13 ± 4	7 ± 3	15 ± 4	1
XMMXCS J004200.6-091933.1	$0.086^{+0.040}_{-0.040}$	0.068 ± 0.015	-0.019 ± 0.019	1.124 ± 0.333	0.036	9 ± 3	12 ± 4	7 ± 3	13 ± 4	1
XMMXCS J004207.1-093022.6	$0.405^{+0.064}_{-0.064}$	0.421 ± 0.042	-0.283 ± 0.076	7.371 ± 1.494	0.001	7 ± 3	33 ± 6	7 ± 3	28 ± 6	1
XMMXCS J004253.5-093413.5	$0.409^{+0.076}_{-0.074}$	0.445 ± 0.064	-0.335 ± 0.058	8.647 ± 1.150	0.500	8 ± 3	10 ± 4	7 ± 3	11 ± 4	1
XMMXCS J004307.6-095136.2	$0.091^{+0.059}_{-0.059}$	0.075 ± 0.030	-0.021 ± 0.025	1.079 ± 0.420	0.043	5 ± 2	5 ± 2	4 ± 2	4 ± 2	1
XMMXCS J004307.6-095136.5	$0.091^{+0.059}_{-0.059}$	0.075 ± 0.030	-0.021 ± 0.025	1.079 ± 0.420	0.043	5 ± 2	5 ± 2	4 ± 2	4 ± 2	1
XMMXCS J004730.2-251340.4	$0.391^{+0.089}_{-0.087}$	0.352 ± 0.063	-0.247 ± 0.068	6.436 ± 1.331	0.001	3 ± 2	6 ± 3	4 ± 2	5 ± 3	1
XMMXCS J012304.3-345456.5	$0.436^{+0.065}_{-0.065}$	0.408 ± 0.054	-0.032 ± 0.071	2.974 ± 1.311	0.070	8 ± 3	24 ± 5	8 ± 3	23 ± 5	1
XMMXCS J013136.6-134500.5	$0.186^{+0.076}_{-0.076}$	0.184 ± 0.021	-0.010 ± 0.012	1.348 ± 0.217	0.001	6 ± 3	4 ± 2	6 ± 2	1 ± 1	1
XMMXCS J013152.9-133647.2	$0.182^{+0.061}_{-0.061}$	0.208 ± 0.024	-0.034 ± 0.023	1.822 ± 0.428	0.086	35 ± 6	37 ± 6	55 ± 8	57 ± 8	1
XMMXCS J013205.1-134000.0	$0.203^{+0.069}_{-0.070}$	0.211 ± 0.035	-0.031 ± 0.043	1.869 ± 0.796	0.060	12 ± 4	10 ± 3	13 ± 4	8 ± 3	1

Table 5.5 *A sample table of GMPhoRCC characterisations for the preliminary XCS DR2 sources using ATLAS optical data. Of the* 970 *with coverage, characterisations were found for* 272 *with* 64 *in the clean subset.*

name	z_{RS}	z_{BCG}	cmr_{grad}	cmr_{inter}	cmr_{wid}	n_{gals-c}	n_{gals-l}	n_{200-c}	n_{200-l}	qual
XMMXCS J020046.49-064223.1	$0.363^{+0.089}_{-0.090}$	0.327 ± 0.089	-0.036 ± 0.012	2.044 ± 0.224	0.038	8 ± 3	8 ± 3	8 ± 3	7 ± 3	1
XMMXCS J020049.61-064026.8	$0.360^{+0.088}_{-0.089}$	0.327 ± 0.089	-0.024 ± 0.018	1.783 ± 0.357	0.074	9 ± 3	36 ± 6	6 ± 3	9 ± 4	1
XMMXCS J020213.89-070113.1	$0.114^{+0.063}_{-0.064}$	0.093 ± 0.060	0.004 ± 0.027	0.518 ± 0.472	0.088	7 ± 3	1 ± 1	3 ± 2	0 ± 1	1
XMMXCS J020230.52-063119.7	$0.339^{+0.088}_{-0.088}$	0.327 ± 0.089	-0.022 ± 0.024	1.638 ± 0.463	0.091	15 ± 4	13 ± 4	15 ± 4	12 ± 4	1
XMMXCS J020254.37-073858.3	$0.151^{+0.077}_{-0.077}$	0.141 ± 0.077	-0.079 ± 0.018	2.052 ± 0.322	0.061	9 ± 3	10 ± 3	7 ± 3	8 ± 3	1
XMMXCS J020255.3-073906.6	$0.136^{+0.076}_{-0.076}$	0.141 ± 0.077	-0.045 ± 0.017	1.511 ± 0.279	0.025	5 ± 2	5 ± 2	4 ± 2	5 ± 2	1
XMMXCS J020328.76-045740.6	$0.477^{+0.094}_{-0.096}$	0.445 ± 0.095	-0.017 ± 0.016	0.792 ± 0.337	0.079	8 ± 4	7 ± 4	6 ± 3	3 ± 3	1
XMMXCS J020341.31-074708.4	$0.470^{+0.097}_{-0.097}$	0.448 ± 0.097	-0.018 ± 0.011	1.141 ± 0.232	0.068	20 ± 5	21 ± 5	24 ± 6	27 ± 6	1
XMMXCS J020341.6-074705.7	$0.462^{+0.096}_{-0.096}$	0.448 ± 0.097	-0.011 ± 0.012	0.985 ± 0.255	0.075	23 ± 5	26 ± 6	27 ± 6	32 ± 7	1
XMMXCS J020353.36-050145.3	$0.534^{+0.095}_{-0.098}$	0.507 ± 0.100	-0.026 ± 0.014	1.444 ± 0.309	0.087	23 ± 5	20 ± 5	24 ± 6	23 ± 5	1
XMMXCS J020359.34-042030.9	$0.678^{+0.106}_{-0.108}$	0.632 ± 0.107	-0.003 ± 0.019	1.300 ± 0.428	0.116	8 ± 4	8 ± 4	4 ± 3	5 ± 3	1
XMMXCS J020435.89-061921.4	$0.953^{+0.127}_{-0.127}$	1.000 ± 0.132	-0.032 ± 0.030	1.273 ± 0.706	0.114	6 ± 5	9 ± 6	10 ± 4	11 ± 5	1
XMMXCS J020449.1-072538.2	$0.337^{+0.088}_{-0.088}$	0.288 ± 0.086	-0.076 ± 0.020	2.672 ± 0.368	0.101	11 ± 4	9 ± 4	11 ± 4	7 ± 3	1
XMMXCS J020509.70-061445.9	$0.271^{+0.095}_{-0.097}$	0.276 ± 0.110	-0.062 ± 0.027	1.862 ± 0.497	0.031	7 ± 3	5 ± 3	6 ± 3	5 ± 2	1
XMMXCS J020517.70-043900.7	$0.944^{+0.128}_{-0.128}$	0.896 ± 0.123	0.009 ± 0.021	0.625 ± 0.482	0.074	34 ± 6	33 ± 6	46 ± 8	46 ± 8	1
XMMXCS J020559.64-063736.5	$0.653^{+0.107}_{-0.108}$	0.623 ± 0.130	-0.012 ± 0.014	0.541 ± 0.288	0.072	13 ± 5	9 ± 5	14 ± 5	8 ± 5	1
XMMXCS J020613.35-041616.7	$0.504^{+0.098}_{-0.098}$	0.511 ± 0.099	-0.061 ± 0.049	1.969 ± 1.041	0.067	4 ± 3	5 ± 3	4 ± 2	5 ± 3	1
XMMXCS J020636.17-061133.8	$0.920^{+0.138}_{-0.137}$	0.948 ± 0.135	-0.002 ± 0.030	0.526 ± 0.679	0.110	16 ± 6	15 ± 6	13 ± 7	15 ± 7	1
XMMXCS J020644.78-065810.1	$0.432^{+0.093}_{-0.094}$	0.399 ± 0.093	-0.009 ± 0.013	1.613 ± 0.267	0.081	26 ± 5	26 ± 5	27 ± 6	30 ± 6	1
XMMXCS J020647.58-065651.0	$0.442^{+0.095}_{-0.095}$	0.399 ± 0.093	0.001 ± 0.005	0.676 ± 0.110	0.041	30 ± 6	30 ± 6	30 ± 6	31 ± 6	1

Table 5.6 *A sample table of GMPhoRCC characterisations for the preliminary XCS DR2 sources using CFHTLenS optical data. Of the* 1104 *with coverage, characterisations were found for* 702 *with* 237 *in the clean subset.*

5.4 Summary

Presented in this Chapter is the characterisation of new cluster candidates using GMPhoRCC with preliminary work to extend beyond the SDSS focus thus far. The XMM cluster survey (XCS) (Romer et al., 2001, Lloyd-Davies et al., 2011 and Mehrtens et al., 2012) has provided analysis of observations from the XMM-Newton telescope to give an extensive list of extended X-ray sources as potential cluster candidates. With many of these candidates outside the SDSS DR10 footprint, the need for additional sources of optical data is clear. Optical data provided by the ATLAS catalogue (Shanks & Metcalfe, 2012 and Shanks et al in prep.), was used to provide extra coverage in the southern hemisphere with deeper photometry available from CFHTLenS, (Heymans et al., 2012 and Erben et al., 2013). As the focus of weak lensing studies, CFHTLenS provides the unique opportunity of future research of cluster characterisations as a function of lensing observables.

Without the extensive analysis using mocks, preliminary investigations into accuracy and redshift consistency attained using ATLAS and CFHTLenS were necessary. Without a suitable cluster richness, redshift comparisons with spectra for a small cluster sample were used to drive this analysis. CFHTLenS redshift were found to produce a slight bias with larger scatter than the SDSS. With extensive research to model this bias in the literature, corrections were available. While a slight bias remained, corrections based on Hildebrandt et al. (2012) produced the lowest scatter ($\sigma \sim 0.03$) and bias ($\overline{z_{RS} - z_{spec}} \sim 0.02$) in the estimates and with consideration of the errors, were consistent with spectra. It is noted that with the small cluster sample, a definitive set of corrections could not be selected, study with addition clusters is needed. With regards to ATLAS, the photometric redshifts again produced a larger spread ($\sigma \sim 0.05$) and slight bias ($\overline{z_{RS} - z_{spec}} \sim 0.02$) resulting from the preliminary photometric calibrations. While no correction were applied it is noted that the improvement of these redshifts is the subject of ongoing research.

Considering the redshift consistency, which is designed to use discrepancies between the well understood BCG and overall photometric distribution to identify potential failures, both ATLAS and CFHTLenS required the use of broader checks. It is found in general that the BCG redshift is no more reliable than any other galaxy despite the brightness and with typically larger errors than those in the SDSS the broader cuts were justified. The use of $0.05 \leq |z_{RS} - z_{BCG}| < 0.1$ and

$|z_{RS} - z_{BCG}| \geq 0.1$, as indicators for quality markers 2 and 3 respectively, strikes a good balance in identifying the worst outliers whilst keeping those with good estimates. Again with the small cluster sample these checks are only preliminary, addition investigation is required to give a definitive survey-specific quality marker for ATLAS and CFHTLenS.

With the new quality markers the XCS sources where characterised and presented in Sections 5.3 and Appendix A. Of the 13,956 candidates, 6124 have optical coverage, 5580 in the SDSS, 523 in ATLAS and 819 in CFHTLenS with some overlap. Overall characterisations are found for 4365 candidates, 1893 of which have an associated spectroscopic redshift. The clean subset comprises 1203 candidates, 904 with spectra. Considering XCS DR1, Mehrtens et al. (2012) presented 503 optically confirmed X-ray clusters of which 258 have spectroscopic redshifts and 108 have SDSS characterisations. GMPhoRCC provides characterisations for 360, 232 of which have spectroscopic redshifts. Overall GMPhoRCC provides 260 (149 of which are clean) new SDSS characterisations and 91 (61 of which are clean) new spectroscopic redshifts.

The performance of the characterisations found using SDSS DR10 are well understood with accuracy and selection function explored in Chapter 4. The analysis presented in this chapter gives a preliminary estimation of the performance attained from using ATLAS and CFHTLenS. Further investigations similar to those in Chapter 4 for the SDSS are necessary for a full evaluation.

Chapter 6

Discussion

Presented in this thesis is the **G**aussian **M**ixture full **Ph**otometric **R**ed sequence **C**luster **C**haracteriser (GMPhoRCC), which is designed to take cluster candidates, previously detected, and provide an optical confirmation and characterisation based on the red sequence. GMPhoRCC has been designed specifically to attain estimates of redshift, richness and the red sequence CMR and offers many advantages over existing algorithms including, treatment of multi-modal distributions, treatment of a variable width full CMR red sequence, model independence, richness extrapolation and quality control. One of the most important features developed is the flag and quality control procedure. By flagging issues, particularly low richness and inconsistent red sequence and BCG redshifts, potential catastrophic failures can be identified and removed from cleaner subsets.

Comparisons with other characterisation methods highlights the advantages of GMPhoRCC. Using a sample of 5500 clusters taken from the GMBCG (Hao et al., 2010), NORAS (Böhringer et al., 2000), REFLEX (Böhringer et al., 2004) and XCS (Mehrtens et al., 2012) catalogues, GMPhoRCC redshift estimates are compared to spectra showing low scatter ($\sigma \sim 0.042$) around the actual value. In addition applying the quality control to produce a clean subset removes most outliers giving a much tighter agreement, $\sigma \sim 0.018$ showing significant improvement over maxBCG, $\sigma \sim 0.025$, and XCS, $\sigma \sim 0.050$. The high accuracy of GMPhoRCC is also demonstrated with a significant percentage ($\sim 75\%$) of all redshift estimates from the clean subset agreeing within $|z_{RS} - z_{spec}| < 0.01$.

While richness comparison with existing methods are not trivial the remaining

evaluation of GMPhoRCC proceeded with the use of empirical mock galaxy clusters. These mocks were produced by stacking red sequence galaxies from existing clusters, analysed using data from the Sloan Digital Sky Survey (SDSS), in redshift-richness bins from which new sequences are resampled. This extends the similar approach of maxBCG and GMBCG where only rich clusters are used as seeds to generate mocks with a range of properties. Comparisons with mocks agreed well with real clusters attaining very low redshift scatters ($\sigma \sim 0.01$) with the clean subset removing the majority of outliers. In addition, with a definitive mock value, richness comparisons are possible and although show a larger fractional scatter ($\sigma \sim 0.12$) are centred on the mock value. Richness estimates are shown to be more sensitive to discrepancies in redshift, background fluctuations and poor modelling of the red sequence than redshift.

Assessment of the optical selection function proceeded with the consideration of completeness, the fraction of mocks with characterisations within given bounds of the actual value. First incomplete photometry, simulated by an i-band < 21 cut, is shown to remove members for clusters with $z > 0.45$. Redshift completeness, the fraction of clusters within 0.03 of the mock value, is not immediately hindered by the photometry attaining 93% for $0.05 < z < 0.62$ for clusters with a richness greater than 20, showing improvement over maxBCG (with 90% for $0.1 < z < 0.3$) and a larger range than GMBCG (with 96% for $0.1 < z < 0.46$). With the large scatters in the estimates, richness attains lower completeness rates, however it is noted that other algorithms, particularly GMBCG, suffer from poor richness recovery. While this recovery is not quantified, Hao et al. (2010) remarks that GMBCG fails to match even intermediate richnesses due to projection effects and background fluctuations. The fraction of clusters within 25% of the mock value, defining completeness, is measured as 91% for $0.07 < z < 0.45$ for clusters with richness greater than 20, 78% for those with richness between 10 and 20, and 64% for those with richnesses less than 10.

Additionally evaluation with mocks has confirmed the value of the quality control system showing very high probabilities that given a cluster is in the clean set that the redshift and richness estimates are within a given bound of the mock value. Most importantly it was shown that those with larger, less clean quality markers, indicating less confidence in the characterisation, show much lower probabilities confirming that the quality control is effective in identifying potential catastrophic failures.

With significant understanding of the accuracy and selection function of GM-

PhoRCC, this thesis concluded with the application to characterise new extended X-ray sources from XCS as potential galaxy clusters. This work laid the foundation for using new optical data particularly from the VLT Survey Telescope (VST) ATLAS catalogue (Shanks & Metcalfe, 2012 and Shanks et al in prep.), providing coverage in the southern hemisphere and from the Canada-France-Hawaii Telescope Lensing Survey (CFHTLenS), (Heymans et al., 2012 and Erben et al., 2013) providing much deeper photometry than the SDSS. While it is found in both cases that the galaxy photometric redshifts result in typically larger scatters in the estimates, recalibration of the redshift consistency checks helped to remove only the worst outliers. In addition, while slight biases where found using both datasets, extensive investigation in the literature allows for potential corrections to CFHTLenS, which indeed reduced the observed redshift bias.

Combining the optical data sources resulted in coverage of 6124 of the 13,956 new extended X-ray sources, 5580 in the SDSS, 523 in ATLAS and 819 in CFHTLenS with some overlap. Overall characterisations were found for 4365 candidates, 1893 of which have an associated spectroscopic redshift. The clean subset comprises 1203 candidates, 904 with spectra. Considering XCS DR1, Mehrtens et al. (2012) presented 503 optically confirmed X-ray clusters of which 258 have spectroscopic redshifts and 108 have SDSS characterisations. GMPhoRCC provides characterisations for 360, 232 of which have spectroscopic redshifts. Overall GMPhoRCC provides 260 (149 of which are clean) new SDSS characterisations and 91 (61 of which are clean) new spectroscopic redshifts.

6.1 Future Research

With GMPhoRCC proven as a valuable tool for the optical characterisation of galaxy clusters there is potential for much future research. Particularly on the horizon is the application of GMPhoRCC to determine characterisations for the latest XCS data release. This release is expected to ~ 5 times larger than the current catalogue and with the additional coverage of ATLAS and CFHTLenS, GMPhoRCC is expected to provide characterisations for a significant fraction of these sources.

With access to the substantial catalogue of X-ray detected clusters the possibility to investigate the optical properties as a function of X-ray observables is possible. Of particular interest is the determination of X-ray - optical scaling relations,

which, in work similar to Kloster et al. (2011) and Rykoff et al. (2008), relies on the tight correlation between X-ray observables, such as temperature, to the cluster mass, in order to calibrate the GMPhoRCC richness as an optical mass proxy. This would ultimately allow the investigation and constraint of cosmological models as described in Section 2.1.8, Jenkins et al. (2001), Rozo et al. (2010) and Tinker et al. (2012).

As a preliminary step towards this goal a subset of 134 clean spectroscopic clusters from XCS DR1 are analysed to illustrate the potential research. First considering the correlation between GMPhoRCC richness and X-ray temperature, modeled as power law scaling relation similar to those used by Rykoff et al. (2008) and defined below:

$$T_{\rm x} = e^{\alpha}(n_{200})^{\beta} \ \ {\rm keV} \tag{6.1}$$

or equivalently,

$$\ln(T_{\rm x}) = \alpha + \beta \ln(n_{200}) \tag{6.2}$$

where α and β are constants. Fitting the scaling relation proceeds by stacking the clusters in richness bins and using the BCES method of Section 3.1.3 and Akritas & Bershady (1996) to find the parameters of Equation 6.2 from the average temperatures and n_{200}. While this is a rather simplistic approach for illustration, future analysis is indented using more sophisticated techniques, such as the Bayesian method of Rykoff et al. (2008) and Rozo & Rykoff (2014). Figure 6.1 demonstrates the $T_{\rm x}$ - n_{200} scaling relation finding, $\alpha = -0.06 \pm 0.07$ and $\beta = 0.44 \pm 0.03$ with a scatter $\sigma_{\ln T_{\rm x}|\ln n_{200}} = 0.22$. With X-ray temperatures and luminosities derived using GMPhoRCC redshifts, this analysis can proceed using the upcoming XCS DR2, offering a significant increase in the number of clusters allowing tighter constraints on the scaling relations.

In addition to the X-ray - optical scaling relations, the full characterisation of the red sequence by GMPhoRCC gives the potential to investigate the evolution, effect of environment and comparisons with semi analytical galaxy and cluster formation models. In work similar to Gladders et al. (1998) this could give further insights in to the formation of the clusters and the origin of the red sequence. Again a preliminary analysis using a subset of 134 clean spectroscopic clusters

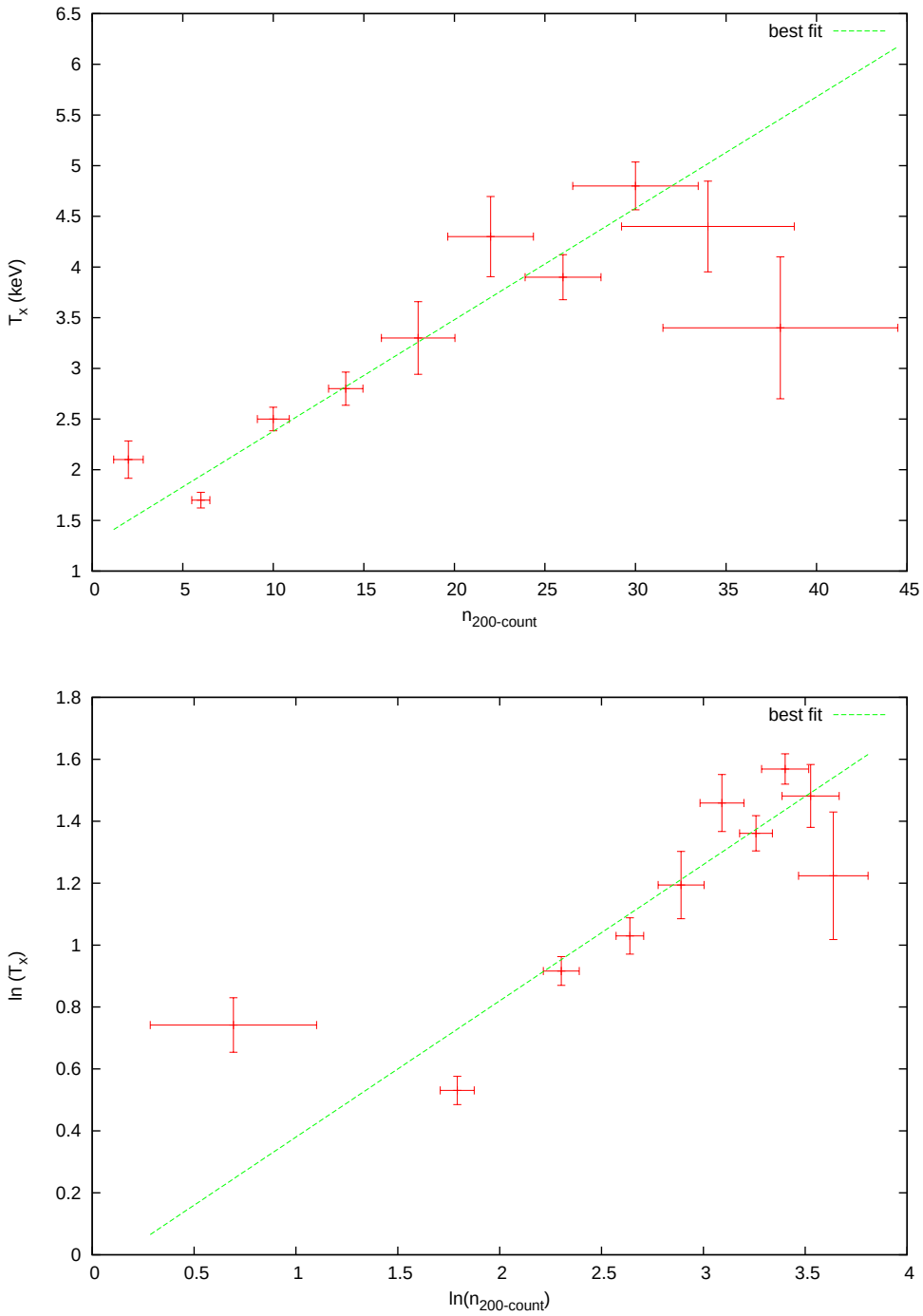

Figure 6.1 *A preliminary analysis of the $T_{\rm x}$ - n_{200} scaling relation produced using a clean spectroscopic subset of XCS DR1. By stacking the clusters in richness bins and using the BCES method of Section 3.1.3 and Akritas & Bershady (1996), a best fit linear model is found from the average temperatures and n_{200}. While the top panel highlights the correlation using a linear model, the bottom panel shows the scaling relation of Equation 6.2 with $\alpha = -0.06 \pm 0.07$, $\beta = 0.44 \pm 0.03$ and a scatter of $\sigma_{\ln T_{\rm x}|\ln n_{200}} = 0.22$*

.

from XCS DR1 provides an illustration of the potential research. While many features of the red sequence can be investigated, such as intrinsic width, this discussion focuses on the CMR slope. First considering redshift dependence, Figure 6.2 shows the evolution of the slope of the red sequence attained by binning clusters in redshift space and averaging. While a slight redshift dependence is found, agreeing with the mass-metallicity evolution suggested by Gladders et al. (1998), further analysis with a larger cluster sample, such as XCS DR2, allows for firmer conclusions to be drawn. Next considering the relation between X-ray temperature and CMR slope, found in a similar manner and shown in Figure 6.3, while a slight dependence is found, the cluster sample is insufficient to contradict the independence on environment found by Hogg et al. (2004) and Hao et al. (2009).

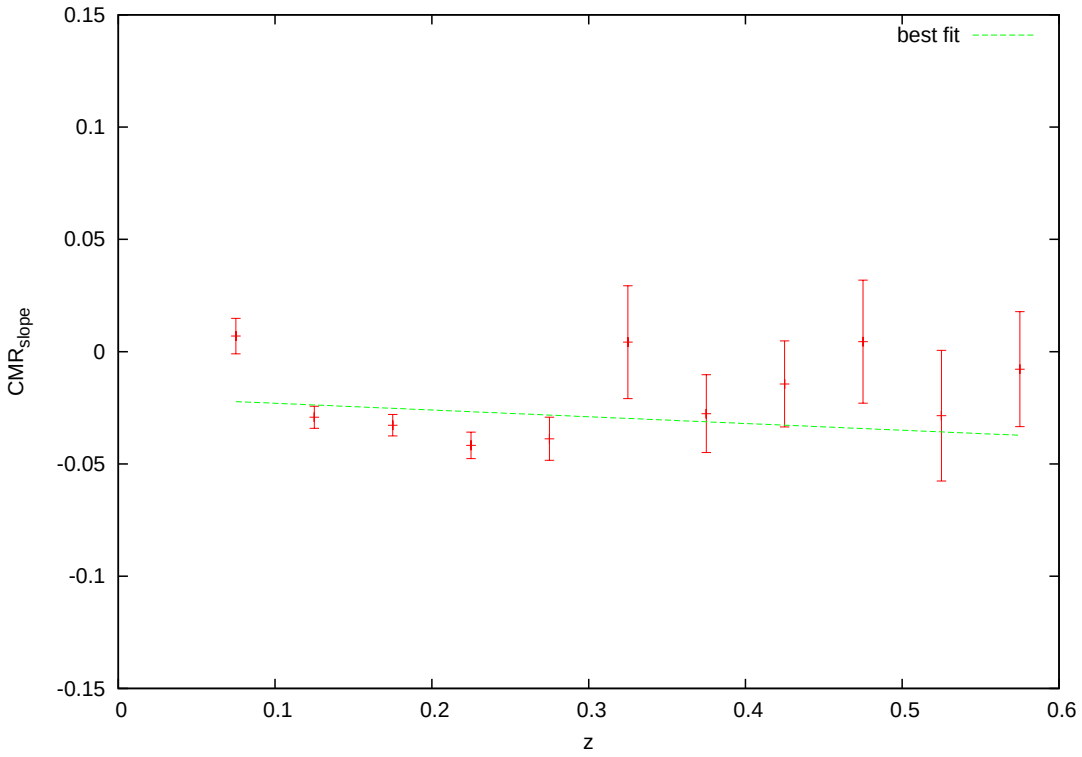

Figure 6.2 *The evolution of the slope of the red sequence attained using a clean spectroscopic subset of XCS DR1. By stacking the clusters in redshift bins and using the BCES method of Section 3.1.3 and Akritas & Bershady (1996), a best fit linear model is found from the average slope and redshift. A slight redshift dependence is found agreeing with the mass-metallicity evolution suggested by Gladders et al. (1998).*

In addition to X-ray based research, access to weak lensing data from CFHTLenS allows for the direct calibration of richness to mass, using a similar approach to the work presented in Sheldon et al. (2009b) and Hansen et al. (2009). With a

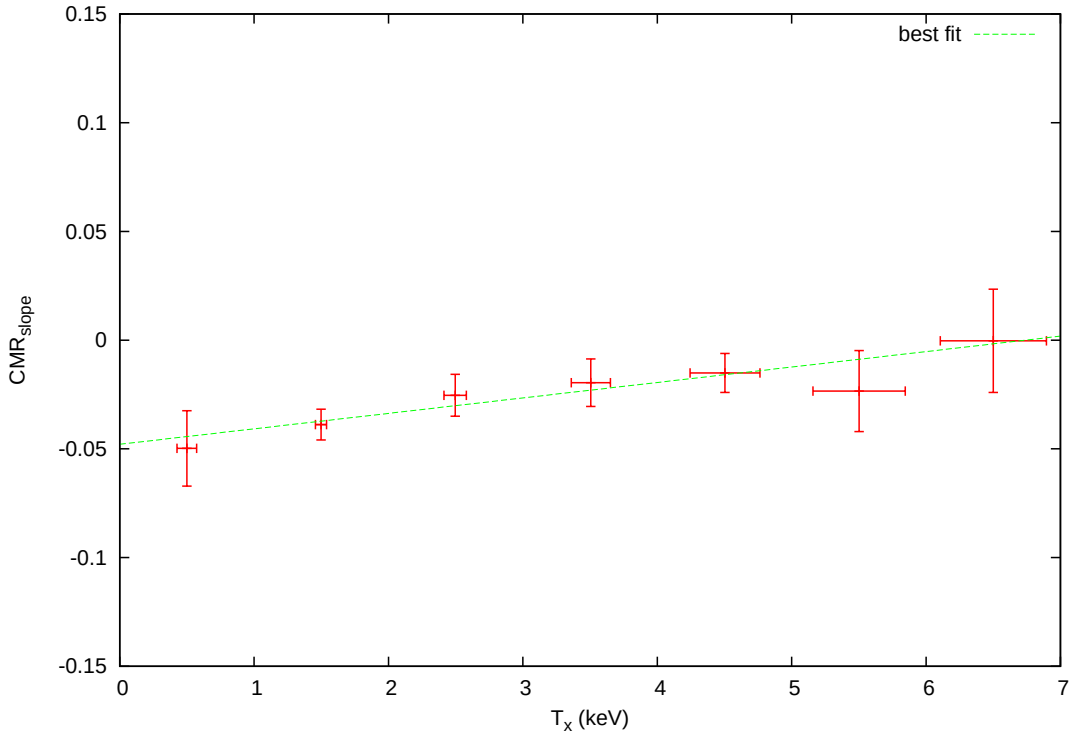

Figure 6.3 *The X-ray temperature dependence of the slope of the red sequence attained using a clean spectroscopic subset of XCS DR1. By stacking the clusters in temperature bins and using the BCES method of Section 3.1.3, a best fit linear model is found from the bin averages. Although a slight dependence is found, the cluster sample is insufficient to contradict the independence on environment found by Hogg et al. (2004) and Hao et al. (2009).*

larger catalogue of clusters this could also improve the richness - radius scaling relation used but GMPhoRCC to determine r_{200} given by Hansen et al. (2009).

With the huge number of available clusters and significant optical coverage it is clear that there is huge scope for further significant research with GMPhoRCC.

Glossary

m_{200} The total cluster mass inside r_{200}.

m_{500} The total cluster mass inside r_{500}.

$n_{200-count}$ The GMPhoRCC estimate of n_{200} obtained by counting the number of red sequence galaxies inside r_{200} and subtracting a background.

$n_{200-lum}$ The GMPhoRCC estimate of n_{200} obtained by fitting and integrating the luminosity function of the red sequence galaxies inside r_{200} and subtracting a background.

n_{200} The number of red sequence cluster members inside r_{200}.

n_{500} The number of red sequence cluster members inside r_{500}.

$n_{gals-count}$ The GMPhoRCC estimate of n_{gals} obtained by counting the number of red sequence galaxies inside $0.5\mathrm{h}^{-1}$Mpc and subtracting a background.

$n_{gals-lum}$ The GMPhoRCC estimate of n_{gals} obtained by fitting and integrating the luminosity function of the red sequence galaxies inside $0.5\mathrm{h}^{-1}$Mpc and subtracting a background.

n_{gals} The number of red sequence cluster members inside $0.5\mathrm{h}^{-1}$Mpc.

r_{200} Characteristic radius of a cluster inside which the average is 200 times greater than the critical density.

r_{500} Characteristic radius of a cluster inside which the average is 500 times greater than the critical density.

z_{BCG} The GMPhoRCC estimate of cluster redshift obtained from the BCG.

z_{RS} The GMPhoRCC estimate of cluster redshift obtained from the peak of the background-subtracted photometric redshift distribution of the red sequence cluster members.

$z_{spec-GMPhoRCC}$ The GMPhoRCC estimate of cluster redshift obtained from red sequence galaxy spectra.

BCG The brightest cluster galaxy.

GMPhoRCC The **G**aussian **M**ixture full **Pho**tometric **R**ed sequence **C**luster **C**haracteriser.

NFW profile The Navarro-Frenk-White profile describing the distribution of dark matter in a cluster.

References

Abazajian, K., et al. 2004, AJ, 128, 502 [ADS]

Abazajian, K. N., et al. 2009, ApJS, 182, 543 [ADS]

Abell, G. O. 1958, ApJS, 3, 211 [ADS]

Ahn, C. P., et al. 2012, ApJS, 203, 21 [ADS]

—. 2013, ArXiv e-prints [ADS]

Akritas, M. G., & Bershady, M. A. 1996, ApJ, 470, 706 [ADS]

Bahcall, N. A., et al. 2003, ApJ, 585, 182 [ADS]

Bartelmann, M. 1996, A&A, 313, 697 [ADS]

Baum, W. A. 1959, in IAU Symposium, Vol. 10, The Hertzsprung-Russell Diagram, ed. J. L. Greenstein, 23–32 [ADS]

Baum, W. A. 1962, in IAU Symposium, Vol. 15, Problems of Extra-Galactic Research, ed. G. C. McVittie, 390 [ADS]

Benítez, N. 2000, ApJ, 536, 571 [ADS]

Bernardi, M., et al. 2003, AJ, 125, 1849 [ADS]

Bertelli, G., Bressan, A., Chiosi, C., Fagotto, F., & Nasi, E. 1994, A&AS, 106, 275 [ADS]

Blanton, M. R. 2006, ApJ, 648, 268 [ADS]

Blanton, M. R., & Roweis, S. 2007, AJ, 133, 734 [ADS]

Blanton, M. R., et al. 2003, ApJ, 592, 819 [ADS]

Böhringer, H., et al. 2000, ApJS, 129, 435 [ADS]

—. 2004, A&A, 425, 367 [ADS]

Bolzonella, M., Miralles, J.-M., & Pelló, R. 2000, A&A, 363, 476 [ADS]

Bower, R. G., Benson, A. J., Malbon, R., Helly, J. C., Frenk, C. S., Baugh, C. M., Cole, S., & Lacey, C. G. 2006, MNRAS, 370, 645 [ADS]

Bower, R. G., Lucey, J. R., & Ellis, R. S. 1992a, MNRAS, 254, 601 [ADS]

—. 1992b, MNRAS, 254, 589 [ADS]

Bruzual, G., & Charlot, S. 2003a, MNRAS, 344, 1000 [ADS]

—. 2003b, MNRAS, 344, 1000 [ADS]

Bruzual A., G., & Charlot, S. 1993, ApJ, 405, 538 [ADS]

Cai, Y.-C., Angulo, R. E., Baugh, C. M., Cole, S., Frenk, C. S., & Jenkins, A. 2009, MNRAS, 395, 1185 [ADS]

Carliles, S., Budavári, T., Heinis, S., Priebe, C., & Szalay, A. S. 2010, ApJ, 712, 511 [ADS]

Chabrier, G. 2003, PASP, 115, 763 [ADS]

Coe, D., Benítez, N., Sánchez, S. F., Jee, M., Bouwens, R., & Ford, H. 2006, AJ, 132, 926 [ADS]

Coleman, G. D., Wu, C.-C., & Weedman, D. W. 1980, ApJS, 43, 393 [ADS]

Conroy, C., & Gunn, J. E. 2010, ApJ, 712, 833 [ADS]

Crawford, S. M., Bershady, M. A., & Hoessel, J. G. 2009, ApJ, 690, 1158 [ADS]

Csabai, I., Dobos, L., Trencséni, M., Herczegh, G., Józsa, P., Purger, N., Budavári, T., & Szalay, A. S. 2007, Astronomische Nachrichten, 328, 852 [ADS]

Eisenstein, D. J., Hu, W., & Tegmark, M. 1998, ApJL, 504, L57 [ADS]

Eisenstein, D. J., et al. 2001, AJ, 122, 2267 [ADS]

Erben, T., et al. 2013, MNRAS, 433, 2545 [ADS]

Ettori, S. 2013, MNRAS, 435, 1265 [ADS]

Finoguenov, A., et al. 2007, ApJS, 172, 182 [ADS]

Garilli, B., et al. 2008, A&A, 486, 683 [ADS]

Gladders, M. D., Lopez-Cruz, O., Yee, H. K. C., & Kodama, T. 1998, ApJ, 501, 571 [ADS]

Gladders, M. D., & Yee, H. K. C. 2000, AJ, 120, 2148 [ADS]

—. 2005, ApJS, 157, 1 [ADS]

Goto, T., et al. 2002, AJ, 123, 1807 [ADS]

Gunn, J. E., & Gott, III, J. R. 1972, ApJ, 176, 1 [ADS]

Hansen, S. M., McKay, T. A., Wechsler, R. H., Annis, J., Sheldon, E. S., & Kimball, A. 2005, ApJ, 633, 122 [ADS]

Hansen, S. M., Sheldon, E. S., Wechsler, R. H., & Koester, B. P. 2009, ApJ, 699, 1333 [ADS]

Hao, J., et al. 2009, ApJ, 702, 745 [ADS]

—. 2010, ApJS, 191, 254 [ADS]

Heymans, C., et al. 2012, MNRAS, 427, 146 [ADS]

High, F. W., et al. 2010, ApJ, 723, 1736 [ADS]

Hildebrandt, H., et al. 2012, MNRAS, 421, 2355 [ADS]

Hilton, M., et al. 2009, ApJ, 697, 436 [ADS]

Hogg, D. W. 1999, ArXiv Astrophysics e-prints [ADS]

Hogg, D. W., Baldry, I. K., Blanton, M. R., & Eisenstein, D. J. 2002, ArXiv Astrophysics e-prints [ADS]

Hogg, D. W., et al. 2004, ApJL, 601, L29 [ADS]

Jenkins, A., Frenk, C. S., White, S. D. M., Colberg, J. M., Cole, S., Evrard, A. E., Couchman, H. M. P., & Yoshida, N. 2001, MNRAS, 321, 372 [ADS]

Johnston, D. E., et al. 2007, ArXiv e-prints [ADS]

Kellogg, E., Murray, S., Giacconi, R., Tananbaum, T., & Gursky, H. 1973, ApJL, 185, L13 [ADS]

Khedekar, S., Majumdar, S., & Das, S. 2010, Phys. Rev. D, 82, 041301 [ADS]

Kloster, D., Rines, K., Svoboda, B. E., Arnold, R. L., Welch, T. J., Finn, R. A., & Vikhlinin, A. 2011, in Bulletin of the American Astronomical Society, Vol. 43, American Astronomical Society Meeting Abstracts 217, 149.12 [ADS]

Kodama, T. 1997, PhD thesis, PhD thesis, Institute of Astronomy, Univ. Tokyo , (1997) [ADS]

Koester, B. P., et al. 2007a, ApJ, 660, 239 [ADS]

—. 2007b, ApJ, 660, 221 [ADS]

Komatsu, E., et al. 2011, ApJS, 192, 18 [ADS]

Kraft, D. 1988, A Software Package for Sequential Quadratic Programming, Deutsche Forschungs- und Versuchsanstalt für Luft- und Raumfahrt Köln: Forschungsbericht (Wiss. Berichtswesen d. DFVLR) [LINK]

Li, L., Zhang, Y., Zhao, Y., & Yang, D. 2006, ArXiv Astrophysics e-prints [ADS]

Lloyd-Davies, E. J., et al. 2011, MNRAS, 418, 14 [ADS]

Magnier, E. A., et al. 2013, ApJS, 205, 20 [ADS]

Maraston, C., Strömbäck, G., Thomas, D., Wake, D. A., & Nichol, R. C. 2009, MNRAS, 394, L107 [ADS]

Marrone, D. P., et al. 2009, ApJL, 701, L114 [ADS]

Mehrtens, N., et al. 2012, MNRAS, 423, 1024 [ADS]

Mei, S., et al. 2009, ApJ, 690, 42 [ADS]

Miller, C. J., et al. 2001, AJ, 122, 3492 [ADS]

—. 2005, AJ, 130, 968 [ADS]

Motl, P. M., Hallman, E. J., Burns, J. O., & Norman, M. L. 2005, ApJL, 623, L63 [ADS]

Murphy, D. N. A., Geach, J. E., & Bower, R. G. 2012, MNRAS, 420, 1861 [ADS]

Navarro, J. F., Frenk, C. S., & White, S. D. M. 1997, ApJ, 490, 493 [ADS]

Newman, J. A., et al. 2013, ApJS, 208, 5 [ADS]

Peacock, J. A. 1999, Cosmological Physics (Cambridge University Press) [ADS]

Peebles, P. J. E. 1980, The large-scale structure of the universe (Princeton University Press) [ADS]

Pierre, M., et al. 2007, MNRAS, 382, 279 [ADS]

Piffaretti, R., Arnaud, M., Pratt, G. W., Pointecouteau, E., & Melin, J.-B. 2011, A&A, 534, A109 [ADS]

Planck Collaboration et al. 2013, ArXiv e-prints [ADS]

Postman, M., Lubin, L. M., Gunn, J. E., Oke, J. B., Hoessel, J. G., Schneider, D. P., & Christensen, J. A. 1996, AJ, 111, 615 [ADS]

Press, W. H., Teukolsky, S. A., Vetterling, W. T., & Flannery, B. P. 2002, Numerical recipes in C++ : the art of scientific computing (Cambridge University Press) [ADS]

Reyes, R., Mandelbaum, R., Hirata, C., Bahcall, N., & Seljak, U. 2008, MNRAS, 390, 1157 [ADS]

Riess, A. G., et al. 1998, AJ, 116, 1009 [ADS]

Roche, N., Bernardi, M., & Hyde, J. 2010, MNRAS, 407, 1231 [ADS]

Romer, A. K., Viana, P. T. P., Liddle, A. R., & Mann, R. G. 2001, ApJ, 547, 594 [ADS]

Rozo, E., & Rykoff, E. S. 2014, ApJ, 783, 80 [ADS]

Rozo, E., et al. 2010, ApJ, 708, 645 [ADS]

Rykoff, E. S., et al. 2008, ApJ, 675, 1106 [ADS]

—. 2012, ApJ, 746, 178 [ADS]

—. 2013, ArXiv e-prints [ADS]

Sarazin, C. L. 1986, Reviews of Modern Physics, 58, 1 [ADS]

Schechter, P. 1976, ApJ, 203, 297 [ADS]

Scranton, R., et al. 2002, ApJ, 579, 48 [ADS]

Shanks, T., & Metcalfe, N. 2012, in Science from the Next Generation Imaging and Spectroscopic Surveys [ADS]

Sheldon, E. S., et al. 2004, AJ, 127, 2544 [ADS]

—. 2009a, ApJ, 703, 2217 [ADS]

—. 2009b, ApJ, 703, 2232 [ADS]

Sheth, R. K., Mo, H. J., & Tormen, G. 2001, MNRAS, 323, 1 [ADS]

Song, J., Mohr, J. J., Barkhouse, W. A., Warren, M. S., Dolag, K., & Rude, C. 2012, ApJ, 747, 58 [ADS]

Springel, V., et al. 2005, Nature, 435, 629 [ADS]

Staniszewski, Z., et al. 2009, ApJ, 701, 32 [ADS]

Sunyaev, R. A., & Zeldovich, Y. B. 1970, AP&SS, 7, 3 [ADS]

Susperregi, M. 2001, ApJ, 546, 85 [ADS]

Tinker, J. L., et al. 2012, ApJ, 745, 16 [ADS]

Tojeiro, R., Percival, W. J., Heavens, A. F., & Jimenez, R. 2011, MNRAS, 413, 434 [ADS]

Vanderlinde, K., et al. 2010, ApJ, 722, 1180 [ADS]

Velander, M., et al. 2014, MNRAS, 437, 2111 [ADS]

Voit, G. M. 2005, Reviews of Modern Physics, 77, 207 [ADS]

Wadadekar, Y. 2005, PASP, 117, 79 [ADS]

Wang, D., Zhang, Y. X., Liu, C., & Zhao, Y. H. 2007, MNRAS, 382, 1601 [ADS]

Wen, Z. L., Han, J. L., & Liu, F. S. 2010, MNRAS, 869 [ADS]

White, S. D. M., Efstathiou, G., & Frenk, C. S. 1993, MNRAS, 262, 1023 [ADS]

Yèche, C., et al. 2010, A&A, 523, A14 [ADS]

York, D. G., et al. 2000, AJ, 120, 1579 [ADS]

Zhang, Y.-Y., Andernach, H., Caretta, C. A., Reiprich, T. H., Böhringer, H., Puchwein, E., Sijacki, D., & Girardi, M. 2011, A&A, 526, A105 [ADS]

Zhang, Y.-Y., Finoguenov, A., Böhringer, H., Kneib, J.-P., Smith, G. P., Kneissl, R., Okabe, N., & Dahle, H. 2008, A&A, 482, 451 [ADS]

Zwicky, F. 1933, Helvetica Physica Acta, 6, 110 [ADS]

Appendix A

Full GMPhoRCC Characterisations of XCS Sources

The GMPhoRCC characterisations of the preliminary XCS DR2 candidates presented in tables of Section 5.3 are sample from 20 sources for illustration where the full characterisations are given in this appendix.

First considering XCS DR1, Mehrtens et al. (2012) presented 503 optically confirmed X-ray clusters of which 258 have spectroscopic redshifts and 108 have SDSS characterisations. GMPhoRCC provides characterisations for 360, 232 of which have spectroscopic redshifts. Overall GMPhoRCC provides 260 (149 of which are clean) new SDSS characterisations and 91 (61 of which are clean) new spectroscopic redshifts shown in Table A.1.

Now considering the preliminary XCS DR2 sources with SDSS DR10 optical data, characterisations where found for 3882 candidates with spectroscopic redshifts found for 1893. The clean subset comprises 1203 extended X-ray sources, 904 with spectra with the complete set shown in Table A.2

Of the 523 sources with ATLAS coverage, GMPhoRCC was able to produce characterisations for 274 with 64 in the clean subset as shown in Table A.3

Using CFHTLenS optical data, GMPhoRCC was able to produce characterisations for 702 of the 819 extended X-ray sources with coverage attaining 237 considered clean as shown in Table A.4.

Table A.1 *A table of GMPhoRCC characterisations for XCS DR1 using SDSS DR10 optical data where* 260 *new clusters are analysed in the addition coverage over DR7, providing* 98 *new spectroscopic redshifts.*

name	z_{RS}	z_{BCG}	z_{spec-g}	cmr_{grad}	cmr_{inter}	cmr_{wid}	n_{gals-c}	n_{gals-l}	n_{200-c}	n_{200-l}	qual
XMMXCS J001116.1+005211.3	$0.364^{+0.061}_{-0.061}$	0.379 ± 0.057	$0.365 \pm 1.2e-04$	-0.128 ± 0.056	4.300 ± 1.070	0.001	9 ± 3	9 ± 4	5 ± 3	5 ± 3	1
XMMXCS J001737.4-005235.4	$0.212^{+0.047}_{-0.048}$	0.229 ± 0.038	$0.211 \pm 3.8e-05$	-0.049 ± 0.016	2.230 ± 0.287	0.054	21 ± 5	19 ± 5	28 ± 6	22 ± 5	1
XMMXCS J002314.1+001201.5	$0.260^{+0.052}_{-0.052}$	0.250 ± 0.039	$0.258 \pm 2.9e-05$	-0.032 ± 0.013	2.020 ± 0.239	0.001	12 ± 4	14 ± 4	12 ± 4	15 ± 4	1
XMMXCS J002650.0+171931.3	$0.474^{+0.115}_{-0.113}$	0.474 ± 0.146	-	-0.058 ± 0.036	1.940 ± 0.724	0.090	6 ± 4	-	5 ± 3	-	1
XMMXCS J002953.9+350507.5	$0.491^{+0.131}_{-0.130}$	0.471 ± 0.086	-	-0.031 ± 0.064	1.470 ± 1.250	0.058	21 ± 5	30 ± 6	20 ± 5	32 ± 7	1
XMMXCS J004119.5+252618.9	$0.137^{+0.031}_{-0.031}$	0.144 ± 0.025	-	-0.011 ± 0.015	1.250 ± 0.266	0.057	20 ± 5	23 ± 5	22 ± 5	26 ± 5	1
XMMXCS J004231.6+005119.9	$0.151^{+0.023}_{-0.024}$	0.159 ± 0.026	$0.151 \pm 2.2e-05$	-0.028 ± 0.009	1.600 ± 0.149	0.006	8 ± 3	8 ± 3	7 ± 3	8 ± 3	1
XMMXCS J004252.6+004303.1	$0.271^{+0.040}_{-0.040}$	0.275 ± 0.042	$0.270 \pm 4.0e-05$	-0.048 ± 0.050	2.320 ± 0.963	0.114	12 ± 4	38 ± 7	12 ± 4	11 ± 5	1
XMMXCS J004333.7+010109.6	$0.195^{+0.030}_{-0.029}$	0.203 ± 0.030	$0.196 \pm 2.1e-05$	-0.073 ± 0.021	2.560 ± 0.372	0.061	8 ± 3	10 ± 4	7 ± 3	8 ± 3	1
XMMXCS J004359.3+000706.8	$0.218^{+0.044}_{-0.045}$	0.226 ± 0.036	$0.218 \pm 2.0e-05$	-0.087 ± 0.030	2.940 ± 0.569	0.031	15 ± 4	17 ± 4	16 ± 4	20 ± 5	1
XMMXCS J005545.8+003840.8	$0.068^{+0.001}_{-0.001}$	0.089 ± 0.023	$0.067 \pm 6.4e-06$	-0.066 ± 0.020	1.910 ± 0.325	0.068	11 ± 3	14 ± 4	11 ± 3	13 ± 4	1
XMMXCS J010608.4+005031.4	$0.258^{+0.050}_{-0.050}$	0.277 ± 0.043	$0.259 \pm 2.8e-05$	-0.049 ± 0.018	2.350 ± 0.340	0.041	22 ± 5	27 ± 6	23 ± 5	37 ± 7	1
XMMXCS J010720.2+141604.2	$0.074^{+0.007}_{-0.008}$	0.073 ± 0.015	$0.074 \pm 1.2e-05$	0.007 ± 0.012	0.782 ± 0.188	0.027	9 ± 3	7 ± 3	7 ± 3	6 ± 3	1
XMMXCS J010858.7+132557.7	$0.146^{+0.025}_{-0.025}$	0.154 ± 0.023	$0.146 \pm 2.1e-05$	-0.037 ± 0.020	1.650 ± 0.342	0.105	6 ± 3	8 ± 3	6 ± 3	9 ± 3	1
XMMXCS J011624.2+325717.0	$0.471^{+0.104}_{-0.102}$	0.475 ± 0.076	-	-0.089 ± 0.061	2.610 ± 1.220	0.094	12 ± 4	19 ± 5	12 ± 4	-	1
XMMXCS J011922.6-011011.7	$0.186^{+0.029}_{-0.029}$	0.190 ± 0.029	$0.186 \pm 2.2e-05$	-0.016 ± 0.020	1.450 ± 0.368	0.071	5 ± 2	9 ± 3	3 ± 2	6 ± 3	1
XMMXCS J014430.3+021237.0	$0.166^{+0.041}_{-0.041}$	0.187 ± 0.031	$0.165 \pm 1.4e-05$	-0.063 ± 0.013	2.270 ± 0.221	0.023	10 ± 3	10 ± 3	10 ± 3	11 ± 3	1
XMMXCS J015315.0+010214.2	$0.059^{+0.001}_{-0.001}$	0.064 ± 0.016	$0.059 \pm 6.7e-06$	-0.011 ± 0.004	1.020 ± 0.054	0.006	6 ± 3	2 ± 2	4 ± 2	3 ± 2	1

Continued on next page

Table A.1 – continued from previous page

name	z_{RS}	z_{BCG}	z_{spec-g}	cmr_{grad}	cmr_{inter}	cmr_{wid}	n_{gals-c}	n_{gals-l}	n_{200-c}	n_{200-l}	qual
XMMXCS J015558.0+053200.8	$0.454^{+0.109}_{-0.108}$	0.499 ± 0.086	$0.450 \pm 1.0e-04$	-0.041 ± 0.024	1.560 ± 0.480	0.001	4 ± 3	13 ± 4	5 ± 3	12 ± 4	1
XMMXCS J020341.6-074705.7	$0.443^{+0.075}_{-0.073}$	0.430 ± 0.066	$0.440 \pm 8.9e-05$	0.107 ± 0.052	-0.071 ± 1.030	0.201	12 ± 4	11 ± 4	13 ± 4	12 ± 4	1
XMMXCS J021012.9-001445.6	$0.282^{+0.051}_{-0.052}$	0.275 ± 0.051	$0.283 \pm 5.1e-05$	0.010 ± 0.014	1.280 ± 0.253	0.024	5 ± 3	4 ± 3	5 ± 2	6 ± 3	1
XMMXCS J021440.9-043321.9	$0.142^{+0.043}_{-0.044}$	0.158 ± 0.026	$0.142 \pm 1.4e-05$	0.003 ± 0.012	1.070 ± 0.204	0.053	17 ± 4	20 ± 5	22 ± 5	32 ± 6	1
XMMXCS J021943.7-045313.8	$0.334^{+0.080}_{-0.079}$	0.365 ± 0.056	$0.318 \pm 5.2e-05$	-0.069 ± 0.150	2.790 ± 3.030	0.179	11 ± 4	10 ± 4	11 ± 4	11 ± 4	1
XMMXCS J022044.8-025227.9	$0.501^{+0.107}_{-0.104}$	0.493 ± 0.074	$0.495 \pm 1.4e-04$	-0.173 ± 0.052	4.150 ± 1.020	0.026	8 ± 4	-	9 ± 4	-	1
XMMXCS J022045.1-032555.0	$0.328^{+0.062}_{-0.063}$	0.339 ± 0.052	$0.328 \pm 6.7e-05$	0.056 ± 0.054	0.680 ± 1.040	0.050	9 ± 3	11 ± 4	8 ± 3	10 ± 4	1
XMMXCS J022145.4-034617.4	$0.434^{+0.085}_{-0.085}$	0.414 ± 0.064	$0.433 \pm 9.9e-05$	-0.021 ± 0.070	2.190 ± 1.370	0.085	27 ± 6	26 ± 6	34 ± 7	35 ± 7	1
XMMXCS J022206.3-030313.6	$0.498^{+0.108}_{-0.107}$	0.483 ± 0.076	$0.496 \pm 1.2e-04$	0.062 ± 0.089	-0.360 ± 1.740	0.096	12 ± 4	66 ± 9	12 ± 4	29 ± 8	1
XMMXCS J022347.6-025129.5	$0.175^{+0.039}_{-0.039}$	0.165 ± 0.038	$0.175 \pm 1.5e-05$	-0.033 ± 0.020	1.730 ± 0.353	0.063	11 ± 4	12 ± 4	10 ± 3	12 ± 4	1
XMMXCS J022356.3-030559.3	$0.296^{+0.036}_{-0.036}$	0.309 ± 0.048	$0.297 \pm 6.1e-05$	0.050 ± 0.026	0.608 ± 0.516	0.045	3 ± 2	6 ± 3	3 ± 2	5 ± 3	1
XMMXCS J022357.6-043518.9	$0.497^{+0.113}_{-0.112}$	0.504 ± 0.080	$0.496 \pm 1.5e-04$	-0.093 ± 0.038	2.690 ± 0.752	0.001	18 ± 5	35 ± 6	20 ± 5	49 ± 8	1
XMMXCS J022406.0-035502.1	$0.565^{+0.104}_{-0.101}$	0.549 ± 0.097	$0.559 \pm 1.4e-04$	0.065 ± 0.093	-0.408 ± 1.930	0.128	5 ± 3	-	4 ± 2	-	1
XMMXCS J022433.8-041432.9	$0.262^{+0.060}_{-0.061}$	0.244 ± 0.043	$0.262 \pm 3.7e-05$	-0.023 ± 0.020	1.810 ± 0.389	0.092	12 ± 4	13 ± 4	12 ± 4	12 ± 4	1
XMMXCS J022722.1-032145.2	$0.331^{+0.079}_{-0.079}$	0.314 ± 0.068	$0.330 \pm 7.2e-05$	0.126 ± 0.065	-0.756 ± 1.220	0.154	6 ± 3	8 ± 4	7 ± 3	8 ± 3	1
XMMXCS J023346.0-085048.5	$0.265^{+0.059}_{-0.059}$	0.285 ± 0.047	$0.265 \pm 4.0e-05$	-0.020 ± 0.019	1.860 ± 0.345	0.001	13 ± 4	27 ± 5	14 ± 4	10 ± 4	1
XMMXCS J024809.8+311516.4	$0.366^{+0.109}_{-0.107}$	0.383 ± 0.058	-	-0.103 ± 0.042	2.610 ± 0.814	0.048	8 ± 4	5 ± 4	10 ± 4	37 ± 6	1
XMMXCS J030253.4-000554.5	$0.446^{+0.151}_{-0.151}$	0.269 ± 0.099	$0.449 \pm 4.9e-05$	0.348 ± 0.227	-6.060 ± 4.630	0.100	5 ± 3	6 ± 3	4 ± 2	6 ± 3	1
XMMXCS J030617.2-000834.6	$0.109^{+0.004}_{-0.004}$	0.126 ± 0.020	$0.109 \pm 1.5e-05$	-0.032 ± 0.012	1.530 ± 0.201	0.033	12 ± 4	13 ± 4	12 ± 4	13 ± 4	1

Continued on next page

Table A.1 – continued from previous page

name	z_{RS}	z_{BCG}	z_{spec-g}	cmr_{grad}	cmr_{inter}	cmr_{wid}	n_{gals-c}	n_{gals-l}	n_{200-c}	n_{200-l}	qual
XMMXCS J030634.0-000423.7	$0.111^{+0.006}_{-0.005}$	0.116 ± 0.022	$0.111 \pm 1.3e-05$	-0.022 ± 0.016	1.310 ± 0.280	0.026	11 ± 3	9 ± 3	10 ± 3	9 ± 3	1
XMMXCS J030644.2-000112.7	$0.111^{+0.001}_{-0.001}$	0.116 ± 0.022	$0.111 \pm 1.4e-05$	-0.049 ± 0.036	1.750 ± 0.620	0.077	14 ± 4	15 ± 4	16 ± 4	11 ± 3	1
XMMXCS J032553.3-061719.9	$0.315^{+0.062}_{-0.064}$	0.323 ± 0.050	-	0.032 ± 0.068	1.040 ± 1.250	0.091	7 ± 3	5 ± 3	7 ± 3	4 ± 3	1
XMMXCS J033351.5+000600.4	$0.353^{+0.088}_{-0.088}$	0.363 ± 0.052	$0.353 \pm 9.4e-05$	0.077 ± 0.131	0.165 ± 2.550	0.165	8 ± 4	10 ± 4	10 ± 4	12 ± 4	1
XMMXCS J033445.3+001707.2	$0.328^{+0.069}_{-0.068}$	0.330 ± 0.050	$0.327 \pm 4.6e-05$	-0.086 ± 0.146	3.030 ± 2.820	0.162	11 ± 4	10 ± 4	8 ± 4	7 ± 4	1
XMMXCS J033556.2+003214.7	$0.429^{+0.092}_{-0.092}$	0.417 ± 0.062	$0.429 \pm 8.9e-05$	-0.005 ± 0.018	0.823 ± 0.350	0.018	13 ± 4	14 ± 5	14 ± 5	16 ± 5	1
XMMXCS J033757.0+002903.4	$0.322^{+0.050}_{-0.051}$	0.321 ± 0.047	$0.323 \pm 4.6e-05$	-0.059 ± 0.019	2.770 ± 0.364	0.001	14 ± 4	16 ± 5	14 ± 4	16 ± 5	1
XMMXCS J041704.8+011330.9	$0.320^{+0.074}_{-0.075}$	0.332 ± 0.051	-	0.020 ± 0.048	1.260 ± 0.902	0.030	13 ± 4	15 ± 4	15 ± 4	18 ± 5	1
XMMXCS J074232.8+651704.5	$0.140^{+0.043}_{-0.041}$	0.149 ± 0.026	-	-0.093 ± 0.069	2.560 ± 1.230	0.121	5 ± 3	6 ± 3	4 ± 2	5 ± 3	1
XMMXCS J075053.1+500316.7	$0.422^{+0.074}_{-0.074}$	0.420 ± 0.061	$0.421 \pm 1.1e-04$	0.178 ± 0.111	-1.640 ± 2.130	0.227	16 ± 5	73 ± 9	24 ± 6	27 ± 8	1
XMMXCS J075427.8+220950.9	$0.399^{+0.060}_{-0.059}$	0.366 ± 0.056	$0.398 \pm 5.5e-05$	-0.028 ± 0.020	1.130 ± 0.390	0.062	13 ± 4	11 ± 4	14 ± 5	10 ± 4	1
XMMXCS J075724.8+392047.7	$0.096^{+0.010}_{-0.010}$	0.111 ± 0.023	$0.096 \pm 1.1e-05$	0.019 ± 0.029	0.616 ± 0.479	0.040	20 ± 5	20 ± 5	24 ± 5	25 ± 5	1
XMMXCS J075839.1+351939.7	$0.174^{+0.022}_{-0.022}$	0.198 ± 0.034	$0.143 \pm 2.1e-05$	-0.077 ± 0.032	2.490 ± 0.516	0.107	5 ± 3	6 ± 3	4 ± 2	4 ± 3	1
XMMXCS J080633.7+153208.6	$0.275^{+0.036}_{-0.037}$	0.276 ± 0.042	$0.274 \pm 3.4e-05$	-0.114 ± 0.063	3.580 ± 1.130	0.110	4 ± 3	2 ± 3	3 ± 2	2 ± 2	1
XMMXCS J080712.8+152701.5	$0.096^{+0.019}_{-0.020}$	0.102 ± 0.017	$0.096 \pm 1.4e-05$	-0.026 ± 0.021	1.370 ± 0.344	0.057	8 ± 3	10 ± 3	9 ± 3	11 ± 3	1
XMMXCS J082135.1+010232.0	$0.100^{+0.017}_{-0.017}$	0.090 ± 0.021	$0.099 \pm 1.4e-05$	-0.019 ± 0.014	1.260 ± 0.233	0.028	8 ± 3	6 ± 3	6 ± 3	4 ± 2	1
XMMXCS J083115.0+523453.9	$0.623^{+0.146}_{-0.143}$	0.608 ± 0.110	$0.611 \pm 1.6e-04$	-0.295 ± 0.064	6.910 ± 1.260	0.001	8 ± 3	182 ± 14	7 ± 3	62 ± 15	1
XMMXCS J083147.8+525036.6	$0.519^{+0.087}_{-0.086}$	0.564 ± 0.090	$0.517 \pm 8.1e-05$	-0.109 ± 0.042	3.040 ± 0.802	0.043	7 ± 3	11 ± 4	6 ± 3	12 ± 4	1
XMMXCS J083454.8+553420.9	$0.266^{+0.069}_{-0.069}$	0.261 ± 0.048	-	-0.086 ± 0.030	3.040 ± 0.571	0.071	20 ± 5	18 ± 5	19 ± 5	16 ± 5	1

Continued on next page

Table A.1 – continued from previous page

name	z_{RS}	z_{BCG}	z_{spec-g}	cmr_{grad}	cmr_{inter}	cmr_{wid}	n_{gals-c}	n_{gals-l}	n_{200-c}	n_{200-l}	qual
XMMXCS J083724.4+553249.8	$0.272^{+0.063}_{-0.065}$	0.269 ± 0.047	$0.273 \pm 5.5e-05$	0.061 ± 0.050	0.426 ± 0.915	0.001	4 ± 2	8 ± 3	3 ± 2	6 ± 3	1
XMMXCS J084044.2+383050.3	$0.174^{+0.033}_{-0.033}$	0.166 ± 0.025	$0.178 \pm 2.4e-05$	-0.007 ± 0.014	1.250 ± 0.253	0.025	7 ± 3	7 ± 3	6 ± 3	6 ± 3	1
XMMXCS J084124.4+004637.7	$0.410^{+0.054}_{-0.053}$	0.382 ± 0.059	$0.408 \pm 1.2e-04$	-0.034 ± 0.098	2.290 ± 1.910	0.001	6 ± 3	5 ± 3	6 ± 3	4 ± 3	1
XMMXCS J084701.4+345112.8	$0.466^{+0.092}_{-0.092}$	0.470 ± 0.068	$0.464 \pm 1.4e-04$	-0.012 ± 0.024	1.040 ± 0.474	0.044	21 ± 5	22 ± 5	25 ± 6	30 ± 7	1
XMMXCS J084848.1+445606.3	$0.572^{+0.126}_{-0.126}$	0.548 ± 0.086	$0.570 \pm 2.1e-04$	-0.008 ± 0.023	1.160 ± 0.441	0.001	11 ± 4	14 ± 5	11 ± 4	14 ± 5	1
XMMXCS J092018.9+370617.7	$0.234^{+0.057}_{-0.057}$	0.242 ± 0.048	$0.235 \pm 2.5e-05$	0.039 ± 0.022	0.703 ± 0.401	0.049	7 ± 3	8 ± 3	7 ± 3	7 ± 3	1
XMMXCS J092052.4+302804.8	$0.290^{+0.068}_{-0.068}$	0.283 ± 0.043	$0.290 \pm 3.9e-05$	-0.009 ± 0.026	1.740 ± 0.489	0.098	27 ± 5	12 ± 4	57 ± 8	13 ± 4	1
XMMXCS J092059.2+303418.6	$0.265^{+0.073}_{-0.075}$	0.268 ± 0.040	$0.273 \pm 4.8e-05$	0.003 ± 0.028	1.430 ± 0.522	0.064	10 ± 4	8 ± 3	10 ± 3	6 ± 3	1
XMMXCS J092114.5+370131.3	$0.234^{+0.072}_{-0.072}$	0.240 ± 0.044	$0.235 \pm 3.0e-05$	-0.059 ± 0.077	2.430 ± 1.400	0.081	8 ± 3	9 ± 4	6 ± 3	8 ± 3	1
XMMXCS J092325.4+225645.7	$0.186^{+0.042}_{-0.041}$	0.188 ± 0.032	$0.186 \pm 4.1e-05$	0.023 ± 0.016	0.801 ± 0.281	0.047	8 ± 3	7 ± 3	6 ± 3	4 ± 2	1
XMMXCS J092545.7+305856.9	$0.478^{+0.123}_{-0.117}$	0.498 ± 0.208	-	0.143 ± 0.064	-2.140 ± 1.320	0.001	9 ± 4	30 ± 6	7 ± 3	12 ± 5	1
XMMXCS J092650.7+310127.3	$0.534^{+0.095}_{-0.094}$	0.559 ± 0.106	-	-0.099 ± 0.017	2.970 ± 0.323	0.001	11 ± 4	23 ± 5	12 ± 4	-	1
XMMXCS J092659.0+361219.1	$0.400^{+0.108}_{-0.106}$	0.378 ± 0.056	$0.382 \pm 8.4e-05$	0.011 ± 0.057	0.500 ± 1.130	0.111	14 ± 5	15 ± 5	15 ± 5	15 ± 5	1
XMMXCS J093205.6+473314.1	$0.225^{+0.047}_{-0.047}$	0.222 ± 0.037	$0.225 \pm 3.6e-05$	-0.036 ± 0.019	1.940 ± 0.334	0.042	5 ± 2	8 ± 3	4 ± 2	4 ± 2	1
XMMXCS J093709.3+611616.2	$0.207^{+0.034}_{-0.034}$	0.211 ± 0.032	$0.208 \pm 4.0e-05$	-0.046 ± 0.020	2.200 ± 0.372	0.059	7 ± 3	7 ± 3	5 ± 2	4 ± 2	1
XMMXCS J093945.5+360057.8	$0.303^{+0.072}_{-0.072}$	0.304 ± 0.046	$0.303 \pm 5.6e-05$	-0.034 ± 0.070	2.050 ± 1.400	0.141	5 ± 3	10 ± 4	4 ± 2	10 ± 4	1
XMMXCS J094034.6+355950.0	$0.300^{+0.054}_{-0.054}$	0.271 ± 0.053	$0.301 \pm 4.6e-05$	0.029 ± 0.031	0.987 ± 0.559	0.001	8 ± 3	15 ± 4	8 ± 3	6 ± 3	1
XMMXCS J094332.3+163954.9	$0.255^{+0.095}_{-0.095}$	0.259 ± 0.041	$0.254 \pm 5.9e-05$	-0.078 ± 0.028	2.840 ± 0.507	0.067	14 ± 4	13 ± 4	17 ± 4	13 ± 4	1
XMMXCS J094358.2+164120.7	$0.203^{+0.071}_{-0.072}$	0.196 ± 0.035	-	0.004 ± 0.027	1.200 ± 0.499	0.087	12 ± 4	14 ± 4	13 ± 4	17 ± 4	1

Continued on next page

Table A.1 – continued from previous page

name	z_{RS}	z_{BCG}	z_{spec-g}	cmr_{grad}	cmr_{inter}	cmr_{wid}	n_{gals-c}	n_{gals-l}	n_{200-c}	n_{200-l}	qual
XMMXCS J094530.5+094631.1	$0.220^{+0.042}_{-0.043}$	0.209 ± 0.035	$0.214 \pm 2.4e-05$	-0.017 ± 0.021	1.660 ± 0.383	0.053	12 ± 4	10 ± 4	12 ± 4	10 ± 4	1
XMMXCS J095105.7+391742.9	$0.477^{+0.050}_{-0.050}$	0.522 ± 0.090	$0.474 \pm 9.7e-05$	-0.070 ± 0.018	2.210 ± 0.342	0.001	11 ± 4	11 ± 4	11 ± 4	11 ± 4	1
XMMXCS J095603.5+410707.1	$0.592^{+0.135}_{-0.135}$	0.590 ± 0.108	$0.589 \pm 3.0e-04$	-0.178 ± 0.104	4.670 ± 2.110	0.001	13 ± 4	34 ± 7	13 ± 4	38 ± 8	1
XMMXCS J095610.9-002157.8	$0.550^{+0.140}_{-0.139}$	0.566 ± 0.101	$0.547 \pm 9.0e-05$	0.155 ± 0.165	-2.000 ± 3.280	0.106	14 ± 4	27 ± 6	19 ± 5	62 ± 9	1
XMMXCS J095737.1+023425.1	$0.377^{+0.088}_{-0.086}$	0.359 ± 0.053	$0.373 \pm 7.0e-05$	-0.000 ± 0.016	0.615 ± 0.316	0.067	23 ± 5	22 ± 6	28 ± 6	29 ± 7	1
XMMXCS J095901.3+024740.5	$0.495^{+0.087}_{-0.086}$	0.499 ± 0.075	$0.501 \pm 1.1e-04$	-0.014 ± 0.042	1.110 ± 0.856	0.080	8 ± 4	10 ± 4	8 ± 3	11 ± 4	1
XMMXCS J095924.7+014616.3	$0.123^{+0.021}_{-0.021}$	0.132 ± 0.025	$0.124 \pm 1.5e-05$	-0.045 ± 0.021	1.790 ± 0.351	0.024	5 ± 2	6 ± 3	5 ± 2	6 ± 3	1
XMMXCS J095931.8+052616.8	$0.226^{+0.076}_{-0.077}$	0.221 ± 0.050	-	-0.008 ± 0.035	1.470 ± 0.654	0.086	3 ± 2	5 ± 3	4 ± 2	6 ± 3	1
XMMXCS J095946.9+025521.9	$0.115^{+0.025}_{-0.026}$	0.095 ± 0.020	$0.103 \pm 1.4e-05$	0.042 ± 0.037	0.279 ± 0.661	0.063	3 ± 2	3 ± 2	4 ± 2	3 ± 2	1
XMMXCS J095951.4+014052.1	$0.375^{+0.097}_{-0.097}$	0.359 ± 0.053	$0.372 \pm 7.8e-05$	-0.058 ± 0.042	2.770 ± 0.801	0.001	4 ± 3	7 ± 3	3 ± 2	6 ± 3	1
XMMXCS J100012.3+021246.7	$0.186^{+0.034}_{-0.034}$	0.175 ± 0.027	$0.185 \pm 3.1e-05$	-0.000 ± 0.001	0.954 ± 0.001	0.500	8 ± 4	7 ± 4	8 ± 3	5 ± 3	1
XMMXCS J100043.2+014607.7	$0.343^{+0.070}_{-0.072}$	0.354 ± 0.053	$0.346 \pm 8.6e-05$	0.051 ± 0.107	0.749 ± 2.040	0.115	6 ± 3	6 ± 3	3 ± 2	5 ± 3	1
XMMXCS J100047.4+013926.9	$0.221^{+0.041}_{-0.041}$	0.229 ± 0.045	$0.221 \pm 4.2e-05$	-0.004 ± 0.038	1.440 ± 0.668	0.033	10 ± 3	10 ± 4	10 ± 3	11 ± 4	1
XMMXCS J100053.2+022831.6	$0.390^{+0.085}_{-0.077}$	0.350 ± 0.053	$0.374 \pm 9.6e-05$	0.062 ± 0.454	0.215 ± 9.290	0.500	6 ± 4	5 ± 4	5 ± 3	1 ± 3	1
XMMXCS J100059.9+683944.9	$0.498^{+0.081}_{-0.080}$	0.498 ± 0.072	$0.497 \pm 1.2e-04$	-0.013 ± 0.047	1.050 ± 0.938	0.042	16 ± 5	91 ± 10	18 ± 5	122 ± 13	1
XMMXCS J100141.7+022539.8	$0.123^{+0.017}_{-0.016}$	0.153 ± 0.028	$0.124 \pm 1.1e-05$	-0.032 ± 0.002	1.610 ± 0.033	0.500	9 ± 4	8 ± 4	7 ± 3	5 ± 3	1
XMMXCS J101507.8+493151.5	$0.316^{+0.076}_{-0.076}$	0.297 ± 0.061	-	-0.056 ± 0.050	2.630 ± 0.953	0.001	10 ± 4	9 ± 4	9 ± 3	9 ± 3	1
XMMXCS J101931.4+080344.5	$0.163^{+0.028}_{-0.029}$	0.173 ± 0.026	$0.174 \pm 3.1e-05$	-0.037 ± 0.007	1.840 ± 0.118	0.012	20 ± 5	19 ± 5	27 ± 5	25 ± 5	1
XMMXCS J102133.7+213748.8	$0.187^{+0.039}_{-0.038}$	0.193 ± 0.029	$0.187 \pm 4.0e-05$	-0.033 ± 0.006	1.840 ± 0.097	0.001	4 ± 2	3 ± 2	3 ± 2	0 ± 1	1

Continued on next page

Table A.1 – continued from previous page

name	z_{RS}	z_{BCG}	z_{spec-g}	cmr_{grad}	cmr_{inter}	cmr_{wid}	n_{gals-c}	n_{gals-l}	n_{200-c}	n_{200-l}	qual
XMMXCS J102136.9+125643.2	$0.324^{+0.054}_{-0.055}$	0.268 ± 0.046	$0.325 \pm 1.0e-04$	0.192 ± 0.079	-1.950 ± 1.470	0.001	5 ± 3	8 ± 3	4 ± 2	7 ± 3	1
XMMXCS J102539.7+470512.6	$0.194^{+0.046}_{-0.045}$	0.187 ± 0.033	$0.191 \pm 3.8e-05$	-0.025 ± 0.022	1.650 ± 0.394	0.075	12 ± 4	11 ± 4	15 ± 4	10 ± 4	1
XMMXCS J103007.0+051950.7	$0.153^{+0.055}_{-0.057}$	0.131 ± 0.041	$0.155 \pm 2.7e-05$	0.011 ± 0.034	0.853 ± 0.621	0.070	5 ± 3	5 ± 3	3 ± 2	4 ± 2	1
XMMXCS J103041.3+650813.2	$0.202^{+0.035}_{-0.035}$	0.207 ± 0.030	$0.202 \pm 4.0e-05$	-0.030 ± 0.048	1.800 ± 0.870	0.064	12 ± 4	10 ± 3	12 ± 4	9 ± 3	1
XMMXCS J103100.1+305134.9	$0.136^{+0.019}_{-0.019}$	0.140 ± 0.021	$0.137 \pm 1.6e-05$	0.008 ± 0.012	0.943 ± 0.199	0.028	10 ± 3	11 ± 4	9 ± 3	11 ± 4	1
XMMXCS J103131.5+311317.2	$0.375^{+0.082}_{-0.080}$	0.358 ± 0.055	$0.373 \pm 1.0e-04$	0.014 ± 0.021	0.392 ± 0.396	0.001	8 ± 4	9 ± 4	4 ± 3	6 ± 3	1
XMMXCS J104044.4+395710.4	$0.137^{+0.028}_{-0.028}$	0.140 ± 0.022	$0.136 \pm 2.4e-05$	-0.033 ± 0.019	1.660 ± 0.332	0.052	15 ± 4	14 ± 4	15 ± 4	14 ± 4	1
XMMXCS J104422.2+213025.2	$0.432^{+0.113}_{-0.113}$	0.422 ± 0.070	$0.517 \pm 2.3e-04$	-0.175 ± 0.176	5.240 ± 3.530	0.001	15 ± 4	18 ± 5	15 ± 5	22 ± 6	1
XMMXCS J105040.6+573741.4	$0.607^{+0.114}_{-0.113}$	0.618 ± 0.103	-	0.026 ± 0.073	0.650 ± 1.410	0.001	3 ± 2	-	4 ± 2	-	1
XMMXCS J105128.6+355124.0	$0.388^{+0.085}_{-0.081}$	0.371 ± 0.078	$0.381 \pm 9.6e-05$	-0.006 ± 0.032	0.700 ± 0.601	0.090	3 ± 3	3 ± 4	3 ± 2	5 ± 3	1
XMMXCS J105655.6+065840.2	$0.281^{+0.074}_{-0.075}$	0.283 ± 0.064	-	-0.046 ± 0.067	2.350 ± 1.270	0.001	10 ± 3	1 ± 2	10 ± 3	3 ± 2	1
XMMXCS J110406.6+354433.0	$0.552^{+0.091}_{-0.091}$	0.596 ± 0.110	$0.537 \pm 1.7e-04$	-0.059 ± 0.098	2.180 ± 1.960	0.133	9 ± 4	12 ± 5	8 ± 3	15 ± 5	1
XMMXCS J110425.9+360026.3	$0.502^{+0.090}_{-0.088}$	0.562 ± 0.126	$0.499 \pm 1.3e-04$	-0.223 ± 0.139	5.220 ± 2.770	0.074	13 ± 4	-	14 ± 4	-	1
XMMXCS J111515.6+531949.5	$0.468^{+0.094}_{-0.093}$	0.493 ± 0.075	$0.467 \pm 7.4e-05$	-0.024 ± 0.022	1.260 ± 0.437	0.015	53 ± 8	58 ± 8	98 ± 11	99 ± 12	1
XMMXCS J111729.8+174451.4	$0.546^{+0.115}_{-0.115}$	0.505 ± 0.078	$0.542 \pm 1.6e-04$	-0.019 ± 0.069	1.330 ± 1.350	0.094	28 ± 6	41 ± 7	35 ± 7	53 ± 9	1
XMMXCS J112054.9+431820.8	$0.184^{+0.025}_{-0.025}$	0.189 ± 0.028	$0.186 \pm 2.3e-05$	-0.047 ± 0.009	2.040 ± 0.164	0.021	10 ± 3	10 ± 3	10 ± 3	9 ± 3	1
XMMXCS J113844.1+031540.5	$0.128^{+0.020}_{-0.020}$	0.134 ± 0.025	$0.128 \pm 1.5e-05$	-0.027 ± 0.017	1.480 ± 0.282	0.033	6 ± 3	5 ± 2	7 ± 3	4 ± 2	1
XMMXCS J115123.8+545008.7	$0.143^{+0.035}_{-0.035}$	0.160 ± 0.026	$0.143 \pm 2.1e-05$	-0.053 ± 0.011	2.010 ± 0.201	0.046	6 ± 3	7 ± 3	7 ± 3	7 ± 3	1
XMMXCS J115851.4+440537.2	$0.290^{+0.041}_{-0.042}$	0.305 ± 0.047	$0.290 \pm 5.8e-05$	-0.030 ± 0.023	2.140 ± 0.424	0.001	14 ± 4	12 ± 4	14 ± 4	12 ± 4	1

Continued on next page

Table A.1 – continued from previous page

name	z_{RS}	z_{BCG}	z_{spec-g}	cmr_{grad}	cmr_{inter}	cmr_{wid}	n_{gals-c}	n_{gals-l}	n_{200-c}	n_{200-l}	qual
XMMXCS J120210.3+442709.2	$0.409^{+0.065}_{-0.064}$	0.406 ± 0.061	$0.408 \pm 8.4e-05$	0.032 ± 0.021	0.085 ± 0.377	0.001	10 ± 4	10 ± 4	11 ± 4	11 ± 4	1
XMMXCS J120313.7+442717.8	$0.345^{+0.067}_{-0.067}$	0.352 ± 0.051	$0.345 \pm 7.6e-05$	-0.020 ± 0.046	2.030 ± 0.923	0.135	7 ± 3	6 ± 4	7 ± 3	6 ± 3	1
XMMXCS J120352.8+014706.5	$0.236^{+0.054}_{-0.053}$	0.245 ± 0.043	$0.247 \pm 2.4e-05$	-0.054 ± 0.019	2.370 ± 0.342	0.009	24 ± 5	25 ± 5	45 ± 7	44 ± 7	1
XMMXCS J120746.9+281320.0	$0.432^{+0.093}_{-0.091}$	0.455 ± 0.079	$0.462 \pm 1.2e-04$	-0.042 ± 0.030	1.560 ± 0.592	0.090	27 ± 6	31 ± 6	40 ± 8	41 ± 8	1
XMMXCS J120801.1+433926.7	$0.265^{+0.059}_{-0.059}$	0.261 ± 0.040	$0.266 \pm 5.6e-05$	-0.030 ± 0.023	2.000 ± 0.430	0.001	6 ± 3	7 ± 3	5 ± 2	5 ± 3	1
XMMXCS J120929.4+392803.6	$0.236^{+0.033}_{-0.033}$	0.237 ± 0.039	$0.237 \pm 5.3e-05$	-0.006 ± 0.014	1.480 ± 0.277	0.055	2 ± 2	2 ± 2	3 ± 2	3 ± 2	1
XMMXCS J120934.2+392232.8	$0.555^{+0.102}_{-0.101}$	0.540 ± 0.089	$0.554 \pm 7.9e-05$	0.024 ± 0.047	0.503 ± 0.937	0.086	15 ± 4	15 ± 5	16 ± 4	15 ± 5	1
XMMXCS J121205.4+131741.4	$0.452^{+0.083}_{-0.081}$	0.449 ± 0.066	$0.450 \pm 1.1e-04$	0.017 ± 0.055	0.384 ± 1.070	0.084	11 ± 4	11 ± 4	10 ± 4	10 ± 4	1
XMMXCS J121334.8+025349.8	$0.408^{+0.084}_{-0.084}$	0.424 ± 0.064	$0.407 \pm 1.5e-04$	-0.023 ± 0.064	2.150 ± 1.260	0.001	20 ± 5	25 ± 6	27 ± 6	-	1
XMMXCS J121744.6+472921.5	$0.270^{+0.061}_{-0.061}$	0.301 ± 0.048	$0.271 \pm 3.7e-05$	-0.043 ± 0.018	2.260 ± 0.353	0.085	21 ± 5	24 ± 5	30 ± 6	32 ± 6	1
XMMXCS J121754.5+472853.8	$0.268^{+0.061}_{-0.061}$	0.301 ± 0.048	$0.271 \pm 3.7e-05$	-0.056 ± 0.017	2.500 ± 0.317	0.008	14 ± 4	19 ± 5	15 ± 4	22 ± 5	1
XMMXCS J122443.8+071103.5	$0.659^{+0.101}_{-0.099}$	0.556 ± 0.090	$0.655 \pm 1.3e-04$	-0.075 ± 0.018	2.640 ± 0.356	0.001	3 ± 2	-	3 ± 2	-	1
XMMXCS J122528.1+004229.1	$0.236^{+0.044}_{-0.044}$	0.239 ± 0.037	$0.237 \pm 3.9e-05$	-0.042 ± 0.011	2.180 ± 0.200	0.068	14 ± 4	15 ± 4	15 ± 4	13 ± 4	1
XMMXCS J122643.3+334549.9	$0.510^{+0.102}_{-0.101}$	0.509 ± 0.081	$0.510 \pm 9.4e-05$	-0.013 ± 0.042	1.240 ± 0.832	0.063	13 ± 4	13 ± 4	16 ± 4	15 ± 5	1
XMMXCS J122656.4+334329.4	$0.504^{+0.100}_{-0.100}$	0.526 ± 0.117	$0.515 \pm 1.1e-04$	-0.015 ± 0.020	1.170 ± 0.403	0.059	18 ± 5	22 ± 5	25 ± 6	30 ± 6	1
XMMXCS J122944.6+133450.6	$0.442^{+0.090}_{-0.088}$	0.462 ± 0.069	$0.437 \pm 1.8e-04$	-0.103 ± 0.027	2.720 ± 0.540	0.041	5 ± 3	13 ± 5	4 ± 3	12 ± 5	1
XMMXCS J123019.6+161634.1	$0.203^{+0.052}_{-0.053}$	0.203 ± 0.033	$0.202 \pm 3.0e-05$	-0.055 ± 0.029	2.250 ± 0.538	0.069	20 ± 5	21 ± 5	22 ± 5	26 ± 5	1
XMMXCS J123105.3+155627.2	$0.191^{+0.043}_{-0.043}$	0.210 ± 0.038	$0.190 \pm 2.2e-05$	-0.065 ± 0.018	2.360 ± 0.314	0.061	25 ± 5	26 ± 5	39 ± 6	43 ± 7	1
XMMXCS J123144.4+413732.0	$0.175^{+0.043}_{-0.043}$	0.177 ± 0.026	$0.174 \pm 2.3e-05$	-0.031 ± 0.012	1.710 ± 0.209	0.001	12 ± 4	13 ± 4	12 ± 4	14 ± 4	1

Continued on next page

Table A.1 – continued from previous page

name	z_{RS}	z_{BCG}	z_{spec-g}	cmr_{grad}	cmr_{inter}	cmr_{wid}	n_{gals-c}	n_{gals-l}	n_{200-c}	n_{200-l}	qual
XMMXCS J123647.4+125614.1	$0.093^{+0.025}_{-0.025}$	0.117 ± 0.038	$0.093 \pm 1.4e-05$	0.060 ± 0.064	-0.169 ± 1.080	0.108	7 ± 3	6 ± 3	5 ± 2	5 ± 2	1
XMMXCS J124128.1-015822.0	$0.153^{+0.036}_{-0.036}$	0.164 ± 0.025	$0.153 \pm 1.8e-05$	-0.042 ± 0.010	1.840 ± 0.160	0.001	14 ± 4	14 ± 4	14 ± 4	14 ± 4	1
XMMXCS J124202.8+332203.7	$0.133^{+0.045}_{-0.044}$	0.122 ± 0.022	$0.141 \pm 1.7e-05$	-0.045 ± 0.025	1.770 ± 0.419	0.084	6 ± 3	7 ± 3	6 ± 3	9 ± 3	1
XMMXCS J124305.2+023312.9	$0.205^{+0.057}_{-0.057}$	0.219 ± 0.049	$0.206 \pm 3.4e-05$	-0.036 ± 0.065	1.970 ± 1.180	0.069	8 ± 3	3 ± 2	5 ± 2	2 ± 2	1
XMMXCS J124425.9+164758.0	$0.235^{+0.048}_{-0.047}$	0.240 ± 0.039	$0.235 \pm 3.7e-05$	-0.057 ± 0.021	2.380 ± 0.373	0.046	4 ± 2	5 ± 3	4 ± 2	5 ± 3	1
XMMXCS J124454.1-003330.3	$0.232^{+0.046}_{-0.046}$	0.248 ± 0.038	$0.232 \pm 3.4e-05$	-0.072 ± 0.022	2.680 ± 0.392	0.001	7 ± 3	7 ± 3	7 ± 3	12 ± 4	1
XMMXCS J125403.0+310150.0	$0.510^{+0.124}_{-0.123}$	0.533 ± 0.088	-	-0.176 ± 0.109	4.500 ± 2.190	0.001	7 ± 3	25 ± 6	8 ± 3	26 ± 6	1
XMMXCS J125621.5+254603.9	$0.224^{+0.063}_{-0.063}$	0.208 ± 0.048	-	-0.048 ± 0.034	2.220 ± 0.630	0.081	10 ± 3	10 ± 4	10 ± 3	10 ± 4	1
XMMXCS J125752.7+283010.6	$0.306^{+0.065}_{-0.065}$	0.306 ± 0.048	-	-0.060 ± 0.055	2.730 ± 1.040	0.001	13 ± 4	14 ± 4	14 ± 4	17 ± 5	1
XMMXCS J130150.1+585753.5	$0.225^{+0.079}_{-0.079}$	0.222 ± 0.061	-	-0.037 ± 0.030	1.980 ± 0.561	0.072	4 ± 2	4 ± 3	5 ± 2	5 ± 3	1
XMMXCS J130534.7+175658.6	$0.550^{+0.110}_{-0.109}$	0.574 ± 0.118	$0.529 \pm 1.2e-04$	-0.174 ± 0.057	4.370 ± 1.140	0.050	19 ± 5	49 ± 8	23 ± 5	186 ± 15	1
XMMXCS J130749.6+292549.2	$0.240^{+0.049}_{-0.050}$	0.242 ± 0.037	$0.241 \pm 5.4e-05$	0.003 ± 0.012	1.410 ± 0.218	0.010	12 ± 4	10 ± 4	12 ± 4	11 ± 4	1
XMMXCS J130832.6+534214.2	$0.321^{+0.088}_{-0.088}$	0.336 ± 0.058	-	-0.201 ± 0.107	5.580 ± 2.130	0.071	13 ± 4	13 ± 4	13 ± 4	13 ± 4	1
XMMXCS J130933.7+573926.3	$0.202^{+0.048}_{-0.047}$	0.192 ± 0.030	-	0.044 ± 0.052	0.415 ± 0.986	0.116	4 ± 2	3 ± 2	4 ± 2	3 ± 2	1
XMMXCS J131302.0+351943.1	$0.299^{+0.053}_{-0.054}$	0.312 ± 0.046	$0.299 \pm 5.8e-05$	-0.035 ± 0.015	2.230 ± 0.275	0.001	13 ± 4	14 ± 4	15 ± 4	11 ± 4	1
XMMXCS J131843.8-004356.7	$0.098^{+0.032}_{-0.032}$	0.094 ± 0.017	$0.099 \pm 1.2e-05$	-0.048 ± 0.013	1.730 ± 0.234	0.040	8 ± 3	8 ± 3	5 ± 2	5 ± 2	1
XMMXCS J132053.8+335521.0	$0.184^{+0.055}_{-0.056}$	0.185 ± 0.028	$0.185 \pm 3.8e-05$	0.004 ± 0.012	1.130 ± 0.227	0.041	12 ± 4	12 ± 4	12 ± 4	12 ± 4	1
XMMXCS J132434.0+053427.1	$0.228^{+0.035}_{-0.035}$	0.235 ± 0.036	$0.228 \pm 2.6e-05$	-0.055 ± 0.009	2.370 ± 0.179	0.012	10 ± 3	12 ± 4	9 ± 3	13 ± 4	1
XMMXCS J132958.9+241124.6	$0.166^{+0.046}_{-0.047}$	0.169 ± 0.030	$0.166 \pm 2.9e-05$	-0.027 ± 0.013	1.590 ± 0.219	0.046	6 ± 3	2 ± 2	5 ± 2	4 ± 2	1

Continued on next page

Table A.1 – continued from previous page

name	z_{RS}	z_{BCG}	z_{spec-g}	cmr_{grad}	cmr_{inter}	cmr_{wid}	n_{gals-c}	n_{gals-l}	n_{200-c}	n_{200-l}	qual
XMMXCS J133107.1-015837.4	$0.208^{+0.056}_{-0.057}$	0.192 ± 0.030	$0.203 \pm 1.9e-05$	0.031 ± 0.035	0.704 ± 0.630	0.077	4 ± 2	5 ± 3	3 ± 2	12 ± 4	1
XMMXCS J133254.8+503153.1	$0.279^{+0.058}_{-0.058}$	0.294 ± 0.044	$0.282 \pm 3.6e-05$	-0.012 ± 0.015	1.800 ± 0.274	0.025	35 ± 6	33 ± 6	75 ± 9	68 ± 9	1
XMMXCS J133505.3+502336.3	$0.088^{+0.012}_{-0.012}$	0.099 ± 0.018	$0.088 \pm 1.4e-05$	-0.048 ± 0.018	1.710 ± 0.296	0.037	10 ± 3	7 ± 3	8 ± 3	5 ± 2	1
XMMXCS J133559.1+375400.8	$0.254^{+0.062}_{-0.062}$	0.269 ± 0.043	$0.252 \pm 4.1e-05$	-0.134 ± 0.013	3.870 ± 0.247	0.001	7 ± 3	9 ± 3	5 ± 2	8 ± 3	1
XMMXCS J133909.2+481152.7	$0.412^{+0.069}_{-0.067}$	0.400 ± 0.072	$0.409 \pm 1.2e-04$	-0.021 ± 0.025	1.010 ± 0.501	0.031	8 ± 4	6 ± 4	7 ± 3	-	1
XMMXCS J134139.3+001733.9	$0.506^{+0.093}_{-0.093}$	0.510 ± 0.076	$0.505 \pm 5.0e-05$	-0.038 ± 0.029	1.650 ± 0.564	0.054	14 ± 4	15 ± 5	15 ± 5	14 ± 5	1
XMMXCS J135358.8+335003.1	$0.470^{+0.090}_{-0.090}$	0.474 ± 0.069	$0.470 \pm 1.2e-04$	-0.008 ± 0.022	0.996 ± 0.425	0.068	14 ± 4	20 ± 5	14 ± 5	22 ± 6	1
XMMXCS J140615.8+283049.1	$0.547^{+0.087}_{-0.086}$	0.564 ± 0.111	$0.546 \pm 1.2e-04$	-0.016 ± 0.059	1.240 ± 1.220	0.001	5 ± 3	-	5 ± 3	-	1
XMMXCS J140646.0+283308.3	$0.117^{+0.019}_{-0.019}$	0.117 ± 0.020	$0.116 \pm 1.5e-05$	-0.053 ± 0.016	1.870 ± 0.290	0.058	9 ± 3	8 ± 3	8 ± 3	7 ± 3	1
XMMXCS J141534.8+282335.2	$0.224^{+0.033}_{-0.033}$	0.236 ± 0.036	$0.224 \pm 2.9e-05$	-0.020 ± 0.031	1.710 ± 0.569	0.067	11 ± 4	10 ± 4	12 ± 4	10 ± 3	1
XMMXCS J141731.2+251139.1	$0.178^{+0.037}_{-0.037}$	0.197 ± 0.030	$0.178 \pm 4.3e-05$	-0.076 ± 0.012	2.480 ± 0.193	0.042	7 ± 3	5 ± 3	4 ± 2	3 ± 2	1
XMMXCS J141832.3+251104.9	$0.290^{+0.056}_{-0.057}$	0.314 ± 0.049	$0.291 \pm 6.7e-05$	-0.000 ± 0.024	1.600 ± 0.442	0.055	21 ± 5	21 ± 5	31 ± 6	30 ± 6	1
XMMXCS J141936.2+064736.8	$0.115^{+0.012}_{-0.012}$	0.125 ± 0.021	$0.115 \pm 1.4e-05$	-0.018 ± 0.005	1.300 ± 0.090	0.022	7 ± 3	8 ± 3	6 ± 3	8 ± 3	1
XMMXCS J142044.6+063101.0	$0.156^{+0.034}_{-0.034}$	0.146 ± 0.031	$0.156 \pm 4.0e-05$	-0.040 ± 0.033	1.770 ± 0.585	0.050	4 ± 2	3 ± 2	4 ± 2	3 ± 2	1
XMMXCS J142305.4+382807.0	$0.452^{+0.086}_{-0.085}$	0.424 ± 0.063	$0.451 \pm 1.4e-04$	0.141 ± 0.073	-2.060 ± 1.440	0.074	13 ± 4	13 ± 4	14 ± 5	-	1
XMMXCS J143102.1+421431.3	$0.427^{+0.080}_{-0.080}$	0.441 ± 0.063	$0.426 \pm 1.5e-04$	-0.008 ± 0.030	0.884 ± 0.576	0.031	20 ± 5	22 ± 5	21 ± 6	24 ± 6	1
XMMXCS J143432.3+033744.4	$0.294^{+0.064}_{-0.064}$	0.314 ± 0.049	$0.294 \pm 7.4e-05$	-0.195 ± 0.045	5.230 ± 0.875	0.001	4 ± 3	14 ± 4	4 ± 2	1 ± 3	1
XMMXCS J143714.4+341517.8	$0.541^{+0.083}_{-0.083}$	0.552 ± 0.108	$0.541 \pm 6.7e-05$	-0.016 ± 0.039	1.290 ± 0.758	0.001	16 ± 4	19 ± 5	18 ± 5	24 ± 6	1
XMMXCS J143724.6+341427.9	$0.362^{+0.063}_{-0.063}$	0.360 ± 0.059	-	0.098 ± 0.064	-0.222 ± 1.290	0.041	17 ± 4	16 ± 5	20 ± 5	20 ± 5	1

Continued on next page

Table A.1 – continued from previous page

name	z_{RS}	z_{BCG}	z_{spec-g}	cmr_{grad}	cmr_{inter}	cmr_{wid}	n_{gals-c}	n_{gals-l}	n_{200-c}	n_{200-l}	qual
XMMXCS J144016.2+034124.4	$0.280^{+0.067}_{-0.072}$	0.271 ± 0.050	$0.295 \pm 3.7e-05$	-0.042 ± 0.032	2.280 ± 0.607	0.085	19 ± 5	20 ± 5	20 ± 5	25 ± 6	1
XMMXCS J145505.6+184148.4	$0.238^{+0.045}_{-0.045}$	0.219 ± 0.044	$0.237 \pm 4.1e-05$	-0.038 ± 0.070	1.880 ± 1.300	0.152	5 ± 3	8 ± 4	4 ± 2	8 ± 3	1
XMMXCS J150215.2+422815.7	$0.242^{+0.062}_{-0.062}$	0.246 ± 0.036	$0.242 \pm 4.8e-05$	-0.064 ± 0.038	2.520 ± 0.699	0.022	8 ± 3	7 ± 3	6 ± 3	6 ± 3	1
XMMXCS J150701.6+010650.5	$0.185^{+0.038}_{-0.037}$	0.182 ± 0.027	$0.188 \pm 3.0e-05$	-0.140 ± 0.046	3.680 ± 0.826	0.059	9 ± 3	7 ± 3	7 ± 3	5 ± 3	1
XMMXCS J150824.8-001531.7	$0.090^{+0.003}_{-0.002}$	0.101 ± 0.021	$0.091 \pm 8.7e-06$	0.011 ± 0.016	0.772 ± 0.241	0.028	16 ± 4	16 ± 4	18 ± 4	18 ± 4	1
XMMXCS J151050.4+670633.0	$0.344^{+0.095}_{-0.095}$	0.361 ± 0.062	-	0.025 ± 0.052	1.110 ± 1.010	0.134	20 ± 5	18 ± 5	31 ± 6	27 ± 6	1
XMMXCS J151618.6+000531.3	$0.117^{+0.022}_{-0.021}$	0.129 ± 0.022	$0.118 \pm 1.3e-05$	-0.012 ± 0.004	1.210 ± 0.063	0.001	24 ± 5	24 ± 5	26 ± 5	26 ± 5	1
XMMXCS J153148.2+044314.4	$0.446^{+0.078}_{-0.074}$	0.399 ± 0.066	$0.442 \pm 2.3e-04$	-0.148 ± 0.035	4.410 ± 0.678	0.001	9 ± 4	17 ± 5	11 ± 4	26 ± 6	1
XMMXCS J153648.2+543718.7	$0.389^{+0.090}_{-0.087}$	0.378 ± 0.059	$0.383 \pm 1.3e-04$	-0.013 ± 0.040	0.865 ± 0.775	0.030	16 ± 5	12 ± 4	17 ± 5	12 ± 4	1
XMMXCS J161040.2+540613.2	$0.327^{+0.074}_{-0.076}$	0.348 ± 0.059	-	-0.044 ± 0.036	2.500 ± 0.698	0.001	15 ± 4	14 ± 4	17 ± 5	16 ± 5	1
XMMXCS J161554.1+121928.9	$0.369^{+0.056}_{-0.058}$	0.376 ± 0.060	$0.370 \pm 6.2e-05$	-0.082 ± 0.081	3.380 ± 1.570	0.001	18 ± 5	16 ± 4	25 ± 5	21 ± 5	1
XMMXCS J170041.9+641257.9	$0.235^{+0.054}_{-0.055}$	0.250 ± 0.038	$0.235 \pm 2.8e-05$	-0.022 ± 0.014	1.830 ± 0.248	0.031	15 ± 4	12 ± 4	18 ± 4	13 ± 4	1
XMMXCS J171437.9+623322.2	$0.176^{+0.029}_{-0.029}$	0.173 ± 0.029	$0.177 \pm 4.5e-05$	-0.012 ± 0.022	1.400 ± 0.393	0.063	6 ± 3	4 ± 2	4 ± 2	4 ± 2	1
XMMXCS J172335.9+341154.5	$0.443^{+0.059}_{-0.058}$	0.413 ± 0.070	$0.443 \pm 6.2e-05$	0.063 ± 0.059	0.581 ± 1.110	0.012	7 ± 3	9 ± 4	5 ± 3	7 ± 3	1
XMMXCS J200759.0-110256.5	$0.292^{+0.069}_{-0.069}$	0.282 ± 0.056	-	-0.030 ± 0.023	2.130 ± 0.437	0.001	6 ± 3	8 ± 3	5 ± 2	7 ± 3	1
XMMXCS J205405.9-154736.5	$0.223^{+0.056}_{-0.056}$	0.233 ± 0.052	-	-0.047 ± 0.027	2.220 ± 0.507	0.078	13 ± 4	14 ± 4	13 ± 4	18 ± 5	1
XMMXCS J213026.9-000032.0	$0.136^{+0.019}_{-0.019}$	0.145 ± 0.022	$0.135 \pm 1.6e-05$	-0.024 ± 0.007	1.470 ± 0.120	0.041	9 ± 3	13 ± 4	8 ± 3	14 ± 4	1
XMMXCS J220621.9-002540.0	$0.323^{+0.078}_{-0.079}$	0.336 ± 0.050	$0.387 \pm 7.7e-05$	-0.046 ± 0.035	2.540 ± 0.674	0.001	10 ± 4	23 ± 5	8 ± 3	6 ± 4	1
XMMXCS J220740.3+101814.4	$0.492^{+0.083}_{-0.083}$	0.501 ± 0.073	$0.492 \pm 7.9e-05$	-0.043 ± 0.025	1.670 ± 0.499	0.018	8 ± 4	14 ± 4	10 ± 4	13 ± 4	1

Continued on next page

Table A.1 – continued from previous page

name	z_{RS}	z_{BCG}	z_{spec-g}	cmr_{grad}	cmr_{inter}	cmr_{wid}	n_{gals-c}	n_{gals-l}	n_{200-c}	n_{200-l}	qual
XMMXCS J222818.7-050752.8	$0.203^{+0.050}_{-0.051}$	0.192 ± 0.030	-	0.036 ± 0.021	0.686 ± 0.347	0.103	5 ± 3	3 ± 3	3 ± 2	2 ± 2	1
XMMXCS J223924.4-054717.9	$0.241^{+0.055}_{-0.055}$	0.250 ± 0.042	-	-0.013 ± 0.028	1.660 ± 0.531	0.086	17 ± 4	18 ± 5	18 ± 5	21 ± 5	1
XMMXCS J223934.0-060017.5	$0.174^{+0.063}_{-0.065}$	0.155 ± 0.044	-	-0.045 ± 0.035	2.040 ± 0.656	0.095	6 ± 3	4 ± 2	5 ± 2	2 ± 2	1
XMMXCS J223939.3-054327.4	$0.256^{+0.058}_{-0.058}$	0.247 ± 0.037	-	-0.012 ± 0.016	1.660 ± 0.309	0.040	22 ± 5	20 ± 5	26 ± 5	23 ± 5	1
XMMXCS J224113.5+032832.5	$0.149^{+0.024}_{-0.024}$	0.171 ± 0.034	$0.162 \pm 1.4e-05$	-0.046 ± 0.017	1.930 ± 0.277	0.500	5 ± 3	6 ± 3	6 ± 3	7 ± 3	1
XMMXCS J232156.0+193807.8	$0.313^{+0.081}_{-0.082}$	0.324 ± 0.073	-	-0.019 ± 0.078	1.950 ± 1.510	0.065	5 ± 3	5 ± 3	5 ± 2	5 ± 3	1
XMMXCS J232221.3+193855.0	$0.184^{+0.045}_{-0.045}$	0.186 ± 0.031	-	-0.035 ± 0.028	1.870 ± 0.523	0.065	4 ± 2	2 ± 2	4 ± 2	2 ± 2	1
XMMXCS J232925.9+052624.1	$0.176^{+0.033}_{-0.033}$	0.188 ± 0.034	$0.177 \pm 2.3e-05$	-0.038 ± 0.009	1.800 ± 0.142	0.001	10 ± 3	14 ± 4	8 ± 3	15 ± 4	1
XMMXCS J233227.5+195822.1	$0.325^{+0.077}_{-0.078}$	0.345 ± 0.051	-	-0.021 ± 0.058	2.030 ± 1.090	0.001	13 ± 4	10 ± 4	13 ± 4	11 ± 4	1
XMMXCS J233757.0+271121.0	$0.122^{+0.039}_{-0.039}$	0.138 ± 0.025	-	-0.018 ± 0.010	1.290 ± 0.164	0.036	10 ± 3	11 ± 4	10 ± 3	11 ± 4	1
XMMXCS J001639.1-010211.5	$0.152^{+0.018}_{-0.018}$	0.166 ± 0.026	$0.152 \pm 1.7e-05$	-0.024 ± 0.002	1.570 ± 0.026	0.001	5 ± 2	5 ± 3	2 ± 2	3 ± 2	2
XMMXCS J010658.7+320934.0	$0.125^{+0.036}_{-0.036}$	0.086 ± 0.027	-	-0.008 ± 0.027	1.110 ± 0.486	0.068	9 ± 3	6 ± 3	9 ± 3	5 ± 2	2
XMMXCS J011632.1+330325.0	$0.413^{+0.165}_{-0.159}$	0.376 ± 0.158	-	0.297 ± 0.002	-4.230 ± 0.031	0.500	1 ± 3	4 ± 3	2 ± 1	3 ± 2	2
XMMXCS J011954.7+141655.1	$0.600^{+0.165}_{-0.166}$	0.551 ± 0.090	-	-0.032 ± 0.112	1.650 ± 2.240	0.130	4 ± 3	10 ± 5	3 ± 2	12 ± 5	2
XMMXCS J012400.0+035110.8	$0.095^{+0.029}_{-0.029}$	0.072 ± 0.028	-	0.093 ± 0.023	-0.721 ± 0.377	0.017	1 ± 1	1 ± 1	1 ± 1	1 ± 1	2
XMMXCS J014449.2-043246.1	$0.118^{+0.042}_{-0.042}$	0.155 ± 0.027	-	-0.090 ± 0.028	2.600 ± 0.459	0.082	3 ± 2	4 ± 2	4 ± 2	5 ± 2	2
XMMXCS J021518.8-003813.2	$0.358^{+0.076}_{-0.071}$	0.362 ± 0.054	$0.349 \pm 5.0e-05$	-0.037 ± 0.049	1.300 ± 0.917	0.001	3 ± 3	5 ± 4	2 ± 2	2 ± 2	2
XMMXCS J022023.2-025025.4	$0.192^{+0.084}_{-0.085}$	0.203 ± 0.069	-	-0.037 ± 0.037	1.860 ± 0.682	0.001	1 ± 1	0 ± 1	1 ± 1	-	2
XMMXCS J022038.8-030145.9	$0.522^{+0.060}_{-0.060}$	0.477 ± 0.073	$0.522 \pm 1.4e-04$	-0.077 ± 0.071	2.400 ± 1.400	0.001	9 ± 4	18 ± 5	7 ± 3	14 ± 5	2

Continued on next page

Table A.1 – continued from previous page

name	z_{RS}	z_{BCG}	z_{spec-g}	cmr_{grad}	cmr_{inter}	cmr_{wid}	n_{gals-c}	n_{gals-l}	n_{200-c}	n_{200-l}	qual
XMMXCS J022204.3-043239.6	$0.320^{+0.092}_{-0.093}$	0.304 ± 0.048	$0.319 \pm 6.3e-05$	-0.110 ± 0.030	3.560 ± 0.582	0.064	4 ± 3	5 ± 3	1 ± 1	4 ± 2	2
XMMXCS J022401.9-050528.4	$0.328^{+0.056}_{-0.053}$	0.320 ± 0.051	$0.324 \pm 5.3e-05$	-0.169 ± 0.014	4.690 ± 0.262	0.500	8 ± 4	7 ± 4	2 ± 3	2 ± 3	2
XMMXCS J022457.8-034851.1	$0.512^{+0.130}_{-0.129}$	0.548 ± 0.182	-	-0.661 ± 0.176	14.600 ± 3.630	0.001	8 ± 3	17 ± 5	9 ± 3	24 ± 6	2
XMMXCS J022618.3-040000.1	$0.168^{+0.061}_{-0.061}$	0.210 ± 0.037	$0.209 \pm 2.7e-05$	0.066 ± 0.082	-0.081 ± 1.520	0.116	5 ± 3	3 ± 2	4 ± 2	3 ± 2	2
XMMXCS J022726.7-043209.1	$0.260^{+0.061}_{-0.061}$	0.222 ± 0.039	-	0.183 ± 0.037	-1.970 ± 0.728	0.097	6 ± 3	8 ± 3	8 ± 3	9 ± 3	2
XMMXCS J022738.5-031801.3	$0.605^{+0.118}_{-0.118}$	0.583 ± 0.124	-	0.751 ± 0.540	-14.30 ± 11.10	0.258	1 ± 2	9 ± 3	1 ± 1	2 ± 2	2
XMMXCS J030332.8-005735.5	$0.661^{+0.177}_{-0.178}$	0.672 ± 0.118	-	-0.046 ± 0.155	2.290 ± 3.040	0.084	3 ± 2	10 ± 4	2 ± 1	11 ± 4	2
XMMXCS J030637.3-001816.7	$0.422^{+0.091}_{-0.090}$	0.464 ± 0.068	$0.458 \pm 2.0e-04$	0.027 ± 0.054	0.216 ± 1.090	0.067	11 ± 4	10 ± 4	11 ± 4	11 ± 4	2
XMMXCS J051545.1-001036.1	$0.523^{+0.128}_{-0.127}$	0.562 ± 0.128	-	0.054 ± 0.072	-0.066 ± 1.460	0.085	8 ± 3	12 ± 4	9 ± 3	12 ± 4	2
XMMXCS J051610.0+010954.0	$0.283^{+0.070}_{-0.070}$	0.313 ± 0.047	-	-0.102 ± 0.027	3.460 ± 0.518	0.072	8 ± 3	6 ± 3	5 ± 3	4 ± 3	2
XMMXCS J064423.6+822626.5	$0.250^{+0.068}_{-0.071}$	0.246 ± 0.043	-	0.002 ± 0.015	1.400 ± 0.284	0.001	2 ± 2	1 ± 2	2 ± 1	2 ± 2	2
XMMXCS J073605.8+433910.2	$0.379^{+0.088}_{-0.087}$	0.443 ± 0.064	$0.428 \pm 6.0e-05$	-0.023 ± 0.045	1.080 ± 0.899	0.088	16 ± 5	14 ± 5	16 ± 5	14 ± 5	2
XMMXCS J074725.2+310146.5	$0.338^{+0.059}_{-0.059}$	0.343 ± 0.054	$0.338 \pm 4.7e-05$	-0.051 ± 0.032	2.670 ± 0.604	0.001	6 ± 3	9 ± 4	2 ± 2	8 ± 3	2
XMMXCS J085741.3+090109.0	$0.205^{+0.114}_{-0.117}$	0.175 ± 0.046	-	-0.101 ± 0.184	2.980 ± 3.550	0.060	3 ± 2	2 ± 2	2 ± 1	0 ± 1	2
XMMXCS J090101.5+600606.2	$0.279^{+0.050}_{-0.050}$	0.318 ± 0.048	$0.279 \pm 5.6e-05$	-0.050 ± 0.030	2.480 ± 0.547	0.061	10 ± 4	13 ± 4	10 ± 3	14 ± 4	2
XMMXCS J091609.0+302718.1	$0.630^{+0.168}_{-0.169}$	0.600 ± 0.099	-	-0.013 ± 0.058	1.310 ± 1.150	0.001	7 ± 3	127 ± 12	7 ± 3	90 ± 13	2
XMMXCS J092111.0+302758.2	$0.395^{+0.085}_{-0.084}$	0.422 ± 0.061	$0.429 \pm 9.7e-05$	-0.052 ± 0.035	2.630 ± 0.675	0.070	28 ± 6	29 ± 6	57 ± 8	56 ± 9	2
XMMXCS J092540.0+362711.1	$0.115^{+0.017}_{-0.017}$	0.127 ± 0.024	$0.112 \pm 1.1e-05$	-0.022 ± 0.006	1.370 ± 0.096	0.001	3 ± 2	4 ± 2	1 ± 1	1 ± 1	2
XMMXCS J093449.2+551023.5	$0.623^{+0.153}_{-0.152}$	0.587 ± 0.241	-	-0.014 ± 0.169	1.430 ± 3.420	0.001	5 ± 3	-	5 ± 2	-	2

Continued on next page

Table A.1 – continued from previous page

name	z_{RS}	z_{BCG}	z_{spec-g}	cmr_{grad}	cmr_{inter}	cmr_{wid}	n_{gals-c}	n_{gals-l}	n_{200-c}	n_{200-l}	qual
XMMXCS J094311.2+480956.1	$0.314^{+0.065}_{-0.065}$	0.300 ± 0.068	$0.309 \pm 6.0e-05$	0.022 ± 0.040	1.160 ± 0.733	0.156	9 ± 4	10 ± 4	10 ± 4	11 ± 4	2
XMMXCS J095904.2+023814.3	$0.365^{+0.074}_{-0.073}$	0.323 ± 0.049	-	0.017 ± 0.152	1.190 ± 2.980	0.070	1 ± 2	1 ± 2	1 ± 1	2 ± 2	2
XMMXCS J095940.8+023111.3	$0.595^{+0.158}_{-0.158}$	0.564 ± 0.282	-	0.201 ± 0.253	-2.720 ± 5.110	0.001	9 ± 3	24 ± 5	9 ± 3	29 ± 6	2
XMMXCS J095957.6+251629.0	$0.092^{+0.025}_{-0.026}$	0.059 ± 0.021	$0.066 \pm 1.3e-05$	0.013 ± 0.045	0.633 ± 0.778	0.063	7 ± 3	4 ± 2	6 ± 3	3 ± 2	2
XMMXCS J100029.2+024137.4	$0.229^{+0.110}_{-0.115}$	0.187 ± 0.132	-	-0.001 ± 0.150	1.300 ± 2.960	0.180	4 ± 3	0 ± 3	3 ± 2	-	2
XMMXCS J100116.2+021655.9	$0.090^{+0.058}_{-0.050}$	0.165 ± 0.037	$0.106 \pm 1.4e-05$	-0.112 ± 0.001	2.520 ± 0.001	0.500	3 ± 2	1 ± 2	3 ± 2	1 ± 1	2
XMMXCS J101041.8+554208.5	$0.168^{+0.044}_{-0.044}$	0.185 ± 0.032	$0.178 \pm 4.0e-05$	-0.037 ± 0.037	1.820 ± 0.698	0.095	1 ± 2	3 ± 2	2 ± 1	3 ± 2	2
XMMXCS J101056.3+555711.5	$0.137^{+0.050}_{-0.050}$	0.150 ± 0.034	$0.174 \pm 1.5e-05$	0.169 ± 0.066	-2.150 ± 1.190	0.108	2 ± 2	1 ± 2	1 ± 1	0 ± 1	2
XMMXCS J103930.7+394743.7	$0.093^{+0.011}_{-0.011}$	0.098 ± 0.019	$0.093 \pm 1.5e-05$	0.012 ± 0.029	0.717 ± 0.500	0.068	3 ± 2	2 ± 2	1 ± 1	3 ± 2	2
XMMXCS J104551.5+213350.5	$0.438^{+0.085}_{-0.083}$	0.481 ± 0.073	$0.472 \pm 2.1e-04$	-0.008 ± 0.046	0.901 ± 0.919	0.116	7 ± 4	7 ± 4	4 ± 3	4 ± 3	2
XMMXCS J105236.6+573054.3	$0.535^{+0.185}_{-0.194}$	0.493 ± 0.112	-	-0.187 ± 0.123	4.660 ± 2.520	0.113	12 ± 4	34 ± 6	12 ± 4	39 ± 8	2
XMMXCS J110954.0+482704.6	$0.515^{+0.155}_{-0.155}$	0.542 ± 0.110	-	0.184 ± 0.078	-2.850 ± 1.590	0.001	15 ± 4	55 ± 8	20 ± 5	92 ± 11	2
XMMXCS J111726.0+074327.7	$0.441^{+0.085}_{-0.085}$	0.475 ± 0.069	-	0.017 ± 0.037	0.432 ± 0.743	0.093	22 ± 5	27 ± 6	30 ± 7	-	2
XMMXCS J111729.7+074632.1	$0.160^{+0.029}_{-0.029}$	0.152 ± 0.024	$0.159 \pm 3.0e-05$	-0.068 ± 0.045	2.220 ± 0.760	0.084	5 ± 3	6 ± 3	2 ± 2	3 ± 2	2
XMMXCS J112259.3+465916.8	$0.448^{+0.102}_{-0.101}$	0.477 ± 0.077	-	-0.052 ± 0.036	1.830 ± 0.721	0.078	17 ± 5	17 ± 5	19 ± 5	19 ± 5	2
XMMXCS J114643.9+472600.8	$0.536^{+0.120}_{-0.116}$	0.573 ± 0.109	-	0.317 ± 0.183	-5.450 ± 3.780	0.124	5 ± 3	9 ± 4	2 ± 2	8 ± 4	2
XMMXCS J115103.3+551124.9	$0.230^{+0.054}_{-0.054}$	0.187 ± 0.087	-	0.005 ± 0.048	1.300 ± 0.901	0.059	5 ± 3	4 ± 3	3 ± 2	5 ± 2	2
XMMXCS J115112.0+550655.5	$0.079^{+0.020}_{-0.019}$	0.075 ± 0.015	$0.078 \pm 1.1e-05$	-0.013 ± 0.007	1.060 ± 0.112	0.032	2 ± 2	3 ± 2	1 ± 1	4 ± 2	2
XMMXCS J115824.6+440533.9	$0.352^{+0.077}_{-0.077}$	0.309 ± 0.105	-	0.072 ± 0.080	0.183 ± 1.590	0.097	8 ± 3	12 ± 4	6 ± 3	12 ± 4	2

Continued on next page

Table A.1 – continued from previous page

name	z_{RS}	z_{BCG}	z_{spec-g}	cmr_{grad}	cmr_{inter}	cmr_{wid}	n_{gals-c}	n_{gals-l}	n_{200-c}	n_{200-l}	qual
XMMXCS J120532.3+441910.3	$0.331^{+0.070}_{-0.071}$	0.359 ± 0.055	$0.334 \pm 9.3e-05$	0.039 ± 0.034	0.950 ± 0.687	0.052	8 ± 3	8 ± 3	9 ± 3	9 ± 3	2
XMMXCS J120606.8+441923.8	$0.281^{+0.051}_{-0.052}$	0.329 ± 0.051	-	0.021 ± 0.087	1.210 ± 1.640	0.041	3 ± 2	0 ± 2	4 ± 2	-	2
XMMXCS J121156.7+502918.8	$0.096^{+0.015}_{-0.015}$	0.106 ± 0.017	$0.089 \pm 1.3e-05$	-0.027 ± 0.022	1.430 ± 0.351	0.051	2 ± 2	1 ± 1	2 ± 1	2 ± 2	2
XMMXCS J123018.7+110102.5	$0.167^{+0.038}_{-0.038}$	0.165 ± 0.024	$0.167 \pm 4.9e-05$	-0.026 ± 0.016	1.610 ± 0.276	0.023	2 ± 2	2 ± 2	2 ± 1	2 ± 2	2
XMMXCS J123236.3+000224.7	$0.656^{+0.126}_{-0.123}$	0.651 ± 0.134	$0.650 \pm 2.0e-04$	0.019 ± 0.120	0.948 ± 2.470	0.112	4 ± 2	-	2 ± 1	-	2
XMMXCS J124024.7-114806.6	$0.160^{+0.046}_{-0.047}$	0.186 ± 0.035	-	-0.027 ± 0.045	1.670 ± 0.848	0.089	1 ± 2	3 ± 2	1 ± 1	2 ± 2	2
XMMXCS J125650.2+254803.2	$0.283^{+0.098}_{-0.098}$	0.279 ± 0.046	$0.283 \pm 3.8e-05$	-0.029 ± 0.029	1.960 ± 0.575	0.084	1 ± 2	4 ± 3	2 ± 1	2 ± 2	2
XMMXCS J125933.2+283039.3	$0.605^{+0.149}_{-0.149}$	0.640 ± 0.132	-	0.087 ± 0.087	-0.435 ± 1.640	0.058	11 ± 3	29 ± 6	11 ± 3	26 ± 6	2
XMMXCS J130106.9+281808.3	$0.218^{+0.067}_{-0.070}$	0.218 ± 0.039	-	-0.006 ± 0.016	1.420 ± 0.289	0.001	6 ± 3	5 ± 3	2 ± 2	0 ± 1	2
XMMXCS J132830.2+470357.2	$0.365^{+0.075}_{-0.074}$	0.398 ± 0.068	-	-0.011 ± 0.017	0.851 ± 0.335	0.022	11 ± 4	12 ± 4	10 ± 4	11 ± 4	2
XMMXCS J134124.3-010204.0	$0.282^{+0.075}_{-0.078}$	0.307 ± 0.047	$0.285 \pm 3.5e-05$	0.007 ± 0.041	1.350 ± 0.768	0.089	7 ± 3	10 ± 4	2 ± 2	9 ± 4	2
XMMXCS J134645.9+264625.7	$0.382^{+0.105}_{-0.104}$	0.426 ± 0.063	$0.427 \pm 1.2e-04$	-0.098 ± 0.070	3.470 ± 1.320	0.001	5 ± 3	-	6 ± 3	-	2
XMMXCS J135541.9+182545.4	$0.302^{+0.074}_{-0.076}$	0.274 ± 0.043	-	-0.006 ± 0.061	1.700 ± 1.140	0.001	8 ± 3	0 ± 2	7 ± 3	-	2
XMMXCS J135546.0+182250.8	$0.311^{+0.070}_{-0.072}$	0.326 ± 0.051	-	-0.021 ± 0.028	1.980 ± 0.539	0.001	5 ± 3	7 ± 3	2 ± 2	4 ± 3	2
XMMXCS J140935.2+262941.9	$0.132^{+0.026}_{-0.026}$	0.136 ± 0.021	$0.131 \pm 1.6e-05$	0.018 ± 0.028	0.762 ± 0.454	0.063	4 ± 2	4 ± 2	1 ± 1	3 ± 2	2
XMMXCS J141313.2-031803.8	$0.307^{+0.059}_{-0.061}$	0.338 ± 0.054	$0.309 \pm 6.3e-05$	-0.030 ± 0.035	2.240 ± 0.664	0.072	6 ± 3	6 ± 3	6 ± 3	7 ± 3	2
XMMXCS J141458.4+440317.5	$0.393^{+0.079}_{-0.078}$	0.362 ± 0.066	-	-0.006 ± 0.036	0.836 ± 0.714	0.001	4 ± 3	5 ± 3	5 ± 2	6 ± 3	2
XMMXCS J142024.0+063241.5	$0.151^{+0.094}_{-0.103}$	0.115 ± 0.020	$0.229 \pm 4.1e-05$	-0.007 ± 0.030	1.030 ± 0.547	0.091	4 ± 2	2 ± 2	2 ± 1	0 ± 1	2
XMMXCS J142551.8+380246.3	$0.488^{+0.090}_{-0.089}$	0.445 ± 0.091	$0.487 \pm 1.4e-04$	0.270 ± 0.269	-4.470 ± 5.320	0.193	16 ± 5	20 ± 5	18 ± 5	20 ± 6	2

Continued on next page

Table A.1 – continued from previous page

name	z_{RS}	z_{BCG}	z_{spec-g}	cmr_{grad}	cmr_{inter}	cmr_{wid}	n_{gals-c}	n_{gals-l}	n_{200-c}	n_{200-l}	qual
XMMXCS J143603.2+632538.0	$0.123^{+0.028}_{-0.028}$	0.169 ± 0.099	$0.124 \pm 1.0e-05$	0.041 ± 0.001	0.265 ± 0.001	0.500	3 ± 3	14 ± 4	4 ± 2	14 ± 4	2
XMMXCS J144940.0+084744.6	$0.280^{+0.067}_{-0.069}$	0.263 ± 0.051	-	0.091 ± 0.110	-0.248 ± 2.140	0.102	2 ± 2	0 ± 2	1 ± 1	-	2
XMMXCS J153455.1+232844.4	$0.066^{+0.023}_{-0.023}$	0.075 ± 0.030	$0.048 \pm 9.4e-06$	0.046 ± 0.013	0.237 ± 0.188	0.077	5 ± 2	7 ± 3	3 ± 2	5 ± 2	2
XMMXCS J154233.1+535919.9	$0.624^{+0.163}_{-0.163}$	0.587 ± 0.153	-	-0.055 ± 0.065	2.440 ± 1.290	0.001	14 ± 4	42 ± 7	14 ± 4	31 ± 7	2
XMMXCS J160129.8+083856.3	$0.188^{+0.042}_{-0.042}$	0.197 ± 0.030	$0.188 \pm 3.3e-05$	-0.029 ± 0.009	1.800 ± 0.153	0.001	4 ± 2	3 ± 2	2 ± 1	0 ± 1	2
XMMXCS J161132.7+541628.3	$0.324^{+0.078}_{-0.078}$	0.355 ± 0.054	-	-0.074 ± 0.029	3.100 ± 0.555	0.071	28 ± 6	26 ± 5	34 ± 6	32 ± 6	2
XMMXCS J163210.3+340022.3	$0.190^{+0.041}_{-0.041}$	0.196 ± 0.030	$0.190 \pm 4.2e-05$	-0.077 ± 0.027	2.620 ± 0.475	0.077	4 ± 2	6 ± 3	2 ± 2	3 ± 2	2
XMMXCS J220605.0-001113.4	$0.389^{+0.073}_{-0.072}$	0.368 ± 0.056	$0.388 \pm 1.0e-04$	-0.015 ± 0.033	1.930 ± 0.661	0.001	2 ± 2	3 ± 3	2 ± 2	4 ± 2	2
XMMXCS J222818.2-053403.4	$0.497^{+0.144}_{-0.144}$	0.528 ± 0.091	-	-0.044 ± 0.092	1.820 ± 1.830	0.111	23 ± 5	47 ± 7	30 ± 6	54 ± 9	2
XMMXCS J230247.7+084355.9	$0.598^{+0.161}_{-0.157}$	0.565 ± 0.165	-	0.131 ± 0.307	-1.510 ± 6.230	0.074	3 ± 2	-	2 ± 1	-	2
XMMXCS J232124.6+194514.8	$0.315^{+0.067}_{-0.068}$	0.355 ± 0.060	-	-0.015 ± 0.020	1.870 ± 0.379	0.001	24 ± 5	22 ± 5	33 ± 6	28 ± 6	2
XMMXCS J235537.0+055129.0	$0.279^{+0.077}_{-0.077}$	0.310 ± 0.048	$0.279 \pm 6.2e-05$	-0.028 ± 0.030	2.010 ± 0.568	0.046	14 ± 4	18 ± 5	14 ± 4	21 ± 5	2
XMMXCS J000626.2+195944.2	$0.464^{+0.078}_{-0.073}$	0.492 ± 0.073	-	-0.473 ± 0.193	10.100 ± 3.780	0.044	4 ± 3	-	2 ± 2	-	3
XMMXCS J005730.1+301321.6	$0.131^{+0.038}_{-0.038}$	0.069 ± 0.027	-	0.026 ± 0.039	0.568 ± 0.684	0.093	4 ± 2	3 ± 3	3 ± 2	2 ± 2	3
XMMXCS J010422.4-063004.5	$0.672^{+0.182}_{-0.180}$	0.577 ± 0.129	-	-11.30 ± 20.30	237 ± 424	1.504	3 ± 2	0 ± 1	2 ± 1	-	3
XMMXCS J011023.8+330544.1	$0.117^{+0.051}_{-0.057}$	0.082 ± 0.017	-	-0.023 ± 0.009	1.200 ± 0.129	0.086	1 ± 2	-	0 ± 0.1	-	3
XMMXCS J014615.5-044031.9	$0.589^{+0.169}_{-0.170}$	0.644 ± 0.128	-	-0.234 ± 0.313	5.990 ± 6.320	0.121	6 ± 3	23 ± 5	3 ± 2	43 ± 7	3
XMMXCS J015653.3+284339.3	$0.242^{+0.071}_{-0.072}$	0.243 ± 0.041	-	-0.006 ± 0.012	1.560 ± 0.212	0.001	0 ± 1	1 ± 2	-	1 ± 1	3
XMMXCS J015746.3+284918.1	$0.323^{+0.107}_{-0.109}$	0.405 ± 0.064	-	-0.324 ± 0.111	8.080 ± 2.320	0.091	4 ± 2	5 ± 3	2 ± 2	3 ± 2	3

Continued on next page

Table A.1 – continued from previous page

name	z_{RS}	z_{BCG}	z_{spec-g}	cmr_{grad}	cmr_{inter}	cmr_{wid}	n_{gals-c}	n_{gals-l}	n_{200-c}	n_{200-l}	qual
XMMXCS J015951.9+001655.4	$0.478^{+0.145}_{-0.150}$	0.346 ± 0.133	-	0.226 ± 0.098	-3.770 ± 1.960	0.117	8 ± 4	9 ± 4	5 ± 3	6 ± 3	3
XMMXCS J020019.1+001931.8	$0.705^{+0.121}_{-0.112}$	0.600 ± 0.116	$0.682 \pm 1.7e-04$	-0.027 ± 0.095	1.680 ± 1.950	0.091	1 ± 2	9 ± 4	0 ± 0.1	10 ± 4	3
XMMXCS J020719.8+292240.4	$0.572^{+0.133}_{-0.129}$	0.661 ± 0.156	-	0.027 ± 0.242	0.392 ± 4.980	0.001	5 ± 3	1 ± 1	5 ± 2	0 ± 1	3
XMMXCS J021020.7-000706.5	$0.246^{+0.074}_{-0.074}$	0.191 ± 0.031	-	0.031 ± 0.042	0.787 ± 0.811	0.105	3 ± 2	2 ± 2	1 ± 1	2 ± 2	3
XMMXCS J021045.5-002202.1	$0.261^{+0.064}_{-0.064}$	0.184 ± 0.104	$0.152 \pm 5.4e-05$	0.253 ± 0.145	-3.610 ± 2.960	0.044	0 ± 2	1 ± 2	-	1 ± 1	3
XMMXCS J021659.3-044920.0	$0.383^{+0.098}_{-0.080}$	0.234 ± 0.081	-	0.005 ± 0.118	1.130 ± 2.340	0.106	1 ± 2	1 ± 3	1 ± 1	2 ± 2	3
XMMXCS J021734.7-051326.9	$0.571^{+0.121}_{-0.120}$	0.197 ± 0.165	$0.546 \pm 1.3e-04$	0.231 ± 0.046	-3.650 ± 0.925	0.001	7 ± 3	12 ± 4	6 ± 3	12 ± 4	3
XMMXCS J021759.3-045215.9	$0.134^{+0.062}_{-0.063}$	0.071 ± 0.046	$0.098 \pm 1.8e-05$	0.081 ± 0.021	-0.425 ± 0.406	0.068	1 ± 1	2 ± 2	0 ± 0.1	0 ± 1	3
XMMXCS J021832.4-050054.1	$0.531^{+0.154}_{-0.154}$	0.332 ± 0.057	$0.515 \pm 1.5e-04$	0.489 ± 0.280	-8.820 ± 5.600	0.231	11 ± 4	26 ± 6	10 ± 4	27 ± 6	3
XMMXCS J022252.8-032831.2	$0.548^{+0.143}_{-0.136}$	0.352 ± 0.077	-	0.233 ± 0.229	-3.710 ± 4.660	0.146	5 ± 3	11 ± 4	0 ± 1	11 ± 4	3
XMMXCS J022307.7-041259.4	$0.562^{+0.102}_{-0.101}$	0.489 ± 0.083	$0.564 \pm 1.2e-04$	0.112 ± 0.169	-1.200 ± 3.360	0.104	5 ± 3	-	3 ± 2	-	3
XMMXCS J022427.3-045028.1	$0.352^{+0.129}_{-0.129}$	0.276 ± 0.105	-	0.155 ± 0.081	-2.550 ± 1.620	0.001	6 ± 3	6 ± 3	2 ± 2	3 ± 3	3
XMMXCS J022509.7-040137.6	$0.173^{+0.032}_{-0.032}$	0.174 ± 0.026	$0.173 \pm 1.7e-05$	-0.058 ± 0.005	2.120 ± 0.092	0.001	1 ± 1	2 ± 2	1 ± 1	3 ± 2	3
XMMXCS J022827.3-042542.2	$0.371^{+0.095}_{-0.095}$	0.444 ± 0.067	$0.434 \pm 7.4e-05$	0.055 ± 0.056	0.542 ± 1.100	0.133	23 ± 5	23 ± 5	24 ± 6	23 ± 6	3
XMMXCS J024835.6+311917.0	$0.343^{+0.083}_{-0.083}$	0.273 ± 0.042	-	0.001 ± 0.109	1.630 ± 2.080	0.056	38 ± 7	37 ± 7	47 ± 8	42 ± 8	3
XMMXCS J030145.5+000335.8	$0.256^{+0.090}_{-0.093}$	0.292 ± 0.078	-	-0.063 ± 0.045	2.650 ± 0.843	0.001	1 ± 1	0 ± 1	0 ± 0.1	-	3
XMMXCS J030205.1-000003.6	$0.593^{+0.147}_{-0.147}$	0.647 ± 0.115	-	-0.021 ± 0.139	1.620 ± 2.840	0.119	12 ± 4	39 ± 7	12 ± 4	56 ± 9	3
XMMXCS J030211.4-000134.3	$0.403^{+0.132}_{-0.131}$	0.249 ± 0.164	-	0.522 ± 0.209	-9.200 ± 4.170	0.211	13 ± 4	82 ± 9	14 ± 5	-	3
XMMXCS J030317.4+001238.4	$0.534^{+0.117}_{-0.115}$	0.464 ± 0.068	$0.605 \pm 2.2e-04$	0.011 ± 0.139	0.730 ± 2.840	0.153	7 ± 3	15 ± 5	7 ± 3	20 ± 6	3

Continued on next page

Table A.1 – continued from previous page

name	z_{RS}	z_{BCG}	z_{spec-g}	cmr_{grad}	cmr_{inter}	cmr_{wid}	n_{gals-c}	n_{gals-l}	n_{200-c}	n_{200-l}	qual
XMMXCS J030659.8+000824.9	$0.204^{+0.085}_{-0.093}$	0.082 ± 0.019	$0.119 \pm 1.6e-05$	0.042 ± 0.062	0.458 ± 1.160	0.118	4 ± 3	4 ± 3	3 ± 2	4 ± 2	3
XMMXCS J064010.9+822902.2	$0.420^{+0.090}_{-0.090}$	0.387 ± 0.059	-	-0.026 ± 0.051	2.330 ± 1.050	0.001	0 ± 2	1 ± 2	-	3 ± 2	3
XMMXCS J073524.1+435311.5	$0.131^{+0.034}_{-0.034}$	0.147 ± 0.032	$0.191 \pm 2.8e-05$	0.007 ± 0.056	0.868 ± 1.040	0.090	7 ± 3	6 ± 3	6 ± 3	5 ± 2	3
XMMXCS J074603.6+305244.5	$0.222^{+0.065}_{-0.066}$	0.213 ± 0.039	$0.224 \pm 2.8e-05$	-0.006 ± 0.034	1.470 ± 0.636	0.075	3 ± 2	4 ± 3	0 ± 1	3 ± 2	3
XMMXCS J083025.9+524128.4	$0.499^{+0.085}_{-0.087}$	0.351 ± 0.100	$0.501 \pm 1.7e-04$	0.604 ± 0.159	-11.30 ± 3.250	0.119	2 ± 3	11 ± 4	0 ± 1	16 ± 5	3
XMMXCS J083855.9+253803.9	$0.167^{+0.075}_{-0.076}$	0.064 ± 0.025	-	0.337 ± 0.062	-5.220 ± 1.140	0.059	1 ± 1	2 ± 2	1 ± 1	0 ± 1	3
XMMXCS J084711.2+344842.4	$0.477^{+0.137}_{-0.137}$	0.578 ± 0.160	-	-0.049 ± 0.028	1.880 ± 0.545	0.113	24 ± 5	25 ± 6	35 ± 7	38 ± 7	3
XMMXCS J091836.8+515041.2	$0.357^{+0.103}_{-0.102}$	0.423 ± 0.062	$0.436 \pm 8.4e-05$	-0.023 ± 0.021	1.070 ± 0.426	0.052	10 ± 4	8 ± 4	8 ± 3	6 ± 3	3
XMMXCS J092641.4+310308.8	$0.205^{+0.085}_{-0.085}$	0.263 ± 0.042	$0.279 \pm 8.6e-05$	-0.163 ± 0.101	4.250 ± 1.930	0.106	5 ± 3	4 ± 3	1 ± 1	1 ± 2	3
XMMXCS J092703.2+310039.2	$0.519^{+0.099}_{-0.098}$	0.616 ± 0.121	-	-0.259 ± 0.032	6.150 ± 0.642	0.001	4 ± 3	8 ± 4	3 ± 2	10 ± 4	3
XMMXCS J093350.2+552620.1	$0.533^{+0.146}_{-0.142}$	0.462 ± 0.142	-	-0.131 ± 0.124	3.430 ± 2.460	0.113	6 ± 3	-	5 ± 3	-	3
XMMXCS J093722.2+611416.7	$0.218^{+0.069}_{-0.072}$	0.211 ± 0.032	$0.208 \pm 4.0e-05$	0.032 ± 0.026	0.676 ± 0.503	0.110	5 ± 3	7 ± 3	0 ± 1	0 ± 2	3
XMMXCS J095343.6+694735.0	$0.241^{+0.072}_{-0.072}$	0.374 ± 0.183	-	-0.001 ± 0.042	1.450 ± 0.813	0.072	14 ± 4	17 ± 4	16 ± 4	20 ± 5	3
XMMXCS J100022.8+021156.2	$0.478^{+0.140}_{-0.140}$	0.402 ± 0.092	-	0.256 ± 0.255	-4.210 ± 5.240	0.133	4 ± 3	3 ± 3	5 ± 2	5 ± 3	3
XMMXCS J100201.7+021332.8	$0.260^{+0.096}_{-0.099}$	0.237 ± 0.055	$0.221 \pm 3.0e-05$	-0.027 ± 0.047	1.790 ± 0.932	0.129	4 ± 3	3 ± 3	0 ± 0.1	1 ± 2	3
XMMXCS J102400.4+040222.6	$0.380^{+0.128}_{-0.127}$	0.324 ± 0.069	-	0.169 ± 0.055	-2.670 ± 1.100	0.042	8 ± 3	9 ± 4	9 ± 3	8 ± 3	3
XMMXCS J102711.1-031905.2	$0.060^{+0.025}_{-0.025}$	0.076 ± 0.041	-	-0.013 ± 0.006	0.992 ± 0.079	0.011	6 ± 3	9 ± 3	5 ± 2	11 ± 3	3
XMMXCS J103254.0+501738.7	$0.472^{+0.104}_{-0.100}$	0.611 ± 0.124	-	0.104 ± 0.199	-1.330 ± 4.150	0.130	6 ± 3	6 ± 3	2 ± 2	2 ± 2	3
XMMXCS J104545.4+063441.3	$0.209^{+0.061}_{-0.062}$	0.213 ± 0.033	$0.212 \pm 5.0e-05$	0.084 ± 0.015	-0.051 ± 0.281	0.001	0 ± 1	1 ± 2	-	1 ± 1	3

Continued on next page

Table A.1 – continued from previous page

name	z_{RS}	z_{BCG}	z_{spec-g}	cmr_{grad}	cmr_{inter}	cmr_{wid}	n_{gals-c}	n_{gals-l}	n_{200-c}	n_{200-l}	qual
XMMXCS J105227.6+441905.1	$0.498^{+0.094}_{-0.094}$	0.448 ± 0.069	$0.480 \pm 6.2e-05$	0.020 ± 0.047	0.522 ± 0.947	0.088	23 ± 5	30 ± 6	34 ± 7	47 ± 8	3
XMMXCS J105318.5+572043.7	$0.294^{+0.082}_{-0.085}$	0.280 ± 0.052	-	-0.054 ± 0.101	2.680 ± 2.010	0.129	1 ± 2	1 ± 2	0 ± 0.1	2 ± 2	3
XMMXCS J111711.5+423610.5	$0.174^{+0.041}_{-0.043}$	0.156 ± 0.030	-	-0.034 ± 0.031	1.850 ± 0.554	0.017	1 ± 1	2 ± 2	0 ± 0.1	1 ± 1	3
XMMXCS J113055.2+311334.1	$0.676^{+0.120}_{-0.105}$	0.680 ± 0.131	-	-0.068 ± 0.140	2.130 ± 2.810	0.105	1 ± 2	-	2 ± 1	-	3
XMMXCS J115131.6+014814.5	$0.166^{+0.052}_{-0.053}$	0.222 ± 0.058	-	-0.031 ± 0.042	1.710 ± 0.772	0.063	6 ± 3	7 ± 3	4 ± 2	5 ± 2	3
XMMXCS J123050.9+413410.8	$0.401^{+0.138}_{-0.144}$	0.239 ± 0.037	-	0.285 ± 5.890	-5.170 ± 123	0.500	0 ± 3	3 ± 4	-	2 ± 2	3
XMMXCS J123338.5+374114.9	$0.100^{+0.047}_{-0.048}$	0.118 ± 0.024	$0.102 \pm 2.6e-05$	-0.064 ± 0.013	2.000 ± 0.211	0.001	0 ± 1	1 ± 1	-	0 ± 1	3
XMMXCS J125047.4+263353.4	$0.415^{+0.098}_{-0.097}$	0.474 ± 0.072	-	-0.065 ± 0.050	1.980 ± 0.971	0.027	10 ± 4	8 ± 4	10 ± 4	12 ± 4	3
XMMXCS J130515.1+180215.5	$0.427^{+0.123}_{-0.122}$	0.310 ± 0.055	-	0.120 ± 0.051	-1.610 ± 0.996	0.092	7 ± 4	14 ± 5	6 ± 3	13 ± 5	3
XMMXCS J130527.1+673519.8	$0.266^{+0.090}_{-0.091}$	0.140 ± 0.068	-	0.148 ± 0.061	-1.510 ± 1.190	0.134	3 ± 3	4 ± 3	2 ± 2	3 ± 2	3
XMMXCS J130601.4+180145.9	$0.099^{+0.026}_{-0.025}$	0.128 ± 0.031	$0.132 \pm 5.8e-06$	0.192 ± 0.014	-2.340 ± 0.230	0.021	2 ± 2	0 ± 1	0 ± 0.1	-	3
XMMXCS J131028.4-011906.9	$0.139^{+0.021}_{-0.021}$	0.084 ± 0.019	$0.112 \pm 1.5e-05$	0.034 ± 0.048	0.386 ± 0.874	0.123	6 ± 3	7 ± 3	6 ± 3	6 ± 3	3
XMMXCS J131058.5+572043.8	$0.514^{+0.107}_{-0.107}$	0.444 ± 0.067	-	0.218 ± 0.131	-3.400 ± 2.610	0.079	18 ± 5	55 ± 8	25 ± 6	98 ± 11	3
XMMXCS J132420.7+301240.3	$0.683^{+0.190}_{-0.190}$	0.665 ± 0.149	-	-0.565 ± 0.081	12.500 ± 1.600	0.001	4 ± 2	11 ± 5	2 ± 2	12 ± 5	3
XMMXCS J132458.2+300723.2	$0.538^{+0.156}_{-0.158}$	0.393 ± 0.101	-	0.051 ± 0.159	-0.042 ± 3.270	0.107	8 ± 3	16 ± 5	3 ± 2	17 ± 5	3
XMMXCS J133439.5+504327.1	$0.251^{+0.089}_{-0.088}$	0.233 ± 0.074	-	-0.027 ± 0.059	2.140 ± 1.190	0.001	1 ± 1	1 ± 2	1 ± 1	1 ± 1	3
XMMXCS J133457.7+375020.3	$0.368^{+0.079}_{-0.079}$	0.292 ± 0.049	$0.383 \pm 7.9e-05$	-0.008 ± 0.043	1.850 ± 0.865	0.116	8 ± 3	11 ± 4	8 ± 3	10 ± 4	3
XMMXCS J133514.1+374905.8	$0.351^{+0.083}_{-0.083}$	0.258 ± 0.053	-	-0.010 ± 0.028	1.810 ± 0.530	0.086	4 ± 3	5 ± 3	0 ± 1	4 ± 3	3
XMMXCS J133605.0+514531.2	$0.350^{+0.100}_{-0.099}$	0.235 ± 0.036	$0.234 \pm 3.6e-05$	0.163 ± 0.149	-1.390 ± 2.550	0.311	7 ± 4	5 ± 4	6 ± 3	18 ± 5	3

Continued on next page

Table A.1 – continued from previous page

name	z_{RS}	z_{BCG}	z_{spec-g}	cmr_{grad}	cmr_{inter}	cmr_{wid}	n_{gals-c}	n_{gals-l}	n_{200-c}	n_{200-l}	qual
XMMXCS J134305.1-000056.8	$0.719^{+0.139}_{-0.137}$	0.648 ± 0.115	-	-0.060 ± 0.032	2.380 ± 0.643	0.001	13 ± 4	54 ± 8	13 ± 4	83 ± 11	3
XMMXCS J134326.9+554648.3	$0.065^{+0.014}_{-0.009}$	0.071 ± 0.015	$0.068 \pm 1.4e-05$	-0.001 ± 0.024	0.917 ± 0.392	0.037	3 ± 2	1 ± 1	1 ± 1	0 ± 1	3
XMMXCS J134825.6+580015.8	$0.128^{+0.022}_{-0.022}$	0.136 ± 0.023	$0.111 \pm 1.6e-05$	-0.026 ± 0.018	1.490 ± 0.280	0.049	3 ± 2	3 ± 2	3 ± 2	4 ± 2	3
XMMXCS J134851.8+600942.5	$0.373^{+0.096}_{-0.096}$	0.436 ± 0.071	-	-0.061 ± 0.094	2.740 ± 1.780	0.001	3 ± 3	3 ± 3	3 ± 2	3 ± 2	3
XMMXCS J134949.7+270605.3	$0.423^{+0.084}_{-0.083}$	0.346 ± 0.053	-	0.080 ± 0.085	-0.049 ± 1.700	0.098	13 ± 4	18 ± 5	14 ± 4	22 ± 6	3
XMMXCS J143743.2+340807.8	$0.544^{+0.042}_{-0.043}$	0.591 ± 0.132	$0.544 \pm 8.4e-05$	-0.045 ± 0.059	1.890 ± 1.130	0.001	6 ± 3	6 ± 4	3 ± 2	4 ± 3	3
XMMXCS J145009.3+090428.8	$0.644^{+0.138}_{-0.135}$	0.511 ± 0.260	-	0.388 ± 0.647	-6.870 ± 13.40	0.119	4 ± 2	1 ± 1	5 ± 2	0 ± 1	3
XMMXCS J150652.9+014424.8	$0.557^{+0.146}_{-0.143}$	0.627 ± 0.201	-	0.374 ± 0.053	-6.710 ± 1.080	0.001	5 ± 2	0 ± 1	6 ± 2	-	3
XMMXCS J150918.3-001432.7	$0.253^{+0.062}_{-0.062}$	0.145 ± 0.023	-	0.038 ± 0.087	0.564 ± 1.650	0.076	11 ± 4	9 ± 4	10 ± 4	8 ± 3	3
XMMXCS J151547.1+001529.3	$0.322^{+0.090}_{-0.085}$	0.131 ± 0.035	-	-0.000 ± 0.001	1.700 ± 0.001	0.500	6 ± 4	8 ± 4	9 ± 4	10 ± 4	3
XMMXCS J153629.7+543920.8	$0.338^{+0.092}_{-0.091}$	0.269 ± 0.046	$0.409 \pm 1.3e-04$	-0.146 ± 0.069	4.360 ± 1.370	0.143	7 ± 3	0 ± 2	5 ± 3	-	3
XMMXCS J154932.2+213302.5	$0.555^{+0.123}_{-0.122}$	0.544 ± 0.103	-	0.152 ± 0.078	-1.930 ± 1.580	0.119	2 ± 2	4 ± 3	-	7 ± 3	3
XMMXCS J163341.0+571420.1	$0.205^{+0.125}_{-0.079}$	0.262 ± 0.056	-	-0.100 ± 0.059	3.270 ± 1.090	0.046	0 ± 1	1 ± 2	-	0 ± 1	3
XMMXCS J171246.1+435334.3	$0.252^{+0.066}_{-0.069}$	0.170 ± 0.039	-	0.003 ± 0.078	1.340 ± 1.530	0.125	2 ± 2	0 ± 1	0 ± 0.1	-	3
XMMXCS J173602.6+655941.1	$0.581^{+0.167}_{-0.168}$	0.487 ± 0.320	-	-0.047 ± 0.158	2.240 ± 3.270	0.137	2 ± 2	-	1 ± 1	-	3
XMMXCS J220550.0-015930.4	$0.522^{+0.145}_{-0.153}$	0.354 ± 0.166	$0.607 \pm 2.0e-04$	-0.011 ± 0.133	0.870 ± 2.680	0.070	4 ± 3	3 ± 4	2 ± 2	9 ± 3	3
XMMXCS J232152.6+195334.9	$0.273^{+0.061}_{-0.061}$	0.127 ± 0.031	-	0.248 ± 0.158	-3.160 ± 2.970	0.193	14 ± 4	14 ± 5	17 ± 5	18 ± 5	3
XMMXCS J232231.6+195043.8	$0.198^{+0.059}_{-0.063}$	0.215 ± 0.046	-	-0.007 ± 0.028	1.380 ± 0.526	0.072	1 ± 2	3 ± 2	0 ± 0.1	0 ± 1	3
XMMXCS J233537.0+021738.1	$0.333^{+0.090}_{-0.090}$	0.377 ± 0.059	$0.384 \pm 6.1e-05$	-0.080 ± 0.046	3.170 ± 0.873	0.001	13 ± 4	15 ± 4	14 ± 4	15 ± 4	3

Table A.2 *A table of GMPhoRCC characterisations for the preliminary XCS DR2 sources using SDSS DR10 optical data. Of the* 7227 *with coverage, characterisations were found for* 3882 *with spectroscopic redshifts found for* 1893*. The clean subset comprises* 1203 *extended X-ray sources,* 904 *with spectra.*

name	z_{RS}	z_{BCG}	z_{spec-g}	cmr_{grad}	cmr_{inter}	cmr_{wid}	n_{gals-c}	n_{gals-l}	n_{200-c}	n_{200-l}	qual
XMMXCS J000349.3+020403.5	$0.116^{+0.030}_{-0.030}$	0.132 ± 0.039	$0.098 \pm 1.4e-05$	-0.023 ± 0.013	1.360 ± 0.217	0.043	15 ± 4	15 ± 4	17 ± 4	23 ± 5	1
XMMXCS J000521.4+201503.1	$0.390^{+0.085}_{-0.085}$	0.408 ± 0.062	-	-0.029 ± 0.098	2.210 ± 1.880	0.021	10 ± 4	10 ± 4	10 ± 4	10 ± 4	1
XMMXCS J001116.1+005211.3	$0.364^{+0.061}_{-0.061}$	0.379 ± 0.057	$0.365 \pm 1.2e-04$	-0.128 ± 0.056	4.300 ± 1.070	0.001	9 ± 3	9 ± 4	5 ± 3	5 ± 3	1
XMMXCS J001737.4-005235.4	$0.212^{+0.047}_{-0.048}$	0.229 ± 0.038	$0.211 \pm 3.8e-05$	-0.049 ± 0.016	2.230 ± 0.287	0.054	21 ± 5	19 ± 5	28 ± 6	22 ± 5	1
XMMXCS J001738.0-004856.5	$0.210^{+0.040}_{-0.041}$	0.223 ± 0.037	$0.200 \pm 3.7e-05$	-0.005 ± 0.021	1.360 ± 0.386	0.089	15 ± 4	15 ± 4	20 ± 5	18 ± 5	1
XMMXCS J001817.2+161744.2	$0.555^{+0.128}_{-0.129}$	0.562 ± 0.092	-	0.082 ± 0.045	-0.489 ± 0.858	0.091	7 ± 3	12 ± 4	6 ± 3	12 ± 4	1
XMMXCS J001847.99+160215.5	$0.541^{+0.100}_{-0.099}$	0.571 ± 0.096	$0.541 \pm 1.9e-04$	-0.039 ± 0.021	1.800 ± 0.391	0.001	14 ± 4	28 ± 6	14 ± 4	49 ± 8	1
XMMXCS J001848.2+160201.7	$0.542^{+0.112}_{-0.111}$	0.571 ± 0.096	$0.541 \pm 1.9e-04$	-0.053 ± 0.018	2.080 ± 0.362	0.001	16 ± 4	32 ± 6	16 ± 5	42 ± 8	1
XMMXCS J001919.91+162445.9	$0.333^{+0.085}_{-0.085}$	0.345 ± 0.051	-	0.052 ± 0.112	0.687 ± 2.160	0.042	11 ± 4	10 ± 4	11 ± 4	11 ± 4	1
XMMXCS J001919.9+162445.9	$0.333^{+0.085}_{-0.085}$	0.345 ± 0.051	-	0.052 ± 0.112	0.687 ± 2.160	0.042	11 ± 4	10 ± 4	11 ± 4	11 ± 4	1
XMMXCS J002113.4-082751.3	$0.093^{+0.062}_{-0.064}$	0.102 ± 0.032	-	0.046 ± 0.001	-0.216 ± 0.013	0.500	3 ± 2	3 ± 2	3 ± 2	3 ± 2	1
XMMXCS J002213.8-150543.3	$0.463^{+0.171}_{-0.171}$	0.485 ± 0.171	-	0.044 ± 0.104	0.006 ± 2.080	0.097	16 ± 5	19 ± 5	19 ± 5	28 ± 6	1
XMMXCS J002314.1+001201.5	$0.260^{+0.052}_{-0.052}$	0.250 ± 0.039	$0.258 \pm 2.9e-05$	-0.032 ± 0.013	2.020 ± 0.239	0.001	12 ± 4	14 ± 4	12 ± 4	15 ± 4	1
XMMXCS J002650.0+171931.3	$0.474^{+0.115}_{-0.113}$	0.474 ± 0.146	-	-0.058 ± 0.036	1.940 ± 0.724	0.090	6 ± 4	-	5 ± 3	-	1
XMMXCS J002742.9+171016.6	$0.141^{+0.029}_{-0.029}$	0.165 ± 0.030	-	-0.035 ± 0.025	1.680 ± 0.436	0.047	6 ± 3	4 ± 2	5 ± 2	4 ± 2	1

Continued on next page

Table A.2 – continued from previous page

name	z_{RS}	z_{BCG}	z_{spec-g}	cmr_{grad}	cmr_{inter}	cmr_{wid}	n_{gals-c}	n_{gals-l}	n_{200-c}	n_{200-l}	qual
XMMXCS J002944.7+045222.1	$0.206^{+0.052}_{-0.053}$	0.210 ± 0.034	$0.206 \pm 3.2e-05$	-0.046 ± 0.029	2.140 ± 0.543	0.061	4 ± 2	5 ± 3	4 ± 2	5 ± 3	1
XMMXCS J002953.9+350507.5	$0.491^{+0.131}_{-0.130}$	0.471 ± 0.086	-	-0.031 ± 0.064	1.470 ± 1.250	0.058	21 ± 5	30 ± 6	21 ± 6	32 ± 7	1
XMMXCS J003054.0+262306.1	$0.508^{+0.152}_{-0.152}$	0.509 ± 0.078	-	-0.062 ± 0.050	2.070 ± 0.995	0.001	5 ± 3	13 ± 4	5 ± 3	12 ± 4	1
XMMXCS J003614.6+091408.9	$0.436^{+0.072}_{-0.072}$	0.439 ± 0.094	$0.436 \pm 1.1e-04$	0.087 ± 0.140	0.248 ± 2.700	0.067	21 ± 5	23 ± 5	30 ± 6	48 ± 8	1
XMMXCS J003647.5+090242.2	$0.389^{+0.093}_{-0.090}$	0.363 ± 0.057	$0.389 \pm 6.0e-05$	0.023 ± 0.042	0.239 ± 0.816	0.001	7 ± 3	6 ± 4	6 ± 3	4 ± 3	1
XMMXCS J003706.3+090924.6	$0.249^{+0.058}_{-0.058}$	0.292 ± 0.047	$0.255 \pm 3.2e-05$	0.031 ± 0.037	0.889 ± 0.684	0.077	37 ± 6	40 ± 7	54 ± 8	59 ± 8	1
XMMXCS J003800.3+091540.1	$0.373^{+0.081}_{-0.081}$	0.352 ± 0.059	$0.373 \pm 9.7e-05$	-0.061 ± 0.045	2.920 ± 0.863	0.025	13 ± 4	11 ± 4	15 ± 4	12 ± 4	1
XMMXCS J003805.1+091241.5	$0.364^{+0.097}_{-0.105}$	0.333 ± 0.055	$0.361 \pm 7.2e-05$	0.127 ± 0.153	-0.922 ± 3.100	0.213	11 ± 4	13 ± 5	10 ± 4	16 ± 5	1
XMMXCS J003841.0+004740.4	$0.556^{+0.094}_{-0.093}$	0.577 ± 0.121	$0.555 \pm 8.0e-05$	-0.112 ± 0.067	3.180 ± 1.330	0.047	7 ± 3	11 ± 4	7 ± 3	11 ± 4	1
XMMXCS J003921.9+411140.1	$0.552^{+0.160}_{-0.159}$	0.573 ± 0.170	-	0.038 ± 0.122	0.183 ± 2.480	0.133	31 ± 7	55 ± 9	68 ± 10	167 ± 16	1
XMMXCS J003922.1+004806.5	$0.414^{+0.056}_{-0.055}$	0.356 ± 0.065	$0.413 \pm 8.3e-05$	-0.028 ± 0.051	2.070 ± 0.947	0.001	14 ± 5	13 ± 5	15 ± 5	13 ± 5	1
XMMXCS J003942.0+411607.1	$0.249^{+0.079}_{-0.080}$	0.264 ± 0.058	-	0.033 ± 0.071	0.806 ± 1.400	0.092	5 ± 3	4 ± 2	4 ± 2	5 ± 2	1
XMMXCS J004038.9+253104.5	$0.169^{+0.055}_{-0.056}$	0.165 ± 0.027	-	-0.031 ± 0.019	1.670 ± 0.352	0.062	12 ± 4	14 ± 4	12 ± 4	16 ± 4	1
XMMXCS J004102.3+252715.9	$0.141^{+0.038}_{-0.039}$	0.144 ± 0.025	-	-0.049 ± 0.020	1.930 ± 0.349	0.030	20 ± 5	22 ± 5	28 ± 5	33 ± 6	1
XMMXCS J004104.3+252254.5	$0.119^{+0.025}_{-0.025}$	0.130 ± 0.021	-	-0.006 ± 0.025	1.060 ± 0.432	0.059	14 ± 4	13 ± 4	17 ± 4	13 ± 4	1
XMMXCS J004110.2+401403.8	$0.263^{+0.100}_{-0.105}$	0.281 ± 0.060	-	-0.051 ± 0.039	2.400 ± 0.751	0.103	7 ± 3	5 ± 3	4 ± 2	2 ± 2	1
XMMXCS J004119.5+252618.9	$0.137^{+0.031}_{-0.031}$	0.144 ± 0.025	-	-0.008 ± 0.015	1.200 ± 0.266	0.056	20 ± 5	22 ± 5	22 ± 5	26 ± 5	1
XMMXCS J004130.5-091548.4	$0.056^{+0.006}_{-0.005}$	0.079 ± 0.022	$0.055 \pm 1.2e-05$	-0.025 ± 0.013	1.220 ± 0.204	0.046	17 ± 4	11 ± 3	17 ± 4	9 ± 3	1
XMMXCS J004134.0-092212.4	$0.057^{+0.044}_{-0.044}$	0.061 ± 0.017	$0.052 \pm 7.9e-06$	-0.025 ± 0.005	1.210 ± 0.080	0.049	16 ± 4	13 ± 4	23 ± 5	15 ± 4	1

Continued on next page

Table A.2 – continued from previous page

name	z_{RS}	z_{BCG}	z_{spec-g}	cmr_{grad}	cmr_{inter}	cmr_{wid}	n_{gals-c}	n_{gals-l}	n_{200-c}	n_{200-l}	qual
XMMXCS J004137.0-091932.1	$0.052^{+0.008}_{-0.008}$	0.075 ± 0.081	$0.053 \pm 1.4e-05$	0.001 ± 0.019	0.823 ± 0.305	0.044	24 ± 5	20 ± 5	32 ± 6	21 ± 5	1
XMMXCS J004144.6-092113.6	$0.057^{+0.045}_{-0.043}$	0.075 ± 0.081	-	-0.008 ± 0.008	0.934 ± 0.139	0.062	22 ± 5	23 ± 5	34 ± 6	33 ± 6	1
XMMXCS J004146.6+401612.6	$0.123^{+0.038}_{-0.039}$	0.112 ± 0.026	-	0.005 ± 0.079	0.935 ± 1.370	0.094	4 ± 2	1 ± 2	4 ± 2	3 ± 2	1
XMMXCS J004148.6-092742.6	$0.056^{+0.007}_{-0.007}$	0.076 ± 0.017	$0.058 \pm 1.2e-05$	-0.017 ± 0.005	1.100 ± 0.085	0.036	16 ± 4	14 ± 4	17 ± 4	14 ± 4	1
XMMXCS J004155.7+253143.0	$0.135^{+0.040}_{-0.040}$	0.120 ± 0.019	-	-0.050 ± 0.019	1.880 ± 0.338	0.053	9 ± 3	13 ± 4	9 ± 3	12 ± 4	1
XMMXCS J004200.6-091933.1	$0.059^{+0.021}_{-0.025}$	0.075 ± 0.081	$0.053 \pm 1.4e-05$	0.016 ± 0.009	0.560 ± 0.148	0.043	21 ± 5	22 ± 5	33 ± 6	31 ± 6	1
XMMXCS J004204.4-091644.6	$0.057^{+0.006}_{-0.006}$	0.075 ± 0.081	$0.061 \pm 9.1e-06$	-0.007 ± 0.002	0.937 ± 0.029	0.001	19 ± 5	18 ± 4	28 ± 5	25 ± 5	1
XMMXCS J004207.1-093022.6	$0.438^{+0.082}_{-0.080}$	0.428 ± 0.066	$0.435 \pm 8.3e-05$	0.114 ± 0.180	-0.586 ± 3.470	0.191	20 ± 5	22 ± 6	23 ± 6	31 ± 7	1
XMMXCS J004220.1+401920.9	$0.650^{+0.194}_{-0.205}$	0.663 ± 0.180	-	0.445 ± 0.126	-7.700 ± 2.570	0.195	6 ± 4	18 ± 6	4 ± 3	36 ± 8	1
XMMXCS J004231.6+005119.9	$0.151^{+0.023}_{-0.024}$	0.159 ± 0.026	$0.151 \pm 2.2e-05$	-0.028 ± 0.009	1.600 ± 0.149	0.006	8 ± 3	8 ± 3	7 ± 3	8 ± 3	1
XMMXCS J004249.3-203307.5	$0.315^{+0.089}_{-0.085}$	0.305 ± 0.049	-	0.385 ± 0.333	-6.000 ± 6.420	0.281	5 ± 3	64 ± 8	4 ± 3	4 ± 7	1
XMMXCS J004252.6+004303.1	$0.271^{+0.040}_{-0.040}$	0.275 ± 0.042	$0.270 \pm 4.0e-05$	-0.048 ± 0.050	2.320 ± 0.963	0.114	12 ± 4	38 ± 7	12 ± 4	11 ± 5	1
XMMXCS J004253.5-093413.5	$0.390^{+0.096}_{-0.096}$	0.401 ± 0.060	-	-0.029 ± 0.056	2.360 ± 1.070	0.001	11 ± 4	14 ± 4	11 ± 4	14 ± 4	1
XMMXCS J004324.6-094449.8	$0.183^{+0.038}_{-0.038}$	0.185 ± 0.028	$0.182 \pm 2.4e-05$	-0.056 ± 0.021	2.160 ± 0.364	0.001	5 ± 2	6 ± 3	6 ± 2	6 ± 3	1
XMMXCS J004333.7+010109.6	$0.196^{+0.033}_{-0.032}$	0.203 ± 0.030	$0.196 \pm 2.1e-05$	-0.079 ± 0.023	2.650 ± 0.420	0.042	8 ± 3	10 ± 3	7 ± 3	8 ± 3	1
XMMXCS J004337.1+403800.2	$0.321^{+0.109}_{-0.110}$	0.322 ± 0.053	-	0.028 ± 0.136	0.826 ± 2.740	0.148	10 ± 4	15 ± 5	11 ± 4	15 ± 5	1
XMMXCS J004338.9-001201.3	$0.397^{+0.091}_{-0.090}$	0.407 ± 0.059	$0.396 \pm 7.2e-05$	-0.043 ± 0.029	1.490 ± 0.565	0.009	15 ± 5	16 ± 5	17 ± 5	18 ± 5	1
XMMXCS J004359.3+000706.8	$0.218^{+0.044}_{-0.045}$	0.226 ± 0.036	$0.218 \pm 2.0e-05$	-0.087 ± 0.030	2.940 ± 0.569	0.031	15 ± 4	17 ± 4	16 ± 4	20 ± 5	1
XMMXCS J004535.8+405156.4	$0.344^{+0.109}_{-0.110}$	0.345 ± 0.056	-	-0.033 ± 0.088	2.250 ± 1.740	0.085	6 ± 3	7 ± 3	5 ± 3	5 ± 3	1

Continued on next page

Table A.2 – continued from previous page

name	z_{RS}	z_{BCG}	z_{spec-g}	cmr_{grad}	cmr_{inter}	cmr_{wid}	n_{gals-c}	n_{gals-l}	n_{200-c}	n_{200-l}	qual
XMMXCS J004602.2+040106.6	$0.217^{+0.082}_{-0.081}$	0.198 ± 0.058	-	0.282 ± 0.096	-4.200 ± 1.870	0.074	3 ± 2	3 ± 2	3 ± 2	2 ± 2	1
XMMXCS J004727.6+415258.6	$0.556^{+0.162}_{-0.163}$	0.551 ± 0.097	-	0.078 ± 0.067	-0.612 ± 1.380	0.132	11 ± 5	48 ± 8	8 ± 4	127 ± 15	1
XMMXCS J004728.3+412455.7	$0.314^{+0.074}_{-0.075}$	0.305 ± 0.051	-	-0.012 ± 0.110	1.770 ± 2.150	0.020	8 ± 3	10 ± 4	6 ± 3	8 ± 3	1
XMMXCS J005259.6-083934.2	$0.314^{+0.066}_{-0.067}$	0.321 ± 0.047	$0.316 \pm 9.4e-05$	0.034 ± 0.039	1.070 ± 0.734	0.001	7 ± 3	6 ± 3	4 ± 2	4 ± 2	1
XMMXCS J005414.6+251508.9	$0.166^{+0.040}_{-0.040}$	0.163 ± 0.028	-	-0.046 ± 0.021	1.920 ± 0.348	0.063	4 ± 2	5 ± 3	3 ± 2	3 ± 2	1
XMMXCS J005545.8+003840.8	$0.068^{+0.001}_{-0.001}$	0.089 ± 0.023	$0.067 \pm 6.4e-06$	-0.066 ± 0.020	1.910 ± 0.325	0.068	11 ± 3	14 ± 4	11 ± 3	13 ± 4	1
XMMXCS J005550.1-012821.8	$0.384^{+0.095}_{-0.094}$	0.374 ± 0.056	$0.418 \pm 1.1e-04$	0.142 ± 0.125	-1.140 ± 2.470	0.181	18 ± 5	19 ± 5	19 ± 5	21 ± 6	1
XMMXCS J005551.6+262449.0	$0.196^{+0.049}_{-0.049}$	0.211 ± 0.052	-	0.0001 ± 0.013	1.240 ± 0.245	0.033	14 ± 4	22 ± 5	19 ± 4	40 ± 7	1
XMMXCS J005557.3+003825.2	$0.066^{+0.035}_{-0.035}$	0.089 ± 0.023	$0.059 \pm 5.7e-06$	-0.019 ± 0.009	1.150 ± 0.155	0.078	9 ± 3	11 ± 3	8 ± 3	11 ± 3	1
XMMXCS J005602.2+262736.0	$0.190^{+0.046}_{-0.046}$	0.212 ± 0.033	-	-0.038 ± 0.024	1.960 ± 0.419	0.048	15 ± 4	19 ± 5	19 ± 4	30 ± 6	1
XMMXCS J005602.3+262300.7	$0.197^{+0.051}_{-0.052}$	0.195 ± 0.051	-	-0.032 ± 0.015	1.850 ± 0.272	0.051	25 ± 5	28 ± 5	48 ± 7	26 ± 5	1
XMMXCS J005606.4-011215.3	$0.044^{+0.003}_{-0.002}$	0.071 ± 0.030	$0.043 \pm 6.6e-06$	-0.009 ± 0.007	0.979 ± 0.091	0.036	20 ± 5	28 ± 5	31 ± 6	39 ± 6	1
XMMXCS J005607.2+004058.6	$0.415^{+0.093}_{-0.091}$	0.399 ± 0.061	-	0.257 ± 0.239	-3.250 ± 4.750	0.137	6 ± 3	7 ± 3	3 ± 2	6 ± 3	1
XMMXCS J005613.6-011507.3	$0.043^{+0.007}_{-0.008}$	0.071 ± 0.030	$0.044 \pm 6.0e-06$	-0.019 ± 0.007	1.110 ± 0.107	0.043	20 ± 5	26 ± 5	31 ± 6	35 ± 6	1
XMMXCS J005614.4-011549.7	$0.043^{+0.007}_{-0.008}$	0.071 ± 0.030	$0.044 \pm 6.0e-06$	-0.019 ± 0.007	1.110 ± 0.107	0.043	19 ± 5	23 ± 5	30 ± 6	31 ± 6	1
XMMXCS J005614.5-011840.9	$0.045^{+0.020}_{-0.020}$	0.071 ± 0.030	$0.044 \pm 1.1e-05$	-0.027 ± 0.007	1.210 ± 0.101	0.045	20 ± 5	27 ± 5	29 ± 6	43 ± 7	1
XMMXCS J005615.3-011444.1	$0.043^{+0.007}_{-0.008}$	0.071 ± 0.030	$0.044 \pm 6.0e-06$	-0.019 ± 0.007	1.110 ± 0.107	0.043	19 ± 5	24 ± 5	30 ± 6	36 ± 6	1
XMMXCS J005615.9-011435.2	$0.043^{+0.009}_{-0.009}$	0.071 ± 0.030	$0.044 \pm 6.0e-06$	-0.020 ± 0.008	1.130 ± 0.112	0.046	19 ± 5	21 ± 5	29 ± 6	29 ± 5	1
XMMXCS J005616.5+262301.8	$0.190^{+0.049}_{-0.050}$	0.205 ± 0.032	-	-0.012 ± 0.031	1.450 ± 0.581	0.042	19 ± 4	18 ± 4	30 ± 6	29 ± 6	1

Continued on next page

Table A.2 – continued from previous page

name	z_{RS}	z_{BCG}	z_{spec-g}	cmr_{grad}	cmr_{inter}	cmr_{wid}	n_{gals-c}	n_{gals-l}	n_{200-c}	n_{200-l}	qual
XMMXCS J005616.6-012414.7	$0.075^{+0.028}_{-0.028}$	0.051 ± 0.018	-	0.068 ± 0.097	-0.476 ± 1.650	0.111	5 ± 2	3 ± 2	3 ± 2	1 ± 1	1
XMMXCS J005622.4-011225.3	$0.043^{+0.012}_{-0.012}$	0.071 ± 0.030	$0.044 \pm 6.0e-06$	-0.015 ± 0.008	1.070 ± 0.122	0.035	20 ± 5	23 ± 5	29 ± 6	32 ± 6	1
XMMXCS J005626.3-011719.1	$0.042^{+0.009}_{-0.009}$	0.071 ± 0.030	$0.041 \pm 7.8e-06$	-0.018 ± 0.005	1.080 ± 0.062	0.066	18 ± 5	19 ± 4	26 ± 6	28 ± 5	1
XMMXCS J010608.4+005031.4	$0.258^{+0.050}_{-0.050}$	0.277 ± 0.043	$0.259 \pm 2.8e-05$	-0.049 ± 0.018	2.350 ± 0.340	0.041	22 ± 5	27 ± 6	23 ± 5	37 ± 7	1
XMMXCS J010720.2+141604.2	$0.074^{+0.007}_{-0.008}$	0.073 ± 0.015	$0.074 \pm 1.2e-05$	0.007 ± 0.012	0.782 ± 0.188	0.027	9 ± 3	7 ± 3	7 ± 3	6 ± 3	1
XMMXCS J010858.7+132557.7	$0.146^{+0.025}_{-0.025}$	0.154 ± 0.023	$0.146 \pm 2.1e-05$	-0.037 ± 0.020	1.650 ± 0.342	0.105	6 ± 3	8 ± 3	6 ± 3	9 ± 3	1
XMMXCS J010918.2+131013.5	$0.091^{+0.027}_{-0.027}$	0.080 ± 0.033	-	0.007 ± 0.015	0.801 ± 0.228	0.093	22 ± 5	25 ± 5	24 ± 5	30 ± 6	1
XMMXCS J011018.0+193825.6	$0.316^{+0.084}_{-0.084}$	0.298 ± 0.061	$0.316 \pm 3.4e-05$	-0.070 ± 0.050	2.770 ± 0.929	0.001	7 ± 3	9 ± 4	6 ± 3	9 ± 4	1
XMMXCS J011036.3+330730.7	$0.093^{+0.027}_{-0.029}$	0.082 ± 0.017	-	0.013 ± 0.015	0.696 ± 0.250	0.086	3 ± 2	4 ± 3	3 ± 2	4 ± 2	1
XMMXCS J011058.7+330906.0	$0.091^{+0.030}_{-0.031}$	0.071 ± 0.019	-	0.018 ± 0.014	0.607 ± 0.193	0.092	8 ± 3	23 ± 5	7 ± 3	34 ± 7	1
XMMXCS J011153.9+331242.3	$0.131^{+0.052}_{-0.052}$	0.152 ± 0.064	-	-0.059 ± 0.021	1.990 ± 0.349	0.044	18 ± 4	17 ± 4	25 ± 5	26 ± 5	1
XMMXCS J011624.2+325717.0	$0.471^{+0.104}_{-0.102}$	0.475 ± 0.076	-	-0.089 ± 0.061	2.610 ± 1.220	0.094	12 ± 4	19 ± 5	12 ± 4	-	1
XMMXCS J011922.6-011011.7	$0.186^{+0.029}_{-0.029}$	0.190 ± 0.029	$0.186 \pm 2.2e-05$	-0.016 ± 0.020	1.450 ± 0.368	0.071	5 ± 2	9 ± 3	3 ± 2	6 ± 3	1
XMMXCS J012329.4+330521.4	$0.257^{+0.065}_{-0.067}$	0.260 ± 0.040	-	0.071 ± 0.109	0.083 ± 2.020	0.127	12 ± 4	12 ± 4	12 ± 4	12 ± 4	1
XMMXCS J012340.2+330548.1	$0.275^{+0.060}_{-0.061}$	0.260 ± 0.040	-	0.028 ± 0.035	0.991 ± 0.650	0.058	10 ± 4	12 ± 4	10 ± 3	13 ± 4	1
XMMXCS J012348.3+330320.2	$0.256^{+0.067}_{-0.070}$	0.241 ± 0.041	-	0.051 ± 0.043	0.495 ± 0.800	0.096	8 ± 3	7 ± 3	6 ± 3	4 ± 3	1
XMMXCS J012352.0+333902.6	$0.245^{+0.060}_{-0.060}$	0.254 ± 0.047	-	-0.038 ± 0.030	2.150 ± 0.589	0.108	19 ± 5	19 ± 5	17 ± 5	20 ± 5	1
XMMXCS J012434.9+040054.2	$0.323^{+0.060}_{-0.053}$	0.335 ± 0.052	$0.380 \pm 3.6e-05$	0.001 ± 0.057	1.630 ± 1.060	0.001	20 ± 5	20 ± 5	27 ± 6	27 ± 6	1
XMMXCS J012459.1+320202.8	$0.330^{+0.053}_{-0.054}$	0.316 ± 0.049	-	-0.027 ± 0.035	2.210 ± 0.666	0.068	3 ± 2	19 ± 5	3 ± 2	5 ± 3	1

Continued on next page

Table A.2 – continued from previous page

name	z_{RS}	z_{BCG}	z_{spec-g}	cmr_{grad}	cmr_{inter}	cmr_{wid}	n_{gals-c}	n_{gals-l}	n_{200-c}	n_{200-l}	qual
XMMXCS J012516.6+321341.5	$0.269^{+0.076}_{-0.077}$	0.265 ± 0.045	-	-0.022 ± 0.032	1.890 ± 0.578	0.035	8 ± 3	9 ± 4	5 ± 2	10 ± 4	1
XMMXCS J012526.2+321453.9	$0.268^{+0.082}_{-0.085}$	0.265 ± 0.045	-	-0.070 ± 0.030	2.750 ± 0.571	0.085	13 ± 4	14 ± 4	14 ± 4	14 ± 4	1
XMMXCS J012526.4+014906.8	$0.058^{+0.047}_{-0.048}$	0.068 ± 0.021	-	-0.036 ± 0.013	1.240 ± 0.181	0.066	11 ± 3	14 ± 4	10 ± 3	14 ± 4	1
XMMXCS J012534.0-011647.3	$0.474^{+0.110}_{-0.109}$	0.456 ± 0.069	-	-0.169 ± 0.259	4.240 ± 5.290	0.069	11 ± 4	13 ± 4	11 ± 4	15 ± 5	1
XMMXCS J012558.0-012105.0	$0.068^{+0.036}_{-0.036}$	0.069 ± 0.032	-	-0.023 ± 0.004	1.070 ± 0.048	0.012	17 ± 4	42 ± 7	19 ± 4	86 ± 10	1
XMMXCS J013221.3+304033.2	$0.514^{+0.158}_{-0.157}$	0.514 ± 0.223	-	-0.236 ± 0.085	5.680 ± 1.750	0.001	15 ± 5	21 ± 5	16 ± 5	25 ± 6	1
XMMXCS J013837.5-175956.8	$0.510^{+0.169}_{-0.170}$	0.513 ± 0.186	-	-0.057 ± 0.093	2.010 ± 1.830	0.001	5 ± 3	2 ± 3	6 ± 3	4 ± 2	1
XMMXCS J014320.9+134900.6	$0.216^{+0.080}_{-0.080}$	0.218 ± 0.040	$0.216 \pm 3.2e-05$	-0.037 ± 0.043	1.960 ± 0.763	0.027	3 ± 2	2 ± 2	3 ± 2	3 ± 2	1
XMMXCS J014430.3+021237.0	$0.166^{+0.041}_{-0.041}$	0.187 ± 0.031	$0.165 \pm 1.4e-05$	-0.063 ± 0.013	2.270 ± 0.221	0.023	10 ± 3	10 ± 3	10 ± 3	11 ± 3	1
XMMXCS J014450.3+165457.9	$0.151^{+0.020}_{-0.019}$	0.166 ± 0.025	$0.152 \pm 1.7e-05$	-0.052 ± 0.018	2.000 ± 0.301	0.059	3 ± 2	3 ± 2	3 ± 2	3 ± 2	1
XMMXCS J014828.6+140200.0	$0.125^{+0.020}_{-0.020}$	0.137 ± 0.025	$0.122 \pm 2.3e-05$	-0.053 ± 0.018	1.910 ± 0.289	0.060	14 ± 4	12 ± 4	13 ± 4	12 ± 4	1
XMMXCS J014839.5+135630.4	$0.432^{+0.076}_{-0.075}$	0.444 ± 0.066	$0.432 \pm 6.8e-05$	0.124 ± 0.149	-0.652 ± 2.890	0.192	16 ± 5	17 ± 5	18 ± 5	19 ± 6	1
XMMXCS J014908.5+135745.1	$0.070^{+0.010}_{-0.011}$	0.085 ± 0.017	$0.070 \pm 7.6e-06$	-0.055 ± 0.017	1.710 ± 0.257	0.071	9 ± 3	12 ± 4	9 ± 3	12 ± 4	1
XMMXCS J015237.1+005632.6	$0.208^{+0.059}_{-0.059}$	0.191 ± 0.036	-	-0.013 ± 0.023	1.550 ± 0.426	0.036	9 ± 3	9 ± 3	6 ± 3	7 ± 3	1
XMMXCS J015242.0+010028.6	$0.231^{+0.052}_{-0.051}$	0.238 ± 0.039	$0.230 \pm 4.0e-05$	-0.035 ± 0.013	2.020 ± 0.240	0.066	25 ± 5	23 ± 5	37 ± 6	36 ± 6	1
XMMXCS J015315.0+010214.2	$0.059^{+0.001}_{-0.001}$	0.064 ± 0.016	$0.059 \pm 6.7e-06$	-0.011 ± 0.004	1.020 ± 0.054	0.006	6 ± 3	2 ± 2	4 ± 2	3 ± 2	1
XMMXCS J015558.0+053200.8	$0.454^{+0.109}_{-0.108}$	0.499 ± 0.086	$0.450 \pm 1.0e-04$	-0.041 ± 0.024	1.560 ± 0.480	0.001	4 ± 3	13 ± 4	5 ± 3	12 ± 4	1
XMMXCS J015720.8+321257.4	$0.108^{+0.021}_{-0.021}$	0.123 ± 0.026	-	0.001 ± 0.008	0.969 ± 0.127	0.042	31 ± 6	31 ± 6	39 ± 6	48 ± 7	1
XMMXCS J015733.3+321211.5	$0.100^{+0.027}_{-0.027}$	0.112 ± 0.025	-	-0.013 ± 0.016	1.130 ± 0.276	0.038	27 ± 5	28 ± 5	32 ± 6	35 ± 6	1

Continued on next page

Table A.2 – continued from previous page

name	z_{RS}	z_{BCG}	z_{spec-g}	cmr_{grad}	cmr_{inter}	cmr_{wid}	n_{gals-c}	n_{gals-l}	n_{200-c}	n_{200-l}	qual
XMMXCS J015916.9+003044.4	$0.387^{+0.081}_{-0.080}$	0.358 ± 0.099	$0.384 \pm 6.6e-05$	0.124 ± 0.091	-0.985 ± 1.810	0.129	9 ± 4	11 ± 4	9 ± 4	10 ± 4	1
XMMXCS J015916.9+003010.9	$0.386^{+0.073}_{-0.072}$	0.358 ± 0.099	$0.384 \pm 6.6e-05$	0.063 ± 0.059	0.239 ± 1.150	0.021	8 ± 4	10 ± 4	4 ± 3	9 ± 4	1
XMMXCS J020046.49-064223.1	$0.338^{+0.075}_{-0.076}$	0.314 ± 0.047	$0.338 \pm 5.2e-05$	0.016 ± 0.055	1.290 ± 1.050	0.001	11 ± 4	10 ± 4	9 ± 4	12 ± 4	1
XMMXCS J020049.61-064026.8	$0.339^{+0.065}_{-0.065}$	0.314 ± 0.047	$0.339 \pm 7.3e-05$	0.068 ± 0.038	0.283 ± 0.743	0.116	10 ± 4	9 ± 4	8 ± 3	6 ± 3	1
XMMXCS J020140.52-050227.9	$0.244^{+0.068}_{-0.068}$	0.234 ± 0.039	-	-0.014 ± 0.024	1.610 ± 0.446	0.065	5 ± 3	7 ± 3	5 ± 2	6 ± 3	1
XMMXCS J020140.52-050205.6	$0.214^{+0.065}_{-0.065}$	0.234 ± 0.039	-	-0.035 ± 0.037	1.940 ± 0.705	0.103	6 ± 3	9 ± 4	5 ± 2	6 ± 3	1
XMMXCS J020213.89-070113.1	$0.069^{+0.021}_{-0.021}$	0.069 ± 0.015	-	-0.051 ± 0.014	1.580 ± 0.206	0.049	5 ± 2	6 ± 3	5 ± 2	6 ± 3	1
XMMXCS J020230.52-063119.7	$0.291^{+0.098}_{-0.097}$	0.327 ± 0.049	$0.314 \pm 4.8e-05$	-0.068 ± 0.052	2.630 ± 1.010	0.121	9 ± 4	0 ± 3	10 ± 4	-	1
XMMXCS J020254.37-073858.3	$0.138^{+0.026}_{-0.026}$	0.133 ± 0.024	$0.137 \pm 1.4e-05$	-0.024 ± 0.025	1.400 ± 0.421	0.077	12 ± 4	14 ± 4	12 ± 4	14 ± 4	1
XMMXCS J020255.3-073906.6	$0.138^{+0.026}_{-0.025}$	0.133 ± 0.024	$0.137 \pm 1.4e-05$	-0.040 ± 0.029	1.700 ± 0.479	0.051	8 ± 3	10 ± 3	8 ± 3	10 ± 3	1
XMMXCS J020303.11-051813.2	$0.134^{+0.031}_{-0.030}$	0.141 ± 0.024	$0.134 \pm 2.0e-05$	-0.141 ± 0.033	3.230 ± 0.547	0.080	2 ± 2	2 ± 2	3 ± 2	4 ± 2	1
XMMXCS J020304.85-070610.5	$0.335^{+0.073}_{-0.069}$	0.288 ± 0.045	$0.333 \pm 4.2e-05$	-0.136 ± 0.071	4.120 ± 1.360	0.114	11 ± 4	12 ± 4	10 ± 4	12 ± 4	1
XMMXCS J020341.31-074708.4	$0.440^{+0.075}_{-0.074}$	0.430 ± 0.066	$0.440 \pm 8.9e-05$	0.104 ± 0.038	0.062 ± 0.744	0.076	10 ± 4	10 ± 4	10 ± 3	10 ± 4	1
XMMXCS J020341.6-074705.7	$0.443^{+0.075}_{-0.073}$	0.430 ± 0.066	$0.440 \pm 8.9e-05$	0.107 ± 0.052	-0.071 ± 1.030	0.201	12 ± 4	11 ± 4	13 ± 4	11 ± 4	1
XMMXCS J020344.4-073739.5	$0.177^{+0.050}_{-0.051}$	0.158 ± 0.026	-	0.016 ± 0.035	0.907 ± 0.652	0.062	5 ± 2	4 ± 2	4 ± 2	3 ± 2	1
XMMXCS J020353.36-050145.3	$0.521^{+0.099}_{-0.098}$	0.544 ± 0.090	$0.521 \pm 1.2e-04$	-0.021 ± 0.029	1.350 ± 0.595	0.001	13 ± 4	15 ± 5	12 ± 4	14 ± 5	1
XMMXCS J020429.21-060131.0	$0.291^{+0.135}_{-0.134}$	0.310 ± 0.050	-	-0.167 ± 0.328	4.680 ± 6.740	0.202	9 ± 4	8 ± 4	5 ± 3	4 ± 3	1
XMMXCS J020634.39-055839.8	$0.281^{+0.073}_{-0.073}$	0.270 ± 0.045	$0.289 \pm 4.3e-05$	0.041 ± 0.061	0.773 ± 1.150	0.102	10 ± 4	7 ± 3	5 ± 3	1 ± 2	1
XMMXCS J020644.78-065810.1	$0.410^{+0.116}_{-0.116}$	0.407 ± 0.060	$0.431 \pm 7.3e-05$	-0.174 ± 0.108	5.110 ± 2.150	0.001	15 ± 5	16 ± 5	17 ± 5	17 ± 5	1

Continued on next page

Table A.2 – continued from previous page

name	z_{RS}	z_{BCG}	z_{spec-g}	cmr_{grad}	cmr_{inter}	cmr_{wid}	n_{gals-c}	n_{gals-l}	n_{200-c}	n_{200-l}	qual
XMMXCS J020647.58-065651.0	$0.432^{+0.075}_{-0.074}$	0.365 ± 0.057	$0.427 \pm 6.3e-05$	0.045 ± 0.064	0.862 ± 1.230	0.089	26 ± 6	23 ± 5	23 ± 6	23 ± 6	1
XMMXCS J020647.93-065727.1	$0.432^{+0.081}_{-0.080}$	0.365 ± 0.057	$0.428 \pm 5.7e-05$	-0.009 ± 0.061	1.900 ± 1.190	0.058	27 ± 6	25 ± 6	22 ± 6	19 ± 6	1
XMMXCS J020737.6+293442.5	$0.115^{+0.026}_{-0.027}$	0.106 ± 0.018	-	-0.032 ± 0.019	1.490 ± 0.321	0.050	8 ± 3	9 ± 3	7 ± 3	7 ± 3	1
XMMXCS J020911.25-062043.8	$0.491^{+0.081}_{-0.081}$	0.490 ± 0.071	$0.491 \pm 1.1e-04$	-0.027 ± 0.020	1.360 ± 0.413	0.001	12 ± 4	12 ± 4	11 ± 4	12 ± 4	1
XMMXCS J021012.9-001445.6	$0.282^{+0.051}_{-0.052}$	0.275 ± 0.051	$0.283 \pm 5.1e-05$	0.010 ± 0.014	1.280 ± 0.253	0.024	5 ± 3	4 ± 3	5 ± 2	6 ± 3	1
XMMXCS J021039.98-055642.2	$0.537^{+0.099}_{-0.098}$	0.474 ± 0.094	$0.535 \pm 8.7e-05$	-0.040 ± 0.056	1.660 ± 1.120	0.066	10 ± 4	15 ± 5	10 ± 4	14 ± 5	1
XMMXCS J021043.73-063451.2	$0.061^{+0.020}_{-0.020}$	0.072 ± 0.022	-	-0.013 ± 0.007	1.010 ± 0.112	0.019	13 ± 4	16 ± 4	13 ± 4	17 ± 4	1
XMMXCS J021051.87-061020.2	$0.428^{+0.083}_{-0.081}$	0.429 ± 0.064	$0.427 \pm 6.5e-05$	-0.137 ± 0.069	4.240 ± 1.340	0.001	17 ± 5	18 ± 5	25 ± 6	27 ± 6	1
XMMXCS J021102.87-045402.1	$0.138^{+0.030}_{-0.031}$	0.139 ± 0.030	$0.137 \pm 1.5e-05$	-0.040 ± 0.022	1.740 ± 0.371	0.036	11 ± 3	10 ± 3	11 ± 3	11 ± 3	1
XMMXCS J021104.15-045323.3	$0.137^{+0.025}_{-0.025}$	0.139 ± 0.030	$0.137 \pm 1.5e-05$	-0.015 ± 0.011	1.320 ± 0.189	0.027	11 ± 3	10 ± 3	11 ± 3	9 ± 3	1
XMMXCS J021109.46-042045.0	$0.445^{+0.081}_{-0.080}$	0.443 ± 0.069	$0.443 \pm 1.8e-04$	0.012 ± 0.040	0.453 ± 0.810	0.093	24 ± 6	25 ± 6	36 ± 7	37 ± 7	1
XMMXCS J021114.47-060950.8	$0.426^{+0.086}_{-0.085}$	0.412 ± 0.059	$0.423 \pm 8.1e-05$	-0.241 ± 0.054	6.280 ± 1.010	0.094	12 ± 4	12 ± 4	13 ± 4	13 ± 5	1
XMMXCS J021116.1-085240.3	$0.244^{+0.050}_{-0.050}$	0.260 ± 0.054	$0.243 \pm 4.1e-05$	-0.036 ± 0.020	2.000 ± 0.359	0.060	6 ± 3	7 ± 3	3 ± 2	4 ± 2	1
XMMXCS J021128.86-061131.5	$0.437^{+0.100}_{-0.095}$	0.441 ± 0.066	$0.428 \pm 7.0e-05$	-0.038 ± 0.060	1.380 ± 1.170	0.053	7 ± 4	6 ± 4	7 ± 3	6 ± 3	1
XMMXCS J021220.86-042015.0	$0.590^{+0.091}_{-0.090}$	0.570 ± 0.118	$0.589 \pm 1.4e-04$	-0.191 ± 0.073	4.870 ± 1.460	0.001	5 ± 3	17 ± 5	6 ± 3	15 ± 5	1
XMMXCS J021225.59-053752.0	$0.299^{+0.065}_{-0.065}$	0.337 ± 0.059	$0.300 \pm 4.0e-05$	-0.067 ± 0.035	2.900 ± 0.670	0.026	24 ± 5	20 ± 5	28 ± 6	23 ± 5	1
XMMXCS J021227.66-060430.5	$0.296^{+0.074}_{-0.074}$	0.306 ± 0.049	$0.297 \pm 5.4e-05$	-0.111 ± 0.029	3.590 ± 0.581	0.110	6 ± 3	5 ± 3	4 ± 2	4 ± 3	1
XMMXCS J021239.63-041622.5	$0.198^{+0.042}_{-0.038}$	0.192 ± 0.041	$0.197 \pm 2.7e-05$	-0.005 ± 0.031	1.340 ± 0.560	0.023	5 ± 2	4 ± 2	3 ± 2	1 ± 1	1
XMMXCS J021321.74-060550.1	$0.698^{+0.133}_{-0.132}$	0.649 ± 0.128	$0.695 \pm 2.3e-04$	-0.121 ± 0.084	3.000 ± 1.650	0.001	15 ± 4	87 ± 10	15 ± 4	110 ± 13	1

Continued on next page

Table A.2 – continued from previous page

name	z_{RS}	z_{BCG}	z_{spec-g}	cmr_{grad}	cmr_{inter}	cmr_{wid}	n_{gals-c}	n_{gals-l}	n_{200-c}	n_{200-l}	qual
XMMXCS J021407.78-053508.0	$0.448^{+0.066}_{-0.065}$	0.404 ± 0.060	$0.447 \pm 7.2e-05$	0.019 ± 0.052	1.240 ± 1.010	0.001	15 ± 5	15 ± 5	16 ± 5	15 ± 5	1
XMMXCS J021427.64-062733.8	$0.236^{+0.046}_{-0.047}$	0.256 ± 0.039	$0.237 \pm 2.8e-05$	-0.019 ± 0.034	1.760 ± 0.610	0.040	18 ± 4	16 ± 4	21 ± 5	46 ± 7	1
XMMXCS J021440.9-043321.9	$0.142^{+0.043}_{-0.044}$	0.158 ± 0.026	$0.142 \pm 1.4e-05$	0.003 ± 0.012	1.070 ± 0.204	0.053	17 ± 4	20 ± 5	22 ± 5	32 ± 6	1
XMMXCS J021441.91-061635.9	$0.241^{+0.056}_{-0.055}$	0.262 ± 0.040	$0.240 \pm 2.6e-05$	-0.058 ± 0.034	2.360 ± 0.638	0.102	10 ± 4	12 ± 4	9 ± 3	12 ± 4	1
XMMXCS J021442.21-043315.3	$0.142^{+0.044}_{-0.045}$	0.158 ± 0.026	$0.142 \pm 1.4e-05$	0.004 ± 0.012	1.070 ± 0.194	0.051	17 ± 4	20 ± 5	23 ± 5	32 ± 6	1
XMMXCS J021453.41-042842.4	$0.136^{+0.029}_{-0.029}$	0.148 ± 0.023	$0.138 \pm 1.2e-05$	-0.012 ± 0.027	1.250 ± 0.467	0.060	14 ± 4	16 ± 4	18 ± 4	23 ± 5	1
XMMXCS J021500.32-035429.3	$0.138^{+0.025}_{-0.025}$	0.146 ± 0.025	$0.138 \pm 1.5e-05$	0.006 ± 0.007	0.967 ± 0.127	0.021	4 ± 2	5 ± 3	3 ± 2	6 ± 3	1
XMMXCS J021502.6-042309.8	$0.195^{+0.076}_{-0.077}$	0.171 ± 0.051	-	-0.013 ± 0.036	1.510 ± 0.651	0.051	4 ± 2	2 ± 2	3 ± 2	4 ± 2	1
XMMXCS J021504.69-055830.0	$0.223^{+0.050}_{-0.051}$	0.243 ± 0.040	-	-0.088 ± 0.026	2.960 ± 0.468	0.001	9 ± 3	10 ± 3	7 ± 3	8 ± 3	1
XMMXCS J021528.34-040258.0	$0.373^{+0.087}_{-0.085}$	0.329 ± 0.053	$0.371 \pm 7.7e-05$	-0.005 ± 0.017	0.695 ± 0.329	0.001	11 ± 4	12 ± 4	11 ± 4	12 ± 4	1
XMMXCS J021528.91-044052.8	$0.353^{+0.085}_{-0.083}$	0.363 ± 0.054	$0.350 \pm 8.2e-05$	-0.036 ± 0.008	1.230 ± 0.156	0.001	24 ± 5	22 ± 5	34 ± 7	36 ± 7	1
XMMXCS J021604.63-032607.0	$0.314^{+0.068}_{-0.067}$	0.325 ± 0.050	$0.313 \pm 5.9e-05$	-0.183 ± 0.041	4.920 ± 0.802	0.091	10 ± 4	7 ± 4	11 ± 4	13 ± 4	1
XMMXCS J021606.40-093517.1	$0.596^{+0.110}_{-0.110}$	0.654 ± 0.115	$0.595 \pm 1.3e-04$	-0.088 ± 0.061	2.870 ± 1.200	0.001	21 ± 5	35 ± 6	27 ± 6	63 ± 9	1
XMMXCS J021611.69-041422.8	$0.150^{+0.032}_{-0.032}$	0.157 ± 0.026	$0.154 \pm 2.2e-05$	-0.073 ± 0.052	2.390 ± 0.932	0.068	7 ± 3	9 ± 3	6 ± 3	10 ± 3	1
XMMXCS J021611.6-041422.8	$0.150^{+0.032}_{-0.032}$	0.157 ± 0.026	$0.154 \pm 2.2e-05$	-0.073 ± 0.052	2.390 ± 0.932	0.068	7 ± 3	9 ± 3	6 ± 3	10 ± 3	1
XMMXCS J021640.9-041843.3	$0.153^{+0.032}_{-0.032}$	0.157 ± 0.032	$0.153 \pm 2.5e-05$	0.005 ± 0.024	0.973 ± 0.414	0.042	8 ± 3	8 ± 3	7 ± 3	7 ± 3	1
XMMXCS J021640.94-041842.4	$0.153^{+0.032}_{-0.032}$	0.157 ± 0.032	$0.153 \pm 2.5e-05$	0.005 ± 0.024	0.973 ± 0.414	0.042	8 ± 3	8 ± 3	7 ± 3	7 ± 3	1
XMMXCS J021650.8-043600.9	$0.291^{+0.075}_{-0.075}$	0.320 ± 0.049	$0.363 \pm 4.7e-05$	-0.065 ± 0.055	2.760 ± 1.030	0.001	7 ± 3	7 ± 3	4 ± 2	5 ± 3	1
XMMXCS J021653.14-041725.5	$0.152^{+0.037}_{-0.037}$	0.157 ± 0.032	$0.153 \pm 2.5e-05$	0.016 ± 0.010	0.807 ± 0.161	0.001	6 ± 3	5 ± 3	3 ± 2	4 ± 2	1

Continued on next page

Table A.2 – continued from previous page

name	z_{RS}	z_{BCG}	z_{spec-g}	cmr_{grad}	cmr_{inter}	cmr_{wid}	n_{gals-c}	n_{gals-l}	n_{200-c}	n_{200-l}	qual
XMMXCS J021739.38-034827.7	$0.290^{+0.070}_{-0.070}$	0.314 ± 0.090	$0.291 \pm 3.0e-05$	$5.65e- \pm 0.022$	1.470 ± 0.417	0.001	6 ± 3	6 ± 3	7 ± 3	8 ± 3	1
XMMXCS J021803.27-055527.7	$0.391^{+0.064}_{-0.064}$	0.340 ± 0.057	$0.389 \pm 6.2e-05$	0.210 ± 0.156	-2.220 ± 2.920	0.206	5 ± 3	-	5 ± 3	-	1
XMMXCS J021803.8-055525.3	$0.391^{+0.064}_{-0.064}$	0.340 ± 0.057	$0.389 \pm 6.2e-05$	0.210 ± 0.156	-2.220 ± 2.920	0.206	5 ± 3	-	5 ± 3	-	1
XMMXCS J021837.90-054037.0	$0.280^{+0.068}_{-0.069}$	0.283 ± 0.046	$0.332 \pm 5.9e-05$	-0.036 ± 0.023	2.200 ± 0.441	0.057	12 ± 4	9 ± 4	12 ± 4	4 ± 3	1
XMMXCS J021837.8-054037.0	$0.280^{+0.068}_{-0.069}$	0.283 ± 0.046	$0.332 \pm 5.9e-05$	-0.036 ± 0.023	2.200 ± 0.441	0.057	12 ± 4	9 ± 4	12 ± 4	4 ± 3	1
XMMXCS J021843.72-053253.3	$0.383^{+0.064}_{-0.063}$	0.358 ± 0.069	$0.382 \pm 5.9e-05$	0.346 ± 0.315	-4.970 ± 6.090	0.235	10 ± 4	-	11 ± 4	-	1
XMMXCS J021943.7-045313.8	$0.334^{+0.079}_{-0.078}$	0.365 ± 0.056	$0.318 \pm 5.2e-05$	-0.087 ± 0.155	3.170 ± 3.120	0.186	11 ± 4	10 ± 4	11 ± 4	11 ± 4	1
XMMXCS J021944.29-045326.8	$0.353^{+0.087}_{-0.086}$	0.365 ± 0.056	$0.318 \pm 5.2e-05$	-0.087 ± 0.236	3.070 ± 4.800	0.190	10 ± 4	11 ± 4	11 ± 4	11 ± 4	1
XMMXCS J022002.9-052754.6	$0.382^{+0.061}_{-0.059}$	0.350 ± 0.056	$0.380 \pm 6.3e-05$	-0.135 ± 0.076	4.160 ± 1.430	0.001	7 ± 3	9 ± 4	5 ± 3	8 ± 4	1
XMMXCS J022042.69-030119.2	$0.250^{+0.090}_{-0.092}$	0.229 ± 0.063	-	0.046 ± 0.072	0.399 ± 1.320	0.072	3 ± 2	4 ± 3	3 ± 2	3 ± 2	1
XMMXCS J022042.8-030119.0	$0.250^{+0.090}_{-0.092}$	0.229 ± 0.063	-	0.046 ± 0.072	0.399 ± 1.320	0.072	3 ± 2	4 ± 3	3 ± 2	4 ± 2	1
XMMXCS J022044.8-025227.9	$0.501^{+0.107}_{-0.104}$	0.493 ± 0.074	$0.495 \pm 1.4e-04$	-0.173 ± 0.052	4.150 ± 1.020	0.026	8 ± 4	-	9 ± 4	-	1
XMMXCS J022045.03-025226.4	$0.501^{+0.107}_{-0.104}$	0.493 ± 0.074	$0.495 \pm 1.4e-04$	-0.173 ± 0.052	4.150 ± 1.020	0.026	8 ± 4	-	9 ± 4	-	1
XMMXCS J022045.12-032555.3	$0.328^{+0.062}_{-0.063}$	0.339 ± 0.052	$0.328 \pm 6.7e-05$	0.056 ± 0.054	0.680 ± 1.040	0.050	9 ± 3	11 ± 4	8 ± 3	10 ± 4	1
XMMXCS J022045.1-032555.0	$0.328^{+0.062}_{-0.063}$	0.339 ± 0.052	$0.328 \pm 6.7e-05$	0.056 ± 0.054	0.680 ± 1.040	0.050	9 ± 3	11 ± 4	8 ± 3	10 ± 4	1
XMMXCS J022126.8-043402.2	$0.158^{+0.036}_{-0.037}$	0.161 ± 0.027	$0.159 \pm 2.0e-05$	0.021 ± 0.020	0.794 ± 0.345	0.044	5 ± 2	4 ± 2	4 ± 2	3 ± 2	1
XMMXCS J022129.25-040554.1	$0.137^{+0.029}_{-0.029}$	0.142 ± 0.022	-	-0.040 ± 0.024	1.720 ± 0.394	0.020	4 ± 2	4 ± 2	3 ± 2	3 ± 2	1
XMMXCS J022141.18-034645.7	$0.408^{+0.100}_{-0.099}$	0.414 ± 0.064	$0.433 \pm 9.9e-05$	0.005 ± 0.016	0.591 ± 0.314	0.023	23 ± 5	21 ± 5	32 ± 7	27 ± 6	1
XMMXCS J022143.61-034612.9	$0.433^{+0.086}_{-0.085}$	0.414 ± 0.064	$0.433 \pm 9.9e-05$	-0.023 ± 0.064	2.200 ± 1.240	0.092	27 ± 6	26 ± 6	34 ± 7	34 ± 7	1

Continued on next page

Table A.2 – continued from previous page

name	z_{RS}	z_{BCG}	z_{spec-g}	cmr_{grad}	cmr_{inter}	cmr_{wid}	n_{gals-c}	n_{gals-l}	n_{200-c}	n_{200-l}	qual
XMMXCS J022145.4-034617.4	$0.434^{+0.085}_{-0.085}$	0.414 ± 0.064	$0.433 \pm 9.9e-05$	-0.021 ± 0.070	2.190 ± 1.370	0.085	27 ± 6	26 ± 6	34 ± 7	35 ± 7	1
XMMXCS J022148.0-034607.1	$0.433^{+0.078}_{-0.078}$	0.414 ± 0.064	$0.433 \pm 9.9e-05$	-0.036 ± 0.035	2.490 ± 0.666	0.016	23 ± 5	22 ± 5	34 ± 7	32 ± 6	1
XMMXCS J022153.2-054447.1	$0.258^{+0.054}_{-0.055}$	0.262 ± 0.051	$0.259 \pm 2.4e-05$	-0.056 ± 0.035	2.500 ± 0.664	0.041	9 ± 3	9 ± 3	9 ± 3	8 ± 3	1
XMMXCS J022154.83-054519.0	$0.259^{+0.050}_{-0.050}$	0.262 ± 0.051	$0.259 \pm 2.4e-05$	-0.029 ± 0.011	1.970 ± 0.222	0.023	10 ± 3	10 ± 4	9 ± 3	8 ± 3	1
XMMXCS J022154.8-054519.0	$0.259^{+0.050}_{-0.050}$	0.262 ± 0.051	$0.259 \pm 2.4e-05$	-0.029 ± 0.011	1.970 ± 0.222	0.023	10 ± 3	10 ± 4	9 ± 3	8 ± 3	1
XMMXCS J022159.6-054322.8	$0.256^{+0.069}_{-0.070}$	0.262 ± 0.051	$0.259 \pm 3.1e-05$	-0.014 ± 0.023	1.700 ± 0.438	0.044	8 ± 3	7 ± 3	5 ± 2	4 ± 2	1
XMMXCS J022201.7-054330.4	$0.257^{+0.072}_{-0.073}$	0.262 ± 0.051	$0.259 \pm 3.1e-05$	-0.027 ± 0.029	1.930 ± 0.537	0.039	9 ± 3	8 ± 3	5 ± 3	4 ± 3	1
XMMXCS J022205.92-030313.0	$0.500^{+0.077}_{-0.074}$	0.483 ± 0.076	$0.496 \pm 1.2e-04$	-0.010 ± 0.062	0.911 ± 1.220	0.131	17 ± 5	48 ± 8	15 ± 5	37 ± 9	1
XMMXCS J022206.3-030313.6	$0.501^{+0.092}_{-0.087}$	0.483 ± 0.076	$0.496 \pm 1.2e-04$	0.090 ± 0.116	-0.972 ± 2.280	0.167	12 ± 4	43 ± 7	13 ± 4	35 ± 9	1
XMMXCS J022218.56-041651.9	$0.234^{+0.067}_{-0.068}$	0.246 ± 0.075	-	0.067 ± 0.019	0.153 ± 0.354	0.031	5 ± 2	4 ± 2	3 ± 2	0 ± 1	1
XMMXCS J022218.5-041651.8	$0.234^{+0.067}_{-0.068}$	0.246 ± 0.075	-	0.067 ± 0.019	0.153 ± 0.354	0.031	5 ± 2	4 ± 2	3 ± 2	0 ± 1	1
XMMXCS J022250.94-041641.1	$0.244^{+0.113}_{-0.117}$	0.203 ± 0.065	$0.238 \pm 3.0e-05$	-0.014 ± 0.046	1.500 ± 0.889	0.128	3 ± 2	5 ± 3	3 ± 2	3 ± 2	1
XMMXCS J022258.8-040636.0	$0.285^{+0.076}_{-0.076}$	0.295 ± 0.101	-	-0.099 ± 0.058	3.320 ± 1.080	0.089	10 ± 4	11 ± 4	11 ± 4	11 ± 4	1
XMMXCS J022259.03-040633.1	$0.291^{+0.095}_{-0.096}$	0.295 ± 0.101	-	-0.047 ± 0.051	2.260 ± 0.998	0.135	13 ± 4	13 ± 4	12 ± 4	12 ± 4	1
XMMXCS J022318.30-051209.8	$0.331^{+0.046}_{-0.046}$	0.331 ± 0.049	$0.330 \pm 3.6e-05$	-0.005 ± 0.051	1.730 ± 0.963	0.118	5 ± 3	7 ± 3	6 ± 3	9 ± 3	1
XMMXCS J022318.37-052707.6	$0.213^{+0.067}_{-0.066}$	0.201 ± 0.032	-	-0.062 ± 0.029	2.420 ± 0.534	0.054	6 ± 3	5 ± 3	4 ± 2	4 ± 2	1
XMMXCS J022319.5-052710.9	$0.212^{+0.059}_{-0.060}$	0.201 ± 0.032	-	-0.032 ± 0.013	1.870 ± 0.242	0.041	5 ± 3	4 ± 3	3 ± 2	4 ± 2	1
XMMXCS J022324.1+062202.9	$0.347^{+0.065}_{-0.064}$	0.363 ± 0.122	-	-0.002 ± 0.042	1.630 ± 0.828	0.001	3 ± 3	4 ± 3	3 ± 2	3 ± 2	1
XMMXCS J022338.0-030144.6	$0.494^{+0.087}_{-0.087}$	0.451 ± 0.090	$0.493 \pm 9.1e-05$	0.007 ± 0.034	0.639 ± 0.683	0.001	11 ± 4	16 ± 5	11 ± 4	20 ± 5	1

Continued on next page

Table A.2 – continued from previous page

name	z_{RS}	z_{BCG}	z_{spec-g}	cmr_{grad}	cmr_{inter}	cmr_{wid}	n_{gals-c}	n_{gals-l}	n_{200-c}	n_{200-l}	qual
XMMXCS J022347.50-025134.4	$0.175^{+0.039}_{-0.039}$	0.165 ± 0.038	$0.175 \pm 1.5e-05$	-0.033 ± 0.020	1.730 ± 0.353	0.063	11 ± 4	12 ± 4	10 ± 3	12 ± 4	1
XMMXCS J022347.6-025129.5	$0.175^{+0.035}_{-0.035}$	0.165 ± 0.038	$0.175 \pm 1.5e-05$	-0.042 ± 0.015	1.890 ± 0.264	0.058	11 ± 4	13 ± 4	10 ± 3	13 ± 4	1
XMMXCS J022350.88-053643.9	$0.496^{+0.084}_{-0.084}$	0.503 ± 0.074	$0.497 \pm 1.1e-04$	-0.018 ± 0.047	1.210 ± 0.932	0.064	19 ± 5	21 ± 5	21 ± 5	23 ± 6	1
XMMXCS J022352.59-082125.4	$0.229^{+0.051}_{-0.051}$	0.230 ± 0.035	$0.244 \pm 2.6e-05$	0.020 ± 0.018	1.000 ± 0.320	0.071	14 ± 4	15 ± 4	14 ± 4	15 ± 4	1
XMMXCS J022356.3-030559.3	$0.296^{+0.036}_{-0.036}$	0.309 ± 0.048	$0.297 \pm 6.1e-05$	0.050 ± 0.026	0.608 ± 0.516	0.045	3 ± 2	6 ± 3	3 ± 2	5 ± 3	1
XMMXCS J022356.32-030556.8	$0.296^{+0.036}_{-0.036}$	0.309 ± 0.048	$0.297 \pm 6.1e-05$	0.050 ± 0.026	0.608 ± 0.516	0.045	3 ± 2	6 ± 3	3 ± 2	5 ± 3	1
XMMXCS J022357.59-043519.7	$0.497^{+0.113}_{-0.112}$	0.504 ± 0.080	$0.496 \pm 1.5e-04$	-0.093 ± 0.038	2.690 ± 0.752	0.001	18 ± 5	35 ± 6	20 ± 5	49 ± 8	1
XMMXCS J022357.6-043518.9	$0.497^{+0.113}_{-0.112}$	0.504 ± 0.080	$0.496 \pm 1.5e-04$	-0.093 ± 0.038	2.690 ± 0.752	0.001	18 ± 5	35 ± 6	20 ± 5	49 ± 8	1
XMMXCS J022359.25-083544.0	$0.269^{+0.060}_{-0.060}$	0.269 ± 0.041	$0.269 \pm 3.0e-05$	-0.009 ± 0.020	1.620 ± 0.376	0.019	26 ± 5	27 ± 5	32 ± 6	31 ± 6	1
XMMXCS J022401.5-044033.9	$0.403^{+0.147}_{-0.147}$	0.401 ± 0.095	-	0.228 ± 0.027	-2.580 ± 0.506	0.001	12 ± 4	14 ± 4	12 ± 4	15 ± 4	1
XMMXCS J022401.9-050528.4	$0.327^{+0.058}_{-0.054}$	0.320 ± 0.051	$0.324 \pm 5.3e-05$	-0.297 ± 0.014	7.220 ± 0.268	0.500	8 ± 4	7 ± 4	3 ± 3	2 ± 3	1
XMMXCS J022406.0-035502.1	$0.565^{+0.104}_{-0.101}$	0.549 ± 0.097	$0.559 \pm 1.4e-04$	0.065 ± 0.093	-0.408 ± 1.930	0.128	5 ± 3	-	4 ± 2	-	1
XMMXCS J022414.79-024322.3	$0.076^{+0.028}_{-0.029}$	0.074 ± 0.013	-	-0.051 ± 0.019	1.660 ± 0.294	0.051	6 ± 3	9 ± 3	6 ± 2	9 ± 3	1
XMMXCS J022415.1-024333.2	$0.076^{+0.028}_{-0.029}$	0.074 ± 0.013	-	-0.051 ± 0.019	1.660 ± 0.294	0.051	6 ± 3	9 ± 3	6 ± 2	9 ± 3	1
XMMXCS J022433.23-041423.8	$0.262^{+0.061}_{-0.061}$	0.244 ± 0.043	$0.262 \pm 3.7e-05$	0.031 ± 0.035	0.829 ± 0.647	0.068	12 ± 4	13 ± 4	12 ± 4	13 ± 4	1
XMMXCS J022433.8-041432.9	$0.262^{+0.060}_{-0.060}$	0.244 ± 0.043	$0.262 \pm 3.7e-05$	-0.047 ± 0.029	2.260 ± 0.552	0.095	11 ± 4	12 ± 4	11 ± 4	12 ± 4	1
XMMXCS J022455.00-050835.9	$0.086^{+0.034}_{-0.033}$	0.088 ± 0.018	-	-0.021 ± 0.019	1.250 ± 0.309	0.045	5 ± 2	3 ± 2	6 ± 2	3 ± 2	1
XMMXCS J022455.8-050809.6	$0.086^{+0.034}_{-0.034}$	0.088 ± 0.018	-	-0.021 ± 0.019	1.250 ± 0.309	0.045	5 ± 2	2 ± 2	6 ± 2	2 ± 2	1
XMMXCS J022457.8-034851.1	$0.525^{+0.126}_{-0.125}$	0.548 ± 0.182	-	-0.397 ± 0.140	9.140 ± 2.890	0.001	10 ± 4	20 ± 5	11 ± 4	25 ± 6	1

Continued on next page

Table A.2 – continued from previous page

name	z_{RS}	z_{BCG}	z_{spec-g}	cmr_{grad}	cmr_{inter}	cmr_{wid}	n_{gals-c}	n_{gals-l}	n_{200-c}	n_{200-l}	qual
XMMXCS J022505.29-095008.2	$0.157^{+0.030}_{-0.030}$	0.174 ± 0.027	$0.160 \pm 1.9e-05$	-0.021 ± 0.008	1.510 ± 0.148	0.001	14 ± 4	15 ± 4	15 ± 4	16 ± 4	1
XMMXCS J022508.61-040835.1	$0.626^{+0.129}_{-0.127}$	0.158 ± 0.128	$0.622 \pm 2.4e-04$	0.287 ± 0.163	-4.810 ± 3.300	0.001	4 ± 2	17 ± 5	3 ± 2	23 ± 5	1
XMMXCS J022512.16-062307.9	$0.204^{+0.046}_{-0.046}$	0.220 ± 0.034	$0.204 \pm 2.8e-05$	-0.047 ± 0.015	2.130 ± 0.247	0.065	12 ± 4	13 ± 4	12 ± 4	13 ± 4	1
XMMXCS J022538.7-042153.2	$0.155^{+0.037}_{-0.037}$	0.143 ± 0.027	$0.141 \pm 1.6e-05$	-0.055 ± 0.003	1.990 ± 0.052	0.500	10 ± 4	5 ± 3	10 ± 4	5 ± 3	1
XMMXCS J022539.1-031125.2	$0.141^{+0.040}_{-0.040}$	0.148 ± 0.024	$0.141 \pm 1.6e-05$	-0.027 ± 0.012	1.550 ± 0.205	0.010	18 ± 4	16 ± 4	18 ± 4	17 ± 4	1
XMMXCS J022539.11-031126.2	$0.141^{+0.040}_{-0.040}$	0.148 ± 0.024	$0.141 \pm 1.6e-05$	-0.027 ± 0.012	1.550 ± 0.205	0.010	18 ± 4	16 ± 4	18 ± 4	17 ± 4	1
XMMXCS J022542.8-042840.3	$0.197^{+0.067}_{-0.071}$	0.225 ± 0.047	$0.205 \pm 3.1e-05$	-0.065 ± 0.040	2.570 ± 0.743	0.075	2 ± 2	3 ± 2	3 ± 2	3 ± 2	1
XMMXCS J022543.80-031147.4	$0.141^{+0.050}_{-0.050}$	0.148 ± 0.024	$0.141 \pm 1.6e-05$	-0.029 ± 0.015	1.590 ± 0.270	0.031	18 ± 4	16 ± 4	21 ± 5	19 ± 4	1
XMMXCS J022543.8-031148.4	$0.141^{+0.042}_{-0.043}$	0.148 ± 0.024	$0.141 \pm 1.6e-05$	-0.001 ± 0.015	1.090 ± 0.260	0.028	18 ± 4	16 ± 4	21 ± 5	18 ± 4	1
XMMXCS J022549.02-055339.3	$0.233^{+0.055}_{-0.055}$	0.239 ± 0.044	$0.232 \pm 2.2e-05$	-0.015 ± 0.022	1.620 ± 0.411	0.064	11 ± 4	12 ± 4	10 ± 3	12 ± 4	1
XMMXCS J022549.0-055339.2	$0.233^{+0.055}_{-0.055}$	0.239 ± 0.044	$0.232 \pm 2.2e-05$	-0.015 ± 0.022	1.620 ± 0.411	0.064	11 ± 4	12 ± 4	10 ± 3	12 ± 4	1
XMMXCS J022549.58-055338.1	$0.233^{+0.066}_{-0.067}$	0.239 ± 0.044	$0.232 \pm 2.2e-05$	-0.055 ± 0.013	2.330 ± 0.256	0.054	13 ± 4	13 ± 4	13 ± 4	13 ± 4	1
XMMXCS J022556.24-053825.0	$0.195^{+0.055}_{-0.056}$	0.204 ± 0.033	$0.195 \pm 2.6e-05$	-0.050 ± 0.015	2.110 ± 0.262	0.054	8 ± 3	7 ± 3	5 ± 2	4 ± 2	1
XMMXCS J022556.2-053825.0	$0.195^{+0.055}_{-0.056}$	0.204 ± 0.033	$0.195 \pm 2.6e-05$	-0.050 ± 0.015	2.110 ± 0.262	0.054	8 ± 3	7 ± 3	5 ± 2	4 ± 2	1
XMMXCS J022610.3-045805.8	$0.113^{+0.055}_{-0.056}$	0.088 ± 0.029	$0.053 \pm 1.4e-05$	0.048 ± 0.015	0.044 ± 0.233	0.062	5 ± 2	7 ± 3	3 ± 2	7 ± 3	1
XMMXCS J022610.37-045805.3	$0.112^{+0.056}_{-0.056}$	0.088 ± 0.029	$0.053 \pm 1.4e-05$	0.048 ± 0.015	0.044 ± 0.233	0.062	5 ± 2	7 ± 3	3 ± 2	7 ± 3	1
XMMXCS J022620.1-040025.9	$0.210^{+0.050}_{-0.049}$	0.233 ± 0.051	$0.209 \pm 2.0e-05$	-0.043 ± 0.056	1.980 ± 1.020	0.121	10 ± 4	20 ± 5	9 ± 3	9 ± 4	1
XMMXCS J022621.29-031725.3	$0.152^{+0.055}_{-0.054}$	0.170 ± 0.052	-	0.101 ± 0.021	-0.733 ± 0.376	0.013	4 ± 2	3 ± 2	3 ± 2	3 ± 2	1
XMMXCS J022632.50-054651.9	$0.322^{+0.055}_{-0.054}$	0.340 ± 0.053	$0.318 \pm 6.0e-05$	-0.041 ± 0.049	2.330 ± 0.920	0.072	6 ± 3	8 ± 4	5 ± 3	8 ± 3	1

Continued on next page

Table A.2 – continued from previous page

name	z_{RS}	z_{BCG}	z_{spec-g}	cmr_{grad}	cmr_{inter}	cmr_{wid}	n_{gals-c}	n_{gals-l}	n_{200-c}	n_{200-l}	qual
XMMXCS J022648.0-041422.5	$0.208^{+0.060}_{-0.060}$	0.177 ± 0.046	$0.210 \pm 1.9e-05$	0.092 ± 0.025	-0.420 ± 0.446	0.094	7 ± 3	1 ± 2	6 ± 3	2 ± 2	1
XMMXCS J022659.58-043521.6	$0.084^{+0.038}_{-0.040}$	0.082 ± 0.020	-	-0.033 ± 0.017	1.330 ± 0.259	0.066	5 ± 2	6 ± 3	4 ± 2	5 ± 2	1
XMMXCS J022711.83-031838.6	$0.330^{+0.088}_{-0.088}$	0.346 ± 0.052	$0.329 \pm 5.3e-05$	-0.103 ± 0.126	3.510 ± 2.440	0.001	4 ± 3	11 ± 4	3 ± 2	4 ± 3	1
XMMXCS J022722.1-032145.2	$0.331^{+0.079}_{-0.079}$	0.314 ± 0.068	$0.330 \pm 7.2e-05$	0.126 ± 0.065	-0.756 ± 1.220	0.154	6 ± 3	8 ± 4	7 ± 3	8 ± 3	1
XMMXCS J022722.40-032141.4	$0.331^{+0.076}_{-0.076}$	0.314 ± 0.068	$0.330 \pm 7.2e-05$	0.124 ± 0.079	-0.718 ± 1.480	0.158	5 ± 3	7 ± 3	5 ± 3	8 ± 3	1
XMMXCS J022726.38-043206.8	$0.309^{+0.039}_{-0.039}$	0.335 ± 0.058	$0.308 \pm 4.9e-05$	-0.002 ± 0.066	1.610 ± 1.270	0.129	12 ± 4	11 ± 4	12 ± 4	11 ± 4	1
XMMXCS J022732.99-055730.7	$0.231^{+0.057}_{-0.058}$	0.256 ± 0.047	$0.232 \pm 3.1e-05$	0.060 ± 0.038	0.249 ± 0.726	0.073	12 ± 4	9 ± 4	12 ± 4	8 ± 3	1
XMMXCS J022801.28-085857.9	$0.525^{+0.107}_{-0.106}$	0.520 ± 0.078	$0.523 \pm 1.5e-04$	-0.013 ± 0.064	1.130 ± 1.290	0.096	14 ± 4	21 ± 5	15 ± 5	27 ± 6	1
XMMXCS J022802.7-045101.7	$0.295^{+0.074}_{-0.074}$	0.304 ± 0.048	$0.295 \pm 3.1e-05$	-0.212 ± 0.129	5.550 ± 2.430	0.134	12 ± 4	12 ± 4	12 ± 4	12 ± 4	1
XMMXCS J022802.85-045101.1	$0.295^{+0.074}_{-0.074}$	0.304 ± 0.048	$0.295 \pm 3.1e-05$	-0.212 ± 0.129	5.550 ± 2.430	0.134	12 ± 4	12 ± 4	12 ± 4	12 ± 4	1
XMMXCS J022828.2-040045.7	$0.330^{+0.084}_{-0.086}$	0.334 ± 0.053	$0.329 \pm 6.3e-05$	-0.053 ± 0.072	2.630 ± 1.380	0.001	6 ± 3	8 ± 3	4 ± 2	5 ± 3	1
XMMXCS J022828.2-040045.6	$0.330^{+0.084}_{-0.086}$	0.334 ± 0.053	$0.329 \pm 6.3e-05$	-0.053 ± 0.072	2.630 ± 1.380	0.001	6 ± 3	8 ± 3	4 ± 2	5 ± 3	1
XMMXCS J022829.83-031257.2	$0.313^{+0.054}_{-0.054}$	0.328 ± 0.049	$0.404 \pm 5.6e-05$	-0.023 ± 0.031	2.020 ± 0.612	0.090	6 ± 3	8 ± 3	3 ± 2	6 ± 3	1
XMMXCS J022830.26-044358.0	$0.612^{+0.101}_{-0.100}$	0.586 ± 0.137	$0.611 \pm 1.3e-04$	0.016 ± 0.099	0.855 ± 1.940	0.057	9 ± 3	12 ± 4	10 ± 3	11 ± 4	1
XMMXCS J022831.83-094934.9	$0.371^{+0.074}_{-0.074}$	0.354 ± 0.055	-	0.035 ± 0.088	1.130 ± 1.710	0.064	20 ± 5	21 ± 5	26 ± 6	25 ± 6	1
XMMXCS J022917.00-055401.1	$0.292^{+0.070}_{-0.070}$	0.304 ± 0.047	$0.292 \pm 4.8e-05$	-0.045 ± 0.019	2.360 ± 0.337	0.001	8 ± 3	4 ± 3	4 ± 2	6 ± 3	1
XMMXCS J022933.47-055306.1	$0.281^{+0.061}_{-0.062}$	0.269 ± 0.045	$0.285 \pm 2.6e-05$	-0.058 ± 0.025	2.580 ± 0.478	0.001	11 ± 4	10 ± 4	12 ± 4	11 ± 4	1
XMMXCS J023008.87-054034.5	$0.499^{+0.105}_{-0.105}$	0.477 ± 0.085	$0.498 \pm 1.2e-04$	0.021 ± 0.035	0.467 ± 0.658	0.090	12 ± 4	17 ± 5	12 ± 4	16 ± 5	1
XMMXCS J023024.8-004946.4	$0.370^{+0.066}_{-0.062}$	0.341 ± 0.054	$0.363 \pm 4.5e-05$	-0.000 ± 0.001	1.000 ± 0.001	0.500	8 ± 4	8 ± 5	7 ± 4	7 ± 4	1

Continued on next page

Table A.2 – continued from previous page

name	z_{RS}	z_{BCG}	z_{spec-g}	cmr_{grad}	cmr_{inter}	cmr_{wid}	n_{gals-c}	n_{gals-l}	n_{200-c}	n_{200-l}	qual
XMMXCS J023026.62-043443.3	$0.294^{+0.061}_{-0.061}$	0.296 ± 0.046	$0.294 \pm 2.8e-05$	-0.045 ± 0.023	2.380 ± 0.426	0.001	14 ± 4	18 ± 5	14 ± 4	19 ± 5	1
XMMXCS J023027.22-051325.0	$0.188^{+0.052}_{-0.052}$	0.204 ± 0.031	$0.188 \pm 2.4e-05$	-0.016 ± 0.032	1.550 ± 0.567	0.027	6 ± 3	5 ± 3	5 ± 2	5 ± 2	1
XMMXCS J023027.23-051325.2	$0.188^{+0.052}_{-0.052}$	0.204 ± 0.031	$0.188 \pm 2.4e-05$	-0.016 ± 0.032	1.550 ± 0.567	0.027	6 ± 3	5 ± 3	5 ± 2	5 ± 2	1
XMMXCS J023035.12-043801.9	$0.290^{+0.068}_{-0.069}$	0.296 ± 0.046	$0.292 \pm 4.6e-05$	0.043 ± 0.036	0.727 ± 0.693	0.088	5 ± 3	5 ± 3	3 ± 2	2 ± 2	1
XMMXCS J023036.75-045930.4	$0.294^{+0.070}_{-0.070}$	0.312 ± 0.047	$0.292 \pm 3.8e-05$	-0.027 ± 0.037	2.030 ± 0.678	0.001	18 ± 5	20 ± 5	17 ± 5	18 ± 5	1
XMMXCS J023050.58-072901.3	$0.179^{+0.033}_{-0.033}$	0.174 ± 0.036	$0.179 \pm 2.4e-05$	-0.089 ± 0.052	2.720 ± 0.887	0.074	6 ± 3	5 ± 3	4 ± 2	4 ± 2	1
XMMXCS J023050.5-072901.2	$0.179^{+0.033}_{-0.033}$	0.174 ± 0.036	$0.179 \pm 2.4e-05$	-0.089 ± 0.052	2.720 ± 0.887	0.074	6 ± 3	5 ± 3	4 ± 2	4 ± 2	1
XMMXCS J023104.8-071849.7	$0.187^{+0.052}_{-0.052}$	0.205 ± 0.038	$0.187 \pm 2.8e-05$	-0.013 ± 0.017	1.430 ± 0.308	0.074	13 ± 4	14 ± 4	14 ± 4	15 ± 4	1
XMMXCS J023142.25-045253.7	$0.185^{+0.054}_{-0.054}$	0.199 ± 0.041	$0.186 \pm 1.7e-05$	-0.029 ± 0.010	1.770 ± 0.189	0.045	29 ± 5	36 ± 6	34 ± 6	47 ± 7	1
XMMXCS J023142.36-045311.6	$0.185^{+0.054}_{-0.054}$	0.199 ± 0.041	$0.186 \pm 1.7e-05$	-0.023 ± 0.011	1.670 ± 0.205	0.042	29 ± 5	36 ± 6	33 ± 6	46 ± 7	1
XMMXCS J023143.3-072800.1	$0.180^{+0.035}_{-0.034}$	0.167 ± 0.027	$0.180 \pm 4.4e-05$	-0.040 ± 0.043	1.780 ± 0.786	0.137	4 ± 2	3 ± 2	3 ± 2	2 ± 2	1
XMMXCS J023146.67-045229.6	$0.195^{+0.054}_{-0.055}$	0.199 ± 0.041	$0.186 \pm 1.7e-05$	-0.053 ± 0.010	2.210 ± 0.183	0.001	29 ± 6	37 ± 6	35 ± 6	53 ± 8	1
XMMXCS J023152.77-072905.3	$0.178^{+0.046}_{-0.047}$	0.172 ± 0.029	$0.179 \pm 2.7e-05$	0.033 ± 0.041	0.550 ± 0.753	0.098	4 ± 2	5 ± 3	4 ± 2	4 ± 2	1
XMMXCS J023152.7-072905.3	$0.178^{+0.046}_{-0.047}$	0.172 ± 0.029	$0.179 \pm 2.7e-05$	0.033 ± 0.041	0.550 ± 0.753	0.098	4 ± 2	5 ± 3	4 ± 2	4 ± 2	1
XMMXCS J023153.34-045125.5	$0.189^{+0.057}_{-0.058}$	0.199 ± 0.041	$0.189 \pm 1.8e-05$	-0.033 ± 0.010	1.840 ± 0.175	0.055	14 ± 4	22 ± 5	18 ± 4	37 ± 6	1
XMMXCS J023234.11-044552.3	$0.277^{+0.070}_{-0.070}$	0.291 ± 0.043	$0.277 \pm 3.9e-05$	-0.065 ± 0.024	2.690 ± 0.442	0.001	10 ± 4	13 ± 4	11 ± 4	14 ± 4	1
XMMXCS J023234.4-073104.0	$0.364^{+0.101}_{-0.093}$	0.352 ± 0.053	$0.358 \pm 1.1e-04$	-0.036 ± 0.001	2.030 ± 0.002	0.500	8 ± 4	7 ± 4	6 ± 4	5 ± 3	1
XMMXCS J023325.87-054043.8	$0.417^{+0.111}_{-0.110}$	0.484 ± 0.081	$0.437 \pm 8.8e-05$	-0.056 ± 0.032	1.860 ± 0.656	0.078	9 ± 4	11 ± 4	5 ± 3	11 ± 4	1
XMMXCS J023346.0-085048.5	$0.265^{+0.059}_{-0.059}$	0.285 ± 0.047	$0.265 \pm 4.0e-05$	-0.020 ± 0.019	1.860 ± 0.345	0.001	13 ± 4	27 ± 5	14 ± 4	10 ± 4	1

Continued on next page

Table A.2 – continued from previous page

name	z_{RS}	z_{BCG}	z_{spec-g}	cmr_{grad}	cmr_{inter}	cmr_{wid}	n_{gals-c}	n_{gals-l}	n_{200-c}	n_{200-l}	qual
XMMXCS J023432.5-053404.9	$0.228^{+0.072}_{-0.070}$	0.217 ± 0.036	$0.223 \pm 2.9e-05$	-0.115 ± 0.038	3.290 ± 0.729	0.072	8 ± 3	9 ± 4	4 ± 2	7 ± 3	1
XMMXCS J023458.5-085058.8	$0.138^{+0.028}_{-0.028}$	0.138 ± 0.022	$0.138 \pm 2.2e-05$	-0.036 ± 0.007	1.630 ± 0.116	0.022	4 ± 2	4 ± 2	4 ± 2	3 ± 2	1
XMMXCS J024747.5-032412.1	$0.137^{+0.031}_{-0.032}$	0.147 ± 0.023	$0.136 \pm 9.5e-06$	-0.134 ± 0.071	3.270 ± 1.170	0.059	10 ± 3	9 ± 3	9 ± 3	8 ± 3	1
XMMXCS J024749.5-033638.3	$0.214^{+0.045}_{-0.045}$	0.217 ± 0.040	-	-0.058 ± 0.018	2.380 ± 0.318	0.031	6 ± 3	7 ± 3	5 ± 2	5 ± 3	1
XMMXCS J024759.7-032235.4	$0.137^{+0.022}_{-0.022}$	0.147 ± 0.023	$0.136 \pm 9.5e-06$	-0.051 ± 0.021	1.900 ± 0.359	0.067	8 ± 3	9 ± 3	8 ± 3	9 ± 3	1
XMMXCS J024803.2-033143.4	$0.182^{+0.040}_{-0.040}$	0.196 ± 0.036	-	-0.013 ± 0.015	1.460 ± 0.280	0.058	17 ± 4	17 ± 4	21 ± 5	21 ± 5	1
XMMXCS J024809.8+311516.4	$0.366^{+0.109}_{-0.107}$	0.383 ± 0.058	-	-0.103 ± 0.042	2.610 ± 0.814	0.048	8 ± 4	5 ± 4	10 ± 4	37 ± 6	1
XMMXCS J024855.9-032840.2	$0.665^{+0.113}_{-0.111}$	0.569 ± 0.091	$0.667 \pm 1.4e-04$	-0.311 ± 0.185	6.510 ± 3.670	0.179	9 ± 3	2 ± 2	9 ± 3	32 ± 6	1
XMMXCS J025629.2+000753.0	$0.362^{+0.073}_{-0.072}$	0.384 ± 0.057	$0.363 \pm 5.6e-05$	-0.042 ± 0.029	2.480 ± 0.574	0.001	37 ± 6	36 ± 6	52 ± 8	51 ± 8	1
XMMXCS J025633.0+000558.2	$0.362^{+0.066}_{-0.066}$	0.384 ± 0.057	$0.363 \pm 5.6e-05$	-0.035 ± 0.015	1.280 ± 0.281	0.026	45 ± 7	45 ± 7	51 ± 8	54 ± 9	1
XMMXCS J025748.2+055718.8	$0.041^{+0.183}_{-0.041}$	0.061 ± 0.019	-	-0.105 ± 0.060	2.050 ± 0.904	0.500	19 ± 5	16 ± 4	26 ± 5	17 ± 4	1
XMMXCS J025826.2+060210.3	$0.207^{+0.112}_{-0.112}$	0.214 ± 0.037	-	-0.244 ± 0.100	5.850 ± 1.890	0.133	2 ± 2	1 ± 2	3 ± 2	1 ± 1	1
XMMXCS J025827.4+055935.3	$0.077^{+0.055}_{-0.056}$	0.091 ± 0.025	-	-0.008 ± 0.021	0.846 ± 0.351	0.103	7 ± 3	11 ± 4	4 ± 2	10 ± 3	1
XMMXCS J030016.7+370151.3	$0.201^{+0.067}_{-0.067}$	0.204 ± 0.044	-	-0.025 ± 0.027	1.730 ± 0.458	0.020	5 ± 3	8 ± 3	5 ± 2	7 ± 3	1
XMMXCS J030210.6+001053.4	$0.660^{+0.137}_{-0.135}$	0.656 ± 0.102	$0.652 \pm 1.7e-04$	-0.302 ± 0.078	7.100 ± 1.550	0.001	9 ± 3	14 ± 5	8 ± 3	12 ± 5	1
XMMXCS J030253.4-000554.5	$0.446^{+0.151}_{-0.151}$	0.269 ± 0.099	$0.449 \pm 4.9e-05$	0.348 ± 0.227	-6.060 ± 4.630	0.100	5 ± 3	6 ± 3	4 ± 2	6 ± 3	1
XMMXCS J030317.4+001238.4	$0.607^{+0.099}_{-0.098}$	0.626 ± 0.149	$0.605 \pm 2.2e-04$	-0.054 ± 0.056	2.150 ± 1.120	0.001	5 ± 3	11 ± 4	4 ± 2	12 ± 4	1
XMMXCS J030617.2-000834.6	$0.109^{+0.004}_{-0.004}$	0.126 ± 0.020	$0.109 \pm 1.5e-05$	-0.032 ± 0.012	1.530 ± 0.201	0.033	12 ± 4	13 ± 4	12 ± 4	13 ± 4	1
XMMXCS J030634.0-000423.7	$0.111^{+0.006}_{-0.005}$	0.116 ± 0.022	$0.111 \pm 1.3e-05$	-0.022 ± 0.016	1.310 ± 0.280	0.026	11 ± 3	9 ± 3	10 ± 3	9 ± 3	1

Continued on next page

Table A.2 – continued from previous page

name	z_{RS}	z_{BCG}	z_{spec-g}	cmr_{grad}	cmr_{inter}	cmr_{wid}	n_{gals-c}	n_{gals-l}	n_{200-c}	n_{200-l}	qual
XMMXCS J030644.2-000112.7	$0.111^{+0.001}_{-0.001}$	0.116 ± 0.022	$0.111 \pm 1.4e-05$	-0.049 ± 0.036	1.750 ± 0.620	0.077	14 ± 4	15 ± 4	16 ± 4	11 ± 3	1
XMMXCS J031528.4+420536.4	$0.444^{+0.109}_{-0.109}$	0.457 ± 0.184	-	-0.011 ± 0.024	1.020 ± 0.465	0.077	23 ± 5	22 ± 5	29 ± 6	27 ± 6	1
XMMXCS J031606.1+421044.1	$0.154^{+0.037}_{-0.038}$	0.134 ± 0.026	-	-0.033 ± 0.028	1.710 ± 0.525	0.064	7 ± 3	6 ± 3	6 ± 3	2 ± 2	1
XMMXCS J031907.7+412550.4	$0.029^{+0.015}_{-0.016}$	0.072 ± 0.021	$0.017 \pm 4.2e-06$	-0.068 ± 0.012	1.740 ± 0.159	0.032	20 ± 5	15 ± 4	33 ± 6	19 ± 4	1
XMMXCS J032253.8+413701.1	$0.134^{+0.038}_{-0.038}$	0.132 ± 0.021	$0.133 \pm 2.0e-05$	-0.161 ± 0.055	3.700 ± 0.925	0.071	2 ± 2	3 ± 2	3 ± 2	4 ± 2	1
XMMXCS J032347.6+413730.3	$0.134^{+0.045}_{-0.046}$	0.156 ± 0.028	$0.134 \pm 2.3e-05$	-0.009 ± 0.032	1.320 ± 0.548	0.116	7 ± 3	6 ± 3	8 ± 3	6 ± 3	1
XMMXCS J032538.2-055530.4	$0.203^{+0.051}_{-0.051}$	0.203 ± 0.031	$0.203 \pm 3.5e-05$	-0.003 ± 0.021	1.300 ± 0.393	0.055	5 ± 3	4 ± 3	3 ± 2	3 ± 2	1
XMMXCS J032553.3-061719.9	$0.315^{+0.062}_{-0.064}$	0.323 ± 0.050	-	0.032 ± 0.068	1.040 ± 1.250	0.091	7 ± 3	5 ± 3	7 ± 3	4 ± 3	1
XMMXCS J033351.5+000600.4	$0.353^{+0.088}_{-0.088}$	0.363 ± 0.052	$0.353 \pm 9.4e-05$	0.077 ± 0.131	0.165 ± 2.550	0.165	8 ± 4	10 ± 4	10 ± 4	12 ± 4	1
XMMXCS J033445.3+001707.2	$0.328^{+0.069}_{-0.068}$	0.330 ± 0.050	$0.327 \pm 4.6e-05$	-0.086 ± 0.146	3.030 ± 2.820	0.162	11 ± 4	10 ± 4	8 ± 4	7 ± 4	1
XMMXCS J033556.2+003214.7	$0.429^{+0.092}_{-0.092}$	0.417 ± 0.062	$0.429 \pm 8.9e-05$	-0.005 ± 0.018	0.823 ± 0.350	0.018	13 ± 4	14 ± 5	14 ± 5	16 ± 5	1
XMMXCS J033751.5+002759.1	$0.320^{+0.061}_{-0.062}$	0.321 ± 0.047	$0.323 \pm 4.6e-05$	-0.082 ± 0.029	3.210 ± 0.556	0.001	10 ± 4	9 ± 4	9 ± 3	8 ± 3	1
XMMXCS J033757.0+002903.4	$0.322^{+0.050}_{-0.051}$	0.321 ± 0.047	$0.323 \pm 4.6e-05$	-0.059 ± 0.019	2.770 ± 0.364	0.001	14 ± 4	16 ± 5	14 ± 4	16 ± 5	1
XMMXCS J033757.9+002901.1	$0.322^{+0.050}_{-0.051}$	0.321 ± 0.047	$0.323 \pm 4.6e-05$	-0.059 ± 0.019	2.770 ± 0.364	0.001	14 ± 4	3 ± 3	15 ± 4	10 ± 3	1
XMMXCS J041644.8+010537.2	$0.256^{+0.077}_{-0.080}$	0.253 ± 0.051	-	-0.018 ± 0.034	1.770 ± 0.655	0.101	10 ± 4	9 ± 4	7 ± 3	8 ± 3	1
XMMXCS J041652.0+010818.2	$0.325^{+0.080}_{-0.080}$	0.315 ± 0.048	-	-0.041 ± 0.042	2.370 ± 0.821	0.001	12 ± 4	13 ± 4	12 ± 4	13 ± 4	1
XMMXCS J041658.4+010740.1	$0.332^{+0.085}_{-0.086}$	0.315 ± 0.048	-	0.052 ± 0.063	0.653 ± 1.190	0.048	9 ± 4	11 ± 4	8 ± 3	11 ± 4	1
XMMXCS J041704.8+011330.9	$0.320^{+0.074}_{-0.075}$	0.332 ± 0.051	-	0.020 ± 0.048	1.260 ± 0.902	0.030	13 ± 4	15 ± 4	15 ± 4	18 ± 5	1
XMMXCS J043200.6-045528.1	$0.325^{+0.090}_{-0.091}$	0.321 ± 0.049	-	-0.137 ± 0.054	4.180 ± 1.050	0.085	6 ± 3	6 ± 3	7 ± 3	6 ± 3	1

Continued on next page

Table A.2 – continued from previous page

name	z_{RS}	z_{BCG}	z_{spec-g}	cmr_{grad}	cmr_{inter}	cmr_{wid}	n_{gals-c}	n_{gals-l}	n_{200-c}	n_{200-l}	qual
XMMXCS J044757.8-061530.5	$0.466^{+0.097}_{-0.097}$	0.481 ± 0.071	-	-0.061 ± 0.032	2.060 ± 0.617	0.001	7 ± 3	109 ± 11	6 ± 3	47 ± 10	1
XMMXCS J051537.1-000353.7	$0.141^{+0.033}_{-0.033}$	0.141 ± 0.031	-	0.149 ± 0.047	-1.600 ± 0.837	0.056	4 ± 2	4 ± 2	4 ± 2	4 ± 2	1
XMMXCS J051628.7-001836.1	$0.265^{+0.080}_{-0.080}$	0.268 ± 0.089	-	-0.089 ± 0.054	3.000 ± 1.060	0.001	2 ± 2	2 ± 2	3 ± 2	3 ± 2	1
XMMXCS J073422.3+265141.1	$0.078^{+0.057}_{-0.059}$	0.092 ± 0.018	$0.076 \pm 1.0e-05$	0.011 ± 0.015	0.744 ± 0.241	0.044	5 ± 2	4 ± 2	3 ± 2	3 ± 2	1
XMMXCS J073546.2+652629.3	$0.592^{+0.133}_{-0.132}$	0.570 ± 0.124	-	-0.142 ± 0.263	4.090 ± 5.380	0.194	4 ± 2	6 ± 4	4 ± 2	7 ± 3	1
XMMXCS J073608.2+435143.7	$0.147^{+0.067}_{-0.068}$	0.099 ± 0.028	$0.134 \pm 2.2e-05$	-0.041 ± 0.013	1.560 ± 0.244	0.500	3 ± 3	4 ± 3	5 ± 2	4 ± 2	1
XMMXCS J074232.8+651704.5	$0.140^{+0.043}_{-0.041}$	0.149 ± 0.026	-	-0.093 ± 0.069	2.560 ± 1.230	0.121	5 ± 3	6 ± 3	4 ± 2	5 ± 3	1
XMMXCS J074616.8+310228.1	$0.073^{+0.067}_{-0.071}$	0.058 ± 0.019	$0.056 \pm 8.3e-06$	-0.019 ± 0.009	1.060 ± 0.162	0.078	10 ± 3	14 ± 4	10 ± 3	16 ± 4	1
XMMXCS J074632.7+310118.3	$0.050^{+0.100}_{-0.050}$	0.058 ± 0.019	$0.056 \pm 7.9e-06$	-0.032 ± 0.023	1.230 ± 0.338	0.001	5 ± 2	0 ± 1	4 ± 2	-	1
XMMXCS J074643.2+305957.6	$0.058^{+0.007}_{-0.007}$	0.058 ± 0.019	$0.056 \pm 7.9e-06$	-0.026 ± 0.032	1.250 ± 0.472	0.048	12 ± 4	8 ± 3	12 ± 4	10 ± 3	1
XMMXCS J075046.2+144513.9	$0.108^{+0.020}_{-0.020}$	0.108 ± 0.018	$0.108 \pm 1.4e-05$	-0.015 ± 0.018	1.190 ± 0.299	0.036	9 ± 3	9 ± 3	9 ± 3	9 ± 3	1
XMMXCS J075053.1+500316.7	$0.422^{+0.074}_{-0.074}$	0.420 ± 0.061	$0.421 \pm 1.1e-04$	0.178 ± 0.111	-1.640 ± 2.130	0.227	16 ± 5	73 ± 9	24 ± 6	27 ± 8	1
XMMXCS J075427.8+220950.9	$0.399^{+0.060}_{-0.059}$	0.366 ± 0.056	$0.398 \pm 5.5e-05$	-0.028 ± 0.020	1.130 ± 0.390	0.062	13 ± 4	11 ± 4	14 ± 5	10 ± 4	1
XMMXCS J075724.8+392047.7	$0.096^{+0.010}_{-0.010}$	0.111 ± 0.023	$0.096 \pm 1.1e-05$	0.019 ± 0.029	0.616 ± 0.479	0.040	20 ± 5	20 ± 5	24 ± 5	25 ± 5	1
XMMXCS J075839.1+351939.7	$0.174^{+0.022}_{-0.022}$	0.198 ± 0.034	$0.143 \pm 2.1e-05$	-0.077 ± 0.032	2.490 ± 0.516	0.107	5 ± 3	6 ± 3	4 ± 2	4 ± 3	1
XMMXCS J080239.6+644942.1	$0.136^{+0.032}_{-0.032}$	0.119 ± 0.021	-	-0.117 ± 0.029	3.060 ± 0.528	0.073	7 ± 3	6 ± 3	4 ± 2	3 ± 2	1
XMMXCS J080352.1+651011.8	$0.356^{+0.075}_{-0.076}$	0.351 ± 0.052	-	-0.021 ± 0.027	2.140 ± 0.503	0.001	12 ± 4	13 ± 4	12 ± 4	13 ± 4	1
XMMXCS J080633.7+153208.6	$0.275^{+0.036}_{-0.037}$	0.276 ± 0.042	$0.274 \pm 3.4e-05$	-0.114 ± 0.063	3.580 ± 1.130	0.110	4 ± 3	2 ± 3	3 ± 2	2 ± 2	1
XMMXCS J080712.8+152701.5	$0.096^{+0.019}_{-0.020}$	0.102 ± 0.017	$0.096 \pm 1.4e-05$	-0.026 ± 0.021	1.370 ± 0.344	0.057	8 ± 3	10 ± 3	9 ± 3	11 ± 3	1

Continued on next page

Table A.2 – continued from previous page

name	z_{RS}	z_{BCG}	z_{spec-g}	cmr_{grad}	cmr_{inter}	cmr_{wid}	n_{gals-c}	n_{gals-l}	n_{200-c}	n_{200-l}	qual
XMMXCS J080724.6+391138.5	$0.319^{+0.105}_{-0.114}$	0.310 ± 0.141	$0.514 \pm 1.5e-04$	-0.006 ± 0.068	1.550 ± 1.310	0.001	11 ± 4	10 ± 4	10 ± 4	7 ± 3	1
XMMXCS J081020.3+482050.6	$0.536^{+0.128}_{-0.127}$	0.531 ± 0.081	$0.530 \pm 7.7e-05$	0.164 ± 0.148	-2.260 ± 2.980	0.110	25 ± 5	35 ± 6	32 ± 6	57 ± 9	1
XMMXCS J081058.2+500530.4	$0.406^{+0.082}_{-0.079}$	0.389 ± 0.062	$0.413 \pm 5.9e-05$	-0.008 ± 0.037	0.762 ± 0.730	0.059	16 ± 5	16 ± 5	16 ± 5	16 ± 5	1
XMMXCS J082135.1+010232.0	$0.100^{+0.017}_{-0.017}$	0.090 ± 0.021	$0.099 \pm 1.4e-05$	-0.019 ± 0.014	1.260 ± 0.233	0.028	7 ± 3	5 ± 2	4 ± 2	4 ± 2	1
XMMXCS J082139.6+012315.5	$0.241^{+0.060}_{-0.061}$	0.251 ± 0.041	$0.241 \pm 2.7e-05$	-0.049 ± 0.018	2.300 ± 0.319	0.090	10 ± 3	9 ± 4	8 ± 3	7 ± 3	1
XMMXCS J082151.5+011202.1	$0.090^{+0.038}_{-0.037}$	0.114 ± 0.020	$0.091 \pm 1.7e-05$	-0.010 ± 0.011	1.090 ± 0.189	0.037	20 ± 5	20 ± 5	26 ± 5	26 ± 5	1
XMMXCS J082152.9+011138.6	$0.091^{+0.035}_{-0.036}$	0.114 ± 0.020	$0.091 \pm 1.7e-05$	-0.022 ± 0.007	1.280 ± 0.125	0.028	20 ± 5	21 ± 5	26 ± 5	28 ± 5	1
XMMXCS J082215.5+011033.1	$0.108^{+0.069}_{-0.069}$	0.111 ± 0.025	-	-0.033 ± 0.024	1.500 ± 0.376	0.078	8 ± 3	10 ± 3	7 ± 3	6 ± 3	1
XMMXCS J082613.6+262605.6	$0.457^{+0.114}_{-0.111}$	0.446 ± 0.103	$0.449 \pm 1.3e-04$	-0.225 ± 0.093	5.280 ± 1.880	0.103	4 ± 3	-	3 ± 2	-	1
XMMXCS J082613.7+262605.4	$0.457^{+0.114}_{-0.111}$	0.446 ± 0.103	$0.449 \pm 1.3e-04$	-0.225 ± 0.093	5.280 ± 1.880	0.103	4 ± 3	-	3 ± 2	-	1
XMMXCS J082747.9+263505.4	$0.395^{+0.085}_{-0.083}$	0.402 ± 0.061	$0.394 \pm 5.4e-05$	-0.044 ± 0.035	1.490 ± 0.653	0.001	19 ± 5	42 ± 7	21 ± 6	20 ± 7	1
XMMXCS J083057.0+655059.2	$0.199^{+0.043}_{-0.042}$	0.209 ± 0.037	-	-0.012 ± 0.007	1.460 ± 0.128	0.043	37 ± 6	38 ± 6	87 ± 10	86 ± 10	1
XMMXCS J083115.0+523453.9	$0.623^{+0.146}_{-0.143}$	0.608 ± 0.110	$0.611 \pm 1.6e-04$	-0.295 ± 0.064	6.910 ± 1.260	0.001	8 ± 3	182 ± 14	7 ± 3	62 ± 15	1
XMMXCS J083147.8+525036.6	$0.518^{+0.087}_{-0.086}$	0.564 ± 0.090	$0.517 \pm 8.1e-05$	-0.107 ± 0.046	3.020 ± 0.894	0.060	8 ± 4	13 ± 5	8 ± 3	12 ± 5	1
XMMXCS J083227.4+524204.1	$0.629^{+0.102}_{-0.097}$	0.152 ± 0.194	$0.620 \pm 1.4e-04$	0.102 ± 0.066	-1.110 ± 1.350	0.001	4 ± 2	-	3 ± 2	-	1
XMMXCS J083454.8+553420.9	$0.264^{+0.071}_{-0.070}$	0.261 ± 0.048	-	-0.080 ± 0.030	2.930 ± 0.568	0.071	20 ± 5	17 ± 5	19 ± 5	16 ± 5	1
XMMXCS J083724.4+553249.8	$0.272^{+0.063}_{-0.065}$	0.269 ± 0.047	$0.273 \pm 5.5e-05$	0.061 ± 0.050	0.426 ± 0.915	0.001	4 ± 2	8 ± 3	3 ± 2	6 ± 3	1
XMMXCS J083726.6+145102.5	$0.215^{+0.051}_{-0.051}$	0.226 ± 0.039	$0.215 \pm 4.3e-05$	0.0004 ± 0.022	1.320 ± 0.409	0.059	8 ± 3	9 ± 3	6 ± 3	7 ± 3	1
XMMXCS J083840.4+255007.4	$0.269^{+0.081}_{-0.082}$	0.264 ± 0.102	-	0.029 ± 0.022	0.818 ± 0.424	0.052	6 ± 3	6 ± 3	4 ± 2	5 ± 3	1

Continued on next page

Table A.2 – continued from previous page

name	z_{RS}	z_{BCG}	z_{spec-g}	cmr_{grad}	cmr_{inter}	cmr_{wid}	n_{gals-c}	n_{gals-l}	n_{200-c}	n_{200-l}	qual
XMMXCS J083932.5+575621.3	$0.471^{+0.113}_{-0.114}$	0.471 ± 0.068	$0.472 \pm 1.1e-04$	0.077 ± 0.057	-0.573 ± 1.060	0.105	8 ± 4	11 ± 4	8 ± 3	11 ± 4	1
XMMXCS J084025.8+004237.2	$0.386^{+0.125}_{-0.135}$	0.404 ± 0.061	$0.406 \pm 1.1e-04$	0.027 ± 0.075	0.320 ± 1.460	0.134	4 ± 3	3 ± 3	3 ± 2	2 ± 2	1
XMMXCS J084044.2+383050.3	$0.174^{+0.033}_{-0.033}$	0.166 ± 0.025	$0.178 \pm 2.4e-05$	-0.007 ± 0.014	1.250 ± 0.253	0.025	7 ± 3	7 ± 3	6 ± 3	6 ± 3	1
XMMXCS J084110.5+003737.0	$0.378^{+0.115}_{-0.113}$	0.383 ± 0.059	$0.362 \pm 1.2e-04$	-0.076 ± 0.043	1.980 ± 0.834	0.070	15 ± 5	13 ± 5	13 ± 5	13 ± 5	1
XMMXCS J084124.4+004637.7	$0.410^{+0.055}_{-0.053}$	0.382 ± 0.059	$0.408 \pm 1.2e-04$	-0.034 ± 0.098	2.290 ± 1.910	0.001	6 ± 3	5 ± 3	6 ± 3	4 ± 3	1
XMMXCS J084623.0+345338.4	$0.377^{+0.080}_{-0.080}$	0.392 ± 0.059	-	0.019 ± 0.071	1.330 ± 1.380	0.001	6 ± 3	8 ± 4	6 ± 3	8 ± 3	1
XMMXCS J084647.4+343618.4	$0.351^{+0.136}_{-0.129}$	0.359 ± 0.148	-	0.059 ± 0.232	-0.066 ± 4.650	0.001	4 ± 3	3 ± 3	3 ± 2	1 ± 2	1
XMMXCS J084701.4+345112.8	$0.466^{+0.092}_{-0.092}$	0.470 ± 0.068	$0.464 \pm 1.4e-04$	-0.012 ± 0.024	1.040 ± 0.474	0.044	21 ± 5	22 ± 5	25 ± 6	30 ± 7	1
XMMXCS J084702.1+345120.2	$0.465^{+0.091}_{-0.090}$	0.470 ± 0.068	$0.464 \pm 1.4e-04$	-0.010 ± 0.025	0.993 ± 0.485	0.044	20 ± 5	21 ± 5	25 ± 6	26 ± 6	1
XMMXCS J084740.2+185116.7	$0.295^{+0.074}_{-0.072}$	0.305 ± 0.047	$0.292 \pm 5.8e-05$	-0.083 ± 0.037	2.960 ± 0.682	0.500	2 ± 3	1 ± 3	4 ± 2	2 ± 2	1
XMMXCS J084749.1+345749.0	$0.545^{+0.115}_{-0.115}$	0.554 ± 0.088	-	-0.046 ± 0.059	1.940 ± 1.140	0.001	10 ± 4	-	9 ± 3	-	1
XMMXCS J084848.1+445606.3	$0.572^{+0.126}_{-0.126}$	0.548 ± 0.086	$0.570 \pm 2.1e-04$	-0.008 ± 0.023	1.160 ± 0.441	0.001	11 ± 4	14 ± 5	11 ± 4	14 ± 5	1
XMMXCS J085216.53-010138.9	$0.456^{+0.084}_{-0.084}$	0.445 ± 0.089	$0.459 \pm 7.7e-05$	-0.034 ± 0.011	1.460 ± 0.207	0.001	25 ± 6	26 ± 6	38 ± 7	40 ± 7	1
XMMXCS J085234.8+161825.7	$0.100^{+0.022}_{-0.022}$	0.104 ± 0.016	$0.100 \pm 1.4e-05$	0.0001 ± 0.005	0.953 ± 0.075	0.001	6 ± 3	5 ± 2	3 ± 2	3 ± 2	1
XMMXCS J085236.7+161534.3	$0.099^{+0.023}_{-0.024}$	0.104 ± 0.016	$0.100 \pm 1.4e-05$	-0.039 ± 0.019	1.570 ± 0.317	0.063	6 ± 3	5 ± 2	7 ± 3	4 ± 2	1
XMMXCS J085253.54-013642.5	$0.332^{+0.074}_{-0.074}$	0.307 ± 0.048	-	0.040 ± 0.052	0.853 ± 0.997	0.091	10 ± 4	8 ± 4	10 ± 4	9 ± 4	1
XMMXCS J085302.9+180640.0	$0.290^{+0.048}_{-0.048}$	0.280 ± 0.050	$0.290 \pm 3.5e-05$	-0.030 ± 0.031	2.100 ± 0.609	0.065	5 ± 3	7 ± 3	3 ± 2	4 ± 3	1
XMMXCS J085332.0+150136.1	$0.429^{+0.049}_{-0.048}$	0.438 ± 0.064	$0.391 \pm 6.1e-05$	-0.044 ± 0.014	1.510 ± 0.273	0.016	6 ± 4	7 ± 4	4 ± 3	5 ± 3	1
XMMXCS J085337.6+180133.0	$0.180^{+0.054}_{-0.054}$	0.195 ± 0.041	$0.179 \pm 2.5e-05$	0.017 ± 0.027	0.867 ± 0.504	0.097	10 ± 3	9 ± 3	9 ± 3	6 ± 3	1

Continued on next page

Table A.2 – continued from previous page

name	z_{RS}	z_{BCG}	z_{spec-g}	cmr_{grad}	cmr_{inter}	cmr_{wid}	n_{gals-c}	n_{gals-l}	n_{200-c}	n_{200-l}	qual
XMMXCS J085412.98-022100.7	$0.371^{+0.066}_{-0.065}$	0.361 ± 0.057	-	-0.007 ± 0.011	0.787 ± 0.223	0.051	16 ± 5	16 ± 5	23 ± 5	21 ± 5	1
XMMXCS J085447.73-012150.9	$0.353^{+0.062}_{-0.063}$	0.348 ± 0.053	$0.353 \pm 6.0e-05$	-0.010 ± 0.027	1.910 ± 0.519	0.063	23 ± 5	23 ± 5	22 ± 5	22 ± 6	1
XMMXCS J085504.8+145459.8	$0.334^{+0.059}_{-0.060}$	0.359 ± 0.055	$0.336 \pm 9.7e-05$	0.018 ± 0.041	1.310 ± 0.815	0.058	6 ± 3	6 ± 3	4 ± 2	4 ± 3	1
XMMXCS J085612.7+375559.8	$0.412^{+0.081}_{-0.080}$	0.419 ± 0.062	$0.411 \pm 1.2e-04$	-0.001 ± 0.019	0.686 ± 0.381	0.025	39 ± 7	36 ± 7	62 ± 9	63 ± 9	1
XMMXCS J085744.6+280122.2	$0.258^{+0.068}_{-0.069}$	0.268 ± 0.041	-	-0.014 ± 0.056	1.610 ± 1.070	0.087	8 ± 3	1 ± 2	7 ± 3	1 ± 1	1
XMMXCS J085757.6+170416.5	$0.320^{+0.074}_{-0.075}$	0.344 ± 0.056	$0.322 \pm 4.3e-05$	-0.015 ± 0.067	2.020 ± 1.250	0.001	6 ± 3	7 ± 3	7 ± 3	7 ± 3	1
XMMXCS J085822.6+165715.3	$0.364^{+0.091}_{-0.089}$	0.383 ± 0.061	-	-0.014 ± 0.033	0.911 ± 0.658	0.071	19 ± 5	18 ± 5	32 ± 6	30 ± 6	1
XMMXCS J085845.4+170956.3	$0.330^{+0.067}_{-0.067}$	0.333 ± 0.050	$0.330 \pm 5.3e-05$	-0.091 ± 0.085	3.330 ± 1.630	0.097	10 ± 4	11 ± 4	10 ± 4	12 ± 4	1
XMMXCS J085904.5+275748.6	$0.309^{+0.059}_{-0.057}$	0.283 ± 0.047	$0.306 \pm 7.2e-05$	-0.059 ± 0.065	2.520 ± 1.220	0.090	4 ± 3	7 ± 3	3 ± 2	5 ± 3	1
XMMXCS J090019.5+391434.4	$0.097^{+0.006}_{-0.006}$	0.092 ± 0.021	$0.096 \pm 9.7e-06$	-0.000 ± 0.001	0.668 ± 0.001	0.500	9 ± 3	5 ± 3	8 ± 3	2 ± 2	1
XMMXCS J090036.9+205340.3	$0.246^{+0.069}_{-0.069}$	0.269 ± 0.043	$0.237 \pm 3.7e-05$	-0.032 ± 0.029	2.000 ± 0.553	0.001	9 ± 3	11 ± 4	10 ± 3	11 ± 4	1
XMMXCS J090121.7+204354.3	$0.440^{+0.100}_{-0.099}$	0.454 ± 0.114	-	-0.095 ± 0.070	2.690 ± 1.400	0.001	4 ± 3	3 ± 3	4 ± 2	4 ± 2	1
XMMXCS J090145.85-013823.6	$0.309^{+0.068}_{-0.069}$	0.285 ± 0.049	-	0.013 ± 0.023	1.330 ± 0.426	0.001	11 ± 4	11 ± 4	11 ± 4	12 ± 4	1
XMMXCS J090147.47-014323.6	$0.231^{+0.063}_{-0.063}$	0.224 ± 0.036	-	-0.090 ± 0.026	2.990 ± 0.466	0.051	7 ± 3	8 ± 3	8 ± 3	8 ± 3	1
XMMXCS J090359.7+552520.6	$0.307^{+0.101}_{-0.101}$	0.317 ± 0.054	-	-0.032 ± 0.040	2.140 ± 0.802	0.082	8 ± 3	0 ± 2	5 ± 3	-	1
XMMXCS J090953.5+543438.0	$0.142^{+0.022}_{-0.022}$	0.147 ± 0.022	$0.142 \pm 1.7e-05$	-0.071 ± 0.008	2.260 ± 0.135	0.010	4 ± 2	4 ± 2	4 ± 2	3 ± 2	1
XMMXCS J091255.9+415556.4	$0.153^{+0.029}_{-0.030}$	0.155 ± 0.025	$0.155 \pm 2.0e-05$	0.024 ± 0.021	0.769 ± 0.369	0.086	13 ± 4	10 ± 3	13 ± 4	9 ± 3	1
XMMXCS J091345.7+405627.1	$0.435^{+0.080}_{-0.079}$	0.447 ± 0.074	-	-0.149 ± 0.126	4.670 ± 2.540	0.106	24 ± 5	22 ± 5	28 ± 6	-	1
XMMXCS J091601.3+292749.2	$0.499^{+0.112}_{-0.111}$	0.510 ± 0.135	-	0.027 ± 0.055	0.373 ± 1.090	0.089	17 ± 5	20 ± 5	18 ± 5	23 ± 6	1

Continued on next page

Table A.2 – continued from previous page

name	z_{RS}	z_{BCG}	z_{spec-g}	cmr_{grad}	cmr_{inter}	cmr_{wid}	n_{gals-c}	n_{gals-l}	n_{200-c}	n_{200-l}	qual
XMMXCS J091752.3+514331.6	$0.224^{+0.057}_{-0.057}$	0.228 ± 0.035	$0.226 \pm 2.1e-05$	-0.022 ± 0.013	1.800 ± 0.245	0.063	56 ± 8	56 ± 8	81 ± 10	82 ± 10	1
XMMXCS J091759.1+514113.4	$0.224^{+0.051}_{-0.051}$	0.228 ± 0.035	$0.223 \pm 2.5e-05$	-0.043 ± 0.010	2.130 ± 0.179	0.071	45 ± 7	47 ± 7	82 ± 10	80 ± 10	1
XMMXCS J091809.3+514225.2	$0.226^{+0.046}_{-0.047}$	0.228 ± 0.035	$0.223 \pm 2.5e-05$	-0.035 ± 0.017	1.960 ± 0.321	0.068	46 ± 7	48 ± 7	90 ± 10	88 ± 10	1
XMMXCS J091932.1+303205.5	$0.404^{+0.098}_{-0.094}$	0.427 ± 0.063	$0.427 \pm 1.2e-04$	-0.052 ± 0.025	1.730 ± 0.513	0.094	9 ± 4	9 ± 4	9 ± 4	9 ± 4	1
XMMXCS J091934.7+303234.8	$0.430^{+0.084}_{-0.083}$	0.427 ± 0.063	$0.427 \pm 1.2e-04$	0.018 ± 0.044	1.460 ± 0.869	0.006	17 ± 5	14 ± 4	19 ± 5	15 ± 5	1
XMMXCS J091934.9+303156.9	$0.439^{+0.107}_{-0.104}$	0.427 ± 0.063	$0.427 \pm 1.2e-04$	-0.037 ± 0.011	1.360 ± 0.201	0.001	10 ± 4	10 ± 4	11 ± 4	11 ± 4	1
XMMXCS J091935.2+303153.4	$0.439^{+0.107}_{-0.104}$	0.427 ± 0.063	$0.427 \pm 1.2e-04$	-0.037 ± 0.011	1.360 ± 0.201	0.001	10 ± 4	10 ± 4	10 ± 4	10 ± 4	1
XMMXCS J091939.6+370755.2	$0.107^{+0.008}_{-0.008}$	0.106 ± 0.019	$0.108 \pm 1.3e-05$	0.007 ± 0.015	0.826 ± 0.259	0.048	4 ± 2	4 ± 2	3 ± 2	2 ± 2	1
XMMXCS J091952.1+301656.6	$0.361^{+0.089}_{-0.089}$	0.370 ± 0.069	-	-0.012 ± 0.091	1.840 ± 1.820	0.001	6 ± 3	8 ± 4	6 ± 3	6 ± 3	1
XMMXCS J091952.4+301655.4	$0.357^{+0.089}_{-0.089}$	0.370 ± 0.069	-	-0.026 ± 0.090	2.150 ± 1.800	0.001	7 ± 3	8 ± 3	6 ± 3	7 ± 3	1
XMMXCS J092018.9+370617.7	$0.234^{+0.057}_{-0.057}$	0.242 ± 0.048	$0.235 \pm 2.5e-05$	0.039 ± 0.022	0.703 ± 0.401	0.049	7 ± 3	8 ± 3	7 ± 3	7 ± 3	1
XMMXCS J092021.1+303013.8	$0.293^{+0.052}_{-0.053}$	0.317 ± 0.050	$0.294 \pm 3.6e-05$	-0.029 ± 0.016	2.070 ± 0.291	0.023	40 ± 7	42 ± 7	86 ± 10	89 ± 10	1
XMMXCS J092021.2+303005.7	$0.293^{+0.052}_{-0.052}$	0.317 ± 0.050	$0.294 \pm 3.6e-05$	-0.048 ± 0.021	2.440 ± 0.398	0.040	40 ± 7	42 ± 7	83 ± 10	87 ± 10	1
XMMXCS J092031.8+303305.9	$0.290^{+0.072}_{-0.074}$	0.306 ± 0.046	$0.304 \pm 6.8e-05$	-0.067 ± 0.037	2.840 ± 0.694	0.070	16 ± 4	18 ± 5	21 ± 5	23 ± 5	1
XMMXCS J092052.4+302804.8	$0.290^{+0.068}_{-0.068}$	0.283 ± 0.043	$0.290 \pm 3.9e-05$	-0.009 ± 0.026	1.740 ± 0.489	0.098	27 ± 5	12 ± 4	57 ± 8	13 ± 4	1
XMMXCS J092052.6+302802.3	$0.290^{+0.068}_{-0.068}$	0.283 ± 0.043	$0.290 \pm 3.9e-05$	-0.009 ± 0.026	1.740 ± 0.489	0.098	27 ± 5	12 ± 4	56 ± 8	31 ± 6	1
XMMXCS J092059.1+303506.7	$0.272^{+0.065}_{-0.065}$	0.268 ± 0.040	$0.273 \pm 4.8e-05$	-0.073 ± 0.021	2.860 ± 0.387	0.056	11 ± 4	10 ± 4	12 ± 4	3 ± 2	1
XMMXCS J092059.2+303418.6	$0.265^{+0.073}_{-0.075}$	0.268 ± 0.040	$0.273 \pm 4.8e-05$	0.003 ± 0.028	1.430 ± 0.522	0.064	10 ± 4	8 ± 3	10 ± 3	6 ± 3	1
XMMXCS J092114.5+370131.3	$0.234^{+0.072}_{-0.072}$	0.240 ± 0.044	$0.235 \pm 3.0e-05$	-0.059 ± 0.077	2.430 ± 1.400	0.081	8 ± 3	9 ± 4	6 ± 3	8 ± 3	1

Continued on next page

Table A.2 – continued from previous page

name	z_{RS}	z_{BCG}	z_{spec-g}	cmr_{grad}	cmr_{inter}	cmr_{wid}	n_{gals-c}	n_{gals-l}	n_{200-c}	n_{200-l}	qual
XMMXCS J092129.1+370059.9	$0.235^{+0.056}_{-0.056}$	0.240 ± 0.044	$0.235 \pm 3.0e-05$	-0.030 ± 0.023	1.890 ± 0.429	0.070	8 ± 3	10 ± 4	4 ± 2	7 ± 3	1
XMMXCS J092133.8+370339.1	$0.216^{+0.059}_{-0.059}$	0.214 ± 0.034	-	-0.008 ± 0.137	1.400 ± 2.630	0.079	5 ± 3	5 ± 3	3 ± 2	0 ± 1	1
XMMXCS J092325.4+225645.7	$0.186^{+0.042}_{-0.041}$	0.188 ± 0.032	$0.186 \pm 4.1e-05$	0.007 ± 0.015	1.070 ± 0.270	0.056	8 ± 3	7 ± 3	6 ± 3	4 ± 2	1
XMMXCS J092333.2+225740.4	$0.186^{+0.047}_{-0.047}$	0.188 ± 0.032	$0.186 \pm 4.1e-05$	-0.029 ± 0.017	1.730 ± 0.312	0.066	5 ± 2	5 ± 3	3 ± 2	4 ± 2	1
XMMXCS J092424.0+520711.8	$0.493^{+0.137}_{-0.136}$	0.492 ± 0.150	-	-0.059 ± 0.145	2.170 ± 2.890	0.098	4 ± 3	-	4 ± 2	-	1
XMMXCS J092545.7+305856.9	$0.478^{+0.123}_{-0.117}$	0.498 ± 0.208	-	0.143 ± 0.064	-2.140 ± 1.320	0.001	9 ± 4	30 ± 6	7 ± 3	12 ± 5	1
XMMXCS J092621.9+362140.7	$0.658^{+0.103}_{-0.101}$	0.625 ± 0.108	$0.607 \pm 1.3e-04$	-0.004 ± 0.043	1.190 ± 0.825	0.001	6 ± 3	11 ± 4	5 ± 2	12 ± 4	1
XMMXCS J092650.6+310127.3	$0.534^{+0.095}_{-0.094}$	0.559 ± 0.106	-	-0.099 ± 0.017	2.970 ± 0.323	0.001	11 ± 4	23 ± 5	12 ± 4	-	1
XMMXCS J092650.7+310127.3	$0.534^{+0.095}_{-0.094}$	0.559 ± 0.106	-	-0.099 ± 0.017	2.970 ± 0.323	0.001	11 ± 4	23 ± 5	12 ± 4	-	1
XMMXCS J092659.0+361219.1	$0.400^{+0.108}_{-0.106}$	0.378 ± 0.056	$0.382 \pm 8.4e-05$	0.011 ± 0.057	0.500 ± 1.130	0.111	14 ± 5	15 ± 5	15 ± 5	15 ± 5	1
XMMXCS J093205.6+473314.1	$0.225^{+0.054}_{-0.054}$	0.222 ± 0.037	$0.225 \pm 3.6e-05$	-0.044 ± 0.015	2.100 ± 0.283	0.047	5 ± 2	8 ± 3	4 ± 2	4 ± 2	1
XMMXCS J093709.3+611616.2	$0.207^{+0.034}_{-0.034}$	0.211 ± 0.032	$0.208 \pm 4.0e-05$	-0.046 ± 0.020	2.200 ± 0.372	0.059	7 ± 3	7 ± 3	5 ± 2	4 ± 2	1
XMMXCS J093945.5+360057.8	$0.303^{+0.072}_{-0.072}$	0.304 ± 0.046	$0.303 \pm 5.6e-05$	-0.034 ± 0.070	2.050 ± 1.400	0.141	5 ± 3	10 ± 4	4 ± 2	10 ± 4	1
XMMXCS J094024.8+032144.7	$0.587^{+0.108}_{-0.107}$	0.541 ± 0.143	$0.586 \pm 1.0e-04$	-0.246 ± 0.073	5.940 ± 1.460	0.001	14 ± 4	17 ± 5	16 ± 4	-	1
XMMXCS J094034.6+355950.0	$0.300^{+0.054}_{-0.054}$	0.271 ± 0.053	$0.301 \pm 4.6e-05$	0.029 ± 0.031	0.987 ± 0.559	0.001	8 ± 3	15 ± 4	8 ± 3	6 ± 3	1
XMMXCS J094055.5+032310.3	$0.506^{+0.105}_{-0.101}$	0.451 ± 0.114	$0.503 \pm 7.9e-05$	-0.002 ± 0.041	0.804 ± 0.804	0.094	14 ± 5	23 ± 6	17 ± 5	17 ± 6	1
XMMXCS J094055.5+032310.4	$0.506^{+0.105}_{-0.101}$	0.451 ± 0.114	$0.503 \pm 7.9e-05$	-0.002 ± 0.041	0.804 ± 0.804	0.094	14 ± 5	23 ± 6	17 ± 5	17 ± 6	1
XMMXCS J094117.1+033617.7	$0.290^{+0.072}_{-0.073}$	0.345 ± 0.054	$0.292 \pm 5.5e-05$	-0.073 ± 0.093	2.930 ± 1.730	0.001	5 ± 3	10 ± 4	4 ± 2	10 ± 4	1
XMMXCS J094129.5+033526.0	$0.230^{+0.053}_{-0.053}$	0.219 ± 0.036	$0.290 \pm 9.7e-05$	-0.001 ± 0.033	1.280 ± 0.630	0.058	1 ± 2	1 ± 2	3 ± 2	0 ± 1	1

Continued on next page

Table A.2 – continued from previous page

name	z_{RS}	z_{BCG}	z_{spec-g}	cmr_{grad}	cmr_{inter}	cmr_{wid}	n_{gals-c}	n_{gals-l}	n_{200-c}	n_{200-l}	qual
XMMXCS J094247.5+475450.3	$0.519^{+0.090}_{-0.089}$	0.503 ± 0.075	$0.519 \pm 1.3e-04$	-0.049 ± 0.034	1.840 ± 0.654	0.066	14 ± 4	19 ± 5	15 ± 5	16 ± 5	1
XMMXCS J094252.1+464638.6	$0.358^{+0.088}_{-0.089}$	0.349 ± 0.054	-	0.176 ± 0.039	-1.640 ± 0.756	0.001	3 ± 2	-	3 ± 2	-	1
XMMXCS J094300.1+465937.3	$0.325^{+0.082}_{-0.083}$	0.309 ± 0.062	-	0.066 ± 0.041	0.358 ± 0.810	0.098	33 ± 6	32 ± 6	55 ± 8	57 ± 8	1
XMMXCS J094314.0+475451.0	$0.441^{+0.096}_{-0.095}$	0.462 ± 0.069	$0.438 \pm 1.7e-04$	-0.098 ± 0.154	3.520 ± 2.980	0.086	10 ± 4	10 ± 4	10 ± 4	10 ± 4	1
XMMXCS J094315.4+165210.2	$0.162^{+0.042}_{-0.042}$	0.175 ± 0.027	$0.162 \pm 2.1e-05$	-0.017 ± 0.026	1.430 ± 0.470	0.056	7 ± 3	10 ± 3	6 ± 3	10 ± 3	1
XMMXCS J094332.3+163954.9	$0.255^{+0.095}_{-0.095}$	0.259 ± 0.041	$0.254 \pm 5.9e-05$	-0.078 ± 0.028	2.840 ± 0.507	0.067	14 ± 4	13 ± 4	17 ± 4	13 ± 4	1
XMMXCS J094344.5+164421.6	$0.179^{+0.045}_{-0.046}$	0.186 ± 0.028	$0.179 \pm 3.0e-05$	0.013 ± 0.026	0.993 ± 0.467	0.078	18 ± 4	14 ± 4	22 ± 5	16 ± 4	1
XMMXCS J094358.2+164120.7	$0.203^{+0.071}_{-0.072}$	0.196 ± 0.035	-	0.004 ± 0.027	1.200 ± 0.499	0.087	12 ± 4	14 ± 4	13 ± 4	17 ± 4	1
XMMXCS J094530.5+094631.1	$0.220^{+0.042}_{-0.043}$	0.209 ± 0.035	$0.214 \pm 2.4e-05$	-0.017 ± 0.021	1.660 ± 0.383	0.053	12 ± 4	10 ± 4	12 ± 4	10 ± 4	1
XMMXCS J095105.7+391742.9	$0.477^{+0.050}_{-0.050}$	0.522 ± 0.090	$0.474 \pm 9.7e-05$	-0.070 ± 0.018	2.210 ± 0.342	0.001	11 ± 4	11 ± 4	11 ± 4	11 ± 4	1
XMMXCS J095236.9-013717.3	$0.489^{+0.123}_{-0.120}$	0.548 ± 0.195	$0.479 \pm 1.0e-04$	-0.042 ± 0.043	1.560 ± 0.842	0.091	10 ± 4	12 ± 5	10 ± 4	12 ± 5	1
XMMXCS J095338.4+014207.7	$0.101^{+0.010}_{-0.010}$	0.112 ± 0.020	$0.099 \pm 1.5e-05$	-0.031 ± 0.013	1.450 ± 0.202	0.054	7 ± 3	4 ± 2	5 ± 2	3 ± 2	1
XMMXCS J095341.5+014202.1	$0.100^{+0.019}_{-0.019}$	0.112 ± 0.020	$0.099 \pm 1.5e-05$	-0.028 ± 0.010	1.400 ± 0.150	0.060	7 ± 3	3 ± 2	5 ± 2	3 ± 2	1
XMMXCS J095354.5+694453.2	$0.220^{+0.057}_{-0.058}$	0.182 ± 0.057	$0.214 \pm 6.1e-05$	-0.009 ± 0.031	1.490 ± 0.594	0.039	10 ± 3	8 ± 3	8 ± 3	4 ± 2	1
XMMXCS J095420.0+173547.9	$0.383^{+0.067}_{-0.067}$	0.343 ± 0.063	$0.381 \pm 6.5e-05$	-0.016 ± 0.056	2.010 ± 1.090	0.101	14 ± 4	17 ± 5	13 ± 4	19 ± 5	1
XMMXCS J095529.6+692640.7	$0.599^{+0.136}_{-0.134}$	0.606 ± 0.101	-	-0.054 ± 0.025	2.130 ± 0.475	0.001	6 ± 3	9 ± 4	6 ± 3	11 ± 4	1
XMMXCS J095603.5+410707.1	$0.592^{+0.135}_{-0.135}$	0.590 ± 0.108	$0.589 \pm 3.0e-04$	-0.178 ± 0.104	4.670 ± 2.110	0.001	13 ± 4	34 ± 7	13 ± 4	38 ± 8	1
XMMXCS J095610.9-002157.8	$0.550^{+0.140}_{-0.139}$	0.566 ± 0.101	$0.547 \pm 9.0e-05$	0.155 ± 0.165	-2.000 ± 3.280	0.106	14 ± 4	27 ± 6	19 ± 5	62 ± 9	1
XMMXCS J095638.8-002132.5	$0.088^{+0.002}_{-0.002}$	0.091 ± 0.017	$0.090 \pm 1.4e-05$	-0.022 ± 0.011	1.260 ± 0.168	0.028	8 ± 3	5 ± 2	9 ± 3	4 ± 2	1

Continued on next page

Table A.2 – continued from previous page

name	z_{RS}	z_{BCG}	z_{spec-g}	cmr_{grad}	cmr_{inter}	cmr_{wid}	n_{gals-c}	n_{gals-l}	n_{200-c}	n_{200-l}	qual
XMMXCS J095715.2+411643.0	$0.409^{+0.068}_{-0.066}$	0.380 ± 0.060	$0.408 \pm 1.5e-04$	0.040 ± 0.033	-0.166 ± 0.642	0.071	12 ± 4	12 ± 5	12 ± 4	12 ± 5	1
XMMXCS J095737.07+023428.5	$0.376^{+0.088}_{-0.087}$	0.359 ± 0.053	$0.373 \pm 7.0e-05$	-0.001 ± 0.015	0.647 ± 0.277	0.031	17 ± 5	144 ± 12	22 ± 5	42 ± 12	1
XMMXCS J095737.1+023425.1	$0.377^{+0.088}_{-0.087}$	0.359 ± 0.053	$0.373 \pm 7.0e-05$	-0.000 ± 0.016	0.615 ± 0.316	0.067	23 ± 5	22 ± 6	28 ± 6	29 ± 7	1
XMMXCS J095751.7+020744.3	$0.126^{+0.016}_{-0.017}$	0.106 ± 0.024	$0.125 \pm 1.0e-05$	0.172 ± 0.062	-2.190 ± 1.110	0.073	3 ± 2	2 ± 2	4 ± 2	2 ± 2	1
XMMXCS J095751.86+020746.3	$0.126^{+0.016}_{-0.017}$	0.106 ± 0.024	$0.125 \pm 1.0e-05$	0.172 ± 0.062	-2.190 ± 1.110	0.073	3 ± 2	2 ± 2	4 ± 2	2 ± 2	1
XMMXCS J095813.8+013149.3	$0.432^{+0.140}_{-0.150}$	0.435 ± 0.071	-	-0.754 ± 2.070	16.700 ± 43.00	0.500	5 ± 4	6 ± 4	5 ± 3	2 ± 3	1
XMMXCS J095823.49+024920.2	$0.344^{+0.069}_{-0.070}$	0.359 ± 0.055	$0.347 \pm 5.8e-05$	0.072 ± 0.115	0.370 ± 2.190	0.158	9 ± 4	11 ± 4	9 ± 3	11 ± 4	1
XMMXCS J095832.3+024858.9	$0.367^{+0.060}_{-0.060}$	0.359 ± 0.055	$0.345 \pm 6.9e-05$	-0.004 ± 0.076	1.740 ± 1.450	0.001	7 ± 3	8 ± 4	4 ± 2	5 ± 3	1
XMMXCS J095832.40+024900.6	$0.360^{+0.063}_{-0.058}$	0.359 ± 0.055	$0.345 \pm 6.9e-05$	-0.004 ± 0.076	1.740 ± 1.450	0.001	7 ± 3	8 ± 4	3 ± 2	5 ± 3	1
XMMXCS J095837.67+020434.4	$0.325^{+0.058}_{-0.059}$	0.328 ± 0.072	-	-0.043 ± 0.053	2.440 ± 1.070	0.095	6 ± 3	-	3 ± 2	-	1
XMMXCS J095838.1+020439.3	$0.325^{+0.058}_{-0.059}$	0.328 ± 0.072	-	-0.043 ± 0.053	2.440 ± 1.070	0.095	7 ± 3	8 ± 3	3 ± 2	3 ± 2	1
XMMXCS J095839.5+020504.6	$0.317^{+0.059}_{-0.060}$	0.328 ± 0.072	-	0.059 ± 0.072	0.453 ± 1.410	0.085	7 ± 3	4 ± 3	3 ± 2	4 ± 2	1
XMMXCS J095901.3+024740.5	$0.495^{+0.087}_{-0.086}$	0.499 ± 0.075	$0.501 \pm 1.1e-04$	-0.014 ± 0.042	1.110 ± 0.856	0.080	8 ± 4	10 ± 4	8 ± 3	11 ± 4	1
XMMXCS J095902.73+025544.3	$0.348^{+0.065}_{-0.065}$	0.356 ± 0.053	$0.349 \pm 7.6e-05$	-0.040 ± 0.060	2.590 ± 1.210	0.118	7 ± 3	7 ± 3	5 ± 3	5 ± 3	1
XMMXCS J095902.7+025544.3	$0.348^{+0.065}_{-0.065}$	0.356 ± 0.053	$0.349 \pm 7.6e-05$	-0.040 ± 0.060	2.590 ± 1.210	0.118	7 ± 3	7 ± 3	5 ± 3	5 ± 3	1
XMMXCS J095905.5+130459.6	$0.397^{+0.078}_{-0.077}$	0.392 ± 0.059	$0.396 \pm 1.1e-04$	-0.160 ± 0.094	4.760 ± 1.810	0.099	18 ± 5	22 ± 5	20 ± 5	-	1
XMMXCS J095924.12+014620.6	$0.123^{+0.021}_{-0.021}$	0.132 ± 0.025	$0.124 \pm 1.5e-05$	-0.045 ± 0.021	1.790 ± 0.351	0.024	4 ± 2	5 ± 2	4 ± 2	5 ± 2	1
XMMXCS J095924.7+014616.3	$0.123^{+0.021}_{-0.021}$	0.132 ± 0.025	$0.124 \pm 1.5e-05$	-0.045 ± 0.021	1.790 ± 0.351	0.024	5 ± 2	6 ± 3	5 ± 2	6 ± 3	1
XMMXCS J095931.8+052616.8	$0.226^{+0.076}_{-0.077}$	0.221 ± 0.050	-	-0.008 ± 0.035	1.470 ± 0.654	0.086	3 ± 2	5 ± 3	4 ± 2	6 ± 3	1

Continued on next page

Table A.2 – continued from previous page

name	z_{RS}	z_{BCG}	z_{spec-g}	cmr_{grad}	cmr_{inter}	cmr_{wid}	n_{gals-c}	n_{gals-l}	n_{200-c}	n_{200-l}	qual
XMMXCS J095939.93+023106.9	$0.584^{+0.161}_{-0.161}$	0.564 ± 0.282	-	0.354 ± 0.148	-5.780 ± 3.040	0.001	9 ± 3	17 ± 4	8 ± 3	18 ± 5	1
XMMXCS J095944.68+023619.8	$0.345^{+0.057}_{-0.056}$	0.359 ± 0.055	$0.344 \pm 6.8e-05$	-0.356 ± 0.076	8.440 ± 1.490	0.001	4 ± 3	5 ± 3	6 ± 3	6 ± 3	1
XMMXCS J095944.7+023621.7	$0.348^{+0.120}_{-0.120}$	0.359 ± 0.055	$0.344 \pm 6.8e-05$	-0.334 ± 0.173	7.940 ± 3.470	0.001	6 ± 3	6 ± 3	4 ± 2	5 ± 3	1
XMMXCS J095946.92+025522.3	$0.115^{+0.025}_{-0.026}$	0.095 ± 0.020	$0.103 \pm 1.4e-05$	0.042 ± 0.037	0.279 ± 0.661	0.063	3 ± 2	3 ± 2	4 ± 2	3 ± 2	1
XMMXCS J095946.9+025521.9	$0.115^{+0.025}_{-0.026}$	0.095 ± 0.020	$0.103 \pm 1.4e-05$	0.042 ± 0.037	0.279 ± 0.661	0.063	3 ± 2	3 ± 2	4 ± 2	3 ± 2	1
XMMXCS J095946.9+025521.6	$0.115^{+0.025}_{-0.026}$	0.095 ± 0.020	$0.103 \pm 1.4e-05$	0.042 ± 0.037	0.279 ± 0.661	0.063	3 ± 2	3 ± 2	4 ± 2	3 ± 2	1
XMMXCS J095951.33+014051.5	$0.375^{+0.097}_{-0.097}$	0.359 ± 0.053	$0.372 \pm 7.8e-05$	-0.058 ± 0.042	2.770 ± 0.801	0.001	4 ± 3	7 ± 3	3 ± 2	6 ± 3	1
XMMXCS J095951.4+014052.1	$0.375^{+0.097}_{-0.097}$	0.359 ± 0.053	$0.372 \pm 7.8e-05$	-0.058 ± 0.042	2.770 ± 0.801	0.001	4 ± 3	7 ± 3	4 ± 2	6 ± 3	1
XMMXCS J100012.3+021246.7	$0.186^{+0.034}_{-0.034}$	0.175 ± 0.027	$0.185 \pm 3.1e-05$	-0.000 ± 0.001	0.954 ± 0.001	0.500	8 ± 4	7 ± 4	8 ± 3	5 ± 3	1
XMMXCS J100012.40+021246.0	$0.186^{+0.034}_{-0.034}$	0.175 ± 0.027	$0.185 \pm 3.1e-05$	-0.000 ± 0.001	0.954 ± 0.001	0.500	8 ± 4	7 ± 4	8 ± 3	5 ± 3	1
XMMXCS J100012.9+023522.9	$0.502^{+0.137}_{-0.138}$	0.539 ± 0.086	$0.504 \pm 1.0e-04$	0.012 ± 0.077	0.709 ± 1.540	0.001	4 ± 3	22 ± 5	4 ± 2	9 ± 4	1
XMMXCS J100013.7+022239.2	$0.220^{+0.047}_{-0.048}$	0.224 ± 0.034	$0.221 \pm 2.5e-05$	-0.033 ± 0.013	1.950 ± 0.242	0.042	8 ± 3	9 ± 3	4 ± 2	6 ± 3	1
XMMXCS J100013.85+022239.7	$0.220^{+0.048}_{-0.049}$	0.224 ± 0.034	$0.221 \pm 2.5e-05$	-0.044 ± 0.014	2.160 ± 0.252	0.042	8 ± 3	9 ± 3	4 ± 2	6 ± 3	1
XMMXCS J100021.72+022329.3	$0.220^{+0.056}_{-0.057}$	0.224 ± 0.034	$0.220 \pm 2.4e-05$	-0.001 ± 0.025	1.390 ± 0.469	0.034	12 ± 4	13 ± 4	12 ± 4	13 ± 4	1
XMMXCS J100021.7+022329.0	$0.220^{+0.056}_{-0.057}$	0.224 ± 0.034	$0.220 \pm 2.4e-05$	-0.001 ± 0.025	1.390 ± 0.469	0.034	12 ± 4	13 ± 4	12 ± 4	13 ± 4	1
XMMXCS J100022.6+022406.7	$0.221^{+0.040}_{-0.040}$	0.224 ± 0.034	$0.220 \pm 2.4e-05$	-0.060 ± 0.021	2.440 ± 0.366	0.024	12 ± 4	14 ± 4	14 ± 4	15 ± 4	1
XMMXCS J100023.11+022354.2	$0.221^{+0.039}_{-0.039}$	0.224 ± 0.034	$0.220 \pm 2.4e-05$	-0.057 ± 0.016	2.380 ± 0.295	0.021	13 ± 4	15 ± 4	12 ± 4	14 ± 4	1
XMMXCS J100025.8+050852.1	$0.348^{+0.058}_{-0.059}$	0.345 ± 0.052	$0.348 \pm 6.6e-05$	-0.026 ± 0.052	2.200 ± 0.998	0.043	6 ± 3	7 ± 3	4 ± 2	5 ± 3	1
XMMXCS J100027.1+022133.9	$0.220^{+0.034}_{-0.034}$	0.224 ± 0.034	$0.220 \pm 2.4e-05$	-0.044 ± 0.026	2.150 ± 0.468	0.001	13 ± 4	12 ± 4	14 ± 4	11 ± 4	1

Continued on next page

Table A.2 – continued from previous page

name	z_{RS}	z_{BCG}	z_{spec-g}	cmr_{grad}	cmr_{inter}	cmr_{wid}	n_{gals-c}	n_{gals-l}	n_{200-c}	n_{200-l}	qual
XMMXCS J100027.26+022135.9	$0.220^{+0.034}_{-0.034}$	0.224 ± 0.034	$0.220 \pm 2.4e-05$	-0.044 ± 0.026	2.150 ± 0.468	0.001	13 ± 4	12 ± 4	14 ± 4	11 ± 4	1
XMMXCS J100027.9+024114.7	$0.348^{+0.068}_{-0.069}$	0.358 ± 0.053	$0.349 \pm 4.0e-05$	0.003 ± 0.033	1.610 ± 0.642	0.078	8 ± 3	10 ± 4	7 ± 3	9 ± 4	1
XMMXCS J100028.37+024114.3	$0.348^{+0.068}_{-0.069}$	0.358 ± 0.053	$0.349 \pm 4.0e-05$	-0.001 ± 0.034	1.680 ± 0.642	0.078	8 ± 3	11 ± 4	7 ± 3	9 ± 4	1
XMMXCS J100029.2+024137.4	$0.353^{+0.089}_{-0.087}$	0.358 ± 0.053	$0.350 \pm 4.2e-05$	-0.073 ± 0.062	2.880 ± 1.200	0.139	5 ± 3	12 ± 4	7 ± 3	12 ± 4	1
XMMXCS J100042.95+014553.4	$0.344^{+0.072}_{-0.072}$	0.354 ± 0.053	$0.346 \pm 8.6e-05$	0.084 ± 0.124	0.130 ± 2.350	0.142	5 ± 3	3 ± 3	4 ± 2	4 ± 2	1
XMMXCS J100043.2+014607.7	$0.343^{+0.070}_{-0.072}$	0.354 ± 0.053	$0.346 \pm 8.6e-05$	0.051 ± 0.107	0.749 ± 2.040	0.115	6 ± 3	6 ± 3	3 ± 2	5 ± 3	1
XMMXCS J100046.98+013925.2	$0.221^{+0.041}_{-0.041}$	0.229 ± 0.045	$0.221 \pm 4.2e-05$	-0.004 ± 0.038	1.440 ± 0.668	0.033	10 ± 3	10 ± 4	10 ± 3	11 ± 4	1
XMMXCS J100047.4+013926.9	$0.221^{+0.041}_{-0.041}$	0.229 ± 0.045	$0.221 \pm 4.2e-05$	-0.004 ± 0.038	1.440 ± 0.668	0.033	10 ± 3	10 ± 4	10 ± 3	11 ± 4	1
XMMXCS J100051.1+683348.4	$0.247^{+0.065}_{-0.066}$	0.249 ± 0.040	$0.248 \pm 4.3e-05$	-0.068 ± 0.040	2.670 ± 0.741	0.041	9 ± 3	11 ± 4	8 ± 3	9 ± 3	1
XMMXCS J100053.1+014129.2	$0.220^{+0.050}_{-0.051}$	0.229 ± 0.045	$0.221 \pm 4.2e-05$	-0.028 ± 0.026	1.860 ± 0.480	0.054	11 ± 3	10 ± 4	9 ± 3	8 ± 3	1
XMMXCS J100053.2+022831.6	$0.390^{+0.085}_{-0.077}$	0.350 ± 0.053	$0.374 \pm 9.6e-05$	0.062 ± 0.454	0.215 ± 9.290	0.500	6 ± 4	5 ± 4	5 ± 3	1 ± 3	1
XMMXCS J100053.32+022832.3	$0.390^{+0.085}_{-0.077}$	0.350 ± 0.053	$0.374 \pm 9.6e-05$	0.062 ± 0.454	0.215 ± 9.290	0.500	6 ± 4	5 ± 4	5 ± 3	1 ± 3	1
XMMXCS J100059.9+683944.9	$0.498^{+0.081}_{-0.080}$	0.498 ± 0.072	$0.497 \pm 1.2e-04$	-0.013 ± 0.047	1.050 ± 0.938	0.042	16 ± 5	91 ± 10	18 ± 5	122 ± 13	1
XMMXCS J100109.0+013338.9	$0.365^{+0.070}_{-0.068}$	0.318 ± 0.080	$0.363 \pm 4.4e-05$	-0.008 ± 0.047	0.556 ± 0.882	0.068	11 ± 4	12 ± 4	11 ± 4	12 ± 5	1
XMMXCS J100109.18+013336.0	$0.365^{+0.070}_{-0.068}$	0.318 ± 0.080	$0.363 \pm 4.4e-05$	-0.008 ± 0.047	0.556 ± 0.882	0.068	11 ± 4	12 ± 4	11 ± 4	12 ± 5	1
XMMXCS J100115.5+021359.8	$0.405^{+0.148}_{-0.152}$	0.406 ± 0.066	-	0.045 ± 0.206	0.432 ± 4.210	0.118	4 ± 3	4 ± 3	3 ± 2	-	1
XMMXCS J100115.6+021359.5	$0.405^{+0.148}_{-0.152}$	0.406 ± 0.066	-	0.045 ± 0.206	0.432 ± 4.210	0.118	4 ± 3	4 ± 3	3 ± 2	-	1
XMMXCS J100118.7+285030.3	$0.090^{+0.009}_{-0.010}$	0.102 ± 0.023	$0.089 \pm 1.6e-05$	-0.043 ± 0.012	1.600 ± 0.184	0.040	11 ± 3	7 ± 3	11 ± 3	4 ± 2	1
XMMXCS J100122.1+021334.7	$0.369^{+0.100}_{-0.092}$	0.352 ± 0.052	-	-0.041 ± 0.047	1.350 ± 0.938	0.097	7 ± 4	8 ± 4	6 ± 3	-	1

Continued on next page

Table A.2 – continued from previous page

name	z_{RS}	z_{BCG}	z_{spec-g}	cmr_{grad}	cmr_{inter}	cmr_{wid}	n_{gals-c}	n_{gals-l}	n_{200-c}	n_{200-l}	qual
XMMXCS J100141.45+022309.4	$0.128^{+0.036}_{-0.033}$	0.153 ± 0.028	$0.124 \pm 1.1e-05$	0.009 ± 0.025	0.900 ± 0.424	0.110	9 ± 3	6 ± 3	7 ± 3	3 ± 2	1
XMMXCS J100141.4+022309.5	$0.128^{+0.036}_{-0.033}$	0.153 ± 0.028	$0.124 \pm 1.1e-05$	0.009 ± 0.025	0.900 ± 0.424	0.110	9 ± 3	6 ± 3	7 ± 3	3 ± 2	1
XMMXCS J100141.70+022534.9	$0.123^{+0.017}_{-0.016}$	0.153 ± 0.028	$0.124 \pm 1.1e-05$	-0.032 ± 0.002	1.610 ± 0.033	0.500	9 ± 4	8 ± 4	7 ± 3	5 ± 3	1
XMMXCS J100141.7+022539.8	$0.123^{+0.017}_{-0.016}$	0.153 ± 0.028	$0.124 \pm 1.1e-05$	-0.032 ± 0.002	1.610 ± 0.033	0.500	9 ± 4	8 ± 4	7 ± 3	5 ± 3	1
XMMXCS J100146.58+020256.7	$0.318^{+0.093}_{-0.095}$	0.353 ± 0.055	$0.323 \pm 6.6e-05$	-0.062 ± 0.082	2.730 ± 1.630	0.077	8 ± 3	8 ± 4	6 ± 3	3 ± 2	1
XMMXCS J100146.5+020256.6	$0.318^{+0.093}_{-0.095}$	0.353 ± 0.055	$0.323 \pm 6.6e-05$	-0.062 ± 0.082	2.730 ± 1.630	0.077	8 ± 3	8 ± 4	6 ± 3	3 ± 2	1
XMMXCS J100219.7+015613.4	$0.310^{+0.058}_{-0.057}$	0.316 ± 0.048	$0.308 \pm 5.5e-05$	-0.040 ± 0.052	2.230 ± 1.010	0.110	3 ± 3	3 ± 3	4 ± 2	4 ± 2	1
XMMXCS J100236.0+324236.7	$0.050^{+0.004}_{-0.004}$	0.066 ± 0.021	$0.052 \pm 9.3e-06$	-0.010 ± 0.010	1.030 ± 0.149	0.042	5 ± 2	2 ± 2	4 ± 2	2 ± 2	1
XMMXCS J100237.0+324256.8	$0.050^{+0.004}_{-0.004}$	0.066 ± 0.021	$0.052 \pm 9.3e-06$	-0.010 ± 0.010	1.030 ± 0.149	0.042	5 ± 2	2 ± 2	3 ± 2	2 ± 2	1
XMMXCS J100259.9+022038.9	$0.176^{+0.031}_{-0.031}$	0.198 ± 0.038	$0.177 \pm 2.3e-05$	0.053 ± 0.034	0.338 ± 0.581	0.053	6 ± 3	6 ± 3	3 ± 2	5 ± 2	1
XMMXCS J100303.7+325329.1	$0.424^{+0.083}_{-0.083}$	0.403 ± 0.060	$0.419 \pm 8.2e-05$	-0.092 ± 0.047	3.480 ± 0.901	0.001	26 ± 6	31 ± 6	29 ± 7	34 ± 7	1
XMMXCS J100304.5+325340.6	$0.424^{+0.079}_{-0.077}$	0.408 ± 0.062	$0.423 \pm 1.1e-04$	-0.018 ± 0.025	1.060 ± 0.474	0.018	21 ± 5	24 ± 6	26 ± 6	30 ± 7	1
XMMXCS J100339.0+683825.0	$0.383^{+0.081}_{-0.075}$	0.360 ± 0.053	$0.369 \pm 6.6e-05$	-0.059 ± 0.001	3.050 ± 0.002	0.500	7 ± 4	8 ± 4	7 ± 3	8 ± 4	1
XMMXCS J100403.4+410015.3	$0.363^{+0.075}_{-0.074}$	0.356 ± 0.056	$0.361 \pm 8.5e-05$	-0.011 ± 0.013	0.786 ± 0.246	0.001	7 ± 4	8 ± 4	8 ± 3	9 ± 4	1
XMMXCS J100434.5+411238.1	$0.682^{+0.126}_{-0.124}$	0.556 ± 0.150	$0.679 \pm 1.7e-04$	0.231 ± 0.050	-3.430 ± 1.010	0.001	5 ± 2	28 ± 6	4 ± 2	-	1
XMMXCS J100828.9+535407.5	$0.408^{+0.100}_{-0.091}$	0.405 ± 0.065	-	0.102 ± 0.001	-0.449 ± 0.003	0.500	8 ± 4	7 ± 4	5 ± 3	2 ± 3	1
XMMXCS J101119.6+533430.4	$0.390^{+0.078}_{-0.078}$	0.380 ± 0.055	$0.390 \pm 9.0e-05$	0.029 ± 0.082	1.200 ± 1.560	0.073	25 ± 5	25 ± 5	30 ± 6	28 ± 6	1
XMMXCS J101335.9+493330.9	$0.133^{+0.020}_{-0.020}$	0.142 ± 0.022	$0.133 \pm 1.6e-05$	-0.019 ± 0.010	1.390 ± 0.169	0.035	9 ± 3	11 ± 4	9 ± 3	11 ± 4	1
XMMXCS J101345.6-000718.4	$0.096^{+0.013}_{-0.013}$	0.108 ± 0.020	$0.094 \pm 1.6e-05$	-0.018 ± 0.004	1.230 ± 0.061	0.010	14 ± 4	19 ± 4	15 ± 4	19 ± 5	1

Continued on next page

Table A.2 – continued from previous page

name	z_{RS}	z_{BCG}	z_{spec-g}	cmr_{grad}	cmr_{inter}	cmr_{wid}	n_{gals-c}	n_{gals-l}	n_{200-c}	n_{200-l}	qual
XMMXCS J101351.1-001119.9	$0.089^{+0.053}_{-0.054}$	0.114 ± 0.019	$0.094 \pm 1.6e-05$	-0.021 ± 0.006	1.250 ± 0.103	0.017	8 ± 3	7 ± 3	8 ± 3	7 ± 3	1
XMMXCS J101358.0-001500.5	$0.229^{+0.064}_{-0.072}$	0.204 ± 0.036	-	0.077 ± 0.040	-0.100 ± 0.757	0.093	7 ± 3	10 ± 4	5 ± 2	10 ± 4	1
XMMXCS J101503.6+492633.6	$0.159^{+0.031}_{-0.031}$	0.168 ± 0.025	$0.158 \pm 2.5e-05$	-0.036 ± 0.021	1.720 ± 0.374	0.043	10 ± 3	8 ± 3	10 ± 3	7 ± 3	1
XMMXCS J101504.8+492749.4	$0.159^{+0.042}_{-0.041}$	0.168 ± 0.025	$0.158 \pm 2.5e-05$	-0.059 ± 0.012	2.120 ± 0.212	0.035	10 ± 3	7 ± 3	9 ± 3	5 ± 2	1
XMMXCS J101507.8+493151.5	$0.316^{+0.076}_{-0.076}$	0.297 ± 0.061	-	-0.056 ± 0.050	2.630 ± 0.953	0.001	10 ± 4	9 ± 4	9 ± 3	9 ± 3	1
XMMXCS J101514.7+493249.9	$0.265^{+0.076}_{-0.077}$	0.275 ± 0.059	-	-0.006 ± 0.051	1.550 ± 0.997	0.120	7 ± 3	1 ± 2	7 ± 3	1 ± 1	1
XMMXCS J101703.5+390250.5	$0.204^{+0.076}_{-0.076}$	0.204 ± 0.034	$0.205 \pm 3.8e-05$	-0.011 ± 0.015	1.490 ± 0.285	0.058	17 ± 4	18 ± 4	27 ± 5	26 ± 5	1
XMMXCS J101737.1+593349.7	$0.289^{+0.054}_{-0.053}$	0.269 ± 0.051	$0.289 \pm 5.1e-05$	-0.055 ± 0.020	2.550 ± 0.391	0.085	48 ± 7	48 ± 7	79 ± 10	79 ± 10	1
XMMXCS J101931.4+080344.5	$0.163^{+0.028}_{-0.029}$	0.173 ± 0.026	$0.174 \pm 3.1e-05$	-0.037 ± 0.007	1.840 ± 0.118	0.012	20 ± 5	19 ± 5	27 ± 5	25 ± 5	1
XMMXCS J102107.0+215937.7	$0.500^{+0.099}_{-0.096}$	0.461 ± 0.069	$0.495 \pm 2.0e-04$	0.032 ± 0.057	0.127 ± 1.150	0.001	4 ± 3	9 ± 4	3 ± 2	12 ± 4	1
XMMXCS J102133.7+213748.8	$0.187^{+0.039}_{-0.038}$	0.193 ± 0.029	$0.187 \pm 4.0e-05$	-0.033 ± 0.006	1.840 ± 0.097	0.001	4 ± 2	3 ± 2	3 ± 2	0 ± 1	1
XMMXCS J102136.9+125643.2	$0.324^{+0.054}_{-0.055}$	0.268 ± 0.046	$0.325 \pm 1.0e-04$	0.192 ± 0.079	-1.950 ± 1.470	0.001	5 ± 3	8 ± 3	4 ± 2	7 ± 3	1
XMMXCS J102202.8+130006.7	$0.126^{+0.025}_{-0.025}$	0.132 ± 0.021	$0.126 \pm 1.7e-05$	-0.011 ± 0.012	1.220 ± 0.211	0.031	3 ± 2	3 ± 2	4 ± 2	5 ± 2	1
XMMXCS J102235.5+131048.6	$0.709^{+0.116}_{-0.114}$	0.696 ± 0.135	$0.705 \pm 2.4e-04$	-0.042 ± 0.039	2.020 ± 0.735	0.001	3 ± 2	35 ± 6	4 ± 2	52 ± 8	1
XMMXCS J102236.5+041222.1	$0.516^{+0.096}_{-0.094}$	0.496 ± 0.073	$0.512 \pm 1.0e-04$	-0.111 ± 0.055	3.080 ± 1.110	0.067	5 ± 3	8 ± 4	4 ± 2	8 ± 4	1
XMMXCS J102339.8+041112.9	$0.285^{+0.063}_{-0.063}$	0.288 ± 0.043	$0.289 \pm 5.1e-05$	0.011 ± 0.073	1.340 ± 1.420	0.079	22 ± 5	22 ± 5	30 ± 6	28 ± 6	1
XMMXCS J102539.7+470512.6	$0.194^{+0.046}_{-0.045}$	0.187 ± 0.033	$0.191 \pm 3.8e-05$	-0.025 ± 0.022	1.650 ± 0.394	0.075	12 ± 4	11 ± 4	15 ± 4	10 ± 4	1
XMMXCS J102547.5+383414.7	$0.318^{+0.070}_{-0.070}$	0.334 ± 0.050	$0.319 \pm 7.9e-05$	-0.012 ± 0.086	1.840 ± 1.690	0.093	8 ± 3	7 ± 3	8 ± 3	9 ± 3	1
XMMXCS J103007.0+051950.7	$0.154^{+0.053}_{-0.054}$	0.131 ± 0.041	$0.155 \pm 2.7e-05$	-0.028 ± 0.020	1.560 ± 0.363	0.049	6 ± 3	5 ± 3	3 ± 2	4 ± 2	1

Continued on next page

Table A.2 – continued from previous page

name	z_{RS}	z_{BCG}	z_{spec-g}	cmr_{grad}	cmr_{inter}	cmr_{wid}	n_{gals-c}	n_{gals-l}	n_{200-c}	n_{200-l}	qual
XMMXCS J103007.1-030642.6	$0.442^{+0.078}_{-0.076}$	0.421 ± 0.063	$0.440 \pm 4.9e-05$	0.027 ± 0.067	1.300 ± 1.280	0.051	18 ± 5	16 ± 5	17 ± 5	16 ± 5	1
XMMXCS J103013.3-030820.8	$0.060^{+0.022}_{-0.023}$	0.059 ± 0.023	-	0.023 ± 0.026	0.420 ± 0.426	0.040	7 ± 3	5 ± 2	3 ± 2	2 ± 2	1
XMMXCS J103027.6+305805.6	$0.236^{+0.061}_{-0.063}$	0.227 ± 0.041	-	0.167 ± 0.165	-1.700 ± 3.000	0.171	4 ± 3	5 ± 3	4 ± 2	2 ± 2	1
XMMXCS J103041.3+650813.2	$0.202^{+0.035}_{-0.035}$	0.207 ± 0.030	$0.202 \pm 4.0e-05$	-0.030 ± 0.048	1.800 ± 0.870	0.064	12 ± 4	10 ± 3	12 ± 4	9 ± 3	1
XMMXCS J103046.8+052752.0	$0.380^{+0.078}_{-0.076}$	0.343 ± 0.053	$0.377 \pm 7.4e-05$	-0.007 ± 0.039	0.749 ± 0.742	0.036	3 ± 3	8 ± 4	3 ± 2	5 ± 3	1
XMMXCS J103100.1+305134.9	$0.136^{+0.019}_{-0.019}$	0.140 ± 0.021	$0.137 \pm 1.6e-05$	0.008 ± 0.012	0.943 ± 0.199	0.028	10 ± 3	11 ± 4	9 ± 3	11 ± 4	1
XMMXCS J103104.9+052628.1	$0.328^{+0.059}_{-0.060}$	0.327 ± 0.048	$0.328 \pm 1.4e-04$	0.009 ± 0.039	1.510 ± 0.743	0.069	6 ± 3	8 ± 3	5 ± 2	7 ± 3	1
XMMXCS J103114.2+051717.8	$0.296^{+0.058}_{-0.058}$	0.279 ± 0.057	$0.297 \pm 5.4e-05$	-0.019 ± 0.030	1.870 ± 0.578	0.061	8 ± 3	10 ± 4	8 ± 3	9 ± 4	1
XMMXCS J103129.9+645306.0	$0.354^{+0.075}_{-0.075}$	0.374 ± 0.057	-	-0.050 ± 0.026	2.650 ± 0.492	0.001	4 ± 3	3 ± 3	3 ± 2	4 ± 2	1
XMMXCS J103131.5+311317.2	$0.375^{+0.082}_{-0.080}$	0.358 ± 0.055	$0.373 \pm 1.0e-04$	0.014 ± 0.021	0.392 ± 0.396	0.001	8 ± 4	9 ± 4	4 ± 3	5 ± 3	1
XMMXCS J103131.9+310530.9	$0.553^{+0.173}_{-0.180}$	0.540 ± 0.188	-	0.273 ± 0.059	-4.670 ± 1.220	0.001	3 ± 2	-	3 ± 2	-	1
XMMXCS J103513.0+595625.9	$0.545^{+0.145}_{-0.145}$	0.556 ± 0.091	-	-0.043 ± 0.029	1.890 ± 0.557	0.001	9 ± 3	16 ± 5	7 ± 3	15 ± 5	1
XMMXCS J103524.65+575049.5	$0.362^{+0.133}_{-0.129}$	0.364 ± 0.055	-	0.101 ± 0.034	-1.320 ± 0.677	0.095	13 ± 4	11 ± 4	14 ± 4	9 ± 4	1
XMMXCS J103524.6+575049.6	$0.362^{+0.133}_{-0.129}$	0.364 ± 0.055	-	0.101 ± 0.034	-1.320 ± 0.677	0.095	13 ± 4	11 ± 4	14 ± 4	9 ± 4	1
XMMXCS J103801.3+414619.0	$0.124^{+0.019}_{-0.019}$	0.131 ± 0.021	$0.124 \pm 1.7e-05$	-0.002 ± 0.006	1.100 ± 0.104	0.016	8 ± 3	8 ± 3	5 ± 2	5 ± 2	1
XMMXCS J103826.1+414818.8	$0.124^{+0.022}_{-0.022}$	0.123 ± 0.020	$0.124 \pm 1.3e-05$	-0.029 ± 0.014	1.490 ± 0.234	0.060	8 ± 3	8 ± 3	5 ± 2	6 ± 3	1
XMMXCS J104044.2+400000.4	$0.141^{+0.028}_{-0.028}$	0.158 ± 0.025	$0.142 \pm 1.8e-05$	-0.025 ± 0.022	1.480 ± 0.401	0.056	11 ± 3	12 ± 4	11 ± 3	11 ± 4	1
XMMXCS J104044.4+395710.4	$0.137^{+0.028}_{-0.028}$	0.140 ± 0.022	$0.136 \pm 2.4e-05$	-0.033 ± 0.019	1.660 ± 0.332	0.052	15 ± 4	14 ± 4	15 ± 4	14 ± 4	1
XMMXCS J104210.8+061715.6	$0.448^{+0.119}_{-0.118}$	0.445 ± 0.064	$0.457 \pm 8.2e-05$	-0.002 ± 0.072	0.812 ± 1.380	0.001	8 ± 4	9 ± 4	9 ± 3	14 ± 4	1

Continued on next page

Table A.2 – continued from previous page

name	z_{RS}	z_{BCG}	z_{spec-g}	cmr_{grad}	cmr_{inter}	cmr_{wid}	n_{gals-c}	n_{gals-l}	n_{200-c}	n_{200-l}	qual
XMMXCS J104225.5+582649.6	$0.388^{+0.093}_{-0.088}$	0.388 ± 0.069	-	0.002 ± 0.043	1.510 ± 0.848	0.001	4 ± 3	-	3 ± 2	-	1
XMMXCS J104412.5+064533.0	$0.298^{+0.053}_{-0.053}$	0.322 ± 0.050	$0.299 \pm 3.7e-05$	0.023 ± 0.036	1.110 ± 0.679	0.059	11 ± 4	10 ± 4	11 ± 4	11 ± 4	1
XMMXCS J104422.2+213025.2	$0.432^{+0.113}_{-0.113}$	0.422 ± 0.070	$0.517 \pm 2.3e-04$	-0.175 ± 0.176	5.240 ± 3.530	0.001	15 ± 4	18 ± 5	15 ± 5	22 ± 6	1
XMMXCS J104502.4+585452.7	$0.359^{+0.077}_{-0.074}$	0.350 ± 0.051	$0.355 \pm 1.3e-04$	-0.047 ± 0.028	1.440 ± 0.543	0.061	5 ± 3	17 ± 5	5 ± 3	14 ± 5	1
XMMXCS J104519.0-012146.2	$0.462^{+0.153}_{-0.153}$	0.461 ± 0.126	-	0.024 ± 0.267	0.494 ± 5.450	0.077	8 ± 4	8 ± 4	4 ± 3	3 ± 3	1
XMMXCS J104544.8+525023.8	$0.258^{+0.038}_{-0.038}$	0.258 ± 0.041	$0.257 \pm 4.6e-05$	-0.112 ± 0.032	3.460 ± 0.565	0.001	7 ± 3	8 ± 3	6 ± 3	7 ± 3	1
XMMXCS J104622.8+484327.8	$0.370^{+0.106}_{-0.104}$	0.389 ± 0.067	-	0.084 ± 0.209	-0.061 ± 4.050	0.135	9 ± 4	9 ± 4	8 ± 3	8 ± 3	1
XMMXCS J105040.6+573741.4	$0.607^{+0.114}_{-0.113}$	0.618 ± 0.103	-	0.026 ± 0.073	0.650 ± 1.410	0.001	3 ± 2	-	4 ± 2	-	1
XMMXCS J105041.8+573730.2	$0.607^{+0.114}_{-0.113}$	0.618 ± 0.103	-	0.026 ± 0.073	0.650 ± 1.410	0.001	4 ± 2	6 ± 3	3 ± 2	-	1
XMMXCS J105048.1+572524.2	$0.364^{+0.079}_{-0.078}$	0.342 ± 0.054	-	-0.132 ± 0.106	4.230 ± 2.120	0.141	7 ± 3	9 ± 4	8 ± 3	9 ± 4	1
XMMXCS J105121.1+335739.8	$0.222^{+0.052}_{-0.052}$	0.210 ± 0.041	-	0.023 ± 0.024	0.881 ± 0.440	0.043	4 ± 2	3 ± 2	3 ± 2	2 ± 2	1
XMMXCS J105128.6+355124.0	$0.388^{+0.085}_{-0.081}$	0.371 ± 0.078	$0.381 \pm 9.6e-05$	-0.006 ± 0.032	0.700 ± 0.601	0.090	3 ± 3	3 ± 4	3 ± 2	5 ± 3	1
XMMXCS J105201.5+435730.6	$0.444^{+0.093}_{-0.091}$	0.455 ± 0.074	$0.440 \pm 9.6e-05$	0.004 ± 0.050	1.490 ± 0.928	0.146	10 ± 4	10 ± 4	10 ± 4	10 ± 4	1
XMMXCS J105319.9+440811.6	$0.511^{+0.083}_{-0.081}$	0.521 ± 0.093	$0.527 \pm 1.2e-04$	0.058 ± 0.072	-0.295 ± 1.430	0.103	12 ± 4	13 ± 5	11 ± 4	16 ± 5	1
XMMXCS J105655.6+065840.2	$0.281^{+0.074}_{-0.075}$	0.283 ± 0.064	-	-0.046 ± 0.067	2.350 ± 1.270	0.001	10 ± 3	1 ± 2	10 ± 3	3 ± 2	1
XMMXCS J105706.9+065345.0	$0.156^{+0.031}_{-0.032}$	0.174 ± 0.029	$0.156 \pm 1.7e-05$	-0.002 ± 0.026	1.110 ± 0.477	0.096	9 ± 3	9 ± 3	8 ± 3	8 ± 3	1
XMMXCS J105707.5+065606.8	$0.162^{+0.019}_{-0.019}$	0.174 ± 0.029	$0.162 \pm 2.2e-05$	-0.098 ± 0.046	2.730 ± 0.763	0.065	4 ± 2	6 ± 3	3 ± 2	4 ± 2	1
XMMXCS J105708.9+065337.7	$0.155^{+0.033}_{-0.033}$	0.174 ± 0.029	$0.156 \pm 1.7e-05$	0.001 ± 0.025	1.060 ± 0.444	0.093	9 ± 3	9 ± 3	7 ± 3	8 ± 3	1
XMMXCS J105922.6+242905.8	$0.279^{+0.062}_{-0.061}$	0.288 ± 0.047	$0.277 \pm 5.7e-05$	-0.094 ± 0.070	3.140 ± 1.360	0.157	6 ± 3	6 ± 3	4 ± 2	3 ± 2	1

Continued on next page

Table A.2 – continued from previous page

name	z_{RS}	z_{BCG}	z_{spec-g}	cmr_{grad}	cmr_{inter}	cmr_{wid}	n_{gals-c}	n_{gals-l}	n_{200-c}	n_{200-l}	qual
XMMXCS J110303.1+355208.7	$0.239^{+0.067}_{-0.069}$	0.260 ± 0.065	-	-0.047 ± 0.050	2.250 ± 0.950	0.108	5 ± 3	4 ± 3	5 ± 2	2 ± 2	1
XMMXCS J110341.6+380510.1	$0.074^{+0.010}_{-0.009}$	0.099 ± 0.022	$0.074 \pm 1.0e-05$	-0.026 ± 0.016	1.330 ± 0.263	0.029	2 ± 2	1 ± 1	3 ± 2	3 ± 2	1
XMMXCS J110345.2+360505.5	$0.498^{+0.097}_{-0.096}$	0.515 ± 0.078	$0.497 \pm 9.7e-05$	-0.095 ± 0.026	2.760 ± 0.505	0.087	15 ± 4	23 ± 5	17 ± 5	39 ± 7	1
XMMXCS J110358.6+381400.7	$0.540^{+0.094}_{-0.092}$	0.508 ± 0.075	$0.538 \pm 1.4e-04$	0.182 ± 0.066	-2.690 ± 1.340	0.072	6 ± 3	16 ± 5	5 ± 3	12 ± 5	1
XMMXCS J110406.6+354433.0	$0.571^{+0.098}_{-0.097}$	0.596 ± 0.110	$0.548 \pm 1.3e-04$	-0.182 ± 0.076	4.700 ± 1.490	0.112	8 ± 3	15 ± 5	8 ± 3	21 ± 6	1
XMMXCS J110410.7+354725.3	$0.561^{+0.123}_{-0.118}$	0.557 ± 0.100	$0.569 \pm 1.1e-04$	0.046 ± 0.068	0.042 ± 1.370	0.121	5 ± 3	6 ± 4	3 ± 2	11 ± 4	1
XMMXCS J110425.9+360026.3	$0.502^{+0.090}_{-0.088}$	0.562 ± 0.126	$0.499 \pm 1.3e-04$	-0.223 ± 0.139	5.220 ± 2.770	0.074	13 ± 4	-	14 ± 4	-	1
XMMXCS J110632.7-182640.3	$0.510^{+0.138}_{-0.136}$	0.515 ± 0.082	-	0.089 ± 0.106	-0.859 ± 2.130	0.091	6 ± 3	32 ± 6	4 ± 2	20 ± 6	1
XMMXCS J111109.4+664955.3	$0.136^{+0.024}_{-0.024}$	0.142 ± 0.024	$0.137 \pm 1.3e-05$	-0.011 ± 0.004	1.250 ± 0.067	0.001	7 ± 3	10 ± 3	7 ± 3	10 ± 3	1
XMMXCS J111515.6+531949.5	$0.468^{+0.094}_{-0.093}$	0.493 ± 0.075	$0.467 \pm 7.4e-05$	-0.024 ± 0.022	1.260 ± 0.437	0.015	53 ± 8	58 ± 8	98 ± 11	100 ± 12	1
XMMXCS J111725.0+180922.3	$0.582^{+0.094}_{-0.093}$	0.614 ± 0.115	$0.579 \pm 1.1e-04$	-0.050 ± 0.068	1.970 ± 1.340	0.025	8 ± 3	50 ± 8	7 ± 3	10 ± 7	1
XMMXCS J111727.7+074755.9	$0.160^{+0.039}_{-0.039}$	0.152 ± 0.024	$0.159 \pm 3.0e-05$	0.003 ± 0.022	0.986 ± 0.406	0.052	4 ± 2	3 ± 2	3 ± 2	3 ± 2	1
XMMXCS J111729.8+174451.4	$0.546^{+0.115}_{-0.115}$	0.505 ± 0.078	$0.542 \pm 1.6e-04$	-0.019 ± 0.069	1.330 ± 1.350	0.094	28 ± 6	41 ± 7	34 ± 7	53 ± 9	1
XMMXCS J111744.9+073814.0	$0.500^{+0.094}_{-0.094}$	0.495 ± 0.073	$0.500 \pm 1.7e-04$	-0.058 ± 0.020	2.010 ± 0.401	0.001	8 ± 4	8 ± 4	8 ± 3	8 ± 4	1
XMMXCS J111749.9+073939.1	$0.497^{+0.096}_{-0.097}$	0.495 ± 0.073	$0.500 \pm 1.7e-04$	0.067 ± 0.127	-0.381 ± 2.480	0.074	6 ± 3	7 ± 4	5 ± 3	9 ± 4	1
XMMXCS J111750.8+075709.8	$0.406^{+0.134}_{-0.135}$	0.426 ± 0.113	-	0.090 ± 0.056	-1.370 ± 1.110	0.071	7 ± 4	7 ± 4	5 ± 3	5 ± 3	1
XMMXCS J111805.9+440921.1	$0.351^{+0.075}_{-0.075}$	0.341 ± 0.052	-	-0.108 ± 0.044	3.750 ± 0.854	0.001	8 ± 3	8 ± 4	8 ± 3	10 ± 4	1
XMMXCS J111813.1+441132.1	$0.365^{+0.155}_{-0.156}$	0.349 ± 0.054	-	0.212 ± 0.095	-3.570 ± 1.890	0.116	5 ± 3	6 ± 4	3 ± 2	6 ± 3	1
XMMXCS J111834.5+074431.5	$0.486^{+0.096}_{-0.094}$	0.467 ± 0.073	$0.483 \pm 1.6e-04$	-0.135 ± 0.069	3.490 ± 1.360	0.031	5 ± 3	-	4 ± 2	-	1

Continued on next page

Table A.2 – continued from previous page

name	z_{RS}	z_{BCG}	z_{spec-g}	cmr_{grad}	cmr_{inter}	cmr_{wid}	n_{gals-c}	n_{gals-l}	n_{200-c}	n_{200-l}	qual
XMMXCS J111846.0+075504.0	$0.128^{+0.014}_{-0.014}$	0.138 ± 0.023	$0.127 \pm 2.3e-05$	-0.077 ± 0.043	2.290 ± 0.717	0.053	5 ± 2	3 ± 2	4 ± 2	2 ± 2	1
XMMXCS J111926.1+210645.1	$0.175^{+0.028}_{-0.028}$	0.185 ± 0.028	$0.176 \pm 2.7e-05$	-0.139 ± 0.033	3.550 ± 0.558	0.056	11 ± 4	9 ± 3	11 ± 4	9 ± 3	1
XMMXCS J112007.3+431803.1	$0.613^{+0.098}_{-0.096}$	0.614 ± 0.112	$0.609 \pm 1.5e-04$	-0.253 ± 0.024	6.080 ± 0.474	0.001	9 ± 3	15 ± 5	8 ± 3	-	1
XMMXCS J112023.5+134805.0	$0.126^{+0.033}_{-0.035}$	0.133 ± 0.022	$0.149 \pm 1.8e-05$	0.035 ± 0.035	0.491 ± 0.598	0.108	5 ± 3	5 ± 3	3 ± 2	3 ± 2	1
XMMXCS J112054.9+431820.8	$0.184^{+0.025}_{-0.025}$	0.189 ± 0.028	$0.186 \pm 2.3e-05$	-0.047 ± 0.009	2.040 ± 0.164	0.021	10 ± 3	10 ± 3	10 ± 3	9 ± 3	1
XMMXCS J112213.6+241811.9	$0.026^{+0.011}_{-0.012}$	0.050 ± 0.020	$0.026 \pm 7.8e-06$	-0.014 ± 0.009	1.000 ± 0.128	0.039	3 ± 2	0 ± 1	3 ± 2	-	1
XMMXCS J112228.0+241746.4	$0.027^{+0.014}_{-0.014}$	0.050 ± 0.020	$0.027 \pm 6.2e-06$	-0.022 ± 0.008	1.110 ± 0.112	0.033	3 ± 2	0 ± 1	3 ± 2	-	1
XMMXCS J112434.2+384814.9	$0.387^{+0.142}_{-0.145}$	0.402 ± 0.075	-	-0.152 ± 0.014	3.270 ± 0.288	0.001	7 ± 3	10 ± 4	4 ± 2	-	1
XMMXCS J112447.9+385930.2	$0.300^{+0.045}_{-0.045}$	0.326 ± 0.053	$0.301 \pm 3.9e-05$	-0.003 ± 0.027	1.660 ± 0.507	0.049	9 ± 3	9 ± 4	9 ± 3	9 ± 3	1
XMMXCS J112524.2+385400.2	$0.555^{+0.112}_{-0.111}$	0.499 ± 0.076	$0.553 \pm 1.4e-04$	-0.067 ± 0.022	2.230 ± 0.426	0.001	14 ± 4	24 ± 6	15 ± 4	26 ± 6	1
XMMXCS J112737.1+583735.6	$0.196^{+0.055}_{-0.056}$	0.199 ± 0.029	$0.197 \pm 3.1e-05$	0.016 ± 0.028	0.951 ± 0.517	0.081	9 ± 3	16 ± 4	8 ± 3	9 ± 4	1
XMMXCS J113753.0+215839.9	$0.200^{+0.075}_{-0.080}$	0.219 ± 0.034	$0.208 \pm 4.3e-05$	0.005 ± 0.048	1.230 ± 0.900	0.073	10 ± 3	9 ± 3	10 ± 3	9 ± 3	1
XMMXCS J113844.1+031540.5	$0.128^{+0.020}_{-0.020}$	0.134 ± 0.025	$0.128 \pm 1.5e-05$	-0.027 ± 0.017	1.480 ± 0.282	0.033	6 ± 3	5 ± 2	7 ± 3	4 ± 2	1
XMMXCS J114450.2+194140.8	$0.033^{+0.009}_{-0.009}$	0.047 ± 0.025	$0.020 \pm 5.6e-06$	-0.036 ± 0.066	1.230 ± 0.988	0.076	4 ± 2	1 ± 1	3 ± 2	0 ± 1	1
XMMXCS J114506.2+195811.5	$0.020^{+0.023}_{-0.020}$	0.043 ± 0.015	$0.017 \pm 6.6e-06$	-0.039 ± 0.039	1.120 ± 0.677	0.105	5 ± 2	0 ± 1	4 ± 2	-	1
XMMXCS J114546.3+194623.5	$0.026^{+0.028}_{-0.026}$	0.051 ± 0.021	$0.018 \pm 7.9e-06$	-0.023 ± 0.010	1.090 ± 0.124	0.023	9 ± 3	3 ± 2	8 ± 3	1 ± 1	1
XMMXCS J114555.8+522154.3	$0.457^{+0.087}_{-0.085}$	0.451 ± 0.064	$0.455 \pm 1.4e-04$	0.017 ± 0.032	0.403 ± 0.626	0.050	25 ± 6	24 ± 6	27 ± 6	22 ± 6	1
XMMXCS J115011.6+013848.7	$0.454^{+0.090}_{-0.089}$	0.440 ± 0.065	$0.451 \pm 1.4e-04$	-0.003 ± 0.026	0.795 ± 0.495	0.001	10 ± 4	16 ± 5	8 ± 4	14 ± 5	1
XMMXCS J115123.8+545008.7	$0.143^{+0.035}_{-0.035}$	0.160 ± 0.026	$0.143 \pm 2.1e-05$	-0.053 ± 0.011	2.010 ± 0.201	0.046	6 ± 3	7 ± 3	7 ± 3	7 ± 3	1

Continued on next page

Table A.2 – continued from previous page

name	z_{RS}	z_{BCG}	z_{spec-g}	cmr_{grad}	cmr_{inter}	cmr_{wid}	n_{gals-c}	n_{gals-l}	n_{200-c}	n_{200-l}	qual
XMMXCS J115517.4+233838.8	$0.129^{+0.039}_{-0.050}$	0.139 ± 0.023	$0.123 \pm 1.6e-05$	0.025 ± 0.056	0.437 ± 1.030	0.116	8 ± 3	6 ± 3	5 ± 2	5 ± 2	1
XMMXCS J115518.6+232418.4	$0.139^{+0.031}_{-0.031}$	0.152 ± 0.037	$0.144 \pm 2.7e-05$	-0.038 ± 0.009	1.660 ± 0.151	0.043	32 ± 6	33 ± 6	46 ± 7	46 ± 7	1
XMMXCS J115524.8+231927.8	$0.143^{+0.044}_{-0.042}$	0.140 ± 0.023	$0.165 \pm 1.7e-05$	-0.032 ± 0.022	1.610 ± 0.393	0.062	22 ± 5	24 ± 5	33 ± 6	36 ± 6	1
XMMXCS J115530.8+232324.5	$0.133^{+0.044}_{-0.044}$	0.152 ± 0.037	$0.139 \pm 3.2e-05$	-0.053 ± 0.017	1.930 ± 0.292	0.058	23 ± 5	21 ± 5	39 ± 6	35 ± 6	1
XMMXCS J115533.7+545804.5	$0.220^{+0.074}_{-0.075}$	0.237 ± 0.043	-	-0.143 ± 0.019	3.930 ± 0.344	0.080	2 ± 2	5 ± 3	4 ± 2	5 ± 3	1
XMMXCS J115622.3+524232.8	$0.484^{+0.088}_{-0.087}$	0.499 ± 0.074	$0.482 \pm 1.3e-04$	-0.060 ± 0.014	1.990 ± 0.279	0.001	11 ± 4	10 ± 4	12 ± 4	10 ± 4	1
XMMXCS J115738.6+435031.9	$0.108^{+0.040}_{-0.034}$	0.089 ± 0.030	$0.076 \pm 1.1e-05$	0.020 ± 0.013	0.476 ± 0.214	0.037	5 ± 2	4 ± 2	5 ± 2	4 ± 2	1
XMMXCS J115758.7+441012.7	$0.290^{+0.050}_{-0.051}$	0.291 ± 0.042	$0.292 \pm 5.1e-05$	-0.052 ± 0.030	2.550 ± 0.569	0.001	7 ± 3	8 ± 3	7 ± 3	8 ± 3	1
XMMXCS J115851.4+440537.2	$0.290^{+0.041}_{-0.042}$	0.305 ± 0.047	$0.290 \pm 5.8e-05$	-0.030 ± 0.023	2.140 ± 0.424	0.001	14 ± 4	12 ± 4	14 ± 4	12 ± 4	1
XMMXCS J115949.2-033420.4	$0.447^{+0.099}_{-0.094}$	0.427 ± 0.062	$0.436 \pm 1.2e-04$	0.041 ± 0.110	0.997 ± 2.090	0.259	12 ± 4	14 ± 5	13 ± 5	15 ± 5	1
XMMXCS J120045.8+342447.8	$0.263^{+0.047}_{-0.047}$	0.256 ± 0.045	$0.263 \pm 3.3e-05$	0.033 ± 0.038	0.860 ± 0.699	0.050	8 ± 3	9 ± 3	8 ± 3	9 ± 3	1
XMMXCS J120047.3-033646.9	$0.256^{+0.080}_{-0.082}$	0.258 ± 0.086	-	-0.167 ± 0.018	4.550 ± 0.370	0.001	5 ± 3	4 ± 3	3 ± 2	2 ± 2	1
XMMXCS J120048.8-032726.7	$0.396^{+0.059}_{-0.059}$	0.395 ± 0.063	$0.395 \pm 9.7e-05$	0.152 ± 0.082	-1.110 ± 1.560	0.090	15 ± 4	20 ± 5	17 ± 5	2 ± 3	1
XMMXCS J120115.0+342542.4	$0.222^{+0.067}_{-0.067}$	0.210 ± 0.034	$0.235 \pm 3.0e-05$	-0.042 ± 0.027	2.080 ± 0.510	0.089	6 ± 3	6 ± 3	5 ± 2	5 ± 3	1
XMMXCS J120124.5+342041.6	$0.255^{+0.070}_{-0.071}$	0.265 ± 0.046	$0.257 \pm 2.9e-05$	-0.021 ± 0.021	1.870 ± 0.403	0.054	7 ± 3	8 ± 3	5 ± 2	7 ± 3	1
XMMXCS J120131.7+341513.4	$0.289^{+0.049}_{-0.049}$	0.291 ± 0.050	$0.289 \pm 5.9e-05$	-0.060 ± 0.024	2.640 ± 0.453	0.044	13 ± 4	13 ± 4	13 ± 4	4 ± 3	1
XMMXCS J120210.3+442709.2	$0.409^{+0.065}_{-0.064}$	0.406 ± 0.061	$0.408 \pm 8.4e-05$	0.032 ± 0.021	0.085 ± 0.377	0.001	10 ± 4	10 ± 4	11 ± 4	11 ± 4	1
XMMXCS J120313.7+442717.8	$0.345^{+0.067}_{-0.067}$	0.352 ± 0.051	$0.345 \pm 7.6e-05$	-0.020 ± 0.046	2.030 ± 0.923	0.135	7 ± 3	6 ± 4	7 ± 3	6 ± 3	1
XMMXCS J120352.8+014706.5	$0.236^{+0.054}_{-0.053}$	0.245 ± 0.043	$0.247 \pm 2.4e-05$	-0.054 ± 0.019	2.370 ± 0.342	0.009	24 ± 5	25 ± 5	45 ± 7	44 ± 7	1

Continued on next page

Table A.2 – continued from previous page

name	z_{RS}	z_{BCG}	z_{spec-g}	cmr_{grad}	cmr_{inter}	cmr_{wid}	n_{gals-c}	n_{gals-l}	n_{200-c}	n_{200-l}	qual
XMMXCS J120405.0+280333.9	$0.166^{+0.034}_{-0.034}$	0.189 ± 0.030	$0.165 \pm 1.5e-05$	-0.031 ± 0.015	1.650 ± 0.270	0.064	14 ± 4	14 ± 4	17 ± 4	17 ± 4	1
XMMXCS J120439.0+352233.2	$0.190^{+0.039}_{-0.040}$	0.193 ± 0.029	$0.190 \pm 2.2e-05$	-0.019 ± 0.017	1.570 ± 0.302	0.029	10 ± 3	10 ± 3	10 ± 3	10 ± 3	1
XMMXCS J120545.3+350950.6	$0.076^{+0.025}_{-0.025}$	0.077 ± 0.020	$0.079 \pm 9.5e-06$	0.113 ± 0.038	-1.150 ± 0.616	0.500	3 ± 2	1 ± 1	3 ± 2	1 ± 1	1
XMMXCS J120619.8+282254.6	$0.167^{+0.042}_{-0.044}$	0.178 ± 0.030	$0.159 \pm 2.0e-05$	0.024 ± 0.021	0.730 ± 0.380	0.067	7 ± 3	8 ± 3	7 ± 3	8 ± 3	1
XMMXCS J120622.7+281041.8	$0.205^{+0.036}_{-0.036}$	0.229 ± 0.046	$0.205 \pm 3.8e-05$	-0.044 ± 0.011	2.080 ± 0.202	0.036	8 ± 3	6 ± 3	7 ± 3	6 ± 3	1
XMMXCS J120622.86+281041.1	$0.205^{+0.036}_{-0.036}$	0.229 ± 0.046	$0.205 \pm 3.8e-05$	-0.044 ± 0.011	2.080 ± 0.202	0.036	8 ± 3	6 ± 3	7 ± 3	6 ± 3	1
XMMXCS J120630.5+282310.1	$0.169^{+0.035}_{-0.035}$	0.178 ± 0.030	$0.169 \pm 2.1e-05$	-0.071 ± 0.027	2.400 ± 0.475	0.015	8 ± 3	9 ± 3	8 ± 3	8 ± 3	1
XMMXCS J120732.67+280607.6	$0.590^{+0.158}_{-0.158}$	0.605 ± 0.164	-	0.199 ± 0.088	-2.880 ± 1.780	0.095	8 ± 3	22 ± 5	8 ± 3	36 ± 7	1
XMMXCS J120733.3+280647.5	$0.602^{+0.162}_{-0.162}$	0.605 ± 0.164	-	0.125 ± 0.081	-1.420 ± 1.650	0.095	10 ± 3	-	10 ± 3	-	1
XMMXCS J120746.9+281320.0	$0.432^{+0.093}_{-0.091}$	0.455 ± 0.079	$0.462 \pm 1.2e-04$	-0.042 ± 0.030	1.560 ± 0.592	0.090	27 ± 6	31 ± 6	40 ± 8	41 ± 8	1
XMMXCS J120801.1+433926.7	$0.265^{+0.059}_{-0.059}$	0.261 ± 0.040	$0.266 \pm 5.6e-05$	-0.030 ± 0.023	2.000 ± 0.430	0.001	6 ± 3	7 ± 3	5 ± 2	5 ± 3	1
XMMXCS J120929.4+392803.6	$0.236^{+0.033}_{-0.033}$	0.237 ± 0.039	$0.237 \pm 5.3e-05$	-0.006 ± 0.014	1.480 ± 0.277	0.055	2 ± 2	2 ± 2	3 ± 2	3 ± 2	1
XMMXCS J120934.2+392232.8	$0.555^{+0.102}_{-0.101}$	0.540 ± 0.089	$0.554 \pm 7.9e-05$	0.024 ± 0.047	0.503 ± 0.937	0.086	15 ± 4	15 ± 5	16 ± 4	15 ± 5	1
XMMXCS J120936.9+434338.0	$0.494^{+0.136}_{-0.135}$	0.499 ± 0.246	-	0.028 ± 0.016	0.290 ± 0.302	0.028	9 ± 4	10 ± 4	9 ± 4	11 ± 4	1
XMMXCS J120952.3+393738.0	$0.218^{+0.070}_{-0.070}$	0.241 ± 0.037	-	-0.000 ± 0.001	1.270 ± 0.001	0.500	3 ± 3	4 ± 3	3 ± 2	2 ± 2	1
XMMXCS J121108.5+391257.5	$0.319^{+0.074}_{-0.075}$	0.326 ± 0.055	$0.314 \pm 3.6e-05$	0.018 ± 0.046	1.320 ± 0.889	0.110	17 ± 4	42 ± 7	18 ± 5	32 ± 7	1
XMMXCS J121113.8+501846.2	$0.349^{+0.066}_{-0.066}$	0.358 ± 0.053	$0.349 \pm 5.5e-05$	-0.068 ± 0.018	2.970 ± 0.344	0.001	15 ± 4	34 ± 6	16 ± 5	21 ± 6	1
XMMXCS J121115.4+391136.7	$0.336^{+0.080}_{-0.082}$	0.326 ± 0.055	$0.338 \pm 5.1e-05$	-0.053 ± 0.022	2.700 ± 0.420	0.019	14 ± 4	14 ± 4	15 ± 4	15 ± 4	1
XMMXCS J121130.5+130539.5	$0.376^{+0.061}_{-0.061}$	0.346 ± 0.051	$0.375 \pm 1.3e-04$	0.059 ± 0.052	0.534 ± 0.984	0.054	3 ± 3	3 ± 3	3 ± 2	0 ± 1	1

Continued on next page

Table A.2 – continued from previous page

name	z_{RS}	z_{BCG}	z_{spec-g}	cmr_{grad}	cmr_{inter}	cmr_{wid}	n_{gals-c}	n_{gals-l}	n_{200-c}	n_{200-l}	qual
XMMXCS J121205.4+131741.4	$0.451^{+0.083}_{-0.082}$	0.449 ± 0.066	$0.450 \pm 1.1e-04$	0.024 ± 0.056	0.262 ± 1.080	0.055	8 ± 4	9 ± 4	8 ± 3	8 ± 4	1
XMMXCS J121221.0+503429.3	$0.561^{+0.152}_{-0.152}$	0.537 ± 0.119	-	0.143 ± 0.090	-1.910 ± 1.800	0.001	13 ± 4	37 ± 7	13 ± 4	41 ± 8	1
XMMXCS J121321.1+291415.7	$0.141^{+0.032}_{-0.033}$	0.152 ± 0.025	$0.141 \pm 1.5e-05$	-0.011 ± 0.019	1.240 ± 0.332	0.071	18 ± 4	18 ± 4	25 ± 5	24 ± 5	1
XMMXCS J121334.8+025349.8	$0.408^{+0.084}_{-0.084}$	0.424 ± 0.064	$0.407 \pm 1.5e-04$	-0.023 ± 0.064	2.150 ± 1.260	0.001	20 ± 5	25 ± 6	27 ± 6	-	1
XMMXCS J121448.1+140552.6	$0.100^{+0.038}_{-0.039}$	0.082 ± 0.025	$0.106 \pm 1.4e-05$	-0.001 ± 0.022	0.910 ± 0.342	0.500	7 ± 3	8 ± 4	5 ± 3	8 ± 3	1
XMMXCS J121451.7+140533.5	$0.081^{+0.001}_{-0.001}$	0.082 ± 0.025	$0.081 \pm 1.3e-05$	-0.070 ± 0.052	1.980 ± 0.824	0.087	7 ± 3	2 ± 2	3 ± 2	2 ± 2	1
XMMXCS J121521.8+363449.0	$0.358^{+0.059}_{-0.077}$	0.327 ± 0.051	$0.366 \pm 4.9e-05$	-0.071 ± 0.050	2.900 ± 0.934	0.106	9 ± 4	13 ± 4	8 ± 3	13 ± 4	1
XMMXCS J121658.1+065830.8	$0.486^{+0.135}_{-0.135}$	0.483 ± 0.071	$0.484 \pm 1.7e-04$	-0.037 ± 0.017	1.530 ± 0.316	0.001	11 ± 4	22 ± 5	11 ± 4	19 ± 6	1
XMMXCS J121731.3+033655.2	$0.079^{+0.005}_{-0.005}$	0.100 ± 0.017	$0.077 \pm 9.7e-06$	-0.031 ± 0.010	1.410 ± 0.154	0.030	29 ± 6	30 ± 6	37 ± 6	37 ± 6	1
XMMXCS J121741.3+033935.0	$0.078^{+0.004}_{-0.004}$	0.100 ± 0.017	$0.077 \pm 9.3e-06$	-0.027 ± 0.007	1.360 ± 0.109	0.019	19 ± 5	24 ± 5	29 ± 6	38 ± 6	1
XMMXCS J121744.6+472921.5	$0.270^{+0.061}_{-0.061}$	0.301 ± 0.048	$0.271 \pm 3.7e-05$	-0.043 ± 0.018	2.260 ± 0.353	0.085	21 ± 5	24 ± 5	30 ± 6	32 ± 6	1
XMMXCS J121753.2+034132.6	$0.079^{+0.004}_{-0.004}$	0.100 ± 0.017	$0.076 \pm 1.0e-05$	-0.028 ± 0.014	1.380 ± 0.238	0.027	19 ± 4	20 ± 5	28 ± 5	32 ± 6	1
XMMXCS J121754.5+472853.8	$0.268^{+0.061}_{-0.061}$	0.301 ± 0.048	$0.271 \pm 3.7e-05$	-0.057 ± 0.016	2.510 ± 0.296	0.007	14 ± 4	19 ± 5	15 ± 4	22 ± 5	1
XMMXCS J121759.8+295704.8	$0.358^{+0.062}_{-0.063}$	0.355 ± 0.053	$0.361 \pm 7.0e-05$	0.026 ± 0.059	1.220 ± 1.130	0.080	7 ± 3	0 ± 2	3 ± 2	-	1
XMMXCS J121805.9+295811.1	$0.360^{+0.067}_{-0.067}$	0.355 ± 0.053	$0.360 \pm 7.5e-05$	-0.080 ± 0.049	3.240 ± 0.942	0.062	6 ± 3	7 ± 3	7 ± 3	6 ± 3	1
XMMXCS J121822.9+033316.4	$0.396^{+0.074}_{-0.073}$	0.397 ± 0.079	$0.395 \pm 8.2e-05$	0.113 ± 0.091	-0.569 ± 1.770	0.140	5 ± 3	6 ± 4	3 ± 2	4 ± 3	1
XMMXCS J121832.3+470944.3	$0.530^{+0.130}_{-0.114}$	0.510 ± 0.203	-	0.032 ± 0.124	0.143 ± 2.490	0.120	4 ± 3	7 ± 4	3 ± 2	6 ± 3	1
XMMXCS J121858.7+294304.7	$0.456^{+0.136}_{-0.132}$	0.473 ± 0.071	-	0.146 ± 0.081	-2.190 ± 1.640	0.096	6 ± 3	6 ± 3	4 ± 3	6 ± 3	1
XMMXCS J121917.9+060206.2	$0.353^{+0.092}_{-0.093}$	0.342 ± 0.055	$0.353 \pm 5.8e-05$	-0.014 ± 0.137	1.850 ± 2.570	0.001	6 ± 3	5 ± 3	3 ± 2	2 ± 2	1

Continued on next page

Table A.2 – continued from previous page

name	z_{RS}	z_{BCG}	z_{spec-g}	cmr_{grad}	cmr_{inter}	cmr_{wid}	n_{gals-c}	n_{gals-l}	n_{200-c}	n_{200-l}	qual
XMMXCS J121919.3+295318.9	$0.105^{+0.004}_{-0.004}$	0.094 ± 0.018	$0.104 \pm 1.2e-05$	0.068 ± 0.015	-0.182 ± 0.259	0.034	5 ± 2	4 ± 2	5 ± 2	3 ± 2	1
XMMXCS J122018.2+290559.2	$0.132^{+0.023}_{-0.023}$	0.130 ± 0.022	$0.132 \pm 2.0e-05$	-0.040 ± 0.022	1.720 ± 0.384	0.029	6 ± 3	5 ± 2	6 ± 2	4 ± 2	1
XMMXCS J122235.8+143535.3	$0.500^{+0.081}_{-0.081}$	0.510 ± 0.108	$0.503 \pm 1.3e-04$	0.016 ± 0.132	0.647 ± 2.590	0.001	14 ± 4	20 ± 5	15 ± 4	21 ± 5	1
XMMXCS J122446.9+070604.6	$0.191^{+0.055}_{-0.056}$	0.181 ± 0.029	$0.179 \pm 4.1e-05$	0.014 ± 0.071	0.894 ± 1.310	0.098	7 ± 3	3 ± 2	6 ± 3	2 ± 2	1
XMMXCS J122526.00+122803.9	$0.312^{+0.069}_{-0.071}$	0.322 ± 0.048	$0.317 \pm 6.2e-05$	-0.019 ± 0.053	2.020 ± 1.010	0.001	6 ± 3	5 ± 3	6 ± 3	5 ± 3	1
XMMXCS J122526.0+122803.9	$0.312^{+0.069}_{-0.071}$	0.322 ± 0.048	$0.317 \pm 6.2e-05$	-0.019 ± 0.053	2.020 ± 1.010	0.001	6 ± 3	5 ± 3	6 ± 3	5 ± 3	1
XMMXCS J122528.1+004229.1	$0.237^{+0.040}_{-0.040}$	0.239 ± 0.037	$0.237 \pm 3.9e-05$	-0.056 ± 0.019	2.410 ± 0.343	0.064	13 ± 4	13 ± 4	13 ± 4	14 ± 4	1
XMMXCS J122552.2+334454.1	$0.503^{+0.105}_{-0.103}$	0.501 ± 0.084	$0.501 \pm 8.7e-05$	-0.034 ± 0.044	1.510 ± 0.863	0.092	12 ± 4	17 ± 5	11 ± 4	30 ± 6	1
XMMXCS J122553.5+334625.8	$0.507^{+0.088}_{-0.087}$	0.501 ± 0.084	$0.503 \pm 6.7e-05$	-0.016 ± 0.026	1.170 ± 0.512	0.053	13 ± 4	15 ± 5	12 ± 4	14 ± 5	1
XMMXCS J122643.3+334549.9	$0.510^{+0.102}_{-0.101}$	0.509 ± 0.081	$0.510 \pm 9.4e-05$	-0.013 ± 0.042	1.240 ± 0.832	0.063	13 ± 4	13 ± 4	16 ± 4	15 ± 5	1
XMMXCS J122656.4+334329.4	$0.504^{+0.100}_{-0.100}$	0.526 ± 0.117	$0.515 \pm 1.1e-04$	-0.015 ± 0.020	1.170 ± 0.403	0.059	18 ± 5	22 ± 5	25 ± 6	30 ± 6	1
XMMXCS J122701.2+331847.5	$0.257^{+0.050}_{-0.051}$	0.252 ± 0.039	$0.280 \pm 4.2e-05$	0.007 ± 0.025	1.320 ± 0.468	0.064	11 ± 4	13 ± 4	11 ± 3	15 ± 4	1
XMMXCS J122703.6+334527.0	$0.500^{+0.095}_{-0.094}$	0.503 ± 0.084	$0.499 \pm 1.6e-04$	-0.029 ± 0.025	1.450 ± 0.485	0.001	4 ± 3	-	3 ± 2	-	1
XMMXCS J122750.3+333940.6	$0.337^{+0.057}_{-0.056}$	0.343 ± 0.052	$0.338 \pm 5.3e-05$	0.133 ± 0.111	-0.714 ± 2.080	0.177	12 ± 4	13 ± 4	12 ± 4	143 ± 12	1
XMMXCS J122806.41+135511.5	$0.256^{+0.052}_{-0.052}$	0.240 ± 0.044	-	0.063 ± 0.058	0.317 ± 1.050	0.107	10 ± 4	10 ± 4	10 ± 4	10 ± 4	1
XMMXCS J122902.2+015013.8	$0.314^{+0.073}_{-0.067}$	0.317 ± 0.047	$0.314 \pm 5.4e-05$	0.044 ± 0.050	0.821 ± 0.997	0.039	5 ± 3	0 ± 2	4 ± 2	-	1
XMMXCS J122944.6+133450.6	$0.442^{+0.090}_{-0.088}$	0.462 ± 0.069	$0.437 \pm 1.8e-04$	-0.103 ± 0.027	2.720 ± 0.540	0.041	5 ± 3	13 ± 5	4 ± 3	12 ± 5	1
XMMXCS J122945.27+133450.5	$0.441^{+0.090}_{-0.089}$	0.462 ± 0.069	$0.437 \pm 1.8e-04$	-0.100 ± 0.029	2.670 ± 0.573	0.044	5 ± 3	13 ± 5	4 ± 3	13 ± 5	1
XMMXCS J122948.1+132534.5	$0.087^{+0.069}_{-0.068}$	0.103 ± 0.030	$0.008 \pm 5.3e-05$	-0.005 ± 0.009	0.949 ± 0.116	0.082	6 ± 3	35 ± 6	3 ± 2	100 ± 10	1

Continued on next page

Table A.2 – continued from previous page

name	z_{RS}	z_{BCG}	z_{spec-g}	cmr_{grad}	cmr_{inter}	cmr_{wid}	n_{gals-c}	n_{gals-l}	n_{200-c}	n_{200-l}	qual
XMMXCS J122951.5+105827.3	$0.378^{+0.089}_{-0.087}$	0.361 ± 0.060	-	0.044 ± 0.086	0.780 ± 1.690	0.081	11 ± 4	9 ± 4	9 ± 4	9 ± 4	1
XMMXCS J123019.6+161634.1	$0.203^{+0.052}_{-0.053}$	0.203 ± 0.033	$0.202 \pm 3.0e-05$	-0.055 ± 0.029	2.250 ± 0.538	0.069	19 ± 5	20 ± 5	22 ± 5	24 ± 5	1
XMMXCS J123041.2+105930.0	$0.294^{+0.113}_{-0.094}$	0.294 ± 0.071	-	-0.012 ± 0.085	1.760 ± 1.640	0.075	7 ± 3	0 ± 2	5 ± 2	-	1
XMMXCS J123045.80+105624.1	$0.251^{+0.062}_{-0.062}$	0.227 ± 0.049	-	-0.005 ± 0.076	1.540 ± 1.460	0.067	7 ± 3	7 ± 3	8 ± 3	8 ± 3	1
XMMXCS J123105.3+155627.2	$0.191^{+0.043}_{-0.043}$	0.210 ± 0.038	$0.190 \pm 2.2e-05$	-0.065 ± 0.018	2.360 ± 0.314	0.061	25 ± 5	26 ± 5	39 ± 6	43 ± 7	1
XMMXCS J123144.4+413732.0	$0.175^{+0.043}_{-0.043}$	0.177 ± 0.026	$0.174 \pm 2.3e-05$	-0.031 ± 0.012	1.710 ± 0.209	0.001	12 ± 4	13 ± 4	12 ± 4	14 ± 4	1
XMMXCS J123150.71+120001.3	$0.249^{+0.054}_{-0.054}$	0.252 ± 0.038	$0.250 \pm 3.3e-05$	-0.032 ± 0.019	1.940 ± 0.329	0.001	7 ± 3	9 ± 4	4 ± 2	8 ± 3	1
XMMXCS J123324.3+641529.8	$0.208^{+0.036}_{-0.037}$	0.209 ± 0.032	$0.208 \pm 2.7e-05$	-0.036 ± 0.018	1.940 ± 0.345	0.064	6 ± 3	7 ± 3	4 ± 2	6 ± 3	1
XMMXCS J123331.4+153311.6	$0.298^{+0.058}_{-0.058}$	0.322 ± 0.051	$0.298 \pm 4.6e-05$	0.021 ± 0.062	1.180 ± 1.170	0.113	6 ± 3	8 ± 4	6 ± 3	7 ± 3	1
XMMXCS J123347.2+151448.7	$0.311^{+0.104}_{-0.107}$	0.290 ± 0.052	$0.293 \pm 5.1e-05$	-0.058 ± 0.033	2.590 ± 0.648	0.085	10 ± 4	9 ± 4	7 ± 3	6 ± 3	1
XMMXCS J123354.3+151219.1	$0.284^{+0.067}_{-0.068}$	0.306 ± 0.050	$0.284 \pm 3.2e-05$	-0.038 ± 0.020	2.150 ± 0.380	0.085	24 ± 5	44 ± 7	38 ± 7	64 ± 9	1
XMMXCS J123355.9+152607.6	$0.234^{+0.048}_{-0.048}$	0.228 ± 0.036	$0.234 \pm 3.0e-05$	-0.020 ± 0.011	1.720 ± 0.203	0.001	15 ± 4	17 ± 4	16 ± 4	20 ± 5	1
XMMXCS J123414.9+151447.7	$0.288^{+0.060}_{-0.061}$	0.313 ± 0.047	$0.288 \pm 4.6e-05$	-0.020 ± 0.030	1.870 ± 0.585	0.088	32 ± 6	33 ± 6	56 ± 8	61 ± 9	1
XMMXCS J123423.7+151856.3	$0.264^{+0.054}_{-0.055}$	0.260 ± 0.039	$0.284 \pm 5.7e-05$	-0.059 ± 0.029	2.580 ± 0.537	0.001	18 ± 4	14 ± 4	24 ± 5	16 ± 4	1
XMMXCS J123508.9-033339.8	$0.057^{+0.039}_{-0.037}$	0.067 ± 0.015	$0.059 \pm 1.4e-05$	0.013 ± 0.020	0.653 ± 0.307	0.056	3 ± 2	0 ± 1	4 ± 2	-	1
XMMXCS J123517.70+122501.5	$0.507^{+0.088}_{-0.088}$	0.509 ± 0.076	$0.508 \pm 9.6e-05$	0.037 ± 0.035	0.215 ± 0.678	0.001	5 ± 3	5 ± 3	4 ± 2	6 ± 3	1
XMMXCS J123517.6+122501.5	$0.507^{+0.088}_{-0.088}$	0.509 ± 0.076	$0.508 \pm 9.6e-05$	0.037 ± 0.035	0.215 ± 0.678	0.001	5 ± 3	5 ± 3	4 ± 2	6 ± 3	1
XMMXCS J123526.09+121938.0	$0.360^{+0.076}_{-0.073}$	0.332 ± 0.052	$0.356 \pm 6.8e-05$	-0.077 ± 0.019	2.050 ± 0.363	0.045	7 ± 4	7 ± 4	3 ± 3	9 ± 4	1
XMMXCS J123526.0+121938.0	$0.360^{+0.076}_{-0.073}$	0.332 ± 0.052	$0.356 \pm 6.8e-05$	-0.077 ± 0.019	2.050 ± 0.363	0.045	7 ± 4	7 ± 4	3 ± 3	9 ± 4	1

Continued on next page

Table A.2 – continued from previous page

name	z_{RS}	z_{BCG}	z_{spec-g}	cmr_{grad}	cmr_{inter}	cmr_{wid}	n_{gals-c}	n_{gals-l}	n_{200-c}	n_{200-l}	qual
XMMXCS J123551.1+620733.2	$0.474^{+0.126}_{-0.124}$	0.473 ± 0.076	$0.472 \pm 1.2e-04$	0.024 ± 0.037	0.390 ± 0.712	0.001	11 ± 4	12 ± 4	11 ± 4	12 ± 4	1
XMMXCS J123601.9+263816.2	$0.210^{+0.062}_{-0.062}$	0.206 ± 0.034	$0.210 \pm 4.2e-05$	-0.066 ± 0.040	2.490 ± 0.748	0.074	10 ± 3	9 ± 3	9 ± 3	9 ± 3	1
XMMXCS J123629.8+262313.6	$0.243^{+0.068}_{-0.069}$	0.226 ± 0.043	-	0.029 ± 0.053	0.849 ± 0.979	0.081	3 ± 2	3 ± 3	5 ± 2	4 ± 2	1
XMMXCS J123647.4+125614.1	$0.093^{+0.025}_{-0.025}$	0.117 ± 0.038	$0.093 \pm 1.4e-05$	0.060 ± 0.064	-0.169 ± 1.080	0.108	7 ± 3	6 ± 3	5 ± 2	5 ± 2	1
XMMXCS J123647.55+125613.7	$0.093^{+0.025}_{-0.025}$	0.117 ± 0.038	$0.093 \pm 1.4e-05$	0.060 ± 0.064	-0.169 ± 1.080	0.108	7 ± 3	6 ± 3	5 ± 2	5 ± 2	1
XMMXCS J123650.5+255218.0	$0.162^{+0.040}_{-0.040}$	0.184 ± 0.028	$0.175 \pm 2.2e-05$	-0.053 ± 0.032	2.110 ± 0.601	0.082	7 ± 3	9 ± 3	8 ± 3	8 ± 3	1
XMMXCS J123659.5+631121.8	$0.291^{+0.064}_{-0.065}$	0.309 ± 0.051	$0.302 \pm 7.8e-05$	-0.038 ± 0.012	2.270 ± 0.213	0.001	40 ± 6	38 ± 6	72 ± 9	68 ± 9	1
XMMXCS J123728.1+631024.9	$0.291^{+0.072}_{-0.073}$	0.286 ± 0.045	$0.297 \pm 5.0e-05$	-0.026 ± 0.025	1.990 ± 0.479	0.033	21 ± 5	19 ± 5	35 ± 6	32 ± 6	1
XMMXCS J123840.6+092837.6	$0.230^{+0.031}_{-0.031}$	0.247 ± 0.043	$0.230 \pm 3.6e-05$	-0.040 ± 0.010	2.070 ± 0.175	0.008	15 ± 4	13 ± 4	19 ± 5	14 ± 4	1
XMMXCS J123900.5-113458.0	$0.317^{+0.073}_{-0.074}$	0.306 ± 0.046	-	0.029 ± 0.057	1.010 ± 1.080	0.055	10 ± 4	8 ± 3	8 ± 3	3 ± 2	1
XMMXCS J124059.7+330123.4	$0.156^{+0.032}_{-0.032}$	0.159 ± 0.031	$0.215 \pm 2.0e-05$	-0.224 ± 0.062	5.080 ± 1.140	0.500	3 ± 2	3 ± 2	3 ± 2	3 ± 2	1
XMMXCS J124059.9+183227.0	$0.071^{+0.012}_{-0.013}$	0.078 ± 0.017	$0.072 \pm 7.8e-06$	-0.014 ± 0.007	1.110 ± 0.117	0.033	16 ± 4	23 ± 5	24 ± 5	35 ± 6	1
XMMXCS J124119.2+183437.0	$0.072^{+0.003}_{-0.004}$	0.084 ± 0.042	$0.071 \pm 8.0e-06$	-0.015 ± 0.008	1.080 ± 0.126	0.038	22 ± 5	31 ± 6	31 ± 6	44 ± 7	1
XMMXCS J124124.4+183323.6	$0.071^{+0.027}_{-0.027}$	0.084 ± 0.042	$0.071 \pm 8.0e-06$	-0.007 ± 0.013	0.964 ± 0.222	0.050	23 ± 5	31 ± 6	31 ± 6	44 ± 7	1
XMMXCS J124128.1-015822.0	$0.153^{+0.036}_{-0.036}$	0.164 ± 0.025	$0.153 \pm 1.9e-05$	-0.042 ± 0.010	1.840 ± 0.160	0.001	14 ± 4	14 ± 4	14 ± 4	14 ± 4	1
XMMXCS J124133.4+325022.1	$0.372^{+0.073}_{-0.073}$	0.371 ± 0.056	$0.396 \pm 1.2e-04$	0.030 ± 0.030	1.130 ± 0.584	0.049	24 ± 5	28 ± 6	39 ± 7	50 ± 8	1
XMMXCS J124202.8+332203.7	$0.133^{+0.045}_{-0.044}$	0.122 ± 0.022	$0.141 \pm 1.7e-05$	-0.045 ± 0.025	1.770 ± 0.419	0.084	6 ± 3	7 ± 3	6 ± 3	9 ± 3	1
XMMXCS J124214.9+333017.6	$0.201^{+0.105}_{-0.109}$	0.211 ± 0.034	$0.224 \pm 4.7e-05$	-0.307 ± 0.018	7.150 ± 0.354	0.500	6 ± 3	9 ± 4	3 ± 2	5 ± 3	1
XMMXCS J124234.4+024354.0	$0.075^{+0.050}_{-0.056}$	0.094 ± 0.018	$0.086 \pm 9.2e-06$	0.017 ± 0.017	0.670 ± 0.285	0.050	5 ± 2	8 ± 3	3 ± 2	7 ± 3	1

Continued on next page

Table A.2 – continued from previous page

name	z_{RS}	z_{BCG}	z_{spec-g}	cmr_{grad}	cmr_{inter}	cmr_{wid}	n_{gals-c}	n_{gals-l}	n_{200-c}	n_{200-l}	qual
XMMXCS J124241.1+141747.9	$0.054^{+0.027}_{-0.030}$	0.057 ± 0.016	$0.001 \pm 7.3e-06$	0.051 ± 0.007	0.066 ± 0.099	0.500	2 ± 2	2 ± 2	4 ± 2	6 ± 3	1
XMMXCS J124241.5-112843.5	$0.064^{+0.036}_{-0.035}$	0.080 ± 0.023	-	-0.056 ± 0.015	1.690 ± 0.236	0.044	8 ± 3	8 ± 3	7 ± 3	8 ± 3	1
XMMXCS J124246.9+331914.7	$0.244^{+0.040}_{-0.041}$	0.258 ± 0.040	$0.244 \pm 3.5e-05$	-0.032 ± 0.013	2.010 ± 0.230	0.001	5 ± 2	2 ± 2	4 ± 2	2 ± 2	1
XMMXCS J124259.9+141807.9	$0.518^{+0.088}_{-0.086}$	0.517 ± 0.080	$0.539 \pm 1.3e-04$	-0.072 ± 0.007	2.300 ± 0.123	0.001	9 ± 4	58 ± 8	8 ± 3	42 ± 9	1
XMMXCS J124305.2+023312.9	$0.205^{+0.057}_{-0.057}$	0.219 ± 0.049	$0.206 \pm 3.4e-05$	-0.036 ± 0.065	1.970 ± 1.180	0.069	8 ± 3	3 ± 2	5 ± 2	2 ± 2	1
XMMXCS J124309.8+142024.9	$0.334^{+0.113}_{-0.113}$	0.314 ± 0.054	-	0.056 ± 0.130	0.406 ± 2.560	0.001	9 ± 4	9 ± 4	7 ± 3	8 ± 3	1
XMMXCS J124401.7+165345.8	$0.554^{+0.116}_{-0.115}$	0.549 ± 0.086	$0.557 \pm 7.6e-05$	-0.038 ± 0.037	1.670 ± 0.729	0.127	25 ± 6	44 ± 7	37 ± 7	92 ± 12	1
XMMXCS J124403.9+165148.5	$0.558^{+0.114}_{-0.113}$	0.527 ± 0.083	$0.556 \pm 1.2e-04$	-0.076 ± 0.058	2.510 ± 1.160	0.070	24 ± 5	41 ± 7	41 ± 7	69 ± 10	1
XMMXCS J124425.9+164758.0	$0.235^{+0.048}_{-0.047}$	0.240 ± 0.039	$0.235 \pm 3.7e-05$	-0.057 ± 0.021	2.380 ± 0.373	0.046	4 ± 2	5 ± 3	4 ± 2	5 ± 3	1
XMMXCS J124454.1-003330.3	$0.232^{+0.046}_{-0.046}$	0.248 ± 0.038	$0.232 \pm 3.4e-05$	-0.072 ± 0.022	2.680 ± 0.392	0.001	7 ± 3	7 ± 3	7 ± 3	12 ± 4	1
XMMXCS J124928.4-060007.2	$0.347^{+0.068}_{-0.068}$	0.342 ± 0.052	-	0.080 ± 0.111	0.125 ± 2.160	0.001	4 ± 3	4 ± 2	4 ± 2	3 ± 2	1
XMMXCS J124956.1+264336.0	$0.427^{+0.138}_{-0.138}$	0.440 ± 0.064	$0.452 \pm 1.2e-04$	-0.014 ± 0.084	0.964 ± 1.650	0.001	6 ± 3	6 ± 4	4 ± 3	4 ± 3	1
XMMXCS J125312.2+310712.2	$0.303^{+0.047}_{-0.047}$	0.311 ± 0.065	$0.303 \pm 7.5e-05$	-0.084 ± 0.027	3.100 ± 0.521	0.001	2 ± 2	1 ± 2	3 ± 2	1 ± 1	1
XMMXCS J125314.6+155530.9	$0.277^{+0.070}_{-0.069}$	0.281 ± 0.044	$0.275 \pm 7.2e-05$	-0.148 ± 0.032	4.210 ± 0.618	0.061	11 ± 4	9 ± 4	11 ± 4	9 ± 3	1
XMMXCS J125344.8+305808.9	$0.117^{+0.050}_{-0.050}$	0.077 ± 0.023	$0.103 \pm 1.6e-05$	-0.117 ± 0.001	2.890 ± 0.001	0.500	5 ± 3	4 ± 2	3 ± 2	2 ± 2	1
XMMXCS J125403.0+310150.0	$0.510^{+0.124}_{-0.123}$	0.533 ± 0.088	-	-0.176 ± 0.109	4.500 ± 2.190	0.001	8 ± 3	25 ± 6	7 ± 3	26 ± 6	1
XMMXCS J125422.6+101953.0	$0.183^{+0.061}_{-0.064}$	0.192 ± 0.029	-	-0.051 ± 0.023	2.130 ± 0.427	0.069	4 ± 2	2 ± 2	3 ± 2	2 ± 2	1
XMMXCS J125602.4+255645.5	$0.232^{+0.052}_{-0.052}$	0.225 ± 0.040	$0.233 \pm 4.2e-05$	-0.035 ± 0.012	2.020 ± 0.235	0.064	10 ± 3	9 ± 3	9 ± 3	8 ± 3	1
XMMXCS J125621.5+254603.9	$0.224^{+0.062}_{-0.062}$	0.208 ± 0.048	-	-0.048 ± 0.034	2.220 ± 0.630	0.081	10 ± 3	10 ± 4	10 ± 3	10 ± 4	1

Continued on next page

Table A.2 – continued from previous page

name	z_{RS}	z_{BCG}	z_{spec-g}	cmr_{grad}	cmr_{inter}	cmr_{wid}	n_{gals-c}	n_{gals-l}	n_{200-c}	n_{200-l}	qual
XMMXCS J125752.7+283010.6	$0.306^{+0.065}_{-0.065}$	0.306 ± 0.048	-	-0.060 ± 0.055	2.730 ± 1.040	0.001	13 ± 4	14 ± 4	14 ± 4	17 ± 5	1
XMMXCS J125834.2-014328.5	$0.086^{+0.018}_{-0.018}$	0.110 ± 0.046	$0.089 \pm 1.8e-05$	-0.018 ± 0.007	1.210 ± 0.111	0.039	19 ± 5	24 ± 5	29 ± 6	38 ± 6	1
XMMXCS J125901.7+280653.8	$0.026^{+0.004}_{-0.003}$	0.055 ± 0.020	$0.023 \pm 4.7e-06$	-0.050 ± 0.007	1.500 ± 0.119	0.500	12 ± 4	0 ± 1	12 ± 4	-	1
XMMXCS J125912.9-015013.0	$0.083^{+0.003}_{-0.003}$	0.090 ± 0.018	$0.084 \pm 1.1e-05$	-0.044 ± 0.026	1.620 ± 0.440	0.037	6 ± 3	8 ± 3	3 ± 2	5 ± 2	1
XMMXCS J125938.8+275743.6	$0.025^{+0.004}_{-0.004}$	0.043 ± 0.016	$0.022 \pm 5.1e-06$	0.001 ± 0.002	0.785 ± 0.020	0.011	14 ± 4	3 ± 2	18 ± 5	2 ± 2	1
XMMXCS J125946.5+275854.6	$0.023^{+0.002}_{-0.002}$	0.043 ± 0.016	$0.023 \pm 5.1e-06$	-0.002 ± 0.004	0.820 ± 0.046	0.018	8 ± 3	2 ± 2	4 ± 2	1 ± 1	1
XMMXCS J125951.2+275939.0	$0.025^{+0.003}_{-0.003}$	0.076 ± 0.049	$0.023 \pm 5.3e-06$	-0.009 ± 0.019	0.908 ± 0.269	0.027	18 ± 5	7 ± 3	22 ± 5	7 ± 3	1
XMMXCS J130006.2+281029.2	$0.025^{+0.022}_{-0.023}$	0.049 ± 0.021	$0.025 \pm 5.8e-06$	-0.013 ± 0.011	0.904 ± 0.178	0.076	11 ± 3	1 ± 1	11 ± 3	0 ± 1	1
XMMXCS J130010.1+281017.4	$0.022^{+0.032}_{-0.022}$	0.049 ± 0.021	$0.025 \pm 5.8e-06$	-0.003 ± 0.012	0.773 ± 0.191	0.039	5 ± 2	0 ± 1	5 ± 2	-	1
XMMXCS J130014.8+283624.3	$0.179^{+0.032}_{-0.033}$	0.185 ± 0.031	$0.179 \pm 3.2e-05$	0.045 ± 0.015	0.476 ± 0.270	0.079	4 ± 2	3 ± 2	4 ± 2	3 ± 2	1
XMMXCS J130017.1+281210.0	$0.031^{+0.006}_{-0.006}$	0.049 ± 0.021	$0.025 \pm 6.5e-06$	-0.066 ± 0.019	1.670 ± 0.274	0.071	20 ± 5	19 ± 4	29 ± 6	20 ± 5	1
XMMXCS J130017.5+275719.5	$0.024^{+0.003}_{-0.003}$	0.076 ± 0.049	$0.023 \pm 6.0e-06$	-0.031 ± 0.003	1.160 ± 0.031	0.028	11 ± 4	4 ± 2	11 ± 4	4 ± 2	1
XMMXCS J130028.7+275913.7	$0.025^{+0.003}_{-0.003}$	0.052 ± 0.022	$0.024 \pm 4.5e-06$	-0.013 ± 0.015	0.935 ± 0.220	0.038	4 ± 2	0 ± 1	3 ± 2	-	1
XMMXCS J130118.6+282039.1	$0.222^{+0.044}_{-0.044}$	0.190 ± 0.037	$0.222 \pm 4.6e-05$	0.049 ± 0.060	0.374 ± 1.100	0.070	7 ± 3	6 ± 3	5 ± 2	4 ± 2	1
XMMXCS J130119.0+281955.5	$0.210^{+0.044}_{-0.044}$	0.218 ± 0.039	-	-0.089 ± 0.033	2.930 ± 0.608	0.018	4 ± 2	3 ± 2	4 ± 2	5 ± 2	1
XMMXCS J130119.7+281904.8	$0.213^{+0.047}_{-0.047}$	0.218 ± 0.039	-	-0.033 ± 0.070	1.900 ± 1.280	0.001	4 ± 2	3 ± 2	4 ± 2	5 ± 2	1
XMMXCS J130150.1+585753.5	$0.225^{+0.079}_{-0.079}$	0.222 ± 0.061	-	-0.037 ± 0.030	1.980 ± 0.561	0.072	4 ± 2	4 ± 3	5 ± 2	5 ± 3	1
XMMXCS J130235.8-023044.2	$0.083^{+0.008}_{-0.008}$	0.081 ± 0.016	$0.081 \pm 1.2e-05$	-0.016 ± 0.016	1.140 ± 0.259	0.065	9 ± 3	12 ± 4	8 ± 3	13 ± 4	1
XMMXCS J130240.0+672840.5	$0.105^{+0.015}_{-0.015}$	0.114 ± 0.018	$0.107 \pm 1.6e-05$	-0.038 ± 0.007	1.590 ± 0.114	0.029	10 ± 3	12 ± 4	9 ± 3	12 ± 4	1

Continued on next page

Table A.2 – continued from previous page

name	z_{RS}	z_{BCG}	z_{spec-g}	cmr_{grad}	cmr_{inter}	cmr_{wid}	n_{gals-c}	n_{gals-l}	n_{200-c}	n_{200-l}	qual
XMMXCS J130244.0+281305.9	$0.247^{+0.058}_{-0.058}$	0.244 ± 0.042	$0.252 \pm 7.4e-05$	0.061 ± 0.059	0.258 ± 1.080	0.111	8 ± 3	7 ± 3	7 ± 3	6 ± 3	1
XMMXCS J130250.3-022712.1	$0.082^{+0.014}_{-0.014}$	0.085 ± 0.016	$0.085 \pm 1.0e-05$	-0.011 ± 0.004	1.070 ± 0.066	0.012	17 ± 4	17 ± 4	23 ± 5	22 ± 5	1
XMMXCS J130301.4+672513.1	$0.107^{+0.020}_{-0.020}$	0.123 ± 0.031	$0.108 \pm 2.0e-05$	0.038 ± 0.015	0.370 ± 0.242	0.044	10 ± 3	14 ± 4	10 ± 3	10 ± 3	1
XMMXCS J130304.8-022142.0	$0.084^{+0.009}_{-0.009}$	0.083 ± 0.015	$0.086 \pm 1.0e-05$	0.027 ± 0.031	0.440 ± 0.513	0.045	14 ± 4	14 ± 4	16 ± 4	16 ± 4	1
XMMXCS J130328.8+672710.8	$0.207^{+0.063}_{-0.064}$	0.214 ± 0.033	-	-0.027 ± 0.016	1.820 ± 0.301	0.072	24 ± 5	22 ± 5	39 ± 7	34 ± 6	1
XMMXCS J130330.9+534344.7	$0.303^{+0.065}_{-0.065}$	0.286 ± 0.046	-	0.075 ± 0.075	0.091 ± 1.470	0.130	7 ± 3	7 ± 3	7 ± 3	1 ± 2	1
XMMXCS J130339.3+674350.8	$0.184^{+0.049}_{-0.050}$	0.183 ± 0.049	$0.222 \pm 4.4e-05$	-0.001 ± 0.055	1.220 ± 1.030	0.086	6 ± 3	6 ± 3	3 ± 2	2 ± 2	1
XMMXCS J130358.0+673055.1	$0.221^{+0.057}_{-0.057}$	0.231 ± 0.036	$0.220 \pm 3.9e-05$	-0.015 ± 0.026	1.610 ± 0.473	0.106	25 ± 5	28 ± 6	55 ± 8	57 ± 8	1
XMMXCS J130526.8+181155.9	$0.443^{+0.078}_{-0.076}$	0.445 ± 0.066	$0.443 \pm 6.9e-05$	0.006 ± 0.037	0.562 ± 0.730	0.080	17 ± 5	26 ± 6	21 ± 6	36 ± 7	1
XMMXCS J130534.7+175658.6	$0.550^{+0.110}_{-0.109}$	0.574 ± 0.118	$0.529 \pm 1.2e-04$	-0.174 ± 0.057	4.370 ± 1.140	0.050	19 ± 5	49 ± 8	23 ± 5	186 ± 15	1
XMMXCS J130553.3+181441.7	$0.443^{+0.076}_{-0.075}$	0.432 ± 0.063	$0.441 \pm 6.3e-05$	-0.023 ± 0.017	1.160 ± 0.317	0.001	18 ± 5	19 ± 5	23 ± 6	27 ± 6	1
XMMXCS J130636.5+175558.9	$0.111^{+0.014}_{-0.014}$	0.121 ± 0.021	$0.108 \pm 8.7e-06$	-0.024 ± 0.081	1.200 ± 1.340	0.142	6 ± 3	6 ± 3	5 ± 2	6 ± 3	1
XMMXCS J130741.7+292627.9	$0.240^{+0.051}_{-0.051}$	0.242 ± 0.037	$0.241 \pm 5.4e-05$	-0.013 ± 0.016	1.660 ± 0.295	0.032	12 ± 4	10 ± 4	12 ± 4	13 ± 4	1
XMMXCS J130745.1+292323.1	$0.240^{+0.053}_{-0.053}$	0.242 ± 0.037	$0.241 \pm 5.4e-05$	-0.005 ± 0.015	1.490 ± 0.281	0.060	18 ± 4	21 ± 5	17 ± 4	18 ± 5	1
XMMXCS J130749.6+292549.2	$0.240^{+0.049}_{-0.050}$	0.242 ± 0.037	$0.241 \pm 5.4e-05$	0.003 ± 0.012	1.410 ± 0.218	0.010	12 ± 4	10 ± 4	12 ± 4	11 ± 4	1
XMMXCS J130832.6+534214.2	$0.321^{+0.088}_{-0.088}$	0.336 ± 0.058	-	-0.201 ± 0.107	5.580 ± 2.130	0.071	13 ± 4	13 ± 4	13 ± 4	13 ± 4	1
XMMXCS J130851.2+574257.9	$0.343^{+0.067}_{-0.067}$	0.347 ± 0.051	$0.343 \pm 1.0e-04$	-0.022 ± 0.046	2.000 ± 0.932	0.086	5 ± 3	5 ± 3	4 ± 2	0 ± 2	1
XMMXCS J130852.4+293303.8	$0.318^{+0.053}_{-0.053}$	0.333 ± 0.051	$0.317 \pm 6.0e-05$	-0.086 ± 0.061	3.100 ± 1.170	0.063	4 ± 3	4 ± 3	4 ± 2	4 ± 2	1
XMMXCS J130903.5+081737.7	$0.469^{+0.100}_{-0.098}$	0.418 ± 0.065	$0.464 \pm 8.3e-05$	-0.047 ± 0.042	1.700 ± 0.827	0.062	11 ± 4	14 ± 5	12 ± 4	16 ± 5	1

Continued on next page

Table A.2 – continued from previous page

name	z_{RS}	z_{BCG}	z_{spec-g}	cmr_{grad}	cmr_{inter}	cmr_{wid}	n_{gals-c}	n_{gals-l}	n_{200-c}	n_{200-l}	qual
XMMXCS J130920.6+212640.4	$0.280^{+0.064}_{-0.062}$	0.258 ± 0.084	$0.342 \pm 7.9e-05$	0.110 ± 0.004	-0.915 ± 0.072	0.500	3 ± 3	1 ± 4	4 ± 2	5 ± 3	1
XMMXCS J130933.7+573926.3	$0.202^{+0.048}_{-0.047}$	0.192 ± 0.030	-	0.044 ± 0.052	0.415 ± 0.986	0.116	4 ± 2	3 ± 2	4 ± 2	3 ± 2	1
XMMXCS J130947.3+573011.6	$0.244^{+0.101}_{-0.100}$	0.236 ± 0.073	-	0.072 ± 0.074	-0.027 ± 1.300	0.500	11 ± 4	5 ± 4	12 ± 4	12 ± 4	1
XMMXCS J130956.8+322220.0	$0.293^{+0.057}_{-0.058}$	0.309 ± 0.058	$0.293 \pm 5.7e-05$	-0.038 ± 0.031	2.280 ± 0.578	0.001	10 ± 4	19 ± 5	10 ± 3	10 ± 4	1
XMMXCS J131021.3+322204.4	$0.411^{+0.117}_{-0.118}$	0.428 ± 0.134	-	0.079 ± 0.049	0.033 ± 0.909	0.106	11 ± 4	12 ± 4	6 ± 3	11 ± 4	1
XMMXCS J131029.7+314424.0	$0.146^{+0.041}_{-0.042}$	0.183 ± 0.030	$0.169 \pm 3.0e-05$	-0.086 ± 0.042	2.660 ± 0.726	0.075	5 ± 3	4 ± 2	4 ± 2	3 ± 2	1
XMMXCS J131036.1+081800.1	$0.202^{+0.057}_{-0.057}$	0.215 ± 0.034	$0.219 \pm 4.5e-05$	-0.058 ± 0.024	2.330 ± 0.448	0.069	7 ± 3	5 ± 3	7 ± 3	5 ± 2	1
XMMXCS J131056.1+215808.7	$0.269^{+0.066}_{-0.066}$	0.270 ± 0.046	-	-0.007 ± 0.047	1.620 ± 0.916	0.066	15 ± 4	16 ± 4	16 ± 4	17 ± 5	1
XMMXCS J131119.6+274409.4	$0.540^{+0.110}_{-0.112}$	0.535 ± 0.094	$0.544 \pm 1.3e-04$	0.136 ± 0.056	-1.630 ± 1.120	0.001	5 ± 3	13 ± 4	4 ± 2	17 ± 5	1
XMMXCS J131125.2-012338.6	$0.174^{+0.039}_{-0.039}$	0.204 ± 0.033	$0.183 \pm 2.4e-05$	-0.056 ± 0.026	2.190 ± 0.477	0.052	31 ± 6	27 ± 5	62 ± 8	49 ± 7	1
XMMXCS J131126.7-012427.6	$0.174^{+0.046}_{-0.046}$	0.204 ± 0.033	$0.183 \pm 2.4e-05$	-0.062 ± 0.020	2.320 ± 0.356	0.042	25 ± 5	23 ± 5	46 ± 7	39 ± 6	1
XMMXCS J131129.9-012024.4	$0.188^{+0.034}_{-0.034}$	0.185 ± 0.044	$0.174 \pm 3.6e-05$	0.005 ± 0.012	1.160 ± 0.209	0.050	64 ± 8	65 ± 8	98 ± 10	90 ± 10	1
XMMXCS J131145.1+220206.2	$0.171^{+0.040}_{-0.040}$	0.173 ± 0.026	$0.171 \pm 1.9e-05$	-0.013 ± 0.007	1.360 ± 0.129	0.019	11 ± 3	10 ± 3	11 ± 3	11 ± 3	1
XMMXCS J131145.3-011828.4	$0.182^{+0.037}_{-0.036}$	0.209 ± 0.036	$0.195 \pm 1.9e-05$	-0.026 ± 0.015	1.660 ± 0.264	0.028	27 ± 5	26 ± 5	66 ± 8	57 ± 8	1
XMMXCS J131154.4+352242.6	$0.183^{+0.029}_{-0.029}$	0.176 ± 0.027	$0.183 \pm 2.3e-05$	0.018 ± 0.031	0.859 ± 0.579	0.081	9 ± 3	8 ± 3	8 ± 3	8 ± 3	1
XMMXCS J131223.6-012013.2	$0.173^{+0.056}_{-0.056}$	0.158 ± 0.027	-	-0.060 ± 0.058	2.200 ± 1.070	0.109	5 ± 3	4 ± 3	4 ± 2	5 ± 2	1
XMMXCS J131243.9+350622.8	$0.281^{+0.066}_{-0.066}$	0.299 ± 0.044	$0.279 \pm 6.5e-05$	-0.097 ± 0.062	3.290 ± 1.210	0.104	10 ± 4	7 ± 3	10 ± 4	3 ± 2	1
XMMXCS J131302.0+351943.1	$0.299^{+0.053}_{-0.054}$	0.312 ± 0.046	$0.299 \pm 5.8e-05$	-0.035 ± 0.015	2.230 ± 0.275	0.001	13 ± 4	14 ± 4	15 ± 4	11 ± 4	1
XMMXCS J131843.8-004356.7	$0.098^{+0.032}_{-0.032}$	0.094 ± 0.017	$0.099 \pm 1.2e-05$	-0.048 ± 0.013	1.730 ± 0.234	0.040	8 ± 3	8 ± 3	5 ± 2	5 ± 2	1

Continued on next page

Table A.2 – continued from previous page

name	z_{RS}	z_{BCG}	z_{spec-g}	cmr_{grad}	cmr_{inter}	cmr_{wid}	n_{gals-c}	n_{gals-l}	n_{200-c}	n_{200-l}	qual
XMMXCS J131914.6-005911.6	$0.083^{+0.016}_{-0.016}$	0.120 ± 0.022	$0.085 \pm 7.8e-06$	-0.021 ± 0.010	1.290 ± 0.151	0.038	20 ± 5	20 ± 5	25 ± 5	25 ± 5	1
XMMXCS J131919.9-005430.3	$0.083^{+0.006}_{-0.006}$	0.090 ± 0.019	$0.083 \pm 1.1e-05$	-0.009 ± 0.012	1.060 ± 0.186	0.035	19 ± 5	18 ± 4	25 ± 5	23 ± 5	1
XMMXCS J132014.0+330805.7	$0.037^{+0.011}_{-0.011}$	0.054 ± 0.017	$0.038 \pm 8.8e-06$	-0.020 ± 0.012	1.070 ± 0.170	0.031	9 ± 3	3 ± 2	8 ± 3	4 ± 2	1
XMMXCS J132014.7+330844.1	$0.666^{+0.126}_{-0.121}$	0.399 ± 0.318	$0.657 \pm 2.9e-04$	-0.040 ± 0.087	1.840 ± 1.790	0.091	10 ± 3	29 ± 6	6 ± 3	35 ± 7	1
XMMXCS J132042.0+331022.8	$0.289^{+0.076}_{-0.075}$	0.270 ± 0.045	$0.289 \pm 7.7e-05$	-0.042 ± 0.028	2.270 ± 0.537	0.084	17 ± 5	14 ± 4	18 ± 5	14 ± 4	1
XMMXCS J132053.8+335521.0	$0.184^{+0.055}_{-0.056}$	0.185 ± 0.028	$0.185 \pm 3.8e-05$	0.004 ± 0.012	1.130 ± 0.227	0.041	12 ± 4	12 ± 4	12 ± 4	12 ± 4	1
XMMXCS J132434.0+053427.1	$0.228^{+0.035}_{-0.035}$	0.235 ± 0.036	$0.228 \pm 2.6e-05$	-0.055 ± 0.009	2.370 ± 0.179	0.012	10 ± 3	12 ± 4	9 ± 3	13 ± 4	1
XMMXCS J132508.7+655027.9	$0.182^{+0.039}_{-0.039}$	0.195 ± 0.030	$0.201 \pm 3.1e-05$	0.048 ± 0.079	0.341 ± 1.410	0.093	12 ± 4	12 ± 4	12 ± 4	12 ± 4	1
XMMXCS J132703.9+012009.8	$0.080^{+0.002}_{-0.002}$	0.096 ± 0.025	$0.080 \pm 8.3e-06$	-0.017 ± 0.022	1.140 ± 0.344	0.054	7 ± 3	7 ± 3	5 ± 2	4 ± 2	1
XMMXCS J132716.6+315107.0	$0.236^{+0.060}_{-0.060}$	0.247 ± 0.060	$0.235 \pm 6.3e-05$	-0.047 ± 0.020	2.200 ± 0.373	0.065	16 ± 4	15 ± 4	22 ± 5	19 ± 5	1
XMMXCS J132924.4+114523.2	$0.038^{+0.024}_{-0.024}$	0.058 ± 0.025	$0.024 \pm 6.7e-06$	-0.050 ± 0.015	1.450 ± 0.204	0.048	9 ± 3	7 ± 3	9 ± 3	10 ± 3	1
XMMXCS J132946.5+114107.4	$0.203^{+0.048}_{-0.048}$	0.219 ± 0.035	$0.204 \pm 2.8e-05$	-0.027 ± 0.007	1.770 ± 0.127	0.023	3 ± 2	3 ± 2	3 ± 2	3 ± 2	1
XMMXCS J132958.9+241124.6	$0.166^{+0.046}_{-0.047}$	0.169 ± 0.030	$0.166 \pm 2.9e-05$	-0.027 ± 0.013	1.590 ± 0.219	0.046	6 ± 3	2 ± 2	5 ± 2	4 ± 2	1
XMMXCS J132959.3+583414.5	$0.301^{+0.073}_{-0.073}$	0.311 ± 0.047	$0.301 \pm 6.6e-05$	-0.081 ± 0.073	3.020 ± 1.440	0.156	8 ± 3	7 ± 4	8 ± 3	6 ± 3	1
XMMXCS J133046.3+334626.6	$0.450^{+0.041}_{-0.040}$	0.454 ± 0.069	$0.449 \pm 2.0e-04$	-0.247 ± 0.042	5.570 ± 0.843	0.023	7 ± 3	10 ± 4	6 ± 3	10 ± 4	1
XMMXCS J133048.6-015150.2	$0.086^{+0.004}_{-0.004}$	0.109 ± 0.020	$0.088 \pm 9.4e-06$	0.0003 ± 0.011	0.968 ± 0.158	0.023	16 ± 4	15 ± 4	18 ± 4	16 ± 4	1
XMMXCS J133052.7-014904.9	$0.086^{+0.011}_{-0.011}$	0.109 ± 0.020	$0.088 \pm 9.4e-06$	-0.021 ± 0.008	1.300 ± 0.124	0.032	18 ± 4	18 ± 4	22 ± 5	22 ± 5	1
XMMXCS J133054.9-014111.2	$0.083^{+0.013}_{-0.013}$	0.095 ± 0.016	$0.081 \pm 1.1e-05$	-0.010 ± 0.017	1.060 ± 0.284	0.069	9 ± 3	6 ± 3	6 ± 3	5 ± 2	1
XMMXCS J133056.2-013818.9	$0.110^{+0.089}_{-0.089}$	0.082 ± 0.017	$0.083 \pm 1.3e-05$	-0.079 ± 0.037	2.330 ± 0.673	0.105	9 ± 3	6 ± 3	8 ± 3	8 ± 3	1

Continued on next page

Table A.2 – continued from previous page

name	z_{RS}	z_{BCG}	z_{spec-g}	cmr_{grad}	cmr_{inter}	cmr_{wid}	n_{gals-c}	n_{gals-l}	n_{200-c}	n_{200-l}	qual
XMMXCS J133057.1+581535.0	$0.307^{+0.070}_{-0.072}$	0.313 ± 0.047	$0.309 \pm 5.4e-05$	-0.002 ± 0.031	1.640 ± 0.578	0.023	14 ± 4	14 ± 4	13 ± 4	15 ± 4	1
XMMXCS J133058.2+581447.9	$0.310^{+0.057}_{-0.057}$	0.313 ± 0.047	$0.311 \pm 5.6e-05$	-0.041 ± 0.037	2.410 ± 0.710	0.048	16 ± 4	15 ± 4	15 ± 4	12 ± 4	1
XMMXCS J133100.8-014748.8	$0.084^{+0.055}_{-0.056}$	0.088 ± 0.016	$0.086 \pm 1.1e-05$	-0.027 ± 0.011	1.360 ± 0.196	0.055	17 ± 4	14 ± 4	20 ± 5	16 ± 4	1
XMMXCS J133107.1-015837.4	$0.207^{+0.055}_{-0.056}$	0.192 ± 0.030	$0.203 \pm 1.9e-05$	0.031 ± 0.035	0.704 ± 0.630	0.077	4 ± 2	5 ± 3	3 ± 2	11 ± 4	1
XMMXCS J133108.5-014340.5	$0.083^{+0.024}_{-0.023}$	0.071 ± 0.020	$0.083 \pm 9.1e-06$	-0.020 ± 0.007	1.190 ± 0.124	0.056	14 ± 4	21 ± 5	18 ± 4	34 ± 6	1
XMMXCS J133117.5+582928.3	$0.480^{+0.106}_{-0.105}$	0.470 ± 0.072	$0.479 \pm 2.0e-04$	0.004 ± 0.032	0.686 ± 0.645	0.011	15 ± 4	15 ± 5	19 ± 5	-	1
XMMXCS J133119.0-014640.9	$0.081^{+0.048}_{-0.050}$	0.071 ± 0.020	$0.084 \pm 9.8e-06$	-0.015 ± 0.007	1.130 ± 0.127	0.051	13 ± 4	17 ± 4	14 ± 4	28 ± 5	1
XMMXCS J133124.1-015132.8	$0.239^{+0.055}_{-0.055}$	0.228 ± 0.041	$0.240 \pm 2.6e-05$	-0.067 ± 0.022	2.610 ± 0.414	0.069	7 ± 3	6 ± 3	8 ± 3	6 ± 3	1
XMMXCS J133233.9+502449.9	$0.272^{+0.060}_{-0.060}$	0.285 ± 0.049	$0.273 \pm 4.1e-05$	-0.003 ± 0.013	1.560 ± 0.257	0.052	18 ± 4	13 ± 4	23 ± 5	21 ± 5	1
XMMXCS J133244.2+503242.9	$0.286^{+0.065}_{-0.066}$	0.301 ± 0.045	$0.279 \pm 3.9e-05$	-0.043 ± 0.052	2.390 ± 1.000	0.048	51 ± 7	49 ± 7	90 ± 10	91 ± 10	1
XMMXCS J133254.8+503153.1	$0.279^{+0.058}_{-0.058}$	0.294 ± 0.044	$0.282 \pm 3.6e-05$	-0.012 ± 0.015	1.800 ± 0.274	0.025	35 ± 6	33 ± 6	75 ± 9	68 ± 9	1
XMMXCS J133421.5+503057.6	$0.489^{+0.138}_{-0.138}$	0.477 ± 0.120	-	-0.018 ± 0.097	1.340 ± 1.940	0.022	15 ± 4	17 ± 5	17 ± 5	26 ± 6	1
XMMXCS J133444.6+410207.9	$0.233^{+0.047}_{-0.047}$	0.253 ± 0.062	-	-0.001 ± 0.018	1.360 ± 0.338	0.068	13 ± 4	14 ± 4	13 ± 4	15 ± 4	1
XMMXCS J133453.1+405654.5	$0.238^{+0.033}_{-0.033}$	0.243 ± 0.037	$0.236 \pm 2.3e-05$	-0.037 ± 0.018	2.010 ± 0.315	0.038	29 ± 6	27 ± 5	56 ± 8	48 ± 7	1
XMMXCS J133505.3+502336.3	$0.088^{+0.012}_{-0.012}$	0.099 ± 0.018	$0.088 \pm 1.4e-05$	-0.048 ± 0.018	1.710 ± 0.296	0.037	10 ± 3	7 ± 3	8 ± 3	5 ± 2	1
XMMXCS J133514.7+405429.4	$0.209^{+0.055}_{-0.056}$	0.214 ± 0.033	-	-0.021 ± 0.025	1.730 ± 0.464	0.068	7 ± 3	6 ± 3	3 ± 2	3 ± 2	1
XMMXCS J133516.8+410416.6	$0.229^{+0.041}_{-0.041}$	0.221 ± 0.038	$0.230 \pm 3.0e-05$	-0.040 ± 0.021	2.070 ± 0.377	0.086	9 ± 3	11 ± 4	3 ± 2	10 ± 4	1
XMMXCS J133519.5+410004.3	$0.233^{+0.053}_{-0.054}$	0.257 ± 0.040	$0.230 \pm 2.6e-05$	-0.035 ± 0.013	2.030 ± 0.255	0.074	49 ± 7	46 ± 7	109 ± 11	105 ± 11	1
XMMXCS J133521.4+410340.1	$0.225^{+0.049}_{-0.048}$	0.227 ± 0.034	$0.231 \pm 3.5e-05$	-0.029 ± 0.015	1.860 ± 0.289	0.082	15 ± 4	17 ± 5	24 ± 5	33 ± 6	1

Continued on next page

Table A.2 – continued from previous page

name	z_{RS}	z_{BCG}	z_{spec-g}	cmr_{grad}	cmr_{inter}	cmr_{wid}	n_{gals-c}	n_{gals-l}	n_{200-c}	n_{200-l}	qual
XMMXCS J133529.7+380346.1	$0.497^{+0.132}_{-0.131}$	0.501 ± 0.076	$0.414 \pm 1.1e-04$	0.172 ± 0.159	-2.510 ± 3.190	0.114	3 ± 3	3 ± 3	5 ± 2	5 ± 3	1
XMMXCS J133530.9+374526.5	$0.300^{+0.062}_{-0.062}$	0.320 ± 0.049	$0.304 \pm 5.0e-05$	-0.060 ± 0.035	2.750 ± 0.689	0.103	7 ± 3	6 ± 3	6 ± 3	4 ± 3	1
XMMXCS J133544.8+375139.8	$0.236^{+0.077}_{-0.077}$	0.240 ± 0.073	-	0.069 ± 0.073	-0.145 ± 1.400	0.128	4 ± 3	5 ± 3	4 ± 2	5 ± 3	1
XMMXCS J133559.1+375400.8	$0.254^{+0.062}_{-0.062}$	0.269 ± 0.043	$0.252 \pm 4.1e-05$	-0.134 ± 0.013	3.870 ± 0.247	0.001	7 ± 3	9 ± 3	5 ± 2	8 ± 3	1
XMMXCS J133611.7+410455.5	$0.234^{+0.062}_{-0.061}$	0.234 ± 0.035	$0.233 \pm 4.9e-05$	-0.076 ± 0.018	2.760 ± 0.334	0.055	8 ± 3	7 ± 3	9 ± 3	8 ± 3	1
XMMXCS J133649.5+241312.8	$0.605^{+0.143}_{-0.143}$	0.620 ± 0.118	$0.602 \pm 1.5e-04$	-0.037 ± 0.086	1.880 ± 1.720	0.070	5 ± 3	45 ± 7	4 ± 2	46 ± 8	1
XMMXCS J133655.1+514447.7	$0.291^{+0.073}_{-0.075}$	0.279 ± 0.041	-	-0.050 ± 0.047	2.490 ± 0.874	0.001	8 ± 3	8 ± 3	5 ± 3	12 ± 4	1
XMMXCS J133759.3+280145.8	$0.252^{+0.044}_{-0.044}$	0.243 ± 0.040	$0.251 \pm 5.4e-05$	-0.070 ± 0.010	2.700 ± 0.180	0.001	2 ± 2	1 ± 2	3 ± 2	3 ± 2	1
XMMXCS J133909.2+481152.7	$0.412^{+0.069}_{-0.067}$	0.400 ± 0.072	$0.409 \pm 1.2e-04$	-0.021 ± 0.025	1.010 ± 0.501	0.031	8 ± 4	6 ± 4	7 ± 3	-	1
XMMXCS J133933.7-001700.3	$0.145^{+0.023}_{-0.023}$	0.153 ± 0.025	$0.146 \pm 1.6e-05$	-0.035 ± 0.007	1.690 ± 0.113	0.015	13 ± 4	14 ± 4	13 ± 4	15 ± 4	1
XMMXCS J134139.3+001733.9	$0.506^{+0.093}_{-0.093}$	0.510 ± 0.076	$0.505 \pm 5.0e-05$	-0.038 ± 0.029	1.650 ± 0.564	0.054	14 ± 4	15 ± 5	15 ± 5	14 ± 5	1
XMMXCS J134152.8+262228.7	$0.073^{+0.008}_{-0.008}$	0.081 ± 0.017	$0.072 \pm 9.4e-06$	0.003 ± 0.004	0.845 ± 0.066	0.001	16 ± 4	17 ± 4	15 ± 4	20 ± 5	1
XMMXCS J134323.5+560047.0	$0.484^{+0.133}_{-0.132}$	0.488 ± 0.072	$0.481 \pm 1.5e-04$	0.005 ± 0.039	0.794 ± 0.762	0.053	9 ± 4	9 ± 4	9 ± 3	9 ± 4	1
XMMXCS J134405.2+000005.0	$0.523^{+0.141}_{-0.140}$	0.555 ± 0.128	$0.539 \pm 1.1e-04$	-0.005 ± 0.042	0.963 ± 0.855	0.104	8 ± 4	11 ± 4	7 ± 3	11 ± 4	1
XMMXCS J134446.4-003018.4	$0.581^{+0.131}_{-0.131}$	0.588 ± 0.106	$0.580 \pm 8.6e-05$	0.011 ± 0.083	0.932 ± 1.630	0.098	4 ± 3	10 ± 4	4 ± 2	11 ± 4	1
XMMXCS J134500.0-002045.2	$0.434^{+0.106}_{-0.102}$	0.412 ± 0.063	$0.382 \pm 1.1e-04$	-0.039 ± 0.051	1.560 ± 1.030	0.147	13 ± 5	12 ± 5	13 ± 5	13 ± 5	1
XMMXCS J134515.0+335658.3	$0.514^{+0.144}_{-0.142}$	0.491 ± 0.090	$0.505 \pm 1.0e-04$	-0.310 ± 0.053	7.000 ± 1.090	0.018	3 ± 3	7 ± 4	5 ± 2	7 ± 3	1
XMMXCS J134730.8+643520.5	$0.519^{+0.123}_{-0.119}$	0.511 ± 0.080	$0.509 \pm 1.2e-04$	0.006 ± 0.090	0.667 ± 1.810	0.150	9 ± 4	89 ± 10	8 ± 4	19 ± 10	1
XMMXCS J134742.7+264537.3	$0.231^{+0.060}_{-0.061}$	0.240 ± 0.036	$0.251 \pm 3.6e-05$	-0.013 ± 0.054	1.620 ± 1.020	0.099	3 ± 2	4 ± 3	4 ± 2	3 ± 2	1

Continued on next page

Table A.2 – continued from previous page

name	z_{RS}	z_{BCG}	z_{spec-g}	cmr_{grad}	cmr_{inter}	cmr_{wid}	n_{gals-c}	n_{gals-l}	n_{200-c}	n_{200-l}	qual
XMMXCS J134752.7+600350.3	$0.401^{+0.080}_{-0.075}$	0.406 ± 0.059	-	0.373 ± 0.002	-5.880 ± 0.041	0.500	5 ± 4	4 ± 4	4 ± 3	4 ± 3	1
XMMXCS J134819.7+263218.6	$0.065^{+0.007}_{-0.007}$	0.074 ± 0.020	$0.065 \pm 1.1e-05$	0.037 ± 0.108	0.125 ± 1.830	0.127	5 ± 2	3 ± 2	3 ± 2	0 ± 1	1
XMMXCS J134825.6+263220.0	$0.074^{+0.021}_{-0.022}$	0.077 ± 0.015	$0.082 \pm 9.6e-06$	-0.071 ± 0.030	2.010 ± 0.491	0.032	7 ± 3	7 ± 3	6 ± 3	5 ± 2	1
XMMXCS J134835.6+262405.8	$0.063^{+0.004}_{-0.003}$	0.081 ± 0.017	$0.064 \pm 7.6e-06$	-0.031 ± 0.005	1.350 ± 0.083	0.008	5 ± 3	4 ± 2	3 ± 2	1 ± 1	1
XMMXCS J134837.5+263431.2	$0.062^{+0.013}_{-0.013}$	0.086 ± 0.018	$0.080 \pm 8.4e-06$	-0.037 ± 0.021	1.540 ± 0.365	0.069	9 ± 3	6 ± 3	7 ± 3	5 ± 2	1
XMMXCS J134842.9+264231.3	$0.066^{+0.052}_{-0.053}$	0.065 ± 0.017	$0.065 \pm 1.1e-05$	-0.018 ± 0.031	1.190 ± 0.568	0.066	5 ± 2	3 ± 2	3 ± 2	1 ± 1	1
XMMXCS J134844.7+263622.8	$0.066^{+0.013}_{-0.013}$	0.077 ± 0.018	$0.066 \pm 9.9e-06$	-0.057 ± 0.018	1.840 ± 0.303	0.050	8 ± 3	6 ± 3	6 ± 2	3 ± 2	1
XMMXCS J134847.2+264137.6	$0.066^{+0.024}_{-0.024}$	0.065 ± 0.017	$0.066 \pm 1.5e-05$	-0.047 ± 0.013	1.650 ± 0.233	0.050	5 ± 2	3 ± 2	3 ± 2	1 ± 1	1
XMMXCS J134851.6+263438.7	$0.075^{+0.021}_{-0.021}$	0.079 ± 0.015	$0.080 \pm 8.5e-06$	-0.051 ± 0.021	1.750 ± 0.369	0.058	15 ± 4	15 ± 4	16 ± 4	15 ± 4	1
XMMXCS J134854.8+264426.1	$0.249^{+0.058}_{-0.058}$	0.255 ± 0.041	$0.248 \pm 3.4e-05$	-0.053 ± 0.030	2.340 ± 0.579	0.076	8 ± 3	8 ± 3	7 ± 3	8 ± 3	1
XMMXCS J134905.5+264042.5	$0.065^{+0.016}_{-0.016}$	0.068 ± 0.017	$0.065 \pm 1.3e-05$	-0.020 ± 0.022	1.180 ± 0.370	0.051	7 ± 3	5 ± 2	3 ± 2	1 ± 1	1
XMMXCS J134910.9+263751.4	$0.062^{+0.020}_{-0.021}$	0.068 ± 0.017	$0.061 \pm 1.7e-05$	0.004 ± 0.028	0.764 ± 0.468	0.069	6 ± 3	5 ± 2	4 ± 2	2 ± 2	1
XMMXCS J134915.0+601127.5	$0.059^{+0.077}_{-0.059}$	0.064 ± 0.020	-	0.002 ± 0.026	0.687 ± 0.325	0.084	3 ± 2	28 ± 5	4 ± 2	41 ± 7	1
XMMXCS J135019.1+265027.3	$0.423^{+0.081}_{-0.079}$	0.374 ± 0.056	$0.421 \pm 1.1e-04$	0.057 ± 0.035	-0.478 ± 0.683	0.001	6 ± 3	6 ± 3	6 ± 3	-	1
XMMXCS J135358.8+335003.1	$0.470^{+0.090}_{-0.090}$	0.474 ± 0.069	$0.470 \pm 1.2e-04$	-0.008 ± 0.022	0.996 ± 0.425	0.068	14 ± 4	20 ± 5	14 ± 5	22 ± 6	1
XMMXCS J135403.4+334601.7	$0.385^{+0.082}_{-0.080}$	0.378 ± 0.056	$0.382 \pm 6.7e-05$	-0.064 ± 0.038	1.850 ± 0.728	0.025	15 ± 4	21 ± 5	15 ± 5	18 ± 5	1
XMMXCS J135417.3-022149.7	$0.548^{+0.104}_{-0.104}$	0.522 ± 0.084	$0.548 \pm 1.6e-04$	0.025 ± 0.035	0.581 ± 0.695	0.050	22 ± 5	56 ± 8	23 ± 5	55 ± 9	1
XMMXCS J135503.6+382951.5	$0.582^{+0.107}_{-0.103}$	0.564 ± 0.100	$0.576 \pm 1.6e-04$	0.261 ± 0.243	-4.350 ± 4.950	0.161	8 ± 3	-	8 ± 3	-	1
XMMXCS J135649.1+653509.5	$0.214^{+0.083}_{-0.081}$	0.250 ± 0.073	$0.230 \pm 4.7e-05$	-0.067 ± 0.033	2.420 ± 0.606	0.071	5 ± 3	4 ± 3	3 ± 2	1 ± 2	1

Continued on next page

Table A.2 – continued from previous page

name	z_{RS}	z_{BCG}	z_{spec-g}	cmr_{grad}	cmr_{inter}	cmr_{wid}	n_{gals-c}	n_{gals-l}	n_{200-c}	n_{200-l}	qual
XMMXCS J140032.2+025426.3	$0.251^{+0.056}_{-0.056}$	0.214 ± 0.033	$0.250 \pm 3.2e-05$	0.015 ± 0.024	1.080 ± 0.440	0.072	16 ± 4	15 ± 4	18 ± 5	17 ± 5	1
XMMXCS J140045.8+025336.5	$0.249^{+0.064}_{-0.065}$	0.255 ± 0.039	$0.249 \pm 4.0e-05$	-0.019 ± 0.017	1.760 ± 0.323	0.070	15 ± 4	17 ± 4	21 ± 5	28 ± 6	1
XMMXCS J140051.4+025351.5	$0.248^{+0.067}_{-0.067}$	0.226 ± 0.039	$0.251 \pm 2.9e-05$	-0.058 ± 0.021	2.490 ± 0.403	0.053	24 ± 5	29 ± 6	55 ± 8	63 ± 8	1
XMMXCS J140053.1+025053.4	$0.251^{+0.059}_{-0.060}$	0.290 ± 0.044	$0.260 \pm 2.7e-05$	-0.016 ± 0.017	1.750 ± 0.328	0.063	25 ± 5	26 ± 5	51 ± 7	55 ± 8	1
XMMXCS J140058.1+025728.7	$0.251^{+0.064}_{-0.064}$	0.226 ± 0.039	$0.253 \pm 3.7e-05$	-0.036 ± 0.024	2.080 ± 0.452	0.060	26 ± 5	26 ± 5	48 ± 7	45 ± 7	1
XMMXCS J140101.9+025236.8	$0.245^{+0.050}_{-0.050}$	0.226 ± 0.036	$0.252 \pm 2.7e-05$	-0.069 ± 0.041	2.730 ± 0.768	0.050	36 ± 6	41 ± 7	64 ± 8	71 ± 9	1
XMMXCS J140104.5+025542.6	$0.249^{+0.057}_{-0.057}$	0.226 ± 0.039	$0.249 \pm 3.5e-05$	0.003 ± 0.051	1.370 ± 0.947	0.052	25 ± 5	28 ± 6	50 ± 7	54 ± 8	1
XMMXCS J140108.9+025128.0	$0.252^{+0.054}_{-0.054}$	0.226 ± 0.036	$0.262 \pm 2.3e-05$	-0.027 ± 0.029	1.920 ± 0.537	0.065	33 ± 6	32 ± 6	72 ± 9	68 ± 9	1
XMMXCS J140114.0+025119.3	$0.247^{+0.056}_{-0.056}$	0.226 ± 0.036	$0.253 \pm 3.0e-05$	-0.005 ± 0.019	1.520 ± 0.360	0.070	19 ± 5	20 ± 5	33 ± 6	39 ± 7	1
XMMXCS J140125.6-110913.7	$0.085^{+0.023}_{-0.023}$	0.093 ± 0.027	-	-0.014 ± 0.008	1.130 ± 0.134	0.043	18 ± 4	19 ± 5	23 ± 5	26 ± 5	1
XMMXCS J140127.2+025505.5	$0.219^{+0.054}_{-0.054}$	0.198 ± 0.034	-	0.022 ± 0.060	0.986 ± 1.150	0.001	9 ± 3	8 ± 3	8 ± 3	6 ± 3	1
XMMXCS J140134.8-110204.3	$0.086^{+0.037}_{-0.038}$	0.095 ± 0.021	-	0.001 ± 0.022	0.822 ± 0.399	0.067	10 ± 3	10 ± 3	11 ± 3	10 ± 3	1
XMMXCS J140136.0-111003.2	$0.082^{+0.043}_{-0.044}$	0.093 ± 0.028	-	-0.029 ± 0.009	1.400 ± 0.150	0.035	20 ± 5	18 ± 4	23 ± 5	20 ± 5	1
XMMXCS J140137.7-110720.4	$0.092^{+0.026}_{-0.026}$	0.093 ± 0.027	-	0.010 ± 0.004	0.760 ± 0.060	0.023	21 ± 5	21 ± 5	27 ± 5	25 ± 5	1
XMMXCS J140139.2-111838.3	$0.077^{+0.049}_{-0.051}$	0.064 ± 0.018	-	-0.008 ± 0.005	0.957 ± 0.074	0.001	7 ± 3	6 ± 3	3 ± 2	2 ± 2	1
XMMXCS J140615.8+283049.1	$0.547^{+0.087}_{-0.086}$	0.564 ± 0.111	$0.546 \pm 1.2e-04$	-0.016 ± 0.059	1.240 ± 1.220	0.001	5 ± 3	-	5 ± 3	-	1
XMMXCS J140653.8+283420.4	$0.117^{+0.028}_{-0.028}$	0.117 ± 0.020	$0.117 \pm 2.2e-05$	0.020 ± 0.024	0.608 ± 0.455	0.064	8 ± 3	7 ± 3	3 ± 2	3 ± 2	1
XMMXCS J140659.9+282134.4	$0.506^{+0.098}_{-0.097}$	0.525 ± 0.085	$0.504 \pm 1.2e-04$	-0.128 ± 0.063	3.400 ± 1.270	0.001	7 ± 3	9 ± 4	6 ± 3	7 ± 4	1
XMMXCS J140852.0+260640.6	$0.585^{+0.109}_{-0.104}$	0.498 ± 0.130	$0.574 \pm 9.3e-05$	0.239 ± 0.210	-3.940 ± 4.150	0.211	6 ± 3	-	4 ± 2	-	1

Continued on next page

Table A.2 – continued from previous page

name	z_{RS}	z_{BCG}	z_{spec-g}	cmr_{grad}	cmr_{inter}	cmr_{wid}	n_{gals-c}	n_{gals-l}	n_{200-c}	n_{200-l}	qual
XMMXCS J141319.2+440442.7	$0.565^{+0.115}_{-0.114}$	0.541 ± 0.102	$0.561 \pm 1.7e-04$	-0.058 ± 0.038	2.130 ± 0.739	0.001	5 ± 3	63 ± 8	4 ± 2	11 ± 7	1
XMMXCS J141359.1-002626.6	$0.134^{+0.027}_{-0.026}$	0.121 ± 0.031	$0.133 \pm 1.8e-05$	0.014 ± 0.027	0.716 ± 0.477	0.068	10 ± 3	8 ± 3	8 ± 3	5 ± 3	1
XMMXCS J141408.4-001613.4	$0.140^{+0.025}_{-0.025}$	0.152 ± 0.025	$0.140 \pm 2.7e-05$	-0.021 ± 0.027	1.460 ± 0.462	0.037	11 ± 3	10 ± 3	11 ± 3	9 ± 3	1
XMMXCS J141424.8-002235.1	$0.138^{+0.024}_{-0.023}$	0.150 ± 0.026	$0.138 \pm 1.5e-05$	-0.034 ± 0.014	1.630 ± 0.247	0.031	23 ± 5	27 ± 5	33 ± 6	43 ± 7	1
XMMXCS J141446.39+544710.1	$0.581^{+0.133}_{-0.133}$	0.601 ± 0.122	-	-0.078 ± 0.029	2.710 ± 0.587	0.071	22 ± 5	64 ± 8	33 ± 6	87 ± 11	1
XMMXCS J141451.5-002553.3	$0.141^{+0.043}_{-0.044}$	0.146 ± 0.023	$0.143 \pm 1.8e-05$	-0.029 ± 0.016	1.530 ± 0.298	0.064	21 ± 5	23 ± 5	37 ± 6	44 ± 7	1
XMMXCS J141457.5+281744.2	$0.472^{+0.096}_{-0.095}$	0.468 ± 0.107	-	0.221 ± 0.136	-3.620 ± 2.760	0.095	10 ± 4	-	9 ± 4	-	1
XMMXCS J141458.0-002057.0	$0.139^{+0.024}_{-0.025}$	0.159 ± 0.026	$0.142 \pm 1.7e-05$	-0.052 ± 0.013	1.970 ± 0.223	0.031	24 ± 5	23 ± 5	34 ± 6	32 ± 6	1
XMMXCS J141506.7-002927.7	$0.139^{+0.014}_{-0.015}$	0.151 ± 0.024	$0.142 \pm 1.5e-05$	-0.033 ± 0.005	1.610 ± 0.090	0.027	23 ± 5	27 ± 5	33 ± 6	37 ± 6	1
XMMXCS J141514.1+111903.8	$0.304^{+0.068}_{-0.068}$	0.263 ± 0.045	$0.304 \pm 3.2e-05$	-0.035 ± 0.023	2.150 ± 0.452	0.074	5 ± 3	6 ± 3	5 ± 2	5 ± 3	1
XMMXCS J141534.8+282335.2	$0.224^{+0.033}_{-0.033}$	0.236 ± 0.036	$0.224 \pm 2.9e-05$	-0.020 ± 0.031	1.710 ± 0.569	0.067	11 ± 4	10 ± 4	12 ± 4	10 ± 3	1
XMMXCS J141553.7+281720.2	$0.139^{+0.037}_{-0.037}$	0.132 ± 0.025	$0.139 \pm 1.9e-05$	-0.003 ± 0.023	1.080 ± 0.399	0.062	3 ± 2	3 ± 2	3 ± 2	3 ± 2	1
XMMXCS J141610.3+264631.6	$0.333^{+0.071}_{-0.072}$	0.308 ± 0.095	$0.386 \pm 8.6e-05$	-0.053 ± 0.060	2.640 ± 1.200	0.127	6 ± 3	5 ± 3	3 ± 2	2 ± 2	1
XMMXCS J141627.7+231526.5	$0.138^{+0.029}_{-0.029}$	0.145 ± 0.023	$0.137 \pm 2.1e-05$	-0.029 ± 0.010	1.520 ± 0.173	0.086	7 ± 3	8 ± 3	4 ± 2	6 ± 3	1
XMMXCS J141645.1+232315.3	$0.139^{+0.013}_{-0.013}$	0.146 ± 0.024	$0.140 \pm 1.4e-05$	-0.045 ± 0.010	1.830 ± 0.171	0.011	8 ± 3	9 ± 3	7 ± 3	8 ± 3	1
XMMXCS J141702.3+450509.5	$0.445^{+0.053}_{-0.052}$	0.430 ± 0.068	$0.491 \pm 7.9e-05$	-0.037 ± 0.058	2.530 ± 1.100	0.091	2 ± 3	4 ± 3	3 ± 2	4 ± 3	1
XMMXCS J141723.9+270338.4	$0.485^{+0.116}_{-0.115}$	0.475 ± 0.069	$0.482 \pm 6.9e-05$	-0.097 ± 0.027	2.720 ± 0.529	0.001	3 ± 3	7 ± 4	4 ± 2	5 ± 3	1
XMMXCS J141731.2+251139.1	$0.178^{+0.037}_{-0.037}$	0.197 ± 0.030	$0.178 \pm 4.3e-05$	-0.076 ± 0.012	2.480 ± 0.193	0.042	7 ± 3	5 ± 3	4 ± 2	3 ± 2	1
XMMXCS J141823.26+522710.6	$0.285^{+0.074}_{-0.073}$	0.296 ± 0.044	$0.281 \pm 6.7e-05$	-0.052 ± 0.144	2.400 ± 2.790	0.085	4 ± 3	4 ± 3	3 ± 2	3 ± 2	1

Continued on next page

Table A.2 – continued from previous page

name	z_{RS}	z_{BCG}	z_{spec-g}	cmr_{grad}	cmr_{inter}	cmr_{wid}	n_{gals-c}	n_{gals-l}	n_{200-c}	n_{200-l}	qual
XMMXCS J141823.2+522710.6	$0.285^{+0.074}_{-0.073}$	0.296 ± 0.044	$0.281 \pm 6.7e-05$	-0.052 ± 0.144	2.400 ± 2.790	0.085	4 ± 3	4 ± 3	3 ± 2	3 ± 2	1
XMMXCS J141832.3+251104.9	$0.290^{+0.056}_{-0.057}$	0.314 ± 0.049	$0.291 \pm 6.7e-05$	-0.000 ± 0.024	1.600 ± 0.442	0.055	21 ± 5	21 ± 5	31 ± 6	30 ± 6	1
XMMXCS J141936.2+064736.8	$0.115^{+0.012}_{-0.012}$	0.125 ± 0.021	$0.115 \pm 1.4e-05$	-0.018 ± 0.005	1.300 ± 0.090	0.022	7 ± 3	8 ± 3	6 ± 3	8 ± 3	1
XMMXCS J141937.4+064707.7	$0.114^{+0.016}_{-0.016}$	0.125 ± 0.021	$0.115 \pm 1.4e-05$	-0.015 ± 0.006	1.250 ± 0.098	0.019	7 ± 3	8 ± 3	5 ± 2	8 ± 3	1
XMMXCS J141939.0+062847.4	$0.565^{+0.082}_{-0.081}$	0.569 ± 0.094	$0.564 \pm 7.8e-05$	-0.166 ± 0.060	4.290 ± 1.200	0.001	10 ± 4	16 ± 5	9 ± 3	17 ± 5	1
XMMXCS J142044.6+063101.0	$0.156^{+0.034}_{-0.034}$	0.146 ± 0.031	$0.156 \pm 4.0e-05$	-0.040 ± 0.033	1.770 ± 0.585	0.050	4 ± 2	3 ± 2	4 ± 2	3 ± 2	1
XMMXCS J142305.4+382807.0	$0.452^{+0.086}_{-0.085}$	0.424 ± 0.063	$0.451 \pm 1.4e-04$	0.141 ± 0.073	-2.060 ± 1.440	0.074	13 ± 4	13 ± 4	14 ± 5	-	1
XMMXCS J142505.3+375731.8	$0.163^{+0.033}_{-0.033}$	0.172 ± 0.027	$0.163 \pm 2.2e-05$	-0.030 ± 0.005	1.680 ± 0.088	0.001	15 ± 4	15 ± 4	19 ± 5	17 ± 4	1
XMMXCS J142601.0+374936.4	$0.170^{+0.027}_{-0.027}$	0.175 ± 0.029	$0.171 \pm 3.4e-05$	-0.019 ± 0.021	1.520 ± 0.365	0.037	36 ± 6	36 ± 6	55 ± 8	56 ± 8	1
XMMXCS J142605.6+375315.0	$0.170^{+0.036}_{-0.037}$	0.184 ± 0.032	$0.169 \pm 2.8e-05$	-0.037 ± 0.010	1.840 ± 0.176	0.047	25 ± 5	24 ± 5	42 ± 7	41 ± 7	1
XMMXCS J142632.4+375535.7	$0.155^{+0.034}_{-0.034}$	0.174 ± 0.026	$0.171 \pm 3.3e-05$	-0.124 ± 0.026	3.350 ± 0.461	0.070	8 ± 3	9 ± 3	6 ± 3	6 ± 3	1
XMMXCS J142725.5+423419.5	$0.130^{+0.032}_{-0.032}$	0.135 ± 0.022	$0.134 \pm 1.8e-05$	-0.024 ± 0.011	1.460 ± 0.182	0.001	11 ± 3	10 ± 3	11 ± 3	10 ± 3	1
XMMXCS J142741.8+264029.1	$0.440^{+0.092}_{-0.088}$	0.442 ± 0.065	$0.440 \pm 4.8e-05$	-0.130 ± 0.063	3.200 ± 1.240	0.114	2 ± 3	2 ± 3	3 ± 2	3 ± 2	1
XMMXCS J142747.7+423417.3	$0.132^{+0.018}_{-0.019}$	0.152 ± 0.025	$0.131 \pm 1.9e-05$	-0.076 ± 0.029	2.360 ± 0.510	0.053	7 ± 3	7 ± 3	6 ± 3	6 ± 3	1
XMMXCS J142901.6+424717.0	$0.162^{+0.035}_{-0.035}$	0.148 ± 0.026	$0.151 \pm 3.2e-05$	-0.014 ± 0.030	1.410 ± 0.558	0.048	2 ± 2	3 ± 2	3 ± 2	3 ± 2	1
XMMXCS J142919.3+474452.1	$0.188^{+0.044}_{-0.045}$	0.208 ± 0.034	$0.193 \pm 1.9e-05$	0.020 ± 0.029	0.890 ± 0.534	0.098	13 ± 4	10 ± 4	13 ± 4	13 ± 4	1
XMMXCS J143100.6-001213.5	$0.123^{+0.010}_{-0.011}$	0.131 ± 0.025	$0.123 \pm 1.6e-05$	0.028 ± 0.039	0.460 ± 0.676	0.063	7 ± 3	6 ± 3	6 ± 3	4 ± 2	1
XMMXCS J143102.1+421431.3	$0.426^{+0.079}_{-0.078}$	0.441 ± 0.063	$0.426 \pm 1.5e-04$	-0.010 ± 0.028	0.919 ± 0.544	0.027	20 ± 5	22 ± 5	21 ± 6	24 ± 6	1
XMMXCS J143120.8-005346.2	$0.405^{+0.067}_{-0.066}$	0.393 ± 0.059	$0.403 \pm 1.4e-04$	-0.032 ± 0.173	2.300 ± 3.370	0.157	15 ± 5	18 ± 5	17 ± 5	19 ± 5	1

Continued on next page

Table A.2 – continued from previous page

name	z_{RS}	z_{BCG}	z_{spec-g}	cmr_{grad}	cmr_{inter}	cmr_{wid}	n_{gals-c}	n_{gals-l}	n_{200-c}	n_{200-l}	qual
XMMXCS J143151.8+281300.6	$0.368^{+0.053}_{-0.053}$	0.354 ± 0.053	$0.371 \pm 5.1e-05$	-0.039 ± 0.057	2.480 ± 1.080	0.057	8 ± 3	8 ± 4	7 ± 3	9 ± 3	1
XMMXCS J143432.3+033744.4	$0.294^{+0.064}_{-0.064}$	0.314 ± 0.049	$0.294 \pm 7.4e-05$	-0.195 ± 0.045	5.230 ± 0.875	0.001	4 ± 3	14 ± 4	4 ± 2	2 ± 3	1
XMMXCS J143448.6+033740.4	$0.146^{+0.018}_{-0.019}$	0.150 ± 0.023	$0.146 \pm 1.8e-05$	-0.020 ± 0.008	1.430 ± 0.137	0.032	9 ± 3	5 ± 3	7 ± 3	5 ± 2	1
XMMXCS J143548.3+034149.2	$0.306^{+0.057}_{-0.057}$	0.310 ± 0.045	$0.343 \pm 4.3e-05$	0.020 ± 0.035	1.220 ± 0.640	0.068	4 ± 3	4 ± 3	3 ± 2	4 ± 2	1
XMMXCS J143714.4+341517.8	$0.541^{+0.083}_{-0.083}$	0.552 ± 0.108	$0.541 \pm 6.7e-05$	-0.016 ± 0.039	1.290 ± 0.758	0.001	16 ± 4	19 ± 5	18 ± 5	24 ± 6	1
XMMXCS J143724.6+341427.9	$0.362^{+0.063}_{-0.063}$	0.360 ± 0.059	-	0.098 ± 0.064	-0.222 ± 1.290	0.041	17 ± 4	16 ± 5	20 ± 5	20 ± 5	1
XMMXCS J143833.1+642850.1	$0.142^{+0.038}_{-0.038}$	0.142 ± 0.023	$0.143 \pm 1.8e-05$	-0.008 ± 0.017	1.220 ± 0.293	0.020	8 ± 3	7 ± 3	7 ± 3	6 ± 3	1
XMMXCS J143850.4+341550.0	$0.340^{+0.055}_{-0.056}$	0.342 ± 0.050	$0.341 \pm 9.4e-05$	-0.049 ± 0.008	2.650 ± 0.157	0.001	13 ± 4	13 ± 4	12 ± 4	13 ± 4	1
XMMXCS J143859.0+642321.0	$0.143^{+0.033}_{-0.033}$	0.154 ± 0.027	$0.143 \pm 1.4e-05$	-0.048 ± 0.007	1.880 ± 0.123	0.023	8 ± 3	10 ± 3	6 ± 3	10 ± 3	1
XMMXCS J144016.2+034124.4	$0.280^{+0.067}_{-0.072}$	0.271 ± 0.050	$0.295 \pm 3.7e-05$	-0.042 ± 0.032	2.280 ± 0.607	0.085	19 ± 5	20 ± 5	20 ± 5	25 ± 6	1
XMMXCS J144027.3+033650.6	$0.295^{+0.103}_{-0.102}$	0.338 ± 0.053	$0.291 \pm 6.8e-05$	-0.417 ± 0.071	9.330 ± 1.420	0.001	3 ± 2	2 ± 2	3 ± 2	4 ± 2	1
XMMXCS J144720.5+631626.7	$0.198^{+0.053}_{-0.053}$	0.199 ± 0.030	$0.198 \pm 2.5e-05$	-0.018 ± 0.027	1.520 ± 0.485	0.081	9 ± 3	9 ± 3	8 ± 3	9 ± 3	1
XMMXCS J144932.0+085951.5	$0.427^{+0.204}_{-0.186}$	0.424 ± 0.223	-	0.279 ± 0.181	-4.670 ± 3.680	0.001	8 ± 3	-	6 ± 3	-	1
XMMXCS J145204.5+165154.1	$0.117^{+0.026}_{-0.027}$	0.130 ± 0.020	$0.094 \pm 1.2e-05$	-0.027 ± 0.050	1.360 ± 0.878	0.103	4 ± 2	6 ± 3	4 ± 2	6 ± 3	1
XMMXCS J145234.4+165156.9	$0.058^{+0.024}_{-0.019}$	0.069 ± 0.020	$0.046 \pm 6.7e-06$	-0.011 ± 0.024	0.980 ± 0.362	0.060	15 ± 4	9 ± 3	22 ± 5	5 ± 2	1
XMMXCS J145256.1+164215.3	$0.044^{+0.002}_{-0.002}$	0.070 ± 0.033	$0.044 \pm 6.9e-06$	-0.014 ± 0.018	1.010 ± 0.271	0.040	15 ± 4	8 ± 3	16 ± 4	8 ± 3	1
XMMXCS J145258.1+163830.6	$0.044^{+0.002}_{-0.002}$	0.070 ± 0.033	$0.044 \pm 6.9e-06$	-0.041 ± 0.030	1.430 ± 0.459	0.022	15 ± 4	9 ± 3	16 ± 4	8 ± 3	1
XMMXCS J145317.3+033446.7	$0.371^{+0.069}_{-0.068}$	0.349 ± 0.051	$0.371 \pm 5.3e-05$	0.218 ± 0.134	-2.440 ± 2.580	0.184	9 ± 4	11 ± 4	8 ± 3	11 ± 4	1
XMMXCS J145351.1+032313.4	$0.368^{+0.057}_{-0.056}$	0.344 ± 0.052	$0.370 \pm 4.5e-05$	-0.099 ± 0.084	3.620 ± 1.680	0.001	5 ± 3	9 ± 4	5 ± 3	7 ± 3	1

Continued on next page

Table A.2 – continued from previous page

name	z_{RS}	z_{BCG}	z_{spec-g}	cmr_{grad}	cmr_{inter}	cmr_{wid}	n_{gals-c}	n_{gals-l}	n_{200-c}	n_{200-l}	qual
XMMXCS J145405.7+033501.7	$0.552^{+0.134}_{-0.134}$	0.557 ± 0.156	-	-0.341 ± 0.178	7.840 ± 3.570	0.001	5 ± 3	3 ± 3	3 ± 2	7 ± 3	1
XMMXCS J145431.8+183835.3	$0.066^{+0.013}_{-0.014}$	0.066 ± 0.015	$0.058 \pm 9.0e-06$	-0.073 ± 0.029	2.090 ± 0.480	0.037	7 ± 3	3 ± 2	7 ± 3	2 ± 2	1
XMMXCS J145435.5+184110.0	$0.059^{+0.002}_{-0.001}$	0.072 ± 0.015	$0.058 \pm 8.6e-06$	-0.020 ± 0.004	1.190 ± 0.061	0.009	13 ± 4	8 ± 3	13 ± 4	9 ± 3	1
XMMXCS J145505.6+184148.4	$0.237^{+0.041}_{-0.041}$	0.219 ± 0.044	$0.237 \pm 4.1e-05$	0.041 ± 0.063	0.566 ± 1.190	0.106	3 ± 2	7 ± 3	4 ± 2	2 ± 2	1
XMMXCS J145710.8+221843.0	$0.258^{+0.069}_{-0.069}$	0.263 ± 0.041	$0.259 \pm 3.2e-05$	-0.052 ± 0.018	2.410 ± 0.337	0.046	12 ± 4	15 ± 4	12 ± 4	13 ± 4	1
XMMXCS J145715.1+222031.7	$0.264^{+0.074}_{-0.074}$	0.263 ± 0.041	$0.259 \pm 3.2e-05$	-0.020 ± 0.017	1.820 ± 0.335	0.044	19 ± 5	19 ± 5	22 ± 5	23 ± 5	1
XMMXCS J145727.1-010115.8	$0.555^{+0.113}_{-0.112}$	0.562 ± 0.124	$0.547 \pm 8.3e-05$	-0.182 ± 0.039	4.650 ± 0.772	0.052	10 ± 4	20 ± 5	9 ± 3	16 ± 5	1
XMMXCS J145847.2+493455.7	$0.430^{+0.083}_{-0.082}$	0.414 ± 0.065	-	-0.015 ± 0.024	1.060 ± 0.477	0.001	22 ± 5	23 ± 5	24 ± 6	26 ± 6	1
XMMXCS J150034.4+015200.0	$0.421^{+0.071}_{-0.071}$	0.401 ± 0.060	$0.421 \pm 9.4e-05$	0.009 ± 0.035	0.522 ± 0.674	0.021	19 ± 5	18 ± 5	23 ± 6	24 ± 6	1
XMMXCS J150049.8+422053.3	$0.333^{+0.095}_{-0.094}$	0.346 ± 0.144	-	0.099 ± 0.116	-0.599 ± 2.340	0.068	4 ± 3	5 ± 3	4 ± 2	5 ± 3	1
XMMXCS J150113.9+423426.2	$0.217^{+0.063}_{-0.064}$	0.225 ± 0.038	$0.243 \pm 3.2e-05$	-0.040 ± 0.028	2.090 ± 0.513	0.065	7 ± 3	8 ± 3	7 ± 3	8 ± 3	1
XMMXCS J150122.5+422042.0	$0.283^{+0.072}_{-0.072}$	0.309 ± 0.047	$0.267 \pm 5.2e-05$	-0.045 ± 0.039	2.370 ± 0.751	0.095	33 ± 6	11 ± 4	46 ± 7	10 ± 4	1
XMMXCS J150215.2+422815.7	$0.242^{+0.062}_{-0.062}$	0.246 ± 0.036	$0.242 \pm 4.8e-05$	-0.064 ± 0.038	2.520 ± 0.699	0.022	8 ± 3	7 ± 3	6 ± 3	6 ± 3	1
XMMXCS J150353.6-025106.9	$0.222^{+0.066}_{-0.067}$	0.197 ± 0.032	-	0.018 ± 0.028	0.993 ± 0.529	0.053	11 ± 4	14 ± 4	10 ± 3	19 ± 5	1
XMMXCS J150407.6-024814.8	$0.232^{+0.059}_{-0.059}$	0.260 ± 0.046	$0.219 \pm 3.2e-05$	-0.026 ± 0.041	1.870 ± 0.759	0.052	26 ± 5	24 ± 5	36 ± 6	31 ± 6	1
XMMXCS J150419.0-024833.4	$0.218^{+0.053}_{-0.053}$	0.260 ± 0.046	$0.220 \pm 2.5e-05$	-0.030 ± 0.025	1.920 ± 0.462	0.078	17 ± 4	18 ± 5	23 ± 5	26 ± 5	1
XMMXCS J150420.1+474756.2	$0.619^{+0.161}_{-0.162}$	0.613 ± 0.105	-	-0.026 ± 0.033	1.650 ± 0.673	0.001	7 ± 3	45 ± 7	6 ± 3	11 ± 6	1
XMMXCS J150701.6+010650.5	$0.185^{+0.038}_{-0.037}$	0.182 ± 0.027	$0.188 \pm 3.0e-05$	-0.140 ± 0.046	3.680 ± 0.826	0.059	9 ± 3	7 ± 3	7 ± 3	5 ± 3	1
XMMXCS J150824.8-001531.7	$0.090^{+0.003}_{-0.002}$	0.101 ± 0.021	$0.091 \pm 8.7e-06$	0.011 ± 0.016	0.772 ± 0.241	0.028	16 ± 4	16 ± 4	18 ± 4	18 ± 4	1

Continued on next page

Table A.2 – continued from previous page

name	z_{RS}	z_{BCG}	z_{spec-g}	cmr_{grad}	cmr_{inter}	cmr_{wid}	n_{gals-c}	n_{gals-l}	n_{200-c}	n_{200-l}	qual
XMMXCS J150854.7+073450.1	$0.272^{+0.070}_{-0.070}$	0.271 ± 0.042	$0.272 \pm 6.2e-05$	0.025 ± 0.041	0.945 ± 0.792	0.081	5 ± 3	4 ± 3	3 ± 2	1 ± 2	1
XMMXCS J150924.6+073510.1	$0.077^{+0.014}_{-0.014}$	0.089 ± 0.028	$0.078 \pm 8.0e-06$	-0.038 ± 0.010	1.510 ± 0.162	0.054	15 ± 4	17 ± 4	19 ± 5	21 ± 5	1
XMMXCS J150932.0+073004.2	$0.077^{+0.009}_{-0.009}$	0.089 ± 0.028	$0.077 \pm 1.0e-05$	-0.014 ± 0.010	1.100 ± 0.164	0.046	12 ± 4	12 ± 4	12 ± 4	12 ± 4	1
XMMXCS J151009.5+332517.9	$0.115^{+0.017}_{-0.017}$	0.133 ± 0.024	$0.118 \pm 1.3e-05$	-0.030 ± 0.011	1.500 ± 0.187	0.049	28 ± 5	30 ± 6	47 ± 7	48 ± 7	1
XMMXCS J151012.2+333057.5	$0.114^{+0.018}_{-0.018}$	0.133 ± 0.024	$0.111 \pm 1.3e-05$	-0.010 ± 0.007	1.180 ± 0.111	0.039	29 ± 5	30 ± 6	51 ± 7	55 ± 8	1
XMMXCS J151012.5+332511.7	$0.115^{+0.012}_{-0.012}$	0.133 ± 0.024	$0.118 \pm 1.3e-05$	-0.023 ± 0.009	1.380 ± 0.138	0.048	27 ± 5	28 ± 5	44 ± 7	46 ± 7	1
XMMXCS J151014.8+054127.9	$0.349^{+0.054}_{-0.053}$	0.343 ± 0.061	-	-0.006 ± 0.110	1.780 ± 2.090	0.129	8 ± 3	8 ± 4	5 ± 3	6 ± 3	1
XMMXCS J151029.0+054449.3	$0.361^{+0.103}_{-0.103}$	0.374 ± 0.100	$0.249 \pm 2.6e+00$	0.094 ± 0.068	-0.880 ± 1.240	0.154	6 ± 3	-	5 ± 3	-	1
XMMXCS J151036.6+054040.9	$0.076^{+0.015}_{-0.015}$	0.087 ± 0.015	$0.077 \pm 9.2e-06$	-0.035 ± 0.009	1.460 ± 0.151	0.021	14 ± 4	12 ± 4	20 ± 5	13 ± 4	1
XMMXCS J151036.7+053949.0	$0.079^{+0.013}_{-0.013}$	0.087 ± 0.015	$0.076 \pm 9.1e-06$	-0.040 ± 0.018	1.550 ± 0.280	0.032	13 ± 4	13 ± 4	16 ± 4	14 ± 4	1
XMMXCS J151038.6+053555.7	$0.080^{+0.004}_{-0.005}$	0.087 ± 0.015	$0.081 \pm 9.9e-06$	-0.068 ± 0.017	2.000 ± 0.265	0.028	12 ± 4	11 ± 3	12 ± 4	11 ± 3	1
XMMXCS J151041.2+053733.7	$0.077^{+0.007}_{-0.007}$	0.087 ± 0.015	$0.078 \pm 9.5e-06$	-0.098 ± 0.017	2.480 ± 0.279	0.035	15 ± 4	18 ± 4	18 ± 5	18 ± 4	1
XMMXCS J151050.4+670633.0	$0.344^{+0.095}_{-0.095}$	0.361 ± 0.062	-	0.025 ± 0.052	1.110 ± 1.010	0.134	20 ± 5	18 ± 5	32 ± 6	27 ± 6	1
XMMXCS J151051.4+054937.2	$0.075^{+0.014}_{-0.014}$	0.109 ± 0.021	$0.076 \pm 1.0e-05$	-0.020 ± 0.037	1.250 ± 0.633	0.048	17 ± 4	19 ± 4	23 ± 5	26 ± 5	1
XMMXCS J151051.5+054934.5	$0.075^{+0.002}_{-0.002}$	0.090 ± 0.016	$0.077 \pm 1.2e-05$	0.020 ± 0.038	0.589 ± 0.653	0.046	11 ± 3	13 ± 4	10 ± 3	13 ± 4	1
XMMXCS J151052.4+053715.7	$0.078^{+0.006}_{-0.007}$	0.089 ± 0.017	$0.079 \pm 9.7e-06$	-0.093 ± 0.018	2.410 ± 0.281	0.033	17 ± 4	16 ± 4	23 ± 5	18 ± 4	1
XMMXCS J151055.8+054437.8	$0.077^{+0.016}_{-0.016}$	0.081 ± 0.027	$0.076 \pm 9.9e-06$	0.008 ± 0.022	0.759 ± 0.375	0.083	27 ± 5	27 ± 5	36 ± 7	38 ± 6	1
XMMXCS J151056.1+054438.1	$0.077^{+0.016}_{-0.016}$	0.081 ± 0.027	$0.076 \pm 9.9e-06$	0.008 ± 0.022	0.759 ± 0.375	0.083	27 ± 5	27 ± 5	36 ± 7	38 ± 6	1
XMMXCS J151100.0+053819.0	$0.080^{+0.015}_{-0.014}$	0.089 ± 0.017	$0.080 \pm 9.6e-06$	-0.025 ± 0.017	1.280 ± 0.286	0.065	22 ± 5	19 ± 4	30 ± 6	22 ± 5	1

Continued on next page

Table A.2 – continued from previous page

name	z_{RS}	z_{BCG}	z_{spec-g}	cmr_{grad}	cmr_{inter}	cmr_{wid}	n_{gals-c}	n_{gals-l}	n_{200-c}	n_{200-l}	qual
XMMXCS J151100.5+054914.5	$0.077^{+0.018}_{-0.017}$	0.109 ± 0.021	$0.076 \pm 9.3e-06$	-0.051 ± 0.010	1.750 ± 0.174	0.043	22 ± 5	21 ± 5	32 ± 6	29 ± 5	1
XMMXCS J151101.3+054914.4	$0.077^{+0.013}_{-0.013}$	0.109 ± 0.021	$0.076 \pm 9.3e-06$	-0.045 ± 0.012	1.640 ± 0.203	0.044	22 ± 5	21 ± 5	32 ± 6	28 ± 5	1
XMMXCS J151102.9+055242.4	$0.077^{+0.004}_{-0.004}$	0.100 ± 0.023	$0.076 \pm 8.5e-06$	-0.018 ± 0.036	1.180 ± 0.581	0.032	11 ± 4	13 ± 4	12 ± 4	14 ± 4	1
XMMXCS J151103.1+054921.9	$0.079^{+0.015}_{-0.015}$	0.109 ± 0.021	$0.076 \pm 9.3e-06$	-0.047 ± 0.015	1.670 ± 0.249	0.045	22 ± 5	21 ± 5	34 ± 6	28 ± 5	1
XMMXCS J151106.1+053849.9	$0.082^{+0.012}_{-0.014}$	0.089 ± 0.017	$0.080 \pm 9.6e-06$	-0.092 ± 0.024	2.370 ± 0.383	0.048	21 ± 5	17 ± 4	32 ± 6	22 ± 5	1
XMMXCS J151107.0+055124.2	$0.076^{+0.010}_{-0.010}$	0.081 ± 0.021	$0.074 \pm 7.9e-06$	-0.025 ± 0.015	1.290 ± 0.250	0.038	12 ± 4	14 ± 4	12 ± 4	18 ± 4	1
XMMXCS J151108.6+054042.7	$0.080^{+0.011}_{-0.011}$	0.089 ± 0.017	$0.083 \pm 1.0e-05$	-0.015 ± 0.017	1.130 ± 0.283	0.043	20 ± 5	17 ± 4	32 ± 6	27 ± 5	1
XMMXCS J151111.5+054736.8	$0.077^{+0.010}_{-0.010}$	0.109 ± 0.021	$0.078 \pm 9.4e-06$	-0.036 ± 0.013	1.480 ± 0.229	0.036	20 ± 5	19 ± 4	29 ± 6	26 ± 5	1
XMMXCS J151118.6+055138.9	$0.076^{+0.006}_{-0.006}$	0.081 ± 0.021	$0.075 \pm 9.5e-06$	-0.022 ± 0.013	1.250 ± 0.213	0.036	11 ± 4	10 ± 3	11 ± 4	9 ± 3	1
XMMXCS J151119.5+055140.8	$0.076^{+0.005}_{-0.006}$	0.081 ± 0.021	$0.075 \pm 9.5e-06$	-0.027 ± 0.014	1.330 ± 0.221	0.035	11 ± 4	10 ± 3	11 ± 4	9 ± 3	1
XMMXCS J151119.6+053917.4	$0.085^{+0.014}_{-0.022}$	0.080 ± 0.026	$0.084 \pm 1.3e-05$	-0.134 ± 0.053	3.050 ± 0.877	0.067	12 ± 4	10 ± 3	12 ± 4	12 ± 4	1
XMMXCS J151119.8+054415.3	$0.075^{+0.038}_{-0.039}$	0.056 ± 0.016	$0.076 \pm 9.7e-06$	-0.016 ± 0.009	1.140 ± 0.151	0.017	13 ± 4	15 ± 4	16 ± 4	20 ± 5	1
XMMXCS J151120.1+054411.3	$0.077^{+0.015}_{-0.015}$	0.056 ± 0.016	$0.078 \pm 1.3e-05$	0.031 ± 0.020	0.329 ± 0.341	0.038	14 ± 4	17 ± 4	19 ± 5	22 ± 5	1
XMMXCS J151120.2+053920.1	$0.085^{+0.014}_{-0.022}$	0.080 ± 0.026	$0.084 \pm 1.3e-05$	-0.134 ± 0.053	3.050 ± 0.877	0.067	12 ± 4	11 ± 4	12 ± 4	9 ± 3	1
XMMXCS J151120.7+054425.5	$0.077^{+0.016}_{-0.016}$	0.056 ± 0.016	$0.078 \pm 1.3e-05$	0.024 ± 0.018	0.452 ± 0.312	0.038	15 ± 4	18 ± 4	20 ± 5	22 ± 5	1
XMMXCS J151424.8+363708.5	$0.374^{+0.084}_{-0.082}$	0.252 ± 0.046	$0.372 \pm 4.1e-05$	0.043 ± 0.006	-0.220 ± 0.112	0.001	11 ± 4	13 ± 5	9 ± 4	14 ± 5	1
XMMXCS J151618.6+000531.3	$0.117^{+0.022}_{-0.021}$	0.129 ± 0.022	$0.118 \pm 1.3e-05$	-0.012 ± 0.004	1.210 ± 0.063	0.001	24 ± 5	24 ± 5	26 ± 5	26 ± 5	1
XMMXCS J151624.6-004953.5	$0.377^{+0.069}_{-0.070}$	0.366 ± 0.054	$0.376 \pm 8.7e-05$	-0.011 ± 0.017	0.782 ± 0.334	0.069	6 ± 4	10 ± 4	9 ± 3	12 ± 4	1
XMMXCS J151627.3-005546.8	$0.119^{+0.019}_{-0.019}$	0.130 ± 0.022	$0.119 \pm 1.8e-05$	-0.034 ± 0.047	1.520 ± 0.822	0.071	11 ± 4	11 ± 3	12 ± 4	10 ± 3	1

Continued on next page

Table A.2 – continued from previous page

name	z_{RS}	z_{BCG}	z_{spec-g}	cmr_{grad}	cmr_{inter}	cmr_{wid}	n_{gals-c}	n_{gals-l}	n_{200-c}	n_{200-l}	qual
XMMXCS J151643.8+065704.7	$0.034^{+0.031}_{-0.032}$	0.019 ± 0.027	$0.032 \pm 8.2e-06$	-0.017 ± 0.008	1.080 ± 0.116	0.045	8 ± 3	6 ± 3	8 ± 3	6 ± 3	1
XMMXCS J151644.4-005822.7	$0.118^{+0.037}_{-0.038}$	0.138 ± 0.025	$0.123 \pm 1.8e-05$	-0.018 ± 0.006	1.320 ± 0.091	0.015	19 ± 4	19 ± 5	31 ± 6	32 ± 6	1
XMMXCS J151645.6-010231.4	$0.119^{+0.022}_{-0.022}$	0.130 ± 0.023	$0.118 \pm 1.6e-05$	-0.030 ± 0.022	1.500 ± 0.398	0.065	21 ± 5	24 ± 5	26 ± 5	34 ± 6	1
XMMXCS J151650.3-005211.3	$0.118^{+0.029}_{-0.029}$	0.120 ± 0.025	$0.120 \pm 1.4e-05$	-0.053 ± 0.011	1.920 ± 0.204	0.021	15 ± 4	14 ± 4	18 ± 4	17 ± 4	1
XMMXCS J151651.5-005655.3	$0.120^{+0.034}_{-0.034}$	0.138 ± 0.025	$0.121 \pm 1.4e-05$	-0.020 ± 0.007	1.330 ± 0.117	0.043	17 ± 4	19 ± 5	22 ± 5	27 ± 5	1
XMMXCS J151658.1-010635.9	$0.099^{+0.032}_{-0.032}$	0.130 ± 0.022	$0.116 \pm 1.5e-05$	-0.020 ± 0.023	1.290 ± 0.395	0.066	9 ± 3	9 ± 3	8 ± 3	8 ± 3	1
XMMXCS J151700.4-005433.3	$0.119^{+0.034}_{-0.035}$	0.120 ± 0.025	$0.120 \pm 1.4e-05$	-0.017 ± 0.012	1.280 ± 0.199	0.077	16 ± 4	14 ± 4	22 ± 5	19 ± 5	1
XMMXCS J151707.7-004936.3	$0.108^{+0.030}_{-0.030}$	0.128 ± 0.021	$0.128 \pm 1.7e-05$	-0.063 ± 0.036	2.040 ± 0.630	0.047	9 ± 3	10 ± 3	5 ± 2	5 ± 2	1
XMMXCS J151822.9+062023.3	$0.101^{+0.033}_{-0.033}$	0.116 ± 0.020	$0.101 \pm 1.3e-05$	-0.037 ± 0.006	1.560 ± 0.092	0.009	10 ± 3	14 ± 4	9 ± 3	18 ± 4	1
XMMXCS J151831.9+062409.3	$0.103^{+0.036}_{-0.036}$	0.116 ± 0.019	$0.104 \pm 1.6e-05$	-0.031 ± 0.011	1.460 ± 0.183	0.035	8 ± 3	8 ± 3	6 ± 3	6 ± 3	1
XMMXCS J152125.5+074342.1	$0.044^{+0.005}_{-0.005}$	0.079 ± 0.018	$0.045 \pm 6.9e-06$	-0.036 ± 0.008	1.390 ± 0.126	0.040	8 ± 3	5 ± 2	8 ± 3	5 ± 2	1
XMMXCS J152151.1+074218.1	$0.045^{+0.004}_{-0.004}$	0.071 ± 0.018	$0.046 \pm 7.1e-06$	-0.014 ± 0.006	1.080 ± 0.084	0.020	13 ± 4	11 ± 3	12 ± 4	11 ± 3	1
XMMXCS J152206.6+074129.2	$0.043^{+0.034}_{-0.034}$	0.071 ± 0.018	$0.045 \pm 8.3e-06$	0.005 ± 0.009	0.769 ± 0.132	0.064	11 ± 4	9 ± 3	11 ± 4	10 ± 3	1
XMMXCS J152214.0+274939.5	$0.075^{+0.008}_{-0.008}$	0.085 ± 0.017	$0.076 \pm 9.1e-06$	-0.013 ± 0.031	1.060 ± 0.512	0.070	23 ± 5	22 ± 5	41 ± 7	35 ± 6	1
XMMXCS J152219.4+274013.6	$0.073^{+0.017}_{-0.016}$	0.098 ± 0.032	$0.069 \pm 1.7e-05$	-0.027 ± 0.007	1.310 ± 0.109	0.037	45 ± 7	47 ± 7	66 ± 9	68 ± 8	1
XMMXCS J152221.0+274117.6	$0.078^{+0.020}_{-0.020}$	0.080 ± 0.024	$0.067 \pm 2.5e-05$	0.064 ± 0.039	-0.226 ± 0.668	0.037	34 ± 6	33 ± 6	50 ± 8	47 ± 7	1
XMMXCS J152225.7+274337.3	$0.075^{+0.018}_{-0.018}$	0.098 ± 0.032	$0.069 \pm 1.7e-05$	-0.028 ± 0.005	1.330 ± 0.074	0.035	52 ± 7	52 ± 7	68 ± 9	70 ± 9	1
XMMXCS J152254.0+274004.6	$0.073^{+0.007}_{-0.006}$	0.082 ± 0.018	$0.073 \pm 1.2e-05$	-0.048 ± 0.016	1.660 ± 0.262	0.065	33 ± 6	31 ± 6	57 ± 8	55 ± 8	1
XMMXCS J152302.2+274151.1	$0.070^{+0.003}_{-0.004}$	0.072 ± 0.015	$0.070 \pm 1.1e-05$	-0.089 ± 0.041	2.320 ± 0.659	0.028	7 ± 3	6 ± 3	6 ± 2	4 ± 2	1

Continued on next page

Table A.2 – continued from previous page

name	z_{RS}	z_{BCG}	z_{spec-g}	cmr_{grad}	cmr_{inter}	cmr_{wid}	n_{gals-c}	n_{gals-l}	n_{200-c}	n_{200-l}	qual
XMMXCS J152312.6+084201.2	$0.219^{+0.048}_{-0.048}$	0.211 ± 0.035	-	-0.051 ± 0.049	2.260 ± 0.882	0.074	10 ± 3	9 ± 3	9 ± 3	7 ± 3	1
XMMXCS J153148.2+044314.4	$0.446^{+0.078}_{-0.074}$	0.399 ± 0.066	$0.442 \pm 2.3e-04$	-0.148 ± 0.035	4.410 ± 0.678	0.001	9 ± 4	17 ± 5	11 ± 4	26 ± 6	1
XMMXCS J153253.9+302058.0	$0.349^{+0.096}_{-0.097}$	0.361 ± 0.057	$0.358 \pm 7.9e-05$	-0.051 ± 0.084	2.670 ± 1.710	0.066	14 ± 4	18 ± 5	16 ± 4	24 ± 5	1
XMMXCS J153422.5+554341.5	$0.426^{+0.058}_{-0.057}$	0.408 ± 0.062	$0.425 \pm 1.4e-04$	-0.038 ± 0.022	1.410 ± 0.442	0.031	13 ± 4	13 ± 4	16 ± 5	16 ± 5	1
XMMXCS J153503.2+012034.6	$0.321^{+0.068}_{-0.069}$	0.306 ± 0.048	$0.317 \pm 3.5e-05$	0.109 ± 0.109	-0.461 ± 2.050	0.143	23 ± 5	3 ± 3	27 ± 6	2 ± 2	1
XMMXCS J153644.2+543736.3	$0.388^{+0.095}_{-0.092}$	0.378 ± 0.059	$0.383 \pm 1.3e-04$	-0.006 ± 0.043	0.740 ± 0.832	0.040	17 ± 5	0 ± 3	20 ± 5	-	1
XMMXCS J153648.2+543718.7	$0.389^{+0.090}_{-0.087}$	0.378 ± 0.059	$0.383 \pm 1.3e-04$	-0.013 ± 0.040	0.865 ± 0.775	0.030	16 ± 5	12 ± 4	17 ± 5	12 ± 4	1
XMMXCS J154405.8+534708.3	$0.499^{+0.094}_{-0.092}$	0.508 ± 0.074	$0.497 \pm 1.2e-04$	-0.013 ± 0.041	1.150 ± 0.791	0.112	11 ± 4	19 ± 5	9 ± 4	17 ± 5	1
XMMXCS J155812.7+270837.1	$0.089^{+0.013}_{-0.013}$	0.090 ± 0.017	$0.091 \pm 1.4e-05$	-0.035 ± 0.022	1.520 ± 0.381	0.030	27 ± 5	26 ± 5	46 ± 7	44 ± 7	1
XMMXCS J155813.9+271506.4	$0.097^{+0.033}_{-0.033}$	0.115 ± 0.019	$0.091 \pm 1.6e-05$	-0.018 ± 0.011	1.300 ± 0.188	0.014	41 ± 7	42 ± 7	81 ± 9	80 ± 9	1
XMMXCS J155819.4+271403.3	$0.088^{+0.018}_{-0.019}$	0.115 ± 0.019	$0.091 \pm 1.6e-05$	0.005 ± 0.011	0.927 ± 0.168	0.044	34 ± 6	34 ± 6	62 ± 8	56 ± 8	1
XMMXCS J155852.1+272405.3	$0.090^{+0.004}_{-0.003}$	0.116 ± 0.048	$0.089 \pm 1.7e-05$	0.025 ± 0.001	0.407 ± 0.001	0.500	8 ± 4	6 ± 3	6 ± 3	4 ± 2	1
XMMXCS J155914.7+350923.4	$0.490^{+0.082}_{-0.081}$	0.468 ± 0.071	$0.490 \pm 1.2e-04$	-0.026 ± 0.049	1.290 ± 0.994	0.096	8 ± 4	6 ± 4	6 ± 3	6 ± 3	1
XMMXCS J160214.4+155808.0	$0.036^{+0.009}_{-0.008}$	0.052 ± 0.014	$0.038 \pm 7.9e-06$	-0.002 ± 0.007	0.836 ± 0.108	0.024	10 ± 4	6 ± 3	10 ± 4	3 ± 2	1
XMMXCS J160515.7+325341.6	$0.153^{+0.085}_{-0.081}$	0.172 ± 0.026	$0.084 \pm 2.3e-05$	0.037 ± 0.022	0.605 ± 0.411	0.067	4 ± 2	4 ± 2	5 ± 2	6 ± 3	1
XMMXCS J160527.2+174859.3	$0.034^{+0.002}_{-0.002}$	0.076 ± 0.036	$0.034 \pm 7.8e-06$	0.008 ± 0.029	0.677 ± 0.399	0.043	12 ± 4	5 ± 2	13 ± 4	2 ± 2	1
XMMXCS J160540.0+324438.1	$0.130^{+0.006}_{-0.005}$	0.115 ± 0.025	$0.129 \pm 1.0e-05$	0.101 ± 0.012	-0.726 ± 0.203	0.042	4 ± 2	4 ± 2	4 ± 2	7 ± 3	1
XMMXCS J160927.0+264450.0	$0.477^{+0.142}_{-0.141}$	0.446 ± 0.065	$0.471 \pm 1.4e-04$	0.179 ± 0.060	-2.760 ± 1.200	0.082	6 ± 3	7 ± 4	4 ± 2	6 ± 3	1
XMMXCS J161040.2+540613.2	$0.327^{+0.074}_{-0.076}$	0.348 ± 0.059	-	-0.044 ± 0.036	2.500 ± 0.698	0.001	15 ± 4	14 ± 4	17 ± 5	16 ± 5	1

Continued on next page

Table A.2 – continued from previous page

name	z_{RS}	z_{BCG}	z_{spec-g}	cmr_{grad}	cmr_{inter}	cmr_{wid}	n_{gals-c}	n_{gals-l}	n_{200-c}	n_{200-l}	qual
XMMXCS J161554.1+121928.9	$0.369^{+0.056}_{-0.058}$	0.376 ± 0.060	$0.370 \pm 6.2e-05$	-0.082 ± 0.081	3.380 ± 1.570	0.001	18 ± 5	16 ± 4	25 ± 5	21 ± 5	1
XMMXCS J162335.1+263417.6	$0.407^{+0.073}_{-0.073}$	0.433 ± 0.064	$0.434 \pm 7.2e-05$	0.015 ± 0.088	1.430 ± 1.720	0.133	37 ± 7	31 ± 6	68 ± 9	58 ± 9	1
XMMXCS J162700.2+552825.4	$0.137^{+0.037}_{-0.037}$	0.151 ± 0.025	-	-0.026 ± 0.008	1.510 ± 0.145	0.060	24 ± 5	24 ± 5	31 ± 6	33 ± 6	1
XMMXCS J162736.2+394022.7	$0.515^{+0.096}_{-0.093}$	0.505 ± 0.077	$0.507 \pm 6.0e-05$	-0.020 ± 0.055	1.330 ± 1.080	0.089	11 ± 4	15 ± 5	9 ± 4	22 ± 5	1
XMMXCS J162822.9+393849.2	$0.513^{+0.120}_{-0.118}$	0.578 ± 0.117	$0.508 \pm 8.0e-05$	-0.060 ± 0.059	2.020 ± 1.210	0.076	10 ± 4	-	9 ± 4	-	1
XMMXCS J162826.0+393348.9	$0.029^{+0.006}_{-0.006}$	0.091 ± 0.044	$0.029 \pm 6.7e-06$	-0.014 ± 0.009	1.010 ± 0.129	0.035	12 ± 4	5 ± 2	12 ± 4	3 ± 2	1
XMMXCS J162837.08+393253.0	$0.028^{+0.004}_{-0.004}$	0.091 ± 0.044	$0.029 \pm 6.7e-06$	-0.010 ± 0.015	0.960 ± 0.199	0.040	9 ± 3	3 ± 2	8 ± 3	4 ± 2	1
XMMXCS J162837.0+393252.9	$0.028^{+0.004}_{-0.004}$	0.091 ± 0.044	$0.029 \pm 6.7e-06$	-0.010 ± 0.015	0.960 ± 0.199	0.040	9 ± 3	3 ± 2	8 ± 3	4 ± 2	1
XMMXCS J162857.0+393300.7	$0.377^{+0.078}_{-0.078}$	0.357 ± 0.060	-	0.182 ± 0.132	-1.950 ± 2.610	0.053	12 ± 4	11 ± 4	13 ± 4	11 ± 4	1
XMMXCS J163133.4+374903.2	$0.417^{+0.109}_{-0.108}$	0.372 ± 0.056	$0.415 \pm 7.2e-05$	-0.265 ± 0.074	6.910 ± 1.460	0.107	11 ± 4	-	11 ± 4	-	1
XMMXCS J163141.5+340438.5	$0.122^{+0.033}_{-0.033}$	0.119 ± 0.028	$0.123 \pm 2.2e-05$	0.003 ± 0.005	0.933 ± 0.093	0.016	8 ± 3	6 ± 3	6 ± 3	4 ± 2	1
XMMXCS J163305.8+571124.0	$0.241^{+0.060}_{-0.060}$	0.251 ± 0.044	-	-0.049 ± 0.024	2.300 ± 0.423	0.012	6 ± 3	9 ± 3	5 ± 2	6 ± 3	1
XMMXCS J164020.3+464226.2	$0.229^{+0.046}_{-0.045}$	0.243 ± 0.047	$0.229 \pm 3.4e-05$	-0.021 ± 0.013	1.760 ± 0.247	0.070	47 ± 7	43 ± 7	95 ± 10	90 ± 10	1
XMMXCS J164102.2+363742.4	$0.182^{+0.050}_{-0.049}$	0.166 ± 0.035	$0.186 \pm 2.8e-05$	0.034 ± 0.066	0.442 ± 1.200	0.059	3 ± 2	2 ± 2	4 ± 2	3 ± 2	1
XMMXCS J164115.9+385414.0	$0.310^{+0.049}_{-0.049}$	0.318 ± 0.062	$0.311 \pm 3.3e-05$	0.006 ± 0.052	1.480 ± 0.999	0.117	4 ± 3	0 ± 2	3 ± 2	-	1
XMMXCS J165758.3+275109.5	$0.064^{+0.037}_{-0.038}$	0.072 ± 0.025	-	-0.015 ± 0.030	0.937 ± 0.421	0.121	17 ± 4	28 ± 5	20 ± 5	49 ± 7	1
XMMXCS J165944.0+323654.3	$0.100^{+0.015}_{-0.015}$	0.113 ± 0.021	$0.099 \pm 1.5e-05$	-0.024 ± 0.008	1.350 ± 0.128	0.024	12 ± 4	12 ± 4	12 ± 4	12 ± 4	1
XMMXCS J170011.4+323513.4	$0.097^{+0.011}_{-0.011}$	0.109 ± 0.026	$0.097 \pm 1.2e-05$	-0.141 ± 0.048	3.150 ± 0.788	0.118	13 ± 4	9 ± 4	13 ± 4	13 ± 4	1
XMMXCS J170017.8+784036.1	$0.072^{+0.022}_{-0.023}$	0.083 ± 0.017	-	-0.040 ± 0.018	1.460 ± 0.298	0.052	24 ± 5	22 ± 5	55 ± 8	45 ± 7	1

Continued on next page

Table A.2 – continued from previous page

name	z_{RS}	z_{BCG}	z_{spec-g}	cmr_{grad}	cmr_{inter}	cmr_{wid}	n_{gals-c}	n_{gals-l}	n_{200-c}	n_{200-l}	qual
XMMXCS J170041.22+641239.9	$0.235^{+0.058}_{-0.058}$	0.250 ± 0.038	$0.235 \pm 2.8e-05$	-0.027 ± 0.015	1.900 ± 0.264	0.037	16 ± 4	17 ± 4	18 ± 4	16 ± 4	1
XMMXCS J170041.9+641257.9	$0.235^{+0.054}_{-0.055}$	0.250 ± 0.038	$0.235 \pm 2.8e-05$	-0.022 ± 0.014	1.830 ± 0.248	0.031	15 ± 4	12 ± 4	18 ± 4	13 ± 4	1
XMMXCS J170102.3+784148.0	$0.075^{+0.022}_{-0.023}$	0.073 ± 0.033	-	-0.006 ± 0.083	0.873 ± 1.340	0.115	41 ± 7	40 ± 6	84 ± 10	80 ± 9	1
XMMXCS J170112.5+783707.0	$0.073^{+0.019}_{-0.020}$	0.071 ± 0.018	-	-0.040 ± 0.008	1.500 ± 0.126	0.022	30 ± 6	28 ± 5	67 ± 9	61 ± 8	1
XMMXCS J170118.9+641422.9	$0.455^{+0.090}_{-0.089}$	0.459 ± 0.069	$0.452 \pm 1.0e-04$	0.014 ± 0.032	0.450 ± 0.636	0.081	28 ± 6	30 ± 6	39 ± 7	42 ± 8	1
XMMXCS J170257.8+783914.2	$0.078^{+0.025}_{-0.025}$	0.080 ± 0.020	-	-0.027 ± 0.006	1.300 ± 0.104	0.024	61 ± 8	59 ± 8	108 ± 11	121 ± 12	1
XMMXCS J170306.4+783934.1	$0.079^{+0.028}_{-0.028}$	0.080 ± 0.020	-	-0.035 ± 0.007	1.430 ± 0.105	0.021	62 ± 8	61 ± 8	109 ± 11	122 ± 12	1
XMMXCS J170326.6+783906.1	$0.083^{+0.023}_{-0.023}$	0.089 ± 0.022	-	-0.051 ± 0.002	1.670 ± 0.026	0.001	58 ± 8	59 ± 8	114 ± 11	136 ± 12	1
XMMXCS J170353.1+783833.8	$0.080^{+0.029}_{-0.028}$	0.089 ± 0.022	-	-0.016 ± 0.004	1.130 ± 0.057	0.022	56 ± 8	63 ± 8	110 ± 11	137 ± 12	1
XMMXCS J170404.1+783704.4	$0.084^{+0.036}_{-0.036}$	0.089 ± 0.022	-	-0.014 ± 0.003	1.090 ± 0.052	0.021	54 ± 7	60 ± 8	115 ± 11	149 ± 13	1
XMMXCS J170411.8+783822.1	$0.082^{+0.032}_{-0.032}$	0.089 ± 0.022	-	-0.021 ± 0.004	1.210 ± 0.071	0.026	56 ± 8	64 ± 8	118 ± 12	146 ± 12	1
XMMXCS J170419.7+783435.8	$0.103^{+0.041}_{-0.041}$	0.089 ± 0.022	-	-0.025 ± 0.014	1.310 ± 0.246	0.001	50 ± 7	60 ± 8	117 ± 11	170 ± 14	1
XMMXCS J170423.0+783046.3	$0.074^{+0.042}_{-0.042}$	0.092 ± 0.017	-	-0.037 ± 0.011	1.470 ± 0.181	0.067	26 ± 5	23 ± 5	59 ± 8	51 ± 7	1
XMMXCS J170426.5+783903.5	$0.081^{+0.039}_{-0.039}$	0.089 ± 0.022	-	-0.022 ± 0.005	1.220 ± 0.080	0.031	57 ± 8	64 ± 8	118 ± 12	146 ± 12	1
XMMXCS J170431.6+783729.0	$0.083^{+0.035}_{-0.036}$	0.089 ± 0.022	-	-0.024 ± 0.005	1.260 ± 0.075	0.035	53 ± 7	61 ± 8	116 ± 11	150 ± 13	1
XMMXCS J170438.4+783710.3	$0.082^{+0.029}_{-0.029}$	0.089 ± 0.022	-	-0.017 ± 0.004	1.140 ± 0.064	0.033	54 ± 7	61 ± 8	115 ± 11	147 ± 12	1
XMMXCS J170745.2+783936.1	$0.082^{+0.024}_{-0.025}$	0.078 ± 0.015	-	-0.019 ± 0.019	1.170 ± 0.303	0.037	17 ± 4	21 ± 5	23 ± 5	38 ± 6	1
XMMXCS J171215.4+640209.7	$0.081^{+0.011}_{-0.011}$	0.093 ± 0.017	$0.083 \pm 9.2e-06$	-0.018 ± 0.012	1.210 ± 0.202	0.050	24 ± 5	21 ± 5	41 ± 7	35 ± 6	1
XMMXCS J171415.02+434100.7	$0.086^{+0.039}_{-0.039}$	0.090 ± 0.082	-	-0.005 ± 0.012	0.941 ± 0.161	0.068	10 ± 3	13 ± 4	11 ± 3	14 ± 4	1

Continued on next page

Table A.2 – continued from previous page

name	z_{RS}	z_{BCG}	z_{spec-g}	cmr_{grad}	cmr_{inter}	cmr_{wid}	n_{gals-c}	n_{gals-l}	n_{200-c}	n_{200-l}	qual
XMMXCS J171415.0+434100.8	$0.086^{+0.039}_{-0.039}$	0.090 ± 0.082	-	-0.005 ± 0.012	0.941 ± 0.161	0.068	10 ± 3	13 ± 4	11 ± 3	14 ± 4	1
XMMXCS J171424.9+624708.6	$0.177^{+0.031}_{-0.031}$	0.200 ± 0.030	$0.176 \pm 2.9e-05$	-0.054 ± 0.006	2.100 ± 0.108	0.015	9 ± 3	11 ± 4	8 ± 3	11 ± 4	1
XMMXCS J171437.9+623322.2	$0.176^{+0.029}_{-0.029}$	0.173 ± 0.029	$0.177 \pm 4.5e-05$	-0.012 ± 0.022	1.400 ± 0.393	0.063	6 ± 3	4 ± 2	4 ± 2	4 ± 2	1
XMMXCS J171945.4+262618.6	$0.172^{+0.032}_{-0.032}$	0.185 ± 0.028	$0.175 \pm 2.3e-05$	-0.030 ± 0.043	1.650 ± 0.772	0.097	12 ± 4	11 ± 4	12 ± 4	10 ± 4	1
XMMXCS J172010.0+263724.7	$0.160^{+0.035}_{-0.035}$	0.190 ± 0.088	$0.161 \pm 2.0e-05$	0.026 ± 0.009	0.644 ± 0.152	0.063	20 ± 5	18 ± 5	23 ± 5	21 ± 5	1
XMMXCS J172012.1+263423.1	$0.164^{+0.037}_{-0.037}$	0.170 ± 0.025	$0.162 \pm 2.7e-05$	-0.051 ± 0.020	2.050 ± 0.351	0.062	10 ± 3	11 ± 4	7 ± 3	9 ± 3	1
XMMXCS J172014.4+584529.1	$0.587^{+0.148}_{-0.148}$	0.592 ± 0.108	-	0.380 ± 0.046	-6.440 ± 0.901	0.001	5 ± 2	23 ± 5	4 ± 2	27 ± 6	1
XMMXCS J172016.7+584502.9	$0.587^{+0.148}_{-0.148}$	0.592 ± 0.108	-	0.380 ± 0.046	-6.440 ± 0.901	0.001	5 ± 2	23 ± 5	3 ± 2	19 ± 5	1
XMMXCS J172211.4+320642.5	$0.230^{+0.054}_{-0.054}$	0.232 ± 0.041	$0.228 \pm 2.2e-05$	0.002 ± 0.020	1.350 ± 0.374	0.078	36 ± 6	33 ± 6	76 ± 9	66 ± 9	1
XMMXCS J172226.8+320754.3	$0.223^{+0.048}_{-0.048}$	0.227 ± 0.043	$0.225 \pm 2.7e-05$	-0.013 ± 0.011	1.640 ± 0.205	0.001	34 ± 6	33 ± 6	68 ± 9	64 ± 8	1
XMMXCS J172256.7+321928.8	$0.244^{+0.095}_{-0.097}$	0.235 ± 0.058	-	0.066 ± 0.041	0.042 ± 0.776	0.001	6 ± 3	7 ± 3	5 ± 2	7 ± 3	1
XMMXCS J172335.9+341154.5	$0.443^{+0.059}_{-0.058}$	0.413 ± 0.070	$0.443 \pm 6.2e-05$	0.063 ± 0.059	0.581 ± 1.110	0.012	7 ± 3	9 ± 4	5 ± 3	7 ± 3	1
XMMXCS J173302.32+434542.3	$0.075^{+0.042}_{-0.043}$	0.062 ± 0.023	-	-0.012 ± 0.009	0.975 ± 0.146	0.058	11 ± 3	22 ± 5	11 ± 3	35 ± 6	1
XMMXCS J173302.4+434540.7	$0.075^{+0.042}_{-0.043}$	0.062 ± 0.023	-	-0.012 ± 0.009	0.975 ± 0.146	0.058	13 ± 4	27 ± 5	13 ± 4	36 ± 6	1
XMMXCS J174328.5+634154.9	$0.334^{+0.076}_{-0.077}$	0.344 ± 0.053	-	-0.033 ± 0.024	2.300 ± 0.452	0.063	28 ± 6	27 ± 6	38 ± 7	35 ± 7	1
XMMXCS J200759.0-110256.5	$0.292^{+0.068}_{-0.069}$	0.282 ± 0.056	-	-0.030 ± 0.023	2.130 ± 0.437	0.001	6 ± 3	8 ± 3	5 ± 2	7 ± 3	1
XMMXCS J205405.9-154736.5	$0.223^{+0.056}_{-0.056}$	0.233 ± 0.052	-	-0.047 ± 0.027	2.220 ± 0.507	0.078	13 ± 4	14 ± 4	13 ± 4	18 ± 5	1
XMMXCS J210104.3+103928.2	$0.544^{+0.474}_{-0.474}$	0.551 ± 0.102	-	0.785 ± 0.047	-14.90 ± 0.973	0.500	7 ± 4	23 ± 6	4 ± 3	40 ± 8	1
XMMXCS J210109.0+103855.3	$0.487^{+0.161}_{-0.172}$	0.501 ± 0.094	-	-0.154 ± 0.041	3.860 ± 0.808	0.001	7 ± 3	7 ± 4	4 ± 3	5 ± 3	1

Continued on next page

Table A.2 – continued from previous page

name	z_{RS}	z_{BCG}	z_{spec-g}	cmr_{grad}	cmr_{inter}	cmr_{wid}	n_{gals-c}	n_{gals-l}	n_{200-c}	n_{200-l}	qual
XMMXCS J211429.3+061513.6	$0.205^{+0.034}_{-0.034}$	0.190 ± 0.029	$0.205 \pm 2.9e-05$	-0.086 ± 0.029	2.840 ± 0.539	0.061	3 ± 2	5 ± 3	3 ± 2	3 ± 2	1
XMMXCS J212242.0+165120.1	$0.510^{+0.126}_{-0.124}$	0.518 ± 0.184	-	0.198 ± 0.071	-3.220 ± 1.470	0.077	5 ± 3	5 ± 3	3 ± 2	4 ± 3	1
XMMXCS J212939.4+000813.1	$0.235^{+0.049}_{-0.049}$	0.238 ± 0.051	$0.235 \pm 3.5e-05$	-0.019 ± 0.012	1.710 ± 0.218	0.050	13 ± 4	14 ± 4	14 ± 4	18 ± 5	1
XMMXCS J212939.7+000516.9	$0.235^{+0.039}_{-0.039}$	0.238 ± 0.051	$0.235 \pm 3.5e-05$	-0.012 ± 0.010	1.610 ± 0.169	0.001	23 ± 5	24 ± 5	27 ± 5	28 ± 6	1
XMMXCS J213026.9-000032.0	$0.136^{+0.019}_{-0.019}$	0.145 ± 0.022	$0.135 \pm 1.6e-05$	-0.024 ± 0.007	1.470 ± 0.120	0.041	9 ± 3	13 ± 4	8 ± 3	14 ± 4	1
XMMXCS J213038.0+045521.0	$0.642^{+0.118}_{-0.117}$	0.658 ± 0.111	$0.640 \pm 1.7e-04$	0.037 ± 0.100	0.438 ± 2.020	0.001	6 ± 3	12 ± 4	5 ± 2	12 ± 4	1
XMMXCS J214605.0+042309.1	$0.531^{+0.108}_{-0.108}$	0.552 ± 0.159	$0.524 \pm 9.2e-05$	0.089 ± 0.074	-0.752 ± 1.440	0.062	14 ± 4	21 ± 5	14 ± 4	20 ± 6	1
XMMXCS J215343.1+172915.1	$0.226^{+0.049}_{-0.052}$	0.269 ± 0.086	$0.229 \pm 5.3e-05$	0.044 ± 0.021	0.596 ± 0.380	0.014	4 ± 2	6 ± 3	4 ± 2	4 ± 2	1
XMMXCS J215439.0-091513.5	$0.075^{+0.014}_{-0.014}$	0.101 ± 0.020	$0.072 \pm 1.4e-05$	-0.060 ± 0.022	1.820 ± 0.342	0.092	3 ± 2	2 ± 2	3 ± 2	1 ± 1	1
XMMXCS J215651.3-074558.5	$0.059^{+0.004}_{-0.004}$	0.082 ± 0.024	$0.061 \pm 9.1e-06$	-0.163 ± 0.030	3.350 ± 0.458	0.062	14 ± 4	9 ± 3	17 ± 4	6 ± 3	1
XMMXCS J215659.9-074901.4	$0.061^{+0.010}_{-0.011}$	0.070 ± 0.017	$0.061 \pm 7.4e-06$	-0.033 ± 0.012	1.370 ± 0.189	0.036	20 ± 5	21 ± 5	24 ± 5	25 ± 5	1
XMMXCS J215714.0-075038.6	$0.058^{+0.003}_{-0.003}$	0.070 ± 0.017	$0.059 \pm 9.0e-06$	-0.011 ± 0.005	0.997 ± 0.084	0.028	20 ± 5	19 ± 4	30 ± 6	26 ± 5	1
XMMXCS J215729.1-074800.3	$0.058^{+0.006}_{-0.005}$	0.074 ± 0.028	$0.058 \pm 8.7e-06$	-0.004 ± 0.007	0.924 ± 0.105	0.027	21 ± 5	19 ± 4	27 ± 5	21 ± 5	1
XMMXCS J215740.4-074627.5	$0.058^{+0.006}_{-0.006}$	0.074 ± 0.028	$0.057 \pm 1.0e-05$	-0.025 ± 0.013	1.240 ± 0.187	0.051	17 ± 4	14 ± 4	24 ± 5	18 ± 4	1
XMMXCS J220059.13+012544.0	$0.235^{+0.054}_{-0.054}$	0.222 ± 0.041	$0.253 \pm 2.6e-05$	0.020 ± 0.031	1.000 ± 0.568	0.111	6 ± 3	6 ± 3	3 ± 2	2 ± 2	1
XMMXCS J220621.9-002540.0	$0.323^{+0.078}_{-0.079}$	0.336 ± 0.050	$0.387 \pm 7.7e-05$	-0.046 ± 0.035	2.540 ± 0.674	0.001	10 ± 4	23 ± 5	8 ± 3	6 ± 4	1
XMMXCS J220625.01+013913.6	$0.281^{+0.060}_{-0.061}$	0.275 ± 0.043	$0.282 \pm 3.7e-05$	-0.029 ± 0.029	2.050 ± 0.542	0.001	8 ± 3	8 ± 3	8 ± 3	7 ± 3	1
XMMXCS J220740.3+101814.4	$0.492^{+0.083}_{-0.083}$	0.501 ± 0.073	$0.492 \pm 7.9e-05$	-0.043 ± 0.025	1.670 ± 0.499	0.018	8 ± 4	14 ± 4	10 ± 4	13 ± 4	1
XMMXCS J221449.28+004706.7	$0.318^{+0.072}_{-0.072}$	0.186 ± 0.088	$0.318 \pm 1.3e-04$	0.067 ± 0.060	0.097 ± 1.170	0.139	5 ± 3	6 ± 4	4 ± 2	4 ± 3	1

Continued on next page

Table A.2 – continued from previous page

name	z_{RS}	z_{BCG}	z_{spec-g}	cmr_{grad}	cmr_{inter}	cmr_{wid}	n_{gals-c}	n_{gals-l}	n_{200-c}	n_{200-l}	qual
XMMXCS J221508.14+003513.5	$0.354^{+0.093}_{-0.092}$	0.328 ± 0.051	$0.351 \pm 5.3e-05$	-0.013 ± 0.032	0.832 ± 0.616	0.032	9 ± 4	9 ± 4	10 ± 4	10 ± 4	1
XMMXCS J221608.82+001105.9	$0.107^{+0.019}_{-0.020}$	0.103 ± 0.019	$0.108 \pm 1.3e-05$	-0.043 ± 0.040	1.610 ± 0.639	0.093	4 ± 2	3 ± 2	3 ± 2	2 ± 2	1
XMMXCS J221743.7+141221.6	$0.254^{+0.110}_{-0.111}$	0.234 ± 0.080	$0.241 \pm 2.7e-05$	-0.037 ± 0.040	1.920 ± 0.770	0.098	6 ± 3	4 ± 3	4 ± 2	4 ± 2	1
XMMXCS J222314.6-013937.7	$0.295^{+0.065}_{-0.065}$	0.300 ± 0.044	$0.296 \pm 5.6e-05$	-0.026 ± 0.027	2.020 ± 0.531	0.081	17 ± 5	3 ± 3	19 ± 5	25 ± 5	1
XMMXCS J222353.1-013711.0	$0.102^{+0.023}_{-0.024}$	0.107 ± 0.019	-	-0.014 ± 0.006	1.180 ± 0.105	0.048	33 ± 6	37 ± 6	53 ± 8	66 ± 8	1
XMMXCS J222414.5-013105.6	$0.104^{+0.022}_{-0.023}$	0.121 ± 0.027	-	-0.027 ± 0.009	1.400 ± 0.146	0.036	22 ± 5	22 ± 5	36 ± 6	41 ± 6	1
XMMXCS J222811.2+203456.0	$0.311^{+0.065}_{-0.066}$	0.325 ± 0.052	$0.311 \pm 3.7e-05$	-0.017 ± 0.031	1.960 ± 0.603	0.044	20 ± 5	18 ± 5	27 ± 6	26 ± 6	1
XMMXCS J222818.7-050752.8	$0.203^{+0.050}_{-0.051}$	0.192 ± 0.030	-	0.036 ± 0.021	0.686 ± 0.347	0.103	5 ± 3	3 ± 3	3 ± 2	2 ± 2	1
XMMXCS J222854.7+203919.9	$0.415^{+0.081}_{-0.079}$	0.377 ± 0.060	$0.411 \pm 5.2e-05$	-0.004 ± 0.044	0.721 ± 0.840	0.001	17 ± 5	17 ± 5	22 ± 6	22 ± 6	1
XMMXCS J223924.4-054717.9	$0.241^{+0.055}_{-0.055}$	0.250 ± 0.042	-	-0.013 ± 0.028	1.660 ± 0.531	0.086	17 ± 4	18 ± 5	18 ± 5	21 ± 5	1
XMMXCS J223939.3-054327.4	$0.256^{+0.058}_{-0.058}$	0.247 ± 0.037	-	-0.012 ± 0.016	1.660 ± 0.309	0.040	22 ± 5	20 ± 5	26 ± 5	23 ± 5	1
XMMXCS J224040.0+081020.6	$0.146^{+0.056}_{-0.057}$	0.166 ± 0.030	-	0.030 ± 0.022	0.523 ± 0.399	0.087	9 ± 3	13 ± 4	8 ± 3	12 ± 4	1
XMMXCS J224113.5+032832.5	$0.149^{+0.024}_{-0.024}$	0.171 ± 0.034	$0.162 \pm 1.4e-05$	-0.046 ± 0.017	1.930 ± 0.277	0.500	5 ± 3	6 ± 3	6 ± 3	7 ± 3	1
XMMXCS J224321.44-093550.5	$0.442^{+0.095}_{-0.094}$	0.436 ± 0.067	-	0.0004 ± 0.028	0.730 ± 0.573	0.073	67 ± 9	64 ± 8	169 ± 15	157 ± 14	1
XMMXCS J224413.00-093427.9	$0.448^{+0.076}_{-0.075}$	0.464 ± 0.085	$0.447 \pm 9.6e-05$	0.066 ± 0.038	-0.543 ± 0.749	0.069	18 ± 5	19 ± 5	26 ± 6	27 ± 6	1
XMMXCS J230803.9-021343.5	$0.300^{+0.053}_{-0.053}$	0.289 ± 0.043	$0.301 \pm 3.5e-05$	-0.033 ± 0.025	2.150 ± 0.485	0.001	10 ± 4	11 ± 4	9 ± 3	10 ± 4	1
XMMXCS J231333.5+003355.8	$0.369^{+0.065}_{-0.066}$	0.376 ± 0.055	$0.371 \pm 6.8e-05$	-0.029 ± 0.054	2.340 ± 1.050	0.001	19 ± 5	2 ± 3	19 ± 5	8 ± 3	1
XMMXCS J231932.9+081807.9	$0.066^{+0.025}_{-0.027}$	0.065 ± 0.026	-	-0.221 ± 0.001	4.140 ± 0.001	0.500	4 ± 3	11 ± 4	3 ± 2	11 ± 4	1
XMMXCS J232005.3+081129.1	$0.080^{+0.034}_{-0.034}$	0.082 ± 0.039	-	-0.013 ± 0.010	1.010 ± 0.130	0.040	5 ± 2	16 ± 4	5 ± 2	17 ± 4	1

Continued on next page

Table A.2 – continued from previous page

name	z_{RS}	z_{BCG}	z_{spec-g}	cmr_{grad}	cmr_{inter}	cmr_{wid}	n_{gals-c}	n_{gals-l}	n_{200-c}	n_{200-l}	qual
XMMXCS J232029.9+082342.6	$0.352^{+0.083}_{-0.085}$	0.333 ± 0.119	-	-0.003 ± 0.059	1.660 ± 1.090	0.001	9 ± 4	10 ± 4	6 ± 3	9 ± 4	1
XMMXCS J232143.5+195458.3	$0.681^{+0.202}_{-0.210}$	0.668 ± 0.212	-	0.317 ± 0.391	-5.170 ± 7.910	0.154	7 ± 3	31 ± 6	5 ± 2	32 ± 7	1
XMMXCS J232156.0+193807.8	$0.313^{+0.081}_{-0.082}$	0.324 ± 0.073	-	-0.019 ± 0.078	1.950 ± 1.510	0.065	5 ± 3	5 ± 3	5 ± 2	5 ± 3	1
XMMXCS J232221.3+193855.0	$0.184^{+0.045}_{-0.045}$	0.186 ± 0.031	-	-0.035 ± 0.028	1.870 ± 0.523	0.065	4 ± 2	2 ± 2	4 ± 2	2 ± 2	1
XMMXCS J232356.8+164630.5	$0.071^{+0.021}_{-0.021}$	0.079 ± 0.023	-	-0.012 ± 0.005	1.030 ± 0.067	0.026	26 ± 5	31 ± 6	30 ± 6	42 ± 7	1
XMMXCS J232356.8+164625.9	$0.071^{+0.021}_{-0.021}$	0.079 ± 0.023	-	-0.012 ± 0.005	1.030 ± 0.067	0.026	26 ± 5	31 ± 6	31 ± 6	43 ± 7	1
XMMXCS J232411.4+165724.5	$0.254^{+0.081}_{-0.080}$	0.272 ± 0.053	-	0.005 ± 0.037	1.310 ± 0.713	0.079	4 ± 3	5 ± 3	4 ± 2	5 ± 3	1
XMMXCS J232419.9+163905.9	$0.081^{+0.031}_{-0.034}$	0.066 ± 0.023	-	0.034 ± 0.017	0.272 ± 0.278	0.096	9 ± 3	11 ± 3	7 ± 3	11 ± 3	1
XMMXCS J232421.9+164642.3	$0.075^{+0.063}_{-0.070}$	0.069 ± 0.020	-	-0.024 ± 0.006	1.180 ± 0.106	0.073	15 ± 4	18 ± 4	22 ± 5	31 ± 6	1
XMMXCS J232727.6-020441.5	$0.703^{+0.125}_{-0.124}$	0.611 ± 0.115	$0.700 \pm 1.5e-04$	0.009 ± 0.022	0.424 ± 0.410	0.001	18 ± 5	131 ± 12	23 ± 5	214 ± 18	1
XMMXCS J232851.2+145307.7	$0.499^{+0.079}_{-0.079}$	0.492 ± 0.071	$0.499 \pm 1.5e-04$	-0.026 ± 0.020	1.400 ± 0.373	0.001	18 ± 5	0 ± 2	20 ± 5	-	1
XMMXCS J232851.4+145305.7	$0.499^{+0.079}_{-0.079}$	0.492 ± 0.071	$0.499 \pm 1.5e-04$	-0.026 ± 0.020	1.400 ± 0.373	0.001	18 ± 5	0 ± 2	20 ± 5	-	1
XMMXCS J232918.8+052200.5	$0.217^{+0.059}_{-0.059}$	0.204 ± 0.033	$0.217 \pm 3.0e-05$	-0.052 ± 0.030	2.220 ± 0.542	0.050	7 ± 3	9 ± 3	8 ± 3	9 ± 3	1
XMMXCS J232925.9+052624.1	$0.176^{+0.033}_{-0.033}$	0.188 ± 0.034	$0.177 \pm 2.3e-05$	-0.038 ± 0.009	1.800 ± 0.142	0.001	10 ± 3	14 ± 4	8 ± 3	15 ± 4	1
XMMXCS J232926.3+051932.0	$0.219^{+0.070}_{-0.070}$	0.204 ± 0.033	-	-0.036 ± 0.032	1.920 ± 0.582	0.077	10 ± 3	15 ± 4	5 ± 3	11 ± 4	1
XMMXCS J232928.6+052405.4	$0.189^{+0.066}_{-0.067}$	0.188 ± 0.034	$0.177 \pm 2.3e-05$	0.013 ± 0.033	0.978 ± 0.577	0.088	14 ± 4	19 ± 5	18 ± 5	25 ± 6	1
XMMXCS J233219.2+195457.7	$0.235^{+0.083}_{-0.083}$	0.245 ± 0.040	-	-0.031 ± 0.023	1.950 ± 0.415	0.001	7 ± 3	4 ± 3	6 ± 3	4 ± 2	1
XMMXCS J233227.5+195822.1	$0.325^{+0.077}_{-0.078}$	0.345 ± 0.051	-	-0.021 ± 0.058	2.030 ± 1.090	0.001	13 ± 4	10 ± 4	13 ± 4	11 ± 4	1
XMMXCS J233402.6+485108.6	$0.275^{+0.086}_{-0.087}$	0.298 ± 0.097	-	-0.085 ± 0.067	3.200 ± 1.330	0.062	19 ± 5	19 ± 5	28 ± 6	30 ± 6	1

Continued on next page

Table A.2 – continued from previous page

name	z_{RS}	z_{BCG}	z_{spec-g}	cmr_{grad}	cmr_{inter}	cmr_{wid}	n_{gals-c}	n_{gals-l}	n_{200-c}	n_{200-l}	qual
XMMXCS J233625.1+211023.8	$0.071^{+0.020}_{-0.021}$	0.075 ± 0.018	-	0.009 ± 0.015	0.719 ± 0.233	0.058	21 ± 5	28 ± 5	32 ± 6	43 ± 7	1
XMMXCS J233630.1+210837.3	$0.072^{+0.021}_{-0.022}$	0.075 ± 0.018	-	0.009 ± 0.013	0.711 ± 0.205	0.059	20 ± 5	29 ± 6	29 ± 6	47 ± 7	1
XMMXCS J233638.6+210921.4	$0.070^{+0.020}_{-0.020}$	0.075 ± 0.018	-	0.016 ± 0.016	0.585 ± 0.259	0.049	20 ± 5	26 ± 5	29 ± 6	38 ± 6	1
XMMXCS J233732.2+210904.1	$0.186^{+0.062}_{-0.062}$	0.200 ± 0.031	-	-0.006 ± 0.022	1.340 ± 0.387	0.043	8 ± 3	10 ± 3	6 ± 3	10 ± 3	1
XMMXCS J233738.5+001614.0	$0.276^{+0.055}_{-0.055}$	0.304 ± 0.048	$0.276 \pm 3.3e-05$	-0.035 ± 0.021	2.240 ± 0.391	0.001	34 ± 6	31 ± 6	63 ± 8	52 ± 8	1
XMMXCS J233745.1+270423.4	$0.065^{+0.023}_{-0.024}$	0.050 ± 0.017	-	-0.056 ± 0.022	1.670 ± 0.367	0.054	7 ± 3	4 ± 2	5 ± 2	3 ± 2	1
XMMXCS J233757.0+271121.0	$0.122^{+0.039}_{-0.039}$	0.138 ± 0.025	-	-0.018 ± 0.010	1.290 ± 0.164	0.036	10 ± 3	11 ± 4	10 ± 3	11 ± 4	1
XMMXCS J233826.3+270101.2	$0.066^{+0.022}_{-0.022}$	0.068 ± 0.018	-	-0.030 ± 0.008	1.240 ± 0.104	0.026	30 ± 6	39 ± 7	50 ± 8	100 ± 10	1
XMMXCS J233830.4+270144.5	$0.062^{+0.022}_{-0.023}$	0.068 ± 0.018	-	-0.010 ± 0.003	0.971 ± 0.047	0.011	31 ± 6	37 ± 6	54 ± 8	95 ± 10	1
XMMXCS J233831.2+462106.6	$0.415^{+0.083}_{-0.082}$	0.428 ± 0.062	-	0.062 ± 0.050	-0.512 ± 0.983	0.064	12 ± 4	16 ± 5	12 ± 4	16 ± 5	1
XMMXCS J233837.5+001340.5	$0.277^{+0.055}_{-0.055}$	0.265 ± 0.041	$0.277 \pm 5.7e-05$	0.038 ± 0.053	0.767 ± 1.000	0.096	5 ± 3	7 ± 3	5 ± 2	7 ± 3	1
XMMXCS J233838.8+270040.4	$0.066^{+0.025}_{-0.025}$	0.068 ± 0.018	-	-0.022 ± 0.006	1.130 ± 0.087	0.022	25 ± 5	35 ± 6	48 ± 7	91 ± 10	1
XMMXCS J233858.6+270602.3	$0.059^{+0.022}_{-0.022}$	0.058 ± 0.016	-	0.009 ± 0.004	0.686 ± 0.052	0.017	33 ± 6	40 ± 6	47 ± 8	79 ± 9	1
XMMXCS J233901.2+270007.8	$0.051^{+0.021}_{-0.022}$	0.064 ± 0.035	-	-0.024 ± 0.024	1.160 ± 0.372	0.021	7 ± 3	3 ± 2	5 ± 2	2 ± 2	1
XMMXCS J234341.7+001830.9	$0.265^{+0.070}_{-0.070}$	0.286 ± 0.051	$0.270 \pm 3.3e-05$	-0.059 ± 0.018	2.530 ± 0.333	0.015	28 ± 5	31 ± 6	54 ± 8	53 ± 8	1
XMMXCS J234455.3+091146.8	$0.071^{+0.031}_{-0.031}$	0.077 ± 0.018	-	-0.032 ± 0.013	1.340 ± 0.196	0.024	19 ± 4	23 ± 5	23 ± 5	33 ± 6	1
XMMXCS J234517.3+091555.8	$0.079^{+0.031}_{-0.031}$	0.082 ± 0.018	-	-0.048 ± 0.013	1.580 ± 0.197	0.043	9 ± 3	16 ± 4	7 ± 3	20 ± 5	1
XMMXCS J234808.1+004828.6	$0.281^{+0.056}_{-0.056}$	0.279 ± 0.041	$0.279 \pm 5.2e-05$	-0.036 ± 0.039	2.130 ± 0.728	0.065	10 ± 4	19 ± 5	8 ± 3	23 ± 5	1
XMMXCS J235109.4+201540.1	$0.217^{+0.079}_{-0.079}$	0.234 ± 0.051	-	-0.039 ± 0.026	2.000 ± 0.474	0.041	8 ± 3	6 ± 3	8 ± 3	6 ± 3	1

Continued on next page

Table A.2 – continued from previous page

name	z_{RS}	z_{BCG}	z_{spec-g}	cmr_{grad}	cmr_{inter}	cmr_{wid}	n_{gals-c}	n_{gals-l}	n_{200-c}	n_{200-l}	qual
XMMXCS J235117.1+201352.9	$0.210^{+0.076}_{-0.076}$	0.234 ± 0.051	-	-0.040 ± 0.030	2.020 ± 0.523	0.001	9 ± 3	8 ± 3	7 ± 3	3 ± 2	1
XMMXCS J235124.6+200642.7	$0.085^{+0.049}_{-0.049}$	0.069 ± 0.029	-	0.022 ± 0.021	0.280 ± 0.309	0.109	4 ± 2	11 ± 3	4 ± 2	10 ± 3	1
XMMXCS J235139.4+204233.8	$0.422^{+0.137}_{-0.139}$	0.417 ± 0.124	-	1.580 ± 0.594	-30.20 ± 12.30	0.001	5 ± 3	10 ± 3	3 ± 2	10 ± 3	1
XMMXCS J235149.5+201555.4	$0.488^{+0.153}_{-0.154}$	0.485 ± 0.083	-	0.248 ± 0.192	-3.880 ± 3.780	0.001	5 ± 3	14 ± 4	5 ± 2	13 ± 4	1
XMMXCS J235400.4-102534.3	$0.079^{+0.017}_{-0.017}$	0.077 ± 0.018	$0.070 \pm 1.8e-05$	-0.009 ± 0.013	1.020 ± 0.212	0.061	30 ± 6	31 ± 6	56 ± 8	54 ± 7	1
XMMXCS J235412.7-102503.8	$0.079^{+0.020}_{-0.020}$	0.077 ± 0.018	$0.070 \pm 1.8e-05$	-0.013 ± 0.018	1.110 ± 0.289	0.071	31 ± 6	32 ± 6	55 ± 8	52 ± 7	1
XMMXCS J235414.4-100957.7	$0.062^{+0.059}_{-0.062}$	0.070 ± 0.015	$0.072 \pm 1.1e-05$	-0.013 ± 0.002	1.050 ± 0.039	0.500	11 ± 4	4 ± 2	11 ± 4	2 ± 2	1
XMMXCS J235420.6-101844.7	$0.079^{+0.009}_{-0.010}$	0.073 ± 0.013	$0.073 \pm 1.5e-05$	-0.012 ± 0.028	1.090 ± 0.455	0.026	29 ± 5	25 ± 5	41 ± 7	38 ± 6	1
XMMXCS J235424.0-101606.9	$0.076^{+0.003}_{-0.004}$	0.063 ± 0.028	$0.077 \pm 9.1e-06$	0.088 ± 0.018	-0.568 ± 0.277	0.017	21 ± 5	17 ± 4	28 ± 5	22 ± 5	1
XMMXCS J235529.3+055322.0	$0.276^{+0.077}_{-0.079}$	0.257 ± 0.043	$0.280 \pm 4.2e-05$	0.102 ± 0.094	-0.405 ± 1.750	0.137	14 ± 4	16 ± 5	14 ± 4	17 ± 5	1
XMMXCS J000335.6+020530.2	$0.101^{+0.018}_{-0.017}$	0.132 ± 0.039	-	-0.025 ± 0.012	1.350 ± 0.184	0.067	14 ± 4	17 ± 4	17 ± 4	23 ± 5	2
XMMXCS J000349.6+020750.2	$0.098^{+0.031}_{-0.031}$	0.132 ± 0.039	$0.098 \pm 1.4e-05$	-0.042 ± 0.008	1.690 ± 0.157	0.034	14 ± 4	15 ± 4	16 ± 4	17 ± 4	2
XMMXCS J000612.7+201553.7	$0.310^{+0.060}_{-0.056}$	0.334 ± 0.053	-	0.292 ± 0.276	-4.160 ± 5.380	0.209	2 ± 2	-	1 ± 1	-	2
XMMXCS J001034.5+005644.2	$0.480^{+0.126}_{-0.126}$	0.502 ± 0.096	-	-0.066 ± 0.007	2.150 ± 0.138	0.500	6 ± 4	7 ± 4	1 ± 2	2 ± 3	2
XMMXCS J001541.3+172736.3	$0.254^{+0.068}_{-0.073}$	0.301 ± 0.047	-	-0.018 ± 0.038	1.800 ± 0.719	0.097	8 ± 3	17 ± 4	2 ± 2	8 ± 3	2
XMMXCS J001639.1-010211.5	$0.152^{+0.018}_{-0.018}$	0.166 ± 0.026	$0.152 \pm 1.7e-05$	-0.024 ± 0.002	1.570 ± 0.026	0.001	5 ± 2	5 ± 3	2 ± 2	3 ± 2	2
XMMXCS J001745.6-004247.5	$0.578^{+0.078}_{-0.075}$	0.542 ± 0.087	$0.574 \pm 1.4e-04$	-0.086 ± 0.122	2.740 ± 2.450	0.001	2 ± 2	-	1 ± 1	-	2
XMMXCS J001835.95+163621.9	$0.330^{+0.153}_{-0.140}$	0.315 ± 0.168	-	-0.070 ± 0.084	2.470 ± 1.700	0.001	2 ± 2	2 ± 2	1 ± 1	0 ± 1	2
XMMXCS J001835.9+163621.8	$0.330^{+0.153}_{-0.140}$	0.315 ± 0.168	-	-0.070 ± 0.084	2.470 ± 1.700	0.001	2 ± 2	2 ± 2	1 ± 1	0 ± 1	2

Continued on next page

Table A.2 – continued from previous page

name	z_{RS}	z_{BCG}	z_{spec-g}	cmr_{grad}	cmr_{inter}	cmr_{wid}	n_{gals-c}	n_{gals-l}	n_{200-c}	n_{200-l}	qual
XMMXCS J001908.38+163105.9	$0.315^{+0.071}_{-0.071}$	0.351 ± 0.055	-	0.397 ± 0.002	-6.010 ± 0.040	0.500	6 ± 4	7 ± 4	4 ± 3	4 ± 3	2
XMMXCS J001908.3+163105.8	$0.315^{+0.071}_{-0.071}$	0.351 ± 0.055	-	0.397 ± 0.002	-6.010 ± 0.040	0.500	6 ± 4	7 ± 4	4 ± 3	4 ± 3	2
XMMXCS J002134.1-145544.5	$0.390^{+0.118}_{-0.118}$	0.418 ± 0.085	-	-0.075 ± 0.210	1.800 ± 4.310	0.004	4 ± 3	4 ± 3	1 ± 1	1 ± 2	2
XMMXCS J002139.3-150429.1	$0.546^{+0.129}_{-0.129}$	0.593 ± 0.112	-	-0.068 ± 0.048	2.460 ± 0.973	0.001	10 ± 4	33 ± 6	11 ± 4	50 ± 8	2
XMMXCS J002234.6-151339.7	$0.372^{+0.177}_{-0.186}$	0.335 ± 0.141	-	0.078 ± 0.150	-0.416 ± 3.010	0.001	5 ± 3	-	5 ± 2	-	2
XMMXCS J002615.8+170328.6	$0.217^{+0.108}_{-0.110}$	0.259 ± 0.042	-	-0.134 ± 0.043	3.770 ± 0.837	0.101	2 ± 2	3 ± 2	2 ± 1	1 ± 1	2
XMMXCS J002635.7+103443.5	$0.221^{+0.053}_{-0.054}$	0.224 ± 0.037	-	-0.029 ± 0.017	1.880 ± 0.303	0.052	5 ± 3	7 ± 3	1 ± 1	5 ± 3	2
XMMXCS J002635.8+170930.5	$0.380^{+0.087}_{-0.087}$	0.406 ± 0.062	-	-0.010 ± 0.014	0.839 ± 0.270	0.006	37 ± 7	40 ± 7	56 ± 9	60 ± 9	2
XMMXCS J002656.1+103452.1	$0.221^{+0.056}_{-0.056}$	0.216 ± 0.034	-	-0.053 ± 0.031	2.250 ± 0.542	0.025	4 ± 2	5 ± 3	1 ± 1	2 ± 2	2
XMMXCS J002715.2+170920.1	$0.385^{+0.111}_{-0.111}$	0.367 ± 0.059	-	-0.145 ± 0.141	4.430 ± 2.820	0.001	4 ± 3	9 ± 4	1 ± 1	10 ± 4	2
XMMXCS J002904.0-001312.7	$0.163^{+0.019}_{-0.020}$	0.168 ± 0.027	$0.163 \pm 2.5e-05$	0.014 ± 0.019	0.923 ± 0.344	0.034	1 ± 1	1 ± 2	1 ± 1	1 ± 1	2
XMMXCS J003101.6+262633.1	$0.588^{+0.116}_{-0.114}$	0.538 ± 0.087	-	0.145 ± 0.182	-1.820 ± 3.640	0.120	5 ± 3	12 ± 4	5 ± 2	12 ± 4	2
XMMXCS J003104.8+260817.2	$0.163^{+0.049}_{-0.049}$	0.144 ± 0.023	-	-0.054 ± 0.007	1.950 ± 0.125	0.001	3 ± 2	4 ± 2	1 ± 1	1 ± 1	2
XMMXCS J003111.3+261302.9	$0.306^{+0.078}_{-0.079}$	0.312 ± 0.048	-	-0.193 ± 0.043	5.290 ± 0.852	0.012	1 ± 2	2 ± 2	2 ± 1	3 ± 2	2
XMMXCS J003313.8+393133.7	$0.390^{+0.116}_{-0.112}$	0.440 ± 0.067	-	-0.006 ± 0.056	0.804 ± 1.110	0.001	5 ± 3	-	2 ± 2	-	2
XMMXCS J003648.5+092109.9	$0.268^{+0.111}_{-0.112}$	0.309 ± 0.053	-	-0.133 ± 0.079	3.910 ± 1.530	0.001	3 ± 2	4 ± 3	2 ± 1	2 ± 2	2
XMMXCS J003832.5+405005.7	$0.435^{+0.188}_{-0.186}$	0.474 ± 0.076	-	0.044 ± 0.220	-0.035 ± 4.550	0.111	38 ± 7	38 ± 7	122 ± 13	115 ± 13	2
XMMXCS J003910.5+410330.5	$0.374^{+0.120}_{-0.119}$	0.421 ± 0.062	-	0.043 ± 0.036	-0.144 ± 0.718	0.090	27 ± 6	33 ± 7	59 ± 9	78 ± 10	2
XMMXCS J003956.7+065118.6	$0.565^{+0.128}_{-0.120}$	0.496 ± 0.074	$0.504 \pm 8.2e-05$	0.074 ± 0.064	-0.549 ± 1.290	0.113	4 ± 3	711 ± 27	1 ± 1	39 ± 25	2

Continued on next page

Table A.2 – continued from previous page

name	z_{RS}	z_{BCG}	z_{spec-g}	cmr_{grad}	cmr_{inter}	cmr_{wid}	n_{gals-c}	n_{gals-l}	n_{200-c}	n_{200-l}	qual
XMMXCS J004013.8+412938.1	$0.344^{+0.143}_{-0.140}$	0.319 ± 0.092	-	0.118 ± 0.121	-1.100 ± 2.490	0.001	2 ± 3	1 ± 3	1 ± 1	1 ± 1	2
XMMXCS J004123.0+401207.2	$0.270^{+0.069}_{-0.070}$	0.304 ± 0.046	-	-0.049 ± 0.035	2.420 ± 0.673	0.072	17 ± 4	13 ± 4	20 ± 5	13 ± 4	2
XMMXCS J004151.0-091816.7	$0.044^{+0.038}_{-0.027}$	0.075 ± 0.081	$0.053 \pm 1.4e-05$	0.017 ± 0.011	0.558 ± 0.160	0.055	19 ± 4	13 ± 4	23 ± 5	12 ± 4	2
XMMXCS J004203.9-094413.4	$0.073^{+0.035}_{-0.035}$	0.082 ± 0.015	$0.088 \pm 1.3e-05$	-0.064 ± 0.001	1.880 ± 0.001	0.500	3 ± 2	1 ± 1	1 ± 1	1 ± 1	2
XMMXCS J004247.5+402518.4	$0.609^{+0.244}_{-0.261}$	0.654 ± 0.136	-	0.581 ± 0.642	-10.30 ± 13.20	0.210	12 ± 4	22 ± 6	12 ± 4	40 ± 8	2
XMMXCS J004307.6-095136.2	$0.297^{+0.117}_{-0.115}$	0.291 ± 0.095	-	0.024 ± 0.064	0.824 ± 1.200	0.056	2 ± 2	4 ± 3	2 ± 1	2 ± 2	2
XMMXCS J004307.6-095136.5	$0.297^{+0.117}_{-0.115}$	0.291 ± 0.095	-	0.024 ± 0.064	0.824 ± 1.200	0.056	2 ± 2	4 ± 3	2 ± 1	2 ± 2	2
XMMXCS J004349.7+404421.3	$0.393^{+0.155}_{-0.154}$	0.438 ± 0.068	-	0.042 ± 0.034	-0.114 ± 0.695	0.113	12 ± 5	14 ± 5	15 ± 5	22 ± 6	2
XMMXCS J004349.9+004720.5	$0.430^{+0.106}_{-0.105}$	0.396 ± 0.078	-	-0.160 ± 0.158	4.780 ± 3.120	0.041	20 ± 5	25 ± 6	25 ± 6	25 ± 6	2
XMMXCS J004350.0+004720.7	$0.430^{+0.106}_{-0.105}$	0.396 ± 0.078	-	-0.160 ± 0.158	4.780 ± 3.120	0.041	20 ± 5	25 ± 6	25 ± 6	25 ± 6	2
XMMXCS J004404.6+010152.8	$0.110^{+0.021}_{-0.022}$	0.113 ± 0.021	$0.110 \pm 1.3e-05$	-0.023 ± 0.049	1.190 ± 0.881	0.088	2 ± 2	3 ± 2	1 ± 1	4 ± 2	2
XMMXCS J004604.4+410530.0	$0.462^{+0.156}_{-0.156}$	0.431 ± 0.263	-	-0.174 ± 0.158	4.490 ± 3.290	0.112	14 ± 5	10 ± 4	20 ± 6	8 ± 4	2
XMMXCS J004923.5+320024.3	$0.389^{+0.098}_{-0.095}$	0.353 ± 0.064	-	-0.128 ± 0.042	4.150 ± 0.839	0.001	1 ± 2	-	2 ± 1	-	2
XMMXCS J005348.2-084219.7	$0.257^{+0.076}_{-0.078}$	0.303 ± 0.087	$0.262 \pm 5.9e-05$	-0.008 ± 0.037	1.470 ± 0.710	0.096	4 ± 3	3 ± 3	1 ± 1	1 ± 2	2
XMMXCS J005511.8+263529.0	$0.164^{+0.063}_{-0.063}$	0.176 ± 0.032	-	-0.212 ± 0.040	4.920 ± 0.726	0.027	1 ± 1	1 ± 1	1 ± 1	0 ± 1	2
XMMXCS J005559.0+261949.2	$0.201^{+0.059}_{-0.059}$	0.236 ± 0.038	-	-0.075 ± 0.009	2.630 ± 0.161	0.008	26 ± 5	27 ± 5	42 ± 7	48 ± 7	2
XMMXCS J005611.3+263529.8	$0.314^{+0.068}_{-0.070}$	0.361 ± 0.053	-	-0.024 ± 0.094	2.110 ± 1.800	0.020	5 ± 3	4 ± 3	2 ± 2	0 ± 1	2
XMMXCS J010658.7+320934.0	$0.125^{+0.036}_{-0.036}$	0.086 ± 0.027	-	-0.008 ± 0.027	1.110 ± 0.486	0.068	9 ± 3	6 ± 3	9 ± 3	5 ± 2	2
XMMXCS J010707.2+142154.3	$0.083^{+0.016}_{-0.015}$	0.086 ± 0.017	$0.083 \pm 1.2e-05$	0.001 ± 0.049	0.849 ± 0.853	0.085	5 ± 3	3 ± 2	1 ± 1	0 ± 1	2

Continued on next page

Table A.2 – continued from previous page

name	z_{RS}	z_{BCG}	z_{spec-g}	cmr_{grad}	cmr_{inter}	cmr_{wid}	n_{gals-c}	n_{gals-l}	n_{200-c}	n_{200-l}	qual
XMMXCS J011045.2+332136.4	$0.260^{+0.147}_{-0.141}$	0.297 ± 0.053	-	-0.263 ± 0.061	6.380 ± 1.230	0.055	3 ± 2	2 ± 2	1 ± 1	0 ± 1	2
XMMXCS J011124.1+330151.9	$0.102^{+0.020}_{-0.020}$	0.093 ± 0.019	-	0.009 ± 0.011	0.815 ± 0.177	0.010	4 ± 2	4 ± 2	2 ± 2	2 ± 2	2
XMMXCS J011632.1+330325.0	$0.425^{+0.164}_{-0.158}$	0.376 ± 0.158	-	0.297 ± 0.002	-4.230 ± 0.031	0.500	1 ± 3	5 ± 3	2 ± 1	3 ± 2	2
XMMXCS J011954.7+141655.1	$0.600^{+0.165}_{-0.166}$	0.551 ± 0.090	-	-0.032 ± 0.112	1.650 ± 2.240	0.130	4 ± 3	10 ± 5	3 ± 2	12 ± 5	2
XMMXCS J012312.6+071231.4	$0.082^{+0.035}_{-0.035}$	0.100 ± 0.018	$0.082 \pm 1.2e-05$	-0.029 ± 0.009	1.400 ± 0.155	0.021	3 ± 2	2 ± 2	2 ± 1	1 ± 1	2
XMMXCS J012400.0+035110.8	$0.095^{+0.029}_{-0.029}$	0.072 ± 0.028	-	0.093 ± 0.023	-0.721 ± 0.377	0.017	1 ± 1	1 ± 1	1 ± 1	1 ± 1	2
XMMXCS J012414.3+035635.2	$0.240^{+0.117}_{-0.117}$	0.278 ± 0.080	-	-0.095 ± 0.081	3.120 ± 1.560	0.001	3 ± 2	3 ± 2	1 ± 1	1 ± 1	2
XMMXCS J012420.8+330530.1	$0.188^{+0.069}_{-0.066}$	0.168 ± 0.041	-	-0.068 ± 0.021	2.140 ± 0.360	0.100	1 ± 2	1 ± 2	1 ± 1	1 ± 1	2
XMMXCS J012444.8+320956.9	$0.282^{+0.178}_{-0.168}$	0.234 ± 0.072	-	0.002 ± 0.037	1.120 ± 0.713	0.001	3 ± 2	2 ± 2	3 ± 2	1 ± 1	2
XMMXCS J012549.6-011717.0	$0.192^{+0.082}_{-0.086}$	0.197 ± 0.056	-	-0.024 ± 0.033	1.670 ± 0.631	0.001	3 ± 2	3 ± 2	1 ± 1	1 ± 1	2
XMMXCS J014359.4+171420.3	$0.665^{+0.112}_{-0.103}$	0.629 ± 0.127	$0.647 \pm 1.7e-04$	0.039 ± 0.187	0.324 ± 3.770	0.107	3 ± 2	15 ± 5	2 ± 1	10 ± 5	2
XMMXCS J014440.3-043335.9	$0.120^{+0.044}_{-0.046}$	0.155 ± 0.027	-	-0.037 ± 0.027	1.690 ± 0.463	0.079	5 ± 2	5 ± 2	2 ± 2	2 ± 2	2
XMMXCS J014449.2-043246.1	$0.118^{+0.042}_{-0.042}$	0.155 ± 0.027	-	-0.090 ± 0.028	2.600 ± 0.459	0.082	3 ± 2	4 ± 2	4 ± 2	5 ± 2	2
XMMXCS J014511.5-044736.3	$0.186^{+0.067}_{-0.056}$	0.161 ± 0.042	-	-0.000 ± 0.001	1.260 ± 0.001	0.500	5 ± 3	13 ± 4	2 ± 2	7 ± 4	2
XMMXCS J014522.3-042307.2	$0.598^{+0.119}_{-0.111}$	0.577 ± 0.091	-	-0.056 ± 0.107	2.230 ± 2.120	0.153	1 ± 2	2 ± 3	1 ± 1	-	2
XMMXCS J014526.1-044750.1	$0.142^{+0.042}_{-0.042}$	0.126 ± 0.029	-	-0.009 ± 0.009	1.130 ± 0.154	0.023	2 ± 2	4 ± 2	1 ± 1	2 ± 2	2
XMMXCS J015038.7-071413.7	$0.393^{+0.106}_{-0.096}$	0.421 ± 0.063	-	-0.074 ± 0.044	3.000 ± 0.869	0.500	5 ± 4	3 ± 4	2 ± 3	4 ± 3	2
XMMXCS J015112.4+223527.8	$0.108^{+0.066}_{-0.070}$	0.066 ± 0.039	-	0.122 ± 0.001	-0.915 ± 0.003	0.500	2 ± 2	3 ± 2	2 ± 1	1 ± 1	2
XMMXCS J015335.6+010353.6	$0.188^{+0.060}_{-0.060}$	0.210 ± 0.039	-	-0.186 ± 0.031	4.600 ± 0.599	0.086	2 ± 2	2 ± 2	1 ± 1	2 ± 2	2

Continued on next page

Table A.2 – continued from previous page

name	z_{RS}	z_{BCG}	z_{spec-g}	cmr_{grad}	cmr_{inter}	cmr_{wid}	n_{gals-c}	n_{gals-l}	n_{200-c}	n_{200-l}	qual
XMMXCS J015702.8+320002.4	$0.109^{+0.051}_{-0.051}$	0.092 ± 0.021	-	-0.013 ± 0.011	1.130 ± 0.185	0.050	4 ± 2	4 ± 2	1 ± 1	1 ± 1	2
XMMXCS J020011.40-093127.4	$0.283^{+0.054}_{-0.055}$	0.309 ± 0.046	$0.286 \pm 5.5e-05$	-0.029 ± 0.044	2.060 ± 0.829	0.100	4 ± 3	4 ± 3	1 ± 1	0 ± 1	2
XMMXCS J020011.3-093127.4	$0.283^{+0.054}_{-0.055}$	0.309 ± 0.046	$0.286 \pm 5.5e-05$	-0.029 ± 0.044	2.060 ± 0.829	0.100	4 ± 3	4 ± 3	1 ± 1	0 ± 1	2
XMMXCS J020232.0-073345.2	$0.525^{+0.102}_{-0.102}$	0.567 ± 0.148	$0.523 \pm 1.4e-04$	0.037 ± 0.036	0.230 ± 0.734	0.067	10 ± 4	43 ± 7	8 ± 3	28 ± 7	2
XMMXCS J020232.45-073346.7	$0.525^{+0.104}_{-0.104}$	0.567 ± 0.148	$0.523 \pm 1.4e-04$	0.038 ± 0.036	0.222 ± 0.736	0.057	8 ± 3	11 ± 4	9 ± 3	11 ± 4	2
XMMXCS J020319.9-073438.4	$0.539^{+0.094}_{-0.094}$	0.572 ± 0.089	$0.538 \pm 1.3e-04$	0.060 ± 0.069	-0.228 ± 1.370	0.094	11 ± 4	33 ± 6	11 ± 4	36 ± 7	2
XMMXCS J020411.60-051034.3	$0.139^{+0.090}_{-0.091}$	0.140 ± 0.023	-	-0.017 ± 0.018	1.290 ± 0.341	0.039	1 ± 1	1 ± 1	1 ± 1	1 ± 1	2
XMMXCS J020423.79-073527.1	$0.137^{+0.027}_{-0.027}$	0.121 ± 0.029	$0.136 \pm 2.4e-05$	0.020 ± 0.082	0.686 ± 1.430	0.116	2 ± 2	2 ± 2	2 ± 1	2 ± 2	2
XMMXCS J020502.12-062441.2	$0.293^{+0.087}_{-0.087}$	0.327 ± 0.051	$0.423 \pm 1.3e-04$	-0.123 ± 0.068	3.860 ± 1.270	0.001	2 ± 2	1 ± 2	2 ± 1	0 ± 1	2
XMMXCS J020517.70-043900.7	$0.203^{+0.066}_{-0.061}$	0.199 ± 0.036	-	-0.158 ± 0.111	3.870 ± 2.170	0.143	2 ± 2	1 ± 2	1 ± 1	1 ± 1	2
XMMXCS J020525.15-073541.6	$0.421^{+0.099}_{-0.098}$	0.388 ± 0.070	$0.415 \pm 7.4e-05$	0.200 ± 0.110	-2.340 ± 2.210	0.161	19 ± 5	20 ± 5	25 ± 6	26 ± 6	2
XMMXCS J020612.94-071217.1	$0.238^{+0.104}_{-0.110}$	0.199 ± 0.032	-	0.053 ± 0.028	0.336 ± 0.534	0.001	5 ± 2	4 ± 3	3 ± 2	3 ± 2	2
XMMXCS J020717.8+022042.8	$0.180^{+0.079}_{-0.083}$	0.219 ± 0.042	$0.187 \pm 3.3e-05$	-0.036 ± 0.013	1.840 ± 0.241	0.061	3 ± 2	1 ± 2	2 ± 1	1 ± 1	2
XMMXCS J020719.8+292240.4	$0.625^{+0.133}_{-0.132}$	0.661 ± 0.156	-	0.024 ± 0.646	0.730 ± 13.40	0.001	5 ± 3	12 ± 4	4 ± 2	12 ± 4	2
XMMXCS J020722.2+023134.2	$0.692^{+0.166}_{-0.168}$	0.661 ± 0.127	$0.666 \pm 2.4e-04$	0.050 ± 0.134	0.207 ± 2.770	0.099	8 ± 3	29 ± 6	7 ± 3	46 ± 8	2
XMMXCS J020725.5+020702.5	$0.090^{+0.042}_{-0.042}$	0.057 ± 0.020	-	-0.003 ± 0.009	0.763 ± 0.144	0.065	4 ± 2	17 ± 4	3 ± 2	19 ± 4	2
XMMXCS J020733.5+292413.1	$0.526^{+0.121}_{-0.104}$	0.486 ± 0.074	-	1.180 ± 0.767	-23.20 ± 15.70	0.341	3 ± 3	11 ± 4	1 ± 1	11 ± 4	2
XMMXCS J020750.8-051224.4	$0.118^{+0.025}_{-0.025}$	0.092 ± 0.032	-	-0.116 ± 0.111	2.840 ± 1.940	0.500	4 ± 3	2 ± 2	3 ± 2	1 ± 1	2
XMMXCS J020755.76-055215.6	$0.448^{+0.103}_{-0.099}$	0.439 ± 0.065	$0.441 \pm 5.8e-05$	0.079 ± 0.047	-0.807 ± 0.925	0.099	5 ± 3	-	2 ± 2	-	2

Continued on next page

Table A.2 – continued from previous page

name	z_{RS}	z_{BCG}	z_{spec-g}	cmr_{grad}	cmr_{inter}	cmr_{wid}	n_{gals-c}	n_{gals-l}	n_{200-c}	n_{200-l}	qual
XMMXCS J020800.5+023059.9	$0.389^{+0.111}_{-0.109}$	0.359 ± 0.057	-	0.062 ± 0.043	-0.525 ± 0.836	0.001	11 ± 4	10 ± 4	10 ± 4	10 ± 4	2
XMMXCS J020901.42-060936.0	$0.288^{+0.071}_{-0.074}$	0.247 ± 0.085	-	0.018 ± 0.045	1.100 ± 0.869	0.082	6 ± 3	9 ± 4	5 ± 2	7 ± 3	2
XMMXCS J020922.25-062543.4	$0.283^{+0.090}_{-0.093}$	0.248 ± 0.044	$0.273 \pm 3.7e-05$	-0.050 ± 0.102	2.430 ± 1.950	0.001	4 ± 2	4 ± 3	1 ± 1	2 ± 2	2
XMMXCS J020951.69-060658.7	$0.251^{+0.079}_{-0.079}$	0.276 ± 0.043	-	-0.154 ± 0.051	4.410 ± 1.010	0.077	2 ± 2	1 ± 2	2 ± 1	1 ± 1	2
XMMXCS J020956.03-043751.0	$0.261^{+0.083}_{-0.084}$	0.230 ± 0.054	-	-0.052 ± 0.060	2.380 ± 1.150	0.130	3 ± 2	4 ± 3	3 ± 2	4 ± 2	2
XMMXCS J020957.96-051751.2	$0.128^{+0.030}_{-0.029}$	0.105 ± 0.035	-	0.137 ± 0.136	-1.390 ± 2.290	0.500	3 ± 2	4 ± 3	1 ± 1	1 ± 2	2
XMMXCS J021027.64-042232.7	$0.149^{+0.074}_{-0.072}$	0.146 ± 0.029	$0.138 \pm 2.0e-05$	-0.005 ± 0.106	1.190 ± 2.030	0.126	2 ± 2	3 ± 2	1 ± 1	1 ± 1	2
XMMXCS J021033.6-002552.5	$0.232^{+0.073}_{-0.075}$	0.262 ± 0.059	-	-0.042 ± 0.043	2.130 ± 0.840	0.106	2 ± 2	2 ± 2	1 ± 1	1 ± 1	2
XMMXCS J021057.28-061153.5	$0.385^{+0.094}_{-0.094}$	0.429 ± 0.064	$0.427 \pm 6.5e-05$	-0.120 ± 0.036	4.000 ± 0.693	0.001	25 ± 5	27 ± 6	36 ± 7	37 ± 7	2
XMMXCS J021114.60-034356.1	$0.555^{+0.138}_{-0.132}$	0.515 ± 0.131	$0.548 \pm 1.4e-04$	0.731 ± 0.189	-13.40 ± 3.850	0.215	5 ± 3	19 ± 4	2 ± 2	23 ± 5	2
XMMXCS J021252.79-061205.7	$0.416^{+0.093}_{-0.091}$	0.367 ± 0.058	-	-0.000 ± 0.048	0.714 ± 0.918	0.069	13 ± 4	12 ± 4	13 ± 4	13 ± 4	2
XMMXCS J021324.44-042009.3	$0.585^{+0.132}_{-0.134}$	0.618 ± 0.108	-	-0.145 ± 0.142	4.190 ± 2.920	0.076	3 ± 2	-	2 ± 1	-	2
XMMXCS J021329.09-081309.2	$0.237^{+0.053}_{-0.053}$	0.235 ± 0.045	$0.236 \pm 5.4e-05$	-0.052 ± 0.046	2.250 ± 0.826	0.101	5 ± 3	4 ± 3	2 ± 2	2 ± 2	2
XMMXCS J021402.2-003954.4	$0.486^{+0.097}_{-0.088}$	0.523 ± 0.115	$0.466 \pm 1.2e-04$	0.034 ± 0.138	0.152 ± 2.730	0.102	3 ± 3	2 ± 3	1 ± 1	-	2
XMMXCS J021446.34-035630.1	$0.138^{+0.033}_{-0.033}$	0.161 ± 0.030	$0.139 \pm 1.6e-05$	0.0001 ± 0.007	1.100 ± 0.125	0.036	5 ± 3	7 ± 3	1 ± 1	3 ± 2	2
XMMXCS J021446.3-035633.7	$0.139^{+0.035}_{-0.036}$	0.161 ± 0.030	$0.140 \pm 2.0e-05$	-0.004 ± 0.008	1.170 ± 0.154	0.037	6 ± 3	7 ± 3	2 ± 2	3 ± 2	2
XMMXCS J021447.4-005424.4	$0.261^{+0.065}_{-0.068}$	0.271 ± 0.045	$0.265 \pm 4.4e-05$	0.069 ± 0.040	0.245 ± 0.721	0.001	1 ± 2	2 ± 2	1 ± 1	0 ± 1	2
XMMXCS J021452.68-042331.7	$0.219^{+0.141}_{-0.155}$	0.171 ± 0.051	-	0.017 ± 0.098	0.959 ± 1.920	0.112	5 ± 3	5 ± 3	1 ± 1	2 ± 2	2
XMMXCS J021516.76-062236.1	$0.611^{+0.126}_{-0.118}$	0.506 ± 0.077	$0.586 \pm 1.5e-04$	0.211 ± 0.082	-3.200 ± 1.640	0.093	1 ± 2	3 ± 3	1 ± 1	-	2

Continued on next page

Table A.2 – continued from previous page

name	z_{RS}	z_{BCG}	z_{spec-g}	cmr_{grad}	cmr_{inter}	cmr_{wid}	n_{gals-c}	n_{gals-l}	n_{200-c}	n_{200-l}	qual
XMMXCS J021518.8-003813.2	$0.358^{+0.076}_{-0.071}$	0.362 ± 0.054	$0.349 \pm 5.0e-05$	-0.037 ± 0.049	1.300 ± 0.917	0.001	3 ± 3	5 ± 4	2 ± 2	2 ± 2	2
XMMXCS J021537.71-055853.4	$0.300^{+0.085}_{-0.087}$	0.252 ± 0.047	$0.279 \pm 3.4e-05$	-0.013 ± 0.029	1.760 ± 0.563	0.061	5 ± 3	8 ± 3	2 ± 2	2 ± 2	2
XMMXCS J021538.17-055857.9	$0.302^{+0.085}_{-0.086}$	0.252 ± 0.047	$0.279 \pm 3.4e-05$	-0.008 ± 0.031	1.670 ± 0.590	0.064	6 ± 3	8 ± 4	1 ± 2	2 ± 2	2
XMMXCS J021542.84-065418.0	$0.256^{+0.061}_{-0.060}$	0.237 ± 0.039	$0.255 \pm 4.5e-05$	0.020 ± 0.037	0.917 ± 0.693	0.500	2 ± 3	-	1 ± 1	-	2
XMMXCS J021602.03-033138.3	$0.169^{+0.047}_{-0.047}$	0.201 ± 0.034	-	0.028 ± 0.074	0.584 ± 1.360	0.102	1 ± 2	1 ± 2	1 ± 1	1 ± 1	2
XMMXCS J021605.61-034319.1	$0.189^{+0.071}_{-0.073}$	0.156 ± 0.065	$0.263 \pm 4.4e-05$	0.056 ± 0.069	-0.314 ± 1.250	0.500	5 ± 3	4 ± 3	2 ± 2	2 ± 2	2
XMMXCS J021611.9-044626.2	$0.324^{+0.166}_{-0.165}$	0.354 ± 0.061	-	-0.626 ± 0.133	14.000 ± 2.680	0.001	5 ± 3	4 ± 3	2 ± 2	0 ± 1	2
XMMXCS J021619.99-060539.6	$0.198^{+0.067}_{-0.063}$	0.156 ± 0.036	-	0.011 ± 0.020	0.874 ± 0.355	0.500	3 ± 3	4 ± 3	2 ± 2	3 ± 2	2
XMMXCS J021619.9-060539.5	$0.198^{+0.067}_{-0.063}$	0.156 ± 0.036	-	0.011 ± 0.020	0.874 ± 0.355	0.500	3 ± 3	4 ± 3	2 ± 2	3 ± 2	2
XMMXCS J021717.0-052837.5	$0.372^{+0.076}_{-0.076}$	0.336 ± 0.094	-	-0.024 ± 0.020	2.040 ± 0.371	0.500	2 ± 3	1 ± 3	1 ± 1	1 ± 2	2
XMMXCS J021718.61-052922.3	$0.326^{+0.115}_{-0.118}$	0.336 ± 0.094	-	-0.157 ± 0.077	4.420 ± 1.510	0.024	3 ± 2	5 ± 3	1 ± 1	2 ± 2	2
XMMXCS J021719.1-052917.1	$0.307^{+0.162}_{-0.178}$	0.261 ± 0.075	-	0.0 ± -1.00	1.930 ± -1.00	0.500	1 ± 3	2 ± 3	2 ± 1	1 ± 2	2
XMMXCS J021720.90-053925.5	$0.373^{+0.077}_{-0.078}$	0.349 ± 0.053	-	0.055 ± 0.125	0.622 ± 2.440	0.001	3 ± 2	3 ± 3	2 ± 2	3 ± 2	2
XMMXCS J021725.8-050936.4	$0.426^{+0.118}_{-0.121}$	0.429 ± 0.071	-	1.120 ± 0.804	-21.50 ± 16.00	0.302	5 ± 3	17 ± 4	2 ± 2	23 ± 5	2
XMMXCS J021808.0-044049.9	$0.279^{+0.093}_{-0.095}$	0.246 ± 0.042	-	-0.003 ± 0.073	1.410 ± 1.490	0.049	2 ± 2	1 ± 2	1 ± 1	1 ± 1	2
XMMXCS J021808.30-044050.2	$0.268^{+0.089}_{-0.090}$	0.246 ± 0.042	-	0.002 ± 0.071	1.310 ± 1.450	0.057	2 ± 2	0 ± 1	1 ± 1	-	2
XMMXCS J021837.40-060451.1	$0.231^{+0.138}_{-0.109}$	0.234 ± 0.041	-	-0.676 ± 0.702	14.400 ± 13.30	0.223	1 ± 2	0 ± 2	1 ± 1	-	2
XMMXCS J021911.32-034416.1	$0.410^{+0.128}_{-0.122}$	0.360 ± 0.062	-	-0.386 ± 0.363	9.050 ± 7.390	0.227	6 ± 4	6 ± 4	4 ± 3	5 ± 3	2
XMMXCS J021911.3-034416.0	$0.400^{+0.135}_{-0.132}$	0.360 ± 0.062	-	-0.571 ± 0.342	12.700 ± 7.050	0.232	6 ± 4	6 ± 4	6 ± 3	6 ± 3	2

Continued on next page

Table A.2 – continued from previous page

name	z_{RS}	z_{BCG}	z_{spec-g}	cmr_{grad}	cmr_{inter}	cmr_{wid}	n_{gals-c}	n_{gals-l}	n_{200-c}	n_{200-l}	qual
XMMXCS J021919.1-040453.9	$0.615^{+0.151}_{-0.151}$	0.599 ± 0.104	-	-0.266 ± 0.208	6.720 ± 4.290	0.001	6 ± 3	-	2 ± 2	-	2
XMMXCS J021933.77-061230.8	$0.224^{+0.054}_{-0.055}$	0.223 ± 0.061	$0.225 \pm 3.6e-05$	0.007 ± 0.028	1.200 ± 0.525	0.066	4 ± 2	4 ± 3	1 ± 1	1 ± 2	2
XMMXCS J021938.4-040024.2	$0.207^{+0.074}_{-0.074}$	0.199 ± 0.096	$0.204 \pm 2.3e-05$	-0.001 ± 0.020	1.130 ± 0.343	0.001	1 ± 2	0 ± 2	2 ± 1	-	2
XMMXCS J021939.41-040025.0	$0.207^{+0.074}_{-0.074}$	0.199 ± 0.096	$0.204 \pm 2.3e-05$	-0.001 ± 0.020	1.130 ± 0.343	0.001	1 ± 2	0 ± 2	2 ± 1	-	2
XMMXCS J021940.78-055043.7	$0.652^{+0.140}_{-0.139}$	0.619 ± 0.120	$0.648 \pm 2.0e-04$	0.183 ± 0.148	-2.380 ± 2.940	0.130	3 ± 2	15 ± 4	2 ± 1	14 ± 4	2
XMMXCS J021951.16-033233.6	$0.180^{+0.057}_{-0.058}$	0.177 ± 0.028	$0.181 \pm 3.9e-05$	0.006 ± 0.018	1.070 ± 0.321	0.043	2 ± 2	2 ± 2	1 ± 1	1 ± 1	2
XMMXCS J021951.1-033234.3	$0.180^{+0.057}_{-0.058}$	0.177 ± 0.028	$0.181 \pm 3.9e-05$	0.006 ± 0.018	1.070 ± 0.321	0.043	2 ± 2	2 ± 2	1 ± 1	1 ± 1	2
XMMXCS J021958.6-045219.7	$0.330^{+0.068}_{-0.071}$	0.330 ± 0.057	$0.334 \pm 5.7e-05$	0.069 ± 0.055	0.270 ± 1.050	0.106	2 ± 2	3 ± 3	1 ± 1	12 ± 4	2
XMMXCS J022012.07-034111.8	$0.333^{+0.077}_{-0.083}$	0.307 ± 0.049	-	0.066 ± 0.154	0.439 ± 2.990	0.001	4 ± 2	4 ± 3	1 ± 1	2 ± 2	2
XMMXCS J022023.2-025025.4	$0.192^{+0.084}_{-0.085}$	0.203 ± 0.069	-	-0.037 ± 0.037	1.860 ± 0.682	0.001	1 ± 1	0 ± 1	1 ± 1	-	2
XMMXCS J022038.8-030145.9	$0.522^{+0.060}_{-0.060}$	0.477 ± 0.073	$0.522 \pm 1.4e-04$	-0.077 ± 0.071	2.400 ± 1.400	0.001	9 ± 4	18 ± 5	7 ± 3	14 ± 5	2
XMMXCS J022058.70-043918.1	$0.111^{+0.045}_{-0.045}$	0.076 ± 0.026	-	0.028 ± 0.031	0.455 ± 0.538	0.070	2 ± 2	1 ± 2	2 ± 1	0 ± 1	2
XMMXCS J022103.3-050611.1	$0.249^{+0.060}_{-0.061}$	0.265 ± 0.040	-	-0.136 ± 0.057	4.030 ± 1.080	0.026	1 ± 2	1 ± 2	2 ± 1	3 ± 2	2
XMMXCS J022108.6+195812.4	$0.384^{+0.115}_{-0.115}$	0.412 ± 0.122	-	0.220 ± 0.135	-2.700 ± 2.600	0.154	24 ± 5	25 ± 6	34 ± 7	33 ± 7	2
XMMXCS J022118.36-042238.0	$0.086^{+0.026}_{-0.028}$	0.082 ± 0.016	-	-0.007 ± 0.039	0.911 ± 0.642	0.500	5 ± 3	3 ± 2	1 ± 1	2 ± 2	2
XMMXCS J022119.2-043754.1	$0.086^{+0.039}_{-0.039}$	0.076 ± 0.026	-	-0.004 ± 0.016	0.886 ± 0.260	0.068	4 ± 2	5 ± 2	1 ± 1	2 ± 2	2
XMMXCS J022137.91-043440.5	$0.193^{+0.100}_{-0.101}$	0.166 ± 0.033	-	-0.136 ± 0.041	3.670 ± 0.807	0.101	5 ± 3	6 ± 3	2 ± 2	3 ± 2	2
XMMXCS J022204.3-043239.6	$0.320^{+0.092}_{-0.093}$	0.304 ± 0.048	$0.319 \pm 6.3e-05$	-0.110 ± 0.030	3.560 ± 0.582	0.064	4 ± 3	5 ± 3	1 ± 1	4 ± 2	2
XMMXCS J022205.2-054307.7	$0.266^{+0.088}_{-0.088}$	0.275 ± 0.043	-	-0.023 ± 0.063	1.830 ± 1.200	0.095	4 ± 3	4 ± 3	1 ± 1	1 ± 2	2

Continued on next page

Table A.2 – continued from previous page

name	z_{RS}	z_{BCG}	z_{spec-g}	cmr_{grad}	cmr_{inter}	cmr_{wid}	n_{gals-c}	n_{gals-l}	n_{200-c}	n_{200-l}	qual
XMMXCS J022323.7-025526.1	$0.281^{+0.081}_{-0.077}$	0.297 ± 0.070	-	-0.011 ± 0.064	1.570 ± 1.220	0.131	3 ± 3	2 ± 3	2 ± 2	2 ± 2	2
XMMXCS J022402.8-044131.1	$0.061^{+0.067}_{-0.061}$	0.066 ± 0.021	-	0.093 ± 0.001	-0.503 ± 0.002	0.500	4 ± 3	8 ± 3	1 ± 1	6 ± 3	2
XMMXCS J022416.9-050315.7	$0.142^{+0.035}_{-0.036}$	0.132 ± 0.023	$0.143 \pm 2.3e-05$	0.011 ± 0.035	0.930 ± 0.628	0.115	1 ± 2	1 ± 2	1 ± 1	2 ± 2	2
XMMXCS J022421.2-040356.1	$0.567^{+0.107}_{-0.101}$	0.542 ± 0.138	-	-0.095 ± 0.242	2.920 ± 4.870	0.089	1 ± 2	5 ± 3	1 ± 1	9 ± 3	2
XMMXCS J022457.31-034859.1	$0.517^{+0.133}_{-0.132}$	0.548 ± 0.182	-	-0.695 ± 0.229	15.300 ± 4.710	0.001	9 ± 3	18 ± 5	8 ± 3	20 ± 5	2
XMMXCS J022519.81-041842.3	$0.142^{+0.028}_{-0.028}$	0.143 ± 0.027	$0.142 \pm 1.2e-05$	0.008 ± 0.011	0.952 ± 0.190	0.034	2 ± 2	2 ± 2	2 ± 1	3 ± 2	2
XMMXCS J022519.8-041842.3	$0.142^{+0.028}_{-0.028}$	0.143 ± 0.027	$0.142 \pm 1.2e-05$	0.008 ± 0.011	0.952 ± 0.190	0.034	2 ± 2	2 ± 2	2 ± 1	3 ± 2	2
XMMXCS J022524.72-044043.9	$0.263^{+0.071}_{-0.071}$	0.261 ± 0.042	$0.264 \pm 4.6e-05$	-0.003 ± 0.024	1.540 ± 0.447	0.046	4 ± 2	6 ± 3	2 ± 2	8 ± 3	2
XMMXCS J022524.7-044043.9	$0.263^{+0.071}_{-0.071}$	0.261 ± 0.042	$0.264 \pm 4.6e-05$	-0.003 ± 0.024	1.540 ± 0.447	0.046	4 ± 2	6 ± 3	2 ± 2	8 ± 3	2
XMMXCS J022529.1-041519.6	$0.140^{+0.073}_{-0.076}$	0.146 ± 0.024	$0.143 \pm 2.3e-05$	-0.018 ± 0.025	1.380 ± 0.469	0.062	3 ± 2	2 ± 2	2 ± 1	1 ± 1	2
XMMXCS J022529.75-041432.7	$0.142^{+0.063}_{-0.064}$	0.146 ± 0.024	$0.143 \pm 2.3e-05$	-0.011 ± 0.011	1.260 ± 0.200	0.017	3 ± 2	2 ± 2	2 ± 1	1 ± 1	2
XMMXCS J022530.7-041419.0	$0.143^{+0.040}_{-0.040}$	0.146 ± 0.024	$0.143 \pm 2.3e-05$	-0.035 ± 0.018	1.670 ± 0.314	0.001	3 ± 2	2 ± 2	2 ± 1	1 ± 1	2
XMMXCS J022539.6-042210.1	$0.167^{+0.055}_{-0.058}$	0.143 ± 0.027	$0.141 \pm 1.6e-05$	0.053 ± 0.019	0.218 ± 0.332	0.029	5 ± 2	4 ± 2	2 ± 2	3 ± 2	2
XMMXCS J022601.17-030116.1	$0.357^{+0.160}_{-0.177}$	0.332 ± 0.084	-	0.109 ± 0.095	-1.330 ± 1.880	0.125	2 ± 2	3 ± 3	1 ± 1	1 ± 2	2
XMMXCS J022607.8-041843.7	$0.319^{+0.115}_{-0.121}$	0.330 ± 0.059	$0.495 \pm 1.2e-04$	-0.000 ± 0.001	0.790 ± 0.001	0.500	3 ± 3	0 ± 3	1 ± 2	-	2
XMMXCS J022616.47-050443.8	$0.083^{+0.026}_{-0.026}$	0.116 ± 0.031	$0.053 \pm 1.4e-05$	0.072 ± 0.016	-0.369 ± 0.241	0.069	9 ± 3	11 ± 3	9 ± 3	11 ± 3	2
XMMXCS J022618.3-040000.1	$0.168^{+0.061}_{-0.061}$	0.210 ± 0.037	$0.209 \pm 2.7e-05$	0.066 ± 0.082	-0.081 ± 1.520	0.116	5 ± 3	3 ± 2	4 ± 2	3 ± 2	2
XMMXCS J022630.88-034236.3	$0.302^{+0.070}_{-0.067}$	0.289 ± 0.049	$0.299 \pm 4.4e-05$	-0.059 ± 0.057	2.460 ± 1.150	0.137	3 ± 3	3 ± 3	2 ± 2	3 ± 2	2
XMMXCS J022639.7-041647.0	$0.186^{+0.050}_{-0.048}$	0.172 ± 0.035	-	0.005 ± 0.029	1.000 ± 0.536	0.114	3 ± 2	1 ± 2	1 ± 1	-	2

Continued on next page

Table A.2 – continued from previous page

name	z_{RS}	z_{BCG}	z_{spec-g}	cmr_{grad}	cmr_{inter}	cmr_{wid}	n_{gals-c}	n_{gals-l}	n_{200-c}	n_{200-l}	qual
XMMXCS J022648.5-041157.9	$0.205^{+0.049}_{-0.052}$	0.177 ± 0.046	$0.210 \pm 1.9e-05$	0.041 ± 0.035	0.602 ± 0.657	0.093	7 ± 3	7 ± 3	1 ± 1	0 ± 2	2
XMMXCS J022651.2-054138.1	$0.315^{+0.071}_{-0.074}$	0.265 ± 0.055	-	0.001 ± 0.043	1.570 ± 0.825	0.083	2 ± 2	-	1 ± 1	-	2
XMMXCS J022726.7-043209.1	$0.260^{+0.061}_{-0.061}$	0.222 ± 0.039	-	0.183 ± 0.037	-1.970 ± 0.728	0.097	6 ± 3	8 ± 3	8 ± 3	9 ± 3	2
XMMXCS J022737.78-031810.9	$0.585^{+0.150}_{-0.128}$	0.583 ± 0.124	-	0.529 ± 0.381	-9.660 ± 7.760	0.204	1 ± 2	6 ± 3	1 ± 1	0 ± 1	2
XMMXCS J022738.5-031801.3	$0.609^{+0.107}_{-0.107}$	0.583 ± 0.124	-	0.751 ± 0.540	-14.30 ± 11.10	0.258	2 ± 2	10 ± 3	1 ± 1	5 ± 2	2
XMMXCS J022808.41-053553.2	$0.192^{+0.034}_{-0.034}$	0.179 ± 0.028	$0.192 \pm 2.2e-05$	-0.018 ± 0.019	1.540 ± 0.341	0.042	1 ± 2	2 ± 2	2 ± 1	2 ± 2	2
XMMXCS J022808.4-053553.2	$0.192^{+0.034}_{-0.034}$	0.179 ± 0.028	$0.192 \pm 2.2e-05$	-0.018 ± 0.019	1.540 ± 0.341	0.042	1 ± 2	2 ± 2	2 ± 1	2 ± 2	2
XMMXCS J022829.38-045125.6	$0.141^{+0.054}_{-0.053}$	0.155 ± 0.026	$0.142 \pm 2.1e-05$	-0.059 ± 0.023	2.060 ± 0.391	0.072	1 ± 1	1 ± 2	1 ± 1	1 ± 1	2
XMMXCS J022846.8-050315.7	$0.218^{+0.074}_{-0.075}$	0.245 ± 0.066	-	-0.046 ± 0.030	2.180 ± 0.577	0.080	2 ± 2	2 ± 2	3 ± 2	2 ± 2	2
XMMXCS J023040.76-040753.5	$0.172^{+0.152}_{-0.092}$	0.139 ± 0.059	-	0.416 ± 0.001	-7.150 ± 0.005	0.500	2 ± 2	0 ± 2	1 ± 1	-	2
XMMXCS J023052.30-045121.9	$0.293^{+0.060}_{-0.061}$	0.257 ± 0.055	$0.294 \pm 6.4e-05$	0.007 ± 0.011	1.380 ± 0.209	0.026	3 ± 2	5 ± 3	2 ± 2	5 ± 3	2
XMMXCS J023052.60-042117.6	$0.141^{+0.042}_{-0.042}$	0.138 ± 0.023	$0.141 \pm 2.0e-05$	-0.027 ± 0.013	1.480 ± 0.216	0.069	2 ± 2	2 ± 2	1 ± 1	1 ± 1	2
XMMXCS J023103.4-072226.4	$0.172^{+0.040}_{-0.039}$	0.180 ± 0.043	-	-0.030 ± 0.055	1.710 ± 0.999	0.106	5 ± 2	5 ± 3	1 ± 1	2 ± 2	2
XMMXCS J023145.4-044534.6	$0.171^{+0.034}_{-0.035}$	0.175 ± 0.029	-	-0.021 ± 0.027	1.540 ± 0.474	0.032	5 ± 2	5 ± 3	2 ± 1	2 ± 2	2
XMMXCS J023150.20-054106.3	$0.342^{+0.050}_{-0.050}$	0.344 ± 0.053	$0.341 \pm 5.1e-05$	-0.075 ± 0.026	3.000 ± 0.474	0.001	2 ± 2	2 ± 3	2 ± 2	-	2
XMMXCS J023226.53-041359.0	$0.226^{+0.087}_{-0.088}$	0.256 ± 0.042	-	-0.088 ± 0.078	3.000 ± 1.450	0.035	4 ± 2	3 ± 2	3 ± 2	3 ± 2	2
XMMXCS J023304.54-045554.9	$0.475^{+0.219}_{-0.216}$	0.505 ± 0.126	-	-0.069 ± 0.101	2.290 ± 2.050	0.066	3 ± 3	3 ± 3	1 ± 1	-	2
XMMXCS J023333.48-041233.2	$0.251^{+0.072}_{-0.073}$	0.245 ± 0.040	-	0.077 ± 0.092	-0.134 ± 1.810	0.079	2 ± 2	3 ± 2	2 ± 1	1 ± 1	2
XMMXCS J023337.65-053026.5	$0.389^{+0.105}_{-0.104}$	0.408 ± 0.060	$0.430 \pm 9.4e-05$	-0.036 ± 0.038	1.390 ± 0.753	0.095	24 ± 5	25 ± 6	29 ± 7	30 ± 7	2

Continued on next page

Table A.2 – continued from previous page

name	z_{RS}	z_{BCG}	z_{spec-g}	cmr_{grad}	cmr_{inter}	cmr_{wid}	n_{gals-c}	n_{gals-l}	n_{200-c}	n_{200-l}	qual
XMMXCS J023436.23-041922.7	$0.151^{+0.069}_{-0.072}$	0.162 ± 0.030	-	0.007 ± 0.023	0.915 ± 0.418	0.088	1 ± 2	3 ± 2	1 ± 1	0 ± 1	2
XMMXCS J024220.9+000852.6	$0.494^{+0.121}_{-0.126}$	0.527 ± 0.081	$0.511 \pm 9.7e-05$	0.074 ± 0.074	-0.508 ± 1.470	0.105	4 ± 3	3 ± 3	2 ± 2	2 ± 2	2
XMMXCS J024227.5+000356.0	$0.649^{+0.081}_{-0.078}$	0.519 ± 0.181	$0.644 \pm 1.0e-04$	0.030 ± 0.062	0.499 ± 1.240	0.001	3 ± 2	5 ± 3	1 ± 1	1 ± 2	2
XMMXCS J024748.3-032845.2	$0.254^{+0.059}_{-0.060}$	0.218 ± 0.034	-	0.014 ± 0.031	1.230 ± 0.589	0.001	8 ± 3	6 ± 3	5 ± 2	4 ± 2	2
XMMXCS J024846.6-033653.6	$0.117^{+0.041}_{-0.041}$	0.128 ± 0.021	-	-0.007 ± 0.029	1.130 ± 0.504	0.068	2 ± 2	1 ± 2	1 ± 1	0 ± 1	2
XMMXCS J025808.2+055910.1	$0.120^{+0.085}_{-0.088}$	0.091 ± 0.025	-	-0.007 ± 0.019	0.810 ± 0.338	0.108	5 ± 3	14 ± 4	3 ± 2	24 ± 5	2
XMMXCS J030332.8-005735.5	$0.661^{+0.177}_{-0.178}$	0.672 ± 0.118	-	-0.046 ± 0.155	2.290 ± 3.040	0.084	3 ± 2	10 ± 4	2 ± 1	11 ± 4	2
XMMXCS J030604.4+001123.6	$0.629^{+0.123}_{-0.115}$	0.588 ± 0.095	$0.608 \pm 1.7e-04$	0.287 ± 0.341	-4.810 ± 6.960	0.139	3 ± 2	24 ± 6	1 ± 1	85 ± 10	2
XMMXCS J030614.4-000535.8	$0.389^{+0.101}_{-0.098}$	0.370 ± 0.056	-	0.007 ± 0.039	0.411 ± 0.794	0.001	1 ± 2	-	1 ± 1	-	2
XMMXCS J030637.3-001816.7	$0.422^{+0.091}_{-0.090}$	0.464 ± 0.068	$0.458 \pm 2.0e-04$	0.027 ± 0.054	0.216 ± 1.090	0.067	11 ± 4	10 ± 4	11 ± 4	11 ± 4	2
XMMXCS J031146.2+412110.7	$0.660^{+0.167}_{-0.165}$	0.709 ± 0.133	-	-0.266 ± 0.077	6.700 ± 1.540	0.001	2 ± 2	0 ± 1	1 ± 1	-	2
XMMXCS J031937.0+411500.6	$0.250^{+0.087}_{-0.087}$	0.275 ± 0.055	-	-0.346 ± 0.169	8.020 ± 3.290	0.001	2 ± 2	1 ± 2	1 ± 1	0 ± 1	2
XMMXCS J032050.9+414830.5	$0.118^{+0.052}_{-0.051}$	0.101 ± 0.033	-	-0.108 ± 0.083	2.940 ± 1.440	0.500	3 ± 3	2 ± 3	1 ± 1	-	2
XMMXCS J032141.3+414636.7	$0.192^{+0.080}_{-0.081}$	0.196 ± 0.033	-	-0.028 ± 0.033	1.630 ± 0.626	0.105	3 ± 2	5 ± 3	1 ± 1	3 ± 2	2
XMMXCS J032347.0+412859.7	$0.133^{+0.082}_{-0.088}$	0.158 ± 0.029	-	-0.000 ± 0.001	0.708 ± 0.001	0.500	5 ± 3	6 ± 3	5 ± 3	5 ± 3	2
XMMXCS J033729.5+004228.0	$0.478^{+0.109}_{-0.094}$	0.478 ± 0.071	$0.477 \pm 1.3e-04$	-0.078 ± 0.062	2.310 ± 1.240	0.001	1 ± 3	6 ± 4	1 ± 1	-	2
XMMXCS J041645.5+010758.2	$0.315^{+0.091}_{-0.090}$	0.285 ± 0.045	-	-0.031 ± 0.043	2.100 ± 0.816	0.023	6 ± 3	6 ± 3	3 ± 2	7 ± 3	2
XMMXCS J041715.0+005554.3	$0.255^{+0.077}_{-0.079}$	0.210 ± 0.037	-	0.078 ± 0.043	-0.055 ± 0.828	0.098	6 ± 3	-	5 ± 2	-	2
XMMXCS J044713.8-063502.3	$0.552^{+0.191}_{-0.191}$	0.547 ± 0.087	-	0.029 ± 0.179	0.495 ± 3.560	0.001	2 ± 2	-	1 ± 1	-	2

Continued on next page

Table A.2 – continued from previous page

name	z_{RS}	z_{BCG}	z_{spec-g}	cmr_{grad}	cmr_{inter}	cmr_{wid}	n_{gals-c}	n_{gals-l}	n_{200-c}	n_{200-l}	qual
XMMXCS J044842.0-062547.8	$0.339^{+0.084}_{-0.083}$	0.368 ± 0.056	-	-0.760 ± 0.283	16.700 ± 5.680	0.001	5 ± 3	5 ± 3	3 ± 2	3 ± 2	2
XMMXCS J051545.1-001036.1	$0.523^{+0.128}_{-0.127}$	0.562 ± 0.128	-	0.054 ± 0.072	-0.066 ± 1.460	0.085	8 ± 3	12 ± 4	9 ± 3	12 ± 4	2
XMMXCS J051610.0+010954.0	$0.283^{+0.070}_{-0.070}$	0.313 ± 0.047	-	-0.102 ± 0.027	3.460 ± 0.518	0.072	8 ± 3	6 ± 3	5 ± 3	4 ± 3	2
XMMXCS J064423.6+822626.5	$0.250^{+0.068}_{-0.071}$	0.246 ± 0.043	-	0.002 ± 0.015	1.400 ± 0.284	0.001	2 ± 2	1 ± 2	2 ± 1	2 ± 2	2
XMMXCS J073344.2+314723.3	$0.413^{+0.097}_{-0.095}$	0.429 ± 0.064	$0.463 \pm 1.0e-04$	-0.023 ± 0.061	1.130 ± 1.200	0.101	9 ± 4	141 ± 12	8 ± 4	-	2
XMMXCS J073605.8+433910.2	$0.379^{+0.088}_{-0.086}$	0.443 ± 0.064	$0.428 \pm 6.0e-05$	-0.023 ± 0.045	1.080 ± 0.899	0.088	15 ± 5	14 ± 5	15 ± 5	14 ± 5	2
XMMXCS J073626.4+434406.6	$0.112^{+0.026}_{-0.026}$	0.128 ± 0.028	$0.112 \pm 1.7e-05$	-0.073 ± 0.036	2.120 ± 0.645	0.072	1 ± 1	2 ± 2	1 ± 1	0 ± 1	2
XMMXCS J073631.1+434757.2	$0.112^{+0.030}_{-0.026}$	0.115 ± 0.019	$0.098 \pm 1.1e-05$	0.072 ± 0.041	-0.232 ± 0.674	0.069	5 ± 3	5 ± 3	2 ± 2	3 ± 2	2
XMMXCS J074222.4+494147.2	$0.237^{+0.086}_{-0.090}$	0.195 ± 0.039	-	0.033 ± 0.135	0.746 ± 2.490	0.120	3 ± 2	4 ± 3	2 ± 1	1 ± 2	2
XMMXCS J074711.0+305448.7	$0.384^{+0.119}_{-0.116}$	0.322 ± 0.051	$0.370 \pm 9.4e-05$	-0.387 ± 0.034	9.100 ± 0.690	0.001	1 ± 2	2 ± 3	2 ± 1	2 ± 2	2
XMMXCS J074725.2+310146.5	$0.338^{+0.059}_{-0.059}$	0.343 ± 0.054	$0.338 \pm 4.7e-05$	-0.051 ± 0.032	2.670 ± 0.604	0.001	6 ± 3	9 ± 4	2 ± 2	8 ± 3	2
XMMXCS J075037.7+180532.4	$0.508^{+0.157}_{-0.157}$	0.555 ± 0.153	-	-1.270 ± 0.386	27.000 ± 7.840	0.500	1 ± 3	6 ± 4	1 ± 1	12 ± 4	2
XMMXCS J075152.7+180935.7	$0.380^{+0.095}_{-0.084}$	0.383 ± 0.059	$0.395 \pm 6.2e-05$	-0.065 ± 0.031	1.910 ± 0.616	0.080	1 ± 3	2 ± 3	1 ± 1	2 ± 2	2
XMMXCS J075602.0+215848.6	$0.153^{+0.038}_{-0.041}$	0.163 ± 0.029	$0.156 \pm 1.3e-05$	0.038 ± 0.061	0.413 ± 1.090	0.155	4 ± 2	3 ± 2	2 ± 2	1 ± 1	2
XMMXCS J075845.7+352356.9	$0.474^{+0.123}_{-0.125}$	0.458 ± 0.137	$0.482 \pm 1.4e-04$	0.007 ± 0.032	0.779 ± 0.633	0.001	1 ± 2	-	1 ± 1	-	2
XMMXCS J080615.0+153032.9	$0.083^{+0.026}_{-0.023}$	0.101 ± 0.018	$0.095 \pm 1.2e-05$	0.075 ± 0.001	-0.420 ± 0.003	0.500	2 ± 2	1 ± 2	2 ± 1	2 ± 2	2
XMMXCS J080615.8+153154.9	$0.094^{+0.033}_{-0.035}$	0.101 ± 0.018	$0.095 \pm 1.2e-05$	0.001 ± 0.020	0.861 ± 0.365	0.080	2 ± 2	2 ± 2	1 ± 1	1 ± 1	2
XMMXCS J080624.0+151532.0	$0.410^{+0.078}_{-0.078}$	0.447 ± 0.065	$0.514 \pm 8.8e-05$	0.120 ± 0.121	-0.799 ± 2.460	0.114	3 ± 3	3 ± 3	2 ± 2	2 ± 2	2
XMMXCS J080821.8+390118.2	$0.194^{+0.059}_{-0.059}$	0.213 ± 0.059	$0.196 \pm 4.1e-05$	0.079 ± 0.010	-0.099 ± 0.181	0.001	3 ± 2	4 ± 2	1 ± 1	2 ± 2	2

Continued on next page

Table A.2 – continued from previous page

name	z_{RS}	z_{BCG}	z_{spec-g}	cmr_{grad}	cmr_{inter}	cmr_{wid}	n_{gals-c}	n_{gals-l}	n_{200-c}	n_{200-l}	qual
XMMXCS J082413.0+300438.1	$0.287^{+0.076}_{-0.076}$	0.247 ± 0.050	-	-0.037 ± 0.040	2.220 ± 0.769	0.018	11 ± 4	7 ± 3	11 ± 4	5 ± 3	2
XMMXCS J082426.1+295833.0	$0.362^{+0.106}_{-0.118}$	0.405 ± 0.068	-	0.016 ± 0.081	1.300 ± 1.560	0.001	3 ± 2	3 ± 3	1 ± 1	1 ± 2	2
XMMXCS J082436.8+295306.9	$0.412^{+0.156}_{-0.156}$	0.368 ± 0.134	-	0.312 ± 0.192	-5.590 ± 3.810	0.090	7 ± 4	5 ± 3	6 ± 3	10 ± 4	2
XMMXCS J082501.8+300302.5	$0.324^{+0.101}_{-0.099}$	0.315 ± 0.112	$0.520 \pm 1.2e-04$	0.006 ± 0.106	1.210 ± 2.090	0.001	6 ± 3	-	2 ± 2	-	2
XMMXCS J083037.0+655247.7	$0.182^{+0.041}_{-0.041}$	0.209 ± 0.037	-	-0.013 ± 0.011	1.420 ± 0.193	0.073	37 ± 6	38 ± 6	89 ± 10	90 ± 10	2
XMMXCS J083037.6+525530.0	$0.205^{+0.071}_{-0.076}$	0.229 ± 0.037	$0.212 \pm 2.6e-05$	-0.078 ± 0.066	2.660 ± 1.300	0.101	3 ± 2	2 ± 2	2 ± 1	1 ± 1	2
XMMXCS J083150.7+525821.0	$0.420^{+0.124}_{-0.109}$	0.451 ± 0.078	-	0.035 ± 0.106	-0.068 ± 2.140	0.112	4 ± 3	5 ± 3	2 ± 2	3 ± 3	2
XMMXCS J083259.8+524020.5	$0.576^{+0.172}_{-0.175}$	0.553 ± 0.087	$0.642 \pm 8.3e-05$	0.060 ± 0.070	-0.082 ± 1.420	0.500	3 ± 3	4 ± 4	3 ± 2	4 ± 3	2
XMMXCS J083905.8+254446.9	$0.344^{+0.069}_{-0.068}$	0.328 ± 0.059	-	0.221 ± 0.202	-2.810 ± 4.070	0.145	2 ± 3	1 ± 3	1 ± 1	0 ± 1	2
XMMXCS J083926.4+193654.5	$0.378^{+0.087}_{-0.086}$	0.339 ± 0.051	$0.375 \pm 4.7e-05$	-0.106 ± 0.042	3.630 ± 0.743	0.069	8 ± 3	8 ± 4	5 ± 3	0 ± 2	2
XMMXCS J084011.6+511324.0	$0.569^{+0.139}_{-0.121}$	0.606 ± 0.123	$0.580 \pm 3.8e-04$	0.190 ± 0.183	-2.910 ± 3.620	0.182	1 ± 2	1 ± 3	1 ± 1	11 ± 4	2
XMMXCS J084012.2+295250.8	$0.508^{+0.110}_{-0.109}$	0.557 ± 0.093	$0.510 \pm 1.7e-04$	-0.069 ± 0.048	2.330 ± 0.975	0.127	15 ± 4	18 ± 5	16 ± 5	27 ± 6	2
XMMXCS J084646.4+184849.0	$0.244^{+0.067}_{-0.071}$	0.267 ± 0.041	-	-0.007 ± 0.037	1.510 ± 0.710	0.081	2 ± 2	3 ± 2	2 ± 1	1 ± 1	2
XMMXCS J084736.5+184711.9	$0.277^{+0.076}_{-0.078}$	0.278 ± 0.053	-	0.013 ± 0.181	1.130 ± 3.530	0.095	1 ± 2	1 ± 2	1 ± 1	1 ± 1	2
XMMXCS J084823.2+445857.2	$0.338^{+0.118}_{-0.108}$	0.327 ± 0.126	-	0.832 ± 0.027	-15.10 ± 0.557	0.500	1 ± 2	1 ± 3	2 ± 1	2 ± 2	2
XMMXCS J084913.91-025242.0	$0.229^{+0.062}_{-0.064}$	0.262 ± 0.045	-	0.007 ± 0.031	1.200 ± 0.595	0.095	8 ± 3	9 ± 3	9 ± 3	9 ± 3	2
XMMXCS J084932.1+450105.5	$0.578^{+0.162}_{-0.163}$	0.540 ± 0.150	$0.566 \pm 2.2e-04$	0.416 ± 0.246	-7.350 ± 4.950	0.001	1 ± 2	3 ± 3	2 ± 1	6 ± 3	2
XMMXCS J085232.8+175125.9	$0.203^{+0.043}_{-0.043}$	0.208 ± 0.033	-	-0.100 ± 0.047	3.130 ± 0.867	0.074	2 ± 2	2 ± 2	1 ± 1	2 ± 2	2
XMMXCS J085235.3+181122.4	$0.104^{+0.030}_{-0.032}$	0.128 ± 0.022	$0.105 \pm 1.3e-05$	0.072 ± 0.035	-0.186 ± 0.609	0.076	2 ± 2	4 ± 2	1 ± 1	3 ± 2	2

Continued on next page

Table A.2 – continued from previous page

name	z_{RS}	z_{BCG}	z_{spec-g}	cmr_{grad}	cmr_{inter}	cmr_{wid}	n_{gals-c}	n_{gals-l}	n_{200-c}	n_{200-l}	qual
XMMXCS J085658.0+374747.3	$0.380^{+0.124}_{-0.130}$	0.397 ± 0.061	-	0.104 ± 0.111	-0.504 ± 2.160	0.125	3 ± 3	8 ± 4	2 ± 2	2 ± 3	2
XMMXCS J085741.3+090109.0	$0.205^{+0.114}_{-0.117}$	0.175 ± 0.046	-	-0.101 ± 0.184	2.980 ± 3.550	0.060	3 ± 2	2 ± 2	2 ± 1	0 ± 1	2
XMMXCS J085815.3+275018.2	$0.302^{+0.116}_{-0.115}$	0.268 ± 0.116	-	0.073 ± 0.168	-0.209 ± 3.350	0.001	1 ± 2	2 ± 2	1 ± 1	3 ± 2	2
XMMXCS J085819.4+134454.4	$0.121^{+0.051}_{-0.052}$	0.127 ± 0.021	$0.122 \pm 1.2e-05$	0.040 ± 0.037	0.215 ± 0.643	0.116	3 ± 2	3 ± 2	2 ± 1	2 ± 2	2
XMMXCS J085908.5+274814.2	$0.461^{+0.121}_{-0.110}$	0.480 ± 0.255	-	0.135 ± 0.065	-1.910 ± 1.290	0.104	5 ± 3	-	2 ± 2	-	2
XMMXCS J090101.5+600606.2	$0.279^{+0.050}_{-0.050}$	0.318 ± 0.048	$0.279 \pm 5.6e-05$	-0.050 ± 0.030	2.480 ± 0.547	0.061	10 ± 4	13 ± 4	10 ± 3	14 ± 4	2
XMMXCS J090130.07-013859.6	$0.309^{+0.074}_{-0.075}$	0.338 ± 0.050	-	-0.072 ± 0.018	2.970 ± 0.357	0.001	23 ± 5	25 ± 5	34 ± 6	34 ± 7	2
XMMXCS J090138.59-015856.5	$0.320^{+0.064}_{-0.065}$	0.345 ± 0.053	-	0.156 ± 0.179	-1.280 ± 3.340	0.235	7 ± 3	8 ± 4	9 ± 3	8 ± 4	2
XMMXCS J090434.2+555037.3	$0.246^{+0.088}_{-0.086}$	0.218 ± 0.063	-	0.131 ± 0.067	-1.380 ± 1.290	0.091	2 ± 2	2 ± 2	1 ± 1	1 ± 1	2
XMMXCS J090730.0+620814.2	$0.379^{+0.088}_{-0.088}$	0.330 ± 0.210	-	-0.124 ± 0.178	3.590 ± 3.550	0.072	4 ± 3	5 ± 3	3 ± 2	2 ± 2	2
XMMXCS J090915.6+543021.9	$0.607^{+0.163}_{-0.163}$	0.652 ± 0.135	-	0.038 ± 0.113	0.299 ± 2.310	0.065	2 ± 2	1 ± 3	3 ± 2	5 ± 2	2
XMMXCS J090956.6+544200.9	$0.175^{+0.036}_{-0.037}$	0.171 ± 0.026	$0.175 \pm 2.2e-05$	-0.049 ± 0.022	1.950 ± 0.391	0.001	3 ± 2	3 ± 2	2 ± 1	2 ± 2	2
XMMXCS J091128.9+542906.0	$0.157^{+0.063}_{-0.066}$	0.175 ± 0.032	-	-0.072 ± 0.010	2.420 ± 0.192	0.001	2 ± 2	1 ± 1	1 ± 1	1 ± 1	2
XMMXCS J091535.4+441044.7	$0.468^{+0.115}_{-0.113}$	0.497 ± 0.074	-	-0.018 ± 0.037	1.170 ± 0.736	0.034	18 ± 5	19 ± 5	24 ± 6	25 ± 6	2
XMMXCS J091609.0+302718.1	$0.630^{+0.168}_{-0.169}$	0.600 ± 0.099	-	-0.013 ± 0.058	1.310 ± 1.150	0.001	7 ± 3	127 ± 12	7 ± 3	90 ± 13	2
XMMXCS J091714.6+301739.0	$0.515^{+0.125}_{-0.125}$	0.488 ± 0.146	-	-0.017 ± 0.048	1.250 ± 0.944	0.098	9 ± 4	13 ± 5	8 ± 3	16 ± 5	2
XMMXCS J091828.3+513932.0	$0.208^{+0.044}_{-0.041}$	0.197 ± 0.050	-	-0.008 ± 0.027	1.430 ± 0.502	0.076	3 ± 2	1 ± 2	1 ± 1	0 ± 1	2
XMMXCS J091854.8+513933.0	$0.184^{+0.056}_{-0.056}$	0.180 ± 0.035	$0.186 \pm 3.4e-05$	0.026 ± 0.031	0.689 ± 0.566	0.105	5 ± 3	10 ± 4	1 ± 1	5 ± 3	2
XMMXCS J092102.2+300533.0	$0.529^{+0.114}_{-0.113}$	0.498 ± 0.074	-	-0.039 ± 0.050	1.740 ± 1.000	0.001	11 ± 4	16 ± 5	11 ± 4	26 ± 6	2

Continued on next page

Table A.2 – continued from previous page

name	z_{RS}	z_{BCG}	z_{spec-g}	cmr_{grad}	cmr_{inter}	cmr_{wid}	n_{gals-c}	n_{gals-l}	n_{200-c}	n_{200-l}	qual
XMMXCS J092111.0+302758.2	$0.395^{+0.085}_{-0.084}$	0.422 ± 0.061	$0.429 \pm 9.7e-05$	-0.052 ± 0.035	2.630 ± 0.675	0.070	28 ± 6	29 ± 6	57 ± 8	56 ± 9	2
XMMXCS J092111.8+302757.0	$0.390^{+0.085}_{-0.085}$	0.422 ± 0.061	$0.429 \pm 9.7e-05$	-0.071 ± 0.036	2.970 ± 0.700	0.073	29 ± 6	30 ± 6	57 ± 8	53 ± 8	2
XMMXCS J092206.8+301155.0	$0.164^{+0.034}_{-0.034}$	0.136 ± 0.028	$0.128 \pm 1.2e-05$	0.046 ± 0.036	0.141 ± 0.620	0.116	3 ± 2	1 ± 2	1 ± 1	2 ± 2	2
XMMXCS J092212.8+300718.3	$0.263^{+0.049}_{-0.050}$	0.213 ± 0.035	-	0.031 ± 0.048	0.918 ± 0.947	0.093	8 ± 3	8 ± 4	9 ± 3	8 ± 3	2
XMMXCS J092540.0+362711.1	$0.115^{+0.017}_{-0.017}$	0.127 ± 0.024	$0.112 \pm 1.1e-05$	-0.022 ± 0.006	1.370 ± 0.096	0.001	3 ± 2	4 ± 2	1 ± 1	1 ± 1	2
XMMXCS J092553.9+304932.1	$0.551^{+0.123}_{-0.123}$	0.579 ± 0.114	-	-0.055 ± 0.062	2.170 ± 1.220	0.001	14 ± 4	38 ± 7	14 ± 4	57 ± 9	2
XMMXCS J092607.5+363413.1	$0.103^{+0.067}_{-0.072}$	0.114 ± 0.026	$0.112 \pm 1.6e-05$	-0.037 ± 0.038	1.580 ± 0.666	0.115	2 ± 2	0 ± 1	1 ± 1	-	2
XMMXCS J092744.6+362436.3	$0.106^{+0.027}_{-0.029}$	0.107 ± 0.022	$0.098 \pm 1.6e-05$	0.017 ± 0.037	0.681 ± 0.669	0.095	2 ± 2	1 ± 1	1 ± 1	1 ± 1	2
XMMXCS J093157.9+472719.7	$0.257^{+0.083}_{-0.091}$	0.225 ± 0.062	-	0.008 ± 0.010	1.040 ± 0.176	0.074	4 ± 2	12 ± 4	4 ± 2	11 ± 4	2
XMMXCS J093449.2+551023.5	$0.623^{+0.153}_{-0.152}$	0.587 ± 0.241	-	-0.014 ± 0.169	1.430 ± 3.420	0.001	5 ± 3	-	5 ± 2	-	2
XMMXCS J094036.2+034038.0	$0.579^{+0.135}_{-0.130}$	0.568 ± 0.101	$0.562 \pm 1.8e-04$	-0.080 ± 0.075	2.470 ± 1.510	0.100	3 ± 3	15 ± 5	2 ± 2	13 ± 5	2
XMMXCS J094059.9+384527.3	$0.287^{+0.078}_{-0.078}$	0.292 ± 0.045	$0.287 \pm 3.3e-05$	-0.096 ± 0.045	3.250 ± 0.872	0.001	3 ± 2	5 ± 3	2 ± 2	5 ± 3	2
XMMXCS J094102.0+150244.8	$0.296^{+0.140}_{-0.144}$	0.320 ± 0.049	$0.361 \pm 4.3e-05$	-0.142 ± 0.079	4.080 ± 1.570	0.001	4 ± 3	6 ± 3	2 ± 2	3 ± 2	2
XMMXCS J094105.2+033256.9	$0.386^{+0.160}_{-0.161}$	0.336 ± 0.094	-	-0.087 ± 0.243	2.740 ± 4.890	0.001	8 ± 4	9 ± 4	8 ± 3	8 ± 4	2
XMMXCS J094203.6+470031.5	$0.410^{+0.189}_{-0.107}$	0.345 ± 0.058	$0.470 \pm 9.0e-05$	-0.031 ± 0.044	1.340 ± 0.890	0.110	2 ± 3	3 ± 3	1 ± 1	-	2
XMMXCS J094226.0+470315.0	$0.421^{+0.116}_{-0.116}$	0.395 ± 0.061	$0.547 \pm 1.4e-04$	-0.013 ± 0.051	1.880 ± 1.000	0.001	8 ± 4	20 ± 5	10 ± 4	21 ± 6	2
XMMXCS J094251.7+470519.2	$0.186^{+0.108}_{-0.117}$	0.141 ± 0.028	-	-0.023 ± 0.032	1.500 ± 0.637	0.038	1 ± 1	0 ± 1	1 ± 1	-	2
XMMXCS J094310.4+465245.5	$0.234^{+0.079}_{-0.085}$	0.246 ± 0.042	-	-0.245 ± 0.001	6.440 ± 0.017	0.500	6 ± 3	5 ± 3	2 ± 2	2 ± 2	2
XMMXCS J094311.2+480956.1	$0.314^{+0.065}_{-0.065}$	0.300 ± 0.068	$0.309 \pm 6.0e-05$	0.022 ± 0.040	1.160 ± 0.733	0.156	9 ± 4	10 ± 4	10 ± 4	11 ± 4	2

Continued on next page

Table A.2 – continued from previous page

name	z_{RS}	z_{BCG}	z_{spec-g}	cmr_{grad}	cmr_{inter}	cmr_{wid}	n_{gals-c}	n_{gals-l}	n_{200-c}	n_{200-l}	qual
XMMXCS J094437.6+040041.6	$0.343^{+0.067}_{-0.070}$	0.382 ± 0.056	-	-0.017 ± 0.044	2.120 ± 0.849	0.001	5 ± 3	4 ± 3	1 ± 1	0 ± 1	2
XMMXCS J095245.3+013416.1	$0.643^{+0.126}_{-0.121}$	0.557 ± 0.089	$0.628 \pm 1.6e-04$	0.021 ± 0.111	0.732 ± 2.280	0.001	1 ± 2	-	1 ± 1	-	2
XMMXCS J095414.8+013901.6	$0.093^{+0.035}_{-0.035}$	0.110 ± 0.021	$0.088 \pm 1.1e-05$	-0.019 ± 0.069	1.180 ± 1.200	0.141	3 ± 2	1 ± 2	1 ± 1	1 ± 1	2
XMMXCS J095508.3+694339.6	$0.195^{+0.093}_{-0.092}$	0.235 ± 0.177	-	0.041 ± 0.048	0.060 ± 0.905	0.083	3 ± 2	4 ± 3	1 ± 1	0 ± 1	2
XMMXCS J095517.8+653551.6	$0.432^{+0.132}_{-0.132}$	0.461 ± 0.088	-	0.028 ± 0.166	1.290 ± 3.140	0.001	21 ± 5	22 ± 5	23 ± 6	24 ± 6	2
XMMXCS J095729.3+410636.8	$0.453^{+0.074}_{-0.069}$	0.403 ± 0.062	$0.444 \pm 1.3e-04$	0.005 ± 0.049	0.658 ± 0.936	0.082	1 ± 3	1 ± 3	1 ± 1	37 ± 6	2
XMMXCS J095740.83+021908.8	$0.533^{+0.141}_{-0.139}$	0.550 ± 0.085	-	-3.890 ± 3.860	82.100 ± 80.10	0.500	3 ± 2	0 ± 1	2 ± 2	-	2
XMMXCS J095740.8+021909.8	$0.536^{+0.142}_{-0.139}$	0.550 ± 0.085	-	-4.510 ± 2.590	94.800 ± 53.70	0.513	2 ± 2	0 ± 1	2 ± 1	-	2
XMMXCS J095746.4+023257.4	$0.361^{+0.109}_{-0.108}$	0.402 ± 0.087	-	0.162 ± 0.140	-1.690 ± 2.790	0.001	10 ± 4	11 ± 4	8 ± 3	11 ± 4	2
XMMXCS J095746.5+022057.4	$0.451^{+0.142}_{-0.144}$	0.467 ± 0.080	-	0.157 ± 0.093	-2.220 ± 1.860	0.065	2 ± 2	2 ± 2	1 ± 1	0 ± 1	2
XMMXCS J095813.1+025707.8	$0.348^{+0.055}_{-0.053}$	0.348 ± 0.060	$0.344 \pm 7.3e-05$	-0.495 ± 0.003	11.200 ± 0.061	0.500	3 ± 3	16 ± 5	1 ± 2	3 ± 4	2
XMMXCS J095819.8+022904.6	$0.374^{+0.057}_{-0.053}$	0.354 ± 0.064	-	-0.201 ± 0.039	5.560 ± 0.759	0.001	1 ± 2	-	1 ± 1	-	2
XMMXCS J095821.86+020924.5	$0.257^{+0.071}_{-0.071}$	0.241 ± 0.040	$0.283 \pm 7.4e-05$	-0.258 ± 0.001	6.290 ± 0.012	0.500	3 ± 3	3 ± 3	1 ± 2	2 ± 2	2
XMMXCS J095821.8+020924.4	$0.257^{+0.071}_{-0.071}$	0.241 ± 0.040	$0.283 \pm 7.4e-05$	-0.258 ± 0.001	6.290 ± 0.012	0.500	3 ± 3	3 ± 3	1 ± 2	2 ± 2	2
XMMXCS J095822.4+020831.8	$0.314^{+0.073}_{-0.072}$	0.278 ± 0.054	-	-0.236 ± 0.066	5.950 ± 1.320	0.069	1 ± 2	3 ± 3	1 ± 1	2 ± 2	2
XMMXCS J095827.7+025607.8	$0.230^{+0.089}_{-0.089}$	0.263 ± 0.047	-	-0.328 ± 0.007	7.630 ± 0.132	0.500	1 ± 2	2 ± 3	2 ± 1	1 ± 2	2
XMMXCS J095835.8+694016.7	$0.402^{+0.073}_{-0.074}$	0.439 ± 0.065	-	-0.098 ± 0.103	3.880 ± 1.980	0.001	11 ± 4	10 ± 4	10 ± 4	10 ± 4	2
XMMXCS J095841.28+023731.8	$0.520^{+0.191}_{-0.218}$	0.553 ± 0.123	-	0.068 ± 0.075	-0.505 ± 1.530	0.066	1 ± 2	0 ± 1	1 ± 1	-	2
XMMXCS J095848.91+023441.7	$0.350^{+0.127}_{-0.137}$	0.301 ± 0.083	-	0.310 ± 0.139	-5.080 ± 2.780	0.175	3 ± 3	1 ± 3	1 ± 1	1 ± 1	2

Continued on next page

Table A.2 – continued from previous page

name	z_{RS}	z_{BCG}	z_{spec-g}	cmr_{grad}	cmr_{inter}	cmr_{wid}	n_{gals-c}	n_{gals-l}	n_{200-c}	n_{200-l}	qual
XMMXCS J095848.9+023441.6	$0.350^{+0.127}_{-0.137}$	0.301 ± 0.083	-	0.310 ± 0.139	-5.080 ± 2.780	0.175	3 ± 3	1 ± 3	1 ± 1	1 ± 1	2
XMMXCS J095850.7+022417.6	$0.359^{+0.084}_{-0.084}$	0.328 ± 0.059	-	0.035 ± 0.096	0.949 ± 1.830	0.138	7 ± 3	7 ± 4	3 ± 2	-	2
XMMXCS J095852.14+021123.5	$0.648^{+0.101}_{-0.092}$	0.644 ± 0.111	$0.631 \pm 1.9e-04$	0.210 ± 0.235	-3.140 ± 4.670	0.155	1 ± 2	11 ± 4	1 ± 1	11 ± 4	2
XMMXCS J095853.24+023748.2	$0.286^{+0.060}_{-0.062}$	0.324 ± 0.088	$0.270 \pm 6.1e-05$	-0.041 ± 0.093	2.260 ± 1.800	0.065	6 ± 3	6 ± 3	2 ± 2	2 ± 2	2
XMMXCS J095857.7+015706.9	$0.434^{+0.097}_{-0.092}$	0.465 ± 0.095	-	0.006 ± 0.084	0.594 ± 1.690	0.125	8 ± 4	8 ± 4	2 ± 3	2 ± 3	2
XMMXCS J095900.1+025338.7	$0.285^{+0.096}_{-0.096}$	0.285 ± 0.058	-	0.018 ± 0.047	1.020 ± 0.919	0.155	4 ± 3	4 ± 3	2 ± 2	1 ± 2	2
XMMXCS J095900.7+021957.6	$0.291^{+0.076}_{-0.078}$	0.261 ± 0.086	-	-0.002 ± 0.054	1.580 ± 1.040	0.001	6 ± 3	5 ± 3	5 ± 2	4 ± 2	2
XMMXCS J095902.9+021905.0	$0.308^{+0.080}_{-0.083}$	0.261 ± 0.086	-	-0.048 ± 0.044	2.450 ± 0.858	0.047	9 ± 3	7 ± 3	8 ± 3	9 ± 3	2
XMMXCS J095904.18+023813.6	$0.365^{+0.074}_{-0.073}$	0.323 ± 0.049	-	0.017 ± 0.152	1.190 ± 2.980	0.070	1 ± 2	1 ± 2	1 ± 1	2 ± 2	2
XMMXCS J095904.2+023814.3	$0.366^{+0.075}_{-0.074}$	0.323 ± 0.049	-	0.017 ± 0.152	1.190 ± 2.980	0.070	1 ± 2	1 ± 2	1 ± 1	2 ± 2	2
XMMXCS J095928.5+021950.4	$0.381^{+0.104}_{-0.098}$	0.385 ± 0.057	-	0.005 ± 0.061	0.584 ± 1.200	0.111	3 ± 3	3 ± 3	1 ± 1	-	2
XMMXCS J095939.7+023108.9	$0.607^{+0.150}_{-0.149}$	0.564 ± 0.282	-	0.548 ± 0.277	-9.660 ± 5.670	0.001	7 ± 3	19 ± 5	7 ± 3	19 ± 5	2
XMMXCS J095940.8+023111.3	$0.595^{+0.158}_{-0.158}$	0.564 ± 0.282	-	0.201 ± 0.253	-2.720 ± 5.110	0.001	9 ± 3	24 ± 5	9 ± 3	29 ± 6	2
XMMXCS J095943.1+251523.9	$0.102^{+0.023}_{-0.020}$	0.134 ± 0.048	$0.115 \pm 1.5e-05$	-0.094 ± 0.026	2.370 ± 0.389	0.089	8 ± 3	7 ± 3	6 ± 3	4 ± 2	2
XMMXCS J095957.6+251629.0	$0.092^{+0.025}_{-0.026}$	0.059 ± 0.021	$0.066 \pm 1.3e-05$	0.013 ± 0.045	0.633 ± 0.778	0.063	7 ± 3	4 ± 2	6 ± 3	3 ± 2	2
XMMXCS J100025.4+015851.2	$0.340^{+0.101}_{-0.102}$	0.345 ± 0.054	-	-0.081 ± 0.106	3.200 ± 2.070	0.001	3 ± 2	4 ± 3	2 ± 2	3 ± 2	2
XMMXCS J100034.6+013633.6	$0.283^{+0.098}_{-0.097}$	0.239 ± 0.107	-	0.028 ± 0.044	0.648 ± 0.855	0.102	2 ± 2	0 ± 2	1 ± 1	-	2
XMMXCS J100034.73+024255.3	$0.302^{+0.143}_{-0.141}$	0.358 ± 0.053	$0.350 \pm 4.2e-05$	-0.120 ± 0.296	3.800 ± 6.130	0.001	2 ± 2	4 ± 3	1 ± 1	3 ± 2	2
XMMXCS J100038.84+023656.7	$0.380^{+0.134}_{-0.141}$	0.367 ± 0.054	-	-0.091 ± 0.072	2.780 ± 1.410	0.500	4 ± 4	4 ± 4	2 ± 2	3 ± 3	2

Continued on next page

Table A.2 – continued from previous page

name	z_{RS}	z_{BCG}	z_{spec-g}	cmr_{grad}	cmr_{inter}	cmr_{wid}	n_{gals-c}	n_{gals-l}	n_{200-c}	n_{200-l}	qual
XMMXCS J100039.2+023655.9	$0.402^{+0.126}_{-0.119}$	0.367 ± 0.054	-	-0.091 ± 0.072	2.780 ± 1.410	0.500	3 ± 4	4 ± 4	2 ± 2	3 ± 3	2
XMMXCS J100056.5+285411.0	$0.099^{+0.009}_{-0.008}$	0.105 ± 0.018	$0.098 \pm 1.5e-05$	-0.022 ± 0.011	1.320 ± 0.183	0.016	6 ± 3	4 ± 2	2 ± 2	1 ± 1	2
XMMXCS J100114.2+554835.3	$0.349^{+0.056}_{-0.054}$	0.344 ± 0.051	$0.348 \pm 6.3e-05$	-0.079 ± 0.034	3.110 ± 0.641	0.028	2 ± 2	6 ± 3	2 ± 1	5 ± 3	2
XMMXCS J100115.83+023607.7	$0.203^{+0.095}_{-0.092}$	0.163 ± 0.044	-	0.016 ± 0.039	0.400 ± 0.753	0.102	1 ± 1	1 ± 2	2 ± 1	1 ± 1	2
XMMXCS J100116.2+021655.9	$0.090^{+0.058}_{-0.050}$	0.165 ± 0.037	$0.106 \pm 1.4e-05$	-0.112 ± 0.001	2.520 ± 0.001	0.500	3 ± 2	1 ± 2	3 ± 2	1 ± 1	2
XMMXCS J100124.6+250655.9	$0.578^{+0.142}_{-0.140}$	0.565 ± 0.122	-	-0.053 ± 0.212	2.200 ± 4.340	0.138	3 ± 2	11 ± 4	1 ± 1	12 ± 4	2
XMMXCS J100148.0+021447.2	$0.190^{+0.054}_{-0.055}$	0.180 ± 0.101	-	0.018 ± 0.106	0.809 ± 1.890	0.072	3 ± 2	2 ± 2	1 ± 1	2 ± 2	2
XMMXCS J100148.1+020342.5	$0.369^{+0.098}_{-0.097}$	0.353 ± 0.055	$0.442 \pm 5.8e-05$	-0.035 ± 0.071	2.220 ± 1.430	0.079	10 ± 4	17 ± 5	10 ± 4	2 ± 3	2
XMMXCS J100149.7+023852.9	$0.225^{+0.051}_{-0.051}$	0.227 ± 0.038	-	-0.035 ± 0.035	1.960 ± 0.641	0.001	3 ± 2	2 ± 2	2 ± 1	1 ± 1	2
XMMXCS J100156.4+554134.1	$0.038^{+0.067}_{-0.038}$	0.099 ± 0.031	$0.004 \pm 9.9e-06$	0.034 ± 0.001	-0.111 ± 0.001	0.500	7 ± 3	1 ± 1	7 ± 3	5 ± 2	2
XMMXCS J100205.2+023729.2	$0.347^{+0.070}_{-0.070}$	0.366 ± 0.054	$0.347 \pm 6.9e-05$	-0.013 ± 0.095	1.940 ± 1.810	0.133	3 ± 3	3 ± 3	1 ± 1	1 ± 2	2
XMMXCS J100210.9+023031.3	$0.194^{+0.081}_{-0.088}$	0.187 ± 0.059	-	-0.028 ± 0.069	1.670 ± 1.340	0.115	2 ± 2	2 ± 2	1 ± 1	1 ± 1	2
XMMXCS J100218.82+015551.2	$0.259^{+0.057}_{-0.057}$	0.316 ± 0.048	$0.308 \pm 5.5e-05$	-0.127 ± 0.042	3.870 ± 0.776	0.001	2 ± 2	3 ± 2	2 ± 1	3 ± 2	2
XMMXCS J100330.6+684420.5	$0.085^{+0.072}_{-0.072}$	0.076 ± 0.018	-	-0.020 ± 0.008	0.589 ± 0.109	0.095	1 ± 1	-	1 ± 1	-	2
XMMXCS J100346.5+324856.9	$0.176^{+0.074}_{-0.074}$	0.189 ± 0.100	-	0.122 ± 0.065	-1.280 ± 1.230	0.132	2 ± 2	3 ± 2	1 ± 1	1 ± 1	2
XMMXCS J100635.4+124949.8	$0.692^{+0.157}_{-0.152}$	0.621 ± 0.105	$0.652 \pm 2.4e-04$	-0.069 ± 0.033	2.440 ± 0.643	0.028	2 ± 2	20 ± 5	1 ± 1	5 ± 4	2
XMMXCS J100655.6+123903.8	$0.420^{+0.088}_{-0.089}$	0.452 ± 0.074	-	0.032 ± 0.096	1.180 ± 1.880	0.001	6 ± 3	6 ± 3	4 ± 2	4 ± 3	2
XMMXCS J100815.1+124229.0	$0.289^{+0.067}_{-0.067}$	0.267 ± 0.063	-	-0.061 ± 0.078	2.650 ± 1.480	0.074	4 ± 3	16 ± 5	1 ± 1	15 ± 5	2
XMMXCS J101020.2+553701.0	$0.142^{+0.051}_{-0.051}$	0.185 ± 0.052	-	0.009 ± 0.056	0.726 ± 1.070	0.111	1 ± 1	0 ± 1	1 ± 1	-	2

Continued on next page

Table A.2 – continued from previous page

name	z_{RS}	z_{BCG}	z_{spec-g}	cmr_{grad}	cmr_{inter}	cmr_{wid}	n_{gals-c}	n_{gals-l}	n_{200-c}	n_{200-l}	qual
XMMXCS J101041.8+554208.5	$0.168^{+0.044}_{-0.044}$	0.185 ± 0.032	$0.178 \pm 4.0e-05$	-0.037 ± 0.037	1.820 ± 0.698	0.095	1 ± 2	3 ± 2	2 ± 1	3 ± 2	2
XMMXCS J101056.3+555711.5	$0.137^{+0.050}_{-0.050}$	0.150 ± 0.034	$0.174 \pm 1.5e-05$	0.169 ± 0.066	-2.150 ± 1.190	0.108	2 ± 2	1 ± 2	1 ± 1	0 ± 1	2
XMMXCS J101103.6+533945.1	$0.314^{+0.060}_{-0.061}$	0.330 ± 0.051	-	-0.040 ± 0.067	2.350 ± 1.360	0.001	3 ± 2	6 ± 3	2 ± 2	7 ± 3	2
XMMXCS J101106.9+462252.4	$0.214^{+0.096}_{-0.096}$	0.166 ± 0.035	-	-0.131 ± 0.056	3.630 ± 1.120	0.079	1 ± 1	0 ± 1	2 ± 1	-	2
XMMXCS J101640.9+385451.0	$0.203^{+0.072}_{-0.072}$	0.168 ± 0.041	$0.185 \pm 2.7e-05$	-0.176 ± 0.255	4.390 ± 5.090	0.500	1 ± 3	4 ± 3	1 ± 1	0 ± 2	2
XMMXCS J101730.6+213353.4	$0.188^{+0.062}_{-0.062}$	0.186 ± 0.030	$0.187 \pm 2.4e-05$	-0.032 ± 0.011	1.780 ± 0.207	0.028	5 ± 3	7 ± 3	2 ± 2	4 ± 2	2
XMMXCS J101738.5+214118.7	$0.148^{+0.118}_{-0.128}$	0.116 ± 0.128	-	-0.008 ± 0.048	0.804 ± 0.830	0.080	22 ± 5	23 ± 5	22 ± 5	26 ± 5	2
XMMXCS J102142.6+130649.2	$0.068^{+0.019}_{-0.019}$	0.054 ± 0.031	$0.061 \pm 7.1e-06$	0.165 ± 0.005	-1.830 ± 0.083	0.001	4 ± 2	2 ± 2	3 ± 2	2 ± 2	2
XMMXCS J102148.5+213916.5	$0.185^{+0.053}_{-0.055}$	0.193 ± 0.029	$0.187 \pm 4.0e-05$	-0.019 ± 0.029	1.530 ± 0.557	0.078	4 ± 2	2 ± 2	1 ± 1	0 ± 1	2
XMMXCS J102235.9+041034.3	$0.375^{+0.116}_{-0.098}$	0.344 ± 0.115	-	0.0001 ± 0.071	1.200 ± 1.420	0.114	6 ± 4	8 ± 4	6 ± 3	5 ± 3	2
XMMXCS J102245.8+194737.7	$0.198^{+0.099}_{-0.099}$	0.206 ± 0.082	$0.189 \pm 2.4e-05$	0.007 ± 0.025	1.110 ± 0.451	0.001	5 ± 2	7 ± 3	1 ± 1	1 ± 2	2
XMMXCS J102327.6+040950.5	$0.224^{+0.057}_{-0.057}$	0.205 ± 0.059	-	0.054 ± 0.091	0.256 ± 1.720	0.070	5 ± 2	5 ± 3	2 ± 1	3 ± 2	2
XMMXCS J102352.3+003115.5	$0.784^{+0.142}_{-0.123}$	0.642 ± 0.144	$0.736 \pm 2.5e-04$	-0.244 ± 0.157	5.510 ± 3.110	0.052	2 ± 2	40 ± 7	1 ± 1	43 ± 8	2
XMMXCS J102355.1+004728.4	$0.583^{+0.166}_{-0.166}$	0.618 ± 0.124	-	1.670 ± 1.120	-33.60 ± 23.20	0.181	4 ± 2	1 ± 1	2 ± 1	0 ± 1	2
XMMXCS J102417.7+041656.1	$0.537^{+0.109}_{-0.110}$	0.505 ± 0.079	$0.539 \pm 1.5e-04$	0.122 ± 0.060	-1.420 ± 1.190	0.001	4 ± 3	5 ± 3	1 ± 1	5 ± 3	2
XMMXCS J102732.9+383718.6	$0.192^{+0.041}_{-0.032}$	0.208 ± 0.038	-	-0.250 ± 0.052	5.690 ± 0.908	0.500	1 ± 2	0 ± 2	1 ± 1	-	2
XMMXCS J103012.4-031601.8	$0.063^{+0.084}_{-0.063}$	0.074 ± 0.023	-	-0.134 ± 0.113	2.800 ± 2.080	0.001	5 ± 2	7 ± 3	2 ± 1	5 ± 2	2
XMMXCS J103024.4+052343.7	$0.219^{+0.056}_{-0.051}$	0.228 ± 0.048	$0.202 \pm 3.4e-05$	-0.000 ± 0.001	0.868 ± 0.001	0.500	2 ± 3	4 ± 4	1 ± 1	2 ± 2	2
XMMXCS J103024.8+051849.4	$0.533^{+0.100}_{-0.089}$	0.570 ± 0.129	-	0.073 ± 0.052	-0.598 ± 1.050	0.104	5 ± 3	8 ± 3	1 ± 1	7 ± 3	2

Continued on next page

Table A.2 – continued from previous page

name	z_{RS}	z_{BCG}	z_{spec-g}	cmr_{grad}	cmr_{inter}	cmr_{wid}	n_{gals-c}	n_{gals-l}	n_{200-c}	n_{200-l}	qual
XMMXCS J103027.8+310801.0	$0.456^{+0.126}_{-0.127}$	0.471 ± 0.070	$0.462 \pm 1.7e-04$	0.074 ± 0.065	-0.533 ± 1.300	0.131	1 ± 3	3 ± 3	1 ± 1	0 ± 1	2
XMMXCS J103042.9-031033.6	$0.103^{+0.067}_{-0.068}$	0.067 ± 0.029	-	-0.072 ± 0.001	1.960 ± 0.001	0.500	8 ± 3	15 ± 5	7 ± 3	18 ± 5	2
XMMXCS J103046.3-030653.3	$0.082^{+0.031}_{-0.032}$	0.129 ± 0.035	-	-0.099 ± 0.144	2.320 ± 2.460	0.112	3 ± 2	1 ± 1	1 ± 1	0 ± 1	2
XMMXCS J103103.3+052504.3	$0.329^{+0.054}_{-0.054}$	0.327 ± 0.048	$0.328 \pm 1.4e-04$	-0.030 ± 0.027	2.190 ± 0.517	0.023	3 ± 2	8 ± 3	2 ± 2	6 ± 3	2
XMMXCS J103243.3+573524.1	$0.592^{+0.124}_{-0.116}$	0.612 ± 0.105	-	0.132 ± 0.068	-1.660 ± 1.350	0.095	3 ± 2	0 ± 1	2 ± 1	-	2
XMMXCS J103405.64+575627.8	$0.199^{+0.086}_{-0.086}$	0.181 ± 0.052	-	0.013 ± 0.024	0.812 ± 0.452	0.021	3 ± 2	1 ± 1	2 ± 1	0 ± 1	2
XMMXCS J103405.6+575627.7	$0.199^{+0.086}_{-0.086}$	0.181 ± 0.052	-	0.013 ± 0.024	0.812 ± 0.452	0.021	3 ± 2	1 ± 1	2 ± 1	0 ± 1	2
XMMXCS J103448.7+574652.9	$0.528^{+0.122}_{-0.120}$	0.484 ± 0.178	-	0.076 ± 0.052	-0.590 ± 1.020	0.001	7 ± 3	14 ± 4	5 ± 3	13 ± 4	2
XMMXCS J103500.6+595022.5	$0.400^{+0.131}_{-0.128}$	0.419 ± 0.063	$0.428 \pm 1.2e-04$	0.018 ± 0.044	0.334 ± 0.897	0.121	5 ± 4	6 ± 4	3 ± 2	3 ± 3	2
XMMXCS J103612.09+580854.6	$0.174^{+0.046}_{-0.044}$	0.146 ± 0.030	-	0.110 ± 0.017	-0.888 ± 0.298	0.085	4 ± 2	5 ± 3	2 ± 1	2 ± 2	2
XMMXCS J103612.2+580853.6	$0.174^{+0.046}_{-0.044}$	0.146 ± 0.030	-	0.110 ± 0.017	-0.888 ± 0.298	0.085	4 ± 2	5 ± 3	2 ± 1	2 ± 2	2
XMMXCS J103930.7+394743.7	$0.093^{+0.011}_{-0.011}$	0.098 ± 0.019	$0.093 \pm 1.5e-05$	0.012 ± 0.029	0.717 ± 0.500	0.068	3 ± 2	2 ± 2	1 ± 1	3 ± 2	2
XMMXCS J104052.7+400659.4	$0.534^{+0.148}_{-0.151}$	0.563 ± 0.100	$0.546 \pm 1.5e-04$	0.131 ± 0.073	-1.420 ± 1.480	0.001	6 ± 3	7 ± 3	2 ± 2	4 ± 2	2
XMMXCS J104053.6+062111.3	$0.272^{+0.156}_{-0.157}$	0.246 ± 0.092	-	-0.223 ± 0.088	5.440 ± 1.750	0.064	1 ± 1	1 ± 2	1 ± 1	0 ± 1	2
XMMXCS J104148.6+061848.6	$0.464^{+0.096}_{-0.094}$	0.458 ± 0.092	$0.484 \pm 9.1e-05$	0.014 ± 0.049	0.530 ± 0.965	0.001	4 ± 3	4 ± 3	1 ± 1	2 ± 2	2
XMMXCS J104344.4+212918.3	$0.227^{+0.083}_{-0.087}$	0.231 ± 0.037	-	0.017 ± 0.060	0.993 ± 1.170	0.092	5 ± 2	5 ± 3	2 ± 2	3 ± 2	2
XMMXCS J104550.6+485649.7	$0.397^{+0.091}_{-0.089}$	0.423 ± 0.072	-	-0.022 ± 0.031	1.100 ± 0.604	0.065	5 ± 3	7 ± 4	5 ± 3	-	2
XMMXCS J104551.5+213350.5	$0.438^{+0.085}_{-0.083}$	0.481 ± 0.073	$0.472 \pm 2.1e-04$	-0.008 ± 0.046	0.901 ± 0.919	0.116	7 ± 4	7 ± 4	4 ± 3	4 ± 3	2
XMMXCS J104619.5+483634.9	$0.135^{+0.051}_{-0.050}$	0.138 ± 0.026	-	-0.026 ± 0.035	1.520 ± 0.643	0.059	5 ± 2	4 ± 2	2 ± 2	2 ± 2	2

Continued on next page

Table A.2 – continued from previous page

name	z_{RS}	z_{BCG}	z_{spec-g}	cmr_{grad}	cmr_{inter}	cmr_{wid}	n_{gals-c}	n_{gals-l}	n_{200-c}	n_{200-l}	qual
XMMXCS J105008.1+325857.9	$0.409^{+0.128}_{-0.129}$	0.371 ± 0.057	-	-0.128 ± 0.106	4.140 ± 2.070	0.044	6 ± 3	6 ± 4	6 ± 3	25 ± 5	2
XMMXCS J105236.6+573054.3	$0.535^{+0.185}_{-0.194}$	0.493 ± 0.112	-	-0.187 ± 0.123	4.660 ± 2.520	0.113	12 ± 4	34 ± 6	12 ± 4	39 ± 8	2
XMMXCS J105250.2+335503.3	$0.498^{+0.133}_{-0.130}$	0.527 ± 0.226	-	0.210 ± 0.124	-3.380 ± 2.530	0.109	1 ± 2	0 ± 1	1 ± 1	-	2
XMMXCS J105251.8+573156.0	$0.512^{+0.159}_{-0.167}$	0.493 ± 0.112	-	-0.056 ± 0.091	2.020 ± 1.840	0.131	1 ± 2	-	1 ± 1	-	2
XMMXCS J105307.4+571503.5	$0.591^{+0.142}_{-0.140}$	0.608 ± 0.253	-	-0.342 ± 0.153	8.110 ± 3.140	0.053	4 ± 2	10 ± 3	2 ± 2	10 ± 3	2
XMMXCS J105421.0+572542.8	$0.217^{+0.087}_{-0.088}$	0.171 ± 0.035	-	-0.022 ± 0.044	1.450 ± 0.858	0.090	1 ± 2	2 ± 2	2 ± 1	1 ± 1	2
XMMXCS J105543.8+572718.5	$0.271^{+0.056}_{-0.057}$	0.229 ± 0.051	-	0.146 ± 0.060	-1.200 ± 1.110	0.001	6 ± 3	9 ± 3	1 ± 1	3 ± 2	2
XMMXCS J105602.2+065140.4	$0.444^{+0.064}_{-0.064}$	0.414 ± 0.063	$0.443 \pm 1.4e-04$	0.001 ± 0.031	0.714 ± 0.611	0.001	6 ± 3	5 ± 3	5 ± 3	5 ± 3	2
XMMXCS J105630.8+070356.1	$0.161^{+0.026}_{-0.026}$	0.175 ± 0.033	$0.132 \pm 1.6e-05$	-0.086 ± 0.044	2.440 ± 0.810	0.097	3 ± 2	3 ± 2	2 ± 1	1 ± 1	2
XMMXCS J110327.6+360358.8	$0.658^{+0.183}_{-0.183}$	0.704 ± 0.120	-	-0.229 ± 0.394	6.170 ± 8.170	0.001	2 ± 2	0 ± 1	1 ± 1	-	2
XMMXCS J110359.0+381505.7	$0.540^{+0.094}_{-0.092}$	0.508 ± 0.075	$0.538 \pm 1.4e-04$	0.182 ± 0.066	-2.690 ± 1.340	0.072	5 ± 3	13 ± 4	2 ± 2	12 ± 4	2
XMMXCS J110402.7+375949.4	$0.200^{+0.074}_{-0.071}$	0.178 ± 0.030	$0.196 \pm 3.0e-05$	0.052 ± 0.001	0.319 ± 0.001	0.500	5 ± 3	4 ± 3	1 ± 2	1 ± 2	2
XMMXCS J110420.7+380554.9	$0.153^{+0.021}_{-0.021}$	0.148 ± 0.024	$0.153 \pm 1.7e-05$	-0.054 ± 0.006	2.000 ± 0.104	0.009	2 ± 2	4 ± 2	1 ± 1	2 ± 2	2
XMMXCS J110428.5+355241.3	$0.101^{+0.029}_{-0.029}$	0.100 ± 0.024	$0.101 \pm 2.3e-05$	-0.005 ± 0.026	1.020 ± 0.446	0.068	3 ± 2	2 ± 2	1 ± 1	1 ± 1	2
XMMXCS J110438.7+382500.5	$0.532^{+0.128}_{-0.129}$	0.531 ± 0.206	$0.510 \pm 1.5e-04$	-0.111 ± 0.138	3.260 ± 2.760	0.083	2 ± 2	5 ± 3	1 ± 1	3 ± 2	2
XMMXCS J110550.8+251748.4	$0.323^{+0.083}_{-0.082}$	0.331 ± 0.063	-	-0.131 ± 0.090	3.940 ± 1.770	0.001	2 ± 2	2 ± 2	2 ± 1	0 ± 1	2
XMMXCS J110811.6+770155.2	$0.205^{+0.065}_{-0.065}$	0.176 ± 0.031	-	0.042 ± 0.084	0.362 ± 1.640	0.149	3 ± 2	5 ± 3	3 ± 2	3 ± 2	2
XMMXCS J110945.9+612203.0	$0.360^{+0.091}_{-0.089}$	0.378 ± 0.064	-	-0.226 ± 0.334	6.090 ± 6.710	0.142	3 ± 3	2 ± 3	1 ± 1	-	2
XMMXCS J110954.0+482704.6	$0.511^{+0.156}_{-0.156}$	0.542 ± 0.110	-	0.184 ± 0.078	-2.850 ± 1.590	0.001	15 ± 4	52 ± 8	20 ± 5	83 ± 10	2

Continued on next page

Table A.2 – continued from previous page

name	z_{RS}	z_{BCG}	z_{spec-g}	cmr_{grad}	cmr_{inter}	cmr_{wid}	n_{gals-c}	n_{gals-l}	n_{200-c}	n_{200-l}	qual
XMMXCS J111021.6+612819.0	$0.247^{+0.066}_{-0.067}$	0.274 ± 0.043	-	-0.032 ± 0.039	2.010 ± 0.724	0.056	7 ± 3	8 ± 3	5 ± 2	5 ± 3	2
XMMXCS J111237.9+062307.7	$0.388^{+0.107}_{-0.110}$	0.352 ± 0.053	-	-0.000 ± 0.276	1.600 ± 5.520	0.091	4 ± 3	3 ± 3	1 ± 2	1 ± 2	2
XMMXCS J111253.4+062321.1	$0.386^{+0.106}_{-0.102}$	0.399 ± 0.155	$0.433 \pm 1.5e-04$	-1.440 ± 0.189	30.500 ± 3.890	0.500	1 ± 3	3 ± 3	1 ± 1	2 ± 2	2
XMMXCS J111538.5+424356.8	$0.629^{+0.193}_{-0.207}$	0.608 ± 0.135	-	0.214 ± 0.151	-3.110 ± 3.050	0.001	3 ± 2	-	2 ± 1	-	2
XMMXCS J111658.6+174940.7	$0.440^{+0.068}_{-0.067}$	0.409 ± 0.061	$0.439 \pm 9.0e-05$	0.013 ± 0.015	0.476 ± 0.293	0.001	4 ± 3	6 ± 3	2 ± 2	-	2
XMMXCS J111726.0+074327.7	$0.441^{+0.085}_{-0.085}$	0.475 ± 0.069	-	0.017 ± 0.037	0.432 ± 0.743	0.093	23 ± 5	28 ± 6	30 ± 7	-	2
XMMXCS J111729.7+074632.1	$0.160^{+0.029}_{-0.029}$	0.152 ± 0.024	$0.159 \pm 3.0e-05$	-0.068 ± 0.045	2.220 ± 0.760	0.084	5 ± 3	6 ± 3	2 ± 2	3 ± 2	2
XMMXCS J111741.1+073535.9	$0.493^{+0.125}_{-0.124}$	0.530 ± 0.088	-	-0.077 ± 0.029	2.420 ± 0.582	0.041	3 ± 3	1 ± 3	1 ± 1	2 ± 2	2
XMMXCS J111748.1+074619.3	$0.141^{+0.064}_{-0.072}$	0.180 ± 0.106	$0.140 \pm 2.6e-05$	-0.071 ± 0.061	2.150 ± 1.120	0.500	4 ± 3	2 ± 2	2 ± 2	1 ± 1	2
XMMXCS J111749.0+410901.0	$0.325^{+0.063}_{-0.062}$	0.286 ± 0.045	-	0.187 ± 0.042	-2.050 ± 0.835	0.001	6 ± 3	7 ± 3	3 ± 2	6 ± 3	2
XMMXCS J111754.1+440611.6	$0.328^{+0.078}_{-0.085}$	0.360 ± 0.054	-	-0.065 ± 0.040	2.910 ± 0.753	0.057	3 ± 2	2 ± 2	1 ± 1	-	2
XMMXCS J111820.1+401757.9	$0.153^{+0.022}_{-0.022}$	0.136 ± 0.029	$0.152 \pm 1.1e-05$	0.031 ± 0.046	0.093 ± 0.804	0.091	2 ± 2	2 ± 2	1 ± 1	2 ± 2	2
XMMXCS J111823.3+403501.2	$0.256^{+0.120}_{-0.119}$	0.294 ± 0.135	-	2.280 ± 0.451	-43.10 ± 8.870	0.116	1 ± 1	0 ± 1	1 ± 1	-	2
XMMXCS J112004.3+211519.5	$0.125^{+0.037}_{-0.039}$	0.135 ± 0.027	$0.114 \pm 1.8e-05$	0.007 ± 0.039	0.843 ± 0.695	0.063	2 ± 2	1 ± 1	2 ± 1	0 ± 1	2
XMMXCS J112216.7+052146.4	$0.333^{+0.082}_{-0.083}$	0.297 ± 0.045	$0.332 \pm 6.8e-05$	-0.018 ± 0.060	1.890 ± 1.140	0.001	16 ± 4	16 ± 5	19 ± 5	18 ± 5	2
XMMXCS J112259.3+465916.8	$0.448^{+0.102}_{-0.101}$	0.477 ± 0.077	-	-0.052 ± 0.036	1.830 ± 0.721	0.078	17 ± 5	17 ± 5	19 ± 5	19 ± 5	2
XMMXCS J112410.2+062235.0	$0.270^{+0.095}_{-0.095}$	0.314 ± 0.051	$0.308 \pm 6.2e-05$	-0.038 ± 0.136	2.170 ± 2.720	0.102	6 ± 3	4 ± 3	3 ± 2	1 ± 2	2
XMMXCS J112419.6+470000.1	$0.530^{+0.118}_{-0.118}$	0.496 ± 0.073	-	0.099 ± 0.018	-0.958 ± 0.360	0.001	11 ± 4	49 ± 7	11 ± 4	87 ± 10	2
XMMXCS J113109.4-035838.7	$0.161^{+0.047}_{-0.048}$	0.125 ± 0.025	-	-0.101 ± 0.092	2.930 ± 1.700	0.095	2 ± 2	1 ± 1	2 ± 1	1 ± 1	2

Continued on next page

Table A.2 – continued from previous page

name	z_{RS}	z_{BCG}	z_{spec-g}	cmr_{grad}	cmr_{inter}	cmr_{wid}	n_{gals-c}	n_{gals-l}	n_{200-c}	n_{200-l}	qual
XMMXCS J113313.8+662243.9	$0.116^{+0.020}_{-0.020}$	0.145 ± 0.030	$0.118 \pm 1.7e-05$	-0.018 ± 0.005	1.320 ± 0.080	0.004	18 ± 4	20 ± 5	22 ± 5	25 ± 5	2
XMMXCS J113908.5+030433.1	$0.156^{+0.076}_{-0.090}$	0.121 ± 0.023	$0.107 \pm 2.1e-05$	-0.023 ± 0.043	1.590 ± 0.796	0.116	3 ± 2	2 ± 2	2 ± 1	0 ± 1	2
XMMXCS J114025.1+030619.9	$0.247^{+0.070}_{-0.074}$	0.207 ± 0.039	-	0.073 ± 0.077	0.018 ± 1.450	0.049	4 ± 2	3 ± 2	3 ± 2	4 ± 2	2
XMMXCS J114035.8-015243.6	$0.147^{+0.018}_{-0.017}$	0.147 ± 0.031	$0.144 \pm 2.2e-05$	-0.161 ± 0.046	3.500 ± 0.828	0.500	1 ± 2	0 ± 2	1 ± 1	-	2
XMMXCS J114344.2+195850.1	$0.377^{+0.070}_{-0.073}$	0.368 ± 0.121	$0.382 \pm 6.4e-05$	-0.032 ± 0.013	2.300 ± 0.247	0.022	5 ± 3	8 ± 4	1 ± 2	3 ± 3	2
XMMXCS J114643.9+472600.8	$0.538^{+0.120}_{-0.115}$	0.573 ± 0.109	-	0.317 ± 0.183	-5.450 ± 3.780	0.124	5 ± 3	10 ± 4	2 ± 2	7 ± 4	2
XMMXCS J115012.9+014549.5	$0.317^{+0.128}_{-0.133}$	0.288 ± 0.127	-	-0.008 ± 0.094	1.310 ± 1.830	0.001	1 ± 2	1 ± 2	1 ± 1	0 ± 1	2
XMMXCS J115042.7+545636.8	$0.228^{+0.078}_{-0.078}$	0.230 ± 0.034	$0.228 \pm 6.1e-05$	-0.030 ± 0.022	1.900 ± 0.400	0.001	2 ± 2	1 ± 2	2 ± 1	1 ± 1	2
XMMXCS J115103.3+551124.9	$0.230^{+0.054}_{-0.054}$	0.187 ± 0.087	-	0.005 ± 0.048	1.300 ± 0.901	0.059	5 ± 3	4 ± 3	3 ± 2	5 ± 2	2
XMMXCS J115112.0+550655.5	$0.079^{+0.020}_{-0.019}$	0.075 ± 0.015	$0.078 \pm 1.1e-05$	-0.013 ± 0.007	1.060 ± 0.112	0.032	2 ± 2	3 ± 2	1 ± 1	4 ± 2	2
XMMXCS J115516.2+231651.8	$0.134^{+0.032}_{-0.031}$	0.110 ± 0.024	$0.100 \pm 1.9e-05$	0.045 ± 0.025	0.218 ± 0.441	0.061	18 ± 4	18 ± 4	27 ± 5	26 ± 5	2
XMMXCS J115559.1+064520.9	$0.048^{+0.042}_{-0.043}$	0.077 ± 0.045	-	0.039 ± 0.044	-0.092 ± 0.609	0.065	4 ± 2	2 ± 2	4 ± 2	5 ± 2	2
XMMXCS J115818.7+440901.0	$0.294^{+0.076}_{-0.078}$	0.253 ± 0.041	-	-0.029 ± 0.036	2.040 ± 0.682	0.060	9 ± 3	10 ± 4	6 ± 3	9 ± 4	2
XMMXCS J115824.6+440533.9	$0.352^{+0.077}_{-0.077}$	0.309 ± 0.105	-	0.072 ± 0.080	0.183 ± 1.590	0.097	8 ± 3	12 ± 4	6 ± 3	12 ± 4	2
XMMXCS J115854.7+435118.0	$0.222^{+0.075}_{-0.074}$	0.213 ± 0.045	-	0.014 ± 0.038	0.920 ± 0.751	0.097	2 ± 2	1 ± 2	1 ± 1	1 ± 1	2
XMMXCS J115952.4+553204.9	$0.081^{+0.019}_{-0.019}$	0.091 ± 0.016	$0.081 \pm 1.1e-05$	-0.010 ± 0.033	1.060 ± 0.561	0.082	3 ± 2	1 ± 1	2 ± 1	0 ± 1	2
XMMXCS J120040.5+342241.4	$0.261^{+0.059}_{-0.061}$	0.256 ± 0.045	$0.263 \pm 3.3e-05$	0.004 ± 0.017	1.370 ± 0.328	0.043	5 ± 3	7 ± 3	1 ± 1	2 ± 2	2
XMMXCS J120156.0+341730.1	$0.366^{+0.085}_{-0.086}$	0.387 ± 0.058	-	0.007 ± 0.068	1.470 ± 1.360	0.114	1 ± 2	1 ± 2	1 ± 1	0 ± 1	2
XMMXCS J120409.6+202035.8	$0.024^{+0.001}_{-0.001}$	0.052 ± 0.019	$0.024 \pm 5.5e-06$	-0.018 ± 0.005	1.020 ± 0.078	0.019	5 ± 2	0 ± 1	2 ± 1	-	2

Continued on next page

Table A.2 – continued from previous page

name	z_{RS}	z_{BCG}	z_{spec-g}	cmr_{grad}	cmr_{inter}	cmr_{wid}	n_{gals-c}	n_{gals-l}	n_{200-c}	n_{200-l}	qual
XMMXCS J120449.1+020452.4	$0.102^{+0.055}_{-0.077}$	0.069 ± 0.029	$0.066 \pm 1.3e-05$	-0.013 ± 0.015	1.020 ± 0.215	0.094	3 ± 2	6 ± 3	1 ± 1	5 ± 3	2
XMMXCS J120532.3+441910.3	$0.331^{+0.070}_{-0.071}$	0.359 ± 0.055	$0.334 \pm 9.3e-05$	0.039 ± 0.034	0.950 ± 0.687	0.052	8 ± 3	8 ± 3	9 ± 3	9 ± 3	2
XMMXCS J120550.2+444309.1	$0.396^{+0.109}_{-0.107}$	0.354 ± 0.176	-	0.096 ± 0.041	-1.330 ± 0.828	0.094	10 ± 4	8 ± 4	9 ± 4	8 ± 4	2
XMMXCS J120551.7+352349.3	$0.494^{+0.145}_{-0.144}$	0.463 ± 0.130	-	0.174 ± 0.071	-2.510 ± 1.450	0.105	4 ± 3	5 ± 3	1 ± 1	-	2
XMMXCS J120606.8+441923.8	$0.281^{+0.051}_{-0.052}$	0.329 ± 0.051	-	0.021 ± 0.087	1.210 ± 1.640	0.041	3 ± 2	0 ± 2	4 ± 2	-	2
XMMXCS J120746.97+281318.9	$0.406^{+0.103}_{-0.102}$	0.455 ± 0.079	$0.462 \pm 1.2e-04$	-0.052 ± 0.029	1.750 ± 0.569	0.090	27 ± 6	28 ± 6	38 ± 7	-	2
XMMXCS J120815.5+250004.3	$0.062^{+0.039}_{-0.040}$	0.056 ± 0.026	$0.023 \pm 5.2e-06$	-0.029 ± 0.016	1.230 ± 0.276	0.082	5 ± 2	5 ± 2	5 ± 2	6 ± 3	2
XMMXCS J120958.5+392455.8	$0.137^{+0.050}_{-0.059}$	0.162 ± 0.026	$0.160 \pm 2.8e-05$	0.019 ± 0.019	0.766 ± 0.356	0.069	4 ± 2	2 ± 2	1 ± 1	1 ± 1	2
XMMXCS J121029.0+391749.3	$0.206^{+0.098}_{-0.103}$	0.234 ± 0.052	-	-0.041 ± 0.048	1.980 ± 0.957	0.126	1 ± 2	1 ± 2	1 ± 1	1 ± 1	2
XMMXCS J121034.3+393041.8	$0.572^{+0.123}_{-0.122}$	0.598 ± 0.101	-	-0.047 ± 0.085	2.010 ± 1.730	0.001	2 ± 2	5 ± 3	1 ± 1	-	2
XMMXCS J121039.4+391155.8	$0.640^{+0.162}_{-0.162}$	0.680 ± 0.151	-	-0.028 ± 0.394	1.880 ± 8.160	0.001	7 ± 3	29 ± 6	6 ± 3	30 ± 6	2
XMMXCS J121048.2+393745.6	$0.197^{+0.052}_{-0.051}$	0.205 ± 0.062	$0.197 \pm 1.0e-05$	0.063 ± 0.040	0.014 ± 0.750	0.500	1 ± 2	0 ± 2	2 ± 1	-	2
XMMXCS J121111.6+391234.1	$0.304^{+0.083}_{-0.085}$	0.258 ± 0.047	$0.301 \pm 4.3e-05$	-0.022 ± 0.039	2.050 ± 0.757	0.083	12 ± 4	14 ± 4	13 ± 4	12 ± 4	2
XMMXCS J121120.1+391441.0	$0.306^{+0.086}_{-0.086}$	0.258 ± 0.047	$0.264 \pm 3.4e-05$	-0.043 ± 0.035	2.350 ± 0.684	0.118	6 ± 3	4 ± 3	2 ± 2	1 ± 2	2
XMMXCS J121156.7+502918.8	$0.096^{+0.015}_{-0.015}$	0.106 ± 0.017	$0.089 \pm 1.3e-05$	-0.027 ± 0.022	1.430 ± 0.351	0.051	2 ± 2	1 ± 1	2 ± 1	2 ± 2	2
XMMXCS J121731.5+294430.0	$0.575^{+0.149}_{-0.142}$	0.531 ± 0.086	-	0.017 ± 0.107	0.592 ± 2.130	0.067	2 ± 2	2 ± 3	1 ± 1	-	2
XMMXCS J121804.7+294236.3	$0.234^{+0.071}_{-0.071}$	0.215 ± 0.060	-	0.004 ± 0.062	1.270 ± 1.140	0.098	1 ± 2	3 ± 2	1 ± 1	3 ± 2	2
XMMXCS J121859.3+472820.5	$0.581^{+0.110}_{-0.109}$	0.570 ± 0.110	-	0.067 ± 0.047	-0.297 ± 0.926	0.001	3 ± 2	5 ± 3	2 ± 2	6 ± 3	2
XMMXCS J121904.8+053858.0	$0.312^{+0.067}_{-0.071}$	0.342 ± 0.066	$0.291 \pm 6.7e-05$	0.050 ± 0.071	0.561 ± 1.360	0.084	3 ± 2	3 ± 3	1 ± 1	-	2

Continued on next page

Table A.2 – continued from previous page

name	z_{RS}	z_{BCG}	z_{spec-g}	cmr_{grad}	cmr_{inter}	cmr_{wid}	n_{gals-c}	n_{gals-l}	n_{200-c}	n_{200-l}	qual
XMMXCS J121910.3+470535.9	$0.590^{+0.139}_{-0.132}$	0.554 ± 0.114	-	-0.638 ± 0.327	14.200 ± 6.750	0.500	10 ± 4	38 ± 7	8 ± 4	88 ± 12	2
XMMXCS J121934.1+063040.5	$0.270^{+0.097}_{-0.099}$	0.323 ± 0.051	$0.298 \pm 5.2e-05$	-0.192 ± 0.153	4.960 ± 2.960	0.075	5 ± 3	5 ± 3	1 ± 1	0 ± 1	2
XMMXCS J122107.9+281619.5	$0.222^{+0.082}_{-0.082}$	0.204 ± 0.043	-	0.017 ± 0.048	1.020 ± 0.927	0.045	1 ± 1	1 ± 2	2 ± 1	0 ± 1	2
XMMXCS J122122.8+143251.6	$0.424^{+0.112}_{-0.115}$	0.431 ± 0.065	-	0.078 ± 0.047	-0.812 ± 0.948	0.092	4 ± 3	2 ± 3	2 ± 2	0 ± 1	2
XMMXCS J122226.8+142820.7	$0.239^{+0.079}_{-0.079}$	0.199 ± 0.048	-	0.058 ± 0.106	0.265 ± 1.960	0.049	6 ± 3	6 ± 3	4 ± 2	4 ± 2	2
XMMXCS J122443.8+071103.5	$0.658^{+0.102}_{-0.099}$	0.556 ± 0.090	$0.655 \pm 1.3e-04$	-0.075 ± 0.018	2.640 ± 0.356	0.001	3 ± 2	-	2 ± 2	-	2
XMMXCS J122454.2+045903.7	$0.174^{+0.054}_{-0.056}$	0.165 ± 0.025	-	0.111 ± 0.054	-0.808 ± 0.973	0.069	4 ± 2	3 ± 2	1 ± 1	0 ± 1	2
XMMXCS J122534.3+175854.3	$0.463^{+0.111}_{-0.113}$	0.400 ± 0.157	$0.469 \pm 1.1e-04$	0.200 ± 0.108	-3.070 ± 2.160	0.077	5 ± 3	5 ± 3	2 ± 2	-	2
XMMXCS J122547.5+322236.4	$0.614^{+0.150}_{-0.150}$	0.636 ± 0.158	-	0.179 ± 0.478	-2.800 ± 9.830	0.115	2 ± 2	0 ± 1	2 ± 1	-	2
XMMXCS J122558.4+333627.9	$0.240^{+0.067}_{-0.072}$	0.197 ± 0.031	-	0.034 ± 0.072	0.678 ± 1.380	0.086	2 ± 2	2 ± 2	1 ± 1	0 ± 1	2
XMMXCS J122600.5+333347.3	$0.307^{+0.075}_{-0.071}$	0.320 ± 0.054	-	-0.035 ± 0.203	2.020 ± 4.030	0.500	1 ± 3	0 ± 3	2 ± 1	-	2
XMMXCS J122608.09+130654.0	$0.389^{+0.069}_{-0.069}$	0.352 ± 0.053	-	-0.029 ± 0.052	2.250 ± 1.010	0.001	6 ± 3	6 ± 3	1 ± 2	2 ± 2	2
XMMXCS J122719.5+435810.4	$0.383^{+0.072}_{-0.070}$	0.376 ± 0.067	-	0.001 ± 0.055	0.629 ± 1.080	0.042	3 ± 3	-	2 ± 2	-	2
XMMXCS J122833.0+015550.6	$0.197^{+0.095}_{-0.105}$	0.160 ± 0.040	-	0.018 ± 0.030	0.694 ± 0.570	0.031	3 ± 2	2 ± 2	2 ± 1	0 ± 1	2
XMMXCS J122859.4+021132.3	$0.074^{+0.063}_{-0.069}$	0.086 ± 0.019	$0.081 \pm 1.0e-05$	-0.025 ± 0.017	1.210 ± 0.302	0.058	2 ± 2	0 ± 1	1 ± 1	-	2
XMMXCS J122903.6+015240.3	$0.305^{+0.069}_{-0.073}$	0.317 ± 0.047	$0.314 \pm 5.4e-05$	-0.065 ± 0.047	2.850 ± 0.918	0.069	5 ± 3	6 ± 3	2 ± 2	-	2
XMMXCS J122912.1+075655.1	$0.129^{+0.049}_{-0.048}$	0.130 ± 0.022	$0.127 \pm 1.1e-05$	0.063 ± 0.067	-0.126 ± 1.190	0.102	4 ± 2	4 ± 2	2 ± 2	2 ± 2	2
XMMXCS J122934.8+080038.7	$0.050^{+0.024}_{-0.024}$	0.064 ± 0.022	$0.066 \pm 1.6e-05$	0.069 ± 0.001	-0.568 ± 0.004	0.500	1 ± 2	0 ± 1	1 ± 1	-	2
XMMXCS J123009.5+640350.9	$0.123^{+0.030}_{-0.031}$	0.098 ± 0.024	$0.105 \pm 1.2e-05$	0.053 ± 0.042	-0.089 ± 0.690	0.082	4 ± 2	5 ± 3	1 ± 1	1 ± 1	2

Continued on next page

Table A.2 – continued from previous page

name	z_{RS}	z_{BCG}	z_{spec-g}	cmr_{grad}	cmr_{inter}	cmr_{wid}	n_{gals-c}	n_{gals-l}	n_{200-c}	n_{200-l}	qual
XMMXCS J123018.7+110102.5	$0.167^{+0.038}_{-0.038}$	0.165 ± 0.024	$0.167 \pm 4.9e-05$	-0.026 ± 0.016	1.610 ± 0.276	0.023	2 ± 2	1 ± 2	2 ± 1	2 ± 2	2
XMMXCS J123018.81+110101.7	$0.167^{+0.038}_{-0.038}$	0.165 ± 0.024	$0.167 \pm 4.9e-05$	-0.026 ± 0.016	1.610 ± 0.276	0.023	2 ± 2	1 ± 2	2 ± 1	2 ± 2	2
XMMXCS J123024.02+111126.9	$0.407^{+0.142}_{-0.158}$	0.396 ± 0.088	-	0.161 ± 0.093	-1.930 ± 1.850	0.155	4 ± 3	4 ± 3	1 ± 2	-	2
XMMXCS J123032.97+105720.1	$0.297^{+0.064}_{-0.064}$	0.294 ± 0.071	-	-0.046 ± 0.053	2.420 ± 1.010	0.068	3 ± 2	4 ± 3	1 ± 1	0 ± 1	2
XMMXCS J123052.3+211415.8	$0.076^{+0.031}_{-0.033}$	0.077 ± 0.017	$0.056 \pm 5.8e-06$	-0.013 ± 0.050	0.904 ± 0.841	0.155	2 ± 2	1 ± 1	2 ± 1	2 ± 2	2
XMMXCS J123101.0+160833.7	$0.173^{+0.077}_{-0.077}$	0.147 ± 0.030	-	-0.005 ± 0.051	1.150 ± 0.975	0.100	2 ± 2	1 ± 1	1 ± 1	-	2
XMMXCS J123205.0+215254.2	$0.343^{+0.130}_{-0.128}$	0.329 ± 0.101	-	0.068 ± 0.080	-0.194 ± 1.640	0.037	2 ± 2	2 ± 2	2 ± 1	3 ± 2	2
XMMXCS J123208.40+143505.4	$0.214^{+0.065}_{-0.069}$	0.247 ± 0.069	-	0.037 ± 0.081	0.607 ± 1.520	0.090	4 ± 2	5 ± 3	4 ± 2	5 ± 3	2
XMMXCS J123208.3+143505.3	$0.214^{+0.065}_{-0.069}$	0.247 ± 0.069	-	0.037 ± 0.081	0.607 ± 1.520	0.090	4 ± 2	5 ± 3	4 ± 2	5 ± 3	2
XMMXCS J123236.3+000224.7	$0.656^{+0.126}_{-0.123}$	0.651 ± 0.134	$0.650 \pm 2.0e-04$	0.019 ± 0.120	0.948 ± 2.470	0.112	4 ± 2	-	2 ± 1	-	2
XMMXCS J123538.7+620913.4	$0.424^{+0.094}_{-0.093}$	0.467 ± 0.112	-	-0.062 ± 0.044	1.990 ± 0.894	0.074	10 ± 4	9 ± 4	8 ± 3	6 ± 3	2
XMMXCS J123554.7+274304.0	$0.398^{+0.074}_{-0.067}$	0.401 ± 0.062	$0.385 \pm 1.8e-04$	-0.070 ± 0.055	2.890 ± 1.080	0.135	3 ± 3	3 ± 3	2 ± 2	2 ± 2	2
XMMXCS J123555.1+373224.1	$0.614^{+0.134}_{-0.128}$	0.476 ± 0.182	$0.571 \pm 1.9e-04$	0.235 ± 0.089	-3.810 ± 1.780	0.001	1 ± 2	1 ± 3	1 ± 1	0 ± 1	2
XMMXCS J123600.6+620158.6	$0.196^{+0.073}_{-0.076}$	0.216 ± 0.048	-	0.021 ± 0.079	0.827 ± 1.470	0.102	3 ± 2	0 ± 1	2 ± 1	-	2
XMMXCS J123600.9+274340.1	$0.399^{+0.070}_{-0.064}$	0.426 ± 0.066	-	-0.136 ± 0.027	4.280 ± 0.511	0.001	1 ± 2	-	1 ± 1	-	2
XMMXCS J123602.0+263459.8	$0.176^{+0.080}_{-0.082}$	0.206 ± 0.034	$0.210 \pm 4.2e-05$	-0.031 ± 0.063	1.770 ± 1.250	0.001	1 ± 2	1 ± 2	1 ± 1	2 ± 2	2
XMMXCS J123615.7+255437.2	$0.550^{+0.158}_{-0.158}$	0.507 ± 0.152	-	-0.127 ± 0.070	3.470 ± 1.430	0.110	19 ± 5	26 ± 6	23 ± 6	31 ± 7	2
XMMXCS J123634.6+274813.9	$0.700^{+0.145}_{-0.132}$	0.684 ± 0.125	-	-0.380 ± 0.346	8.460 ± 7.050	0.193	1 ± 2	-	1 ± 1	-	2
XMMXCS J123703.2+621547.9	$0.355^{+0.120}_{-0.115}$	0.307 ± 0.060	-	0.044 ± 0.056	-0.483 ± 1.120	0.099	1 ± 3	2 ± 3	1 ± 1	1 ± 2	2

Continued on next page

Table A.2 – continued from previous page

name	z_{RS}	z_{BCG}	z_{spec-g}	cmr_{grad}	cmr_{inter}	cmr_{wid}	n_{gals-c}	n_{gals-l}	n_{200-c}	n_{200-l}	qual
XMMXCS J123735.4+615838.5	$0.501^{+0.162}_{-0.162}$	0.529 ± 0.082	-	-0.147 ± 0.079	3.830 ± 1.570	0.001	5 ± 3	8 ± 4	5 ± 3	10 ± 4	2
XMMXCS J123800.5+621336.6	$0.431^{+0.085}_{-0.080}$	0.478 ± 0.073	-	0.761 ± 0.258	-13.60 ± 5.210	0.114	4 ± 3	7 ± 3	1 ± 1	4 ± 2	2
XMMXCS J123904.1+621615.1	$0.377^{+0.089}_{-0.089}$	0.412 ± 0.073	-	0.077 ± 0.113	0.360 ± 2.180	0.088	1 ± 2	3 ± 2	2 ± 1	3 ± 2	2
XMMXCS J123909.8-114612.6	$0.358^{+0.107}_{-0.108}$	0.310 ± 0.144	-	0.105 ± 0.074	-1.410 ± 1.480	0.012	5 ± 3	6 ± 3	3 ± 2	4 ± 3	2
XMMXCS J123937.7+093041.8	$0.130^{+0.027}_{-0.028}$	0.132 ± 0.021	$0.129 \pm 3.0e-05$	-0.117 ± 0.030	2.990 ± 0.532	0.066	2 ± 2	0 ± 1	2 ± 1	-	2
XMMXCS J124024.7-114806.6	$0.160^{+0.046}_{-0.047}$	0.186 ± 0.035	-	-0.027 ± 0.045	1.670 ± 0.848	0.089	1 ± 2	3 ± 2	1 ± 1	2 ± 2	2
XMMXCS J124052.5-113310.0	$0.162^{+0.072}_{-0.071}$	0.160 ± 0.025	-	0.002 ± 0.028	1.010 ± 0.517	0.110	2 ± 2	1 ± 2	1 ± 1	2 ± 2	2
XMMXCS J124107.0-020932.4	$0.336^{+0.079}_{-0.081}$	0.310 ± 0.059	-	0.015 ± 0.041	1.270 ± 0.802	0.038	4 ± 3	2 ± 3	1 ± 1	-	2
XMMXCS J124214.5+330324.2	$0.132^{+0.017}_{-0.016}$	0.136 ± 0.025	$0.132 \pm 1.6e-05$	0.070 ± 0.076	-0.556 ± 1.350	0.500	1 ± 2	0 ± 1	1 ± 1	-	2
XMMXCS J124235.4-112410.8	$0.072^{+0.024}_{-0.024}$	0.063 ± 0.017	-	-0.028 ± 0.003	1.250 ± 0.046	0.500	4 ± 3	3 ± 2	1 ± 1	2 ± 2	2
XMMXCS J124250.8+022750.2	$0.608^{+0.106}_{-0.103}$	0.571 ± 0.095	$0.601 \pm 1.5e-04$	-0.069 ± 0.139	2.500 ± 2.780	0.001	4 ± 3	9 ± 4	2 ± 2	11 ± 4	2
XMMXCS J124304.5+024118.1	$0.203^{+0.217}_{-0.203}$	0.183 ± 0.096	-	-0.031 ± 0.146	1.590 ± 2.720	0.001	3 ± 2	3 ± 2	1 ± 1	1 ± 1	2
XMMXCS J124325.4+112734.1	$0.203^{+0.131}_{-0.133}$	0.227 ± 0.039	-	-0.273 ± 0.117	6.440 ± 2.410	0.001	1 ± 1	0 ± 1	1 ± 1	-	2
XMMXCS J124329.9+023039.5	$0.621^{+0.079}_{-0.075}$	0.600 ± 0.185	$0.615 \pm 1.0e-04$	-0.015 ± 0.054	1.420 ± 1.060	0.095	1 ± 2	4 ± 3	1 ± 1	-	2
XMMXCS J124450.1+672704.9	$0.465^{+0.136}_{-0.136}$	0.510 ± 0.079	-	-0.037 ± 0.035	1.610 ± 0.693	0.019	5 ± 3	-	2 ± 2	-	2
XMMXCS J124510.7-002824.8	$0.116^{+0.056}_{-0.076}$	0.146 ± 0.036	-	0.038 ± 0.008	0.134 ± 0.099	0.500	4 ± 3	33 ± 6	2 ± 2	70 ± 10	2
XMMXCS J124616.4+671928.3	$0.472^{+0.113}_{-0.112}$	0.443 ± 0.151	-	0.239 ± 0.079	-4.010 ± 1.540	0.001	1 ± 2	0 ± 2	1 ± 1	-	2
XMMXCS J124721.0+022934.2	$0.304^{+0.072}_{-0.072}$	0.246 ± 0.039	$0.313 \pm 4.1e-05$	0.071 ± 0.068	0.236 ± 1.300	0.001	1 ± 2	2 ± 2	1 ± 1	2 ± 2	2
XMMXCS J124750.1-055104.3	$0.119^{+0.040}_{-0.041}$	0.117 ± 0.025	-	0.016 ± 0.024	0.722 ± 0.387	0.064	1 ± 2	1 ± 2	1 ± 1	1 ± 1	2

Continued on next page

Table A.2 – continued from previous page

name	z_{RS}	z_{BCG}	z_{spec-g}	cmr_{grad}	cmr_{inter}	cmr_{wid}	n_{gals-c}	n_{gals-l}	n_{200-c}	n_{200-l}	qual
XMMXCS J124919.9-054202.2	$0.607^{+0.104}_{-0.094}$	0.618 ± 0.104	-	2.450 ± 1.870	-49.40 ± 38.60	0.399	3 ± 2	1 ± 1	1 ± 1	0 ± 1	2
XMMXCS J125007.9+253551.3	$0.260^{+0.085}_{-0.084}$	0.293 ± 0.084	-	-0.186 ± 0.056	4.960 ± 1.100	0.001	3 ± 2	1 ± 2	2 ± 1	0 ± 1	2
XMMXCS J125012.9+264405.8	$0.383^{+0.105}_{-0.098}$	0.349 ± 0.128	-	0.199 ± 0.163	-2.620 ± 3.260	0.142	6 ± 3	6 ± 3	6 ± 3	6 ± 3	2
XMMXCS J125025.2+001317.8	$0.079^{+0.043}_{-0.043}$	0.057 ± 0.022	$0.064 \pm 7.8e-06$	-0.078 ± 0.040	2.060 ± 0.662	0.090	3 ± 2	1 ± 2	3 ± 2	3 ± 2	2
XMMXCS J125042.4+272612.1	$0.038^{+0.051}_{-0.038}$	0.066 ± 0.021	$0.032 \pm 9.2e-06$	0.022 ± 0.011	0.293 ± 0.158	0.083	1 ± 1	0 ± 1	1 ± 1	-	2
XMMXCS J125141.3+273730.6	$0.439^{+0.097}_{-0.089}$	0.436 ± 0.068	-	-0.136 ± 0.041	3.300 ± 0.782	0.066	3 ± 3	4 ± 3	2 ± 2	5 ± 3	2
XMMXCS J125439.5+262001.1	$0.066^{+0.024}_{-0.024}$	0.079 ± 0.016	$0.057 \pm 9.1e-06$	-0.003 ± 0.030	0.863 ± 0.503	0.072	3 ± 2	0 ± 1	1 ± 1	-	2
XMMXCS J125505.7+255257.0	$0.218^{+0.069}_{-0.069}$	0.171 ± 0.052	-	0.040 ± 0.042	0.500 ± 0.801	0.090	9 ± 3	9 ± 3	7 ± 3	7 ± 3	2
XMMXCS J125638.6+281037.0	$0.506^{+0.168}_{-0.168}$	0.485 ± 0.142	-	-0.008 ± 0.035	1.120 ± 0.692	0.001	5 ± 3	8 ± 4	1 ± 1	3 ± 3	2
XMMXCS J125650.2+254803.2	$0.283^{+0.098}_{-0.098}$	0.279 ± 0.046	$0.283 \pm 3.8e-05$	-0.029 ± 0.029	1.960 ± 0.575	0.084	1 ± 2	4 ± 3	2 ± 1	2 ± 2	2
XMMXCS J125712.8+215418.1	$0.151^{+0.066}_{-0.066}$	0.154 ± 0.042	$0.187 \pm 3.2e-05$	-0.018 ± 0.063	1.200 ± 1.160	0.137	2 ± 2	1 ± 1	1 ± 1	1 ± 1	2
XMMXCS J125736.1+272826.5	$0.063^{+-1.063}_{-1.063}$	0.085 ± 0.031	$0.024 \pm 5.0e-06$	0.011 ± 0.012	0.726 ± 0.187	0.053	9 ± 3	18 ± 5	6 ± 3	7 ± 4	2
XMMXCS J125746.1+265628.9	$0.241^{+0.061}_{-0.061}$	0.211 ± 0.040	-	0.103 ± 0.038	-0.583 ± 0.701	0.035	2 ± 2	2 ± 2	2 ± 1	3 ± 2	2
XMMXCS J125749.2+265751.4	$0.216^{+0.052}_{-0.051}$	0.211 ± 0.040	-	0.023 ± 0.035	0.862 ± 0.643	0.066	3 ± 2	2 ± 2	1 ± 1	2 ± 2	2
XMMXCS J125841.7-014530.2	$0.082^{+0.023}_{-0.023}$	0.110 ± 0.046	$0.082 \pm 1.7e-05$	-0.004 ± 0.007	0.995 ± 0.133	0.038	20 ± 5	25 ± 5	21 ± 5	34 ± 6	2
XMMXCS J125850.5-014545.1	$0.085^{+0.016}_{-0.016}$	0.110 ± 0.046	$0.082 \pm 1.7e-05$	-0.033 ± 0.042	1.450 ± 0.721	0.024	21 ± 5	27 ± 5	25 ± 5	38 ± 6	2
XMMXCS J125857.7+275559.1	$0.062^{+0.045}_{-0.045}$	0.048 ± 0.017	$0.023 \pm 4.8e-06$	0.014 ± 0.019	0.563 ± 0.298	0.107	20 ± 5	19 ± 4	33 ± 6	27 ± 5	2
XMMXCS J125912.9-013407.8	$0.083^{+0.018}_{-0.018}$	0.067 ± 0.022	$0.095 \pm 1.5e-05$	0.023 ± 0.046	0.392 ± 0.801	0.101	3 ± 2	1 ± 1	1 ± 1	0 ± 1	2
XMMXCS J125933.2+283039.3	$0.605^{+0.149}_{-0.149}$	0.640 ± 0.132	-	0.087 ± 0.087	-0.435 ± 1.640	0.058	11 ± 3	29 ± 6	11 ± 3	26 ± 6	2

Continued on next page

Table A.2 – continued from previous page

name	z_{RS}	z_{BCG}	z_{spec-g}	cmr_{grad}	cmr_{inter}	cmr_{wid}	n_{gals-c}	n_{gals-l}	n_{200-c}	n_{200-l}	qual
XMMXCS J125943.1+280216.1	$0.025^{+0.004}_{-0.004}$	0.048 ± 0.015	$0.026 \pm 4.5e-06$	-0.044 ± 0.046	1.380 ± 0.622	0.074	2 ± 1	0 ± 1	1 ± 1	-	2
XMMXCS J130058.3+280216.0	$0.021^{+0.006}_{-0.005}$	0.044 ± 0.016	$0.020 \pm 6.4e-06$	-0.031 ± 0.009	1.190 ± 0.122	0.023	3 ± 2	0 ± 1	1 ± 1	-	2
XMMXCS J130106.9+281808.3	$0.218^{+0.067}_{-0.070}$	0.218 ± 0.039	-	-0.006 ± 0.016	1.420 ± 0.289	0.001	6 ± 3	5 ± 3	2 ± 2	0 ± 1	2
XMMXCS J130108.7+283446.7	$0.592^{+0.180}_{-0.181}$	0.594 ± 0.256	-	-0.511 ± 0.112	12.000 ± 2.410	0.238	3 ± 2	-	1 ± 1	-	2
XMMXCS J130126.2+275309.7	$0.356^{+0.068}_{-0.068}$	0.315 ± 0.052	-	0.123 ± 0.095	-0.760 ± 1.850	0.001	5 ± 3	18 ± 5	2 ± 2	13 ± 4	2
XMMXCS J130230.9-023202.5	$0.486^{+0.100}_{-0.096}$	0.467 ± 0.070	$0.476 \pm 1.7e-04$	0.093 ± 0.164	-0.973 ± 3.140	0.154	1 ± 3	3 ± 3	2 ± 1	10 ± 4	2
XMMXCS J130252.0-023054.9	$0.084^{+0.011}_{-0.010}$	0.124 ± 0.022	$0.094 \pm 1.2e-05$	-0.028 ± 0.021	1.390 ± 0.366	0.040	9 ± 3	11 ± 3	9 ± 3	9 ± 3	2
XMMXCS J130431.6+673535.0	$0.224^{+0.074}_{-0.075}$	0.226 ± 0.036	-	-0.016 ± 0.032	1.610 ± 0.606	0.076	7 ± 3	6 ± 3	2 ± 2	1 ± 2	2
XMMXCS J130441.9+175914.0	$0.178^{+0.045}_{-0.046}$	0.173 ± 0.028	-	0.013 ± 0.037	0.986 ± 0.688	0.085	4 ± 2	3 ± 2	1 ± 1	0 ± 1	2
XMMXCS J130514.4+181421.8	$0.366^{+0.060}_{-0.060}$	0.370 ± 0.088	$0.368 \pm 1.2e-04$	0.015 ± 0.079	1.540 ± 1.490	0.001	1 ± 2	-	1 ± 1	-	2
XMMXCS J130545.2+175318.2	$0.557^{+0.105}_{-0.105}$	0.511 ± 0.079	$0.541 \pm 1.4e-04$	-0.062 ± 0.030	2.150 ± 0.589	0.066	4 ± 3	4 ± 3	3 ± 2	6 ± 3	2
XMMXCS J130816.2+213325.2	$0.138^{+0.053}_{-0.052}$	0.151 ± 0.039	-	-0.019 ± 0.064	1.330 ± 1.160	0.500	1 ± 2	1 ± 2	1 ± 1	0 ± 1	2
XMMXCS J130824.7+292457.6	$0.123^{+0.015}_{-0.015}$	0.137 ± 0.022	$0.123 \pm 2.0e-05$	-0.018 ± 0.007	1.360 ± 0.109	0.001	2 ± 1	1 ± 1	2 ± 1	3 ± 2	2
XMMXCS J130836.7+113841.6	$0.435^{+0.106}_{-0.100}$	0.425 ± 0.136	$0.428 \pm 1.2e-04$	0.057 ± 0.026	-0.397 ± 0.517	0.085	1 ± 3	-	1 ± 1	-	2
XMMXCS J130848.0+533246.0	$0.175^{+0.097}_{-0.099}$	0.175 ± 0.027	$0.180 \pm 5.1e-05$	-0.105 ± 0.025	3.050 ± 0.465	0.073	5 ± 2	6 ± 3	2 ± 1	2 ± 2	2
XMMXCS J130918.8-013726.6	$0.082^{+0.004}_{-0.004}$	0.093 ± 0.019	$0.082 \pm 1.1e-05$	-0.010 ± 0.001	1.100 ± 0.016	0.001	5 ± 3	8 ± 3	2 ± 2	6 ± 3	2
XMMXCS J131018.7+322840.2	$0.193^{+0.059}_{-0.055}$	0.169 ± 0.028	$0.186 \pm 2.5e-05$	-0.026 ± 0.040	1.490 ± 0.772	0.139	7 ± 3	7 ± 3	2 ± 2	4 ± 3	2
XMMXCS J131052.4+275708.9	$0.356^{+0.055}_{-0.058}$	0.383 ± 0.061	-	-0.045 ± 0.083	2.600 ± 1.620	0.001	2 ± 2	2 ± 2	2 ± 1	3 ± 2	2
XMMXCS J131113.5+573121.6	$0.369^{+0.177}_{-0.172}$	0.363 ± 0.204	-	-0.345 ± 0.113	8.090 ± 2.270	0.001	4 ± 3	1 ± 2	1 ± 1	-	2

Continued on next page

Table A.2 – continued from previous page

name	z_{RS}	z_{BCG}	z_{spec-g}	cmr_{grad}	cmr_{inter}	cmr_{wid}	n_{gals-c}	n_{gals-l}	n_{200-c}	n_{200-l}	qual
XMMXCS J131117.8+215834.2	$0.216^{+0.074}_{-0.074}$	0.161 ± 0.030	$0.171 \pm 2.6e-05$	0.081 ± 0.035	-0.353 ± 0.657	0.012	5 ± 2	5 ± 3	2 ± 2	2 ± 2	2
XMMXCS J131200.3+350901.3	$0.263^{+0.070}_{-0.068}$	0.313 ± 0.048	$0.308 \pm 7.0e-05$	-0.075 ± 0.054	2.780 ± 1.060	0.093	2 ± 2	1 ± 2	1 ± 1	-	2
XMMXCS J131209.5+350241.6	$0.230^{+0.048}_{-0.048}$	0.194 ± 0.030	-	0.092 ± 0.019	-0.333 ± 0.333	0.039	3 ± 2	0 ± 2	2 ± 1	-	2
XMMXCS J131228.3+315318.9	$0.188^{+0.106}_{-0.116}$	0.188 ± 0.038	-	-0.060 ± 0.060	2.290 ± 1.190	0.068	3 ± 2	1 ± 2	1 ± 1	0 ± 1	2
XMMXCS J131243.8+230955.4	$0.323^{+0.106}_{-0.107}$	0.293 ± 0.044	-	-0.100 ± 0.060	3.320 ± 1.160	0.001	2 ± 2	2 ± 2	2 ± 1	2 ± 2	2
XMMXCS J131610.0+290031.3	$0.239^{+0.081}_{-0.082}$	0.302 ± 0.050	$0.275 \pm 7.7e-05$	-0.130 ± 0.161	3.790 ± 3.100	0.124	8 ± 3	8 ± 3	4 ± 2	3 ± 2	2
XMMXCS J131955.4+331853.6	$0.230^{+0.059}_{-0.060}$	0.263 ± 0.047	-	-0.104 ± 0.025	3.410 ± 0.493	0.040	5 ± 2	7 ± 3	2 ± 2	3 ± 2	2
XMMXCS J131957.0+325744.8	$0.255^{+0.060}_{-0.056}$	0.311 ± 0.058	$0.302 \pm 8.2e-05$	-0.004 ± 0.086	1.350 ± 1.600	0.128	6 ± 3	3 ± 3	3 ± 2	0 ± 1	2
XMMXCS J132009.3+330418.3	$0.037^{+0.025}_{-0.026}$	0.061 ± 0.017	$0.039 \pm 1.3e-05$	-0.009 ± 0.015	0.889 ± 0.256	0.069	3 ± 2	0 ± 1	1 ± 1	-	2
XMMXCS J132338.5+033156.1	$0.116^{+0.040}_{-0.040}$	0.100 ± 0.018	$0.138 \pm 2.2e-05$	-0.028 ± 0.020	1.430 ± 0.354	0.052	2 ± 2	1 ± 1	1 ± 1	2 ± 2	2
XMMXCS J132352.0+301720.6	$0.198^{+0.060}_{-0.063}$	0.216 ± 0.039	-	-0.013 ± 0.036	1.490 ± 0.685	0.054	2 ± 2	1 ± 2	1 ± 1	0 ± 1	2
XMMXCS J132353.2+300648.7	$0.390^{+0.119}_{-0.111}$	0.380 ± 0.071	-	0.028 ± 0.069	0.039 ± 1.350	0.093	2 ± 3	3 ± 3	1 ± 1	1 ± 2	2
XMMXCS J132449.0+301131.5	$0.502^{+0.179}_{-0.192}$	0.541 ± 0.131	-	0.188 ± 0.008	-2.300 ± 0.144	0.500	5 ± 4	10 ± 4	4 ± 3	11 ± 4	2
XMMXCS J132454.2+053328.1	$0.172^{+0.045}_{-0.048}$	0.166 ± 0.026	$0.175 \pm 2.8e-05$	0.024 ± 0.025	0.785 ± 0.468	0.094	1 ± 2	4 ± 2	1 ± 1	3 ± 2	2
XMMXCS J132631.0+074504.0	$0.534^{+0.073}_{-0.073}$	0.476 ± 0.157	$0.534 \pm 1.6e-04$	-0.107 ± 0.012	3.140 ± 0.233	0.001	2 ± 2	-	2 ± 2	-	2
XMMXCS J132644.4+010819.1	$0.083^{+0.009}_{-0.009}$	0.096 ± 0.019	$0.082 \pm 9.4e-06$	-0.061 ± 0.024	1.860 ± 0.387	0.036	2 ± 2	1 ± 2	1 ± 1	1 ± 1	2
XMMXCS J132656.8+655935.0	$0.115^{+0.055}_{-0.054}$	0.107 ± 0.115	$0.131 \pm 1.2e-05$	-0.023 ± 0.011	0.946 ± 0.208	0.055	1 ± 1	0 ± 1	1 ± 1	-	2
XMMXCS J132830.2+470357.2	$0.365^{+0.075}_{-0.074}$	0.398 ± 0.068	-	-0.011 ± 0.017	0.851 ± 0.335	0.022	11 ± 4	12 ± 4	10 ± 4	11 ± 4	2
XMMXCS J132832.8+583717.4	$0.304^{+0.065}_{-0.064}$	0.287 ± 0.043	-	0.001 ± 0.046	1.500 ± 0.896	0.092	1 ± 2	1 ± 2	1 ± 1	0 ± 1	2

Continued on next page

Table A.2 – continued from previous page

name	z_{RS}	z_{BCG}	z_{spec-g}	cmr_{grad}	cmr_{inter}	cmr_{wid}	n_{gals-c}	n_{gals-l}	n_{200-c}	n_{200-l}	qual
XMMXCS J132949.0+335150.1	$0.256^{+0.072}_{-0.079}$	0.279 ± 0.059	-	-0.024 ± 0.035	1.930 ± 0.649	0.081	2 ± 2	-	1 ± 1	-	2
XMMXCS J132958.6+242436.8	$0.315^{+0.159}_{-0.174}$	0.326 ± 0.107	-	-0.029 ± 0.037	1.510 ± 0.750	0.096	2 ± 2	0 ± 2	1 ± 1	-	2
XMMXCS J133000.9+465822.6	$0.658^{+0.155}_{-0.150}$	0.641 ± 0.136	-	0.422 ± 0.219	-7.680 ± 4.530	0.001	1 ± 1	6 ± 3	1 ± 1	3 ± 2	2
XMMXCS J133005.1+240652.4	$0.541^{+0.118}_{-0.117}$	0.521 ± 0.082	$0.537 \pm 1.1e-04$	0.088 ± 0.108	-0.830 ± 2.160	0.053	3 ± 2	13 ± 4	2 ± 2	11 ± 4	2
XMMXCS J133018.6+472215.4	$0.514^{+0.136}_{-0.131}$	0.487 ± 0.075	-	-0.119 ± 0.053	3.280 ± 1.080	0.076	4 ± 3	7 ± 4	2 ± 2	2 ± 3	2
XMMXCS J133415.6+502812.5	$0.134^{+0.061}_{-0.062}$	0.097 ± 0.017	$0.085 \pm 1.4e-05$	0.014 ± 0.030	0.850 ± 0.537	0.142	4 ± 2	4 ± 2	2 ± 2	2 ± 2	2
XMMXCS J133420.0+503526.3	$0.613^{+0.123}_{-0.119}$	0.593 ± 0.113	-	0.015 ± 0.038	0.855 ± 0.778	0.001	2 ± 2	6 ± 3	1 ± 1	5 ± 3	2
XMMXCS J133435.1+375655.4	$0.279^{+0.058}_{-0.058}$	0.301 ± 0.047	$0.310 \pm 6.1e-05$	-0.029 ± 0.063	2.020 ± 1.230	0.098	17 ± 4	18 ± 5	18 ± 5	16 ± 5	2
XMMXCS J133437.7+375602.5	$0.284^{+0.066}_{-0.066}$	0.301 ± 0.047	$0.310 \pm 6.1e-05$	-0.061 ± 0.034	2.620 ± 0.644	0.110	15 ± 4	12 ± 4	16 ± 4	12 ± 4	2
XMMXCS J133523.3+515148.6	$0.535^{+0.143}_{-0.144}$	0.571 ± 0.185	-	-0.002 ± 0.146	1.160 ± 2.940	0.115	2 ± 2	4 ± 3	2 ± 1	-	2
XMMXCS J133630.7+514713.9	$0.129^{+0.069}_{-0.058}$	0.173 ± 0.026	$0.175 \pm 2.8e-05$	-0.354 ± 0.001	7.160 ± 0.002	0.500	2 ± 2	2 ± 2	2 ± 1	1 ± 1	2
XMMXCS J133650.3+515514.8	$0.242^{+0.066}_{-0.070}$	0.237 ± 0.039	-	-0.025 ± 0.024	1.920 ± 0.459	0.072	2 ± 2	1 ± 2	1 ± 1	0 ± 1	2
XMMXCS J133753.2+515257.3	$0.303^{+0.069}_{-0.071}$	0.273 ± 0.053	-	0.014 ± 0.035	1.250 ± 0.660	0.055	8 ± 3	8 ± 3	5 ± 3	1 ± 2	2
XMMXCS J133855.7+281116.1	$0.445^{+0.202}_{-0.194}$	0.467 ± 0.283	-	-0.027 ± 0.071	1.390 ± 1.410	0.094	5 ± 3	3 ± 3	1 ± 2	-	2
XMMXCS J134003.8+273346.9	$0.145^{+0.043}_{-0.042}$	0.150 ± 0.034	-	-0.030 ± 0.082	1.500 ± 1.460	0.115	2 ± 2	1 ± 1	2 ± 1	0 ± 1	2
XMMXCS J134124.3-010204.0	$0.281^{+0.073}_{-0.075}$	0.307 ± 0.047	$0.285 \pm 3.5e-05$	0.024 ± 0.044	1.040 ± 0.827	0.101	6 ± 3	10 ± 4	2 ± 2	9 ± 4	2
XMMXCS J134316.7+555810.8	$0.445^{+0.105}_{-0.102}$	0.488 ± 0.072	$0.481 \pm 1.5e-04$	-0.013 ± 0.067	1.040 ± 1.330	0.103	16 ± 5	20 ± 5	18 ± 5	22 ± 6	2
XMMXCS J134645.9+264625.7	$0.382^{+0.105}_{-0.104}$	0.426 ± 0.063	$0.427 \pm 1.2e-04$	-0.098 ± 0.070	3.470 ± 1.320	0.001	5 ± 3	-	6 ± 3	-	2
XMMXCS J134755.7+264230.5	$0.105^{+0.056}_{-0.057}$	0.062 ± 0.021	$0.069 \pm 7.9e-06$	0.032 ± 0.027	0.215 ± 0.468	0.122	6 ± 3	3 ± 2	4 ± 2	1 ± 1	2

Continued on next page

Table A.2 – continued from previous page

name	z_{RS}	z_{BCG}	z_{spec-g}	cmr_{grad}	cmr_{inter}	cmr_{wid}	n_{gals-c}	n_{gals-l}	n_{200-c}	n_{200-l}	qual
XMMXCS J134807.2+261648.7	$0.599^{+0.123}_{-0.119}$	0.630 ± 0.132	-	-0.114 ± 0.138	3.400 ± 2.760	0.091	2 ± 2	9 ± 4	2 ± 1	10 ± 4	2
XMMXCS J134855.2+263832.8	$0.066^{+0.010}_{-0.010}$	0.101 ± 0.024	$0.067 \pm 1.3e-05$	-0.024 ± 0.020	1.290 ± 0.332	0.014	3 ± 2	1 ± 1	1 ± 1	0 ± 1	2
XMMXCS J135049.4+600707.4	$0.399^{+0.134}_{-0.136}$	0.368 ± 0.178	-	-0.349 ± 0.183	8.320 ± 3.750	0.143	3 ± 3	4 ± 3	2 ± 2	3 ± 2	2
XMMXCS J135153.2+642214.5	$0.100^{+0.063}_{-0.069}$	0.060 ± 0.086	$0.100 \pm 2.1e-05$	-0.053 ± 0.001	1.490 ± 0.001	0.500	1 ± 2	1 ± 2	2 ± 1	2 ± 2	2
XMMXCS J135244.9+400536.6	$0.528^{+0.112}_{-0.109}$	0.554 ± 0.095	$0.554 \pm 6.2e-05$	-0.026 ± 0.051	1.430 ± 1.010	0.120	5 ± 3	9 ± 4	2 ± 2	11 ± 4	2
XMMXCS J135320.1+335802.8	$0.370^{+0.089}_{-0.079}$	0.341 ± 0.058	-	-0.032 ± 0.030	1.210 ± 0.606	0.072	2 ± 3	1 ± 3	1 ± 1	0 ± 1	2
XMMXCS J135405.1+333513.3	$0.042^{+0.046}_{-0.042}$	0.072 ± 0.020	$0.046 \pm 8.3e-06$	0.034 ± 0.011	0.216 ± 0.191	0.040	2 ± 1	0 ± 1	1 ± 1	-	2
XMMXCS J135439.4-021208.1	$0.529^{+0.111}_{-0.110}$	0.522 ± 0.129	-	0.282 ± 0.171	-4.860 ± 3.480	0.001	3 ± 2	-	2 ± 2	-	2
XMMXCS J135541.9+182545.4	$0.302^{+0.074}_{-0.076}$	0.274 ± 0.043	-	-0.006 ± 0.061	1.700 ± 1.140	0.001	8 ± 3	0 ± 2	7 ± 3	-	2
XMMXCS J135546.0+182250.8	$0.311^{+0.070}_{-0.072}$	0.326 ± 0.051	-	-0.021 ± 0.028	1.980 ± 0.539	0.001	5 ± 3	7 ± 3	2 ± 2	4 ± 3	2
XMMXCS J135933.5+621901.4	$0.328^{+0.060}_{-0.060}$	0.292 ± 0.068	-	0.086 ± 0.058	0.035 ± 1.100	0.024	17 ± 4	15 ± 4	24 ± 5	31 ± 6	2
XMMXCS J140129.6+025639.2	$0.225^{+0.073}_{-0.075}$	0.198 ± 0.034	-	-0.057 ± 0.048	2.440 ± 0.890	0.016	9 ± 3	8 ± 3	7 ± 3	6 ± 3	2
XMMXCS J140532.6+091326.4	$0.429^{+0.144}_{-0.151}$	0.481 ± 0.072	$0.476 \pm 6.9e-05$	0.002 ± 0.062	0.703 ± 1.220	0.103	5 ± 3	6 ± 4	3 ± 2	4 ± 3	2
XMMXCS J140536.5+255141.2	$0.202^{+0.039}_{-0.036}$	0.161 ± 0.032	-	0.035 ± 0.040	0.696 ± 0.771	0.500	1 ± 2	0 ± 2	1 ± 1	-	2
XMMXCS J140935.2+262941.9	$0.132^{+0.026}_{-0.026}$	0.136 ± 0.021	$0.131 \pm 1.6e-05$	0.018 ± 0.028	0.762 ± 0.454	0.063	4 ± 2	4 ± 2	1 ± 1	3 ± 2	2
XMMXCS J141223.6-030932.9	$0.662^{+0.116}_{-0.107}$	0.584 ± 0.095	$0.644 \pm 1.8e-04$	0.086 ± 0.159	-0.558 ± 3.180	0.001	2 ± 2	8 ± 4	2 ± 1	3 ± 3	2
XMMXCS J141252.5-031744.3	$0.376^{+0.112}_{-0.126}$	0.374 ± 0.082	-	-0.129 ± 0.191	3.400 ± 3.850	0.150	3 ± 3	4 ± 3	2 ± 2	2 ± 2	2
XMMXCS J141303.9+440709.5	$0.181^{+0.070}_{-0.072}$	0.150 ± 0.025	-	-0.087 ± 0.106	2.810 ± 2.020	0.147	4 ± 2	1 ± 2	2 ± 2	1 ± 1	2
XMMXCS J141313.2-031803.8	$0.307^{+0.059}_{-0.061}$	0.338 ± 0.054	$0.309 \pm 6.3e-05$	-0.030 ± 0.035	2.240 ± 0.664	0.072	6 ± 3	6 ± 3	6 ± 3	7 ± 3	2

Continued on next page

Table A.2 – continued from previous page

name	z_{RS}	z_{BCG}	z_{spec-g}	cmr_{grad}	cmr_{inter}	cmr_{wid}	n_{gals-c}	n_{gals-l}	n_{200-c}	n_{200-l}	qual
XMMXCS J141314.6-031719.3	$0.308^{+0.049}_{-0.050}$	0.338 ± 0.054	$0.322 \pm 4.2e-05$	0.023 ± 0.062	1.240 ± 1.150	0.001	7 ± 3	6 ± 3	4 ± 2	8 ± 3	2
XMMXCS J141455.7+112351.9	$0.219^{+0.064}_{-0.064}$	0.248 ± 0.037	$0.252 \pm 4.1e-05$	-0.080 ± 0.019	2.790 ± 0.363	0.078	9 ± 3	11 ± 4	7 ± 3	12 ± 4	2
XMMXCS J141458.4+440317.5	$0.393^{+0.079}_{-0.078}$	0.362 ± 0.066	-	-0.006 ± 0.036	0.836 ± 0.714	0.001	4 ± 3	5 ± 3	5 ± 2	6 ± 3	2
XMMXCS J141504.6+111945.4	$0.264^{+0.056}_{-0.054}$	0.263 ± 0.045	$0.287 \pm 2.6e-05$	-0.033 ± 0.025	2.080 ± 0.467	0.089	6 ± 3	7 ± 3	6 ± 3	9 ± 3	2
XMMXCS J141504.74+545450.9	$0.225^{+0.069}_{-0.071}$	0.251 ± 0.041	$0.228 \pm 4.9e-05$	-0.082 ± 0.042	2.850 ± 0.820	0.138	6 ± 3	4 ± 3	2 ± 2	1 ± 2	2
XMMXCS J141511.0+361204.9	$0.153^{+0.066}_{-0.062}$	0.191 ± 0.049	$0.210 \pm 1.5e-05$	-0.475 ± 0.001	9.520 ± 0.001	0.500	2 ± 2	0 ± 2	1 ± 1	-	2
XMMXCS J141511.7+361125.4	$0.148^{+0.052}_{-0.050}$	0.191 ± 0.049	$0.210 \pm 1.5e-05$	-0.475 ± 0.001	9.520 ± 0.001	0.500	2 ± 2	0 ± 2	1 ± 1	-	2
XMMXCS J141520.3+361022.4	$0.099^{+0.041}_{-0.041}$	0.101 ± 0.032	$0.063 \pm 6.7e-06$	0.207 ± 0.033	-2.780 ± 0.537	0.500	2 ± 2	2 ± 2	1 ± 1	1 ± 1	2
XMMXCS J141544.4+522511.5	$0.466^{+0.163}_{-0.173}$	0.442 ± 0.067	-	0.025 ± 0.079	0.272 ± 1.570	0.001	3 ± 3	3 ± 3	2 ± 2	1 ± 2	2
XMMXCS J141544.45+522511.7	$0.466^{+0.163}_{-0.173}$	0.442 ± 0.067	-	0.025 ± 0.079	0.272 ± 1.570	0.001	3 ± 3	3 ± 3	2 ± 2	1 ± 2	2
XMMXCS J141544.4+522511.7	$0.466^{+0.163}_{-0.173}$	0.442 ± 0.067	-	0.025 ± 0.079	0.272 ± 1.570	0.001	3 ± 3	3 ± 3	2 ± 2	1 ± 2	2
XMMXCS J141558.9+450012.2	$0.364^{+0.056}_{-0.056}$	0.319 ± 0.054	-	0.117 ± 0.086	-0.587 ± 1.640	0.094	3 ± 3	4 ± 3	1 ± 1	2 ± 2	2
XMMXCS J141613.2+230207.6	$0.095^{+0.034}_{-0.035}$	0.071 ± 0.017	$0.088 \pm 1.3e-05$	-0.030 ± 0.034	1.410 ± 0.572	0.097	5 ± 3	4 ± 2	4 ± 2	3 ± 2	2
XMMXCS J141643.6+105306.9	$0.026^{+0.008}_{-0.008}$	0.052 ± 0.017	$0.026 \pm 1.1e-05$	-0.030 ± 0.011	1.200 ± 0.162	0.038	1 ± 1	0 ± 1	1 ± 1	-	2
XMMXCS J141923.1+063834.9	$0.540^{+0.127}_{-0.117}$	0.515 ± 0.090	-	0.253 ± 0.165	-3.980 ± 3.260	0.135	15 ± 4	29 ± 6	14 ± 4	46 ± 8	2
XMMXCS J142017.8+064633.9	$0.543^{+0.098}_{-0.094}$	0.525 ± 0.083	$0.543 \pm 1.1e-04$	-0.009 ± 0.058	1.080 ± 1.190	0.052	5 ± 3	16 ± 5	2 ± 2	13 ± 5	2
XMMXCS J142024.0+063241.5	$0.151^{+0.094}_{-0.103}$	0.115 ± 0.020	$0.229 \pm 4.1e-05$	-0.007 ± 0.030	1.030 ± 0.547	0.091	4 ± 2	2 ± 2	2 ± 1	0 ± 1	2
XMMXCS J142449.3+382307.6	$0.425^{+0.130}_{-0.127}$	0.396 ± 0.114	-	0.239 ± 0.101	-4.160 ± 2.060	0.069	5 ± 3	4 ± 3	4 ± 2	3 ± 2	2
XMMXCS J142516.0+374446.4	$0.184^{+0.036}_{-0.035}$	0.172 ± 0.027	$0.164 \pm 2.8e-05$	-0.070 ± 0.036	2.430 ± 0.672	0.058	1 ± 2	2 ± 2	1 ± 1	2 ± 2	2

Continued on next page

Table A.2 – continued from previous page

name	z_{RS}	z_{BCG}	z_{spec-g}	cmr_{grad}	cmr_{inter}	cmr_{wid}	n_{gals-c}	n_{gals-l}	n_{200-c}	n_{200-l}	qual
XMMXCS J142551.8+380246.3	$0.488^{+0.090}_{-0.089}$	0.445 ± 0.091	$0.487 \pm 1.4e-04$	0.270 ± 0.269	-4.470 ± 5.320	0.193	16 ± 5	20 ± 5	18 ± 5	20 ± 6	2
XMMXCS J142730.7+262901.3	$0.368^{+0.072}_{-0.072}$	0.330 ± 0.050	$0.369 \pm 7.3e-05$	0.0002 ± 0.084	1.750 ± 1.600	0.001	6 ± 3	12 ± 4	6 ± 3	12 ± 4	2
XMMXCS J142822.1+424050.4	$0.129^{+0.030}_{-0.030}$	0.145 ± 0.046	$0.129 \pm 1.7e-05$	0.150 ± 0.026	-1.770 ± 0.482	0.026	3 ± 2	3 ± 2	1 ± 1	1 ± 1	2
XMMXCS J142859.6+424750.6	$0.162^{+0.032}_{-0.032}$	0.148 ± 0.026	$0.151 \pm 3.2e-05$	-0.031 ± 0.043	1.720 ± 0.774	0.050	2 ± 2	3 ± 2	2 ± 1	3 ± 2	2
XMMXCS J142903.5+474524.1	$0.196^{+0.047}_{-0.046}$	0.148 ± 0.029	-	0.037 ± 0.035	0.569 ± 0.677	0.070	5 ± 2	5 ± 3	3 ± 2	4 ± 2	2
XMMXCS J142934.9+423451.2	$0.535^{+0.096}_{-0.091}$	0.488 ± 0.073	$0.528 \pm 1.1e-04$	0.128 ± 0.047	-1.670 ± 0.944	0.075	4 ± 3	6 ± 4	1 ± 1	3 ± 3	2
XMMXCS J143006.1+012217.8	$0.261^{+0.071}_{-0.072}$	0.277 ± 0.070	$0.245 \pm 3.6e-05$	0.002 ± 0.038	1.430 ± 0.701	0.046	2 ± 2	3 ± 2	1 ± 1	2 ± 2	2
XMMXCS J143113.2-005240.9	$0.359^{+0.081}_{-0.081}$	0.393 ± 0.059	$0.403 \pm 1.4e-04$	-0.016 ± 0.082	2.090 ± 1.560	0.026	7 ± 3	6 ± 3	2 ± 2	0 ± 1	2
XMMXCS J143137.7+280743.2	$0.250^{+0.114}_{-0.115}$	0.270 ± 0.067	-	-0.013 ± 0.075	1.670 ± 1.450	0.001	2 ± 2	0 ± 1	1 ± 1	-	2
XMMXCS J143603.2+632538.0	$0.123^{+0.028}_{-0.028}$	0.169 ± 0.099	$0.124 \pm 1.0e-05$	0.041 ± 0.001	0.265 ± 0.001	0.500	3 ± 3	14 ± 4	4 ± 2	14 ± 4	2
XMMXCS J143625.0+484922.7	$0.529^{+0.123}_{-0.112}$	0.546 ± 0.091	-	0.476 ± 0.250	-8.420 ± 4.990	0.184	2 ± 2	-	1 ± 1	-	2
XMMXCS J143731.0+341850.5	$0.347^{+0.073}_{-0.073}$	0.377 ± 0.067	$0.395 \pm 5.8e-05$	0.093 ± 0.156	-0.203 ± 3.090	0.111	5 ± 3	6 ± 3	5 ± 3	5 ± 3	2
XMMXCS J143925.1+642150.0	$0.141^{+0.059}_{-0.060}$	0.154 ± 0.027	$0.144 \pm 1.9e-05$	0.035 ± 0.046	0.416 ± 0.845	0.089	4 ± 2	3 ± 2	1 ± 1	1 ± 1	2
XMMXCS J143929.0+024606.6	$0.145^{+0.030}_{-0.030}$	0.143 ± 0.023	$0.145 \pm 1.7e-05$	-0.015 ± 0.014	1.310 ± 0.241	0.053	5 ± 2	5 ± 3	2 ± 1	3 ± 2	2
XMMXCS J143936.8+642053.4	$0.141^{+0.048}_{-0.049}$	0.119 ± 0.021	-	0.135 ± 0.032	-1.390 ± 0.592	0.078	3 ± 2	2 ± 2	2 ± 1	0 ± 1	2
XMMXCS J144141.7+352030.7	$0.188^{+0.087}_{-0.097}$	0.210 ± 0.044	-	-0.087 ± 0.027	2.770 ± 0.533	0.085	2 ± 2	0 ± 1	1 ± 1	-	2
XMMXCS J144456.6+062509.4	$0.269^{+0.058}_{-0.059}$	0.287 ± 0.055	$0.277 \pm 3.3e-05$	0.004 ± 0.036	1.340 ± 0.715	0.075	6 ± 3	8 ± 3	3 ± 2	5 ± 3	2
XMMXCS J144801.8+632550.2	$0.260^{+0.060}_{-0.061}$	0.286 ± 0.059	-	-0.059 ± 0.026	2.600 ± 0.480	0.001	3 ± 2	7 ± 3	1 ± 1	3 ± 2	2
XMMXCS J144858.9+090741.1	$0.270^{+0.061}_{-0.062}$	0.287 ± 0.045	$0.272 \pm 3.5e-05$	-0.073 ± 0.075	2.760 ± 1.480	0.138	1 ± 2	1 ± 2	1 ± 1	1 ± 1	2

Continued on next page

Table A.2 – continued from previous page

name	z_{RS}	z_{BCG}	z_{spec-g}	cmr_{grad}	cmr_{inter}	cmr_{wid}	n_{gals-c}	n_{gals-l}	n_{200-c}	n_{200-l}	qual
XMMXCS J144940.0+084744.6	$0.280^{+0.067}_{-0.069}$	0.263 ± 0.051	-	0.091 ± 0.110	-0.248 ± 2.140	0.102	2 ± 2	0 ± 2	1 ± 1	-	2
XMMXCS J145209.2+164603.3	$0.169^{+0.081}_{-0.081}$	0.165 ± 0.044	-	-0.036 ± 0.033	1.760 ± 0.651	0.057	2 ± 2	2 ± 2	2 ± 1	1 ± 1	2
XMMXCS J145316.4+033733.9	$0.396^{+0.102}_{-0.091}$	0.354 ± 0.055	$0.371 \pm 6.6e-05$	0.017 ± 0.035	0.223 ± 0.691	0.068	5 ± 4	11 ± 4	2 ± 2	11 ± 4	2
XMMXCS J145325.9+033545.7	$0.349^{+0.082}_{-0.081}$	0.349 ± 0.051	$0.371 \pm 8.3e-05$	0.094 ± 0.104	-0.232 ± 2.040	0.134	6 ± 3	6 ± 3	2 ± 2	2 ± 2	2
XMMXCS J145352.8+184853.7	$0.434^{+0.082}_{-0.079}$	0.444 ± 0.076	$0.430 \pm 1.9e-04$	0.020 ± 0.147	1.100 ± 2.880	0.154	6 ± 4	4 ± 4	2 ± 2	3 ± 2	2
XMMXCS J145423.6+183513.3	$0.099^{+0.045}_{-0.028}$	0.062 ± 0.016	$0.076 \pm 9.8e-06$	0.014 ± 0.024	0.694 ± 0.378	0.086	14 ± 4	14 ± 4	18 ± 5	21 ± 5	2
XMMXCS J145617.9+222228.2	$0.108^{+0.014}_{-0.014}$	0.107 ± 0.018	$0.109 \pm 1.1e-05$	-0.016 ± 0.014	1.210 ± 0.250	0.040	4 ± 2	4 ± 2	2 ± 2	3 ± 2	2
XMMXCS J145658.3+222943.4	$0.090^{+0.033}_{-0.034}$	0.110 ± 0.027	$0.123 \pm 2.8e-05$	-0.173 ± 0.048	3.650 ± 0.789	0.101	2 ± 2	1 ± 2	2 ± 1	1 ± 1	2
XMMXCS J145709.0-010057.7	$0.143^{+0.078}_{-0.083}$	0.156 ± 0.024	$0.150 \pm 2.3e-05$	-0.016 ± 0.016	1.350 ± 0.300	0.058	2 ± 2	1 ± 1	1 ± 1	0 ± 1	2
XMMXCS J145713.6+223257.4	$0.343^{+0.098}_{-0.093}$	0.383 ± 0.126	$0.418 \pm 1.3e-04$	0.482 ± 0.257	-7.830 ± 5.060	0.335	8 ± 4	11 ± 4	8 ± 4	12 ± 4	2
XMMXCS J150205.9+421149.7	$0.548^{+0.110}_{-0.107}$	0.523 ± 0.144	$0.542 \pm 2.7e-04$	-0.036 ± 0.036	1.700 ± 0.717	0.001	1 ± 2	2 ± 3	1 ± 1	-	2
XMMXCS J150244.8+422005.3	$0.235^{+0.045}_{-0.048}$	0.235 ± 0.036	-	0.050 ± 0.057	0.494 ± 1.080	0.036	4 ± 2	4 ± 2	1 ± 1	0 ± 1	2
XMMXCS J150414.9-024119.2	$0.281^{+0.063}_{-0.055}$	0.232 ± 0.037	-	-0.039 ± 0.904	1.920 ± 17.50	0.128	4 ± 3	-	2 ± 2	-	2
XMMXCS J150421.9-023943.0	$0.276^{+0.111}_{-0.114}$	0.232 ± 0.037	-	-0.030 ± 0.049	1.930 ± 0.953	0.072	3 ± 2	0 ± 2	1 ± 1	-	2
XMMXCS J150559.4+014147.0	$0.239^{+0.050}_{-0.048}$	0.194 ± 0.042	$0.236 \pm 1.7e-05$	-0.167 ± 0.032	4.060 ± 0.600	0.001	2 ± 2	1 ± 2	2 ± 1	0 ± 1	2
XMMXCS J150637.5+002523.0	$0.512^{+0.150}_{-0.145}$	0.466 ± 0.276	-	0.163 ± 0.056	-2.530 ± 1.140	0.001	3 ± 3	13 ± 4	4 ± 2	12 ± 4	2
XMMXCS J150953.0+073608.6	$0.086^{+0.081}_{-0.081}$	0.067 ± 0.018	$0.076 \pm 2.3e-05$	0.005 ± 0.027	0.709 ± 0.498	0.088	5 ± 2	3 ± 2	1 ± 1	0 ± 1	2
XMMXCS J151602.4+561642.7	$0.103^{+0.087}_{-0.098}$	0.080 ± 0.028	$0.001 \pm 1.1e-05$	-0.035 ± 0.029	1.480 ± 0.542	0.500	3 ± 2	31 ± 6	2 ± 2	47 ± 8	2
XMMXCS J151647.7+071228.6	$0.070^{+0.018}_{-0.018}$	0.055 ± 0.022	$0.039 \pm 6.8e-06$	0.426 ± 0.001	-5.530 ± 0.001	0.500	14 ± 4	15 ± 4	18 ± 5	20 ± 5	2

Continued on next page

Table A.2 – continued from previous page

name	z_{RS}	z_{BCG}	z_{spec-g}	cmr_{grad}	cmr_{inter}	cmr_{wid}	n_{gals-c}	n_{gals-l}	n_{200-c}	n_{200-l}	qual
XMMXCS J151724.1+312220.6	$0.100^{+0.027}_{-0.027}$	0.100 ± 0.023	$0.099 \pm 1.2e-05$	-0.077 ± 0.050	1.950 ± 0.885	0.084	2 ± 2	1 ± 2	2 ± 1	1 ± 1	2
XMMXCS J151858.9+312935.1	$0.657^{+0.163}_{-0.170}$	0.619 ± 0.215	-	0.281 ± 0.290	-4.850 ± 5.980	0.001	3 ± 2	1 ± 1	2 ± 1	0 ± 1	2
XMMXCS J152140.9+075237.2	$0.112^{+0.036}_{-0.036}$	0.076 ± 0.021	$0.086 \pm 9.7e-06$	0.162 ± 0.001	-1.810 ± 0.001	0.500	7 ± 4	7 ± 4	5 ± 3	3 ± 3	2
XMMXCS J152223.8+073747.5	$0.573^{+0.140}_{-0.138}$	0.504 ± 0.082	$0.526 \pm 1.1e-04$	0.146 ± 0.141	-2.010 ± 2.850	0.036	7 ± 3	12 ± 4	6 ± 3	12 ± 4	2
XMMXCS J152324.7+273055.9	$0.470^{+0.232}_{-0.205}$	0.430 ± 0.161	-	-0.061 ± 0.171	2.130 ± 3.560	0.001	7 ± 3	10 ± 4	2 ± 2	7 ± 3	2
XMMXCS J153144.9+043407.1	$0.039^{+0.020}_{-0.020}$	0.058 ± 0.022	$0.039 \pm 6.9e-06$	-0.025 ± 0.023	1.190 ± 0.376	0.043	2 ± 1	0 ± 1	1 ± 1	-	2
XMMXCS J153352.3+302129.5	$0.361^{+0.070}_{-0.070}$	0.386 ± 0.064	-	-0.049 ± 0.031	2.620 ± 0.596	0.067	4 ± 3	-	2 ± 2	-	2
XMMXCS J153406.5+232922.6	$0.065^{+0.038}_{-0.038}$	0.078 ± 0.021	$0.049 \pm 7.5e-06$	-0.034 ± 0.001	1.280 ± 0.001	0.500	2 ± 2	1 ± 1	1 ± 1	0 ± 1	2
XMMXCS J153455.1+232844.4	$0.065^{+0.025}_{-0.025}$	0.075 ± 0.030	$0.048 \pm 9.4e-06$	0.046 ± 0.013	0.237 ± 0.188	0.077	5 ± 2	7 ± 3	3 ± 2	5 ± 2	2
XMMXCS J153540.8+552719.6	$0.218^{+0.100}_{-0.108}$	0.173 ± 0.045	-	0.006 ± 0.042	1.080 ± 0.804	0.074	2 ± 2	1 ± 2	1 ± 1	1 ± 1	2
XMMXCS J153629.6+580139.8	$0.478^{+0.153}_{-0.144}$	0.446 ± 0.067	-	0.427 ± 0.138	-7.670 ± 2.810	0.128	4 ± 3	7 ± 3	2 ± 2	2 ± 2	2
XMMXCS J154233.1+535919.9	$0.624^{+0.163}_{-0.163}$	0.587 ± 0.153	-	-0.055 ± 0.065	2.440 ± 1.290	0.001	14 ± 4	42 ± 7	14 ± 4	31 ± 7	2
XMMXCS J160129.8+083856.3	$0.188^{+0.042}_{-0.042}$	0.197 ± 0.030	$0.188 \pm 3.3e-05$	-0.029 ± 0.009	1.800 ± 0.153	0.001	4 ± 2	3 ± 2	2 ± 1	0 ± 1	2
XMMXCS J160423.8+325217.6	$0.397^{+0.100}_{-0.100}$	0.384 ± 0.082	$0.553 \pm 1.5e-04$	-0.180 ± 0.730	5.260 ± 14.90	0.001	4 ± 3	5 ± 3	1 ± 1	-	2
XMMXCS J160439.9+425950.2	$0.263^{+0.044}_{-0.041}$	0.224 ± 0.040	$0.273 \pm 5.6e-05$	-0.030 ± 0.025	1.930 ± 0.462	0.065	5 ± 3	6 ± 3	2 ± 2	3 ± 2	2
XMMXCS J160538.2+323838.2	$0.291^{+0.068}_{-0.074}$	0.296 ± 0.045	$0.301 \pm 4.3e-05$	0.009 ± 0.029	1.470 ± 0.580	0.001	3 ± 2	3 ± 2	2 ± 1	1 ± 1	2
XMMXCS J160544.7+325402.4	$0.587^{+0.147}_{-0.145}$	0.539 ± 0.103	$0.569 \pm 1.8e-04$	-0.288 ± 0.113	6.770 ± 2.310	0.016	1 ± 2	3 ± 3	1 ± 1	-	2
XMMXCS J160740.4+112532.6	$0.491^{+0.124}_{-0.114}$	0.450 ± 0.066	-	-0.027 ± 0.086	1.410 ± 1.730	0.111	4 ± 3	6 ± 4	2 ± 2	1 ± 2	2
XMMXCS J160934.4+542027.2	$0.451^{+0.118}_{-0.101}$	0.484 ± 0.071	-	-0.003 ± 0.051	0.705 ± 1.030	0.107	4 ± 3	-	2 ± 2	-	2

Continued on next page

Table A.2 – continued from previous page

name	z_{RS}	z_{BCG}	z_{spec-g}	cmr_{grad}	cmr_{inter}	cmr_{wid}	n_{gals-c}	n_{gals-l}	n_{200-c}	n_{200-l}	qual
XMMXCS J160947.2+263032.8	$0.086^{+0.049}_{-0.044}$	0.110 ± 0.029	$0.076 \pm 2.1e-05$	-0.027 ± 0.022	1.220 ± 0.394	0.093	4 ± 2	2 ± 2	2 ± 1	0 ± 1	2
XMMXCS J161132.7+541628.3	$0.324^{+0.078}_{-0.078}$	0.355 ± 0.054	-	-0.074 ± 0.029	3.100 ± 0.555	0.071	28 ± 6	26 ± 5	34 ± 6	32 ± 6	2
XMMXCS J161544.0+121708.7	$0.172^{+0.039}_{-0.040}$	0.201 ± 0.117	-	-0.017 ± 0.042	1.510 ± 0.786	0.072	4 ± 2	4 ± 2	3 ± 2	3 ± 2	2
XMMXCS J161603.5+350149.2	$0.532^{+0.132}_{-0.135}$	0.507 ± 0.133	-	-0.216 ± 0.105	5.340 ± 2.170	0.001	2 ± 2	7 ± 3	1 ± 1	1 ± 1	2
XMMXCS J161622.6+345600.0	$0.060^{+0.041}_{-0.033}$	0.082 ± 0.018	$0.082 \pm 8.8e-06$	-0.705 ± 0.001	11.900 ± 0.001	0.500	6 ± 3	0 ± 1	4 ± 2	-	2
XMMXCS J161714.1+123810.5	$0.199^{+0.029}_{-0.028}$	0.209 ± 0.040	$0.199 \pm 4.5e-05$	-0.082 ± 0.046	2.660 ± 0.824	0.100	2 ± 2	3 ± 2	2 ± 1	2 ± 2	2
XMMXCS J162659.6+552140.6	$0.126^{+0.058}_{-0.060}$	0.120 ± 0.026	-	-0.011 ± 0.014	1.200 ± 0.254	0.062	3 ± 2	4 ± 2	1 ± 1	1 ± 1	2
XMMXCS J162739.9+553434.3	$0.128^{+0.033}_{-0.033}$	0.124 ± 0.028	-	0.160 ± 0.030	-1.970 ± 0.535	0.034	3 ± 2	3 ± 2	1 ± 1	1 ± 1	2
XMMXCS J162820.3+551031.5	$0.270^{+0.163}_{-0.169}$	0.235 ± 0.047	-	-0.106 ± 0.080	3.200 ± 1.600	0.081	3 ± 2	3 ± 2	3 ± 2	3 ± 2	2
XMMXCS J163210.3+340022.3	$0.190^{+0.041}_{-0.041}$	0.196 ± 0.030	$0.190 \pm 4.2e-05$	-0.077 ± 0.027	2.620 ± 0.475	0.077	4 ± 2	6 ± 3	2 ± 2	3 ± 2	2
XMMXCS J163247.8+373846.6	$0.504^{+0.128}_{-0.125}$	0.530 ± 0.081	-	0.040 ± 0.058	0.051 ± 1.170	0.107	1 ± 2	-	2 ± 1	-	2
XMMXCS J163300.7+054442.8	$0.150^{+0.058}_{-0.059}$	0.145 ± 0.024	-	-0.039 ± 0.022	1.800 ± 0.403	0.026	2 ± 2	1 ± 1	1 ± 1	-	2
XMMXCS J163325.8+571139.2	$0.240^{+0.050}_{-0.050}$	0.251 ± 0.044	-	0.006 ± 0.019	1.290 ± 0.347	0.001	3 ± 2	7 ± 3	1 ± 1	2 ± 2	2
XMMXCS J163936.7+464946.2	$0.206^{+0.073}_{-0.072}$	0.234 ± 0.046	-	-0.099 ± 0.104	3.050 ± 1.980	0.082	4 ± 2	5 ± 3	1 ± 1	2 ± 2	2
XMMXCS J164142.0+390738.8	$0.454^{+0.108}_{-0.111}$	0.410 ± 0.157	$0.535 \pm 1.1e-04$	0.212 ± 0.096	-3.300 ± 1.870	0.130	5 ± 3	8 ± 4	2 ± 2	9 ± 4	2
XMMXCS J165429.0+142045.6	$0.593^{+0.146}_{-0.145}$	0.570 ± 0.185	-	0.041 ± 0.191	0.358 ± 3.900	0.141	2 ± 2	10 ± 4	2 ± 1	11 ± 4	2
XMMXCS J165724.2+785221.8	$0.608^{+0.195}_{-0.195}$	0.623 ± 0.214	-	0.232 ± 0.272	-3.300 ± 5.420	0.001	3 ± 2	9 ± 4	2 ± 1	6 ± 3	2
XMMXCS J165728.4+275106.9	$0.035^{+0.032}_{-0.032}$	0.073 ± 0.026	$0.034 \pm 7.0e-06$	-0.005 ± 0.012	0.846 ± 0.201	0.041	3 ± 2	0 ± 1	1 ± 1	-	2
XMMXCS J165901.0+322930.5	$0.061^{+0.004}_{-0.003}$	0.099 ± 0.023	$0.061 \pm 1.1e-05$	-0.033 ± 0.005	1.380 ± 0.085	0.016	6 ± 3	4 ± 2	5 ± 2	5 ± 2	2

Continued on next page

Table A.2 – continued from previous page

name	z_{RS}	z_{BCG}	z_{spec-g}	cmr_{grad}	cmr_{inter}	cmr_{wid}	n_{gals-c}	n_{gals-l}	n_{200-c}	n_{200-l}	qual
XMMXCS J170427.9+453913.1	$0.281^{+0.063}_{-0.064}$	0.311 ± 0.048	-	-0.049 ± 0.044	2.360 ± 0.848	0.120	2 ± 2	-	2 ± 1	-	2
XMMXCS J170625.3+784241.8	$0.123^{+0.098}_{-0.105}$	0.078 ± 0.015	-	0.006 ± 0.021	0.710 ± 0.368	0.099	22 ± 5	23 ± 5	44 ± 7	49 ± 7	2
XMMXCS J171226.9+591147.6	$0.226^{+0.088}_{-0.075}$	0.202 ± 0.066	-	0.364 ± 0.001	-5.630 ± 0.002	0.500	4 ± 3	2 ± 3	2 ± 2	0 ± 1	2
XMMXCS J171245.86+640343.7	$0.080^{+0.008}_{-0.008}$	0.112 ± 0.025	$0.081 \pm 1.3e-05$	0.002 ± 0.011	0.905 ± 0.177	0.054	31 ± 6	35 ± 6	50 ± 7	55 ± 7	2
XMMXCS J171249.0+640347.6	$0.079^{+0.009}_{-0.009}$	0.112 ± 0.025	$0.081 \pm 1.3e-05$	-0.005 ± 0.010	1.000 ± 0.162	0.056	31 ± 6	34 ± 6	51 ± 7	56 ± 8	2
XMMXCS J171328.8+640248.2	$0.079^{+0.014}_{-0.015}$	0.112 ± 0.025	$0.081 \pm 1.3e-05$	-0.032 ± 0.018	1.420 ± 0.285	0.050	26 ± 5	28 ± 5	45 ± 7	49 ± 7	2
XMMXCS J171359.19+434438.1	$0.524^{+0.147}_{-0.147}$	0.522 ± 0.182	-	-0.087 ± 0.075	2.750 ± 1.520	0.077	3 ± 2	4 ± 3	1 ± 1	2 ± 2	2
XMMXCS J171416.9+573101.5	$0.076^{+0.034}_{-0.037}$	0.045 ± 0.017	$0.057 \pm 9.2e-06$	0.062 ± 0.045	-0.135 ± 0.772	0.122	3 ± 2	3 ± 2	3 ± 2	4 ± 2	2
XMMXCS J171418.9+623513.6	$0.174^{+0.043}_{-0.044}$	0.173 ± 0.029	$0.177 \pm 4.5e-05$	0.026 ± 0.063	0.727 ± 1.130	0.098	5 ± 3	5 ± 3	1 ± 1	0 ± 1	2
XMMXCS J171817.9+584903.7	$0.176^{+0.067}_{-0.074}$	0.175 ± 0.049	-	-0.069 ± 0.043	2.470 ± 0.795	0.062	4 ± 2	3 ± 2	2 ± 1	1 ± 1	2
XMMXCS J171953.5+263003.1	$0.159^{+0.046}_{-0.047}$	0.164 ± 0.025	$0.166 \pm 3.2e-05$	-0.006 ± 0.015	1.250 ± 0.271	0.063	5 ± 3	7 ± 3	1 ± 1	2 ± 2	2
XMMXCS J172039.3+262552.8	$0.148^{+0.029}_{-0.028}$	0.179 ± 0.034	$0.162 \pm 1.7e-05$	-0.013 ± 0.046	1.280 ± 0.804	0.093	5 ± 3	5 ± 3	1 ± 1	0 ± 1	2
XMMXCS J172120.6+263656.4	$0.165^{+0.058}_{-0.058}$	0.189 ± 0.033	$0.173 \pm 3.9e-05$	-0.100 ± 0.048	2.900 ± 0.900	0.075	4 ± 2	3 ± 2	1 ± 1	2 ± 2	2
XMMXCS J172731.7+703554.6	$0.311^{+0.072}_{-0.072}$	0.337 ± 0.050	-	-0.069 ± 0.035	2.890 ± 0.657	0.040	29 ± 6	27 ± 6	40 ± 7	40 ± 7	2
XMMXCS J173710.6+660316.3	$0.269^{+0.071}_{-0.071}$	0.296 ± 0.108	-	0.284 ± 0.069	-4.310 ± 1.380	0.107	4 ± 2	4 ± 3	4 ± 2	3 ± 2	2
XMMXCS J180026.6+080527.6	$0.157^{+0.102}_{-0.106}$	0.187 ± 0.148	-	-0.312 ± 0.520	7.220 ± 10.20	0.500	1 ± 2	0 ± 2	1 ± 1	-	2
XMMXCS J180032.2+080629.9	$0.149^{+0.096}_{-0.111}$	0.175 ± 0.035	-	0.398 ± 0.021	-5.960 ± 0.355	0.500	2 ± 3	4 ± 3	1 ± 1	2 ± 2	2
XMMXCS J180032.5+080720.3	$0.148^{+0.097}_{-0.115}$	0.175 ± 0.035	-	0.398 ± 0.021	-5.960 ± 0.355	0.500	1 ± 2	4 ± 3	1 ± 1	1 ± 2	2
XMMXCS J183716.5+794048.1	$0.319^{+0.059}_{-0.058}$	0.295 ± 0.059	-	0.076 ± 0.071	0.009 ± 1.370	0.001	2 ± 2	-	2 ± 1	-	2

Continued on next page

Table A.2 – continued from previous page

name	z_{RS}	z_{BCG}	z_{spec-g}	cmr_{grad}	cmr_{inter}	cmr_{wid}	n_{gals-c}	n_{gals-l}	n_{200-c}	n_{200-l}	qual
XMMXCS J184406.9+793908.3	$0.417^{+0.144}_{-0.144}$	0.373 ± 0.073	-	-1.240 ± 0.809	26.600 ± 16.50	0.641	9 ± 4	10 ± 4	7 ± 4	9 ± 4	2
XMMXCS J210702.1+233111.2	$0.625^{+0.111}_{-0.110}$	0.588 ± 0.111	-	0.232 ± 0.086	-3.500 ± 1.730	0.095	2 ± 2	-	1 ± 1	-	2
XMMXCS J211422.9+060053.4	$0.206^{+0.044}_{-0.044}$	0.190 ± 0.029	-	-0.000 ± 0.043	1.270 ± 0.760	0.001	2 ± 2	2 ± 2	2 ± 1	4 ± 2	2
XMMXCS J214411.5+281020.4	$0.204^{+0.055}_{-0.055}$	0.245 ± 0.043	-	-0.007 ± 0.020	1.420 ± 0.365	0.066	2 ± 2	6 ± 3	1 ± 1	5 ± 3	2
XMMXCS J215040.3-054104.8	$0.395^{+0.118}_{-0.112}$	0.420 ± 0.062	-	0.043 ± 0.134	0.738 ± 2.630	0.139	6 ± 3	10 ± 4	3 ± 2	5 ± 3	2
XMMXCS J215336.9+174146.4	$0.263^{+0.069}_{-0.069}$	0.227 ± 0.044	$0.229 \pm 3.0e-05$	-0.002 ± 0.034	1.490 ± 0.625	0.049	40 ± 6	45 ± 7	74 ± 9	76 ± 9	2
XMMXCS J215713.2-074241.0	$0.418^{+0.119}_{-0.116}$	0.466 ± 0.068	-	-0.081 ± 0.059	3.220 ± 1.180	0.132	12 ± 4	12 ± 4	12 ± 4	12 ± 4	2
XMMXCS J220357.6+190155.1	$0.368^{+0.139}_{-0.138}$	0.346 ± 0.055	-	-0.515 ± 0.659	11.800 ± 13.60	0.184	3 ± 3	6 ± 3	1 ± 1	2 ± 2	2
XMMXCS J220605.0-001113.4	$0.389^{+0.073}_{-0.072}$	0.368 ± 0.056	$0.388 \pm 1.0e-04$	-0.015 ± 0.033	1.930 ± 0.661	0.001	2 ± 2	3 ± 3	2 ± 2	4 ± 2	2
XMMXCS J221211.3+000830.4	$0.283^{+0.089}_{-0.091}$	0.340 ± 0.058	$0.331 \pm 5.8e-05$	-0.038 ± 0.058	2.210 ± 1.120	0.001	3 ± 2	2 ± 2	2 ± 2	2 ± 2	2
XMMXCS J222143.88-005307.7	$0.334^{+0.059}_{-0.060}$	0.338 ± 0.072	$0.335 \pm 5.5e-05$	0.099 ± 0.042	-0.030 ± 0.737	0.001	2 ± 2	-	2 ± 1	-	2
XMMXCS J222818.2-053403.4	$0.497^{+0.144}_{-0.144}$	0.528 ± 0.091	-	-0.044 ± 0.092	1.820 ± 1.830	0.111	23 ± 5	47 ± 7	30 ± 6	54 ± 9	2
XMMXCS J222831.6+203730.6	$0.388^{+0.079}_{-0.079}$	0.434 ± 0.071	$0.408 \pm 8.8e-05$	0.025 ± 0.084	1.310 ± 1.630	0.120	39 ± 7	51 ± 7	78 ± 10	85 ± 10	2
XMMXCS J223546.6+335243.8	$0.255^{+0.100}_{-0.102}$	0.234 ± 0.090	-	0.100 ± 0.077	-0.548 ± 1.470	0.148	7 ± 3	8 ± 3	2 ± 2	2 ± 2	2
XMMXCS J223604.1+134950.8	$0.265^{+0.076}_{-0.077}$	0.287 ± 0.098	-	0.181 ± 0.074	-2.160 ± 1.420	0.001	2 ± 2	-	1 ± 1	-	2
XMMXCS J223934.0-060017.5	$0.181^{+0.059}_{-0.060}$	0.155 ± 0.044	-	-0.036 ± 0.037	1.880 ± 0.702	0.097	6 ± 3	5 ± 3	5 ± 2	5 ± 2	2
XMMXCS J223939.1+080557.9	$0.384^{+0.099}_{-0.097}$	0.417 ± 0.064	-	-0.121 ± 0.038	2.970 ± 0.732	0.065	12 ± 4	12 ± 5	12 ± 4	14 ± 5	2
XMMXCS J224240.91-092746.0	$0.596^{+0.201}_{-0.242}$	0.643 ± 0.154	-	0.149 ± 0.086	-1.950 ± 1.710	0.001	3 ± 2	7 ± 3	2 ± 1	0 ± 1	2
XMMXCS J224334.01-092214.2	$0.217^{+0.070}_{-0.075}$	0.253 ± 0.043	-	-0.093 ± 0.135	2.960 ± 2.630	0.141	1 ± 2	1 ± 2	2 ± 1	2 ± 2	2

Continued on next page

Table A.2 – continued from previous page

name	z_{RS}	z_{BCG}	z_{spec-g}	cmr_{grad}	cmr_{inter}	cmr_{wid}	n_{gals-c}	n_{gals-l}	n_{200-c}	n_{200-l}	qual
XMMXCS J230247.7+084355.9	$0.597^{+0.161}_{-0.157}$	0.565 ± 0.165	-	0.131 ± 0.307	-1.510 ± 6.230	0.074	3 ± 2	-	2 ± 1	-	2
XMMXCS J230821.7-021127.6	$0.289^{+0.072}_{-0.073}$	0.322 ± 0.065	$0.305 \pm 6.8e-05$	-0.016 ± 0.016	1.830 ± 0.298	0.037	54 ± 8	54 ± 8	84 ± 10	82 ± 10	2
XMMXCS J230824.8-022049.6	$0.302^{+0.078}_{-0.078}$	0.313 ± 0.052	$0.304 \pm 5.0e-05$	-0.036 ± 0.025	2.270 ± 0.465	0.001	2 ± 2	4 ± 3	2 ± 1	2 ± 2	2
XMMXCS J232124.6+194514.8	$0.315^{+0.067}_{-0.068}$	0.355 ± 0.060	-	-0.015 ± 0.020	1.870 ± 0.379	0.001	24 ± 5	22 ± 5	33 ± 6	28 ± 6	2
XMMXCS J232329.4+164154.5	$0.406^{+0.084}_{-0.083}$	0.447 ± 0.065	-	-0.052 ± 0.051	2.680 ± 0.995	0.090	15 ± 4	16 ± 5	16 ± 5	17 ± 5	2
XMMXCS J232356.0+163314.3	$0.374^{+0.088}_{-0.082}$	0.355 ± 0.053	-	0.017 ± 0.038	0.289 ± 0.762	0.001	3 ± 3	-	1 ± 1	-	2
XMMXCS J232829.0+150443.5	$0.599^{+0.164}_{-0.179}$	0.560 ± 0.193	-	0.300 ± 0.126	-5.090 ± 2.550	0.115	5 ± 3	45 ± 7	4 ± 2	52 ± 9	2
XMMXCS J232832.9+051817.7	$0.175^{+0.057}_{-0.055}$	0.215 ± 0.160	-	0.548 ± 0.208	-9.160 ± 3.820	0.500	3 ± 2	2 ± 3	3 ± 2	0 ± 1	2
XMMXCS J233400.3+485252.8	$0.255^{+0.081}_{-0.082}$	0.286 ± 0.044	-	0.019 ± 0.035	1.040 ± 0.682	0.083	21 ± 5	23 ± 5	30 ± 6	36 ± 6	2
XMMXCS J233743.9+000412.0	$0.472^{+0.112}_{-0.111}$	0.473 ± 0.070	$0.470 \pm 1.3e-04$	-0.006 ± 0.036	0.927 ± 0.716	0.001	7 ± 3	6 ± 4	2 ± 2	1 ± 2	2
XMMXCS J233802.8+265630.8	$0.084^{+0.040}_{-0.042}$	0.049 ± 0.015	-	0.151 ± 0.028	-1.570 ± 0.462	0.057	3 ± 2	4 ± 3	1 ± 1	1 ± 2	2
XMMXCS J233928.4+270245.2	$0.107^{+0.033}_{-0.031}$	0.058 ± 0.025	-	0.033 ± 0.002	0.229 ± 0.030	0.500	5 ± 3	5 ± 3	1 ± 2	2 ± 2	2
XMMXCS J234715.0-022054.9	$0.340^{+0.059}_{-0.059}$	0.367 ± 0.061	-	0.077 ± 0.064	0.037 ± 1.330	0.079	1 ± 2	2 ± 3	1 ± 1	2 ± 2	2
XMMXCS J235036.8+362204.9	$0.223^{+0.084}_{-0.091}$	0.247 ± 0.103	-	0.045 ± 0.001	0.210 ± 0.001	0.500	2 ± 3	1 ± 3	2 ± 2	1 ± 1	2
XMMXCS J235145.8+201643.9	$0.475^{+0.132}_{-0.130}$	0.485 ± 0.083	-	0.090 ± 0.109	-0.872 ± 2.180	0.104	3 ± 3	5 ± 4	1 ± 1	1 ± 2	2
XMMXCS J235537.0+055129.0	$0.279^{+0.077}_{-0.077}$	0.310 ± 0.048	$0.279 \pm 6.2e-05$	-0.028 ± 0.030	2.010 ± 0.568	0.046	14 ± 4	18 ± 5	14 ± 4	21 ± 5	2
XMMXCS J235557.2+055935.2	$0.257^{+0.062}_{-0.061}$	0.231 ± 0.039	$0.257 \pm 2.9e-05$	-0.046 ± 0.019	2.220 ± 0.354	0.001	3 ± 2	5 ± 3	2 ± 1	2 ± 2	2
XMMXCS J000532.7+200714.1	$0.234^{+0.082}_{-0.082}$	0.112 ± 0.060	-	-0.009 ± 0.001	1.640 ± 0.001	0.500	1 ± 2	0 ± 2	1 ± 1	-	3
XMMXCS J000616.5+201415.5	$0.347^{+0.085}_{-0.086}$	0.347 ± 0.052	-	0.036 ± 0.122	0.988 ± 2.320	0.116	0 ± 2	3 ± 3	-	1 ± 2	3

Continued on next page

Table A.2 – continued from previous page

name	z_{RS}	z_{BCG}	z_{spec-g}	cmr_{grad}	cmr_{inter}	cmr_{wid}	n_{gals-c}	n_{gals-l}	n_{200-c}	n_{200-l}	qual
XMMXCS J000618.1+200915.3	$0.345^{+0.052}_{-0.052}$	0.289 ± 0.070	-	0.062 ± 0.070	0.470 ± 1.370	0.036	1 ± 2	1 ± 2	1 ± 1	2 ± 2	3
XMMXCS J000621.6+201119.8	$0.361^{+0.079}_{-0.080}$	0.289 ± 0.070	-	-0.007 ± 0.068	1.830 ± 1.320	0.049	1 ± 2	1 ± 2	1 ± 1	0 ± 1	3
XMMXCS J000626.2+195944.2	$0.464^{+0.078}_{-0.073}$	0.492 ± 0.073	-	-0.473 ± 0.193	10.100 ± 3.780	0.044	4 ± 3	-	2 ± 2	-	3
XMMXCS J000635.3+201814.8	$0.351^{+0.079}_{-0.076}$	0.291 ± 0.045	-	-0.087 ± 0.077	3.200 ± 1.500	0.077	3 ± 3	2 ± 3	0 ± 1	1 ± 2	3
XMMXCS J001015.6+005445.6	$0.288^{+0.067}_{-0.067}$	0.160 ± 0.030	$0.199 \pm 2.4e-05$	0.366 ± 0.208	-5.700 ± 4.090	0.204	1 ± 3	4 ± 3	0 ± 0.1	2 ± 2	3
XMMXCS J001040.4+004258.1	$0.355^{+0.112}_{-0.108}$	0.163 ± 0.035	-	0.015 ± 0.153	0.965 ± 3.080	0.130	3 ± 3	4 ± 4	2 ± 2	3 ± 3	3
XMMXCS J001100.0+005939.4	$0.461^{+0.098}_{-0.096}$	0.444 ± 0.066	$0.457 \pm 1.9e-04$	0.155 ± 0.078	-2.330 ± 1.580	0.108	6 ± 4	7 ± 4	0 ± 2	4 ± 3	3
XMMXCS J001308.8-193125.2	$0.076^{+0.027}_{-0.027}$	0.087 ± 0.017	-	-0.045 ± 0.026	1.590 ± 0.446	0.086	16 ± 4	13 ± 4	19 ± 4	13 ± 4	3
XMMXCS J001335.6-192931.7	$0.115^{+0.030}_{-0.029}$	0.123 ± 0.021	-	-0.001 ± 0.017	0.964 ± 0.259	0.079	41 ± 6	40 ± 6	54 ± 8	62 ± 8	3
XMMXCS J001347.0-193501.1	$0.086^{+0.029}_{-0.029}$	0.095 ± 0.028	-	0.009 ± 0.038	0.716 ± 0.638	0.078	19 ± 4	16 ± 4	28 ± 5	22 ± 5	3
XMMXCS J001356.1-193119.8	$0.081^{+0.025}_{-0.025}$	0.096 ± 0.043	-	0.035 ± 0.049	0.332 ± 0.794	0.065	25 ± 5	22 ± 5	38 ± 6	31 ± 6	3
XMMXCS J001424.9-193010.3	$0.091^{+0.024}_{-0.024}$	0.095 ± 0.018	-	-0.035 ± 0.014	1.470 ± 0.231	0.051	9 ± 3	9 ± 3	7 ± 3	7 ± 3	3
XMMXCS J001604.7+173417.5	$0.304^{+0.118}_{-0.091}$	0.184 ± 0.086	-	0.342 ± 0.252	-5.310 ± 4.830	0.190	5 ± 3	7 ± 4	3 ± 2	7 ± 3	3
XMMXCS J001802.1+163614.5	$0.191^{+0.079}_{-0.087}$	0.119 ± 0.019	-	0.043 ± 0.031	0.299 ± 0.564	0.122	0 ± 1	2 ± 2	-	0 ± 1	3
XMMXCS J001816.70+161737.8	$0.577^{+0.142}_{-0.143}$	0.562 ± 0.092	-	0.106 ± 0.032	-0.888 ± 0.622	0.091	7 ± 3	13 ± 4	6 ± 3	12 ± 4	3
XMMXCS J001816.6+161737.8	$0.577^{+0.142}_{-0.143}$	0.562 ± 0.092	-	0.106 ± 0.032	-0.888 ± 0.622	0.091	7 ± 3	13 ± 4	6 ± 3	12 ± 4	3
XMMXCS J001833.13+162609.1	$0.545^{+0.122}_{-0.121}$	0.601 ± 0.112	-	-0.099 ± 0.036	2.970 ± 0.721	0.001	27 ± 6	46 ± 7	38 ± 7	87 ± 11	3
XMMXCS J001833.1+162609.1	$0.545^{+0.122}_{-0.121}$	0.601 ± 0.112	-	-0.099 ± 0.036	2.970 ± 0.721	0.001	27 ± 6	46 ± 7	38 ± 7	87 ± 11	3
XMMXCS J001835.15+163801.6	$0.268^{+0.156}_{-0.141}$	0.143 ± 0.030	-	0.191 ± 0.080	-2.700 ± 1.560	0.070	0 ± 1	1 ± 2	-	0 ± 1	3

Continued on next page

Table A.2 – continued from previous page

name	z_{RS}	z_{BCG}	z_{spec-g}	cmr_{grad}	cmr_{inter}	cmr_{wid}	n_{gals-c}	n_{gals-l}	n_{200-c}	n_{200-l}	qual
XMMXCS J001835.1+163801.6	$0.268^{+0.156}_{-0.141}$	0.143 ± 0.030	-	0.191 ± 0.080	-2.700 ± 1.560	0.070	0 ± 1	1 ± 2	-	0 ± 1	3
XMMXCS J001854.96+162947.6	$0.297^{+0.089}_{-0.088}$	0.102 ± 0.027	-	0.340 ± 0.219	-4.990 ± 4.330	0.207	11 ± 4	8 ± 4	8 ± 4	3 ± 3	3
XMMXCS J001854.9+162947.6	$0.297^{+0.089}_{-0.088}$	0.102 ± 0.027	-	0.340 ± 0.219	-4.990 ± 4.330	0.207	11 ± 4	8 ± 4	8 ± 4	3 ± 3	3
XMMXCS J001905.94+162838.3	$0.293^{+0.075}_{-0.078}$	0.490 ± 0.172	-	0.096 ± 0.084	-0.386 ± 1.600	0.151	7 ± 3	7 ± 3	2 ± 2	2 ± 2	3
XMMXCS J001905.9+162838.2	$0.293^{+0.075}_{-0.078}$	0.490 ± 0.172	-	0.096 ± 0.084	-0.386 ± 1.600	0.151	7 ± 3	7 ± 3	2 ± 2	2 ± 2	3
XMMXCS J002029.3+215634.5	$0.200^{+0.041}_{-0.034}$	0.051 ± 0.022	-	-0.009 ± 0.019	1.270 ± 0.309	0.500	0 ± 2	2 ± 3	-	453 ± 21	3
XMMXCS J002054.5-021114.7	$0.346^{+0.080}_{-0.076}$	0.159 ± 0.027	$0.340 \pm 8.1e-05$	0.271 ± 0.007	-4.320 ± 0.142	0.500	2 ± 4	1 ± 4	3 ± 2	2 ± 2	3
XMMXCS J002121.7-083956.0	$0.419^{+0.083}_{-0.082}$	0.347 ± 0.063	-	0.160 ± 0.089	-1.220 ± 1.700	0.001	4 ± 3	4 ± 3	3 ± 2	3 ± 2	3
XMMXCS J002136.1-083608.3	$0.386^{+0.081}_{-0.080}$	0.294 ± 0.058	-	0.039 ± 0.043	-0.121 ± 0.840	0.001	5 ± 3	4 ± 3	4 ± 2	2 ± 2	3
XMMXCS J002144.4+001905.9	$0.281^{+0.100}_{-0.104}$	0.245 ± 0.056	-	0.062 ± 0.028	0.135 ± 0.546	0.001	0 ± 1	2 ± 2	-	1 ± 1	3
XMMXCS J002247.4-145438.7	$0.246^{+0.082}_{-0.083}$	0.125 ± 0.035	-	0.115 ± 0.022	-1.030 ± 0.429	0.500	3 ± 3	0 ± 3	1 ± 1	-	3
XMMXCS J002309.1+001520.7	$0.262^{+0.069}_{-0.069}$	0.280 ± 0.043	$0.264 \pm 4.1e-05$	-0.033 ± 0.016	2.010 ± 0.304	0.059	3 ± 2	0 ± 2	0 ± 0.1	-	3
XMMXCS J002710.5+170540.8	$0.222^{+0.084}_{-0.096}$	0.184 ± 0.039	-	-0.000 ± 0.001	0.642 ± 0.001	0.500	3 ± 3	4 ± 4	2 ± 2	0 ± 2	3
XMMXCS J002713.3+165939.6	$0.171^{+0.036}_{-0.032}$	0.081 ± 0.026	-	0.026 ± 0.010	0.746 ± 0.181	0.500	4 ± 3	4 ± 4	2 ± 2	1 ± 2	3
XMMXCS J002901.9+350822.3	$0.513^{+0.141}_{-0.139}$	0.457 ± 0.068	-	0.041 ± 0.054	-0.006 ± 1.100	0.106	10 ± 4	11 ± 4	10 ± 4	10 ± 4	3
XMMXCS J002912.4+350857.9	$0.508^{+0.169}_{-0.179}$	0.530 ± 0.084	-	0.014 ± 0.048	0.606 ± 0.968	0.088	2 ± 3	13 ± 4	0 ± 1	12 ± 4	3
XMMXCS J002928.8-001250.7	$0.132^{+0.068}_{-0.069}$	0.068 ± 0.013	$0.060 \pm 9.3e-06$	0.043 ± 0.016	0.317 ± 0.252	0.099	14 ± 4	22 ± 5	17 ± 4	34 ± 6	3
XMMXCS J002932.7+262344.3	$0.213^{+0.065}_{-0.066}$	0.086 ± 0.015	-	0.052 ± 0.053	0.299 ± 1.000	0.137	6 ± 3	8 ± 4	3 ± 2	6 ± 3	3
XMMXCS J003026.5+260915.5	$0.659^{+0.141}_{-0.133}$	0.651 ± 0.151	-	0.008 ± 0.149	1.050 ± 3.090	0.001	2 ± 2	7 ± 3	1 ± 1	5 ± 2	3

Continued on next page

Table A.2 – continued from previous page

name	z_{RS}	z_{BCG}	z_{spec-g}	cmr_{grad}	cmr_{inter}	cmr_{wid}	n_{gals-c}	n_{gals-l}	n_{200-c}	n_{200-l}	qual
XMMXCS J003033.9+261807.4	$0.339^{+0.133}_{-0.130}$	0.529 ± 0.085	-	-0.065 ± 0.145	2.860 ± 2.880	0.001	8 ± 3	10 ± 4	5 ± 3	10 ± 4	3
XMMXCS J003047.5+045811.0	$0.603^{+0.151}_{-0.146}$	0.534 ± 0.120	-	0.095 ± 0.184	-0.929 ± 3.650	0.141	3 ± 2	-	0 ± 1	-	3
XMMXCS J003109.4+261004.4	$0.126^{+0.041}_{-0.041}$	0.106 ± 0.028	-	-0.046 ± 0.074	1.590 ± 1.290	0.071	0 ± 1	2 ± 2	-	1 ± 1	3
XMMXCS J003119.0+262456.2	$0.516^{+0.143}_{-0.139}$	0.385 ± 0.113	-	0.363 ± 0.257	-6.350 ± 5.080	0.273	5 ± 4	6 ± 4	1 ± 2	-	3
XMMXCS J003317.9-212459.2	$0.160^{+0.058}_{-0.059}$	0.062 ± 0.017	-	0.157 ± 0.028	-1.720 ± 0.507	0.500	15 ± 4	12 ± 4	14 ± 4	12 ± 4	3
XMMXCS J003413.6-052214.4	$0.498^{+0.155}_{-0.156}$	0.380 ± 0.095	-	0.590 ± 0.222	-11.20 ± 4.600	0.148	5 ± 3	7 ± 4	2 ± 2	4 ± 3	3
XMMXCS J003416.4-212623.0	$0.076^{+0.036}_{-0.035}$	0.128 ± 0.056	-	0.048 ± 0.022	-0.016 ± 0.273	0.117	6 ± 3	11 ± 3	5 ± 2	10 ± 3	3
XMMXCS J003428.3-213649.5	$0.210^{+0.078}_{-0.078}$	0.166 ± 0.045	-	0.001 ± 0.055	1.190 ± 1.050	0.124	4 ± 2	4 ± 3	0 ± 1	0 ± 1	3
XMMXCS J003631.6+091316.0	$0.445^{+0.135}_{-0.134}$	0.247 ± 0.075	$0.635 \pm 2.2e-04$	0.168 ± 0.081	-1.950 ± 1.650	0.001	3 ± 3	2 ± 3	2 ± 2	-	3
XMMXCS J003730.6+092257.7	$0.228^{+0.081}_{-0.088}$	0.193 ± 0.086	-	0.117 ± 0.131	-0.890 ± 2.490	0.105	5 ± 3	4 ± 3	0 ± 0.1	0 ± 1	3
XMMXCS J003814.8+400305.9	$0.578^{+0.165}_{-0.165}$	0.655 ± 0.127	-	0.031 ± 0.047	0.429 ± 0.969	0.126	26 ± 6	76 ± 10	78 ± 10	668 ± 28	3
XMMXCS J003819.3+005110.2	$0.456^{+0.098}_{-0.097}$	0.331 ± 0.136	-	0.231 ± 0.122	-3.830 ± 2.410	0.001	6 ± 3	5 ± 3	3 ± 2	3 ± 2	3
XMMXCS J003819.7+405638.4	$0.510^{+0.145}_{-0.142}$	0.400 ± 0.122	-	0.294 ± 0.305	-5.180 ± 6.330	0.073	13 ± 5	17 ± 6	13 ± 5	-	3
XMMXCS J003834.3+400219.4	$0.560^{+0.160}_{-0.160}$	0.475 ± 0.276	-	0.027 ± 0.205	0.612 ± 4.180	0.159	32 ± 6	63 ± 9	83 ± 10	346 ± 21	3
XMMXCS J003836.8+010104.0	$0.387^{+0.066}_{-0.057}$	0.293 ± 0.052	-	-0.053 ± 0.057	2.700 ± 1.110	0.113	2 ± 3	-	0 ± 0.1	-	3
XMMXCS J003837.3+004413.0	$0.294^{+0.113}_{-0.113}$	0.214 ± 0.041	$0.192 \pm 2.3e-05$	-0.061 ± 0.240	2.460 ± 4.850	0.128	6 ± 3	1 ± 3	4 ± 3	0 ± 1	3
XMMXCS J003846.6+400447.5	$0.609^{+0.168}_{-0.169}$	0.461 ± 0.149	-	1.360 ± 0.441	-27.10 ± 9.130	0.174	21 ± 5	2 ± 2	49 ± 8	1 ± 1	3
XMMXCS J003856.2+003836.0	$0.298^{+0.078}_{-0.083}$	0.275 ± 0.046	-	-0.020 ± 0.058	1.880 ± 1.110	0.073	1 ± 2	2 ± 3	-	0 ± 1	3
XMMXCS J003916.8+405115.1	$0.572^{+0.238}_{-0.243}$	0.452 ± 0.254	-	0.779 ± 0.471	-14.20 ± 9.620	0.318	36 ± 7	63 ± 9	143 ± 13	380 ± 21	3

Continued on next page

Table A.2 – continued from previous page

name	z_{RS}	z_{BCG}	z_{spec-g}	cmr_{grad}	cmr_{inter}	cmr_{wid}	n_{gals-c}	n_{gals-l}	n_{200-c}	n_{200-l}	qual
XMMXCS J003924.6+405026.2	$0.657^{+0.174}_{-0.173}$	0.680 ± 0.126	-	0.424 ± 0.169	-7.080 ± 3.440	0.202	13 ± 4	82 ± 10	16 ± 5	367 ± 22	3
XMMXCS J003926.4+410529.1	$0.310^{+0.139}_{-0.138}$	0.164 ± 0.035	-	0.119 ± 0.138	-1.110 ± 2.780	0.110	11 ± 4	10 ± 4	10 ± 4	7 ± 4	3
XMMXCS J003927.2+411919.7	$0.343^{+0.129}_{-0.127}$	0.214 ± 0.042	-	0.100 ± 0.059	-0.478 ± 1.180	0.123	8 ± 4	10 ± 4	8 ± 3	6 ± 4	3
XMMXCS J003934.7+410930.3	$0.539^{+0.158}_{-0.158}$	0.443 ± 0.136	-	0.097 ± 0.051	-1.030 ± 1.030	0.072	25 ± 6	55 ± 8	72 ± 10	155 ± 15	3
XMMXCS J003942.1+401817.4	$0.348^{+0.166}_{-0.160}$	0.182 ± 0.060	-	-0.047 ± 0.058	2.340 ± 1.150	0.001	19 ± 5	17 ± 5	29 ± 6	26 ± 6	3
XMMXCS J003954.4+400856.0	$0.521^{+0.223}_{-0.182}$	0.654 ± 0.198	-	0.038 ± 0.346	0.242 ± 7.210	0.116	6 ± 4	0 ± 1	0 ± 2	-	3
XMMXCS J004001.1+410057.0	$0.566^{+0.142}_{-0.143}$	0.669 ± 0.134	-	0.267 ± 0.209	-4.150 ± 4.260	0.200	16 ± 5	49 ± 8	22 ± 6	115 ± 14	3
XMMXCS J004030.3+065500.6	$0.064^{+0.017}_{-0.017}$	0.062 ± 0.018	-	-0.018 ± 0.003	1.110 ± 0.053	0.012	16 ± 4	19 ± 4	20 ± 5	30 ± 6	3
XMMXCS J004049.2+415212.5	$0.299^{+0.091}_{-0.093}$	0.118 ± 0.128	-	0.322 ± 0.262	-4.850 ± 5.200	0.250	8 ± 4	6 ± 4	9 ± 3	7 ± 3	3
XMMXCS J004128.0+252959.0	$0.114^{+0.027}_{-0.028}$	0.056 ± 0.028	-	0.017 ± 0.008	0.613 ± 0.127	0.094	12 ± 4	11 ± 4	12 ± 4	10 ± 4	3
XMMXCS J004149.6-094704.9	$0.179^{+0.033}_{-0.033}$	0.099 ± 0.032	-	1.270 ± 0.018	-22.90 ± 0.349	0.500	0 ± 1	1 ± 2	-	0 ± 1	3
XMMXCS J004152.5+401911.3	$0.561^{+0.195}_{-0.192}$	0.575 ± 0.150	-	0.150 ± 0.201	-1.780 ± 4.090	0.049	7 ± 4	-	1 ± 2	-	3
XMMXCS J004153.1+402117.2	$0.064^{+0.031}_{-0.032}$	0.051 ± 0.015	-	-0.022 ± 0.002	0.908 ± 0.034	0.500	1 ± 1	0 ± 1	1 ± 1	-	3
XMMXCS J004157.1+402126.6	$0.066^{+0.038}_{-0.038}$	0.051 ± 0.015	-	-0.036 ± 0.044	1.210 ± 0.720	0.109	2 ± 1	0 ± 1	1 ± 1	-	3
XMMXCS J004203.6+402413.6	$0.391^{+0.117}_{-0.118}$	0.454 ± 0.071	-	0.089 ± 0.104	-1.040 ± 2.120	0.001	4 ± 3	3 ± 3	4 ± 2	3 ± 2	3
XMMXCS J004205.9-093606.4	$0.285^{+0.073}_{-0.071}$	0.159 ± 0.047	-	-0.292 ± 0.001	7.190 ± 0.020	0.500	2 ± 3	3 ± 3	2 ± 2	5 ± 3	3
XMMXCS J004253.6+401331.9	$0.383^{+0.099}_{-0.093}$	0.218 ± 0.035	-	-0.003 ± 0.142	0.529 ± 2.860	0.078	1 ± 3	6 ± 4	0 ± 0.1	3 ± 3	3
XMMXCS J004302.2-092714.9	$0.188^{+0.043}_{-0.044}$	0.192 ± 0.036	$0.188 \pm 5.5e-05$	-0.007 ± 0.063	1.390 ± 1.120	0.073	3 ± 2	2 ± 2	2 ± 1	2 ± 2	3
XMMXCS J004302.2-092715.0	$0.188^{+0.043}_{-0.044}$	0.192 ± 0.036	$0.188 \pm 5.5e-05$	-0.007 ± 0.063	1.390 ± 1.120	0.073	3 ± 2	2 ± 2	2 ± 1	2 ± 2	3

Continued on next page

Table A.2 – continued from previous page

name	z_{RS}	z_{BCG}	z_{spec-g}	cmr_{grad}	cmr_{inter}	cmr_{wid}	n_{gals-c}	n_{gals-l}	n_{200-c}	n_{200-l}	qual
XMMXCS J004303.5+403714.2	$0.403^{+0.172}_{-0.170}$	0.220 ± 0.038	-	-0.074 ± 0.093	2.850 ± 1.900	0.018	35 ± 7	30 ± 7	75 ± 11	60 ± 10	3
XMMXCS J004307.9-203147.9	$0.276^{+0.077}_{-0.079}$	0.264 ± 0.053	-	0.050 ± 0.044	0.473 ± 0.853	0.065	5 ± 3	3 ± 3	4 ± 2	1 ± 2	3
XMMXCS J004312.6+005604.7	$0.311^{+0.052}_{-0.048}$	0.282 ± 0.047	$0.306 \pm 3.6e-05$	-0.272 ± 0.071	6.380 ± 1.320	0.037	3 ± 2	1 ± 2	0 ± 0.1	-	3
XMMXCS J004313.3-203439.0	$0.304^{+0.073}_{-0.074}$	0.299 ± 0.051	-	0.088 ± 0.073	-0.043 ± 1.370	0.149	29 ± 6	29 ± 6	56 ± 8	56 ± 8	3
XMMXCS J004313.8+403425.1	$0.371^{+0.164}_{-0.161}$	0.306 ± 0.051	-	-0.027 ± 0.051	2.030 ± 0.997	0.059	10 ± 4	11 ± 5	8 ± 4	10 ± 4	3
XMMXCS J004324.7-203726.6	$0.285^{+0.078}_{-0.079}$	0.306 ± 0.049	-	-0.058 ± 0.017	2.580 ± 0.306	0.051	37 ± 6	40 ± 7	55 ± 8	56 ± 8	3
XMMXCS J004326.7+004255.2	$0.374^{+0.121}_{-0.123}$	0.184 ± 0.070	-	-0.040 ± 0.048	1.200 ± 0.964	0.129	8 ± 4	10 ± 5	2 ± 3	9 ± 4	3
XMMXCS J004327.8+004314.2	$0.441^{+0.128}_{-0.108}$	0.272 ± 0.122	$0.550 \pm 1.8e-04$	-0.114 ± 0.057	3.430 ± 1.110	0.001	3 ± 3	5 ± 4	0 ± 1	1 ± 2	3
XMMXCS J004327.9+403414.7	$0.445^{+0.167}_{-0.168}$	0.288 ± 0.048	-	0.104 ± 0.024	-1.360 ± 0.485	0.124	18 ± 6	16 ± 6	40 ± 8	29 ± 7	3
XMMXCS J004536.0+040712.3	$0.407^{+0.121}_{-0.118}$	0.310 ± 0.102	-	0.187 ± 0.058	-3.000 ± 1.160	0.093	2 ± 3	-	0 ± 1	-	3
XMMXCS J004537.0+035509.4	$0.390^{+0.154}_{-0.160}$	0.271 ± 0.073	-	0.175 ± 0.100	-2.810 ± 2.000	0.113	2 ± 3	2 ± 3	3 ± 2	6 ± 3	3
XMMXCS J004545.8+040715.2	$0.366^{+0.068}_{-0.065}$	0.377 ± 0.061	$0.361 \pm 5.3e-05$	-0.005 ± 0.032	0.708 ± 0.617	0.043	3 ± 3	3 ± 3	1 ± 1	3 ± 2	3
XMMXCS J004617.7+405436.5	$0.485^{+0.130}_{-0.127}$	0.489 ± 0.140	-	0.031 ± 0.086	0.239 ± 1.740	0.124	7 ± 4	-	0 ± 2	-	3
XMMXCS J004620.0+412420.5	$0.439^{+0.136}_{-0.136}$	0.577 ± 0.141	-	-0.107 ± 0.400	3.690 ± 8.220	0.001	28 ± 6	22 ± 6	56 ± 10	32 ± 8	3
XMMXCS J004717.5+422124.1	$0.436^{+0.136}_{-0.135}$	0.311 ± 0.066	-	0.034 ± 0.033	0.103 ± 0.664	0.118	7 ± 4	6 ± 4	3 ± 3	-	3
XMMXCS J004730.4+415324.9	$0.533^{+0.153}_{-0.152}$	0.655 ± 0.178	-	0.030 ± 0.060	0.362 ± 1.230	0.118	17 ± 5	79 ± 10	28 ± 7	277 ± 20	3
XMMXCS J004746.9+421422.6	$0.332^{+0.156}_{-0.153}$	0.427 ± 0.081	-	-0.406 ± 0.162	9.770 ± 3.290	0.161	12 ± 4	15 ± 4	12 ± 4	17 ± 5	3
XMMXCS J005325.3-083423.1	$0.401^{+0.120}_{-0.126}$	0.290 ± 0.110	-	0.248 ± 0.128	-4.300 ± 2.590	0.001	5 ± 3	-	2 ± 2	-	3
XMMXCS J005325.4-083423.0	$0.401^{+0.120}_{-0.126}$	0.290 ± 0.110	-	0.248 ± 0.128	-4.300 ± 2.590	0.001	5 ± 3	-	2 ± 2	-	3

Continued on next page

Table A.2 – continued from previous page

name	z_{RS}	z_{BCG}	z_{spec-g}	cmr_{grad}	cmr_{inter}	cmr_{wid}	n_{gals-c}	n_{gals-l}	n_{200-c}	n_{200-l}	qual
XMMXCS J005451.8+261728.3	$0.278^{+0.090}_{-0.097}$	0.274 ± 0.068	-	0.005 ± 0.046	1.280 ± 0.867	0.056	5 ± 3	6 ± 3	0 ± 1	1 ± 2	3
XMMXCS J005455.6+253220.5	$0.279^{+0.069}_{-0.074}$	0.194 ± 0.038	-	0.177 ± 0.148	-1.940 ± 2.880	0.069	2 ± 2	-	3 ± 2	-	3
XMMXCS J005527.8+263219.4	$0.194^{+0.051}_{-0.051}$	0.197 ± 0.031	-	-0.022 ± 0.013	1.650 ± 0.227	0.032	3 ± 2	4 ± 2	0 ± 0.1	0 ± 1	3
XMMXCS J005534.3+262711.0	$0.197^{+0.070}_{-0.070}$	0.213 ± 0.041	-	-0.142 ± 0.021	3.780 ± 0.400	0.004	10 ± 3	7 ± 3	10 ± 3	13 ± 4	3
XMMXCS J005555.6-011449.3	$0.091^{+0.096}_{-0.091}$	0.060 ± 0.019	$0.040 \pm 6.4e-06$	0.013 ± 0.014	0.556 ± 0.257	0.092	29 ± 6	36 ± 6	57 ± 8	98 ± 10	3
XMMXCS J005603.1-012039.2	$0.134^{+0.072}_{-0.075}$	0.064 ± 0.017	-	0.097 ± 0.001	-0.505 ± 0.019	0.500	19 ± 5	24 ± 6	40 ± 7	80 ± 10	3
XMMXCS J005620.4+263059.3	$0.418^{+0.114}_{-0.112}$	0.511 ± 0.101	-	-0.026 ± 0.048	1.250 ± 0.959	0.098	9 ± 4	10 ± 4	8 ± 4	10 ± 4	3
XMMXCS J005624.4-011936.1	$0.309^{+0.075}_{-0.077}$	0.269 ± 0.045	$0.277 \pm 3.6e-05$	0.025 ± 0.044	1.100 ± 0.816	0.088	5 ± 3	5 ± 3	3 ± 2	3 ± 2	3
XMMXCS J005637.7-011536.8	$0.036^{+0.020}_{-0.018}$	0.059 ± 0.015	$0.038 \pm 1.1e-05$	-0.067 ± 0.037	1.730 ± 0.490	0.056	13 ± 4	7 ± 3	16 ± 4	8 ± 3	3
XMMXCS J005655.7-011201.3	$0.302^{+0.082}_{-0.084}$	0.144 ± 0.025	$0.142 \pm 3.5e-05$	-0.304 ± 0.013	7.290 ± 0.264	0.500	7 ± 4	-	4 ± 3	-	3
XMMXCS J005659.5-010547.6	$0.079^{+0.028}_{-0.028}$	0.059 ± 0.014	$0.053 \pm 1.9e-05$	0.018 ± 0.037	0.559 ± 0.599	0.115	2 ± 2	2 ± 2	0 ± 0.1	0 ± 1	3
XMMXCS J005730.1+301321.6	$0.131^{+0.038}_{-0.038}$	0.069 ± 0.027	-	0.026 ± 0.039	0.568 ± 0.684	0.093	4 ± 2	3 ± 3	3 ± 2	2 ± 2	3
XMMXCS J005732.8+301647.7	$0.127^{+0.046}_{-0.046}$	0.069 ± 0.027	-	0.009 ± 0.008	0.719 ± 0.100	0.086	1 ± 2	-	0 ± 0.1	-	3
XMMXCS J010417.5-064447.7	$0.530^{+0.120}_{-0.119}$	0.589 ± 0.143	-	-0.107 ± 0.107	3.150 ± 2.190	0.001	5 ± 3	-	5 ± 2	-	3
XMMXCS J010422.4-063004.5	$0.672^{+0.182}_{-0.180}$	0.577 ± 0.129	-	-11.30 ± 20.30	237 ± 424	1.504	3 ± 2	0 ± 1	2 ± 1	-	3
XMMXCS J010647.3+005622.0	$0.172^{+0.058}_{-0.062}$	0.080 ± 0.020	$0.131 \pm 1.5e-05$	0.046 ± 0.046	0.254 ± 0.861	0.119	2 ± 2	1 ± 3	0 ± 0.1	1 ± 1	3
XMMXCS J010749.7+135803.5	$0.510^{+0.127}_{-0.127}$	0.576 ± 0.147	-	-0.042 ± 0.069	1.800 ± 1.350	0.111	3 ± 3	3 ± 3	4 ± 2	-	3
XMMXCS J011023.8+330544.1	$0.117^{+0.051}_{-0.057}$	0.082 ± 0.017	-	-0.023 ± 0.009	1.200 ± 0.129	0.086	1 ± 2	-	0 ± 0.1	-	3
XMMXCS J011126.6+330226.7	$0.099^{+0.021}_{-0.021}$	0.093 ± 0.019	-	-0.010 ± 0.015	1.100 ± 0.226	0.037	6 ± 3	6 ± 3	5 ± 2	5 ± 2	3

Continued on next page

Table A.2 – continued from previous page

name	z_{RS}	z_{BCG}	z_{spec-g}	cmr_{grad}	cmr_{inter}	cmr_{wid}	n_{gals-c}	n_{gals-l}	n_{200-c}	n_{200-l}	qual
XMMXCS J011713.1+331143.0	$0.670^{+0.186}_{-0.187}$	0.740 ± 0.274	-	0.070 ± 0.142	0.129 ± 2.770	0.105	4 ± 2	9 ± 4	2 ± 1	11 ± 4	3
XMMXCS J011849.3-011040.0	$0.343^{+0.127}_{-0.129}$	0.230 ± 0.044	-	0.110 ± 0.056	-0.582 ± 1.060	0.001	2 ± 2	4 ± 3	0 ± 0.1	-	3
XMMXCS J011926.0-005610.5	$0.603^{+0.144}_{-0.138}$	0.457 ± 0.092	$0.571 \pm 1.6e-04$	0.190 ± 0.081	-2.850 ± 1.590	0.001	3 ± 2	7 ± 3	0 ± 1	4 ± 3	3
XMMXCS J012005.9+032502.7	$0.173^{+0.048}_{-0.045}$	0.060 ± 0.021	-	0.005 ± 0.014	0.711 ± 0.154	0.500	3 ± 3	15 ± 5	1 ± 1	15 ± 5	3
XMMXCS J012335.8+325939.8	$0.681^{+0.179}_{-0.180}$	0.608 ± 0.212	-	0.140 ± 0.131	-1.390 ± 2.590	0.001	2 ± 2	10 ± 4	-	11 ± 4	3
XMMXCS J012341.0+072325.0	$0.110^{+0.033}_{-0.033}$	0.075 ± 0.035	-	-0.000 ± 0.001	0.724 ± 0.001	0.500	0 ± 1	1 ± 2	-	0 ± 1	3
XMMXCS J012355.3+331559.8	$0.183^{+0.049}_{-0.050}$	0.213 ± 0.038	-	-0.099 ± 0.013	3.080 ± 0.236	0.001	2 ± 2	1 ± 2	2 ± 1	1 ± 1	3
XMMXCS J012426.6+334756.7	$0.073^{+0.034}_{-0.034}$	0.105 ± 0.039	-	-0.037 ± 0.025	1.210 ± 0.322	0.119	2 ± 2	5 ± 3	3 ± 2	3 ± 2	3
XMMXCS J012435.0+034729.7	$0.087^{+0.075}_{-0.077}$	0.103 ± 0.095	-	-0.029 ± 0.016	1.140 ± 0.192	0.087	2 ± 2	13 ± 4	1 ± 1	14 ± 4	3
XMMXCS J012435.2+320827.9	$0.521^{+0.134}_{-0.123}$	0.509 ± 0.128	-	0.175 ± 0.082	-2.750 ± 1.650	0.116	1 ± 3	12 ± 5	-	12 ± 5	3
XMMXCS J012501.4+321836.8	$0.498^{+0.205}_{-0.222}$	0.361 ± 0.055	-	0.682 ± 0.608	-12.80 ± 12.60	0.320	3 ± 3	1 ± 3	1 ± 2	-	3
XMMXCS J012502.4+322031.4	$0.105^{+0.027}_{-0.027}$	0.090 ± 0.024	-	0.111 ± 0.041	-0.970 ± 0.709	0.038	4 ± 2	3 ± 2	3 ± 2	1 ± 1	3
XMMXCS J012513.9+034603.5	$0.398^{+0.095}_{-0.096}$	0.467 ± 0.078	$0.385 \pm 8.4e-05$	-0.038 ± 0.033	1.450 ± 0.662	0.073	4 ± 3	6 ± 3	1 ± 2	2 ± 2	3
XMMXCS J012531.2+014531.6	$0.362^{+0.101}_{-0.106}$	0.370 ± 0.119	-	0.074 ± 0.043	0.445 ± 0.793	0.061	3 ± 2	18 ± 5	-	7 ± 3	3
XMMXCS J012535.9-012545.6	$0.132^{+0.047}_{-0.048}$	0.057 ± 0.016	-	0.020 ± 0.011	0.599 ± 0.150	0.095	6 ± 3	20 ± 5	2 ± 2	25 ± 6	3
XMMXCS J012615.7+315803.8	$0.388^{+0.143}_{-0.126}$	0.389 ± 0.066	-	-0.100 ± 0.040	2.600 ± 0.804	0.090	1 ± 3	1 ± 3	0 ± 1	1 ± 2	3
XMMXCS J012725.8+191410.0	$0.083^{+0.037}_{-0.040}$	0.084 ± 0.017	-	0.017 ± 0.024	0.635 ± 0.363	0.112	4 ± 2	7 ± 3	1 ± 1	3 ± 2	3
XMMXCS J012753.3+185910.3	$0.057^{+0.021}_{-0.022}$	0.058 ± 0.017	-	-0.170 ± 0.024	3.530 ± 0.401	0.058	1 ± 1	1 ± 1	0 ± 0.1	0 ± 1	3
XMMXCS J013146.8+302157.0	$0.421^{+0.146}_{-0.296}$	0.371 ± 0.057	-	-0.000 ± 0.001	0.835 ± 0.001	0.500	0 ± 3	2 ± 4	-	1 ± 2	3

Continued on next page

Table A.2 – continued from previous page

name	z_{RS}	z_{BCG}	z_{spec-g}	cmr_{grad}	cmr_{inter}	cmr_{wid}	n_{gals-c}	n_{gals-l}	n_{200-c}	n_{200-l}	qual
XMMXCS J013154.2+302940.2	$0.269^{+0.122}_{-0.111}$	0.094 ± 0.035	-	0.060 ± 0.054	-0.329 ± 1.030	0.099	5 ± 3	3 ± 3	2 ± 2	0 ± 1	3
XMMXCS J013223.3+304747.8	$0.446^{+0.113}_{-0.110}$	0.357 ± 0.106	-	0.664 ± 0.259	-11.70 ± 5.180	0.170	14 ± 5	13 ± 5	17 ± 5	14 ± 5	3
XMMXCS J013229.7+303617.0	$0.588^{+0.155}_{-0.154}$	0.513 ± 0.109	-	0.757 ± 0.832	-14.30 ± 17.20	0.116	4 ± 2	1 ± 1	0 ± 1	-	3
XMMXCS J013309.1+301221.6	$0.434^{+0.157}_{-0.157}$	0.280 ± 0.059	-	0.155 ± 0.095	-2.250 ± 1.930	0.118	19 ± 5	20 ± 5	26 ± 6	26 ± 6	3
XMMXCS J013529.1+304213.0	$0.502^{+0.152}_{-0.145}$	0.435 ± 0.068	-	0.093 ± 0.134	-1.290 ± 2.690	0.050	17 ± 5	22 ± 6	22 ± 6	38 ± 7	3
XMMXCS J013551.6+304452.7	$0.394^{+0.181}_{-0.196}$	0.348 ± 0.056	-	0.045 ± 0.104	-0.281 ± 2.010	0.106	2 ± 3	2 ± 3	0 ± 1	1 ± 2	3
XMMXCS J013811.6-175415.6	$0.578^{+0.166}_{-0.191}$	0.417 ± 0.231	-	0.323 ± 0.173	-5.640 ± 3.470	0.137	4 ± 3	11 ± 4	2 ± 2	11 ± 4	3
XMMXCS J014042.9+062154.2	$0.254^{+0.387}_{-0.254}$	0.244 ± 0.044	$0.276 \pm 4.3e-05$	0.029 ± 0.053	0.884 ± 1.020	0.096	1 ± 2	1 ± 2	0 ± 0.1	0 ± 1	3
XMMXCS J014438.1-043056.1	$0.114^{+0.041}_{-0.043}$	0.058 ± 0.017	-	-0.026 ± 0.034	1.460 ± 0.610	0.115	5 ± 3	5 ± 3	3 ± 2	4 ± 2	3
XMMXCS J014450.9-042523.4	$0.270^{+0.071}_{-0.073}$	0.194 ± 0.030	-	-0.015 ± 0.038	1.690 ± 0.726	0.120	7 ± 3	7 ± 3	4 ± 2	1 ± 2	3
XMMXCS J014459.9-043642.6	$0.196^{+0.050}_{-0.050}$	0.176 ± 0.053	-	-0.072 ± 0.087	2.590 ± 1.610	0.024	1 ± 1	0 ± 1	0 ± 0.1	-	3
XMMXCS J014534.9-044711.4	$0.117^{+0.037}_{-0.037}$	0.126 ± 0.029	-	-0.008 ± 0.016	1.100 ± 0.282	0.035	2 ± 2	2 ± 2	0 ± 0.1	0 ± 1	3
XMMXCS J014547.5-042211.8	$0.217^{+0.181}_{-0.163}$	0.062 ± 0.022	-	0.007 ± 0.017	0.736 ± 0.248	0.500	6 ± 4	1 ± 4	5 ± 3	0 ± 1	3
XMMXCS J014550.7-042513.9	$0.075^{+0.041}_{-0.045}$	0.062 ± 0.022	-	-0.022 ± 0.004	0.737 ± 0.067	0.500	3 ± 2	2 ± 2	0 ± 1	0 ± 1	3
XMMXCS J014557.5-043418.7	$0.403^{+0.104}_{-0.090}$	0.280 ± 0.120	-	-0.023 ± 0.041	0.878 ± 0.819	0.059	2 ± 3	6 ± 3	0 ± 0.1	2 ± 2	3
XMMXCS J014613.5-042641.7	$0.300^{+0.106}_{-0.107}$	0.338 ± 0.097	-	-0.048 ± 0.036	1.820 ± 0.676	0.001	0 ± 1	1 ± 2	-	1 ± 1	3
XMMXCS J014615.5-044031.9	$0.589^{+0.169}_{-0.170}$	0.644 ± 0.128	-	-0.234 ± 0.313	5.990 ± 6.320	0.121	6 ± 3	23 ± 5	3 ± 2	43 ± 7	3
XMMXCS J014857.3+055420.9	$0.195^{+0.057}_{-0.043}$	0.138 ± 0.126	-	-0.039 ± 0.001	0.756 ± 0.001	0.500	3 ± 2	12 ± 4	3 ± 2	12 ± 4	3
XMMXCS J015234.3+010705.1	$0.145^{+0.046}_{-0.047}$	0.147 ± 0.023	-	-0.046 ± 0.022	1.910 ± 0.387	0.065	1 ± 1	1 ± 1	0 ± 0.1	0 ± 1	3

Continued on next page

Table A.2 – continued from previous page

name	z_{RS}	z_{BCG}	z_{spec-g}	cmr_{grad}	cmr_{inter}	cmr_{wid}	n_{gals-c}	n_{gals-l}	n_{200-c}	n_{200-l}	qual
XMMXCS J015456.2-090104.4	$0.679^{+0.145}_{-0.142}$	0.632 ± 0.128	-	0.302 ± 0.274	-4.510 ± 5.550	0.001	3 ± 2	12 ± 4	-	12 ± 4	3
XMMXCS J015653.3+284339.3	$0.242^{+0.071}_{-0.072}$	0.243 ± 0.041	-	-0.006 ± 0.012	1.560 ± 0.212	0.001	0 ± 1	1 ± 2	-	1 ± 1	3
XMMXCS J015657.0+320106.3	$0.417^{+0.155}_{-0.152}$	0.299 ± 0.117	-	-0.099 ± 0.090	3.050 ± 1.820	0.154	6 ± 4	7 ± 4	1 ± 2	7 ± 4	3
XMMXCS J015746.3+284918.1	$0.323^{+0.107}_{-0.109}$	0.405 ± 0.064	-	-0.324 ± 0.111	8.080 ± 2.320	0.091	4 ± 2	5 ± 3	2 ± 2	3 ± 2	3
XMMXCS J015750.9+322302.8	$0.230^{+0.072}_{-0.081}$	0.220 ± 0.054	-	0.145 ± 0.112	-1.360 ± 2.110	0.176	3 ± 2	-	0 ± 0.1	-	3
XMMXCS J015800.7+284256.3	$0.307^{+0.100}_{-0.100}$	0.478 ± 0.077	-	0.019 ± 0.153	0.974 ± 3.040	0.152	3 ± 3	3 ± 3	0 ± 1	0 ± 1	3
XMMXCS J015830.3+080822.2	$0.277^{+0.125}_{-0.126}$	0.151 ± 0.047	-	0.023 ± 0.003	0.684 ± 0.054	0.500	2 ± 3	4 ± 4	1 ± 2	1 ± 2	3
XMMXCS J015951.9+001655.4	$0.478^{+0.145}_{-0.150}$	0.346 ± 0.133	-	0.226 ± 0.098	-3.770 ± 1.960	0.117	8 ± 4	9 ± 4	5 ± 3	6 ± 3	3
XMMXCS J015952.5+001654.2	$0.522^{+0.145}_{-0.141}$	0.346 ± 0.133	-	0.310 ± 0.148	-5.450 ± 2.950	0.169	6 ± 3	11 ± 5	1 ± 2	9 ± 4	3
XMMXCS J020001.26-092305.3	$0.236^{+0.121}_{-0.124}$	0.213 ± 0.036	-	0.0 ± -1.00	0.546 ± -1.00	0.500	0 ± 2	2 ± 3	-	1 ± 2	3
XMMXCS J020001.2-092305.2	$0.236^{+0.121}_{-0.124}$	0.213 ± 0.036	-	0.0 ± -1.00	0.546 ± -1.00	0.500	0 ± 2	2 ± 3	-	1 ± 2	3
XMMXCS J020008.2+001932.6	$0.527^{+0.112}_{-0.108}$	0.527 ± 0.080	$0.514 \pm 1.1e-04$	-0.017 ± 0.090	1.220 ± 1.810	0.082	2 ± 2	7 ± 4	0 ± 1	2 ± 3	3
XMMXCS J020019.1+001931.8	$0.705^{+0.121}_{-0.112}$	0.600 ± 0.116	$0.682 \pm 1.7e-04$	-0.027 ± 0.095	1.680 ± 1.950	0.091	1 ± 2	9 ± 4	0 ± 0.1	10 ± 4	3
XMMXCS J020119.03-064952.9	$0.305^{+0.069}_{-0.070}$	0.397 ± 0.066	$0.282 \pm 5.0e-05$	-0.015 ± 0.059	1.870 ± 1.120	0.083	12 ± 4	11 ± 4	13 ± 4	12 ± 4	3
XMMXCS J020139.05-062256.7	$0.285^{+0.097}_{-0.098}$	0.313 ± 0.049	$0.338 \pm 5.6e-05$	-0.068 ± 0.079	2.670 ± 1.570	0.120	6 ± 3	5 ± 3	5 ± 3	5 ± 3	3
XMMXCS J020155.93-063427.5	$0.130^{+0.038}_{-0.037}$	0.124 ± 0.025	$0.129 \pm 2.7e-05$	-0.009 ± 0.031	1.050 ± 0.556	0.084	1 ± 2	0 ± 1	0 ± 0.1	-	3
XMMXCS J020156.2-052058.7	$0.218^{+0.066}_{-0.068}$	0.219 ± 0.041	-	-0.176 ± 0.066	4.740 ± 1.290	0.001	0 ± 1	1 ± 1	-	0 ± 1	3
XMMXCS J020202.46-062850.5	$0.226^{+0.049}_{-0.052}$	0.188 ± 0.041	-	0.340 ± 0.076	-5.170 ± 1.480	0.064	4 ± 2	2 ± 2	2 ± 1	-	3
XMMXCS J020214.9-074142.2	$0.429^{+0.158}_{-0.157}$	0.307 ± 0.088	-	0.288 ± 0.174	-5.340 ± 3.500	0.141	3 ± 3	4 ± 4	3 ± 2	2 ± 2	3

Continued on next page

Table A.2 – continued from previous page

name	z_{RS}	z_{BCG}	z_{spec-g}	cmr_{grad}	cmr_{inter}	cmr_{wid}	n_{gals-c}	n_{gals-l}	n_{200-c}	n_{200-l}	qual
XMMXCS J020305.38-041856.2	$0.410^{+0.146}_{-0.156}$	0.338 ± 0.061	-	0.002 ± 0.057	0.591 ± 1.140	0.042	4 ± 3	10 ± 4	-	11 ± 4	3
XMMXCS J020309.31-043707.5	$0.440^{+0.147}_{-0.149}$	0.526 ± 0.088	-	-0.040 ± 0.478	1.640 ± 9.800	0.154	6 ± 3	9 ± 4	3 ± 2	4 ± 3	3
XMMXCS J020318.46-043956.8	$0.531^{+0.179}_{-0.184}$	0.451 ± 0.290	-	1.070 ± 0.635	-21.30 ± 13.20	0.001	1 ± 2	0 ± 1	1 ± 1	-	3
XMMXCS J020340.0-073633.5	$0.202^{+0.086}_{-0.092}$	0.092 ± 0.019	-	0.152 ± 0.003	-1.530 ± 0.061	0.500	3 ± 3	5 ± 4	1 ± 1	3 ± 3	3
XMMXCS J020342.24-050722.9	$0.431^{+0.121}_{-0.120}$	0.237 ± 0.057	-	0.129 ± 0.071	-1.930 ± 1.410	0.112	14 ± 5	-	14 ± 5	-	3
XMMXCS J020423.62-050611.2	$0.357^{+0.094}_{-0.092}$	0.321 ± 0.100	-	0.067 ± 0.058	0.196 ± 1.120	0.001	6 ± 3	7 ± 3	4 ± 2	-	3
XMMXCS J020425.3+295837.7	$0.642^{+0.155}_{-0.148}$	0.679 ± 0.132	-	-0.089 ± 0.305	3.080 ± 6.230	0.179	2 ± 2	14 ± 5	-	18 ± 6	3
XMMXCS J020439.65-042752.2	$0.656^{+0.138}_{-0.130}$	0.555 ± 0.100	$0.615 \pm 2.5e-04$	0.278 ± 0.084	-4.220 ± 1.680	0.500	2 ± 2	5 ± 4	-	4 ± 3	3
XMMXCS J020446.66-072111.8	$0.236^{+0.052}_{-0.050}$	0.220 ± 0.036	$0.235 \pm 3.2e-05$	0.002 ± 0.042	1.220 ± 0.800	0.137	3 ± 2	1 ± 2	0 ± 0.1	0 ± 1	3
XMMXCS J020449.1-072538.2	$0.334^{+0.080}_{-0.080}$	0.220 ± 0.036	$0.235 \pm 3.2e-05$	0.072 ± 0.083	0.139 ± 1.630	0.001	5 ± 3	5 ± 3	3 ± 2	5 ± 3	3
XMMXCS J020509.70-061445.9	$0.228^{+0.086}_{-0.085}$	0.144 ± 0.043	-	-0.138 ± 0.097	3.440 ± 1.820	0.059	4 ± 2	5 ± 3	4 ± 2	5 ± 2	3
XMMXCS J020555.29-040544.8	$0.464^{+0.122}_{-0.120}$	0.290 ± 0.221	-	0.322 ± 0.194	-5.940 ± 3.980	0.001	4 ± 3	1 ± 1	5 ± 2	0 ± 1	3
XMMXCS J020605.49-051129.5	$0.489^{+0.137}_{-0.133}$	0.566 ± 0.158	-	0.094 ± 0.141	-1.090 ± 2.900	0.001	4 ± 3	-	2 ± 2	-	3
XMMXCS J020607.3+293253.2	$0.148^{+0.119}_{-0.119}$	0.251 ± 0.100	-	-0.054 ± 0.084	2.280 ± 1.640	0.139	2 ± 1	0 ± 1	0 ± 0.1	-	3
XMMXCS J020611.78-061131.4	$0.574^{+0.144}_{-0.119}$	0.406 ± 0.076	-	1.490 ± 0.440	-29.60 ± 8.950	0.500	4 ± 3	-	3 ± 2	-	3
XMMXCS J020613.35-041616.7	$0.192^{+0.061}_{-0.062}$	0.298 ± 0.051	-	-0.120 ± 0.096	3.660 ± 1.810	0.001	1 ± 1	0 ± 1	1 ± 1	-	3
XMMXCS J020614.59-054407.5	$0.196^{+0.028}_{-0.027}$	0.380 ± 0.149	$0.196 \pm 3.2e-05$	-0.039 ± 0.016	1.930 ± 0.287	0.033	2 ± 2	5 ± 3	2 ± 1	4 ± 2	3
XMMXCS J020623.24-071841.3	$0.198^{+0.063}_{-0.065}$	0.128 ± 0.026	-	-0.086 ± 0.040	2.640 ± 0.792	0.500	1 ± 3	-	0 ± 0.1	-	3
XMMXCS J020623.58-053821.1	$0.602^{+0.084}_{-0.081}$	0.563 ± 0.086	$0.597 \pm 1.8e-04$	-0.024 ± 0.059	1.430 ± 1.120	0.120	4 ± 3	37 ± 7	1 ± 1	34 ± 8	3

Continued on next page

Table A.2 – continued from previous page

name	z_{RS}	z_{BCG}	z_{spec-g}	cmr_{grad}	cmr_{inter}	cmr_{wid}	n_{gals-c}	n_{gals-l}	n_{200-c}	n_{200-l}	qual
XMMXCS J020627.47-054526.9	$0.636^{+0.187}_{-0.190}$	0.552 ± 0.132	-	-0.118 ± 0.442	4.420 ± 9.340	0.500	2 ± 2	7 ± 3	2 ± 1	7 ± 3	3
XMMXCS J020635.56-073352.5	$0.291^{+0.079}_{-0.080}$	0.126 ± 0.023	$0.205 \pm 2.9e-05$	0.092 ± 0.089	-0.327 ± 1.700	0.141	6 ± 3	8 ± 4	6 ± 3	7 ± 3	3
XMMXCS J020636.17-061133.8	$0.229^{+0.082}_{-0.081}$	0.091 ± 0.029	-	-0.091 ± 0.001	3.120 ± 0.003	0.500	1 ± 3	-	2 ± 1	-	3
XMMXCS J020653.58-065206.8	$0.233^{+0.050}_{-0.046}$	0.208 ± 0.069	-	0.088 ± 0.094	-0.400 ± 1.730	0.102	4 ± 2	2 ± 2	0 ± 0.1	0 ± 1	3
XMMXCS J020702.77-072203.2	$0.093^{+0.060}_{-0.067}$	0.104 ± 0.025	-	0.047 ± 0.030	-0.057 ± 0.533	0.100	3 ± 2	1 ± 1	0 ± 0.1	0 ± 1	3
XMMXCS J020724.8+291914.7	$0.500^{+0.122}_{-0.123}$	0.377 ± 0.142	-	0.191 ± 0.093	-3.090 ± 1.900	0.001	4 ± 3	13 ± 5	2 ± 2	12 ± 5	3
XMMXCS J020725.25-045603.3	$0.185^{+0.088}_{-0.091}$	0.098 ± 0.025	-	0.089 ± 0.008	-0.631 ± 0.162	0.024	2 ± 2	1 ± 2	1 ± 1	1 ± 1	3
XMMXCS J020727.49-074055.7	$0.655^{+0.165}_{-0.183}$	0.493 ± 0.312	-	-0.749 ± 0.215	15.600 ± 4.420	0.001	2 ± 2	13 ± 4	1 ± 1	13 ± 4	3
XMMXCS J020732.7-040903.5	$0.137^{+0.074}_{-0.080}$	0.064 ± 0.022	-	0.019 ± 0.011	0.291 ± 0.177	0.053	2 ± 2	2 ± 2	1 ± 1	1 ± 1	3
XMMXCS J020736.5+020711.7	$0.062^{+0.022}_{-0.022}$	0.053 ± 0.016	-	-0.040 ± 0.002	1.300 ± 0.036	0.012	4 ± 2	13 ± 4	3 ± 2	13 ± 4	3
XMMXCS J020749.7+020919.4	$0.147^{+0.059}_{-0.063}$	0.073 ± 0.026	-	0.010 ± 0.019	0.758 ± 0.331	0.500	9 ± 4	39 ± 7	6 ± 3	76 ± 10	3
XMMXCS J020754.52-062914.1	$0.096^{+0.053}_{-0.066}$	0.066 ± 0.027	-	-0.050 ± 0.025	1.450 ± 0.382	0.093	2 ± 2	1 ± 2	0 ± 0.1	0 ± 1	3
XMMXCS J020809.6-053839.2	$0.317^{+0.091}_{-0.089}$	0.267 ± 0.049	-	-0.020 ± 0.054	1.770 ± 1.030	0.092	2 ± 2	3 ± 3	0 ± 0.1	1 ± 2	3
XMMXCS J020811.82-055803.5	$0.292^{+0.120}_{-0.115}$	0.130 ± 0.088	-	0.602 ± 0.682	-11.00 ± 13.90	0.210	4 ± 2	7 ± 3	1 ± 1	4 ± 2	3
XMMXCS J020828.1-051159.8	$0.135^{+0.035}_{-0.035}$	0.137 ± 0.021	-	-0.144 ± 0.009	3.530 ± 0.149	0.001	1 ± 1	1 ± 1	0 ± 0.1	0 ± 1	3
XMMXCS J020852.23-063404.0	$0.147^{+0.045}_{-0.043}$	0.082 ± 0.019	-	-0.056 ± 0.056	1.870 ± 0.957	0.129	3 ± 2	3 ± 2	2 ± 1	0 ± 1	3
XMMXCS J020900.13-060904.2	$0.405^{+0.114}_{-0.119}$	0.282 ± 0.053	-	-0.020 ± 0.120	1.870 ± 2.310	0.068	6 ± 3	10 ± 4	1 ± 2	10 ± 4	3
XMMXCS J020908.35-063640.4	$0.350^{+0.076}_{-0.071}$	0.187 ± 0.041	$0.345 \pm 6.2e-05$	0.057 ± 0.039	-0.458 ± 0.776	0.071	5 ± 3	5 ± 4	3 ± 2	3 ± 3	3
XMMXCS J020959.0-001522.9	$0.542^{+0.093}_{-0.087}$	0.449 ± 0.112	$0.523 \pm 7.1e-05$	0.027 ± 0.058	0.366 ± 1.130	0.102	0 ± 2	25 ± 6	-	36 ± 7	3

Continued on next page

Table A.2 – continued from previous page

name	z_{RS}	z_{BCG}	z_{spec-g}	cmr_{grad}	cmr_{inter}	cmr_{wid}	n_{gals-c}	n_{gals-l}	n_{200-c}	n_{200-l}	qual
XMMXCS J021005.45-050909.1	$0.297^{+0.074}_{-0.074}$	0.148 ± 0.037	-	0.290 ± 0.368	-4.140 ± 7.170	0.135	5 ± 3	6 ± 3	2 ± 2	2 ± 2	3
XMMXCS J021010.12-062738.4	$0.330^{+0.079}_{-0.082}$	0.268 ± 0.099	-	0.035 ± 0.107	0.871 ± 2.070	0.051	4 ± 3	11 ± 4	0 ± 1	11 ± 4	3
XMMXCS J021015.6-034446.1	$0.356^{+0.114}_{-0.099}$	0.220 ± 0.184	-	0.203 ± 0.109	-3.370 ± 2.250	0.086	3 ± 2	1 ± 2	1 ± 1	-	3
XMMXCS J021020.7-000706.5	$0.246^{+0.074}_{-0.074}$	0.191 ± 0.031	-	0.031 ± 0.042	0.787 ± 0.811	0.105	3 ± 2	2 ± 2	1 ± 1	2 ± 2	3
XMMXCS J021022.74-035132.7	$0.393^{+0.076}_{-0.077}$	0.328 ± 0.066	-	0.061 ± 0.136	0.534 ± 2.750	0.001	5 ± 3	6 ± 3	2 ± 2	-	3
XMMXCS J021029.24-034345.4	$0.355^{+0.086}_{-0.089}$	0.452 ± 0.069	$0.442 \pm 1.1e-04$	-0.037 ± 0.056	2.370 ± 1.020	0.001	4 ± 3	3 ± 3	0 ± 0.1	1 ± 2	3
XMMXCS J021037.97-060504.3	$0.346^{+0.126}_{-0.130}$	0.205 ± 0.032	$0.462 \pm 1.1e-04$	0.008 ± 0.091	1.210 ± 1.780	0.097	1 ± 2	2 ± 3	1 ± 1	1 ± 2	3
XMMXCS J021045.5-002202.1	$0.261^{+0.064}_{-0.064}$	0.184 ± 0.104	$0.152 \pm 5.4e-05$	0.253 ± 0.145	-3.610 ± 2.960	0.044	0 ± 2	1 ± 2	-	1 ± 1	3
XMMXCS J021051.23-034208.7	$0.405^{+0.034}_{-0.020}$	0.324 ± 0.051	-	-0.004 ± 0.078	0.911 ± 1.510	0.500	4 ± 4	4 ± 4	5 ± 3	5 ± 3	3
XMMXCS J021051.7-003209.7	$0.314^{+0.102}_{-0.097}$	0.254 ± 0.039	$0.458 \pm 1.4e-04$	0.113 ± 0.132	-0.740 ± 2.550	0.181	7 ± 3	7 ± 4	5 ± 3	6 ± 3	3
XMMXCS J021059.55-095048.6	$0.590^{+0.156}_{-0.155}$	0.650 ± 0.127	-	-0.032 ± 0.154	1.800 ± 3.130	0.001	3 ± 2	-	3 ± 2	-	3
XMMXCS J021059.5-095048.6	$0.590^{+0.156}_{-0.155}$	0.650 ± 0.127	-	-0.032 ± 0.154	1.800 ± 3.130	0.001	3 ± 2	-	3 ± 2	-	3
XMMXCS J021106.15-034650.9	$0.517^{+0.139}_{-0.134}$	0.365 ± 0.075	$0.359 \pm 8.1e-05$	0.263 ± 0.097	-4.230 ± 1.940	0.082	4 ± 3	5 ± 3	3 ± 2	18 ± 5	3
XMMXCS J021110.13-052144.8	$0.102^{+0.027}_{-0.028}$	0.069 ± 0.016	-	0.146 ± 0.013	-1.550 ± 0.221	0.500	1 ± 2	0 ± 1	1 ± 1	-	3
XMMXCS J021111.5-035208.9	$0.388^{+0.075}_{-0.077}$	0.338 ± 0.051	-	-0.025 ± 0.095	2.170 ± 1.860	0.001	1 ± 2	1 ± 2	0 ± 0.1	0 ± 1	3
XMMXCS J021151.79-050159.1	$0.397^{+0.127}_{-0.118}$	0.585 ± 0.156	-	-0.000 ± 0.001	0.770 ± 0.001	0.500	2 ± 4	1 ± 4	0 ± 1	1 ± 2	3
XMMXCS J021221.3-041201.7	$0.479^{+0.104}_{-0.099}$	0.389 ± 0.062	-	0.045 ± 0.037	-0.092 ± 0.741	0.105	6 ± 3	10 ± 4	2 ± 2	7 ± 4	3
XMMXCS J021223.26-041430.6	$0.503^{+0.112}_{-0.095}$	0.485 ± 0.081	$0.462 \pm 1.7e-04$	0.160 ± 0.112	-2.450 ± 2.230	0.134	3 ± 3	-	0 ± 1	-	3
XMMXCS J021224.16-040814.8	$0.510^{+0.116}_{-0.109}$	0.501 ± 0.081	$0.482 \pm 9.2e-05$	0.054 ± 0.027	-0.197 ± 0.533	0.090	5 ± 3	7 ± 4	0 ± 1	2 ± 3	3

Continued on next page

Table A.2 – continued from previous page

name	z_{RS}	z_{BCG}	z_{spec-g}	cmr_{grad}	cmr_{inter}	cmr_{wid}	n_{gals-c}	n_{gals-l}	n_{200-c}	n_{200-l}	qual
XMMXCS J021225.5-054440.3	$0.446^{+0.186}_{-0.187}$	0.369 ± 0.062	-	0.022 ± 0.119	0.560 ± 2.330	0.187	3 ± 3	6 ± 3	0 ± 1	-	3
XMMXCS J021225.99-041033.3	$0.479^{+0.100}_{-0.097}$	0.501 ± 0.081	$0.472 \pm 8.9e-05$	-0.016 ± 0.038	1.110 ± 0.739	0.098	4 ± 3	39 ± 7	0 ± 1	19 ± 7	3
XMMXCS J021250.50-043601.7	$0.153^{+0.030}_{-0.030}$	0.162 ± 0.030	-	-0.218 ± 0.088	5.060 ± 1.590	0.069	1 ± 1	1 ± 1	0 ± 0.1	0 ± 1	3
XMMXCS J021255.79-044013.7	$0.661^{+0.087}_{-0.077}$	0.589 ± 0.110	$0.641 \pm 1.7e-04$	-0.024 ± 0.028	1.510 ± 0.499	0.048	0 ± 1	11 ± 4	-	3 ± 3	3
XMMXCS J021300.96-060811.1	$0.139^{+0.032}_{-0.033}$	0.142 ± 0.024	$0.139 \pm 1.2e-05$	-0.028 ± 0.018	1.520 ± 0.294	0.001	0 ± 1	1 ± 1	-	1 ± 1	3
XMMXCS J021316.08-051033.2	$0.274^{+0.075}_{-0.074}$	0.218 ± 0.067	$0.297 \pm 7.5e-05$	0.064 ± 0.149	0.125 ± 2.920	0.133	3 ± 2	3 ± 2	1 ± 1	2 ± 2	3
XMMXCS J021321.18-042600.8	$0.770^{+0.121}_{-0.095}$	0.613 ± 0.111	$0.664 \pm 2.2e-04$	0.139 ± 0.039	-2.210 ± 0.778	0.001	0 ± 1	313 ± 18	-	21 ± 13	3
XMMXCS J021334.13-032154.5	$0.275^{+0.087}_{-0.086}$	0.179 ± 0.033	-	0.182 ± 0.022	-2.020 ± 0.409	0.500	4 ± 4	4 ± 4	5 ± 3	5 ± 3	3
XMMXCS J021334.1-032154.4	$0.275^{+0.087}_{-0.086}$	0.179 ± 0.033	-	0.182 ± 0.022	-2.020 ± 0.409	0.500	4 ± 4	4 ± 4	5 ± 3	5 ± 3	3
XMMXCS J021343.4-005140.1	$0.464^{+0.073}_{-0.074}$	0.466 ± 0.067	$0.465 \pm 1.0e-04$	0.060 ± 0.012	-0.263 ± 0.230	0.001	2 ± 2	2 ± 3	1 ± 1	-	3
XMMXCS J021344.68-051856.4	$0.400^{+0.115}_{-0.116}$	0.264 ± 0.089	-	0.074 ± 0.072	-0.737 ± 1.470	0.091	3 ± 3	-	0 ± 1	-	3
XMMXCS J021346.00-041506.3	$0.577^{+0.147}_{-0.151}$	0.477 ± 0.145	-	0.109 ± 0.057	-1.560 ± 1.170	0.109	2 ± 2	13 ± 5	1 ± 1	11 ± 5	3
XMMXCS J021355.01-055121.1	$0.326^{+0.082}_{-0.079}$	0.368 ± 0.057	$0.356 \pm 5.8e-05$	-0.073 ± 0.081	2.900 ± 1.600	0.104	5 ± 3	5 ± 3	0 ± 0.1	0 ± 2	3
XMMXCS J021358.96-054436.1	$0.334^{+0.117}_{-0.114}$	0.255 ± 0.087	-	0.663 ± 0.150	-12.30 ± 3.050	0.500	4 ± 3	3 ± 3	3 ± 2	2 ± 2	3
XMMXCS J021359.12-051115.8	$0.439^{+0.128}_{-0.129}$	0.336 ± 0.051	$0.354 \pm 6.4e-05$	-0.032 ± 0.064	1.390 ± 1.280	0.123	3 ± 3	-	0 ± 1	-	3
XMMXCS J021404.03-050805.2	$0.234^{+0.094}_{-0.095}$	0.215 ± 0.062	-	0.016 ± 0.028	0.897 ± 0.547	0.084	3 ± 2	4 ± 3	0 ± 0.1	0 ± 1	3
XMMXCS J021437.8-033745.0	$0.469^{+0.098}_{-0.095}$	0.382 ± 0.123	$0.462 \pm 1.3e-04$	-0.013 ± 0.037	1.010 ± 0.730	0.046	4 ± 3	3 ± 3	0 ± 1	-	3
XMMXCS J021438.04-033739.4	$0.469^{+0.122}_{-0.122}$	0.382 ± 0.123	$0.462 \pm 1.3e-04$	0.067 ± 0.054	-0.521 ± 1.090	0.114	5 ± 3	5 ± 4	4 ± 3	12 ± 4	3
XMMXCS J021443.40-053458.5	$0.690^{+0.173}_{-0.163}$	0.627 ± 0.143	-	0.439 ± 0.297	-7.610 ± 6.020	0.186	4 ± 2	-	2 ± 1	-	3

Continued on next page

Table A.2 – continued from previous page

name	z_{RS}	z_{BCG}	z_{spec-g}	cmr_{grad}	cmr_{inter}	cmr_{wid}	n_{gals-c}	n_{gals-l}	n_{200-c}	n_{200-l}	qual
XMMXCS J021443.47-034921.2	$0.151^{+0.038}_{-0.038}$	0.152 ± 0.026	-	-0.105 ± 0.039	2.980 ± 0.722	0.038	1 ± 1	0 ± 1	0 ± 0.1	-	3
XMMXCS J021504.51-044618.0	$0.283^{+0.076}_{-0.081}$	0.311 ± 0.047	$0.295 \pm 5.7e-05$	-0.002 ± 0.057	1.570 ± 1.070	0.082	4 ± 2	3 ± 3	0 ± 1	-	3
XMMXCS J021522.82-034344.5	$0.182^{+0.065}_{-0.063}$	0.052 ± 0.021	-	0.067 ± 0.034	-0.567 ± 0.666	0.056	0 ± 1	1 ± 1	-	1 ± 1	3
XMMXCS J021522.8-034344.4	$0.182^{+0.065}_{-0.063}$	0.052 ± 0.021	-	0.067 ± 0.034	-0.567 ± 0.666	0.056	0 ± 1	1 ± 1	-	1 ± 1	3
XMMXCS J021528.66-061551.8	$0.308^{+0.100}_{-0.102}$	0.362 ± 0.092	-	0.053 ± 0.056	0.456 ± 1.080	0.127	2 ± 2	0 ± 2	0 ± 1	-	3
XMMXCS J021530.86-042238.9	$0.366^{+0.088}_{-0.089}$	0.374 ± 0.076	-	-0.179 ± 0.174	5.010 ± 3.540	0.001	3 ± 2	3 ± 3	0 ± 0.1	0 ± 1	3
XMMXCS J021534.66-050502.1	$0.379^{+0.100}_{-0.091}$	0.338 ± 0.053	$0.348 \pm 6.3e-05$	-0.013 ± 0.021	0.703 ± 0.415	0.078	0 ± 2	1 ± 3	-	2 ± 2	3
XMMXCS J021534.6-050502.4	$0.379^{+0.100}_{-0.091}$	0.338 ± 0.053	$0.348 \pm 6.3e-05$	-0.013 ± 0.021	0.703 ± 0.415	0.078	0 ± 2	1 ± 3	-	2 ± 2	3
XMMXCS J021608.00-050308.8	$0.350^{+0.077}_{-0.076}$	0.339 ± 0.052	$0.348 \pm 6.4e-05$	-0.035 ± 0.017	1.230 ± 0.311	0.001	0 ± 2	2 ± 3	-	2 ± 2	3
XMMXCS J021613.53-094225.7	$0.323^{+0.118}_{-0.116}$	0.229 ± 0.068	-	0.086 ± 0.063	-0.810 ± 1.280	0.077	2 ± 2	1 ± 2	0 ± 0.1	-	3
XMMXCS J021633.52-043319.3	$0.325^{+0.055}_{-0.056}$	0.427 ± 0.067	-	0.012 ± 0.036	1.390 ± 0.724	0.001	7 ± 3	7 ± 3	5 ± 2	5 ± 3	3
XMMXCS J021633.7-043328.0	$0.325^{+0.055}_{-0.056}$	0.427 ± 0.067	-	0.012 ± 0.036	1.390 ± 0.724	0.001	6 ± 3	6 ± 3	4 ± 2	3 ± 2	3
XMMXCS J021638.9-051053.7	$0.668^{+0.120}_{-0.085}$	0.506 ± 0.081	-	0.161 ± 0.125	-2.440 ± 2.550	0.107	2 ± 2	8 ± 4	1 ± 1	7 ± 3	3
XMMXCS J021648.3-043321.0	$0.309^{+0.186}_{-0.097}$	0.293 ± 0.055	$0.446 \pm 1.2e-04$	-0.028 ± 0.042	2.170 ± 0.820	0.001	4 ± 2	5 ± 3	0 ± 1	0 ± 1	3
XMMXCS J021648.43-091832.2	$0.655^{+0.102}_{-0.099}$	0.550 ± 0.140	$0.652 \pm 1.3e-04$	0.011 ± 0.095	0.718 ± 1.900	0.059	4 ± 2	3 ± 3	5 ± 2	8 ± 3	3
XMMXCS J021659.3-044920.0	$0.383^{+0.098}_{-0.080}$	0.234 ± 0.081	-	0.005 ± 0.118	1.130 ± 2.340	0.106	1 ± 2	1 ± 3	1 ± 1	2 ± 2	3
XMMXCS J021701.8-042616.4	$0.203^{+0.073}_{-0.070}$	0.311 ± 0.068	-	0.018 ± 0.065	0.629 ± 1.230	0.111	2 ± 2	1 ± 1	1 ± 1	0 ± 1	3
XMMXCS J021709.8-053441.4	$0.436^{+0.177}_{-0.171}$	0.367 ± 0.111	-	0.579 ± 0.289	-11.30 ± 5.970	0.161	3 ± 3	0 ± 1	3 ± 2	-	3
XMMXCS J021713.83-064743.1	$0.213^{+0.090}_{-0.087}$	0.126 ± 0.033	-	0.0 ± -1.00	1.060 ± -1.00	0.500	1 ± 3	3 ± 4	1 ± 1	-	3

Continued on next page

Table A.2 – continued from previous page

name	z_{RS}	z_{BCG}	z_{spec-g}	cmr_{grad}	cmr_{inter}	cmr_{wid}	n_{gals-c}	n_{gals-l}	n_{200-c}	n_{200-l}	qual
XMMXCS J021716.2-050734.5	$0.672^{+0.151}_{-0.140}$	0.581 ± 0.108	$0.627 \pm 1.9e-04$	-0.596 ± 0.198	12.600 ± 4.080	0.001	1 ± 2	8 ± 4	-	6 ± 3	3
XMMXCS J021723.32-041844.1	$0.346^{+0.081}_{-0.085}$	0.296 ± 0.061	-	0.013 ± 0.076	1.250 ± 1.470	0.001	3 ± 2	3 ± 3	1 ± 1	-	3
XMMXCS J021723.8-051310.2	$0.583^{+0.141}_{-0.137}$	0.467 ± 0.087	-	0.254 ± 0.131	-4.130 ± 2.620	0.112	2 ± 2	0 ± 1	1 ± 1	-	3
XMMXCS J021724.1-051314.3	$0.583^{+0.142}_{-0.137}$	0.467 ± 0.087	-	0.254 ± 0.131	-4.130 ± 2.620	0.112	2 ± 2	0 ± 1	1 ± 1	-	3
XMMXCS J021725.6-051801.0	$0.432^{+0.112}_{-0.110}$	0.300 ± 0.049	$0.492 \pm 8.2e-05$	-0.004 ± 0.062	0.767 ± 1.220	0.117	4 ± 3	8 ± 4	1 ± 2	3 ± 3	3
XMMXCS J021733.67-051315.2	$0.554^{+0.112}_{-0.111}$	0.197 ± 0.165	$0.546 \pm 1.3e-04$	0.086 ± 0.092	-0.813 ± 1.840	0.039	7 ± 3	12 ± 4	7 ± 3	12 ± 4	3
XMMXCS J021734.7-051326.9	$0.571^{+0.121}_{-0.120}$	0.197 ± 0.165	$0.546 \pm 1.3e-04$	0.231 ± 0.046	-3.650 ± 0.925	0.001	7 ± 3	12 ± 4	6 ± 3	12 ± 4	3
XMMXCS J021735.1-051306.5	$0.573^{+0.121}_{-0.118}$	0.197 ± 0.165	$0.546 \pm 1.3e-04$	0.188 ± 0.105	-2.840 ± 2.090	0.051	6 ± 3	12 ± 4	5 ± 2	11 ± 4	3
XMMXCS J021736.4-045925.7	$0.354^{+0.090}_{-0.089}$	0.550 ± 0.113	-	-0.818 ± 0.888	18.300 ± 18.10	0.074	2 ± 2	2 ± 2	3 ± 2	0 ± 1	3
XMMXCS J021741.26-045144.1	$0.430^{+0.127}_{-0.127}$	0.315 ± 0.151	-	0.091 ± 0.060	-1.050 ± 1.150	0.001	1 ± 2	0 ± 2	2 ± 1	-	3
XMMXCS J021743.43-034539.2	$0.289^{+0.082}_{-0.085}$	0.168 ± 0.032	-	-0.014 ± 0.043	1.600 ± 0.844	0.110	1 ± 2	1 ± 2	0 ± 0.1	0 ± 1	3
XMMXCS J021754.95-045011.6	$0.257^{+0.071}_{-0.073}$	0.315 ± 0.067	-	-0.164 ± 0.097	4.500 ± 1.870	0.083	2 ± 2	0 ± 2	1 ± 1	-	3
XMMXCS J021759.3-045215.9	$0.134^{+0.062}_{-0.063}$	0.071 ± 0.046	$0.098 \pm 1.8e-05$	0.081 ± 0.021	-0.425 ± 0.406	0.068	1 ± 1	2 ± 2	0 ± 0.1	0 ± 1	3
XMMXCS J021805.68-033927.6	$0.203^{+0.032}_{-0.032}$	0.214 ± 0.034	$0.203 \pm 3.4e-05$	-0.049 ± 0.005	2.170 ± 0.089	0.001	9 ± 3	8 ± 3	5 ± 2	3 ± 2	3
XMMXCS J021805.6-033927.6	$0.203^{+0.032}_{-0.032}$	0.214 ± 0.034	$0.203 \pm 3.4e-05$	-0.049 ± 0.005	2.170 ± 0.089	0.001	9 ± 3	8 ± 3	5 ± 2	3 ± 2	3
XMMXCS J021807.88-054557.3	$0.363^{+0.184}_{-0.187}$	0.360 ± 0.110	-	0.077 ± 0.086	-0.742 ± 1.700	0.001	1 ± 2	2 ± 2	0 ± 0.1	2 ± 2	3
XMMXCS J021809.13-035856.2	$0.639^{+0.158}_{-0.160}$	0.658 ± 0.118	-	0.118 ± 0.319	-1.240 ± 6.600	0.029	1 ± 1	0 ± 1	1 ± 1	-	3
XMMXCS J021825.98-045942.7	$0.542^{+0.132}_{-0.127}$	0.459 ± 0.188	-	0.290 ± 0.225	-4.890 ± 4.510	0.156	5 ± 3	-	0 ± 1	-	3
XMMXCS J021831.7-041351.4	$0.306^{+0.103}_{-0.108}$	0.311 ± 0.138	-	0.087 ± 0.024	-0.692 ± 0.461	0.001	1 ± 2	0 ± 2	0 ± 0.1	-	3

Continued on next page

Table A.2 – continued from previous page

name	z_{RS}	z_{BCG}	z_{spec-g}	cmr_{grad}	cmr_{inter}	cmr_{wid}	n_{gals-c}	n_{gals-l}	n_{200-c}	n_{200-l}	qual
XMMXCS J021832.4-050054.1	$0.531^{+0.154}_{-0.154}$	0.332 ± 0.057	$0.515 \pm 1.5e-04$	0.489 ± 0.280	-8.820 ± 5.600	0.231	11 ± 4	26 ± 6	10 ± 4	27 ± 6	3
XMMXCS J021832.83-050053.3	$0.531^{+0.154}_{-0.154}$	0.332 ± 0.057	$0.515 \pm 1.5e-04$	0.489 ± 0.280	-8.820 ± 5.600	0.231	11 ± 4	26 ± 6	10 ± 4	27 ± 6	3
XMMXCS J021842.9-050439.0	$0.504^{+0.076}_{-0.075}$	0.504 ± 0.076	$0.504 \pm 1.1e-04$	-0.065 ± 0.016	2.180 ± 0.325	0.001	4 ± 3	4 ± 3	2 ± 2	2 ± 2	3
XMMXCS J021842.98-061834.5	$0.304^{+0.078}_{-0.079}$	0.147 ± 0.166	-	0.103 ± 0.092	-0.516 ± 1.780	0.118	6 ± 3	-	0 ± 1	-	3
XMMXCS J021855.7-053305.5	$0.326^{+0.115}_{-0.117}$	0.213 ± 0.037	-	-0.059 ± 0.231	2.660 ± 4.390	0.154	6 ± 3	14 ± 4	4 ± 2	7 ± 4	3
XMMXCS J021859.89-034606.5	$0.163^{+0.031}_{-0.030}$	0.164 ± 0.031	-	-0.023 ± 0.078	1.520 ± 1.340	0.041	3 ± 2	5 ± 3	0 ± 0.1	1 ± 1	3
XMMXCS J021900.96-032742.0	$0.730^{+0.093}_{-0.066}$	0.621 ± 0.127	-	0.671 ± 0.177	-13.20 ± 3.690	0.500	1 ± 1	0 ± 1	1 ± 1	-	3
XMMXCS J021900.9-032742.0	$0.730^{+0.093}_{-0.066}$	0.621 ± 0.127	-	0.671 ± 0.177	-13.20 ± 3.690	0.500	1 ± 1	0 ± 1	1 ± 1	-	3
XMMXCS J021905.2-053657.6	$0.171^{+0.041}_{-0.041}$	0.113 ± 0.019	$0.198 \pm 2.9e-05$	-0.012 ± 0.042	1.350 ± 0.798	0.109	3 ± 2	3 ± 2	2 ± 1	10 ± 3	3
XMMXCS J021911.83-045056.6	$0.394^{+0.073}_{-0.072}$	0.315 ± 0.061	$0.398 \pm 7.0e-05$	0.048 ± 0.029	-0.236 ± 0.549	0.061	2 ± 3	12 ± 4	2 ± 2	12 ± 4	3
XMMXCS J021912.2-045104.7	$0.428^{+0.083}_{-0.069}$	0.315 ± 0.061	$0.398 \pm 7.0e-05$	-0.043 ± 0.069	1.460 ± 1.300	0.079	0 ± 3	20 ± 5	-	14 ± 5	3
XMMXCS J021914.45-045053.2	$0.360^{+0.090}_{-0.087}$	0.337 ± 0.058	-	-0.633 ± 0.051	14.300 ± 1.060	0.500	1 ± 3	1 ± 3	0 ± 1	-	3
XMMXCS J021914.4-045053.2	$0.360^{+0.090}_{-0.087}$	0.337 ± 0.058	-	-0.633 ± 0.051	14.300 ± 1.060	0.500	1 ± 3	1 ± 3	0 ± 1	-	3
XMMXCS J021929.61-043312.2	$0.151^{+0.023}_{-0.023}$	0.160 ± 0.034	$0.151 \pm 1.6e-05$	-0.028 ± 0.029	1.540 ± 0.485	0.001	2 ± 2	3 ± 2	0 ± 0.1	1 ± 1	3
XMMXCS J021929.6-043312.2	$0.151^{+0.023}_{-0.023}$	0.160 ± 0.034	$0.151 \pm 1.6e-05$	-0.028 ± 0.029	1.540 ± 0.485	0.001	2 ± 2	3 ± 2	0 ± 0.1	1 ± 1	3
XMMXCS J021938.3-032511.7	$0.526^{+0.086}_{-0.084}$	0.550 ± 0.142	-	-0.070 ± 0.045	2.290 ± 0.877	0.056	1 ± 2	12 ± 4	0 ± 0.1	12 ± 4	3
XMMXCS J021946.1-050748.1	$0.510^{+0.131}_{-0.131}$	0.577 ± 0.311	$0.508 \pm 1.3e-04$	0.176 ± 0.087	-2.640 ± 1.740	0.061	7 ± 3	9 ± 4	8 ± 3	10 ± 4	3
XMMXCS J021958.8-052343.5	$0.082^{+0.033}_{-0.033}$	0.066 ± 0.019	-	0.030 ± 0.056	0.063 ± 0.936	0.089	1 ± 1	0 ± 1	0 ± 0.1	-	3
XMMXCS J022002.6-045144.6	$0.362^{+0.091}_{-0.079}$	0.330 ± 0.057	$0.334 \pm 5.7e-05$	-0.027 ± 0.028	1.070 ± 0.545	0.107	0 ± 3	2 ± 3	-	5 ± 3	3

Continued on next page

Table A.2 – continued from previous page

name	z_{RS}	z_{BCG}	z_{spec-g}	cmr_{grad}	cmr_{inter}	cmr_{wid}	n_{gals-c}	n_{gals-l}	n_{200-c}	n_{200-l}	qual
XMMXCS J022023.19-025025.8	$0.203^{+0.087}_{-0.087}$	0.203 ± 0.069	-	-0.011 ± 0.040	1.400 ± 0.725	0.001	0 ± 1	1 ± 2	-	1 ± 1	3
XMMXCS J022035.72-032045.3	$0.186^{+0.057}_{-0.057}$	0.242 ± 0.059	$0.325 \pm 4.7e-05$	-0.027 ± 0.090	1.560 ± 1.680	0.158	5 ± 3	3 ± 3	1 ± 1	1 ± 2	3
XMMXCS J022036.5-054328.8	$0.417^{+0.111}_{-0.085}$	0.300 ± 0.094	-	0.012 ± 0.068	0.943 ± 1.360	0.093	1 ± 3	2 ± 3	0 ± 0.1	1 ± 2	3
XMMXCS J022042.64-052549.9	$0.517^{+0.149}_{-0.147}$	0.370 ± 0.160	-	1.070 ± 0.829	-20.80 ± 16.80	0.286	11 ± 4	87 ± 10	10 ± 4	18 ± 10	3
XMMXCS J022048.27-084248.8	$0.416^{+0.136}_{-0.136}$	0.540 ± 0.084	$0.525 \pm 1.1e-04$	-0.291 ± 0.041	6.640 ± 0.822	0.031	12 ± 4	12 ± 4	12 ± 4	12 ± 4	3
XMMXCS J022105.4-043933.4	$0.161^{+0.108}_{-0.111}$	0.076 ± 0.026	-	0.056 ± 0.013	-0.084 ± 0.186	0.106	4 ± 2	16 ± 4	0 ± 1	15 ± 4	3
XMMXCS J022105.3-043933.9	$0.161^{+0.108}_{-0.111}$	0.076 ± 0.026	-	0.056 ± 0.013	-0.084 ± 0.186	0.106	4 ± 2	16 ± 4	0 ± 1	15 ± 4	3
XMMXCS J022118.10-033129.7	$0.519^{+0.190}_{-0.187}$	0.435 ± 0.264	-	-0.105 ± 0.026	3.040 ± 0.530	0.001	4 ± 3	12 ± 4	0 ± 1	12 ± 4	3
XMMXCS J022118.2-033130.3	$0.526^{+0.189}_{-0.190}$	0.435 ± 0.264	-	-0.105 ± 0.026	3.040 ± 0.530	0.001	4 ± 3	13 ± 4	1 ± 1	12 ± 4	3
XMMXCS J022118.26-035848.1	$0.115^{+0.059}_{-0.066}$	0.135 ± 0.037	-	-0.108 ± 0.001	2.560 ± 0.001	0.500	0 ± 1	1 ± 1	-	0 ± 1	3
XMMXCS J022118.7-032327.6	$0.144^{+0.029}_{-0.029}$	0.108 ± 0.044	-	-0.087 ± 0.001	2.990 ± 0.005	0.500	1 ± 1	0 ± 1	0 ± 0.1	-	3
XMMXCS J022152.01-043152.8	$0.289^{+0.096}_{-0.093}$	0.209 ± 0.082	-	-0.075 ± 0.047	2.540 ± 0.884	0.001	3 ± 2	3 ± 2	2 ± 1	0 ± 1	3
XMMXCS J022159.14-034400.7	$0.357^{+0.084}_{-0.077}$	0.241 ± 0.106	-	0.035 ± 0.045	-0.170 ± 0.879	0.092	2 ± 3	4 ± 4	0 ± 1	1 ± 2	3
XMMXCS J022201.33-025416.1	$0.253^{+0.066}_{-0.068}$	0.254 ± 0.067	-	-0.067 ± 0.025	2.620 ± 0.464	0.001	2 ± 2	2 ± 2	3 ± 2	5 ± 2	3
XMMXCS J022204.54-043246.3	$0.320^{+0.097}_{-0.096}$	0.226 ± 0.036	$0.319 \pm 6.3e-05$	-0.097 ± 0.046	3.290 ± 0.922	0.077	4 ± 3	7 ± 3	2 ± 2	1 ± 2	3
XMMXCS J022208.0-031104.6	$0.235^{+0.091}_{-0.088}$	0.221 ± 0.084	-	0.151 ± 0.043	-1.820 ± 0.804	0.109	0 ± 1	1 ± 2	-	1 ± 1	3
XMMXCS J022225.2-043730.2	$0.587^{+0.143}_{-0.140}$	0.447 ± 0.284	-	0.054 ± 0.105	-0.129 ± 2.140	0.093	4 ± 2	1 ± 1	2 ± 1	0 ± 1	3
XMMXCS J022231.0-042639.1	$0.344^{+0.125}_{-0.128}$	0.394 ± 0.069	-	-0.004 ± 0.206	1.360 ± 4.120	0.151	2 ± 2	-	2 ± 2	-	3
XMMXCS J022246.3-035150.5	$0.085^{+0.039}_{-0.040}$	0.104 ± 0.025	$0.085 \pm 1.6e-05$	-0.018 ± 0.005	1.240 ± 0.087	0.001	4 ± 2	0 ± 1	1 ± 1	-	3

Continued on next page

Table A.2 – continued from previous page

name	z_{RS}	z_{BCG}	z_{spec-g}	cmr_{grad}	cmr_{inter}	cmr_{wid}	n_{gals-c}	n_{gals-l}	n_{200-c}	n_{200-l}	qual
XMMXCS J022246.55-035141.4	$0.085^{+0.039}_{-0.040}$	0.104 ± 0.025	$0.085 \pm 1.6e-05$	-0.018 ± 0.005	1.240 ± 0.087	0.001	4 ± 2	0 ± 1	1 ± 1	-	3
XMMXCS J022252.73-032830.3	$0.549^{+0.143}_{-0.136}$	0.352 ± 0.077	-	0.233 ± 0.229	-3.710 ± 4.660	0.146	5 ± 3	12 ± 4	0 ± 1	12 ± 4	3
XMMXCS J022252.8-032831.2	$0.548^{+0.143}_{-0.136}$	0.352 ± 0.077	-	0.233 ± 0.229	-3.710 ± 4.660	0.146	5 ± 3	11 ± 4	0 ± 1	11 ± 4	3
XMMXCS J022300.2-054830.8	$0.318^{+0.096}_{-0.095}$	0.209 ± 0.070	-	0.235 ± 0.028	-3.290 ± 0.579	0.001	1 ± 2	0 ± 2	0 ± 0.1	-	3
XMMXCS J022305.09-035816.1	$0.644^{+0.096}_{-0.092}$	0.551 ± 0.117	$0.637 \pm 1.8e-04$	0.189 ± 0.182	-2.700 ± 3.630	0.060	2 ± 2	-	1 ± 1	-	3
XMMXCS J022306.5-035025.6	$0.305^{+0.110}_{-0.115}$	0.366 ± 0.059	-	-0.025 ± 0.077	2.030 ± 1.480	0.001	0 ± 1	1 ± 2	-	0 ± 1	3
XMMXCS J022307.7-041259.4	$0.562^{+0.102}_{-0.101}$	0.489 ± 0.083	$0.564 \pm 1.2e-04$	0.112 ± 0.169	-1.200 ± 3.360	0.104	5 ± 3	-	3 ± 2	-	3
XMMXCS J022317.1-024328.5	$0.384^{+0.051}_{-0.052}$	0.396 ± 0.059	$0.385 \pm 5.1e-05$	-0.024 ± 0.011	2.230 ± 0.216	0.001	3 ± 2	3 ± 3	0 ± 1	-	3
XMMXCS J022319.6-051957.2	$0.361^{+0.091}_{-0.084}$	0.370 ± 0.062	$0.331 \pm 5.4e-05$	0.008 ± 0.046	0.499 ± 0.895	0.103	4 ± 3	9 ± 4	-	6 ± 3	3
XMMXCS J022328.1-042149.1	$0.270^{+0.100}_{-0.108}$	0.258 ± 0.100	-	-0.004 ± 0.077	1.400 ± 1.470	0.111	3 ± 2	3 ± 3	0 ± 1	1 ± 2	3
XMMXCS J022336.6+062425.7	$0.409^{+0.102}_{-0.097}$	0.331 ± 0.051	-	-0.003 ± 0.112	1.680 ± 2.190	0.030	0 ± 2	1 ± 3	-	0 ± 1	3
XMMXCS J022336.83-040941.4	$0.321^{+0.095}_{-0.085}$	0.077 ± 0.022	$0.143 \pm 2.7e-05$	0.085 ± 0.057	-0.475 ± 1.100	0.125	2 ± 3	60 ± 8	0 ± 0.1	-	3
XMMXCS J022337.0-034507.1	$0.561^{+0.172}_{-0.177}$	0.488 ± 0.103	-	0.483 ± 0.320	-8.710 ± 6.530	0.140	1 ± 2	-	2 ± 1	-	3
XMMXCS J022341.6-023941.6	$0.277^{+0.132}_{-0.131}$	0.152 ± 0.038	-	-0.224 ± 0.059	5.750 ± 1.180	0.500	3 ± 3	3 ± 4	3 ± 2	4 ± 3	3
XMMXCS J022341.8-043037.8	$0.374^{+0.076}_{-0.074}$	0.423 ± 0.062	$0.436 \pm 9.4e-05$	-0.039 ± 0.021	1.390 ± 0.418	0.030	8 ± 4	9 ± 4	6 ± 3	8 ± 4	3
XMMXCS J022342.0-040013.0	$0.235^{+0.102}_{-0.108}$	0.256 ± 0.045	-	-0.111 ± 0.026	3.590 ± 0.504	0.001	1 ± 1	0 ± 1	0 ± 0.1	-	3
XMMXCS J022342.3-050200.3	$0.171^{+0.040}_{-0.041}$	0.144 ± 0.028	-	0.096 ± 0.033	-0.580 ± 0.583	0.051	2 ± 2	3 ± 2	0 ± 0.1	1 ± 1	3
XMMXCS J022353.9-044812.8	$0.283^{+0.066}_{-0.066}$	0.303 ± 0.048	-	-0.065 ± 0.037	2.830 ± 0.697	0.001	0 ± 1	1 ± 2	-	0 ± 1	3
XMMXCS J022400.87-044129.2	$0.460^{+0.113}_{-0.105}$	0.401 ± 0.095	-	0.052 ± 0.029	-0.260 ± 0.575	0.097	6 ± 4	5 ± 3	4 ± 3	117 ± 11	3

Continued on next page

Table A.2 – continued from previous page

name	z_{RS}	z_{BCG}	z_{spec-g}	cmr_{grad}	cmr_{inter}	cmr_{wid}	n_{gals-c}	n_{gals-l}	n_{200-c}	n_{200-l}	qual
XMMXCS J022401.09-050542.2	$0.330^{+0.062}_{-0.057}$	0.320 ± 0.051	$0.324 \pm 5.3e-05$	-0.000 ± 0.001	1.450 ± 0.001	0.500	4 ± 4	3 ± 4	0 ± 2	3 ± 3	3
XMMXCS J022403.6-041912.9	$0.275^{+0.114}_{-0.120}$	0.416 ± 0.066	-	-0.446 ± 0.216	10.400 ± 4.430	0.150	1 ± 1	1 ± 2	0 ± 0.1	1 ± 1	3
XMMXCS J022413.31-052725.8	$0.273^{+0.088}_{-0.093}$	0.223 ± 0.040	-	0.146 ± 0.137	-1.430 ± 2.660	0.116	4 ± 2	2 ± 2	2 ± 2	0 ± 1	3
XMMXCS J022419.6-062142.9	$0.172^{+0.069}_{-0.074}$	0.151 ± 0.033	-	-0.005 ± 0.032	1.090 ± 0.621	0.102	1 ± 1	0 ± 1	0 ± 0.1	-	3
XMMXCS J022420.3-045725.5	$0.350^{+0.108}_{-0.096}$	0.299 ± 0.048	-	0.005 ± 0.018	0.474 ± 0.348	0.100	0 ± 3	2 ± 3	-	2 ± 2	3
XMMXCS J022420.3-042202.0	$0.181^{+0.057}_{-0.057}$	0.152 ± 0.037	$0.268 \pm 3.6e-05$	0.173 ± 0.001	-1.930 ± 0.001	0.500	0 ± 2	1 ± 3	-	4 ± 2	3
XMMXCS J022423.8-050417.2	$0.142^{+0.035}_{-0.035}$	0.132 ± 0.023	$0.143 \pm 2.3e-05$	0.065 ± 0.021	0.017 ± 0.347	0.042	1 ± 1	1 ± 1	1 ± 1	1 ± 1	3
XMMXCS J022424.2-040109.6	$0.359^{+0.114}_{-0.126}$	0.271 ± 0.059	-	-0.077 ± 0.107	2.990 ± 2.190	0.066	0 ± 2	1 ± 2	-	0 ± 1	3
XMMXCS J022427.3-045028.1	$0.352^{+0.129}_{-0.129}$	0.276 ± 0.105	-	0.155 ± 0.081	-2.550 ± 1.620	0.001	6 ± 3	6 ± 3	2 ± 2	4 ± 3	3
XMMXCS J022427.40-045025.7	$0.389^{+0.135}_{-0.135}$	0.251 ± 0.116	-	0.164 ± 0.092	-2.740 ± 1.870	0.001	8 ± 4	6 ± 4	6 ± 3	4 ± 3	3
XMMXCS J022438.1-045335.9	$0.262^{+0.090}_{-0.091}$	0.388 ± 0.147	-	-1.060 ± 0.007	21.700 ± 0.133	0.500	2 ± 2	-	1 ± 1	-	3
XMMXCS J022453.8-032847.0	$0.172^{+0.061}_{-0.063}$	0.189 ± 0.030	$0.174 \pm 2.3e-05$	0.034 ± 0.038	0.583 ± 0.712	0.119	3 ± 2	2 ± 2	0 ± 1	0 ± 1	3
XMMXCS J022453.88-032847.6	$0.172^{+0.061}_{-0.063}$	0.189 ± 0.030	$0.174 \pm 2.3e-05$	0.034 ± 0.038	0.583 ± 0.712	0.119	3 ± 2	2 ± 2	0 ± 1	0 ± 1	3
XMMXCS J022509.7-040137.6	$0.173^{+0.032}_{-0.032}$	0.174 ± 0.026	$0.173 \pm 1.7e-05$	-0.058 ± 0.005	2.120 ± 0.092	0.001	1 ± 1	2 ± 2	1 ± 1	3 ± 2	3
XMMXCS J022512.31-053112.3	$0.343^{+0.090}_{-0.081}$	0.291 ± 0.052	-	0.477 ± 0.001	-8.030 ± 0.023	0.500	1 ± 3	-	0 ± 0.1	-	3
XMMXCS J022517.8-042225.2	$0.323^{+0.109}_{-0.116}$	0.246 ± 0.040	-	-0.109 ± 0.101	3.480 ± 1.990	0.067	0 ± 2	2 ± 3	-	1 ± 2	3
XMMXCS J022519.72-054415.4	$0.147^{+0.132}_{-0.135}$	0.064 ± 0.018	-	0.034 ± 0.036	0.172 ± 0.686	0.102	4 ± 2	5 ± 3	3 ± 2	4 ± 2	3
XMMXCS J022519.7-054415.4	$0.147^{+0.132}_{-0.135}$	0.064 ± 0.018	-	0.034 ± 0.036	0.172 ± 0.686	0.102	4 ± 2	5 ± 3	3 ± 2	4 ± 2	3
XMMXCS J022525.01-061854.8	$0.443^{+0.083}_{-0.067}$	0.563 ± 0.135	-	-0.066 ± 0.038	2.850 ± 0.754	0.051	3 ± 3	1 ± 1	0 ± 1	-	3

Continued on next page

Table A.2 – continued from previous page

name	z_{RS}	z_{BCG}	z_{spec-g}	cmr_{grad}	cmr_{inter}	cmr_{wid}	n_{gals-c}	n_{gals-l}	n_{200-c}	n_{200-l}	qual
XMMXCS J022532.0-035509.9	$0.547^{+0.134}_{-0.130}$	0.518 ± 0.101	$0.562 \pm 1.5e-04$	-0.119 ± 0.112	3.500 ± 2.260	0.182	4 ± 3	8 ± 4	3 ± 2	4 ± 3	3
XMMXCS J022532.42-035502.4	$0.556^{+0.116}_{-0.117}$	0.518 ± 0.101	$0.562 \pm 1.5e-04$	0.029 ± 0.141	0.518 ± 2.920	0.001	4 ± 2	-	2 ± 2	-	3
XMMXCS J022536.2-030231.9	$0.510^{+0.128}_{-0.130}$	0.326 ± 0.164	-	0.003 ± 0.087	0.918 ± 1.770	0.111	1 ± 2	-	1 ± 1	-	3
XMMXCS J022536.97-025222.2	$0.427^{+0.085}_{-0.085}$	0.309 ± 0.074	-	0.070 ± 0.096	0.068 ± 1.840	0.065	1 ± 3	2 ± 3	1 ± 1	-	3
XMMXCS J022538.3-042829.1	$0.196^{+0.120}_{-0.125}$	0.111 ± 0.036	-	-0.022 ± 0.029	1.170 ± 0.555	0.081	1 ± 1	1 ± 2	0 ± 0.1	0 ± 1	3
XMMXCS J022544.6-051234.9	$0.155^{+0.077}_{-0.074}$	0.070 ± 0.019	-	0.059 ± 0.037	-0.016 ± 0.677	0.129	4 ± 2	4 ± 3	1 ± 1	1 ± 2	3
XMMXCS J022553.6-031748.6	$0.124^{+0.060}_{-0.066}$	0.212 ± 0.046	-	0.011 ± 0.019	0.813 ± 0.366	0.084	4 ± 2	3 ± 2	2 ± 1	1 ± 1	3
XMMXCS J022559.68-024932.4	$0.264^{+0.065}_{-0.066}$	0.151 ± 0.025	-	0.306 ± 0.193	-4.370 ± 3.710	0.184	8 ± 4	5 ± 3	10 ± 4	5 ± 3	3
XMMXCS J022559.7-024932.7	$0.264^{+0.065}_{-0.066}$	0.151 ± 0.025	-	0.306 ± 0.193	-4.370 ± 3.710	0.184	8 ± 4	5 ± 3	10 ± 4	5 ± 3	3
XMMXCS J022600.21-044413.1	$0.086^{+0.029}_{-0.031}$	0.106 ± 0.028	-	-0.115 ± 0.064	2.560 ± 1.120	0.500	0 ± 1	1 ± 1	-	0 ± 1	3
XMMXCS J022600.2-044413.0	$0.086^{+0.029}_{-0.031}$	0.106 ± 0.028	-	-0.115 ± 0.064	2.560 ± 1.120	0.500	0 ± 1	1 ± 1	-	0 ± 1	3
XMMXCS J022608.8-051550.6	$0.200^{+0.079}_{-0.080}$	0.218 ± 0.035	-	-0.029 ± 0.038	1.730 ± 0.703	0.072	1 ± 2	1 ± 2	0 ± 0.1	0 ± 1	3
XMMXCS J022616.2-023954.5	$0.289^{+0.072}_{-0.077}$	0.169 ± 0.119	$0.370 \pm 1.5e-04$	-0.134 ± 0.079	4.130 ± 1.590	0.097	3 ± 2	5 ± 3	0 ± 1	2 ± 2	3
XMMXCS J022616.24-023954.2	$0.289^{+0.072}_{-0.077}$	0.169 ± 0.119	$0.370 \pm 1.5e-04$	-0.134 ± 0.079	4.130 ± 1.590	0.097	3 ± 2	4 ± 3	0 ± 1	67 ± 8	3
XMMXCS J022617.8-050406.1	$0.054^{+0.018}_{-0.018}$	0.116 ± 0.031	$0.054 \pm 8.5e-06$	0.063 ± 0.015	-0.194 ± 0.228	0.068	7 ± 3	2 ± 2	5 ± 2	1 ± 1	3
XMMXCS J022618.03-050405.7	$0.054^{+0.018}_{-0.018}$	0.116 ± 0.031	$0.054 \pm 8.5e-06$	0.063 ± 0.015	-0.194 ± 0.228	0.068	7 ± 3	2 ± 2	5 ± 2	1 ± 1	3
XMMXCS J022627.42-043711.8	$0.518^{+0.154}_{-0.153}$	0.595 ± 0.132	$0.585 \pm 3.5e-04$	0.047 ± 0.053	-0.149 ± 1.030	0.078	2 ± 3	13 ± 4	1 ± 1	12 ± 4	3
XMMXCS J022627.7-034156.4	$0.193^{+0.108}_{-0.109}$	0.209 ± 0.044	-	0.024 ± 0.029	0.708 ± 0.558	0.013	0 ± 1	1 ± 1	-	1 ± 1	3
XMMXCS J022627.78-034157.4	$0.193^{+0.108}_{-0.109}$	0.209 ± 0.044	-	0.024 ± 0.029	0.708 ± 0.558	0.013	0 ± 1	1 ± 1	-	1 ± 1	3

Continued on next page

Table A.2 – continued from previous page

name	z_{RS}	z_{BCG}	z_{spec-g}	cmr_{grad}	cmr_{inter}	cmr_{wid}	n_{gals-c}	n_{gals-l}	n_{200-c}	n_{200-l}	qual
XMMXCS J022628.67-054234.7	$0.359^{+0.059}_{-0.059}$	0.337 ± 0.050	$0.357 \pm 5.6e-05$	0.085 ± 0.088	0.200 ± 1.610	0.150	2 ± 2	2 ± 2	0 ± 0.1	0 ± 1	3
XMMXCS J022628.98-045253.4	$0.289^{+0.067}_{-0.065}$	0.105 ± 0.032	$0.317 \pm 4.3e-05$	0.121 ± 0.084	-0.965 ± 1.540	0.500	5 ± 4	5 ± 4	0 ± 2	2 ± 3	3
XMMXCS J022628.9-045253.3	$0.289^{+0.067}_{-0.065}$	0.105 ± 0.032	$0.317 \pm 4.3e-05$	0.121 ± 0.084	-0.965 ± 1.540	0.500	5 ± 4	5 ± 4	0 ± 2	2 ± 3	3
XMMXCS J022633.65-042216.0	$0.128^{+0.052}_{-0.058}$	0.100 ± 0.022	-	0.062 ± 0.014	-0.043 ± 0.237	0.001	1 ± 1	0 ± 1	0 ± 0.1	-	3
XMMXCS J022639.92-041641.5	$0.181^{+0.079}_{-0.075}$	0.076 ± 0.024	-	-0.054 ± 0.025	1.770 ± 0.476	0.064	2 ± 2	0 ± 1	1 ± 1	-	3
XMMXCS J022702.06-040512.4	$0.622^{+0.157}_{-0.158}$	0.563 ± 0.138	-	-0.070 ± 0.170	2.520 ± 3.480	0.001	3 ± 2	0 ± 1	2 ± 1	-	3
XMMXCS J022702.1-040511.5	$0.622^{+0.157}_{-0.158}$	0.563 ± 0.138	-	-0.070 ± 0.170	2.520 ± 3.480	0.001	3 ± 2	0 ± 1	2 ± 1	-	3
XMMXCS J022702.94-041509.5	$0.172^{+0.048}_{-0.045}$	0.177 ± 0.046	$0.209 \pm 2.9e-05$	-0.046 ± 0.008	1.880 ± 0.149	0.056	1 ± 1	0 ± 1	0 ± 0.1	-	3
XMMXCS J022705.30-041214.9	$0.202^{+0.052}_{-0.057}$	0.166 ± 0.059	-	-0.155 ± 0.001	3.780 ± 0.001	0.500	1 ± 2	1 ± 3	0 ± 0.1	0 ± 1	3
XMMXCS J022708.5-043226.3	$0.346^{+0.124}_{-0.125}$	0.286 ± 0.094	-	-0.136 ± 0.088	3.680 ± 1.820	0.083	8 ± 3	10 ± 4	5 ± 3	11 ± 4	3
XMMXCS J022708.64-043228.0	$0.348^{+0.124}_{-0.124}$	0.286 ± 0.094	-	-0.136 ± 0.088	3.680 ± 1.820	0.083	10 ± 4	12 ± 4	11 ± 4	12 ± 4	3
XMMXCS J022714.2-042647.5	$0.086^{+0.042}_{-0.052}$	0.064 ± 0.014	-	0.003 ± 0.023	0.780 ± 0.354	0.500	0 ± 2	1 ± 2	-	0 ± 1	3
XMMXCS J022714.3-042648.6	$0.086^{+0.042}_{-0.052}$	0.064 ± 0.014	-	0.003 ± 0.023	0.780 ± 0.354	0.500	0 ± 2	1 ± 2	-	0 ± 1	3
XMMXCS J022722.0-045226.1	$0.319^{+0.087}_{-0.089}$	0.244 ± 0.057	-	0.019 ± 0.059	1.150 ± 1.150	0.067	5 ± 3	6 ± 3	1 ± 1	1 ± 2	3
XMMXCS J022725.01-041127.0	$0.639^{+0.123}_{-0.119}$	0.568 ± 0.088	$0.634 \pm 1.3e-04$	-0.083 ± 0.084	2.790 ± 1.690	0.001	4 ± 2	-	0 ± 1	-	3
XMMXCS J022725.1-041125.8	$0.623^{+0.119}_{-0.115}$	0.568 ± 0.088	$0.634 \pm 1.3e-04$	-0.078 ± 0.102	2.660 ± 2.060	0.102	4 ± 2	-	0 ± 1	-	3
XMMXCS J022727.52-042712.5	$0.406^{+0.096}_{-0.084}$	0.268 ± 0.065	-	-0.032 ± 0.157	1.400 ± 3.230	0.500	5 ± 3	-	3 ± 2	-	3
XMMXCS J022728.3-084810.5	$0.346^{+0.081}_{-0.081}$	0.403 ± 0.060	-	-0.117 ± 0.047	3.930 ± 0.915	0.001	8 ± 3	12 ± 4	6 ± 3	12 ± 4	3
XMMXCS J022731.8-043750.3	$0.304^{+0.086}_{-0.091}$	0.328 ± 0.075	$0.308 \pm 3.4e-05$	-0.107 ± 0.044	3.540 ± 0.851	0.090	2 ± 2	4 ± 3	0 ± 1	3 ± 2	3

Continued on next page

Table A.2 – continued from previous page

name	z_{RS}	z_{BCG}	z_{spec-g}	cmr_{grad}	cmr_{inter}	cmr_{wid}	n_{gals-c}	n_{gals-l}	n_{200-c}	n_{200-l}	qual
XMMXCS J022731.86-043750.4	$0.304^{+0.086}_{-0.091}$	0.328 ± 0.075	$0.308 \pm 3.4e-05$	-0.107 ± 0.044	3.540 ± 0.851	0.090	2 ± 2	4 ± 3	0 ± 1	3 ± 2	3
XMMXCS J022734.3-043553.2	$0.306^{+0.083}_{-0.085}$	0.328 ± 0.075	$0.308 \pm 3.4e-05$	-0.092 ± 0.054	3.230 ± 1.030	0.071	6 ± 3	7 ± 3	0 ± 1	2 ± 2	3
XMMXCS J022735.37-032634.5	$0.239^{+0.052}_{-0.052}$	0.277 ± 0.051	$0.278 \pm 5.2e-05$	0.050 ± 0.049	0.435 ± 0.912	0.094	1 ± 2	1 ± 2	0 ± 0.1	0 ± 1	3
XMMXCS J022740.86-045743.1	$0.054^{+0.021}_{-0.023}$	0.072 ± 0.019	$0.055 \pm 9.9e-06$	-0.022 ± 0.035	0.971 ± 0.638	0.500	1 ± 1	0 ± 1	0 ± 0.1	-	3
XMMXCS J022744.92-034413.8	$0.357^{+0.182}_{-0.190}$	0.328 ± 0.157	-	0.362 ± 0.252	-7.480 ± 5.190	0.001	2 ± 1	3 ± 2	0 ± 0.1	1 ± 1	3
XMMXCS J022744.9-034413.7	$0.357^{+0.182}_{-0.190}$	0.328 ± 0.157	-	0.362 ± 0.252	-7.480 ± 5.190	0.001	2 ± 1	3 ± 2	0 ± 0.1	1 ± 1	3
XMMXCS J022750.6-025406.4	$0.208^{+0.069}_{-0.074}$	0.174 ± 0.030	-	0.020 ± 0.052	0.863 ± 0.966	0.146	1 ± 2	1 ± 2	0 ± 0.1	0 ± 1	3
XMMXCS J022752.85-054756.9	$0.222^{+0.074}_{-0.079}$	0.059 ± 0.017	$0.298 \pm 4.6e-05$	0.011 ± 0.001	1.100 ± 0.011	0.500	0 ± 3	1 ± 3	-	0 ± 1	3
XMMXCS J022759.29-034828.8	$0.311^{+0.125}_{-0.140}$	0.191 ± 0.035	-	-0.024 ± 0.028	1.630 ± 0.531	0.001	1 ± 2	-	0 ± 0.1	-	3
XMMXCS J022759.2-034828.8	$0.311^{+0.125}_{-0.140}$	0.191 ± 0.035	-	-0.024 ± 0.028	1.630 ± 0.531	0.001	1 ± 2	-	0 ± 0.1	-	3
XMMXCS J022804.6-041818.6	$0.339^{+0.040}_{-0.040}$	0.346 ± 0.052	$0.338 \pm 6.9e-05$	0.024 ± 0.058	1.250 ± 1.070	0.001	4 ± 3	7 ± 3	1 ± 1	2 ± 2	3
XMMXCS J022805.60-051934.5	$0.242^{+0.088}_{-0.092}$	0.220 ± 0.041	$0.318 \pm 8.9e-05$	0.010 ± 0.120	1.160 ± 2.420	0.128	3 ± 2	3 ± 3	0 ± 1	1 ± 2	3
XMMXCS J022805.5-051934.5	$0.242^{+0.088}_{-0.092}$	0.220 ± 0.041	$0.318 \pm 8.9e-05$	0.010 ± 0.120	1.160 ± 2.420	0.128	3 ± 2	3 ± 3	0 ± 1	1 ± 2	3
XMMXCS J022807.23-030939.3	$0.315^{+0.051}_{-0.048}$	0.280 ± 0.050	-	0.023 ± 0.075	1.120 ± 1.410	0.038	1 ± 2	1 ± 2	0 ± 0.1	0 ± 1	3
XMMXCS J022807.98-031627.4	$0.065^{+0.021}_{-0.021}$	0.070 ± 0.015	-	-0.022 ± 0.008	1.150 ± 0.142	0.028	2 ± 2	0 ± 1	2 ± 1	-	3
XMMXCS J022808.1-031625.1	$0.065^{+0.021}_{-0.021}$	0.070 ± 0.015	-	-0.022 ± 0.008	1.150 ± 0.142	0.028	2 ± 2	0 ± 1	2 ± 1	-	3
XMMXCS J022811.29-041140.6	$0.422^{+0.120}_{-0.114}$	0.327 ± 0.176	-	0.528 ± 1.050	-9.110 ± 21.20	0.500	2 ± 4	6 ± 4	1 ± 2	7 ± 4	3
XMMXCS J022811.7-041136.6	$0.414^{+0.125}_{-0.122}$	0.327 ± 0.176	-	0.528 ± 1.050	-9.110 ± 21.20	0.500	2 ± 4	3 ± 4	1 ± 2	2 ± 2	3
XMMXCS J022812.4-043234.6	$0.507^{+0.113}_{-0.100}$	0.373 ± 0.103	-	4.650 ± 2.440	-95.60 ± 51.00	0.500	2 ± 2	0 ± 1	0 ± 1	-	3

Continued on next page

Table A.2 – continued from previous page

name	z_{RS}	z_{BCG}	z_{spec-g}	cmr_{grad}	cmr_{inter}	cmr_{wid}	n_{gals-c}	n_{gals-l}	n_{200-c}	n_{200-l}	qual
XMMXCS J022824.6-030927.6	$0.139^{+0.061}_{-0.061}$	0.090 ± 0.036	-	-0.124 ± 0.059	2.610 ± 0.964	0.105	2 ± 2	4 ± 3	1 ± 1	8 ± 3	3
XMMXCS J022827.28-042542.5	$0.371^{+0.095}_{-0.095}$	0.444 ± 0.067	$0.434 \pm 7.4e-05$	0.055 ± 0.056	0.542 ± 1.100	0.133	23 ± 5	23 ± 5	24 ± 6	23 ± 6	3
XMMXCS J022827.3-042542.2	$0.375^{+0.094}_{-0.094}$	0.444 ± 0.067	$0.434 \pm 7.4e-05$	0.039 ± 0.050	0.892 ± 0.974	0.087	18 ± 5	19 ± 5	20 ± 5	22 ± 5	3
XMMXCS J022829.6-031257.0	$0.267^{+0.067}_{-0.068}$	0.267 ± 0.045	-	-0.001 ± 0.079	1.430 ± 1.510	0.001	3 ± 2	5 ± 3	1 ± 1	1 ± 2	3
XMMXCS J022841.25-035700.6	$0.223^{+0.093}_{-0.095}$	0.173 ± 0.035	-	-0.014 ± 0.040	1.380 ± 0.774	0.110	1 ± 2	2 ± 2	0 ± 0.1	1 ± 1	3
XMMXCS J022844.7-041339.8	$0.143^{+0.060}_{-0.064}$	0.132 ± 0.023	-	0.009 ± 0.034	0.946 ± 0.627	0.088	1 ± 2	1 ± 2	0 ± 0.1	1 ± 1	3
XMMXCS J022851.4-051224.4	$0.300^{+0.084}_{-0.074}$	0.109 ± 0.025	-	-0.081 ± 0.096	2.580 ± 1.790	0.087	3 ± 3	1 ± 3	2 ± 2	1 ± 1	3
XMMXCS J022856.65-085721.2	$0.357^{+0.164}_{-0.165}$	0.288 ± 0.047	-	-0.124 ± 0.165	3.650 ± 3.380	0.166	2 ± 3	-	1 ± 1	-	3
XMMXCS J022858.05-055409.5	$0.305^{+0.078}_{-0.074}$	0.237 ± 0.061	-	0.138 ± 0.044	-1.250 ± 0.845	0.119	3 ± 3	2 ± 3	0 ± 1	0 ± 1	3
XMMXCS J022912.41-060124.3	$0.366^{+0.091}_{-0.089}$	0.298 ± 0.070	-	0.530 ± 0.120	-8.670 ± 2.410	0.229	7 ± 3	9 ± 4	4 ± 3	8 ± 4	3
XMMXCS J022929.14-040846.7	$0.451^{+0.225}_{-0.202}$	0.579 ± 0.304	-	-0.950 ± 0.433	20.300 ± 8.890	0.001	1 ± 2	-	0 ± 0.1	-	3
XMMXCS J022933.28-043953.8	$0.379^{+0.110}_{-0.105}$	0.272 ± 0.084	-	1.810 ± 0.639	-36.20 ± 13.10	0.500	1 ± 3	1 ± 3	2 ± 1	0 ± 1	3
XMMXCS J022940.9-060426.0	$0.289^{+0.099}_{-0.092}$	0.150 ± 0.027	-	0.025 ± 0.041	0.627 ± 0.810	0.124	2 ± 2	0 ± 2	0 ± 0.1	-	3
XMMXCS J022954.19-054954.1	$0.306^{+0.093}_{-0.083}$	0.232 ± 0.073	-	-0.066 ± 0.069	2.360 ± 1.360	0.100	0 ± 2	2 ± 3	-	0 ± 1	3
XMMXCS J023007.35-043125.6	$0.503^{+0.109}_{-0.105}$	0.464 ± 0.091	-	0.046 ± 0.048	-0.111 ± 0.920	0.001	4 ± 3	3 ± 3	3 ± 2	2 ± 2	3
XMMXCS J023009.8-005915.4	$0.318^{+0.083}_{-0.081}$	0.191 ± 0.030	-	0.103 ± 0.149	-0.639 ± 2.920	0.098	5 ± 3	9 ± 4	5 ± 2	4 ± 3	3
XMMXCS J023035.76-052604.9	$0.242^{+0.086}_{-0.086}$	0.144 ± 0.041	-	0.058 ± 0.054	-0.070 ± 1.050	0.136	1 ± 2	-	0 ± 0.1	-	3
XMMXCS J023057.21-044252.5	$0.158^{+0.044}_{-0.046}$	0.071 ± 0.018	$0.031 \pm 1.4e-05$	-0.107 ± 0.140	3.090 ± 2.640	0.500	1 ± 2	0 ± 3	0 ± 0.1	-	3
XMMXCS J023103.19-040345.2	$0.164^{+0.039}_{-0.040}$	0.125 ± 0.027	-	-0.007 ± 0.103	1.220 ± 1.880	0.098	2 ± 2	3 ± 2	0 ± 0.1	0 ± 1	3

Continued on next page

Table A.2 – continued from previous page

name	z_{RS}	z_{BCG}	z_{spec-g}	cmr_{grad}	cmr_{inter}	cmr_{wid}	n_{gals-c}	n_{gals-l}	n_{200-c}	n_{200-l}	qual
XMMXCS J023103.42-051345.9	$0.128^{+0.044}_{-0.044}$	0.121 ± 0.028	$0.127 \pm 1.7e-05$	-0.076 ± 0.010	2.130 ± 0.167	0.067	0 ± 1	1 ± 1	-	1 ± 1	3
XMMXCS J023105.55-041322.8	$0.522^{+0.090}_{-0.087}$	0.527 ± 0.080	$0.516 \pm 1.1e-04$	0.112 ± 0.163	-1.330 ± 3.210	0.138	0 ± 2	6 ± 4	-	8 ± 3	3
XMMXCS J023113.45-054126.1	$0.587^{+0.133}_{-0.118}$	0.482 ± 0.157	-	0.284 ± 0.424	-4.930 ± 8.770	0.001	1 ± 1	0 ± 1	1 ± 1	-	3
XMMXCS J023133.04-071507.8	$0.212^{+0.074}_{-0.075}$	0.190 ± 0.035	$0.189 \pm 3.0e-05$	0.075 ± 0.140	-0.178 ± 2.680	0.149	0 ± 2	2 ± 2	-	1 ± 1	3
XMMXCS J023133.0-071507.8	$0.212^{+0.074}_{-0.075}$	0.190 ± 0.035	$0.189 \pm 3.0e-05$	0.075 ± 0.140	-0.178 ± 2.680	0.149	0 ± 2	2 ± 2	-	1 ± 1	3
XMMXCS J023141.5-042955.3	$0.395^{+0.130}_{-0.131}$	0.337 ± 0.086	-	-0.117 ± 0.070	2.910 ± 1.350	0.077	2 ± 3	3 ± 3	2 ± 2	3 ± 2	3
XMMXCS J023204.92-053309.4	$0.599^{+0.126}_{-0.124}$	0.537 ± 0.084	$0.589 \pm 2.3e-04$	-0.159 ± 0.067	4.170 ± 1.330	0.001	13 ± 4	21 ± 5	12 ± 4	31 ± 7	3
XMMXCS J023220.9-055843.4	$0.310^{+0.096}_{-0.106}$	0.315 ± 0.051	-	-0.120 ± 0.220	3.790 ± 4.470	0.133	1 ± 2	0 ± 2	0 ± 0.1	-	3
XMMXCS J023247.47-045147.4	$0.197^{+0.070}_{-0.069}$	0.091 ± 0.026	-	-0.005 ± 0.027	1.030 ± 0.485	0.112	1 ± 2	3 ± 3	0 ± 0.1	-	3
XMMXCS J023249.43-055026.6	$0.326^{+0.119}_{-0.131}$	0.259 ± 0.057	-	-0.343 ± 0.166	7.960 ± 3.430	0.062	0 ± 2	1 ± 2	-	0 ± 1	3
XMMXCS J023249.96-044345.4	$0.255^{+0.067}_{-0.069}$	0.254 ± 0.046	-	-0.077 ± 0.033	2.880 ± 0.636	0.101	1 ± 2	1 ± 2	0 ± 0.1	0 ± 1	3
XMMXCS J023300.88-050951.0	$0.244^{+0.074}_{-0.081}$	0.163 ± 0.035	$0.250 \pm 4.3e-05$	-0.000 ± 0.001	1.390 ± 0.001	0.500	7 ± 4	5 ± 4	3 ± 3	3 ± 3	3
XMMXCS J023308.59-050250.3	$0.210^{+0.084}_{-0.084}$	0.071 ± 0.022	-	-0.352 ± 0.001	7.710 ± 0.009	0.500	7 ± 4	5 ± 4	3 ± 3	2 ± 2	3
XMMXCS J023321.06-053644.6	$0.436^{+0.083}_{-0.075}$	0.301 ± 0.052	$0.299 \pm 4.9e-05$	0.034 ± 0.041	0.966 ± 0.783	0.042	0 ± 2	15 ± 5	-	22 ± 5	3
XMMXCS J023333.45-060009.6	$0.181^{+0.054}_{-0.055}$	0.185 ± 0.033	$0.183 \pm 2.6e-05$	0.001 ± 0.038	1.060 ± 0.735	0.106	1 ± 2	3 ± 2	1 ± 1	3 ± 2	3
XMMXCS J023346.36-055402.5	$0.266^{+0.064}_{-0.058}$	0.197 ± 0.076	-	0.026 ± 0.068	0.810 ± 1.270	0.137	2 ± 3	3 ± 3	0 ± 0.1	2 ± 2	3
XMMXCS J023356.94-050815.9	$0.413^{+0.121}_{-0.121}$	0.387 ± 0.129	-	0.111 ± 0.264	-0.910 ± 5.280	0.132	2 ± 3	11 ± 4	0 ± 1	11 ± 4	3
XMMXCS J023357.24-055812.9	$0.699^{+0.129}_{-0.127}$	0.553 ± 0.144	$0.692 \pm 2.6e-04$	-0.001 ± 0.069	1.240 ± 1.320	0.059	2 ± 2	-	1 ± 1	-	3
XMMXCS J023358.22-053632.1	$0.621^{+0.161}_{-0.156}$	0.600 ± 0.135	-	2.810 ± 0.145	-57.20 ± 3.140	0.123	2 ± 2	0 ± 1	1 ± 1	-	3

Continued on next page

Table A.2 – continued from previous page

name	z_{RS}	z_{BCG}	z_{spec-g}	cmr_{grad}	cmr_{inter}	cmr_{wid}	n_{gals-c}	n_{gals-l}	n_{200-c}	n_{200-l}	qual
XMMXCS J023406.90-051121.7	$0.144^{+0.041}_{-0.040}$	0.174 ± 0.048	-	0.068 ± 0.067	-0.325 ± 1.200	0.128	2 ± 2	2 ± 2	0 ± 0.1	0 ± 1	3
XMMXCS J023418.87-060107.9	$0.304^{+0.064}_{-0.066}$	0.413 ± 0.065	-	-0.142 ± 0.101	4.400 ± 2.000	0.087	1 ± 2	1 ± 2	0 ± 0.1	1 ± 1	3
XMMXCS J023424.01-042920.7	$0.155^{+0.078}_{-0.085}$	0.080 ± 0.028	$0.182 \pm 2.7e-05$	-0.000 ± 0.001	1.100 ± 0.001	0.500	2 ± 3	2 ± 3	1 ± 1	1 ± 2	3
XMMXCS J024113.6-082653.8	$0.292^{+0.105}_{-0.106}$	0.181 ± 0.038	-	-0.064 ± 0.125	2.500 ± 2.520	0.001	2 ± 2	1 ± 2	1 ± 1	-	3
XMMXCS J024128.1-081648.7	$0.186^{+0.101}_{-0.106}$	0.186 ± 0.039	-	-0.123 ± 0.037	3.330 ± 0.723	0.108	0 ± 1	2 ± 2	-	1 ± 1	3
XMMXCS J024134.8-082508.0	$0.550^{+0.126}_{-0.103}$	0.496 ± 0.079	-	0.106 ± 0.161	-1.370 ± 3.220	0.149	4 ± 3	8 ± 4	0 ± 1	5 ± 3	3
XMMXCS J024141.1-081416.6	$0.136^{+0.060}_{-0.063}$	0.131 ± 0.023	$0.139 \pm 1.8e-05$	-0.025 ± 0.027	1.330 ± 0.507	0.092	0 ± 1	1 ± 1	-	1 ± 1	3
XMMXCS J024156.9-000534.0	$0.356^{+0.090}_{-0.093}$	0.332 ± 0.062	$0.369 \pm 1.0e-04$	-0.038 ± 0.073	2.420 ± 1.440	0.001	2 ± 2	4 ± 3	0 ± 0.1	1 ± 2	3
XMMXCS J024204.6+000815.3	$0.393^{+0.104}_{-0.100}$	0.221 ± 0.052	-	0.073 ± 0.371	-0.111 ± 7.580	0.001	1 ± 2	0 ± 2	1 ± 1	-	3
XMMXCS J024239.8+000614.2	$0.366^{+0.103}_{-0.101}$	0.283 ± 0.115	-	10.100 ± 17.20	-203.0 ± 349	0.727	3 ± 2	0 ± 1	4 ± 2	-	3
XMMXCS J024255.0+424113.5	$0.137^{+0.044}_{-0.042}$	0.080 ± 0.024	-	0.242 ± 0.077	-3.470 ± 1.450	0.500	3 ± 2	3 ± 3	1 ± 1	2 ± 2	3
XMMXCS J024317.7-000746.8	$0.738^{+0.123}_{-0.114}$	0.645 ± 0.166	$0.717 \pm 1.6e-04$	0.063 ± 0.105	-0.042 ± 2.100	0.111	3 ± 2	30 ± 6	-	33 ± 7	3
XMMXCS J024754.6+311323.3	$0.226^{+0.063}_{-0.074}$	0.220 ± 0.066	-	0.006 ± 0.035	1.070 ± 0.668	0.108	2 ± 2	1 ± 2	0 ± 0.1	1 ± 1	3
XMMXCS J024824.5-041633.3	$0.247^{+0.107}_{-0.109}$	0.118 ± 0.022	-	0.036 ± 0.028	0.415 ± 0.532	0.105	2 ± 2	3 ± 3	2 ± 2	1 ± 2	3
XMMXCS J024826.3-032932.1	$0.277^{+0.057}_{-0.057}$	0.205 ± 0.049	-	0.108 ± 0.039	-0.610 ± 0.716	0.105	15 ± 4	14 ± 4	18 ± 5	16 ± 5	3
XMMXCS J024835.6+311917.0	$0.347^{+0.089}_{-0.089}$	0.501 ± 0.088	-	-0.090 ± 0.112	3.420 ± 2.160	0.084	35 ± 6	2 ± 3	44 ± 8	1 ± 2	3
XMMXCS J024901.8-081902.5	$0.494^{+0.151}_{-0.151}$	0.594 ± 0.104	-	-0.291 ± 0.141	7.010 ± 2.740	0.192	9 ± 4	24 ± 6	6 ± 3	17 ± 6	3
XMMXCS J025405.2+413606.2	$0.219^{+0.082}_{-0.090}$	0.176 ± 0.069	-	0.081 ± 0.074	-0.249 ± 1.340	0.116	3 ± 2	6 ± 3	4 ± 2	8 ± 3	3
XMMXCS J025444.3+413139.6	$0.190^{+0.094}_{-0.095}$	0.174 ± 0.029	-	-0.019 ± 0.047	1.510 ± 0.852	0.001	3 ± 2	4 ± 2	3 ± 2	3 ± 2	3

Continued on next page

Table A.2 – continued from previous page

name	z_{RS}	z_{BCG}	z_{spec-g}	cmr_{grad}	cmr_{inter}	cmr_{wid}	n_{gals-c}	n_{gals-l}	n_{200-c}	n_{200-l}	qual
XMMXCS J025447.0+413007.0	$0.117^{+0.067}_{-0.065}$	0.066 ± 0.018	-	0.043 ± 0.005	0.311 ± 0.060	0.500	1 ± 3	4 ± 4	0 ± 0.1	3 ± 3	3
XMMXCS J025502.8+413654.8	$0.255^{+0.079}_{-0.079}$	0.172 ± 0.116	-	-0.197 ± 0.244	5.290 ± 4.600	0.283	4 ± 3	4 ± 3	0 ± 1	1 ± 2	3
XMMXCS J025502.8+413442.4	$0.323^{+0.072}_{-0.073}$	0.244 ± 0.095	-	0.042 ± 0.022	0.813 ± 0.439	0.001	6 ± 3	6 ± 3	3 ± 2	3 ± 2	3
XMMXCS J025512.1-001101.0	$0.028^{+0.005}_{-0.004}$	0.097 ± 0.022	$0.029 \pm 4.5e-06$	-0.000 ± 0.001	1.290 ± 0.001	0.500	1 ± 1	0 ± 1	2 ± 1	-	3
XMMXCS J025716.8+000312.9	$0.288^{+0.116}_{-0.117}$	0.166 ± 0.028	$0.386 \pm 1.5e-04$	-0.006 ± 0.030	1.220 ± 0.595	0.073	2 ± 2	2 ± 3	0 ± 0.1	0 ± 1	3
XMMXCS J025722.5+001139.4	$0.495^{+0.142}_{-0.130}$	0.443 ± 0.066	-	0.126 ± 0.081	-1.760 ± 1.600	0.134	1 ± 3	454 ± 21	2 ± 1	43 ± 20	3
XMMXCS J025724.0-000248.6	$0.355^{+0.159}_{-0.162}$	0.412 ± 0.177	-	0.518 ± 0.410	-9.920 ± 8.250	0.308	10 ± 4	12 ± 5	10 ± 4	11 ± 5	3
XMMXCS J025804.5+060215.6	$0.315^{+0.093}_{-0.095}$	0.227 ± 0.039	-	0.113 ± 0.113	-0.595 ± 2.290	0.001	2 ± 2	4 ± 3	2 ± 1	1 ± 2	3
XMMXCS J025820.8+060543.4	$0.258^{+0.129}_{-0.132}$	0.080 ± 0.042	-	0.213 ± 0.128	-2.900 ± 2.500	0.152	2 ± 3	4 ± 4	2 ± 2	1 ± 2	3
XMMXCS J030054.5+370000.2	$0.388^{+0.104}_{-0.100}$	0.412 ± 0.061	-	0.037 ± 0.123	-0.044 ± 2.390	0.071	3 ± 3	5 ± 3	1 ± 1	5 ± 3	3
XMMXCS J030145.5+000335.8	$0.256^{+0.090}_{-0.093}$	0.292 ± 0.078	-	-0.063 ± 0.045	2.650 ± 0.843	0.001	1 ± 1	0 ± 1	0 ± 0.1	-	3
XMMXCS J030159.3-000216.5	$0.454^{+0.139}_{-0.138}$	0.621 ± 0.163	-	-0.084 ± 0.042	2.450 ± 0.843	0.060	6 ± 3	5 ± 3	1 ± 2	1 ± 2	3
XMMXCS J030204.3+001626.6	$0.360^{+0.208}_{-0.221}$	0.408 ± 0.338	-	0.617 ± 0.197	-11.80 ± 4.010	0.127	1 ± 2	0 ± 2	0 ± 0.1	-	3
XMMXCS J030205.1-000003.6	$0.593^{+0.147}_{-0.147}$	0.647 ± 0.115	-	-0.021 ± 0.139	1.620 ± 2.840	0.119	12 ± 4	39 ± 7	12 ± 4	56 ± 9	3
XMMXCS J030206.7-000121.5	$0.516^{+0.172}_{-0.172}$	0.358 ± 0.053	-	0.279 ± 0.192	-4.710 ± 3.880	0.116	12 ± 4	35 ± 6	12 ± 4	20 ± 6	3
XMMXCS J030211.4-000134.3	$0.403^{+0.132}_{-0.131}$	0.249 ± 0.164	-	0.522 ± 0.209	-9.200 ± 4.170	0.211	13 ± 4	82 ± 9	14 ± 5	-	3
XMMXCS J030244.7+002149.7	$0.416^{+0.126}_{-0.117}$	0.512 ± 0.082	$0.379 \pm 3.7e-05$	-0.159 ± 0.166	4.300 ± 3.360	0.150	6 ± 4	6 ± 4	0 ± 2	-	3
XMMXCS J030401.0-010655.3	$0.429^{+0.125}_{-0.117}$	0.198 ± 0.068	$0.356 \pm 5.4e-05$	0.195 ± 0.173	-3.030 ± 3.500	0.164	0 ± 2	2 ± 3	-	0 ± 1	3
XMMXCS J030433.9-005406.9	$0.560^{+0.137}_{-0.136}$	0.614 ± 0.110	$0.703 \pm 1.7e-04$	-0.262 ± 0.063	6.310 ± 1.260	0.001	8 ± 3	42 ± 7	8 ± 3	-	3

Continued on next page

Table A.2 – continued from previous page

name	z_{RS}	z_{BCG}	z_{spec-g}	cmr_{grad}	cmr_{inter}	cmr_{wid}	n_{gals-c}	n_{gals-l}	n_{200-c}	n_{200-l}	qual
XMMXCS J030436.5-005506.8	$0.394^{+0.074}_{-0.075}$	0.375 ± 0.056	-	0.013 ± 0.045	1.580 ± 0.900	0.001	3 ± 2	4 ± 3	0 ± 1	2 ± 2	3
XMMXCS J030542.7-001145.1	$0.117^{+0.049}_{-0.049}$	0.082 ± 0.035	$0.079 \pm 1.3e-05$	-0.058 ± 0.038	1.880 ± 0.611	0.500	8 ± 4	13 ± 4	6 ± 3	12 ± 4	3
XMMXCS J030551.0-000557.4	$0.116^{+0.033}_{-0.035}$	0.119 ± 0.019	$0.107 \pm 1.9e-05$	-0.022 ± 0.020	1.330 ± 0.344	0.052	2 ± 2	1 ± 1	0 ± 0.1	1 ± 1	3
XMMXCS J030614.0-000540.2	$0.436^{+0.068}_{-0.062}$	0.399 ± 0.063	$0.425 \pm 1.1e-04$	0.004 ± 0.033	1.630 ± 0.634	0.001	1 ± 3	1 ± 3	0 ± 0.1	-	3
XMMXCS J030615.7+001254.7	$0.137^{+0.035}_{-0.037}$	0.062 ± 0.015	$0.112 \pm 1.3e-05$	-0.022 ± 0.060	1.210 ± 1.020	0.126	1 ± 2	3 ± 2	0 ± 0.1	2 ± 2	3
XMMXCS J030626.7+001307.0	$0.155^{+0.001}_{-0.001}$	0.161 ± 0.027	$0.156 \pm 2.3e-05$	-0.094 ± 0.005	2.760 ± 0.083	0.001	1 ± 1	0 ± 1	1 ± 1	-	3
XMMXCS J030631.7+000113.0	$0.316^{+0.090}_{-0.089}$	0.237 ± 0.036	$0.236 \pm 4.3e-05$	0.025 ± 0.055	0.994 ± 1.050	0.111	8 ± 3	5 ± 3	6 ± 3	1 ± 2	3
XMMXCS J030659.8+000824.9	$0.204^{+0.085}_{-0.093}$	0.082 ± 0.019	$0.119 \pm 1.6e-05$	0.042 ± 0.062	0.458 ± 1.160	0.118	4 ± 3	4 ± 3	3 ± 2	4 ± 2	3
XMMXCS J030800.3+404654.7	$0.522^{+0.178}_{-0.163}$	0.374 ± 0.063	-	0.584 ± 0.439	-10.90 ± 8.990	0.045	1 ± 2	3 ± 2	1 ± 1	0 ± 1	3
XMMXCS J031357.5+411522.8	$0.180^{+0.081}_{-0.086}$	0.136 ± 0.023	-	0.026 ± 0.039	0.629 ± 0.695	0.084	1 ± 2	4 ± 3	-	2 ± 2	3
XMMXCS J031627.1+413209.9	$0.357^{+0.088}_{-0.085}$	0.421 ± 0.325	-	-0.117 ± 0.053	2.970 ± 1.080	0.092	3 ± 3	5 ± 3	0 ± 1	1 ± 2	3
XMMXCS J031842.1+414208.4	$0.224^{+0.097}_{-0.103}$	0.097 ± 0.050	-	0.043 ± 0.034	0.323 ± 0.610	0.088	2 ± 2	11 ± 4	0 ± 0.1	3 ± 3	3
XMMXCS J032031.8+413045.8	$0.293^{+0.124}_{-0.122}$	0.424 ± 0.100	-	-0.143 ± 0.097	4.170 ± 1.970	0.169	6 ± 3	11 ± 4	3 ± 2	10 ± 4	3
XMMXCS J032041.6+414414.3	$0.206^{+0.103}_{-0.107}$	0.108 ± 0.024	-	0.009 ± 0.036	0.986 ± 0.704	0.124	9 ± 3	13 ± 4	9 ± 3	14 ± 4	3
XMMXCS J032050.2+414322.3	$0.124^{+0.088}_{-0.084}$	0.054 ± 0.025	$0.017 \pm 4.9e-06$	-0.001 ± 0.064	0.998 ± 1.080	0.106	4 ± 3	10 ± 4	5 ± 2	10 ± 4	3
XMMXCS J032103.0+411802.4	$0.194^{+0.062}_{-0.066}$	0.217 ± 0.038	-	-0.007 ± 0.046	1.380 ± 0.901	0.086	0 ± 1	1 ± 2	-	1 ± 1	3
XMMXCS J032118.3+412046.2	$0.113^{+0.082}_{-0.091}$	0.058 ± 0.018	$0.021 \pm 8.9e-06$	0.042 ± 0.036	0.070 ± 0.634	0.053	4 ± 2	5 ± 3	1 ± 1	2 ± 2	3
XMMXCS J032133.5+414746.9	$0.154^{+0.071}_{-0.073}$	0.070 ± 0.022	$0.019 \pm 7.5e-06$	0.006 ± 0.040	0.941 ± 0.740	0.108	3 ± 2	0 ± 2	1 ± 1	-	3
XMMXCS J032133.6+415612.2	$0.140^{+0.059}_{-0.060}$	0.059 ± 0.030	$0.010 \pm 5.4e-06$	-0.084 ± 0.001	2.420 ± 0.017	0.500	7 ± 4	17 ± 6	7 ± 3	14 ± 6	3

Continued on next page

Table A.2 – continued from previous page

name	z_{RS}	z_{BCG}	z_{spec-g}	cmr_{grad}	cmr_{inter}	cmr_{wid}	n_{gals-c}	n_{gals-l}	n_{200-c}	n_{200-l}	qual
XMMXCS J032455.3-055931.1	$0.222^{+0.081}_{-0.093}$	0.086 ± 0.016	$0.085 \pm 2.1e-05$	0.124 ± 0.077	-0.999 ± 1.460	0.098	5 ± 3	5 ± 3	3 ± 2	2 ± 2	3
XMMXCS J032511.7-061051.8	$0.103^{+0.047}_{-0.048}$	0.088 ± 0.042	$0.101 \pm 1.6e-05$	0.074 ± 0.005	-0.261 ± 0.068	0.001	3 ± 2	3 ± 2	1 ± 1	1 ± 1	3
XMMXCS J032609.0-061603.6	$0.469^{+0.110}_{-0.091}$	0.442 ± 0.068	-	-0.009 ± 0.037	0.804 ± 0.731	0.100	1 ± 3	4 ± 3	0 ± 1	2 ± 2	3
XMMXCS J033557.4+003417.8	$0.254^{+0.078}_{-0.080}$	0.297 ± 0.045	$0.305 \pm 5.3e-05$	-0.110 ± 0.026	3.510 ± 0.473	0.001	1 ± 2	3 ± 2	1 ± 1	1 ± 2	3
XMMXCS J033622.0+004416.3	$0.217^{+0.056}_{-0.058}$	0.098 ± 0.026	$0.109 \pm 1.5e-05$	-0.000 ± 0.001	1.540 ± 0.001	0.500	1 ± 3	0 ± 3	3 ± 2	-	3
XMMXCS J033740.7+004350.3	$0.682^{+0.144}_{-0.136}$	0.607 ± 0.129	$0.623 \pm 1.4e-04$	0.255 ± 0.166	-3.960 ± 3.390	0.140	2 ± 2	16 ± 5	1 ± 1	37 ± 7	3
XMMXCS J033753.8+001832.0	$0.525^{+0.125}_{-0.120}$	0.423 ± 0.067	$0.430 \pm 1.1e-04$	0.020 ± 0.137	0.334 ± 2.790	0.096	7 ± 3	38 ± 7	8 ± 3	51 ± 9	3
XMMXCS J033753.8+001831.5	$0.525^{+0.125}_{-0.120}$	0.423 ± 0.067	$0.430 \pm 1.1e-04$	0.020 ± 0.137	0.334 ± 2.790	0.096	7 ± 3	38 ± 7	8 ± 3	51 ± 9	3
XMMXCS J040727.9-120511.5	$0.472^{+0.136}_{-0.128}$	0.507 ± 0.080	-	-0.147 ± 0.090	3.740 ± 1.740	0.500	17 ± 5	20 ± 5	23 ± 6	30 ± 7	3
XMMXCS J042505.9-083954.6	$0.195^{+0.071}_{-0.072}$	0.190 ± 0.034	-	0.184 ± 0.146	-1.970 ± 2.570	0.161	8 ± 3	9 ± 4	9 ± 3	10 ± 4	3
XMMXCS J042602.3-084129.4	$0.417^{+0.161}_{-0.161}$	0.405 ± 0.066	-	-0.140 ± 0.154	3.990 ± 3.110	0.042	8 ± 4	-	5 ± 3	-	3
XMMXCS J042602.8-084219.1	$0.660^{+0.192}_{-0.213}$	0.568 ± 0.095	-	0.929 ± 0.371	-17.50 ± 7.470	0.188	3 ± 2	22 ± 5	1 ± 1	150 ± 12	3
XMMXCS J042603.8-084330.4	$0.600^{+0.233}_{-0.239}$	0.568 ± 0.095	-	1.080 ± 0.476	-20.50 ± 9.660	0.321	0 ± 1	7 ± 3	-	7 ± 3	3
XMMXCS J043127.1-051933.9	$0.473^{+0.151}_{-0.161}$	0.308 ± 0.049	-	0.030 ± 0.112	0.043 ± 2.200	0.001	1 ± 3	1 ± 3	1 ± 1	0 ± 1	3
XMMXCS J043709.7+004349.0	$0.276^{+0.062}_{-0.062}$	0.220 ± 0.060	-	-0.008 ± 0.029	1.640 ± 0.566	0.081	31 ± 6	28 ± 6	54 ± 8	50 ± 8	3
XMMXCS J044723.3-061609.0	$0.419^{+0.123}_{-0.114}$	0.337 ± 0.053	-	0.132 ± 0.077	-1.330 ± 1.560	0.152	3 ± 3	-	1 ± 2	-	3
XMMXCS J044739.4-063647.4	$0.253^{+0.077}_{-0.072}$	0.151 ± 0.024	-	0.075 ± 0.039	-0.190 ± 0.714	0.110	1 ± 2	1 ± 3	0 ± 0.1	0 ± 1	3
XMMXCS J051552.7+010407.4	$0.163^{+0.071}_{-0.073}$	0.218 ± 0.053	-	-0.097 ± 0.038	2.930 ± 0.706	0.076	6 ± 3	4 ± 2	3 ± 2	1 ± 1	3
XMMXCS J051635.9-001806.7	$0.269^{+0.076}_{-0.080}$	0.332 ± 0.051	-	-0.131 ± 0.069	3.760 ± 1.350	0.132	3 ± 3	1 ± 3	0 ± 1	-	3

Continued on next page

Table A.2 – continued from previous page

name	z_{RS}	z_{BCG}	z_{spec-g}	cmr_{grad}	cmr_{inter}	cmr_{wid}	n_{gals-c}	n_{gals-l}	n_{200-c}	n_{200-l}	qual
XMMXCS J051638.8-001000.8	$0.467^{+0.097}_{-0.096}$	0.535 ± 0.118	-	-0.030 ± 0.072	1.550 ± 1.410	0.122	5 ± 3	7 ± 4	0 ± 1	2 ± 3	3
XMMXCS J051646.7-000154.9	$0.582^{+0.154}_{-0.154}$	0.523 ± 0.188	-	0.096 ± 0.055	-0.746 ± 1.060	0.124	6 ± 3	116 ± 11	4 ± 2	43 ± 11	3
XMMXCS J053727.8-024005.7	$0.196^{+0.075}_{-0.076}$	0.110 ± 0.030	-	0.047 ± 0.056	0.203 ± 0.957	0.039	7 ± 3	10 ± 4	4 ± 2	7 ± 3	3
XMMXCS J055432.4+461441.1	$0.117^{+0.037}_{-0.037}$	0.159 ± 0.044	-	-0.069 ± 0.021	2.070 ± 0.346	0.001	3 ± 2	4 ± 2	2 ± 1	1 ± 1	3
XMMXCS J055437.2+461440.5	$0.152^{+0.048}_{-0.048}$	0.165 ± 0.028	-	-0.055 ± 0.027	1.900 ± 0.478	0.065	3 ± 2	4 ± 2	0 ± 0.1	3 ± 2	3
XMMXCS J064010.9+822902.2	$0.420^{+0.090}_{-0.090}$	0.387 ± 0.059	-	-0.026 ± 0.051	2.330 ± 1.050	0.001	0 ± 2	1 ± 2	-	3 ± 2	3
XMMXCS J072028.4+660844.5	$0.227^{+0.092}_{-0.094}$	0.188 ± 0.051	-	-0.057 ± 0.158	2.200 ± 3.110	0.159	2 ± 1	0 ± 1	0 ± 0.1	-	3
XMMXCS J072949.3+370630.3	$0.592^{+0.073}_{-0.069}$	0.470 ± 0.075	$0.588 \pm 1.7e-04$	0.024 ± 0.070	0.435 ± 1.430	0.001	1 ± 2	-	1 ± 1	-	3
XMMXCS J073227.2+215654.7	$0.253^{+0.104}_{-0.114}$	0.150 ± 0.106	-	0.093 ± 0.064	-0.721 ± 1.250	0.140	2 ± 1	0 ± 1	0 ± 0.1	-	3
XMMXCS J073229.5+220038.7	$0.133^{+0.070}_{-0.076}$	0.128 ± 0.026	-	-0.020 ± 0.044	1.380 ± 0.753	0.094	1 ± 1	1 ± 2	0 ± 0.1	0 ± 1	3
XMMXCS J073241.7+215326.3	$0.232^{+0.103}_{-0.101}$	0.287 ± 0.046	-	0.006 ± 0.051	1.190 ± 0.953	0.124	5 ± 3	5 ± 3	1 ± 1	1 ± 2	3
XMMXCS J073249.2+220500.0	$0.527^{+0.165}_{-0.166}$	0.509 ± 0.093	-	0.365 ± 0.457	-6.570 ± 9.360	0.085	6 ± 3	1 ± 1	4 ± 2	0 ± 1	3
XMMXCS J073436.1+653606.8	$0.276^{+0.098}_{-0.097}$	0.169 ± 0.033	-	0.141 ± 0.151	-1.320 ± 2.990	0.065	1 ± 2	0 ± 2	0 ± 0.1	-	3
XMMXCS J073508.4+265134.8	$0.132^{+0.066}_{-0.069}$	0.072 ± 0.014	$0.073 \pm 1.3e-05$	0.159 ± 0.171	-2.400 ± 3.220	0.500	2 ± 2	2 ± 2	1 ± 1	1 ± 1	3
XMMXCS J073513.3+435748.5	$0.337^{+0.132}_{-0.133}$	0.230 ± 0.097	-	0.271 ± 0.154	-4.250 ± 3.010	0.139	0 ± 2	2 ± 3	-	4 ± 2	3
XMMXCS J073524.1+435311.5	$0.131^{+0.034}_{-0.034}$	0.147 ± 0.032	$0.191 \pm 2.8e-05$	0.007 ± 0.056	0.868 ± 1.040	0.090	7 ± 3	6 ± 3	6 ± 3	5 ± 2	3
XMMXCS J073528.1+434434.4	$0.565^{+0.099}_{-0.091}$	0.382 ± 0.102	-	0.543 ± 0.376	-9.910 ± 7.500	0.204	3 ± 2	6 ± 4	0 ± 1	2 ± 2	3
XMMXCS J073542.3+653104.5	$0.501^{+0.087}_{-0.084}$	0.482 ± 0.071	-	-0.029 ± 0.043	1.460 ± 0.820	0.001	2 ± 2	2 ± 3	0 ± 1	0 ± 1	3
XMMXCS J073603.8+433252.9	$0.342^{+0.105}_{-0.113}$	0.255 ± 0.049	-	-0.185 ± 0.056	5.090 ± 1.120	0.106	6 ± 3	19 ± 5	1 ± 2	16 ± 5	3

Continued on next page

Table A.2 – continued from previous page

name	z_{RS}	z_{BCG}	z_{spec-g}	cmr_{grad}	cmr_{inter}	cmr_{wid}	n_{gals-c}	n_{gals-l}	n_{200-c}	n_{200-l}	qual
XMMXCS J073631.2+654812.3	$0.252^{+0.047}_{-0.048}$	0.283 ± 0.053	-	-0.046 ± 0.011	2.320 ± 0.208	0.001	3 ± 2	1 ± 2	3 ± 2	0 ± 1	3
XMMXCS J073709.7+653942.0	$0.187^{+0.073}_{-0.092}$	0.103 ± 0.077	-	-0.043 ± 0.001	0.850 ± 0.008	0.500	1 ± 1	0 ± 1	0 ± 0.1	-	3
XMMXCS J073859.0+654455.0	$0.367^{+0.069}_{-0.063}$	0.299 ± 0.109	-	0.034 ± 0.034	0.785 ± 0.621	0.084	0 ± 2	1 ± 3	-	0 ± 1	3
XMMXCS J073903.4+653147.2	$0.229^{+0.057}_{-0.057}$	0.193 ± 0.037	-	0.078 ± 0.038	-0.255 ± 0.695	0.116	1 ± 2	1 ± 2	0 ± 0.1	1 ± 1	3
XMMXCS J074218.7+493727.1	$0.231^{+0.070}_{-0.073}$	0.215 ± 0.037	$0.218 \pm 4.2e-05$	0.046 ± 0.108	0.328 ± 2.150	0.114	2 ± 2	2 ± 2	0 ± 0.1	0 ± 1	3
XMMXCS J074344.3+645646.7	$0.436^{+0.087}_{-0.085}$	0.424 ± 0.065	-	0.074 ± 0.034	-0.723 ± 0.680	0.001	8 ± 3	8 ± 4	8 ± 3	8 ± 3	3
XMMXCS J074603.6+305244.5	$0.223^{+0.063}_{-0.064}$	0.213 ± 0.039	$0.224 \pm 2.8e-05$	-0.023 ± 0.030	1.780 ± 0.581	0.074	3 ± 2	3 ± 3	0 ± 1	2 ± 2	3
XMMXCS J074713.1+305228.2	$0.283^{+0.105}_{-0.114}$	0.216 ± 0.039	-	0.079 ± 0.073	-0.134 ± 1.360	0.091	8 ± 3	6 ± 3	5 ± 3	5 ± 3	3
XMMXCS J075122.0+501200.0	$0.091^{+0.027}_{-0.027}$	0.065 ± 0.019	$0.022 \pm 6.3e-06$	-0.034 ± 0.007	1.260 ± 0.122	0.082	13 ± 4	8 ± 3	13 ± 4	9 ± 3	3
XMMXCS J075145.6+144707.0	$0.344^{+0.115}_{-0.115}$	0.373 ± 0.055	$0.405 \pm 7.6e-05$	-0.235 ± 0.400	6.220 ± 8.110	0.145	7 ± 3	9 ± 4	4 ± 2	8 ± 3	3
XMMXCS J080440.9+645436.5	$0.290^{+0.072}_{-0.072}$	0.346 ± 0.185	-	0.070 ± 0.096	0.087 ± 1.900	0.103	2 ± 2	2 ± 2	0 ± 0.1	0 ± 1	3
XMMXCS J080549.7+244949.6	$0.513^{+0.105}_{-0.108}$	0.444 ± 0.107	-	-0.043 ± 0.050	1.910 ± 1.020	0.001	2 ± 2	0 ± 1	1 ± 1	-	3
XMMXCS J080604.3+152707.5	$0.278^{+0.094}_{-0.095}$	0.093 ± 0.022	-	0.044 ± 0.048	0.361 ± 0.925	0.120	4 ± 3	5 ± 3	0 ± 1	1 ± 2	3
XMMXCS J080613.6+153053.0	$0.095^{+0.019}_{-0.020}$	0.101 ± 0.018	$0.095 \pm 1.2e-05$	0.016 ± 0.001	0.502 ± 0.001	0.500	0 ± 2	2 ± 2	-	3 ± 2	3
XMMXCS J080616.5+153115.9	$0.095^{+0.031}_{-0.031}$	0.101 ± 0.018	$0.095 \pm 1.2e-05$	-0.000 ± 0.001	0.785 ± 0.001	0.500	0 ± 2	2 ± 2	-	3 ± 2	3
XMMXCS J080625.5+152752.0	$0.303^{+0.075}_{-0.076}$	0.248 ± 0.039	-	0.040 ± 0.059	0.809 ± 1.130	0.021	4 ± 2	5 ± 3	2 ± 2	0 ± 1	3
XMMXCS J080628.9+151847.8	$0.527^{+0.092}_{-0.090}$	0.515 ± 0.081	$0.525 \pm 2.7e-04$	0.042 ± 0.060	0.117 ± 1.200	0.093	5 ± 3	17 ± 5	0 ± 1	20 ± 5	3
XMMXCS J080633.1+151550.4	$0.527^{+0.076}_{-0.068}$	0.506 ± 0.077	$0.514 \pm 8.8e-05$	-0.204 ± 0.030	4.840 ± 0.574	0.031	3 ± 3	47 ± 7	0 ± 1	1 ± 5	3
XMMXCS J080641.8+151817.4	$0.371^{+0.122}_{-0.123}$	0.284 ± 0.059	-	-0.076 ± 0.052	2.080 ± 1.020	0.069	3 ± 3	11 ± 4	3 ± 2	1 ± 3	3

Continued on next page

Table A.2 – continued from previous page

name	z_{RS}	z_{BCG}	z_{spec-g}	cmr_{grad}	cmr_{inter}	cmr_{wid}	n_{gals-c}	n_{gals-l}	n_{200-c}	n_{200-l}	qual
XMMXCS J080651.9+153219.8	$0.370^{+0.145}_{-0.145}$	0.214 ± 0.063	-	-0.166 ± 0.079	4.570 ± 1.540	0.097	2 ± 3	3 ± 3	0 ± 1	1 ± 2	3
XMMXCS J081004.6+501742.1	$0.250^{+0.075}_{-0.087}$	0.183 ± 0.033	-	0.046 ± 0.082	0.629 ± 1.570	0.153	1 ± 2	-	1 ± 1	-	3
XMMXCS J081012.7+495914.9	$0.120^{+0.030}_{-0.030}$	0.123 ± 0.023	$0.120 \pm 3.0e-05$	-0.206 ± 0.079	4.490 ± 1.370	0.081	1 ± 1	1 ± 2	2 ± 1	0 ± 1	3
XMMXCS J081035.6+275734.4	$0.432^{+0.118}_{-0.120}$	0.289 ± 0.092	-	-0.046 ± 0.086	2.520 ± 1.700	0.086	6 ± 4	7 ± 4	2 ± 2	3 ± 3	3
XMMXCS J081103.1+480840.4	$0.458^{+0.103}_{-0.091}$	0.365 ± 0.066	-	0.185 ± 0.086	-2.910 ± 1.690	0.500	3 ± 4	8 ± 5	2 ± 2	3 ± 3	3
XMMXCS J081938.4+210647.0	$0.048^{+0.032}_{-0.043}$	0.071 ± 0.042	$0.018 \pm 1.3e-05$	0.002 ± 0.016	0.781 ± 0.209	0.039	5 ± 2	3 ± 2	3 ± 2	0 ± 1	3
XMMXCS J082025.8+210844.6	$0.076^{+0.041}_{-0.040}$	0.044 ± 0.016	$0.072 \pm 1.1e-05$	0.021 ± 0.006	0.588 ± 0.084	0.030	2 ± 2	0 ± 2	3 ± 2	-	3
XMMXCS J082258.0+404537.5	$0.249^{+0.064}_{-0.067}$	0.266 ± 0.042	$0.260 \pm 4.6e-05$	-0.010 ± 0.037	1.670 ± 0.695	0.098	4 ± 2	5 ± 3	0 ± 1	3 ± 2	3
XMMXCS J082351.5-045454.3	$0.527^{+0.141}_{-0.140}$	0.588 ± 0.192	-	-0.005 ± 0.047	1.030 ± 0.943	0.047	6 ± 3	14 ± 4	6 ± 3	11 ± 4	3
XMMXCS J082432.6+294754.7	$0.205^{+0.073}_{-0.076}$	0.211 ± 0.033	$0.209 \pm 3.8e-05$	-0.027 ± 0.045	1.730 ± 0.817	0.102	1 ± 2	2 ± 2	0 ± 0.1	1 ± 2	3
XMMXCS J082640.3+263113.5	$0.262^{+0.108}_{-0.116}$	0.175 ± 0.109	$0.182 \pm 2.7e-05$	0.035 ± 0.114	0.435 ± 2.220	0.500	10 ± 4	9 ± 4	9 ± 4	7 ± 4	3
XMMXCS J082805.1+500750.8	$0.203^{+0.084}_{-0.085}$	0.398 ± 0.283	-	-0.050 ± 0.096	2.130 ± 1.870	0.132	0 ± 1	1 ± 2	-	2 ± 2	3
XMMXCS J082902.4+495524.9	$0.332^{+0.095}_{-0.090}$	0.284 ± 0.127	-	0.064 ± 0.157	-0.059 ± 3.110	0.001	1 ± 2	1 ± 2	0 ± 0.1	0 ± 1	3
XMMXCS J083025.9+524128.4	$0.499^{+0.085}_{-0.087}$	0.351 ± 0.100	$0.501 \pm 1.7e-04$	0.604 ± 0.159	-11.30 ± 3.250	0.119	2 ± 3	11 ± 4	0 ± 1	16 ± 5	3
XMMXCS J083026.0+524126.8	$0.498^{+0.086}_{-0.087}$	0.351 ± 0.100	$0.501 \pm 1.7e-04$	0.604 ± 0.159	-11.30 ± 3.250	0.119	1 ± 2	15 ± 5	0 ± 0.1	15 ± 5	3
XMMXCS J083207.9+524744.5	$0.639^{+0.155}_{-0.155}$	0.543 ± 0.091	-	0.331 ± 0.179	-5.790 ± 3.620	0.139	1 ± 2	8 ± 4	1 ± 1	11 ± 4	3
XMMXCS J083208.0+525544.8	$0.238^{+0.107}_{-0.115}$	0.231 ± 0.050	-	-0.086 ± 0.211	2.970 ± 4.260	0.001	1 ± 1	2 ± 2	0 ± 0.1	1 ± 1	3
XMMXCS J083234.1+523417.2	$0.663^{+0.154}_{-0.145}$	0.573 ± 0.191	-	-0.360 ± 0.194	7.840 ± 4.010	0.001	3 ± 2	59 ± 8	1 ± 1	14 ± 9	3
XMMXCS J083234.1+525726.2	$0.370^{+0.096}_{-0.095}$	0.295 ± 0.046	-	-0.027 ± 0.359	2.150 ± 7.330	0.087	2 ± 3	2 ± 3	2 ± 2	2 ± 2	3

Continued on next page

Table A.2 – continued from previous page

name	z_{RS}	z_{BCG}	z_{spec-g}	cmr_{grad}	cmr_{inter}	cmr_{wid}	n_{gals-c}	n_{gals-l}	n_{200-c}	n_{200-l}	qual
XMMXCS J083234.3+523418.9	$0.664^{+0.153}_{-0.145}$	0.573 ± 0.191	-	-0.360 ± 0.194	7.840 ± 4.010	0.001	3 ± 2	59 ± 8	1 ± 1	13 ± 9	3
XMMXCS J083237.9+524646.5	$0.462^{+0.156}_{-0.203}$	0.518 ± 0.228	-	-0.688 ± 0.001	14.700 ± 0.025	0.500	8 ± 4	5 ± 4	7 ± 4	13 ± 4	3
XMMXCS J083459.0+250928.7	$0.389^{+0.114}_{-0.102}$	0.318 ± 0.057	-	-0.104 ± 0.102	3.250 ± 2.100	0.500	3 ± 4	4 ± 4	2 ± 2	2 ± 3	3
XMMXCS J083516.6+251143.1	$0.189^{+0.062}_{-0.061}$	0.138 ± 0.022	$0.132 \pm 1.8e-05$	0.078 ± 0.001	-0.305 ± 0.001	0.500	8 ± 4	6 ± 4	6 ± 3	3 ± 3	3
XMMXCS J083524.2+553607.2	$0.242^{+0.065}_{-0.065}$	0.227 ± 0.087	-	-0.003 ± 0.032	1.410 ± 0.600	0.082	1 ± 2	2 ± 2	0 ± 0.1	1 ± 1	3
XMMXCS J083534.1+244718.1	$0.346^{+0.073}_{-0.075}$	0.311 ± 0.050	-	0.013 ± 0.058	1.370 ± 1.170	0.001	2 ± 2	-	0 ± 0.1	-	3
XMMXCS J083622.9+250507.3	$0.173^{+0.056}_{-0.058}$	0.075 ± 0.031	$0.078 \pm 1.8e-05$	0.021 ± 0.116	0.572 ± 2.210	0.500	3 ± 3	9 ± 4	1 ± 1	-	3
XMMXCS J083737.0+255151.5	$0.145^{+0.068}_{-0.078}$	0.121 ± 0.033	$0.092 \pm 1.4e-05$	0.118 ± 0.001	-0.986 ± 0.001	0.500	0 ± 2	3 ± 3	-	3 ± 2	3
XMMXCS J083743.5+145235.6	$0.270^{+0.069}_{-0.070}$	0.340 ± 0.056	-	-0.073 ± 0.064	2.920 ± 1.210	0.063	10 ± 3	10 ± 4	7 ± 3	7 ± 3	3
XMMXCS J083810.8+250552.4	$0.419^{+0.075}_{-0.060}$	0.345 ± 0.053	$0.379 \pm 8.4e-05$	-0.027 ± 0.047	1.050 ± 0.924	0.085	0 ± 3	4 ± 4	-	5 ± 3	3
XMMXCS J083823.8+254617.1	$0.136^{+0.156}_{-0.136}$	0.052 ± 0.024	$0.052 \pm 1.1e-05$	0.007 ± 0.017	0.638 ± 0.251	0.118	2 ± 2	1 ± 3	0 ± 0.1	0 ± 1	3
XMMXCS J083855.9+253803.9	$0.169^{+0.074}_{-0.076}$	0.064 ± 0.025	-	0.337 ± 0.062	-5.220 ± 1.140	0.059	1 ± 1	2 ± 2	1 ± 1	0 ± 1	3
XMMXCS J083859.7+484816.7	$0.271^{+0.077}_{-0.068}$	0.187 ± 0.042	-	0.046 ± 0.081	0.399 ± 1.550	0.155	1 ± 2	-	1 ± 1	-	3
XMMXCS J083947.5+300100.6	$0.146^{+0.045}_{-0.029}$	0.073 ± 0.018	$0.134 \pm 1.3e-05$	-0.019 ± 0.002	1.550 ± 0.039	0.500	1 ± 2	4 ± 3	0 ± 0.1	2 ± 2	3
XMMXCS J084001.1+385013.0	$0.160^{+0.064}_{-0.064}$	0.217 ± 0.044	-	-0.214 ± 0.110	5.010 ± 2.140	0.500	1 ± 2	-	0 ± 0.1	-	3
XMMXCS J084004.6+294546.1	$0.459^{+0.167}_{-0.166}$	0.587 ± 0.123	$0.564 \pm 1.2e-04$	-0.135 ± 0.057	3.670 ± 1.130	0.001	7 ± 3	5 ± 3	6 ± 3	3 ± 2	3
XMMXCS J084018.9+293733.2	$0.270^{+0.070}_{-0.059}$	0.084 ± 0.017	$0.077 \pm 2.3e-05$	-0.006 ± 0.027	1.040 ± 0.490	0.093	0 ± 2	1 ± 3	-	5 ± 2	3
XMMXCS J084036.0+511838.7	$0.495^{+0.116}_{-0.103}$	0.332 ± 0.109	-	0.136 ± 0.059	-2.060 ± 1.180	0.116	2 ± 3	4 ± 4	1 ± 1	2 ± 2	3
XMMXCS J084048.2+194007.3	$0.598^{+0.162}_{-0.166}$	0.634 ± 0.148	-	0.244 ± 0.208	-3.960 ± 4.180	0.001	1 ± 2	4 ± 3	-	7 ± 3	3

Continued on next page

Table A.2 – continued from previous page

name	z_{RS}	z_{BCG}	z_{spec-g}	cmr_{grad}	cmr_{inter}	cmr_{wid}	n_{gals-c}	n_{gals-l}	n_{200-c}	n_{200-l}	qual
XMMXCS J084128.5+383137.9	$0.291^{+0.108}_{-0.108}$	0.205 ± 0.046	-	0.018 ± 0.053	0.970 ± 1.020	0.112	7 ± 3	8 ± 4	7 ± 3	7 ± 3	3
XMMXCS J084141.6+544314.5	$0.401^{+0.111}_{-0.103}$	0.236 ± 0.098	$0.403 \pm 6.9e-05$	0.021 ± 0.031	0.236 ± 0.603	0.061	5 ± 3	8 ± 4	0 ± 2	-	3
XMMXCS J084313.1+544942.6	$0.263^{+0.143}_{-0.151}$	0.086 ± 0.028	-	0.042 ± 0.061	0.193 ± 1.230	0.136	2 ± 2	4 ± 3	0 ± 0.1	0 ± 2	3
XMMXCS J084551.7+184847.6	$0.401^{+0.097}_{-0.097}$	0.369 ± 0.056	-	-0.070 ± 0.062	3.120 ± 1.200	0.001	5 ± 3	5 ± 3	0 ± 1	1 ± 2	3
XMMXCS J084604.9+185524.3	$0.370^{+0.129}_{-0.130}$	0.294 ± 0.055	-	0.084 ± 0.048	-0.991 ± 0.934	0.001	0 ± 2	1 ± 2	-	1 ± 1	3
XMMXCS J084626.9+344908.5	$0.355^{+0.193}_{-0.205}$	0.245 ± 0.089	-	0.107 ± 0.037	-1.530 ± 0.735	0.074	0 ± 2	1 ± 3	-	1 ± 1	3
XMMXCS J084631.0+184022.0	$0.367^{+0.058}_{-0.056}$	0.360 ± 0.054	$0.366 \pm 7.8e-05$	-0.021 ± 0.012	0.969 ± 0.227	0.001	2 ± 3	0 ± 3	0 ± 1	-	3
XMMXCS J084637.8+185458.2	$0.511^{+0.134}_{-0.131}$	0.547 ± 0.088	-	0.030 ± 0.059	0.279 ± 1.220	0.115	2 ± 2	1 ± 3	0 ± 1	-	3
XMMXCS J084706.6+344426.9	$0.242^{+0.117}_{-0.117}$	0.194 ± 0.031	-	-0.072 ± 0.032	2.560 ± 0.634	0.122	0 ± 2	1 ± 2	-	0 ± 1	3
XMMXCS J084711.0+344845.2	$0.476^{+0.138}_{-0.137}$	0.578 ± 0.160	-	-0.050 ± 0.027	1.890 ± 0.529	0.110	25 ± 6	27 ± 6	38 ± 7	40 ± 8	3
XMMXCS J084711.2+344842.4	$0.477^{+0.137}_{-0.137}$	0.578 ± 0.160	-	-0.049 ± 0.028	1.880 ± 0.545	0.113	24 ± 5	25 ± 6	35 ± 7	38 ± 7	3
XMMXCS J084747.6+345323.9	$0.406^{+0.092}_{-0.091}$	0.482 ± 0.077	-	-0.065 ± 0.040	2.030 ± 0.801	0.025	16 ± 5	11 ± 4	18 ± 5	10 ± 4	3
XMMXCS J084748.4+345326.4	$0.406^{+0.091}_{-0.091}$	0.482 ± 0.077	-	-0.065 ± 0.040	2.030 ± 0.801	0.025	17 ± 5	12 ± 4	17 ± 5	11 ± 4	3
XMMXCS J084756.1+345517.3	$0.396^{+0.138}_{-0.138}$	0.529 ± 0.083	-	-0.344 ± 0.288	8.730 ± 5.870	0.001	6 ± 3	8 ± 3	4 ± 2	5 ± 3	3
XMMXCS J084858.28-020554.7	$0.415^{+0.114}_{-0.109}$	0.245 ± 0.084	-	0.333 ± 0.166	-5.300 ± 3.320	0.181	5 ± 3	3 ± 3	4 ± 3	4 ± 3	3
XMMXCS J085006.81-014943.0	$0.241^{+0.092}_{-0.100}$	0.074 ± 0.019	-	-0.042 ± 0.001	1.770 ± 0.002	0.500	3 ± 3	11 ± 5	1 ± 2	11 ± 5	3
XMMXCS J085009.8+444713.5	$0.204^{+0.071}_{-0.072}$	0.153 ± 0.054	-	0.198 ± 0.048	-2.820 ± 0.963	0.500	3 ± 2	2 ± 2	2 ± 1	1 ± 1	3
XMMXCS J085210.0+115530.0	$0.239^{+0.072}_{-0.075}$	0.336 ± 0.054	-	-0.030 ± 0.055	1.940 ± 1.070	0.079	1 ± 1	1 ± 1	0 ± 0.1	0 ± 1	3
XMMXCS J085220.69-011023.7	$0.404^{+0.091}_{-0.091}$	0.332 ± 0.061	-	-0.038 ± 0.298	2.110 ± 6.030	0.096	3 ± 3	4 ± 3	0 ± 1	2 ± 2	3

Continued on next page

Table A.2 – continued from previous page

name	z_{RS}	z_{BCG}	z_{spec-g}	cmr_{grad}	cmr_{inter}	cmr_{wid}	n_{gals-c}	n_{gals-l}	n_{200-c}	n_{200-l}	qual
XMMXCS J085301.38-015050.9	$0.506^{+0.170}_{-0.223}$	0.445 ± 0.264	-	-0.141 ± 0.061	3.610 ± 1.220	0.066	6 ± 3	7 ± 4	4 ± 2	-	3
XMMXCS J085307.9+180340.4	$0.290^{+0.101}_{-0.102}$	0.204 ± 0.044	-	0.005 ± 0.077	1.300 ± 1.530	0.128	4 ± 3	-	4 ± 2	-	3
XMMXCS J085317.6+174747.2	$0.102^{+0.022}_{-0.022}$	0.085 ± 0.029	$0.102 \pm 9.5e-06$	0.007 ± 0.051	0.518 ± 0.881	0.063	1 ± 1	0 ± 1	0 ± 0.1	-	3
XMMXCS J085319.14-014510.4	$0.559^{+0.145}_{-0.146}$	0.506 ± 0.084	-	0.045 ± 0.056	0.137 ± 1.110	0.086	9 ± 3	40 ± 7	9 ± 3	52 ± 8	3
XMMXCS J085339.2+150254.2	$0.271^{+0.203}_{-0.203}$	0.087 ± 0.017	$0.077 \pm 1.5e-05$	-0.016 ± 0.050	1.100 ± 0.937	0.001	5 ± 3	10 ± 4	1 ± 1	10 ± 4	3
XMMXCS J085451.4+195827.2	$0.464^{+0.098}_{-0.130}$	0.377 ± 0.126	-	0.004 ± 0.029	0.623 ± 0.573	0.106	5 ± 3	7 ± 4	1 ± 2	8 ± 4	3
XMMXCS J085512.1+200437.3	$0.264^{+0.093}_{-0.090}$	0.262 ± 0.112	-	0.080 ± 0.096	-0.373 ± 1.880	0.001	0 ± 1	1 ± 2	-	0 ± 1	3
XMMXCS J085530.0+200633.5	$0.241^{+0.114}_{-0.121}$	0.174 ± 0.046	$0.307 \pm 4.3e-05$	0.154 ± 0.110	-1.900 ± 2.130	0.153	1 ± 2	0 ± 2	1 ± 1	-	3
XMMXCS J085533.0+201439.4	$0.271^{+0.061}_{-0.062}$	0.214 ± 0.069	-	0.023 ± 0.065	0.924 ± 1.270	0.127	1 ± 2	2 ± 2	1 ± 1	1 ± 1	3
XMMXCS J085545.0+374500.7	$0.419^{+0.082}_{-0.078}$	0.425 ± 0.061	$0.412 \pm 1.7e-04$	0.027 ± 0.038	0.183 ± 0.735	0.073	6 ± 3	-	1 ± 2	-	3
XMMXCS J085643.21-005931.6	$0.232^{+0.067}_{-0.069}$	0.285 ± 0.095	-	-0.096 ± 0.045	3.130 ± 0.864	0.078	2 ± 2	1 ± 2	1 ± 1	0 ± 1	3
XMMXCS J085739.2+275250.4	$0.368^{+0.147}_{-0.137}$	0.233 ± 0.093	-	0.202 ± 0.172	-2.760 ± 3.390	0.144	7 ± 4	4 ± 3	5 ± 3	1 ± 2	3
XMMXCS J085750.9+275638.3	$0.419^{+0.100}_{-0.098}$	0.321 ± 0.049	-	0.668 ± 0.173	-11.00 ± 3.440	0.436	6 ± 3	6 ± 4	7 ± 3	7 ± 3	3
XMMXCS J085757.4+274539.7	$0.430^{+0.158}_{-0.151}$	0.432 ± 0.137	-	0.003 ± 0.043	1.250 ± 0.861	0.001	4 ± 3	3 ± 3	2 ± 2	1 ± 2	3
XMMXCS J085810.1+275051.6	$0.333^{+0.141}_{-0.138}$	0.268 ± 0.116	-	-0.112 ± 0.058	3.250 ± 1.140	0.001	3 ± 2	3 ± 3	1 ± 1	2 ± 2	3
XMMXCS J085815.0+274633.5	$0.323^{+0.078}_{-0.087}$	0.297 ± 0.045	-	0.022 ± 0.043	1.170 ± 0.813	0.001	1 ± 2	3 ± 3	0 ± 0.1	-	3
XMMXCS J085829.1+273630.8	$0.283^{+0.095}_{-0.095}$	0.192 ± 0.041	-	0.007 ± 0.160	1.250 ± 3.090	0.107	5 ± 3	5 ± 3	4 ± 2	6 ± 3	3
XMMXCS J085841.5+140943.6	$0.247^{+0.098}_{-0.093}$	0.131 ± 0.021	$0.114 \pm 2.3e-05$	-0.050 ± 0.001	2.420 ± 0.001	0.500	1 ± 3	1 ± 3	2 ± 1	2 ± 2	3
XMMXCS J085846.0+140905.3	$0.365^{+0.121}_{-0.125}$	0.268 ± 0.047	-	-0.059 ± 0.119	2.720 ± 2.430	0.001	8 ± 3	6 ± 3	7 ± 3	6 ± 3	3

Continued on next page

Table A.2 – continued from previous page

name	z_{RS}	z_{BCG}	z_{spec-g}	cmr_{grad}	cmr_{inter}	cmr_{wid}	n_{gals-c}	n_{gals-l}	n_{200-c}	n_{200-l}	qual
XMMXCS J085848.2+274933.0	$0.408^{+0.104}_{-0.100}$	0.332 ± 0.059	-	-0.638 ± 0.574	14.400 ± 11.50	0.500	17 ± 5	20 ± 6	15 ± 5	10 ± 5	3
XMMXCS J085908.9+170704.4	$0.228^{+0.107}_{-0.106}$	0.052 ± 0.016	$0.053 \pm 2.1e-05$	-0.000 ± 0.001	1.270 ± 0.001	0.500	3 ± 3	2 ± 3	2 ± 2	3 ± 2	3
XMMXCS J085911.8+275832.8	$0.241^{+0.104}_{-0.107}$	0.283 ± 0.047	$0.306 \pm 7.2e-05$	-0.135 ± 0.047	3.870 ± 0.946	0.001	3 ± 2	3 ± 2	0 ± 0.1	0 ± 1	3
XMMXCS J085930.7+170858.3	$0.326^{+0.051}_{-0.051}$	0.327 ± 0.052	$0.331 \pm 4.6e-05$	-0.074 ± 0.025	3.040 ± 0.466	0.001	0 ± 2	1 ± 2	-	2 ± 2	3
XMMXCS J090136.5+205446.0	$0.388^{+0.088}_{-0.083}$	0.366 ± 0.057	$0.403 \pm 5.8e-05$	-0.011 ± 0.025	0.860 ± 0.478	0.066	5 ± 3	5 ± 4	0 ± 1	-	3
XMMXCS J090137.37-015432.8	$0.338^{+0.077}_{-0.077}$	0.255 ± 0.043	-	-0.017 ± 0.069	1.890 ± 1.330	0.082	12 ± 4	12 ± 4	12 ± 4	12 ± 4	3
XMMXCS J090434.8+143539.2	$0.467^{+0.117}_{-0.110}$	0.391 ± 0.068	-	0.016 ± 0.123	0.420 ± 2.530	0.064	3 ± 3	4 ± 3	0 ± 1	-	3
XMMXCS J090435.3+144531.3	$0.277^{+0.082}_{-0.077}$	0.085 ± 0.022	-	0.0 ± -1.00	1.360 ± -1.00	0.500	3 ± 3	7 ± 4	4 ± 2	3 ± 3	3
XMMXCS J091008.3+541854.6	$0.274^{+0.092}_{-0.089}$	0.117 ± 0.025	-	-0.032 ± 0.057	1.590 ± 1.110	0.127	2 ± 2	1 ± 3	0 ± 0.1	0 ± 1	3
XMMXCS J091044.7+542200.2	$0.420^{+0.120}_{-0.118}$	0.279 ± 0.065	-	-0.127 ± 0.176	4.020 ± 3.580	0.001	2 ± 3	2 ± 3	0 ± 1	-	3
XMMXCS J091103.8+543425.7	$0.088^{+0.025}_{-0.032}$	0.054 ± 0.016	$0.046 \pm 1.0e-05$	0.025 ± 0.016	0.384 ± 0.270	0.500	1 ± 1	0 ± 1	0 ± 0.1	-	3
XMMXCS J091108.4+543745.1	$0.139^{+0.047}_{-0.047}$	0.190 ± 0.030	$0.183 \pm 2.1e-05$	-0.008 ± 0.200	1.140 ± 3.830	0.134	1 ± 2	0 ± 2	0 ± 0.1	-	3
XMMXCS J091120.1+453339.2	$0.210^{+0.106}_{-0.119}$	0.227 ± 0.046	$0.329 \pm 9.1e-05$	-0.270 ± 0.166	6.260 ± 3.250	0.500	0 ± 2	3 ± 3	-	1 ± 2	3
XMMXCS J091125.3+453534.3	$0.350^{+0.119}_{-0.109}$	0.227 ± 0.046	-	-0.000 ± 0.001	0.700 ± 0.001	0.500	6 ± 4	6 ± 4	1 ± 2	4 ± 3	3
XMMXCS J091435.4+405545.5	$0.331^{+0.052}_{-0.051}$	0.274 ± 0.058	-	-0.012 ± 0.036	1.840 ± 0.672	0.001	1 ± 1	-	1 ± 1	-	3
XMMXCS J091707.2+302421.4	$0.392^{+0.146}_{-0.150}$	0.320 ± 0.139	-	0.004 ± 0.135	0.551 ± 2.730	0.111	6 ± 4	5 ± 4	7 ± 3	8 ± 3	3
XMMXCS J091755.5+513250.4	$0.393^{+0.139}_{-0.114}$	0.278 ± 0.048	-	-0.030 ± 0.139	1.980 ± 2.720	0.096	2 ± 3	-	0 ± 1	-	3
XMMXCS J091819.4+211509.0	$0.201^{+0.077}_{-0.076}$	0.139 ± 0.041	$0.104 \pm 2.6e-05$	-0.159 ± 0.001	3.780 ± 0.001	0.500	1 ± 2	1 ± 2	1 ± 1	2 ± 2	3
XMMXCS J091836.8+515041.2	$0.357^{+0.103}_{-0.102}$	0.423 ± 0.062	$0.436 \pm 8.4e-05$	-0.023 ± 0.021	1.070 ± 0.426	0.052	10 ± 4	8 ± 4	8 ± 3	6 ± 3	3

Continued on next page

Table A.2 – continued from previous page

name	z_{RS}	z_{BCG}	z_{spec-g}	cmr_{grad}	cmr_{inter}	cmr_{wid}	n_{gals-c}	n_{gals-l}	n_{200-c}	n_{200-l}	qual
XMMXCS J091859.9+514734.8	$0.362^{+0.065}_{-0.061}$	0.380 ± 0.057	-	-0.640 ± 0.015	14.500 ± 0.319	0.500	10 ± 4	6 ± 4	7 ± 4	4 ± 3	3
XMMXCS J091911.9+303506.2	$0.338^{+0.181}_{-0.254}$	0.188 ± 0.075	-	0.055 ± 0.036	-0.095 ± 0.693	0.001	1 ± 2	4 ± 3	1 ± 1	0 ± 1	3
XMMXCS J091922.4+303332.8	$0.405^{+0.115}_{-0.106}$	0.437 ± 0.066	-	-0.015 ± 0.091	0.926 ± 1.830	0.086	6 ± 3	7 ± 4	0 ± 2	2 ± 2	3
XMMXCS J091922.5+303336.1	$0.405^{+0.115}_{-0.106}$	0.437 ± 0.066	-	-0.015 ± 0.091	0.926 ± 1.830	0.086	5 ± 3	-	0 ± 0.1	-	3
XMMXCS J091927.4+210823.5	$0.239^{+0.094}_{-0.094}$	0.221 ± 0.077	-	-0.200 ± 0.046	4.950 ± 0.903	0.001	0 ± 0.1	1 ± 1	-	0 ± 1	3
XMMXCS J091931.4+303911.2	$0.225^{+0.075}_{-0.078}$	0.198 ± 0.109	-	-0.030 ± 0.051	1.750 ± 1.010	0.121	2 ± 2	1 ± 2	0 ± 0.1	0 ± 1	3
XMMXCS J091935.4+304135.1	$0.224^{+0.071}_{-0.072}$	0.218 ± 0.042	-	-0.149 ± 0.092	4.160 ± 1.780	0.081	0 ± 1	1 ± 2	-	0 ± 1	3
XMMXCS J092041.8+372514.9	$0.652^{+0.117}_{-0.096}$	0.585 ± 0.103	$0.595 \pm 2.9e-04$	1.440 ± 2.050	-28.10 ± 42.30	0.500	1 ± 2	10 ± 4	-	12 ± 4	3
XMMXCS J092111.4+302653.8	$0.357^{+0.085}_{-0.084}$	0.422 ± 0.061	$0.429 \pm 9.7e-05$	0.057 ± 0.045	0.524 ± 0.885	0.115	26 ± 6	5 ± 3	40 ± 7	14 ± 4	3
XMMXCS J092119.3+371727.2	$0.474^{+0.086}_{-0.079}$	0.327 ± 0.051	$0.435 \pm 1.1e-04$	0.013 ± 0.060	0.569 ± 1.210	0.126	0 ± 2	13 ± 5	-	12 ± 5	3
XMMXCS J092122.6+301238.7	$0.398^{+0.145}_{-0.142}$	0.217 ± 0.034	-	0.069 ± 0.117	0.021 ± 2.260	0.115	13 ± 5	16 ± 5	13 ± 5	24 ± 6	3
XMMXCS J092206.1+302116.8	$0.575^{+0.131}_{-0.126}$	0.740 ± 0.127	-	-0.179 ± 0.121	4.640 ± 2.490	0.001	4 ± 3	8 ± 4	2 ± 2	7 ± 3	3
XMMXCS J092210.3+300355.6	$0.277^{+0.060}_{-0.061}$	0.213 ± 0.035	-	0.005 ± 0.043	1.410 ± 0.841	0.064	6 ± 3	6 ± 3	0 ± 1	0 ± 2	3
XMMXCS J092508.3+520535.6	$0.628^{+0.120}_{-0.109}$	0.553 ± 0.130	-	0.193 ± 0.131	-2.940 ± 2.700	0.001	0 ± 1	5 ± 2	-	0 ± 1	3
XMMXCS J092546.4+363539.6	$0.160^{+0.086}_{-0.087}$	0.105 ± 0.022	$0.111 \pm 2.3e-05$	0.038 ± 0.034	0.303 ± 0.615	0.069	1 ± 1	1 ± 1	0 ± 0.1	0 ± 1	3
XMMXCS J092546.5+363539.1	$0.160^{+0.086}_{-0.087}$	0.105 ± 0.022	$0.111 \pm 2.3e-05$	0.038 ± 0.034	0.303 ± 0.615	0.069	1 ± 1	1 ± 1	0 ± 0.1	0 ± 1	3
XMMXCS J092550.9+361241.3	$0.723^{+0.163}_{-0.203}$	0.647 ± 0.129	-	0.003 ± 0.070	1.070 ± 1.430	0.073	0 ± 1	4 ± 2	-	4 ± 2	3
XMMXCS J092626.3+304209.3	$0.620^{+0.165}_{-0.165}$	0.518 ± 0.087	-	0.109 ± 0.109	-1.120 ± 2.240	0.001	8 ± 3	10 ± 4	7 ± 3	11 ± 4	3
XMMXCS J092628.3+304445.8	$0.522^{+0.123}_{-0.124}$	0.620 ± 0.100	-	0.143 ± 0.159	-1.750 ± 3.160	0.155	4 ± 3	19 ± 5	2 ± 2	14 ± 5	3

Continued on next page

Table A.2 – continued from previous page

name	z_{RS}	z_{BCG}	z_{spec-g}	cmr_{grad}	cmr_{inter}	cmr_{wid}	n_{gals-c}	n_{gals-l}	n_{200-c}	n_{200-l}	qual
XMMXCS J092641.4+310308.8	$0.200^{+0.081}_{-0.081}$	0.263 ± 0.042	$0.279 \pm 8.6e-05$	-0.210 ± 0.099	5.180 ± 1.900	0.104	6 ± 3	5 ± 3	3 ± 2	0 ± 1	3
XMMXCS J092641.4+310308.9	$0.200^{+0.081}_{-0.081}$	0.263 ± 0.042	$0.279 \pm 8.6e-05$	-0.210 ± 0.099	5.180 ± 1.900	0.104	6 ± 3	5 ± 3	3 ± 2	0 ± 1	3
XMMXCS J092643.4+361211.9	$0.450^{+0.108}_{-0.105}$	0.352 ± 0.088	-	0.080 ± 0.135	-0.813 ± 2.720	0.060	5 ± 3	5 ± 3	2 ± 2	1 ± 2	3
XMMXCS J092703.2+310039.2	$0.519^{+0.099}_{-0.098}$	0.616 ± 0.121	-	-0.259 ± 0.032	6.150 ± 0.642	0.001	4 ± 3	8 ± 4	3 ± 2	10 ± 4	3
XMMXCS J092722.7+362706.0	$0.349^{+0.094}_{-0.093}$	0.272 ± 0.131	-	0.250 ± 0.123	-3.550 ± 2.420	0.001	3 ± 2	2 ± 2	3 ± 2	3 ± 2	3
XMMXCS J093201.0+472749.7	$0.213^{+0.063}_{-0.062}$	0.160 ± 0.077	-	0.025 ± 0.039	0.811 ± 0.665	0.500	3 ± 3	-	4 ± 2	-	3
XMMXCS J093350.2+552620.1	$0.533^{+0.146}_{-0.142}$	0.462 ± 0.142	-	-0.131 ± 0.124	3.430 ± 2.460	0.113	6 ± 3	-	5 ± 3	-	3
XMMXCS J093530.7+495430.7	$0.395^{+0.126}_{-0.123}$	0.248 ± 0.158	-	0.269 ± 0.273	-4.180 ± 5.600	0.107	5 ± 3	5 ± 3	3 ± 2	3 ± 2	3
XMMXCS J093551.8+551108.2	$0.447^{+0.132}_{-0.127}$	0.343 ± 0.084	-	0.381 ± 0.187	-6.990 ± 3.830	0.081	2 ± 3	-	1 ± 1	-	3
XMMXCS J093556.0+551254.1	$0.483^{+0.142}_{-0.140}$	0.285 ± 0.051	-	0.123 ± 0.094	-1.670 ± 1.900	0.091	3 ± 3	-	1 ± 1	-	3
XMMXCS J093608.1+613250.5	$0.177^{+0.076}_{-0.079}$	0.176 ± 0.028	-	-0.073 ± 0.036	2.450 ± 0.699	0.043	1 ± 1	0 ± 1	0 ± 0.1	-	3
XMMXCS J093608.1+613245.5	$0.164^{+0.066}_{-0.068}$	0.178 ± 0.061	-	-0.030 ± 0.035	1.460 ± 0.662	0.109	1 ± 2	1 ± 2	0 ± 0.1	0 ± 1	3
XMMXCS J093722.2+611416.7	$0.218^{+0.069}_{-0.072}$	0.211 ± 0.032	$0.208 \pm 4.0e-05$	0.032 ± 0.026	0.676 ± 0.503	0.110	5 ± 3	7 ± 3	0 ± 1	0 ± 2	3
XMMXCS J093951.3+355501.4	$0.358^{+0.135}_{-0.136}$	0.274 ± 0.062	-	0.013 ± 0.065	0.309 ± 1.320	0.107	4 ± 3	5 ± 4	1 ± 2	3 ± 3	3
XMMXCS J094019.5+034713.6	$0.535^{+0.119}_{-0.114}$	0.374 ± 0.135	$0.511 \pm 2.0e-04$	-0.125 ± 0.176	3.420 ± 3.670	0.093	5 ± 3	7 ± 4	0 ± 1	2 ± 3	3
XMMXCS J094035.1+032320.9	$0.569^{+0.165}_{-0.169}$	0.528 ± 0.117	-	0.076 ± 0.087	-0.548 ± 1.760	0.110	3 ± 2	-	0 ± 1	-	3
XMMXCS J094100.8+384915.8	$0.300^{+0.116}_{-0.115}$	0.240 ± 0.140	-	0.201 ± 0.029	-2.950 ± 0.556	0.001	2 ± 2	1 ± 2	0 ± 0.1	1 ± 1	3
XMMXCS J094100.9+385317.7	$0.229^{+0.107}_{-0.103}$	0.133 ± 0.028	-	0.043 ± 0.036	0.097 ± 0.712	0.088	2 ± 2	2 ± 2	0 ± 0.1	1 ± 1	3
XMMXCS J094106.8+145904.9	$0.165^{+0.053}_{-0.052}$	0.142 ± 0.031	-	-0.206 ± 0.044	4.690 ± 0.865	0.014	1 ± 1	0 ± 1	0 ± 0.1	-	3

Continued on next page

Table A.2 – continued from previous page

name	z_{RS}	z_{BCG}	z_{spec-g}	cmr_{grad}	cmr_{inter}	cmr_{wid}	n_{gals-c}	n_{gals-l}	n_{200-c}	n_{200-l}	qual
XMMXCS J094204.5+480449.8	$0.137^{+0.072}_{-0.075}$	0.038 ± 0.015	$0.103 \pm 2.2e-05$	-0.028 ± 0.001	1.560 ± 0.002	0.500	5 ± 3	5 ± 3	3 ± 2	2 ± 2	3
XMMXCS J094218.3+385536.2	$0.659^{+0.169}_{-0.240}$	0.595 ± 0.176	-	0.152 ± 0.375	-2.110 ± 7.590	0.001	3 ± 2	3 ± 3	2 ± 1	-	3
XMMXCS J094302.0+385832.3	$0.092^{+0.027}_{-0.027}$	0.094 ± 0.022	$0.093 \pm 9.9e-06$	-0.064 ± 0.018	1.900 ± 0.335	0.046	2 ± 1	0 ± 1	0 ± 0.1	-	3
XMMXCS J094306.1+481620.7	$0.291^{+0.117}_{-0.112}$	0.195 ± 0.046	-	0.042 ± 0.061	0.342 ± 1.200	0.092	1 ± 2	0 ± 2	0 ± 0.1	-	3
XMMXCS J094314.8+470558.9	$0.317^{+0.116}_{-0.114}$	0.224 ± 0.066	-	0.014 ± 0.040	0.975 ± 0.786	0.103	5 ± 3	5 ± 3	4 ± 2	3 ± 2	3
XMMXCS J094359.2+481101.7	$0.435^{+0.139}_{-0.138}$	0.333 ± 0.155	-	0.300 ± 0.243	-4.960 ± 4.920	0.001	5 ± 3	3 ± 3	3 ± 2	2 ± 2	3
XMMXCS J094421.0+481155.6	$0.322^{+0.077}_{-0.077}$	0.175 ± 0.028	-	-0.233 ± 0.219	5.630 ± 4.250	0.123	2 ± 2	1 ± 2	2 ± 1	2 ± 2	3
XMMXCS J094423.6+035951.6	$0.315^{+0.083}_{-0.085}$	0.216 ± 0.055	-	-0.040 ± 0.053	2.130 ± 1.030	0.094	3 ± 3	3 ± 3	0 ± 1	1 ± 2	3
XMMXCS J094523.8+040238.9	$0.289^{+0.067}_{-0.071}$	0.292 ± 0.061	-	0.233 ± 0.125	-2.820 ± 2.320	0.091	3 ± 2	3 ± 2	0 ± 0.1	-	3
XMMXCS J094637.7+095633.7	$0.418^{+0.139}_{-0.139}$	0.414 ± 0.067	-	-0.394 ± 0.140	9.110 ± 2.820	0.134	3 ± 3	3 ± 3	0 ± 0.1	-	3
XMMXCS J095127.7+392011.6	$0.472^{+0.133}_{-0.133}$	0.488 ± 0.173	$0.474 \pm 1.3e-04$	-0.105 ± 0.049	2.890 ± 0.955	0.001	0 ± 2	24 ± 6	-	8 ± 5	3
XMMXCS J095221.8+080232.1	$0.583^{+0.093}_{-0.094}$	0.554 ± 0.085	$0.583 \pm 1.2e-04$	0.189 ± 0.071	-2.460 ± 1.350	0.001	2 ± 2	25 ± 5	2 ± 1	23 ± 5	3
XMMXCS J095239.8+080714.3	$0.096^{+0.024}_{-0.025}$	0.094 ± 0.018	$0.097 \pm 2.3e-05$	-0.008 ± 0.036	1.040 ± 0.606	0.086	1 ± 1	1 ± 1	0 ± 0.1	1 ± 1	3
XMMXCS J095253.0+080800.4	$0.148^{+0.025}_{-0.024}$	0.110 ± 0.025	$0.147 \pm 4.4e-05$	0.018 ± 0.068	0.535 ± 1.150	0.095	3 ± 2	1 ± 2	2 ± 1	1 ± 1	3
XMMXCS J095339.7+013455.3	$0.390^{+0.043}_{-0.025}$	0.273 ± 0.094	-	-0.000 ± 0.001	0.313 ± 0.001	0.500	1 ± 3	1 ± 3	0 ± 0.1	-	3
XMMXCS J095343.6+694735.0	$0.241^{+0.072}_{-0.072}$	0.374 ± 0.183	-	-0.001 ± 0.042	1.450 ± 0.813	0.072	14 ± 4	17 ± 4	16 ± 4	20 ± 5	3
XMMXCS J095408.7+693322.8	$0.147^{+0.037}_{-0.037}$	0.162 ± 0.030	-	0.082 ± 0.001	-0.673 ± 0.001	0.500	0 ± 1	2 ± 2	-	0 ± 1	3
XMMXCS J095409.4+014308.3	$0.208^{+0.086}_{-0.088}$	0.110 ± 0.021	$0.098 \pm 1.9e-05$	-0.006 ± 0.057	1.070 ± 1.110	0.065	2 ± 2	2 ± 2	1 ± 1	1 ± 1	3
XMMXCS J095427.2+173140.2	$0.258^{+0.097}_{-0.101}$	0.343 ± 0.052	-	-0.151 ± 0.070	4.440 ± 1.410	0.045	3 ± 2	0 ± 1	3 ± 2	-	3

Continued on next page

Table A.2 – continued from previous page

name	z_{RS}	z_{BCG}	z_{spec-g}	cmr_{grad}	cmr_{inter}	cmr_{wid}	n_{gals-c}	n_{gals-l}	n_{200-c}	n_{200-l}	qual
XMMXCS J095457.8+694327.3	$0.137^{+0.073}_{-0.072}$	0.149 ± 0.035	$0.145 \pm 3.3e-05$	-0.023 ± 0.025	1.400 ± 0.452	0.107	0 ± 1	1 ± 1	-	1 ± 1	3
XMMXCS J095505.4+175649.6	$0.354^{+0.164}_{-0.189}$	0.508 ± 0.213	-	-0.057 ± 0.123	2.330 ± 2.440	0.089	3 ± 3	4 ± 3	0 ± 1	-	3
XMMXCS J095536.5+173626.8	$0.397^{+0.086}_{-0.088}$	0.361 ± 0.058	$0.382 \pm 7.0e-05$	-0.087 ± 0.063	3.480 ± 1.280	0.001	3 ± 3	3 ± 3	0 ± 1	-	3
XMMXCS J095538.3+653843.2	$0.354^{+0.107}_{-0.106}$	0.416 ± 0.067	-	-0.028 ± 0.091	2.140 ± 1.750	0.091	1 ± 2	2 ± 3	-	2 ± 2	3
XMMXCS J095540.2+411727.9	$0.247^{+0.034}_{-0.034}$	0.228 ± 0.036	$0.247 \pm 6.4e-05$	-0.069 ± 0.018	2.590 ± 0.342	0.060	2 ± 2	1 ± 2	2 ± 1	0 ± 1	3
XMMXCS J095554.6-002616.4	$0.405^{+0.121}_{-0.122}$	0.510 ± 0.212	-	0.394 ± 0.220	-6.810 ± 4.460	0.265	2 ± 3	4 ± 4	0 ± 1	-	3
XMMXCS J095600.6-003117.4	$0.283^{+0.103}_{-0.110}$	0.202 ± 0.032	-	-0.029 ± 0.056	1.840 ± 1.080	0.082	2 ± 2	0 ± 2	1 ± 1	-	3
XMMXCS J095630.2-002702.8	$0.423^{+0.152}_{-0.153}$	0.480 ± 0.074	-	0.137 ± 0.145	-2.010 ± 2.990	0.001	5 ± 3	4 ± 3	2 ± 2	2 ± 2	3
XMMXCS J095632.3-001718.4	$0.446^{+0.109}_{-0.108}$	0.348 ± 0.101	$0.472 \pm 7.4e-05$	-0.052 ± 0.058	1.770 ± 1.170	0.037	23 ± 5	22 ± 5	23 ± 6	21 ± 6	3
XMMXCS J095634.9+410848.5	$0.257^{+0.073}_{-0.074}$	0.286 ± 0.061	-	-0.070 ± 0.026	2.790 ± 0.479	0.001	0 ± 1	1 ± 2	-	0 ± 1	3
XMMXCS J095703.1-002821.0	$0.316^{+0.082}_{-0.078}$	0.234 ± 0.039	-	-0.341 ± 0.003	8.240 ± 0.056	0.500	2 ± 3	1 ± 3	3 ± 2	-	3
XMMXCS J095722.0-001707.7	$0.230^{+0.064}_{-0.065}$	0.086 ± 0.016	$0.088 \pm 9.4e-06$	-0.001 ± 0.109	0.994 ± 2.070	0.133	2 ± 2	5 ± 4	0 ± 1	0 ± 2	3
XMMXCS J095731.9+024304.5	$0.600^{+0.295}_{-0.267}$	0.525 ± 0.270	-	-0.156 ± 0.978	4.500 ± 20.40	0.001	4 ± 2	37 ± 7	1 ± 1	114 ± 11	3
XMMXCS J095735.1+024448.7	$0.386^{+0.184}_{-0.172}$	0.328 ± 0.097	-	1.080 ± 0.594	-21.10 ± 12.10	0.362	1 ± 3	1 ± 3	0 ± 0.1	-	3
XMMXCS J095756.3+022424.8	$0.487^{+0.085}_{-0.082}$	0.447 ± 0.074	$0.482 \pm 8.8e-05$	0.013 ± 0.029	0.440 ± 0.565	0.001	0 ± 2	6 ± 4	-	4 ± 3	3
XMMXCS J095801.08+020440.3	$0.273^{+0.084}_{-0.087}$	0.240 ± 0.047	-	-0.006 ± 0.092	1.520 ± 1.790	0.089	2 ± 2	2 ± 2	0 ± 0.1	1 ± 1	3
XMMXCS J095801.0+020439.9	$0.273^{+0.084}_{-0.087}$	0.240 ± 0.047	-	-0.006 ± 0.092	1.520 ± 1.790	0.089	2 ± 2	2 ± 2	0 ± 0.1	1 ± 1	3
XMMXCS J095804.33+015201.6	$0.522^{+0.115}_{-0.109}$	0.420 ± 0.061	-	0.080 ± 0.089	-0.716 ± 1.780	0.067	2 ± 2	-	1 ± 1	-	3
XMMXCS J095804.3+015201.6	$0.522^{+0.115}_{-0.109}$	0.420 ± 0.061	-	0.080 ± 0.089	-0.716 ± 1.780	0.067	2 ± 2	-	1 ± 1	-	3

Continued on next page

Table A.2 – continued from previous page

name	z_{RS}	z_{BCG}	z_{spec-g}	cmr_{grad}	cmr_{inter}	cmr_{wid}	n_{gals-c}	n_{gals-l}	n_{200-c}	n_{200-l}	qual
XMMXCS J095805.88+014205.3	$0.395^{+0.127}_{-0.110}$	0.381 ± 0.112	$0.571 \pm 2.0e-04$	0.019 ± 0.142	0.771 ± 2.780	0.124	2 ± 3	4 ± 3	0 ± 1	-	3
XMMXCS J095805.9+014205.5	$0.395^{+0.126}_{-0.111}$	0.381 ± 0.112	$0.571 \pm 2.0e-04$	0.019 ± 0.142	0.771 ± 2.780	0.124	2 ± 3	4 ± 3	0 ± 1	-	3
XMMXCS J095815.90+020923.0	$0.440^{+0.092}_{-0.074}$	0.431 ± 0.074	-	-0.510 ± 0.152	11.400 ± 3.070	0.163	0 ± 2	5 ± 4	-	0 ± 2	3
XMMXCS J095817.5+021937.5	$0.125^{+0.013}_{-0.012}$	0.117 ± 0.024	$0.125 \pm 1.7e-05$	-0.160 ± 0.056	3.580 ± 0.950	0.058	5 ± 2	3 ± 2	1 ± 1	1 ± 1	3
XMMXCS J095822.8+024830.5	$0.329^{+0.080}_{-0.079}$	0.261 ± 0.095	-	0.978 ± 0.518	-18.20 ± 10.40	0.260	2 ± 3	1 ± 3	1 ± 1	2 ± 2	3
XMMXCS J095822.88+024717.4	$0.357^{+0.058}_{-0.058}$	0.359 ± 0.055	$0.345 \pm 8.0e-05$	0.049 ± 0.096	0.728 ± 1.840	0.119	4 ± 3	5 ± 3	0 ± 1	3 ± 2	3
XMMXCS J095823.39+020233.4	$0.294^{+0.050}_{-0.054}$	0.247 ± 0.052	-	0.084 ± 0.036	-0.061 ± 0.667	0.033	0 ± 2	2 ± 2	-	3 ± 2	3
XMMXCS J095833.8+022047.7	$0.258^{+0.103}_{-0.115}$	0.098 ± 0.019	$0.125 \pm 1.8e-05$	0.154 ± 0.041	-1.660 ± 0.757	0.078	2 ± 2	2 ± 3	1 ± 1	1 ± 2	3
XMMXCS J095833.89+022049.3	$0.245^{+0.101}_{-0.108}$	0.098 ± 0.019	$0.125 \pm 1.8e-05$	0.099 ± 0.020	-0.642 ± 0.359	0.001	2 ± 2	4 ± 3	1 ± 1	3 ± 2	3
XMMXCS J095835.37+024938.0	$0.358^{+0.074}_{-0.074}$	0.425 ± 0.069	$0.378 \pm 7.9e-05$	-0.066 ± 0.048	2.860 ± 0.913	0.065	2 ± 2	4 ± 3	0 ± 0.1	1 ± 2	3
XMMXCS J095835.7+022101.9	$0.256^{+0.098}_{-0.098}$	0.129 ± 0.020	$0.125 \pm 2.9e-05$	0.037 ± 0.040	0.470 ± 0.742	0.055	0 ± 1	1 ± 2	-	0 ± 1	3
XMMXCS J095841.3+023709.9	$0.286^{+0.055}_{-0.058}$	0.259 ± 0.047	$0.270 \pm 6.1e-05$	-0.020 ± 0.060	1.850 ± 1.170	0.062	4 ± 2	3 ± 3	0 ± 1	0 ± 1	3
XMMXCS J095846.90+021550.8	$0.494^{+0.154}_{-0.154}$	0.366 ± 0.142	-	0.789 ± 0.408	-15.60 ± 8.420	0.164	3 ± 3	1 ± 1	2 ± 2	0 ± 1	3
XMMXCS J095847.9+022628.2	$0.307^{+0.106}_{-0.103}$	0.131 ± 0.021	$0.125 \pm 1.9e-05$	0.073 ± 0.087	-0.050 ± 1.710	0.102	3 ± 3	1 ± 3	0 ± 1	1 ± 1	3
XMMXCS J095847.94+022628.5	$0.307^{+0.106}_{-0.103}$	0.131 ± 0.021	$0.125 \pm 1.9e-05$	0.073 ± 0.087	-0.050 ± 1.710	0.102	3 ± 3	1 ± 3	0 ± 1	1 ± 1	3
XMMXCS J095848.91+023252.0	$0.518^{+0.110}_{-0.096}$	0.461 ± 0.071	$0.477 \pm 1.9e-04$	0.061 ± 0.049	-0.540 ± 0.994	0.127	0 ± 3	20 ± 5	-	16 ± 6	3
XMMXCS J095852.5+025122.6	$0.254^{+0.106}_{-0.115}$	0.071 ± 0.014	$0.072 \pm 1.7e-05$	0.022 ± 0.111	0.719 ± 2.160	0.103	2 ± 2	-	0 ± 1	-	3
XMMXCS J095856.89+021409.6	$0.134^{+0.039}_{-0.038}$	0.151 ± 0.031	$0.128 \pm 1.5e-05$	-0.033 ± 0.023	1.400 ± 0.410	0.001	0 ± 1	1 ± 1	-	0 ± 1	3
XMMXCS J095857.5+021403.6	$0.225^{+0.104}_{-0.118}$	0.151 ± 0.031	$0.128 \pm 1.5e-05$	-0.233 ± 0.002	5.620 ± 0.035	0.500	4 ± 3	7 ± 4	2 ± 2	0 ± 2	3

Continued on next page

Table A.2 – continued from previous page

name	z_{RS}	z_{BCG}	z_{spec-g}	cmr_{grad}	cmr_{inter}	cmr_{wid}	n_{gals-c}	n_{gals-l}	n_{200-c}	n_{200-l}	qual
XMMXCS J095923.4+683940.6	$0.257^{+0.060}_{-0.054}$	0.205 ± 0.043	-	0.041 ± 0.065	0.507 ± 1.240	0.119	3 ± 3	1 ± 3	1 ± 1	5 ± 2	3
XMMXCS J095924.69+020806.7	$0.157^{+0.055}_{-0.062}$	0.168 ± 0.030	$0.165 \pm 2.1e-05$	0.414 ± 0.003	-7.120 ± 0.062	0.500	2 ± 2	4 ± 3	1 ± 1	2 ± 2	3
XMMXCS J095924.7+020806.6	$0.157^{+0.055}_{-0.062}$	0.168 ± 0.030	$0.165 \pm 2.1e-05$	0.414 ± 0.003	-7.120 ± 0.062	0.500	2 ± 2	3 ± 3	1 ± 1	-	3
XMMXCS J095929.8+023410.6	$0.613^{+0.180}_{-0.188}$	0.671 ± 0.107	-	0.129 ± 0.171	-1.340 ± 3.480	0.181	3 ± 2	14 ± 4	1 ± 1	13 ± 4	3
XMMXCS J095931.2+022701.5	$0.319^{+0.100}_{-0.102}$	0.135 ± 0.052	-	0.360 ± 0.095	-5.970 ± 1.960	0.031	2 ± 2	1 ± 2	2 ± 1	2 ± 2	3
XMMXCS J095931.63+022657.2	$0.305^{+0.094}_{-0.097}$	0.135 ± 0.052	-	0.336 ± 0.185	-5.480 ± 3.740	0.040	1 ± 2	0 ± 2	0 ± 0.1	-	3
XMMXCS J095932.7+023038.1	$0.629^{+0.170}_{-0.171}$	0.564 ± 0.282	-	0.043 ± 0.116	0.407 ± 2.360	0.132	6 ± 3	15 ± 4	3 ± 2	14 ± 5	3
XMMXCS J095934.96+015647.3	$0.567^{+0.154}_{-0.163}$	0.586 ± 0.107	-	-0.134 ± 0.039	3.520 ± 0.758	0.001	0 ± 2	1 ± 3	-	0 ± 1	3
XMMXCS J095934.9+015646.8	$0.567^{+0.155}_{-0.163}$	0.586 ± 0.107	-	-0.134 ± 0.039	3.520 ± 0.758	0.001	0 ± 2	1 ± 3	-	0 ± 1	3
XMMXCS J095938.4+684849.2	$0.310^{+0.095}_{-0.098}$	0.258 ± 0.050	-	-0.040 ± 0.097	2.360 ± 1.850	0.098	1 ± 2	1 ± 2	1 ± 1	0 ± 1	3
XMMXCS J095938.5+020443.0	$0.371^{+0.108}_{-0.108}$	0.335 ± 0.086	-	0.047 ± 0.082	0.289 ± 1.610	0.001	2 ± 2	2 ± 3	0 ± 0.1	-	3
XMMXCS J095939.08+021205.2	$0.309^{+0.123}_{-0.117}$	0.186 ± 0.034	-	-0.030 ± 0.057	1.930 ± 1.120	0.134	3 ± 2	2 ± 2	0 ± 1	0 ± 1	3
XMMXCS J095940.18+025248.1	$0.262^{+0.073}_{-0.081}$	0.095 ± 0.020	$0.102 \pm 2.1e-05$	0.108 ± 0.055	-0.913 ± 1.080	0.044	2 ± 2	0 ± 2	1 ± 1	-	3
XMMXCS J095942.4+252214.6	$0.509^{+0.147}_{-0.148}$	0.591 ± 0.171	-	-0.021 ± 0.026	1.440 ± 0.509	0.087	7 ± 3	9 ± 4	5 ± 3	6 ± 3	3
XMMXCS J095947.0+022859.3	$0.161^{+0.069}_{-0.075}$	0.236 ± 0.047	$0.265 \pm 3.9e-05$	-0.071 ± 0.134	2.320 ± 2.760	0.500	0 ± 1	1 ± 2	-	0 ± 1	3
XMMXCS J095954.7+021845.5	$0.312^{+0.084}_{-0.081}$	0.204 ± 0.191	-	0.268 ± 0.151	-4.370 ± 3.120	0.500	2 ± 3	2 ± 3	0 ± 1	1 ± 2	3
XMMXCS J095954.9+021706.6	$0.277^{+0.119}_{-0.128}$	0.243 ± 0.080	-	-0.092 ± 0.070	3.010 ± 1.460	0.122	1 ± 2	1 ± 2	0 ± 0.1	1 ± 1	3
XMMXCS J095955.5+304215.8	$0.315^{+0.110}_{-0.097}$	0.149 ± 0.045	-	0.193 ± 0.119	-2.400 ± 2.220	0.227	6 ± 4	8 ± 4	7 ± 3	8 ± 4	3
XMMXCS J095955.74+021900.9	$0.279^{+0.136}_{-0.137}$	0.204 ± 0.191	-	0.107 ± 0.254	-1.220 ± 5.130	0.001	1 ± 1	2 ± 2	0 ± 0.1	0 ± 1	3

Continued on next page

Table A.2 – continued from previous page

name	z_{RS}	z_{BCG}	z_{spec-g}	cmr_{grad}	cmr_{inter}	cmr_{wid}	n_{gals-c}	n_{gals-l}	n_{200-c}	n_{200-l}	qual
XMMXCS J095957.4+021812.1	$0.261^{+0.137}_{-0.135}$	0.204 ± 0.191	-	0.118 ± 0.100	-1.310 ± 1.990	0.115	1 ± 2	3 ± 2	1 ± 1	1 ± 1	3
XMMXCS J095959.4+021550.4	$0.374^{+0.141}_{-0.144}$	0.216 ± 0.042	-	0.157 ± 0.009	-2.300 ± 0.156	0.500	4 ± 4	4 ± 4	4 ± 3	5 ± 3	3
XMMXCS J100001.3+024847.9	$0.505^{+0.128}_{-0.120}$	0.454 ± 0.074	-	0.257 ± 0.054	-4.350 ± 1.140	0.066	3 ± 2	-	0 ± 1	-	3
XMMXCS J100001.40+024846.7	$0.505^{+0.128}_{-0.120}$	0.454 ± 0.074	-	0.257 ± 0.054	-4.350 ± 1.140	0.066	3 ± 2	-	0 ± 1	-	3
XMMXCS J100001.8+023746.4	$0.332^{+0.109}_{-0.108}$	0.173 ± 0.032	-	-0.225 ± 0.027	5.350 ± 0.551	0.001	3 ± 2	2 ± 2	1 ± 1	2 ± 2	3
XMMXCS J100002.3+021630.7	$0.233^{+0.106}_{-0.105}$	0.204 ± 0.191	-	0.338 ± 0.110	-5.670 ± 2.150	0.060	1 ± 1	1 ± 1	0 ± 0.1	0 ± 1	3
XMMXCS J100002.5+021532.5	$0.390^{+0.164}_{-0.168}$	0.216 ± 0.042	-	0.089 ± 0.058	-1.070 ± 1.080	0.001	1 ± 2	3 ± 3	-	3 ± 2	3
XMMXCS J100005.7+021205.5	$0.191^{+0.049}_{-0.046}$	0.175 ± 0.027	$0.185 \pm 3.1e-05$	-0.069 ± 0.048	2.300 ± 0.900	0.106	4 ± 2	4 ± 3	0 ± 1	0 ± 1	3
XMMXCS J100010.97+024118.0	$0.410^{+0.110}_{-0.113}$	0.233 ± 0.040	$0.328 \pm 4.3e-05$	-0.076 ± 0.066	2.940 ± 1.320	0.153	3 ± 3	-	0 ± 1	-	3
XMMXCS J100013.8+013033.7	$0.479^{+0.091}_{-0.086}$	0.478 ± 0.074	$0.507 \pm 6.5e-05$	-0.104 ± 0.037	2.870 ± 0.742	0.072	4 ± 3	-	0 ± 1	-	3
XMMXCS J100015.5+013144.9	$0.386^{+0.200}_{-0.127}$	0.329 ± 0.125	$0.516 \pm 1.2e-04$	0.137 ± 0.127	-1.280 ± 2.480	0.118	1 ± 3	4 ± 3	1 ± 1	-	3
XMMXCS J100016.0+023511.1	$0.396^{+0.133}_{-0.111}$	0.539 ± 0.086	$0.504 \pm 1.0e-04$	0.034 ± 0.124	0.745 ± 2.450	0.087	2 ± 3	3 ± 3	0 ± 1	1 ± 2	3
XMMXCS J100016.2+023511.7	$0.396^{+0.133}_{-0.111}$	0.539 ± 0.086	$0.504 \pm 1.0e-04$	0.034 ± 0.124	0.745 ± 2.450	0.087	2 ± 3	3 ± 3	0 ± 1	1 ± 2	3
XMMXCS J100021.4+023159.9	$0.296^{+0.088}_{-0.084}$	0.221 ± 0.059	-	0.023 ± 0.095	0.846 ± 1.860	0.146	6 ± 3	6 ± 3	3 ± 2	1 ± 2	3
XMMXCS J100022.8+021156.2	$0.478^{+0.140}_{-0.140}$	0.402 ± 0.092	-	0.256 ± 0.255	-4.210 ± 5.240	0.133	4 ± 3	3 ± 3	5 ± 2	5 ± 3	3
XMMXCS J100023.2+024832.8	$0.266^{+0.136}_{-0.141}$	0.178 ± 0.050	-	-0.002 ± 0.057	1.330 ± 1.060	0.031	1 ± 2	3 ± 2	-	1 ± 1	3
XMMXCS J100024.7+023241.7	$0.329^{+0.120}_{-0.117}$	0.221 ± 0.059	$0.502 \pm 1.3e-04$	0.073 ± 0.071	-0.718 ± 1.440	0.500	7 ± 4	6 ± 4	5 ± 3	7 ± 3	3
XMMXCS J100024.81+023242.7	$0.329^{+0.120}_{-0.117}$	0.221 ± 0.059	$0.502 \pm 1.3e-04$	0.073 ± 0.071	-0.718 ± 1.440	0.500	7 ± 4	6 ± 4	5 ± 3	7 ± 3	3
XMMXCS J100024.82+023956.5	$0.353^{+0.075}_{-0.070}$	0.187 ± 0.132	$0.348 \pm 5.3e-05$	0.158 ± 0.344	-1.810 ± 6.850	0.500	7 ± 4	10 ± 5	2 ± 3	9 ± 5	3

Continued on next page

Table A.2 – continued from previous page

name	z_{RS}	z_{BCG}	z_{spec-g}	cmr_{grad}	cmr_{inter}	cmr_{wid}	n_{gals-c}	n_{gals-l}	n_{200-c}	n_{200-l}	qual
XMMXCS J100032.58+021728.1	$0.316^{+0.112}_{-0.111}$	0.260 ± 0.099	$0.185 \pm 2.8e-05$	-0.045 ± 0.066	2.150 ± 1.280	0.130	5 ± 3	4 ± 3	2 ± 2	5 ± 3	3
XMMXCS J100032.7+021724.9	$0.317^{+0.113}_{-0.110}$	0.260 ± 0.099	$0.185 \pm 2.8e-05$	-0.045 ± 0.066	2.150 ± 1.280	0.130	5 ± 3	4 ± 3	2 ± 2	1 ± 2	3
XMMXCS J100034.56+013632.1	$0.343^{+0.101}_{-0.103}$	0.190 ± 0.050	-	0.021 ± 0.127	1.010 ± 2.580	0.001	5 ± 3	2 ± 3	0 ± 1	0 ± 1	3
XMMXCS J100034.5+250041.2	$0.261^{+0.067}_{-0.067}$	0.250 ± 0.044	-	-0.003 ± 0.041	1.490 ± 0.748	0.001	1 ± 2	0 ± 2	0 ± 0.1	-	3
XMMXCS J100034.8+024256.0	$0.302^{+0.143}_{-0.141}$	0.358 ± 0.053	$0.350 \pm 4.2e-05$	-0.120 ± 0.296	3.800 ± 6.130	0.001	2 ± 2	4 ± 3	0 ± 0.1	3 ± 2	3
XMMXCS J100041.7+685400.0	$0.234^{+0.109}_{-0.109}$	0.088 ± 0.026	-	0.235 ± 0.109	-3.550 ± 2.110	0.053	2 ± 2	2 ± 2	1 ± 1	1 ± 1	3
XMMXCS J100043.1+020636.8	$0.363^{+0.060}_{-0.058}$	0.231 ± 0.062	$0.360 \pm 3.5e-05$	-0.085 ± 0.132	2.880 ± 2.620	0.500	1 ± 3	2 ± 4	3 ± 2	1 ± 2	3
XMMXCS J100047.7+015911.7	$0.457^{+0.095}_{-0.086}$	0.306 ± 0.064	$0.438 \pm 1.3e-04$	0.021 ± 0.060	0.160 ± 1.200	0.094	1 ± 3	51 ± 8	2 ± 2	-	3
XMMXCS J100048.00+020359.0	$0.307^{+0.070}_{-0.069}$	0.182 ± 0.030	$0.185 \pm 3.3e-05$	0.012 ± 0.035	1.370 ± 0.662	0.500	6 ± 4	6 ± 4	3 ± 3	6 ± 3	3
XMMXCS J100051.6+021928.8	$0.170^{+0.054}_{-0.052}$	0.129 ± 0.020	$0.123 \pm 2.6e-05$	0.017 ± 0.051	0.739 ± 0.925	0.112	1 ± 2	0 ± 2	0 ± 0.1	-	3
XMMXCS J100051.67+021928.8	$0.170^{+0.054}_{-0.052}$	0.129 ± 0.020	$0.123 \pm 2.6e-05$	0.017 ± 0.051	0.739 ± 0.925	0.112	1 ± 2	0 ± 2	0 ± 0.1	-	3
XMMXCS J100053.88+021649.0	$0.407^{+0.099}_{-0.095}$	0.323 ± 0.106	-	0.089 ± 0.174	-1.260 ± 3.470	0.120	4 ± 3	-	3 ± 2	-	3
XMMXCS J100058.55+015159.5	$0.533^{+0.107}_{-0.106}$	0.497 ± 0.076	$0.530 \pm 1.5e-04$	0.068 ± 0.106	-0.416 ± 2.130	0.035	1 ± 2	-	0 ± 0.1	-	3
XMMXCS J100058.5+015158.5	$0.533^{+0.107}_{-0.106}$	0.497 ± 0.076	$0.530 \pm 1.5e-04$	0.068 ± 0.106	-0.416 ± 2.130	0.035	1 ± 2	-	0 ± 0.1	-	3
XMMXCS J100103.4+020319.0	$0.176^{+0.078}_{-0.084}$	0.200 ± 0.038	-	-0.068 ± 0.033	2.490 ± 0.618	0.001	1 ± 1	0 ± 1	0 ± 0.1	-	3
XMMXCS J100111.2+285047.8	$0.090^{+0.006}_{-0.006}$	0.102 ± 0.023	$0.086 \pm 1.2e-05$	-0.067 ± 0.023	1.980 ± 0.358	0.039	8 ± 3	5 ± 2	7 ± 3	4 ± 2	3
XMMXCS J100114.72+012946.8	$0.407^{+0.126}_{-0.128}$	0.343 ± 0.107	-	0.138 ± 0.110	-1.220 ± 2.130	0.001	5 ± 3	5 ± 3	4 ± 2	8 ± 3	3
XMMXCS J100117.3+013756.6	$0.328^{+0.103}_{-0.102}$	0.258 ± 0.099	$0.527 \pm 2.0e-04$	0.066 ± 0.047	0.185 ± 0.919	0.086	7 ± 3	9 ± 4	7 ± 3	6 ± 3	3
XMMXCS J100117.6+285108.9	$0.090^{+0.012}_{-0.012}$	0.102 ± 0.023	$0.096 \pm 1.6e-05$	-0.034 ± 0.004	1.480 ± 0.071	0.020	10 ± 3	6 ± 3	9 ± 3	3 ± 2	3

Continued on next page

Table A.2 – continued from previous page

name	z_{RS}	z_{BCG}	z_{spec-g}	cmr_{grad}	cmr_{inter}	cmr_{wid}	n_{gals-c}	n_{gals-l}	n_{200-c}	n_{200-l}	qual
XMMXCS J100120.7+555349.6	$0.357^{+0.068}_{-0.066}$	0.235 ± 0.086	-	0.057 ± 0.040	-0.569 ± 0.796	0.060	5 ± 3	3 ± 3	3 ± 2	2 ± 2	3
XMMXCS J100123.3+022159.3	$0.129^{+0.028}_{-0.027}$	0.112 ± 0.024	$0.123 \pm 1.5e-05$	0.087 ± 0.078	-0.757 ± 1.330	0.096	1 ± 1	0 ± 1	0 ± 0.1	-	3
XMMXCS J100131.0+023251.9	$0.117^{+0.012}_{-0.012}$	0.110 ± 0.021	$0.116 \pm 1.1e-05$	0.057 ± 0.034	-0.047 ± 0.570	0.067	0 ± 1	1 ± 2	-	1 ± 1	3
XMMXCS J100137.0+025418.4	$0.379^{+0.078}_{-0.078}$	0.160 ± 0.031	$0.192 \pm 1.5e-05$	0.043 ± 0.022	-0.287 ± 0.418	0.097	1 ± 3	3 ± 4	0 ± 0.1	0 ± 2	3
XMMXCS J100141.49+021030.8	$0.437^{+0.087}_{-0.082}$	0.333 ± 0.087	-	0.184 ± 0.111	-2.960 ± 2.250	0.094	2 ± 3	3 ± 3	0 ± 1	-	3
XMMXCS J100144.4+021430.2	$0.184^{+0.054}_{-0.038}$	0.180 ± 0.101	$0.221 \pm 3.0e-05$	0.167 ± 0.025	-1.850 ± 0.436	0.500	2 ± 3	4 ± 3	0 ± 1	2 ± 2	3
XMMXCS J100144.5+021428.0	$0.188^{+0.051}_{-0.041}$	0.180 ± 0.101	$0.221 \pm 3.0e-05$	0.167 ± 0.025	-1.850 ± 0.436	0.500	2 ± 3	4 ± 3	0 ± 1	1 ± 2	3
XMMXCS J100145.0+284712.1	$0.185^{+0.034}_{-0.035}$	0.362 ± 0.105	$0.186 \pm 1.8e-05$	-0.007 ± 0.034	1.320 ± 0.636	0.083	6 ± 3	7 ± 3	6 ± 3	6 ± 3	3
XMMXCS J100146.6+020842.1	$0.377^{+0.097}_{-0.093}$	0.429 ± 0.160	-	-0.126 ± 0.090	3.110 ± 1.790	0.001	5 ± 3	5 ± 3	0 ± 1	-	3
XMMXCS J100152.80+021154.0	$0.400^{+0.127}_{-0.128}$	0.378 ± 0.059	-	0.177 ± 0.005	-2.590 ± 0.095	0.001	2 ± 2	3 ± 2	1 ± 1	2 ± 2	3
XMMXCS J100153.1+022431.4	$0.261^{+0.089}_{-0.084}$	0.185 ± 0.033	$0.150 \pm 2.1e-05$	-0.004 ± 0.041	0.923 ± 0.741	0.500	5 ± 4	5 ± 4	4 ± 3	4 ± 3	3
XMMXCS J100156.0+025310.5	$0.192^{+0.038}_{-0.037}$	0.211 ± 0.066	-	0.751 ± 0.247	-13.00 ± 4.550	0.062	2 ± 2	0 ± 1	1 ± 1	-	3
XMMXCS J100156.2+014802.5	$0.279^{+0.077}_{-0.072}$	0.342 ± 0.064	$0.310 \pm 8.7e-05$	-0.165 ± 0.058	4.340 ± 1.100	0.129	0 ± 2	2 ± 3	-	1 ± 2	3
XMMXCS J100200.96+021332.7	$0.247^{+0.094}_{-0.100}$	0.237 ± 0.055	$0.221 \pm 3.0e-05$	-0.081 ± 0.043	2.830 ± 0.861	0.145	3 ± 2	2 ± 3	0 ± 0.1	0 ± 1	3
XMMXCS J100201.7+021332.8	$0.260^{+0.096}_{-0.099}$	0.237 ± 0.055	$0.221 \pm 3.0e-05$	-0.027 ± 0.047	1.790 ± 0.932	0.129	4 ± 3	3 ± 3	0 ± 0.1	1 ± 2	3
XMMXCS J100201.7+283425.5	$0.084^{+0.038}_{-0.039}$	0.075 ± 0.017	$0.113 \pm 6.5e-05$	-0.050 ± 0.021	1.630 ± 0.388	0.015	1 ± 1	0 ± 1	0 ± 0.1	-	3
XMMXCS J100202.9+022435.2	$0.238^{+0.089}_{-0.080}$	0.217 ± 0.087	-	-0.045 ± 0.049	1.760 ± 0.939	0.098	1 ± 2	0 ± 2	0 ± 0.1	-	3
XMMXCS J100204.32+023123.6	$0.431^{+0.128}_{-0.128}$	0.282 ± 0.095	-	0.114 ± 0.038	-1.540 ± 0.752	0.094	0 ± 2	1 ± 3	-	1 ± 1	3
XMMXCS J100204.4+023120.7	$0.433^{+0.110}_{-0.109}$	0.347 ± 0.078	-	0.655 ± 0.303	-12.10 ± 6.100	0.001	2 ± 3	3 ± 3	0 ± 1	2 ± 2	3

Continued on next page

Table A.2 – continued from previous page

name	z_{RS}	z_{BCG}	z_{spec-g}	cmr_{grad}	cmr_{inter}	cmr_{wid}	n_{gals-c}	n_{gals-l}	n_{200-c}	n_{200-l}	qual
XMMXCS J100208.2+024246.7	$0.186^{+0.075}_{-0.073}$	0.248 ± 0.056	$0.239 \pm 3.0e-05$	-0.308 ± 0.005	6.590 ± 0.081	0.500	6 ± 3	5 ± 3	7 ± 3	7 ± 3	3
XMMXCS J100214.2+325657.2	$0.381^{+0.082}_{-0.081}$	0.321 ± 0.054	-	-0.021 ± 0.029	2.050 ± 0.556	0.001	6 ± 3	8 ± 4	4 ± 3	-	3
XMMXCS J100217.5+022958.6	$0.440^{+0.145}_{-0.151}$	0.317 ± 0.112	-	-0.105 ± 0.066	3.200 ± 1.330	0.055	4 ± 3	4 ± 3	1 ± 2	1 ± 2	3
XMMXCS J100219.9+324450.2	$0.050^{+0.028}_{-0.028}$	0.105 ± 0.025	$0.051 \pm 9.9e-06$	0.006 ± 0.023	0.714 ± 0.396	0.104	2 ± 2	1 ± 1	2 ± 1	0 ± 1	3
XMMXCS J100240.1+021600.9	$0.198^{+0.099}_{-0.103}$	0.104 ± 0.027	-	0.024 ± 0.038	0.536 ± 0.735	0.114	3 ± 2	2 ± 2	2 ± 1	0 ± 1	3
XMMXCS J100240.18+023144.4	$0.400^{+0.146}_{-0.148}$	0.213 ± 0.278	-	-0.231 ± 0.070	5.520 ± 1.350	0.164	3 ± 3	5 ± 3	3 ± 2	5 ± 3	3
XMMXCS J100240.1+023144.4	$0.400^{+0.146}_{-0.148}$	0.213 ± 0.278	-	-0.231 ± 0.070	5.520 ± 1.350	0.164	3 ± 3	5 ± 3	3 ± 2	5 ± 3	3
XMMXCS J100240.8+023450.3	$0.451^{+0.107}_{-0.091}$	0.345 ± 0.053	$0.372 \pm 5.8e-05$	-0.009 ± 0.026	0.741 ± 0.527	0.500	8 ± 5	9 ± 5	7 ± 4	8 ± 4	3
XMMXCS J100243.93+024037.0	$0.254^{+0.079}_{-0.075}$	0.253 ± 0.077	-	0.010 ± 0.034	0.905 ± 0.613	0.001	2 ± 2	1 ± 2	0 ± 0.1	1 ± 1	3
XMMXCS J100252.8+025429.8	$0.283^{+0.126}_{-0.221}$	0.160 ± 0.027	$0.178 \pm 2.8e-05$	-0.117 ± 0.076	3.010 ± 1.430	0.089	2 ± 2	2 ± 3	0 ± 0.1	0 ± 1	3
XMMXCS J100254.6+324039.1	$0.050^{+0.002}_{-0.001}$	0.057 ± 0.015	$0.050 \pm 8.0e-06$	0.009 ± 0.005	0.689 ± 0.080	0.007	3 ± 2	1 ± 1	1 ± 1	0 ± 1	3
XMMXCS J100304.4+324859.5	$0.376^{+0.091}_{-0.082}$	0.303 ± 0.045	$0.296 \pm 6.8e-05$	-0.028 ± 0.058	1.850 ± 1.120	0.500	13 ± 5	9 ± 5	14 ± 5	10 ± 5	3
XMMXCS J100305.9+015203.6	$0.427^{+0.086}_{-0.078}$	0.489 ± 0.076	-	-0.025 ± 0.130	1.180 ± 2.670	0.085	4 ± 3	4 ± 3	0 ± 1	1 ± 2	3
XMMXCS J100309.0+024843.6	$0.214^{+0.063}_{-0.064}$	0.226 ± 0.057	$0.218 \pm 3.2e-05$	0.001 ± 0.040	1.390 ± 0.718	0.019	1 ± 1	1 ± 2	0 ± 0.1	1 ± 1	3
XMMXCS J100309.05+024843.3	$0.214^{+0.063}_{-0.064}$	0.226 ± 0.057	$0.218 \pm 3.2e-05$	0.001 ± 0.040	1.390 ± 0.718	0.019	1 ± 1	1 ± 2	0 ± 0.1	1 ± 1	3
XMMXCS J100309.5+554135.1	$0.214^{+0.097}_{-0.102}$	0.155 ± 0.045	$0.146 \pm 8.0e-06$	0.147 ± 0.049	-1.660 ± 0.887	0.001	3 ± 2	3 ± 2	2 ± 1	3 ± 2	3
XMMXCS J100318.6+684400.8	$0.066^{+0.134}_{-0.066}$	0.076 ± 0.018	-	0.035 ± 0.001	0.062 ± 0.001	0.500	2 ± 2	-	2 ± 1	-	3
XMMXCS J100324.7+021831.8	$0.696^{+0.169}_{-0.248}$	0.589 ± 0.147	-	-0.040 ± 0.140	1.870 ± 2.760	0.001	1 ± 2	4 ± 4	1 ± 1	-	3
XMMXCS J100401.9+411858.8	$0.419^{+0.088}_{-0.088}$	0.349 ± 0.101	-	0.548 ± 0.186	-10.40 ± 3.810	0.081	2 ± 3	11 ± 4	0 ± 1	1 ± 3	3

Continued on next page

Table A.2 – continued from previous page

name	z_{RS}	z_{BCG}	z_{spec-g}	cmr_{grad}	cmr_{inter}	cmr_{wid}	n_{gals-c}	n_{gals-l}	n_{200-c}	n_{200-l}	qual
XMMXCS J100554.0+411435.9	$0.448^{+0.132}_{-0.128}$	0.325 ± 0.070	-	0.182 ± 0.096	-2.920 ± 1.920	0.133	6 ± 4	6 ± 4	1 ± 2	-	3
XMMXCS J100710.3+123847.9	$0.506^{+0.075}_{-0.075}$	0.541 ± 0.097	$0.506 \pm 1.4e-04$	-0.041 ± 0.069	1.760 ± 1.330	0.073	2 ± 2	7 ± 4	1 ± 1	9 ± 4	3
XMMXCS J100727.9+534019.6	$0.367^{+0.149}_{-0.141}$	0.305 ± 0.048	-	0.155 ± 0.213	-1.470 ± 4.200	0.206	6 ± 3	5 ± 3	2 ± 2	-	3
XMMXCS J100902.2+533501.9	$0.362^{+0.103}_{-0.106}$	0.448 ± 0.066	-	0.032 ± 0.056	0.119 ± 1.120	0.114	4 ± 3	57 ± 8	0 ± 1	-	3
XMMXCS J100954.3+534425.1	$0.606^{+0.181}_{-0.228}$	0.587 ± 0.162	-	-0.248 ± 0.405	6.140 ± 8.330	0.167	3 ± 2	8 ± 4	0 ± 0.1	-	3
XMMXCS J100955.8+535022.4	$0.438^{+0.116}_{-0.114}$	0.387 ± 0.063	-	-0.002 ± 0.104	0.701 ± 2.000	0.001	2 ± 3	6 ± 3	1 ± 1	3 ± 3	3
XMMXCS J101047.5+554755.6	$0.114^{+0.122}_{-0.114}$	0.185 ± 0.032	$0.178 \pm 4.0e-05$	-0.091 ± 0.052	2.870 ± 1.070	0.106	1 ± 1	1 ± 1	0 ± 0.1	0 ± 1	3
XMMXCS J101123.9+534026.5	$0.244^{+0.117}_{-0.112}$	0.139 ± 0.035	-	0.769 ± 0.069	-13.90 ± 1.350	0.500	3 ± 3	2 ± 3	3 ± 2	2 ± 2	3
XMMXCS J101142.9+555458.4	$0.397^{+0.138}_{-0.144}$	0.487 ± 0.076	-	-0.317 ± 0.228	7.350 ± 4.700	0.144	1 ± 2	1 ± 2	0 ± 0.1	0 ± 1	3
XMMXCS J101353.7+001520.9	$0.364^{+0.088}_{-0.084}$	0.175 ± 0.068	$0.358 \pm 3.3e-05$	0.238 ± 0.094	-4.240 ± 1.880	0.089	3 ± 3	1 ± 3	2 ± 2	2 ± 2	3
XMMXCS J101401.4+492659.6	$0.280^{+0.074}_{-0.079}$	0.145 ± 0.024	$0.133 \pm 3.6e-05$	0.022 ± 0.055	0.912 ± 1.060	0.154	4 ± 3	1 ± 3	1 ± 1	0 ± 1	3
XMMXCS J101412.0+492435.2	$0.122^{+0.082}_{-0.083}$	0.131 ± 0.023	$0.130 \pm 2.8e-05$	0.041 ± 0.017	0.354 ± 0.300	0.040	1 ± 1	1 ± 1	0 ± 0.1	1 ± 1	3
XMMXCS J101412.0+492753.3	$0.301^{+0.116}_{-0.088}$	0.131 ± 0.023	$0.130 \pm 2.8e-05$	0.092 ± 0.088	-0.350 ± 1.700	0.191	3 ± 3	5 ± 4	1 ± 1	7 ± 3	3
XMMXCS J101419.3+493051.9	$0.150^{+0.087}_{-0.093}$	0.077 ± 0.017	$0.116 \pm 1.3e-05$	-0.003 ± 0.008	0.946 ± 0.116	0.500	5 ± 3	6 ± 4	2 ± 2	-	3
XMMXCS J101654.0+385503.2	$0.311^{+0.379}_{-0.311}$	0.168 ± 0.041	$0.185 \pm 2.7e-05$	0.148 ± 0.077	-2.120 ± 1.530	0.500	4 ± 4	7 ± 5	3 ± 2	4 ± 4	3
XMMXCS J101737.2+411928.3	$0.289^{+0.088}_{-0.095}$	0.299 ± 0.076	-	-0.026 ± 0.041	1.840 ± 0.793	0.119	2 ± 2	1 ± 2	0 ± 0.1	0 ± 1	3
XMMXCS J101738.4+413235.5	$0.462^{+0.100}_{-0.100}$	0.270 ± 0.055	$0.271 \pm 5.8e-05$	0.318 ± 0.126	-5.420 ± 2.480	0.105	9 ± 4	-	9 ± 3	-	3
XMMXCS J101746.9+390729.0	$0.342^{+0.108}_{-0.110}$	0.282 ± 0.123	-	0.095 ± 0.050	-0.566 ± 0.957	0.001	1 ± 2	1 ± 2	2 ± 1	2 ± 2	3
XMMXCS J101759.0+215357.7	$0.224^{+0.052}_{-0.054}$	0.308 ± 0.074	-	0.011 ± 0.066	1.180 ± 1.190	0.113	9 ± 3	8 ± 3	8 ± 3	6 ± 3	3

Continued on next page

Table A.2 – continued from previous page

name	z_{RS}	z_{BCG}	z_{spec-g}	cmr_{grad}	cmr_{inter}	cmr_{wid}	n_{gals-c}	n_{gals-l}	n_{200-c}	n_{200-l}	qual
XMMXCS J101852.5+001019.9	$0.620^{+0.188}_{-0.207}$	0.630 ± 0.155	-	-0.384 ± 0.107	8.960 ± 2.180	0.001	1 ± 2	-	0 ± 0.1	-	3
XMMXCS J102121.3+234303.1	$0.501^{+0.115}_{-0.115}$	0.392 ± 0.115	-	0.514 ± 0.223	-9.710 ± 4.540	0.089	5 ± 3	7 ± 4	3 ± 2	6 ± 3	3
XMMXCS J102200.3+214035.3	$0.137^{+0.051}_{-0.051}$	0.134 ± 0.027	-	0.085 ± 0.097	-0.482 ± 1.730	0.120	0 ± 1	1 ± 2	-	0 ± 1	3
XMMXCS J102219.6+213917.2	$0.160^{+0.084}_{-0.077}$	0.185 ± 0.031	-	0.017 ± 0.001	0.924 ± 0.001	0.500	1 ± 2	1 ± 2	0 ± 0.1	1 ± 1	3
XMMXCS J102220.3+213414.5	$0.201^{+0.077}_{-0.077}$	0.189 ± 0.032	-	0.089 ± 0.115	-0.415 ± 2.160	0.069	2 ± 2	2 ± 2	0 ± 0.1	0 ± 1	3
XMMXCS J102227.8+220807.8	$0.197^{+0.064}_{-0.058}$	0.210 ± 0.082	-	-0.106 ± 0.091	2.970 ± 1.770	0.130	0 ± 1	1 ± 2	-	0 ± 1	3
XMMXCS J102231.5+130730.0	$0.608^{+0.132}_{-0.114}$	0.509 ± 0.135	-	0.062 ± 0.092	-0.215 ± 1.870	0.128	2 ± 2	2 ± 3	0 ± 0.1	-	3
XMMXCS J102245.9+041123.9	$0.206^{+0.040}_{-0.037}$	0.196 ± 0.034	$0.200 \pm 3.5e-05$	-0.164 ± 0.028	3.980 ± 0.504	0.077	4 ± 2	6 ± 3	0 ± 1	1 ± 2	3
XMMXCS J102257.9+195316.8	$0.241^{+0.061}_{-0.063}$	0.203 ± 0.051	-	0.276 ± 0.133	-3.990 ± 2.390	0.162	2 ± 2	0 ± 2	0 ± 1	-	3
XMMXCS J102318.8+200243.8	$0.456^{+0.101}_{-0.092}$	0.599 ± 0.099	$0.512 \pm 2.0e-04$	-0.144 ± 0.063	3.640 ± 1.270	0.076	3 ± 3	3 ± 3	1 ± 1	2 ± 2	3
XMMXCS J102319.6+213706.0	$0.210^{+0.069}_{-0.066}$	0.151 ± 0.045	-	0.016 ± 0.035	0.694 ± 0.680	0.120	1 ± 2	1 ± 2	1 ± 1	0 ± 1	3
XMMXCS J102359.5+194432.2	$0.546^{+0.136}_{-0.127}$	0.486 ± 0.291	$0.530 \pm 1.2e-04$	-0.224 ± 0.041	5.190 ± 0.805	0.001	3 ± 3	11 ± 4	4 ± 2	12 ± 4	3
XMMXCS J102400.4+040222.6	$0.379^{+0.128}_{-0.128}$	0.324 ± 0.069	-	0.196 ± 0.050	-3.220 ± 0.995	0.035	8 ± 3	8 ± 4	9 ± 3	9 ± 3	3
XMMXCS J102405.1+194905.5	$0.287^{+0.092}_{-0.092}$	0.359 ± 0.057	-	-0.308 ± 0.472	7.570 ± 8.980	0.136	2 ± 2	1 ± 2	1 ± 1	1 ± 1	3
XMMXCS J102408.9+040049.4	$0.153^{+0.103}_{-0.103}$	0.189 ± 0.045	-	0.016 ± 0.108	0.832 ± 2.150	0.120	1 ± 1	0 ± 1	0 ± 0.1	-	3
XMMXCS J102416.1+041126.5	$0.268^{+0.060}_{-0.061}$	0.238 ± 0.038	-	0.094 ± 0.069	-0.409 ± 1.360	0.089	4 ± 2	-	0 ± 0.1	-	3
XMMXCS J102607.8+384207.3	$0.606^{+0.126}_{-0.124}$	0.556 ± 0.090	-	0.157 ± 0.168	-2.140 ± 3.450	0.001	2 ± 2	0 ± 1	2 ± 1	-	3
XMMXCS J102711.1-031905.2	$0.060^{+0.025}_{-0.025}$	0.076 ± 0.041	-	-0.013 ± 0.006	0.992 ± 0.079	0.011	6 ± 3	9 ± 3	5 ± 2	11 ± 3	3
XMMXCS J102712.1-032640.3	$0.830^{+0.130}_{-0.130}$	0.647 ± 0.226	-	-0.199 ± 0.369	4.540 ± 7.580	0.001	1 ± 1	41 ± 6	-	81 ± 9	3

Continued on next page

Table A.2 – continued from previous page

name	z_{RS}	z_{BCG}	z_{spec-g}	cmr_{grad}	cmr_{inter}	cmr_{wid}	n_{gals-c}	n_{gals-l}	n_{200-c}	n_{200-l}	qual
XMMXCS J102739.8-032415.8	$0.104^{+0.049}_{-0.051}$	0.067 ± 0.023	-	-0.000 ± 0.001	0.322 ± 0.001	0.500	4 ± 3	4 ± 3	4 ± 2	2 ± 2	3
XMMXCS J102748.4+000333.7	$0.423^{+0.112}_{-0.112}$	0.231 ± 0.077	-	0.100 ± 0.154	-0.654 ± 3.080	0.001	6 ± 4	-	6 ± 3	-	3
XMMXCS J102750.9+000040.0	$0.291^{+0.078}_{-0.079}$	0.192 ± 0.046	-	0.042 ± 0.049	0.358 ± 0.951	0.100	4 ± 3	3 ± 3	3 ± 2	-	3
XMMXCS J102806.6+000738.2	$0.415^{+0.143}_{-0.151}$	0.228 ± 0.096	-	0.128 ± 0.128	-1.540 ± 2.610	0.106	4 ± 3	-	1 ± 2	-	3
XMMXCS J102830.3-001231.3	$0.306^{+0.101}_{-0.110}$	0.329 ± 0.049	$0.326 \pm 7.4e-05$	-0.068 ± 0.035	2.890 ± 0.671	0.001	2 ± 2	2 ± 2	0 ± 0.1	0 ± 1	3
XMMXCS J102953.3-032205.5	$0.076^{+0.026}_{-0.025}$	0.111 ± 0.025	-	-0.075 ± 0.022	1.980 ± 0.345	0.031	4 ± 2	6 ± 3	3 ± 2	4 ± 2	3
XMMXCS J103024.0+052433.5	$0.249^{+0.122}_{-0.121}$	0.228 ± 0.048	$0.202 \pm 3.4e-05$	0.086 ± 0.082	-0.330 ± 1.540	0.185	1 ± 2	3 ± 3	0 ± 0.1	-	3
XMMXCS J103040.6+305445.8	$0.357^{+0.118}_{-0.111}$	0.225 ± 0.101	-	0.029 ± 0.030	0.035 ± 0.604	0.088	10 ± 4	11 ± 5	8 ± 4	12 ± 5	3
XMMXCS J103044.0+505929.9	$0.331^{+0.091}_{-0.081}$	0.275 ± 0.100	-	0.286 ± 0.147	-4.420 ± 2.870	0.001	1 ± 2	-	1 ± 1	-	3
XMMXCS J103056.2+645724.3	$0.137^{+0.054}_{-0.057}$	0.199 ± 0.031	-	-0.108 ± 0.191	3.010 ± 3.480	0.137	0 ± 1	1 ± 1	-	0 ± 1	3
XMMXCS J103121.5+052314.2	$0.412^{+0.095}_{-0.093}$	0.313 ± 0.110	-	0.311 ± 0.335	-4.940 ± 6.810	0.177	1 ± 3	4 ± 3	1 ± 1	-	3
XMMXCS J103126.6+305619.6	$0.377^{+0.086}_{-0.081}$	0.340 ± 0.051	-	0.019 ± 0.058	1.190 ± 1.140	0.111	0 ± 2	1 ± 3	-	0 ± 1	3
XMMXCS J103131.8+052836.0	$0.304^{+0.123}_{-0.132}$	0.293 ± 0.060	-	0.064 ± 0.154	0.290 ± 3.070	0.001	1 ± 2	1 ± 2	0 ± 0.1	0 ± 1	3
XMMXCS J103200.5+650239.7	$0.160^{+0.113}_{-0.113}$	0.184 ± 0.059	-	-0.105 ± 0.053	2.930 ± 0.981	0.075	1 ± 1	1 ± 1	0 ± 0.1	0 ± 1	3
XMMXCS J103203.6+501028.5	$0.121^{+0.021}_{-0.022}$	0.115 ± 0.021	-	0.115 ± 0.019	-1.000 ± 0.339	0.500	2 ± 2	1 ± 1	2 ± 1	0 ± 1	3
XMMXCS J103214.1+504813.6	$0.205^{+0.063}_{-0.067}$	0.231 ± 0.059	-	-0.079 ± 0.033	2.740 ± 0.616	0.001	1 ± 1	2 ± 2	0 ± 0.1	1 ± 1	3
XMMXCS J103254.0+501738.7	$0.472^{+0.104}_{-0.100}$	0.611 ± 0.124	-	0.104 ± 0.199	-1.330 ± 4.150	0.130	6 ± 3	6 ± 3	2 ± 2	2 ± 2	3
XMMXCS J103354.5+394839.3	$0.148^{+0.039}_{-0.040}$	0.141 ± 0.022	$0.148 \pm 3.1e-05$	-0.010 ± 0.015	1.210 ± 0.281	0.052	2 ± 2	3 ± 2	0 ± 0.1	0 ± 1	3
XMMXCS J103403.5+394025.8	$0.471^{+0.121}_{-0.106}$	0.421 ± 0.092	-	0.128 ± 0.067	-1.870 ± 1.370	0.084	3 ± 3	-	2 ± 2	-	3

Continued on next page

Table A.2 – continued from previous page

name	z_{RS}	z_{BCG}	z_{spec-g}	cmr_{grad}	cmr_{inter}	cmr_{wid}	n_{gals-c}	n_{gals-l}	n_{200-c}	n_{200-l}	qual
XMMXCS J103512.70+575027.0	$0.473^{+0.105}_{-0.103}$	0.396 ± 0.061	-	0.043 ± 0.072	0.020 ± 1.430	0.123	9 ± 4	15 ± 5	7 ± 3	17 ± 5	3
XMMXCS J103512.7+575027.0	$0.473^{+0.105}_{-0.103}$	0.396 ± 0.061	-	0.043 ± 0.072	0.020 ± 1.430	0.123	9 ± 4	15 ± 5	7 ± 3	17 ± 5	3
XMMXCS J103526.9+574204.9	$0.266^{+0.123}_{-0.147}$	0.357 ± 0.144	-	-0.115 ± 0.049	3.320 ± 0.971	0.092	4 ± 2	3 ± 3	0 ± 0.1	1 ± 2	3
XMMXCS J103539.5+575713.9	$0.556^{+0.112}_{-0.104}$	0.368 ± 0.057	$0.396 \pm 1.0e-04$	0.156 ± 0.208	-1.860 ± 4.100	0.500	2 ± 3	2 ± 4	3 ± 2	72 ± 9	3
XMMXCS J103840.3+413554.0	$0.460^{+0.107}_{-0.104}$	0.436 ± 0.068	-	0.075 ± 0.073	-0.697 ± 1.450	0.102	5 ± 3	50 ± 7	0 ± 1	12 ± 6	3
XMMXCS J103853.8+413430.8	$0.448^{+0.106}_{-0.100}$	0.254 ± 0.109	-	0.255 ± 0.135	-3.830 ± 2.670	0.241	1 ± 2	4 ± 2	1 ± 1	2 ± 2	3
XMMXCS J103905.5+395710.9	$0.096^{+0.048}_{-0.050}$	0.084 ± 0.016	$0.110 \pm 1.7e-05$	0.029 ± 0.031	0.343 ± 0.561	0.124	1 ± 2	1 ± 2	0 ± 0.1	0 ± 1	3
XMMXCS J103947.53+585418.0	$0.352^{+0.095}_{-0.094}$	0.327 ± 0.051	$0.352 \pm 1.4e-04$	0.005 ± 0.084	1.430 ± 1.600	0.150	2 ± 3	2 ± 3	0 ± 1	2 ± 2	3
XMMXCS J104034.5+394510.8	$0.471^{+0.124}_{-0.123}$	0.615 ± 0.184	-	-0.173 ± 0.106	4.270 ± 2.100	0.064	2 ± 3	11 ± 4	3 ± 2	11 ± 4	3
XMMXCS J104113.4+061921.8	$0.070^{+0.052}_{-0.063}$	0.042 ± 0.016	$0.041 \pm 9.6e-06$	0.042 ± 0.016	0.297 ± 0.267	0.111	1 ± 2	7 ± 3	2 ± 1	7 ± 3	3
XMMXCS J104126.0+061606.9	$0.054^{+0.053}_{-0.054}$	0.065 ± 0.026	$0.038 \pm 4.5e-06$	0.046 ± 0.014	-0.208 ± 0.244	0.078	1 ± 1	0 ± 1	0 ± 0.1	-	3
XMMXCS J104207.3+060822.2	$0.569^{+0.122}_{-0.100}$	0.369 ± 0.224	-	0.178 ± 0.189	-2.860 ± 3.860	0.079	2 ± 2	6 ± 4	0 ± 0.1	4 ± 3	3
XMMXCS J104211.0+061030.7	$0.448^{+0.140}_{-0.142}$	0.667 ± 0.131	$0.640 \pm 1.9e-04$	-1.360 ± 0.578	29.300 ± 12.00	0.133	4 ± 3	16 ± 5	2 ± 2	-	3
XMMXCS J104303.7+582717.4	$0.370^{+0.517}_{-0.370}$	0.221 ± 0.076	-	0.461 ± 0.228	-9.070 ± 4.510	0.500	2 ± 2	4 ± 3	0 ± 1	4 ± 2	3
XMMXCS J104407.9-012724.9	$0.471^{+0.421}_{-0.421}$	0.320 ± 0.095	-	-0.058 ± 0.078	1.580 ± 1.550	0.113	1 ± 3	3 ± 3	-	1 ± 2	3
XMMXCS J104418.5+212839.1	$0.457^{+0.125}_{-0.121}$	0.422 ± 0.070	-	-0.062 ± 0.067	2.050 ± 1.360	0.120	3 ± 3	-	0 ± 1	-	3
XMMXCS J104442.6+590242.8	$0.321^{+0.089}_{-0.077}$	0.227 ± 0.069	-	0.049 ± 0.067	0.310 ± 1.340	0.150	0 ± 2	1 ± 3	-	0 ± 1	3
XMMXCS J104443.5+590247.8	$0.346^{+0.084}_{-0.074}$	0.227 ± 0.069	-	0.073 ± 0.083	-0.160 ± 1.650	0.174	2 ± 3	1 ± 3	0 ± 1	0 ± 1	3
XMMXCS J104449.3+213141.4	$0.441^{+0.123}_{-0.124}$	0.358 ± 0.071	-	0.116 ± 0.064	-1.680 ± 1.280	0.110	2 ± 3	11 ± 4	0 ± 1	1 ± 3	3

Continued on next page

Table A.2 – continued from previous page

name	z_{RS}	z_{BCG}	z_{spec-g}	cmr_{grad}	cmr_{inter}	cmr_{wid}	n_{gals-c}	n_{gals-l}	n_{200-c}	n_{200-l}	qual
XMMXCS J104451.0+214500.1	$0.083^{+0.045}_{-0.052}$	0.057 ± 0.017	$0.066 \pm 1.1e-05$	-0.414 ± 0.001	7.610 ± 0.001	0.500	0 ± 1	1 ± 2	-	1 ± 1	3
XMMXCS J104451.8+063548.2	$0.073^{+0.034}_{-0.026}$	0.053 ± 0.026	$0.068 \pm 1.0e-05$	0.022 ± 0.013	0.404 ± 0.181	0.500	2 ± 2	0 ± 1	1 ± 1	-	3
XMMXCS J104452.2+585444.9	$0.317^{+0.075}_{-0.078}$	0.350 ± 0.051	$0.355 \pm 1.3e-04$	-0.135 ± 0.108	4.210 ± 2.190	0.154	3 ± 3	5 ± 3	0 ± 0.1	1 ± 2	3
XMMXCS J104453.6-013251.4	$0.654^{+0.150}_{-0.149}$	0.630 ± 0.232	-	0.075 ± 0.140	-0.431 ± 2.900	0.001	3 ± 2	16 ± 5	-	13 ± 5	3
XMMXCS J104455.1+585450.9	$0.306^{+0.147}_{-0.143}$	0.179 ± 0.044	-	0.065 ± 0.090	0.018 ± 1.790	0.001	1 ± 2	1 ± 2	1 ± 1	1 ± 1	3
XMMXCS J104455.4-013126.0	$0.444^{+0.160}_{-0.196}$	0.341 ± 0.129	-	0.177 ± 0.119	-2.150 ± 2.330	0.001	2 ± 3	4 ± 3	0 ± 1	0 ± 2	3
XMMXCS J104456.1+214035.3	$0.090^{+0.036}_{-0.036}$	0.057 ± 0.017	$0.077 \pm 1.2e-05$	-0.100 ± 0.001	2.440 ± 0.001	0.500	2 ± 2	0 ± 1	0 ± 0.1	-	3
XMMXCS J104507.8-013617.4	$0.613^{+0.176}_{-0.183}$	0.517 ± 0.122	-	0.536 ± 0.298	-9.820 ± 6.060	0.001	3 ± 2	12 ± 4	1 ± 1	12 ± 4	3
XMMXCS J104513.0+213202.4	$0.499^{+0.120}_{-0.122}$	0.323 ± 0.059	$0.507 \pm 9.0e-05$	0.443 ± 0.320	-7.670 ± 6.410	0.181	4 ± 2	3 ± 3	0 ± 1	-	3
XMMXCS J104526.9-012317.5	$0.237^{+0.076}_{-0.082}$	0.231 ± 0.036	-	-0.015 ± 0.038	1.680 ± 0.698	0.066	4 ± 2	4 ± 3	0 ± 1	4 ± 2	3
XMMXCS J104545.4+063441.3	$0.209^{+0.061}_{-0.062}$	0.213 ± 0.033	$0.212 \pm 5.0e-05$	0.084 ± 0.015	-0.051 ± 0.281	0.001	0 ± 1	1 ± 2	-	1 ± 1	3
XMMXCS J104549.3+213100.1	$0.508^{+0.115}_{-0.115}$	0.593 ± 0.127	-	-0.029 ± 0.028	1.510 ± 0.543	0.001	8 ± 3	38 ± 7	8 ± 3	86 ± 10	3
XMMXCS J104614.5+484813.9	$0.371^{+0.100}_{-0.099}$	0.424 ± 0.062	$0.434 \pm 1.4e-04$	0.013 ± 0.028	0.429 ± 0.556	0.070	11 ± 4	9 ± 4	11 ± 4	8 ± 4	3
XMMXCS J104919.4+572333.8	$0.394^{+0.140}_{-0.141}$	0.333 ± 0.061	-	-0.080 ± 0.063	3.120 ± 1.260	0.090	4 ± 3	4 ± 3	0 ± 1	1 ± 2	3
XMMXCS J104948.5+572403.5	$0.291^{+0.088}_{-0.084}$	0.269 ± 0.127	-	-0.001 ± 0.051	1.290 ± 0.997	0.118	2 ± 2	-	0 ± 1	-	3
XMMXCS J105034.2+572356.9	$0.318^{+0.124}_{-0.119}$	0.375 ± 0.057	-	-0.789 ± 0.634	17.600 ± 13.20	0.500	5 ± 3	3 ± 3	4 ± 2	0 ± 1	3
XMMXCS J105130.9+573439.3	$0.073^{+0.012}_{-0.012}$	0.083 ± 0.019	$0.074 \pm 1.2e-05$	-0.039 ± 0.012	1.490 ± 0.213	0.025	1 ± 1	0 ± 1	1 ± 1	-	3
XMMXCS J105137.2+335614.0	$0.330^{+0.149}_{-0.154}$	0.403 ± 0.152	-	-0.221 ± 0.043	5.530 ± 0.838	0.001	2 ± 2	0 ± 2	0 ± 0.1	-	3
XMMXCS J105137.2+573757.5	$0.090^{+0.026}_{-0.027}$	0.083 ± 0.019	$0.095 \pm 1.1e-05$	-0.019 ± 0.016	1.180 ± 0.275	0.029	1 ± 1	1 ± 1	0 ± 0.1	0 ± 1	3

Continued on next page

Table A.2 – continued from previous page

name	z_{RS}	z_{BCG}	z_{spec-g}	cmr_{grad}	cmr_{inter}	cmr_{wid}	n_{gals-c}	n_{gals-l}	n_{200-c}	n_{200-l}	qual
XMMXCS J105146.0+353851.9	$0.133^{+0.028}_{-0.029}$	0.107 ± 0.022	$0.128 \pm 1.7e-05$	-0.027 ± 0.036	1.530 ± 0.643	0.084	2 ± 2	2 ± 2	2 ± 1	2 ± 2	3
XMMXCS J105223.5+441852.1	$0.499^{+0.097}_{-0.096}$	0.381 ± 0.141	$0.472 \pm 7.4e-05$	-0.003 ± 0.053	0.901 ± 1.090	0.115	31 ± 6	39 ± 7	47 ± 8	60 ± 10	3
XMMXCS J105225.0+440833.2	$0.081^{+0.108}_{-0.081}$	0.095 ± 0.062	$0.071 \pm 5.9e-06$	0.007 ± 0.019	0.606 ± 0.306	0.001	1 ± 1	0 ± 1	1 ± 1	-	3
XMMXCS J105227.6+441905.1	$0.498^{+0.094}_{-0.094}$	0.448 ± 0.069	$0.480 \pm 6.2e-05$	0.020 ± 0.047	0.522 ± 0.947	0.088	23 ± 5	30 ± 6	34 ± 7	47 ± 8	3
XMMXCS J105241.7+573036.6	$0.507^{+0.164}_{-0.178}$	0.314 ± 0.052	-	0.029 ± 0.135	0.194 ± 2.780	0.102	8 ± 4	10 ± 4	8 ± 3	9 ± 4	3
XMMXCS J105246.0+574040.2	$0.148^{+0.091}_{-0.094}$	0.142 ± 0.047	$0.208 \pm 2.6e-05$	0.044 ± 0.029	0.059 ± 0.527	0.001	1 ± 1	1 ± 1	1 ± 1	1 ± 1	3
XMMXCS J105255.8+341845.5	$0.658^{+0.090}_{-0.089}$	0.612 ± 0.101	$0.656 \pm 1.4e-04$	-0.089 ± 0.058	2.970 ± 1.190	0.001	4 ± 2	3 ± 3	2 ± 2	-	3
XMMXCS J105257.9+572400.9	$0.327^{+0.102}_{-0.099}$	0.289 ± 0.127	-	0.092 ± 0.022	-0.289 ± 0.414	0.001	0 ± 1	1 ± 2	-	1 ± 1	3
XMMXCS J105310.2+574228.5	$0.760^{+0.111}_{-0.111}$	0.659 ± 0.266	-	-0.433 ± 0.379	8.940 ± 7.620	0.001	1 ± 1	46 ± 7	-	85 ± 10	3
XMMXCS J105312.9+574151.5	$0.394^{+0.169}_{-0.158}$	0.419 ± 0.169	-	0.072 ± 0.059	-0.737 ± 1.150	0.001	1 ± 2	0 ± 2	0 ± 0.1	-	3
XMMXCS J105318.5+572043.7	$0.294^{+0.082}_{-0.085}$	0.280 ± 0.052	-	-0.054 ± 0.101	2.680 ± 2.010	0.129	1 ± 2	1 ± 2	0 ± 0.1	2 ± 2	3
XMMXCS J105320.5+571517.0	$0.569^{+0.119}_{-0.119}$	0.622 ± 0.137	-	-0.477 ± 0.291	10.900 ± 6.050	0.030	1 ± 2	0 ± 1	0 ± 0.1	-	3
XMMXCS J105333.4+574240.6	$0.476^{+0.131}_{-0.129}$	0.306 ± 0.054	-	0.042 ± 0.051	-0.072 ± 1.040	0.102	1 ± 3	9 ± 4	-	9 ± 4	3
XMMXCS J105339.4+573524.5	$0.693^{+0.124}_{-0.108}$	0.652 ± 0.149	-	0.340 ± 0.214	-5.870 ± 4.460	0.106	2 ± 2	18 ± 4	0 ± 0.1	18 ± 4	3
XMMXCS J105400.0+573409.9	$0.513^{+0.107}_{-0.109}$	0.330 ± 0.160	-	1.310 ± 0.130	-26.20 ± 2.720	0.001	4 ± 2	1 ± 1	1 ± 1	0 ± 1	3
XMMXCS J105422.7+572635.8	$0.207^{+0.077}_{-0.076}$	0.195 ± 0.057	-	0.021 ± 0.035	0.573 ± 0.669	0.040	1 ± 1	0 ± 1	0 ± 0.1	-	3
XMMXCS J105618.4+065636.7	$0.675^{+0.139}_{-0.127}$	0.589 ± 0.107	$0.621 \pm 1.9e-04$	0.798 ± 0.573	-15.00 ± 11.80	0.303	2 ± 2	23 ± 6	1 ± 1	8 ± 5	3
XMMXCS J105623.4+070258.3	$0.141^{+0.039}_{-0.038}$	0.175 ± 0.033	$0.132 \pm 1.6e-05$	-0.003 ± 0.065	0.987 ± 1.120	0.088	0 ± 1	3 ± 2	-	2 ± 2	3
XMMXCS J105624.1-033523.9	$0.495^{+0.127}_{-0.126}$	0.550 ± 0.164	-	0.225 ± 0.285	-3.660 ± 5.740	0.001	5 ± 3	4 ± 3	3 ± 2	3 ± 2	3

Continued on next page

Table A.2 – continued from previous page

name	z_{RS}	z_{BCG}	z_{spec-g}	cmr_{grad}	cmr_{inter}	cmr_{wid}	n_{gals-c}	n_{gals-l}	n_{200-c}	n_{200-l}	qual
XMMXCS J105632.8+070436.4	$0.162^{+0.040}_{-0.039}$	0.112 ± 0.033	$0.123 \pm 1.3e-05$	0.011 ± 0.050	0.769 ± 0.881	0.088	7 ± 3	8 ± 3	5 ± 2	6 ± 3	3
XMMXCS J105637.0+070742.8	$0.370^{+0.153}_{-0.157}$	0.445 ± 0.255	-	-0.031 ± 0.051	1.230 ± 1.000	0.106	11 ± 4	10 ± 4	10 ± 4	-	3
XMMXCS J105651.0+065419.1	$0.258^{+0.121}_{-0.127}$	0.363 ± 0.101	-	0.019 ± 0.038	0.612 ± 0.721	0.089	10 ± 4	9 ± 4	11 ± 4	9 ± 4	3
XMMXCS J105655.1+070358.0	$0.229^{+0.048}_{-0.046}$	0.185 ± 0.042	-	0.158 ± 0.160	-1.920 ± 3.140	0.157	1 ± 2	0 ± 2	0 ± 0.1	-	3
XMMXCS J105720.0+065956.1	$0.246^{+0.056}_{-0.059}$	0.328 ± 0.096	-	-0.061 ± 0.130	2.530 ± 2.540	0.147	2 ± 2	1 ± 2	0 ± 0.1	0 ± 1	3
XMMXCS J110000.5+242245.2	$0.213^{+0.081}_{-0.082}$	0.121 ± 0.020	$0.120 \pm 2.2e-05$	0.081 ± 0.052	-0.355 ± 0.991	0.082	3 ± 2	1 ± 2	2 ± 1	2 ± 2	3
XMMXCS J110054.3+285551.7	$0.402^{+0.096}_{-0.100}$	0.295 ± 0.076	-	0.366 ± 0.242	-6.550 ± 4.860	0.175	3 ± 3	14 ± 5	0 ± 1	21 ± 6	3
XMMXCS J110242.7+355940.7	$0.148^{+0.071}_{-0.077}$	0.046 ± 0.015	$0.090 \pm 5.7e-06$	-0.002 ± 0.078	1.020 ± 1.340	0.500	3 ± 2	2 ± 2	1 ± 1	2 ± 2	3
XMMXCS J110252.6+355100.6	$0.205^{+0.106}_{-0.111}$	0.260 ± 0.065	-	-0.053 ± 0.032	2.210 ± 0.625	0.085	1 ± 1	0 ± 1	0 ± 0.1	-	3
XMMXCS J110337.3+355506.6	$0.221^{+0.089}_{-0.086}$	0.158 ± 0.036	$0.140 \pm 2.7e-05$	0.063 ± 0.082	0.124 ± 1.530	0.107	2 ± 2	4 ± 3	0 ± 0.1	1 ± 2	3
XMMXCS J110342.7+360014.6	$0.172^{+0.067}_{-0.068}$	0.219 ± 0.082	-	-0.026 ± 0.050	1.670 ± 0.923	0.001	2 ± 2	3 ± 2	1 ± 1	2 ± 2	3
XMMXCS J110353.9+360018.3	$0.306^{+0.068}_{-0.067}$	0.219 ± 0.082	-	0.050 ± 0.137	0.425 ± 2.650	0.127	4 ± 3	4 ± 3	4 ± 2	3 ± 2	3
XMMXCS J110355.2+380525.3	$0.070^{+0.022}_{-0.015}$	0.099 ± 0.022	$0.074 \pm 1.0e-05$	-0.013 ± 0.019	1.120 ± 0.320	0.029	1 ± 1	1 ± 1	0 ± 0.1	0 ± 1	3
XMMXCS J110359.5+380508.9	$0.070^{+0.022}_{-0.015}$	0.099 ± 0.022	$0.074 \pm 1.0e-05$	-0.013 ± 0.019	1.120 ± 0.320	0.029	1 ± 1	1 ± 1	0 ± 0.1	0 ± 1	3
XMMXCS J110405.4+380644.4	$0.139^{+0.031}_{-0.024}$	0.067 ± 0.017	$0.114 \pm 2.3e-05$	-0.086 ± 0.037	2.320 ± 0.633	0.500	1 ± 2	2 ± 2	0 ± 0.1	0 ± 1	3
XMMXCS J110412.8+360448.0	$0.218^{+0.060}_{-0.069}$	0.124 ± 0.046	$0.188 \pm 3.0e-05$	0.131 ± 0.032	-1.320 ± 0.608	0.097	2 ± 2	3 ± 2	0 ± 0.1	0 ± 1	3
XMMXCS J110414.2+382158.8	$0.534^{+0.144}_{-0.141}$	0.523 ± 0.172	-	0.206 ± 0.112	-3.320 ± 2.330	0.086	2 ± 2	1 ± 3	0 ± 1	0 ± 1	3
XMMXCS J110425.7+354354.5	$0.263^{+0.092}_{-0.097}$	0.172 ± 0.031	-	0.330 ± 0.052	-5.470 ± 1.030	0.500	1 ± 3	0 ± 3	0 ± 1	-	3
XMMXCS J110430.2+360015.7	$0.502^{+0.125}_{-0.126}$	0.319 ± 0.094	$0.405 \pm 1.0e-04$	0.037 ± 0.080	0.195 ± 1.630	0.095	12 ± 4	25 ± 6	12 ± 4	29 ± 7	3

Continued on next page

Table A.2 – continued from previous page

name	z_{RS}	z_{BCG}	z_{spec-g}	cmr_{grad}	cmr_{inter}	cmr_{wid}	n_{gals-c}	n_{gals-l}	n_{200-c}	n_{200-l}	qual
XMMXCS J110433.5+380236.3	$0.234^{+0.092}_{-0.093}$	0.148 ± 0.024	$0.153 \pm 2.8e-05$	0.059 ± 0.091	0.035 ± 1.790	0.157	1 ± 2	-	1 ± 1	-	3
XMMXCS J110434.2+382457.2	$0.474^{+0.155}_{-0.155}$	0.531 ± 0.206	$0.510 \pm 1.5e-04$	-0.152 ± 0.114	4.080 ± 2.290	0.098	3 ± 3	4 ± 3	1 ± 1	0 ± 2	3
XMMXCS J110437.0+382533.8	$0.565^{+0.146}_{-0.144}$	0.438 ± 0.314	-	0.963 ± 0.477	-18.70 ± 9.830	0.020	3 ± 2	0 ± 1	1 ± 1	-	3
XMMXCS J110448.5+382116.6	$0.528^{+0.084}_{-0.080}$	0.413 ± 0.066	-	0.071 ± 0.068	-0.513 ± 1.360	0.098	0 ± 2	3 ± 2	-	0 ± 1	3
XMMXCS J110522.2+381105.8	$0.432^{+0.184}_{-0.205}$	0.409 ± 0.067	-	-0.123 ± 0.076	3.140 ± 1.540	0.001	1 ± 2	0 ± 2	0 ± 0.1	-	3
XMMXCS J110547.3+380946.5	$0.571^{+0.127}_{-0.104}$	0.430 ± 0.065	-	0.112 ± 0.135	-1.520 ± 2.690	0.176	2 ± 3	5 ± 4	1 ± 1	6 ± 3	3
XMMXCS J110617.4-181511.5	$0.226^{+0.073}_{-0.073}$	0.174 ± 0.086	-	0.022 ± 0.058	0.721 ± 1.130	0.106	1 ± 2	0 ± 2	1 ± 1	-	3
XMMXCS J111132.2+062628.2	$0.100^{+0.033}_{-0.033}$	0.057 ± 0.018	$0.097 \pm 9.9e-06$	-0.052 ± 0.024	1.600 ± 0.353	0.500	3 ± 2	2 ± 2	0 ± 0.1	0 ± 1	3
XMMXCS J111145.3+062359.7	$0.404^{+0.133}_{-0.142}$	0.320 ± 0.049	-	0.125 ± 0.122	-1.940 ± 2.460	0.133	2 ± 3	1 ± 3	3 ± 2	-	3
XMMXCS J111153.2+022855.0	$0.092^{+0.022}_{-0.022}$	0.099 ± 0.031	$0.092 \pm 1.6e-05$	-0.061 ± 0.019	1.870 ± 0.298	0.044	0 ± 1	1 ± 1	-	1 ± 1	3
XMMXCS J111205.6+664341.2	$0.318^{+0.058}_{-0.058}$	0.279 ± 0.050	-	0.013 ± 0.034	1.300 ± 0.608	0.001	1 ± 2	0 ± 2	1 ± 1	-	3
XMMXCS J111206.6+061240.7	$0.254^{+0.077}_{-0.076}$	0.149 ± 0.035	$0.216 \pm 3.0e-05$	-0.000 ± 0.001	1.310 ± 0.001	0.500	0 ± 3	1 ± 4	-	0 ± 1	3
XMMXCS J111209.2+062448.8	$0.560^{+0.122}_{-0.095}$	0.422 ± 0.190	-	0.421 ± 0.280	-7.820 ± 5.670	0.128	0 ± 2	12 ± 5	-	12 ± 5	3
XMMXCS J111217.7+665959.7	$0.124^{+0.107}_{-0.112}$	0.130 ± 0.025	-	-0.299 ± 0.021	6.650 ± 0.415	0.500	1 ± 1	0 ± 1	0 ± 0.1	-	3
XMMXCS J111246.7+060725.7	$0.478^{+0.084}_{-0.083}$	0.313 ± 0.068	$0.478 \pm 1.6e-04$	0.406 ± 0.157	-7.140 ± 3.170	0.153	3 ± 3	8 ± 4	4 ± 2	6 ± 3	3
XMMXCS J111252.6+061139.8	$0.492^{+0.104}_{-0.092}$	0.303 ± 0.127	$0.470 \pm 1.4e-04$	0.099 ± 0.095	-1.200 ± 1.910	0.111	3 ± 3	5 ± 4	0 ± 1	-	3
XMMXCS J111504.2+424415.9	$0.193^{+0.127}_{-0.092}$	0.225 ± 0.040	-	-0.116 ± 0.071	3.580 ± 1.370	0.111	1 ± 1	1 ± 2	0 ± 0.1	0 ± 1	3
XMMXCS J111554.0+422727.3	$0.310^{+0.073}_{-0.073}$	0.217 ± 0.059	-	0.241 ± 0.155	-3.370 ± 3.130	0.173	4 ± 3	5 ± 3	0 ± 0.1	0 ± 2	3
XMMXCS J111619.6+425047.4	$0.449^{+0.133}_{-0.132}$	0.506 ± 0.080	-	0.012 ± 0.093	0.526 ± 1.890	0.001	8 ± 4	8 ± 4	4 ± 3	4 ± 3	3

Continued on next page

Table A.2 – continued from previous page

name	z_{RS}	z_{BCG}	z_{spec-g}	cmr_{grad}	cmr_{inter}	cmr_{wid}	n_{gals-c}	n_{gals-l}	n_{200-c}	n_{200-l}	qual
XMMXCS J111703.5+174440.7	$0.410^{+0.131}_{-0.130}$	0.451 ± 0.072	$0.450 \pm 7.8e-05$	0.052 ± 0.054	-0.340 ± 1.070	0.115	4 ± 3	4 ± 4	0 ± 1	-	3
XMMXCS J111711.5+423610.5	$0.174^{+0.041}_{-0.043}$	0.156 ± 0.030	-	-0.034 ± 0.031	1.850 ± 0.554	0.017	1 ± 1	2 ± 2	0 ± 0.1	1 ± 1	3
XMMXCS J111730.3+441701.0	$0.326^{+0.091}_{-0.081}$	0.339 ± 0.066	-	0.088 ± 0.078	-0.755 ± 1.490	0.001	2 ± 2	-	1 ± 1	-	3
XMMXCS J111735.9+074249.5	$0.480^{+0.097}_{-0.097}$	0.563 ± 0.101	$0.515 \pm 2.1e-04$	0.033 ± 0.055	0.171 ± 1.120	0.071	17 ± 5	25 ± 6	26 ± 6	51 ± 8	3
XMMXCS J111800.9+175125.9	$0.708^{+0.129}_{-0.129}$	0.589 ± 0.255	-	0.137 ± 0.088	-2.090 ± 1.820	0.001	1 ± 1	0 ± 1	1 ± 1	-	3
XMMXCS J111802.4+402733.7	$0.129^{+0.025}_{-0.025}$	0.127 ± 0.033	-	-0.243 ± 0.001	4.960 ± 0.001	0.500	1 ± 2	0 ± 2	0 ± 0.1	-	3
XMMXCS J111804.4+403452.4	$0.336^{+0.062}_{-0.063}$	0.405 ± 0.060	-	-0.087 ± 0.061	3.390 ± 1.200	0.001	6 ± 3	6 ± 3	5 ± 2	6 ± 3	3
XMMXCS J111817.9+075829.3	$0.475^{+0.125}_{-0.125}$	0.540 ± 0.081	-	0.031 ± 0.092	0.253 ± 1.850	0.078	7 ± 3	13 ± 4	2 ± 2	-	3
XMMXCS J111857.8+431551.8	$0.300^{+0.061}_{-0.062}$	0.298 ± 0.045	-	0.005 ± 0.083	1.420 ± 1.580	0.001	4 ± 3	1 ± 2	1 ± 1	2 ± 2	3
XMMXCS J111907.0+130029.2	$0.602^{+0.171}_{-0.172}$	0.516 ± 0.199	-	1.220 ± 0.471	-24.20 ± 9.750	0.001	2 ± 2	0 ± 1	1 ± 1	-	3
XMMXCS J111932.8+212313.7	$0.367^{+0.094}_{-0.094}$	0.304 ± 0.069	-	-0.036 ± 0.076	2.210 ± 1.510	0.001	5 ± 3	7 ± 3	4 ± 2	31 ± 6	3
XMMXCS J111942.8+212646.5	$0.172^{+0.100}_{-0.102}$	0.081 ± 0.021	$0.071 \pm 1.3e-05$	0.0 ± -1.00	0.294 ± -1.00	0.500	0 ± 2	1 ± 3	-	1 ± 2	3
XMMXCS J111955.0+211733.5	$0.177^{+0.056}_{-0.055}$	0.135 ± 0.027	$0.114 \pm 1.8e-05$	0.029 ± 0.045	0.421 ± 0.833	0.064	1 ± 2	2 ± 2	0 ± 0.1	1 ± 1	3
XMMXCS J112012.9+132632.8	$0.270^{+0.049}_{-0.050}$	0.245 ± 0.043	$0.271 \pm 5.4e-05$	-0.015 ± 0.028	1.760 ± 0.507	0.001	1 ± 2	2 ± 2	0 ± 0.1	0 ± 1	3
XMMXCS J112013.6+133405.5	$0.063^{+0.053}_{-0.053}$	0.098 ± 0.031	-	-0.065 ± 0.021	1.460 ± 0.289	0.500	7 ± 3	43 ± 7	6 ± 3	56 ± 8	3
XMMXCS J112055.1+134523.2	$0.215^{+0.068}_{-0.064}$	0.132 ± 0.039	-	0.886 ± 0.003	-15.80 ± 0.046	0.500	3 ± 2	1 ± 2	3 ± 2	0 ± 1	3
XMMXCS J112224.4+053601.0	$0.424^{+0.104}_{-0.103}$	0.336 ± 0.128	-	0.068 ± 0.168	0.330 ± 3.340	0.070	4 ± 3	27 ± 6	0 ± 1	6 ± 4	3
XMMXCS J112225.6+242234.5	$0.561^{+0.131}_{-0.130}$	0.422 ± 0.091	-	1.020 ± 0.460	-19.60 ± 9.350	0.096	4 ± 2	1 ± 1	5 ± 2	6 ± 3	3
XMMXCS J112324.9+054307.2	$0.530^{+0.147}_{-0.148}$	0.471 ± 0.071	-	0.499 ± 0.235	-9.140 ± 4.770	0.146	0 ± 2	4 ± 3	-	3 ± 2	3

Continued on next page

Table A.2 – continued from previous page

name	z_{RS}	z_{BCG}	z_{spec-g}	cmr_{grad}	cmr_{inter}	cmr_{wid}	n_{gals-c}	n_{gals-l}	n_{200-c}	n_{200-l}	qual
XMMXCS J112348.3+053525.0	$0.519^{+0.109}_{-0.108}$	0.424 ± 0.068	-	-0.016 ± 0.202	1.230 ± 4.170	0.104	8 ± 4	14 ± 5	7 ± 3	16 ± 5	3
XMMXCS J112515.7+385434.6	$0.420^{+0.121}_{-0.122}$	0.499 ± 0.076	$0.426 \pm 7.2e-05$	-0.109 ± 0.094	3.700 ± 1.910	0.141	10 ± 4	9 ± 4	10 ± 4	-	3
XMMXCS J112551.9+384414.9	$0.334^{+0.096}_{-0.089}$	0.201 ± 0.065	-	-0.762 ± 5.400	16.100 ± 111	0.500	6 ± 4	3 ± 3	3 ± 3	1 ± 2	3
XMMXCS J112843.3+582803.6	$0.229^{+0.065}_{-0.066}$	0.243 ± 0.048	-	-0.076 ± 0.026	2.810 ± 0.467	0.116	1 ± 2	4 ± 3	0 ± 0.1	0 ± 1	3
XMMXCS J113010.5-042039.9	$0.157^{+0.065}_{-0.066}$	0.223 ± 0.054	-	-0.074 ± 0.008	2.360 ± 0.149	0.500	2 ± 3	4 ± 3	2 ± 2	3 ± 2	3
XMMXCS J113055.2+311334.1	$0.676^{+0.120}_{-0.105}$	0.680 ± 0.131	-	-0.068 ± 0.140	2.130 ± 2.810	0.105	1 ± 2	-	2 ± 1	-	3
XMMXCS J113138.9-034713.7	$0.333^{+0.081}_{-0.080}$	0.160 ± 0.026	-	0.129 ± 0.093	-1.100 ± 1.900	0.095	8 ± 3	0 ± 2	5 ± 3	-	3
XMMXCS J113140.6-040915.7	$0.401^{+0.136}_{-0.148}$	0.348 ± 0.094	-	0.516 ± 0.291	-8.870 ± 5.900	0.262	1 ± 3	-	0 ± 1	-	3
XMMXCS J113239.4-035052.2	$0.584^{+0.119}_{-0.119}$	0.452 ± 0.191	-	0.020 ± 0.105	0.711 ± 2.140	0.128	10 ± 4	132 ± 12	9 ± 3	32 ± 11	3
XMMXCS J113421.8+662731.4	$0.116^{+0.089}_{-0.103}$	0.151 ± 0.044	$0.113 \pm 2.4e-05$	-0.006 ± 0.016	1.080 ± 0.296	0.033	1 ± 1	2 ± 2	0 ± 0.1	0 ± 1	3
XMMXCS J113755.9+215640.9	$0.255^{+0.120}_{-0.121}$	0.171 ± 0.107	-	-0.231 ± 0.229	5.750 ± 4.490	0.164	9 ± 3	10 ± 4	8 ± 3	8 ± 3	3
XMMXCS J113804.2+031534.6	$0.343^{+0.080}_{-0.080}$	0.257 ± 0.052	-	0.033 ± 0.067	0.912 ± 1.300	0.001	7 ± 3	8 ± 4	5 ± 3	8 ± 3	3
XMMXCS J113958.9+025846.9	$0.121^{+0.021}_{-0.022}$	0.128 ± 0.023	$0.120 \pm 2.2e-05$	-0.018 ± 0.064	1.270 ± 1.060	0.084	2 ± 2	1 ± 1	0 ± 0.1	1 ± 1	3
XMMXCS J114022.1+660811.9	$0.158^{+0.056}_{-0.054}$	0.174 ± 0.037	-	0.043 ± 0.053	-0.035 ± 1.020	0.110	0 ± 1	1 ± 1	-	0 ± 1	3
XMMXCS J114037.9+030801.6	$0.204^{+0.060}_{-0.063}$	0.146 ± 0.102	-	0.127 ± 0.121	-1.290 ± 2.280	0.010	1 ± 1	1 ± 2	2 ± 1	2 ± 2	3
XMMXCS J114126.7+655613.0	$0.251^{+0.077}_{-0.082}$	0.339 ± 0.061	-	0.021 ± 0.112	0.963 ± 2.110	0.159	1 ± 1	0 ± 1	0 ± 0.1	-	3
XMMXCS J114349.2+195806.0	$0.377^{+0.060}_{-0.064}$	0.368 ± 0.121	$0.385 \pm 1.1e-04$	-0.007 ± 0.021	1.890 ± 0.366	0.001	2 ± 2	6 ± 3	0 ± 1	1 ± 2	3
XMMXCS J114438.9+194522.7	$0.137^{+0.106}_{-0.110}$	0.065 ± 0.025	$0.027 \pm 1.2e-05$	0.017 ± 0.017	0.353 ± 0.310	0.107	9 ± 3	22 ± 5	6 ± 3	34 ± 7	3
XMMXCS J114447.6+194703.0	$0.042^{+0.021}_{-0.018}$	0.065 ± 0.025	$0.024 \pm 7.8e-06$	-0.062 ± 0.032	1.570 ± 0.446	0.075	19 ± 5	18 ± 4	30 ± 6	30 ± 6	3

Continued on next page

Table A.2 – continued from previous page

name	z_{RS}	z_{BCG}	z_{spec-g}	cmr_{grad}	cmr_{inter}	cmr_{wid}	n_{gals-c}	n_{gals-l}	n_{200-c}	n_{200-l}	qual
XMMXCS J114515.3+202055.6	$0.192^{+0.063}_{-0.065}$	0.043 ± 0.018	$0.079 \pm 1.2e-05$	-0.098 ± 0.004	2.990 ± 0.073	0.500	5 ± 3	-	4 ± 3	-	3
XMMXCS J114628.0+522106.2	$0.331^{+0.109}_{-0.107}$	0.192 ± 0.035	$0.234 \pm 3.9e-05$	0.066 ± 0.042	0.200 ± 0.882	0.082	4 ± 3	4 ± 3	3 ± 2	4 ± 2	3
XMMXCS J114638.2+202201.7	$0.804^{+0.109}_{-0.109}$	0.630 ± 0.230	-	-0.914 ± 0.588	19.100 ± 12.10	0.137	2 ± 1	0 ± 1	1 ± 1	-	3
XMMXCS J114946.6+550609.0	$0.229^{+0.051}_{-0.050}$	0.201 ± 0.035	-	-0.004 ± 0.026	1.370 ± 0.480	0.091	1 ± 2	1 ± 2	0 ± 0.1	0 ± 1	3
XMMXCS J115005.4+013851.5	$0.359^{+0.124}_{-0.123}$	0.256 ± 0.077	-	0.006 ± 0.096	1.210 ± 1.880	0.001	2 ± 2	3 ± 3	1 ± 1	3 ± 2	3
XMMXCS J115008.0+550745.0	$0.214^{+0.056}_{-0.055}$	0.143 ± 0.025	$0.228 \pm 7.3e-05$	0.032 ± 0.043	0.664 ± 0.797	0.096	11 ± 4	10 ± 4	10 ± 3	9 ± 3	3
XMMXCS J115037.6+284504.0	$0.240^{+0.064}_{-0.066}$	0.184 ± 0.034	-	0.055 ± 0.042	0.222 ± 0.764	0.108	2 ± 2	1 ± 2	1 ± 1	-	3
XMMXCS J115041.0+551453.0	$0.171^{+0.075}_{-0.077}$	0.238 ± 0.039	-	-0.078 ± 0.030	2.580 ± 0.585	0.079	1 ± 1	0 ± 1	0 ± 0.1	-	3
XMMXCS J115053.3+015714.7	$0.478^{+0.451}_{-0.451}$	0.468 ± 0.286	-	0.007 ± 0.079	0.539 ± 1.660	0.108	0 ± 3	20 ± 5	-	5 ± 5	3
XMMXCS J115107.2+550440.7	$0.080^{+0.020}_{-0.018}$	0.075 ± 0.015	$0.079 \pm 1.5e-05$	0.002 ± 0.016	0.798 ± 0.279	0.048	2 ± 2	2 ± 2	0 ± 0.1	3 ± 2	3
XMMXCS J115116.7+014611.5	$0.153^{+0.047}_{-0.047}$	0.106 ± 0.030	$0.131 \pm 9.7e-06$	0.0 ± -1.00	1.560 ± -1.00	0.500	3 ± 2	3 ± 2	0 ± 0.1	0 ± 1	3
XMMXCS J115131.6+014814.5	$0.166^{+0.052}_{-0.053}$	0.222 ± 0.058	-	-0.031 ± 0.042	1.710 ± 0.772	0.063	6 ± 3	7 ± 3	4 ± 2	5 ± 2	3
XMMXCS J115211.7+551411.2	$0.487^{+0.117}_{-0.107}$	0.330 ± 0.148	-	0.086 ± 0.071	-0.988 ± 1.400	0.075	2 ± 3	11 ± 4	-	12 ± 4	3
XMMXCS J115225.9+370428.7	$0.249^{+0.107}_{-0.110}$	0.166 ± 0.026	$0.163 \pm 3.7e-05$	-0.038 ± 0.028	1.790 ± 0.537	0.090	1 ± 2	4 ± 3	0 ± 0.1	-	3
XMMXCS J115436.6+521108.2	$0.366^{+0.143}_{-0.142}$	0.289 ± 0.087	-	-0.344 ± 0.108	7.580 ± 2.220	0.001	2 ± 2	2 ± 2	2 ± 1	0 ± 1	3
XMMXCS J115530.2+233820.8	$0.153^{+0.074}_{-0.074}$	0.101 ± 0.026	-	0.014 ± 0.038	0.481 ± 0.730	0.089	2 ± 2	1 ± 1	0 ± 0.1	0 ± 1	3
XMMXCS J115554.5+232409.4	$0.189^{+0.040}_{-0.036}$	0.184 ± 0.031	$0.176 \pm 3.6e-05$	-0.376 ± 0.894	7.590 ± 15.70	0.500	1 ± 3	4 ± 3	0 ± 0.1	2 ± 2	3
XMMXCS J115628.5+550735.3	$0.073^{+0.007}_{-0.007}$	0.057 ± 0.038	$0.060 \pm 1.0e-05$	0.037 ± 0.008	0.252 ± 0.111	0.061	3 ± 2	3 ± 2	1 ± 1	2 ± 2	3
XMMXCS J115641.0+524322.9	$0.395^{+0.125}_{-0.123}$	0.242 ± 0.045	-	0.104 ± 0.060	-0.586 ± 1.170	0.106	10 ± 4	11 ± 4	11 ± 4	12 ± 4	3

Continued on next page

Table A.2 – continued from previous page

name	z_{RS}	z_{BCG}	z_{spec-g}	cmr_{grad}	cmr_{inter}	cmr_{wid}	n_{gals-c}	n_{gals-l}	n_{200-c}	n_{200-l}	qual
XMMXCS J115700.2+435702.8	$0.445^{+0.091}_{-0.087}$	0.374 ± 0.061	-	-0.342 ± 0.142	8.350 ± 2.910	0.072	2 ± 3	3 ± 3	-	0 ± 2	3
XMMXCS J115710.4+553452.6	$0.135^{+0.060}_{-0.060}$	0.061 ± 0.028	$0.134 \pm 1.9e-05$	-0.002 ± 0.001	0.598 ± 0.001	0.500	2 ± 3	1 ± 3	2 ± 2	2 ± 2	3
XMMXCS J115736.0+435303.9	$0.128^{+0.045}_{-0.044}$	0.079 ± 0.021	$0.134 \pm 2.2e-05$	-0.081 ± 0.020	2.180 ± 0.343	0.024	1 ± 1	1 ± 1	0 ± 0.1	0 ± 1	3
XMMXCS J115755.0+434751.7	$0.088^{+0.019}_{-0.020}$	0.089 ± 0.030	$0.083 \pm 1.2e-05$	0.046 ± 0.023	0.150 ± 0.349	0.071	5 ± 3	5 ± 3	2 ± 2	8 ± 3	3
XMMXCS J115755.8+434853.5	$0.088^{+0.020}_{-0.020}$	0.089 ± 0.030	$0.083 \pm 1.2e-05$	-0.006 ± 0.019	0.942 ± 0.326	0.059	5 ± 2	4 ± 2	2 ± 2	3 ± 2	3
XMMXCS J115817.9+524131.3	$0.513^{+0.170}_{-0.170}$	0.605 ± 0.129	-	-0.084 ± 0.034	2.670 ± 0.664	0.004	12 ± 4	15 ± 4	11 ± 4	17 ± 5	3
XMMXCS J115849.0+435144.0	$0.221^{+0.071}_{-0.071}$	0.235 ± 0.037	$0.264 \pm 3.5e-05$	0.192 ± 0.036	-2.560 ± 0.698	0.500	1 ± 3	0 ± 3	0 ± 1	-	3
XMMXCS J115849.5+441008.8	$0.305^{+0.099}_{-0.108}$	0.216 ± 0.053	-	0.101 ± 0.070	-0.605 ± 1.370	0.145	3 ± 3	-	0 ± 1	-	3
XMMXCS J115914.5+435419.8	$0.321^{+0.087}_{-0.091}$	0.386 ± 0.085	-	-1.200 ± 0.070	26.300 ± 1.450	0.500	1 ± 1	1 ± 2	1 ± 1	1 ± 1	3
XMMXCS J115941.9+435804.5	$0.252^{+0.117}_{-0.120}$	0.217 ± 0.084	-	-0.047 ± 0.030	2.090 ± 0.584	0.001	1 ± 1	0 ± 1	0 ± 0.1	-	3
XMMXCS J115955.3-032737.2	$0.279^{+0.097}_{-0.101}$	0.294 ± 0.090	-	0.187 ± 0.090	-2.510 ± 1.760	0.063	0 ± 1	1 ± 2	-	0 ± 1	3
XMMXCS J120003.0+341428.5	$0.440^{+0.129}_{-0.120}$	0.330 ± 0.059	-	-0.086 ± 0.129	3.310 ± 2.570	0.172	2 ± 3	2 ± 3	0 ± 0.1	0 ± 1	3
XMMXCS J120023.5-031904.4	$0.394^{+0.132}_{-0.134}$	0.313 ± 0.049	-	0.275 ± 0.162	-3.560 ± 3.010	0.241	6 ± 3	6 ± 4	5 ± 3	4 ± 3	3
XMMXCS J120027.5-031523.4	$0.298^{+0.134}_{-0.165}$	0.201 ± 0.031	-	0.033 ± 0.052	0.630 ± 1.020	0.100	5 ± 3	4 ± 3	0 ± 1	1 ± 2	3
XMMXCS J120033.4+341535.3	$0.353^{+0.063}_{-0.061}$	0.327 ± 0.061	-	0.003 ± 0.014	0.560 ± 0.284	0.001	1 ± 2	1 ± 3	0 ± 0.1	-	3
XMMXCS J120045.5+064639.0	$0.110^{+0.046}_{-0.042}$	0.068 ± 0.020	$0.105 \pm 1.9e-05$	0.051 ± 0.007	0.064 ± 0.102	0.001	1 ± 1	1 ± 1	0 ± 0.1	0 ± 1	3
XMMXCS J120050.3+341853.8	$0.454^{+0.123}_{-0.113}$	0.388 ± 0.061	$0.485 \pm 1.3e-04$	0.114 ± 0.117	-1.390 ± 2.320	0.107	3 ± 3	3 ± 3	1 ± 1	-	3
XMMXCS J120053.4-031922.5	$0.249^{+0.087}_{-0.086}$	0.191 ± 0.029	-	-0.038 ± 0.051	1.920 ± 1.000	0.073	3 ± 2	2 ± 2	2 ± 1	1 ± 1	3
XMMXCS J120053.8+553330.3	$0.207^{+0.090}_{-0.090}$	0.202 ± 0.056	-	0.005 ± 0.028	1.020 ± 0.541	0.118	3 ± 2	4 ± 3	0 ± 1	1 ± 2	3

Continued on next page

Table A.2 – continued from previous page

name	z_{RS}	z_{BCG}	z_{spec-g}	cmr_{grad}	cmr_{inter}	cmr_{wid}	n_{gals-c}	n_{gals-l}	n_{200-c}	n_{200-l}	qual
XMMXCS J120108.0-031626.1	$0.233^{+0.074}_{-0.067}$	0.183 ± 0.047	-	0.267 ± 0.520	-4.060 ± 9.890	0.030	1 ± 1	1 ± 1	0 ± 0.1	0 ± 1	3
XMMXCS J120109.6-033708.1	$0.210^{+0.082}_{-0.092}$	0.137 ± 0.022	$0.142 \pm 2.9e-05$	0.058 ± 0.034	0.065 ± 0.623	0.036	3 ± 2	3 ± 2	3 ± 2	2 ± 2	3
XMMXCS J120115.3-033954.8	$0.327^{+0.124}_{-0.126}$	0.137 ± 0.022	$0.142 \pm 2.9e-05$	0.222 ± 0.281	-2.810 ± 5.340	0.158	0 ± 2	1 ± 3	-	16 ± 4	3
XMMXCS J120228.0+442711.6	$0.415^{+0.101}_{-0.102}$	0.333 ± 0.053	-	-0.007 ± 0.099	1.830 ± 1.940	0.001	5 ± 3	7 ± 4	0 ± 1	2 ± 2	3
XMMXCS J120340.5+443737.0	$0.337^{+0.041}_{-0.042}$	0.346 ± 0.051	$0.337 \pm 7.9e-05$	-0.030 ± 0.009	2.250 ± 0.156	0.001	2 ± 2	1 ± 2	1 ± 1	1 ± 1	3
XMMXCS J120349.1+020556.7	$0.077^{+0.035}_{-0.038}$	0.111 ± 0.025	$0.089 \pm 1.2e-05$	0.032 ± 0.084	0.458 ± 1.580	0.129	1 ± 2	2 ± 2	0 ± 0.1	0 ± 1	3
XMMXCS J120439.7+351212.1	$0.642^{+0.122}_{-0.154}$	0.535 ± 0.158	-	0.147 ± 0.094	-1.910 ± 1.890	0.136	1 ± 2	7 ± 3	1 ± 1	7 ± 3	3
XMMXCS J120550.8+442904.8	$0.449^{+0.121}_{-0.124}$	0.560 ± 0.091	-	-0.009 ± 0.067	1.840 ± 1.310	0.001	14 ± 5	14 ± 5	19 ± 5	18 ± 5	3
XMMXCS J120553.0+351130.1	$0.112^{+0.064}_{-0.066}$	0.077 ± 0.020	$0.079 \pm 9.5e-06$	-0.006 ± 0.144	1.100 ± 2.800	0.500	2 ± 2	4 ± 3	2 ± 1	4 ± 2	3
XMMXCS J120638.92+281025.5	$0.081^{+0.031}_{-0.041}$	0.059 ± 0.024	$0.048 \pm 7.9e-06$	-0.028 ± 0.012	1.240 ± 0.213	0.075	7 ± 3	5 ± 2	5 ± 2	4 ± 2	3
XMMXCS J120638.9+281026.3	$0.081^{+0.031}_{-0.041}$	0.059 ± 0.024	$0.048 \pm 7.9e-06$	-0.028 ± 0.012	1.240 ± 0.213	0.075	7 ± 3	5 ± 2	5 ± 2	4 ± 2	3
XMMXCS J120703.1+652401.5	$0.171^{+0.061}_{-0.062}$	0.142 ± 0.053	-	0.186 ± 0.197	-2.640 ± 3.740	0.100	0 ± 0.1	1 ± 1	-	0 ± 1	3
XMMXCS J120713.5+251641.6	$0.381^{+0.097}_{-0.101}$	0.380 ± 0.056	$0.391 \pm 1.1e-04$	-0.044 ± 0.055	2.510 ± 1.110	0.093	4 ± 3	2 ± 3	0 ± 1	-	3
XMMXCS J120833.5+433152.0	$0.103^{+0.022}_{-0.023}$	0.135 ± 0.031	$0.091 \pm 1.7e-05$	-0.279 ± 0.001	5.440 ± 0.001	0.500	4 ± 3	2 ± 2	2 ± 2	3 ± 2	3
XMMXCS J120850.9+452950.8	$0.319^{+0.069}_{-0.072}$	0.276 ± 0.041	$0.269 \pm 5.5e-05$	-0.002 ± 0.039	1.610 ± 0.755	0.001	4 ± 3	6 ± 3	0 ± 1	1 ± 2	3
XMMXCS J120900.6+250551.1	$0.202^{+0.062}_{-0.061}$	0.111 ± 0.021	$0.152 \pm 3.2e-05$	0.107 ± 0.031	-0.865 ± 0.601	0.077	3 ± 2	5 ± 3	2 ± 2	5 ± 3	3
XMMXCS J120943.2+391440.3	$0.131^{+0.029}_{-0.029}$	0.180 ± 0.028	$0.187 \pm 3.5e-05$	-0.074 ± 0.007	2.270 ± 0.126	0.500	1 ± 2	0 ± 2	0 ± 0.1	-	3
XMMXCS J120943.4+393643.5	$0.210^{+0.069}_{-0.071}$	0.241 ± 0.037	-	-0.025 ± 0.044	1.700 ± 0.836	0.081	1 ± 2	2 ± 2	-	1 ± 1	3
XMMXCS J121009.9+393019.2	$0.635^{+0.126}_{-0.118}$	0.550 ± 0.211	-	-0.005 ± 0.093	1.080 ± 1.890	0.061	1 ± 2	0 ± 1	1 ± 1	-	3

Continued on next page

Table A.2 – continued from previous page

name	z_{RS}	z_{BCG}	z_{spec-g}	cmr_{grad}	cmr_{inter}	cmr_{wid}	n_{gals-c}	n_{gals-l}	n_{200-c}	n_{200-l}	qual
XMMXCS J121020.8+503215.3	$0.517^{+0.101}_{-0.097}$	0.400 ± 0.127	-	0.074 ± 0.076	-0.640 ± 1.520	0.086	2 ± 3	4 ± 3	2 ± 2	6 ± 3	3
XMMXCS J121030.8+390859.7	$0.266^{+0.021}_{-0.021}$	0.214 ± 0.036	-	-0.000 ± 0.001	0.929 ± 0.001	0.500	0 ± 2	6 ± 2	-	2 ± 1	3
XMMXCS J121031.2+423035.6	$0.294^{+0.095}_{-0.096}$	0.155 ± 0.077	-	0.235 ± 0.139	-3.420 ± 2.710	0.106	2 ± 2	1 ± 2	1 ± 1	1 ± 1	3
XMMXCS J121047.8+392957.1	$0.589^{+0.146}_{-0.144}$	0.615 ± 0.112	-	0.031 ± 0.182	0.351 ± 3.750	0.001	4 ± 2	1 ± 1	0 ± 1	-	3
XMMXCS J121054.7+393608.3	$0.144^{+0.031}_{-0.024}$	0.101 ± 0.025	$0.147 \pm 6.8e-06$	0.305 ± 0.149	-4.580 ± 2.580	0.500	1 ± 2	1 ± 2	0 ± 0.1	1 ± 1	3
XMMXCS J121110.5+502546.6	$0.333^{+0.075}_{-0.075}$	0.280 ± 0.069	-	-0.029 ± 0.097	2.070 ± 1.900	0.001	1 ± 2	0 ± 2	1 ± 1	-	3
XMMXCS J121131.2+391626.1	$0.199^{+0.070}_{-0.073}$	0.227 ± 0.052	$0.208 \pm 7.1e-05$	-0.022 ± 0.018	1.770 ± 0.336	0.006	1 ± 1	0 ± 1	0 ± 0.1	-	3
XMMXCS J121218.1+502046.8	$0.314^{+0.101}_{-0.100}$	0.324 ± 0.052	-	-0.098 ± 0.045	3.480 ± 0.897	0.075	3 ± 2	1 ± 2	0 ± 0.1	0 ± 1	3
XMMXCS J121238.8+130306.5	$0.153^{+0.028}_{-0.024}$	0.158 ± 0.027	$0.149 \pm 3.1e-05$	0.116 ± 0.003	-1.400 ± 0.054	0.500	3 ± 3	1 ± 2	0 ± 0.1	1 ± 1	3
XMMXCS J121239.0+131457.8	$0.301^{+0.083}_{-0.082}$	0.369 ± 0.059	$0.394 \pm 1.1e-04$	-0.282 ± 0.053	6.900 ± 1.030	0.001	4 ± 3	6 ± 3	2 ± 2	5 ± 3	3
XMMXCS J121327.9+140444.1	$0.200^{+0.079}_{-0.076}$	0.155 ± 0.034	$0.123 \pm 1.4e-05$	-0.087 ± 0.001	2.210 ± 0.001	0.500	1 ± 3	2 ± 3	0 ± 1	0 ± 1	3
XMMXCS J121331.9+135526.7	$0.412^{+0.149}_{-0.162}$	0.355 ± 0.077	-	0.005 ± 0.043	0.661 ± 0.845	0.122	3 ± 3	3 ± 3	0 ± 1	1 ± 2	3
XMMXCS J121355.6+140245.0	$0.154^{+0.025}_{-0.025}$	0.158 ± 0.025	$0.154 \pm 1.8e-05$	-0.039 ± 0.029	1.790 ± 0.493	0.099	1 ± 2	4 ± 2	0 ± 0.1	3 ± 2	3
XMMXCS J121408.5+140935.7	$0.046^{+0.069}_{-0.046}$	0.059 ± 0.019	$0.051 \pm 7.6e-06$	-0.024 ± 0.024	1.190 ± 0.333	0.096	3 ± 2	0 ± 1	2 ± 1	-	3
XMMXCS J121415.3+135059.6	$0.210^{+0.091}_{-0.108}$	0.178 ± 0.045	-	0.066 ± 0.030	-0.017 ± 0.566	0.093	1 ± 2	2 ± 2	-	0 ± 1	3
XMMXCS J121440.9+140326.3	$0.153^{+0.120}_{-0.120}$	0.082 ± 0.025	$0.106 \pm 1.4e-05$	-0.004 ± 0.020	0.993 ± 0.337	0.089	6 ± 3	9 ± 4	3 ± 2	9 ± 4	3
XMMXCS J121443.8+140305.5	$0.157^{+0.029}_{-0.029}$	0.082 ± 0.025	$0.106 \pm 1.4e-05$	0.003 ± 0.025	0.927 ± 0.420	0.114	9 ± 3	13 ± 4	9 ± 3	15 ± 5	3
XMMXCS J121502.4+140203.1	$0.118^{+0.040}_{-0.063}$	0.045 ± 0.022	$0.044 \pm 1.4e-05$	-0.000 ± 0.001	0.658 ± 0.001	0.500	9 ± 4	12 ± 5	2 ± 2	12 ± 5	3
XMMXCS J121558.5-032759.4	$0.101^{+0.013}_{-0.013}$	0.125 ± 0.021	$0.102 \pm 1.1e-05$	-0.019 ± 0.046	1.210 ± 0.787	0.107	1 ± 2	3 ± 2	0 ± 0.1	1 ± 1	3

Continued on next page

Table A.2 – continued from previous page

name	z_{RS}	z_{BCG}	z_{spec-g}	cmr_{grad}	cmr_{inter}	cmr_{wid}	n_{gals-c}	n_{gals-l}	n_{200-c}	n_{200-l}	qual
XMMXCS J121651.9+375437.1	$0.223^{+0.046}_{-0.043}$	0.211 ± 0.053	$0.215 \pm 3.3e-05$	-0.754 ± 0.017	15.000 ± 0.318	0.500	2 ± 3	4 ± 3	0 ± 1	2 ± 2	3
XMMXCS J121657.2+071215.6	$0.415^{+0.146}_{-0.146}$	0.314 ± 0.163	-	0.474 ± 0.484	-8.660 ± 10.10	0.001	3 ± 3	-	0 ± 1	-	3
XMMXCS J121700.3+471511.8	$0.371^{+0.095}_{-0.083}$	0.453 ± 0.070	-	0.279 ± 0.054	-5.510 ± 1.130	0.500	3 ± 3	-	0 ± 1	-	3
XMMXCS J121708.6+034049.3	$0.033^{+0.030}_{-0.030}$	0.029 ± 0.013	$0.007 \pm 5.9e-06$	-0.040 ± 0.013	0.933 ± 0.168	0.500	1 ± 1	0 ± 1	0 ± 0.1	-	3
XMMXCS J121753.0+470540.8	$0.231^{+0.102}_{-0.108}$	0.207 ± 0.044	-	0.005 ± 0.042	1.080 ± 0.804	0.174	1 ± 2	4 ± 3	0 ± 0.1	0 ± 1	3
XMMXCS J121758.7+374842.7	$0.431^{+0.120}_{-0.116}$	0.438 ± 0.069	-	0.210 ± 0.103	-3.410 ± 2.050	0.118	5 ± 3	5 ± 3	0 ± 1	-	3
XMMXCS J121806.6+295848.8	$0.290^{+0.126}_{-0.120}$	0.118 ± 0.045	-	0.585 ± 0.060	-10.40 ± 1.200	0.500	10 ± 4	7 ± 4	10 ± 4	7 ± 4	3
XMMXCS J121810.7+471530.3	$0.290^{+0.099}_{-0.100}$	0.165 ± 0.031	-	-0.018 ± 0.072	1.660 ± 1.410	0.155	0 ± 2	1 ± 3	-	0 ± 1	3
XMMXCS J121816.9+295010.2	$0.367^{+0.123}_{-0.120}$	0.292 ± 0.092	-	-0.092 ± 0.046	3.100 ± 0.948	0.111	7 ± 3	4 ± 3	2 ± 2	1 ± 2	3
XMMXCS J121828.0+034359.7	$0.545^{+0.137}_{-0.137}$	0.544 ± 0.109	-	0.099 ± 0.137	-0.998 ± 2.760	0.001	6 ± 3	24 ± 5	4 ± 2	18 ± 5	3
XMMXCS J121847.3+472023.6	$0.089^{+0.062}_{-0.065}$	0.099 ± 0.029	-	-0.017 ± 0.001	0.965 ± 0.010	0.500	8 ± 3	17 ± 5	7 ± 3	62 ± 9	3
XMMXCS J121849.1+294014.9	$0.483^{+0.148}_{-0.148}$	0.576 ± 0.134	-	-0.076 ± 0.051	2.450 ± 1.020	0.062	5 ± 3	-	3 ± 2	-	3
XMMXCS J121850.6+472032.7	$0.089^{+0.063}_{-0.067}$	0.099 ± 0.029	-	-0.017 ± 0.001	0.965 ± 0.010	0.500	8 ± 3	4 ± 3	7 ± 3	19 ± 5	3
XMMXCS J121858.2+471823.1	$0.030^{+0.051}_{-0.030}$	0.099 ± 0.029	-	-0.000 ± 0.001	0.388 ± 0.001	0.500	4 ± 2	2 ± 2	5 ± 2	12 ± 4	3
XMMXCS J121906.2+293842.9	$0.585^{+0.153}_{-0.150}$	0.523 ± 0.136	-	-0.399 ± 0.399	9.310 ± 8.300	0.001	2 ± 2	0 ± 1	1 ± 1	-	3
XMMXCS J121912.8+290838.5	$0.173^{+0.069}_{-0.066}$	0.144 ± 0.027	-	0.158 ± 0.026	-1.820 ± 0.486	0.064	1 ± 1	1 ± 1	0 ± 0.1	0 ± 1	3
XMMXCS J121914.4+295756.6	$0.085^{+0.025}_{-0.029}$	0.056 ± 0.022	$0.079 \pm 1.1e-05$	0.058 ± 0.072	-0.093 ± 1.160	0.092	2 ± 2	2 ± 2	1 ± 1	1 ± 1	3
XMMXCS J121916.1+294606.9	$0.100^{+0.049}_{-0.055}$	0.112 ± 0.020	$0.090 \pm 1.5e-05$	0.025 ± 0.001	0.580 ± 0.001	0.500	1 ± 2	0 ± 1	0 ± 0.1	-	3
XMMXCS J121918.6+295426.8	$0.295^{+0.083}_{-0.081}$	0.114 ± 0.033	-	0.341 ± 0.268	-5.480 ± 5.250	0.190	3 ± 3	1 ± 3	2 ± 2	1 ± 1	3

Continued on next page

Table A.2 – continued from previous page

name	z_{RS}	z_{BCG}	z_{spec-g}	cmr_{grad}	cmr_{inter}	cmr_{wid}	n_{gals-c}	n_{gals-l}	n_{200-c}	n_{200-l}	qual
XMMXCS J121946.6+064852.4	$0.532^{+0.084}_{-0.084}$	0.545 ± 0.097	$0.531 \pm 1.6e-04$	0.105 ± 0.153	-1.150 ± 3.070	0.097	3 ± 3	4 ± 3	2 ± 2	-	3
XMMXCS J121950.5+472727.8	$0.211^{+0.101}_{-0.105}$	0.139 ± 0.027	-	0.018 ± 0.021	0.732 ± 0.408	0.079	2 ± 2	1 ± 2	0 ± 0.1	1 ± 1	3
XMMXCS J122009.4+290839.0	$0.281^{+0.087}_{-0.087}$	0.304 ± 0.045	-	-0.042 ± 0.031	2.290 ± 0.593	0.081	5 ± 3	6 ± 3	0 ± 1	1 ± 2	3
XMMXCS J122016.6+064116.5	$0.435^{+0.110}_{-0.110}$	0.558 ± 0.166	-	-0.014 ± 0.150	1.500 ± 3.040	0.126	2 ± 3	-	0 ± 0.1	-	3
XMMXCS J122036.2+291800.5	$0.051^{+0.024}_{-0.024}$	0.066 ± 0.033	$0.046 \pm 1.7e-05$	0.027 ± 0.008	0.462 ± 0.104	0.500	0 ± 2	1 ± 1	-	4 ± 2	3
XMMXCS J122050.5+291152.1	$0.177^{+0.074}_{-0.074}$	0.130 ± 0.022	$0.151 \pm 2.2e-05$	-0.113 ± 0.044	3.020 ± 0.874	0.086	3 ± 2	4 ± 2	3 ± 2	2 ± 2	3
XMMXCS J122112.9+143924.9	$0.297^{+0.057}_{-0.057}$	0.285 ± 0.048	$0.297 \pm 5.5e-05$	-0.002 ± 0.034	1.550 ± 0.618	0.001	1 ± 2	-	0 ± 0.1	-	3
XMMXCS J122118.4+275721.8	$0.607^{+0.145}_{-0.142}$	0.679 ± 0.125	-	-0.196 ± 0.121	5.100 ± 2.460	0.043	5 ± 3	4 ± 3	0 ± 1	2 ± 2	3
XMMXCS J122123.5+275707.4	$0.598^{+0.142}_{-0.139}$	0.679 ± 0.125	-	-0.229 ± 0.123	5.730 ± 2.500	0.001	5 ± 3	4 ± 3	2 ± 2	1 ± 2	3
XMMXCS J122124.6+275419.6	$0.642^{+0.137}_{-0.135}$	0.567 ± 0.175	-	-0.139 ± 0.237	4.000 ± 4.820	0.001	5 ± 3	15 ± 5	5 ± 2	20 ± 5	3
XMMXCS J122124.6+144423.8	$0.554^{+0.155}_{-0.159}$	0.401 ± 0.062	-	0.200 ± 0.328	-3.050 ± 6.750	0.143	3 ± 3	10 ± 4	0 ± 1	10 ± 4	3
XMMXCS J122126.6+142230.4	$0.374^{+0.079}_{-0.073}$	0.222 ± 0.052	$0.364 \pm 1.3e-04$	-0.045 ± 0.002	2.460 ± 0.033	0.500	2 ± 4	3 ± 4	3 ± 2	3 ± 3	3
XMMXCS J122218.3+154023.4	$0.226^{+0.047}_{-0.047}$	0.225 ± 0.035	$0.232 \pm 3.3e-05$	0.081 ± 0.033	-0.063 ± 0.612	0.100	1 ± 2	2 ± 2	1 ± 1	3 ± 2	3
XMMXCS J122306.9+103714.0	$0.038^{+0.047}_{-0.038}$	0.072 ± 0.021	$0.025 \pm 1.1e-05$	-0.073 ± 0.110	1.940 ± 2.050	0.128	1 ± 1	0 ± 1	0 ± 0.1	-	3
XMMXCS J122435.8+321423.5	$0.485^{+0.131}_{-0.129}$	0.358 ± 0.080	-	-0.010 ± 0.172	1.090 ± 3.480	0.136	4 ± 3	-	2 ± 2	-	3
XMMXCS J122439.5+332435.5	$0.357^{+0.126}_{-0.128}$	0.336 ± 0.101	-	-0.000 ± 0.049	0.476 ± 0.976	0.092	3 ± 3	4 ± 3	0 ± 1	0 ± 2	3
XMMXCS J122503.3+332845.5	$0.411^{+0.084}_{-0.084}$	0.462 ± 0.079	-	0.230 ± 0.462	-2.770 ± 9.390	0.001	1 ± 2	1 ± 2	1 ± 1	0 ± 1	3
XMMXCS J122513.4+321357.9	$0.059^{+0.012}_{-0.012}$	0.066 ± 0.016	$0.059 \pm 1.3e-05$	-0.001 ± 0.016	0.909 ± 0.225	0.092	3 ± 2	1 ± 1	2 ± 1	1 ± 1	3
XMMXCS J122513.82+123949.7	$0.355^{+0.062}_{-0.063}$	0.195 ± 0.048	-	0.292 ± 0.099	-3.900 ± 1.960	0.013	3 ± 2	4 ± 3	2 ± 2	10 ± 3	3

Continued on next page

Table A.2 – continued from previous page

name	z_{RS}	z_{BCG}	z_{spec-g}	cmr_{grad}	cmr_{inter}	cmr_{wid}	n_{gals-c}	n_{gals-l}	n_{200-c}	n_{200-l}	qual
XMMXCS J122514.8+124003.1	$0.314^{+0.085}_{-0.085}$	0.195 ± 0.048	-	0.040 ± 0.125	0.794 ± 2.430	0.155	3 ± 3	3 ± 3	3 ± 2	5 ± 3	3
XMMXCS J122524.5+071956.9	$0.418^{+0.169}_{-0.183}$	0.251 ± 0.054	$0.547 \pm 2.4e-04$	-0.295 ± 0.352	7.050 ± 7.240	0.001	7 ± 4	6 ± 4	3 ± 3	2 ± 3	3
XMMXCS J122530.6+320729.9	$0.441^{+0.128}_{-0.129}$	0.268 ± 0.101	-	0.018 ± 0.095	1.150 ± 1.870	0.122	9 ± 4	9 ± 4	6 ± 3	6 ± 3	3
XMMXCS J122532.6+332528.4	$0.598^{+0.080}_{-0.073}$	0.350 ± 0.272	$0.587 \pm 9.5e-05$	0.074 ± 0.035	-0.714 ± 0.685	0.001	1 ± 2	10 ± 4	0 ± 0.1	11 ± 4	3
XMMXCS J122534.2+180240.3	$0.409^{+0.171}_{-0.247}$	0.349 ± 0.115	-	0.314 ± 0.101	-6.230 ± 2.050	0.041	3 ± 2	-	3 ± 2	-	3
XMMXCS J122542.7+044939.9	$0.287^{+0.102}_{-0.103}$	0.261 ± 0.059	-	0.022 ± 0.025	0.952 ± 0.503	0.001	1 ± 2	2 ± 2	-	1 ± 1	3
XMMXCS J122546.67+123941.6	$0.060^{+0.056}_{-0.058}$	0.068 ± 0.035	$0.009 \pm 1.8e-05$	-0.018 ± 0.007	0.896 ± 0.101	0.058	1 ± 1	0 ± 2	0 ± 0.1	-	3
XMMXCS J122549.5+312319.4	$0.335^{+0.057}_{-0.056}$	0.346 ± 0.055	-	0.107 ± 0.061	-0.441 ± 1.180	0.001	2 ± 2	3 ± 2	0 ± 0.1	1 ± 1	3
XMMXCS J122550.7+334130.5	$0.452^{+0.124}_{-0.124}$	0.541 ± 0.088	-	-0.166 ± 0.047	4.180 ± 0.943	0.062	10 ± 4	22 ± 5	9 ± 4	-	3
XMMXCS J122556.27+131732.9	$0.649^{+0.153}_{-0.146}$	0.641 ± 0.141	-	-0.722 ± 0.242	16.100 ± 4.940	0.001	1 ± 1	3 ± 2	1 ± 1	4 ± 2	3
XMMXCS J122556.2+131732.9	$0.649^{+0.153}_{-0.146}$	0.641 ± 0.141	-	-0.722 ± 0.242	16.100 ± 4.940	0.001	1 ± 1	3 ± 2	1 ± 1	4 ± 2	3
XMMXCS J122601.2+180347.0	$0.238^{+0.069}_{-0.075}$	0.227 ± 0.036	-	-0.007 ± 0.053	1.600 ± 1.030	0.001	1 ± 1	2 ± 2	0 ± 0.1	0 ± 1	3
XMMXCS J122602.6+333244.1	$0.302^{+0.072}_{-0.074}$	0.320 ± 0.054	-	-0.004 ± 0.058	1.580 ± 1.190	0.106	3 ± 2	1 ± 2	2 ± 2	-	3
XMMXCS J122731.0+332317.2	$0.335^{+0.055}_{-0.055}$	0.276 ± 0.046	-	0.077 ± 0.081	0.166 ± 1.520	0.079	2 ± 2	6 ± 3	1 ± 1	2 ± 2	3
XMMXCS J122747.3+334429.7	$0.283^{+0.046}_{-0.046}$	0.322 ± 0.050	$0.293 \pm 6.9e-05$	0.103 ± 0.112	-0.327 ± 2.150	0.096	4 ± 2	3 ± 3	0 ± 1	-	3
XMMXCS J122754.0+332522.9	$0.127^{+0.052}_{-0.054}$	0.179 ± 0.044	-	-0.047 ± 0.046	1.670 ± 0.881	0.108	1 ± 1	0 ± 1	0 ± 0.1	-	3
XMMXCS J122807.1+012747.9	$0.110^{+0.026}_{-0.026}$	0.098 ± 0.019	$0.110 \pm 3.2e-05$	-0.192 ± 0.042	4.200 ± 0.757	0.084	0 ± 0.1	1 ± 1	-	0 ± 1	3
XMMXCS J122811.7+020105.0	$0.133^{+0.068}_{-0.071}$	0.112 ± 0.029	$0.090 \pm 1.6e-05$	0.010 ± 0.040	0.815 ± 0.722	0.082	0 ± 1	3 ± 2	-	0 ± 1	3
XMMXCS J122820.2+333621.6	$0.447^{+0.115}_{-0.108}$	0.311 ± 0.070	-	0.188 ± 0.078	-2.960 ± 1.550	0.122	3 ± 3	2 ± 3	1 ± 1	1 ± 2	3

Continued on next page

Table A.2 – continued from previous page

name	z_{RS}	z_{BCG}	z_{spec-g}	cmr_{grad}	cmr_{inter}	cmr_{wid}	n_{gals-c}	n_{gals-l}	n_{200-c}	n_{200-l}	qual
XMMXCS J122821.6+015914.5	$0.426^{+0.112}_{-0.106}$	0.313 ± 0.134	-	0.009 ± 0.103	0.491 ± 2.060	0.059	6 ± 4	-	3 ± 3	-	3
XMMXCS J122827.1+435141.0	$0.455^{+0.113}_{-0.097}$	0.372 ± 0.058	-	0.018 ± 0.026	0.310 ± 0.518	0.057	2 ± 3	4 ± 3	0 ± 1	1 ± 2	3
XMMXCS J122828.4+015449.4	$0.173^{+0.065}_{-0.071}$	0.160 ± 0.040	-	0.032 ± 0.038	0.402 ± 0.705	0.036	0 ± 1	1 ± 1	-	0 ± 1	3
XMMXCS J122840.9+441517.3	$0.360^{+0.065}_{-0.066}$	0.352 ± 0.052	-	-0.123 ± 0.121	4.420 ± 2.330	0.001	0 ± 0.1	2 ± 2	-	1 ± 1	3
XMMXCS J122849.1+015552.2	$0.335^{+0.119}_{-0.117}$	0.243 ± 0.089	-	-0.006 ± 0.115	1.310 ± 2.300	0.126	3 ± 3	3 ± 3	2 ± 2	2 ± 2	3
XMMXCS J122850.4+440716.2	$0.666^{+0.137}_{-0.136}$	0.655 ± 0.130	$0.664 \pm 2.8e-04$	0.044 ± 0.048	0.459 ± 0.956	0.001	3 ± 2	-	2 ± 1	-	3
XMMXCS J122903.9+014858.2	$0.365^{+0.095}_{-0.095}$	0.317 ± 0.047	$0.314 \pm 5.4e-05$	-0.074 ± 0.088	3.130 ± 1.730	0.001	10 ± 4	0 ± 2	10 ± 4	-	3
XMMXCS J122904.6+440252.7	$0.270^{+0.083}_{-0.078}$	0.159 ± 0.027	-	-0.084 ± 0.794	2.930 ± 16.60	0.500	1 ± 3	1 ± 3	1 ± 1	0 ± 1	3
XMMXCS J122909.6+020040.2	$0.182^{+0.059}_{-0.058}$	0.182 ± 0.040	-	-0.072 ± 0.003	2.520 ± 0.055	0.500	1 ± 2	0 ± 2	0 ± 0.1	-	3
XMMXCS J122911.7+020218.2	$0.202^{+0.068}_{-0.069}$	0.182 ± 0.040	-	-0.056 ± 0.114	2.330 ± 2.200	0.113	0 ± 1	1 ± 2	-	1 ± 1	3
XMMXCS J122915.1+015241.2	$0.249^{+0.091}_{-0.098}$	0.150 ± 0.024	$0.158 \pm 1.9e-05$	0.053 ± 0.061	0.131 ± 1.140	0.146	2 ± 2	0 ± 3	0 ± 1	-	3
XMMXCS J122919.2+075446.7	$0.125^{+0.105}_{-0.105}$	0.048 ± 0.028	$0.090 \pm 1.6e-05$	0.014 ± 0.026	0.503 ± 0.405	0.096	3 ± 2	5 ± 3	0 ± 1	0 ± 1	3
XMMXCS J122932.0+020828.5	$0.655^{+0.133}_{-0.111}$	0.628 ± 0.142	-	0.435 ± 0.335	-7.770 ± 6.820	0.176	1 ± 2	7 ± 4	0 ± 0.1	5 ± 3	3
XMMXCS J122932.7+080218.2	$0.192^{+0.038}_{-0.024}$	0.064 ± 0.022	$0.005 \pm 7.6e-06$	-0.072 ± 0.012	1.930 ± 0.181	0.001	2 ± 2	-	1 ± 1	-	3
XMMXCS J122938.6+020243.0	$0.154^{+0.090}_{-0.089}$	0.046 ± 0.028	$0.006 \pm 3.6e-05$	0.045 ± 0.037	-0.280 ± 0.714	0.050	1 ± 1	0 ± 1	0 ± 0.1	-	3
XMMXCS J122942.4+015524.6	$0.204^{+0.045}_{-0.046}$	0.151 ± 0.030	-	0.084 ± 0.046	-0.447 ± 0.834	0.099	2 ± 2	1 ± 2	1 ± 1	0 ± 1	3
XMMXCS J122944.0+075529.5	$0.431^{+0.281}_{-0.201}$	0.551 ± 0.195	-	2.150 ± 0.838	-43.30 ± 17.30	0.462	4 ± 3	0 ± 1	2 ± 2	-	3
XMMXCS J122946.8+075443.4	$0.266^{+0.177}_{-0.166}$	0.238 ± 0.195	-	0.872 ± 0.348	-16.70 ± 7.110	0.179	1 ± 1	1 ± 1	0 ± 0.1	0 ± 1	3
XMMXCS J122954.81+140042.6	$0.337^{+0.130}_{-0.132}$	0.508 ± 0.089	-	-0.210 ± 0.080	5.640 ± 1.600	0.001	2 ± 2	2 ± 3	2 ± 2	2 ± 2	3

Continued on next page

Table A.2 – continued from previous page

name	z_{RS}	z_{BCG}	z_{spec-g}	cmr_{grad}	cmr_{inter}	cmr_{wid}	n_{gals-c}	n_{gals-l}	n_{200-c}	n_{200-l}	qual
XMMXCS J122958.6+161957.3	$0.199^{+0.067}_{-0.067}$	0.204 ± 0.042	-	-0.002 ± 0.051	1.270 ± 0.965	0.042	1 ± 1	1 ± 1	0 ± 0.1	0 ± 1	3
XMMXCS J122959.8+123811.9	$0.267^{+0.082}_{-0.093}$	0.222 ± 0.062	-	0.027 ± 0.041	0.496 ± 0.770	0.128	1 ± 2	1 ± 3	0 ± 0.1	2 ± 2	3
XMMXCS J123000.5+152201.2	$0.469^{+0.098}_{-0.096}$	0.451 ± 0.067	$0.467 \pm 8.6e-05$	-0.011 ± 0.095	0.931 ± 1.860	0.052	4 ± 3	11 ± 4	2 ± 2	12 ± 4	3
XMMXCS J123001.08+110712.3	$0.352^{+0.128}_{-0.119}$	0.238 ± 0.108	$0.501 \pm 1.3e-04$	-0.059 ± 0.053	2.300 ± 1.060	0.100	0 ± 2	44 ± 7	-	7 ± 6	3
XMMXCS J123008.5+132521.8	$0.065^{+0.027}_{-0.027}$	0.071 ± 0.032	$0.058 \pm 2.0e-05$	-0.006 ± 0.011	0.927 ± 0.157	0.060	2 ± 2	0 ± 1	2 ± 1	-	3
XMMXCS J123014.02+121857.4	$0.123^{+0.184}_{-0.123}$	0.058 ± 0.030	$0.085 \pm 1.6e-05$	0.008 ± 0.026	0.413 ± 0.523	0.001	1 ± 1	1 ± 2	0 ± 0.1	0 ± 1	3
XMMXCS J123014.0+642445.3	$0.161^{+0.065}_{-0.066}$	0.071 ± 0.023	$0.094 \pm 2.4e-05$	-0.033 ± 0.006	1.600 ± 0.105	0.500	0 ± 2	2 ± 3	-	4 ± 2	3
XMMXCS J123017.09+121928.4	$0.200^{+0.127}_{-0.133}$	0.058 ± 0.030	-	0.030 ± 0.016	0.089 ± 0.271	0.087	4 ± 2	6 ± 3	3 ± 2	2 ± 2	3
XMMXCS J123017.3+105127.6	$0.235^{+0.058}_{-0.057}$	0.220 ± 0.035	$0.232 \pm 4.8e-05$	-0.005 ± 0.029	1.340 ± 0.551	0.078	2 ± 2	2 ± 2	0 ± 0.1	0 ± 1	3
XMMXCS J123024.6+143932.7	$0.528^{+0.124}_{-0.114}$	0.368 ± 0.073	-	0.124 ± 0.056	-1.620 ± 1.090	0.095	5 ± 3	33 ± 6	3 ± 2	10 ± 6	3
XMMXCS J123027.9+641025.2	$0.171^{+0.067}_{-0.078}$	0.184 ± 0.058	-	0.022 ± 0.078	0.767 ± 1.480	0.110	0 ± 1	1 ± 2	-	1 ± 1	3
XMMXCS J123032.0+132643.1	$0.167^{+0.064}_{-0.060}$	0.083 ± 0.018	$0.083 \pm 8.9e-06$	0.093 ± 0.009	-0.558 ± 0.150	0.500	2 ± 3	-	0 ± 0.1	-	3
XMMXCS J123033.6+415123.3	$0.434^{+0.088}_{-0.089}$	0.510 ± 0.118	-	-0.014 ± 0.219	2.190 ± 4.490	0.001	1 ± 2	0 ± 1	1 ± 1	-	3
XMMXCS J123045.91+111131.4	$0.308^{+0.103}_{-0.104}$	0.231 ± 0.052	-	-0.031 ± 0.028	1.910 ± 0.538	0.114	1 ± 2	1 ± 3	0 ± 0.1	1 ± 1	3
XMMXCS J123046.6+111123.5	$0.271^{+0.087}_{-0.086}$	0.231 ± 0.052	-	-0.034 ± 0.033	1.980 ± 0.627	0.108	0 ± 2	2 ± 3	-	0 ± 1	3
XMMXCS J123050.9+413410.8	$0.401^{+0.138}_{-0.144}$	0.239 ± 0.037	-	0.285 ± 5.890	-5.170 ± 123	0.500	0 ± 3	3 ± 4	-	2 ± 2	3
XMMXCS J123056.3+160905.4	$0.190^{+0.062}_{-0.061}$	0.147 ± 0.030	-	-0.076 ± 0.108	2.540 ± 1.990	0.114	3 ± 2	2 ± 2	0 ± 0.1	0 ± 1	3
XMMXCS J123057.02+123400.2	$0.429^{+0.141}_{-0.149}$	0.489 ± 0.136	-	-0.307 ± 0.135	7.200 ± 2.780	0.001	1 ± 2	-	0 ± 0.1	-	3
XMMXCS J123059.7+214320.5	$0.738^{+0.183}_{-0.212}$	0.719 ± 0.256	$0.660 \pm 1.6e-04$	0.056 ± 0.088	0.130 ± 1.810	0.001	1 ± 1	13 ± 4	1 ± 1	13 ± 4	3

Continued on next page

Table A.2 – continued from previous page

name	z_{RS}	z_{BCG}	z_{spec-g}	cmr_{grad}	cmr_{inter}	cmr_{wid}	n_{gals-c}	n_{gals-l}	n_{200-c}	n_{200-l}	qual
XMMXCS J123100.7+174433.9	$0.484^{+0.122}_{-0.121}$	0.415 ± 0.086	-	0.670 ± 0.108	-13.00 ± 2.260	0.001	1 ± 2	5 ± 2	0 ± 0.1	3 ± 2	3
XMMXCS J123101.04+121539.1	$0.568^{+0.135}_{-0.134}$	0.584 ± 0.097	$0.559 \pm 1.2e-04$	-0.080 ± 0.070	2.590 ± 1.360	0.001	2 ± 2	8 ± 4	-	8 ± 4	3
XMMXCS J123103.1+163105.3	$0.279^{+0.098}_{-0.098}$	0.137 ± 0.032	-	0.255 ± 0.047	-3.550 ± 0.899	0.050	2 ± 2	3 ± 2	2 ± 1	2 ± 2	3
XMMXCS J123106.9+174234.1	$0.240^{+0.112}_{-0.112}$	0.196 ± 0.029	$0.203 \pm 3.5e-05$	0.244 ± 0.163	-3.190 ± 3.010	0.202	0 ± 2	2 ± 3	-	7 ± 3	3
XMMXCS J123110.9+214315.8	$0.612^{+0.182}_{-0.189}$	0.567 ± 0.118	-	1.000 ± 0.502	-19.60 ± 10.30	0.127	2 ± 2	8 ± 3	0 ± 0.1	8 ± 3	3
XMMXCS J123113.4+154545.0	$0.610^{+0.186}_{-0.189}$	0.690 ± 0.180	-	-10.10 ± 33.30	211 ± 693	1.537	3 ± 2	1 ± 1	4 ± 2	0 ± 1	3
XMMXCS J123114.5+110829.3	$0.251^{+0.131}_{-0.132}$	0.185 ± 0.046	-	0.189 ± 0.221	-2.710 ± 4.350	0.083	2 ± 2	0 ± 2	2 ± 1	-	3
XMMXCS J123120.1+205454.8	$0.269^{+0.070}_{-0.070}$	0.150 ± 0.032	-	0.056 ± 0.065	0.087 ± 1.150	0.092	1 ± 2	0 ± 2	1 ± 1	-	3
XMMXCS J123125.44+121854.3	$0.506^{+0.157}_{-0.161}$	0.346 ± 0.185	-	0.093 ± 0.071	-0.951 ± 1.400	0.145	1 ± 2	-	2 ± 1	-	3
XMMXCS J123125.46+121800.2	$0.587^{+0.175}_{-0.179}$	0.438 ± 0.333	-	0.356 ± 0.057	-6.410 ± 1.100	0.001	2 ± 2	2 ± 3	1 ± 1	-	3
XMMXCS J123127.48+135447.1	$0.425^{+0.130}_{-0.130}$	0.573 ± 0.214	-	0.054 ± 0.294	0.400 ± 5.800	0.112	13 ± 5	11 ± 4	13 ± 5	10 ± 4	3
XMMXCS J123129.8+254912.4	$0.307^{+0.080}_{-0.080}$	0.204 ± 0.136	-	0.068 ± 0.100	0.168 ± 1.990	0.117	3 ± 3	5 ± 3	3 ± 2	5 ± 3	3
XMMXCS J123134.9+161939.2	$0.583^{+0.155}_{-0.154}$	0.567 ± 0.162	-	-0.328 ± 0.190	7.850 ± 3.970	0.001	1 ± 2	5 ± 2	-	2 ± 2	3
XMMXCS J123135.5+255742.3	$0.663^{+0.161}_{-0.159}$	0.632 ± 0.152	-	-0.086 ± 0.245	2.990 ± 5.050	0.001	2 ± 2	7 ± 4	0 ± 0.1	0 ± 2	3
XMMXCS J123139.1+640152.9	$0.393^{+0.126}_{-0.124}$	0.275 ± 0.046	-	-0.106 ± 0.207	2.810 ± 4.150	0.098	5 ± 3	4 ± 3	3 ± 2	-	3
XMMXCS J123156.8+253615.6	$0.231^{+0.046}_{-0.046}$	0.231 ± 0.036	$0.234 \pm 2.3e-05$	-0.035 ± 0.030	1.890 ± 0.575	0.121	5 ± 3	7 ± 3	3 ± 2	4 ± 3	3
XMMXCS J123255.6-000612.7	$0.153^{+0.056}_{-0.056}$	0.191 ± 0.034	-	-0.224 ± 0.040	5.140 ± 0.735	0.058	2 ± 2	2 ± 2	0 ± 0.1	0 ± 1	3
XMMXCS J123305.7+153213.0	$0.300^{+0.126}_{-0.128}$	0.229 ± 0.092	-	-0.107 ± 0.138	3.090 ± 2.790	0.001	0 ± 1	1 ± 2	-	2 ± 2	3
XMMXCS J123311.3+001126.6	$0.362^{+0.101}_{-0.101}$	0.447 ± 0.092	-	-0.522 ± 0.335	12.200 ± 6.850	0.108	6 ± 3	7 ± 3	5 ± 2	6 ± 3	3

Continued on next page

Table A.2 – continued from previous page

name	z_{RS}	z_{BCG}	z_{spec-g}	cmr_{grad}	cmr_{inter}	cmr_{wid}	n_{gals-c}	n_{gals-l}	n_{200-c}	n_{200-l}	qual
XMMXCS J123311.43+123515.0	$0.160^{+0.060}_{-0.061}$	0.213 ± 0.037	$0.237 \pm 4.7e-05$	-0.031 ± 0.043	1.620 ± 0.817	0.112	1 ± 2	0 ± 1	1 ± 1	-	3
XMMXCS J123312.7+001209.8	$0.301^{+0.084}_{-0.080}$	0.192 ± 0.029	$0.410 \pm 1.7e-04$	0.019 ± 0.041	0.943 ± 0.778	0.102	1 ± 2	0 ± 2	0 ± 0.1	-	3
XMMXCS J123332.3+001413.8	$0.192^{+0.057}_{-0.056}$	0.189 ± 0.032	-	0.025 ± 0.033	0.691 ± 0.597	0.101	4 ± 2	5 ± 3	0 ± 1	1 ± 2	3
XMMXCS J123338.5+374114.9	$0.100^{+0.047}_{-0.048}$	0.118 ± 0.024	$0.102 \pm 2.6e-05$	-0.064 ± 0.013	2.000 ± 0.211	0.001	0 ± 1	1 ± 1	-	0 ± 1	3
XMMXCS J123338.8+073143.6	$0.416^{+0.048}_{-0.045}$	0.307 ± 0.047	-	0.021 ± 0.059	1.310 ± 1.110	0.001	2 ± 3	7 ± 4	0 ± 1	-	3
XMMXCS J123409.4+153219.9	$0.295^{+0.082}_{-0.079}$	0.244 ± 0.042	$0.231 \pm 3.4e-05$	0.075 ± 0.085	-0.149 ± 1.640	0.178	2 ± 3	2 ± 3	0 ± 1	1 ± 2	3
XMMXCS J123434.3-034235.9	$0.495^{+0.161}_{-0.164}$	0.569 ± 0.112	-	-0.047 ± 0.054	1.790 ± 1.070	0.111	7 ± 3	9 ± 4	4 ± 3	11 ± 4	3
XMMXCS J123509.1-033547.8	$0.044^{+0.086}_{-0.044}$	0.067 ± 0.015	$0.061 \pm 7.5e-06$	-0.024 ± 0.017	1.160 ± 0.282	0.102	1 ± 1	0 ± 1	1 ± 1	-	3
XMMXCS J123534.6+391141.1	$0.617^{+0.094}_{-0.091}$	0.569 ± 0.094	$0.606 \pm 7.9e-05$	0.293 ± 0.175	-4.680 ± 3.440	0.115	1 ± 2	29 ± 6	1 ± 1	17 ± 5	3
XMMXCS J123536.9+122129.7	$0.067^{+0.050}_{-0.050}$	0.036 ± 0.019	$0.080 \pm 1.2e-05$	0.007 ± 0.017	0.683 ± 0.279	0.070	2 ± 2	1 ± 1	0 ± 0.1	1 ± 1	3
XMMXCS J123540.6+621722.7	$0.135^{+0.054}_{-0.056}$	0.122 ± 0.021	-	-0.073 ± 0.021	2.250 ± 0.390	0.068	1 ± 1	1 ± 1	0 ± 0.1	0 ± 1	3
XMMXCS J123542.9+374426.2	$0.307^{+0.065}_{-0.067}$	0.214 ± 0.073	-	0.031 ± 0.040	0.887 ± 0.788	0.111	0 ± 1	1 ± 2	-	0 ± 1	3
XMMXCS J123557.4+261839.3	$0.414^{+0.083}_{-0.073}$	0.222 ± 0.071	-	-0.056 ± 0.056	2.690 ± 1.110	0.500	4 ± 4	8 ± 5	1 ± 2	7 ± 4	3
XMMXCS J123612.5+260123.0	$0.132^{+0.177}_{-0.132}$	0.099 ± 0.053	-	0.003 ± 0.001	0.619 ± 0.009	0.001	1 ± 1	11 ± 3	0 ± 0.1	11 ± 3	3
XMMXCS J123618.2+255943.1	$0.073^{+0.064}_{-0.067}$	0.055 ± 0.025	$0.004 \pm 6.8e-06$	0.018 ± 0.022	0.620 ± 0.363	0.103	3 ± 2	32 ± 6	4 ± 2	55 ± 8	3
XMMXCS J123619.1+260027.8	$0.072^{+0.054}_{-0.055}$	0.055 ± 0.025	$0.004 \pm 6.8e-06$	0.012 ± 0.020	0.691 ± 0.334	0.094	2 ± 2	24 ± 5	3 ± 2	33 ± 6	3
XMMXCS J123619.23+132314.3	$0.515^{+0.153}_{-0.153}$	0.357 ± 0.062	-	0.206 ± 0.081	-3.160 ± 1.650	0.096	9 ± 4	11 ± 4	10 ± 4	12 ± 4	3
XMMXCS J123619.2+132314.2	$0.515^{+0.153}_{-0.153}$	0.357 ± 0.062	-	0.206 ± 0.081	-3.160 ± 1.650	0.096	9 ± 4	11 ± 4	10 ± 4	12 ± 4	3
XMMXCS J123624.9+622112.9	$0.351^{+0.104}_{-0.100}$	0.477 ± 0.070	-	-0.197 ± 0.134	4.640 ± 2.740	0.029	2 ± 2	3 ± 2	-	1 ± 1	3

Continued on next page

Table A.2 – continued from previous page

name	z_{RS}	z_{BCG}	z_{spec-g}	cmr_{grad}	cmr_{inter}	cmr_{wid}	n_{gals-c}	n_{gals-l}	n_{200-c}	n_{200-l}	qual
XMMXCS J123627.9+260914.4	$0.484^{+0.142}_{-0.142}$	0.411 ± 0.145	-	0.192 ± 0.124	-3.160 ± 2.530	0.099	5 ± 3	6 ± 4	0 ± 2	-	3
XMMXCS J123631.9+280221.1	$0.466^{+0.135}_{-0.134}$	0.558 ± 0.138	-	0.071 ± 0.103	-0.606 ± 2.070	0.045	9 ± 4	13 ± 4	6 ± 3	14 ± 4	3
XMMXCS J123643.0+263654.5	$0.178^{+0.103}_{-0.074}$	0.250 ± 0.053	-	-0.219 ± 0.001	5.230 ± 0.001	0.500	3 ± 3	3 ± 3	1 ± 1	0 ± 1	3
XMMXCS J123651.4+275828.0	$0.481^{+0.096}_{-0.096}$	0.381 ± 0.119	-	0.051 ± 0.029	-0.177 ± 0.594	0.046	9 ± 4	14 ± 5	8 ± 3	13 ± 5	3
XMMXCS J123705.9+621616.1	$0.247^{+0.164}_{-0.163}$	0.230 ± 0.084	-	-0.161 ± 0.172	4.160 ± 3.350	0.001	2 ± 1	1 ± 1	1 ± 1	0 ± 1	3
XMMXCS J123716.5+114111.4	$0.324^{+0.079}_{-0.084}$	0.334 ± 0.051	-	-0.131 ± 0.084	4.160 ± 1.660	0.084	3 ± 2	4 ± 3	0 ± 1	2 ± 2	3
XMMXCS J123756.6+621516.6	$0.357^{+0.084}_{-0.082}$	0.252 ± 0.060	-	0.376 ± 0.229	-5.590 ± 4.350	0.230	4 ± 3	-	4 ± 2	-	3
XMMXCS J123803.0+092249.8	$0.192^{+0.076}_{-0.078}$	0.229 ± 0.050	-	-0.224 ± 0.246	5.460 ± 4.540	0.203	1 ± 2	2 ± 2	0 ± 0.1	1 ± 1	3
XMMXCS J123833.6+620352.0	$0.137^{+0.014}_{-0.014}$	0.137 ± 0.021	$0.136 \pm 2.2e-05$	-0.013 ± 0.020	1.250 ± 0.323	0.001	2 ± 2	2 ± 2	1 ± 1	1 ± 1	3
XMMXCS J123837.4+091515.4	$0.358^{+0.134}_{-0.138}$	0.236 ± 0.046	-	0.132 ± 0.055	-1.940 ± 1.100	0.116	0 ± 2	1 ± 3	-	0 ± 1	3
XMMXCS J123850.1+091511.7	$0.590^{+0.156}_{-0.157}$	0.653 ± 0.116	-	-0.125 ± 0.299	3.930 ± 6.090	0.001	5 ± 2	-	3 ± 2	-	3
XMMXCS J124003.0-020110.8	$0.240^{+0.054}_{-0.054}$	0.069 ± 0.018	$0.064 \pm 1.1e-05$	0.334 ± 0.228	-4.770 ± 4.340	0.131	1 ± 2	-	1 ± 1	-	3
XMMXCS J124033.4-014756.3	$0.152^{+0.039}_{-0.040}$	0.154 ± 0.024	$0.153 \pm 3.2e-05$	-0.035 ± 0.044	1.770 ± 0.789	0.118	1 ± 2	2 ± 2	0 ± 0.1	1 ± 1	3
XMMXCS J124058.9-020006.6	$0.226^{+0.072}_{-0.075}$	0.091 ± 0.021	-	0.223 ± 0.026	-3.340 ± 0.490	0.001	1 ± 1	0 ± 1	2 ± 1	-	3
XMMXCS J124112.2-020626.2	$0.311^{+0.053}_{-0.053}$	0.327 ± 0.056	-	-0.059 ± 0.027	2.690 ± 0.505	0.026	1 ± 2	1 ± 2	0 ± 0.1	0 ± 1	3
XMMXCS J124130.3+182526.8	$0.444^{+0.072}_{-0.068}$	0.419 ± 0.061	-	0.277 ± 0.178	-3.610 ± 3.500	0.165	4 ± 3	4 ± 3	0 ± 1	-	3
XMMXCS J124135.7+332625.0	$0.213^{+0.083}_{-0.083}$	0.139 ± 0.026	-	0.030 ± 0.070	0.646 ± 1.340	0.104	2 ± 2	3 ± 2	2 ± 1	3 ± 2	3
XMMXCS J124140.5+332452.6	$0.127^{+0.085}_{-0.088}$	0.035 ± 0.028	$0.023 \pm 7.4e-06$	-0.000 ± 0.001	0.847 ± 0.001	0.500	4 ± 3	5 ± 3	3 ± 2	3 ± 2	3
XMMXCS J124144.2+332333.9	$0.098^{+0.032}_{-0.063}$	0.035 ± 0.028	$0.086 \pm 1.7e-05$	-0.000 ± 0.001	0.805 ± 0.001	0.500	7 ± 3	5 ± 2	6 ± 3	5 ± 2	3

Continued on next page

Table A.2 – continued from previous page

name	z_{RS}	z_{BCG}	z_{spec-g}	cmr_{grad}	cmr_{inter}	cmr_{wid}	n_{gals-c}	n_{gals-l}	n_{200-c}	n_{200-l}	qual
XMMXCS J124145.0+331700.7	$0.104^{+0.053}_{-0.065}$	0.135 ± 0.021	$0.133 \pm 2.3e-05$	0.045 ± 0.053	0.367 ± 0.948	0.120	0 ± 1	1 ± 1	-	0 ± 1	3
XMMXCS J124154.8-111909.6	$0.351^{+0.148}_{-0.154}$	0.185 ± 0.063	-	0.280 ± 0.456	-5.430 ± 9.320	0.230	1 ± 2	0 ± 2	2 ± 1	-	3
XMMXCS J124155.9+024329.0	$0.098^{+0.026}_{-0.025}$	0.089 ± 0.051	$0.098 \pm 1.5e-05$	0.070 ± 0.029	-0.559 ± 0.528	0.067	2 ± 2	1 ± 1	2 ± 1	1 ± 1	3
XMMXCS J124207.4+325946.7	$0.124^{+0.030}_{-0.029}$	0.128 ± 0.043	$0.138 \pm 1.1e-05$	0.012 ± 0.101	0.422 ± 1.780	0.073	1 ± 1	0 ± 1	0 ± 0.1	-	3
XMMXCS J124213.7+322848.9	$0.679^{+0.150}_{-0.136}$	0.668 ± 0.126	-	0.191 ± 0.484	-3.900 ± 9.860	0.001	1 ± 1	0 ± 1	0 ± 0.1	-	3
XMMXCS J124219.9-112404.7	$0.072^{+0.034}_{-0.036}$	0.063 ± 0.017	-	-0.043 ± 0.026	1.470 ± 0.444	0.070	3 ± 2	3 ± 2	1 ± 1	1 ± 1	3
XMMXCS J124222.7+141049.9	$0.144^{+0.062}_{-0.067}$	0.167 ± 0.031	$0.157 \pm 1.4e-05$	0.080 ± 0.024	-0.390 ± 0.446	0.073	2 ± 2	3 ± 2	0 ± 0.1	2 ± 2	3
XMMXCS J124223.0+322235.0	$0.351^{+0.110}_{-0.100}$	0.256 ± 0.063	-	-0.420 ± 0.004	9.910 ± 0.067	0.500	5 ± 4	-	0 ± 2	-	3
XMMXCS J124232.9+332505.1	$0.447^{+0.126}_{-0.128}$	0.249 ± 0.103	-	0.101 ± 0.068	-1.360 ± 1.380	0.108	5 ± 4	5 ± 4	0 ± 1	-	3
XMMXCS J124238.2+142616.5	$0.623^{+0.149}_{-0.149}$	0.568 ± 0.137	-	0.396 ± 0.087	-6.610 ± 1.730	0.001	4 ± 2	7 ± 3	5 ± 2	8 ± 3	3
XMMXCS J124241.0+024645.2	$0.086^{+-1.086}_{-1.086}$	0.094 ± 0.018	$0.059 \pm 7.3e-05$	-0.003 ± 0.013	0.989 ± 0.195	0.038	6 ± 3	11 ± 3	4 ± 2	10 ± 3	3
XMMXCS J124244.0+113907.1	$0.144^{+0.070}_{-0.071}$	0.103 ± 0.025	$0.118 \pm 2.9e-05$	0.224 ± 0.067	-3.280 ± 1.220	0.111	1 ± 1	0 ± 1	0 ± 0.1	-	3
XMMXCS J124246.1+324317.3	$0.337^{+0.145}_{-0.142}$	0.242 ± 0.040	-	0.083 ± 0.038	-0.101 ± 0.721	0.001	1 ± 2	-	0 ± 0.1	-	3
XMMXCS J124252.8+112842.4	$0.066^{+0.054}_{-0.054}$	0.066 ± 0.026	-	0.010 ± 0.003	0.660 ± 0.046	0.019	0 ± 1	2 ± 2	-	3 ± 2	3
XMMXCS J124254.7+023343.4	$0.206^{+0.061}_{-0.061}$	0.219 ± 0.049	$0.206 \pm 3.4e-05$	-0.037 ± 0.041	1.920 ± 0.747	0.090	5 ± 3	6 ± 3	0 ± 1	1 ± 2	3
XMMXCS J124258.6+332350.9	$0.438^{+0.109}_{-0.105}$	0.496 ± 0.126	-	-0.012 ± 0.070	0.970 ± 1.400	0.117	11 ± 4	16 ± 5	9 ± 4	18 ± 6	3
XMMXCS J124259.0+024105.7	$0.086^{+0.026}_{-0.028}$	0.061 ± 0.051	$0.087 \pm 2.4e-05$	0.043 ± 0.001	0.065 ± 0.001	0.500	6 ± 3	17 ± 5	3 ± 2	21 ± 5	3
XMMXCS J124259.0+024032.3	$0.129^{+0.121}_{-0.121}$	0.061 ± 0.051	$0.087 \pm 2.4e-05$	0.020 ± 0.001	0.699 ± 0.009	0.500	3 ± 3	4 ± 4	2 ± 2	2 ± 2	3
XMMXCS J124259.8+332600.7	$0.404^{+0.169}_{-0.176}$	0.253 ± 0.248	-	0.290 ± 0.088	-5.270 ± 1.750	0.001	4 ± 3	4 ± 3	4 ± 2	4 ± 3	3

Continued on next page

Table A.2 – continued from previous page

name	z_{RS}	z_{BCG}	z_{spec-g}	cmr_{grad}	cmr_{inter}	cmr_{wid}	n_{gals-c}	n_{gals-l}	n_{200-c}	n_{200-l}	qual
XMMXCS J124300.1+023934.1	$0.104^{+0.158}_{-0.104}$	0.023 ± 0.028	$0.207 \pm 3.5e-05$	0.027 ± 0.030	0.687 ± 0.515	0.117	4 ± 2	7 ± 3	0 ± 1	0 ± 1	3
XMMXCS J124304.0+331836.7	$0.091^{+0.029}_{-0.029}$	0.048 ± 0.022	$0.083 \pm 1.2e-05$	0.125 ± 0.045	-1.170 ± 0.808	0.080	1 ± 1	2 ± 2	1 ± 1	1 ± 1	3
XMMXCS J124308.7+331530.9	$0.167^{+0.067}_{-0.067}$	0.109 ± 0.023	$0.092 \pm 1.3e-05$	0.032 ± 0.040	0.363 ± 0.721	0.123	3 ± 2	2 ± 2	3 ± 2	1 ± 1	3
XMMXCS J124312.3+131306.8	$0.803^{+0.148}_{-0.143}$	0.606 ± 0.126	$0.790 \pm 2.6e-04$	-0.003 ± 0.028	0.821 ± 0.524	0.001	0 ± 1	7 ± 4	-	10 ± 4	3
XMMXCS J124342.4+142350.4	$0.291^{+0.066}_{-0.069}$	0.262 ± 0.055	-	0.031 ± 0.046	0.902 ± 0.870	0.060	3 ± 2	2 ± 2	0 ± 1	0 ± 1	3
XMMXCS J124357.2+113619.6	$0.359^{+0.084}_{-0.099}$	0.377 ± 0.059	$0.398 \pm 6.9e-05$	0.079 ± 0.047	-0.722 ± 0.949	0.001	0 ± 2	3 ± 3	-	5 ± 3	3
XMMXCS J124411.6+112424.0	$0.373^{+0.148}_{-0.157}$	0.245 ± 0.080	-	0.824 ± 0.288	-14.80 ± 5.850	0.284	2 ± 3	1 ± 3	2 ± 2	2 ± 2	3
XMMXCS J124423.6+113536.2	$0.577^{+0.100}_{-0.099}$	0.598 ± 0.113	$0.576 \pm 2.1e-04$	-0.038 ± 0.086	1.870 ± 1.730	0.001	5 ± 3	8 ± 4	3 ± 2	-	3
XMMXCS J124448.6-001951.4	$0.473^{+0.066}_{-0.061}$	0.394 ± 0.061	$0.469 \pm 1.0e-04$	-0.215 ± 0.037	4.900 ± 0.758	0.068	3 ± 3	7 ± 4	1 ± 1	10 ± 4	3
XMMXCS J124527.2+672438.6	$0.204^{+0.054}_{-0.050}$	0.144 ± 0.025	-	0.369 ± 0.015	-5.470 ± 0.274	0.500	2 ± 3	3 ± 3	3 ± 2	2 ± 2	3
XMMXCS J124728.9+672159.2	$0.106^{+0.037}_{-0.037}$	0.115 ± 0.018	$0.107 \pm 1.3e-05$	-0.071 ± 0.018	2.140 ± 0.288	0.094	0 ± 1	1 ± 1	-	1 ± 1	3
XMMXCS J124829.5-055501.5	$0.395^{+0.117}_{-0.110}$	0.306 ± 0.123	-	0.124 ± 0.174	-1.130 ± 3.430	0.127	8 ± 4	5 ± 4	6 ± 3	-	3
XMMXCS J124900.1-060159.7	$0.420^{+0.117}_{-0.121}$	0.333 ± 0.070	-	-0.292 ± 0.253	7.250 ± 5.150	0.001	2 ± 3	3 ± 3	1 ± 1	1 ± 2	3
XMMXCS J124901.8-060004.5	$0.462^{+0.126}_{-0.119}$	0.400 ± 0.059	-	0.294 ± 0.105	-5.130 ± 2.160	0.098	4 ± 3	11 ± 4	0 ± 1	-	3
XMMXCS J124923.7-060422.8	$0.424^{+0.106}_{-0.091}$	0.354 ± 0.102	-	0.220 ± 0.145	-4.170 ± 2.960	0.156	2 ± 3	2 ± 3	1 ± 1	-	3
XMMXCS J124956.2+405851.2	$0.231^{+0.054}_{-0.058}$	0.195 ± 0.032	-	0.070 ± 0.036	0.106 ± 0.687	0.076	2 ± 2	2 ± 2	0 ± 0.1	0 ± 1	3
XMMXCS J125007.9+410335.1	$0.273^{+0.094}_{-0.093}$	0.103 ± 0.030	$0.271 \pm 3.1e-05$	0.226 ± 0.109	-3.250 ± 2.110	0.046	4 ± 2	2 ± 2	3 ± 2	4 ± 2	3
XMMXCS J125038.0+411046.1	$0.094^{+0.022}_{-0.022}$	0.106 ± 0.062	$0.086 \pm 1.0e-05$	-0.000 ± 0.028	0.558 ± 0.432	0.500	1 ± 2	1 ± 2	0 ± 0.1	0 ± 1	3
XMMXCS J125047.4+263353.4	$0.415^{+0.098}_{-0.097}$	0.474 ± 0.072	-	-0.065 ± 0.050	1.980 ± 0.971	0.027	10 ± 4	8 ± 4	10 ± 4	12 ± 4	3

Continued on next page

Table A.2 – continued from previous page

name	z_{RS}	z_{BCG}	z_{spec-g}	cmr_{grad}	cmr_{inter}	cmr_{wid}	n_{gals-c}	n_{gals-l}	n_{200-c}	n_{200-l}	qual
XMMXCS J125057.0+412125.6	$0.244^{+0.088}_{-0.085}$	0.204 ± 0.035	$0.190 \pm 3.2e-05$	-0.003 ± 0.219	1.110 ± 4.360	0.152	2 ± 2	3 ± 3	0 ± 0.1	0 ± 1	3
XMMXCS J125058.2+273458.4	$0.219^{+0.092}_{-0.090}$	0.113 ± 0.031	-	0.180 ± 0.185	-2.560 ± 3.540	0.132	1 ± 1	1 ± 2	0 ± 0.1	0 ± 1	3
XMMXCS J125318.2+311133.6	$0.305^{+0.110}_{-0.096}$	0.246 ± 0.114	-	0.018 ± 0.038	0.768 ± 0.737	0.070	1 ± 2	0 ± 2	0 ± 0.1	-	3
XMMXCS J125329.8+100659.6	$0.214^{+0.062}_{-0.061}$	0.124 ± 0.029	$0.193 \pm 1.9e-05$	-0.000 ± 0.001	1.180 ± 0.001	0.500	1 ± 3	3 ± 3	4 ± 2	4 ± 3	3
XMMXCS J125345.1+101139.8	$0.450^{+0.146}_{-0.146}$	0.333 ± 0.167	-	0.479 ± 0.053	-9.070 ± 1.110	0.001	5 ± 3	5 ± 3	7 ± 3	7 ± 3	3
XMMXCS J125348.5+100920.7	$0.360^{+0.126}_{-0.119}$	0.501 ± 0.160	-	0.091 ± 0.135	-0.382 ± 2.650	0.032	4 ± 3	4 ± 3	1 ± 1	1 ± 2	3
XMMXCS J125456.2+271510.4	$0.253^{+0.056}_{-0.060}$	0.238 ± 0.038	$0.257 \pm 3.8e-05$	-0.031 ± 0.031	1.950 ± 0.565	0.022	1 ± 2	-	0 ± 0.1	-	3
XMMXCS J125538.1+272721.8	$0.285^{+0.098}_{-0.098}$	0.193 ± 0.076	-	0.007 ± 0.045	1.240 ± 0.876	0.123	6 ± 3	5 ± 3	4 ± 2	1 ± 2	3
XMMXCS J125553.3+272404.2	$0.321^{+0.064}_{-0.060}$	0.188 ± 0.030	$0.258 \pm 3.3e-05$	0.0 ± -1.00	1.160 ± -1.00	0.500	4 ± 4	3 ± 4	4 ± 3	3 ± 3	3
XMMXCS J125622.0+215852.5	$0.362^{+0.088}_{-0.074}$	0.320 ± 0.102	-	0.383 ± 0.387	-6.260 ± 7.650	0.121	4 ± 3	4 ± 3	0 ± 1	-	3
XMMXCS J125626.6+220722.1	$0.354^{+0.077}_{-0.079}$	0.375 ± 0.056	-	-0.157 ± 0.065	4.850 ± 1.300	0.001	3 ± 2	4 ± 3	2 ± 2	1 ± 2	3
XMMXCS J125626.7+215408.4	$0.399^{+0.065}_{-0.071}$	0.377 ± 0.112	-	0.011 ± 0.113	1.490 ± 2.230	0.001	3 ± 2	-	0 ± 1	-	3
XMMXCS J125639.4+272903.3	$0.619^{+0.148}_{-0.143}$	0.460 ± 0.220	-	0.140 ± 0.039	-1.690 ± 0.747	0.075	1 ± 1	0 ± 1	1 ± 1	-	3
XMMXCS J125648.4+570346.8	$0.213^{+0.077}_{-0.069}$	0.173 ± 0.036	-	-0.042 ± 0.054	1.570 ± 1.040	0.088	2 ± 1	1 ± 1	0 ± 0.1	0 ± 1	3
XMMXCS J125653.6+215124.8	$0.164^{+0.049}_{-0.047}$	0.118 ± 0.034	$0.162 \pm 1.6e-05$	-0.080 ± 0.105	2.430 ± 2.030	0.500	1 ± 2	2 ± 2	0 ± 0.1	0 ± 1	3
XMMXCS J125704.3+275112.8	$0.169^{+0.070}_{-0.071}$	0.093 ± 0.021	$0.085 \pm 2.0e-05$	0.028 ± 0.137	0.430 ± 2.590	0.083	2 ± 2	0 ± 2	1 ± 1	-	3
XMMXCS J125716.3+264837.9	$0.210^{+0.062}_{-0.062}$	0.211 ± 0.035	-	0.009 ± 0.048	1.120 ± 0.924	0.071	2 ± 2	2 ± 2	0 ± 0.1	0 ± 1	3
XMMXCS J125719.8+272920.8	$0.024^{+0.002}_{-0.002}$	0.085 ± 0.031	$0.025 \pm 4.8e-06$	-0.050 ± 0.008	1.500 ± 0.108	0.015	1 ± 2	0 ± 1	0 ± 0.1	-	3
XMMXCS J125723.7+281347.2	$0.111^{+0.074}_{-0.087}$	0.054 ± 0.015	$0.088 \pm 3.4e-05$	0.039 ± 0.046	-0.093 ± 0.844	0.056	3 ± 2	3 ± 2	0 ± 0.1	0 ± 1	3

Continued on next page

Table A.2 – continued from previous page

name	z_{RS}	z_{BCG}	z_{spec-g}	cmr_{grad}	cmr_{inter}	cmr_{wid}	n_{gals-c}	n_{gals-l}	n_{200-c}	n_{200-l}	qual
XMMXCS J125740.4+283056.1	$0.319^{+0.083}_{-0.082}$	0.220 ± 0.041	-	0.094 ± 0.086	-0.286 ± 1.640	0.088	12 ± 4	58 ± 8	11 ± 4	31 ± 7	3
XMMXCS J125749.1+281033.9	$0.056^{+0.045}_{-0.012}$	0.041 ± 0.016	$0.023 \pm 8.6e-06$	-0.150 ± 0.001	2.990 ± 0.008	0.500	2 ± 3	1 ± 2	0 ± 1	0 ± 1	3
XMMXCS J125751.3+565350.3	$0.339^{+0.080}_{-0.081}$	0.286 ± 0.051	-	-0.020 ± 0.056	1.930 ± 1.070	0.001	4 ± 3	6 ± 3	3 ± 2	7 ± 3	3
XMMXCS J125805.2+281441.3	$0.459^{+0.139}_{-0.140}$	0.587 ± 0.125	-	0.062 ± 0.036	-0.283 ± 0.661	0.001	2 ± 2	2 ± 2	0 ± 1	0 ± 1	3
XMMXCS J125808.8+271112.1	$0.375^{+0.084}_{-0.076}$	0.283 ± 0.111	-	-0.013 ± 0.112	1.750 ± 2.300	0.500	1 ± 4	-	3 ± 2	-	3
XMMXCS J125823.1+015031.8	$0.357^{+0.052}_{-0.052}$	0.381 ± 0.064	$0.358 \pm 8.3e-05$	0.082 ± 0.085	0.224 ± 1.570	0.142	8 ± 3	9 ± 4	6 ± 3	7 ± 3	3
XMMXCS J125834.5+271547.1	$0.151^{+0.059}_{-0.057}$	0.141 ± 0.024	$0.153 \pm 2.4e-05$	0.025 ± 0.060	0.591 ± 1.030	0.108	1 ± 2	2 ± 2	0 ± 0.1	2 ± 2	3
XMMXCS J125835.6+273547.1	$0.301^{+0.058}_{-0.058}$	0.240 ± 0.044	-	-0.028 ± 0.045	2.060 ± 0.866	0.096	1 ± 2	-	0 ± 0.1	-	3
XMMXCS J125923.4+275630.7	$0.022^{+0.004}_{-0.003}$	0.043 ± 0.016	$0.022 \pm 5.1e-06$	0.002 ± 0.003	0.770 ± 0.035	0.012	2 ± 2	1 ± 1	0 ± 0.1	1 ± 1	3
XMMXCS J125923.7+275437.6	$0.022^{+0.003}_{-0.003}$	0.043 ± 0.016	$0.021 \pm 5.0e-06$	-0.029 ± 0.007	1.190 ± 0.109	0.030	2 ± 2	0 ± 1	0 ± 0.1	-	3
XMMXCS J125930.7+275024.2	$0.312^{+0.105}_{-0.108}$	0.236 ± 0.067	-	-0.085 ± 0.062	2.830 ± 1.180	0.047	4 ± 3	1 ± 2	3 ± 2	-	3
XMMXCS J125932.1+274845.5	$0.210^{+0.124}_{-0.124}$	0.048 ± 0.024	$0.015 \pm 1.9e-05$	0.075 ± 0.040	-0.735 ± 0.780	0.092	9 ± 3	10 ± 4	8 ± 3	9 ± 4	3
XMMXCS J125933.0+281741.4	$0.172^{+0.095}_{-0.095}$	0.050 ± 0.025	$0.062 \pm 9.7e-06$	0.061 ± 0.017	-0.283 ± 0.307	0.081	2 ± 2	5 ± 3	1 ± 1	-	3
XMMXCS J125936.1+275714.8	$0.022^{+0.002}_{-0.002}$	0.043 ± 0.016	$0.022 \pm 5.1e-06$	-0.004 ± 0.003	0.850 ± 0.038	0.011	5 ± 3	1 ± 1	0 ± 1	1 ± 1	3
XMMXCS J125937.4+281434.7	$0.087^{+0.040}_{-0.040}$	0.050 ± 0.025	$0.075 \pm 9.5e-06$	0.040 ± 0.066	0.022 ± 1.020	0.500	7 ± 3	7 ± 3	5 ± 3	2 ± 2	3
XMMXCS J125938.5+283028.7	$0.640^{+0.147}_{-0.147}$	0.640 ± 0.132	-	0.141 ± 0.134	-1.460 ± 2.710	0.001	9 ± 3	15 ± 4	7 ± 3	14 ± 4	3
XMMXCS J125947.7+283530.8	$0.342^{+0.128}_{-0.110}$	0.221 ± 0.092	-	0.060 ± 0.063	-0.084 ± 1.240	0.128	1 ± 2	-	0 ± 0.1	-	3
XMMXCS J125949.4+275008.0	$0.492^{+0.121}_{-0.120}$	0.575 ± 0.104	-	-0.110 ± 0.040	3.100 ± 0.773	0.069	12 ± 4	30 ± 6	12 ± 4	41 ± 8	3
XMMXCS J125950.0+274924.2	$0.449^{+0.144}_{-0.144}$	0.575 ± 0.104	-	-0.164 ± 0.070	4.060 ± 1.420	0.028	6 ± 3	6 ± 3	7 ± 3	13 ± 4	3

Continued on next page

Table A.2 – continued from previous page

name	z_{RS}	z_{BCG}	z_{spec-g}	cmr_{grad}	cmr_{inter}	cmr_{wid}	n_{gals-c}	n_{gals-l}	n_{200-c}	n_{200-l}	qual
XMMXCS J125956.4+281155.8	$0.114^{+0.126}_{-0.114}$	0.070 ± 0.034	$0.024 \pm 7.2e-06$	-0.012 ± 0.013	0.849 ± 0.228	0.080	9 ± 3	12 ± 4	9 ± 3	12 ± 4	3
XMMXCS J125957.0+274803.0	$0.548^{+0.116}_{-0.114}$	0.397 ± 0.178	-	0.066 ± 0.134	-0.404 ± 2.730	0.064	7 ± 3	13 ± 4	6 ± 3	14 ± 5	3
XMMXCS J130000.6+274757.0	$0.099^{+0.058}_{-0.072}$	0.042 ± 0.014	$0.024 \pm 6.0e-06$	-0.017 ± 0.006	0.968 ± 0.103	0.034	16 ± 4	22 ± 5	26 ± 5	43 ± 7	3
XMMXCS J130003.1+281109.9	$0.162^{+0.049}_{-0.049}$	0.049 ± 0.021	$0.025 \pm 5.0e-06$	-0.000 ± 0.001	0.796 ± 0.001	0.500	9 ± 4	19 ± 6	5 ± 3	22 ± 7	3
XMMXCS J130005.9+274428.6	$0.085^{+0.050}_{-0.049}$	0.047 ± 0.029	$0.026 \pm 2.0e-05$	-0.757 ± 0.001	13.800 ± 0.011	0.500	1 ± 2	2 ± 2	1 ± 1	3 ± 2	3
XMMXCS J130017.3+280406.0	$0.179^{+0.140}_{-0.140}$	0.047 ± 0.016	$0.024 \pm 4.6e-06$	0.002 ± 0.001	0.848 ± 0.001	0.500	13 ± 5	35 ± 7	13 ± 5	97 ± 12	3
XMMXCS J130020.1+282524.8	$0.217^{+0.092}_{-0.093}$	0.395 ± 0.112	-	-0.312 ± 0.091	7.420 ± 1.760	0.108	2 ± 1	1 ± 1	1 ± 1	0 ± 1	3
XMMXCS J130026.9+283616.9	$0.360^{+0.118}_{-0.114}$	0.276 ± 0.071	-	0.085 ± 0.105	-1.220 ± 2.140	0.064	2 ± 3	0 ± 3	0 ± 0.1	-	3
XMMXCS J130027.2+281004.2	$0.026^{+0.024}_{-0.025}$	0.049 ± 0.021	$0.025 \pm 5.8e-06$	0.029 ± 0.009	0.401 ± 0.139	0.045	16 ± 4	5 ± 2	20 ± 5	3 ± 2	3
XMMXCS J130043.5+282500.4	$0.122^{+0.063}_{-0.053}$	0.044 ± 0.017	$0.063 \pm 1.0e-05$	-0.005 ± 0.003	1.140 ± 0.056	0.500	3 ± 3	3 ± 5	3 ± 2	1 ± 2	3
XMMXCS J130054.1+283515.9	$0.610^{+0.159}_{-0.172}$	0.453 ± 0.244	-	-0.053 ± 0.091	1.940 ± 1.820	0.001	5 ± 3	18 ± 5	1 ± 1	21 ± 6	3
XMMXCS J130106.7+282942.6	$0.117^{+0.042}_{-0.041}$	0.041 ± 0.013	$0.028 \pm 4.0e-06$	-0.009 ± 0.039	0.778 ± 0.705	0.500	1 ± 2	0 ± 1	2 ± 1	-	3
XMMXCS J130115.6+282818.3	$0.147^{+0.055}_{-0.038}$	0.040 ± 0.017	$0.039 \pm 8.3e-06$	0.270 ± 0.244	-3.720 ± 4.390	0.500	2 ± 3	1 ± 3	1 ± 1	1 ± 2	3
XMMXCS J130128.6+282541.7	$0.588^{+0.150}_{-0.151}$	0.671 ± 0.135	-	0.068 ± 0.168	-0.357 ± 3.400	0.151	0 ± 2	6 ± 3	-	0 ± 1	3
XMMXCS J130246.0+590542.1	$0.263^{+0.074}_{-0.062}$	0.265 ± 0.098	-	-0.063 ± 0.063	2.170 ± 1.210	0.100	3 ± 2	2 ± 2	0 ± 0.1	1 ± 1	3
XMMXCS J130318.6-022020.9	$0.085^{+0.006}_{-0.007}$	0.113 ± 0.028	$0.084 \pm 1.5e-05$	0.086 ± 0.021	-0.517 ± 0.335	0.019	8 ± 3	6 ± 3	6 ± 3	5 ± 2	3
XMMXCS J130323.5+535653.4	$0.128^{+0.032}_{-0.033}$	0.156 ± 0.044	-	0.006 ± 0.079	0.906 ± 1.460	0.124	1 ± 1	1 ± 1	0 ± 0.1	0 ± 1	3
XMMXCS J130458.8+175452.9	$0.129^{+0.123}_{-0.129}$	0.084 ± 0.025	$0.103 \pm 4.3e-06$	0.134 ± 0.129	-1.850 ± 2.530	0.116	3 ± 2	1 ± 1	0 ± 0.1	0 ± 1	3
XMMXCS J130515.1+180215.5	$0.427^{+0.123}_{-0.122}$	0.310 ± 0.055	-	0.120 ± 0.051	-1.610 ± 0.996	0.092	7 ± 4	14 ± 5	6 ± 3	13 ± 5	3

Continued on next page

Table A.2 – continued from previous page

name	z_{RS}	z_{BCG}	z_{spec-g}	cmr_{grad}	cmr_{inter}	cmr_{wid}	n_{gals-c}	n_{gals-l}	n_{200-c}	n_{200-l}	qual
XMMXCS J130527.1+673519.8	$0.266^{+0.090}_{-0.091}$	0.140 ± 0.068	-	0.148 ± 0.061	-1.510 ± 1.190	0.134	3 ± 3	4 ± 3	2 ± 2	3 ± 2	3
XMMXCS J130532.4+175537.8	$0.505^{+0.104}_{-0.103}$	0.383 ± 0.111	$0.544 \pm 9.1e-05$	0.125 ± 0.070	-1.750 ± 1.400	0.121	23 ± 5	35 ± 7	29 ± 6	64 ± 10	3
XMMXCS J130544.8+180454.0	$0.164^{+0.049}_{-0.052}$	0.148 ± 0.024	$0.156 \pm 1.2e-05$	0.056 ± 0.035	0.085 ± 0.648	0.118	1 ± 2	3 ± 3	0 ± 0.1	0 ± 1	3
XMMXCS J130558.3+180526.5	$0.368^{+0.081}_{-0.078}$	0.321 ± 0.093	-	0.004 ± 0.099	1.470 ± 1.980	0.131	3 ± 3	3 ± 3	0 ± 1	-	3
XMMXCS J130601.4+180145.9	$0.099^{+0.026}_{-0.025}$	0.128 ± 0.031	$0.132 \pm 5.8e-06$	0.192 ± 0.014	-2.340 ± 0.230	0.021	2 ± 2	0 ± 1	0 ± 0.1	-	3
XMMXCS J130609.9+672314.6	$0.178^{+0.094}_{-0.092}$	0.127 ± 0.028	$0.132 \pm 2.5e-05$	-0.211 ± 0.077	5.100 ± 1.420	0.500	5 ± 3	7 ± 3	5 ± 3	5 ± 3	3
XMMXCS J130614.0+175023.6	$0.431^{+0.076}_{-0.065}$	0.395 ± 0.061	$0.406 \pm 8.9e-05$	-0.100 ± 0.048	2.510 ± 0.979	0.105	3 ± 3	5 ± 4	0 ± 0.1	-	3
XMMXCS J130739.4+212347.5	$0.365^{+0.273}_{-0.185}$	0.172 ± 0.082	$0.516 \pm 1.2e-04$	0.308 ± 0.159	-5.320 ± 3.100	0.150	3 ± 3	3 ± 3	1 ± 2	3 ± 2	3
XMMXCS J130749.7+293305.6	$0.383^{+0.163}_{-0.170}$	0.279 ± 0.103	-	0.080 ± 0.143	-0.524 ± 2.850	0.117	2 ± 3	2 ± 3	0 ± 1	0 ± 1	3
XMMXCS J130800.3+213048.3	$0.105^{+0.028}_{-0.029}$	0.118 ± 0.025	$0.094 \pm 1.2e-05$	0.015 ± 0.054	0.589 ± 1.020	0.103	1 ± 1	0 ± 1	0 ± 0.1	-	3
XMMXCS J130803.6+212124.1	$0.574^{+0.104}_{-0.100}$	0.564 ± 0.102	$0.564 \pm 2.3e-04$	0.041 ± 0.059	0.273 ± 1.130	0.113	0 ± 2	1 ± 3	-	2 ± 2	3
XMMXCS J130820.8+211614.1	$0.113^{+0.090}_{-0.091}$	0.072 ± 0.026	-	-0.010 ± 0.056	0.890 ± 1.020	0.105	1 ± 1	0 ± 1	0 ± 0.1	-	3
XMMXCS J130821.9+213128.7	$0.266^{+0.103}_{-0.087}$	0.151 ± 0.039	$0.298 \pm 6.2e-05$	-0.000 ± 0.001	1.130 ± 0.001	0.500	5 ± 4	7 ± 4	2 ± 2	3 ± 3	3
XMMXCS J130828.4+533512.9	$0.175^{+0.066}_{-0.068}$	0.175 ± 0.027	$0.180 \pm 5.1e-05$	-0.029 ± 0.026	1.650 ± 0.484	0.014	3 ± 2	4 ± 2	0 ± 0.1	1 ± 1	3
XMMXCS J130849.6+291245.6	$0.102^{+0.049}_{-0.053}$	0.092 ± 0.020	$0.113 \pm 2.2e-05$	-0.009 ± 0.028	1.100 ± 0.540	0.082	1 ± 1	0 ± 1	0 ± 0.1	-	3
XMMXCS J130904.1+322817.3	$0.600^{+0.155}_{-0.154}$	0.655 ± 0.135	-	-0.159 ± 0.121	4.270 ± 2.420	0.073	3 ± 2	12 ± 4	2 ± 2	12 ± 4	3
XMMXCS J130924.8+082509.0	$0.267^{+0.166}_{-0.164}$	0.153 ± 0.046	-	0.231 ± 0.416	-3.870 ± 8.470	0.085	1 ± 1	0 ± 1	1 ± 1	-	3
XMMXCS J130939.4+322503.1	$0.353^{+0.127}_{-0.130}$	0.436 ± 0.171	-	0.063 ± 0.072	0.244 ± 1.400	0.001	1 ± 2	2 ± 3	2 ± 1	5 ± 3	3
XMMXCS J130942.6+322650.4	$0.509^{+0.150}_{-0.148}$	0.585 ± 0.104	-	0.987 ± 0.579	-19.40 ± 12.00	0.155	7 ± 3	1 ± 1	6 ± 3	0 ± 1	3

Continued on next page

Table A.2 – continued from previous page

name	z_{RS}	z_{BCG}	z_{spec-g}	cmr_{grad}	cmr_{inter}	cmr_{wid}	n_{gals-c}	n_{gals-l}	n_{200-c}	n_{200-l}	qual
XMMXCS J130955.6+321123.0	$0.296^{+0.101}_{-0.099}$	0.230 ± 0.038	-	-0.126 ± 0.031	3.710 ± 0.589	0.093	3 ± 2	-	1 ± 1	-	3
XMMXCS J131022.1+081938.2	$0.208^{+0.052}_{-0.061}$	0.113 ± 0.023	$0.093 \pm 1.5e-05$	0.028 ± 0.023	0.639 ± 0.431	0.115	8 ± 3	13 ± 4	4 ± 2	16 ± 5	3
XMMXCS J131024.0+573948.5	$0.280^{+0.072}_{-0.061}$	0.140 ± 0.041	-	-0.163 ± 0.132	3.980 ± 2.550	0.081	1 ± 2	1 ± 2	1 ± 1	0 ± 1	3
XMMXCS J131025.3+272205.4	$0.419^{+0.086}_{-0.092}$	0.249 ± 0.062	-	-0.015 ± 0.018	1.010 ± 0.367	0.001	2 ± 2	1 ± 2	0 ± 1	0 ± 1	3
XMMXCS J131028.4-011906.9	$0.139^{+0.021}_{-0.021}$	0.084 ± 0.019	$0.112 \pm 1.5e-05$	0.034 ± 0.048	0.386 ± 0.874	0.123	7 ± 3	7 ± 3	6 ± 3	6 ± 3	3
XMMXCS J131039.3+302057.5	$0.517^{+0.134}_{-0.140}$	0.379 ± 0.106	-	0.022 ± 0.221	0.077 ± 4.540	0.151	1 ± 2	0 ± 1	1 ± 1	-	3
XMMXCS J131041.0+322055.5	$0.512^{+0.127}_{-0.122}$	0.402 ± 0.129	-	-1.540 ± 0.357	33.100 ± 7.570	0.500	4 ± 3	1 ± 1	2 ± 2	0 ± 1	3
XMMXCS J131047.1+220910.1	$0.314^{+0.140}_{-0.133}$	0.205 ± 0.052	-	0.145 ± 0.118	-1.640 ± 2.360	0.205	3 ± 3	2 ± 3	1 ± 1	-	3
XMMXCS J131047.7+322956.9	$0.160^{+0.051}_{-0.052}$	0.186 ± 0.028	$0.186 \pm 3.4e-05$	-0.072 ± 0.017	2.420 ± 0.302	0.075	0 ± 1	1 ± 2	-	0 ± 1	3
XMMXCS J131058.0+314625.9	$0.674^{+0.148}_{-0.148}$	0.569 ± 0.222	-	-0.020 ± 0.074	1.320 ± 1.430	0.001	0 ± 1	6 ± 3	-	3 ± 2	3
XMMXCS J131058.5+572043.8	$0.514^{+0.107}_{-0.107}$	0.444 ± 0.067	-	0.218 ± 0.131	-3.400 ± 2.610	0.079	18 ± 5	55 ± 8	25 ± 6	98 ± 11	3
XMMXCS J131100.6+272057.0	$0.122^{+0.064}_{-0.069}$	0.067 ± 0.017	$0.070 \pm 1.4e-05$	-0.188 ± 0.036	4.380 ± 0.685	0.500	2 ± 2	3 ± 3	0 ± 0.1	-	3
XMMXCS J131101.7+314230.3	$0.144^{+0.043}_{-0.044}$	0.105 ± 0.021	$0.111 \pm 3.6e-05$	0.003 ± 0.029	0.812 ± 0.533	0.074	1 ± 1	1 ± 1	0 ± 0.1	0 ± 1	3
XMMXCS J131112.0+280020.6	$0.509^{+0.150}_{-0.151}$	0.439 ± 0.065	-	0.019 ± 0.159	0.518 ± 3.250	0.068	4 ± 3	4 ± 3	2 ± 2	3 ± 2	3
XMMXCS J131114.4-013139.0	$0.132^{+0.032}_{-0.030}$	0.122 ± 0.022	$0.102 \pm 1.3e-05$	-0.434 ± 0.045	8.070 ± 0.742	0.500	2 ± 2	4 ± 3	0 ± 1	2 ± 2	3
XMMXCS J131114.9+320303.9	$0.157^{+0.039}_{-0.040}$	0.178 ± 0.027	$0.179 \pm 2.7e-05$	-0.093 ± 0.034	2.810 ± 0.611	0.091	0 ± 1	1 ± 2	-	0 ± 1	3
XMMXCS J131124.0+172735.0	$0.174^{+0.060}_{-0.047}$	0.151 ± 0.025	$0.145 \pm 1.5e-05$	0.070 ± 0.022	-0.197 ± 0.385	0.500	0 ± 2	1 ± 2	-	1 ± 1	3
XMMXCS J131137.1+232130.6	$0.158^{+0.055}_{-0.057}$	0.142 ± 0.032	$0.152 \pm 2.3e-05$	0.096 ± 0.152	-0.774 ± 2.830	0.146	0 ± 1	1 ± 2	-	1 ± 1	3
XMMXCS J131139.4+232011.6	$0.305^{+0.078}_{-0.075}$	0.209 ± 0.032	-	0.126 ± 0.034	-0.938 ± 0.642	0.097	4 ± 3	3 ± 3	0 ± 1	-	3

Continued on next page

Table A.2 – continued from previous page

name	z_{RS}	z_{BCG}	z_{spec-g}	cmr_{grad}	cmr_{inter}	cmr_{wid}	n_{gals-c}	n_{gals-l}	n_{200-c}	n_{200-l}	qual
XMMXCS J131143.8-013042.1	$0.329^{+0.081}_{-0.085}$	0.371 ± 0.059	$0.340 \pm 7.4e-05$	-0.090 ± 0.078	3.380 ± 1.510	0.001	1 ± 2	1 ± 2	0 ± 0.1	0 ± 1	3
XMMXCS J131144.6+371257.6	$0.430^{+0.119}_{-0.113}$	0.425 ± 0.066	$0.408 \pm 2.1e-04$	0.034 ± 0.041	0.042 ± 0.823	0.089	3 ± 3	-	0 ± 1	-	3
XMMXCS J131208.9-012941.4	$0.178^{+0.087}_{-0.069}$	0.114 ± 0.029	-	0.008 ± 0.024	0.857 ± 0.440	0.500	0 ± 2	1 ± 2	-	2 ± 2	3
XMMXCS J131213.9-011135.6	$0.114^{+0.031}_{-0.030}$	0.110 ± 0.027	$0.110 \pm 2.8e-05$	-0.059 ± 0.016	1.790 ± 0.284	0.041	2 ± 1	1 ± 1	0 ± 0.1	0 ± 1	3
XMMXCS J131245.9+352047.5	$0.270^{+0.061}_{-0.061}$	0.218 ± 0.040	-	-0.038 ± 0.037	2.170 ± 0.714	0.098	2 ± 2	1 ± 2	0 ± 0.1	0 ± 1	3
XMMXCS J131247.1+230820.8	$0.215^{+0.085}_{-0.088}$	0.076 ± 0.019	$0.149 \pm 2.5e-05$	0.0 ± -1.00	1.040 ± -1.00	0.500	8 ± 4	4 ± 4	6 ± 3	1 ± 2	3
XMMXCS J131256.6+231121.8	$0.362^{+0.083}_{-0.084}$	0.364 ± 0.062	-	0.015 ± 0.062	1.330 ± 1.210	0.077	2 ± 2	2 ± 3	0 ± 1	0 ± 1	3
XMMXCS J131602.8+285507.3	$0.298^{+0.118}_{-0.118}$	0.356 ± 0.066	-	-0.484 ± 0.087	11.000 ± 1.750	0.001	3 ± 2	1 ± 2	3 ± 2	2 ± 2	3
XMMXCS J131741.4+323143.8	$0.483^{+0.163}_{-0.187}$	0.553 ± 0.099	-	-0.723 ± 0.050	15.600 ± 1.010	0.500	5 ± 4	3 ± 4	4 ± 3	5 ± 3	3
XMMXCS J131822.3+323228.1	$0.117^{+0.041}_{-0.042}$	0.058 ± 0.017	$0.092 \pm 9.9e-06$	-0.069 ± 0.001	1.900 ± 0.019	0.500	1 ± 2	-	1 ± 1	-	3
XMMXCS J131842.1-005722.6	$0.380^{+0.125}_{-0.122}$	0.256 ± 0.054	-	0.107 ± 0.083	-0.749 ± 1.640	0.139	5 ± 3	-	2 ± 2	-	3
XMMXCS J131901.9+330908.2	$0.173^{+0.107}_{-0.110}$	0.087 ± 0.038	-	-0.091 ± 0.034	2.570 ± 0.668	0.066	2 ± 1	1 ± 1	0 ± 0.1	0 ± 1	3
XMMXCS J131902.1-010627.8	$0.255^{+0.139}_{-0.143}$	0.096 ± 0.028	-	0.244 ± 0.235	-3.670 ± 4.640	0.158	3 ± 2	4 ± 3	0 ± 1	0 ± 1	3
XMMXCS J131942.5+330139.4	$0.348^{+0.140}_{-0.142}$	0.231 ± 0.054	-	-0.265 ± 0.523	6.390 ± 10.60	0.001	2 ± 2	1 ± 2	0 ± 0.1	0 ± 1	3
XMMXCS J132028.4+331605.7	$0.243^{+0.080}_{-0.079}$	0.072 ± 0.035	-	0.128 ± 0.083	-1.280 ± 1.590	0.131	4 ± 3	4 ± 3	3 ± 2	4 ± 2	3
XMMXCS J132056.3-203804.8	$0.590^{+0.155}_{-0.149}$	0.674 ± 0.168	-	-9.060 ± 34.30	189 ± 712	1.191	5 ± 3	1 ± 1	2 ± 2	0 ± 1	3
XMMXCS J132057.1+330532.2	$0.352^{+0.102}_{-0.102}$	0.335 ± 0.052	$0.302 \pm 4.7e-05$	0.005 ± 0.102	1.550 ± 1.990	0.136	11 ± 4	11 ± 4	11 ± 4	11 ± 4	3
XMMXCS J132110.6+340440.6	$0.297^{+0.087}_{-0.089}$	0.199 ± 0.036	-	0.015 ± 0.068	1.200 ± 1.320	0.122	3 ± 3	4 ± 3	0 ± 0.1	-	3
XMMXCS J132307.7+655444.7	$0.556^{+0.145}_{-0.143}$	0.468 ± 0.124	-	0.131 ± 0.087	-1.620 ± 1.760	0.078	4 ± 3	14 ± 4	0 ± 1	15 ± 5	3

Continued on next page

Table A.2 – continued from previous page

name	z_{RS}	z_{BCG}	z_{spec-g}	cmr_{grad}	cmr_{inter}	cmr_{wid}	n_{gals-c}	n_{gals-l}	n_{200-c}	n_{200-l}	qual
XMMXCS J132312.4+031719.6	$0.143^{+0.035}_{-0.036}$	0.191 ± 0.045	$0.165 \pm 3.0e-05$	-0.080 ± 0.051	2.550 ± 0.931	0.103	2 ± 2	3 ± 2	0 ± 0.1	2 ± 2	3
XMMXCS J132346.0+140509.6	$0.347^{+0.106}_{-0.109}$	0.205 ± 0.036	$0.209 \pm 3.2e-05$	0.018 ± 0.053	1.130 ± 1.010	0.103	4 ± 3	10 ± 4	0 ± 1	0 ± 2	3
XMMXCS J132349.9+301138.2	$0.190^{+0.070}_{-0.071}$	0.227 ± 0.041	-	-0.003 ± 0.047	1.200 ± 0.908	0.130	3 ± 2	1 ± 2	0 ± 0.1	0 ± 1	3
XMMXCS J132410.0+135834.8	$0.168^{+0.136}_{-0.136}$	0.062 ± 0.026	$0.024 \pm 1.3e-05$	0.032 ± 0.017	0.234 ± 0.326	0.001	9 ± 3	11 ± 4	7 ± 3	10 ± 3	3
XMMXCS J132419.0+300041.9	$0.215^{+0.134}_{-0.143}$	0.197 ± 0.070	-	-0.022 ± 0.032	1.230 ± 0.619	0.101	1 ± 1	1 ± 2	0 ± 0.1	0 ± 1	3
XMMXCS J132420.7+301240.3	$0.683^{+0.190}_{-0.190}$	0.665 ± 0.149	-	-0.565 ± 0.081	12.500 ± 1.600	0.001	4 ± 2	11 ± 5	2 ± 2	12 ± 5	3
XMMXCS J132435.9+300339.3	$0.564^{+0.171}_{-0.186}$	0.471 ± 0.226	-	0.317 ± 0.162	-5.540 ± 3.310	0.044	3 ± 2	17 ± 5	0 ± 1	35 ± 7	3
XMMXCS J132458.2+300723.2	$0.538^{+0.156}_{-0.158}$	0.393 ± 0.101	-	0.051 ± 0.159	-0.042 ± 3.270	0.107	8 ± 3	16 ± 5	3 ± 2	17 ± 5	3
XMMXCS J132503.2+302415.4	$0.365^{+0.124}_{-0.121}$	0.430 ± 0.077	$0.435 \pm 1.5e-04$	-0.039 ± 0.027	1.370 ± 0.524	0.075	7 ± 4	5 ± 4	5 ± 3	9 ± 4	3
XMMXCS J132503.2+302415.6	$0.365^{+0.124}_{-0.121}$	0.430 ± 0.077	$0.435 \pm 1.5e-04$	-0.039 ± 0.027	1.370 ± 0.524	0.075	7 ± 4	5 ± 4	5 ± 3	9 ± 4	3
XMMXCS J132605.3+315800.9	$0.252^{+0.099}_{-0.101}$	0.196 ± 0.058	-	0.022 ± 0.053	0.778 ± 1.020	0.001	4 ± 2	2 ± 2	2 ± 1	1 ± 1	3
XMMXCS J132629.6+314621.8	$0.283^{+0.117}_{-0.262}$	0.220 ± 0.099	-	0.012 ± 0.049	0.892 ± 0.966	0.112	2 ± 2	1 ± 3	0 ± 1	-	3
XMMXCS J132633.8+314427.2	$0.195^{+0.123}_{-0.143}$	0.058 ± 0.017	$0.053 \pm 8.7e-06$	0.037 ± 0.032	0.302 ± 0.624	0.114	3 ± 2	7 ± 4	0 ± 1	5 ± 3	3
XMMXCS J132658.8+315424.7	$0.216^{+0.053}_{-0.054}$	0.165 ± 0.044	-	0.030 ± 0.036	0.752 ± 0.681	0.065	3 ± 2	7 ± 3	0 ± 0.1	3 ± 2	3
XMMXCS J132704.3+315122.1	$0.224^{+0.063}_{-0.062}$	0.294 ± 0.100	-	-0.017 ± 0.029	1.710 ± 0.542	0.056	8 ± 3	11 ± 4	6 ± 3	11 ± 4	3
XMMXCS J132735.1+013015.9	$0.076^{+0.041}_{-0.043}$	0.072 ± 0.020	$0.079 \pm 2.5e-05$	-0.081 ± 0.019	2.240 ± 0.348	0.066	0 ± 1	1 ± 1	-	0 ± 1	3
XMMXCS J132835.7+471653.7	$0.198^{+0.109}_{-0.131}$	0.259 ± 0.096	-	0.088 ± 0.144	-0.685 ± 2.690	0.084	1 ± 1	1 ± 1	0 ± 0.1	0 ± 1	3
XMMXCS J132836.6+471602.0	$0.276^{+0.046}_{-0.046}$	0.199 ± 0.038	-	-0.360 ± 0.141	7.700 ± 2.630	0.500	4 ± 4	43 ± 7	0 ± 1	-	3
XMMXCS J132844.1+583457.1	$0.284^{+0.057}_{-0.056}$	0.253 ± 0.057	-	0.052 ± 0.051	0.482 ± 0.998	0.078	2 ± 2	1 ± 2	0 ± 0.1	1 ± 1	3

Continued on next page

Table A.2 – continued from previous page

name	z_{RS}	z_{BCG}	z_{spec-g}	cmr_{grad}	cmr_{inter}	cmr_{wid}	n_{gals-c}	n_{gals-l}	n_{200-c}	n_{200-l}	qual
XMMXCS J132854.6+470809.2	$0.356^{+0.068}_{-0.069}$	0.356 ± 0.057	-	0.068 ± 0.109	0.393 ± 2.130	0.001	4 ± 3	3 ± 3	0 ± 1	-	3
XMMXCS J132910.2+472213.1	$0.289^{+0.067}_{-0.068}$	0.395 ± 0.188	-	-0.015 ± 0.050	1.790 ± 0.965	0.105	2 ± 2	1 ± 2	1 ± 1	2 ± 2	3
XMMXCS J132919.4+334537.1	$0.195^{+0.057}_{-0.055}$	0.205 ± 0.032	-	-0.028 ± 0.073	1.460 ± 1.390	0.500	1 ± 2	3 ± 3	0 ± 0.1	0 ± 1	3
XMMXCS J132943.6+241120.3	$0.353^{+0.133}_{-0.131}$	0.195 ± 0.090	-	0.087 ± 0.111	-0.550 ± 2.250	0.037	7 ± 3	7 ± 3	6 ± 3	5 ± 3	3
XMMXCS J132951.9+115714.9	$0.190^{+0.071}_{-0.071}$	0.212 ± 0.043	-	-0.123 ± 0.125	3.490 ± 2.320	0.034	1 ± 1	0 ± 1	2 ± 1	-	3
XMMXCS J133007.2+113728.8	$0.252^{+0.063}_{-0.067}$	0.238 ± 0.040	$0.260 \pm 4.1e-05$	-0.042 ± 0.027	2.230 ± 0.523	0.041	2 ± 2	1 ± 2	0 ± 0.1	0 ± 1	3
XMMXCS J133011.6+581616.0	$0.147^{+0.034}_{-0.035}$	0.164 ± 0.037	-	-0.076 ± 0.067	2.490 ± 1.200	0.078	2 ± 2	2 ± 2	0 ± 0.1	0 ± 1	3
XMMXCS J133034.2+333616.7	$0.200^{+0.082}_{-0.081}$	0.181 ± 0.029	-	-0.025 ± 0.016	1.600 ± 0.314	0.065	1 ± 1	0 ± 1	0 ± 0.1	-	3
XMMXCS J133040.1-013831.3	$0.300^{+0.238}_{-0.193}$	0.172 ± 0.073	-	0.667 ± 1.600	-12.50 ± 32.60	0.001	2 ± 2	-	0 ± 0.1	-	3
XMMXCS J133040.5+241758.3	$0.277^{+0.055}_{-0.055}$	0.330 ± 0.089	-	0.050 ± 0.062	0.423 ± 1.220	0.098	3 ± 2	2 ± 2	0 ± 1	0 ± 1	3
XMMXCS J133055.0+111405.8	$0.080^{+0.040}_{-0.040}$	0.059 ± 0.029	$0.051 \pm 1.2e-05$	-0.009 ± 0.016	0.815 ± 0.257	0.093	2 ± 2	8 ± 3	2 ± 1	8 ± 3	3
XMMXCS J133055.5+240343.8	$0.359^{+0.132}_{-0.131}$	0.199 ± 0.043	-	-0.184 ± 0.141	4.780 ± 2.860	0.084	2 ± 3	2 ± 3	1 ± 1	0 ± 1	3
XMMXCS J133056.2+242718.0	$0.136^{+0.063}_{-0.062}$	0.118 ± 0.039	-	0.026 ± 0.025	0.228 ± 0.472	0.043	1 ± 1	0 ± 1	0 ± 0.1	-	3
XMMXCS J133103.2+470617.0	$0.248^{+0.097}_{-0.090}$	0.105 ± 0.017	$0.090 \pm 1.5e-05$	0.080 ± 0.001	-0.321 ± 0.001	0.500	5 ± 4	5 ± 4	2 ± 2	3 ± 3	3
XMMXCS J133113.0-013938.8	$0.084^{+0.003}_{-0.003}$	0.052 ± 0.028	$0.022 \pm 7.2e-06$	0.021 ± 0.013	0.538 ± 0.212	0.066	15 ± 4	28 ± 5	16 ± 4	37 ± 6	3
XMMXCS J133123.1+470757.8	$0.282^{+0.075}_{-0.078}$	0.312 ± 0.107	-	0.005 ± 0.045	1.390 ± 0.887	0.118	2 ± 2	-	0 ± 0.1	-	3
XMMXCS J133129.5+110756.1	$0.405^{+0.116}_{-0.110}$	0.383 ± 0.058	$0.410 \pm 1.3e-04$	-0.061 ± 0.047	1.820 ± 0.932	0.070	3 ± 3	-	0 ± 1	-	3
XMMXCS J133147.1-015406.9	$0.083^{+0.026}_{-0.027}$	0.054 ± 0.027	$0.054 \pm 1.1e-05$	-0.002 ± 0.031	0.822 ± 0.527	0.107	13 ± 4	16 ± 4	14 ± 4	18 ± 4	3
XMMXCS J133149.6+292047.1	$0.144^{+0.076}_{-0.073}$	0.114 ± 0.030	$0.093 \pm 5.1e-05$	-0.002 ± 0.026	1.030 ± 0.489	0.126	1 ± 1	0 ± 1	0 ± 0.1	-	3

Continued on next page

Table A.2 – continued from previous page

name	z_{RS}	z_{BCG}	z_{spec-g}	cmr_{grad}	cmr_{inter}	cmr_{wid}	n_{gals-c}	n_{gals-l}	n_{200-c}	n_{200-l}	qual
XMMXCS J133149.7+503024.1	$0.250^{+0.059}_{-0.060}$	0.288 ± 0.043	$0.278 \pm 6.0e-05$	-0.002 ± 0.042	1.500 ± 0.805	0.093	4 ± 2	3 ± 2	0 ± 1	-	3
XMMXCS J133154.4+291951.7	$0.414^{+0.119}_{-0.114}$	0.402 ± 0.191	-	-0.164 ± 0.150	4.040 ± 3.080	0.090	4 ± 3	4 ± 3	0 ± 1	1 ± 2	3
XMMXCS J133155.4+110333.3	$0.372^{+0.068}_{-0.062}$	0.279 ± 0.046	$0.256 \pm 5.3e-05$	0.052 ± 0.277	0.841 ± 5.390	0.500	3 ± 4	54 ± 8	3 ± 2	0 ± 8	3
XMMXCS J133157.3-014749.2	$0.385^{+0.076}_{-0.075}$	0.332 ± 0.054	$0.364 \pm 5.8e-05$	-0.020 ± 0.040	2.010 ± 0.754	0.059	7 ± 3	8 ± 4	6 ± 3	15 ± 4	3
XMMXCS J133229.2+291222.7	$0.098^{+0.031}_{-0.035}$	0.120 ± 0.025	$0.136 \pm 1.0e-05$	0.385 ± 0.115	-5.890 ± 1.950	0.500	0 ± 1	1 ± 1	-	0 ± 1	3
XMMXCS J133437.1+502738.6	$0.086^{+0.010}_{-0.010}$	0.068 ± 0.021	$0.067 \pm 1.1e-05$	-0.062 ± 0.020	1.890 ± 0.322	0.090	9 ± 3	10 ± 3	9 ± 3	10 ± 3	3
XMMXCS J133439.5+504327.1	$0.251^{+0.089}_{-0.088}$	0.233 ± 0.074	-	-0.027 ± 0.059	2.140 ± 1.190	0.001	1 ± 1	1 ± 2	1 ± 1	1 ± 1	3
XMMXCS J133457.7+375020.3	$0.368^{+0.079}_{-0.079}$	0.292 ± 0.049	$0.383 \pm 7.9e-05$	-0.008 ± 0.043	1.850 ± 0.865	0.116	8 ± 3	11 ± 4	8 ± 3	10 ± 4	3
XMMXCS J133458.7+380429.0	$0.240^{+0.077}_{-0.075}$	0.185 ± 0.047	-	-0.028 ± 0.056	1.420 ± 1.150	0.101	1 ± 2	0 ± 2	0 ± 0.1	-	3
XMMXCS J133507.5+501841.5	$0.412^{+0.093}_{-0.075}$	0.283 ± 0.106	-	0.034 ± 0.033	-0.246 ± 0.649	0.082	0 ± 2	2 ± 3	-	2 ± 2	3
XMMXCS J133510.0+411127.4	$0.188^{+0.052}_{-0.053}$	0.217 ± 0.070	-	-0.129 ± 0.098	3.650 ± 1.800	0.054	0 ± 1	1 ± 1	-	1 ± 1	3
XMMXCS J133514.1+374905.8	$0.351^{+0.083}_{-0.083}$	0.258 ± 0.053	-	-0.010 ± 0.028	1.810 ± 0.530	0.086	4 ± 3	5 ± 3	0 ± 1	4 ± 3	3
XMMXCS J133516.1+375239.2	$0.237^{+0.137}_{-0.172}$	0.041 ± 0.039	-	0.354 ± 0.385	-5.850 ± 7.690	0.166	1 ± 2	-	0 ± 0.1	-	3
XMMXCS J133534.1+410602.6	$0.168^{+0.056}_{-0.056}$	0.167 ± 0.058	$0.218 \pm 2.5e-05$	0.107 ± 0.075	-0.984 ± 1.470	0.040	1 ± 1	1 ± 1	0 ± 0.1	1 ± 1	3
XMMXCS J133605.0+514531.2	$0.350^{+0.100}_{-0.099}$	0.235 ± 0.036	$0.234 \pm 3.6e-05$	0.163 ± 0.149	-1.390 ± 2.550	0.311	7 ± 4	5 ± 4	5 ± 3	18 ± 5	3
XMMXCS J133628.3+520614.2	$0.584^{+0.138}_{-0.127}$	0.509 ± 0.151	-	0.143 ± 0.078	-1.880 ± 1.550	0.112	5 ± 3	-	0 ± 1	-	3
XMMXCS J133650.7+241247.1	$0.528^{+0.118}_{-0.118}$	0.338 ± 0.220	-	0.483 ± 0.202	-8.990 ± 4.160	0.060	6 ± 3	8 ± 3	6 ± 3	9 ± 3	3
XMMXCS J133709.6+241114.3	$0.378^{+0.112}_{-0.110}$	0.289 ± 0.059	-	-0.111 ± 0.056	2.750 ± 1.110	0.088	2 ± 3	3 ± 3	0 ± 1	1 ± 2	3
XMMXCS J133723.9+520649.0	$0.436^{+0.115}_{-0.103}$	0.550 ± 0.084	-	-0.205 ± 0.001	5.130 ± 0.023	0.500	8 ± 4	-	7 ± 4	-	3

Continued on next page

Table A.2 – continued from previous page

name	z_{RS}	z_{BCG}	z_{spec-g}	cmr_{grad}	cmr_{inter}	cmr_{wid}	n_{gals-c}	n_{gals-l}	n_{200-c}	n_{200-l}	qual
XMMXCS J133727.8+482048.7	$0.561^{+0.143}_{-0.144}$	0.466 ± 0.137	-	1.840 ± 0.286	-36.80 ± 5.890	0.084	2 ± 2	0 ± 1	1 ± 1	-	3
XMMXCS J133739.1+514751.3	$0.222^{+0.074}_{-0.076}$	0.168 ± 0.031	-	-0.005 ± 0.041	1.270 ± 0.795	0.111	1 ± 2	-	0 ± 0.1	-	3
XMMXCS J133809.6+043618.0	$0.337^{+0.092}_{-0.081}$	0.406 ± 0.062	$0.412 \pm 9.1e-05$	-0.136 ± 0.035	3.900 ± 0.674	0.070	1 ± 2	1 ± 3	0 ± 0.1	0 ± 1	3
XMMXCS J133814.8+275738.9	$0.297^{+0.082}_{-0.084}$	0.234 ± 0.037	-	-0.101 ± 0.091	3.500 ± 1.810	0.117	1 ± 2	-	1 ± 1	-	3
XMMXCS J133817.5+481636.0	$0.353^{+0.074}_{-0.069}$	0.355 ± 0.058	$0.346 \pm 1.0e-04$	0.047 ± 0.025	-0.303 ± 0.499	0.029	3 ± 3	6 ± 4	0 ± 0.1	1 ± 2	3
XMMXCS J133818.6+390534.6	$0.235^{+0.053}_{-0.052}$	0.196 ± 0.032	$0.288 \pm 5.5e-05$	-0.137 ± 0.090	3.970 ± 1.700	0.118	0 ± 2	1 ± 2	-	1 ± 1	3
XMMXCS J133834.1+273007.6	$0.548^{+0.141}_{-0.137}$	0.571 ± 0.102	-	0.025 ± 0.044	0.390 ± 0.884	0.082	1 ± 2	1 ± 3	0 ± 0.1	-	3
XMMXCS J133852.2+044248.9	$0.735^{+0.164}_{-0.162}$	0.716 ± 0.115	$0.726 \pm 3.6e-04$	0.223 ± 0.291	-3.140 ± 5.950	0.001	3 ± 2	-	2 ± 1	-	3
XMMXCS J133853.6+482029.6	$0.597^{+0.152}_{-0.151}$	0.519 ± 0.130	-	-0.221 ± 0.019	5.510 ± 0.386	0.001	2 ± 2	3 ± 3	2 ± 1	-	3
XMMXCS J133923.1+272328.2	$0.195^{+0.062}_{-0.065}$	0.182 ± 0.028	-	0.0002 ± 0.009	1.220 ± 0.168	0.001	3 ± 2	3 ± 2	3 ± 2	2 ± 2	3
XMMXCS J134029.9-005208.4	$0.172^{+0.076}_{-0.082}$	0.115 ± 0.025	-	0.036 ± 0.025	0.175 ± 0.491	0.055	2 ± 2	2 ± 2	1 ± 1	0 ± 1	3
XMMXCS J134106.7-004813.0	$0.164^{+0.031}_{-0.028}$	0.157 ± 0.035	$0.161 \pm 1.4e-05$	-0.053 ± 0.040	1.800 ± 0.698	0.100	0 ± 1	1 ± 2	-	0 ± 1	3
XMMXCS J134120.0+261543.6	$0.072^{+0.025}_{-0.026}$	0.074 ± 0.017	$0.072 \pm 1.0e-05$	-0.082 ± 0.022	2.150 ± 0.359	0.090	3 ± 2	4 ± 2	0 ± 0.1	0 ± 1	3
XMMXCS J134126.4+262410.1	$0.406^{+0.180}_{-0.193}$	0.210 ± 0.093	-	0.423 ± 0.258	-7.650 ± 5.290	0.129	3 ± 3	5 ± 3	1 ± 1	1 ± 2	3
XMMXCS J134215.0+261102.6	$0.070^{+0.004}_{-0.004}$	0.071 ± 0.015	$0.066 \pm 1.0e-05$	-0.004 ± 0.007	0.931 ± 0.104	0.020	6 ± 3	6 ± 3	2 ± 2	4 ± 2	3
XMMXCS J134246.3-003545.4	$0.200^{+0.076}_{-0.064}$	0.062 ± 0.034	$0.086 \pm 1.3e-05$	0.172 ± 0.001	-2.900 ± 0.013	0.500	1 ± 2	4 ± 3	0 ± 0.1	-	3
XMMXCS J134247.3+403012.7	$0.726^{+0.131}_{-0.124}$	0.635 ± 0.245	-	-0.080 ± 0.084	2.890 ± 1.730	0.116	3 ± 2	-	1 ± 1	-	3
XMMXCS J134249.5+402824.7	$0.606^{+0.173}_{-0.174}$	0.411 ± 0.336	-	-0.062 ± 0.145	2.340 ± 2.960	0.076	11 ± 4	19 ± 5	10 ± 3	25 ± 6	3
XMMXCS J134305.1-000056.8	$0.719^{+0.139}_{-0.137}$	0.648 ± 0.115	-	-0.060 ± 0.032	2.380 ± 0.643	0.001	13 ± 4	54 ± 8	13 ± 4	83 ± 11	3

Continued on next page

Table A.2 – continued from previous page

name	z_{RS}	z_{BCG}	z_{spec-g}	cmr_{grad}	cmr_{inter}	cmr_{wid}	n_{gals-c}	n_{gals-l}	n_{200-c}	n_{200-l}	qual
XMMXCS J134326.6+402331.7	$0.421^{+0.097}_{-0.097}$	0.234 ± 0.061	-	-0.059 ± 0.047	2.650 ± 0.943	0.099	4 ± 3	5 ± 3	0 ± 1	2 ± 2	3
XMMXCS J134326.9+554648.3	$0.065^{+0.014}_{-0.009}$	0.071 ± 0.015	$0.068 \pm 1.4e-05$	-0.001 ± 0.024	0.917 ± 0.392	0.037	3 ± 2	1 ± 1	1 ± 1	0 ± 1	3
XMMXCS J134352.5+402635.3	$0.174^{+0.037}_{-0.039}$	0.179 ± 0.031	$0.178 \pm 2.7e-05$	0.093 ± 0.014	-0.317 ± 0.236	0.045	3 ± 2	1 ± 2	0 ± 0.1	0 ± 1	3
XMMXCS J134636.5+173641.4	$0.068^{+0.001}_{-0.001}$	0.071 ± 0.026	$0.068 \pm 8.6e-06$	0.024 ± 0.016	0.434 ± 0.254	0.031	1 ± 1	1 ± 1	1 ± 1	2 ± 2	3
XMMXCS J134655.0+173214.7	$0.364^{+0.109}_{-0.103}$	0.511 ± 0.125	$0.474 \pm 1.3e-04$	-0.102 ± 0.006	2.700 ± 0.112	0.500	3 ± 3	2 ± 4	4 ± 2	3 ± 2	3
XMMXCS J134659.3+173940.4	$0.483^{+0.146}_{-0.145}$	0.557 ± 0.099	$0.524 \pm 1.0e-04$	0.067 ± 0.137	-0.574 ± 2.690	0.134	5 ± 3	4 ± 3	7 ± 3	7 ± 3	3
XMMXCS J134800.2+075220.6	$0.361^{+0.113}_{-0.113}$	0.437 ± 0.064	-	-0.041 ± 0.066	1.520 ± 1.310	0.044	3 ± 2	2 ± 2	2 ± 2	2 ± 2	3
XMMXCS J134800.5+601702.7	$0.322^{+0.124}_{-0.122}$	0.399 ± 0.118	-	-0.218 ± 0.252	5.830 ± 5.120	0.024	0 ± 1	1 ± 2	-	0 ± 1	3
XMMXCS J134807.2-035352.2	$0.297^{+0.092}_{-0.094}$	0.191 ± 0.029	-	0.126 ± 0.267	-0.882 ± 5.210	0.099	5 ± 3	5 ± 3	4 ± 2	4 ± 3	3
XMMXCS J134812.7+581331.3	$0.155^{+0.057}_{-0.070}$	0.061 ± 0.017	$0.119 \pm 1.8e-05$	-0.002 ± 0.017	0.966 ± 0.306	0.064	2 ± 2	0 ± 2	1 ± 1	-	3
XMMXCS J134825.6+580015.8	$0.128^{+0.022}_{-0.022}$	0.136 ± 0.023	$0.111 \pm 1.6e-05$	-0.026 ± 0.018	1.490 ± 0.280	0.049	3 ± 2	3 ± 2	3 ± 2	4 ± 2	3
XMMXCS J134842.8+263732.2	$0.054^{+0.090}_{-0.054}$	0.077 ± 0.018	$0.066 \pm 9.9e-06$	0.038 ± 0.039	0.193 ± 0.705	0.096	1 ± 1	0 ± 1	0 ± 0.1	-	3
XMMXCS J134848.1+074723.5	$0.281^{+0.085}_{-0.087}$	0.205 ± 0.065	-	0.159 ± 0.049	-2.070 ± 0.991	0.093	1 ± 2	0 ± 2	0 ± 0.1	-	3
XMMXCS J134851.8+600942.5	$0.373^{+0.096}_{-0.096}$	0.436 ± 0.071	-	-0.061 ± 0.094	2.740 ± 1.780	0.001	3 ± 3	3 ± 3	3 ± 2	3 ± 2	3
XMMXCS J134903.8+642305.0	$0.539^{+0.090}_{-0.090}$	0.507 ± 0.074	$0.539 \pm 1.3e-04$	0.016 ± 0.019	0.686 ± 0.378	0.034	1 ± 2	0 ± 2	0 ± 0.1	-	3
XMMXCS J134922.0+261655.3	$0.469^{+0.142}_{-0.138}$	0.428 ± 0.064	-	0.211 ± 0.093	-3.480 ± 1.880	0.116	2 ± 3	2 ± 3	0 ± 1	-	3
XMMXCS J134923.2+075351.5	$0.373^{+0.097}_{-0.095}$	0.406 ± 0.065	-	-1.950 ± 0.345	41.400 ± 6.620	0.500	5 ± 3	3 ± 3	1 ± 1	-	3
XMMXCS J134936.4+643920.9	$0.572^{+0.235}_{-0.230}$	0.552 ± 0.228	-	-0.062 ± 0.327	3.010 ± 6.550	0.001	1 ± 1	1 ± 1	0 ± 0.1	-	3
XMMXCS J134945.0-034959.4	$0.486^{+0.236}_{-0.236}$	0.467 ± 0.099	-	-76.20 ± 616	1590 ± 12800	8.472	6 ± 3	0 ± 1	2 ± 2	-	3

Continued on next page

Table A.2 – continued from previous page

name	z_{RS}	z_{BCG}	z_{spec-g}	cmr_{grad}	cmr_{inter}	cmr_{wid}	n_{gals-c}	n_{gals-l}	n_{200-c}	n_{200-l}	qual
XMMXCS J134949.7+270605.3	$0.423^{+0.084}_{-0.083}$	0.346 ± 0.053	-	0.080 ± 0.085	-0.049 ± 1.700	0.098	13 ± 4	18 ± 5	14 ± 4	22 ± 6	3
XMMXCS J135005.5+265610.0	$0.307^{+0.117}_{-0.108}$	0.139 ± 0.038	-	-0.008 ± 0.187	1.690 ± 3.670	0.500	4 ± 3	3 ± 4	3 ± 2	1 ± 2	3
XMMXCS J135117.8+634257.1	$0.316^{+0.105}_{-0.101}$	0.240 ± 0.096	-	0.219 ± 0.014	-3.040 ± 0.274	0.500	2 ± 3	1 ± 3	3 ± 2	-	3
XMMXCS J135349.8+634415.9	$0.150^{+0.188}_{-0.124}$	0.209 ± 0.069	-	-0.015 ± 0.038	1.420 ± 0.715	0.050	1 ± 1	0 ± 1	0 ± 0.1	-	3
XMMXCS J135407.8+633802.3	$0.148^{+0.121}_{-0.137}$	0.085 ± 0.020	$0.080 \pm 1.2e-05$	0.013 ± 0.059	0.660 ± 1.020	0.500	0 ± 2	1 ± 2	-	1 ± 1	3
XMMXCS J135412.2+634129.9	$0.143^{+0.034}_{-0.038}$	0.122 ± 0.025	-	0.040 ± 0.086	0.484 ± 1.560	0.095	0 ± 1	1 ± 1	-	0 ± 1	3
XMMXCS J135422.9+633852.9	$0.165^{+0.049}_{-0.041}$	0.085 ± 0.020	$0.080 \pm 1.2e-05$	0.175 ± 0.011	-1.950 ± 0.187	0.500	5 ± 3	3 ± 3	2 ± 2	1 ± 2	3
XMMXCS J135502.5+382519.3	$0.276^{+0.076}_{-0.074}$	0.192 ± 0.035	-	0.056 ± 0.047	0.246 ± 0.859	0.100	2 ± 2	2 ± 3	0 ± 0.1	-	3
XMMXCS J135526.9+634243.3	$0.269^{+0.102}_{-0.124}$	0.194 ± 0.044	-	-0.025 ± 0.073	1.690 ± 1.380	0.001	3 ± 2	2 ± 2	1 ± 1	0 ± 1	3
XMMXCS J135556.4+653249.0	$0.242^{+0.065}_{-0.059}$	0.235 ± 0.073	-	-0.062 ± 0.047	2.290 ± 0.893	0.116	3 ± 2	2 ± 2	0 ± 1	0 ± 1	3
XMMXCS J135609.1+382244.1	$0.310^{+0.086}_{-0.090}$	0.238 ± 0.064	-	0.095 ± 0.062	-0.564 ± 1.220	0.075	1 ± 2	1 ± 2	0 ± 0.1	0 ± 1	3
XMMXCS J135623.8+652616.1	$0.218^{+0.061}_{-0.059}$	0.245 ± 0.049	-	-0.041 ± 0.071	1.930 ± 1.290	0.500	0 ± 2	1 ± 2	-	2 ± 2	3
XMMXCS J135753.4+651541.3	$0.059^{+0.039}_{-0.043}$	0.062 ± 0.020	$0.059 \pm 7.3e-06$	0.061 ± 0.016	-0.091 ± 0.253	0.050	2 ± 1	0 ± 1	1 ± 1	-	3
XMMXCS J140045.7-013316.0	$0.128^{+0.078}_{-0.084}$	0.168 ± 0.049	$0.156 \pm 9.9e-06$	0.054 ± 0.034	-0.274 ± 0.601	0.114	1 ± 1	1 ± 1	0 ± 0.1	1 ± 1	3
XMMXCS J140048.7-014454.4	$0.149^{+0.032}_{-0.032}$	0.145 ± 0.040	$0.149 \pm 1.2e-05$	-0.093 ± 0.333	2.520 ± 6.010	0.500	0 ± 2	1 ± 2	-	2 ± 2	3
XMMXCS J140052.7-014512.3	$0.149^{+0.030}_{-0.029}$	0.145 ± 0.040	$0.147 \pm 2.4e-05$	-0.307 ± 0.001	6.320 ± 0.010	0.500	1 ± 2	4 ± 3	0 ± 0.1	0 ± 1	3
XMMXCS J140129.1-110248.0	$0.279^{+0.111}_{-0.109}$	0.190 ± 0.036	-	-0.174 ± 0.043	4.490 ± 0.832	0.023	3 ± 2	3 ± 3	4 ± 2	4 ± 2	3
XMMXCS J140204.2-110541.1	$0.311^{+0.179}_{-0.179}$	0.114 ± 0.020	-	-0.174 ± 0.161	4.270 ± 3.350	0.062	0 ± 2	2 ± 2	-	1 ± 1	3
XMMXCS J140354.81+540848.8	$0.111^{+0.023}_{-0.023}$	0.118 ± 0.028	$0.110 \pm 1.4e-05$	0.073 ± 0.150	-0.408 ± 2.650	0.086	1 ± 1	1 ± 1	0 ± 0.1	0 ± 1	3

Continued on next page

Table A.2 – continued from previous page

name	z_{RS}	z_{BCG}	z_{spec-g}	cmr_{grad}	cmr_{inter}	cmr_{wid}	n_{gals-c}	n_{gals-l}	n_{200-c}	n_{200-l}	qual
XMMXCS J140354.8+540848.8	$0.111^{+0.023}_{-0.023}$	0.118 ± 0.028	$0.110 \pm 1.4e-05$	0.073 ± 0.150	-0.408 ± 2.650	0.086	1 ± 1	1 ± 1	0 ± 0.1	0 ± 1	3
XMMXCS J140412.8+260003.7	$0.364^{+0.101}_{-0.101}$	0.429 ± 0.095	$0.440 \pm 6.5e-05$	-0.118 ± 0.091	4.030 ± 1.720	0.001	2 ± 2	2 ± 2	2 ± 1	2 ± 2	3
XMMXCS J140456.3+542355.5	$0.371^{+0.128}_{-0.107}$	0.349 ± 0.150	-	0.009 ± 0.074	0.916 ± 1.460	0.117	5 ± 3	3 ± 3	1 ± 2	-	3
XMMXCS J140456.2+542355.4	$0.371^{+0.128}_{-0.107}$	0.349 ± 0.150	-	0.009 ± 0.074	0.916 ± 1.460	0.117	5 ± 3	3 ± 3	1 ± 2	-	3
XMMXCS J140602.0+221821.1	$0.591^{+0.088}_{-0.087}$	0.554 ± 0.141	$0.590 \pm 1.1e-04$	-0.053 ± 0.013	2.090 ± 0.256	0.001	6 ± 3	20 ± 5	4 ± 2	25 ± 6	3
XMMXCS J140637.3+283930.3	$0.485^{+0.033}_{-0.033}$	0.357 ± 0.113	$0.484 \pm 1.1e-04$	0.008 ± 0.058	0.663 ± 1.130	0.001	2 ± 3	8 ± 4	1 ± 1	10 ± 4	3
XMMXCS J140646.0+283308.3	$0.478^{+0.138}_{-0.138}$	0.281 ± 0.058	-	0.059 ± 0.160	-0.500 ± 3.320	0.122	11 ± 4	10 ± 5	10 ± 4	10 ± 4	3
XMMXCS J140719.3+281813.0	$0.342^{+0.076}_{-0.075}$	0.146 ± 0.028	$0.351 \pm 5.7e-05$	0.219 ± 0.151	-2.520 ± 2.850	0.189	18 ± 5	16 ± 5	22 ± 5	29 ± 6	3
XMMXCS J140908.1+261406.7	$0.472^{+0.124}_{-0.123}$	0.346 ± 0.126	-	0.438 ± 0.271	-8.000 ± 5.540	0.174	1 ± 3	-	0 ± 0.1	-	3
XMMXCS J140927.7+262233.6	$0.609^{+0.166}_{-0.163}$	0.697 ± 0.143	$0.674 \pm 2.2e-04$	-0.203 ± 0.442	5.050 ± 9.060	0.001	3 ± 2	24 ± 6	2 ± 2	-	3
XMMXCS J141235.3+435532.1	$0.145^{+0.028}_{-0.024}$	0.113 ± 0.024	$0.137 \pm 2.1e-05$	-0.208 ± 0.035	4.480 ± 0.628	0.500	0 ± 2	2 ± 2	-	1 ± 1	3
XMMXCS J141256.5-032416.7	$0.389^{+0.113}_{-0.111}$	0.281 ± 0.084	-	0.041 ± 0.066	0.587 ± 1.290	0.001	5 ± 3	5 ± 3	5 ± 3	5 ± 3	3
XMMXCS J141257.1+440223.2	$0.571^{+0.143}_{-0.142}$	0.517 ± 0.088	-	0.278 ± 0.361	-4.450 ± 7.230	0.001	4 ± 2	11 ± 4	-	11 ± 4	3
XMMXCS J141321.7-030654.1	$0.309^{+0.089}_{-0.089}$	0.256 ± 0.052	$0.386 \pm 4.9e-05$	-0.011 ± 0.070	1.730 ± 1.330	0.083	7 ± 3	-	0 ± 1	-	3
XMMXCS J141453.0+361228.5	$0.346^{+0.091}_{-0.090}$	0.261 ± 0.070	-	-0.116 ± 0.137	3.780 ± 2.710	0.001	2 ± 2	1 ± 2	3 ± 2	2 ± 2	3
XMMXCS J141511.3+114004.6	$0.183^{+0.062}_{-0.061}$	0.178 ± 0.069	-	0.359 ± 0.060	-5.610 ± 1.110	0.076	3 ± 2	2 ± 2	1 ± 1	0 ± 1	3
XMMXCS J141525.0+113641.5	$0.155^{+0.043}_{-0.042}$	0.151 ± 0.028	$0.155 \pm 2.1e-05$	-0.050 ± 0.011	1.930 ± 0.182	0.001	1 ± 1	3 ± 2	0 ± 0.1	3 ± 2	3
XMMXCS J141531.9+112749.1	$0.169^{+0.085}_{-0.087}$	0.142 ± 0.038	$0.171 \pm 1.9e-05$	0.001 ± 0.050	0.738 ± 0.988	0.127	0 ± 0.1	2 ± 2	-	0 ± 1	3
XMMXCS J141534.5-001827.6	$0.141^{+0.023}_{-0.023}$	0.155 ± 0.027	$0.141 \pm 3.8e-05$	-0.032 ± 0.012	1.630 ± 0.220	0.001	2 ± 2	2 ± 2	1 ± 1	1 ± 1	3

Continued on next page

Table A.2 – continued from previous page

name	z_{RS}	z_{BCG}	z_{spec-g}	cmr_{grad}	cmr_{inter}	cmr_{wid}	n_{gals-c}	n_{gals-l}	n_{200-c}	n_{200-l}	qual
XMMXCS J141541.0+114130.5	$0.565^{+0.163}_{-0.173}$	0.573 ± 0.135	-	0.027 ± 0.128	0.469 ± 2.630	0.135	1 ± 2	5 ± 3	0 ± 0.1	5 ± 3	3
XMMXCS J141542.2+522206.7	$0.483^{+0.147}_{-0.152}$	0.312 ± 0.049	-	-0.110 ± 0.114	2.990 ± 2.330	0.143	8 ± 4	12 ± 5	2 ± 3	11 ± 5	3
XMMXCS J141549.9+282149.7	$0.256^{+0.081}_{-0.086}$	0.220 ± 0.037	-	0.044 ± 0.041	0.556 ± 0.792	0.110	2 ± 2	1 ± 2	0 ± 0.1	-	3
XMMXCS J141559.4+361605.7	$0.079^{+0.083}_{-0.076}$	0.065 ± 0.027	$0.038 \pm 2.3e-05$	0.135 ± 0.023	-1.530 ± 0.401	0.035	1 ± 1	0 ± 1	1 ± 1	-	3
XMMXCS J141620.6+264301.8	$0.392^{+0.103}_{-0.103}$	0.228 ± 0.040	-	0.459 ± 0.211	-7.410 ± 4.260	0.158	15 ± 4	17 ± 5	16 ± 5	19 ± 5	3
XMMXCS J141627.7+444644.5	$0.399^{+0.063}_{-0.063}$	0.330 ± 0.054	-	0.052 ± 0.071	0.679 ± 1.390	0.052	26 ± 5	30 ± 6	32 ± 6	40 ± 7	3
XMMXCS J141629.01+522701.3	$0.319^{+0.067}_{-0.062}$	0.229 ± 0.038	-	0.228 ± 0.181	-2.860 ± 3.520	0.157	2 ± 2	-	0 ± 0.1	-	3
XMMXCS J141629.0+522701.3	$0.319^{+0.067}_{-0.062}$	0.229 ± 0.038	-	0.228 ± 0.181	-2.860 ± 3.520	0.157	2 ± 2	-	0 ± 0.1	-	3
XMMXCS J141639.3+522845.3	$0.346^{+0.102}_{-0.094}$	0.231 ± 0.039	-	0.573 ± 0.350	-9.250 ± 6.530	0.534	0 ± 3	2 ± 3	-	1 ± 2	3
XMMXCS J141652.4+522052.9	$0.289^{+0.086}_{-0.081}$	0.250 ± 0.075	-	0.038 ± 0.035	0.498 ± 0.673	0.128	3 ± 3	5 ± 3	0 ± 1	4 ± 3	3
XMMXCS J141653.63+522102.2	$0.397^{+0.088}_{-0.082}$	0.250 ± 0.075	-	0.096 ± 0.059	-0.385 ± 1.050	0.160	3 ± 3	4 ± 3	1 ± 2	1 ± 2	3
XMMXCS J141656.7+521514.9	$0.352^{+0.140}_{-0.130}$	0.336 ± 0.123	-	0.061 ± 0.072	0.044 ± 1.410	0.138	0 ± 2	1 ± 3	-	0 ± 1	3
XMMXCS J141720.3+445625.5	$0.112^{+0.025}_{-0.026}$	0.122 ± 0.042	$0.114 \pm 1.0e-05$	-0.032 ± 0.016	1.190 ± 0.297	0.500	0 ± 2	2 ± 2	-	3 ± 2	3
XMMXCS J141731.73+523200.3	$0.242^{+0.095}_{-0.099}$	0.242 ± 0.053	-	-0.012 ± 0.053	1.610 ± 1.020	0.001	0 ± 1	1 ± 1	-	0 ± 1	3
XMMXCS J141731.7+523200.2	$0.242^{+0.095}_{-0.099}$	0.242 ± 0.053	-	-0.012 ± 0.053	1.610 ± 1.020	0.001	0 ± 1	1 ± 1	-	0 ± 1	3
XMMXCS J141759.5+445156.1	$0.414^{+0.141}_{-0.133}$	0.428 ± 0.187	-	0.045 ± 0.139	0.342 ± 2.830	0.150	4 ± 3	3 ± 3	0 ± 1	0 ± 1	3
XMMXCS J141803.0+264721.7	$0.238^{+0.065}_{-0.081}$	0.278 ± 0.057	-	-0.065 ± 0.157	2.660 ± 3.150	0.167	1 ± 1	0 ± 1	0 ± 0.1	-	3
XMMXCS J141812.5+251139.8	$0.291^{+0.061}_{-0.064}$	0.241 ± 0.041	$0.296 \pm 4.3e-05$	0.030 ± 0.076	0.918 ± 1.450	0.073	4 ± 3	3 ± 3	0 ± 1	0 ± 1	3
XMMXCS J141838.7+522359.0	$0.293^{+0.083}_{-0.077}$	0.299 ± 0.045	-	-0.121 ± 0.245	3.500 ± 4.600	0.500	5 ± 3	-	0 ± 2	-	3

Continued on next page

Table A.2 – continued from previous page

name	z_{RS}	z_{BCG}	z_{spec-g}	cmr_{grad}	cmr_{inter}	cmr_{wid}	n_{gals-c}	n_{gals-l}	n_{200-c}	n_{200-l}	qual
XMMXCS J141857.7+250949.5	$0.417^{+0.117}_{-0.118}$	0.281 ± 0.046	-	0.019 ± 0.025	1.180 ± 0.475	0.081	5 ± 3	6 ± 3	1 ± 2	-	3
XMMXCS J141923.5+063140.9	$0.512^{+0.135}_{-0.135}$	0.390 ± 0.147	-	-0.016 ± 0.032	0.802 ± 0.639	0.054	3 ± 2	1 ± 1	1 ± 1	-	3
XMMXCS J141956.2+063434.1	$0.536^{+0.145}_{-0.145}$	0.474 ± 0.207	-	0.198 ± 0.091	-3.050 ± 1.820	0.001	15 ± 4	37 ± 7	17 ± 5	62 ± 9	3
XMMXCS J141956.2+063434.2	$0.536^{+0.145}_{-0.145}$	0.474 ± 0.207	-	0.198 ± 0.091	-3.050 ± 1.820	0.001	15 ± 4	37 ± 7	17 ± 5	62 ± 9	3
XMMXCS J142005.9+062521.2	$0.337^{+0.129}_{-0.106}$	0.173 ± 0.029	-	0.032 ± 0.045	0.619 ± 0.937	0.128	0 ± 2	2 ± 3	-	1 ± 2	3
XMMXCS J142030.2+064746.3	$0.182^{+0.089}_{-0.091}$	0.226 ± 0.151	-	-0.036 ± 0.023	1.700 ± 0.444	0.098	1 ± 2	1 ± 2	0 ± 0.1	1 ± 1	3
XMMXCS J142030.3+064746.3	$0.182^{+0.089}_{-0.091}$	0.226 ± 0.151	-	-0.036 ± 0.023	1.700 ± 0.444	0.098	1 ± 2	1 ± 2	0 ± 0.1	1 ± 1	3
XMMXCS J142040.2+063453.2	$0.228^{+0.092}_{-0.097}$	0.161 ± 0.053	-	0.041 ± 0.052	0.271 ± 0.929	0.127	2 ± 2	1 ± 2	0 ± 0.1	0 ± 1	3
XMMXCS J142449.1+422047.7	$0.378^{+0.111}_{-0.124}$	0.414 ± 0.064	$0.456 \pm 8.1e-05$	0.082 ± 0.063	-0.751 ± 1.220	0.001	2 ± 2	2 ± 2	0 ± 0.1	0 ± 1	3
XMMXCS J142634.2+380157.4	$0.154^{+0.047}_{-0.049}$	0.146 ± 0.027	-	0.062 ± 0.060	-0.047 ± 1.220	0.145	1 ± 1	1 ± 2	0 ± 0.1	0 ± 1	3
XMMXCS J142700.2+264308.6	$0.589^{+0.123}_{-0.122}$	0.398 ± 0.277	-	1.110 ± 0.474	-21.20 ± 9.560	0.001	1 ± 1	0 ± 1	1 ± 1	-	3
XMMXCS J142733.1+264127.2	$0.242^{+0.054}_{-0.048}$	0.237 ± 0.036	$0.229 \pm 3.6e-05$	-0.057 ± 0.108	2.240 ± 2.040	0.075	1 ± 2	0 ± 2	0 ± 0.1	-	3
XMMXCS J142814.7+423600.9	$0.232^{+0.062}_{-0.062}$	0.209 ± 0.052	-	0.083 ± 0.013	-0.378 ± 0.240	0.001	1 ± 1	1 ± 2	0 ± 0.1	0 ± 1	3
XMMXCS J142821.0+422637.0	$0.500^{+0.132}_{-0.117}$	0.319 ± 0.049	-	0.175 ± 0.055	-2.800 ± 1.120	0.126	2 ± 3	7 ± 4	1 ± 1	7 ± 4	3
XMMXCS J142823.8+422641.1	$0.494^{+0.166}_{-0.247}$	0.319 ± 0.049	-	0.326 ± 0.097	-5.920 ± 1.980	0.113	2 ± 3	5 ± 4	2 ± 2	7 ± 3	3
XMMXCS J142829.8+423217.0	$0.332^{+0.100}_{-0.101}$	0.262 ± 0.044	-	-0.152 ± 0.052	4.480 ± 1.050	0.119	4 ± 3	-	3 ± 2	-	3
XMMXCS J142832.2+262733.8	$0.300^{+0.090}_{-0.088}$	0.195 ± 0.030	$0.202 \pm 3.2e-05$	-0.000 ± 0.037	1.260 ± 0.658	0.001	5 ± 3	4 ± 3	1 ± 1	1 ± 2	3
XMMXCS J142839.8+424849.2	$0.335^{+0.104}_{-0.099}$	0.243 ± 0.046	-	-0.321 ± 0.002	7.710 ± 0.049	0.500	0 ± 3	1 ± 4	-	3 ± 2	3
XMMXCS J142841.1+425148.7	$0.232^{+0.094}_{-0.101}$	0.165 ± 0.039	-	0.219 ± 0.001	-3.220 ± 0.025	0.500	5 ± 3	5 ± 4	1 ± 2	1 ± 2	3

Continued on next page

Table A.2 – continued from previous page

name	z_{RS}	z_{BCG}	z_{spec-g}	cmr_{grad}	cmr_{inter}	cmr_{wid}	n_{gals-c}	n_{gals-l}	n_{200-c}	n_{200-l}	qual
XMMXCS J142854.3+425135.4	$0.184^{+0.074}_{-0.076}$	0.119 ± 0.024	$0.167 \pm 2.1e-05$	-0.234 ± 0.001	5.460 ± 0.023	0.500	4 ± 3	6 ± 4	0 ± 1	0 ± 2	3
XMMXCS J142855.5+474224.0	$0.227^{+0.083}_{-0.104}$	0.161 ± 0.026	-	-0.018 ± 0.044	1.440 ± 0.826	0.085	4 ± 2	4 ± 3	1 ± 1	1 ± 2	3
XMMXCS J142904.5+012220.2	$0.243^{+0.071}_{-0.072}$	0.144 ± 0.047	$0.101 \pm 1.2e-05$	0.171 ± 0.073	-2.040 ± 1.430	0.054	3 ± 2	1 ± 2	1 ± 1	3 ± 2	3
XMMXCS J142917.6+012057.9	$0.204^{+0.077}_{-0.077}$	0.125 ± 0.025	$0.128 \pm 1.4e-05$	-0.012 ± 0.029	1.100 ± 0.536	0.116	4 ± 3	0 ± 2	0 ± 1	-	3
XMMXCS J142923.3+011357.2	$0.437^{+0.096}_{-0.093}$	0.273 ± 0.120	$0.373 \pm 4.6e-05$	-0.139 ± 0.044	4.050 ± 0.827	0.001	5 ± 4	7 ± 4	1 ± 2	3 ± 3	3
XMMXCS J143521.3+034803.8	$0.455^{+0.101}_{-0.087}$	0.495 ± 0.157	-	0.071 ± 0.084	-0.716 ± 1.650	0.103	2 ± 3	4 ± 4	0 ± 0.1	-	3
XMMXCS J143529.8+484529.0	$0.586^{+0.128}_{-0.127}$	0.722 ± 0.156	-	0.013 ± 0.029	0.753 ± 0.544	0.001	9 ± 3	15 ± 5	9 ± 3	22 ± 6	3
XMMXCS J143536.5+034116.0	$0.100^{+0.043}_{-0.044}$	0.070 ± 0.027	$0.028 \pm 9.2e-06$	-0.004 ± 0.003	0.885 ± 0.036	0.500	2 ± 2	1 ± 2	0 ± 0.1	0 ± 1	3
XMMXCS J143609.0+485115.9	$0.364^{+0.118}_{-0.112}$	0.184 ± 0.032	-	-0.040 ± 0.109	1.300 ± 2.170	0.151	8 ± 4	11 ± 5	9 ± 4	11 ± 5	3
XMMXCS J143707.7+341843.9	$0.122^{+0.016}_{-0.017}$	0.063 ± 0.016	$0.096 \pm 1.1e-05$	0.024 ± 0.040	0.678 ± 0.644	0.096	4 ± 2	8 ± 3	4 ± 2	8 ± 3	3
XMMXCS J143743.2+340807.8	$0.544^{+0.042}_{-0.043}$	0.591 ± 0.132	$0.544 \pm 8.4e-05$	-0.045 ± 0.059	1.890 ± 1.130	0.001	6 ± 3	6 ± 4	3 ± 2	4 ± 3	3
XMMXCS J143836.3+001959.5	$0.406^{+0.104}_{-0.109}$	0.327 ± 0.049	$0.556 \pm 1.2e-04$	0.028 ± 0.087	1.200 ± 1.640	0.001	8 ± 3	9 ± 4	7 ± 3	8 ± 3	3
XMMXCS J143920.4+642402.3	$0.229^{+0.090}_{-0.088}$	0.154 ± 0.027	$0.144 \pm 1.9e-05$	0.075 ± 0.099	-0.015 ± 1.920	0.500	6 ± 4	6 ± 4	3 ± 2	2 ± 3	3
XMMXCS J143933.9+001357.5	$0.329^{+0.082}_{-0.077}$	0.297 ± 0.047	$0.320 \pm 4.0e-05$	-0.111 ± 0.069	3.440 ± 1.330	0.088	2 ± 3	-	0 ± 0.1	-	3
XMMXCS J143954.6+030005.5	$0.214^{+0.047}_{-0.049}$	0.244 ± 0.041	-	-0.140 ± 0.107	4.060 ± 2.050	0.041	2 ± 2	1 ± 2	0 ± 0.1	-	3
XMMXCS J144009.8+000918.6	$0.304^{+0.056}_{-0.055}$	0.248 ± 0.059	-	0.021 ± 0.046	1.120 ± 0.893	0.099	2 ± 2	2 ± 3	0 ± 1	-	3
XMMXCS J144017.73+533228.3	$0.423^{+0.142}_{-0.155}$	0.518 ± 0.178	-	0.018 ± 0.032	0.300 ± 0.646	0.085	3 ± 3	4 ± 3	0 ± 1	2 ± 2	3
XMMXCS J144100.5+642318.6	$0.510^{+0.182}_{-0.184}$	0.490 ± 0.122	-	2.370 ± 2.210	-46.70 ± 44.50	0.242	3 ± 2	2 ± 1	3 ± 2	1 ± 1	3
XMMXCS J144103.49+534042.4	$0.752^{+0.104}_{-0.104}$	0.595 ± 0.097	-	0.017 ± 0.185	0.202 ± 3.760	0.001	0 ± 1	23 ± 5	-	100 ± 11	3

Continued on next page

Table A.2 – continued from previous page

name	z_{RS}	z_{BCG}	z_{spec-g}	cmr_{grad}	cmr_{inter}	cmr_{wid}	n_{gals-c}	n_{gals-l}	n_{200-c}	n_{200-l}	qual
XMMXCS J144216.8+353139.4	$0.299^{+0.124}_{-0.159}$	0.317 ± 0.157	-	0.051 ± 0.054	0.380 ± 1.020	0.048	3 ± 2	4 ± 3	0 ± 1	1 ± 2	3
XMMXCS J144238.3+353713.5	$0.487^{+0.122}_{-0.133}$	0.353 ± 0.118	-	0.108 ± 0.086	-1.490 ± 1.750	0.118	2 ± 3	5 ± 4	1 ± 1	5 ± 3	3
XMMXCS J144643.4+025810.1	$0.444^{+0.193}_{-0.188}$	0.512 ± 0.225	-	0.013 ± 0.027	0.561 ± 0.531	0.001	2 ± 3	3 ± 3	2 ± 2	3 ± 2	3
XMMXCS J144926.4+085812.7	$0.509^{+0.161}_{-0.160}$	0.515 ± 0.110	$0.507 \pm 1.5e-04$	0.232 ± 0.037	-3.770 ± 0.759	0.001	7 ± 3	8 ± 4	4 ± 2	6 ± 3	3
XMMXCS J144934.8+090023.6	$0.609^{+0.182}_{-0.376}$	0.497 ± 0.151	-	0.254 ± 0.167	-4.150 ± 3.390	0.147	0 ± 2	3 ± 3	-	2 ± 2	3
XMMXCS J145009.3+090428.8	$0.644^{+0.138}_{-0.135}$	0.511 ± 0.260	-	0.388 ± 0.647	-6.870 ± 13.40	0.119	4 ± 2	1 ± 1	5 ± 2	0 ± 1	3
XMMXCS J145015.2+270831.7	$0.305^{+0.092}_{-0.091}$	0.124 ± 0.022	$0.143 \pm 3.0e-05$	0.137 ± 0.031	-1.280 ± 0.615	0.030	0 ± 2	2 ± 3	-	0 ± 1	3
XMMXCS J145339.9+183600.9	$0.254^{+0.105}_{-0.109}$	0.191 ± 0.030	$0.272 \pm 5.4e-05$	-0.048 ± 0.039	2.140 ± 0.730	0.128	0 ± 2	1 ± 2	-	0 ± 1	3
XMMXCS J145356.5+033243.7	$0.070^{+0.032}_{-0.035}$	0.079 ± 0.050	$0.061 \pm 9.4e-06$	0.045 ± 0.010	0.091 ± 0.135	0.038	1 ± 1	2 ± 2	0 ± 0.1	0 ± 1	3
XMMXCS J145404.5+185040.9	$0.140^{+0.083}_{-0.083}$	0.073 ± 0.017	$0.117 \pm 1.1e-05$	-0.020 ± 0.025	1.530 ± 0.428	0.500	3 ± 3	3 ± 3	1 ± 1	2 ± 2	3
XMMXCS J150320.8-025543.7	$0.615^{+0.138}_{-0.138}$	0.558 ± 0.118	-	-0.020 ± 0.107	1.670 ± 2.040	0.038	4 ± 2	8 ± 4	2 ± 2	9 ± 4	3
XMMXCS J150332.4+102157.6	$0.245^{+0.042}_{-0.041}$	0.098 ± 0.022	$0.123 \pm 1.4e-05$	0.133 ± 0.078	-1.200 ± 1.410	0.500	12 ± 5	14 ± 5	11 ± 5	168 ± 14	3
XMMXCS J150413.1-024310.6	$0.262^{+0.089}_{-0.091}$	0.178 ± 0.037	-	0.006 ± 0.053	1.230 ± 1.030	0.097	2 ± 2	2 ± 2	2 ± 1	2 ± 2	3
XMMXCS J150415.5-024056.3	$0.294^{+0.142}_{-0.157}$	0.232 ± 0.037	-	-0.577 ± 0.009	12.300 ± 0.189	0.500	5 ± 4	3 ± 4	3 ± 2	-	3
XMMXCS J150415.6-030210.0	$0.337^{+0.167}_{-0.165}$	0.188 ± 0.029	-	-0.019 ± 0.096	1.640 ± 1.720	0.001	1 ± 2	3 ± 3	-	0 ± 1	3
XMMXCS J150418.1-023944.4	$0.498^{+0.092}_{-0.085}$	0.386 ± 0.075	$0.489 \pm 2.3e-04$	-0.030 ± 0.074	1.250 ± 1.490	0.001	4 ± 3	5 ± 3	4 ± 2	4 ± 3	3
XMMXCS J150420.9-024040.5	$0.213^{+0.067}_{-0.072}$	0.232 ± 0.037	-	-0.092 ± 0.056	3.140 ± 1.070	0.001	1 ± 1	1 ± 2	0 ± 0.1	1 ± 1	3
XMMXCS J150422.8-023913.2	$0.252^{+0.060}_{-0.061}$	0.232 ± 0.037	$0.335 \pm 4.3e-05$	0.099 ± 0.032	-0.474 ± 0.613	0.001	1 ± 2	2 ± 2	0 ± 0.1	1 ± 1	3
XMMXCS J150452.5+474130.2	$0.383^{+0.115}_{-0.118}$	0.330 ± 0.053	-	-0.143 ± 0.082	4.260 ± 1.600	0.001	4 ± 3	5 ± 3	0 ± 1	1 ± 2	3

Continued on next page

Table A.2 – continued from previous page

name	z_{RS}	z_{BCG}	z_{spec-g}	cmr_{grad}	cmr_{inter}	cmr_{wid}	n_{gals-c}	n_{gals-l}	n_{200-c}	n_{200-l}	qual
XMMXCS J150627.4+030618.1	$0.173^{+0.047}_{-0.046}$	0.057 ± 0.015	$0.086 \pm 9.1e-06$	-0.000 ± 0.001	0.768 ± 0.001	0.500	8 ± 4	9 ± 4	6 ± 3	4 ± 3	3
XMMXCS J150652.9+014424.8	$0.557^{+0.146}_{-0.143}$	0.627 ± 0.201	-	0.374 ± 0.053	-6.710 ± 1.080	0.001	5 ± 2	0 ± 1	6 ± 2	-	3
XMMXCS J150817.4+012043.8	$0.173^{+0.067}_{-0.068}$	0.113 ± 0.018	$0.105 \pm 1.3e-05$	0.057 ± 0.019	0.099 ± 0.346	0.097	0 ± 2	5 ± 3	-	0 ± 1	3
XMMXCS J150843.4+010724.3	$0.282^{+0.066}_{-0.065}$	0.099 ± 0.018	$0.093 \pm 2.3e-05$	0.276 ± 0.079	-4.190 ± 1.580	0.500	10 ± 5	7 ± 5	10 ± 4	4 ± 4	3
XMMXCS J150918.3-001432.7	$0.253^{+0.062}_{-0.062}$	0.145 ± 0.023	-	0.038 ± 0.087	0.564 ± 1.650	0.076	11 ± 4	9 ± 4	10 ± 4	8 ± 3	3
XMMXCS J150944.1+072214.4	$0.369^{+0.095}_{-0.081}$	0.221 ± 0.045	-	0.051 ± 0.030	-0.356 ± 0.559	0.083	0 ± 2	1 ± 3	-	1 ± 1	3
XMMXCS J150944.6+074618.1	$0.073^{+0.032}_{-0.023}$	0.063 ± 0.021	$0.081 \pm 5.7e-06$	0.286 ± 0.095	-4.100 ± 1.590	0.100	2 ± 2	3 ± 2	2 ± 1	1 ± 1	3
XMMXCS J151014.4+054121.2	$0.276^{+0.061}_{-0.062}$	0.343 ± 0.061	-	-0.068 ± 0.110	2.760 ± 2.120	0.106	3 ± 2	3 ± 3	2 ± 2	2 ± 2	3
XMMXCS J151027.2+054519.3	$0.343^{+0.154}_{-0.160}$	0.165 ± 0.046	-	0.240 ± 0.338	-3.870 ± 6.830	0.202	3 ± 3	3 ± 3	1 ± 2	3 ± 2	3
XMMXCS J151029.7+054459.4	$0.364^{+0.127}_{-0.126}$	0.495 ± 0.262	$0.249 \pm 2.6e+00$	0.953 ± 0.327	-18.20 ± 6.710	0.001	5 ± 3	5 ± 3	3 ± 2	2 ± 2	3
XMMXCS J151038.0+053419.9	$0.422^{+0.114}_{-0.106}$	0.289 ± 0.058	-	0.015 ± 0.038	0.401 ± 0.750	0.113	4 ± 3	4 ± 4	0 ± 2	0 ± 2	3
XMMXCS J151043.7+053509.0	$0.080^{+0.006}_{-0.007}$	0.091 ± 0.021	$0.082 \pm 1.2e-05$	-0.212 ± 0.001	4.370 ± 0.001	0.500	9 ± 4	9 ± 3	6 ± 3	6 ± 3	3
XMMXCS J151132.1+053324.1	$0.140^{+0.098}_{-0.111}$	0.059 ± 0.018	$0.084 \pm 8.4e-06$	-0.004 ± 0.013	0.889 ± 0.239	0.058	4 ± 3	5 ± 3	1 ± 1	1 ± 2	3
XMMXCS J151142.8+055246.9	$0.069^{+0.018}_{-0.016}$	0.076 ± 0.020	$0.069 \pm 1.2e-05$	0.038 ± 0.043	0.092 ± 0.727	0.095	5 ± 2	3 ± 2	0 ± 0.1	0 ± 1	3
XMMXCS J151441.5+364448.9	$0.370^{+0.128}_{-0.130}$	0.345 ± 0.201	-	0.181 ± 0.076	-3.510 ± 1.520	0.100	1 ± 2	2 ± 2	0 ± 0.1	1 ± 1	3
XMMXCS J151526.3+000021.9	$0.301^{+0.065}_{-0.065}$	0.210 ± 0.048	-	0.013 ± 0.191	1.130 ± 3.840	0.154	4 ± 3	-	0 ± 1	-	3
XMMXCS J151528.9+370102.8	$0.213^{+0.063}_{-0.066}$	0.184 ± 0.047	-	-0.082 ± 0.034	2.590 ± 0.631	0.500	2 ± 3	0 ± 3	0 ± 1	-	3
XMMXCS J151534.7+000421.2	$0.431^{+0.128}_{-0.092}$	0.367 ± 0.077	-	0.164 ± 0.093	-1.610 ± 1.830	0.119	1 ± 2	15 ± 5	-	27 ± 6	3
XMMXCS J151536.6+364648.1	$0.165^{+0.045}_{-0.044}$	0.073 ± 0.027	-	-0.009 ± 0.001	1.100 ± 0.001	0.500	5 ± 3	3 ± 3	6 ± 3	2 ± 2	3

Continued on next page

Table A.2 – continued from previous page

name	z_{RS}	z_{BCG}	z_{spec-g}	cmr_{grad}	cmr_{inter}	cmr_{wid}	n_{gals-c}	n_{gals-l}	n_{200-c}	n_{200-l}	qual
XMMXCS J151547.1+001529.3	$0.322^{+0.090}_{-0.085}$	0.131 ± 0.035	-	-0.000 ± 0.001	1.700 ± 0.001	0.500	6 ± 4	8 ± 4	9 ± 4	10 ± 4	3
XMMXCS J151556.7-000222.0	$0.147^{+0.038}_{-0.082}$	0.060 ± 0.017	$0.053 \pm 8.5e-06$	0.237 ± 0.197	-3.330 ± 3.470	0.108	4 ± 3	3 ± 3	1 ± 1	1 ± 2	3
XMMXCS J151602.3-010856.0	$0.119^{+0.024}_{-0.024}$	0.124 ± 0.021	$0.119 \pm 4.0e-05$	-0.050 ± 0.032	1.810 ± 0.558	0.051	1 ± 1	2 ± 2	0 ± 0.1	1 ± 1	3
XMMXCS J151604.3+562806.8	$0.237^{+0.103}_{-0.116}$	0.207 ± 0.038	-	-0.061 ± 0.070	2.360 ± 1.380	0.060	1 ± 1	0 ± 1	0 ± 0.1	-	3
XMMXCS J151610.2+065744.8	$0.032^{+0.008}_{-0.008}$	0.053 ± 0.018	$0.031 \pm 6.7e-06$	-0.049 ± 0.016	1.520 ± 0.253	0.029	1 ± 1	0 ± 1	0 ± 0.1	-	3
XMMXCS J151627.2+065504.4	$0.655^{+0.129}_{-0.125}$	0.682 ± 0.141	-	-0.232 ± 0.083	6.060 ± 1.660	0.001	2 ± 1	1 ± 1	0 ± 0.1	-	3
XMMXCS J151637.2+065754.7	$0.094^{+0.063}_{-0.068}$	0.069 ± 0.018	$0.033 \pm 6.0e-06$	-0.025 ± 0.016	1.210 ± 0.287	0.074	18 ± 5	37 ± 6	29 ± 6	83 ± 10	3
XMMXCS J151644.2+070108.5	$0.033^{+0.012}_{-0.012}$	0.069 ± 0.018	$0.033 \pm 6.0e-06$	-0.018 ± 0.013	1.090 ± 0.167	0.033	9 ± 3	6 ± 3	8 ± 3	6 ± 3	3
XMMXCS J151645.4+070320.5	$0.516^{+0.117}_{-0.115}$	0.513 ± 0.135	$0.509 \pm 1.6e-04$	0.013 ± 0.109	0.548 ± 2.200	0.054	3 ± 3	8 ± 4	2 ± 2	-	3
XMMXCS J151651.7+070833.3	$0.542^{+0.189}_{-0.247}$	0.444 ± 0.153	-	0.086 ± 0.147	-0.874 ± 2.990	0.080	4 ± 3	-	0 ± 0.1	-	3
XMMXCS J151653.5+065627.9	$0.163^{+0.109}_{-0.113}$	0.075 ± 0.046	-	0.447 ± 0.041	-8.330 ± 0.851	0.500	1 ± 1	0 ± 1	0 ± 0.1	-	3
XMMXCS J151655.1+070156.0	$0.435^{+0.109}_{-0.099}$	0.437 ± 0.065	-	-0.120 ± 0.124	3.660 ± 2.490	0.001	3 ± 3	-	2 ± 2	-	3
XMMXCS J151655.3-000606.8	$0.392^{+0.126}_{-0.125}$	0.293 ± 0.147	-	-0.070 ± 0.036	1.950 ± 0.725	0.050	5 ± 3	-	1 ± 2	-	3
XMMXCS J151722.4+313547.6	$0.371^{+0.153}_{-0.156}$	0.308 ± 0.167	-	-0.034 ± 0.055	1.900 ± 1.090	0.001	3 ± 3	17 ± 5	2 ± 2	4 ± 4	3
XMMXCS J151734.5+314008.6	$0.445^{+0.112}_{-0.108}$	0.276 ± 0.084	-	0.337 ± 0.177	-6.030 ± 3.580	0.161	6 ± 4	9 ± 4	0 ± 2	7 ± 4	3
XMMXCS J151743.8+070121.0	$0.581^{+0.165}_{-0.168}$	0.673 ± 0.227	-	0.347 ± 0.186	-5.880 ± 3.740	0.500	4 ± 3	42 ± 7	4 ± 2	73 ± 11	3
XMMXCS J151756.7+312729.8	$0.634^{+0.110}_{-0.110}$	0.475 ± 0.194	-	0.105 ± 0.127	-1.360 ± 2.570	0.001	2 ± 2	1 ± 3	2 ± 1	-	3
XMMXCS J151839.3+424638.7	$0.189^{+0.057}_{-0.065}$	0.150 ± 0.025	$0.208 \pm 1.6e-05$	0.036 ± 0.025	0.572 ± 0.472	0.078	0 ± 1	2 ± 2	-	1 ± 1	3
XMMXCS J151852.5+062601.2	$0.067^{+0.031}_{-0.033}$	0.056 ± 0.022	$0.033 \pm 1.4e-05$	0.013 ± 0.059	0.636 ± 1.060	0.108	2 ± 2	0 ± 1	0 ± 0.1	-	3

Continued on next page

Table A.2 – continued from previous page

name	z_{RS}	z_{BCG}	z_{spec-g}	cmr_{grad}	cmr_{inter}	cmr_{wid}	n_{gals-c}	n_{gals-l}	n_{200-c}	n_{200-l}	qual
XMMXCS J152130.3+274419.3	$0.188^{+0.094}_{-0.096}$	0.084 ± 0.025	$0.071 \pm 3.2e-05$	0.018 ± 0.023	0.452 ± 0.457	0.112	2 ± 2	5 ± 3	0 ± 0.1	1 ± 2	3
XMMXCS J152149.8+672830.7	$0.521^{+0.164}_{-0.171}$	0.523 ± 0.238	-	0.071 ± 0.111	-0.722 ± 2.140	0.500	11 ± 4	12 ± 5	11 ± 4	11 ± 5	3
XMMXCS J152154.3+074803.2	$0.162^{+0.154}_{-0.154}$	0.058 ± 0.015	$0.045 \pm 9.9e-06$	-0.050 ± 0.019	1.610 ± 0.345	0.082	8 ± 3	9 ± 4	4 ± 2	6 ± 3	3
XMMXCS J152155.4+073824.4	$0.045^{+0.004}_{-0.004}$	0.060 ± 0.015	$0.045 \pm 7.9e-06$	-0.000 ± 0.006	0.854 ± 0.092	0.012	6 ± 3	3 ± 2	5 ± 2	1 ± 1	3
XMMXCS J152222.5+073325.5	$0.549^{+0.133}_{-0.133}$	0.607 ± 0.108	-	0.027 ± 0.128	0.632 ± 2.510	0.105	2 ± 2	-	2 ± 1	-	3
XMMXCS J152246.4+275255.9	$0.277^{+0.067}_{-0.065}$	0.202 ± 0.031	-	0.151 ± 0.078	-1.380 ± 1.520	0.001	5 ± 3	4 ± 3	1 ± 1	0 ± 1	3
XMMXCS J152252.4+083737.3	$0.186^{+0.121}_{-0.125}$	0.075 ± 0.036	$0.035 \pm 6.4e-06$	0.001 ± 0.036	0.900 ± 0.688	0.131	17 ± 5	21 ± 6	20 ± 5	34 ± 7	3
XMMXCS J152258.5+275235.9	$0.312^{+0.087}_{-0.085}$	0.202 ± 0.031	$0.427 \pm 4.6e-05$	-0.552 ± 0.192	12.500 ± 4.020	0.500	8 ± 4	6 ± 4	4 ± 3	3 ± 3	3
XMMXCS J152300.3+275306.3	$0.062^{+0.016}_{-0.015}$	0.082 ± 0.021	$0.057 \pm 6.0e-06$	0.559 ± 0.100	-8.350 ± 1.630	0.039	1 ± 1	0 ± 1	0 ± 0.1	-	3
XMMXCS J152305.4+083640.3	$0.035^{+0.003}_{-0.003}$	0.075 ± 0.036	$0.035 \pm 6.6e-06$	0.011 ± 0.007	0.662 ± 0.101	0.024	14 ± 4	6 ± 3	15 ± 4	7 ± 3	3
XMMXCS J152309.5+083849.5	$0.033^{+0.038}_{-0.033}$	0.075 ± 0.036	$0.035 \pm 6.7e-06$	-0.001 ± 0.009	0.836 ± 0.128	0.067	13 ± 4	4 ± 2	13 ± 4	5 ± 2	3
XMMXCS J152441.7+513414.5	$0.324^{+0.143}_{-0.129}$	0.156 ± 0.028	-	0.218 ± 0.097	-3.120 ± 1.930	0.124	2 ± 2	2 ± 3	0 ± 0.1	-	3
XMMXCS J152519.2+512914.8	$0.293^{+0.119}_{-0.110}$	0.310 ± 0.110	-	0.082 ± 0.074	-0.566 ± 1.480	0.087	2 ± 2	0 ± 1	0 ± 0.1	-	3
XMMXCS J152525.8+513049.6	$0.435^{+0.138}_{-0.123}$	0.533 ± 0.088	-	-0.462 ± 0.036	9.850 ± 0.732	0.500	3 ± 3	3 ± 3	2 ± 2	2 ± 2	3
XMMXCS J152609.7+513437.3	$0.233^{+0.086}_{-0.086}$	0.192 ± 0.082	-	0.167 ± 0.094	-1.930 ± 1.790	0.056	1 ± 1	0 ± 1	0 ± 0.1	-	3
XMMXCS J152652.0+512753.6	$0.228^{+0.085}_{-0.091}$	0.197 ± 0.032	-	-0.095 ± 0.195	3.140 ± 4.010	0.118	1 ± 1	0 ± 1	0 ± 0.1	-	3
XMMXCS J153159.6+044629.0	$0.384^{+0.094}_{-0.097}$	0.316 ± 0.055	$0.579 \pm 3.0e-04$	0.009 ± 0.059	1.460 ± 1.140	0.001	1 ± 2	2 ± 3	0 ± 0.1	-	3
XMMXCS J153209.5+044438.0	$0.432^{+0.134}_{-0.133}$	0.344 ± 0.118	-	0.407 ± 0.209	-7.080 ± 4.230	0.118	6 ± 4	6 ± 4	3 ± 2	3 ± 3	3
XMMXCS J153231.4+044047.5	$0.218^{+0.111}_{-0.119}$	0.062 ± 0.022	$0.039 \pm 1.1e-05$	0.025 ± 0.056	0.513 ± 1.070	0.049	5 ± 3	8 ± 4	4 ± 2	7 ± 3	3

Continued on next page

Table A.2 – continued from previous page

name	z_{RS}	z_{BCG}	z_{spec-g}	cmr_{grad}	cmr_{inter}	cmr_{wid}	n_{gals-c}	n_{gals-l}	n_{200-c}	n_{200-l}	qual
XMMXCS J153235.5+044436.2	$0.318^{+0.116}_{-0.111}$	0.137 ± 0.022	$0.135 \pm 1.8e-05$	0.009 ± 0.030	0.979 ± 0.564	0.113	10 ± 4	10 ± 4	9 ± 4	126 ± 12	3
XMMXCS J153242.1+044454.5	$0.342^{+0.126}_{-0.124}$	0.412 ± 0.120	-	0.059 ± 0.035	0.099 ± 0.649	0.148	17 ± 5	42 ± 7	18 ± 5	24 ± 8	3
XMMXCS J153245.1+324245.5	$0.592^{+0.083}_{-0.082}$	0.382 ± 0.134	$0.590 \pm 2.4e-04$	0.524 ± 0.123	-9.330 ± 2.430	0.045	2 ± 2	9 ± 3	-	9 ± 3	3
XMMXCS J153306.2+044631.1	$0.038^{+0.025}_{-0.026}$	0.058 ± 0.016	$0.039 \pm 8.6e-06$	-0.026 ± 0.004	1.190 ± 0.066	0.001	2 ± 1	0 ± 1	0 ± 0.1	-	3
XMMXCS J153308.1+043104.3	$0.449^{+0.099}_{-0.097}$	0.425 ± 0.062	-	0.039 ± 0.040	0.092 ± 0.778	0.129	2 ± 3	-	0 ± 1	-	3
XMMXCS J153311.4+301450.0	$0.305^{+0.095}_{-0.096}$	0.309 ± 0.049	$0.276 \pm 4.9e-05$	0.012 ± 0.033	1.240 ± 0.652	0.108	2 ± 2	-	0 ± 0.1	-	3
XMMXCS J153457.4+233010.3	$0.070^{+0.034}_{-0.033}$	0.075 ± 0.030	$0.048 \pm 9.4e-06$	0.044 ± 0.008	0.262 ± 0.141	0.071	4 ± 2	8 ± 3	4 ± 2	6 ± 3	3
XMMXCS J153512.7-140823.5	$0.341^{+0.139}_{-0.126}$	0.281 ± 0.157	-	0.190 ± 0.212	-2.610 ± 4.220	0.001	3 ± 2	-	1 ± 1	-	3
XMMXCS J153609.8+553202.1	$0.258^{+0.087}_{-0.089}$	0.236 ± 0.044	-	0.004 ± 0.060	1.420 ± 1.070	0.001	0 ± 0.1	1 ± 2	-	0 ± 1	3
XMMXCS J153629.7+543920.8	$0.338^{+0.092}_{-0.091}$	0.269 ± 0.046	$0.409 \pm 1.3e-04$	-0.146 ± 0.069	4.360 ± 1.370	0.143	8 ± 4	10 ± 4	6 ± 3	1 ± 2	3
XMMXCS J153708.1+544418.4	$0.349^{+0.064}_{-0.062}$	0.361 ± 0.056	-	0.022 ± 0.060	1.230 ± 1.190	0.100	5 ± 3	7 ± 3	0 ± 0.1	0 ± 2	3
XMMXCS J153713.2+542951.4	$0.401^{+0.070}_{-0.067}$	0.587 ± 0.125	-	0.075 ± 0.042	0.307 ± 0.810	0.001	1 ± 2	1 ± 2	0 ± 0.1	-	3
XMMXCS J153804.3+543015.2	$0.591^{+0.114}_{-0.102}$	0.528 ± 0.105	-	0.022 ± 0.115	0.369 ± 2.320	0.001	1 ± 2	3 ± 3	1 ± 1	1 ± 2	3
XMMXCS J153814.2+533332.2	$0.373^{+0.085}_{-0.085}$	0.355 ± 0.063	$0.291 \pm 8.4e-05$	0.049 ± 0.060	0.751 ± 1.180	0.105	20 ± 5	20 ± 5	26 ± 6	26 ± 6	3
XMMXCS J154417.0+535522.1	$0.433^{+0.096}_{-0.094}$	0.491 ± 0.082	-	-0.143 ± 0.066	4.530 ± 1.330	0.068	18 ± 5	17 ± 5	22 ± 5	19 ± 5	3
XMMXCS J154932.2+213302.5	$0.555^{+0.123}_{-0.122}$	0.544 ± 0.103	-	0.152 ± 0.078	-1.930 ± 1.580	0.119	2 ± 2	4 ± 3	-	7 ± 3	3
XMMXCS J155539.6+111035.1	$0.367^{+0.097}_{-0.095}$	0.437 ± 0.097	$0.434 \pm 8.2e-05$	-0.130 ± 0.189	4.190 ± 3.820	0.163	3 ± 3	4 ± 3	0 ± 1	-	3
XMMXCS J155936.5+351352.1	$0.159^{+0.038}_{-0.037}$	0.152 ± 0.025	$0.158 \pm 2.7e-05$	-0.071 ± 0.036	2.290 ± 0.606	0.073	3 ± 2	2 ± 2	1 ± 1	1 ± 1	3
XMMXCS J160408.8+431455.9	$0.420^{+0.111}_{-0.115}$	0.295 ± 0.082	$0.349 \pm 1.0e-04$	-0.122 ± 0.434	3.980 ± 8.930	0.130	3 ± 3	4 ± 3	1 ± 1	1 ± 2	3

Continued on next page

Table A.2 – continued from previous page

name	z_{RS}	z_{BCG}	z_{spec-g}	cmr_{grad}	cmr_{inter}	cmr_{wid}	n_{gals-c}	n_{gals-l}	n_{200-c}	n_{200-l}	qual
XMMXCS J160434.5+174346.0	$0.259^{+0.101}_{-0.092}$	0.084 ± 0.061	-	0.143 ± 0.089	-1.190 ± 1.740	0.175	7 ± 3	5 ± 3	0 ± 1	1 ± 2	3
XMMXCS J160435.9+173318.6	$0.087^{+0.045}_{-0.046}$	0.056 ± 0.019	$0.034 \pm 8.7e-06$	0.019 ± 0.009	0.290 ± 0.164	0.066	2 ± 2	2 ± 2	0 ± 0.1	0 ± 1	3
XMMXCS J160504.2+324831.5	$0.352^{+0.101}_{-0.102}$	0.257 ± 0.149	-	-0.438 ± 0.410	10.700 ± 8.430	0.272	3 ± 2	4 ± 3	0 ± 1	-	3
XMMXCS J160508.9+174414.0	$0.033^{+0.001}_{-0.001}$	0.088 ± 0.023	$0.033 \pm 5.1e-06$	-0.060 ± 0.055	1.690 ± 0.803	0.102	9 ± 3	3 ± 2	9 ± 3	6 ± 3	3
XMMXCS J160512.6+174313.6	$0.440^{+0.082}_{-0.081}$	0.341 ± 0.071	-	-0.080 ± 0.248	3.340 ± 4.940	0.001	3 ± 3	-	2 ± 2	-	3
XMMXCS J160516.3+235902.0	$0.289^{+0.084}_{-0.087}$	0.276 ± 0.073	-	0.320 ± 0.132	-5.090 ± 2.690	0.073	1 ± 2	0 ± 2	0 ± 0.1	-	3
XMMXCS J160531.0+325327.3	$0.207^{+0.144}_{-0.156}$	0.117 ± 0.021	$0.136 \pm 2.3e-05$	-0.006 ± 0.037	1.210 ± 0.718	0.090	4 ± 2	5 ± 3	0 ± 1	1 ± 2	3
XMMXCS J160601.3+174742.5	$0.145^{+0.062}_{-0.058}$	0.073 ± 0.022	-	0.009 ± 0.041	0.542 ± 0.748	0.047	1 ± 1	0 ± 1	0 ± 0.1	-	3
XMMXCS J160719.7+081559.1	$0.284^{+0.062}_{-0.056}$	0.213 ± 0.037	-	-0.036 ± 0.043	2.010 ± 0.824	0.133	1 ± 2	0 ± 2	0 ± 0.1	-	3
XMMXCS J160808.9+601406.8	$0.341^{+0.173}_{-0.173}$	0.220 ± 0.045	-	-0.034 ± 0.200	1.790 ± 4.060	0.001	0 ± 2	1 ± 2	-	1 ± 1	3
XMMXCS J160815.1+263824.2	$0.362^{+0.102}_{-0.104}$	0.379 ± 0.130	-	-0.408 ± 0.107	8.980 ± 2.190	0.023	1 ± 1	-	0 ± 0.1	-	3
XMMXCS J160842.7+263459.4	$0.278^{+0.128}_{-0.151}$	0.105 ± 0.017	-	0.065 ± 0.080	-0.094 ± 1.480	0.133	2 ± 2	5 ± 3	0 ± 0.1	4 ± 3	3
XMMXCS J160932.0+602914.1	$0.225^{+0.060}_{-0.060}$	0.251 ± 0.040	-	-0.018 ± 0.023	1.670 ± 0.433	0.071	4 ± 2	2 ± 2	0 ± 1	1 ± 1	3
XMMXCS J160953.7+602529.3	$0.313^{+0.108}_{-0.103}$	0.157 ± 0.059	-	-0.014 ± 0.043	1.320 ± 0.870	0.001	1 ± 2	1 ± 2	1 ± 1	1 ± 1	3
XMMXCS J161000.7+601641.3	$0.239^{+0.071}_{-0.072}$	0.293 ± 0.106	-	-0.019 ± 0.029	1.700 ± 0.525	0.068	5 ± 3	3 ± 3	4 ± 2	1 ± 2	3
XMMXCS J161003.6+263555.8	$0.211^{+0.058}_{-0.059}$	0.192 ± 0.038	-	-0.060 ± 0.062	2.410 ± 1.150	0.129	2 ± 2	2 ± 2	0 ± 0.1	1 ± 1	3
XMMXCS J161026.4+542335.8	$0.447^{+0.119}_{-0.119}$	0.334 ± 0.141	-	0.035 ± 0.107	0.195 ± 2.090	0.001	2 ± 2	8 ± 4	1 ± 1	4 ± 3	3
XMMXCS J161113.7+540205.7	$0.253^{+0.078}_{-0.082}$	0.335 ± 0.058	-	-0.085 ± 0.067	3.100 ± 1.390	0.001	0 ± 1	1 ± 2	-	1 ± 1	3
XMMXCS J161213.8+540938.9	$0.103^{+0.026}_{-0.026}$	0.082 ± 0.026	-	0.105 ± 0.026	-1.050 ± 0.431	0.086	1 ± 1	1 ± 1	0 ± 0.1	0 ± 1	3

Continued on next page

Table A.2 – continued from previous page

name	z_{RS}	z_{BCG}	z_{spec-g}	cmr_{grad}	cmr_{inter}	cmr_{wid}	n_{gals-c}	n_{gals-l}	n_{200-c}	n_{200-l}	qual
XMMXCS J161638.2+345429.7	$0.485^{+0.183}_{-0.181}$	0.331 ± 0.121	-	0.608 ± 0.299	-11.50 ± 6.170	0.092	2 ± 2	2 ± 3	0 ± 1	-	3
XMMXCS J161759.4+060722.9	$0.307^{+0.121}_{-0.114}$	0.383 ± 0.150	-	-0.408 ± 0.444	9.440 ± 9.000	0.258	1 ± 3	-	2 ± 1	-	3
XMMXCS J161807.1+350227.2	$0.444^{+0.085}_{-0.087}$	0.391 ± 0.192	$0.446 \pm 2.2e-05$	-0.016 ± 0.035	1.040 ± 0.678	0.089	1 ± 3	-	0 ± 0.1	-	3
XMMXCS J161841.2+600203.0	$0.197^{+0.067}_{-0.068}$	0.134 ± 0.061	-	0.109 ± 0.047	-0.860 ± 0.865	0.061	0 ± 1	1 ± 2	-	2 ± 2	3
XMMXCS J162739.6+392747.1	$0.234^{+0.047}_{-0.234}$	0.122 ± 0.026	$0.122 \pm 2.3e-05$	-0.005 ± 0.025	0.804 ± 0.397	0.053	3 ± 2	1 ± 2	0 ± 0.1	0 ± 1	3
XMMXCS J162902.6+780510.1	$0.364^{+0.126}_{-0.122}$	0.412 ± 0.068	-	-0.158 ± 0.146	3.690 ± 2.980	0.077	0 ± 2	1 ± 3	-	0 ± 1	3
XMMXCS J162930.07+391737.6	$0.262^{+0.110}_{-0.108}$	0.201 ± 0.040	-	-0.021 ± 0.029	1.560 ± 0.557	0.066	1 ± 2	2 ± 2	2 ± 1	2 ± 2	3
XMMXCS J162933.81+404710.6	$0.401^{+0.081}_{-0.080}$	0.369 ± 0.055	-	0.279 ± 0.182	-3.650 ± 3.580	0.107	2 ± 2	2 ± 2	0 ± 0.1	1 ± 1	3
XMMXCS J162933.8+404710.6	$0.401^{+0.081}_{-0.080}$	0.369 ± 0.055	-	0.279 ± 0.182	-3.650 ± 3.580	0.107	2 ± 2	2 ± 2	0 ± 0.1	1 ± 1	3
XMMXCS J163008.16+392226.0	$0.211^{+0.093}_{-0.094}$	0.074 ± 0.034	-	-0.146 ± 0.032	3.840 ± 0.618	0.500	1 ± 2	1 ± 3	3 ± 2	4 ± 2	3
XMMXCS J163234.3+411418.6	$0.662^{+0.153}_{-0.150}$	0.486 ± 0.182	-	0.229 ± 0.328	-3.460 ± 6.590	0.001	4 ± 2	7 ± 3	2 ± 1	-	3
XMMXCS J163256.1+054211.8	$0.201^{+0.066}_{-0.069}$	0.186 ± 0.043	-	0.170 ± 0.016	-1.900 ± 0.310	0.043	1 ± 1	2 ± 2	2 ± 1	1 ± 1	3
XMMXCS J163258.4+054545.6	$0.105^{+0.038}_{-0.040}$	0.068 ± 0.038	-	0.282 ± 0.001	-3.670 ± 0.001	0.500	3 ± 2	5 ± 3	0 ± 1	2 ± 2	3
XMMXCS J163341.0+571420.1	$0.205^{+0.125}_{-0.079}$	0.262 ± 0.056	-	-0.100 ± 0.059	3.270 ± 1.090	0.046	0 ± 1	1 ± 2	-	0 ± 1	3
XMMXCS J163358.6+635447.1	$0.591^{+0.176}_{-0.291}$	0.655 ± 0.221	-	-0.080 ± 0.096	2.560 ± 1.920	0.093	2 ± 2	30 ± 6	-	4 ± 5	3
XMMXCS J163401.6+340608.8	$0.290^{+0.099}_{-0.092}$	0.221 ± 0.060	-	0.030 ± 0.033	0.392 ± 0.636	0.101	3 ± 2	2 ± 2	0 ± 0.1	-	3
XMMXCS J163651.5+184512.2	$0.646^{+0.168}_{-0.171}$	0.622 ± 0.109	$0.843 \pm 2.8e-04$	0.102 ± 0.443	-0.928 ± 9.100	0.133	5 ± 3	15 ± 5	4 ± 2	32 ± 6	3
XMMXCS J163653.0+184143.4	$0.300^{+0.062}_{-0.062}$	0.238 ± 0.055	-	0.027 ± 0.042	0.891 ± 0.811	0.145	8 ± 4	7 ± 4	8 ± 3	5 ± 3	3
XMMXCS J164031.18+362327.4	$0.484^{+0.127}_{-0.125}$	0.538 ± 0.125	-	0.051 ± 0.073	-0.272 ± 1.480	0.032	1 ± 2	2 ± 3	1 ± 1	-	3

Continued on next page

Table A.2 – continued from previous page

name	z_{RS}	z_{BCG}	z_{spec-g}	cmr_{grad}	cmr_{inter}	cmr_{wid}	n_{gals-c}	n_{gals-l}	n_{200-c}	n_{200-l}	qual
XMMXCS J164031.1+362327.4	$0.484^{+0.127}_{-0.125}$	0.538 ± 0.125	-	0.051 ± 0.073	-0.272 ± 1.480	0.032	1 ± 2	2 ± 3	1 ± 1	-	3
XMMXCS J164042.65+363057.1	$0.506^{+0.066}_{-0.065}$	0.485 ± 0.074	$0.505 \pm 8.3e-05$	0.034 ± 0.072	0.271 ± 1.440	0.104	2 ± 2	3 ± 3	1 ± 1	-	3
XMMXCS J164042.6+363057.1	$0.506^{+0.066}_{-0.065}$	0.485 ± 0.074	$0.505 \pm 8.3e-05$	0.034 ± 0.072	0.271 ± 1.440	0.104	2 ± 2	3 ± 3	1 ± 1	-	3
XMMXCS J164106.3+363847.6	$0.153^{+0.050}_{-0.048}$	0.166 ± 0.035	$0.142 \pm 2.2e-05$	-0.106 ± 0.073	2.810 ± 1.280	0.123	4 ± 2	3 ± 2	0 ± 1	0 ± 1	3
XMMXCS J164140.4+390811.4	$0.507^{+0.119}_{-0.105}$	0.410 ± 0.157	$0.535 \pm 1.1e-04$	-0.079 ± 0.110	2.450 ± 2.240	0.500	0 ± 3	4 ± 4	-	9 ± 4	3
XMMXCS J164831.9+271006.7	$0.172^{+0.085}_{-0.089}$	0.058 ± 0.014	$0.058 \pm 1.0e-05$	-0.011 ± 0.031	1.100 ± 0.606	0.092	2 ± 2	7 ± 4	0 ± 0.1	5 ± 3	3
XMMXCS J165108.3+045929.9	$0.158^{+0.036}_{-0.036}$	0.180 ± 0.032	-	-0.030 ± 0.028	1.700 ± 0.491	0.078	5 ± 2	5 ± 3	4 ± 2	4 ± 2	3
XMMXCS J165258.8+022404.6	$0.395^{+0.095}_{-0.092}$	0.322 ± 0.143	-	0.361 ± 0.195	-5.310 ± 3.890	0.084	3 ± 3	6 ± 3	0 ± 0.1	3 ± 2	3
XMMXCS J165332.2+023519.0	$0.382^{+0.122}_{-0.121}$	0.394 ± 0.101	-	0.470 ± 0.189	-9.130 ± 3.830	0.095	6 ± 3	-	2 ± 2	-	3
XMMXCS J165430.8+395417.3	$0.145^{+0.055}_{-0.059}$	0.134 ± 0.021	-	0.037 ± 0.028	0.456 ± 0.509	0.118	3 ± 2	1 ± 2	0 ± 1	0 ± 1	3
XMMXCS J165841.9+790719.2	$0.184^{+0.054}_{-0.056}$	0.065 ± 0.018	-	0.206 ± 0.149	-2.410 ± 2.610	0.183	3 ± 3	10 ± 4	3 ± 2	5 ± 3	3
XMMXCS J170934.9+781852.0	$0.242^{+0.078}_{-0.078}$	0.216 ± 0.058	-	-0.025 ± 0.029	1.800 ± 0.567	0.099	2 ± 2	5 ± 3	0 ± 0.1	0 ± 1	3
XMMXCS J171246.1+435334.3	$0.252^{+0.066}_{-0.069}$	0.170 ± 0.039	-	0.003 ± 0.078	1.340 ± 1.530	0.125	2 ± 2	0 ± 1	0 ± 0.1	-	3
XMMXCS J171256.9+590747.2	$0.287^{+0.093}_{-0.097}$	0.254 ± 0.058	-	-0.045 ± 0.018	1.670 ± 0.349	0.500	3 ± 3	-	0 ± 1	-	3
XMMXCS J171840.8+585236.7	$0.111^{+0.024}_{-0.025}$	0.112 ± 0.017	$0.112 \pm 2.7e-05$	0.111 ± 0.062	-0.841 ± 1.080	0.103	0 ± 1	1 ± 2	-	0 ± 1	3
XMMXCS J171854.5+585921.4	$0.430^{+0.127}_{-0.117}$	0.588 ± 0.115	-	0.261 ± 0.195	-3.680 ± 3.920	0.001	4 ± 3	5 ± 3	0 ± 1	1 ± 2	3
XMMXCS J171911.6+583717.7	$0.195^{+0.052}_{-0.052}$	0.240 ± 0.045	-	-0.109 ± 0.044	3.240 ± 0.834	0.084	1 ± 1	0 ± 1	0 ± 0.1	-	3
XMMXCS J171954.0+583605.9	$0.447^{+0.139}_{-0.138}$	0.521 ± 0.082	-	-0.031 ± 0.061	2.170 ± 1.180	0.103	1 ± 3	5 ± 4	-	6 ± 3	3
XMMXCS J171955.7+265028.6	$0.177^{+0.030}_{-0.030}$	0.105 ± 0.018	$0.133 \pm 1.7e-05$	0.065 ± 0.068	-0.242 ± 1.230	0.101	1 ± 2	0 ± 2	0 ± 0.1	-	3

Continued on next page

Table A.2 – continued from previous page

name	z_{RS}	z_{BCG}	z_{spec-g}	cmr_{grad}	cmr_{inter}	cmr_{wid}	n_{gals-c}	n_{gals-l}	n_{200-c}	n_{200-l}	qual
XMMXCS J172052.7+590152.4	$0.326^{+0.075}_{-0.074}$	0.182 ± 0.029	-	0.066 ± 0.033	0.162 ± 0.653	0.500	2 ± 3	0 ± 3	3 ± 2	-	3
XMMXCS J172127.2+584226.9	$0.273^{+0.108}_{-0.148}$	0.098 ± 0.025	$0.109 \pm 2.9e-05$	0.059 ± 0.028	-0.026 ± 0.503	0.127	3 ± 3	1 ± 3	2 ± 2	2 ± 2	3
XMMXCS J172131.0+584403.2	$0.435^{+0.169}_{-0.172}$	0.424 ± 0.198	-	-0.034 ± 0.071	1.820 ± 1.330	0.001	2 ± 3	3 ± 3	2 ± 2	2 ± 2	3
XMMXCS J173104.6+365802.2	$0.353^{+0.134}_{-0.127}$	0.318 ± 0.122	-	-0.147 ± 0.028	3.870 ± 0.586	0.023	0 ± 2	1 ± 2	-	0 ± 1	3
XMMXCS J173602.6+655941.1	$0.581^{+0.167}_{-0.168}$	0.487 ± 0.320	-	-0.047 ± 0.158	2.240 ± 3.270	0.137	2 ± 2	-	1 ± 1	-	3
XMMXCS J173654.4+655845.8	$0.247^{+0.070}_{-0.070}$	0.230 ± 0.037	-	0.124 ± 0.053	-1.070 ± 1.030	0.101	2 ± 2	1 ± 2	0 ± 0.1	0 ± 1	3
XMMXCS J173701.6+660035.6	$0.259^{+0.112}_{-0.110}$	0.296 ± 0.108	-	0.375 ± 0.243	-6.340 ± 4.890	0.158	1 ± 2	2 ± 2	0 ± 0.1	1 ± 1	3
XMMXCS J173809.4+681658.0	$0.221^{+0.083}_{-0.096}$	0.310 ± 0.078	-	-0.011 ± 0.067	1.440 ± 1.300	0.125	3 ± 2	1 ± 2	0 ± 0.1	-	3
XMMXCS J173928.4+651329.6	$0.323^{+0.126}_{-0.107}$	0.213 ± 0.038	-	-0.000 ± 0.001	0.996 ± 0.001	0.500	10 ± 4	-	8 ± 4	-	3
XMMXCS J174124.4+634246.0	$0.335^{+0.089}_{-0.087}$	0.191 ± 0.047	-	0.028 ± 0.088	0.935 ± 1.650	0.188	2 ± 3	4 ± 3	0 ± 1	6 ± 3	3
XMMXCS J174145.7+650422.4	$0.358^{+0.080}_{-0.081}$	0.382 ± 0.076	-	0.012 ± 0.060	1.690 ± 1.220	0.001	6 ± 3	4 ± 3	2 ± 2	0 ± 1	3
XMMXCS J180030.9+080414.7	$0.251^{+0.128}_{-0.124}$	0.091 ± 0.098	-	0.072 ± 0.047	-0.664 ± 0.854	0.128	5 ± 3	6 ± 3	2 ± 2	0 ± 2	3
XMMXCS J180031.0+081830.0	$0.122^{+0.111}_{-0.112}$	0.109 ± 0.040	-	0.024 ± 0.024	0.363 ± 0.432	0.096	2 ± 2	2 ± 2	0 ± 0.1	0 ± 1	3
XMMXCS J180033.0+080827.5	$0.192^{+0.080}_{-0.078}$	0.175 ± 0.035	-	0.398 ± 0.021	-5.960 ± 0.355	0.500	0 ± 2	3 ± 3	-	1 ± 2	3
XMMXCS J180036.9+081142.1	$0.662^{+0.173}_{-0.178}$	0.492 ± 0.304	-	-0.110 ± 0.030	2.490 ± 0.587	0.001	1 ± 1	0 ± 1	1 ± 1	-	3
XMMXCS J180056.8+081559.6	$0.093^{+0.101}_{-0.093}$	0.143 ± 0.032	-	-0.057 ± 0.059	1.850 ± 1.080	0.095	1 ± 1	0 ± 1	0 ± 0.1	-	3
XMMXCS J181758.0+142221.4	$0.188^{+0.137}_{-0.144}$	0.138 ± 0.114	-	0.059 ± 0.034	-0.336 ± 0.625	0.001	1 ± 1	0 ± 2	0 ± 0.1	-	3
XMMXCS J183932.3+793443.0	$0.210^{+0.100}_{-0.101}$	0.198 ± 0.040	-	-0.132 ± 0.094	3.590 ± 1.760	0.115	0 ± 2	3 ± 3	-	2 ± 2	3
XMMXCS J195923.8+114008.4	$0.236^{+0.152}_{-0.152}$	0.054 ± 0.125	-	-0.040 ± 0.031	1.750 ± 0.551	0.500	8 ± 5	6 ± 4	6 ± 4	6 ± 4	3

Continued on next page

Table A.2 – continued from previous page

name	z_{RS}	z_{BCG}	z_{spec-g}	cmr_{grad}	cmr_{inter}	cmr_{wid}	n_{gals-c}	n_{gals-l}	n_{200-c}	n_{200-l}	qual
XMMXCS J200750.5-110238.1	$0.309^{+0.118}_{-0.117}$	0.232 ± 0.061	-	-0.045 ± 0.073	2.270 ± 1.380	0.145	10 ± 4	14 ± 5	8 ± 4	15 ± 5	3
XMMXCS J202251.0-205611.3	$0.069^{+0.049}_{-0.049}$	0.057 ± 0.021	-	-0.019 ± 0.010	1.130 ± 0.163	0.045	7 ± 3	8 ± 3	6 ± 2	7 ± 3	3
XMMXCS J202259.2-205652.5	$0.070^{+0.029}_{-0.028}$	0.057 ± 0.021	-	0.036 ± 0.010	0.305 ± 0.152	0.019	10 ± 3	11 ± 3	7 ± 3	9 ± 3	3
XMMXCS J210101.6+104003.3	$0.354^{+0.233}_{-0.190}$	0.275 ± 0.045	-	0.058 ± 0.090	-0.398 ± 1.810	0.078	1 ± 2	1 ± 3	1 ± 1	0 ± 1	3
XMMXCS J210439.5-122016.6	$0.258^{+0.118}_{-0.178}$	0.069 ± 0.016	-	0.022 ± 0.022	0.695 ± 0.352	0.001	3 ± 2	4 ± 3	0 ± 0.1	1 ± 2	3
XMMXCS J210502.0-121008.3	$0.167^{+0.105}_{-0.111}$	0.221 ± 0.051	-	-0.047 ± 0.086	1.950 ± 1.730	0.103	1 ± 1	1 ± 2	0 ± 0.1	1 ± 1	3
XMMXCS J210650.9+232416.1	$0.317^{+0.086}_{-0.088}$	0.307 ± 0.068	-	0.068 ± 0.123	0.487 ± 2.340	0.223	1 ± 2	2 ± 3	0 ± 0.1	-	3
XMMXCS J210714.8+233146.7	$0.435^{+0.109}_{-0.101}$	0.400 ± 0.226	-	-0.024 ± 0.047	2.270 ± 0.932	0.500	0 ± 3	11 ± 5	-	12 ± 5	3
XMMXCS J210731.9+233531.6	$0.659^{+0.169}_{-0.166}$	0.717 ± 0.225	-	0.979 ± 0.663	-18.90 ± 13.80	0.001	4 ± 2	0 ± 1	2 ± 1	-	3
XMMXCS J210757.7+232900.7	$0.461^{+0.126}_{-0.122}$	0.528 ± 0.126	-	-0.066 ± 0.107	2.000 ± 2.100	0.079	1 ± 3	18 ± 5	-	0 ± 3	3
XMMXCS J211359.1+060710.8	$0.619^{+0.219}_{-0.232}$	0.536 ± 0.261	-	0.177 ± 0.323	-2.290 ± 6.530	0.119	3 ± 2	7 ± 3	1 ± 1	9 ± 3	3
XMMXCS J211441.4+061328.5	$0.239^{+0.055}_{-0.056}$	0.190 ± 0.029	$0.205 \pm 2.9e-05$	-0.018 ± 0.099	1.760 ± 1.850	0.182	3 ± 3	5 ± 3	0 ± 1	2 ± 2	3
XMMXCS J211442.4+060838.5	$0.180^{+0.109}_{-0.133}$	0.194 ± 0.031	-	-0.094 ± 0.053	3.080 ± 1.030	0.042	0 ± 1	1 ± 1	-	0 ± 1	3
XMMXCS J211448.8+061858.5	$0.089^{+0.036}_{-0.040}$	0.064 ± 0.063	-	-0.000 ± 0.001	0.310 ± 0.001	0.500	2 ± 2	1 ± 1	0 ± 0.1	0 ± 1	3
XMMXCS J211512.3+055840.5	$0.217^{+0.048}_{-0.049}$	0.223 ± 0.037	$0.218 \pm 2.2e-05$	-0.016 ± 0.005	1.640 ± 0.091	0.001	7 ± 3	5 ± 3	7 ± 3	9 ± 3	3
XMMXCS J211515.6+060928.3	$0.500^{+0.137}_{-0.137}$	0.523 ± 0.101	$0.593 \pm 8.4e-05$	-0.028 ± 0.109	1.440 ± 2.160	0.121	1 ± 2	9 ± 4	0 ± 0.1	-	3
XMMXCS J212258.8+171620.6	$0.313^{+0.131}_{-0.118}$	0.252 ± 0.110	-	0.093 ± 0.067	-0.695 ± 1.320	0.128	1 ± 2	2 ± 3	0 ± 0.1	1 ± 2	3
XMMXCS J212320.3-053957.4	$0.334^{+0.081}_{-0.079}$	0.232 ± 0.088	-	0.126 ± 0.089	-0.746 ± 1.670	0.154	2 ± 2	6 ± 3	0 ± 1	-	3
XMMXCS J212355.9-053716.2	$0.185^{+0.128}_{-0.136}$	0.227 ± 0.039	-	-0.078 ± 0.161	2.810 ± 3.160	0.159	0 ± 1	1 ± 2	-	1 ± 1	3

Continued on next page

Table A.2 – continued from previous page

name	z_{RS}	z_{BCG}	z_{spec-g}	cmr_{grad}	cmr_{inter}	cmr_{wid}	n_{gals-c}	n_{gals-l}	n_{200-c}	n_{200-l}	qual
XMMXCS J212904.3+000124.2	$0.148^{+0.042}_{-0.043}$	0.131 ± 0.021	$0.138 \pm 1.7e-05$	-0.070 ± 0.053	2.090 ± 0.974	0.107	1 ± 2	2 ± 2	0 ± 0.1	1 ± 1	3
XMMXCS J212924.4+001655.3	$0.412^{+0.115}_{-0.113}$	0.245 ± 0.090	-	0.352 ± 0.085	-6.360 ± 1.730	0.034	7 ± 3	11 ± 4	8 ± 3	11 ± 4	3
XMMXCS J212925.0+001416.8	$0.343^{+0.072}_{-0.071}$	0.222 ± 0.041	-	0.232 ± 0.127	-2.930 ± 2.460	0.181	8 ± 4	120 ± 11	4 ± 3	34 ± 10	3
XMMXCS J212931.1+001708.2	$0.381^{+0.121}_{-0.118}$	0.245 ± 0.090	-	0.113 ± 0.089	-1.880 ± 1.790	0.108	6 ± 3	5 ± 3	2 ± 2	2 ± 2	3
XMMXCS J212945.8-000828.2	$0.135^{+0.013}_{-0.013}$	0.135 ± 0.022	$0.135 \pm 2.2e-05$	0.072 ± 0.047	-0.216 ± 0.821	0.050	3 ± 2	4 ± 2	2 ± 1	3 ± 2	3
XMMXCS J213055.0+050857.8	$0.357^{+0.087}_{-0.085}$	0.218 ± 0.109	-	0.277 ± 0.043	-3.890 ± 0.855	0.155	1 ± 2	-	1 ± 1	-	3
XMMXCS J213100.0+045754.7	$0.630^{+0.158}_{-0.157}$	0.444 ± 0.247	-	0.492 ± 0.269	-9.300 ± 5.570	0.070	2 ± 2	0 ± 1	1 ± 1	-	3
XMMXCS J213341.1-003842.7	$0.210^{+0.057}_{-0.058}$	0.218 ± 0.033	$0.215 \pm 4.5e-05$	-0.084 ± 0.032	2.930 ± 0.602	0.053	3 ± 2	6 ± 3	1 ± 1	2 ± 2	3
XMMXCS J214330.4+064259.7	$0.149^{+0.056}_{-0.048}$	0.118 ± 0.023	-	-0.000 ± 0.001	0.891 ± 0.001	0.500	1 ± 2	2 ± 2	0 ± 0.1	1 ± 1	3
XMMXCS J214427.2+282333.1	$0.453^{+0.139}_{-0.133}$	0.316 ± 0.160	-	2.720 ± 2.310	-56.30 ± 47.50	0.744	4 ± 3	6 ± 3	1 ± 2	0 ± 1	3
XMMXCS J214503.3+281401.4	$0.196^{+0.103}_{-0.106}$	0.260 ± 0.229	-	0.008 ± 0.073	0.761 ± 1.390	0.153	1 ± 2	-	1 ± 1	-	3
XMMXCS J214539.9+041308.3	$0.526^{+0.064}_{-0.064}$	0.537 ± 0.087	$0.526 \pm 1.4e-04$	-0.012 ± 0.076	1.210 ± 1.470	0.031	3 ± 3	20 ± 5	2 ± 2	15 ± 5	3
XMMXCS J215154.5+135536.5	$0.388^{+0.107}_{-0.105}$	0.505 ± 0.188	-	0.224 ± 0.171	-2.710 ± 3.280	0.001	4 ± 3	6 ± 3	2 ± 2	5 ± 3	3
XMMXCS J215213.4+140348.6	$0.184^{+0.048}_{-0.047}$	0.072 ± 0.046	-	0.088 ± 0.069	-0.504 ± 1.280	0.121	9 ± 3	10 ± 4	7 ± 3	9 ± 4	3
XMMXCS J215217.9+141513.5	$0.316^{+0.117}_{-0.116}$	0.239 ± 0.057	-	0.051 ± 0.128	0.504 ± 2.440	0.001	2 ± 2	5 ± 3	1 ± 1	2 ± 2	3
XMMXCS J215352.3+172824.0	$0.285^{+0.075}_{-0.075}$	0.269 ± 0.086	$0.229 \pm 5.3e-05$	0.046 ± 0.042	0.508 ± 0.786	0.001	5 ± 3	8 ± 4	3 ± 2	6 ± 3	3
XMMXCS J220127.7+012301.3	$0.212^{+0.073}_{-0.077}$	0.165 ± 0.075	-	0.011 ± 0.059	1.030 ± 1.160	0.125	1 ± 1	2 ± 2	0 ± 0.1	1 ± 1	3
XMMXCS J220401.6+190030.6	$0.295^{+0.120}_{-0.115}$	0.169 ± 0.035	-	0.145 ± 0.081	-1.520 ± 1.520	0.182	3 ± 3	5 ± 3	3 ± 2	2 ± 2	3
XMMXCS J220515.8-015825.5	$0.156^{+0.062}_{-0.060}$	0.117 ± 0.021	-	-0.024 ± 0.202	1.170 ± 3.860	0.161	0 ± 2	2 ± 3	-	0 ± 1	3

Continued on next page

Table A.2 – continued from previous page

name	z_{RS}	z_{BCG}	z_{spec-g}	cmr_{grad}	cmr_{inter}	cmr_{wid}	n_{gals-c}	n_{gals-l}	n_{200-c}	n_{200-l}	qual
XMMXCS J220550.0-015930.4	$0.522^{+0.145}_{-0.153}$	0.354 ± 0.166	$0.607 \pm 2.0e-04$	-0.011 ± 0.133	0.870 ± 2.680	0.070	4 ± 3	3 ± 4	2 ± 2	9 ± 3	3
XMMXCS J220559.2-015821.7	$0.658^{+0.136}_{-0.125}$	0.614 ± 0.146	-	0.171 ± 0.127	-2.310 ± 2.540	0.126	2 ± 2	0 ± 1	0 ± 0.1	-	3
XMMXCS J220620.37-002559.0	$0.137^{+0.071}_{-0.074}$	0.092 ± 0.021	$0.115 \pm 2.9e-05$	0.021 ± 0.027	0.504 ± 0.511	0.108	3 ± 2	2 ± 2	2 ± 1	1 ± 1	3
XMMXCS J221105.8+021322.9	$0.190^{+0.120}_{-0.140}$	0.180 ± 0.038	-	-0.025 ± 0.046	1.450 ± 0.897	0.094	1 ± 1	0 ± 1	0 ± 0.1	-	3
XMMXCS J221354.26-002051.9	$0.124^{+0.043}_{-0.044}$	0.131 ± 0.023	$0.133 \pm 1.6e-05$	-0.019 ± 0.063	1.290 ± 1.070	0.142	3 ± 2	4 ± 2	0 ± 0.1	1 ± 1	3
XMMXCS J221406.59-001607.0	$0.131^{+0.011}_{-0.011}$	0.081 ± 0.029	$0.126 \pm 1.5e-05$	0.198 ± 0.100	-2.660 ± 1.780	0.085	2 ± 2	2 ± 2	0 ± 0.1	0 ± 1	3
XMMXCS J221456.8+004317.9	$0.227^{+0.064}_{-0.071}$	0.231 ± 0.038	$0.214 \pm 4.3e-05$	-0.004 ± 0.027	1.460 ± 0.506	0.090	1 ± 2	1 ± 2	0 ± 0.1	0 ± 1	3
XMMXCS J221512.8+003947.7	$0.117^{+0.082}_{-0.086}$	0.185 ± 0.051	$0.204 \pm 2.1e-05$	-0.071 ± 0.067	2.080 ± 1.310	0.088	0 ± 0.1	2 ± 2	-	0 ± 1	3
XMMXCS J221525.43+004424.4	$0.384^{+0.071}_{-0.073}$	0.396 ± 0.064	-	0.090 ± 0.049	-1.100 ± 0.977	0.055	3 ± 2	2 ± 3	0 ± 0.1	-	3
XMMXCS J221538.36+004532.7	$0.582^{+0.095}_{-0.084}$	0.518 ± 0.174	$0.561 \pm 1.5e-04$	0.143 ± 0.142	-1.970 ± 2.880	0.137	3 ± 3	6 ± 4	-	7 ± 3	3
XMMXCS J221538.97-002705.0	$0.391^{+0.079}_{-0.079}$	0.356 ± 0.176	-	0.134 ± 0.074	-2.020 ± 1.450	0.001	4 ± 3	4 ± 3	2 ± 2	2 ± 2	3
XMMXCS J221546.25-001808.9	$0.440^{+0.100}_{-0.098}$	0.255 ± 0.053	-	-0.074 ± 0.085	2.220 ± 1.710	0.093	1 ± 3	13 ± 5	-	12 ± 5	3
XMMXCS J221659.5+002506.5	$0.285^{+0.115}_{-0.111}$	0.233 ± 0.064	$0.251 \pm 2.6e-05$	0.029 ± 0.035	0.581 ± 0.663	0.001	0 ± 1	1 ± 2	-	0 ± 1	3
XMMXCS J221705.3+002638.7	$0.276^{+0.090}_{-0.095}$	0.233 ± 0.064	$0.251 \pm 2.6e-05$	0.032 ± 0.076	0.538 ± 1.480	0.001	1 ± 2	2 ± 2	-	2 ± 2	3
XMMXCS J221705.50+002634.0	$0.280^{+0.090}_{-0.092}$	0.233 ± 0.064	$0.251 \pm 2.6e-05$	0.027 ± 0.079	0.641 ± 1.540	0.001	0 ± 2	2 ± 2	-	3 ± 2	3
XMMXCS J221735.3+000926.4	$0.253^{+0.130}_{-0.142}$	0.287 ± 0.083	-	-0.294 ± 0.178	6.970 ± 3.380	0.086	0 ± 1	1 ± 2	-	0 ± 1	3
XMMXCS J221741.42-003023.6	$0.549^{+0.141}_{-0.136}$	0.536 ± 0.085	-	0.798 ± 0.635	-15.30 ± 13.10	0.239	1 ± 2	10 ± 3	-	8 ± 3	3
XMMXCS J221745.1+002958.2	$0.533^{+0.092}_{-0.089}$	0.517 ± 0.085	$0.530 \pm 1.3e-04$	0.070 ± 0.120	-0.476 ± 2.380	0.001	3 ± 3	16 ± 5	0 ± 1	14 ± 5	3
XMMXCS J221748.1+001228.2	$0.392^{+0.103}_{-0.103}$	0.369 ± 0.083	-	-0.077 ± 0.038	1.820 ± 0.705	0.001	1 ± 2	5 ± 3	-	2 ± 2	3

Continued on next page

Table A.2 – continued from previous page

name	z_{RS}	z_{BCG}	z_{spec-g}	cmr_{grad}	cmr_{inter}	cmr_{wid}	n_{gals-c}	n_{gals-l}	n_{200-c}	n_{200-l}	qual
XMMXCS J221830.29+001213.7	$0.252^{+0.060}_{-0.063}$	0.172 ± 0.026	$0.293 \pm 1.8e-05$	0.074 ± 0.074	-0.017 ± 1.410	0.117	5 ± 3	4 ± 3	3 ± 2	4 ± 2	3
XMMXCS J221830.2+001213.6	$0.252^{+0.060}_{-0.063}$	0.172 ± 0.026	$0.293 \pm 1.8e-05$	0.074 ± 0.074	-0.017 ± 1.410	0.117	5 ± 3	4 ± 3	3 ± 2	4 ± 2	3
XMMXCS J221853.8+121336.3	$0.504^{+0.144}_{-0.142}$	0.640 ± 0.131	-	10.400 ± 338	-214.0 ± 6980	1.206	2 ± 2	0 ± 1	1 ± 1	-	3
XMMXCS J221948.19+004023.4	$0.421^{+0.140}_{-0.147}$	0.352 ± 0.057	-	0.199 ± 0.082	-3.200 ± 1.650	0.109	1 ± 2	0 ± 1	2 ± 1	-	3
XMMXCS J222007.8+002003.7	$0.326^{+0.131}_{-0.111}$	0.162 ± 0.033	$0.434 \pm 9.3e-05$	0.379 ± 0.141	-5.950 ± 2.640	0.500	2 ± 3	0 ± 3	3 ± 2	-	3
XMMXCS J222007.82-002003.7	$0.231^{+0.049}_{-0.048}$	0.340 ± 0.115	-	-0.002 ± 0.067	1.340 ± 1.260	0.094	5 ± 3	4 ± 3	1 ± 1	2 ± 2	3
XMMXCS J222008.3+002335.2	$0.580^{+0.153}_{-0.148}$	0.515 ± 0.332	-	-0.476 ± 0.033	10.600 ± 0.654	0.500	2 ± 3	19 ± 6	0 ± 1	1 ± 5	3
XMMXCS J222117.15-010037.0	$0.262^{+0.074}_{-0.075}$	0.135 ± 0.029	-	0.282 ± 0.162	-4.140 ± 3.210	0.097	9 ± 3	7 ± 3	9 ± 3	3 ± 2	3
XMMXCS J222330.7-012817.9	$0.300^{+0.089}_{-0.088}$	0.280 ± 0.103	-	0.062 ± 0.079	-0.242 ± 1.560	0.001	1 ± 2	1 ± 2	0 ± 0.1	1 ± 1	3
XMMXCS J222736.0-052126.2	$0.112^{+0.037}_{-0.037}$	0.095 ± 0.026	-	0.143 ± 0.001	-1.760 ± 0.001	0.500	2 ± 2	1 ± 2	0 ± 0.1	0 ± 1	3
XMMXCS J222737.2-052105.4	$0.111^{+0.037}_{-0.037}$	0.095 ± 0.026	-	0.143 ± 0.001	-1.760 ± 0.001	0.500	2 ± 2	1 ± 2	0 ± 0.1	1 ± 1	3
XMMXCS J222759.8-052859.9	$0.453^{+0.114}_{-0.113}$	0.381 ± 0.062	-	0.391 ± 0.249	-7.030 ± 5.050	0.149	10 ± 4	8 ± 4	8 ± 4	8 ± 4	3
XMMXCS J222820.9-051324.1	$0.566^{+0.196}_{-0.196}$	0.476 ± 0.069	-	0.214 ± 0.134	-2.960 ± 2.730	0.220	6 ± 3	11 ± 4	4 ± 2	11 ± 4	3
XMMXCS J222824.2-051949.7	$0.344^{+0.077}_{-0.077}$	0.195 ± 0.055	-	0.287 ± 0.091	-3.790 ± 1.750	0.198	6 ± 3	8 ± 4	6 ± 3	8 ± 3	3
XMMXCS J222833.4-052827.4	$0.164^{+0.029}_{-0.029}$	0.168 ± 0.029	-	-0.014 ± 0.018	1.370 ± 0.288	0.012	7 ± 3	9 ± 3	4 ± 2	7 ± 3	3
XMMXCS J222837.3-051235.3	$0.241^{+0.103}_{-0.107}$	0.155 ± 0.037	-	0.107 ± 0.064	-0.749 ± 1.190	0.101	2 ± 2	3 ± 3	3 ± 2	3 ± 2	3
XMMXCS J222905.5+203541.9	$0.261^{+0.068}_{-0.068}$	0.264 ± 0.041	-	-0.072 ± 0.122	2.820 ± 2.310	0.112	2 ± 2	3 ± 2	2 ± 1	2 ± 2	3
XMMXCS J222915.2-051715.5	$0.135^{+0.068}_{-0.065}$	0.084 ± 0.026	-	0.172 ± 0.048	-2.160 ± 0.872	0.034	1 ± 1	1 ± 1	0 ± 0.1	1 ± 1	3
XMMXCS J222917.6-052559.2	$0.789^{+0.157}_{-0.157}$	0.660 ± 0.194	-	-0.173 ± 0.129	4.060 ± 2.600	0.173	1 ± 1	0 ± 1	1 ± 1	-	3

Continued on next page

Table A.2 – continued from previous page

name	z_{RS}	z_{BCG}	z_{spec-g}	cmr_{grad}	cmr_{inter}	cmr_{wid}	n_{gals-c}	n_{gals-l}	n_{200-c}	n_{200-l}	qual
XMMXCS J223633.7+343000.4	$0.497^{+0.117}_{-0.117}$	0.583 ± 0.129	-	-0.020 ± 0.071	1.290 ± 1.410	0.047	5 ± 3	-	3 ± 2	-	3
XMMXCS J223719.7+342652.9	$0.073^{+0.033}_{-0.033}$	0.068 ± 0.019	-	-0.051 ± 0.008	1.550 ± 0.129	0.030	3 ± 2	11 ± 3	3 ± 2	11 ± 3	3
XMMXCS J223925.6+032055.0	$0.306^{+0.073}_{-0.075}$	0.237 ± 0.085	-	0.577 ± 0.182	-9.690 ± 3.730	0.001	0 ± 2	2 ± 2	-	1 ± 1	3
XMMXCS J223925.9+032147.5	$0.296^{+0.115}_{-0.113}$	0.190 ± 0.043	-	-0.116 ± 0.140	3.340 ± 2.700	0.128	2 ± 3	3 ± 3	1 ± 1	5 ± 3	3
XMMXCS J224259.9+293403.1	$0.419^{+0.164}_{-0.157}$	0.364 ± 0.169	-	0.068 ± 0.103	-0.441 ± 2.070	0.148	5 ± 3	37 ± 7	3 ± 2	12 ± 6	3
XMMXCS J224304.3+293729.4	$0.466^{+0.164}_{-0.158}$	0.348 ± 0.055	-	0.126 ± 0.063	-1.620 ± 1.250	0.097	3 ± 3	3 ± 3	3 ± 2	2 ± 2	3
XMMXCS J224410.09-094240.8	$0.145^{+0.031}_{-0.031}$	0.148 ± 0.024	$0.145 \pm 1.9e-05$	-0.014 ± 0.033	1.310 ± 0.568	0.059	2 ± 2	5 ± 2	0 ± 0.1	3 ± 2	3
XMMXCS J225145.4-180531.8	$0.328^{+0.126}_{-0.123}$	0.378 ± 0.115	-	-0.655 ± 0.172	14.500 ± 3.580	0.500	7 ± 3	5 ± 3	7 ± 3	-	3
XMMXCS J225417.0-174044.1	$0.090^{+0.028}_{-0.027}$	0.100 ± 0.035	-	-0.060 ± 0.059	1.500 ± 0.956	0.089	3 ± 2	4 ± 2	4 ± 2	4 ± 2	3
XMMXCS J225549.0-031147.2	$0.200^{+0.130}_{-0.137}$	0.111 ± 0.057	-	0.511 ± 0.006	-8.950 ± 0.133	0.500	4 ± 3	3 ± 3	2 ± 2	2 ± 2	3
XMMXCS J225745.4-022440.0	$0.275^{+0.102}_{-0.100}$	0.113 ± 0.048	-	0.160 ± 0.075	-1.600 ± 1.450	0.112	4 ± 3	2 ± 3	1 ± 1	2 ± 2	3
XMMXCS J230159.1+082243.9	$0.376^{+0.086}_{-0.081}$	0.373 ± 0.117	-	0.400 ± 0.237	-6.760 ± 4.680	0.139	2 ± 3	3 ± 3	0 ± 0.1	1 ± 2	3
XMMXCS J230200.2+084633.4	$0.585^{+0.129}_{-0.108}$	0.461 ± 0.068	-	0.196 ± 0.136	-3.160 ± 2.770	0.103	4 ± 3	4 ± 4	1 ± 1	-	3
XMMXCS J230227.1+083912.2	$0.462^{+0.141}_{-0.136}$	0.427 ± 0.065	-	0.327 ± 0.084	-5.540 ± 1.660	0.001	3 ± 2	-	2 ± 2	-	3
XMMXCS J230300.3+084440.2	$0.620^{+0.143}_{-0.141}$	0.607 ± 0.132	$0.719 \pm 1.7e-04$	0.185 ± 0.295	-2.560 ± 5.970	0.242	1 ± 2	12 ± 4	-	12 ± 4	3
XMMXCS J230515.5+032626.8	$0.460^{+0.160}_{-0.176}$	0.377 ± 0.058	-	0.717 ± 0.517	-13.70 ± 10.60	0.158	1 ± 3	5 ± 3	-	2 ± 2	3
XMMXCS J232100.4+081051.4	$0.120^{+0.062}_{-0.058}$	0.055 ± 0.025	-	0.030 ± 0.038	0.395 ± 0.599	0.111	6 ± 3	7 ± 3	6 ± 3	6 ± 3	3
XMMXCS J232121.5+194709.0	$0.299^{+0.078}_{-0.080}$	0.355 ± 0.060	-	-0.045 ± 0.023	2.400 ± 0.435	0.037	19 ± 5	19 ± 5	25 ± 5	24 ± 6	3
XMMXCS J232123.4+194736.3	$0.300^{+0.077}_{-0.079}$	0.355 ± 0.060	-	-0.041 ± 0.028	2.320 ± 0.535	0.035	17 ± 4	18 ± 5	21 ± 5	23 ± 5	3

Continued on next page

Table A.2 – continued from previous page

name	z_{RS}	z_{BCG}	z_{spec-g}	cmr_{grad}	cmr_{inter}	cmr_{wid}	n_{gals-c}	n_{gals-l}	n_{200-c}	n_{200-l}	qual
XMMXCS J232152.6+195334.9	$0.273^{+0.061}_{-0.061}$	0.127 ± 0.031	-	0.248 ± 0.158	-3.160 ± 2.970	0.193	15 ± 5	15 ± 5	17 ± 5	17 ± 5	3
XMMXCS J232209.0+194347.6	$0.478^{+0.115}_{-0.113}$	0.541 ± 0.093	-	-0.005 ± 0.051	0.948 ± 1.030	0.090	15 ± 5	22 ± 5	19 ± 5	30 ± 7	3
XMMXCS J232231.6+195043.8	$0.198^{+0.059}_{-0.063}$	0.215 ± 0.046	-	-0.007 ± 0.028	1.380 ± 0.526	0.072	1 ± 2	2 ± 2	0 ± 0.1	0 ± 1	3
XMMXCS J232353.4+163825.3	$0.442^{+0.327}_{-0.327}$	0.325 ± 0.081	-	0.050 ± 0.070	-0.516 ± 1.360	0.123	2 ± 3	-	0 ± 1	-	3
XMMXCS J232353.8+163826.9	$0.441^{+0.326}_{-0.326}$	0.325 ± 0.081	-	0.050 ± 0.070	-0.516 ± 1.360	0.123	2 ± 3	-	1 ± 1	-	3
XMMXCS J232405.8+164343.2	$0.095^{+0.080}_{-0.081}$	0.057 ± 0.023	-	0.016 ± 0.030	0.428 ± 0.560	0.057	1 ± 1	0 ± 1	0 ± 0.1	-	3
XMMXCS J232450.8+164842.2	$0.234^{+0.083}_{-0.091}$	0.182 ± 0.035	-	0.039 ± 0.038	0.492 ± 0.709	0.096	2 ± 2	1 ± 2	0 ± 0.1	0 ± 1	3
XMMXCS J232730.0+084519.8	$0.152^{+0.044}_{-0.045}$	0.155 ± 0.025	-	-0.008 ± 0.024	1.260 ± 0.442	0.047	1 ± 1	2 ± 2	0 ± 0.1	0 ± 1	3
XMMXCS J232810.0+144447.5	$0.094^{+0.043}_{-0.043}$	0.063 ± 0.021	$0.089 \pm 9.3e-06$	0.077 ± 0.039	-0.639 ± 0.678	0.042	1 ± 1	0 ± 1	0 ± 0.1	-	3
XMMXCS J232824.9+144512.2	$0.419^{+0.118}_{-0.122}$	0.358 ± 0.072	-	-0.026 ± 0.032	1.080 ± 0.654	0.130	1 ± 3	3 ± 3	1 ± 1	-	3
XMMXCS J232830.4+150254.6	$0.561^{+0.164}_{-0.169}$	0.515 ± 0.100	-	0.149 ± 0.081	-2.050 ± 1.620	0.037	4 ± 3	10 ± 4	0 ± 1	10 ± 4	3
XMMXCS J232834.1+144855.2	$0.275^{+0.114}_{-0.108}$	0.296 ± 0.047	-	-0.064 ± 0.154	3.140 ± 3.130	0.263	2 ± 2	1 ± 2	0 ± 0.1	0 ± 1	3
XMMXCS J232845.0+052535.2	$0.563^{+0.168}_{-0.169}$	0.614 ± 0.153	-	0.880 ± 0.520	-16.50 ± 10.50	0.202	8 ± 3	13 ± 4	8 ± 3	15 ± 4	3
XMMXCS J232846.1+050710.4	$0.088^{+0.062}_{-0.068}$	0.103 ± 0.018	$0.083 \pm 1.6e-05$	-0.183 ± 0.013	4.070 ± 0.273	0.500	1 ± 2	0 ± 1	0 ± 0.1	-	3
XMMXCS J232846.7+050428.2	$0.265^{+0.113}_{-0.113}$	0.213 ± 0.084	-	0.131 ± 0.154	-1.300 ± 3.020	0.001	4 ± 2	4 ± 3	2 ± 2	2 ± 2	3
XMMXCS J232849.7+150139.9	$0.592^{+0.123}_{-0.122}$	0.537 ± 0.161	-	0.051 ± 0.086	0.084 ± 1.750	0.001	6 ± 3	54 ± 8	5 ± 2	35 ± 8	3
XMMXCS J232908.7+144215.7	$0.578^{+0.159}_{-0.206}$	0.480 ± 0.092	-	0.142 ± 0.213	-1.900 ± 4.360	0.134	2 ± 2	13 ± 4	-	12 ± 4	3
XMMXCS J232931.6+033618.2	$0.538^{+0.111}_{-0.088}$	0.599 ± 0.120	-	-0.008 ± 0.044	0.821 ± 0.880	0.070	4 ± 2	0 ± 1	2 ± 2	-	3
XMMXCS J232937.9+145724.8	$0.405^{+0.128}_{-0.131}$	0.578 ± 0.145	-	0.069 ± 0.202	-0.548 ± 4.040	0.059	5 ± 3	5 ± 3	4 ± 2	4 ± 2	3

Continued on next page

Table A.2 – continued from previous page

name	z_{RS}	z_{BCG}	z_{spec-g}	cmr_{grad}	cmr_{inter}	cmr_{wid}	n_{gals-c}	n_{gals-l}	n_{200-c}	n_{200-l}	qual
XMMXCS J233122.1+194959.6	$0.699^{+0.184}_{-0.189}$	0.581 ± 0.208	-	0.581 ± 0.220	-10.30 ± 4.530	0.001	2 ± 2	13 ± 4	1 ± 1	19 ± 5	3
XMMXCS J233146.2+192412.4	$0.318^{+0.217}_{-0.165}$	0.241 ± 0.044	-	-0.090 ± 0.048	3.180 ± 0.937	0.062	2 ± 2	1 ± 2	1 ± 1	1 ± 1	3
XMMXCS J233230.7+195108.7	$0.198^{+0.097}_{-0.087}$	0.096 ± 0.029	-	0.014 ± 0.022	0.241 ± 0.403	0.001	1 ± 1	1 ± 2	1 ± 1	4 ± 2	3
XMMXCS J233231.4+485408.5	$0.298^{+0.073}_{-0.073}$	0.317 ± 0.063	-	-0.086 ± 0.026	3.090 ± 0.441	0.001	7 ± 3	8 ± 3	7 ± 3	7 ± 3	3
XMMXCS J233241.2+152720.3	$0.188^{+0.086}_{-0.106}$	0.237 ± 0.069	-	0.403 ± 0.001	-6.820 ± 0.029	0.500	2 ± 2	0 ± 2	1 ± 1	-	3
XMMXCS J233246.9+484419.7	$0.336^{+0.153}_{-0.131}$	0.183 ± 0.075	-	0.026 ± 0.169	0.588 ± 3.340	0.128	5 ± 3	5 ± 3	3 ± 2	3 ± 2	3
XMMXCS J233340.9+485715.1	$0.216^{+0.103}_{-0.105}$	0.154 ± 0.027	-	-0.028 ± 0.035	1.680 ± 0.670	0.089	3 ± 2	4 ± 3	2 ± 1	1 ± 2	3
XMMXCS J233537.0+021738.1	$0.334^{+0.093}_{-0.093}$	0.377 ± 0.059	$0.384 \pm 6.1e-05$	-0.077 ± 0.044	3.120 ± 0.838	0.001	13 ± 4	15 ± 4	14 ± 4	16 ± 5	3
XMMXCS J233539.5+210424.8	$0.442^{+0.177}_{-0.266}$	0.273 ± 0.129	-	-0.011 ± 0.077	0.617 ± 1.580	0.111	2 ± 3	3 ± 4	1 ± 1	0 ± 2	3
XMMXCS J233715.4+211516.5	$0.193^{+0.087}_{-0.081}$	0.079 ± 0.017	-	0.087 ± 0.067	-0.573 ± 1.130	0.141	3 ± 3	3 ± 3	0 ± 1	0 ± 2	3
XMMXCS J233823.0+271309.3	$0.061^{+0.028}_{-0.028}$	0.050 ± 0.021	-	0.054 ± 0.058	-0.105 ± 0.934	0.080	3 ± 2	1 ± 1	3 ± 2	1 ± 1	3
XMMXCS J233831.3+002131.4	$0.178^{+0.100}_{-0.099}$	0.314 ± 0.110	-	-0.072 ± 0.058	2.540 ± 1.110	0.102	2 ± 2	1 ± 2	0 ± 0.1	1 ± 1	3
XMMXCS J234305.4+002248.8	$0.575^{+0.152}_{-0.153}$	0.566 ± 0.239	-	-0.400 ± 0.204	9.470 ± 4.190	0.001	1 ± 2	2 ± 3	1 ± 1	-	3
XMMXCS J234357.4+002828.2	$0.184^{+0.053}_{-0.053}$	0.196 ± 0.030	$0.185 \pm 3.1e-05$	-0.037 ± 0.038	1.850 ± 0.695	0.001	0 ± 1	1 ± 2	-	1 ± 1	3
XMMXCS J234400.0+094124.2	$0.316^{+0.106}_{-0.105}$	0.212 ± 0.052	-	-0.158 ± 0.222	4.530 ± 4.490	0.078	0 ± 2	1 ± 2	-	1 ± 1	3
XMMXCS J234405.5+090300.9	$0.067^{+0.024}_{-0.024}$	0.071 ± 0.018	-	-0.064 ± 0.011	1.740 ± 0.156	0.007	7 ± 3	12 ± 4	4 ± 2	12 ± 4	3
XMMXCS J234636.5-021137.6	$0.191^{+0.090}_{-0.092}$	0.057 ± 0.015	-	-0.000 ± 0.001	1.200 ± 0.001	0.500	3 ± 3	7 ± 4	4 ± 2	5 ± 3	3
XMMXCS J234652.8+005402.0	$0.315^{+0.124}_{-0.127}$	0.211 ± 0.038	$0.142 \pm 2.7e-05$	0.015 ± 0.045	0.930 ± 0.880	0.108	3 ± 3	3 ± 3	2 ± 2	1 ± 2	3
XMMXCS J234705.6+010630.2	$0.209^{+0.058}_{-0.057}$	0.254 ± 0.075	$0.201 \pm 2.8e-05$	-0.110 ± 0.068	3.060 ± 1.280	0.001	2 ± 2	2 ± 2	0 ± 0.1	0 ± 1	3

Continued on next page

Table A.2 – continued from previous page

name	z_{RS}	z_{BCG}	z_{spec-g}	cmr_{grad}	cmr_{inter}	cmr_{wid}	n_{gals-c}	n_{gals-l}	n_{200-c}	n_{200-l}	qual
XMMXCS J234732.4-022314.9	$0.288^{+0.119}_{-0.132}$	0.212 ± 0.051	-	-0.053 ± 0.034	2.360 ± 0.674	0.102	0 ± 2	1 ± 2	-	0 ± 1	3
XMMXCS J234803.5-022500.9	$0.445^{+0.119}_{-0.116}$	0.290 ± 0.108	-	0.029 ± 0.068	0.012 ± 1.340	0.110	3 ± 4	5 ± 4	0 ± 1	2 ± 3	3
XMMXCS J234811.6+005707.3	$0.283^{+0.161}_{-0.161}$	0.274 ± 0.042	$0.279 \pm 6.7e-05$	-0.005 ± 0.054	1.640 ± 1.010	0.012	3 ± 2	2 ± 2	0 ± 1	1 ± 1	3
XMMXCS J235001.8+362521.8	$0.136^{+0.067}_{-0.068}$	0.165 ± 0.028	-	-0.061 ± 0.020	2.160 ± 0.354	0.001	6 ± 3	7 ± 3	5 ± 2	5 ± 2	3
XMMXCS J235147.0+202635.9	$0.511^{+0.190}_{-0.195}$	0.558 ± 0.181	-	0.291 ± 0.330	-4.780 ± 6.660	0.184	3 ± 3	7 ± 4	0 ± 1	-	3
XMMXCS J235147.0+195336.3	$0.449^{+0.173}_{-0.181}$	0.278 ± 0.136	-	-0.196 ± 0.123	5.040 ± 2.470	0.001	10 ± 4	12 ± 5	9 ± 4	-	3
XMMXCS J235148.1+200629.9	$0.150^{+0.028}_{-0.029}$	0.162 ± 0.037	-	-0.038 ± 0.007	1.780 ± 0.125	0.026	3 ± 2	3 ± 2	2 ± 1	2 ± 2	3
XMMXCS J235412.9-103634.1	$0.386^{+0.111}_{-0.105}$	0.228 ± 0.039	-	0.089 ± 0.075	-0.421 ± 1.480	0.136	1 ± 3	6 ± 4	1 ± 1	6 ± 3	3
XMMXCS J235534.2+494727.6	$0.256^{+0.127}_{-0.127}$	0.088 ± 0.023	-	0.376 ± 0.216	-5.770 ± 4.060	0.232	4 ± 2	4 ± 3	0 ± 1	-	3
XMMXCS J235558.1+055443.8	$0.248^{+0.052}_{-0.055}$	0.251 ± 0.040	-	-0.013 ± 0.028	1.640 ± 0.524	0.109	2 ± 2	2 ± 2	0 ± 0.1	0 ± 1	3

Table A.3 *A table of GMPhoRCC characterisations for the preliminary XCS DR2 sources using ATLAS optical data. Of the* 970 *with coverage, characterisations were found for* 272 *with* 64 *in the clean subset.*

name	z_{RS}	z_{BCG}	cmr_{grad}	cmr_{inter}	cmr_{wid}	n_{gals-c}	n_{gals-l}	n_{200-c}	n_{200-l}	qual
XMMXCS J001328.5-272319.0	$0.436^{+0.058}_{-0.056}$	0.392 ± 0.047	0.090 ± 0.147	0.115 ± 2.900	0.026	8 ± 3	8 ± 3	6 ± 3	7 ± 3	1
XMMXCS J001415.6-302251.3	$0.267^{+0.134}_{-0.133}$	0.243 ± 0.078	-0.063 ± 0.059	2.550 ± 1.150	0.001	18 ± 4	18 ± 5	34 ± 6	9 ± 4	1
XMMXCS J001436.6-390012.8	$0.374^{+0.075}_{-0.075}$	0.361 ± 0.066	0.113 ± 0.055	-0.211 ± 1.030	0.001	5 ± 2	25 ± 5	4 ± 2	24 ± 5	1
XMMXCS J001956.5-253517.1	$0.113^{+0.054}_{-0.054}$	0.107 ± 0.029	0.020 ± 0.067	0.358 ± 1.150	0.108	3 ± 2	2 ± 2	3 ± 2	0 ± 1	1
XMMXCS J002041.4-254252.3	$0.147^{+0.088}_{-0.088}$	0.153 ± 0.042	-0.062 ± 0.019	2.090 ± 0.349	0.038	16 ± 4	19 ± 5	22 ± 5	24 ± 5	1
XMMXCS J002531.7-330246.4	$0.103^{+0.037}_{-0.038}$	0.095 ± 0.035	0.038 ± 0.018	0.276 ± 0.300	0.060	6 ± 3	6 ± 3	4 ± 2	5 ± 2	1
XMMXCS J003652.4-333905.3	$0.263^{+0.102}_{-0.101}$	0.308 ± 0.082	-0.043 ± 0.032	2.100 ± 0.595	0.036	7 ± 3	8 ± 3	5 ± 2	7 ± 3	1
XMMXCS J004134.0-092212.4	$0.087^{+0.051}_{-0.050}$	0.067 ± 0.033	-0.028 ± 0.018	1.210 ± 0.302	0.079	8 ± 3	12 ± 4	8 ± 3	14 ± 4	1
XMMXCS J004137.0-091932.1	$0.095^{+0.055}_{-0.055}$	0.068 ± 0.015	-0.024 ± 0.018	1.160 ± 0.320	0.061	16 ± 4	20 ± 5	16 ± 4	21 ± 5	1
XMMXCS J004144.6-092113.6	$0.087^{+0.045}_{-0.045}$	0.067 ± 0.033	-0.040 ± 0.015	1.440 ± 0.255	0.068	9 ± 3	13 ± 4	7 ± 3	15 ± 4	1
XMMXCS J004200.6-091933.1	$0.086^{+0.040}_{-0.040}$	0.068 ± 0.015	-0.019 ± 0.019	1.120 ± 0.333	0.036	9 ± 3	12 ± 4	7 ± 3	13 ± 4	1
XMMXCS J004207.1-093022.6	$0.405^{+0.064}_{-0.064}$	0.421 ± 0.042	-0.283 ± 0.076	7.370 ± 1.490	0.001	7 ± 3	33 ± 6	7 ± 3	28 ± 6	1
XMMXCS J004253.5-093413.5	$0.409^{+0.076}_{-0.074}$	0.445 ± 0.064	-0.335 ± 0.058	8.650 ± 1.150	0.500	8 ± 3	10 ± 4	7 ± 3	11 ± 4	1
XMMXCS J004307.6-095136.2	$0.091^{+0.059}_{-0.059}$	0.075 ± 0.030	-0.021 ± 0.025	1.080 ± 0.420	0.043	5 ± 2	5 ± 2	4 ± 2	4 ± 2	1
XMMXCS J004307.6-095136.5	$0.091^{+0.059}_{-0.059}$	0.075 ± 0.030	-0.021 ± 0.025	1.080 ± 0.420	0.043	5 ± 2	5 ± 2	4 ± 2	4 ± 2	1
XMMXCS J004730.2-251340.4	$0.391^{+0.089}_{-0.087}$	0.352 ± 0.063	-0.247 ± 0.068	6.440 ± 1.330	0.001	3 ± 2	6 ± 3	4 ± 2	5 ± 3	1
XMMXCS J012304.3-345456.5	$0.436^{+0.065}_{-0.065}$	0.408 ± 0.054	-0.032 ± 0.071	2.970 ± 1.310	0.070	8 ± 3	24 ± 5	8 ± 3	23 ± 5	1
XMMXCS J013136.6-134500.5	$0.186^{+0.076}_{-0.076}$	0.184 ± 0.021	-0.011 ± 0.012	1.350 ± 0.217	0.001	6 ± 3	4 ± 2	6 ± 2	1 ± 1	1

Continued on next page

Table A.3 – continued from previous page

name	z_{RS}	z_{BCG}	cmr_{grad}	cmr_{inter}	cmr_{wid}	n_{gals-c}	n_{gals-l}	n_{200-c}	n_{200-l}	qual
XMMXCS J013152.9-133647.2	$0.182^{+0.061}_{-0.061}$	0.208 ± 0.024	-0.034 ± 0.023	1.820 ± 0.428	0.086	35 ± 6	37 ± 6	55 ± 8	57 ± 8	1
XMMXCS J013205.1-134000.0	$0.203^{+0.069}_{-0.070}$	0.211 ± 0.035	-0.031 ± 0.043	1.870 ± 0.796	0.060	12 ± 4	10 ± 3	13 ± 4	8 ± 3	1
XMMXCS J022505.29-095008.2	$0.171^{+0.043}_{-0.042}$	0.157 ± 0.059	0.022 ± 0.054	0.677 ± 0.978	0.057	16 ± 4	14 ± 4	16 ± 4	14 ± 4	1
XMMXCS J022521.6-292615.1	$0.183^{+0.056}_{-0.057}$	0.186 ± 0.073	0.009 ± 0.013	1.050 ± 0.224	0.001	3 ± 2	5 ± 3	4 ± 2	5 ± 2	1
XMMXCS J022523.8-292741.3	$0.180^{+0.049}_{-0.050}$	0.186 ± 0.073	0.003 ± 0.008	1.160 ± 0.146	0.001	4 ± 2	1 ± 2	4 ± 2	0 ± 1	1
XMMXCS J022831.83-094934.9	$0.388^{+0.067}_{-0.068}$	0.413 ± 0.059	-0.206 ± 0.054	6.160 ± 1.050	0.001	11 ± 3	12 ± 4	11 ± 3	12 ± 4	1
XMMXCS J022858.7-100444.1	$0.380^{+0.068}_{-0.067}$	0.382 ± 0.060	-0.060 ± 0.038	3.240 ± 0.673	0.001	6 ± 3	7 ± 3	5 ± 2	0 ± 1	1
XMMXCS J022859.0-100436.2	$0.380^{+0.067}_{-0.067}$	0.382 ± 0.060	-0.060 ± 0.038	3.240 ± 0.673	0.001	6 ± 3	7 ± 3	6 ± 2	0 ± 1	1
XMMXCS J030701.9-283959.5	$0.318^{+0.097}_{-0.097}$	0.309 ± 0.100	0.072 ± 0.046	0.112 ± 0.880	0.082	16 ± 4	3 ± 2	23 ± 5	5 ± 3	1
XMMXCS J033223.4-273107.0	$0.134^{+0.041}_{-0.041}$	0.165 ± 0.034	-0.093 ± 0.026	2.630 ± 0.456	0.044	5 ± 2	5 ± 2	5 ± 2	4 ± 2	1
XMMXCS J033226.2-273102.8	$0.134^{+0.040}_{-0.040}$	0.165 ± 0.034	-0.085 ± 0.022	2.490 ± 0.390	0.036	5 ± 2	5 ± 2	5 ± 2	4 ± 2	1
XMMXCS J033237.9-273947.3	$0.140^{+0.063}_{-0.063}$	0.109 ± 0.039	0.014 ± 0.055	0.705 ± 1.020	0.111	6 ± 3	10 ± 3	4 ± 2	10 ± 3	1
XMMXCS J033241.2-273955.2	$0.133^{+0.051}_{-0.052}$	0.109 ± 0.039	-0.009 ± 0.044	1.070 ± 0.762	0.112	6 ± 3	3 ± 2	4 ± 2	4 ± 2	1
XMMXCS J033245.5-274131.9	$0.142^{+0.065}_{-0.067}$	0.109 ± 0.039	0.032 ± 0.021	0.348 ± 0.364	0.091	5 ± 2	7 ± 3	4 ± 2	4 ± 2	1
XMMXCS J033728.5-344257.8	$0.427^{+0.100}_{-0.095}$	0.393 ± 0.201	0.240 ± 0.513	-3.940 ± 10.30	0.500	3 ± 2	1 ± 1	4 ± 2	0 ± 1	1
XMMXCS J101432.0-041344.3	$0.495^{+0.082}_{-0.079}$	0.488 ± 0.087	0.026 ± 0.036	0.289 ± 0.711	0.001	4 ± 2	35 ± 6	3 ± 2	61 ± 8	1
XMMXCS J102739.8-032415.8	$0.112^{+0.042}_{-0.042}$	0.130 ± 0.056	-0.032 ± 0.009	1.330 ± 0.178	0.500	5 ± 2	4 ± 2	4 ± 2	3 ± 2	1
XMMXCS J103554.6-033153.6	$0.463^{+0.072}_{-0.071}$	0.443 ± 0.076	0.039 ± 0.015	-0.012 ± 0.299	0.001	4 ± 2	23 ± 5	3 ± 2	21 ± 5	1
XMMXCS J105609.6-045949.6	$0.299^{+0.081}_{-0.081}$	0.273 ± 0.093	-0.011 ± 0.042	1.620 ± 0.787	0.091	13 ± 4	12 ± 4	12 ± 4	12 ± 4	1

Continued on next page

Table A.3 – continued from previous page

name	z_{RS}	z_{BCG}	cmr_{grad}	cmr_{inter}	cmr_{wid}	n_{gals-c}	n_{gals-l}	n_{200-c}	n_{200-l}	qual
XMMXCS J120522.6-075552.1	$0.416^{+0.108}_{-0.106}$	0.459 ± 0.064	-0.118 ± 0.056	2.980 ± 1.060	0.001	4 ± 3	5 ± 3	4 ± 2	-	1
XMMXCS J125846.6-041235.6	$0.127^{+0.052}_{-0.053}$	0.103 ± 0.022	0.011 ± 0.027	0.770 ± 0.477	0.095	15 ± 4	18 ± 5	22 ± 5	28 ± 6	1
XMMXCS J150407.6-024814.8	$0.259^{+0.089}_{-0.090}$	0.245 ± 0.037	-0.058 ± 0.069	2.500 ± 1.300	0.087	25 ± 5	25 ± 5	30 ± 6	30 ± 6	1
XMMXCS J150419.0-024833.4	$0.264^{+0.088}_{-0.088}$	0.245 ± 0.037	-0.105 ± 0.031	3.360 ± 0.565	0.013	14 ± 4	26 ± 5	19 ± 5	27 ± 6	1
XMMXCS J214859.7-303826.4	$0.429^{+0.196}_{-0.192}$	0.397 ± 0.244	0.057 ± 0.015	-0.237 ± 0.286	0.059	15 ± 4	15 ± 4	19 ± 5	20 ± 5	1
XMMXCS J215134.3-302624.8	$0.540^{+0.151}_{-0.151}$	0.526 ± 0.182	-0.144 ± 0.102	3.840 ± 1.970	0.097	10 ± 3	0 ± 2	9 ± 3	-	1
XMMXCS J221728.5-353242.1	$0.147^{+0.052}_{-0.052}$	0.161 ± 0.022	-0.057 ± 0.073	2.080 ± 1.260	0.060	12 ± 4	9 ± 3	12 ± 4	12 ± 4	1
XMMXCS J221745.5-354327.8	$0.174^{+0.059}_{-0.059}$	0.194 ± 0.037	-0.004 ± 0.024	1.230 ± 0.421	0.031	16 ± 4	6 ± 3	21 ± 5	12 ± 4	1
XMMXCS J221754.9-354757.2	$0.157^{+0.045}_{-0.046}$	0.107 ± 0.044	0.121 ± 0.024	-1.120 ± 0.427	0.038	9 ± 3	9 ± 3	8 ± 3	7 ± 3	1
XMMXCS J221755.1-354438.1	$0.170^{+0.050}_{-0.050}$	0.194 ± 0.037	-0.037 ± 0.017	1.790 ± 0.296	0.029	17 ± 4	18 ± 4	24 ± 5	24 ± 5	1
XMMXCS J221839.4-385356.7	$0.185^{+0.102}_{-0.102}$	0.220 ± 0.112	-0.040 ± 0.018	1.790 ± 0.323	0.022	25 ± 5	33 ± 6	32 ± 6	42 ± 7	1
XMMXCS J223412.9-373558.8	$0.125^{+0.072}_{-0.075}$	0.168 ± 0.070	-0.036 ± 0.021	1.670 ± 0.368	0.001	4 ± 2	4 ± 2	3 ± 2	2 ± 2	1
XMMXCS J223429.0-374414.3	$0.196^{+0.103}_{-0.103}$	0.182 ± 0.058	0.006 ± 0.021	0.941 ± 0.382	0.051	9 ± 3	11 ± 4	7 ± 3	9 ± 3	1
XMMXCS J223433.9-374603.8	$0.162^{+0.075}_{-0.075}$	0.171 ± 0.035	0.044 ± 0.024	0.269 ± 0.430	0.001	7 ± 3	8 ± 3	3 ± 2	7 ± 3	1
XMMXCS J233126.9-362936.7	$0.121^{+0.033}_{-0.032}$	0.138 ± 0.025	-0.046 ± 0.019	1.720 ± 0.328	0.060	8 ± 3	5 ± 3	5 ± 2	2 ± 2	1
XMMXCS J234033.3-113044.2	$0.146^{+0.047}_{-0.047}$	0.107 ± 0.037	-0.032 ± 0.047	1.220 ± 0.836	0.500	6 ± 3	5 ± 3	4 ± 2	2 ± 2	1
XMMXCS J234721.0-280416.7	$0.104^{+0.057}_{-0.058}$	0.114 ± 0.049	-0.022 ± 0.024	1.040 ± 0.408	0.103	9 ± 3	10 ± 3	7 ± 3	8 ± 3	1
XMMXCS J234727.4-281150.8	$0.378^{+0.137}_{-0.137}$	0.355 ± 0.037	0.850 ± 1.170	-16.70 ± 23.50	0.123	4 ± 2	0 ± 1	4 ± 2	-	1
XMMXCS J234742.9-280826.4	$0.124^{+0.047}_{-0.047}$	0.102 ± 0.040	-0.032 ± 0.010	1.240 ± 0.171	0.012	6 ± 3	6 ± 3	6 ± 2	15 ± 4	1

Continued on next page

Table A.3 – continued from previous page

name	z_{RS}	z_{BCG}	cmr_{grad}	cmr_{inter}	cmr_{wid}	n_{gals-c}	n_{gals-l}	n_{200-c}	n_{200-l}	qual
XMMXCS J234747.7-281329.5	$0.114^{+0.054}_{-0.054}$	0.101 ± 0.033	-0.027 ± 0.048	1.190 ± 0.804	0.078	6 ± 3	5 ± 3	4 ± 2	2 ± 2	1
XMMXCS J234754.1-281128.8	$0.117^{+0.043}_{-0.042}$	0.102 ± 0.040	0.005 ± 0.015	0.687 ± 0.243	0.073	8 ± 3	9 ± 3	6 ± 3	6 ± 3	1
XMMXCS J235139.6-260459.9	$0.225^{+0.099}_{-0.100}$	0.219 ± 0.060	-0.057 ± 0.037	2.300 ± 0.700	0.079	21 ± 5	23 ± 5	25 ± 5	28 ± 6	1
XMMXCS J235216.8-260503.1	$0.283^{+0.125}_{-0.123}$	0.301 ± 0.120	0.048 ± 0.050	0.385 ± 0.958	0.051	6 ± 3	6 ± 3	3 ± 2	0 ± 1	1
XMMXCS J235400.4-102534.3	$0.095^{+0.037}_{-0.038}$	0.096 ± 0.023	0.048 ± 0.024	0.057 ± 0.407	0.018	11 ± 3	10 ± 3	11 ± 3	10 ± 3	1
XMMXCS J235412.7-102503.8	$0.113^{+0.048}_{-0.048}$	0.127 ± 0.043	-0.005 ± 0.013	0.983 ± 0.221	0.037	24 ± 5	20 ± 5	29 ± 6	24 ± 5	1
XMMXCS J235420.6-101844.7	$0.109^{+0.034}_{-0.035}$	0.129 ± 0.026	-0.031 ± 0.014	1.400 ± 0.228	0.034	17 ± 4	17 ± 4	26 ± 5	26 ± 5	1
XMMXCS J235424.0-101606.9	$0.097^{+0.031}_{-0.032}$	0.091 ± 0.025	-0.066 ± 0.001	1.690 ± 0.002	0.500	9 ± 3	10 ± 3	9 ± 3	8 ± 3	1
XMMXCS J000010.1-315951.2	$0.245^{+0.112}_{-0.112}$	0.167 ± 0.033	0.029 ± 0.079	0.675 ± 1.510	0.109	2 ± 2	3 ± 2	1 ± 1	2 ± 2	2
XMMXCS J000029.8-251211.4	$0.106^{+0.031}_{-0.032}$	0.123 ± 0.040	0.003 ± 0.083	0.765 ± 1.460	0.090	4 ± 2	3 ± 2	2 ± 1	0 ± 1	2
XMMXCS J000257.0-295525.3	$0.102^{+0.046}_{-0.046}$	0.108 ± 0.048	0.049 ± 0.031	0.013 ± 0.534	0.065	3 ± 2	4 ± 2	2 ± 1	3 ± 2	2
XMMXCS J000300.6-295153.4	$0.197^{+0.093}_{-0.093}$	0.118 ± 0.038	0.0 ± -1.00	1.100 ± -1.00	0.500	1 ± 2	4 ± 3	2 ± 1	4 ± 2	2
XMMXCS J000322.3-260019.4	$0.173^{+0.105}_{-0.105}$	0.119 ± 0.043	-0.232 ± 0.145	5.700 ± 2.950	0.500	1 ± 1	0 ± 1	1 ± 1	-	2
XMMXCS J001326.4-272135.8	$0.441^{+0.076}_{-0.073}$	0.500 ± 0.049	-0.049 ± 0.106	1.570 ± 2.060	0.119	7 ± 3	7 ± 3	7 ± 3	7 ± 3	2
XMMXCS J001345.2-271654.8	$0.267^{+0.033}_{-0.033}$	0.359 ± 0.127	0.176 ± 0.002	-1.130 ± 0.048	0.500	2 ± 2	0 ± 1	1 ± 1	-	2
XMMXCS J001405.4-302034.7	$0.221^{+0.102}_{-0.102}$	0.243 ± 0.078	-0.142 ± 0.101	3.850 ± 1.940	0.001	4 ± 2	5 ± 3	2 ± 1	4 ± 2	2
XMMXCS J001424.1-301501.7	$0.419^{+0.086}_{-0.082}$	0.447 ± 0.061	0.093 ± 0.087	-1.240 ± 1.750	0.127	1 ± 2	1 ± 3	1 ± 1	0 ± 1	2
XMMXCS J001933.2-254147.0	$0.117^{+0.059}_{-0.060}$	0.141 ± 0.060	-0.007 ± 0.014	1.030 ± 0.241	0.001	4 ± 2	3 ± 2	2 ± 1	2 ± 2	2
XMMXCS J003814.5-335031.8	$0.386^{+0.052}_{-0.050}$	0.396 ± 0.058	0.051 ± 0.014	0.973 ± 0.247	0.500	1 ± 2	2 ± 3	1 ± 1	-	2

Continued on next page

Table A.3 – continued from previous page

name	z_{RS}	z_{BCG}	cmr_{grad}	cmr_{inter}	cmr_{wid}	n_{gals-c}	n_{gals-l}	n_{200-c}	n_{200-l}	qual
XMMXCS J004302.2-092714.9	$0.102^{+0.033}_{-0.034}$	0.080 ± 0.036	0.046 ± 0.037	0.053 ± 0.638	0.101	4 ± 2	5 ± 3	2 ± 1	5 ± 2	2
XMMXCS J004302.2-092715.0	$0.102^{+0.033}_{-0.034}$	0.080 ± 0.036	0.046 ± 0.037	0.053 ± 0.638	0.101	4 ± 2	5 ± 3	2 ± 1	5 ± 2	2
XMMXCS J004324.6-094449.8	$0.249^{+0.088}_{-0.089}$	0.193 ± 0.059	0.048 ± 0.036	0.477 ± 0.643	0.001	2 ± 2	3 ± 2	3 ± 2	4 ± 2	2
XMMXCS J004725.3-251645.1	$0.461^{+0.146}_{-0.148}$	0.536 ± 0.049	0.333 ± 0.431	-5.870 ± 8.630	0.070	6 ± 3	9 ± 4	4 ± 2	7 ± 3	2
XMMXCS J004746.8-252512.0	$0.231^{+0.141}_{-0.158}$	0.269 ± 0.124	-0.059 ± 0.062	2.270 ± 1.200	0.091	3 ± 2	1 ± 2	1 ± 1	-	2
XMMXCS J004757.4-251505.2	$0.399^{+0.144}_{-0.140}$	0.492 ± 0.193	1.200 ± 0.111	-22.90 ± 2.260	0.500	5 ± 3	5 ± 3	5 ± 2	-	2
XMMXCS J004801.4-252733.1	$0.206^{+0.101}_{-0.101}$	0.205 ± 0.108	0.042 ± 0.047	0.312 ± 0.895	0.121	6 ± 3	4 ± 3	2 ± 2	2 ± 2	2
XMMXCS J012230.6-283212.6	$0.327^{+0.120}_{-0.119}$	0.246 ± 0.083	-0.113 ± 0.071	3.560 ± 1.430	0.082	4 ± 2	4 ± 3	4 ± 2	1 ± 2	2
XMMXCS J012411.5-345248.9	$0.471^{+0.076}_{-0.073}$	0.407 ± 0.073	0.263 ± 0.049	-4.520 ± 0.966	0.001	6 ± 3	33 ± 6	3 ± 2	13 ± 5	2
XMMXCS J012419.9-345513.5	$0.417^{+0.077}_{-0.071}$	0.514 ± 0.053	0.047 ± 0.023	-0.401 ± 0.424	0.033	2 ± 2	0 ± 1	1 ± 1	-	2
XMMXCS J012441.1-345805.7	$0.455^{+0.067}_{-0.062}$	0.424 ± 0.119	-0.051 ± 0.029	1.540 ± 0.556	0.094	3 ± 2	4 ± 3	1 ± 1	-	2
XMMXCS J015221.8-140513.8	$0.392^{+0.134}_{-0.133}$	0.456 ± 0.140	-0.018 ± 0.066	0.959 ± 1.260	0.127	13 ± 4	14 ± 4	15 ± 4	15 ± 5	2
XMMXCS J015306.4-134539.0	$0.185^{+0.075}_{-0.079}$	0.206 ± 0.083	-0.033 ± 0.050	1.810 ± 0.938	0.090	2 ± 2	2 ± 2	1 ± 1	0 ± 1	2
XMMXCS J015337.2-135100.4	$0.403^{+0.056}_{-0.056}$	0.413 ± 0.078	0.204 ± 0.105	-2.000 ± 2.010	0.089	2 ± 2	3 ± 2	1 ± 1	0 ± 1	2
XMMXCS J021028.7-101531.0	$0.343^{+0.117}_{-0.116}$	0.342 ± 0.094	-0.446 ± 0.251	10.400 ± 5.050	0.101	2 ± 2	3 ± 2	1 ± 1	1 ± 1	2
XMMXCS J021028.6-101530.9	$0.343^{+0.117}_{-0.116}$	0.342 ± 0.094	-0.446 ± 0.251	10.400 ± 5.050	0.101	2 ± 2	3 ± 2	1 ± 1	1 ± 1	2
XMMXCS J021606.40-093517.1	$0.389^{+0.103}_{-0.102}$	0.465 ± 0.034	-0.137 ± 0.071	3.370 ± 1.460	0.001	3 ± 2	4 ± 3	1 ± 1	0 ± 1	2
XMMXCS J022505.9-292636.4	$0.093^{+0.047}_{-0.049}$	0.100 ± 0.031	0.134 ± 0.039	-1.580 ± 0.642	0.500	4 ± 2	6 ± 3	2 ± 1	2 ± 2	2
XMMXCS J022509.5-292843.4	$0.098^{+0.034}_{-0.034}$	0.100 ± 0.031	-0.024 ± 0.022	1.280 ± 0.353	0.037	2 ± 2	3 ± 2	1 ± 1	1 ± 1	2

Continued on next page

Table A.3 – continued from previous page

name	z_{RS}	z_{BCG}	cmr_{grad}	cmr_{inter}	cmr_{wid}	n_{gals-c}	n_{gals-l}	n_{200-c}	n_{200-l}	qual
XMMXCS J022812.5-100538.3	$0.161^{+0.053}_{-0.053}$	0.157 ± 0.026	0.015 ± 0.035	0.842 ± 0.655	0.032	2 ± 2	2 ± 2	2 ± 1	2 ± 2	2
XMMXCS J022849.5-100205.5	$0.372^{+0.098}_{-0.104}$	0.277 ± 0.058	-0.016 ± 0.273	1.900 ± 5.350	0.001	4 ± 2	6 ± 3	2 ± 1	3 ± 2	2
XMMXCS J023022.2-292736.0	$0.289^{+0.071}_{-0.071}$	0.276 ± 0.058	-0.073 ± 0.053	2.870 ± 1.020	0.001	3 ± 2	2 ± 2	2 ± 1	2 ± 2	2
XMMXCS J024901.1-312015.5	$0.136^{+0.041}_{-0.041}$	0.114 ± 0.030	0.002 ± 0.028	0.926 ± 0.473	0.001	4 ± 2	2 ± 2	2 ± 1	1 ± 1	2
XMMXCS J030648.9-285338.4	$0.329^{+0.099}_{-0.097}$	0.368 ± 0.095	-0.304 ± 0.104	7.530 ± 2.090	0.001	3 ± 2	2 ± 2	1 ± 1	1 ± 1	2
XMMXCS J030753.1-283914.1	$0.488^{+0.101}_{-0.100}$	0.498 ± 0.070	-0.092 ± 0.050	2.530 ± 0.997	0.031	2 ± 2	5 ± 3	2 ± 1	-	2
XMMXCS J033210.8-275940.7	$0.096^{+0.040}_{-0.041}$	0.112 ± 0.048	-0.063 ± 0.042	1.880 ± 0.747	0.095	3 ± 2	2 ± 2	2 ± 1	0 ± 1	2
XMMXCS J033618.0-345958.0	$0.258^{+0.072}_{-0.071}$	0.190 ± 0.111	-0.547 ± 0.131	11.900 ± 2.650	0.500	1 ± 2	0 ± 2	2 ± 1	-	2
XMMXCS J033710.0-251606.1	$0.312^{+0.121}_{-0.113}$	0.320 ± 0.077	-0.289 ± 0.132	7.210 ± 2.710	0.062	2 ± 2	1 ± 2	2 ± 1	-	2
XMMXCS J100243.3-080222.8	$0.391^{+0.093}_{-0.093}$	0.337 ± 0.056	-0.117 ± 0.051	3.880 ± 0.945	0.001	4 ± 2	5 ± 3	4 ± 2	6 ± 3	2
XMMXCS J101110.6-044217.2	$0.289^{+0.113}_{-0.113}$	0.318 ± 0.090	-0.168 ± 0.075	4.860 ± 1.510	0.097	3 ± 2	4 ± 2	2 ± 1	1 ± 1	2
XMMXCS J103601.4-035358.4	$0.371^{+0.107}_{-0.103}$	0.446 ± 0.045	-0.058 ± 0.051	1.740 ± 0.987	0.001	5 ± 3	-	1 ± 1	-	2
XMMXCS J104357.9-065616.4	$0.536^{+0.068}_{-0.066}$	0.535 ± 0.033	-0.486 ± 0.086	10.700 ± 1.710	0.001	3 ± 2	-	2 ± 1	-	2
XMMXCS J105420.2-060125.1	$0.405^{+0.164}_{-0.197}$	0.427 ± 0.184	-0.337 ± 0.088	7.820 ± 1.700	0.001	3 ± 2	-	1 ± 1	-	2
XMMXCS J105533.5-050304.5	$0.337^{+0.097}_{-0.097}$	0.313 ± 0.042	0.051 ± 0.155	0.498 ± 3.050	0.114	4 ± 2	4 ± 3	2 ± 2	-	2
XMMXCS J112831.4-042524.7	$0.199^{+0.090}_{-0.090}$	0.099 ± 0.035	-0.000 ± 0.001	1.240 ± 0.001	0.500	1 ± 2	0 ± 2	1 ± 1	-	2
XMMXCS J120608.9-074551.5	$0.141^{+0.056}_{-0.057}$	0.135 ± 0.033	-0.079 ± 0.029	2.120 ± 0.493	0.042	5 ± 2	5 ± 3	1 ± 1	2 ± 2	2
XMMXCS J124919.8-061034.1	$0.174^{+0.084}_{-0.106}$	0.138 ± 0.046	-0.372 ± 0.006	7.800 ± 0.114	0.500	3 ± 2	-	2 ± 1	-	2
XMMXCS J131122.2-054643.9	$0.172^{+0.066}_{-0.066}$	0.189 ± 0.071	0.004 ± 0.011	1.080 ± 0.167	0.001	3 ± 2	4 ± 2	1 ± 1	4 ± 2	2

Continued on next page

Table A.3 – continued from previous page

name	z_{RS}	z_{BCG}	cmr_{grad}	cmr_{inter}	cmr_{wid}	n_{gals-c}	n_{gals-l}	n_{200-c}	n_{200-l}	qual
XMMXCS J140835.9-074454.0	$0.405^{+0.086}_{-0.083}$	0.383 ± 0.060	-0.057 ± 0.160	1.820 ± 3.080	0.085	5 ± 3	4 ± 3	1 ± 1	2 ± 2	2
XMMXCS J140920.3-074220.9	$0.248^{+0.106}_{-0.102}$	0.185 ± 0.027	0.220 ± 0.117	-2.820 ± 2.210	0.500	5 ± 3	8 ± 4	4 ± 2	6 ± 3	2
XMMXCS J150420.9-024040.5	$0.324^{+0.068}_{-0.068}$	0.290 ± 0.052	0.072 ± 0.099	0.164 ± 1.890	0.001	2 ± 2	3 ± 2	1 ± 1	3 ± 2	2
XMMXCS J150421.9-023943.0	$0.275^{+0.076}_{-0.076}$	0.290 ± 0.052	0.121 ± 0.111	-0.837 ± 2.150	0.202	4 ± 3	4 ± 3	1 ± 1	2 ± 2	2
XMMXCS J214907.4-304205.6	$0.376^{+0.183}_{-0.183}$	0.284 ± 0.205	-0.028 ± 0.034	0.978 ± 0.634	0.071	41 ± 7	40 ± 7	77 ± 9	72 ± 9	2
XMMXCS J215122.9-302436.9	$0.490^{+0.178}_{-0.181}$	0.496 ± 0.179	-0.048 ± 0.047	1.830 ± 0.919	0.065	2 ± 2	18 ± 5	1 ± 1	11 ± 4	2
XMMXCS J215137.1-302638.1	$0.501^{+0.172}_{-0.174}$	0.435 ± 0.207	0.047 ± 0.024	-0.094 ± 0.495	0.001	7 ± 3	6 ± 3	7 ± 3	-	2
XMMXCS J215145.7-302325.0	$0.451^{+0.230}_{-0.212}$	0.365 ± 0.230	0.051 ± 0.031	-0.121 ± 0.603	0.036	1 ± 2	3 ± 3	1 ± 1	4 ± 2	2
XMMXCS J215259.8-272534.7	$0.314^{+0.125}_{-0.120}$	0.357 ± 0.059	-0.205 ± 0.033	5.280 ± 0.611	0.001	3 ± 2	4 ± 3	2 ± 2	5 ± 3	2
XMMXCS J215818.1-301219.2	$0.500^{+0.135}_{-0.132}$	0.506 ± 0.145	0.068 ± 0.049	-0.572 ± 0.967	0.001	4 ± 2	14 ± 4	1 ± 1	13 ± 4	2
XMMXCS J215841.6-302317.5	$0.409^{+0.130}_{-0.129}$	0.494 ± 0.176	0.140 ± 0.135	-1.590 ± 2.620	0.001	5 ± 3	5 ± 3	4 ± 2	6 ± 3	2
XMMXCS J215849.1-301521.9	$0.110^{+0.060}_{-0.060}$	0.089 ± 0.035	-0.083 ± 0.024	2.150 ± 0.419	0.042	1 ± 1	1 ± 1	1 ± 1	1 ± 1	2
XMMXCS J215906.7-300622.8	$0.445^{+0.123}_{-0.116}$	0.537 ± 0.059	-0.072 ± 0.086	3.070 ± 1.710	0.001	4 ± 2	3 ± 2	1 ± 1	-	2
XMMXCS J221738.2-355202.0	$0.132^{+0.082}_{-0.083}$	0.115 ± 0.031	-0.065 ± 0.039	2.070 ± 0.669	0.001	2 ± 1	1 ± 1	1 ± 1	0 ± 1	2
XMMXCS J221741.1-385157.9	$0.377^{+0.127}_{-0.116}$	0.459 ± 0.074	-0.300 ± 0.153	7.680 ± 3.020	0.500	6 ± 3	9 ± 3	4 ± 2	1 ± 1	2
XMMXCS J221817.0-354130.0	$0.181^{+0.078}_{-0.077}$	0.168 ± 0.028	0.007 ± 0.048	0.982 ± 0.882	0.089	5 ± 2	6 ± 3	1 ± 1	3 ± 2	2
XMMXCS J221854.0-390430.7	$0.148^{+0.051}_{-0.052}$	0.208 ± 0.094	-0.059 ± 0.033	2.170 ± 0.606	0.001	2 ± 2	1 ± 2	1 ± 1	0 ± 1	2
XMMXCS J223525.8-260522.3	$0.323^{+0.149}_{-0.141}$	0.233 ± 0.093	0.062 ± 0.098	0.192 ± 1.890	0.104	2 ± 2	1 ± 2	1 ± 1	-	2
XMMXCS J223530.3-261139.3	$0.173^{+0.074}_{-0.075}$	0.116 ± 0.038	-0.181 ± 0.214	4.430 ± 3.950	0.500	3 ± 2	1 ± 2	1 ± 1	2 ± 2	2

Continued on next page

Table A.3 – continued from previous page

name	z_{RS}	z_{BCG}	cmr_{grad}	cmr_{inter}	cmr_{wid}	n_{gals-c}	n_{gals-l}	n_{200-c}	n_{200-l}	qual
XMMXCS J224855.4-270730.0	$0.501^{+0.111}_{-0.108}$	0.529 ± 0.066	-0.271 ± 0.219	6.220 ± 4.360	0.151	5 ± 3	46 ± 7	1 ± 1	12 ± 5	2
XMMXCS J225633.9-364024.2	$0.131^{+0.052}_{-0.054}$	0.183 ± 0.027	-0.000 ± 0.001	0.692 ± 0.001	0.500	3 ± 2	4 ± 2	2 ± 1	3 ± 2	2
XMMXCS J232536.7-115928.9	$0.446^{+0.075}_{-0.073}$	0.393 ± 0.047	0.153 ± 0.078	-2.250 ± 1.530	0.119	7 ± 3	8 ± 3	4 ± 2	7 ± 3	2
XMMXCS J233113.5-363043.3	$0.115^{+0.032}_{-0.031}$	0.139 ± 0.026	-0.033 ± 0.031	1.470 ± 0.548	0.062	4 ± 2	6 ± 3	2 ± 1	3 ± 2	2
XMMXCS J233142.2-363325.0	$0.146^{+0.053}_{-0.054}$	0.138 ± 0.025	0.012 ± 0.033	0.732 ± 0.606	0.085	4 ± 2	4 ± 2	1 ± 1	1 ± 1	2
XMMXCS J233154.8-363648.3	$0.155^{+0.056}_{-0.056}$	0.096 ± 0.037	-0.001 ± 0.088	1.050 ± 1.640	0.063	1 ± 1	1 ± 1	1 ± 1	0 ± 1	2
XMMXCS J233939.8-114217.6	$0.099^{+0.048}_{-0.048}$	0.105 ± 0.036	-0.027 ± 0.093	1.330 ± 1.590	0.046	4 ± 2	1 ± 1	1 ± 1	1 ± 1	2
XMMXCS J234025.0-114337.3	$0.189^{+0.056}_{-0.055}$	0.242 ± 0.078	-0.083 ± 0.029	2.730 ± 0.526	0.038	4 ± 2	6 ± 3	4 ± 2	5 ± 2	2
XMMXCS J234708.4-281822.1	$0.179^{+0.068}_{-0.067}$	0.183 ± 0.030	-0.080 ± 0.035	2.570 ± 0.649	0.066	4 ± 2	4 ± 2	1 ± 1	1 ± 1	2
XMMXCS J234732.1-275643.2	$0.111^{+0.039}_{-0.039}$	0.117 ± 0.045	-0.030 ± 0.011	1.210 ± 0.173	0.035	4 ± 2	2 ± 2	1 ± 1	1 ± 1	2
XMMXCS J234812.7-281405.3	$0.158^{+0.037}_{-0.036}$	0.214 ± 0.031	-0.000 ± 0.001	0.707 ± 0.001	0.500	5 ± 3	5 ± 3	2 ± 2	0 ± 1	2
XMMXCS J234817.8-281101.3	$0.166^{+0.042}_{-0.041}$	0.214 ± 0.031	-0.142 ± 0.030	3.660 ± 0.523	0.001	4 ± 2	5 ± 3	2 ± 1	3 ± 2	2
XMMXCS J235140.5-255818.8	$0.228^{+0.075}_{-0.075}$	0.283 ± 0.050	-0.030 ± 0.043	1.850 ± 0.802	0.050	5 ± 2	7 ± 3	3 ± 2	2 ± 2	2
XMMXCS J000003.1-320024.1	$0.226^{+0.103}_{-0.104}$	0.217 ± 0.053	0.002 ± 0.067	1.220 ± 1.260	0.077	1 ± 1	1 ± 2	1 ± 1	1 ± 1	3
XMMXCS J000013.9-251052.1	$0.107^{+0.043}_{-0.044}$	0.123 ± 0.040	0.007 ± 0.027	0.763 ± 0.479	0.070	5 ± 2	4 ± 2	4 ± 2	3 ± 2	3
XMMXCS J000216.5-360401.4	$0.472^{+0.064}_{-0.062}$	0.479 ± 0.040	-0.366 ± 0.036	7.680 ± 0.698	0.001	5 ± 3	5 ± 3	4 ± 2	4 ± 3	3
XMMXCS J000246.9-294955.1	$0.142^{+0.054}_{-0.055}$	0.161 ± 0.124	0.214 ± 0.084	-2.960 ± 1.590	0.001	1 ± 1	1 ± 1	0 ± 0.1	1 ± 1	3
XMMXCS J000317.1-295847.6	$0.255^{+0.064}_{-0.067}$	0.288 ± 0.062	0.075 ± 0.068	0.003 ± 1.260	0.092	2 ± 2	1 ± 2	0 ± 0.1	-	3
XMMXCS J000359.9-261226.9	$0.445^{+0.069}_{-0.061}$	0.409 ± 0.048	-0.018 ± 0.048	0.967 ± 0.924	0.092	0 ± 1	21 ± 5	-	43 ± 7	3

Continued on next page

Table A.3 – continued from previous page

name	z_{RS}	z_{BCG}	cmr_{grad}	cmr_{inter}	cmr_{wid}	n_{gals-c}	n_{gals-l}	n_{200-c}	n_{200-l}	qual
XMMXCS J000952.7-321938.8	$0.208^{+0.067}_{-0.073}$	0.126 ± 0.035	-0.258 ± 0.040	6.080 ± 0.756	0.500	0 ± 2	1 ± 3	-	2 ± 2	3
XMMXCS J001436.5-385910.9	$0.376^{+0.077}_{-0.077}$	0.361 ± 0.066	0.133 ± 0.058	-0.573 ± 1.090	0.019	4 ± 2	0 ± 1	3 ± 2	-	3
XMMXCS J002033.2-255156.5	$0.135^{+0.060}_{-0.060}$	0.192 ± 0.121	-0.008 ± 0.035	1.050 ± 0.644	0.058	1 ± 1	0 ± 1	0 ± 0.1	-	3
XMMXCS J002059.8-253611.8	$0.133^{+0.056}_{-0.056}$	0.167 ± 0.083	-0.098 ± 0.048	2.670 ± 0.840	0.113	1 ± 1	3 ± 2	-	0 ± 1	3
XMMXCS J003645.3-333945.0	$0.242^{+0.126}_{-0.127}$	0.115 ± 0.022	0.176 ± 0.040	-2.320 ± 0.754	0.001	0 ± 1	1 ± 2	-	0 ± 1	3
XMMXCS J003652.4-333319.2	$0.297^{+0.103}_{-0.099}$	0.361 ± 0.131	-0.212 ± 0.052	5.400 ± 1.030	0.001	3 ± 2	4 ± 2	-	0 ± 1	3
XMMXCS J003656.5-333313.9	$0.222^{+0.087}_{-0.088}$	0.361 ± 0.131	-0.280 ± 0.057	6.700 ± 1.120	0.001	2 ± 1	1 ± 1	2 ± 1	0 ± 1	3
XMMXCS J003710.8-333547.0	$0.213^{+0.077}_{-0.079}$	0.220 ± 0.122	-0.085 ± 0.122	2.860 ± 2.360	0.127	2 ± 2	0 ± 1	0 ± 0.1	-	3
XMMXCS J003737.4-334257.5	$0.170^{+0.057}_{-0.061}$	0.120 ± 0.031	-0.000 ± 0.001	1.040 ± 0.001	0.500	1 ± 2	-	0 ± 0.1	-	3
XMMXCS J003741.4-334241.0	$0.115^{+0.052}_{-0.056}$	0.120 ± 0.031	0.117 ± 0.027	-1.110 ± 0.469	0.001	1 ± 1	0 ± 1	0 ± 0.1	-	3
XMMXCS J003747.2-334105.4	$0.123^{+0.059}_{-0.063}$	0.120 ± 0.031	0.088 ± 0.041	-0.602 ± 0.729	0.001	1 ± 1	1 ± 1	0 ± 0.1	0 ± 1	3
XMMXCS J004130.5-091548.4	$0.088^{+0.049}_{-0.049}$	0.113 ± 0.033	-0.033 ± 0.008	1.380 ± 0.143	0.026	5 ± 2	8 ± 3	4 ± 2	7 ± 3	3
XMMXCS J004149.6-094704.9	$0.363^{+0.072}_{-0.066}$	0.254 ± 0.136	1.210 ± 0.225	-21.60 ± 4.350	0.500	1 ± 2	2 ± 3	2 ± 1	-	3
XMMXCS J004151.0-091816.7	$0.082^{+0.032}_{-0.032}$	0.068 ± 0.015	-0.050 ± 0.014	1.620 ± 0.220	0.043	8 ± 3	13 ± 4	6 ± 3	14 ± 4	3
XMMXCS J004204.4-091644.6	$0.075^{+0.038}_{-0.038}$	0.071 ± 0.016	-0.034 ± 0.015	1.400 ± 0.265	0.008	5 ± 2	6 ± 3	0 ± 0.1	1 ± 1	3
XMMXCS J004717.6-251820.2	$0.596^{+0.123}_{-0.155}$	0.400 ± 0.072	0.581 ± 0.313	-10.30 ± 6.200	0.001	2 ± 1	19 ± 4	-	19 ± 4	3
XMMXCS J004719.5-250643.7	$0.096^{+0.068}_{-0.067}$	0.113 ± 0.073	0.062 ± 0.046	-0.359 ± 0.844	0.093	0 ± 0.1	1 ± 1	-	0 ± 1	3
XMMXCS J004719.9-251007.7	$0.216^{+0.098}_{-0.110}$	0.090 ± 0.028	0.428 ± 0.092	-7.110 ± 1.780	0.052	0 ± 0.1	1 ± 2	-	0 ± 1	3
XMMXCS J004720.8-251330.0	$0.367^{+0.079}_{-0.080}$	0.352 ± 0.063	-0.102 ± 0.088	3.580 ± 1.710	0.001	2 ± 2	2 ± 2	0 ± 0.1	-	3

Continued on next page

Table A.3 – continued from previous page

name	z_{RS}	z_{BCG}	cmr_{grad}	cmr_{inter}	cmr_{wid}	n_{gals-c}	n_{gals-l}	n_{200-c}	n_{200-l}	qual
XMMXCS J004727.6-251226.6	$0.357^{+0.078}_{-0.077}$	0.352 ± 0.063	-0.114 ± 0.085	3.860 ± 1.630	0.001	4 ± 2	5 ± 3	0 ± 1	-	3
XMMXCS J004742.6-251503.6	$0.356^{+0.177}_{-0.155}$	0.509 ± 0.107	-3.910 ± 5.100	81.000 ± 105	1.751	3 ± 2	2 ± 2	2 ± 2	2 ± 2	3
XMMXCS J004745.2-251208.7	$0.288^{+0.163}_{-0.128}$	0.378 ± 0.088	-1.930 ± 1.250	39.000 ± 25.20	0.371	1 ± 2	3 ± 2	0 ± 0.1	0 ± 1	3
XMMXCS J004752.2-251548.7	$0.490^{+0.124}_{-0.117}$	0.421 ± 0.052	0.283 ± 0.137	-4.950 ± 2.680	0.500	3 ± 2	6 ± 3	0 ± 0.1	-	3
XMMXCS J004831.3-252351.3	$0.201^{+0.088}_{-0.096}$	0.150 ± 0.022	-0.038 ± 0.122	1.940 ± 2.310	0.179	2 ± 2	2 ± 2	0 ± 0.1	0 ± 1	3
XMMXCS J005803.0-280855.7	$0.277^{+0.117}_{-0.107}$	0.270 ± 0.054	-0.111 ± 0.053	3.530 ± 1.000	0.001	2 ± 2	-	1 ± 1	-	3
XMMXCS J015157.7-134507.5	$0.268^{+0.153}_{-0.143}$	0.118 ± 0.049	0.384 ± 0.100	-6.240 ± 1.960	0.500	2 ± 3	-	2 ± 2	-	3
XMMXCS J015209.2-135023.5	$0.155^{+0.036}_{-0.037}$	0.180 ± 0.027	-0.082 ± 0.046	2.610 ± 0.844	0.001	0 ± 0.1	1 ± 1	-	0 ± 1	3
XMMXCS J015210.6-140820.7	$0.521^{+0.119}_{-0.114}$	0.535 ± 0.115	0.043 ± 0.021	-0.049 ± 0.382	0.001	0 ± 1	7 ± 3	-	8 ± 3	3
XMMXCS J015241.2-140206.2	$0.141^{+0.081}_{-0.098}$	0.111 ± 0.063	0.090 ± 0.003	-1.050 ± 0.053	0.500	0 ± 1	1 ± 2	-	0 ± 1	3
XMMXCS J015243.3-135052.1	$0.277^{+0.085}_{-0.083}$	0.292 ± 0.067	-0.062 ± 0.101	2.510 ± 1.900	0.001	2 ± 2	0 ± 1	0 ± 0.1	-	3
XMMXCS J015301.8-135028.8	$0.237^{+0.065}_{-0.064}$	0.231 ± 0.029	-0.034 ± 0.083	1.920 ± 1.560	0.079	1 ± 1	2 ± 2	-	1 ± 1	3
XMMXCS J015319.7-134759.5	$0.158^{+0.069}_{-0.071}$	0.206 ± 0.083	-0.190 ± 0.139	4.620 ± 2.620	0.500	0 ± 1	1 ± 2	-	1 ± 1	3
XMMXCS J021648.43-091832.2	$0.470^{+0.085}_{-0.070}$	0.418 ± 0.029	0.030 ± 0.065	-0.134 ± 1.260	0.136	0 ± 1	20 ± 5	-	63 ± 8	3
XMMXCS J022451.6-291528.6	$0.199^{+0.074}_{-0.073}$	0.194 ± 0.041	-0.032 ± 0.064	1.760 ± 1.230	0.082	0 ± 0.1	1 ± 2	-	0 ± 1	3
XMMXCS J022600.9-292558.7	$0.104^{+0.047}_{-0.048}$	0.110 ± 0.031	0.008 ± 0.033	0.731 ± 0.570	0.046	1 ± 1	1 ± 1	0 ± 0.1	0 ± 1	3
XMMXCS J022855.5-292717.0	$0.266^{+0.091}_{-0.088}$	0.157 ± 0.032	0.150 ± 0.093	-1.380 ± 1.720	0.107	0 ± 1	2 ± 2	-	2 ± 2	3
XMMXCS J022945.9-293750.5	$0.106^{+0.032}_{-0.034}$	0.165 ± 0.021	-0.516 ± 0.005	9.770 ± 0.085	0.500	1 ± 1	0 ± 1	0 ± 0.1	-	3
XMMXCS J023008.9-292456.5	$0.264^{+0.075}_{-0.074}$	0.276 ± 0.058	-0.121 ± 0.047	3.740 ± 0.897	0.001	1 ± 1	2 ± 2	-	0 ± 1	3

Continued on next page

Table A.3 – continued from previous page

name	z_{RS}	z_{BCG}	cmr_{grad}	cmr_{inter}	cmr_{wid}	n_{gals-c}	n_{gals-l}	n_{200-c}	n_{200-l}	qual
XMMXCS J024034.8-343626.3	$0.146^{+0.074}_{-0.074}$	0.186 ± 0.086	-0.066 ± 0.012	1.980 ± 0.198	0.048	0 ± 0.1	2 ± 2	-	0 ± 1	3
XMMXCS J024103.4-342923.4	$0.268^{+0.065}_{-0.050}$	0.237 ± 0.127	-0.296 ± 0.002	6.360 ± 0.036	0.500	2 ± 3	6 ± 3	1 ± 1	2 ± 2	3
XMMXCS J025035.0-311230.8	$0.404^{+0.108}_{-0.106}$	0.227 ± 0.078	0.008 ± 0.109	0.533 ± 2.120	0.155	3 ± 2	4 ± 3	1 ± 1	2 ± 2	3
XMMXCS J030057.6-111422.3	$0.273^{+0.098}_{-0.082}$	0.100 ± 0.038	-0.161 ± 0.073	4.290 ± 1.420	0.500	1 ± 3	10 ± 4	1 ± 1	11 ± 4	3
XMMXCS J033205.9-275447.4	$0.374^{+0.091}_{-0.084}$	0.196 ± 0.078	-0.186 ± 0.139	5.610 ± 2.750	0.500	4 ± 3	4 ± 3	1 ± 1	2 ± 2	3
XMMXCS J033206.6-274654.8	$0.233^{+0.073}_{-0.070}$	0.093 ± 0.029	-0.000 ± 0.001	0.858 ± 0.001	0.500	3 ± 2	-	2 ± 2	-	3
XMMXCS J033211.6-274240.7	$0.313^{+0.138}_{-0.093}$	0.173 ± 0.090	-0.017 ± 0.096	1.920 ± 1.830	0.500	3 ± 3	2 ± 3	3 ± 2	-	3
XMMXCS J033219.9-280224.9	$0.112^{+0.043}_{-0.043}$	0.112 ± 0.048	-0.079 ± 0.030	2.150 ± 0.546	0.082	1 ± 1	1 ± 2	0 ± 0.1	1 ± 1	3
XMMXCS J033224.0-274128.9	$0.100^{+0.041}_{-0.041}$	0.092 ± 0.031	0.316 ± 0.020	-4.800 ± 0.335	0.500	1 ± 1	1 ± 2	0 ± 0.1	0 ± 1	3
XMMXCS J033224.8-275840.3	$0.092^{+0.039}_{-0.039}$	0.112 ± 0.048	-0.088 ± 0.062	2.300 ± 1.070	0.099	2 ± 1	1 ± 1	1 ± 1	1 ± 1	3
XMMXCS J033227.6-273136.3	$0.126^{+0.050}_{-0.050}$	0.158 ± 0.024	-0.023 ± 0.031	1.370 ± 0.568	0.046	2 ± 2	3 ± 2	0 ± 0.1	1 ± 1	3
XMMXCS J033229.9-274049.9	$0.106^{+0.034}_{-0.034}$	0.109 ± 0.039	-0.026 ± 0.018	1.310 ± 0.304	0.060	0 ± 1	1 ± 1	-	0 ± 1	3
XMMXCS J033231.5-280316.5	$0.115^{+0.064}_{-0.064}$	0.109 ± 0.028	-0.051 ± 0.007	1.720 ± 0.142	0.001	0 ± 0.1	2 ± 2	-	0 ± 1	3
XMMXCS J033239.4-273507.3	$0.194^{+0.071}_{-0.083}$	0.161 ± 0.039	0.118 ± 0.028	-1.250 ± 0.513	0.001	0 ± 1	2 ± 2	-	0 ± 1	3
XMMXCS J033311.0-361732.3	$0.222^{+0.063}_{-0.063}$	0.090 ± 0.029	-0.081 ± 0.076	2.870 ± 1.510	0.500	0 ± 1	1 ± 2	-	2 ± 2	3
XMMXCS J033322.7-274601.5	$0.156^{+0.098}_{-0.098}$	0.139 ± 0.031	-0.093 ± 0.085	2.790 ± 1.640	0.095	1 ± 1	1 ± 2	0 ± 0.1	1 ± 1	3
XMMXCS J033334.6-274211.8	$0.149^{+0.037}_{-0.037}$	0.130 ± 0.061	0.058 ± 0.071	-0.049 ± 1.290	0.096	3 ± 2	3 ± 2	0 ± 0.1	0 ± 1	3
XMMXCS J033420.9-361827.0	$0.356^{+0.066}_{-0.066}$	0.348 ± 0.080	0.063 ± 0.086	0.460 ± 1.620	0.024	2 ± 2	1 ± 2	1 ± 1	-	3
XMMXCS J033422.8-361758.1	$0.356^{+0.066}_{-0.066}$	0.348 ± 0.080	0.063 ± 0.086	0.460 ± 1.620	0.024	2 ± 2	1 ± 2	2 ± 1	2 ± 2	3

Continued on next page

Table A.3 – continued from previous page

name	z_{RS}	z_{BCG}	cmr_{grad}	cmr_{inter}	cmr_{wid}	n_{gals-c}	n_{gals-l}	n_{200-c}	n_{200-l}	qual
XMMXCS J033704.8-350037.3	$0.177^{+0.071}_{-0.073}$	0.349 ± 0.150	0.327 ± 0.052	-5.300 ± 1.010	0.500	2 ± 2	2 ± 2	2 ± 1	0 ± 1	3
XMMXCS J033711.4-344306.8	$0.221^{+0.122}_{-0.118}$	0.220 ± 0.037	-0.148 ± 0.132	4.210 ± 2.570	0.001	0 ± 0.1	1 ± 1	-	0 ± 1	3
XMMXCS J033745.1-252245.5	$0.311^{+0.051}_{-0.053}$	0.416 ± 0.076	-0.288 ± 0.063	7.350 ± 1.240	0.001	0 ± 0.1	1 ± 2	-	1 ± 1	3
XMMXCS J033830.3-345254.2	$0.374^{+0.109}_{-0.117}$	0.343 ± 0.036	-0.053 ± 0.081	2.650 ± 1.540	0.001	3 ± 2	4 ± 3	0 ± 1	1 ± 2	3
XMMXCS J101508.4-042556.7	$0.225^{+0.072}_{-0.065}$	0.073 ± 0.026	0.148 ± 0.001	-1.600 ± 0.017	0.500	0 ± 2	1 ± 2	-	1 ± 1	3
XMMXCS J102711.1-031905.2	$0.078^{+0.102}_{-0.078}$	0.103 ± 0.033	-0.219 ± 0.032	4.570 ± 0.595	0.500	1 ± 1	-	0 ± 0.1	-	3
XMMXCS J103007.1-030642.6	$0.443^{+0.070}_{-0.067}$	0.431 ± 0.038	-0.112 ± 0.044	2.690 ± 0.865	0.107	4 ± 3	33 ± 6	3 ± 2	26 ± 6	3
XMMXCS J103013.3-030820.8	$0.095^{+0.037}_{-0.036}$	0.102 ± 0.032	-0.010 ± 0.004	0.861 ± 0.063	0.001	2 ± 2	2 ± 2	1 ± 1	1 ± 1	3
XMMXCS J103042.9-031033.6	$0.086^{+0.157}_{-0.086}$	0.098 ± 0.033	0.087 ± 0.021	-0.894 ± 0.407	0.001	1 ± 1	0 ± 1	0 ± 0.1	-	3
XMMXCS J103046.3-030653.3	$0.100^{+0.032}_{-0.033}$	0.097 ± 0.037	-0.007 ± 0.072	0.863 ± 1.210	0.500	3 ± 2	1 ± 2	1 ± 1	0 ± 1	3
XMMXCS J103114.6-030638.7	$0.353^{+0.080}_{-0.078}$	0.378 ± 0.099	0.171 ± 0.091	-1.870 ± 1.800	0.001	3 ± 2	4 ± 2	1 ± 1	0 ± 1	3
XMMXCS J103637.6-034348.2	$0.274^{+0.096}_{-0.087}$	0.129 ± 0.074	0.039 ± 0.050	-0.068 ± 0.971	0.001	1 ± 1	1 ± 2	1 ± 1	0 ± 1	3
XMMXCS J104446.5-071511.5	$0.164^{+0.103}_{-0.113}$	0.265 ± 0.161	-0.106 ± 0.043	2.780 ± 0.726	0.001	1 ± 1	1 ± 2	2 ± 1	2 ± 2	3
XMMXCS J105414.4-054409.5	$0.335^{+0.230}_{-0.139}$	0.463 ± 0.089	0.034 ± 0.045	0.764 ± 0.852	0.500	5 ± 3	6 ± 3	2 ± 2	4 ± 3	3
XMMXCS J105437.9-051042.8	$0.296^{+0.126}_{-0.128}$	0.146 ± 0.157	-0.000 ± 0.001	0.234 ± 0.001	0.500	2 ± 2	2 ± 2	1 ± 1	2 ± 2	3
XMMXCS J105528.2-050354.9	$0.186^{+0.043}_{-0.043}$	0.202 ± 0.029	-0.053 ± 0.079	2.090 ± 1.440	0.056	2 ± 2	1 ± 2	0 ± 0.1	0 ± 1	3
XMMXCS J105606.1-050708.9	$0.167^{+0.115}_{-0.115}$	0.214 ± 0.146	-0.108 ± 0.029	3.000 ± 0.575	0.046	1 ± 1	1 ± 1	0 ± 0.1	0 ± 1	3
XMMXCS J105713.2-034640.4	$0.276^{+0.114}_{-0.106}$	0.413 ± 0.152	-0.386 ± 0.117	9.210 ± 2.330	0.001	1 ± 1	1 ± 1	0 ± 0.1	0 ± 1	3
XMMXCS J112908.5-043106.4	$0.318^{+0.130}_{-0.223}$	0.172 ± 0.063	-0.150 ± 0.165	3.940 ± 3.250	0.001	1 ± 1	2 ± 2	0 ± 0.1	-	3

Continued on next page

Table A.3 – continued from previous page

name	z_{RS}	z_{BCG}	cmr_{grad}	cmr_{inter}	cmr_{wid}	n_{gals-c}	n_{gals-l}	n_{200-c}	n_{200-l}	qual
XMMXCS J113140.6-040915.7	$0.285^{+0.141}_{-0.126}$	0.104 ± 0.020	0.125 ± 0.112	-1.190 ± 2.180	0.500	4 ± 3	14 ± 5	2 ± 2	3 ± 3	3
XMMXCS J120602.4-084751.2	$0.423^{+0.097}_{-0.092}$	0.352 ± 0.087	0.131 ± 0.063	-1.980 ± 1.210	0.001	5 ± 3	-	0 ± 1	-	3
XMMXCS J120637.7-085014.0	$0.411^{+0.094}_{-0.090}$	0.414 ± 0.062	-0.230 ± 0.097	5.100 ± 1.930	0.069	1 ± 2	4 ± 2	-	1 ± 1	3
XMMXCS J124900.1-060159.7	$0.115^{+0.032}_{-0.032}$	0.098 ± 0.039	0.044 ± 0.092	0.023 ± 1.600	0.072	1 ± 1	1 ± 1	1 ± 1	1 ± 1	3
XMMXCS J124901.8-060004.5	$0.130^{+0.065}_{-0.070}$	0.117 ± 0.036	-0.000 ± 0.001	0.374 ± 0.001	0.500	1 ± 1	0 ± 1	0 ± 0.1	-	3
XMMXCS J124919.3-054540.2	$0.138^{+0.094}_{-0.099}$	0.129 ± 0.048	0.124 ± 0.045	-1.280 ± 0.857	0.078	1 ± 1	0 ± 1	0 ± 0.1	-	3
XMMXCS J125945.1-042555.2	$0.407^{+0.091}_{-0.085}$	0.320 ± 0.056	0.025 ± 0.001	0.980 ± 0.004	0.500	5 ± 3	6 ± 4	3 ± 2	2 ± 2	3
XMMXCS J145100.2-151709.9	$0.365^{+0.123}_{-0.109}$	0.223 ± 0.138	-0.748 ± 0.007	15.200 ± 0.137	0.500	1 ± 2	15 ± 4	1 ± 1	13 ± 4	3
XMMXCS J145153.3-152133.2	$0.162^{+0.087}_{-0.088}$	0.109 ± 0.025	0.012 ± 0.043	0.816 ± 0.796	0.111	1 ± 1	3 ± 2	0 ± 0.1	1 ± 1	3
XMMXCS J145200.6-151957.0	$0.217^{+0.094}_{-0.094}$	0.109 ± 0.025	0.146 ± 0.041	-1.560 ± 0.769	0.001	2 ± 2	4 ± 2	2 ± 1	3 ± 2	3
XMMXCS J150415.6-030210.0	$0.420^{+0.111}_{-0.113}$	0.268 ± 0.074	0.077 ± 0.073	0.165 ± 1.410	0.082	2 ± 2	3 ± 3	1 ± 1	10 ± 3	3
XMMXCS J150416.5-024033.0	$0.305^{+0.066}_{-0.066}$	0.313 ± 0.059	-0.208 ± 0.259	5.660 ± 5.070	0.101	2 ± 2	0 ± 1	2 ± 1	-	3
XMMXCS J150422.8-023913.2	$0.239^{+0.068}_{-0.070}$	0.290 ± 0.052	-0.110 ± 0.072	3.490 ± 1.340	0.001	2 ± 2	1 ± 2	0 ± 0.1	0 ± 1	3
XMMXCS J214913.3-302855.0	$0.478^{+0.201}_{-0.197}$	0.446 ± 0.206	-0.086 ± 0.117	2.780 ± 2.310	0.103	2 ± 2	3 ± 2	-	0 ± 1	3
XMMXCS J215842.6-301407.5	$0.121^{+0.075}_{-0.077}$	0.089 ± 0.035	0.036 ± 0.039	0.196 ± 0.701	0.109	2 ± 2	1 ± 2	0 ± 0.1	0 ± 1	3
XMMXCS J215844.8-301338.9	$0.120^{+0.095}_{-0.095}$	0.183 ± 0.129	-0.022 ± 0.025	1.020 ± 0.442	0.035	2 ± 1	1 ± 1	0 ± 0.1	1 ± 1	3
XMMXCS J215845.2-301312.1	$0.122^{+0.098}_{-0.098}$	0.183 ± 0.129	-0.013 ± 0.025	0.859 ± 0.438	0.036	2 ± 1	1 ± 1	0 ± 0.1	1 ± 1	3
XMMXCS J215845.5-301414.7	$0.120^{+0.107}_{-0.107}$	0.183 ± 0.129	-0.041 ± 0.032	1.350 ± 0.580	0.040	2 ± 1	1 ± 1	0 ± 0.1	1 ± 1	3
XMMXCS J215850.6-302452.6	$0.282^{+0.140}_{-0.138}$	0.394 ± 0.196	0.027 ± 0.002	0.642 ± 0.041	0.500	5 ± 3	6 ± 4	4 ± 2	6 ± 3	3

Continued on next page

Table A.3 – continued from previous page

name	z_{RS}	z_{BCG}	cmr_{grad}	cmr_{inter}	cmr_{wid}	n_{gals-c}	n_{gals-l}	n_{200-c}	n_{200-l}	qual
XMMXCS J215858.7-301449.7	$0.116^{+0.094}_{-0.094}$	0.089 ± 0.035	0.011 ± 0.026	0.495 ± 0.481	0.083	1 ± 1	2 ± 2	0 ± 0.1	2 ± 2	3
XMMXCS J221716.8-355159.1	$0.147^{+0.075}_{-0.117}$	0.114 ± 0.039	-0.011 ± 0.157	0.878 ± 2.750	0.089	1 ± 1	1 ± 1	0 ± 0.1	0 ± 1	3
XMMXCS J221829.5-355237.0	$0.125^{+0.034}_{-0.035}$	0.137 ± 0.027	-0.032 ± 0.097	1.440 ± 1.720	0.119	1 ± 1	0 ± 1	0 ± 0.1	-	3
XMMXCS J223357.4-373221.8	$0.239^{+0.075}_{-0.073}$	0.145 ± 0.054	0.333 ± 0.088	-4.950 ± 1.630	0.024	4 ± 2	0 ± 1	0 ± 0.1	-	3
XMMXCS J223407.2-373359.2	$0.141^{+0.055}_{-0.059}$	0.168 ± 0.070	0.050 ± 0.108	0.110 ± 1.850	0.090	6 ± 3	5 ± 3	5 ± 2	4 ± 2	3
XMMXCS J223421.3-260050.1	$0.490^{+0.086}_{-0.083}$	0.401 ± 0.158	0.292 ± 0.089	-4.960 ± 1.790	0.065	3 ± 2	5 ± 3	0 ± 0.1	0 ± 1	3
XMMXCS J223544.8-261100.3	$0.118^{+0.055}_{-0.056}$	0.116 ± 0.038	0.106 ± 0.066	-1.060 ± 1.160	0.092	1 ± 1	0 ± 1	1 ± 1	-	3
XMMXCS J223559.0-260120.1	$0.249^{+0.115}_{-0.164}$	0.115 ± 0.042	0.041 ± 0.084	-0.061 ± 1.590	0.071	3 ± 2	3 ± 2	0 ± 0.1	0 ± 1	3
XMMXCS J223612.4-255703.3	$0.436^{+0.098}_{-0.092}$	0.450 ± 0.066	-0.061 ± 0.115	2.680 ± 2.190	0.070	2 ± 2	18 ± 5	-	16 ± 5	3
XMMXCS J225657.2-365724.1	$0.306^{+0.050}_{-0.031}$	0.245 ± 0.195	0.099 ± 0.001	-1.030 ± 0.002	0.500	4 ± 3	6 ± 3	1 ± 1	1 ± 1	3
XMMXCS J225752.8-363537.8	$0.273^{+0.133}_{-0.113}$	0.393 ± 0.100	-0.289 ± 0.098	7.510 ± 2.020	0.001	1 ± 1	2 ± 2	-	0 ± 1	3
XMMXCS J232445.3-115958.3	$0.097^{+0.046}_{-0.045}$	0.093 ± 0.043	0.032 ± 0.015	0.210 ± 0.237	0.001	0 ± 1	1 ± 1	-	1 ± 1	3
XMMXCS J232506.5-121051.5	$0.097^{+0.034}_{-0.034}$	0.109 ± 0.030	-0.078 ± 0.008	2.210 ± 0.137	0.001	3 ± 2	4 ± 2	0 ± 0.1	0 ± 1	3
XMMXCS J232507.0-120823.1	$0.102^{+0.031}_{-0.032}$	0.116 ± 0.035	-0.059 ± 0.009	1.890 ± 0.148	0.001	5 ± 2	7 ± 3	3 ± 2	4 ± 2	3
XMMXCS J232512.0-120839.5	$0.102^{+0.037}_{-0.037}$	0.116 ± 0.035	-0.073 ± 0.011	2.120 ± 0.187	0.009	6 ± 3	7 ± 3	3 ± 2	5 ± 2	3
XMMXCS J232513.6-121056.6	$0.102^{+0.045}_{-0.045}$	0.122 ± 0.046	-0.048 ± 0.022	1.670 ± 0.386	0.001	1 ± 1	3 ± 2	0 ± 0.1	0 ± 1	3
XMMXCS J232514.5-121018.0	$0.103^{+0.037}_{-0.037}$	0.116 ± 0.035	-0.048 ± 0.011	1.690 ± 0.191	0.001	4 ± 2	7 ± 3	0 ± 0.1	5 ± 2	3
XMMXCS J232515.5-121213.7	$0.094^{+0.045}_{-0.045}$	0.109 ± 0.081	0.131 ± 0.032	-1.480 ± 0.563	0.071	2 ± 2	3 ± 2	0 ± 0.1	1 ± 1	3
XMMXCS J232519.6-120727.0	$0.107^{+0.039}_{-0.039}$	0.116 ± 0.035	-0.071 ± 0.011	2.090 ± 0.198	0.008	8 ± 3	8 ± 3	9 ± 3	9 ± 3	3

Continued on next page

Table A.3 – continued from previous page

name	z_{RS}	z_{BCG}	cmr_{grad}	cmr_{inter}	cmr_{wid}	n_{gals-c}	n_{gals-l}	n_{200-c}	n_{200-l}	qual
XMMXCS J232527.4-121128.5	$0.098^{+0.036}_{-0.036}$	0.122 ± 0.046	-0.057 ± 0.016	1.840 ± 0.281	0.001	2 ± 1	2 ± 2	1 ± 1	1 ± 1	3
XMMXCS J233216.1-362336.4	$0.134^{+0.038}_{-0.038}$	0.149 ± 0.027	-0.147 ± 0.077	3.290 ± 1.380	0.500	1 ± 2	0 ± 2	0 ± 0.1	-	3
XMMXCS J233947.1-120644.7	$0.197^{+0.086}_{-0.087}$	0.115 ± 0.027	0.269 ± 0.169	-4.080 ± 3.340	0.139	1 ± 1	3 ± 2	0 ± 0.1	0 ± 1	3
XMMXCS J234014.3-115442.6	$0.127^{+0.036}_{-0.036}$	0.118 ± 0.054	0.147 ± 0.075	-1.700 ± 1.310	0.500	1 ± 1	1 ± 2	0 ± 0.1	1 ± 1	3
XMMXCS J234039.9-112718.6	$0.146^{+0.039}_{-0.039}$	0.095 ± 0.031	0.091 ± 0.125	-0.657 ± 2.370	0.137	1 ± 1	2 ± 2	0 ± 0.1	0 ± 1	3
XMMXCS J234040.1-112822.7	$0.150^{+0.030}_{-0.031}$	0.095 ± 0.031	0.104 ± 0.055	-0.846 ± 1.000	0.064	1 ± 1	1 ± 2	0 ± 0.1	0 ± 1	3
XMMXCS J235205.1-261517.5	$0.274^{+0.115}_{-0.111}$	0.244 ± 0.137	0.087 ± 0.030	-0.630 ± 0.595	0.084	0 ± 1	1 ± 2	-	0 ± 1	3
XMMXCS J235227.0-260250.9	$0.188^{+0.107}_{-0.114}$	0.149 ± 0.035	-0.000 ± 0.042	1.050 ± 0.741	0.001	2 ± 2	1 ± 2	0 ± 0.1	0 ± 1	3
XMMXCS J235939.6-320001.3	$0.295^{+0.070}_{-0.071}$	0.288 ± 0.022	0.097 ± 0.084	-0.322 ± 1.630	0.001	5 ± 2	0 ± 1	2 ± 1	-	3

Table A.4 *A table of GMPhoRCC characterisations for the preliminary XCS DR2 sources using CFHTLenS optical data. Of the* 1104 *with coverage, characterisations were found for* 702 *with* 237 *in the clean subset.*

name	z_{RS}	z_{BCG}	cmr_{grad}	cmr_{inter}	cmr_{wid}	n_{gals-c}	n_{gals-l}	n_{200-c}	n_{200-l}	qual
XMMXCS J020046.49-064223.1	$0.363^{+0.089}_{-0.090}$	0.327 ± 0.089	-0.036 ± 0.012	2.040 ± 0.224	0.038	8 ± 3	8 ± 3	8 ± 3	7 ± 3	1
XMMXCS J020049.61-064026.8	$0.360^{+0.088}_{-0.089}$	0.327 ± 0.089	-0.024 ± 0.018	1.780 ± 0.357	0.074	9 ± 3	36 ± 6	6 ± 3	9 ± 4	1
XMMXCS J020213.89-070113.1	$0.114^{+0.063}_{-0.064}$	0.093 ± 0.060	0.004 ± 0.027	0.518 ± 0.472	0.088	7 ± 3	1 ± 1	3 ± 2	0 ± 1	1
XMMXCS J020230.52-063119.7	$0.339^{+0.088}_{-0.088}$	0.327 ± 0.089	-0.022 ± 0.024	1.640 ± 0.463	0.091	15 ± 4	13 ± 4	15 ± 4	12 ± 4	1
XMMXCS J020254.37-073858.3	$0.151^{+0.077}_{-0.077}$	0.141 ± 0.077	-0.079 ± 0.018	2.050 ± 0.322	0.061	9 ± 3	10 ± 3	7 ± 3	8 ± 3	1
XMMXCS J020255.3-073906.6	$0.136^{+0.076}_{-0.076}$	0.141 ± 0.077	-0.045 ± 0.017	1.510 ± 0.279	0.025	5 ± 2	5 ± 2	4 ± 2	5 ± 2	1
XMMXCS J020328.76-045740.6	$0.477^{+0.094}_{-0.096}$	0.445 ± 0.095	-0.017 ± 0.016	0.792 ± 0.337	0.079	8 ± 4	7 ± 4	6 ± 3	3 ± 3	1
XMMXCS J020341.31-074708.4	$0.470^{+0.097}_{-0.097}$	0.448 ± 0.097	-0.018 ± 0.011	1.140 ± 0.232	0.068	20 ± 5	21 ± 5	24 ± 6	27 ± 6	1
XMMXCS J020341.6-074705.7	$0.462^{+0.096}_{-0.096}$	0.448 ± 0.097	-0.011 ± 0.012	0.985 ± 0.255	0.075	23 ± 5	26 ± 6	27 ± 6	32 ± 7	1
XMMXCS J020353.36-050145.3	$0.534^{+0.095}_{-0.098}$	0.507 ± 0.100	-0.026 ± 0.015	1.440 ± 0.309	0.087	23 ± 5	20 ± 5	24 ± 6	23 ± 5	1
XMMXCS J020359.34-042030.9	$0.678^{+0.106}_{-0.108}$	0.632 ± 0.107	-0.003 ± 0.019	1.300 ± 0.428	0.116	8 ± 4	8 ± 4	4 ± 3	5 ± 3	1
XMMXCS J020435.89-061921.4	$0.953^{+0.127}_{-0.127}$	1.000 ± 0.132	-0.033 ± 0.030	1.270 ± 0.706	0.114	6 ± 5	9 ± 6	10 ± 4	11 ± 5	1
XMMXCS J020449.1-072538.2	$0.337^{+0.088}_{-0.088}$	0.288 ± 0.086	-0.076 ± 0.020	2.670 ± 0.368	0.101	11 ± 4	9 ± 4	11 ± 4	7 ± 3	1
XMMXCS J020509.70-061445.9	$0.271^{+0.095}_{-0.097}$	0.276 ± 0.110	-0.062 ± 0.026	1.860 ± 0.497	0.031	7 ± 3	5 ± 3	6 ± 3	5 ± 2	1
XMMXCS J020517.70-043900.7	$0.944^{+0.128}_{-0.128}$	0.896 ± 0.123	0.009 ± 0.021	0.625 ± 0.482	0.074	34 ± 6	33 ± 6	46 ± 8	46 ± 8	1
XMMXCS J020559.64-063736.5	$0.653^{+0.107}_{-0.108}$	0.623 ± 0.130	-0.012 ± 0.013	0.541 ± 0.288	0.072	13 ± 5	9 ± 5	14 ± 5	8 ± 5	1
XMMXCS J020613.35-041616.7	$0.504^{+0.098}_{-0.098}$	0.511 ± 0.099	-0.061 ± 0.050	1.970 ± 1.040	0.067	4 ± 3	5 ± 3	4 ± 2	5 ± 3	1
XMMXCS J020636.17-061133.8	$0.920^{+0.138}_{-0.137}$	0.948 ± 0.135	-0.002 ± 0.030	0.526 ± 0.679	0.110	16 ± 6	15 ± 6	13 ± 7	15 ± 7	1

Continued on next page

Table A.4 – continued from previous page

name	z_{RS}	z_{BCG}	cmr_{grad}	cmr_{inter}	cmr_{wid}	n_{gals-c}	n_{gals-l}	n_{200-c}	n_{200-l}	qual
XMMXCS J020644.78-065810.1	$0.432^{+0.093}_{-0.094}$	0.399 ± 0.093	-0.009 ± 0.013	1.610 ± 0.267	0.081	26 ± 5	26 ± 5	27 ± 6	30 ± 6	1
XMMXCS J020647.58-065651.0	$0.442^{+0.095}_{-0.095}$	0.399 ± 0.093	0.001 ± 0.005	0.676 ± 0.110	0.041	30 ± 6	30 ± 6	30 ± 6	31 ± 6	1
XMMXCS J020647.93-065727.1	$0.439^{+0.094}_{-0.095}$	0.399 ± 0.093	0.007 ± 0.008	0.568 ± 0.177	0.058	31 ± 6	32 ± 6	29 ± 6	32 ± 7	1
XMMXCS J020849.11-050444.0	$0.745^{+0.114}_{-0.113}$	0.748 ± 0.114	-0.029 ± 0.007	0.853 ± 0.167	0.087	9 ± 5	10 ± 5	8 ± 4	1 ± 4	1
XMMXCS J020852.23-063404.0	$0.705^{+0.114}_{-0.114}$	0.666 ± 0.109	-0.041 ± 0.007	1.170 ± 0.164	0.099	19 ± 6	19 ± 6	28 ± 7	27 ± 8	1
XMMXCS J020900.13-060904.2	$0.333^{+0.092}_{-0.092}$	0.350 ± 0.090	-0.073 ± 0.059	2.370 ± 1.080	0.500	15 ± 5	16 ± 5	14 ± 5	15 ± 5	1
XMMXCS J020911.25-062043.8	$0.486^{+0.097}_{-0.097}$	0.448 ± 0.096	0.032 ± 0.029	0.137 ± 0.600	0.096	16 ± 5	17 ± 5	19 ± 5	20 ± 5	1
XMMXCS J020923.50-055354.0	$0.736^{+0.112}_{-0.113}$	0.695 ± 0.112	-0.011 ± 0.014	0.642 ± 0.308	0.088	16 ± 5	17 ± 6	16 ± 6	16 ± 6	1
XMMXCS J020928.23-063118.7	$0.661^{+0.151}_{-0.147}$	0.692 ± 0.111	-0.031 ± 0.021	0.956 ± 0.454	0.091	8 ± 5	11 ± 5	8 ± 4	11 ± 5	1
XMMXCS J020951.69-060658.7	$0.290^{+0.084}_{-0.085}$	0.278 ± 0.086	-0.063 ± 0.018	2.400 ± 0.353	0.090	11 ± 4	9 ± 3	10 ± 3	9 ± 3	1
XMMXCS J020957.96-051751.2	$0.784^{+0.131}_{-0.131}$	0.821 ± 0.119	-0.036 ± 0.016	1.160 ± 0.362	0.105	20 ± 6	15 ± 6	27 ± 8	23 ± 7	1
XMMXCS J021027.64-042232.7	$0.904^{+0.125}_{-0.125}$	0.871 ± 0.123	-0.036 ± 0.045	1.310 ± 1.040	0.098	4 ± 4	4 ± 5	5 ± 3	6 ± 3	1
XMMXCS J021051.87-061020.2	$0.431^{+0.093}_{-0.093}$	0.472 ± 0.098	-0.021 ± 0.011	1.080 ± 0.225	0.058	20 ± 5	18 ± 5	30 ± 6	24 ± 6	1
XMMXCS J021053.4-063329.7	$0.076^{+0.053}_{-0.054}$	0.054 ± 0.040	-0.014 ± 0.004	0.853 ± 0.062	0.009	4 ± 2	0 ± 1	4 ± 2	-	1
XMMXCS J021057.28-061153.5	$0.429^{+0.093}_{-0.094}$	0.472 ± 0.098	-0.028 ± 0.015	1.250 ± 0.320	0.067	34 ± 6	29 ± 6	63 ± 9	50 ± 8	1
XMMXCS J021102.87-045402.1	$0.164^{+0.078}_{-0.078}$	0.161 ± 0.078	-0.048 ± 0.022	1.690 ± 0.377	0.050	8 ± 3	8 ± 3	7 ± 3	7 ± 3	1
XMMXCS J021104.15-045323.3	$0.167^{+0.078}_{-0.078}$	0.161 ± 0.078	-0.050 ± 0.022	1.730 ± 0.379	0.050	8 ± 3	8 ± 3	6 ± 3	7 ± 3	1
XMMXCS J021109.46-042045.0	$0.412^{+0.088}_{-0.085}$	0.420 ± 0.095	-0.012 ± 0.034	0.602 ± 0.703	0.067	2 ± 2	1 ± 2	3 ± 2	1 ± 1	1
XMMXCS J021114.47-060950.8	$0.430^{+0.093}_{-0.094}$	0.446 ± 0.096	-0.003 ± 0.013	1.530 ± 0.248	0.067	13 ± 4	11 ± 4	13 ± 4	10 ± 4	1

Continued on next page

Table A.4 – continued from previous page

name	z_{RS}	z_{BCG}	cmr_{grad}	cmr_{inter}	cmr_{wid}	n_{gals-c}	n_{gals-l}	n_{200-c}	n_{200-l}	qual
XMMXCS J021128.86-061131.5	$0.414^{+0.089}_{-0.092}$	0.415 ± 0.095	-0.013 ± 0.006	0.955 ± 0.118	0.043	8 ± 3	9 ± 4	8 ± 3	8 ± 3	1
XMMXCS J021225.59-053752.0	$0.318^{+0.086}_{-0.086}$	0.278 ± 0.086	-0.006 ± 0.011	1.390 ± 0.223	0.056	33 ± 6	29 ± 6	49 ± 7	43 ± 7	1
XMMXCS J021227.66-060430.5	$0.719^{+0.111}_{-0.112}$	0.757 ± 0.116	0.005 ± 0.044	0.887 ± 0.985	0.119	4 ± 3	4 ± 3	4 ± 2	3 ± 2	1
XMMXCS J021231.24-044927.0	$0.206^{+0.080}_{-0.080}$	0.229 ± 0.083	-0.053 ± 0.018	1.910 ± 0.327	0.067	8 ± 3	8 ± 3	5 ± 2	5 ± 2	1
XMMXCS J021239.63-041622.5	$0.239^{+0.082}_{-0.083}$	0.190 ± 0.080	0.051 ± 0.017	0.112 ± 0.300	0.042	6 ± 3	6 ± 3	4 ± 2	2 ± 2	1
XMMXCS J021250.50-043601.7	$0.178^{+0.078}_{-0.078}$	0.161 ± 0.078	-0.031 ± 0.010	1.420 ± 0.171	0.053	6 ± 3	5 ± 3	5 ± 2	5 ± 2	1
XMMXCS J021321.74-060550.1	$0.676^{+0.110}_{-0.110}$	0.655 ± 0.109	-0.028 ± 0.015	1.870 ± 0.329	0.088	38 ± 6	43 ± 7	50 ± 8	54 ± 8	1
XMMXCS J021323.6-041308.7	$0.603^{+0.094}_{-0.100}$	0.565 ± 0.102	-0.050 ± 0.038	2.090 ± 0.825	0.118	6 ± 3	5 ± 3	5 ± 3	3 ± 2	1
XMMXCS J021407.78-053508.0	$0.455^{+0.095}_{-0.096}$	0.494 ± 0.100	-0.013 ± 0.009	0.974 ± 0.186	0.066	27 ± 5	26 ± 6	33 ± 6	31 ± 6	1
XMMXCS J021427.64-062733.8	$0.249^{+0.081}_{-0.082}$	0.262 ± 0.085	-0.046 ± 0.010	1.970 ± 0.189	0.058	21 ± 5	20 ± 5	25 ± 5	24 ± 5	1
XMMXCS J021440.9-043321.9	$0.154^{+0.074}_{-0.076}$	0.171 ± 0.079	-0.016 ± 0.014	1.100 ± 0.259	0.062	11 ± 3	11 ± 3	11 ± 3	11 ± 3	1
XMMXCS J021441.91-061635.9	$0.257^{+0.083}_{-0.083}$	0.229 ± 0.083	-0.040 ± 0.019	1.800 ± 0.358	0.065	9 ± 3	8 ± 3	7 ± 3	6 ± 3	1
XMMXCS J021442.21-043315.3	$0.163^{+0.075}_{-0.077}$	0.171 ± 0.079	-0.061 ± 0.030	1.900 ± 0.526	0.067	12 ± 4	14 ± 4	12 ± 4	15 ± 4	1
XMMXCS J021443.40-053458.5	$0.779^{+0.118}_{-0.119}$	0.766 ± 0.116	-0.019 ± 0.013	0.798 ± 0.301	0.113	18 ± 6	15 ± 6	19 ± 7	16 ± 6	1
XMMXCS J021443.47-034921.2	$0.728^{+0.113}_{-0.113}$	0.678 ± 0.111	-0.005 ± 0.014	1.400 ± 0.310	0.083	22 ± 5	22 ± 5	24 ± 6	24 ± 6	1
XMMXCS J021452.68-042331.7	$0.663^{+0.107}_{-0.106}$	0.680 ± 0.111	-0.003 ± 0.010	0.444 ± 0.224	0.053	7 ± 4	9 ± 4	5 ± 3	8 ± 4	1
XMMXCS J021453.41-042842.4	$0.605^{+0.103}_{-0.104}$	0.589 ± 0.104	-0.017 ± 0.020	1.020 ± 0.432	0.092	7 ± 4	6 ± 4	5 ± 3	4 ± 3	1
XMMXCS J021500.32-035429.3	$0.196^{+0.080}_{-0.080}$	0.161 ± 0.078	-0.022 ± 0.013	1.240 ± 0.241	0.036	6 ± 3	10 ± 3	6 ± 3	10 ± 3	1
XMMXCS J021502.6-042309.8	$0.213^{+0.080}_{-0.081}$	0.200 ± 0.081	-0.036 ± 0.025	1.650 ± 0.445	0.055	3 ± 2	3 ± 2	3 ± 2	2 ± 2	1

Continued on next page

Table A.4 – continued from previous page

name	z_{RS}	z_{BCG}	cmr_{grad}	cmr_{inter}	cmr_{wid}	n_{gals-c}	n_{gals-l}	n_{200-c}	n_{200-l}	qual
XMMXCS J021504.69-055830.0	$0.270^{+0.084}_{-0.084}$	0.249 ± 0.084	-0.026 ± 0.013	1.630 ± 0.249	0.062	17 ± 4	18 ± 5	21 ± 5	23 ± 5	1
XMMXCS J021516.76-062236.1	$0.707^{+0.115}_{-0.115}$	0.678 ± 0.110	0.009 ± 0.035	-0.051 ± 0.787	0.107	9 ± 5	9 ± 5	5 ± 4	5 ± 4	1
XMMXCS J021528.91-044052.8	$0.352^{+0.089}_{-0.089}$	0.366 ± 0.092	-0.017 ± 0.011	1.660 ± 0.218	0.063	23 ± 5	23 ± 5	32 ± 6	33 ± 6	1
XMMXCS J021537.71-055853.4	$0.306^{+0.085}_{-0.086}$	0.278 ± 0.086	0.030 ± 0.007	0.654 ± 0.140	0.026	9 ± 3	9 ± 3	6 ± 3	7 ± 3	1
XMMXCS J021538.17-055857.9	$0.306^{+0.085}_{-0.086}$	0.278 ± 0.086	0.030 ± 0.007	0.654 ± 0.140	0.026	9 ± 3	9 ± 3	5 ± 2	4 ± 2	1
XMMXCS J021606.40-093517.1	$0.571^{+0.103}_{-0.103}$	0.559 ± 0.103	-0.017 ± 0.009	1.400 ± 0.189	0.070	36 ± 6	35 ± 6	54 ± 8	56 ± 8	1
XMMXCS J021611.69-041422.8	$0.199^{+0.079}_{-0.079}$	0.180 ± 0.080	0.002 ± 0.024	0.852 ± 0.445	0.048	7 ± 3	5 ± 3	7 ± 3	7 ± 3	1
XMMXCS J021611.6-041422.8	$0.199^{+0.079}_{-0.079}$	0.180 ± 0.080	0.002 ± 0.024	0.852 ± 0.445	0.048	7 ± 3	5 ± 3	7 ± 3	7 ± 3	1
XMMXCS J021619.99-060539.6	$0.397^{+0.090}_{-0.088}$	0.436 ± 0.095	-0.143 ± 0.077	3.760 ± 1.510	0.098	3 ± 3	4 ± 3	5 ± 2	6 ± 3	1
XMMXCS J021619.9-060539.5	$0.397^{+0.090}_{-0.088}$	0.436 ± 0.095	-0.143 ± 0.077	3.760 ± 1.510	0.098	3 ± 3	4 ± 3	5 ± 2	6 ± 3	1
XMMXCS J021633.52-043319.3	$0.359^{+0.089}_{-0.089}$	0.392 ± 0.092	-0.010 ± 0.021	1.510 ± 0.404	0.028	7 ± 3	4 ± 2	6 ± 3	4 ± 2	1
XMMXCS J021633.7-043328.0	$0.359^{+0.089}_{-0.089}$	0.392 ± 0.092	-0.010 ± 0.021	1.510 ± 0.404	0.028	7 ± 3	4 ± 2	6 ± 3	3 ± 2	1
XMMXCS J021640.9-041843.3	$0.524^{+0.098}_{-0.100}$	0.501 ± 0.099	-0.036 ± 0.018	1.560 ± 0.390	0.050	7 ± 3	7 ± 3	6 ± 3	6 ± 3	1
XMMXCS J021640.94-041842.4	$0.179^{+0.076}_{-0.078}$	0.161 ± 0.078	-0.004 ± 0.018	0.955 ± 0.313	0.080	11 ± 4	12 ± 4	11 ± 4	12 ± 4	1
XMMXCS J021653.14-041725.5	$0.203^{+0.080}_{-0.080}$	0.161 ± 0.078	-0.013 ± 0.007	1.130 ± 0.123	0.040	7 ± 3	8 ± 3	3 ± 2	6 ± 3	1
XMMXCS J021704.4-041434.1	$0.202^{+0.080}_{-0.080}$	0.190 ± 0.080	-0.062 ± 0.025	1.830 ± 0.477	0.101	6 ± 3	8 ± 3	3 ± 2	4 ± 2	1
XMMXCS J021709.8-053441.4	$0.646^{+0.106}_{-0.107}$	0.605 ± 0.106	-0.056 ± 0.042	2.190 ± 0.927	0.129	9 ± 4	8 ± 4	7 ± 3	7 ± 4	1
XMMXCS J021735.1-051306.5	$0.639^{+0.107}_{-0.107}$	0.625 ± 0.106	-0.003 ± 0.020	1.200 ± 0.430	0.068	22 ± 5	26 ± 5	31 ± 6	31 ± 6	1
XMMXCS J021736.4-045925.7	$0.468^{+0.094}_{-0.093}$	0.422 ± 0.094	-0.032 ± 0.038	1.260 ± 0.770	0.095	16 ± 5	13 ± 4	16 ± 5	13 ± 5	1

Continued on next page

Table A.4 – continued from previous page

name	z_{RS}	z_{BCG}	cmr_{grad}	cmr_{inter}	cmr_{wid}	n_{gals-c}	n_{gals-l}	n_{200-c}	n_{200-l}	qual
XMMXCS J021738.69-055817.4	$0.797^{+0.119}_{-0.120}$	0.763 ± 0.116	-0.018 ± 0.013	0.692 ± 0.289	0.091	7 ± 5	8 ± 5	4 ± 4	5 ± 4	1
XMMXCS J021739.38-034827.7	$0.314^{+0.086}_{-0.086}$	0.307 ± 0.088	-0.065 ± 0.018	2.440 ± 0.343	0.099	13 ± 4	13 ± 4	13 ± 4	14 ± 4	1
XMMXCS J021755.16-052654.2	$0.690^{+0.110}_{-0.109}$	0.678 ± 0.111	0.007 ± 0.012	0.311 ± 0.267	0.067	15 ± 5	41 ± 7	17 ± 5	18 ± 7	1
XMMXCS J021755.3-052655.2	$0.683^{+0.109}_{-0.110}$	0.729 ± 0.113	0.025 ± 0.029	0.685 ± 0.632	0.108	18 ± 5	34 ± 6	17 ± 5	19 ± 6	1
XMMXCS J021805.8-050327.0	$0.973^{+0.128}_{-0.129}$	0.926 ± 0.129	-0.125 ± 0.044	3.530 ± 1.020	0.117	15 ± 6	-	19 ± 6	-	1
XMMXCS J021807.88-054557.3	$0.660^{+0.105}_{-0.107}$	0.619 ± 0.106	-0.011 ± 0.015	1.440 ± 0.327	0.086	13 ± 4	13 ± 4	13 ± 4	14 ± 4	1
XMMXCS J021837.40-060451.1	$0.903^{+0.125}_{-0.122}$	0.902 ± 0.126	0.040 ± 0.024	-0.604 ± 0.554	0.093	14 ± 6	12 ± 6	19 ± 6	12 ± 6	1
XMMXCS J021842.9-050439.0	$0.556^{+0.095}_{-0.099}$	0.547 ± 0.102	-0.066 ± 0.012	2.180 ± 0.236	0.069	10 ± 4	11 ± 4	9 ± 3	11 ± 4	1
XMMXCS J021907.4-035745.7	$1.047^{+0.157}_{-0.162}$	1.040 ± 0.140	-0.036 ± 0.035	1.410 ± 0.820	0.100	6 ± 5	6 ± 5	8 ± 4	8 ± 4	1
XMMXCS J021911.32-034416.1	$0.750^{+0.114}_{-0.115}$	0.747 ± 0.115	0.022 ± 0.017	-0.010 ± 0.371	0.092	28 ± 6	28 ± 6	26 ± 8	22 ± 8	1
XMMXCS J021911.3-034416.0	$0.752^{+0.115}_{-0.115}$	0.747 ± 0.115	0.023 ± 0.017	-0.022 ± 0.371	0.092	28 ± 6	30 ± 7	28 ± 8	25 ± 8	1
XMMXCS J021938.4-040024.2	$0.634^{+0.104}_{-0.106}$	0.655 ± 0.108	0.106 ± 0.020	-1.150 ± 0.429	0.070	4 ± 3	5 ± 3	4 ± 2	5 ± 3	1
XMMXCS J021940.78-055043.7	$0.661^{+0.108}_{-0.109}$	0.661 ± 0.109	-0.017 ± 0.018	0.642 ± 0.414	0.089	22 ± 6	24 ± 6	35 ± 8	39 ± 8	1
XMMXCS J021943.7-045313.8	$0.371^{+0.090}_{-0.090}$	0.378 ± 0.092	-0.027 ± 0.011	1.840 ± 0.216	0.061	10 ± 3	10 ± 4	10 ± 3	9 ± 3	1
XMMXCS J021944.29-045326.8	$0.359^{+0.089}_{-0.090}$	0.378 ± 0.092	-0.042 ± 0.012	1.460 ± 0.240	0.045	11 ± 4	11 ± 4	11 ± 4	11 ± 4	1
XMMXCS J022002.9-052754.6	$0.278^{+0.084}_{-0.084}$	0.268 ± 0.086	-0.003 ± 0.022	1.220 ± 0.431	0.097	16 ± 4	16 ± 4	15 ± 4	16 ± 4	1
XMMXCS J022103.3-050611.1	$0.343^{+0.088}_{-0.089}$	0.296 ± 0.086	-0.040 ± 0.023	2.000 ± 0.442	0.099	3 ± 2	4 ± 3	4 ± 2	5 ± 3	1
XMMXCS J022105.4-043933.4	$0.761^{+0.112}_{-0.114}$	0.797 ± 0.117	-0.042 ± 0.020	1.380 ± 0.448	0.093	4 ± 4	3 ± 4	6 ± 3	6 ± 3	1
XMMXCS J022105.3-043933.9	$0.761^{+0.112}_{-0.114}$	0.797 ± 0.117	-0.042 ± 0.020	1.380 ± 0.448	0.093	5 ± 4	4 ± 4	7 ± 3	6 ± 3	1

Continued on next page

Table A.4 – continued from previous page

name	z_{RS}	z_{BCG}	cmr_{grad}	cmr_{inter}	cmr_{wid}	n_{gals-c}	n_{gals-l}	n_{200-c}	n_{200-l}	qual
XMMXCS J022118.36-042238.0	$0.779^{+0.120}_{-0.119}$	0.737 ± 0.113	-0.015 ± 0.009	0.635 ± 0.197	0.099	9 ± 5	10 ± 5	6 ± 4	10 ± 5	1
XMMXCS J022119.2-043754.1	$0.179^{+0.076}_{-0.077}$	0.141 ± 0.077	0.335 ± 0.129	-5.400 ± 2.360	0.065	5 ± 2	9 ± 3	5 ± 2	9 ± 3	1
XMMXCS J022126.8-043402.2	$0.179^{+0.078}_{-0.078}$	0.171 ± 0.079	-0.033 ± 0.009	1.470 ± 0.171	0.042	6 ± 3	5 ± 2	5 ± 2	5 ± 2	1
XMMXCS J022130.8-041205.8	$0.867^{+0.125}_{-0.125}$	0.877 ± 0.123	-0.018 ± 0.011	0.721 ± 0.259	0.096	14 ± 6	12 ± 6	16 ± 6	11 ± 6	1
XMMXCS J022141.18-034645.7	$0.435^{+0.094}_{-0.095}$	0.447 ± 0.097	-0.038 ± 0.031	2.320 ± 0.660	0.071	27 ± 5	32 ± 6	36 ± 6	48 ± 7	1
XMMXCS J022143.61-034612.9	$0.445^{+0.095}_{-0.095}$	0.447 ± 0.097	-0.034 ± 0.012	2.230 ± 0.239	0.084	34 ± 6	38 ± 6	48 ± 7	60 ± 8	1
XMMXCS J022145.4-034617.4	$0.455^{+0.096}_{-0.096}$	0.447 ± 0.097	0.001 ± 0.007	0.697 ± 0.130	0.048	41 ± 7	44 ± 7	57 ± 8	63 ± 9	1
XMMXCS J022148.0-034607.1	$0.453^{+0.095}_{-0.095}$	0.447 ± 0.097	-0.009 ± 0.006	0.886 ± 0.118	0.047	38 ± 6	41 ± 7	54 ± 8	61 ± 8	1
XMMXCS J022152.01-043152.8	$0.243^{+0.125}_{-0.109}$	0.222 ± 0.082	-0.000 ± 0.001	0.207 ± 0.001	0.500	4 ± 3	7 ± 3	3 ± 2	5 ± 3	1
XMMXCS J022154.83-054519.0	$0.295^{+0.085}_{-0.086}$	0.268 ± 0.086	0.013 ± 0.014	0.963 ± 0.265	0.044	13 ± 4	19 ± 5	14 ± 4	21 ± 5	1
XMMXCS J022154.8-054519.0	$0.295^{+0.085}_{-0.086}$	0.268 ± 0.086	0.013 ± 0.014	0.963 ± 0.265	0.044	13 ± 4	19 ± 5	14 ± 4	21 ± 5	1
XMMXCS J022218.56-041651.9	$0.819^{+0.119}_{-0.119}$	0.777 ± 0.116	0.024 ± 0.037	0.216 ± 0.841	0.136	12 ± 4	12 ± 5	12 ± 5	12 ± 5	1
XMMXCS J022218.5-041651.8	$0.819^{+0.119}_{-0.119}$	0.777 ± 0.116	0.024 ± 0.037	0.216 ± 0.841	0.136	12 ± 4	12 ± 5	12 ± 5	12 ± 5	1
XMMXCS J022222.8-044043.0	$0.803^{+0.115}_{-0.116}$	0.829 ± 0.120	-0.071 ± 0.018	2.140 ± 0.404	0.113	15 ± 5	18 ± 6	19 ± 6	22 ± 7	1
XMMXCS J022233.0-045803.2	$0.820^{+0.119}_{-0.120}$	0.843 ± 0.121	0.020 ± 0.016	0.266 ± 0.368	0.056	5 ± 3	6 ± 3	7 ± 3	7 ± 3	1
XMMXCS J022233.02-045803.5	$0.815^{+0.119}_{-0.119}$	0.843 ± 0.121	0.019 ± 0.017	0.278 ± 0.375	0.058	3 ± 3	6 ± 3	5 ± 2	6 ± 3	1
XMMXCS J022246.3-035150.5	$0.155^{+0.077}_{-0.077}$	0.132 ± 0.076	0.025 ± 0.021	0.370 ± 0.357	0.047	3 ± 2	3 ± 2	3 ± 2	8 ± 3	1
XMMXCS J022258.8-040636.0	$0.316^{+0.086}_{-0.086}$	0.316 ± 0.088	-0.050 ± 0.019	2.200 ± 0.358	0.057	7 ± 3	9 ± 3	7 ± 3	9 ± 3	1
XMMXCS J022259.03-040633.1	$0.309^{+0.086}_{-0.086}$	0.316 ± 0.088	-0.056 ± 0.016	2.320 ± 0.311	0.057	7 ± 3	9 ± 3	7 ± 3	9 ± 3	1

Continued on next page

Table A.4 – continued from previous page

name	z_{RS}	z_{BCG}	cmr_{grad}	cmr_{inter}	cmr_{wid}	n_{gals-c}	n_{gals-l}	n_{200-c}	n_{200-l}	qual
XMMXCS J022307.7-041259.4	$0.634^{+0.106}_{-0.107}$	0.603 ± 0.105	-0.020 ± 0.019	1.560 ± 0.398	0.093	18 ± 5	20 ± 5	17 ± 5	14 ± 5	1
XMMXCS J022310.13-062231.6	$1.047^{+0.133}_{-0.132}$	1.050 ± 0.134	-0.001 ± 0.029	0.649 ± 0.680	0.105	15 ± 5	15 ± 6	20 ± 6	20 ± 6	1
XMMXCS J022318.37-052707.6	$0.227^{+0.081}_{-0.081}$	0.229 ± 0.083	-0.038 ± 0.009	1.740 ± 0.158	0.030	8 ± 3	7 ± 3	7 ± 3	5 ± 3	1
XMMXCS J022319.5-052710.9	$0.231^{+0.081}_{-0.081}$	0.229 ± 0.083	-0.031 ± 0.005	1.620 ± 0.094	0.024	8 ± 3	7 ± 3	7 ± 3	5 ± 3	1
XMMXCS J022336.55-050832.7	$0.443^{+0.076}_{-0.078}$	0.483 ± 0.097	0.012 ± 0.033	0.681 ± 0.696	0.101	5 ± 3	3 ± 3	3 ± 2	1 ± 2	1
XMMXCS J022337.0-034507.1	$0.706^{+0.115}_{-0.118}$	0.731 ± 0.113	-0.047 ± 0.014	1.360 ± 0.320	0.082	9 ± 5	12 ± 5	5 ± 4	14 ± 5	1
XMMXCS J022341.8-043037.8	$0.475^{+0.096}_{-0.097}$	0.449 ± 0.097	-0.005 ± 0.008	0.804 ± 0.175	0.034	12 ± 4	15 ± 4	12 ± 4	18 ± 5	1
XMMXCS J022342.3-050200.3	$0.854^{+0.121}_{-0.120}$	0.899 ± 0.124	-0.055 ± 0.015	1.790 ± 0.341	0.092	18 ± 6	16 ± 6	21 ± 6	22 ± 6	1
XMMXCS J022350.88-053643.9	$0.514^{+0.099}_{-0.100}$	0.486 ± 0.099	-0.008 ± 0.018	1.000 ± 0.368	0.079	25 ± 5	28 ± 6	31 ± 6	41 ± 7	1
XMMXCS J022352.59-082125.4	$0.245^{+0.082}_{-0.082}$	0.259 ± 0.085	-0.004 ± 0.021	1.200 ± 0.383	0.073	17 ± 4	17 ± 4	17 ± 4	18 ± 5	1
XMMXCS J022357.59-043519.7	$0.504^{+0.097}_{-0.098}$	0.489 ± 0.099	-0.015 ± 0.012	1.120 ± 0.255	0.085	25 ± 5	21 ± 5	38 ± 7	34 ± 6	1
XMMXCS J022357.6-043518.9	$0.501^{+0.097}_{-0.098}$	0.489 ± 0.099	-0.020 ± 0.013	1.220 ± 0.261	0.079	22 ± 5	20 ± 5	32 ± 6	27 ± 6	1
XMMXCS J022359.25-083544.0	$0.315^{+0.087}_{-0.087}$	0.295 ± 0.086	-0.009 ± 0.034	1.400 ± 0.658	0.075	29 ± 6	28 ± 6	42 ± 7	39 ± 7	1
XMMXCS J022402.73-041910.9	$0.810^{+0.118}_{-0.118}$	0.816 ± 0.121	-0.019 ± 0.023	1.040 ± 0.525	0.112	3 ± 3	4 ± 4	3 ± 2	2 ± 2	1
XMMXCS J022416.9-050315.7	$0.202^{+0.079}_{-0.080}$	0.180 ± 0.080	-0.025 ± 0.018	1.370 ± 0.325	0.092	6 ± 3	9 ± 3	4 ± 2	7 ± 3	1
XMMXCS J022433.23-041423.8	$0.285^{+0.085}_{-0.085}$	0.272 ± 0.086	-0.046 ± 0.021	2.050 ± 0.391	0.075	14 ± 4	13 ± 4	15 ± 4	14 ± 4	1
XMMXCS J022433.8-041432.9	$0.284^{+0.084}_{-0.085}$	0.272 ± 0.086	-0.044 ± 0.021	2.000 ± 0.399	0.078	15 ± 4	13 ± 4	14 ± 4	14 ± 4	1
XMMXCS J022438.1-045335.9	$0.315^{+0.078}_{-0.081}$	0.319 ± 0.087	0.594 ± 0.001	-10.40 ± 0.001	0.500	5 ± 3	5 ± 4	3 ± 2	-	1
XMMXCS J022501.6-040753.1	$0.634^{+0.102}_{-0.099}$	0.642 ± 0.107	-0.016 ± 0.021	0.940 ± 0.467	0.095	8 ± 4	8 ± 4	7 ± 3	6 ± 3	1

Continued on next page

Table A.4 – continued from previous page

name	z_{RS}	z_{BCG}	cmr_{grad}	cmr_{inter}	cmr_{wid}	n_{gals-c}	n_{gals-l}	n_{200-c}	n_{200-l}	qual
XMMXCS J022505.29-095008.2	$0.185^{+0.079}_{-0.079}$	0.171 ± 0.079	-0.014 ± 0.011	1.160 ± 0.186	0.034	18 ± 4	15 ± 4	21 ± 5	17 ± 4	1
XMMXCS J022512.16-062307.9	$0.226^{+0.080}_{-0.081}$	0.220 ± 0.082	-0.011 ± 0.021	1.220 ± 0.405	0.045	14 ± 4	15 ± 4	13 ± 4	15 ± 4	1
XMMXCS J022519.81-041842.3	$0.763^{+0.118}_{-0.118}$	0.765 ± 0.115	-0.018 ± 0.006	0.746 ± 0.143	0.098	10 ± 5	12 ± 5	11 ± 5	12 ± 5	1
XMMXCS J022519.8-041842.3	$0.770^{+0.118}_{-0.118}$	0.765 ± 0.115	-0.018 ± 0.006	0.759 ± 0.145	0.100	9 ± 5	13 ± 5	9 ± 4	51 ± 8	1
XMMXCS J022524.72-044043.9	$0.273^{+0.083}_{-0.083}$	0.259 ± 0.085	-0.002 ± 0.021	1.260 ± 0.384	0.069	4 ± 2	4 ± 3	4 ± 2	9 ± 3	1
XMMXCS J022524.7-044043.9	$0.273^{+0.083}_{-0.083}$	0.259 ± 0.085	-0.002 ± 0.021	1.260 ± 0.384	0.069	4 ± 2	4 ± 3	4 ± 2	9 ± 3	1
XMMXCS J022525.01-061854.8	$0.673^{+0.105}_{-0.107}$	0.680 ± 0.110	0.006 ± 0.009	0.276 ± 0.186	0.065	5 ± 4	8 ± 4	5 ± 3	6 ± 4	1
XMMXCS J022529.75-041432.7	$0.170^{+0.077}_{-0.078}$	0.161 ± 0.078	-0.029 ± 0.010	1.350 ± 0.176	0.035	9 ± 3	7 ± 3	8 ± 3	4 ± 2	1
XMMXCS J022530.7-041419.0	$0.170^{+0.077}_{-0.078}$	0.161 ± 0.078	-0.029 ± 0.010	1.350 ± 0.176	0.035	10 ± 3	6 ± 3	7 ± 3	4 ± 2	1
XMMXCS J022539.6-042210.1	$0.155^{+0.085}_{-0.080}$	0.132 ± 0.076	-0.156 ± 0.001	3.460 ± 0.001	0.500	10 ± 4	7 ± 3	10 ± 4	5 ± 3	1
XMMXCS J022542.8-042840.3	$0.261^{+0.083}_{-0.083}$	0.249 ± 0.084	-0.027 ± 0.038	1.540 ± 0.670	0.087	4 ± 3	5 ± 3	4 ± 2	4 ± 2	1
XMMXCS J022544.6-051234.9	$0.146^{+0.075}_{-0.076}$	0.122 ± 0.075	0.139 ± 0.050	-1.630 ± 0.870	0.088	4 ± 2	3 ± 2	3 ± 2	2 ± 2	1
XMMXCS J022610.3-045805.8	$0.134^{+0.071}_{-0.072}$	0.093 ± 0.060	0.040 ± 0.027	-0.086 ± 0.464	0.064	6 ± 3	7 ± 3	5 ± 2	5 ± 2	1
XMMXCS J022618.3-040000.1	$0.222^{+0.079}_{-0.080}$	0.220 ± 0.082	-0.010 ± 0.018	1.170 ± 0.360	0.081	10 ± 3	10 ± 4	10 ± 3	9 ± 3	1
XMMXCS J022620.1-040025.9	$0.207^{+0.075}_{-0.077}$	0.220 ± 0.082	-0.079 ± 0.032	2.250 ± 0.616	0.073	4 ± 2	2 ± 2	3 ± 2	0 ± 1	1
XMMXCS J022626.3-040455.6	$0.339^{+0.087}_{-0.088}$	0.346 ± 0.090	-0.029 ± 0.015	1.880 ± 0.289	0.071	11 ± 4	10 ± 4	11 ± 4	7 ± 3	1
XMMXCS J022634.7-040408.0	$0.360^{+0.089}_{-0.089}$	0.346 ± 0.090	-0.007 ± 0.031	1.440 ± 0.610	0.114	15 ± 4	13 ± 4	15 ± 4	14 ± 4	1
XMMXCS J022634.75-040408.0	$0.360^{+0.089}_{-0.089}$	0.346 ± 0.090	-0.007 ± 0.031	1.440 ± 0.610	0.114	15 ± 4	13 ± 4	15 ± 4	14 ± 4	1
XMMXCS J022639.92-041641.5	$0.960^{+0.128}_{-0.128}$	0.970 ± 0.131	0.008 ± 0.028	0.288 ± 0.637	0.080	8 ± 5	13 ± 5	7 ± 4	13 ± 5	1

Continued on next page

Table A.4 – continued from previous page

name	z_{RS}	z_{BCG}	cmr_{grad}	cmr_{inter}	cmr_{wid}	n_{gals-c}	n_{gals-l}	n_{200-c}	n_{200-l}	qual
XMMXCS J022651.2-054138.1	$0.799^{+0.128}_{-0.128}$	0.756 ± 0.115	-0.016 ± 0.027	0.907 ± 0.612	0.117	12 ± 5	8 ± 5	13 ± 5	5 ± 4	1
XMMXCS J022702.1-040511.5	$0.750^{+0.113}_{-0.113}$	0.746 ± 0.114	-0.072 ± 0.015	2.860 ± 0.338	0.066	2 ± 2	2 ± 2	3 ± 2	1 ± 1	1
XMMXCS J022702.94-041509.5	$0.706^{+0.113}_{-0.115}$	0.669 ± 0.109	-0.026 ± 0.021	0.849 ± 0.457	0.056	3 ± 3	2 ± 4	5 ± 3	4 ± 2	1
XMMXCS J022726.38-043206.8	$0.292^{+0.086}_{-0.085}$	0.298 ± 0.087	-0.002 ± 0.030	1.180 ± 0.590	0.089	9 ± 3	8 ± 3	10 ± 3	8 ± 3	1
XMMXCS J022726.7-043209.1	$0.284^{+0.085}_{-0.085}$	0.284 ± 0.086	0.109 ± 0.018	-0.908 ± 0.336	0.066	7 ± 3	5 ± 3	8 ± 3	4 ± 2	1
XMMXCS J022728.3-084810.5	$0.419^{+0.085}_{-0.082}$	0.407 ± 0.093	0.015 ± 0.025	0.112 ± 0.512	0.131	7 ± 4	7 ± 4	4 ± 3	4 ± 3	1
XMMXCS J022731.8-043750.3	$1.125^{+0.153}_{-0.159}$	1.090 ± 0.136	0.006 ± 0.020	0.555 ± 0.464	0.088	10 ± 4	12 ± 5	6 ± 4	11 ± 5	1
XMMXCS J022731.86-043750.4	$1.125^{+0.153}_{-0.159}$	1.090 ± 0.136	0.006 ± 0.020	0.555 ± 0.464	0.088	10 ± 4	12 ± 5	6 ± 4	11 ± 5	1
XMMXCS J022732.99-055730.7	$0.244^{+0.080}_{-0.081}$	0.229 ± 0.083	-0.016 ± 0.010	1.410 ± 0.200	0.052	10 ± 3	11 ± 4	9 ± 3	11 ± 4	1
XMMXCS J022740.41-045129.9	$0.320^{+0.086}_{-0.086}$	0.278 ± 0.086	-0.014 ± 0.010	1.470 ± 0.190	0.067	11 ± 4	12 ± 4	11 ± 4	12 ± 4	1
XMMXCS J022740.4-045130.3	$0.320^{+0.086}_{-0.086}$	0.278 ± 0.086	-0.014 ± 0.010	1.470 ± 0.190	0.067	11 ± 4	12 ± 4	10 ± 3	12 ± 4	1
XMMXCS J022753.33-051241.4	$0.753^{+0.120}_{-0.121}$	0.797 ± 0.117	-0.004 ± 0.011	0.382 ± 0.249	0.090	8 ± 4	11 ± 5	7 ± 4	12 ± 5	1
XMMXCS J022753.3-051241.4	$0.753^{+0.120}_{-0.121}$	0.797 ± 0.117	-0.004 ± 0.011	0.382 ± 0.249	0.090	8 ± 4	11 ± 5	7 ± 4	12 ± 5	1
XMMXCS J022802.7-045101.7	$0.320^{+0.087}_{-0.087}$	0.288 ± 0.086	-0.028 ± 0.008	1.810 ± 0.157	0.039	10 ± 3	9 ± 3	11 ± 3	9 ± 3	1
XMMXCS J022802.85-045101.1	$0.318^{+0.086}_{-0.086}$	0.288 ± 0.086	-0.027 ± 0.009	1.800 ± 0.171	0.040	10 ± 3	9 ± 3	11 ± 3	9 ± 3	1
XMMXCS J022805.60-051934.5	$0.331^{+0.088}_{-0.088}$	0.317 ± 0.088	-0.027 ± 0.028	1.830 ± 0.499	0.074	8 ± 3	7 ± 3	4 ± 2	4 ± 2	1
XMMXCS J022805.5-051934.5	$0.331^{+0.088}_{-0.088}$	0.317 ± 0.088	-0.027 ± 0.028	1.830 ± 0.499	0.074	8 ± 3	7 ± 3	4 ± 2	4 ± 2	1
XMMXCS J022808.41-053553.2	$0.215^{+0.081}_{-0.081}$	0.200 ± 0.081	-0.004 ± 0.012	1.080 ± 0.207	0.031	4 ± 2	4 ± 3	3 ± 2	3 ± 2	1
XMMXCS J022808.4-053553.2	$0.215^{+0.081}_{-0.081}$	0.200 ± 0.081	-0.004 ± 0.012	1.080 ± 0.207	0.031	4 ± 2	4 ± 3	3 ± 2	3 ± 2	1

Continued on next page

Table A.4 – continued from previous page

name	z_{RS}	z_{BCG}	cmr_{grad}	cmr_{inter}	cmr_{wid}	n_{gals-c}	n_{gals-l}	n_{200-c}	n_{200-l}	qual
XMMXCS J022827.28-042542.5	$0.432^{+0.094}_{-0.094}$	0.430 ± 0.095	-0.030 ± 0.011	2.090 ± 0.223	0.046	21 ± 5	21 ± 5	24 ± 5	23 ± 5	1
XMMXCS J022827.3-042542.2	$0.432^{+0.094}_{-0.094}$	0.430 ± 0.095	-0.030 ± 0.011	2.090 ± 0.223	0.046	21 ± 5	21 ± 5	24 ± 5	23 ± 5	1
XMMXCS J022829.38-045125.6	$0.202^{+0.084}_{-0.084}$	0.180 ± 0.080	-0.031 ± 0.013	1.410 ± 0.229	0.038	4 ± 2	4 ± 2	4 ± 2	4 ± 2	1
XMMXCS J022830.26-044358.0	$0.624^{+0.107}_{-0.107}$	0.673 ± 0.111	-0.031 ± 0.012	1.720 ± 0.254	0.075	26 ± 5	27 ± 6	30 ± 6	33 ± 6	1
XMMXCS J022831.83-094934.9	$0.398^{+0.091}_{-0.092}$	0.382 ± 0.092	-0.014 ± 0.015	1.810 ± 0.313	0.079	24 ± 5	19 ± 5	28 ± 6	29 ± 6	1
XMMXCS J022844.7-041339.8	$1.091^{+0.123}_{-0.109}$	1.080 ± 0.136	0.010 ± 0.023	0.307 ± 0.537	0.104	3 ± 4	4 ± 4	6 ± 3	7 ± 4	1
XMMXCS J022846.8-050315.7	$0.289^{+0.086}_{-0.086}$	0.328 ± 0.089	-0.037 ± 0.039	1.810 ± 0.734	0.117	9 ± 4	5 ± 3	9 ± 3	4 ± 3	1
XMMXCS J022858.05-055409.5	$0.315^{+0.085}_{-0.086}$	0.309 ± 0.086	-0.007 ± 0.023	1.290 ± 0.441	0.105	7 ± 3	5 ± 3	3 ± 2	2 ± 2	1
XMMXCS J022858.7-100444.1	$0.421^{+0.093}_{-0.093}$	0.388 ± 0.092	-0.008 ± 0.027	1.670 ± 0.539	0.086	16 ± 4	31 ± 6	17 ± 5	18 ± 5	1
XMMXCS J022859.0-100436.2	$0.413^{+0.092}_{-0.093}$	0.388 ± 0.092	0.003 ± 0.028	1.410 ± 0.580	0.099	17 ± 4	31 ± 6	17 ± 5	5 ± 4	1
XMMXCS J022915.90-044218.5	$0.607^{+0.105}_{-0.102}$	0.609 ± 0.105	0.030 ± 0.090	0.086 ± 1.920	0.084	11 ± 4	8 ± 4	11 ± 4	8 ± 4	1
XMMXCS J022917.00-055401.1	$0.307^{+0.086}_{-0.086}$	0.298 ± 0.087	-0.045 ± 0.012	2.130 ± 0.227	0.080	10 ± 3	12 ± 4	8 ± 3	12 ± 4	1
XMMXCS J022933.28-043953.8	$0.584^{+0.103}_{-0.104}$	0.604 ± 0.105	-0.021 ± 0.015	1.530 ± 0.318	0.073	14 ± 4	12 ± 4	14 ± 4	12 ± 4	1
XMMXCS J022933.47-055306.1	$0.309^{+0.084}_{-0.085}$	0.321 ± 0.088	-0.014 ± 0.018	1.550 ± 0.350	0.071	14 ± 4	12 ± 4	14 ± 4	12 ± 4	1
XMMXCS J022940.9-060426.0	$1.038^{+0.129}_{-0.127}$	1.010 ± 0.134	0.085 ± 0.029	-1.240 ± 0.654	0.114	12 ± 5	11 ± 5	14 ± 5	11 ± 5	1
XMMXCS J023024.62-044926.2	$0.579^{+0.075}_{-0.090}$	0.532 ± 0.100	0.019 ± 0.023	0.499 ± 0.490	0.109	6 ± 3	3 ± 3	3 ± 2	1 ± 2	1
XMMXCS J023026.62-043443.3	$0.294^{+0.085}_{-0.085}$	0.288 ± 0.086	-0.024 ± 0.020	1.680 ± 0.377	0.092	15 ± 4	19 ± 5	15 ± 4	20 ± 5	1
XMMXCS J023027.22-051325.0	$0.243^{+0.083}_{-0.083}$	0.249 ± 0.084	-0.045 ± 0.013	1.810 ± 0.222	0.042	9 ± 3	12 ± 4	10 ± 3	11 ± 4	1
XMMXCS J023027.23-051325.2	$0.243^{+0.083}_{-0.083}$	0.249 ± 0.084	-0.045 ± 0.013	1.810 ± 0.222	0.042	9 ± 3	12 ± 4	10 ± 3	11 ± 4	1

Continued on next page

Table A.4 – continued from previous page

name	z_{RS}	z_{BCG}	cmr_{grad}	cmr_{inter}	cmr_{wid}	n_{gals-c}	n_{gals-l}	n_{200-c}	n_{200-l}	qual
XMMXCS J023035.61-041039.2	$0.986^{+0.130}_{-0.129}$	0.984 ± 0.132	-0.056 ± 0.032	1.780 ± 0.747	0.092	18 ± 6	20 ± 6	34 ± 8	-	1
XMMXCS J023036.91-040936.1	$0.910^{+0.130}_{-0.129}$	0.955 ± 0.129	-0.015 ± 0.036	0.767 ± 0.837	0.076	17 ± 6	19 ± 6	18 ± 6	18 ± 7	1
XMMXCS J023105.55-041322.8	$0.526^{+0.098}_{-0.089}$	0.551 ± 0.102	0.047 ± 0.002	-0.638 ± 0.041	0.500	4 ± 4	5 ± 4	4 ± 3	6 ± 4	1
XMMXCS J023142.25-045253.7	$0.210^{+0.080}_{-0.080}$	0.239 ± 0.084	-0.023 ± 0.009	1.400 ± 0.171	0.037	39 ± 6	36 ± 6	57 ± 8	52 ± 8	1
XMMXCS J023142.36-045311.6	$0.211^{+0.080}_{-0.080}$	0.239 ± 0.084	-0.022 ± 0.009	1.400 ± 0.170	0.036	41 ± 6	38 ± 6	56 ± 8	54 ± 8	1
XMMXCS J023146.67-045229.6	$0.680^{+0.127}_{-0.126}$	0.703 ± 0.112	-0.092 ± 0.021	2.990 ± 0.470	0.066	10 ± 4	1 ± 2	11 ± 4	1 ± 1	1
XMMXCS J023153.34-045125.5	$0.210^{+0.079}_{-0.080}$	0.200 ± 0.081	-0.023 ± 0.009	1.390 ± 0.162	0.052	22 ± 5	23 ± 5	41 ± 7	38 ± 6	1
XMMXCS J023226.53-041359.0	$0.295^{+0.085}_{-0.085}$	0.279 ± 0.086	-0.004 ± 0.044	1.120 ± 0.864	0.107	9 ± 4	7 ± 3	10 ± 4	8 ± 3	1
XMMXCS J023234.11-044552.3	$0.293^{+0.085}_{-0.085}$	0.317 ± 0.088	-0.017 ± 0.031	1.520 ± 0.614	0.100	17 ± 4	18 ± 5	19 ± 5	20 ± 5	1
XMMXCS J023235.5-041926.6	$0.394^{+0.086}_{-0.085}$	0.440 ± 0.095	-0.062 ± 0.051	2.340 ± 1.030	0.114	8 ± 3	6 ± 3	8 ± 3	6 ± 3	1
XMMXCS J023247.47-045147.4	$0.785^{+0.122}_{-0.122}$	0.831 ± 0.119	-0.033 ± 0.018	1.070 ± 0.399	0.103	25 ± 6	21 ± 6	24 ± 8	20 ± 7	1
XMMXCS J023249.96-044345.4	$0.789^{+0.114}_{-0.115}$	0.804 ± 0.117	-0.022 ± 0.020	0.871 ± 0.452	0.098	7 ± 5	8 ± 5	4 ± 4	5 ± 4	1
XMMXCS J023300.88-050951.0	$0.285^{+0.085}_{-0.085}$	0.268 ± 0.086	-0.021 ± 0.015	1.550 ± 0.277	0.036	5 ± 3	4 ± 3	5 ± 2	4 ± 2	1
XMMXCS J023321.58-040608.7	$0.571^{+0.098}_{-0.094}$	0.533 ± 0.100	-0.055 ± 0.023	1.620 ± 0.504	0.080	6 ± 3	5 ± 3	3 ± 2	0 ± 2	1
XMMXCS J023333.48-041233.2	$0.295^{+0.083}_{-0.084}$	0.278 ± 0.086	-0.043 ± 0.022	1.980 ± 0.398	0.097	5 ± 3	7 ± 3	3 ± 2	1 ± 2	1
XMMXCS J023337.65-053026.5	$0.429^{+0.094}_{-0.094}$	0.424 ± 0.095	-0.020 ± 0.014	1.890 ± 0.292	0.082	31 ± 6	28 ± 6	37 ± 7	32 ± 6	1
XMMXCS J023356.94-050815.9	$0.849^{+0.122}_{-0.123}$	0.883 ± 0.124	-0.052 ± 0.011	1.660 ± 0.246	0.102	13 ± 5	15 ± 6	19 ± 6	22 ± 7	1
XMMXCS J023359.4-042932.1	$0.747^{+0.106}_{-0.096}$	0.706 ± 0.120	0.001 ± 0.012	0.197 ± 0.252	0.072	4 ± 4	3 ± 4	6 ± 3	2 ± 2	1
XMMXCS J023418.41-094003.2	$0.821^{+0.119}_{-0.120}$	0.789 ± 0.117	-0.004 ± 0.011	0.764 ± 0.255	0.080	54 ± 8	54 ± 8	89 ± 11	77 ± 11	1

Continued on next page

Table A.4 – continued from previous page

name	z_{RS}	z_{BCG}	cmr_{grad}	cmr_{inter}	cmr_{wid}	n_{gals-c}	n_{gals-l}	n_{200-c}	n_{200-l}	qual
XMMXCS J023420.21-095112.5	$0.594^{+0.104}_{-0.104}$	0.605 ± 0.106	-0.017 ± 0.014	1.450 ± 0.293	0.088	26 ± 5	27 ± 6	31 ± 6	32 ± 6	1
XMMXCS J023432.5-053404.9	$0.224^{+0.082}_{-0.082}$	0.220 ± 0.082	-0.043 ± 0.018	1.770 ± 0.310	0.049	9 ± 3	7 ± 3	7 ± 3	4 ± 2	1
XMMXCS J085216.06-053332.6	$0.230^{+0.082}_{-0.082}$	0.220 ± 0.082	-0.037 ± 0.016	1.700 ± 0.285	0.041	32 ± 6	32 ± 6	63 ± 8	63 ± 8	1
XMMXCS J085216.53-010138.9	$0.474^{+0.097}_{-0.097}$	0.502 ± 0.099	0.012 ± 0.019	0.535 ± 0.396	0.073	36 ± 6	41 ± 7	57 ± 8	70 ± 9	1
XMMXCS J085220.69-011023.7	$0.625^{+0.108}_{-0.107}$	0.587 ± 0.103	0.029 ± 0.033	0.372 ± 0.702	0.109	5 ± 3	9 ± 4	4 ± 2	4 ± 3	1
XMMXCS J085413.9-053225.3	$0.244^{+0.078}_{-0.081}$	0.200 ± 0.081	0.011 ± 0.034	0.809 ± 0.620	0.096	3 ± 2	1 ± 2	4 ± 2	1 ± 1	1
XMMXCS J085413.94-053225.0	$0.244^{+0.078}_{-0.081}$	0.200 ± 0.081	0.011 ± 0.034	0.809 ± 0.620	0.096	3 ± 2	1 ± 2	4 ± 2	1 ± 1	1
XMMXCS J085447.73-012150.9	$0.361^{+0.089}_{-0.089}$	0.337 ± 0.090	-0.009 ± 0.012	1.560 ± 0.242	0.063	20 ± 5	22 ± 5	21 ± 5	24 ± 5	1
XMMXCS J085820.90-034935.0	$0.742^{+0.129}_{-0.133}$	0.788 ± 0.117	-0.006 ± 0.014	0.434 ± 0.319	0.098	8 ± 5	12 ± 5	5 ± 4	15 ± 5	1
XMMXCS J085822.56-043839.3	$0.653^{+0.109}_{-0.109}$	0.683 ± 0.111	-0.039 ± 0.014	1.970 ± 0.315	0.076	14 ± 4	16 ± 4	15 ± 4	17 ± 5	1
XMMXCS J085851.24-052302.9	$0.102^{+0.062}_{-0.063}$	0.141 ± 0.077	-0.044 ± 0.033	1.470 ± 0.588	0.099	3 ± 2	1 ± 1	3 ± 2	0 ± 1	1
XMMXCS J085917.39-030935.8	$0.301^{+0.091}_{-0.090}$	0.256 ± 0.084	-0.018 ± 0.031	1.110 ± 0.636	0.090	5 ± 3	2 ± 2	4 ± 2	2 ± 2	1
XMMXCS J085957.05-042205.9	$0.161^{+0.077}_{-0.077}$	0.180 ± 0.080	-0.032 ± 0.013	1.440 ± 0.233	0.051	5 ± 2	5 ± 2	5 ± 2	5 ± 2	1
XMMXCS J090130.07-013859.6	$0.346^{+0.089}_{-0.088}$	0.395 ± 0.094	-0.022 ± 0.020	1.760 ± 0.389	0.065	33 ± 6	36 ± 6	53 ± 8	54 ± 8	1
XMMXCS J090138.59-015856.5	$0.333^{+0.087}_{-0.088}$	0.288 ± 0.086	-0.024 ± 0.015	1.800 ± 0.282	0.078	13 ± 4	18 ± 5	13 ± 4	22 ± 5	1
XMMXCS J090145.85-013823.6	$0.333^{+0.087}_{-0.087}$	0.306 ± 0.086	-0.028 ± 0.027	1.800 ± 0.548	0.066	11 ± 4	13 ± 4	11 ± 4	15 ± 4	1
XMMXCS J090147.47-014323.6	$0.292^{+0.084}_{-0.084}$	0.259 ± 0.085	0.003 ± 0.016	1.110 ± 0.309	0.102	16 ± 4	13 ± 4	19 ± 5	14 ± 4	1
XMMXCS J141446.39+544710.1	$0.611^{+0.106}_{-0.106}$	0.597 ± 0.106	-0.027 ± 0.010	1.700 ± 0.221	0.089	65 ± 8	67 ± 8	109 ± 11	101 ± 11	1
XMMXCS J141653.63+522102.2	$0.759^{+0.110}_{-0.109}$	0.750 ± 0.114	-0.008 ± 0.047	0.646 ± 1.070	0.126	10 ± 5	9 ± 5	11 ± 5	8 ± 5	1

Continued on next page

Table A.4 – continued from previous page

name	z_{RS}	z_{BCG}	cmr_{grad}	cmr_{inter}	cmr_{wid}	n_{gals-c}	n_{gals-l}	n_{200-c}	n_{200-l}	qual
XMMXCS J141823.26+522710.6	$0.820^{+0.124}_{-0.122}$	0.866 ± 0.121	-0.026 ± 0.011	0.883 ± 0.252	0.090	7 ± 5	7 ± 5	4 ± 4	2 ± 4	1
XMMXCS J141823.2+522710.6	$0.820^{+0.124}_{-0.122}$	0.866 ± 0.121	-0.026 ± 0.011	0.883 ± 0.252	0.090	7 ± 5	7 ± 5	4 ± 4	2 ± 4	1
XMMXCS J220625.01+013913.6	$0.297^{+0.085}_{-0.085}$	0.307 ± 0.088	-0.044 ± 0.018	2.050 ± 0.347	0.086	12 ± 4	10 ± 3	12 ± 4	9 ± 3	1
XMMXCS J221211.3+000830.4	$0.391^{+0.092}_{-0.092}$	0.349 ± 0.090	0.040 ± 0.025	0.430 ± 0.522	0.093	22 ± 5	21 ± 5	30 ± 6	24 ± 6	1
XMMXCS J221449.28+004706.7	$0.337^{+0.087}_{-0.088}$	0.346 ± 0.090	-0.022 ± 0.012	1.710 ± 0.232	0.060	13 ± 4	14 ± 4	14 ± 4	15 ± 4	1
XMMXCS J221546.25-001808.9	$1.123^{+0.132}_{-0.134}$	1.080 ± 0.134	0.064 ± 0.062	-0.761 ± 1.430	0.093	5 ± 3	-	3 ± 2	-	1
XMMXCS J221657.0+002408.8	$0.956^{+0.136}_{-0.136}$	0.906 ± 0.127	0.010 ± 0.049	0.406 ± 1.150	0.120	14 ± 5	-	15 ± 6	-	1
XMMXCS J221736.16-002319.0	$0.942^{+0.125}_{-0.123}$	0.974 ± 0.135	-0.008 ± 0.038	0.558 ± 0.876	0.107	22 ± 7	19 ± 6	31 ± 9	30 ± 8	1
XMMXCS J222007.8+002003.7	$0.423^{+0.095}_{-0.088}$	0.471 ± 0.097	0.014 ± 0.033	0.306 ± 0.659	0.087	7 ± 3	5 ± 3	6 ± 3	4 ± 3	1
XMMXCS J222007.82-002003.7	$0.098^{+0.059}_{-0.061}$	0.132 ± 0.076	-0.061 ± 0.015	1.650 ± 0.250	0.500	7 ± 3	1 ± 1	4 ± 2	1 ± 1	1
XMMXCS J020056.81-092119.9	$0.322^{+0.075}_{-0.082}$	0.417 ± 0.095	-0.028 ± 0.019	1.810 ± 0.387	0.082	3 ± 2	3 ± 2	1 ± 1	2 ± 2	2
XMMXCS J020056.8-092119.8	$0.322^{+0.075}_{-0.082}$	0.417 ± 0.095	-0.028 ± 0.019	1.810 ± 0.387	0.082	3 ± 2	3 ± 2	1 ± 1	2 ± 2	2
XMMXCS J020119.03-064952.9	$0.331^{+0.082}_{-0.085}$	0.286 ± 0.086	-0.039 ± 0.024	2.010 ± 0.474	0.073	3 ± 2	4 ± 3	1 ± 1	0 ± 1	2
XMMXCS J020119.18-061724.3	$0.899^{+0.117}_{-0.121}$	0.992 ± 0.134	0.003 ± 0.025	0.701 ± 0.585	0.087	5 ± 3	2 ± 3	1 ± 2	3 ± 2	2
XMMXCS J020130.97-070349.5	$0.212^{+0.077}_{-0.078}$	0.279 ± 0.086	-0.112 ± 0.038	2.970 ± 0.743	0.124	2 ± 2	0 ± 1	1 ± 1	-	2
XMMXCS J020139.05-062256.7	$0.353^{+0.088}_{-0.089}$	0.301 ± 0.087	-0.022 ± 0.053	1.650 ± 1.090	0.123	17 ± 5	17 ± 5	18 ± 5	18 ± 5	2
XMMXCS J020140.52-050227.9	$0.750^{+0.126}_{-0.126}$	0.669 ± 0.109	-0.047 ± 0.019	1.470 ± 0.419	0.106	31 ± 7	31 ± 7	36 ± 9	38 ± 9	2
XMMXCS J020140.52-050205.6	$0.753^{+0.123}_{-0.123}$	0.669 ± 0.109	-0.051 ± 0.017	1.560 ± 0.368	0.105	33 ± 7	33 ± 7	35 ± 9	38 ± 9	2
XMMXCS J020155.93-063427.5	$0.194^{+0.080}_{-0.082}$	0.132 ± 0.076	-0.043 ± 0.016	1.470 ± 0.303	0.088	5 ± 3	2 ± 2	2 ± 2	0 ± 1	2

Continued on next page

Table A.4 – continued from previous page

name	z_{RS}	z_{BCG}	cmr_{grad}	cmr_{inter}	cmr_{wid}	n_{gals-c}	n_{gals-l}	n_{200-c}	n_{200-l}	qual
XMMXCS J020222.18-045443.1	$0.282^{+0.088}_{-0.086}$	0.224 ± 0.082	0.034 ± 0.032	-0.008 ± 0.602	0.069	1 ± 2	2 ± 2	1 ± 1	1 ± 1	2
XMMXCS J020232.0-073345.2	$0.551^{+0.101}_{-0.102}$	0.478 ± 0.098	-0.018 ± 0.016	1.330 ± 0.345	0.070	30 ± 6	30 ± 6	46 ± 7	46 ± 7	2
XMMXCS J020232.45-073346.7	$0.553^{+0.102}_{-0.102}$	0.478 ± 0.098	-0.020 ± 0.015	1.360 ± 0.329	0.070	30 ± 6	29 ± 6	46 ± 7	46 ± 7	2
XMMXCS J020304.85-070610.5	$0.334^{+0.087}_{-0.088}$	0.283 ± 0.086	-0.022 ± 0.020	1.690 ± 0.387	0.061	9 ± 3	11 ± 4	8 ± 3	10 ± 4	2
XMMXCS J020312.13-050642.7	$0.969^{+0.124}_{-0.121}$	0.910 ± 0.128	-0.017 ± 0.034	0.867 ± 0.779	0.083	10 ± 5	13 ± 5	11 ± 5	18 ± 6	2
XMMXCS J020319.9-073438.4	$0.593^{+0.104}_{-0.104}$	0.496 ± 0.099	-0.013 ± 0.018	1.290 ± 0.366	0.094	22 ± 5	23 ± 5	23 ± 6	22 ± 5	2
XMMXCS J020413.66-073421.0	$0.713^{+0.101}_{-0.089}$	0.651 ± 0.109	-0.026 ± 0.011	0.881 ± 0.242	0.078	2 ± 4	-	1 ± 2	-	2
XMMXCS J020423.62-050611.2	$0.300^{+0.087}_{-0.086}$	0.202 ± 0.080	0.089 ± 0.041	-1.030 ± 0.834	0.074	2 ± 2	2 ± 2	1 ± 1	0 ± 1	2
XMMXCS J020425.47-063828.4	$1.004^{+0.132}_{-0.132}$	0.944 ± 0.129	-0.013 ± 0.032	0.930 ± 0.737	0.130	32 ± 7	43 ± 8	58 ± 11	73 ± 12	2
XMMXCS J020440.69-073423.6	$0.926^{+0.102}_{-0.102}$	0.971 ± 0.131	-0.060 ± 0.052	1.850 ± 1.170	0.095	3 ± 5	4 ± 5	1 ± 2	4 ± 3	2
XMMXCS J020502.12-062441.2	$0.280^{+0.088}_{-0.081}$	0.180 ± 0.080	0.001 ± 0.045	1.030 ± 0.824	0.500	6 ± 4	10 ± 4	5 ± 3	4 ± 3	2
XMMXCS J020605.49-051129.5	$0.758^{+0.117}_{-0.117}$	0.661 ± 0.108	0.001 ± 0.024	0.405 ± 0.535	0.112	13 ± 5	19 ± 6	13 ± 6	19 ± 7	2
XMMXCS J020612.94-071217.1	$0.420^{+0.089}_{-0.091}$	0.324 ± 0.088	0.022 ± 0.031	0.883 ± 0.631	0.112	10 ± 4	12 ± 4	9 ± 4	12 ± 4	2
XMMXCS J020614.59-054407.5	$0.239^{+0.081}_{-0.082}$	0.210 ± 0.082	-0.043 ± 0.018	1.750 ± 0.311	0.067	4 ± 2	6 ± 3	2 ± 2	5 ± 3	2
XMMXCS J020623.58-053821.1	$0.670^{+0.106}_{-0.108}$	0.615 ± 0.107	0.006 ± 0.008	1.020 ± 0.174	0.075	9 ± 4	3 ± 3	7 ± 3	2 ± 2	2
XMMXCS J020702.77-072203.2	$0.875^{+0.123}_{-0.122}$	0.926 ± 0.129	0.027 ± 0.018	0.219 ± 0.389	0.035	7 ± 3	8 ± 3	5 ± 2	7 ± 3	2
XMMXCS J020710.19-072352.4	$0.143^{+0.049}_{-0.049}$	0.085 ± 0.055	0.036 ± 0.014	-0.098 ± 0.256	0.500	1 ± 1	0 ± 1	1 ± 1	-	2
XMMXCS J020755.76-055215.6	$0.748^{+0.125}_{-0.125}$	0.691 ± 0.111	-0.008 ± 0.009	0.396 ± 0.211	0.090	13 ± 5	13 ± 6	13 ± 6	10 ± 6	2
XMMXCS J020811.82-055803.5	$0.456^{+0.082}_{-0.081}$	0.443 ± 0.096	-0.015 ± 0.021	0.787 ± 0.451	0.092	5 ± 4	3 ± 4	2 ± 2	2 ± 2	2

Continued on next page

Table A.4 – continued from previous page

name	z_{RS}	z_{BCG}	cmr_{grad}	cmr_{inter}	cmr_{wid}	n_{gals-c}	n_{gals-l}	n_{200-c}	n_{200-l}	qual
XMMXCS J020904.27-051816.8	$0.568^{+0.086}_{-0.069}$	0.537 ± 0.101	0.002 ± 0.021	0.369 ± 0.452	0.090	3 ± 3	-	1 ± 1	-	2
XMMXCS J020914.07-035804.6	$0.338^{+0.084}_{-0.078}$	0.242 ± 0.082	0.003 ± 0.024	0.646 ± 0.480	0.070	1 ± 1	1 ± 2	1 ± 1	1 ± 1	2
XMMXCS J020922.25-062543.4	$0.550^{+0.102}_{-0.097}$	0.614 ± 0.106	-0.024 ± 0.065	1.220 ± 1.360	0.146	4 ± 4	4 ± 4	4 ± 3	5 ± 3	2
XMMXCS J020922.50-041206.2	$0.193^{+0.072}_{-0.076}$	0.153 ± 0.077	0.093 ± 0.036	-0.717 ± 0.693	0.094	1 ± 1	0 ± 1	1 ± 1	-	2
XMMXCS J020956.03-043751.0	$0.291^{+0.085}_{-0.085}$	0.235 ± 0.083	0.029 ± 0.033	0.691 ± 0.633	0.058	4 ± 2	9 ± 3	4 ± 2	9 ± 3	2
XMMXCS J021017.13-054326.9	$0.704^{+0.126}_{-0.125}$	0.649 ± 0.107	-0.048 ± 0.043	1.200 ± 1.010	0.105	2 ± 4	1 ± 4	3 ± 2	3 ± 2	2
XMMXCS J021024.48-061737.3	$0.902^{+0.120}_{-0.124}$	0.945 ± 0.130	-0.025 ± 0.014	1.150 ± 0.330	0.105	5 ± 4	7 ± 5	1 ± 2	3 ± 3	2
XMMXCS J021039.98-055642.2	$0.531^{+0.100}_{-0.101}$	0.465 ± 0.097	-0.044 ± 0.019	1.820 ± 0.398	0.062	19 ± 5	20 ± 5	22 ± 5	22 ± 5	2
XMMXCS J021043.73-063451.2	$0.095^{+0.058}_{-0.059}$	0.093 ± 0.060	-0.071 ± 0.027	1.820 ± 0.452	0.054	2 ± 2	0 ± 1	1 ± 1	-	2
XMMXCS J021059.55-095048.6	$0.772^{+0.117}_{-0.117}$	0.679 ± 0.111	-0.029 ± 0.016	1.040 ± 0.359	0.106	27 ± 7	33 ± 7	37 ± 9	50 ± 10	2
XMMXCS J021059.5-095048.6	$0.772^{+0.117}_{-0.117}$	0.679 ± 0.111	-0.029 ± 0.016	1.040 ± 0.359	0.106	27 ± 7	33 ± 7	37 ± 9	50 ± 10	2
XMMXCS J021102.63-055256.4	$0.882^{+0.103}_{-0.114}$	0.955 ± 0.128	0.035 ± 0.036	-0.007 ± 0.826	0.088	4 ± 3	5 ± 3	2 ± 2	-	2
XMMXCS J021105.29-051424.4	$0.830^{+0.114}_{-0.112}$	0.748 ± 0.114	-0.012 ± 0.011	0.557 ± 0.262	0.097	4 ± 5	5 ± 5	1 ± 3	3 ± 3	2
XMMXCS J021114.60-034356.1	$0.742^{+0.115}_{-0.114}$	0.805 ± 0.119	-0.009 ± 0.013	1.510 ± 0.291	0.086	29 ± 6	31 ± 6	35 ± 7	35 ± 7	2
XMMXCS J021151.79-050159.1	$0.353^{+0.086}_{-0.080}$	0.441 ± 0.095	-0.116 ± 0.079	2.720 ± 1.600	0.106	1 ± 3	2 ± 3	1 ± 1	1 ± 2	2
XMMXCS J021220.86-042015.0	$0.606^{+0.105}_{-0.105}$	0.533 ± 0.101	-0.088 ± 0.020	2.760 ± 0.421	0.108	12 ± 4	10 ± 4	12 ± 4	9 ± 4	2
XMMXCS J021225.5-054440.3	$0.677^{+0.108}_{-0.104}$	0.731 ± 0.113	-0.012 ± 0.015	0.518 ± 0.320	0.112	9 ± 5	6 ± 5	8 ± 4	5 ± 4	2
XMMXCS J021252.79-061205.7	$0.407^{+0.089}_{-0.091}$	0.353 ± 0.090	-0.014 ± 0.018	0.955 ± 0.357	0.055	14 ± 4	11 ± 4	13 ± 4	10 ± 4	2
XMMXCS J021254.19-041902.5	$0.958^{+0.133}_{-0.134}$	0.899 ± 0.124	0.032 ± 0.031	-0.252 ± 0.723	0.097	27 ± 7	30 ± 7	50 ± 10	68 ± 11	2

Continued on next page

Table A.4 – continued from previous page

name	z_{RS}	z_{BCG}	cmr_{grad}	cmr_{inter}	cmr_{wid}	n_{gals-c}	n_{gals-l}	n_{200-c}	n_{200-l}	qual
XMMXCS J021310.62-052005.8	$0.742^{+0.112}_{-0.111}$	0.690 ± 0.111	-0.014 ± 0.011	1.030 ± 0.239	0.108	17 ± 5	13 ± 5	21 ± 6	15 ± 5	2
XMMXCS J021329.09-081309.2	$1.115^{+0.138}_{-0.138}$	1.060 ± 0.136	0.015 ± 0.028	0.613 ± 0.642	0.044	3 ± 2	3 ± 2	2 ± 2	2 ± 2	2
XMMXCS J021346.00-041506.3	$1.044^{+0.138}_{-0.138}$	1.050 ± 0.134	0.013 ± 0.014	0.357 ± 0.329	0.105	7 ± 5	-	2 ± 3	-	2
XMMXCS J021346.4-055201.6	$0.956^{+0.130}_{-0.130}$	1.050 ± 0.135	-0.049 ± 0.042	1.800 ± 0.981	0.077	8 ± 4	9 ± 4	7 ± 3	8 ± 4	2
XMMXCS J021355.01-055121.1	$0.355^{+0.089}_{-0.089}$	0.337 ± 0.088	-0.087 ± 0.059	3.020 ± 1.130	0.112	7 ± 3	7 ± 3	2 ± 2	4 ± 2	2
XMMXCS J021358.96-054436.1	$0.365^{+0.088}_{-0.084}$	0.416 ± 0.094	0.0 ± -1.00	1.100 ± -1.00	0.500	7 ± 4	8 ± 4	5 ± 3	9 ± 4	2
XMMXCS J021451.70-052545.2	$0.742^{+0.109}_{-0.106}$	0.805 ± 0.117	-0.018 ± 0.015	0.617 ± 0.334	0.102	12 ± 5	13 ± 5	11 ± 5	13 ± 6	2
XMMXCS J021503.67-062417.1	$0.182^{+0.077}_{-0.076}$	0.102 ± 0.065	-0.003 ± 0.040	0.759 ± 0.743	0.117	4 ± 2	1 ± 2	1 ± 1	0 ± 1	2
XMMXCS J021530.86-042238.9	$0.718^{+0.112}_{-0.111}$	0.654 ± 0.107	-0.003 ± 0.020	0.675 ± 0.463	0.110	7 ± 4	5 ± 4	6 ± 3	2 ± 3	2
XMMXCS J021542.84-065418.0	$0.252^{+0.082}_{-0.083}$	0.239 ± 0.084	0.004 ± 0.013	1.030 ± 0.271	0.056	2 ± 2	2 ± 2	2 ± 1	2 ± 2	2
XMMXCS J021547.28-045031.4	$0.806^{+0.118}_{-0.118}$	0.892 ± 0.124	-0.069 ± 0.026	2.180 ± 0.604	0.104	6 ± 4	8 ± 4	5 ± 3	9 ± 4	2
XMMXCS J021628.9-035138.4	$0.839^{+0.116}_{-0.116}$	0.790 ± 0.119	-0.176 ± 0.069	4.160 ± 1.570	0.072	6 ± 4	17 ± 5	2 ± 3	25 ± 7	2
XMMXCS J021648.43-091832.2	$0.604^{+0.106}_{-0.105}$	0.654 ± 0.109	0.021 ± 0.020	0.624 ± 0.422	0.067	12 ± 4	14 ± 4	13 ± 4	14 ± 4	2
XMMXCS J021650.8-043600.9	$0.335^{+0.086}_{-0.087}$	0.278 ± 0.086	-0.005 ± 0.016	1.350 ± 0.324	0.092	6 ± 3	7 ± 3	4 ± 2	6 ± 3	2
XMMXCS J021659.3-044920.0	$0.548^{+0.098}_{-0.093}$	0.473 ± 0.097	-0.014 ± 0.045	0.909 ± 0.928	0.087	2 ± 3	-	4 ± 2	-	2
XMMXCS J021718.61-052922.3	$0.377^{+0.087}_{-0.088}$	0.281 ± 0.085	0.064 ± 0.028	0.009 ± 0.567	0.092	6 ± 3	6 ± 3	5 ± 2	6 ± 3	2
XMMXCS J021719.1-052917.1	$0.446^{+0.076}_{-0.076}$	0.444 ± 0.094	-0.052 ± 0.017	1.810 ± 0.357	0.093	2 ± 2	2 ± 2	1 ± 1	0 ± 1	2
XMMXCS J021724.1-051314.3	$0.687^{+0.109}_{-0.105}$	0.617 ± 0.105	-0.053 ± 0.013	1.370 ± 0.285	0.087	9 ± 5	7 ± 5	5 ± 4	2 ± 3	2
XMMXCS J021725.8-050936.4	$0.618^{+0.103}_{-0.102}$	0.543 ± 0.101	-0.019 ± 0.014	1.080 ± 0.293	0.088	12 ± 4	11 ± 4	14 ± 5	12 ± 4	2

Continued on next page

Table A.4 – continued from previous page

name	z_{RS}	z_{BCG}	cmr_{grad}	cmr_{inter}	cmr_{wid}	n_{gals-c}	n_{gals-l}	n_{200-c}	n_{200-l}	qual
XMMXCS J021727.25-044836.9	$0.861^{+0.102}_{-0.106}$	0.947 ± 0.130	-0.038 ± 0.025	1.510 ± 0.588	0.109	5 ± 4	6 ± 4	3 ± 3	6 ± 3	2
XMMXCS J021741.26-045144.1	$1.054^{+0.130}_{-0.134}$	0.975 ± 0.132	0.055 ± 0.031	-0.555 ± 0.734	0.084	9 ± 4	7 ± 4	7 ± 4	10 ± 4	2
XMMXCS J021743.43-034539.2	$1.052^{+0.138}_{-0.138}$	1.110 ± 0.137	0.001 ± 0.018	0.736 ± 0.420	0.096	8 ± 4	13 ± 5	6 ± 4	18 ± 6	2
XMMXCS J021754.95-045011.6	$0.978^{+0.138}_{-0.138}$	0.886 ± 0.135	-0.027 ± 0.035	1.200 ± 0.805	0.112	11 ± 5	12 ± 6	10 ± 5	12 ± 6	2
XMMXCS J021803.27-055527.7	$0.438^{+0.093}_{-0.097}$	0.352 ± 0.090	-0.006 ± 0.012	0.743 ± 0.248	0.073	7 ± 3	12 ± 4	7 ± 3	12 ± 4	2
XMMXCS J021803.8-055525.3	$0.703^{+0.114}_{-0.115}$	0.771 ± 0.116	0.009 ± 0.016	0.165 ± 0.347	0.066	14 ± 5	16 ± 5	15 ± 5	16 ± 6	2
XMMXCS J021809.32-044755.5	$0.586^{+0.096}_{-0.100}$	0.541 ± 0.102	-0.034 ± 0.023	1.680 ± 0.485	0.095	4 ± 3	2 ± 3	1 ± 1	-	2
XMMXCS J021831.36-041407.1	$0.437^{+0.098}_{-0.098}$	0.513 ± 0.101	-0.036 ± 0.018	1.160 ± 0.363	0.069	6 ± 3	6 ± 4	4 ± 2	2 ± 2	2
XMMXCS J021831.7-041351.4	$0.414^{+0.086}_{-0.088}$	0.513 ± 0.101	-0.009 ± 0.033	1.090 ± 0.653	0.117	4 ± 3	2 ± 3	5 ± 2	1 ± 2	2
XMMXCS J021837.90-054037.0	$0.348^{+0.085}_{-0.088}$	0.278 ± 0.086	-0.003 ± 0.016	1.300 ± 0.306	0.089	17 ± 4	12 ± 4	21 ± 5	12 ± 4	2
XMMXCS J021837.8-054037.0	$0.348^{+0.085}_{-0.088}$	0.278 ± 0.086	-0.003 ± 0.016	1.300 ± 0.306	0.089	17 ± 4	12 ± 4	21 ± 5	12 ± 4	2
XMMXCS J021843.72-053253.3	$0.407^{+0.092}_{-0.093}$	0.328 ± 0.088	0.010 ± 0.019	1.170 ± 0.383	0.078	13 ± 4	19 ± 5	13 ± 4	18 ± 5	2
XMMXCS J021855.7-053305.5	$0.501^{+0.093}_{-0.096}$	0.485 ± 0.099	-0.037 ± 0.015	1.270 ± 0.331	0.102	7 ± 4	6 ± 4	1 ± 2	2 ± 3	2
XMMXCS J021905.2-053657.6	$0.178^{+0.081}_{-0.082}$	0.132 ± 0.076	-0.017 ± 0.031	1.090 ± 0.539	0.120	3 ± 2	2 ± 2	1 ± 1	0 ± 1	2
XMMXCS J021911.83-045056.6	$1.129^{+0.152}_{-0.152}$	1.080 ± 0.134	-0.021 ± 0.117	1.420 ± 2.770	0.137	15 ± 5	14 ± 5	16 ± 5	14 ± 5	2
XMMXCS J021930.7-044950.4	$1.152^{+0.153}_{-0.158}$	1.060 ± 0.136	0.009 ± 0.015	0.654 ± 0.342	0.111	10 ± 4	10 ± 4	7 ± 4	7 ± 4	2
XMMXCS J021939.41-040025.0	$0.844^{+0.118}_{-0.119}$	0.894 ± 0.124	-0.035 ± 0.031	1.690 ± 0.707	0.086	6 ± 3	-	2 ± 2	-	2
XMMXCS J021951.9-035604.8	$0.885^{+0.132}_{-0.132}$	0.856 ± 0.121	-0.019 ± 0.010	0.909 ± 0.232	0.104	7 ± 5	5 ± 5	2 ± 4	3 ± 3	2
XMMXCS J021958.6-045219.7	$0.925^{+0.125}_{-0.125}$	0.826 ± 0.121	-0.022 ± 0.017	1.140 ± 0.388	0.105	11 ± 5	12 ± 5	9 ± 5	12 ± 5	2

Continued on next page

Table A.4 – continued from previous page

name	z_{RS}	z_{BCG}	cmr_{grad}	cmr_{inter}	cmr_{wid}	n_{gals-c}	n_{gals-l}	n_{200-c}	n_{200-l}	qual
XMMXCS J021958.8-052343.5	$0.167^{+0.079}_{-0.078}$	0.093 ± 0.060	0.045 ± 0.021	-0.234 ± 0.375	0.080	3 ± 2	4 ± 2	1 ± 1	2 ± 2	2
XMMXCS J022042.64-052549.9	$0.481^{+0.112}_{-0.113}$	0.423 ± 0.105	-0.000 ± 0.021	0.420 ± 0.436	0.069	6 ± 3	5 ± 3	5 ± 3	2 ± 2	2
XMMXCS J022129.25-040554.1	$0.875^{+0.122}_{-0.122}$	0.804 ± 0.119	0.044 ± 0.015	-0.100 ± 0.332	0.064	11 ± 4	10 ± 4	11 ± 4	8 ± 3	2
XMMXCS J022129.4-040540.5	$0.892^{+0.124}_{-0.124}$	0.804 ± 0.119	0.048 ± 0.013	-0.194 ± 0.305	0.062	11 ± 4	11 ± 4	11 ± 4	11 ± 4	2
XMMXCS J022153.2-054447.1	$0.782^{+0.121}_{-0.121}$	0.865 ± 0.121	-0.041 ± 0.015	1.330 ± 0.328	0.100	17 ± 6	18 ± 6	18 ± 6	23 ± 7	2
XMMXCS J022159.6-054322.8	$0.794^{+0.120}_{-0.120}$	0.728 ± 0.114	-0.020 ± 0.011	0.870 ± 0.255	0.101	21 ± 6	21 ± 6	36 ± 8	33 ± 8	2
XMMXCS J022201.7-054330.4	$0.807^{+0.121}_{-0.121}$	0.728 ± 0.114	-0.011 ± 0.011	0.665 ± 0.258	0.102	30 ± 7	29 ± 7	41 ± 9	95 ± 12	2
XMMXCS J022204.3-043239.6	$0.339^{+0.088}_{-0.088}$	0.251 ± 0.084	-0.013 ± 0.034	1.480 ± 0.664	0.109	11 ± 4	13 ± 4	11 ± 4	14 ± 4	2
XMMXCS J022204.54-043246.3	$0.337^{+0.088}_{-0.088}$	0.251 ± 0.084	-0.006 ± 0.035	1.340 ± 0.693	0.110	12 ± 4	13 ± 4	12 ± 4	14 ± 4	2
XMMXCS J022213.84-034559.8	$0.495^{+0.084}_{-0.076}$	0.443 ± 0.095	0.025 ± 0.018	0.106 ± 0.384	0.095	3 ± 3	5 ± 3	1 ± 1	3 ± 2	2
XMMXCS J022227.58-035244.6	$0.356^{+0.083}_{-0.076}$	0.426 ± 0.096	-0.007 ± 0.008	0.704 ± 0.159	0.500	8 ± 4	6 ± 4	4 ± 3	-	2
XMMXCS J022231.0-042639.1	$0.580^{+0.091}_{-0.100}$	0.513 ± 0.099	-0.030 ± 0.023	1.410 ± 0.498	0.108	6 ± 3	4 ± 3	4 ± 2	3 ± 2	2
XMMXCS J022242.6-043018.4	$0.861^{+0.122}_{-0.121}$	0.773 ± 0.116	-0.014 ± 0.010	0.727 ± 0.223	0.103	7 ± 5	8 ± 5	1 ± 3	27 ± 6	2
XMMXCS J022302.54-043619.6	$0.929^{+0.125}_{-0.125}$	1.010 ± 0.135	0.012 ± 0.038	0.472 ± 0.860	0.099	12 ± 5	11 ± 4	12 ± 5	10 ± 4	2
XMMXCS J022317.88-052012.6	$0.841^{+0.152}_{-0.157}$	0.915 ± 0.124	-0.008 ± 0.025	0.590 ± 0.571	0.117	11 ± 5	13 ± 6	12 ± 5	13 ± 6	2
XMMXCS J022318.30-051209.8	$0.384^{+0.091}_{-0.091}$	0.319 ± 0.088	-0.100 ± 0.021	3.140 ± 0.377	0.055	7 ± 3	8 ± 3	5 ± 2	7 ± 3	2
XMMXCS J022319.6-051957.2	$0.669^{+0.143}_{-0.168}$	0.673 ± 0.111	-0.160 ± 0.223	3.700 ± 5.030	0.068	5 ± 3	4 ± 3	1 ± 2	1 ± 2	2
XMMXCS J022348.2-051348.0	$0.717^{+0.097}_{-0.105}$	0.707 ± 0.113	-0.024 ± 0.034	1.250 ± 0.766	0.104	3 ± 3	3 ± 4	2 ± 2	-	2
XMMXCS J022401.09-050542.2	$0.323^{+0.085}_{-0.086}$	0.322 ± 0.088	-0.033 ± 0.019	2.010 ± 0.373	0.070	4 ± 2	4 ± 3	1 ± 1	1 ± 2	2

Continued on next page

Table A.4 – continued from previous page

name	z_{RS}	z_{BCG}	cmr_{grad}	cmr_{inter}	cmr_{wid}	n_{gals-c}	n_{gals-l}	n_{200-c}	n_{200-l}	qual
XMMXCS J022401.9-050528.4	$0.325^{+0.085}_{-0.087}$	0.322 ± 0.088	-0.030 ± 0.015	1.940 ± 0.292	0.061	6 ± 3	5 ± 3	2 ± 2	2 ± 2	2
XMMXCS J022403.6-041912.9	$0.855^{+0.128}_{-0.128}$	0.774 ± 0.118	-0.007 ± 0.013	0.613 ± 0.307	0.095	13 ± 5	14 ± 5	15 ± 6	17 ± 6	2
XMMXCS J022421.2-040356.1	$0.544^{+0.282}_{-0.160}$	0.603 ± 0.105	-0.013 ± 0.001	1.060 ± 0.001	0.500	8 ± 4	4 ± 4	4 ± 3	6 ± 3	2
XMMXCS J022424.2-040109.6	$0.789^{+0.136}_{-0.136}$	0.803 ± 0.117	-0.025 ± 0.038	0.913 ± 0.854	0.099	2 ± 4	1 ± 4	2 ± 2	3 ± 2	2
XMMXCS J022426.9-040043.0	$0.308^{+0.086}_{-0.085}$	0.254 ± 0.084	-0.057 ± 0.100	2.180 ± 1.950	0.084	2 ± 2	1 ± 2	3 ± 2	1 ± 1	2
XMMXCS J022443.5-044522.7	$0.736^{+0.108}_{-0.102}$	0.825 ± 0.121	-0.045 ± 0.059	1.740 ± 1.330	0.067	4 ± 3	3 ± 3	5 ± 2	3 ± 2	2
XMMXCS J022452.1-040520.7	$0.804^{+0.112}_{-0.108}$	0.751 ± 0.117	-0.014 ± 0.009	0.646 ± 0.198	0.095	12 ± 5	14 ± 5	13 ± 5	12 ± 5	2
XMMXCS J022452.21-040519.9	$0.806^{+0.114}_{-0.110}$	0.751 ± 0.117	-0.019 ± 0.011	0.754 ± 0.249	0.093	12 ± 5	13 ± 5	13 ± 5	11 ± 5	2
XMMXCS J022455.8-050809.6	$0.128^{+0.072}_{-0.073}$	0.122 ± 0.075	0.022 ± 0.011	0.409 ± 0.179	0.033	1 ± 1	2 ± 2	1 ± 1	1 ± 1	2
XMMXCS J022457.31-034859.1	$0.620^{+0.106}_{-0.107}$	0.524 ± 0.101	0.009 ± 0.025	0.991 ± 0.526	0.073	18 ± 5	25 ± 5	21 ± 5	30 ± 6	2
XMMXCS J022457.8-034851.1	$0.621^{+0.106}_{-0.107}$	0.524 ± 0.101	-0.004 ± 0.023	1.170 ± 0.482	0.100	28 ± 6	22 ± 5	31 ± 6	26 ± 6	2
XMMXCS J022529.1-041519.6	$0.712^{+0.130}_{-0.168}$	0.657 ± 0.109	-0.021 ± 0.014	1.090 ± 0.317	0.101	3 ± 3	8 ± 4	4 ± 2	9 ± 4	2
XMMXCS J022538.7-042153.2	$0.191^{+0.080}_{-0.080}$	0.132 ± 0.076	0.029 ± 0.023	0.344 ± 0.388	0.093	3 ± 2	3 ± 3	2 ± 2	2 ± 2	2
XMMXCS J022549.02-055339.3	$0.300^{+0.085}_{-0.086}$	0.229 ± 0.083	-0.006 ± 0.037	1.250 ± 0.726	0.094	14 ± 4	12 ± 4	13 ± 4	12 ± 4	2
XMMXCS J022549.0-055339.2	$0.300^{+0.085}_{-0.086}$	0.229 ± 0.083	-0.006 ± 0.037	1.250 ± 0.726	0.094	14 ± 4	12 ± 4	13 ± 4	12 ± 4	2
XMMXCS J022549.58-055338.1	$0.297^{+0.085}_{-0.086}$	0.229 ± 0.083	-0.053 ± 0.029	2.110 ± 0.562	0.061	15 ± 4	13 ± 4	16 ± 4	13 ± 4	2
XMMXCS J022607.69-040314.3	$0.227^{+0.078}_{-0.080}$	0.321 ± 0.088	-0.065 ± 0.044	2.130 ± 0.818	0.088	3 ± 2	2 ± 2	1 ± 1	0 ± 1	2
XMMXCS J022627.42-043711.8	$0.547^{+0.091}_{-0.097}$	0.610 ± 0.105	-0.053 ± 0.013	2.030 ± 0.266	0.029	2 ± 2	1 ± 2	1 ± 1	0 ± 1	2
XMMXCS J022627.7-034156.4	$0.350^{+0.050}_{-0.069}$	0.287 ± 0.086	-0.036 ± 0.013	1.180 ± 0.268	0.078	2 ± 3	2 ± 3	2 ± 2	3 ± 2	2

Continued on next page

Table A.4 – continued from previous page

name	z_{RS}	z_{BCG}	cmr_{grad}	cmr_{inter}	cmr_{wid}	n_{gals-c}	n_{gals-l}	n_{200-c}	n_{200-l}	qual
XMMXCS J022630.88-034236.3	$0.324^{+0.087}_{-0.087}$	0.287 ± 0.086	-0.014 ± 0.025	1.470 ± 0.502	0.093	3 ± 2	2 ± 2	2 ± 2	2 ± 2	2
XMMXCS J022639.07-053758.8	$0.338^{+0.089}_{-0.088}$	0.298 ± 0.086	0.050 ± 0.158	-0.256 ± 3.130	0.109	6 ± 3	5 ± 3	2 ± 2	1 ± 2	2
XMMXCS J022648.0-041422.5	$0.720^{+0.113}_{-0.112}$	0.632 ± 0.106	-0.029 ± 0.031	1.390 ± 0.684	0.090	12 ± 4	13 ± 5	13 ± 5	13 ± 5	2
XMMXCS J022702.06-040512.4	$0.718^{+0.113}_{-0.114}$	0.652 ± 0.108	-0.043 ± 0.025	1.360 ± 0.559	0.092	9 ± 5	10 ± 5	10 ± 4	10 ± 5	2
XMMXCS J022706.03-041419.9	$0.811^{+0.127}_{-0.127}$	0.888 ± 0.123	-0.028 ± 0.017	1.140 ± 0.400	0.100	3 ± 4	2 ± 4	2 ± 2	1 ± 2	2
XMMXCS J022706.1-041418.7	$0.809^{+0.126}_{-0.126}$	0.888 ± 0.123	-0.028 ± 0.017	1.140 ± 0.400	0.100	2 ± 4	2 ± 4	1 ± 2	1 ± 2	2
XMMXCS J022709.5-041805.0	$0.944^{+0.126}_{-0.127}$	1.010 ± 0.133	-0.022 ± 0.053	1.210 ± 1.220	0.124	16 ± 5	20 ± 6	20 ± 6	19 ± 6	2
XMMXCS J022722.0-045226.1	$0.386^{+0.083}_{-0.082}$	0.419 ± 0.094	0.046 ± 0.046	0.355 ± 0.909	0.111	5 ± 3	5 ± 3	1 ± 1	2 ± 2	2
XMMXCS J022725.1-041125.8	$0.726^{+0.124}_{-0.125}$	0.786 ± 0.117	-5.610 ± 0.007	124 ± 0.148	0.500	7 ± 3	1 ± 1	4 ± 2	-	2
XMMXCS J022746.0-044518.3	$0.962^{+0.129}_{-0.129}$	0.905 ± 0.124	-0.038 ± 0.013	1.450 ± 0.308	0.097	7 ± 5	9 ± 5	3 ± 3	6 ± 4	2
XMMXCS J022801.28-085857.9	$0.503^{+0.098}_{-0.099}$	0.447 ± 0.096	-0.017 ± 0.008	1.210 ± 0.159	0.053	25 ± 5	24 ± 5	33 ± 6	28 ± 6	2
XMMXCS J022804.6-041818.6	$0.361^{+0.085}_{-0.086}$	0.422 ± 0.095	-0.022 ± 0.016	0.976 ± 0.314	0.068	6 ± 3	6 ± 3	3 ± 2	3 ± 2	2
XMMXCS J022811.29-041140.6	$0.824^{+0.119}_{-0.117}$	0.804 ± 0.120	-0.037 ± 0.012	1.070 ± 0.275	0.049	3 ± 3	5 ± 4	2 ± 2	6 ± 3	2
XMMXCS J022812.5-100538.3	$0.175^{+0.077}_{-0.077}$	0.249 ± 0.084	-0.037 ± 0.012	1.610 ± 0.225	0.035	5 ± 2	4 ± 2	3 ± 2	4 ± 2	2
XMMXCS J022828.2-040045.7	$0.413^{+0.084}_{-0.088}$	0.323 ± 0.088	-0.009 ± 0.008	0.714 ± 0.159	0.086	9 ± 4	15 ± 5	6 ± 3	15 ± 5	2
XMMXCS J022828.2-040045.6	$0.413^{+0.084}_{-0.088}$	0.323 ± 0.088	-0.009 ± 0.008	0.714 ± 0.159	0.086	9 ± 4	15 ± 5	6 ± 3	15 ± 5	2
XMMXCS J022849.5-100205.5	$0.550^{+0.103}_{-0.103}$	0.462 ± 0.097	-0.003 ± 0.015	0.947 ± 0.309	0.065	13 ± 4	14 ± 4	13 ± 4	14 ± 4	2
XMMXCS J022929.14-040846.7	$0.903^{+0.121}_{-0.121}$	0.821 ± 0.121	0.002 ± 0.016	0.438 ± 0.379	0.063	11 ± 5	12 ± 5	12 ± 5	12 ± 5	2
XMMXCS J023005.70-050814.3	$0.185^{+0.089}_{-0.089}$	0.141 ± 0.077	-0.153 ± 0.062	3.510 ± 1.100	0.081	1 ± 2	1 ± 2	1 ± 1	1 ± 1	2

Continued on next page

Table A.4 – continued from previous page

name	z_{RS}	z_{BCG}	cmr_{grad}	cmr_{inter}	cmr_{wid}	n_{gals-c}	n_{gals-l}	n_{200-c}	n_{200-l}	qual
XMMXCS J023035.12-043801.9	$0.282^{+0.085}_{-0.085}$	0.288 ± 0.086	-0.063 ± 0.021	2.380 ± 0.392	0.044	4 ± 2	4 ± 2	2 ± 1	1 ± 1	2
XMMXCS J023036.08-041446.0	$0.407^{+0.092}_{-0.091}$	0.461 ± 0.097	-0.116 ± 0.019	3.500 ± 0.410	0.071	4 ± 2	3 ± 2	2 ± 2	3 ± 2	2
XMMXCS J023052.30-045121.9	$0.302^{+0.086}_{-0.086}$	0.268 ± 0.086	-0.036 ± 0.024	1.800 ± 0.447	0.118	2 ± 2	4 ± 3	1 ± 1	5 ± 3	2
XMMXCS J023052.60-042117.6	$0.161^{+0.077}_{-0.077}$	0.141 ± 0.077	-0.016 ± 0.021	1.060 ± 0.356	0.076	4 ± 2	3 ± 2	1 ± 1	1 ± 1	2
XMMXCS J023055.24-050851.7	$0.586^{+0.103}_{-0.104}$	0.500 ± 0.099	0.006 ± 0.027	0.880 ± 0.576	0.104	4 ± 3	27 ± 6	1 ± 1	31 ± 6	2
XMMXCS J023057.21-044252.5	$0.226^{+0.081}_{-0.081}$	0.188 ± 0.080	-0.003 ± 0.015	0.814 ± 0.285	0.105	4 ± 2	3 ± 2	1 ± 1	1 ± 1	2
XMMXCS J023110.88-044010.3	$1.292^{+0.188}_{-0.192}$	1.350 ± 0.154	0.019 ± 0.033	0.056 ± 0.776	0.085	1 ± 2	2 ± 2	1 ± 1	2 ± 2	2
XMMXCS J023145.4-044534.6	$0.195^{+0.071}_{-0.076}$	0.200 ± 0.081	-0.028 ± 0.011	1.480 ± 0.199	0.043	2 ± 2	4 ± 2	2 ± 1	2 ± 2	2
XMMXCS J023150.20-054106.3	$0.349^{+0.088}_{-0.088}$	0.291 ± 0.086	-0.043 ± 0.027	2.160 ± 0.540	0.069	4 ± 2	4 ± 3	3 ± 2	3 ± 2	2
XMMXCS J023204.92-053309.4	$0.582^{+0.102}_{-0.103}$	0.516 ± 0.100	-0.029 ± 0.014	1.630 ± 0.301	0.079	18 ± 5	22 ± 5	22 ± 5	27 ± 6	2
XMMXCS J023208.99-040943.4	$0.675^{+0.113}_{-0.108}$	0.616 ± 0.105	0.025 ± 0.015	0.134 ± 0.327	0.094	2 ± 3	2 ± 3	1 ± 1	1 ± 2	2
XMMXCS J023234.4-073104.0	$0.352^{+0.087}_{-0.086}$	0.261 ± 0.085	0.277 ± 0.001	-4.470 ± 0.001	0.500	9 ± 4	10 ± 4	8 ± 4	11 ± 4	2
XMMXCS J023301.41-052317.4	$1.031^{+0.129}_{-0.131}$	1.070 ± 0.138	-0.040 ± 0.047	1.790 ± 1.120	0.114	4 ± 3	6 ± 4	2 ± 2	3 ± 3	2
XMMXCS J023346.0-085048.5	$0.275^{+0.084}_{-0.084}$	0.210 ± 0.082	0.011 ± 0.019	0.987 ± 0.372	0.042	15 ± 4	17 ± 4	16 ± 4	18 ± 5	2
XMMXCS J023424.50-051057.6	$0.217^{+0.078}_{-0.074}$	0.153 ± 0.077	-0.692 ± 0.047	13.900 ± 0.901	0.500	3 ± 3	2 ± 3	1 ± 1	2 ± 2	2
XMMXCS J023440.47-052222.8	$0.402^{+0.071}_{-0.067}$	0.325 ± 0.087	0.013 ± 0.017	0.275 ± 0.338	0.106	1 ± 3	0 ± 3	2 ± 1	-	2
XMMXCS J085253.54-013642.5	$0.347^{+0.088}_{-0.089}$	0.278 ± 0.086	-0.010 ± 0.014	1.530 ± 0.278	0.079	17 ± 4	13 ± 4	18 ± 5	13 ± 4	2
XMMXCS J085301.38-015050.9	$0.675^{+0.108}_{-0.107}$	0.580 ± 0.103	-0.070 ± 0.031	2.390 ± 0.694	0.108	10 ± 4	10 ± 4	9 ± 4	9 ± 4	2
XMMXCS J085511.46-052324.5	$0.106^{+0.064}_{-0.064}$	0.102 ± 0.065	-0.033 ± 0.053	1.050 ± 0.944	0.067	2 ± 1	0 ± 1	1 ± 1	-	2

Continued on next page

Table A.4 – continued from previous page

name	z_{RS}	z_{BCG}	cmr_{grad}	cmr_{inter}	cmr_{wid}	n_{gals-c}	n_{gals-l}	n_{200-c}	n_{200-l}	qual
XMMXCS J090137.37-015432.8	$0.324^{+0.087}_{-0.087}$	0.381 ± 0.092	-0.015 ± 0.028	1.510 ± 0.536	0.094	11 ± 4	13 ± 4	11 ± 4	15 ± 4	2
XMMXCS J141647.98+522600.2	$0.988^{+0.132}_{-0.132}$	0.991 ± 0.134	0.052 ± 0.021	-0.275 ± 0.473	0.054	4 ± 2	3 ± 2	2 ± 2	2 ± 2	2
XMMXCS J141647.9+522600.1	$0.988^{+0.132}_{-0.132}$	0.991 ± 0.134	0.052 ± 0.021	-0.275 ± 0.473	0.054	4 ± 2	3 ± 2	2 ± 2	2 ± 2	2
XMMXCS J141652.4+522052.9	$0.370^{+0.088}_{-0.086}$	0.327 ± 0.088	-0.054 ± 0.016	1.430 ± 0.315	0.077	5 ± 3	8 ± 4	1 ± 2	8 ± 4	2
XMMXCS J141731.73+523200.3	$0.519^{+0.065}_{-0.065}$	0.505 ± 0.099	-0.042 ± 0.014	1.330 ± 0.294	0.089	5 ± 3	3 ± 3	2 ± 2	1 ± 2	2
XMMXCS J141731.7+523200.2	$0.519^{+0.065}_{-0.065}$	0.505 ± 0.099	-0.042 ± 0.014	1.330 ± 0.294	0.089	5 ± 3	3 ± 3	2 ± 2	1 ± 2	2
XMMXCS J141749.58+522816.1	$0.812^{+0.120}_{-0.119}$	0.729 ± 0.113	-0.024 ± 0.011	0.885 ± 0.241	0.102	14 ± 6	11 ± 6	27 ± 7	11 ± 6	2
XMMXCS J141749.5+522816.0	$0.812^{+0.120}_{-0.119}$	0.729 ± 0.113	-0.024 ± 0.011	0.885 ± 0.241	0.102	14 ± 6	11 ± 6	27 ± 7	11 ± 6	2
XMMXCS J220059.13+012544.0	$0.674^{+0.099}_{-0.092}$	0.610 ± 0.105	-0.042 ± 0.012	1.120 ± 0.253	0.099	2 ± 3	0 ± 3	1 ± 2	-	2
XMMXCS J221424.97+001208.3	$0.406^{+0.082}_{-0.088}$	0.484 ± 0.099	-0.048 ± 0.021	2.270 ± 0.426	0.106	4 ± 3	1 ± 2	1 ± 1	0 ± 1	2
XMMXCS J221456.8+004317.9	$0.840^{+0.092}_{-0.075}$	0.744 ± 0.114	0.082 ± 0.062	-1.360 ± 1.430	0.073	2 ± 4	-	2 ± 2	-	2
XMMXCS J221508.14+003513.5	$0.368^{+0.088}_{-0.089}$	0.318 ± 0.087	0.006 ± 0.018	1.220 ± 0.369	0.073	6 ± 3	7 ± 3	6 ± 3	7 ± 3	2
XMMXCS J221525.43+004424.4	$0.144^{+0.071}_{-0.071}$	0.151 ± 0.077	-0.006 ± 0.024	0.631 ± 0.424	0.086	2 ± 2	0 ± 1	1 ± 1	-	2
XMMXCS J221608.82+001105.9	$0.169^{+0.083}_{-0.085}$	0.122 ± 0.075	-0.032 ± 0.044	1.240 ± 0.818	0.106	2 ± 2	0 ± 1	1 ± 1	-	2
XMMXCS J221654.0+002415.9	$0.967^{+0.117}_{-0.107}$	0.906 ± 0.127	-0.011 ± 0.018	0.709 ± 0.398	0.098	5 ± 5	6 ± 5	1 ± 3	5 ± 4	2
XMMXCS J221705.50+002634.0	$0.356^{+0.066}_{-0.082}$	0.296 ± 0.105	-0.045 ± 0.011	1.330 ± 0.231	0.096	4 ± 3	1 ± 3	1 ± 2	-	2
XMMXCS J221725.9+002807.6	$0.839^{+0.110}_{-0.106}$	0.767 ± 0.117	-0.007 ± 0.024	0.503 ± 0.542	0.091	4 ± 5	-	2 ± 3	-	2
XMMXCS J221748.1+001228.2	$0.788^{+0.143}_{-0.167}$	0.710 ± 0.113	-0.017 ± 0.013	0.596 ± 0.308	0.079	8 ± 5	9 ± 5	6 ± 4	7 ± 4	2
XMMXCS J221755.1+002910.6	$0.661^{+0.096}_{-0.091}$	0.595 ± 0.105	-0.008 ± 0.025	0.922 ± 0.541	0.115	5 ± 4	1 ± 4	3 ± 3	0 ± 1	2

Continued on next page

Table A.4 – continued from previous page

name	z_{RS}	z_{BCG}	cmr_{grad}	cmr_{inter}	cmr_{wid}	n_{gals-c}	n_{gals-l}	n_{200-c}	n_{200-l}	qual
XMMXCS J221805.2+001242.0	$1.016^{+0.121}_{-0.113}$	0.961 ± 0.130	0.054 ± 0.039	-0.694 ± 0.911	0.084	13 ± 5	16 ± 5	13 ± 5	19 ± 6	2
XMMXCS J221809.0+002721.4	$0.827^{+0.108}_{-0.098}$	0.734 ± 0.114	-0.036 ± 0.026	1.060 ± 0.590	0.104	8 ± 5	10 ± 5	5 ± 4	8 ± 5	2
XMMXCS J221811.77+002648.6	$0.808^{+0.103}_{-0.092}$	0.716 ± 0.113	0.051 ± 0.046	-0.745 ± 1.020	0.094	5 ± 5	-	10 ± 4	-	2
XMMXCS J221830.29+001213.7	$0.296^{+0.086}_{-0.086}$	0.274 ± 0.086	-0.027 ± 0.035	1.570 ± 0.657	0.100	6 ± 3	5 ± 3	2 ± 2	3 ± 2	2
XMMXCS J221830.2+001213.6	$0.296^{+0.086}_{-0.086}$	0.274 ± 0.086	-0.027 ± 0.035	1.570 ± 0.657	0.100	6 ± 3	5 ± 3	2 ± 2	3 ± 2	2
XMMXCS J222117.15-010037.0	$0.345^{+0.089}_{-0.089}$	0.290 ± 0.086	-0.024 ± 0.018	1.710 ± 0.341	0.072	8 ± 3	7 ± 3	4 ± 2	5 ± 3	2
XMMXCS J020115.6-091928.0	$0.833^{+0.115}_{-0.118}$	0.769 ± 0.118	-0.023 ± 0.016	1.320 ± 0.365	0.089	4 ± 3	2 ± 2	0 ± 1	-	3
XMMXCS J020115.5-091927.9	$0.833^{+0.115}_{-0.118}$	0.769 ± 0.118	-0.023 ± 0.016	1.320 ± 0.365	0.089	4 ± 3	2 ± 2	0 ± 1	-	3
XMMXCS J020156.2-052058.7	$0.348^{+0.088}_{-0.088}$	0.248 ± 0.083	-0.001 ± 0.040	1.130 ± 0.781	0.099	5 ± 3	5 ± 3	5 ± 2	8 ± 3	3
XMMXCS J020202.46-062850.5	$0.364^{+0.088}_{-0.081}$	0.233 ± 0.083	-0.094 ± 0.016	2.240 ± 0.311	0.070	6 ± 3	5 ± 4	3 ± 2	3 ± 3	3
XMMXCS J020214.9-074142.2	$1.201^{+0.137}_{-0.132}$	1.330 ± 0.151	-0.117 ± 0.085	3.420 ± 2.000	0.103	4 ± 4	2 ± 4	2 ± 2	-	3
XMMXCS J020303.11-051813.2	$0.107^{+0.065}_{-0.065}$	0.102 ± 0.065	-0.043 ± 0.051	1.340 ± 0.862	0.072	1 ± 1	0 ± 1	1 ± 1	-	3
XMMXCS J020318.46-043956.8	$0.642^{+0.103}_{-0.101}$	0.578 ± 0.105	0.066 ± 0.047	-1.060 ± 1.040	0.059	0 ± 0.1	1 ± 2	-	1 ± 1	3
XMMXCS J020340.0-073633.5	$0.751^{+0.115}_{-0.113}$	0.607 ± 0.105	-0.029 ± 0.121	0.638 ± 2.720	0.088	4 ± 3	5 ± 3	2 ± 2	4 ± 2	3
XMMXCS J020342.24-050722.9	$0.514^{+0.094}_{-0.094}$	0.390 ± 0.092	0.035 ± 0.022	0.042 ± 0.473	0.113	23 ± 5	25 ± 6	27 ± 6	30 ± 7	3
XMMXCS J020344.4-073739.5	$0.836^{+0.122}_{-0.122}$	0.724 ± 0.113	-0.023 ± 0.023	0.642 ± 0.513	0.110	7 ± 5	6 ± 5	6 ± 4	14 ± 5	3
XMMXCS J020353.16-060735.4	$0.878^{+0.118}_{-0.112}$	0.733 ± 0.113	-0.033 ± 0.038	1.040 ± 0.872	0.102	9 ± 6	14 ± 6	8 ± 5	13 ± 6	3
XMMXCS J020411.60-051034.3	$0.366^{+0.085}_{-0.078}$	0.204 ± 0.080	-0.005 ± 0.018	0.649 ± 0.361	0.084	7 ± 4	8 ± 4	7 ± 3	7 ± 3	3
XMMXCS J020414.20-072508.2	$0.267^{+0.090}_{-0.089}$	0.252 ± 0.100	-0.053 ± 0.016	1.650 ± 0.319	0.042	1 ± 1	0 ± 1	0 ± 0.1	-	3

Continued on next page

Table A.4 – continued from previous page

name	z_{RS}	z_{BCG}	cmr_{grad}	cmr_{inter}	cmr_{wid}	n_{gals-c}	n_{gals-l}	n_{200-c}	n_{200-l}	qual
XMMXCS J020423.79-073527.1	$0.637^{+0.108}_{-0.103}$	0.528 ± 0.101	-0.037 ± 0.013	1.560 ± 0.270	0.094	4 ± 3	1 ± 3	0 ± 1	5 ± 3	3
XMMXCS J020429.21-060131.0	$0.605^{+0.103}_{-0.103}$	0.488 ± 0.097	0.010 ± 0.015	0.264 ± 0.311	0.071	8 ± 3	6 ± 3	4 ± 3	4 ± 3	3
XMMXCS J020439.65-042752.2	$0.615^{+0.104}_{-0.104}$	0.549 ± 0.102	-0.040 ± 0.016	1.620 ± 0.343	0.082	2 ± 3	2 ± 3	0 ± 1	1 ± 2	3
XMMXCS J020446.66-072111.8	$0.380^{+0.077}_{-0.085}$	0.274 ± 0.090	-0.024 ± 0.016	1.270 ± 0.325	0.103	2 ± 2	4 ± 3	0 ± 0.1	2 ± 2	3
XMMXCS J020456.65-073823.9	$0.592^{+0.119}_{-0.119}$	0.704 ± 0.113	0.029 ± 0.026	0.132 ± 0.570	0.106	8 ± 4	7 ± 4	10 ± 4	10 ± 4	3
XMMXCS J020525.15-073541.6	$0.422^{+0.087}_{-0.091}$	0.445 ± 0.096	0.005 ± 0.013	1.350 ± 0.270	0.068	4 ± 3	2 ± 2	0 ± 0.1	0 ± 1	3
XMMXCS J020530.88-043621.2	$0.684^{+0.120}_{-0.119}$	0.528 ± 0.101	-0.029 ± 0.007	0.979 ± 0.149	0.094	9 ± 5	9 ± 5	6 ± 4	11 ± 5	3
XMMXCS J020538.36-051255.1	$0.449^{+0.095}_{-0.095}$	0.499 ± 0.099	-0.044 ± 0.034	2.370 ± 0.671	0.048	0 ± 1	1 ± 2	-	0 ± 1	3
XMMXCS J020547.23-070149.4	$1.128^{+0.130}_{-0.123}$	1.090 ± 0.180	0.009 ± 0.019	0.432 ± 0.448	0.105	0 ± 4	3 ± 4	-	1 ± 2	3
XMMXCS J020555.29-040544.8	$0.404^{+0.092}_{-0.079}$	0.310 ± 0.086	0.171 ± 0.001	-2.370 ± 0.001	0.500	1 ± 3	0 ± 3	0 ± 1	-	3
XMMXCS J020605.21-063306.4	$0.421^{+0.086}_{-0.091}$	0.352 ± 0.089	0.004 ± 0.012	1.310 ± 0.223	0.019	2 ± 2	2 ± 2	2 ± 1	0 ± 1	3
XMMXCS J020611.02-060400.0	$0.790^{+0.109}_{-0.113}$	0.851 ± 0.123	0.006 ± 0.020	0.511 ± 0.460	0.092	5 ± 3	7 ± 3	0 ± 1	2 ± 2	3
XMMXCS J020611.78-061131.4	$0.875^{+0.123}_{-0.123}$	0.767 ± 0.116	-0.035 ± 0.012	1.560 ± 0.267	0.071	21 ± 5	22 ± 5	23 ± 6	25 ± 6	3
XMMXCS J020621.16-072718.7	$0.540^{+0.113}_{-0.114}$	0.427 ± 0.094	0.029 ± 0.025	-0.252 ± 0.556	0.064	1 ± 2	0 ± 2	1 ± 1	-	3
XMMXCS J020623.24-071841.3	$0.486^{+0.088}_{-0.092}$	0.317 ± 0.087	-0.014 ± 0.025	0.746 ± 0.537	0.110	3 ± 3	2 ± 4	0 ± 1	-	3
XMMXCS J020630.48-035644.6	$1.188^{+0.191}_{-0.218}$	1.000 ± 0.132	-0.002 ± 0.036	0.719 ± 0.853	0.092	9 ± 4	10 ± 4	8 ± 4	8 ± 4	3
XMMXCS J020634.39-055839.8	$0.414^{+0.093}_{-0.094}$	0.309 ± 0.086	0.018 ± 0.018	1.020 ± 0.370	0.094	7 ± 3	7 ± 3	2 ± 2	2 ± 2	3
XMMXCS J020649.98-055900.4	$0.553^{+0.080}_{-0.091}$	0.353 ± 0.089	-0.010 ± 0.017	0.767 ± 0.353	0.095	7 ± 4	6 ± 4	3 ± 3	4 ± 3	3
XMMXCS J020650.63-061034.7	$0.885^{+0.140}_{-0.138}$	0.733 ± 0.116	-0.021 ± 0.016	1.010 ± 0.362	0.066	2 ± 3	-	0 ± 1	-	3

Continued on next page

Table A.4 – continued from previous page

name	z_{RS}	z_{BCG}	cmr_{grad}	cmr_{inter}	cmr_{wid}	n_{gals-c}	n_{gals-l}	n_{200-c}	n_{200-l}	qual
XMMXCS J020704.93-072132.7	$0.799^{+0.118}_{-0.119}$	0.632 ± 0.106	-0.042 ± 0.023	1.180 ± 0.510	0.087	3 ± 4	5 ± 5	5 ± 3	7 ± 4	3
XMMXCS J020725.25-045603.3	$0.266^{+0.092}_{-0.091}$	0.141 ± 0.077	0.068 ± 0.031	-0.476 ± 0.560	0.098	1 ± 2	-	2 ± 1	-	3
XMMXCS J020727.49-074055.7	$0.867^{+0.113}_{-0.119}$	0.705 ± 0.113	0.013 ± 0.027	0.480 ± 0.607	0.086	14 ± 4	17 ± 5	15 ± 5	1 ± 3	3
XMMXCS J020732.7-040903.5	$0.812^{+0.123}_{-0.123}$	0.644 ± 0.107	0.015 ± 0.025	0.018 ± 0.566	0.080	1 ± 4	-	0 ± 1	-	3
XMMXCS J020828.1-051159.8	$0.137^{+0.075}_{-0.076}$	0.132 ± 0.076	0.002 ± 0.069	0.689 ± 1.220	0.109	2 ± 2	1 ± 1	0 ± 0.1	0 ± 1	3
XMMXCS J020839.6-050711.5	$0.816^{+0.115}_{-0.112}$	0.681 ± 0.111	-0.030 ± 0.026	0.906 ± 0.584	0.099	14 ± 6	11 ± 6	14 ± 6	11 ± 6	3
XMMXCS J020840.5-062718.1	$0.601^{+0.096}_{-0.101}$	0.764 ± 0.116	-0.006 ± 0.028	1.140 ± 0.595	0.106	1 ± 2	7 ± 3	-	0 ± 2	3
XMMXCS J020901.42-060936.0	$0.269^{+0.110}_{-0.115}$	0.122 ± 0.075	0.154 ± 0.001	-1.780 ± 0.001	0.500	12 ± 4	12 ± 5	12 ± 4	12 ± 5	3
XMMXCS J020908.35-063640.4	$0.788^{+0.119}_{-0.120}$	0.611 ± 0.105	0.010 ± 0.011	0.299 ± 0.254	0.111	8 ± 4	9 ± 5	10 ± 4	11 ± 5	3
XMMXCS J021022.74-035132.7	$0.965^{+0.133}_{-0.133}$	0.953 ± 0.130	-0.012 ± 0.020	0.874 ± 0.468	0.120	10 ± 5	10 ± 5	0 ± 4	1 ± 4	3
XMMXCS J021028.7-101531.0	$1.116^{+0.135}_{-0.132}$	0.952 ± 0.130	0.040 ± 0.029	-0.291 ± 0.673	0.086	9 ± 5	8 ± 5	8 ± 4	8 ± 4	3
XMMXCS J021028.6-101530.9	$1.116^{+0.135}_{-0.132}$	0.952 ± 0.130	0.040 ± 0.029	-0.291 ± 0.673	0.086	9 ± 5	8 ± 5	8 ± 4	8 ± 4	3
XMMXCS J021037.97-060504.3	$0.342^{+0.111}_{-0.193}$	0.304 ± 0.105	0.149 ± 0.217	-2.160 ± 4.210	0.113	3 ± 2	4 ± 3	0 ± 1	1 ± 2	3
XMMXCS J021039.1-050039.1	$0.892^{+0.130}_{-0.130}$	0.769 ± 0.117	0.006 ± 0.021	0.197 ± 0.476	0.095	19 ± 6	17 ± 6	17 ± 7	18 ± 7	3
XMMXCS J021106.15-034650.9	$0.748^{+0.139}_{-0.170}$	0.640 ± 0.107	-0.009 ± 0.032	0.374 ± 0.693	0.097	16 ± 5	11 ± 5	17 ± 6	9 ± 5	3
XMMXCS J021110.13-052144.8	$0.609^{+0.098}_{-0.102}$	0.572 ± 0.102	-0.036 ± 0.023	1.360 ± 0.509	0.052	2 ± 2	2 ± 3	0 ± 0.1	0 ± 1	3
XMMXCS J021111.5-035208.9	$0.384^{+0.093}_{-0.090}$	0.432 ± 0.094	0.011 ± 0.033	0.118 ± 0.686	0.062	2 ± 2	2 ± 2	0 ± 0.1	0 ± 1	3
XMMXCS J021116.1-085240.3	$0.403^{+0.116}_{-0.116}$	0.232 ± 0.082	-0.010 ± 0.024	1.270 ± 0.461	0.098	5 ± 3	10 ± 4	5 ± 2	10 ± 4	3
XMMXCS J021141.00-051402.2	$0.920^{+0.107}_{-0.092}$	0.768 ± 0.118	-0.013 ± 0.011	0.649 ± 0.257	0.101	2 ± 5	4 ± 5	0 ± 1	-	3

Continued on next page

Table A.4 – continued from previous page

name	z_{RS}	z_{BCG}	cmr_{grad}	cmr_{inter}	cmr_{wid}	n_{gals-c}	n_{gals-l}	n_{200-c}	n_{200-l}	qual
XMMXCS J021221.3-041201.7	$0.526^{+0.098}_{-0.100}$	0.331 ± 0.087	0.024 ± 0.028	-0.112 ± 0.615	0.105	1 ± 2	1 ± 2	0 ± 0.1	0 ± 1	3
XMMXCS J021223.26-041430.6	$0.458^{+0.094}_{-0.094}$	0.325 ± 0.086	0.032 ± 0.029	-0.250 ± 0.607	0.092	2 ± 2	1 ± 2	0 ± 0.1	1 ± 1	3
XMMXCS J021255.79-044013.7	$0.639^{+0.108}_{-0.108}$	0.662 ± 0.110	-0.014 ± 0.022	1.400 ± 0.473	0.090	6 ± 3	4 ± 3	0 ± 1	0 ± 1	3
XMMXCS J021257.24-040652.6	$0.714^{+0.113}_{-0.113}$	0.545 ± 0.101	-0.025 ± 0.014	0.843 ± 0.308	0.077	15 ± 5	12 ± 5	16 ± 6	12 ± 5	3
XMMXCS J021300.96-060811.1	$0.201^{+0.093}_{-0.089}$	0.138 ± 0.075	0.083 ± 0.034	-1.010 ± 0.664	0.083	1 ± 1	1 ± 1	0 ± 0.1	0 ± 1	3
XMMXCS J021321.13-050831.2	$0.361^{+0.086}_{-0.082}$	0.185 ± 0.079	-0.068 ± 0.020	1.770 ± 0.398	0.066	6 ± 3	4 ± 3	3 ± 2	2 ± 2	3
XMMXCS J021321.18-042600.8	$0.767^{+0.114}_{-0.114}$	0.664 ± 0.110	-0.041 ± 0.018	1.350 ± 0.397	0.091	6 ± 5	5 ± 5	9 ± 4	15 ± 5	3
XMMXCS J021322.83-042134.4	$0.717^{+0.105}_{-0.109}$	0.855 ± 0.123	-0.102 ± 0.052	3.150 ± 1.150	0.074	2 ± 1	1 ± 2	0 ± 0.1	0 ± 1	3
XMMXCS J021324.44-042009.3	$0.704^{+0.102}_{-0.100}$	0.600 ± 0.104	-0.021 ± 0.026	1.460 ± 0.563	0.102	4 ± 3	5 ± 4	0 ± 1	2 ± 2	3
XMMXCS J021344.68-051856.4	$0.734^{+0.116}_{-0.116}$	0.575 ± 0.103	-0.017 ± 0.021	0.669 ± 0.464	0.087	14 ± 5	16 ± 6	14 ± 6	50 ± 9	3
XMMXCS J021359.12-051115.8	$0.239^{+0.094}_{-0.088}$	0.137 ± 0.076	0.113 ± 0.014	-1.150 ± 0.280	0.500	5 ± 3	5 ± 3	4 ± 2	2 ± 2	3
XMMXCS J021404.03-050805.2	$0.727^{+0.129}_{-0.135}$	0.555 ± 0.102	-0.007 ± 0.012	0.423 ± 0.269	0.097	6 ± 5	-	5 ± 4	-	3
XMMXCS J021433.37-060303.1	$0.632^{+0.100}_{-0.091}$	0.663 ± 0.110	-0.065 ± 0.037	2.000 ± 0.724	0.127	1 ± 3	-	0 ± 1	-	3
XMMXCS J021440.99-080219.0	$1.022^{+0.124}_{-0.126}$	0.904 ± 0.122	0.015 ± 0.018	0.142 ± 0.419	0.085	2 ± 4	18 ± 6	1 ± 2	17 ± 6	3
XMMXCS J021444.44-045456.0	$0.960^{+0.122}_{-0.118}$	0.845 ± 0.121	-0.018 ± 0.025	0.944 ± 0.574	0.098	10 ± 5	13 ± 6	12 ± 5	13 ± 6	3
XMMXCS J021446.34-035630.1	$0.173^{+0.078}_{-0.078}$	0.151 ± 0.077	-0.004 ± 0.014	0.953 ± 0.262	0.039	2 ± 2	3 ± 2	0 ± 0.1	1 ± 1	3
XMMXCS J021446.3-035633.7	$0.181^{+0.079}_{-0.079}$	0.190 ± 0.080	-0.094 ± 0.039	2.660 ± 0.728	0.098	1 ± 2	2 ± 2	0 ± 0.1	0 ± 1	3
XMMXCS J021504.51-044618.0	$0.330^{+0.088}_{-0.087}$	0.298 ± 0.087	-0.032 ± 0.017	1.840 ± 0.323	0.096	6 ± 3	8 ± 3	0 ± 1	1 ± 2	3
XMMXCS J021521.25-051121.9	$0.797^{+0.129}_{-0.135}$	0.776 ± 0.117	-0.000 ± 0.016	0.224 ± 0.370	0.090	1 ± 4	0 ± 4	0 ± 0.1	-	3

Continued on next page

Table A.4 – continued from previous page

name	z_{RS}	z_{BCG}	cmr_{grad}	cmr_{inter}	cmr_{wid}	n_{gals-c}	n_{gals-l}	n_{200-c}	n_{200-l}	qual
XMMXCS J021522.82-034344.5	$0.886^{+0.121}_{-0.123}$	0.755 ± 0.117	-0.062 ± 0.023	2.160 ± 0.515	0.081	21 ± 5	20 ± 5	23 ± 6	23 ± 6	3
XMMXCS J021522.8-034344.4	$0.886^{+0.121}_{-0.123}$	0.755 ± 0.117	-0.062 ± 0.023	2.160 ± 0.515	0.081	21 ± 5	20 ± 5	23 ± 6	23 ± 6	3
XMMXCS J021528.34-040258.0	$0.384^{+0.091}_{-0.091}$	0.412 ± 0.095	-0.016 ± 0.010	0.925 ± 0.197	0.046	17 ± 4	14 ± 4	22 ± 5	16 ± 5	3
XMMXCS J021528.66-061551.8	$0.478^{+0.081}_{-0.089}$	0.349 ± 0.089	0.081 ± 0.034	-0.891 ± 0.720	0.080	4 ± 3	5 ± 3	2 ± 2	2 ± 2	3
XMMXCS J021532.90-035124.8	$0.742^{+0.111}_{-0.112}$	0.874 ± 0.123	-0.004 ± 0.010	0.458 ± 0.225	0.099	3 ± 4	5 ± 5	0 ± 2	5 ± 4	3
XMMXCS J021532.8-035124.7	$0.742^{+0.111}_{-0.112}$	0.874 ± 0.123	-0.004 ± 0.010	0.458 ± 0.225	0.099	3 ± 4	5 ± 5	0 ± 2	5 ± 4	3
XMMXCS J021536.3-035454.1	$0.685^{+0.100}_{-0.093}$	0.641 ± 0.107	-0.014 ± 0.013	0.663 ± 0.271	0.093	0 ± 3	1 ± 4	-	0 ± 1	3
XMMXCS J021557.65-045010.7	$0.953^{+0.134}_{-0.134}$	0.795 ± 0.120	-0.077 ± 0.023	2.410 ± 0.515	0.089	8 ± 4	6 ± 4	4 ± 3	5 ± 3	3
XMMXCS J021605.61-034319.1	$0.985^{+0.146}_{-0.153}$	0.856 ± 0.121	0.018 ± 0.019	0.195 ± 0.438	0.120	9 ± 5	10 ± 6	3 ± 4	6 ± 5	3
XMMXCS J021611.9-044626.2	$0.477^{+0.091}_{-0.094}$	0.353 ± 0.089	-0.044 ± 0.019	1.470 ± 0.403	0.108	7 ± 4	10 ± 4	5 ± 3	9 ± 4	3
XMMXCS J021619.2-052558.5	$1.350^{+0.150}_{-0.177}$	1.380 ± 0.153	-0.118 ± 0.033	3.250 ± 0.767	0.044	1 ± 1	-	0 ± 0.1	-	3
XMMXCS J021642.32-055133.6	$0.282^{+0.083}_{-0.084}$	0.285 ± 0.086	-0.098 ± 0.080	3.070 ± 1.540	0.081	1 ± 2	0 ± 1	3 ± 2	-	3
XMMXCS J021647.39-043317.1	$0.389^{+0.079}_{-0.081}$	0.315 ± 0.086	-0.010 ± 0.019	0.815 ± 0.391	0.109	2 ± 2	2 ± 2	0 ± 1	1 ± 1	3
XMMXCS J021658.0-044256.9	$1.022^{+0.131}_{-0.129}$	0.829 ± 0.118	-0.007 ± 0.022	0.719 ± 0.511	0.075	8 ± 5	6 ± 4	4 ± 4	5 ± 3	3
XMMXCS J021701.8-042616.4	$0.764^{+0.120}_{-0.119}$	0.731 ± 0.113	-0.063 ± 0.028	1.600 ± 0.621	0.095	0 ± 4	5 ± 5	-	5 ± 3	3
XMMXCS J021710.10-041143.3	$0.887^{+0.119}_{-0.116}$	0.744 ± 0.114	0.018 ± 0.018	0.039 ± 0.407	0.112	20 ± 6	20 ± 7	24 ± 8	24 ± 8	3
XMMXCS J021710.1-041143.4	$0.903^{+0.118}_{-0.114}$	0.744 ± 0.114	0.013 ± 0.022	0.165 ± 0.487	0.113	20 ± 7	24 ± 7	25 ± 8	23 ± 9	3
XMMXCS J021716.2-050734.5	$0.651^{+0.106}_{-0.107}$	0.658 ± 0.109	-0.045 ± 0.021	2.030 ± 0.449	0.081	2 ± 2	5 ± 3	0 ± 0.1	1 ± 2	3
XMMXCS J021717.0-052837.5	$0.551^{+0.111}_{-0.110}$	0.400 ± 0.092	-0.020 ± 0.019	0.862 ± 0.423	0.107	7 ± 4	5 ± 4	7 ± 3	2 ± 3	3

Continued on next page

Table A.4 – continued from previous page

name	z_{RS}	z_{BCG}	cmr_{grad}	cmr_{inter}	cmr_{wid}	n_{gals-c}	n_{gals-l}	n_{200-c}	n_{200-l}	qual
XMMXCS J021719.25-040332.8	$1.093^{+0.158}_{-0.165}$	0.956 ± 0.128	0.043 ± 0.024	-0.449 ± 0.554	0.092	13 ± 5	14 ± 6	15 ± 6	17 ± 6	3
XMMXCS J021723.32-041844.1	$1.198^{+0.141}_{-0.134}$	1.010 ± 0.134	-0.036 ± 0.039	1.450 ± 0.909	0.087	3 ± 4	6 ± 4	1 ± 2	7 ± 4	3
XMMXCS J021723.8-051310.2	$0.696^{+0.110}_{-0.106}$	0.617 ± 0.105	-0.046 ± 0.014	1.250 ± 0.313	0.096	7 ± 5	10 ± 5	0 ± 3	-	3
XMMXCS J021726.8-045216.7	$1.173^{+0.154}_{-0.157}$	1.000 ± 0.130	0.027 ± 0.021	0.297 ± 0.493	0.118	7 ± 4	7 ± 4	2 ± 2	2 ± 2	3
XMMXCS J021733.67-051315.2	$0.639^{+0.107}_{-0.108}$	0.625 ± 0.106	-0.001 ± 0.020	1.160 ± 0.427	0.062	23 ± 5	29 ± 6	31 ± 6	34 ± 6	3
XMMXCS J021734.7-051326.9	$0.642^{+0.107}_{-0.108}$	0.625 ± 0.106	0.004 ± 0.017	1.080 ± 0.375	0.056	23 ± 5	27 ± 5	29 ± 6	32 ± 6	3
XMMXCS J021741.5-045148.3	$1.085^{+0.139}_{-0.139}$	0.975 ± 0.132	0.044 ± 0.026	-0.296 ± 0.608	0.079	6 ± 4	33 ± 7	7 ± 3	7 ± 6	3
XMMXCS J021747.23-062415.8	$0.214^{+0.079}_{-0.078}$	0.093 ± 0.060	-0.000 ± 0.001	0.692 ± 0.001	0.500	6 ± 3	6 ± 3	4 ± 3	5 ± 3	3
XMMXCS J021756.1-044407.5	$1.097^{+0.136}_{-0.135}$	0.938 ± 0.126	0.065 ± 0.051	-0.814 ± 1.190	0.115	27 ± 6	32 ± 7	46 ± 9	58 ± 10	3
XMMXCS J021759.3-045215.9	$0.544^{+0.096}_{-0.099}$	0.551 ± 0.102	-0.086 ± 0.017	2.670 ± 0.373	0.056	4 ± 2	5 ± 3	3 ± 2	4 ± 2	3
XMMXCS J021801.7-050125.0	$0.657^{+0.075}_{-0.075}$	0.610 ± 0.105	-0.010 ± 0.027	0.740 ± 0.571	0.092	0 ± 2	5 ± 4	-	6 ± 3	3
XMMXCS J021802.41-050135.7	$0.533^{+0.116}_{-0.115}$	0.387 ± 0.090	0.052 ± 0.026	-0.581 ± 0.550	0.067	2 ± 2	11 ± 4	0 ± 1	11 ± 4	3
XMMXCS J021808.0-044049.9	$1.008^{+0.134}_{-0.134}$	0.887 ± 0.123	0.019 ± 0.042	0.171 ± 0.978	0.107	8 ± 5	9 ± 5	7 ± 4	6 ± 4	3
XMMXCS J021808.30-044050.2	$0.998^{+0.122}_{-0.126}$	0.850 ± 0.121	0.0002 ± 0.024	0.089 ± 0.558	0.078	2 ± 2	2 ± 3	0 ± 1	-	3
XMMXCS J021823.0-050605.4	$1.151^{+0.151}_{-0.154}$	0.993 ± 0.132	-0.010 ± 0.023	0.972 ± 0.528	0.115	2 ± 4	39 ± 7	-	29 ± 9	3
XMMXCS J021832.4-050054.1	$0.686^{+0.107}_{-0.109}$	0.516 ± 0.100	-0.024 ± 0.010	0.825 ± 0.210	0.095	23 ± 6	26 ± 7	30 ± 8	30 ± 8	3
XMMXCS J021832.83-050053.3	$0.685^{+0.106}_{-0.109}$	0.516 ± 0.100	-0.022 ± 0.010	0.781 ± 0.213	0.094	21 ± 6	25 ± 6	30 ± 8	33 ± 8	3
XMMXCS J021842.98-061834.5	$0.695^{+0.150}_{-0.157}$	0.507 ± 0.099	-0.017 ± 0.017	0.956 ± 0.372	0.101	4 ± 4	3 ± 4	3 ± 2	-	3
XMMXCS J021849.0-045750.1	$0.934^{+0.111}_{-0.119}$	0.820 ± 0.121	0.065 ± 0.053	-0.936 ± 1.250	0.112	0 ± 4	2 ± 5	-	0 ± 2	3

Continued on next page

Table A.4 – continued from previous page

name	z_{RS}	z_{BCG}	cmr_{grad}	cmr_{inter}	cmr_{wid}	n_{gals-c}	n_{gals-l}	n_{200-c}	n_{200-l}	qual
XMMXCS J021859.89-034606.5	$0.773^{+0.118}_{-0.119}$	0.604 ± 0.104	-0.015 ± 0.021	0.681 ± 0.479	0.104	5 ± 5	4 ± 5	2 ± 3	1 ± 3	3
XMMXCS J021907.63-042316.4	$0.273^{+0.100}_{-0.094}$	0.226 ± 0.082	0.005 ± 0.048	0.870 ± 0.956	0.500	7 ± 4	2 ± 3	4 ± 3	2 ± 2	3
XMMXCS J021912.2-045104.7	$1.004^{+0.142}_{-0.142}$	0.838 ± 0.123	0.003 ± 0.027	0.493 ± 0.637	0.101	7 ± 5	15 ± 6	4 ± 4	30 ± 7	3
XMMXCS J021914.45-045053.2	$1.014^{+0.135}_{-0.136}$	0.826 ± 0.121	0.074 ± 0.028	-0.905 ± 0.630	0.106	10 ± 4	220 ± 15	10 ± 4	128 ± 19	3
XMMXCS J021914.4-045053.2	$1.014^{+0.135}_{-0.136}$	0.826 ± 0.121	0.074 ± 0.028	-0.905 ± 0.630	0.106	10 ± 4	220 ± 15	10 ± 4	128 ± 19	3
XMMXCS J021936.86-042516.6	$0.877^{+0.126}_{-0.126}$	0.705 ± 0.111	-0.004 ± 0.037	0.469 ± 0.854	0.116	13 ± 6	-	13 ± 6	-	3
XMMXCS J021946.1-050748.1	$0.690^{+0.119}_{-0.119}$	0.501 ± 0.099	-0.019 ± 0.015	0.842 ± 0.321	0.093	12 ± 5	11 ± 5	11 ± 5	11 ± 5	3
XMMXCS J022002.6-045144.6	$0.948^{+0.135}_{-0.135}$	0.836 ± 0.121	0.009 ± 0.056	0.350 ± 1.290	0.118	19 ± 6	18 ± 6	28 ± 8	25 ± 7	3
XMMXCS J022005.71-042444.7	$0.863^{+0.126}_{-0.126}$	0.759 ± 0.117	-0.014 ± 0.007	0.621 ± 0.160	0.103	4 ± 5	-	3 ± 3	-	3
XMMXCS J022005.7-042444.7	$0.863^{+0.126}_{-0.126}$	0.759 ± 0.117	-0.014 ± 0.007	0.621 ± 0.160	0.103	4 ± 5	-	3 ± 3	-	3
XMMXCS J022014.46-072325.4	$1.031^{+0.130}_{-0.126}$	0.873 ± 0.124	-0.028 ± 0.046	1.060 ± 1.050	0.115	9 ± 5	11 ± 5	6 ± 4	11 ± 5	3
XMMXCS J022014.98-042931.8	$0.857^{+0.117}_{-0.112}$	0.695 ± 0.113	-0.025 ± 0.013	0.862 ± 0.302	0.098	6 ± 5	9 ± 5	0 ± 2	2 ± 4	3
XMMXCS J022024.13-040305.4	$0.571^{+0.088}_{-0.084}$	0.430 ± 0.094	-0.008 ± 0.012	0.724 ± 0.258	0.105	4 ± 3	0 ± 3	2 ± 2	-	3
XMMXCS J022024.1-040305.4	$0.571^{+0.088}_{-0.084}$	0.430 ± 0.094	-0.008 ± 0.012	0.724 ± 0.258	0.105	4 ± 3	0 ± 3	2 ± 2	-	3
XMMXCS J022025.63-045101.6	$0.822^{+0.133}_{-0.137}$	0.774 ± 0.116	-0.020 ± 0.012	0.791 ± 0.266	0.109	5 ± 5	2 ± 5	0 ± 3	2 ± 2	3
XMMXCS J022028.51-052435.1	$0.503^{+0.073}_{-0.078}$	0.386 ± 0.091	-0.021 ± 0.018	0.909 ± 0.375	0.094	2 ± 3	1 ± 3	1 ± 1	-	3
XMMXCS J022028.5-052435.0	$0.503^{+0.073}_{-0.078}$	0.386 ± 0.091	-0.021 ± 0.018	0.909 ± 0.375	0.094	2 ± 3	1 ± 3	1 ± 1	-	3
XMMXCS J022036.5-054328.8	$0.806^{+0.102}_{-0.111}$	0.990 ± 0.130	0.002 ± 0.016	0.635 ± 0.363	0.105	14 ± 5	29 ± 6	14 ± 5	32 ± 7	3
XMMXCS J022048.27-084248.8	$0.531^{+0.099}_{-0.100}$	0.535 ± 0.101	0.044 ± 0.026	0.024 ± 0.534	0.061	3 ± 2	1 ± 2	0 ± 0.1	1 ± 1	3

Continued on next page

Table A.4 – continued from previous page

name	z_{RS}	z_{BCG}	cmr_{grad}	cmr_{inter}	cmr_{wid}	n_{gals-c}	n_{gals-l}	n_{200-c}	n_{200-l}	qual
XMMXCS J022058.70-043918.1	$0.851^{+0.124}_{-0.125}$	0.668 ± 0.109	-0.019 ± 0.021	0.769 ± 0.481	0.085	7 ± 5	9 ± 5	6 ± 4	9 ± 5	3
XMMXCS J022118.26-035848.1	$0.868^{+0.122}_{-0.121}$	0.756 ± 0.116	0.043 ± 0.032	-0.159 ± 0.752	0.103	4 ± 3	4 ± 3	0 ± 1	0 ± 1	3
XMMXCS J022137.91-043440.5	$0.596^{+0.099}_{-0.101}$	0.470 ± 0.097	0.029 ± 0.019	0.193 ± 0.411	0.106	6 ± 4	9 ± 4	6 ± 3	9 ± 4	3
XMMXCS J022159.14-034400.7	$0.494^{+0.082}_{-0.092}$	0.325 ± 0.087	-0.013 ± 0.010	0.937 ± 0.207	0.089	3 ± 3	4 ± 3	0 ± 0.1	-	3
XMMXCS J022205.2-054307.7	$0.832^{+0.123}_{-0.123}$	0.728 ± 0.114	-0.011 ± 0.011	0.735 ± 0.262	0.110	23 ± 6	19 ± 6	44 ± 9	34 ± 8	3
XMMXCS J022223.72-053851.5	$0.300^{+0.085}_{-0.085}$	0.338 ± 0.088	-0.013 ± 0.039	1.460 ± 0.791	0.126	0 ± 2	1 ± 2	-	0 ± 1	3
XMMXCS J022225.2-043730.2	$0.804^{+0.095}_{-0.081}$	0.777 ± 0.116	0.006 ± 0.023	0.195 ± 0.494	0.096	5 ± 5	6 ± 5	0 ± 2	0 ± 3	3
XMMXCS J022241.9-053619.1	$1.194^{+0.143}_{-0.137}$	1.310 ± 0.148	-0.035 ± 0.052	1.450 ± 1.220	0.098	9 ± 4	8 ± 4	7 ± 4	7 ± 4	3
XMMXCS J022246.55-035141.4	$1.030^{+0.127}_{-0.121}$	0.838 ± 0.119	-0.042 ± 0.020	1.490 ± 0.464	0.102	7 ± 5	7 ± 5	1 ± 3	1 ± 3	3
XMMXCS J022249.5-060123.5	$0.395^{+0.095}_{-0.096}$	0.259 ± 0.085	-0.032 ± 0.015	0.957 ± 0.328	0.084	3 ± 3	2 ± 3	4 ± 2	2 ± 2	3
XMMXCS J022250.94-041641.1	$0.208^{+0.081}_{-0.081}$	0.161 ± 0.078	-0.054 ± 0.033	1.910 ± 0.590	0.068	2 ± 2	4 ± 2	2 ± 1	3 ± 2	3
XMMXCS J022251.9-051420.1	$0.495^{+0.057}_{-0.076}$	0.383 ± 0.090	-0.045 ± 0.036	1.520 ± 0.798	0.099	3 ± 2	1 ± 2	2 ± 1	0 ± 1	3
XMMXCS J022255.46-051818.7	$0.885^{+0.127}_{-0.127}$	0.714 ± 0.113	0.022 ± 0.030	-0.171 ± 0.675	0.125	9 ± 6	9 ± 6	9 ± 5	9 ± 5	3
XMMXCS J022255.4-051818.3	$0.885^{+0.127}_{-0.127}$	0.714 ± 0.113	0.022 ± 0.030	-0.171 ± 0.675	0.125	10 ± 6	10 ± 6	11 ± 5	11 ± 5	3
XMMXCS J022300.2-054830.8	$1.079^{+0.114}_{-0.098}$	0.884 ± 0.123	0.011 ± 0.014	0.279 ± 0.319	0.108	8 ± 5	8 ± 5	7 ± 4	7 ± 4	3
XMMXCS J022305.09-035816.1	$0.705^{+0.115}_{-0.114}$	0.557 ± 0.102	-0.060 ± 0.019	1.620 ± 0.411	0.090	29 ± 6	29 ± 7	29 ± 8	34 ± 9	3
XMMXCS J022313.5-045551.2	$0.537^{+0.084}_{-0.093}$	0.342 ± 0.088	-0.007 ± 0.013	0.670 ± 0.280	0.103	2 ± 3	0 ± 3	0 ± 1	-	3
XMMXCS J022317.7-052011.9	$0.779^{+0.185}_{-0.186}$	0.585 ± 0.103	0.001 ± 0.022	0.304 ± 0.494	0.097	4 ± 4	6 ± 5	0 ± 2	7 ± 4	3
XMMXCS J022320.23-055432.4	$0.389^{+0.070}_{-0.076}$	0.278 ± 0.084	0.032 ± 0.022	0.655 ± 0.442	0.099	1 ± 2	0 ± 2	0 ± 0.1	-	3

Continued on next page

Table A.4 – continued from previous page

name	z_{RS}	z_{BCG}	cmr_{grad}	cmr_{inter}	cmr_{wid}	n_{gals-c}	n_{gals-l}	n_{200-c}	n_{200-l}	qual
XMMXCS J022320.2-055432.3	$0.389^{+0.070}_{-0.076}$	0.278 ± 0.084	0.032 ± 0.022	0.655 ± 0.442	0.099	1 ± 2	0 ± 2	0 ± 0.1	-	3
XMMXCS J022328.51-040138.6	$0.751^{+0.116}_{-0.114}$	0.674 ± 0.109	-0.013 ± 0.028	0.514 ± 0.642	0.100	4 ± 4	7 ± 5	0 ± 2	3 ± 3	3
XMMXCS J022328.7-040135.3	$0.436^{+0.083}_{-0.077}$	0.371 ± 0.090	-0.016 ± 0.021	1.180 ± 0.426	0.092	0 ± 2	1 ± 2	-	1 ± 1	3
XMMXCS J022336.83-040941.4	$0.495^{+0.075}_{-0.076}$	0.457 ± 0.096	-0.014 ± 0.016	0.798 ± 0.337	0.105	3 ± 3	5 ± 3	0 ± 1	2 ± 2	3
XMMXCS J022342.0-040013.0	$0.376^{+0.082}_{-0.077}$	0.256 ± 0.084	-0.061 ± 0.036	2.190 ± 0.695	0.090	7 ± 3	3 ± 3	3 ± 2	2 ± 2	3
XMMXCS J022346.5-042435.1	$0.890^{+0.123}_{-0.124}$	0.765 ± 0.116	-0.035 ± 0.017	1.170 ± 0.387	0.095	10 ± 5	19 ± 6	5 ± 5	19 ± 7	3
XMMXCS J022350.88-044910.3	$1.074^{+0.135}_{-0.135}$	1.110 ± 0.137	0.038 ± 0.034	-0.076 ± 0.779	0.076	4 ± 3	-	3 ± 2	-	3
XMMXCS J022350.9-044914.7	$1.032^{+0.130}_{-0.131}$	1.110 ± 0.137	0.024 ± 0.028	0.260 ± 0.632	0.072	4 ± 3	3 ± 3	3 ± 2	1 ± 2	3
XMMXCS J022351.3-041842.3	$0.699^{+0.112}_{-0.117}$	0.754 ± 0.114	-0.010 ± 0.024	0.551 ± 0.539	0.085	0 ± 3	3 ± 4	-	0 ± 2	3
XMMXCS J022406.0-035502.1	$0.542^{+0.099}_{-0.099}$	0.392 ± 0.092	-0.019 ± 0.016	0.945 ± 0.335	0.081	2 ± 3	3 ± 3	2 ± 2	4 ± 3	3
XMMXCS J022420.3-045725.5	$0.330^{+0.085}_{-0.086}$	0.211 ± 0.080	-0.036 ± 0.019	1.700 ± 0.362	0.092	0 ± 2	2 ± 2	-	2 ± 2	3
XMMXCS J022423.8-050417.2	$0.534^{+0.102}_{-0.103}$	0.512 ± 0.100	-0.015 ± 0.017	1.130 ± 0.345	0.104	2 ± 2	3 ± 3	0 ± 0.1	-	3
XMMXCS J022433.0-040030.9	$0.390^{+0.099}_{-0.099}$	0.407 ± 0.093	-0.082 ± 0.018	2.750 ± 0.360	0.500	3 ± 4	0 ± 3	0 ± 1	-	3
XMMXCS J022441.2-050611.5	$0.576^{+0.085}_{-0.095}$	0.459 ± 0.096	-0.008 ± 0.011	0.846 ± 0.234	0.113	6 ± 4	4 ± 4	3 ± 2	3 ± 2	3
XMMXCS J022441.5-042209.6	$0.556^{+0.100}_{-0.097}$	0.391 ± 0.091	-0.000 ± 0.015	0.372 ± 0.328	0.078	2 ± 2	3 ± 3	0 ± 0.1	1 ± 2	3
XMMXCS J022455.00-050835.9	$0.131^{+0.074}_{-0.074}$	0.259 ± 0.105	0.051 ± 0.038	-0.129 ± 0.695	0.088	2 ± 2	3 ± 2	3 ± 2	2 ± 2	3
XMMXCS J022459.5-040034.1	$0.122^{+0.046}_{-0.052}$	0.180 ± 0.080	-0.019 ± 0.004	0.754 ± 0.072	0.500	1 ± 2	0 ± 1	0 ± 0.1	-	3
XMMXCS J022508.61-040835.1	$0.761^{+0.117}_{-0.118}$	0.642 ± 0.107	-0.006 ± 0.015	0.550 ± 0.342	0.088	15 ± 5	17 ± 6	18 ± 6	-	3
XMMXCS J022509.7-040137.6	$0.177^{+0.079}_{-0.079}$	0.180 ± 0.080	-0.056 ± 0.015	1.860 ± 0.247	0.033	2 ± 2	3 ± 2	2 ± 1	3 ± 2	3

Continued on next page

Table A.4 – continued from previous page

name	z_{RS}	z_{BCG}	cmr_{grad}	cmr_{inter}	cmr_{wid}	n_{gals-c}	n_{gals-l}	n_{200-c}	n_{200-l}	qual
XMMXCS J022510.1-041912.6	$0.638^{+0.108}_{-0.105}$	0.621 ± 0.190	0.027 ± 0.045	-0.217 ± 1.010	0.083	1 ± 2	1 ± 2	0 ± 0.1	1 ± 1	3
XMMXCS J022517.8-042225.2	$0.205^{+0.069}_{-0.078}$	0.132 ± 0.076	-0.008 ± 0.010	1.010 ± 0.192	0.073	1 ± 2	5 ± 3	0 ± 0.1	0 ± 1	3
XMMXCS J022532.0-035509.9	$0.778^{+0.116}_{-0.116}$	0.774 ± 0.116	0.007 ± 0.017	0.347 ± 0.385	0.095	18 ± 5	18 ± 6	19 ± 6	17 ± 6	3
XMMXCS J022532.42-035502.4	$0.774^{+0.117}_{-0.117}$	0.774 ± 0.116	0.005 ± 0.019	0.390 ± 0.420	0.094	18 ± 5	19 ± 6	17 ± 6	17 ± 6	3
XMMXCS J022600.21-044413.1	$1.201^{+0.145}_{-0.141}$	1.040 ± 0.134	-0.051 ± 0.042	1.920 ± 0.987	0.105	1 ± 3	3 ± 3	1 ± 1	2 ± 2	3
XMMXCS J022600.2-044413.0	$1.201^{+0.145}_{-0.141}$	1.040 ± 0.134	-0.051 ± 0.042	1.920 ± 0.987	0.105	1 ± 3	3 ± 3	1 ± 1	2 ± 2	3
XMMXCS J022610.37-045805.3	$0.123^{+0.069}_{-0.070}$	0.093 ± 0.060	0.025 ± 0.041	0.166 ± 0.654	0.070	7 ± 3	7 ± 3	4 ± 2	4 ± 2	3
XMMXCS J022620.07-084322.9	$0.276^{+0.070}_{-0.077}$	0.316 ± 0.088	-0.071 ± 0.018	2.630 ± 0.342	0.056	3 ± 2	2 ± 2	0 ± 0.1	1 ± 1	3
XMMXCS J022621.0-042216.7	$0.224^{+0.081}_{-0.081}$	0.243 ± 0.083	0.021 ± 0.046	0.540 ± 0.880	0.073	0 ± 1	1 ± 2	-	0 ± 1	3
XMMXCS J022632.50-054651.9	$0.245^{+0.091}_{-0.088}$	0.093 ± 0.060	0.037 ± 0.028	-0.073 ± 0.562	0.096	6 ± 3	4 ± 2	3 ± 2	3 ± 2	3
XMMXCS J022633.65-042216.0	$1.100^{+0.143}_{-0.144}$	0.940 ± 0.135	0.033 ± 0.055	-0.177 ± 1.280	0.097	8 ± 4	32 ± 7	11 ± 4	37 ± 8	3
XMMXCS J022639.7-041647.0	$0.962^{+0.128}_{-0.128}$	0.778 ± 0.118	-0.010 ± 0.027	0.714 ± 0.626	0.090	8 ± 5	10 ± 5	7 ± 4	13 ± 5	3
XMMXCS J022648.5-041157.9	$0.275^{+0.079}_{-0.082}$	0.229 ± 0.083	-0.002 ± 0.024	0.970 ± 0.473	0.102	3 ± 2	7 ± 3	0 ± 1	4 ± 3	3
XMMXCS J022659.58-043521.6	$0.098^{+0.059}_{-0.060}$	0.093 ± 0.060	0.048 ± 0.017	-0.212 ± 0.286	0.042	1 ± 1	2 ± 2	0 ± 0.1	0 ± 1	3
XMMXCS J022714.2-042647.5	$0.147^{+0.070}_{-0.071}$	0.102 ± 0.065	-0.000 ± 0.010	0.665 ± 0.173	0.047	1 ± 1	1 ± 1	0 ± 0.1	0 ± 1	3
XMMXCS J022714.3-042648.6	$0.147^{+0.070}_{-0.071}$	0.102 ± 0.065	-0.000 ± 0.010	0.665 ± 0.173	0.047	1 ± 1	1 ± 1	0 ± 0.1	0 ± 1	3
XMMXCS J022725.01-041127.0	$0.667^{+0.105}_{-0.108}$	0.532 ± 0.101	-0.005 ± 0.030	0.958 ± 0.669	0.117	9 ± 4	6 ± 4	7 ± 4	6 ± 3	3
XMMXCS J022727.52-042712.5	$0.448^{+0.048}_{-0.048}$	0.486 ± 0.097	-0.039 ± 0.017	1.130 ± 0.337	0.081	2 ± 2	2 ± 2	0 ± 0.1	0 ± 1	3
XMMXCS J022734.3-043553.2	$1.095^{+0.149}_{-0.152}$	1.120 ± 0.210	-0.023 ± 0.026	1.030 ± 0.608	0.095	3 ± 4	5 ± 5	0 ± 1	1 ± 3	3

Continued on next page

Table A.4 – continued from previous page

name	z_{RS}	z_{BCG}	cmr_{grad}	cmr_{inter}	cmr_{wid}	n_{gals-c}	n_{gals-l}	n_{200-c}	n_{200-l}	qual
XMMXCS J022759.29-034828.8	$0.240^{+0.074}_{-0.067}$	0.180 ± 0.080	-0.019 ± 0.028	0.974 ± 0.529	0.102	1 ± 2	-	0 ± 0.1	-	3
XMMXCS J022759.2-034828.8	$0.240^{+0.074}_{-0.067}$	0.180 ± 0.080	-0.019 ± 0.028	0.974 ± 0.529	0.102	1 ± 2	-	0 ± 0.1	-	3
XMMXCS J022811.63-043844.2	$0.475^{+0.083}_{-0.083}$	0.382 ± 0.091	-0.066 ± 0.019	1.890 ± 0.402	0.086	0 ± 2	1 ± 3	-	0 ± 1	3
XMMXCS J022812.4-043234.6	$0.501^{+0.090}_{-0.095}$	0.532 ± 0.101	-0.012 ± 0.032	1.100 ± 0.653	0.083	2 ± 2	2 ± 2	0 ± 0.1	0 ± 1	3
XMMXCS J022841.25-035700.6	$0.406^{+0.080}_{-0.083}$	0.252 ± 0.083	-0.008 ± 0.013	0.643 ± 0.258	0.084	8 ± 4	8 ± 4	5 ± 3	5 ± 3	3
XMMXCS J022841.4-035658.7	$0.405^{+0.083}_{-0.085}$	0.252 ± 0.083	-0.006 ± 0.013	0.604 ± 0.274	0.088	8 ± 4	9 ± 4	5 ± 3	5 ± 3	3
XMMXCS J022851.4-051224.4	$0.726^{+0.112}_{-0.112}$	0.576 ± 0.103	-0.034 ± 0.010	1.580 ± 0.227	0.106	1 ± 3	-	0 ± 0.1	-	3
XMMXCS J022856.65-085721.2	$0.590^{+0.102}_{-0.103}$	0.393 ± 0.092	-0.026 ± 0.011	1.310 ± 0.237	0.111	7 ± 4	5 ± 4	1 ± 2	1 ± 2	3
XMMXCS J022912.41-060124.3	$1.173^{+0.152}_{-0.153}$	1.070 ± 0.136	-0.084 ± 0.036	2.710 ± 0.847	0.082	17 ± 5	17 ± 5	17 ± 5	18 ± 5	3
XMMXCS J022920.7-044206.2	$0.607^{+0.136}_{-0.135}$	0.441 ± 0.095	-0.044 ± 0.020	1.490 ± 0.429	0.084	8 ± 4	4 ± 4	6 ± 3	0 ± 2	3
XMMXCS J022958.65-042516.0	$0.439^{+0.095}_{-0.094}$	0.240 ± 0.082	-0.025 ± 0.017	0.851 ± 0.355	0.074	2 ± 3	1 ± 3	0 ± 0.1	0 ± 1	3
XMMXCS J022959.47-045716.0	$1.141^{+0.128}_{-0.119}$	0.966 ± 0.130	-0.018 ± 0.078	1.040 ± 1.850	0.092	2 ± 4	5 ± 4	3 ± 2	2 ± 3	3
XMMXCS J023007.35-043125.6	$0.266^{+0.084}_{-0.084}$	0.286 ± 0.086	-0.037 ± 0.052	1.750 ± 0.956	0.138	2 ± 2	1 ± 2	0 ± 0.1	0 ± 1	3
XMMXCS J023022.56-054350.0	$0.304^{+0.070}_{-0.078}$	0.200 ± 0.081	0.201 ± 0.040	-3.220 ± 0.832	0.500	1 ± 3	-	1 ± 1	-	3
XMMXCS J023033.53-045656.3	$0.677^{+0.105}_{-0.107}$	0.651 ± 0.108	0.086 ± 0.042	-0.579 ± 0.861	0.084	3 ± 2	-	0 ± 1	-	3
XMMXCS J023035.76-052604.9	$0.917^{+0.126}_{-0.125}$	1.020 ± 0.136	-0.053 ± 0.036	1.750 ± 0.817	0.115	8 ± 5	31 ± 7	12 ± 5	39 ± 9	3
XMMXCS J023036.75-045930.4	$0.303^{+0.084}_{-0.085}$	0.288 ± 0.086	-0.023 ± 0.019	1.690 ± 0.376	0.080	10 ± 4	6 ± 3	11 ± 4	5 ± 3	3
XMMXCS J023040.76-040753.5	$0.916^{+0.132}_{-0.132}$	1.090 ± 0.140	-0.017 ± 0.009	0.931 ± 0.212	0.109	5 ± 5	4 ± 5	1 ± 3	5 ± 3	3
XMMXCS J023101.66-050546.7	$0.559^{+0.082}_{-0.082}$	0.474 ± 0.097	0.061 ± 0.021	-0.474 ± 0.458	0.107	0 ± 2	2 ± 3	-	0 ± 1	3

Continued on next page

Table A.4 – continued from previous page

name	z_{RS}	z_{BCG}	cmr_{grad}	cmr_{inter}	cmr_{wid}	n_{gals-c}	n_{gals-l}	n_{200-c}	n_{200-l}	qual
XMMXCS J023103.42-051345.9	$0.969^{+0.140}_{-0.140}$	0.868 ± 0.123	0.005 ± 0.031	0.465 ± 0.706	0.080	10 ± 5	12 ± 5	8 ± 4	13 ± 5	3
XMMXCS J023113.45-054126.1	$0.667^{+0.102}_{-0.102}$	0.777 ± 0.116	-0.033 ± 0.011	1.180 ± 0.239	0.096	2 ± 3	2 ± 3	0 ± 0.1	0 ± 1	3
XMMXCS J023138.24-043442.4	$0.864^{+0.134}_{-0.133}$	1.020 ± 0.135	-0.047 ± 0.030	1.710 ± 0.672	0.121	7 ± 4	14 ± 5	9 ± 4	9 ± 5	3
XMMXCS J023141.5-042955.3	$0.495^{+0.088}_{-0.087}$	0.349 ± 0.089	-0.024 ± 0.017	0.946 ± 0.350	0.090	3 ± 3	2 ± 3	2 ± 2	2 ± 2	3
XMMXCS J023214.83-040128.8	$0.254^{+0.085}_{-0.085}$	0.219 ± 0.081	0.002 ± 0.057	0.657 ± 1.080	0.059	2 ± 2	1 ± 1	0 ± 0.1	1 ± 1	3
XMMXCS J023249.43-055026.6	$0.940^{+0.129}_{-0.129}$	0.740 ± 0.114	0.013 ± 0.014	0.154 ± 0.316	0.094	14 ± 6	15 ± 6	13 ± 6	15 ± 6	3
XMMXCS J023308.59-050250.3	$0.326^{+0.086}_{-0.087}$	0.327 ± 0.088	-0.030 ± 0.008	1.900 ± 0.145	0.022	1 ± 1	3 ± 2	0 ± 0.1	0 ± 1	3
XMMXCS J023321.06-053644.6	$1.028^{+0.132}_{-0.132}$	0.860 ± 0.122	0.018 ± 0.043	-0.061 ± 1.020	0.090	10 ± 5	10 ± 5	11 ± 5	11 ± 5	3
XMMXCS J023325.87-054043.8	$0.401^{+0.099}_{-0.099}$	0.235 ± 0.095	0.056 ± 0.069	-0.899 ± 1.400	0.067	2 ± 2	3 ± 2	1 ± 1	2 ± 2	3
XMMXCS J023333.45-060009.6	$0.814^{+0.117}_{-0.114}$	0.693 ± 0.111	-0.033 ± 0.010	1.050 ± 0.233	0.086	11 ± 5	12 ± 5	10 ± 5	12 ± 5	3
XMMXCS J023346.36-055402.5	$0.469^{+0.089}_{-0.089}$	0.282 ± 0.095	0.003 ± 0.017	0.608 ± 0.355	0.111	5 ± 3	4 ± 4	0 ± 2	-	3
XMMXCS J023354.59-042416.6	$0.499^{+0.076}_{-0.076}$	0.435 ± 0.095	-0.016 ± 0.010	0.811 ± 0.195	0.096	0 ± 3	2 ± 3	-	0 ± 1	3
XMMXCS J023406.90-051121.7	$0.721^{+0.139}_{-0.146}$	0.531 ± 0.100	-0.113 ± 0.045	2.700 ± 1.010	0.069	3 ± 4	-	0 ± 1	-	3
XMMXCS J023411.77-042229.2	$0.476^{+0.095}_{-0.092}$	0.493 ± 0.099	-0.047 ± 0.022	1.590 ± 0.432	0.064	0 ± 2	1 ± 2	-	0 ± 1	3
XMMXCS J023418.87-060107.9	$0.449^{+0.090}_{-0.089}$	0.417 ± 0.093	-0.008 ± 0.023	1.500 ± 0.466	0.096	0 ± 2	1 ± 2	-	0 ± 1	3
XMMXCS J023424.01-042920.7	$0.500^{+0.082}_{-0.086}$	0.367 ± 0.090	-0.039 ± 0.018	1.350 ± 0.373	0.103	3 ± 3	4 ± 4	0 ± 1	1 ± 2	3
XMMXCS J023436.23-041922.7	$0.558^{+0.091}_{-0.097}$	0.459 ± 0.096	-0.014 ± 0.023	0.988 ± 0.496	0.088	4 ± 3	4 ± 3	0 ± 1	1 ± 2	3
XMMXCS J023458.5-085058.8	$0.147^{+0.073}_{-0.076}$	0.151 ± 0.077	-0.022 ± 0.009	1.230 ± 0.156	0.030	6 ± 3	4 ± 2	6 ± 3	5 ± 2	3
XMMXCS J023509.35-040242.6	$0.394^{+0.068}_{-0.072}$	0.328 ± 0.088	0.014 ± 0.023	0.582 ± 0.459	0.119	2 ± 3	1 ± 3	0 ± 1	1 ± 1	3

Continued on next page

Table A.4 – continued from previous page

name	z_{RS}	z_{BCG}	cmr_{grad}	cmr_{inter}	cmr_{wid}	n_{gals-c}	n_{gals-l}	n_{200-c}	n_{200-l}	qual
XMMXCS J085006.81-014943.0	$1.153^{+0.153}_{-0.153}$	0.958 ± 0.128	0.007 ± 0.039	0.527 ± 0.911	0.092	12 ± 4	13 ± 5	12 ± 4	13 ± 5	3
XMMXCS J085145.73-044646.3	$0.542^{+0.084}_{-0.091}$	0.471 ± 0.097	0.026 ± 0.023	0.039 ± 0.515	0.110	5 ± 3	3 ± 4	0 ± 2	-	3
XMMXCS J085401.9-033008.2	$0.655^{+0.097}_{-0.095}$	0.753 ± 0.115	-0.017 ± 0.008	0.705 ± 0.179	0.097	2 ± 4	0 ± 4	0 ± 1	-	3
XMMXCS J085739.03-035413.3	$0.412^{+0.130}_{-0.110}$	0.330 ± 0.088	-0.022 ± 0.018	0.976 ± 0.358	0.096	4 ± 3	3 ± 3	0 ± 1	2 ± 2	3
XMMXCS J085845.24-043351.7	$0.897^{+0.118}_{-0.112}$	0.792 ± 0.116	0.013 ± 0.040	0.169 ± 0.925	0.119	10 ± 5	12 ± 5	11 ± 5	12 ± 5	3
XMMXCS J085919.31-041422.6	$0.650^{+0.121}_{-0.122}$	0.542 ± 0.101	-0.047 ± 0.021	1.610 ± 0.457	0.065	1 ± 2	4 ± 3	0 ± 0.1	4 ± 2	3
XMMXCS J090001.64-031538.3	$0.523^{+0.095}_{-0.099}$	0.636 ± 0.106	-0.060 ± 0.068	2.090 ± 1.520	0.111	1 ± 2	-	0 ± 0.1	-	3
XMMXCS J090016.71-031855.8	$0.165^{+0.078}_{-0.078}$	0.161 ± 0.078	-0.006 ± 0.017	1.000 ± 0.287	0.043	2 ± 2	3 ± 2	1 ± 1	2 ± 2	3
XMMXCS J090138.81-030727.7	$0.714^{+0.107}_{-0.101}$	0.533 ± 0.100	-0.019 ± 0.012	0.658 ± 0.256	0.087	1 ± 3	3 ± 4	2 ± 2	4 ± 3	3
XMMXCS J090219.02-021411.1	$1.214^{+0.139}_{-0.130}$	1.150 ± 0.141	0.005 ± 0.029	0.451 ± 0.678	0.075	3 ± 3	2 ± 3	0 ± 1	-	3
XMMXCS J090501.8-033205.0	$0.886^{+0.131}_{-0.132}$	0.773 ± 0.117	-0.023 ± 0.020	1.040 ± 0.450	0.124	13 ± 5	13 ± 5	14 ± 5	16 ± 6	3
XMMXCS J141504.74+545450.9	$0.254^{+0.081}_{-0.082}$	0.141 ± 0.077	-0.011 ± 0.029	1.220 ± 0.551	0.104	6 ± 3	10 ± 4	2 ± 2	8 ± 3	3
XMMXCS J141542.2+522206.7	$0.471^{+0.089}_{-0.087}$	0.378 ± 0.090	-0.070 ± 0.026	1.920 ± 0.553	0.102	3 ± 3	4 ± 3	0 ± 1	2 ± 2	3
XMMXCS J141544.4+522511.5	$0.681^{+0.106}_{-0.103}$	0.504 ± 0.099	0.040 ± 0.042	-0.028 ± 0.908	0.120	2 ± 3	3 ± 4	1 ± 2	1 ± 2	3
XMMXCS J141544.45+522511.7	$0.681^{+0.106}_{-0.103}$	0.504 ± 0.099	0.040 ± 0.042	-0.028 ± 0.908	0.120	2 ± 3	3 ± 4	1 ± 2	1 ± 2	3
XMMXCS J141544.4+522511.7	$0.681^{+0.106}_{-0.103}$	0.504 ± 0.099	0.040 ± 0.042	-0.028 ± 0.908	0.120	2 ± 3	3 ± 4	1 ± 2	1 ± 2	3
XMMXCS J141629.01+522701.3	$0.857^{+0.113}_{-0.104}$	0.746 ± 0.117	-0.016 ± 0.018	0.624 ± 0.424	0.097	9 ± 5	10 ± 5	4 ± 4	7 ± 5	3
XMMXCS J141629.0+522701.3	$0.857^{+0.113}_{-0.104}$	0.746 ± 0.117	-0.016 ± 0.018	0.624 ± 0.424	0.097	9 ± 5	10 ± 5	4 ± 4	7 ± 5	3
XMMXCS J141639.3+522845.3	$0.770^{+0.158}_{-0.160}$	0.584 ± 0.103	0.008 ± 0.020	0.085 ± 0.465	0.099	5 ± 5	7 ± 5	3 ± 3	5 ± 4	3

Continued on next page

Table A.4 – continued from previous page

name	z_{RS}	z_{BCG}	cmr_{grad}	cmr_{inter}	cmr_{wid}	n_{gals-c}	n_{gals-l}	n_{200-c}	n_{200-l}	qual
XMMXCS J141654.3+522040.0	$0.863^{+0.110}_{-0.104}$	0.750 ± 0.114	0.044 ± 0.029	-0.353 ± 0.664	0.093	6 ± 4	1462 ± 38	2 ± 3	-	3
XMMXCS J141656.7+521514.9	$0.833^{+0.119}_{-0.118}$	0.716 ± 0.113	-0.015 ± 0.010	0.615 ± 0.221	0.092	9 ± 5	1 ± 5	5 ± 4	0 ± 1	3
XMMXCS J141728.95+521012.6	$0.770^{+0.112}_{-0.111}$	0.743 ± 0.115	-0.045 ± 0.013	1.320 ± 0.299	0.093	2 ± 4	5 ± 5	0 ± 0.1	-	3
XMMXCS J141728.9+521012.6	$0.770^{+0.112}_{-0.111}$	0.743 ± 0.115	-0.045 ± 0.013	1.320 ± 0.299	0.093	2 ± 4	5 ± 5	0 ± 0.1	-	3
XMMXCS J141757.44+523124.5	$0.751^{+0.110}_{-0.115}$	0.589 ± 0.105	-0.027 ± 0.037	0.849 ± 0.851	0.078	2 ± 4	2 ± 4	1 ± 2	2 ± 2	3
XMMXCS J141757.4+523124.4	$0.751^{+0.110}_{-0.115}$	0.589 ± 0.105	-0.027 ± 0.037	0.849 ± 0.851	0.078	2 ± 4	2 ± 4	1 ± 2	2 ± 2	3
XMMXCS J141825.4+522334.2	$0.935^{+0.105}_{-0.088}$	0.786 ± 0.119	-0.038 ± 0.019	1.320 ± 0.444	0.081	9 ± 5	12 ± 5	5 ± 4	12 ± 5	3
XMMXCS J220127.7+012301.3	$0.900^{+0.122}_{-0.123}$	0.759 ± 0.116	-0.055 ± 0.045	1.760 ± 1.060	0.080	11 ± 5	12 ± 5	11 ± 4	11 ± 5	3
XMMXCS J220217.56+014858.2	$0.665^{+0.141}_{-0.137}$	0.584 ± 0.103	-0.028 ± 0.020	0.785 ± 0.449	0.104	7 ± 4	6 ± 4	0 ± 2	3 ± 3	3
XMMXCS J220645.99+014919.2	$0.098^{+0.057}_{-0.058}$	0.083 ± 0.055	-0.024 ± 0.009	0.881 ± 0.157	0.031	1 ± 1	0 ± 1	1 ± 1	-	3
XMMXCS J221029.5+021559.4	$0.358^{+0.066}_{-0.063}$	0.296 ± 0.086	0.017 ± 0.028	0.189 ± 0.552	0.109	1 ± 3	-	0 ± 0.1	-	3
XMMXCS J221105.8+021322.9	$0.561^{+0.101}_{-0.102}$	0.604 ± 0.105	-0.000 ± 0.026	0.791 ± 0.575	0.085	1 ± 2	0 ± 3	0 ± 0.1	-	3
XMMXCS J221354.26-002051.9	$0.856^{+0.112}_{-0.101}$	0.743 ± 0.114	-0.039 ± 0.014	1.140 ± 0.314	0.105	14 ± 6	-	11 ± 6	-	3
XMMXCS J221512.82-003947.7	$0.350^{+0.079}_{-0.073}$	0.161 ± 0.078	-0.022 ± 0.019	0.738 ± 0.397	0.090	4 ± 3	-	2 ± 2	-	3
XMMXCS J221528.35+001958.1	$0.916^{+0.131}_{-0.132}$	0.884 ± 0.126	0.050 ± 0.036	-0.740 ± 0.830	0.095	5 ± 5	18 ± 6	0 ± 3	17 ± 7	3
XMMXCS J221624.7+000159.4	$1.026^{+0.123}_{-0.118}$	0.859 ± 0.124	-0.007 ± 0.037	0.692 ± 0.870	0.115	8 ± 5	8 ± 5	7 ± 4	6 ± 4	3
XMMXCS J221659.5+002506.5	$1.104^{+0.124}_{-0.112}$	0.958 ± 0.145	0.005 ± 0.026	0.376 ± 0.610	0.111	8 ± 5	14 ± 6	6 ± 4	12 ± 6	3
XMMXCS J221710.83+003922.6	$0.857^{+0.104}_{-0.114}$	0.753 ± 0.116	0.055 ± 0.051	-0.543 ± 1.150	0.111	3 ± 3	4 ± 4	4 ± 2	1 ± 2	3
XMMXCS J221712.80-002503.8	$0.884^{+0.103}_{-0.103}$	0.727 ± 0.114	-0.007 ± 0.010	0.505 ± 0.231	0.101	1 ± 5	2 ± 5	0 ± 0.1	-	3

Continued on next page

Table A.4 – continued from previous page

name	z_{RS}	z_{BCG}	cmr_{grad}	cmr_{inter}	cmr_{wid}	n_{gals-c}	n_{gals-l}	n_{200-c}	n_{200-l}	qual
XMMXCS J221712.8+002503.8	$1.071^{+0.139}_{-0.138}$	0.888 ± 0.126	0.039 ± 0.021	-0.396 ± 0.497	0.086	8 ± 5	9 ± 5	2 ± 3	4 ± 4	3
XMMXCS J221715.11+000542.9	$1.069^{+0.135}_{-0.131}$	0.877 ± 0.124	0.005 ± 0.015	0.303 ± 0.339	0.091	2 ± 4	2 ± 4	0 ± 1	-	3
XMMXCS J221715.1+000542.9	$1.069^{+0.135}_{-0.131}$	0.877 ± 0.124	0.005 ± 0.015	0.303 ± 0.339	0.091	2 ± 4	2 ± 4	0 ± 1	-	3
XMMXCS J221735.3+000926.4	$0.818^{+0.116}_{-0.125}$	0.792 ± 0.119	-0.073 ± 0.025	2.220 ± 0.575	0.084	0 ± 3	1 ± 3	-	0 ± 1	3
XMMXCS J221738.86+001758.0	$0.760^{+0.110}_{-0.104}$	0.585 ± 0.104	-0.003 ± 0.019	0.122 ± 0.425	0.104	0 ± 3	3 ± 4	-	2 ± 2	3
XMMXCS J221741.4+003023.6	$1.062^{+0.144}_{-0.144}$	1.080 ± 0.165	-0.022 ± 0.017	1.020 ± 0.396	0.090	2 ± 4	3 ± 4	0 ± 1	1 ± 2	3
XMMXCS J221741.42-003023.6	$0.794^{+0.117}_{-0.116}$	0.616 ± 0.105	-0.009 ± 0.011	0.487 ± 0.254	0.098	12 ± 6	15 ± 6	12 ± 6	15 ± 6	3
XMMXCS J221745.0+002447.4	$0.846^{+0.120}_{-0.119}$	0.739 ± 0.114	-0.008 ± 0.013	0.551 ± 0.286	0.109	24 ± 7	24 ± 7	38 ± 9	38 ± 9	3
XMMXCS J221745.1+002958.2	$0.851^{+0.123}_{-0.123}$	0.955 ± 0.128	-0.015 ± 0.012	0.916 ± 0.279	0.108	14 ± 5	8 ± 5	16 ± 6	9 ± 4	3
XMMXCS J221752.69+001636.1	$0.489^{+0.095}_{-0.095}$	0.439 ± 0.095	-0.056 ± 0.027	1.840 ± 0.529	0.043	4 ± 3	6 ± 3	0 ± 0.1	-	3
XMMXCS J221752.6+001636.1	$0.489^{+0.095}_{-0.095}$	0.439 ± 0.095	-0.056 ± 0.027	1.840 ± 0.529	0.043	4 ± 3	6 ± 3	0 ± 0.1	-	3
XMMXCS J221804.03-001425.2	$0.828^{+0.068}_{-0.068}$	0.772 ± 0.117	-0.045 ± 0.010	1.100 ± 0.222	0.082	1 ± 3	2 ± 4	0 ± 1	-	3
XMMXCS J221810.48+001920.9	$1.004^{+0.138}_{-0.138}$	0.845 ± 0.123	-0.036 ± 0.037	1.310 ± 0.874	0.115	13 ± 6	13 ± 6	16 ± 6	16 ± 6	3
XMMXCS J221810.4+001920.9	$1.004^{+0.138}_{-0.138}$	0.845 ± 0.123	-0.036 ± 0.037	1.310 ± 0.874	0.115	13 ± 6	13 ± 6	16 ± 6	16 ± 6	3
XMMXCS J221813.3+002620.5	$0.752^{+0.103}_{-0.098}$	0.664 ± 0.110	0.046 ± 0.034	-0.702 ± 0.740	0.109	0 ± 4	10 ± 5	-	4 ± 4	3
XMMXCS J221818.78+002313.5	$0.884^{+0.123}_{-0.121}$	0.687 ± 0.113	0.011 ± 0.032	0.061 ± 0.740	0.099	14 ± 6	17 ± 6	13 ± 6	19 ± 7	3
XMMXCS J221818.7+002313.4	$0.884^{+0.123}_{-0.121}$	0.687 ± 0.113	0.011 ± 0.032	0.061 ± 0.740	0.099	14 ± 6	17 ± 6	13 ± 6	19 ± 7	3
XMMXCS J221824.9+002426.8	$0.867^{+0.120}_{-0.118}$	0.719 ± 0.113	0.011 ± 0.020	0.215 ± 0.463	0.104	12 ± 6	15 ± 6	12 ± 6	18 ± 7	3